



USAMRICD-TR-16-03

Development of an Active Topical Skin
Protectant (aTSP)

Ernest H. Braue, Jr.

February 2016

Approved for public release; distribution unlimited

US Army Medical Research Institute of Chemical Defense
2900 Ricketts Point Road
Aberdeen Proving Ground, MD 21010-5400
an element of the
US Army Medical Research and Materiel Command

DISPOSITION INSTRUCTIONS:

Destroy this report when no longer needed. Do not return to the originator.

DISCLAIMERS:

The views expressed in this technical report are those of the author(s) and do not reflect the official policy of the Department of Army, Department of Defense, or the U.S. Government.

The experimental protocols were approved by the Animal Care and Use Committee at the United States Army Medical Research Institute of Chemical Defense, and all procedures were conducted in accordance with the principles stated in the Guide for the Care and Use of Laboratory Animals and the Animal Welfare Act of 1966 (P.L. 89-544), as amended.

The use of trade names does not constitute an official endorsement or approval of the use of such commercial hardware or software. This document may not be cited for purposes of advertisement.

REPORT DOCUMENTATION PAGE				Form Approved OMB No. 0704-0188	
Public reporting burden for this collection of information is estimated to average 1 hour per response, including the time for reviewing instructions, searching existing data sources, gathering and maintaining the data needed, and completing and reviewing this collection of information. Send comments regarding this burden estimate or any other aspect of this collection of information, including suggestions for reducing this burden to Department of Defense, Washington Headquarters Services, Directorate for Information Operations and Reports (0704-0188), 1215 Jefferson Davis Highway, Suite 1204, Arlington, VA 22202-4302. Respondents should be aware that notwithstanding any other provision of law, no person shall be subject to any penalty for failing to comply with a collection of information if it does not display a currently valid OMB control number. PLEASE DO NOT RETURN YOUR FORM TO THE ABOVE ADDRESS.					
1. REPORT DATE (DD-MM-YYYY) January 2016		2. REPORT TYPE Technical/Review Paper		3. DATES COVERED (From - To) 1994 - 2004	
4. TITLE AND SUBTITLE Development of an Active Topical Skin Protectant (aTSP)				5a. CONTRACT NUMBER	
				5b. GRANT NUMBER	
				5c. PROGRAM ELEMENT NUMBER	
6. AUTHOR(S) Braue, EH, Jr				5d. PROJECT NUMBER	
				5e. TASK NUMBER	
				5f. WORK UNIT NUMBER	
7. PERFORMING ORGANIZATION NAME(S) AND ADDRESS(ES) US Army Medical Research Institute of Chemical Defense ATTN: MCMR-CDT-T 2900 Ricketts Point Road Aberdeen Proving Ground, MD 21010-5400				8. PERFORMING ORGANIZATION REPORT NUMBER USAMRICD-TR-16-03	
9. SPONSORING / MONITORING AGENCY NAME(S) AND ADDRESS(ES) US Army Medical Research Institute of Chemical Defense ATTN: MCMR-CDT-T 2900 Ricketts Point Road Aberdeen Proving Ground, MD 21010-5400				10. SPONSOR/MONITOR'S ACRONYM(S)	
				11. SPONSOR/MONITOR'S REPORT NUMBER(S)	
12. DISTRIBUTION / AVAILABILITY STATEMENT Approved for public release; distribution unlimited.					
13. SUPPLEMENTARY NOTES					
14. ABSTRACT Summary of the research to develop an active topical skin protectant as a follow-on product to Skin Exposure Reduction Paste Against Chemical Warfare Agents (SERPACWA).					
15. SUBJECT TERMS decontamination, Skin Exposure Reduction Paste Against Chemical Warfare Agents (SERPACWA), skin barrier, detoxify, active topical skin protectant, reactive topical skin protectant					
16. SECURITY CLASSIFICATION OF:			17. LIMITATION OF ABSTRACT UNLIMITED	18. NUMBER OF PAGES 1087	19a. NAME OF RESPONSIBLE PERSON USAMRICD Public Affairs Office
a. REPORT UNCLASSIFIED	b. ABSTRACT UNCLASSIFIED	c. THIS PAGE UNCLASSIFIED			19b. TELEPHONE NUMBER (include area code) 410-436-3276

ACKNOWLEDGMENTS

The aTSP program at the USAMRICD was active for 10 years from 1994 to 2004 and was financially supported by the U.S. Army Medical Research and Materiel Command (USAMRMC). The success of the aTSP program was a direct result of all the personnel that contributed their time and talents to support this endeavor. I give my sincere thanks to the following organizations and individuals:

- USAMRICD
 - CPT Stephen Hobson, co-inventor and research scientist
 - Dr. John Graham, Assistant Research Coordinator
 - Dr. Millard Mershon, co-inventor and research scientist
 - Dr. Larry Mitcheltree, pathologist
 - Dr. Carmen Arroyo: EPR spectroscopy
 - MAJ Alan Weir
 - CPT David Sartori, NMR spectroscopy
 - CPT David Johnston, synthesis
 - SGT Marty Litchfield, technician
 - Catherine Braue, co-inventor and biologist
 - SGT Robert Rieder, technician
 - Ruth Way Moretz, co-inventor and biologist
 - Robyn Lee, Statistician
 - Bryce Doxzon, technician
 - Horace Lumpkin, technician
 - Kelly Hanssen Smith, physical scientist
 - Rich Sweeney, bioengineer
 - Rachel Hall, technician
 - Robert Stevenson, biologist
 - Robin Deckert, technician
 - SSG Christopher Maturey, technician
 - SSG James Mitchell, technician
 - Elizabeth Miller, technician
 - SGT Robert Simons, technician
 - Patricia Matterson DiLeonardi, technician
 - Joy Knickman, technician
 - SGT Neil Lewis, technician
 - David Kahler, technician
- Contractors
 - Thomas Snider, research scientist, Battelle
 - Joseph Boecker, co-inventor and technician
- Other Government Labs
 - Dr. Dupont Durst, Edgewood Research, Development and Engineering Center (ERDEC)
 - Dr. Kevin Morrissey, ERDEC
 - Dr. Ray Yin, Army Research Laboratory (ARL)
 - Dr. Dan DeSheppard, ARL

- **Academic Institutions**
 - Professor Craig Hill, Emory University
 - Professor Kenneth Shea, University of California, Irvine
- **Industry**
 - Ms. Ann Grow, Biopraxis,
 - Dr. Cecil Kwong, Southern Research Institute
 - Dr. Chandrika Govardhan, Altus Biologics
 - Dr. Kenneth Klabunde, Nantek Inc, and Nanoscale Materials, Inc.
 - Dr. Back, Mainstream, Inc.
 - Dr. James White, Eltron Research, Inc.
 - Dr. Kenneth Heater, METSS Corp
 - Dr. Brian Smith, TDA Research
 - Dr. John Dankert, HBR Technologies
 - Dr. Emily Reichert, TIAX LLC
 - Mr. James Sheldon, Carogen, Inc.

EXECUTIVE SUMMARY

In 1987, the U.S. Army Chemical School established a new requirement for a barrier cream to protect skin against chemical warfare agents (CWAs). The topical protectant would either augment the protection afforded by the protective over garments or, ideally, redefine the circumstances requiring mission oriented protective posture (MOPP) levels. In response to this requirement the U.S. Army Medical Research Institute of Chemical Defense (USAMRICD), Aberdeen Proving Ground, Maryland, developed Skin Exposure Reduction Paste Against Chemical Warfare Agents (SERPACWA). As candidate formulations for SERPACWA progressed through development, the final formulation received FDA approval in 2002 and became available to U.S. service members in March of 2003.

SERPACWA increased the protection provided by the standard protective suits used by the U.S. service members and extended the window for effective decontamination. While SERPACWA offered several advantages, it was not the ideal barrier cream and had limitations. SERPACWA acted as a passive protective barrier, but it did not neutralize chemical agents into less toxic compounds. In addition, SERPACWA did not provide protection against CWA vapor challenges.

To overcome the limitations of SERPACWA, the USAMRICD began a program to develop an improved SERPACWA. The program started as a Science and Technology Objective in 1994 and transitioned to a Defense Technology Objective in 1999. From FY94 through FY01 the program received a total of 15.9 million dollars mostly for external contracts. This program, known initially as reactive Topical Skin Protectant (rTSP) and later as active Topical Skin Protectant (aTSP), was designed to address the two main limitations of SERPACWA: non-reactivity and inability to protect against an agent vapor threat. Its goal was to develop a formulation that would act as both a protective barrier and an active, destructive matrix to detoxify CWAs.

Candidate formulations were discovered and evaluated through partnerships with external contractors from industry, universities, small businesses, and other government laboratories. The contracts included Broad Agency Announcements (BAA), Small Business Innovation Research (SBIR), Material Transfer Agreements (MTA), Cooperative Research and Development Agreements (CRADA), Short-Term Analysis Services (STAS), and special contracts with Battelle Memorial Institute and the U.S. Army Edgewood Chemical Biological Center (ECBC).

To select the best candidate formulations the USAMRICD developed and implemented a Decision Tree Network (DTN). The DTN was designed for high throughput utilizing *in vitro* modules to rapidly eliminate non-promising candidate formulations. Candidate formulations passing through the *in vitro* tests moved on to the *in vivo* testing modules. The final candidate formulations after *in vivo* testing moved into the advanced testing modules to final down-selection of the two best formulations for transition into advanced development.

Using the two components of SERPACWA, perfluorinated-polyether oil and polytetrafluoroethylene solid as a base cream, USAMRICD scientists evaluated over 150 different active components. Classes of compounds tested included polyalkenimines, enzymes, hybrid organic-inorganic materials, polyoxometalates, inorganic composites, inorganic oxides, metal alloys, and small organic molecules. These compounds were incorporated into the base cream to produce over 500 candidate formulations.

Against sulfur mustard (HD), a total of 17 active moieties demonstrated increased efficacy over SERPACWA: S-330, iodobenzene diacetate (IBDA), nanoreactors, ZE555 resin (M291 SDK powder), polysilsesquioxanes, polyoxometalates (POM), titanium manganese coated metal alloys, gold/copper (Au/Cu) catalysts, magnesium oxide (MgO) nanoparticles, silicon dioxide (SiO₂), ethanolamine matrix, cerium copper (Ce/Cu) salts on TiO₂ nanoparticles, metal precipitates, POM on TiO₂ nanoparticles, POM on MgO nanoparticles, silver (Ag) catalysts, and polyalkenimines.

Against soman (GD), a total of 15 active moieties demonstrated increased efficacy over SERPACWA: nanoreactors, organophosphorus acid anhydrolase (OPAA) enzyme, high test hypochlorite (HTH), metal precipitates, Au/Cu catalysts, Iron/copper/lanthanum (Fe/Cu/La) catalysts, zinc oxide (ZnO) nanoparticles, titanium dioxide (TiO₂) nanoparticles, Calcium oxide (CaO) nanoparticles, MgO nanoparticles, POM on TiO₂ nanoparticles, POM on MgO nanoparticles, Ce/Cu salts on TiO₂ nanoparticles, diethanolamine, and polyalkenimines.

Based on the results of the DTN evaluations, two candidate reactive moieties emerged as the lead compounds for advanced development, polyalkenimines (sold commercially as Lupasols) and S-330. One S-330 and 20 Lupasol and surfactant combinations were formulated at the Army Research Laboratory (ARL) using a commercial extruder to mimic the manufacturing process. These formulations were evaluated using the DTN modules. A special down-selection process was used to find the best candidate formulation. The overall best Lupasol formulation was ICD 3834 containing 38% FOMBLIN Y25 PFPE, 33% F5A PTFE, 13% Lupasol FG, 13% Lupasol WF, 1.5% Fluorolink 7004, and 1.5% Fluorolink 7005. The best S-330 formulation was ICD 4028, and it was selected as the backup formulation for advanced development. It contained 10% S-330, 54% FOMBLIN Y25 PFPE and 36% F5A PTFE.

Both of the products selected for transition to advanced development had limitations. ICD 3834, containing polyalkenimines, compared to SERPACWA did very well against all tested CWAs, but it did not do well in the wash test and thus may be at risk of losing effectiveness during strenuous activity while service members wear it under protective clothing. ICD 4028, containing S-330, compared to SERPACWA performed well against VX and HD and in the wash and wipe tests. It did not, however, react with GD and, thus, did not improve protection against GD compared to SERPACWA. Adding a reactive moiety effective against GD to the S-330 formulation may be a strategy to eliminate this current limitation.

With the current increase in the threats from non-traditional agents, approximately two to three years of additional efficacy studies now would be needed to transition aTSP to advanced development. The Defense Threat Reduction Agency (DTRA) currently (FY16) is not funding any barrier cream efforts, and whether DTRA will fund this research in the future is unknown.

INTRODUCTION

Topical Skin Protectants

The use of topically applied protectants as a means of delaying absorption of toxic substances through the skin has been of interest to the military since World War I (WWI). The purpose of these materials, as with protective suits, was minimizing exposure and prolonging the effective window for decontamination. Applying a topical protectant to vulnerable skin surfaces prior to entry into a chemical combat arena was proposed as a protective measure against percutaneous CWA toxicity soon after the use of sulfur mustard (HD) by Germany at Ypres, Belgium, in 1917 (Papirmeister et al., 1991). In the summer of 1917, the U.S. Army began examining various soaps and ointments for their

protective qualities. Although several simple formulations were found to be effective in reducing skin irritation produced by agents such as hydrogen sulfide, no product was provided to the warfighter before the end of the war (Papirmeister et al., 1991). Research in the area of protective ointments continued after WWI, but this effort did not produce a fielded product before the beginning of World War II (WWII).

During WWII, a concentrated effort to develop ointments for protection against HD took place at the Chemical Warfare Service, Edgewood Arsenal, Md. The Army produced the M-5 protective ointment, which was manufactured in 1943 and 1944. However, because of limited effectiveness, odor, and other cosmetic characteristics, the M-5 ointment was no longer issued to warfighters by the mid-1950s (Romano, 2001).

Between 1950 and the early 1980s, the focus on research shifted to medical countermeasures and away from protective creams. In the late 1980s there was an increased emphasis on the potential military use of vesicant agents. In 1987, the U.S. Army Chemical School established a new requirement for a barrier cream to protect skin against CWAs. In response to this requirement the U.S. Army Medical Research Institute of Chemical Defense (USAMRICD), Aberdeen Proving Ground, Md., developed two non-active barrier skin cream formulations based on a blend of perfluorinated polymers. The two formulations were transferred to advanced development in October 1990 (McCreary, 1997). After extensive testing, the most efficacious formulation was selected and progressed through development with an Investigational New Drug (IND) filed with the Food and Drug Administration (FDA) in 1994; approval of a New Drug Application (NDA) in 2000; and final FDA approval in 2002. It became available to U.S. service members in March of 2003 (Deployment Quarterly, 2003). This new product was called Skin Exposure Reduction Paste Against Chemical Warfare Agents (SERPACWA). SERPACWA consisted of 50% fine particles of polytetrafluoroethylene (PTFE, F5A powder from Ausimont, Morristown, NJ) dispersed in 50% perfluorinated polyether oil (PFPE, FOMBLIM™ Y25 oil also from Ausimont, Morristown, NJ).

SERPACWA was an antipenetrant barrier cream for use by service members to protect against the toxic effects of CWAs, for example, blister (vesicant), nerve agents, and percutaneously active biological agents (T-2 mycotoxin). The excellent barrier properties of SERPACWA were related to the low solubility of most materials in it. SERPACWA, however, acts as a passive barrier and does not neutralize CWAs. When used in conjunction with mission-oriented protective posture (MOPP) gear, SERPACWA prevented, or significantly reduced, the absorption of liquid CWAs into the skin. SERPACWA was much less effective against vapor hazards. It was used as an adjunct to MOPP, not as a substitute. Interestingly, the effective barrier of SERPACWA was found to protect against poison ivy and poison oak.

SERPACWA was used at the direction of each unit commander. Each service member was issued six packets of SERPACWA. The entire contents of one packet would be used in one application. When using SERPACWA in a CWA-contaminated zone, service members were to re-apply the cream every eight hours. A service member's basic load of 6 packets was sufficient to provide protection for two days. SERPACWA was not water-soluble, so it was not easily washed off with water or removed by sweat without brushing and scrubbing. However, SERPACWA did physically wear off with time. Abrasion of SERPACWA by clothing or other contacts, such as sand or dirt, would reduce the effective wear time. SERPACWA needed to be reapplied when the coating was generally embedded with particulate matter (dirt or sand), or the sites were decontaminated. Minimally, the 8-hour rule applied. Insect repellents on the skin, such as DEET, decreased the effectiveness of SERPACWA. If DEET was wiped off using a dry towel, gauze, or piece of cloth before SERPACWA was applied, then SERPACWA would still provide significant protection.

The effectiveness of SERPACWA was dependent on the thickness and integrity of the SERPACWA layer and the length of time between application and agent exposure (wear time). Under normal conditions, SERPACWA was effective when spread over the skin as a thin layer (0.1 millimeter thick or 0.01 ml/square centimeter). One packet of SERPACWA contained 1.35 fluid ounces (about 2.7 weight ounces or 84 grams [gm]). This amount of SERPACWA produced on the skin a smooth coating that had a barely visible cream color and was slightly detectable by touch. The first priority for skin application was to cover those areas adjacent to the closures of the individual protective ensemble (neck, wrists, and lower legs around the top of the boots). If the situation permitted, SERPACWA was to be applied also to the creases and crack of the buttocks and around the waist. It could have been applied to the armpits and groin area, but this was less important because SERPACWA did not provide significant protection against agent vapor. It is not approved for application to open wounds, nor is it approved for application to the entire body. SERPACWA was about 50% occlusive and functioned as a barrier to sweat and could potentially add to the heat stress of the body, especially if worn with MOPP.

The use of SERAPCWA made decontamination easier for those areas that were protected by the barrier because CWA was more easily removed from the SERPACWA layer than from the skin. Service members were still required to perform skin decontamination immediately after chemical contamination because the effectiveness of SERPACWA decreased with time.

SERPACWA had no vapors, so it did not register a false alarm with the automatic vapor detectors, such as the Improved Chemical Agent Monitor (ICAM). It also did not register with systems that detect chemical liquid, such as M8 or M9 paper. The SERPACWA cream on the surface of M8 or M9 paper would prevent CWA absorption by the paper, thereby rendering it ineffective for detecting CWAs.

SERPACWA increased the protection provided by the standard protective suits used by the U.S. service members and extended the window for effective decontamination. While SERPACWA offered several advantages, it was not the ideal barrier cream and had limitations. SERPACWA acted as a passive protective barrier and did not neutralize chemical agents into less toxic compounds. In addition, the evaluation of SERPACWA in animals using a saturated vapor cup model did not demonstrate any efficacy against challenge by HD vapor or GD vapor. In fact, against a minimum HD vapor challenge (saturated vapor cup for a short time) SERPACWA actually produced a significantly worse lesion over non-treated positive control animals. VX had such a low vapor pressure that it was generally not considered a vapor threat.

In a U.S. Army memorandum from the Office of the Army Chief of Staff dated October 9, 2008, the Joint Requirements Office for Chemical, Biological Radiological and Nuclear Defense was informed that the Army no longer recognized the utility of retaining SERPACWA capability within inventory beyond the shelf-life of the current stock. As a consequence of this decision, a Medical Supply Bulletin dated October 31, 2008, was issued to the three storage facilities where SERPACWA was stockpiled (in Kuwait, Korea, and Perry Point, Maryland) requesting that all stocks of SERPACWA be accounted for and quarantined, and that arrangements be made for their destruction. Since the date of manufacture, all supplies of SERPACWA that were stockpiled within the three storage facilities were never issued to individual service members. All SERPACWA lots stored at Perry Point, Kuwait, and Korea have since been destroyed. Also, as a consequence of the Army decision, all corrective and preventive actions which were ongoing and related to the Agency's inspection findings of the SERPACWA contract manufacturing and testing facilities were terminated. At the time of the termination of activities, the mixing procedure development and validation effort had been completed,

and the final report was submitted to the FDA. The results show that all various ages of reconstituted product pass the M8 paper test.

The Office of the Surgeon General (Army) informed the FDA at a November 2008 meeting and in a subsequent letter of its intent to withdraw both the IND and NDA. The Office of the Surgeon General, Department of the Army transferred appropriate sections of the SERPACWA NDA (21-084) and IND (46,876) into a Type V Drug Master File (DMF) and then withdrew both the NDA and IND once the Type V DMF was established in December 2008.

Active Topical Skin Protectants

To overcome the limitations of SERPACWA, the USAMRICD began a program to develop an improved topical skin protectant. The program started as a Science and Technology Objective in 1994 and transitioned to a Defense Technology Objective in 1999. From FY94 through FY01 the program received a total of 15.9 million dollars mostly for external contracts. This program, known initially as reactive Topical Skin Protectant (rTSP) and later as active Topical Skin Protectant (aTSP), was designed to address the two main limitations of SERPACWA: non-reactivity and inability to protect against an agent vapor threat. Its goal was to develop a formulation that would act as both a protective barrier and an active, destructive matrix to detoxify CWAs (Figure 1). The types of molecules that potentially could be used to neutralize or detoxify CWAs were known. The compounds fell into three general classes: oxidizers, reducers, and nucleophiles. An important limitation, however, was that the final formulation could not irritate the skin. This restriction eliminated many of the most reactive species. The aprotic non-polar environment of SERPACWA provided a unique but challenging medium for active moieties to neutralize CWAs. It was necessary for the improved SERPACWA to provide increased protection without degrading a warfighter's performance (Braue, 1999).

***In Vitro* Models for aTSP Evaluation**

The M8 paper test was developed at the USAMRICD under a new protocol. This evaluation model, which had applications for liquid HD and liquid nerve agents, was used at the USAMRICD and later transitioned to Battelle Memorial Institute for routine screening in the aTSP DTN. This test was the initial *in vitro* screen used to evaluate candidate formulations.

The initial analytical method developed for evaluating the effectiveness of TSPs against penetration by HD used Fourier transform infrared (FTIR) spectroscopy and the horizontal attenuated total reflectance (ATR) accessory (Braue et al., 1990 and 1992). This method worked well for aTSPs challenged with liquid HD, but had two major drawbacks: a narrow detection limit and no applicability for evaluating an HD vapor challenge. The USAMRICD developed a better method using a stainless steel Reifenrath Consulting and Research (RCR) low-flow cell (Figure 5). Initial setup used a single cell with nitrogen gas flow into a tenax solid adsorbent collection tube and analysis by a Dynatherm system (CDS Analytical, LLC, Oxford, PA) into a GC-MS. This basic setup was automated using the Miniature Automatic Continuous Air Monitoring System (Minicams, model LM-1001, O.I. Analytical, Birmingham, AL) integrated with a stream selection system so that five samples could be run simultaneously. The Minicams penetration cell test was developed at the USAMRICD and transitioned to Battelle Memorial Institute (Figure 6). Candidate formulations were evaluated for efficacy at both the USAMRICD and Battelle.

The proof-of-neutralization test was used to verify that active TSP formulations actually neutralized CWAs into less toxic materials. This test used the headspace solid phase microextraction

(HS-SPME) technique for the collection of CWAs and was conducted at the ECBC. Solid phase microextraction (SPME) was a relatively new sample preparation technique which was rapid and eliminated the need for extraction solvents. It was first introduced in 1990 (Arthur et al., 1990). The technique of SPME was applied to direct analysis of liquid samples where the fiber was immersed in the sample (IM-SPME). The technique also was applied to analyze the air in the headspace above the sample (HS-SPME). The HS-SPME technique was successfully applied to the analysis of CWAs in various matrices and was the method of choice for screening the effectiveness of aTSP candidates against HD, GD, and VX (Morrissey et al., 1997).

***In Vivo* Models for aTSP Evaluation**

In the late 1980's, with the increased emphasis on the potential military use of vesicant agents, a suitable animal model for evaluating potential anti-vesicant prophylactic and therapeutic compounds was clearly needed. Euthymic hairless guinea pigs [CrI:IAF/HA(hr/hr)Br] were selected for development at the USAMRICD. Vapor HD was delivered to animals under occlusive caps. Gross blistering was not seen after vapor exposure. However, damage to the basal cells, causing microblisters, which resembled lesions of vesicant injury in man without excess fluid in the separation at the dermal-epidermal junction, was observed. Several evaluation techniques, including bioengineering analytical technologies, were used to evaluate skin damage under several protocols. Methods of evaluation included visual grading using a modified visual Draize score (Mershon et al., 1990), erythema measurement using a reflectance colorimeter (Minolta chromameter, models CR-200 and CR-300; Braue et al., 1990 and 1992), edema and microvesicle measurement using high frequency high resolution ultrasound imaging (Dermascan C, Cortex Technology; Braue et al., 1998), dermal-epidermal skin separation using the Nikolsky's sign (Braue et al., 1997), and evaluation of H&E stained histopathology (Bryant et al., 1992; Graham et al., 1994).

The preliminary work demonstrated that the hairless guinea pig offered several advantages over haired guinea pigs as a cutaneous vesicant animal model. These advantages included greater sensitivity to HD, simplified application of both liquid and vapor HD, ease of visualizing and evaluating developing skin lesions, and a higher incidence of microblister formation. In the first three years of one protocol, methodologies for TSPs challenged with HD vapor were developed and validated using the hairless guinea pig model. Many TSP formulations were evaluated and rank ordered. The supply of hairless guinea pigs, however, was interrupted in October 1993 by an outbreak of the pathogenic gram-positive bacteria *Listeria monocytogenes* at the commercial supplier's breeding facility (Colgin et al., 1995), thereby forcing a search for alternative animal models. Both the haired guinea pig and the domestic weanling pig were evaluated as replacement animal models. The haired guinea pig model was used in the validation of a TSP/rTSP screening method against challenge with HD vapor. It was observed to be inferior to the hairless guinea pig because of complications associated with the hair removal process. Research with adult pigs indicated that microblisters developed following cutaneous HD vapor exposure (Mitcheltree et al., 1989). The histological characteristics of pig and human skin were comparable, with similarities in epidermal thickness and composition, pelage density (although follicular diameter was much greater in the pig), dermal structure, lipid content, and general morphology (Dick et al., 1992). In addition, pig skin was antigenically closer to human than rodent skin. EPA guidelines for dermal exposure assessment stated that the percutaneous absorption of many compounds in the pig was similar to that found in humans (EPA, 1992). Klain and co-workers concluded that pig skin was a good model for human skin metabolic studies (Klain et al., 1986). Meyer and co-workers concluded that among the domestic species, the pig provided the most suitable experimental model for dermatological research on humans (Meyer et al., 1978). Development work at the USAMRICD demonstrated that the weanling pig was a viable animal model for use in vesicant injury research.

In comparison with hairless and haired guinea pigs, weanling pig was observed to be more resistant to damage by HD vapor. The pig had a delayed response time and required a longer exposure to achieve similar levels of damage. Maximum erythema response required a vapor exposure of 15 minutes in the pig versus 5 minutes for both the hairless guinea pig (Braue et al., 1992) and haired guinea pig (Braue et al., 1998). Maximum erythema response in the guinea pigs occurred at 5-6 hours post-exposure versus 24 hours in the weanling pig. Given an adequate exposure to HD vapor (e.g., ≥ 15 minutes), erythema determinations made at 24-48 hours post-exposure could be used to reliably and quickly evaluate antivesicant efficacy in the weanling pig. Both the hairless guinea pig and the weanling pig were used to evaluate TSPs and aTSP candidate formulations. Each species offered unique advantages. The hairless guinea pig was very sensitive to HD and was proven to be an excellent model for TSP evaluations challenged with HD vapor. It was limited, however, by the unavailability of animals. The weanling pig was less sensitive to HD than the hairless guinea pig but had skin very similar to that of humans. The weanling pig's large body surface offered many experimental sites, allowing a wide range of doses to be tested on the same animal. It was ideally suited for efficacy testing of aTSPs and was the model of choice for these formulations challenged by HD vapor.

The standard animal model for percutaneously applied nerve agents was the haired guinea pig. A large data base using this model existed. The close-clipped, anesthetized, haired guinea pig was the model of choice for evaluation of TSPs/aTSPs challenged with nerve agents (Braue et al., 2009 Part 1; Braue et al., 2010 Part 2; Braue et al., 2012; Braue et al., 2014 Part 3; Braue et al., 2015 Part 4; Braue et al., 2015 Part 5; Braue et al., 2015 Part 6; Braue et al., 2015 Part 7; Braue et al., 2015 Part 8; Braue et al., 2015 Part 9; Braue et al., 2015 Part 10; Braue et al., 2015 Part 11; and Braue et al., 2015 Part 12). This model, developed at the USAMRICD, was transitioned to Battelle Memorial Institute for routine screening in the aTSP DTN.

The rabbit lesion area ratio (LAR) model was developed at Battelle Memorial Institute for the evaluation of aTSPs challenged with HD liquid. This test was the main *in vivo* evaluation model used in the aTSP DTN for challenge by HD liquid.

Battelle developed a rabbit lethality model for evaluating aTSPs challenged with the liquid nerve agent VX. A pilot study with liquid GD, however, demonstrated that the large volumes of GD needed to penetrate aTSPs in lethal amounts could not be contained reliably within the test site, even when a rubber "O" ring was adhered around the test site. Thus, this model was abandoned for GD challenges, and the guinea pig model developed at the USAMRICD was used. Battelle also developed a rabbit lethality model for evaluating aTSPs challenged with GD vapor.

The improved SERPACWA was ready for advanced development in 2004. However, the U.S. Army Medical Research and Materiel Command decided not to continue development of these improved formulations because SERPACWA provided a partial solution and funds were needed for other advanced development products. If the decision were made to continue advanced development, obtaining FDA approval and bringing this product to market would likely take 7 to 10 years. This new protective product, if fielded, would dramatically improve the protection from CWAs and may reduce the need for a full protective ensemble.

OBJECTIVE

The objective of this technical report is to provide a written summary of the work conducted in the development of aTSP. It includes a publication list of papers, patents, and reports resulting from this

project, a listing of the contracts supporting the project, a description of the experimental modules in the established Decision Tree Network, a listing of all the candidate formulations that were considered, and a summary of the results and conclusions.

MATERIALS AND METHODS

A description of the experimental methods used for this project may be found in the published work listed under references. Summaries will be provided in this report.

Preparing Candidate Formulations

Temperature and mixing shear were monitored to maintain the base cream at the desired consistency and quality. To prepare mixtures, a quantity of base oil (PFPE) was carefully weighed in a small vial, and the powder (PTFE) and active moiety needed for preparation of the desired formulation were weighed out on glassine weighing paper. The solid powders were then slowly mixed into the oil in the vial using a small glass stirring rod. Mixing was slow and deliberate at first to reduce loss of fine particulates into the air. After this initial process, complete mixing of the components in the formulation was achieved by using a mechanical stirrer under low shear or by using a Polytron Mixer (model PCU-11, Brinkmann Instruments) under very high shear. Mixing with the Polytron used a medium head at the setting of 5 for not less than five minutes. During the mixing process the vial got warm. The vial temperature was not allowed to get above what could be comfortably held in the hand. This was achieved by stopping the mixing process until the vial cooled or by placing the vial in a cool water bath. Whichever method was used, the total high shear mixing time was always at least five minutes. Some of the final down-selected formulations were prepared in larger batch sizes using a commercial high shear mixer at the ARL, Aberdeen Proving Ground North, Md.

M8 Chemical Detection Paper Test

M8 paper is packaged as a booklet of 50 2.1 x 9 cm tear-off strips. It contains dyes that appear yellow in contact with G agents, forest green with VX, and red with HD. Prior to each test day, a 2.5 x 14 cm piece of 0.15 mm thick labeling tape was perforated with three 2 cm diameter holes and placed over an M8 paper strip to make a test assembly with three test sites. A station was prepared for each aTSP to be applied onto nine test assemblies (Figures 3 and 4). Each station consisted of three test assemblies adhered to a nylon board, a 1 mL syringe filled with aTSP, and an operator. At a recorder's signal, each operator extruded 0.1 mL of aTSP onto a test site, distributed it using a spatula, and removed any excess with a glass microscope slide. Application times were recorded. Rotation of operators after each application was done to minimize any confounding from the spreading technique with aTSP. Each aTSP application was inspected visually for uniformity and if flawed, corrected.

Up to five test assemblies were placed on a 15 x 15 cm glass table supported by four Teflon[®] legs. Tables were arranged in a row on the floor of a hood, and a mirror was placed at an angle under each table. At 1 hr after application, 8 µL of HD, GD, or VX was dispensed from a repeating pipette at the center of each test site, and the site occluded with a plastic cap (Figure 3). The dosing time was recorded. The undersides of the test assemblies were monitored for up to 6 hr, and the time when a color change in the M8 paper initially became apparent (Figure 4) was recorded, denoting a "breakthrough." If a test site did not exhibit a breakthrough, then 360 min was recorded. Any aTSP that allowed fewer than two CWA breakthroughs among nine dosed test sites passed this screen. A mean breakthrough time was calculated for each aTSP, with 360 min being the highest possible

value. If the process control material allowed more than one HD breakthrough, improper spreading technique was suspected, and results of that test day were invalidated. Initially, ICD 3004 served as the process control material for HD challenges, but later was replaced by ICD 1511 (Krytox[®]). There was no criterion established for process control performance against GD and VX, and results from all test days with nerve agent challenges were accepted.

Minicams Penetration Cell Vapor Challenge Test

On each test day, a cellulose acetate wafer was placed on each of five penetration cells (Figure 6; Battelle used glass cells from Stratacor, Inc., Richmond, CA; the USAMRICD used stainless steel Reifenrath diffusion cells, Reifenrath Consulting and Research, Richmond, CA) in a chemical fume hood. The exposure area in a Stratacor cell was approximately 0.95 cm², while the RCR cell was 0.8 cm². A 0.15 mm thick strip of cellophane tape with a 1 cm diameter perforation was placed over each wafer. Approximately 20 µL of candidate aTSP was placed onto the wafer and distributed with a spatula. A glass microscope slide then was moved over the tape surface to remove excess aTSP (Figure 7). The aTSP surface of each cell was inspected using a magnifying lens for smoothness, and if irregularities were found, the cell was replaced. Two concentric rings of Krytox[®] (ICD 1511, DuPont, Wilmington, DE) lubricant were extruded from a syringe around the edge of each tape perforation, and the cells were placed in an aluminum holding block. Heated (37 °C) water was circulated through channels drilled in the holding block. A 14 mm diameter disk of Whatman paper No. 2 was pressed against the inside top of each of five plastic caps (Evergreen Scientific, Los Angeles, CA, Catalogue Number 300-1006-020) with approximate dimensions of 17 mm OD, 14 mm ID, and 6 mm in height. At 1 hr after each aTSP surface was smoothed, a volume of CWA, either 10 µL of HD or 8 µL of GD, was dosed onto the paper disk in each cap (Figure 8), which then was inverted and pressed into the Krytox[®] rings. The time was recorded.

Five replicate cells per candidate aTSP were monitored in parallel for CWA penetration. Ambient air was pulled from the lower half of each penetration cell and sampled at approximately 40 min intervals by a multi-port automated sampler that rotated among the five ports. Each air sample was adsorbed onto a solid sorbent and, after a prescribed interval, warmed before chromatographic analysis using a MINICAMS[®] (CMS Research Corporation, Birmingham, AL; Figure 3). Analysis data were digitally transferred to a computer for storage and processing. CWA penetration was integrated over a 20 hr exposure, and the time after dosing that the cumulative total of detected CWA exceeded 1000 ng (an endpoint called T1000) was determined. If the cumulative total of detected CWA was less than 1000 ng at the end of the 20 hr monitoring period, then a projected T1000 was estimated by linear extrapolation, with a maximum allowed value of 100,000 min. A low mean T1000 indicated a short time to CA breakthrough, suggesting a low level of protection afforded by a candidate. If the 20 hr total cumulative amount of detected CA exceeded 1000 ng in a cell, a “breakthrough” was noted. The number of breakthroughs was tallied for each candidate. Candidates were assigned a pass/fail result based on both the incidence of breakthroughs and the mean T1000 for five replicate cells relative to that for ICD 3004 (SERPACWA) which was periodically updated and compiled in an historical dataset.

Student’s two-sided t tests were conducted at $\alpha = 0.05$ assuming unequal variances. The statistical relationship between the mean T1000 for each aTSP ($T1000_{aTSP}$) and the current process control mean T1000 for ICD 3004 at the test time ($T1000_{ICD\ 3004}$) was determined as:

- Better, indicating $T1000_{aTSP} > T1000_{ICD\ 3004}$ ($p < 0.05$), and this candidate “passed” the screen if the aTSP allowed fewer than two breakthroughs among the five cells tested.

- Same, indicating $T1000_{aTSP}$ was statistically equivalent to $T1000_{ICD\ 3004}$, and this candidate “failed” the screen; or
- Worse, indicating $T1000_{aTSP} < T1000_{ICD\ 3004}$ ($p < 0.05$), and this candidate “failed” the screen.

This statistical procedure was developed by Battelle and was designed to limit the number of candidate aTSPs that would be evaluated in other DTN tests by identifying aTSPs that not only were better than ICD 3004, but also served as nearly complete barriers over 20 hr of exposure to CWA.

Proof of Neutralization Test

The proof-of-neutralization test was used to verify that aTSP formulations actually neutralized CWAs into less toxic materials. This test used the headspace solid phase microextraction (HS-SPME) technique for the collection of CWAs. A Hewlett-Packard 6890 Series Plus gas chromatograph with 5973 mass selective detector was used for all work performed during this study. Data acquisition was in full scan mode, with electron impact (EI) ionization. Helium was used as the carrier gas. The column was a Hewlett-Packard HP-5TA (30m X 0.32mm X 1 μ m film thickness). The SPME fiber was polydimethylsiloxane (PDMS), with a 100 μ m film thickness. Active TSP formulation, 100 mg, was challenged with 0.1 μ l of neat CWA (HD, GD, or VX) in a 10 mL SPME vial. The capped vial was placed into a 37 °C hot block and allowed to equilibrate for 40 minutes. After that time, the SPME fiber was introduced into the headspace and allowed to collect sample for 30 minutes. The SPME fiber was then removed from the sample vial and placed into the GC/MSD analytical system to determine the amount of CWA remaining in the flask. Efficacy was determined by the percent loss of CWA. Other analytical techniques such as nuclear magnetic resonance (NMR) and Fourier-transform infrared spectrometry (FTIR) also were used in this test. The HS-SPME tests were conducted at the ECBC.

Hairless Guinea Pig HD Vapor Test

Male [CrI:IAF/HA(hr/hr)BR VAF/Plus] euthymic, hairless guinea pigs weighing 250-400 g were used. The back of each animal was carefully cleaned with a soap solution the day before exposure to remove soil and debris. On the day of the experiment, the animals were transferred from the holding area to the laboratory in polycarbonate cages. The exposure sites were outlined using a template that was centered over the animal's back and marked (permanent marker) with dots. There was a total of 6 sites on each animal with 2 contralateral sites on each side to the dorsal midline. Previous work in the hairless guinea pig showed that 6 was the ideal number of sites for this animal model, as additional sites closer to the head are often too red pre-exposure for use. Pre-exposure baseline skin readings were made with a reflectance color meter (Minolta Chromameter models CR-200 or CR-300) using the a^* chromaticity values. Each site had 4 replicate readings. For any given site the mean of the 4 a^* values must have been less than 13. If the mean was greater than 13 a new position for that site was selected. If a satisfactory site could not be found the animal was rejected, and a replacement animal used.

The animals were weighed and anesthetized with one of two anesthesia methods. If the animals were expected to need anesthesia for less than 45 min, a combination of ketamine hydrochloride (30 mg/kg) and xylazine (6 mg/kg) i.m. was used. Injections were administered into the lateral thigh using a tuberculin syringe with a 25-27 gauge needle. If the animals needed anesthesia for greater than 45 min, isoflurane by inhalation was used. For the inhalation anesthesia procedure an anesthesia apparatus (North American Drager, Model SC-V, or similar) was used. Animals were initially placed

in an induction chamber (20 X 12 X 12 cm), and a plane of surgical anesthesia was induced with a 3% isoflurane/oxygen mixture (1.0 L/min). Animals were maintained under anesthesia using a 1.75% isoflurane/oxygen mixture (1.0 L/min) administered through a nose cone. If pain or distress was noted as assessed by decreased activity, anorexia, or self-mutilation, it was alleviated with buprenorphine hydrochloride (0.05 mg/kg, SQ q6-12h) at the PI's or attending veterinarian's discretion. Each animal was draped with polyethylene-backed absorbent sheeting (Kaydry, Kimberly Clark, Roswell, GA). Animals under anesthesia, both in or out of the hood, were kept on heating pads and covered to maintain their body temperature. Tape assemblies were prepared from double-sided carpet tape (ServiStar Fiberglass Professional Outdoor Carpet Tape). Each assembly was 4.0 by 2.5 cm, fitted with a pull tab, and had a center hole 12 mm in diameter. The top protective surface of the carpet tape was not removed until after the templates were placed on the animal and the TSP/aTSP applied. The punched tape assemblies were applied edge to edge and parallel to the spine on each side of an animal's back. This procedure produced two rows of exposure sites. Just prior to exposure the protective coverings were removed with forceps to expose fresh adhesive surfaces to hold the vapor cups.

TSPs/aTSPs were applied at the required thickness between 0.10 to 0.20 mm. Most aTSPs were evaluated at a thickness of 0.15 mm. The required amount of TSP was dispensed from a 50 μ l volumetric syringe (Hamilton gas-tight Luer tip #80901) and spread evenly over the circular exposure site with a spatula. Each TSP/aTSP was allowed to dry for 15 min on the animal's back prior to HD exposure. Immediately following specified HD exposure time, each site was cleaned with a dry cotton-tipped swab to remove the majority of the TSP/aTSP, followed by rinsing with a water-saturated swab (Cat. No. 19-0942-12, PGC Scientific, Frederick, MD). This slightly abrasive cleaning process removed the TSP/aTSP coating from the skin so that it would not interfere with the reflectance color meter readings.

Exposure to HD vapor and liquid was accomplished using the methods developed in our laboratory and described in our safety SOPs. For saturated HD vapor exposures, polyethylene caps (Cat # 300-1006-020, Evergreen Scientific, 2300 E. 49th St. P.O. Box 58248, Los Angeles, CA 90058, phone 1-800-421-6261), with an outer diameter of 17 mm and inner diameter of 14 mm, were fitted with 14 mm discs of Whatman No. 2 filter paper. The filter paper was fixed 5 mm above the cap rim against the bottom inner surface of the cap. The filter paper in each inverted cap was wetted with 10 μ l of neat HD. This quantity of HD was sufficient to completely saturate the filter disc without run-off. Following a short equilibration period (saturated HD vapor pressure of 0.16 mm of Hg at 30 °C with a vapor concentration of 1.4 mg/L), the caps were adhered sequentially to the tape assembly over the exposure sites (holes in tape assembly). Exposure was stopped by removing the cap and tape assembly. Forceps were used to apply the caps or remove caps and tape assemblies from the skin.

For liquid HD exposures, each TSP/aTSP-protected site was challenged using a modified version of the tape assemblies used in the vapor exposures. Tape assemblies were prepared as above, except that the center hole was 9 mm in diameter instead of 12 mm. Centered over the hole in the assembly was placed a 14 mm diameter disc of Whatman No. 2 filter paper. These liquid dosing assemblies were placed onto the dorsal sites with the filter paper in full contact with the skin surface. The filter paper was wetted with 10 μ l of neat HD using a volumetric pipette. Using forceps, an inverted vapor cap (without fitted filter paper) was placed over the wetted filter paper, adhered to the assembly by the carpet tape surrounding the 9 mm hole. Gentle downward pressure was applied to the cap to assure complete contact of the wetted filter with the skin. Previous experimentation with liquid dosing techniques demonstrated that this pressure was necessary to generate uniform lesions. Exposure was stopped by removing the filter disk and tape assembly with forceps. The sites were

then immediately cleaned with a dry cotton-tipped swab to absorb any visible liquid HD remaining on the skin surface and to remove the majority of the TSP, followed by rinsing with a water-saturated swab (Cat. No. 19-0942-12, PGC Scientific, Frederick, MD). The HD liquid exposure technique developed at the USAMRICD was not used in the aTSP DTN.

The skin damage caused by the HD exposure was quantified using three end-points at various times post-exposure: (1) erythema using reflectance color meter, (2) edema using high frequency ultrasound imaging, and (3) testing for Nikolsky's sign (last testing time-point only). In addition, microblister formation was examined using light microscopic examination of hematoxylin and eosin (H&E) stained biopsies taken at 24-72 hours post-exposure. Representative lesions were photographed for future reference.

The reflectance color meter (Minolta Chroma Meter, model CR-300) readings were recorded as previously described (Braue et al., 1990 and 1992). Four replicate readings were taken prior to exposure and just before anesthesia on each experimental site and then again at various time points after HD exposure. Animals were restrained by hand. The a^* chromaticity parameter was used as the indicator of the degree of erythema (redness). On a site by site basis, the difference between the average before and average after readings was calculated to determine the net increase in erythema. The similarly treated sites were averaged on each animal, and a single a^* difference value was calculated for each treatment. The control site was a positive control and was challenged with HD, but was not be protected by a TSP/aTSP. Percent of control was calculated by the equation:

Percent control = [mean Δa^* reflectance value for aTSP site/ mean Δa^* reflectance value for positive control site] x 100

High frequency ultrasound imaging (Dermascan C imaging system, Cortex Technology) was used to determine the degree of edema by measuring the full skin thickness of the animal before exposure and at various time points post-exposure. Guinea pigs were unanesthetized and restrained by hand (note: weanling pigs were placed under anesthesia during ultrasound measurements). On a site by site basis, the difference between the before and after readings was calculated to determine the net increase in edema. A single ultrasound measurement was recorded on each site. In a manner similar to the erythema measurements, replicate sites were averaged on each animal, and a single skin thickness change was calculated for each treatment.

At 24 hours post-exposure, selected sites were tested for the Nikolsky's sign to measure HD-induced damage at the dermal-epidermal junction (Braue et al., 1997). Two procedures were used to test for the Nikolsky's sign. The first procedure used a tape stripping method, and the second procedure used a modified dermal torque meter (DTM, DIA-STRON Limited, 835-837 Sussex Blvd., Broomall, PA 19008-4310).

While the animal was under anesthesia, the skin to be evaluated was first cleansed of dander and loose skin by lightly patting the skin surface with loops of duct tape. Tape stripping was performed using double-sided carpet tape. A small disk (15 mm diameter) of the double-sided tape was placed on the end of a 17 mm metal rod (adhesive centering tool supplied with the DTM). The tape was applied to the animal for 5 sec and pulled off. Each experimental site was tape stripped for 50 replicates or until a positive Nikolsky's sign was observed. After euthanasia, 8 mm skin punches from each site were processed for routine histopathology (H&E stain).

In the DTM procedure, a double-sided adhesive was placed onto the flat surface of six 15 mm diameter DTM torque disks, and a small drop of cyanoacrylate adhesive applied on top of the double-

sided adhesives and spread evenly over the surface with a wooden applicator stick. The assemblies were immediately placed over the center of each of the selected dosing sites, and the cyanoacrylate adhesive was allowed to dry for 5 minutes. While the glue was drying, a double-sided adhesive was placed onto DTM guard rings (48 mm in diameter with a 17 mm diameter hole in the center). After the 5-minute drying time, the guard rings were placed onto the skin surface over each torque disk, leaving a ring gap of 1 mm. The purpose of the guard ring was to keep the skin immediately surrounding the dosing areas stationary and taut while the torque disks over the lesion areas were twisted. Either a modified DTM or a modified 3/4" drill bit placed into a cordless drill supplied the twisting motion to the upper surface of the torque disk. Light downward pressure was applied by hand on the guard rings while the DTM or drill was engaged, thereby twisting off the torque disks from the skin. The guard rings were gently pulled off of the skin, and the area cleansed of dried glue and tape adhesive by rubbing with foam swabs soaked with acetone. Each lesion was visually inspected for a positive Nikolsky's sign, characterized by patches of missing epidermis greater than 1 pinhole. For those sites that produced negative results, the above procedure was repeated. Following the second round of testing for Nikolsky's sign, results were recorded.

Two modifications were made to the standard DTM system. The first modification allowed the torque to be gradually increased (maximum of 50 mNm instead of 30 mNm) with time instead of being applied all at once. The second modification allowed the use of multiple center disk & guard ring assemblies. The DTM parameters used included a center disk of 15 mm, a ring gap of 1 mm, a torque of 30-50 mNm, and a cycle time of 5 sec. A cyanoacrylate adhesive was used to secure the center disk and guard ring to the skin (3 min drying time).

After the lesion evaluations were completed, animals were euthanatized using an inhalation overdose of halothane. Following euthanasia, the skin over the dorsal, thoracic-lumbar area was removed. Circular dermal biopsies (8 mm in diameter) were immediately taken from the center of all exposure sites of each animal. Additional skin biopsies were taken from a back area not exposed to HD to serve as negative controls. The skin biopsies were placed in individually labeled cassettes and then placed in jars containing 10% neutral buffered formalin. Each fixed specimen was embedded in paraffin, sectioned, and stained with H&E for histopathological evaluation by light microscopy. Each site was histopathologically evaluated for the presence or absence of microblisters. In addition, the following histopathological markers were evaluated: epidermal necrosis, pustular epidermitis, follicular damage, vascular damage, dermal hemorrhage, and dermal necrosis. The severity and distribution were combined subjectively into a single number of 0 through 4.

Weanling Pig HD Vapor Test

Weanling pigs were male castrated Yorkshire Cross pigs, *Sus scrofa*, 7-10 kg, purchased from Archer Farms, Belcamp, Md. The HD vapor experiments with weanling pigs were essentially the same as the experiments with hairless guinea pigs except as noted below.

Eighteen to twenty-four hours before agent exposure, the backs of the weanling pigs were closely clipped with electric clippers, followed by shaving with a commercial shaving cream and disposable shaving razor. The shaving procedure was sometimes performed under anesthesia, depending on the animal's response to the process. The shaved skin of anesthetized weanling pigs was exposed to saturated HD vapor for 15-60 minutes. Each animal had 24 exposure sites. A plastic template 8 cm x 12 cm was used for consistent anatomical positioning of the sites. Twelve sites were located on each side of the dorsal midline, in two columns of six sites per side (running anterior to posterior). Each row of sites (e.g., sites at the same anterior-posterior level) was treated the same (positive control or TSP/aTSP). The first row of sites served as positive controls, with no TSPs applied. The

second row of sites had a reference standard (0.2 mm layer of ICD 2289 or 0.1 mm layer of ICD 2650, or some other compound). Candidate aTSPs were applied to the other rows at a thickness of 0.15 mm. Occasionally, other thicknesses were used for the aTSPs. The applied TSP or aTSP was allowed to dry for 15 minutes before HD exposure. Weanling pigs were weighed and anesthetized with intramuscular Telazol[®] (6 mg/kg) and Rompun[®] (2.2 mg/kg). Animals were injected periodically as needed during HD exposure to maintain a level of deep anesthesia. Animals under anesthesia during HD exposure were kept on heating pads and covered to maintain their body temperature. When testing some candidate aTSPs, the first, second, and third rows were challenged with HD vapor for 15 minutes, the fourth row for 30 minutes, the fifth row for 45 minutes, and the sixth row for 60 minutes. In this way, a wide protection range was determined. Preliminary testing of each candidate compound required 6 pigs. For each group of six pigs, the assigned rows were rotated to preclude any site-specific biases within the area covered by the plastic template. If the candidate formulation still showed significant protection, even with a 60 min exposure, additional testing took place using longer exposure times. The actual exposure times used were determined on a case-by-case basis depending on the level of protection observed in the 15 to 60 min screening. This additional testing required 6 weanling pigs. Thus, a maximum of 12 animals were needed per evaluation.

Haired Guinea Pig Nerve Agent Liquid Test

This evaluation test was described in detail in the literature (Braue et al., Technical Report 2009 and Braue et al., COT 2011). Briefly, SERPACWA was applied according to current doctrine. SERPACWA animals were secured to a hold down board in sternal recumbency after animals were under anesthesia. The SERPACWA animals were given an initial i.m. injection of the combination of ketamine (87 mg/kg) and xylazine (13 mg/kg) 5 minutes prior to agent exposure and a second half dose i.m. injection of ketamine (44 mg/kg) and xylazine (7 mg/kg) at 60 minutes post-exposure. A test site received a calculated rate of application of approximately 0.01 mL/cm² of SERPACWA (equivalent to an average depth of approximately 0.1 mm). A 1 mL disposable syringe (no needle) was used to deliver approximately 0.07 ml of SERPACWA to each circular test site, 3.0 cm in diameter. After application, the SERPACWA was uniformly spread over the marked site with a small spatula. Special care was taken to work the SERPACWA under the short hair stubble to obtain a uniform coating. This process was completed within the first 5 minutes after anesthesia injection. The SERPACWA was allowed to dry for an additional 15 minutes. CWA challenge was administered to the SERPACWA-protected skin site 20 minutes after the initial anesthesia injection. Agent remained on the animal for a period of 2 hours. After the 2-hour exposure period, any remaining agent was removed with a dry wipe, and the animal was transferred to the holding cage in the fume hood. Special care was taken to position these animals in the hood so that the exposure site was level prior to CWA application. The maximum volume of CWA that could be applied to SERPACWA-protected skin without the agent running off the site was about 70 µl. If CWA was observed to run off the SERPACWA-protected site during the exposure period, the animal was excluded from the study results. Positive control animals were challenged with CWA in the same way as the treated animals except that they received no treatment. All animals were observed during the first 4 hours and again at 24 hours post-exposure for signs of toxicity and death. The protective ratio (PR, defined as LD₅₀ of the treatment group divided by the LD₅₀ of the untreated positive control animals) was calculated from the derived median lethal dose-response curves established for each treatment group and non-treated positive control animals. Significance was defined as $p < 0.05$. All animals were euthanized 24 hours post-exposure in a halothane or isoflurane-filled chamber IAW USAMRICD SOP-VMSB-301, titled "Animal Euthanasia." After euthanasia, the area of skin receiving CWA was excised down to the fat layer and placed in 5% bleach. The carcasses were disposed of IAW USAMRICD SOP-VMSB-301.

Rabbit Lesion Area Ratio (LAR) HD Liquid Test

Battelle Memorial Institute conducted a pilot study to determine whether the statistical power for detecting the superiority of ICD 2701 (formulation containing S-330) over ICD 3004 (SERPACWA) against HD challenge in the rabbit LAR model could be improved by occluding the dosed test site with a 6 or 12 mm diameter disk of Teflon sheeting (Figure 9). Specific pathogen free (SPF) New Zealand White (albino) male rabbits, each bearing an ear tag, were obtained from Covance, Inc. (Denver, PA). Each rabbit weighed between 2.0 and 4.0 kg and was between 3 and 6 months of age when placed on the study. Rabbits were housed individually in stainless-steel, slotted-floor cages equipped with automatic watering systems. Purina Rabbit Chow[®] was fed. Each animal was anesthetized with a xylazine/ketamine mixture administered by i.m. injection, and then placed on a positioning board. Additional anesthetic was injected as needed. The hair on the dorsum of each animal was clipped. The challenge of HD used on the first and second test days was 1 and 2 μL , respectively. Eight 2.5 x 5 cm contiguous test sites were drawn on each rabbit and labeled A through H using a felt-tipped pen. A 0.19 mL volume of ICD 2701 or ICD 3004 was extruded from a syringe at the center of each designated test site and distributed using a spatula to form an average thickness of 0.15 mm. At 15 min after pretreatment, HD was applied at the center of each site, and the site occluded or not occluded. Pretreatments and occlusions were rotated at sites A through F from rabbit to rabbit to minimize positional effects. Rear test sites consistently were not pretreated and were dosed and occluded with a 6 mm (site G) or a 12 mm (site H) diameter disk. The dosing time was recorded.

Four hours after dosing, a 10 x 10 cm gauze pad was held with tongs in contact with each test site for approximately 5 sec to absorb any residual HD. Another gauze pad was used to wipe off as much aTSP as possible. A third gauze pad was saturated with approximately 3 mL of a 0.5 % aqueous solution of sodium hypochlorite (NaOCl) and held in contact with the test site for approximately 10 sec. The pad was turned over and held at the site for another 10 sec and then discarded. A fourth pad was saturated with approximately 3 mL of distilled water, and the same two-sided process performed as a rinse step. The rinse step then was repeated with a fifth pad.

Decontaminated rabbits were removed from positioning boards and placed in stainless-steel stanchions within the hood for the remainder of the 24-hour experiment. Rabbits were allowed to recover from the anesthetic, and drinking water, but no food, was provided following recovery. On the morning after dosing, a 3% suspension of Trypan blue dye in saline was injected intramuscularly into each rabbit to enhance the visibility of the lesion area. At 24 hr after challenge, the size of the lesion associated with each exposure was estimated with a ruler (Figure 10) and photographed. All surviving rabbits were euthanatized. Lesion size was calculated from the lesion length (l) and width (w) as the area (A_L) of an ellipsoid, i.e., $A_L = \pi lw/4$. Lesion lengths and widths were entered into spreadsheets, and the area was calculated.

Lesion areas at sites A through F occluded with a 6 or 12 mm disk were normalized for individual rabbit sensitivity to HD by dividing the area at site G or site H, depending on occlusive disk diameter. Results were tabulated as descriptive statistics by pretreatment, HD volume, and disk size. For each HD dose volume and disk size, a statistical comparison of LARs was made to determine the sensitivity of the model for detecting the superiority of ICD 2701 over ICD 3004.

The optimized model then was used to perform eight sets of aTSP evaluations against HD over 25 test days involving 24 rabbits per day. The HD challenge dose was 1 μL , and a 12 mm diameter disk of Teflon sheeting was used. Other procedures were the same as in the pilot study. LAR was calculated as the lesion area at each pretreated site divided by the lesion area at the untreated, control site of each rabbit. Results were tabulated as descriptive statistics by aTSP and compared

with concurrent results for ICD 3004, both at fixed sites or, when available, at rotated sites using Dunnett's test. Comparisons against ICD 3004 at rotated sites were preferred in order to remove positional biases. To control for conducting multiple comparisons within each test set, a Bonferroni adjustment to the p value decision level ($\alpha = 0.05/n$, where n is the number of candidates tested in a set) was made. Use of a Bonferroni-adjusted p value reduced the probability of erroneously accepting a false hypothesis that a protective effect was afforded by an aTSP. Thus, a relatively conservative criterion was used to identify candidates that were very likely effective.

Rabbit Lethality Test for Liquid Nerve Agents

The primary endpoint in this model was the 24-hour lethality rate among rabbits pretreated with an aTSP candidate relative to (1) the lethality rate among untreated rabbits to demonstrate aTSP efficacy and (2) lethality rate among rabbits pretreated with ICD 3004 to assess efficacy relative to a standard. Lethality rates were compared statistically using Fisher's exact test at a two-sided, Bonferroni-adjusted decision level of $\alpha = 0.05/n$.

Evaluations of aTSPs against VX were conducted over 50 test days involving nominally 17 rabbits per day. Fifteen rabbits nominally were allocated for pretreatment with one of six aTSPs (two rabbits per group) or a process control material (three rabbits), and two rabbits were not pretreated. Test days were replicated until the sample size was 24 for each aTSP. A 3.8 cm diameter circle was drawn on each rabbit's back on the midline and behind the scapulae to mark a test site. A 0.11 mL volume of aTSP was extruded from a syringe and distributed using a spatula to form an average aTSP thickness of 0.15 mm. At 15 min after aTSP application, a standard challenge of 0.5 mg VX/kg was applied at the center of each site, which remained non-occluded. The dosing time was recorded. The standard challenge was equivalent to the 24 hr median lethal dose (LD_{50}), a dose expected to be lethal to 50% of untreated rabbits. A total of 21 candidate formulations were evaluated for efficacy relative to no pretreatment and relative to ICD 3004.

In add-on work, the protective efficacy of a 0.1 mm thick application of ICD 3004 against 4 hr topical exposures to Russian VX (RVX) was estimated. The objective of the expanded work was to estimate a 24 hr LD_{50} for each challenge material and pretreatment group (untreated or pretreated with ICD 3004) together with 95% confidence intervals calculated by Fieller's method (Finney, 1971). The probit model was fitted, when possible, using the SAS[®] Release 9.1 PROBIT procedure. A protective ratio (PR) of ICD 3004 for each challenge material was computed, when possible, as the LD_{50} for pretreatment with ICD 3004 divided by the untreated LD_{50} . Statistical hypothesis tests were conducted to determine the protective efficacy of ICD 3004 by comparing each estimable PR to unity.

Rabbit Lethality Test for GD Vapor Challenge

This test was similar to the liquid test, except GD was not applied directly onto an aTSP surface but onto Whatman No. 2 paper fitted into the top of a 3.3 cm diameter plastic cap (standard vapor cup challenge). The dosed cap subsequently was inverted over a test site and generated a GD vapor challenge. The maximum GD volume that could be dosed into each cap without the risk of GD dripping onto the test site was approximately 70 μ L, so the standard dose was 28 μ L GD/kg per cap.

An optimization study was conducted to determine whether one, two, or three caps and 2 or 4 hr exposures on rabbits pretreated with ICD 3004 would provide a suitable dynamic range for distinguishing the protective efficacy aTSPs relative to that of ICD 3004 against GD vapor. The objective was to find a regimen in ICD 3004-pretreated rabbits that produced approximately 80% lethality within 24 hr after the start of exposures. Six candidate aTSPs were evaluated relative to ICD

3004 in the first set of tests, but the second set of tests was truncated because of low lethality in ICD 3004-pretreated rabbits. A single vapor cap appeared to be insufficient for discriminating among pretreatments. Results from a second optimization study using rabbits either untreated or pretreated with ICD 3004 or ICD 3834 (lead formulation with polyalkenimines) confirmed that 4 hr exposures to two caps, each dosed with 28 μ L GD/kg, provided a better dynamic range in lethality rate for distinguishing efficacious aTSPs. This model was used to evaluate 28 aTSP candidates.

Weanling Pig Skin aTSP Wash and Wipe Test

TSP Application

Prior to experimentation, each weanling pig was sedated intramuscularly with xylazine HCl (Rompun®; 1.0 mL @ 20 mg/mL) and a combination of tiletamine HCl and zolazepam HCl (Telazol®; weighed out in equal parts, reconstituted to 100 mg/mL, and 0.5 mL administered). Double-sided sticky tabs, with 12 mm diameter circular holes punched through each tab, were applied to the left and right side of the hair-clipped belly of the experimental pig lying in dorsal recumbency. Tabs were applied in three columns of six rows down the ventral surface (some experiments used slightly different numbers of columns and rows as noted in the tables), with the upper covering of each tab left in place protecting the sticky surface. The sets of tabs to each side of the midline were washed with saline, while the midline column acted as a control for comparison, and eventually used in a wipe test. Within the circular opening in each tab, 0.017 ml aTSP was measured out, using a Hamilton gas-tight syringe, and spread evenly to give a 0.15 mm thickness coating of barrier cream. Each site containing an aTSP was allowed to dry for 15 or 60 minutes, and upon completion, the spot was washed with saline solution. Anesthesia was administered as needed in half-doses.

Wash Test

Two 10cc Luer Lok syringes were cut in half, and the plunger, as well as the end containing the dispensing tip, was discarded. The remaining piece of the syringe was used as a base to contain the saline used for washing. The two syringe bases were placed over the first two outlying aTSP sites nearest the anterior end, and a 1.7 ml aliquot of saline solution (0.9%) was pipetted into the open surface of the syringe. Following a 10-second resting time of the fluid, the syringe base was lifted, and the saline was allowed to drain away from the site. Washing was repeated four more times, for a total washing volume of 8.5 ml per site. This procedure was repeated for each of the remaining sites on the ventral surface, moving schematically down the belly toward the posterior end. Following washing, all sites were allowed to dry for a 15-minute period. Upon completion, sites were scored based on how well the aTSP remained intact with the skin. Anesthesia was administered as needed in half-doses.

Wipe Test

The un-wetted sites, running down the center of the ventral surface, were also graded. Foam swabs were swept across the aTSP surface, first with light pressure, followed by heavy pressure. These sites were scored to determine how wiping affected the ability of the aTSP to remain in contact with the skin. Anesthesia was administered as needed in half-doses.

Scoring

Visual scoring of the wash test evaluated the amount of aTSP remaining on the skin and was based on a five-point system (0-4): 0 indicated that no aTSP remained on the skin; 1 indicated that a

majority of the skin was left uncovered by aTSP; 2 indicated that roughly half of the skin was covered; 3 indicated that a majority of the skin was covered, although small breaks in coverage occurred; and 4 indicated total area coverage of the skin.

Visual scoring of the wipe test evaluated the amount of aTSP remaining on the skin and was based on a four-point system (0-3): 0 indicated that all aTSP was removed with light pressure; 1 indicated that aTSP was partially removed with light pressure; 2 indicated that aTSP was removed with heavy pressure, but not with light pressure; and 3 indicated that aTSP was not removed with heavy pressure.

RESULTS

External Contracts

The aTSP program was supported by many external contracts which discovered reactive moieties, developed formulations, and evaluated candidate formulations for efficacy, and safety. The contracts are listed below.

Broad Agency Announcements (BAA)

- SRI: DAMD17-93-C-3186
- Biopraxis
 - Contract 1: DAMD17-08-C-8028
 - Contract 2: DAMD17-01-C-0057
- Altus Biologics: DAMD17-98-C-8029

Small Business Innovation Research (SBIR)

- Nantek : Phases 1 and 2: DAMD17-97-C-7016
- Nanoscale: Phases 1 and 2: DAMA17-99-C-9012
- METSS : Phases 1 and 2: DAMD17-99C-9046
- Cape Cod Research: X81XWH-05-C-0123
- Eltron: DAMD17-99-C-9007
- Mainstream:
 - DAMD17-97-C-7017
 - DAMD17-99-C-9019
- TIAX: Phases 1 and 2: X81XWH-05-C-0131

Material Transfer Agreement (MTA)

- ARL:
- TDA:
- VSP technologies:

STAS/DRC/ORISE/Ke'aki

- Ken Shea, UC Irving: DAAH04-96-C-0086 with Task control No (TCN) 00-089
- Craig Hill, Emory Univ: DAAH04-96-C-0086 with TCN 98-138
- Craig Hill, Emory Univ: DAAH04-96-C-0086 with TCN 01-125

Cooperative Research and Development Agreement (CRDA)

- Carogen: DAMD17-96-0046

OTHER

- SBCCOM SPME analysis
- Battelle Task 3: DAMD17-99-d-0010
- USACHPPM Toxicology safety studies

Many of the final reports for these contracts are very difficult to obtain, so when not prohibited by proprietary restrictions, the final reports are given in Appendix B.

Battelle DTN Contract (Snider, 2005, Government Reports, Task 3 Final Report)

The objective of the Battelle contract was to assist in the development and implementation of a decision tree network (DTN) to compare candidate aTSP formulations to a 0.15 mm thick SERPACWA barrier in providing protection from topical exposure to CWAs. The DTN implementation at Battelle was designed for high throughput in four *in vitro* modules and to screen efficacious candidates in up to three *in vivo* modules. Candidate aTSP formulations were submitted to Battelle without formulary details.

The work was conducted over a five-year period, starting in 2000, under MREF Protocol 166, entitled “Efficacy of Candidate Reactive Topical Skin Protectants on Rabbits against Liquid and Vapor Vesicating and Nerve Agents,” and MREF Protocol 231, entitled “Efficacy of Candidate Active Topical Skin Protectants on Hairless Guinea Pigs against Liquid Nerve Agents.” The protocols describe test models for assessing the protective efficacy of SERPACWA and candidate aTSPs against HD, GD, VX, and RVX, using the New Zealand white rabbit and Hartley guinea pig. Project work was conducted at Battelle Memorial Institute’s Medical Research and Evaluation Facility, Building JM-3, West Jefferson, Ohio 43162. The protocols were attachments to the Battelle final report.

Approximately 195 candidate aTSPs were evaluated *in vitro* in 510 tests conducted between March of 2000 and February 2003. Approximately 59 candidate aTSPs were evaluated in *in vivo* tests conducted over 268 challenge days between March of 2000 and January 2005.

In the Minicams Penetration Cell Vapor Challenge Test, of the 199 candidate aTSPs that were tested against both HD and GD vapor challenges (Table 1) the formulations that were better than the standard ICD 3004 and “passed” this screen were ICD 3523, 3548, 3549, 3551, 3552, 3633, 3664, 3665, 3708, 3717, 3725, 3728, 3729, 3742, 3773, 3775, 3778, 3779, 3782, 3970, 3973, 3974, and 3981.

In the M8 Chemical Detection Paper Test, of the 56 candidate aTSPs that were tested against HD, VX, and GD liquid challenges (Table 2) the formulations that were better than the standard, either ICD 3004 or ICD 1511, and “passed” this screen were ICD 3369, 3371, 3372, 3453, 3520, 3830, 3832, 3833, and 3834.

In the Minicams Penetration Cell Liquid Challenge Test, of the 11 candidate aTSPs that were tested against both HD and GD liquid challenges (Table 3) only ICD 3773 was better than the standard ICD 3004 and “passed” this screen.

In the Rabbit Lesion Area Ratio (LAR) HD Liquid Test of the 34 candidate aTSPs that were tested against an HD liquid challenge (Table 4) the formulations that were better than the standard ICD 3004 and “passed” this screen were ICD 3668, 3768, 3769, 3770, 3790, 3834 (Lot Nos. 020305-ARL, 020807-ARL, and 021029-ARL), 3970, 4020, 4028, 4029, and 4052.

In the Rabbit Lethality Test for Liquid VX (Tables 5, 6, 7, and 8) using a challenge dose of 0.5 mg VX/kg body weight), of the 21 formulations (ICD 3792, 3833, 3834, 3886, 3887, 3903, 3771, 3830, 3832, 3884, 4022, 4028, 3829, 3970, 4020, 4021, 4029, 3773, 4050, 4051, and 4052) all were significantly efficacious compared to no protection, but none were significantly better than ICD 3004. Three aTSPs appeared to be particularly effective, preventing deaths in the pretreated rabbits: ICD 3834 at 0/8 ($p = 0.2421$ versus ICD 3004 at 3/15), ICD 3884 at 0/16 ($p = 0.0712$ versus ICD 3004 at 5/24), and ICD 4029 at 0/14 ($p = 0.2588$ versus ICD 3004 at 3/21). Notably, ICD 3834-pretreated rabbits exhibited no signs of cholinergic intoxication.

In the Rabbit Lethality Test for GD Vapor Challenge (2 GD vapor caps with 28 μ l GD/kg for 4 hours), of the 29 aTSPs that were tested against GD vapor challenge (Tables 9, 10, 11, 12, 13, and 14) the formulations that were better than the standard ICD 3004 and “passed” the test were ICD 3829, 3830, 3832, 3833, 3834, 3886, 4020, 4029, 4050, 4051, and 4052.

In the Haired Guinea Pig GD Liquid Test, the 24 hr LD_{50} for 2 hr exposures to GD in untreated GPs was 30 mg/kg. The LD_{50} values for pretreatment with ICD 3004, 3834, 4028, and 4029 were 32, 249, 85, and 186 mg GD/kg, respectively, and the PRs were 1.1, 8.2, 2.8, and 6.1. At the direction of USAMRICD personnel, a challenge dose of 100 mg GD/kg, predicted by probit analysis to be the 24 hr LD_{91} on ICD 3004-pretreated GPs, was selected for aTSP evaluation of 7 candidate formulations (Table 15). Six of the 7 aTSP formulations (ICD 3834, 4020, 4029, 4050, 4051, and 4052) were significantly efficacious, but only two candidates, ICD 4020 (5 dead/24 dosed) and ICD 4029 (0 dead/10 dosed), were significantly better than ICD 3004 (22 dead/24 dosed).

Research Conducted at the USAMRICD

The research staff at the USAMRICD assigned to the aTSP project collaborated with all of the listed external contractors and formed working partnerships. Some contractors only identified and developed reactive moieties, which were then formulated at the USAMRICD into candidate products, while others developed candidate products and sent them to the USAMRICD for evaluation.

The USAMRICD maintains a data base known as the Drug Assessment Compound Tracking System (DACTS) that is a repository for information and data from many older research programs conducted at the Institute. A great deal of information and data from the aTSP program are available in the DACTS data base. Individual compounds and formulations are referenced by ICD numbers in the DACTS data base.

Table 16 provides a complete listing, by ICD number, of all the candidate aTSP formulations developed and evaluated in the aTSP program. Included in the listing are the individual components, by weight percentage, that were used to make up the candidate formulations. The PI and/or the source of the reactive moieties used in the candidate formulations are provided in the table. Some of the ICD numbers are not final formulations, but represent an individual component used to make a formulation. Formulations typically contain reactive moieties that are listed in two columns and the two base components of SERPACWA, fine particles of polytetrafluoroethylene (PTFE, F5A powder from Ausimont, Morristown, NJ) dispersed in perfluorinated polyether oil (PFPE, FOMBLIM™ Y25 oil also from Ausimont, Morristown, NJ). If the formulation does not include the SERPACWA components, then the component used is listed in the oil and powder column instead of PFPE and PTFE. Some formulations do not contain a reactive moiety, and these formulations have nothing listed in the active moiety columns.

Minicams Penetration Cell Test

Battelle evaluated many of the candidate formulations using the Minicams Penetration Cell Test; however, some testing was done at the USAMRICD using this evaluation method. Table 17 provides a summary of penetration cell results for challenge by HD vapor at the USAMRICD. The table provides the time in minutes (with standard deviation) that it took for 1000 ng of HD vapor to break through candidate formulation. The table also provides the total ng (with standard deviation) of HD that breaks through the candidate formulation in 20 hours. The candidate formulations were spread at a thickness of 0.15 mm. The listed values were calculated by interpolation or extrapolation of the raw data generated from the MINICAMS analysis.

Weanling Pig HD Vapor Test

Candidate TSPs and aTSPs were evaluated for HD vapor challenge in two protocols. The results are summarized in Table 18. This table provides references for the dates of experiments, laboratory notebook numbers, pages in the notebook, weanling pig animal numbers, ICD numbers of candidate formulations, the thickness of applied TSP or aTSP, the duration time of the saturated HD vapor cup exposure (1.4 mg/L), the mean a^* erythema values from reflectance color meter measurements with the corresponding standard error of the mean and standard deviation (N-1 formula), and the percent of positive control ($[\text{mean } a^* \text{ for candidate} / \text{mean } a^* \text{ for positive control}] * 100$). The smaller the % of control value the better the protection provided by the candidate formulation.

Table 19a provides a summary of results in the haired guinea pig and weanling pig HD vapor model from USAMRICD Protocol 1-05-96-000-A-734. All animals were weanling pigs except for the first four experiments dated 12 Feb 97, 19 Feb 97, 4 Mar 97, and 11 Mar 97. The table provides references for the dates of experiments, weanling pig animal numbers, ICD numbers of candidate formulations, the thickness of applied TSP or aTSP, the duration time of the saturated HD vapor cup exposure (1.4 mg/L), the mean a^* erythema values from reflectance color meter measurements with the corresponding standard error of the mean, and the percent of positive control ($[\text{mean } a^* \text{ for candidate} / \text{mean } a^* \text{ for positive control}] * 100$), the mean histology score with corresponding standard error of the mean, and the percent of positive control ($[\text{mean histology score for candidate} / \text{mean histology score for positive control}] * 100$). The smaller the % of control value the better the protection provided by the candidate formulation. Based on statistical analysis of either the erythema data or the histology data, there is a column stating whether the candidate formulation passed the screen (meaning it provided significant protection compared to positive control animals), failed the screen (meaning it provided equivalent protection compared to positive control animals), or failed worse (meaning it produced significantly worse damage compared to positive control animals).

Table 19b is a subset of Table 19a and provides a summary of the results for the weanling pig HD vapor model. The data is ordered by ICD number for easy reference to Table 19a. The table provides references for the dates of experiments, ICD numbers of candidate formulations, the thickness of applied TSP or aTSP, the duration time of the saturated HD vapor cup exposure (1.4 mg/L), the percent of positive control for erythema ($[\text{mean } a^* \text{ for candidate} / \text{mean } a^* \text{ for positive control}] * 100$) and the percent of positive control for histology ($[\text{mean histology score for candidate} / \text{mean histology score for positive control}] * 100$). The smaller the % of control value the better the protection provided by the candidate formulation. Based on statistical analysis of either the erythema data or the histology data, there is a column stating whether the candidate formulation passed the screen (meaning it provided significant protection compared to positive control animals) failed the screen

(meaning it provided equivalent protection compared to positive control animals), or failed worse (meaning it produced significantly worse damage compared to positive control animals).

Weanling Pig Skin aTSP Wash and Wipe Test

The wash and wipe test results are summarized in Tables 20, 21, and 22. Table 20 provides summaries of the wash and wipe test results from USAMRICD Protocol 1-05-96-000-A-734. Experiments were conducted on 19 September 2002 (Notebook #032-02, pp.127-131). These experiments used weanling pigs 446, 447, 449, and 450. The exposure tabs were placed in five columns of nine rows down the ventral surface. The scoring ranges for the wash and wipe tests were 0 to 4 and 0 to 3, respectively. A higher score indicated that more aTSP remained on the skin after the wash or wipe procedure. Table 21 provides a summary of the wash and wipe test results from USAMRICD Protocol 1-05-96-000-A-734. Experiments were conducted on 6 December 2002 (Notebook #069-02, pp.2-8). These experiments used weanling pigs 474 and 475. The exposure tabs were applied in three columns of six rows. The scoring ranges for the wash test and wipe tests were 0 to 4 and 0 to 3, respectively. A higher score indicated that more aTSP remained on the skin after the wash or wipe procedure. A plus sign (+) alongside a visual score indicated that the aTSP was slightly better than the given visual score, but was not effective enough to be given a score of one rank higher. Table 22 provides a summary of wipe test results from USAMRICD Protocol 1-05-96-000-A-734. Experiments were conducted on 6-7 February 2003 (Notebook #069-02, pp.75-79). These experiments used weanling pigs 484, 485, and 486. The exposure tabs were placed in two columns of four rows down the ventral surface. The scoring range for the wipe test was 0 to 3. A higher score indicated that more aTSP remained on the skin after the wipe procedure.

Safety Studies for Acute Eye and Skin Irritation

The initial safety screening for lead candidate formulations was performed at the U.S. Army Center for Health Promotion and Preventive Medicine (USACHPPM). For the skin irritation study, 0.5 g of each candidate formulation was applied to the clipped back of rabbits and left in place for four hours. Following the exposure, animals were observed for seven days, and any signs of toxicity were noted and recorded. For the eye irritation study, 0.1 g of each candidate formulation was applied to the conjunctival sac of one eye. The opposite eye served as an untreated control. Following the exposure, animals were observed intermittently for seven days, and any signs of toxicity were noted and recorded.

The results of the initial safety screening are summarized in Table 23. The experiments were performed on rabbits between 1999 and 2003. Full reports of these studies are available in Appendix B. The only tested aTSP formulation that showed any sign of toxicity was ICD 3833, which contained 26% Lupasol FG, 3% Fluorolink 7004, 38% Fomblin Y25, and 33% F5A PTFE. ICD 3833 produced moderate irritation in the rabbit eye which was resolved within 72 hours. In humans, ICD 3833 should be used with caution around the eyes and mucosa.

DISCUSSION

SERPACWA

The formulation known as SERPACWA (ICD 3004) represents the McKesson product prepared under specified manufacturing procedures. There were many other candidate formulations with the same percentages of F5A powder and FOMBLIM™ Y25 oil prepared in the USAMRICD laboratory.

See Table 16 for a complete listing. ICD 2289 was used as a standard reference formulation for many experiments that compared the efficacy of aTSP candidate formulations to SERPACWA. ICD 2289 was prepared at the USAMRICD using the described procedure in the MATERIALS AND METHODS section. Before August 1996, ICD 2289 showed moderate efficacy against an HD vapor challenge in three models: the hairless guinea pig, the haired guinea pig, and the weanling pig. For example, Figure 11 gives results using the hairless guinea HD vapor evaluation model. ICD 1511 and ICD 2289 were compared to unprotected positive controls. In these experiments, 9 animals (numbers 9-17, 307-329 g) were used, each with 6 experimental sites. The HD vapor challenge was for 4 minutes using a saturated HD vapor cup (1.4 mg/L). Mean erythema values were a* readings of the reflectance color meter (Minolta model CR-200). ICD 1511 was 61% of control and ICD 2289 was 57% of control. The error bars were SEM. These experiments were conducted in June 1993.

In July 1996, another experiment was run using the weanling pig HD vapor model. These experiments (Figure 12) evaluated formulation ICD 2701 and compared results to positive control animals with no protection and the standard formulation, ICD 2289. Six animals (numbers 51-56, 7.7-9.2 kg) with 24 sites per animal were used in the experiment. HD vapor challenge using a saturated HD vapor cup (1.4 mg/L) for positive control and ICD 2289 was 15 minutes. ICD 2701 (S-330) was challenged for 15-60 minutes (as listed). Mean erythema values were a* readings of the reflectance color meter (Minolta model CR-200). Error bars were SEM. ICD 2289 provided protection at a thickness of 0.2 mm and was 54% of control. ICD 2701 (S-330) provided protection at a thickness of 0.15 mm for up to 45 minutes.

The efficacy observed for HD vapor challenges using ICD 2289 in these two sets of experiments was typical of many experiments conducted over several years. ICD 2289 was initially used as the standard for routine screening of candidate formulations for HD vapor challenges in haired guinea pigs, hairless guinea pigs, and weanling pigs.

Something happened, however, between July 1996 and October 1996. All of a sudden, ICD 2289 no longer provided protection against an HD vapor challenge. Figure 13 gives results typical of our observations. In this experiment, the weanling pig HD vapor model evaluated ICD 2730 using ICD 2289 as standard. Six animals (numbers 69-74, 7.3-9.0 kg) with 24 sites per animal were used. HD vapor challenge using a saturated HD vapor cup (1.4 mg/L) for positive control and ICD 2289 was 15 minutes. ICD 2730 (S-330) was challenged for 15-60 minutes (as listed). Mean erythema values were a* readings of the reflectance color meter (Minolta model CR-200). Error bars were SEM. ICD 2289 did not provide protection at a thickness of 0.2 mm and was 122% of control. ICD 2730 (S-330) was observed to provide protection at a thickness of 0.15 mm at 15 minutes but not at 30, 45, or 60 minutes.

This problem with ICD 2289 continued with future formulations of ICD 2289 and ultimately with SERPACWA (ICD 3004). For example, in May 1997 we prepared a series of ICD 2289 samples using new batches of F5A powder (Ausimont lot # 480324) and old batches of Y25 oil (lot # VT590) using slightly different mixing techniques in mixing time and cooling (ICD numbers 2926, 2927, 2928, 2929, 2930, 2931, 2932, and 2933).

A weanling pig HD vapor evaluation conducted 13-15 May 1997 (Figure 14) used ICD 2927, 2928, 2930, and 2933 all spread at a thickness of 0.20 mm. ICD 2650 spread at a thickness of 0.10 mm was used as the standard. These were all compared to unprotected positive controls. Six animals (numbers 121-126, 6.9-9.5 kg) with 24 sites per animal were used in the experiment. HD vapor challenge using a saturated HD vapor cup (1.4 mg/L) was 15 minutes for positive control and candidate formulations. ICD 2650 (S-330) was challenged for 30 minutes. Mean erythema values

were a* readings of the reflectance color meter (Minolta model CR-200). Error bars were SEM. ICD numbers 2927, 2928, 2930, and 2933 were not efficacious and produced worse lesions than the nonprotected positive control animals. The % of control values was 144, 156, 147, and 152, respectively. ICD 2650 (S-330) provided protection with a value of 22% of control.

Another weanling pig HD vapor evaluation conducted 20 May-12 June 1997 (Figure 15) used ICD 2926, 2929, 2931, and 2932 all spread at a thickness of 0.20 mm. ICD 2650 spread at a thickness of 0.10 mm was used as the standard. These were all compared to unprotected positive controls. Six animals (numbers 127-132, 6.6-9.1 kg) with 24 sites per animal were used in the experiment. HD vapor challenge using a saturated HD vapor cup (1.4 mg/L) was 15 minutes for positive control and candidate formulations. ICD 2650 (S-330) was challenged for 30 minutes. Mean erythema values were a* readings of the reflectance color meter (Minolta model CR-200). Error bars were SEM. ICD numbers 2929, 2931, and 2932 were not efficacious compared to the nonprotected positive control animals. The % of control values was 98, 134, and 136, respectively. ICD 2926, however, did show efficacy compared to nonprotected positive control animals with a % of control value of 18. ICD 2650 (S-330) provided protection with a value of 14% of control.

The efficacy observed for ICD 2926 was unexpected. The efficacy evaluation of ICD 2926 was repeated in a similar experiment (data not shown) 12-14 August 1997. The result was the same; ICD 2926 provided protection with a % of control value of 35.

In May of 1999, we evaluated the effect of applying the U.S. Army fielded insect repellent (Extended Duration Topical Insect and Arthropod Repellent, EDTIAR, containing 33% N,N-diethyl-3-methyl-benzamide, DEET) onto the skin prior to applying aTSP formulations (Figure 16). EDTIAR was applied at a rate of 1.9 $\mu\text{L}/\text{cm}^2$ and allowed to dry for 60 minutes. After the 60-minute drying time, ICD formulations 3004 (with and without EDTIAR), 3249, 3250, and 2650 were all spread at a thickness of 0.10 mm and allowed to dry for 15 minutes. Six animals (numbers 189-194, weighing 7.8-11.0 kg) with 24 sites per animal were used in the experiment. An HD vapor challenge of 15 minutes using a saturated HD vapor cup (1.4 mg/L) was used for both positive control and candidate formulations. The standard, ICD 2650 (S-330), was challenged for 30 minutes. Mean erythema values were a* readings of the reflectance color meter (Minolta model CR-200). Error bars were SEM. ICD numbers 3004 (with and without EDTIAR) and ICD 3250 were not efficacious compared to the nonprotected positive control animals. The % of control values was 155, 122, and 64, respectively. ICD 2650 and ICD 3249 were efficacious, with % of control values of 18 and 45. The results of this experiment illustrate that ICD 3004 (SERPACWA) does not provide protection against an HD vapor challenge.

In January of 2001, we again evaluated the efficacy of SERPACWA (ICD 3004, McKesson 300 kg production run, lot # TSP0050498) in the weanling pig HD vapor model (Figure 17). SERPACWA was spread at two thicknesses, 0.1 and 0.2 mm, and challenged with HD vapor for 15 minutes. At the end of the exposure the SERPACWA sites were either cleaned using the normal dry wiping process or cleaned using a special multiple process of dry wiping, wiping with 0.5% bleach, wiping with water, and finally wiping with ethanol. This modification to the normal procedure was to determine if a more thorough cleaning after exposure would make a difference in the observed efficacy. The non-treated positive control also was challenged with HD vapor for 15 minutes. The standard, ICD 2650, was spread at a thickness of 0.1 mm and challenged with HD vapor for 30 minutes. Six animals (numbers 237-242, weighing 8.0-11.1 kg) with 24 sites per animal were used in the experiment. Mean erythema values were a* readings of the reflectance color meter (Minolta model CR-200). Error bars were SEM. SERPACWA sites, with or without the special cleaning procedure, were observed to be significantly worse than the untreated positive control sites with

percent of control values of 343, 355, 348, and 330, respectively. The percent of control value for the standard ICD 2650 was -8.6 and provided good protection. With a mean erythema, for unprotected positive control sites, of only 1.98, this group of animals did not have a large response to HD vapor; nevertheless, applying SERPACWA prior to HD vapor exposure greatly increased the observed skin damage. This result is clearly observed in a photograph of animal number 238 taken 24 hours post-exposure (Figure 18) and is representative of all six animals in this group. These experiments were conducted 17-31 January 2001.

Histopathology of skin lesions also was used occasionally to confirm the efficacy demonstrated with the erythema results. Figure 19 gives the mean histological damage for the experiment described above for weanling pig animal numbers 237-242. After euthanasia at 24 hours post-exposure, skin punches were taken from each exposure site. Mean histological damage scores were determined by the veterinary pathologist from H&E slides. Error bars were SEM. SERPACWA sites, with or without the special cleaning procedure, were observed to be significantly worse than the untreated positive control sites with percent of control values of 403, 381, 370, and 370, respectively. The percent of control value for the standard ICD 2650 was 18, and it provided good protection. The histological scores correlated well with the erythema scores and demonstrated that applying SERPACWA prior to HD vapor exposure greatly increased the observed skin damage.

The experiments described above are representative of the lack of efficacy against HD vapor challenges for SERPACWA, ICD 2289, and formulations like ICD 2289 after October 1996. Table 19b (a summary of all weanling pig HD vapor challenge experiments) gives other examples. A possible explanation for the loss of efficacy against HD vapor for SERPACWA and SERPACWA equivalent formulations after July 1996 is a slight change in the makeup of the F5A PTFE powder. We learned that Ausimont (Morristown, NJ), the supplier of the F5A PTFE powder, switched manufacturing locations during that time frame. Ausimont had the DoD contract to manufacture SERPACWA in sufficient quantities to be used in advanced development and FDA approval. FOMBLIMTM Y25 oil, also from Ausimont, continued to be manufactured in the same facility. Thus, the only difference in the SERPACWA formulations made before and after July 1996 was the manufacturing location of the F5A powder. The new manufacturing facility produced F5A powder that met all the mil specifications for the PTFE component of SERPACWA in the Department of Defense's (DoD) contract; thus, Ausimont continued to manufacture SERPACWA using F5A powder manufactured from the new location. Since the Requirements Document for SERPACWA listed efficacy against HD liquid, but not HD vapor, and an aTSP that provided protection against HD vapor was in research development, the Medical Research and Materiel Command (MRMC) decided to continue the advanced development of SERPACWA, even though it did not protect against HD vapor.

aTSP

Using the two components of SERPACWA, perfluorinated-polyether oil and polytetrafluoroethylene solid, as a base cream, USAMRICD scientists evaluated over 150 different active components. Classes of compounds tested included polyalkenimines, enzymes, hybrid organic-inorganic materials, polyoxometalates, inorganic composites, inorganic oxides, metal alloys, and small organic molecules. These compounds were incorporated into the base cream to produce over 500 candidate formulations (patents by Braue, Hobson, and Hill, 2002, 2004, 2011).

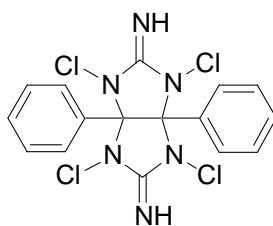
Against HD, a total of 17 active moieties demonstrated increased efficacy over SERPACWA: S-330, iodobenzene diacetate (IBDA), nanoreactors, ZE555 resin (M291 SDK powder), polysilsesquioxanes, polyoxometalates (POM), titanium manganese coated metal alloys, gold/copper (Au/Cu) catalysts, magnesium oxide (MgO) nanoparticles, silicon dioxide (SiO₂), ethanolamine matrix,

cerium copper (Ce/Cu) salts on TiO₂ nanoparticles, metal precipitates, POM on TiO₂ nanoparticles, POM on MgO nanoparticles, silver (Ag) catalysts, and polyalkenimines.

Against GD, a total of 15 active moieties demonstrated increased efficacy over SERPACWA: nanoreactors, organophosphorus acid anhydrolase (OPAA) enzyme, high test hypochlorite (HTH), metal precipitates, Au/Cu catalysts, Iron/copper/lanthanum (Fe/Cu/La) catalysts, zinc oxide (ZnO) nanoparticles, titanium dioxide (TiO₂) nanoparticles, calcium oxide (CaO) nanoparticles, MgO nanoparticles, POM on TiO₂ nanoparticles, POM on MgO nanoparticles, Ce/Cu) salts on TiO₂ nanoparticles, diethanolamine, and polyalkenimines.

The candidate formulations were evaluated for efficacy in both *in vitro* and *in vivo* models. A decision tree network (DTN) approach (Figure 2, Braue, 1999) was used to determine which candidate formulations showed promise and which should be eliminated from consideration.

Based on the results of the DTN evaluations, two candidate reactive moieties emerged as the lead compounds for advanced development, S-330 (Braue et al., patent 2002) and polyalkenimines (Braue et al., patent 2011). An organic molecule, S-330 (Formula 1, Sigma-Aldrich Cat # S706485; CAS # 19103-02-7) was initially discovered to react with HD in the mid-1940s. It was developed and incorporated into a decontamination product and fielded as the M-5 ointment kit at the end of World War II. However, the unacceptable barrier properties and the undesirable cosmetic properties (that is, foul odor and sticky texture) caused the cancellation of this product. S-330 was one of the initial reactive moieties our research team investigated to improve the efficacy of SERPACWA, and it was selected to be grouped with the final list of candidate formulations considered for advanced development.



S-330

Formula 1. S-330

Polyalkenimines were discovered and developed in collaboration with TDA Research (Wheat Ridge, CO). A variety of polyalkenimines (available commercially as Lupasols from BASF Corp, Mount Olive, NJ) were selected for evaluation:

- ICD 3720 Lupasol P, available from BASF Corp., a 50:50 wt % mixture of water and aziridine, homopolymer, CAS # 9002-98-6).
- ICD 3732 Lupasol WF (water free), available from BASF Corp., polyethylenimine (CH₂-CH₂-NH-)_x Product ID # NLE 187702, CAS # 9002-98-6.
- ICD 3733 Lupasol G20 water free, available from BASF Corp., polyethylenimine, Product ID # NLE 555415, CAS # 25987-06-8.
- ICD 3766 Lupasol FG, available from BASF Corp., ethylenediamine-ethylenimine copolymer, (C₂H₈N₂.C₂H₅N)_x Product # NCS 971991, CAS # 25987-06-8.

In addition to Lupasols, surfactants also were observed to increase the efficacy of candidate formulations. Two surfactants were observed to be the most effective:

ICD 3719 Fluorolink 7004, available from Ausimont USA, Inc.; 1, Propene, 1,1,2,3,3,3-hexafluoro-, telomers with chlorotrifluoroethene, oxidized, reduced, ethyl ester, hydrolyzed, CAS # 220182-27-4.

ICD 3730 Fluorolink 7005, available from Ausimont USA, Inc.; a perfluoropolyether derivative (PFPE-CONH-(CH₂)₃-(OCH₂CH₃)₁₈-CH₃) from Ausimont, CAS # not assigned.

One S-330 and 20 Lupasol and surfactant combinations were formulated at the ARL using a commercial extruder. These formulations were evaluated using the DTN modules. A special down-select process was used to find the best candidate formulation. The data were organized into a complete matrix of values for each test compound's result on a damage/undesirable measure. The results were expressed as percentages of the same measurement for SERPACWA. Therefore, lower percentage scores indicate BETTER performance. Table 24 summarizes these values. Data in red with white field was estimated by averaging results from individual components.

Weighting factors were assigned to the various testing modules based on the judgement of the research team. The *in vivo* weighting factors were:

HDV	8 - % of PC for Weanling pig exposed to HD vapor
HDL	5 - Lesion Area Ratio percentage for rabbits exposed to HD liquid
VXL	7 - 24 hr lethality percentage for rabbits exposed to VX liquid
GDV	3 - 24 hr lethality percentage for rabbits exposed to GD vapor

The *in vitro* weighting factors were:

HDL-SPME	2 - Proof of Decontamination of HD liquid
GDL-SPME	2 - Proof of Decontamination of GD liquid
VXL-SPME	2 - Proof of Decontamination of VX liquid
WASH	2 - score for how well a compound washes off skin
WIPE	5 - score for how well compound wipes off skin

Table 25 provides a summary of normalized weighted scores (higher is better). To make higher scores indicate better performance, the raw data percentages were subtracted from 100. The adjusted scores were multiplied by the appropriate normalized weighting factor (weighting factor divided by total of all the weighing factors, 36) to generate the normalized weighted scores reported in this table.

Table 26 provides a summary of compound rankings based on the individual measures listed in Table 24.

Table 27 provides a summary of normalized weighted rank scores (higher is better). To make higher scores indicate better performance, the rank number was subtracted from the 23 (the total number of compounds plus 1). The adjusted scores were multiplied by the appropriate normalized weighting factor (weighting factor divided by total of all the weighing factors, 36) to generate the normalized weighted scores reported in this table.

Table 28 provides a summary of the normalized numerical rankings for groups of measures based on the combined measures. Rankings are given for weighted and un-weight data and *in vivo* and *in vitro* experiments. Note that the highest rank the compound can receive is a 1; the lowest is 22. The table is ordered by the overall best average ranking considering all the different groups measures.

The overall best Lupasol formulation was ICD 3834 containing 38% FOMBLIN Y25 PFPE, 33% F5A PTFE, 13% Lupasol FG, 13% Lupasol WF, 1.5% Fluorolink 7004, and 1.5% Fluorolink 7005. It was rated number 1 in all categories (weighted, unweighted, percentages, ranks, *in vivo*, or *in vitro*) except for the *in vivo* weighted group where it was number 2. Based on these results, ICD 3834 was selected for transition to advanced development.

ICD 3834 had one weakness that presented some risk to its success in advanced development. It did not do well in the wash test. While it did very well in the wipe test, in the wash test it was only 44% of the SERPACWA score and ranked fifteenth out of the 22 Lupasol candidates evaluated. Lupasols, in general, have fair water solubility, which makes the formulations containing them susceptible to washing off under conditions of heavy sweating. The wash test in the DTN poured water directly on to the aTSP protected site. A more relevant test would be to evaluate how well the aTSP remained on human skin during typical military use. The aTSP would be applied to human volunteers using the directions for SERPACWA. The volunteers would then dress in Joint Service Lightweight Integrated Suit Technology (JSLIST) protective clothing and perform normal and strenuous activity. Following this exercise, the skin sites receiving aTSP would be evaluated for how well it remained on the skin. This testing would be accomplished during advanced development.

ICD 4028 was selected as the backup formulation for advanced development. It contained 10% S-330, 54% FOMBLIN Y25 PFPE and 36% F5A PTFE. ICD 4028 is the same formulation as one of the very early S-330 formulations, ICD 2701. The one limitation with S-330 was that it did not react with GD and presumably with the other G-type agents. In DTN testing involving GD, ICD 4028 performed as well as SERPACWA. It was, however, excellent against HD and VX. A possible strategy to improve the S-330 formulation would be to combine it with another reactive moiety that was effective against GD. We did not have time to pursue this strategy before the aTSP program ended.

There was a small research effort initiated on a third generation SERPACWA (SBIR Phase 1 and 2 with TIAX LLC, Award Number: W81XWH-05-C-0131). This new concept would develop a product that could be used as either a pre-exposure barrier cream or a post-exposure decontamination product. Unlike SERPACWA or aTSP that would have active CWA remaining on the surface and require additional decontamination, the new third generation product would consist of a matrix that would dissolve CWAs and rapidly neutralize CWAs into non-toxic products. A large variety of reactive or catalytic materials are available for this type of new product.

CONCLUSIONS

Recent classified discussions have sparked interest in revisiting barrier creams. Due to the classified nature of those discussions, however, details cannot be included in this technical report. Interested readers should review some of the classified reports in the publication list in Appendix A.

In the late 1990s, research was conducted to address some of the limitations of SERPACWA, and development was initiated for an improved product that would act as both a protective barrier and an active destructive matrix to detoxify CWAs. Researchers aimed to find a second generation SERPACWA that added a reactive moiety to the SERPACWA matrix. This new product would

provide increased protection against liquid CWAs and not irritate the skin. It also would expand the capabilities of SERPACWA by providing protection against challenges by HD and GD vapor. This improved SERPACWA became known as active topical skin protectant (aTSP). After conducting numerous years of research and technical studies, two candidate formulations were selected for transition to advanced development in 2004. The first contained a mixture of polyalkenimines, surfactants, and the SERPACWA base cream. The second contained the reactive moiety S-330 and the SERPACWA base cream. The efficacy of these two products compared to SERPACWA is summarized in Figures 20 and 21.

With the increased threat from non-traditional agents, approximately two to three years of additional efficacy studies now would be needed to transition aTSPs to advanced development. The Defense Threat Reduction Agency (DTRA) currently (FY16) is not funding any barrier cream efforts, and it is unknown if DTRA will fund this research in the future.

RECOMMENDATION

Although SERPACWA encountered several technical issues throughout its fielding and was never issued to service members for a chemical attack, barrier creams do offer a unique capability when applied prior to CWA exposure. The active barrier creams chemically or physically react with harmful chemicals such as CWAs to neutralize these chemicals while the barrier properties of the cream prevent penetration of harmful chemicals into the skin. Per the Joint CBR Prophylaxes ICD, dated July 31, 2009, a valid requirement exists for barrier creams such as SERPACWA to prevent or reduce absorption of chemical agents through the skin and/or mucous membrane. Currently, no FDA-approved product exists, but the lead candidate aTSP developed by the USAMRICD could easily transition within 3 years to advanced development. DTRA, however, has no interest in funding barrier creams, currently or within the foreseeable future. Thus, this requirement and capability are likely to remain unmet and unreachable to our service members. The second generation SERPACWA product (aTSP) could be expected to considerably improve protection from CWAs were it fielded and could also potentially limit the need for protective suits if it were applied to all un-covered skin and not just at junction points.

REFERENCES

- Arthur, C.L.; Pawliszyn, J.B., Solid phase microextraction with thermal desorption using fused silica optical fibers. *Anal. Chem.*, 62, 2145-2148, 1990.
- Braue, EH Jr. and Pannella, MG, Topical protectant evaluation by FT-IR spectroscopy. *Appl. Spectrosc.*, 44, 1061-1063, 1990.
- Braue, EH Jr., Mershon, MM, Wade, JV, and Litchfield, MR, *In vivo* assessment of vesicant skin injury using a Minolta chroma meter. *J. Soc. Cosmet. Chem.*, 41, 259-265, 1990.
- Braue, EH, Jr., Koplovitz, I, Mitcheltree, LW, Clayson, ET, Litchfield, MR, and Bangledorf, CR, Characterization of the sulfur mustard vapor induced cutaneous lesions on hairless guinea pigs. *Toxicology Methods*, 2, 242-254, 1992.
- Braue, EH, Jr., Litchfield, MR, Bangledorf, CR, and Rieder, RG, FT-IR/ATR evaluation of topical skin protectants useful for sulfur mustard and related compounds. *SPIE*, 1575, 311-312, 1992.

Braue, EH Jr., Nalls, CR, Way, RA, Zallnick, JE, Rieder, RG, and Mitcheltree, LW, Nikolsky's Sign—A novel way to evaluate damage at the dermal-epidermal junction, *Skin Res. Tech.*, 3, 245-251, 1997.

Braue, EH Jr., Nalls, CR, Way, RA, Zallnick, JE, Rieder, RG, Lee, RB, and Mitcheltree, LW, Characterization of the sulfur mustard vapor induced cutaneous lesions on haired guinea pigs. *Skin Res. Tech.*, 4, 99-108, 1998.

Braue, EH Jr., Development of a reactive topical skin protectant. *J. Appl. Toxicol.*, 19, S47-53, 1999.

Braue, EH Jr., Mershon, MM, Braue, CR, and Way, RA, Active Topical Skin Protectants Containing S-330, U.S. Patent No. 6,472,438, October 29, 2002.

Braue, EH Jr., Hobson, ST, Boecker, JD, and Smith, BM, Active Topical Skin Protectants Containing Amines, Polyalkenimines and/or Derivatives, U.S. Patent No. 7,976,832, July 12, 2011.

Braue, EH, Jr, Hanssen, KA, Doxzon, BF, Lumpkin, HL and Clarkson, ED, Efficacy Sstudies of RSDL, M291 SDK, 0.5% bleach, 1% soapy water and SERPACWA, Part 1: Guinea pigs challenged with VX. *Cutan. Ocul. Toxicol.*, 30 (1): 15-28, 2011.

Braue, EH, Jr, Hanssen, KA, Doxzon, BF, Lumpkin, HL and Clarkson, ED, Efficacy studies of RSDL, M291 SDK, 0.5% bleach, 1% soapy water and SERPACWA, Part 2: Guinea pigs challenged with soman. *Cutan. Ocul. Toxicol.*, 30 (1): 29-37, 2011.

Braue, EH Jr., Hanssen, KA, Doxzon, BF, Lumpkin, HL, and Clarkson, E, Evaluation of RSDL, M291 SDK, 0.5% Bleach, 1% Soapy Water, and SERPACWA; Part 1: Challenge with VX, USAMRICD-TR-09-01. U.S. Army Medical Research Institute of Chemical Defense, Aberdeen Proving Ground, MD, June 2009.

Braue, EH Jr., Hanssen, KA, Doxzon, BF, Lumpkin, HL, and Clarkson, E, Evaluation of RSDL, M291 SDK, 0.5% Bleach, 1% Soapy Water, and SERPACWA; Part 2: Challenge with GD, USAMRICD-TR-10-04. U.S. Army Medical Research Institute of Chemical Defense, Aberdeen Proving Ground, MD, June 2010.

Braue, EH Jr., Hanssen, KA, Doxzon, BF, Lumpkin, HL, and Clarkson, E, Evaluation of RSDL, M291 SDK, 0.5% Bleach, 1% Soapy Water, and SERPACWA; Challenge with Toxic Compounds. USAMRICD-TR-12-03. U.S. Army Medical Research Institute of Chemical Defense, Aberdeen Proving Ground, MD, March 2012.

Braue, EH Jr., Hanssen, KA, Doxzon, BF, Lumpkin, HL, and Clarkson, E, Efficacy S of RSDL, M291 SDK, 0.5% Bleach, 1% Soapy Water and SERPACWA; Part 3: Challenge with EA6033, USAMRICD-TR-14-03. U.S. Army Medical Research Institute of Chemical Defense, Aberdeen Proving Ground, MD, June 2014.

Braue, EH Jr., Smith, KH, Doxzon, BF, Lumpkin, HL, Devorak, JL, and Stevenson, RS, Evaluation of RSDL, M291 SDK, 0.5% Bleach, 1% Soapy Water, and SERPACWA; Part 4: Challenge with EA6030, USAMRICD-TR-15-04. U.S. Army Medical Research Institute of Chemical Defense, Aberdeen Proving Ground, MD, June 2015.

Braue, EH Jr., Smith, KH, Doxzon, BF, Lumpkin, HL, Devorak, JL, and Stevenson, RS, Evaluation of RSDL, M291 SDK, 0.5% Bleach, 1% Soapy Water, and SERPACWA; Part 5: Challenge with EA6032, USAMRICD-TR-15-05. U.S. Army Medical Research Institute of Chemical Defense, Aberdeen Proving Ground, MD, June 2015.

Braue, EH Jr., Smith, KH, Doxzon, BF, Lumpkin, HL, JL, and Stevenson, RS, Evaluation of RSDL, M291 SDK, 0.5% Bleach, 1% Soapy Water, and SERPACWA; Part 6: Challenge with EA6039, USAMRICD-TR-15-06. U.S. Army Medical Research Institute of Chemical Defense, Aberdeen Proving Ground, MD, June 2015,

Braue, EH Jr., Smith, KH, Doxzon, BF, Lumpkin, HL, JL, and Stevenson, RS, Evaluation of RSDL, M291 SDK, 0.5% Bleach, 1% Soapy Water, and SERPACWA; Part 7: Challenge with EA5488, USAMRICD-TR-15-07. U.S. Army Medical Research Institute of Chemical Defense, Aberdeen Proving Ground, MD, June 2015.

Braue, EH Jr., Smith, KH, Doxzon, BF, Devorak, JL, Stevenson, RS, and Lumpkin, HL, Evaluation of RSDL, M291 SDK, 0.5% Bleach, 1% Soapy Water, and SERPACWA; Part 8: Challenge with EA6053, USAMRICD-TR-15-08. U.S. Army Medical Research Institute of Chemical Defense, Aberdeen Proving Ground, MD, June 2015.

Braue, EH Jr., Smith, KH, Doxzon, BF, Lumpkin, HL, Devorak, JL, and Stevenson, RS, Evaluation of RSDL, M291 SDK, 0.5% Bleach, 1% Soapy Water, and SERPACWA; Part 9: Challenge with EA6072, USAMRICD-TR-15-09. U.S. Army Medical Research Institute of Chemical Defense, Aberdeen Proving Ground, MD, June 2015.

Braue, EH Jr., Devorak, JL, Doxzon, BF, Lumpkin, HL, and Azeke, JI, Evaluation of RSDL, M291 SDK, 0.5% Bleach, 1% Soapy Water, and SERPACWA; Part 10: Challenge with EA6048, USAMRICD-TR-15-10. U.S. Army Medical Research Institute of Chemical Defense, Aberdeen Proving Ground, MD, June 2015.

Braue, EH Jr., Doxzon, BF, Lumpkin, HL, Smith, KH, Devorak, JL, and Stevenson, RS, Evaluation of RSDL, M291 SDK, 0.5% Bleach, 1% Soapy Water, and SERPACWA; Part 11: Challenge with EA4243 (VR, Russian VX), USAMRICD-TR-16-01. U.S. Army Medical Research Institute of Chemical Defense, Aberdeen Proving Ground, MD, January 2016.

Braue, EH Jr., Doxzon, BF, Lumpkin, HL, Smith, KH, Devorak, JL, and Stevenson, RS, Evaluation of RSDL, M291 SDK, 0.5% Bleach, 1% Soapy Water, and SERPACWA; Part 12: Challenge with EA1212 (GF, cyclosarin), USAMRICD-TR-16-02. U.S. Army Medical Research Institute of Chemical Defense, Aberdeen Proving Ground, MD, January 2016.

Bryant, MA and Braue EH, Jr., Comparison of fixation and processing methods for hairless guinea pig skin following sulfur mustard exposure. *Toxicology Methods*, 2, 87-100, 1992.

Colgin LM, Nielsen RE, Tucker FS and Okerberg CV, Case report of listerial keratoconjunctivitis in hairless guinea pigs. *Lab. Ani. Sci.* 45(4):435-436, 1995.

Graham, JS, Bryant, MA, and Braue, EH Jr., Effect of sulfur mustard on mast cells in hairless guinea pig skin. *J. Toxicol.-Cut. & Ocular Toxicol.*, 13(1), 47-54, 1994.

Dick IP and Scott RC, Pig ear skin as an in-vitro model for human skin permeability. J. Pharm. Pharmacol. 44:640-645, 1992.

EPA Research and Development-Interim Guidance for Dermal Exposure Assessment, EPA/600/8-91/011B, Jan 1992.

Klain GJ, Bonner SJ and Bell WG, *Swine in Biomedical Research*, pp. 667-671, Ed. Tumbleson ME, Plenum, NY 1986.

Finney, D.J., *Probit Analysis*, Third Edition, Cambridge University Press, 1971.

Lukey, BJ, Slife, HF Jr., Clarkson, E, Hurst, CG, and Braue, EH Jr (corresponding author), Chemical Warfare Agent Decontamination from Skin, In J.A. Romano Jr., B.J. Lukey, and H. Salem, eds., 2nd Edition of *Chemical Warfare Agents: Chemistry, Pharmacology, Toxicology, and Therapeutics*, CRC Press, pp. 611-625, 2008.

Mershon, MM, Wade, JV, Mitcheltree, LW, Petralli, JP, and Braue, EH Jr., Hairless guinea pig bioassay model for vesicant vapor exposures. *Fundam. Appl. Toxicol.* 15, 622-630, 1990.

Meyer W, Schwarz R and Neurand K, Current Problems in Dermatology, Vol 7, pp. 39-52, Ed. Simon GA, Paster Z, Klingberg MA and Kaye M, Karger Basel, 1978.

Mitcheltree LW, Mershon MM, Wall HG, Pulliam JD and Manthei JH, Microblister formation in vesicant-exposed pig skin. *J. Toxicol.-Cut. & Ocular Toxicol.* 8(3):309-319, 1989.

Morrissey, K.M. and Heykamp, L.S., Analysis of Barrier Cream Formulations by Head-Space Solid Phase Microextraction: Proof of Concept, Task A202, EAI Report A202/97/002F, December 1997.

Papirmeister, B., Feister, A.J., Robinson, S.I., and Ford, R.D., *Medical Defense Against Mustard Gas, Toxic Mechanisms and Pharmacological Implications*, Boca Raton, Florida, CRC Press Inc., 92. 1991.

Romano JR, US Army Medical Research Institute of Chemical Defense, Aberdeen Proving Ground, MD, personal communication, 2001.

FIGURES

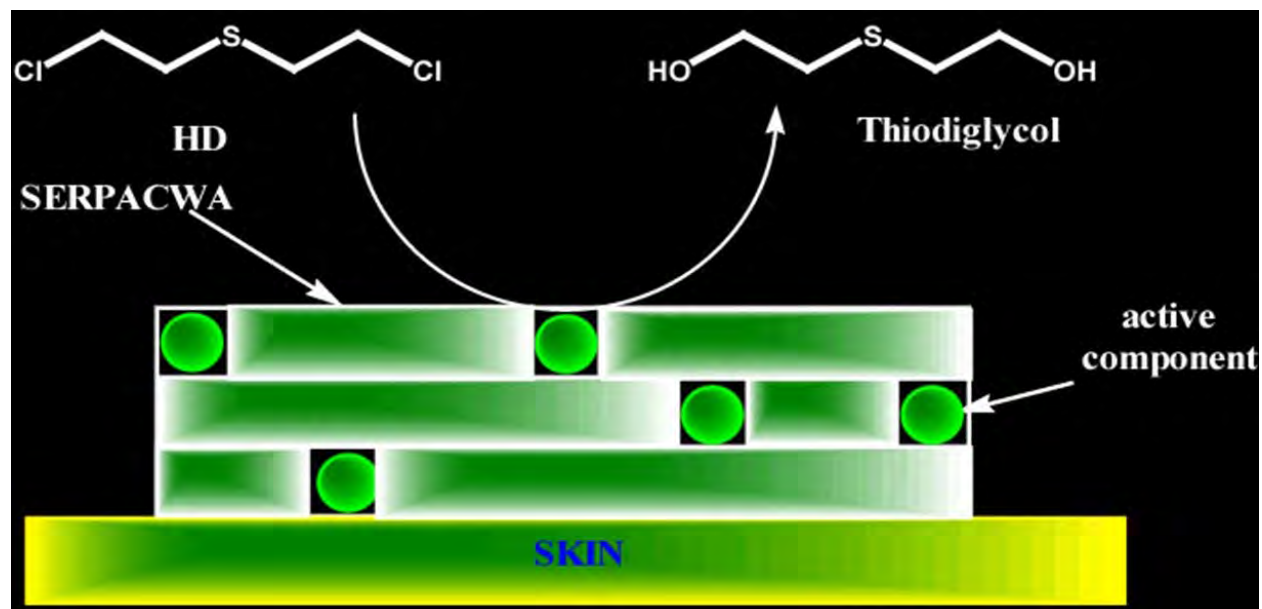


Figure 1. Concept for an aTSP. Pretreatment skin barrier cream formulation provided physical barrier to prevent absorption into the skin and active moieties to neutralize any CWAs that penetrated into the barrier cream.

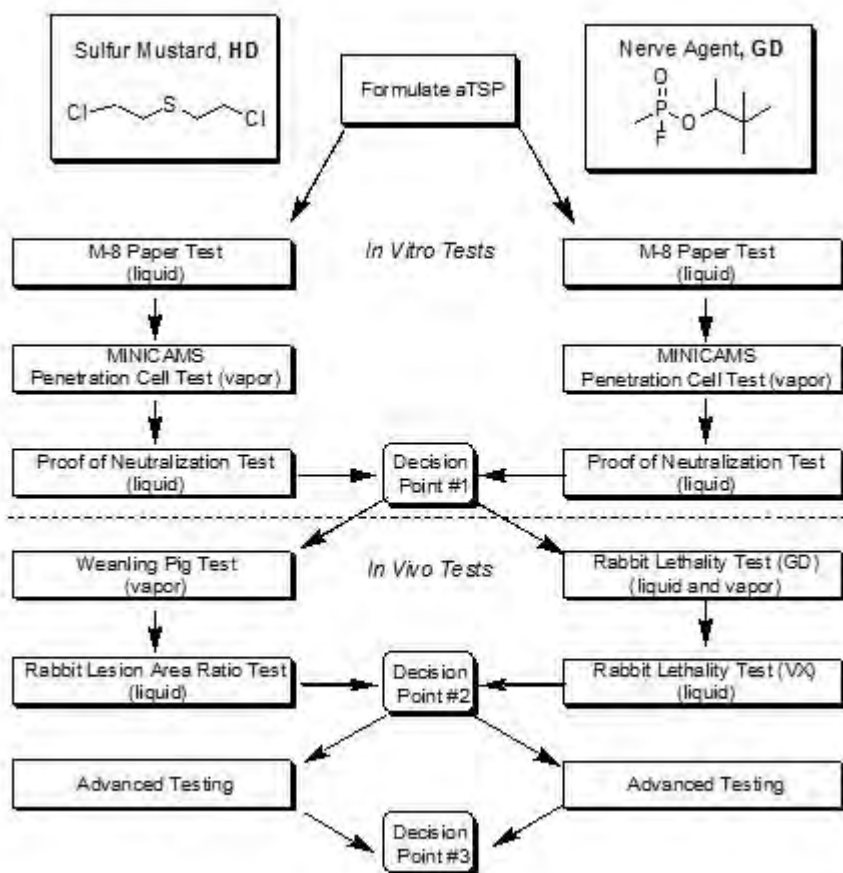


Figure 2. The active topical skin protectant (aTSP) decision tree network (DTN). A flow chart describing the path that candidate aTSPs follow during efficacy evaluation.



Figure 3. M8 test assembly.

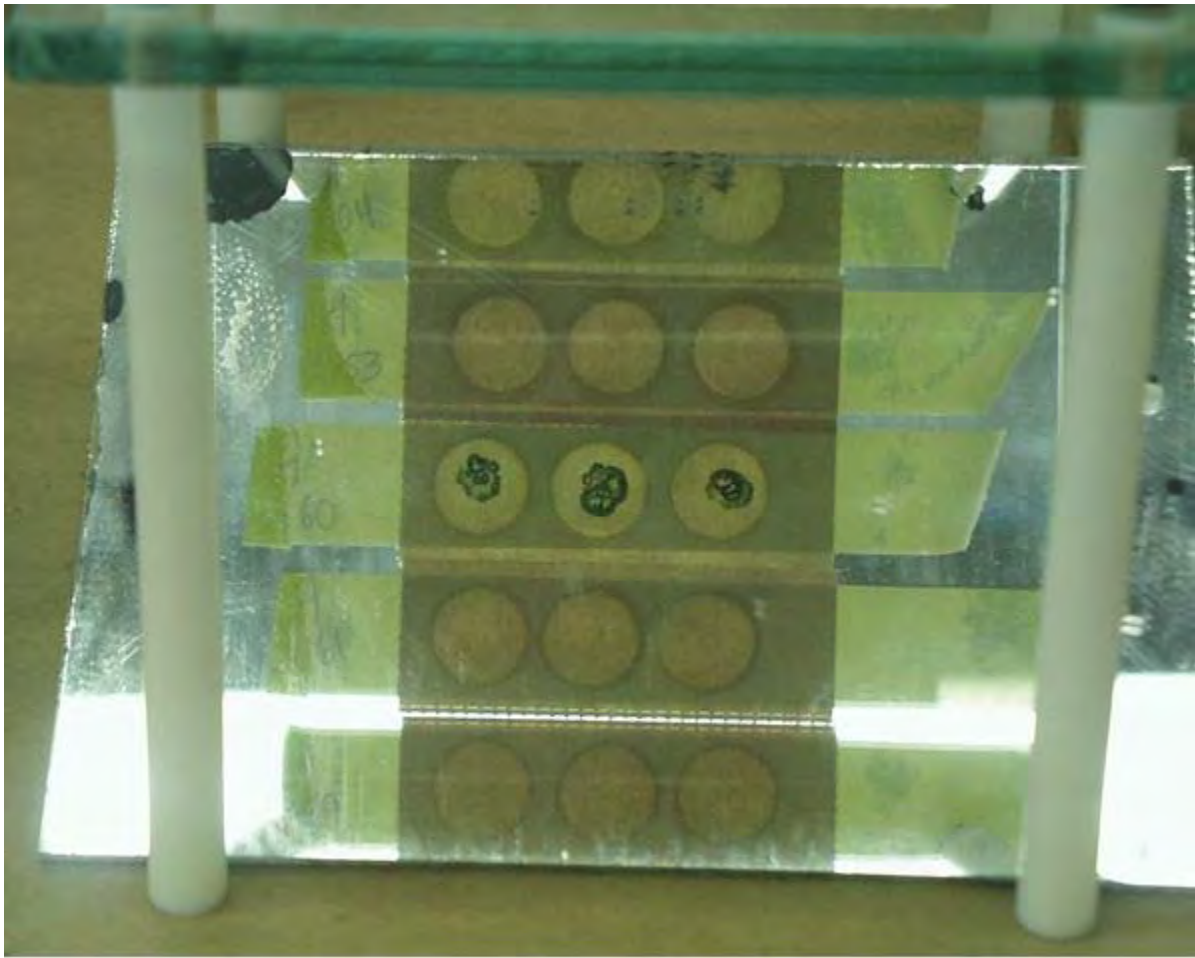


Figure 4. M8 test assembly. Breakthrough was observed from the bottom surface of the M8 paper using a mirror placed on an angle at the bottom of the test assembly.

THE RCR LOW-FLOW CELL

for determining in-vitro percutaneous penetration

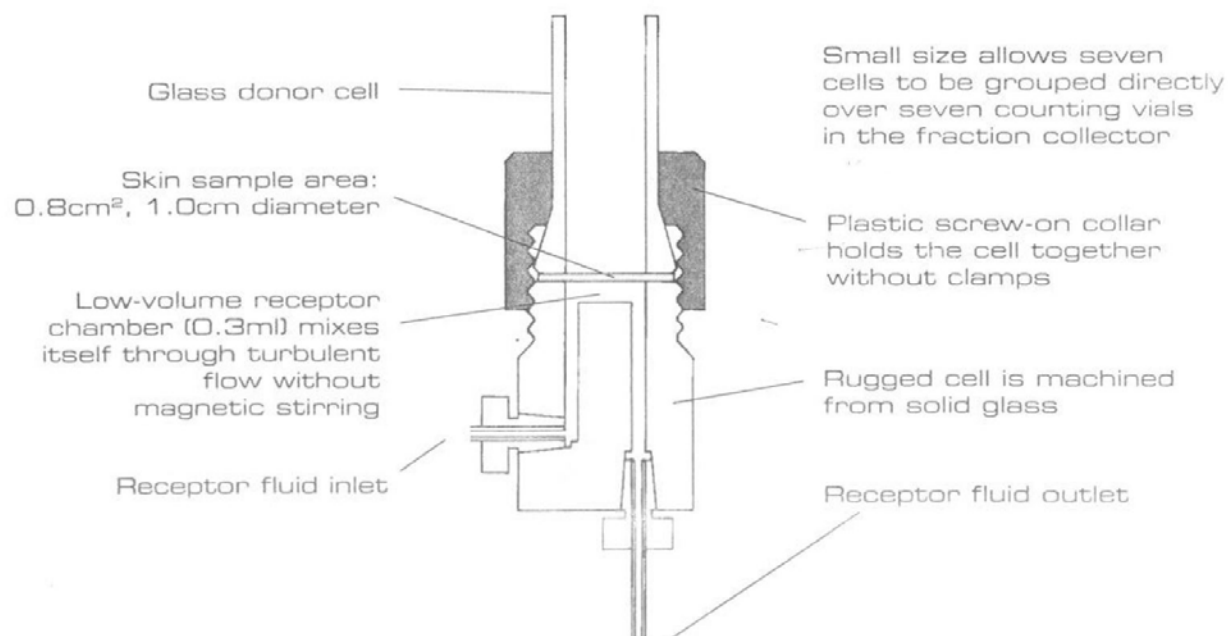


Figure 5. Reifenrath Consulting and Research (RCR) low-flow cell.



Figure 6. Minicams penetration cell test setup in hood.



Figure 7. Removing excess aTSP from a glass penetration cell with cellulose acetate wafer and perforated tape strip.



Figure 8. Penetration cell test. Cell holding assembly and dosing vapor cup with CWA.

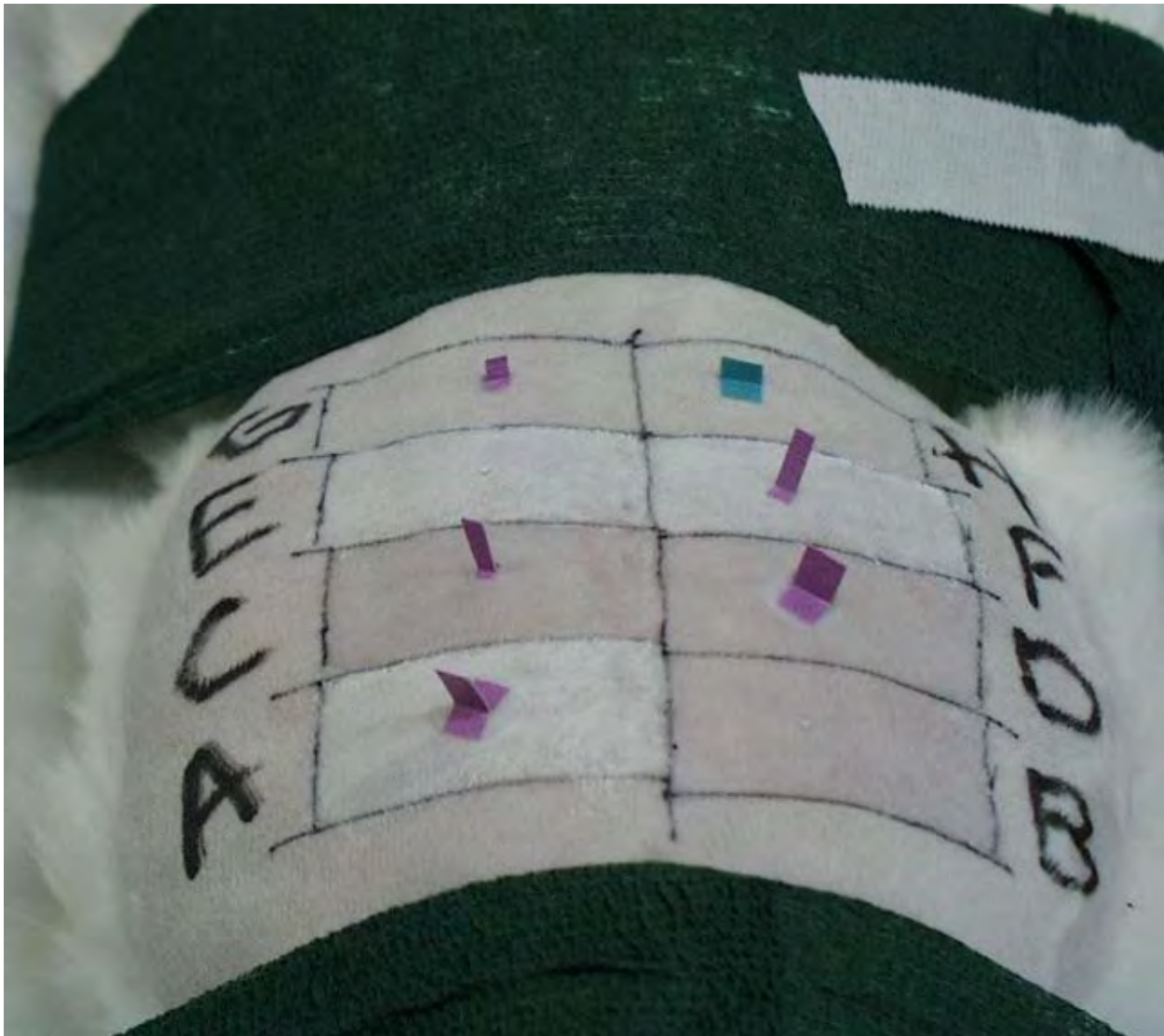


Figure 9. Optimization of the rabbit LAR model. Test sites were untreated or pretreated with ICD 3004 (SERPACWA), challenged with 1 or 2 μ L of HD, and left non-occluded or occluded with 6- or 12-mm diameter Teflon disks.



Figure 10. Rabbit LAR model. Measurement of lesion length and width.

Hairless Guinea Pig Evaluation

4 Min HD Vapor, at 0.2mm thickness

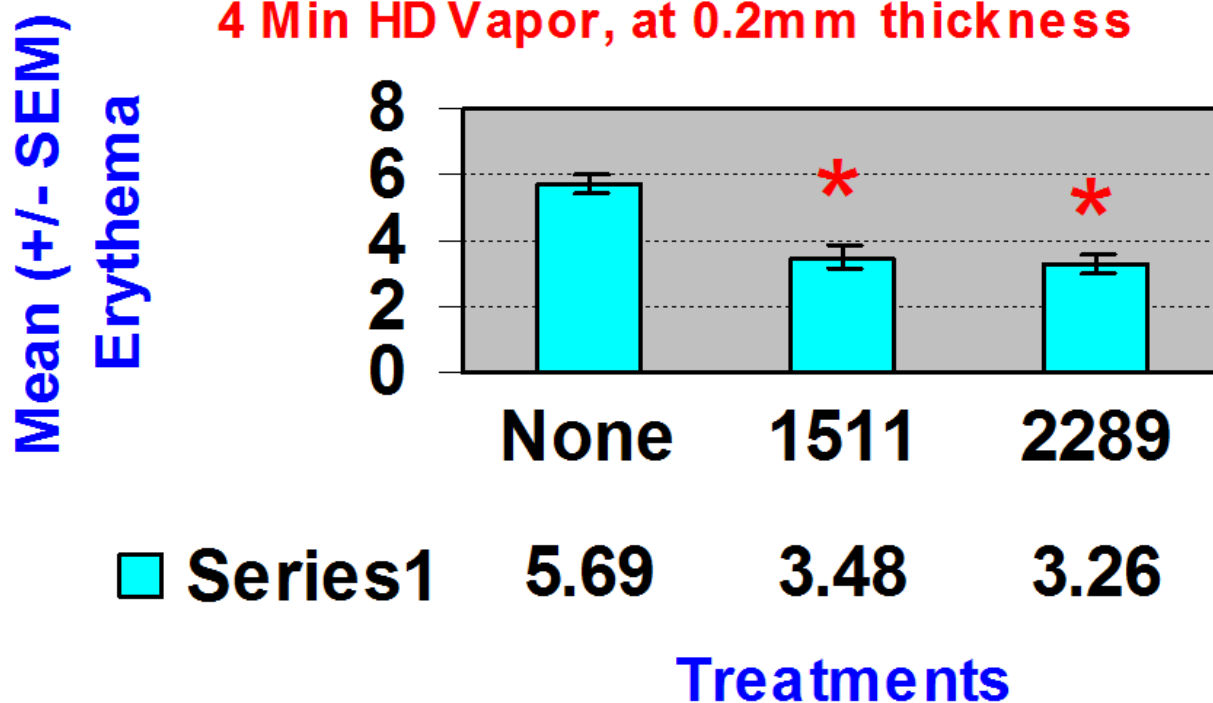


Figure 11. Hairless guinea HD vapor evaluation of ICD 1511 and ICD 2289 compared to unprotected positive controls. Nine animals (numbers 9-17, 307-329 g) using 6 sites per animal. HD challenge for 4 minutes using saturated HD vapor cup (1.4 mg/L). Mean erythema values were a* readings of the reflectance color meter (Minolta model CR-200). ICD 1511 was 61% of control and ICD 2289 was 57% of control. Error bars = SEM. Experiments conducted on 10 June 1993.

Weanling Pig HD Vapor Test

ICD # 2701 (S-330) at 0.1 mm

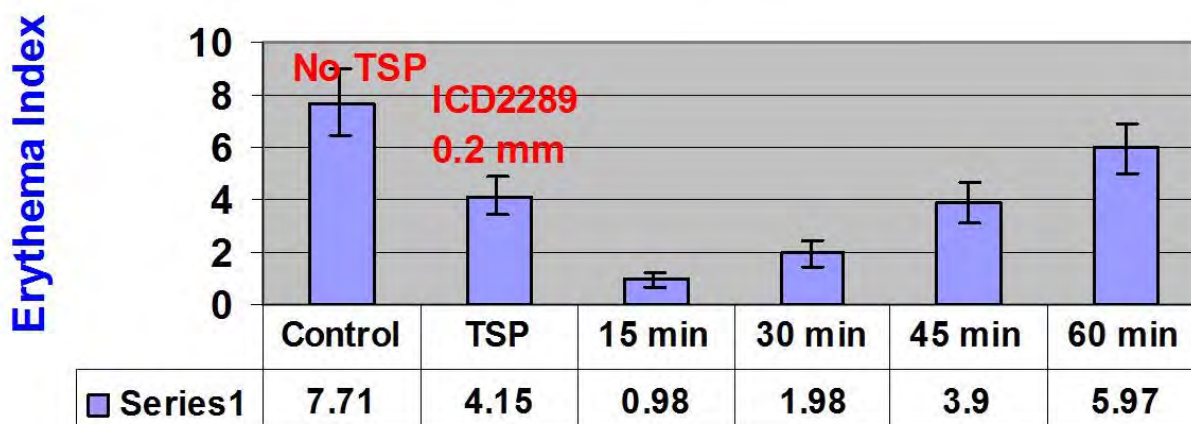


Figure 12. Weanling pig HD vapor evaluation of ICD 2701 and ICD 2289 compared to unprotected positive controls. Six animals (numbers 51-56, 7.7-9.2 kg) with 24 sites per animal were used in the experiment. HD vapor challenge using a saturated HD vapor cup (1.4 mg/L) for positive control and ICD 2289 was 15 minutes. ICD 2701 (S-330) was challenged for 15-60 minutes (as listed). Mean erythema values were a* readings of the reflectance color meter (Minolta model CR-200). Error bars = SEM. ICD 2289 provided significant protection at a thickness of 0.2 mm and was 54% of control. ICD 2701 (S-330) provided significant protection at a thickness of 0.15 mm for up to 45 minutes. Experiments conducted 23-30 July 1996.

Weanling Pig HD Vapor Test

ICD # 2730 (S-330) at 0.1 mm

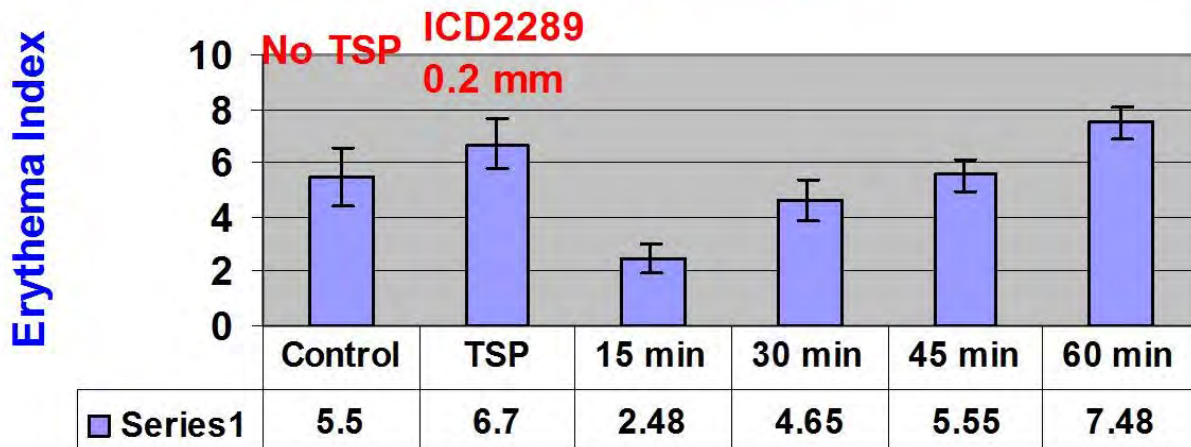


Figure 13. Weanling pig HD vapor evaluation of ICD 2730 and ICD 2289 compared to unprotected positive controls. Six animals (numbers 69-74, 7.3-9.0 kg) with 24 sites per animal were used in the experiment. HD vapor challenge using a saturated HD vapor cup (1.4 mg/L) for positive control and ICD 2289 was 15 minutes. ICD 2730 (S-330) was challenged for 15-60 minutes (as listed). Mean erythema values were a^* readings of the reflectance color meter (Minolta model CR-200). Error bars = SEM. ICD 2289 did not provide significant protection at a thickness of 0.2 mm and was 122% of control. ICD 2730 (S-330) provided significant protection at a thickness of 0.15 mm at 15 minutes but not at 30, 45, or 60 minutes. Experiments conducted 23-31 October 1996.

Weanling Pig HD Vapor Test

ICD # 2927,2928,2930,2933 at 0.2 mm

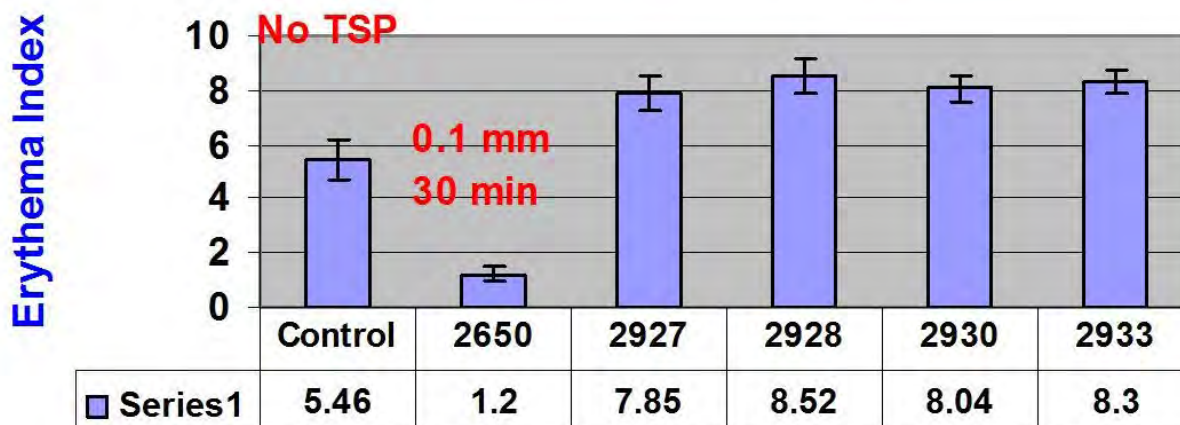


Figure 14. Weanling pig HD vapor evaluation of ICD 2927, 2928, 2930, and 2933 with standard ICD 2650 compared to unprotected positive controls. Six animals (numbers 121-126, 6.9-9.5 kg) with 24 sites per animal were used in the experiment. HD vapor challenge using a saturated HD vapor cup (1.4 mg/L) was 15 minutes for positive control and ICD formulations 2927, 2928, 2930, and 2933 spread at a thickness of 0.2 mm. ICD 2650 (S-330 formulation), spread at a thickness of 0.1 mm, was used as the standard and challenged for 30 minutes. Mean erythema values were a^* readings of the reflectance color meter (Minolta model CR-200). Error bars = SEM. All candidate formulations were like ICD 2289 with 50% new F5A powder, lot #48032450 and old Y25 oil, lot #VT590. Each formulation was mixed with slight variations in mixing time and cooling. None of formulations using the new F5A powder were efficacious and produced significantly worse lesions than the nonprotected positive control animals. The percent of control values were 144, 156, 147, and 152, respectively. ICD 2650 (S-330) provided significant protection with a percent control value of 22. Experiments conducted 13-15 May 1997.

WEANLING PIG EVALUATION

Pig#127-132, ICD# 2926,2929,2931,2932

S = .1mm, T = .2mm

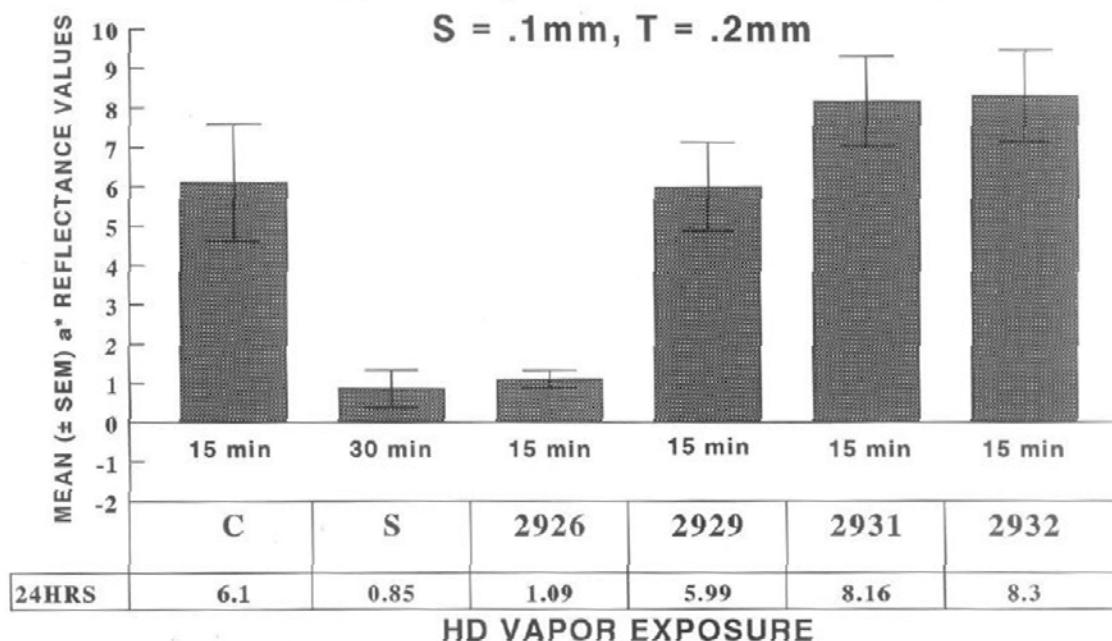


Figure 15. Weanling pig HD vapor evaluation of ICD 2926, 2929, 2931, and 2932 with standard ICD 2650 compared to unprotected positive controls. ICD 2926, 2929, 2931, and 2932 were all spread at a thickness of 0.2 mm. ICD 2650 spread at a thickness of 0.1 mm was used as the standard. These were all compared to unprotected positive controls. Six animals (numbers 127-132, 6.6-9.1 kg) with 24 sites per animal were used in the experiment. HD vapor challenge using a saturated HD vapor cup (1.4 mg/L) was 15 minutes for positive control and candidate formulations. ICD 2650 (S-330 formulation) was challenged for 30 minutes. Mean erythema values were a* readings of the reflectance color meter (Minolta model CR-200). Error bars were SEM. ICD numbers 2929, 2931, and 2932 were not efficacious compared to the nonprotected positive control animals. The percent of control values were 98, 134, and 136, respectively. ICD 2926, however, with a percent of control value of 18 was significant. ICD 2650 (S-330) provided significant protection with a percent of control value of 14. Experiments were conducted 20 May-12 June 1997.

Weanling Pig Evaluation

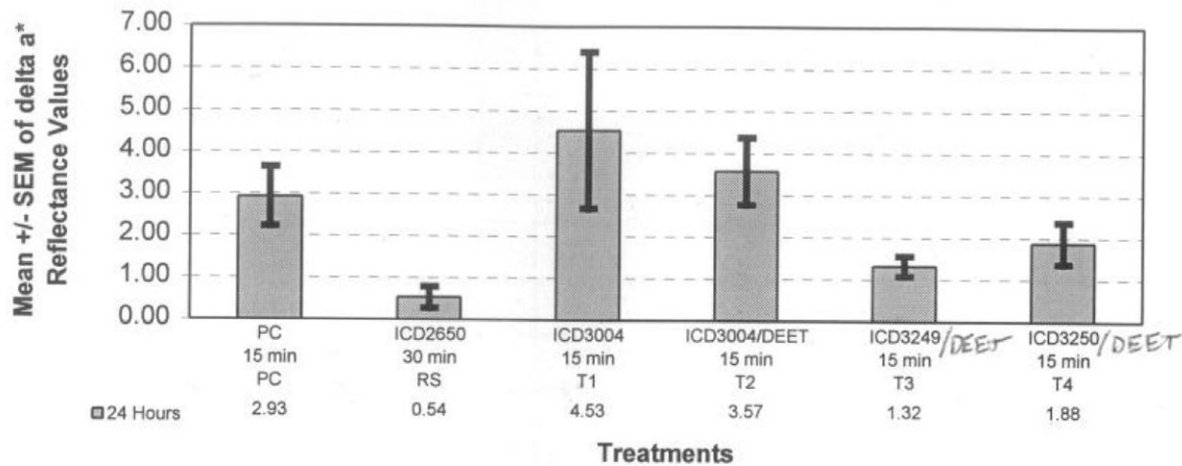


Figure 16. Weanling pig HD vapor evaluation of ICD 3004, 3249, and 3250 with standard ICD 2650 compared to unprotected positive controls. Prior to applying three aTSP formulations (3004, 3249, and 3250) Extended Duration Topical Insect and Arthropod Repellent (EDTIAR) was first applied at a rate of $1.9 \mu\text{l}/\text{cm}^2$ and allowed to dry for 60 minutes. After this drying time, ICD 3004 (with and without EDTIAR), 3249, 3250, and 2650 were all spread at a thickness of 0.1 mm and allowed to dry for 15 minutes. Six animals (numbers 189-194 weighing 7.8-11.0 kg) with 24 sites per animal were used in the experiment. HD vapor challenge, using a saturated HD vapor cup (1.4 mg/L), was 15 minutes for positive control and candidate formulations. The standard, ICD 2650 (S-330 formulation), was challenged for 30 minutes. Mean erythema values were a^* readings of the reflectance color meter (Minolta model CR-200). Error bars were SEM. ICD numbers 3004 (without and with EDTIAR) and 3250 were not efficacious compared to the nonprotected positive control animals. The percent of control values were 155, 122, and 64, respectively. ICD 2650 and 3249 were efficacious, with percent of control values of 18 and 45. Experiments were conducted 4-6 May 1999.

Weanling Pig Erythema Evaluation

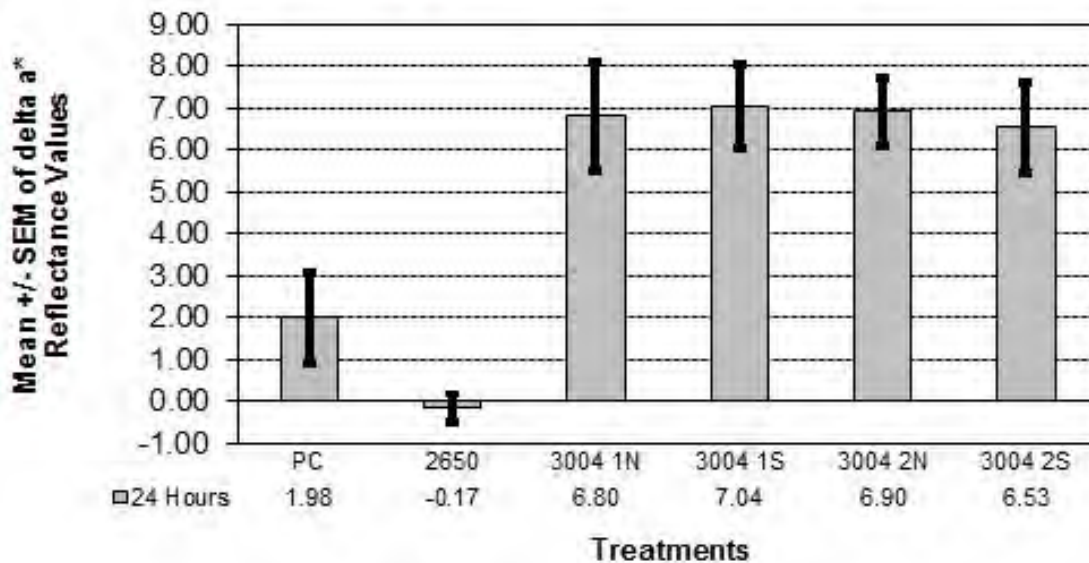


Figure 17. Weanling pig HD vapor evaluation of SERPACWA (ICD 3004, McKesson 300 kg production run, lot # TSP0050498) with standard ICD 2650 compared to unprotected positive controls. SERPACWA was spread at two thicknesses, 0.1 and 0.2 mm, and challenged with HD vapor for 15 minutes. At the end of the exposure the SERPACWA sites were either cleaned using the normal dry wiping process or cleaned using a special multiple process of dry wiping, wiping with 0.5% bleach, wiping with water, and finally wiping with ethanol. This modification to the normal procedure was to determine if a more thorough cleaning after exposure would make a difference in the observed efficacy. The non-treated positive control was also challenged for HD vapor for 15 minutes. The standard, ICD 2650, was spread at a thickness of 0.1 mm and challenged with HD vapor for 30 minutes. Six animals (numbers 237-242, weighing 8.0-11.1 kg) with 24 sites per animal were used in the experiment. Mean erythema values were a* readings of the reflectance color meter (Minolta model CR-200). Error bars were SEM. SERPACWA sites, with or without the special cleaning procedure, were observed to be significantly worse than the untreated positive control sites with percent of control values of 343, 355, 348, and 330, respectively. The percent of control value for the standard ICD 2650 was -8.6 and it provided good protection. With a mean erythema, for unprotected positive control sites, of only 1.98, this group of animals did not have a large response to HD vapor exposure, nevertheless, applying SERPACWA prior to HD vapor exposure greatly increased the observed skin damage. Experiments were conducted 17-31 January 2001.

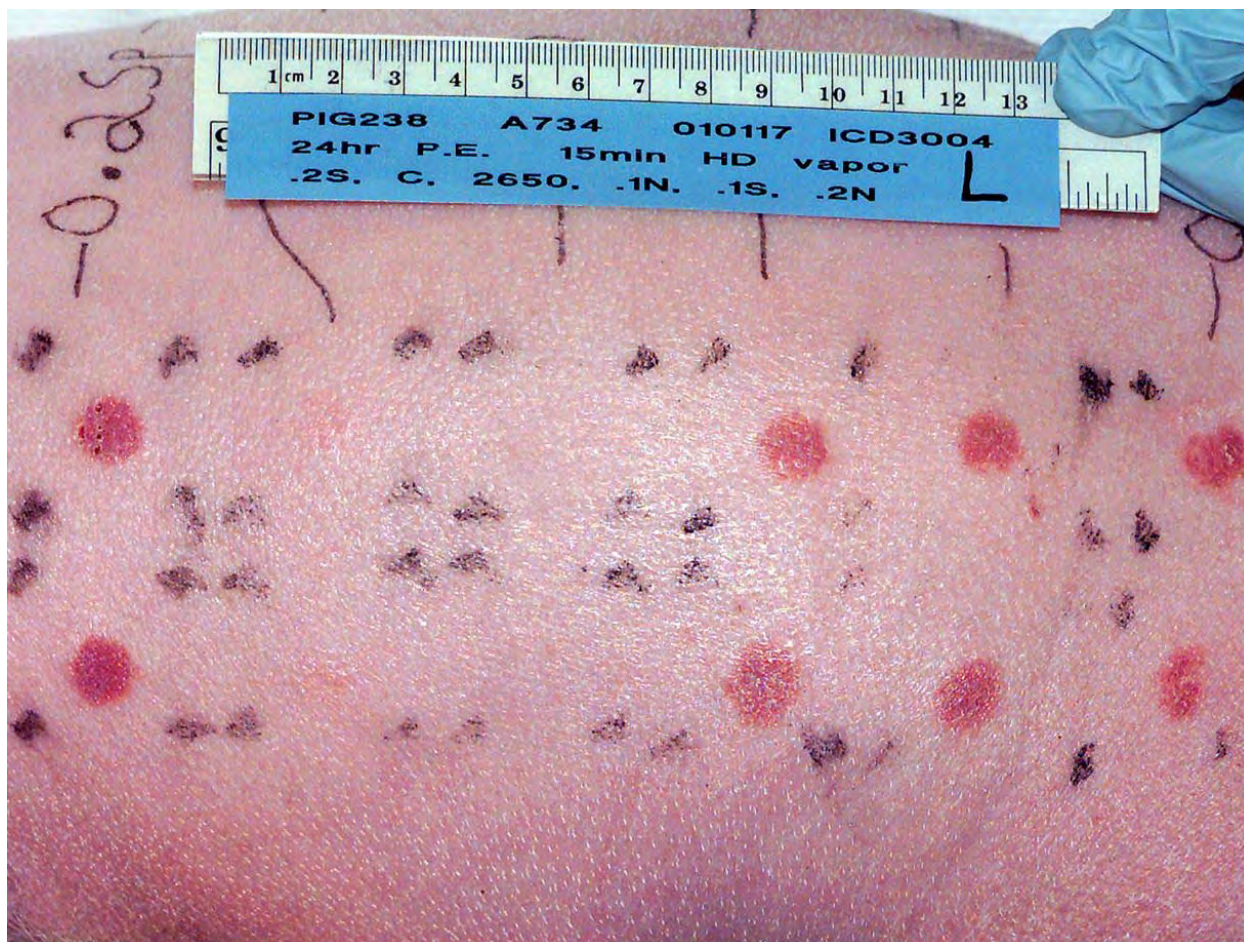


Figure 18. Photograph of animal number 238 (left side) following exposure to HD vapor. Pairs of sites from left to right are ICD 3004 (0.2 mm special cleaning), positive control, standard ICD 2650 (0.1 mm), ICD 3004 (0.1 mm), ICD 3004 (0.1 mm special cleaning), and ICD 3004 (0.2 mm). The positive control and ICD 3004 sites were exposed to HD vapor for 15 minutes. The standard ICD 2650 sites were exposed to HD vapor for 30 minutes. The control sites show slight traces of erythema. The sites protected by standard ICD 2650 showed no evidence of erythema. All the sites protected by SERPACWA showed severe erythema.

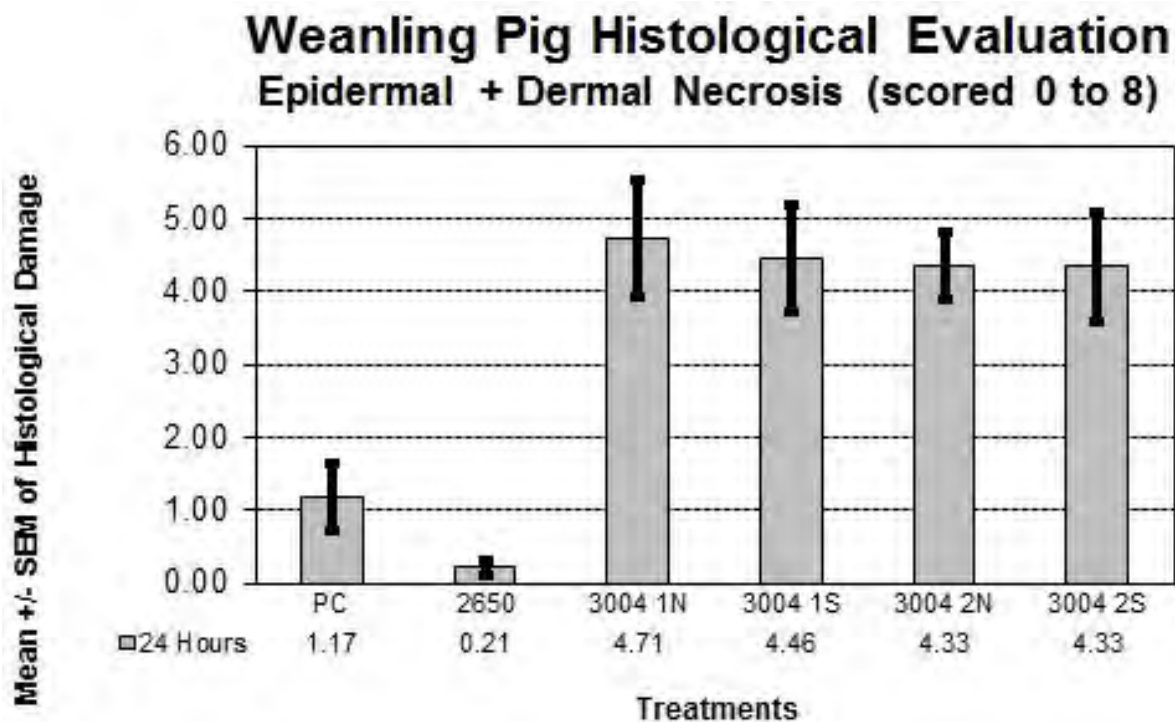


Figure 19. Weanling pig HD vapor evaluation of SERPACWA (ICD 3004, McKesson 300 kg production run, lot # TSP0050498) with standard ICD 2650 compared to unprotected positive controls. SERPACWA was spread at two thicknesses, 0.1 and 0.2 mm, and challenged with HD vapor for 15 minutes. At the end of the exposure the SERPACWA sites were either cleaned using the normal dry wiping process or cleaned using a special multiple process of dry wiping, wiping with 0.5% bleach, wiping with water, and finally wiping with ethanol. This modification to the normal procedure was to determine if a more thorough cleaning after exposure would make a difference in the observed efficacy. The nontreated positive control also was challenged for HD vapor for 15 minutes. The standard, ICD 2650, was spread at a thickness of 0.1 mm and challenged with HD vapor for 30 minutes. Six animals (numbers 237-242, weighing 8.0-11.1 kg) with 24 sites per animal were used in the experiment. After euthanasia at 24 hours post-exposure, skin punches were taken from each exposure site. Mean histological damage scores were determined by the veterinary pathologist from H&E slides. Error bars were SEM. SERPACWA sites, with or without the special cleaning procedure, were observed to be significantly worse than the untreated positive control sites with percent of control values of 403, 381, 370, and 370, respectively. The percent of control value for the standard ICD 2650 was 18 and represents good protection. The histological scores correlated well with the erythema scores and demonstrated that applying SERPACWA prior to HD vapor exposure greatly increased the observed skin damage. Experiments were conducted 17-31 January 2001.

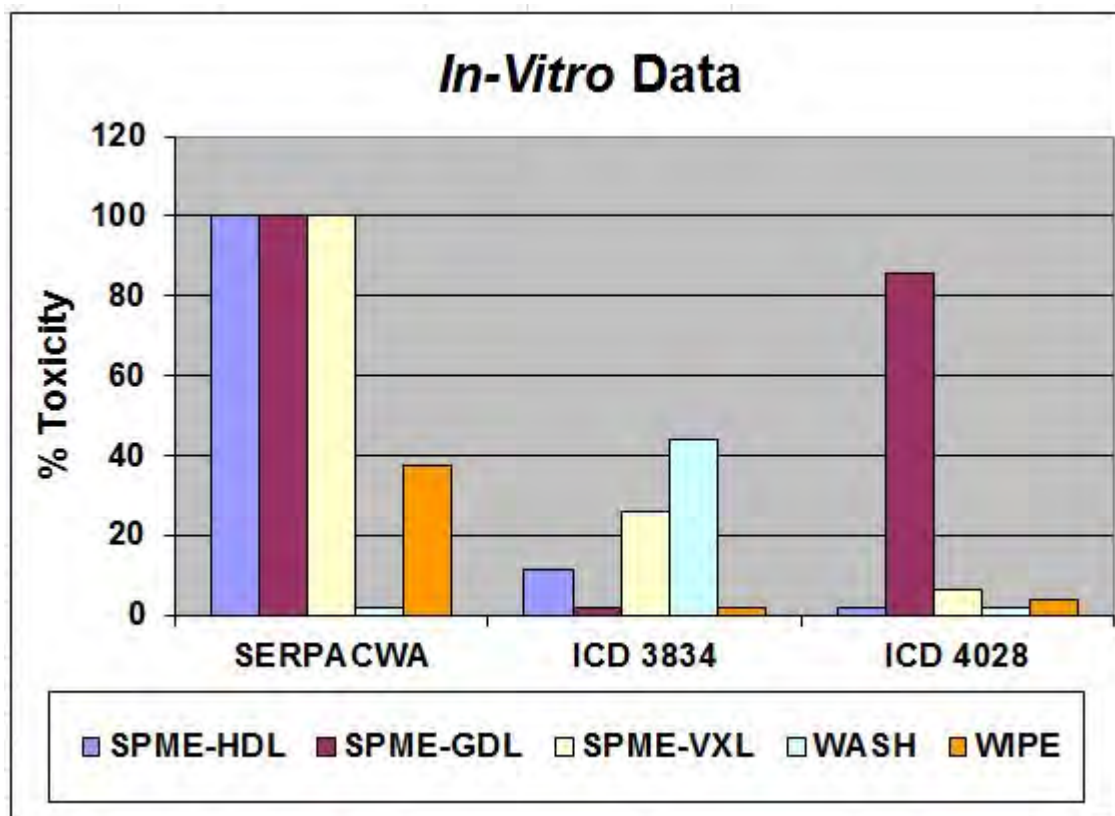


Figure 20. Summary of *in vitro* data for aTSPs selected for transition to advanced development compared to SERPACWA. Smaller bars are more efficacious. Percent toxicity was a normalized efficacy scale where 100 correlates to no destruction of agent in the solid phase microextraction (SPME) headspace tests and easy removal in the wash and wipe tests. “L” with agent name indicates liquid; “V” indicates vapor. The lead formulation containing polyalkenimines and surfactants provided significantly improved protection in every model except for the wash test. The backup formulation, containing S-330, provided improved protection for HD and VX and equivalent protection for GD in the neutralization tests. It also provided improved protection in the wipe test and equivalent protection in the wash test.

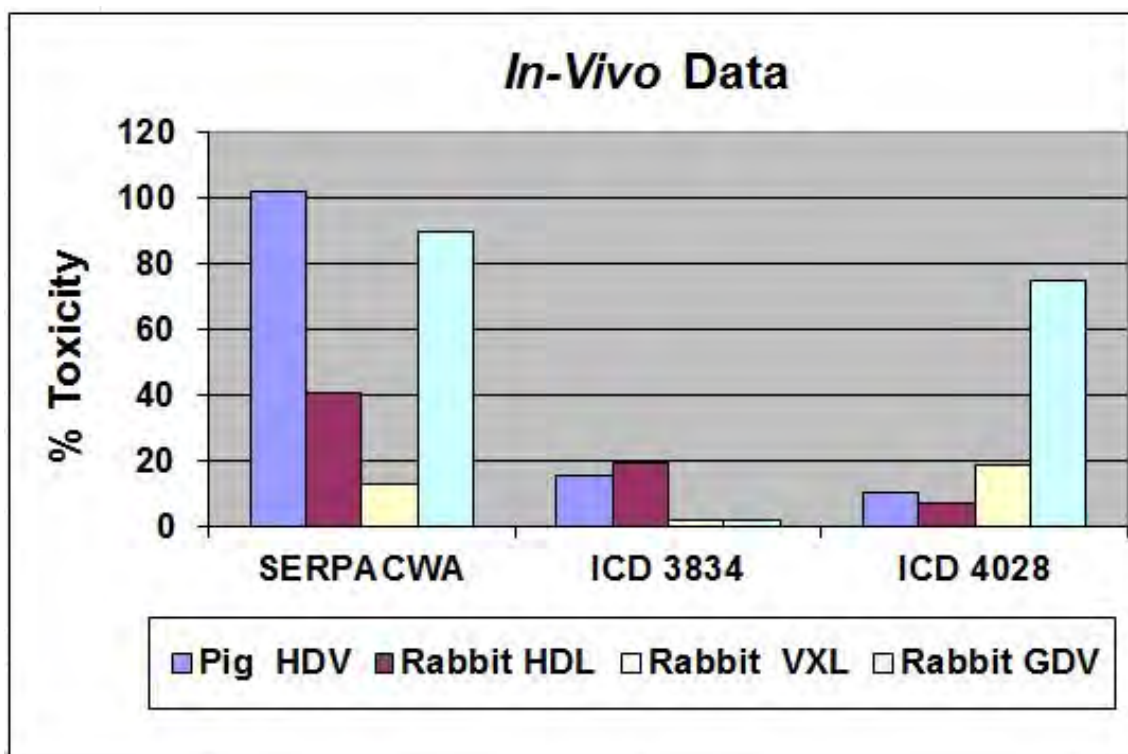


Figure 21. Summary of *in vivo* data for aTSPs selected for transition to advanced development compared to SERPACWA. Smaller bars are more efficacious. Percent toxicity is a normalized efficacy scale where 100 correlates to no protection and 0 is complete protection. “L” with agent name indicates liquid; “V” indicates vapor. The lead formulation containing polyalkenimines and surfactants provided significantly improved protection in every model. The backup formulation, containing S-330, provided improved protection for HD and equivalent protection for VX and GD

TABLES

Table 1. Battelle Module 1 Results: Candidate aTSP in Penetration Cell HD and GD Vapor Challenges

		Challenge Agent							
ICD No.	Alias ICD No.	HD Vapor				GD Vapor			
		A _{20hr} *	T1000**	Candidate Performance Relative To Standard	Test Decision Relative to Standard	A _{20hr} *	T1000**	Candidate Performance Relative to Standard	Test Decision Relative to Standard
2701	3354	193	36036.9	Better	Pass	4746	367.4	Same	Fail
3004	2289	2600	667.4	-	-	5403	434.8	-	-
3214		2520	731.4	Same	Fail	4082	580.0	Better	Fail
3219		3063	614.7	Same	Fail	6599	280.9	Worse	Fail
3220		4771	418.1	Better	Fail	4132	519.7	Better	Fail
3309		2701	680.5	Better	Fail	4369	492.0	Same	Fail
3319		3025	558.5	Same	Fail	3351	736.9	Better	Fail
3328		2120	696.9	Same	Fail	2276	32397.3	Same	Fail
3329		3086	617.3	Same	Fail	3216	416.2	Same	Fail
3330		3937	404.6	Same	Fail	1962	283.6	Same	Fail
3331		3834	294.6	Worse	Fail	1359	2241.2	Same	Fail
3332		4109	354.3	Worse	Fail	1191	1967.8	Same	Fail
3333		1641	804.5	Same	Fail	86	57209.6	Better	Pass
3334		3386	356.3	Worse	Fail	4510	457.1	Same	Fail
3335		3384	394.7	Same	Fail	2751	911.0	Same	Fail
3347	3247	3638	478.0	Same	Fail	4056	533.7	Better	Fail
3348	3248	2741	636.0	Same	Fail	3112	623.8	Better	Fail
3349	3249	1646	956.4	Better	Fail	1539	1017.2	Better	Fail
3350	3250	970	1232.1	Better	Fail	5456	406.3	Better	Fail
3353		2134	1462	Same	Fail				
3354	2701	554	26072.6	Better	Pass	4855	457.7	Better	Fail
3369		1259	1087.5	Better	Fail	5307	411.0	Same	Fail
3370		1577	1007.1	Same	Fail	4687	433.7	Same	Fail
3371		1858	739.6	Better	Fail	4527	484.5	Better	Fail
3372		1265	1057.9	Better	Fail	5966	347.8	Same	Fail
3377		740	1667.8	Better	Fail	3630	576.0	Better	Fail
3378		352	2453.7	Better	Pass	7172	425.8	Same	Fail
3379		427	3111.4	Better	Pass	8174	238.5	Worse	Fail
3380		265	3358.0	Better	Pass	4763	475.7	Same	Fail
3448		3196	886.3	Same	Fail	966	2305.2	Same	Fail

* Cumulative amount of agent detected at 20 hr after dosing.

** Time to Accumulate 1000 ng (min)

		Challenge Agent							
ICD No.	Alias ICD No.	HD Vapor				GD Vapor			
		A _{20hr} *	T1000**	Candidate Performance Relative To Standard	Test Decision Relative to Standard	A _{20hr} *	T1000**	Candidate Performance Relative to Standard	Test Decision Relative to Standard
3449		8750	138.9	Worse	Fail	2391	786.3	Same	Fail
3450	3548	253	2296.5	Better	Pass	4735	1025.6	Same	Fail
3450 2nd test	3548	178	5392.8	Better	Pass	791	2126.1	Better	Pass
3451		16	45106.1	Better	Pass	2383	746.1	Better	Fail
3451 2nd test		1386	1055.1	Better	Fail	2811	598.3	Same	Fail
3452		2602	636.6	Same	Fail	3770	486.0	Same	Fail
3453		2752	663	Better	Fail	4059	506.5	Same	Fail
3454		671	1511.8	Better	Pass	1207	1102.3	Better	Fail
3455		5229	327.0	Worse	Fail	6494	340.7	Same	Fail
3456		3601	517.7	Same	Fail	4495	485.2	Same	Fail
3457		2182	730.2	Better	Fail	4615	451.2	Better	Fail
3458		3124	590.7	Same	Fail	4090	432.5	Same	Fail
3459		2021	792.9	Better	Fail	4067	525.7	Better	Fail
3459 2nd test		2855	657.6	Same	Fail		525.7	Better	Fail
3461		1339	1111.6	Better	Fail	4299	435.9	Same	Fail
3462		943	1301.8	Better	Fail	2281	573.3	Same	Fail
3463		1288	1142.3	Better	Fail	2840	576.3	Same	Fail
3464		1337	1010.5	Better	Fail	3946	551.2	Same	Fail
3465		1264	1074.1	Better	Fail	3506	526.5	Same	Fail
3470		1634	832.6	Better	Fail	11	67600.6	Better	Pass
3470 2nd test						2992	6340.7	Same	Fail
3471		933	1738.1	Same	Fail		82439.4	Better	Pass
3479		1482	990.7	Better	Fail	3674	574.5	Better	Fail
3488		3101	605.0	Same	Fail	5655	454.2	Same	Fail
3496		3632	685.2	Same	Fail	5041	396.8	Same	Fail
3516		2667	757.9	Same	Fail	48	8980.2	Better	Pass
3517		1326	902.8	Same	Fail	5321	397.0	Same	Fail
3518		5878	267.7	Worse	Fail	5822	390.7	Same	Fail
3519		612	1452.5	Better	Pass	2554	711.0	Same	Fail
3520		185	2741.5	Better	Pass	2885	951.7	Same	Fail
3521		1768	944.0	Better	Fail	2379	792.3	Better	Fail
3522		2186	813.1	Better	Fail	3668	723.5	Same	Fail
3523		290	2407.8	Better	Pass	29	39508.0	Better	Pass
3524		55	20192.8	Better	Pass	2723	808.6	Better	Fail
3525		3136	600.2	Same	Fail	3838	536.0	Better	Fail
3526		2412	721.3	Better	Fail	5831	347.6	Same	Fail
3530		1011	1206.8	Better	Fail	1321	994.5	Better	Fail
3531		676	1505.7	Better	Pass	4036	535.3	Same	Fail
3532		782	1423.9	Better	Pass	5194	391.0	Same	Fail
3533		226	3019.6	Better	Pass	1069	1218.6	Same	Fail

* Cumulative amount of agent detected at 20 hr after dosing.

** Time to Accumulate 1000 ng (min)

		Challenge Agent							
ICD No.	Alias ICD No.	HD Vapor				GD Vapor			
		A _{20hr} *	T1000**	Candidate Performance Relative To Standard	Test Decision Relative to Standard	A _{20hr} *	T1000**	Candidate Performance Relative to Standard	Test Decision Relative to Standard
3548	3450	52	12975.3	Better	Pass	429	8240.6	Better	Pass
3549		129	9219.6	Better	Pass	459	2437.6	Better	Pass
3550		943	1311.2	Better	Fail	850	5276.4	Same	Fail
3551		207	2649.9	Better	Pass	801	1329.2	Better	Pass
3552		98	6424.3	Better	Pass	40	12706.5	Better	Pass
3553		1504	981.4	Better	Fail	3416	632.6	Better	Fail
3554		1601	994.1	Better	Fail	1081	1181.7	Better	Fail
3555		1626	962.6	Better	Fail	4391	543.0	Better	Fail
3556		1592	947.9	Better	Fail	4882	437.2	Better	Fail
3564		6997	184.75	Worse	Fail	9480	150.6	Worse	Fail
3565		1275	1079.1	Better	Fail	3219	753.9	Better	Fail
3566		2739	595.8	Same	Fail	5622	444.2	Same	Fail
3567		1307	1074.7	Better	Fail	2905	818.4	Better	Fail
3568		1291	1058.1	Better	Fail	2312	866.3	Better	Fail
3569		1275	1085.4	Better	Fail	4148	604.5	Better	Fail
3570		2338	751.6	Better	Fail	8040	359.9	Same	Fail
3571		1752	906.2	Better	Fail	5289	587.2	Better	Fail
3572		2356	717.7	Same	Fail	7215	469.3	Better	Fail
3573		2361	700.4	Better	Fail	5516	465.9	Same	Fail
3574		1488	992.5	Better	Fail	3940	617.4	Better	Fail
3585		1895	903.8	Better	Fail	3030	661.2	Better	Fail
3598		1566	975.2	Better	Fail	557	2155.0	Better	Pass
3599		2227	792.2	Same	Fail	5119	507.9	Better	Fail
3600		510	1703.7	Better	Pass	5870	979.3	Same	Fail
3601		1307	1083.4	Better	Fail	2294	884.7	Better	Fail
3602		1023	1191.9	Better	Fail	1251	1127.8	Better	Fail
3603		710	1380.3	Better	Pass	4722	540.5	Better	Fail
3609		2571	653.0	Same	Fail	5324	400.8	Same	Fail
3610		2064	786.3	Better	Fail	5042	439.1	Better	Fail
3611		1005	1193.7	Better	Fail	3254	513.7	Same	Fail
3612		2257	745.8	Better	Fail	4559	472.6	Same	Fail
3613		2410	737.9	Same	Fail	5465	394.1	Same	Fail
3622						1564	1041.2	Better	Fail
3623						1623	970.2	Better	Fail
3624						1471	1134.7	Better	Fail
3625						2222	803.8	Better	Fail
3626						2967	734.0	Better	Fail
3627						2512	807.4	Better	Fail
3630		295	2299.0	Better	Pass	4868	446.4	Same	Fail
3631		853	1921.6	Better	Pass	3273	642.1	Same	Fail
3632		1211	1131.2	Better	Fail	1975	935.6	Better	Fail
3633		303	2539.9	Better	Pass	231	2463.9	Better	Pass
3634		1433	1195.9	Same	Fail	52	4117.3	Better	Pass
3664		61	4808.5	Better	Pass	530	2312.6	Better	Pass
3665		114	17664.7	Better	Pass	39	51125.3	Better	Pass
3666		873	1325.9	Better	Fail	2095	820.3	Better	Fail
3667		418	1657.2	Better	Pass	2082	862.6	Better	Fail

* Cumulative amount of agent detected at 20 hr after dosing.

** Time to Accumulate 1000 ng (min)

		Challenge Agent							
ICD No.	Alias ICD No.	HD Vapor				GD Vapor			
		A _{20hr} *	T1000**	Candidate Performance Relative To Standard	Test Decision Relative to Standard	A _{20hr} *	T1000**	Candidate Performance Relative to Standard	Test Decision Relative to Standard
3668		3	57964.9	Better	Pass	3046	651.7	Better	Fail
3669		1138	1125.6	Better	Fail	4121	509.2	Better	Fail
3670		1221	1093.8	Better	Fail	3206	622.4	Better	Fail
3671		1010	1193.6	Better	Fail	2202	785.6	Better	Fail
3672		1179	1108.7	Better	Fail	2137	819.6	Better	Fail
3698		2610	699.5	Same	Fail	5139	464.8	Better	Fail
3699		708	2069.2	Same	Fail	2880	591.9	Same	Fail
3708		738	1279.1	Better	Pass	604	1502.1	Better	Pass
3709		384	1877.4	Better	Pass	873	1202.0	Better	Fail
3710		539	1602.1	Better	Pass	2468	753.0	Better	Fail
3711		746	1396.3	Better	Pass	3433	666.0	Same	Fail
3712		1108	1055.0	Better	Fail		100000.0	Better	Pass
3713		3011	552.3	Same	Fail	1007	1167.5	Better	Fail
3714		1506	982.0	Better	Fail		100000.0	Better	Pass
3715		1411	1016.8	Better	Fail		74643.2	Better	Pass
3716		1261	1064.6	Better	Fail		100000.0	Better	Pass
3717		747	1469.5	Better	Pass	15	61033.1	Better	Pass
3718		1262	1083.3	Better	Fail		100000.0	Better	Pass
3724		1640	935.8	Better	Fail	197	3479.9	Better	Pass
3725		122	2804.5	Better	Pass	22	48559.8	Better	Pass
3726		2573	754.7	Better	Fail	4969	446.0	Same	Fail
3727		775	1321.8	Better	Pass	2319	763.9	Better	Fail
3728		696	1576.4	Better	Pass	58	44549.2	Better	Pass
3729		317	2965.4	Better	Pass	198	3809.9	Better	Pass
3736		1215	1106.6	Better	Fail	4301	489.9	Better	Fail
3737		213	2708.7	Better	Pass	3603	675.6	Same	Fail
3742		250	5514.7	Better	Pass		100000.0	Better	Pass
3743		3431	397.4	Worse	Fail		100000.0	Better	Pass
3744		3077	570.7	Worse	Fail	41	47492.0	Better	Pass
3745		3645	509.2	Worse	Fail	22	42689.0	Better	Pass
3772	3830	1167	1117.9	Better	Fail	2	92000.0	Better	Pass
3773	3790	290	4349.0	Better	Pass		100000.0	Better	Pass
3774		8495	192.1	Worse	Fail	94	5355.7	Better	Pass
3775		204	3687.5	Better	Pass		100000.0	Better	Pass
3778		431	3370.4	Better	Pass	26	9667.4	Better	Pass
3779	3970	105	5262.8	Better	Pass		100000.0	Better	Pass
3780	3792	2503	737.0	Same	Fail		100000.0	Better	Pass
3781		2580	571.2	Same	Fail		100000.0	Better	Pass
3782		531	2228.6	Better	Pass		100000.0	Better	Pass
3818		620	1663.3	Better	Pass	7699	224.4	Worse	Fail
3819		576	2045.7	Better	Pass	7335	278.2	Worse	Fail
3820		1057	1268.6	Better	Fail	9662	193.5	Worse	Fail
3821		363	1913.5	Better	Pass	1419	1429.7	Better	Fail
3825		7374	301.8	Worse	Fail	10	28521.7	Better	Pass
3826		6263	340.5	Worse	Fail	10	47397.7	Better	Pass
3827		6532	302.0	Worse	Fail		100000.0	Better	Pass
3828		3493	626.7	Same	Fail	58	62992.9	Better	Pass

* Cumulative amount of agent detected at 20 hr after dosing.

** Time to Accumulate 1000 ng (min)

		Challenge Agent							
ICD No.	Alias ICD No.	HD Vapor				GD Vapor			
		A _{20hr} *	T1000**	Candidate Performance Relative To Standard	Test Decision Relative to Standard	A _{20hr} *	T1000**	Candidate Performance Relative to Standard	Test Decision Relative to Standard
3829		5231	437.3	Worse	Fail	2	671456.3	Better	Pass
3830	3772	1045	1312.9	Same	Fail	6	245954.2	Better	Pass
3831		7092	206.7	Worse	Fail	1188	1020.8	Better	Fail
3832	3791	11407	169.3	Worse	Fail	223	6953.4	Better	Pass
3833		4953	374.4	Worse	Fail	34	72918.6	Better	Pass
3834		1592	34.1	Same	Fail	6	285215.5	Better	Pass
3836		9869	215.5	Worse	Fail	74	63662.1	Better	Pass
3837		1232	1106.2	Better	Fail	530	1493.2	Better	Pass
3839		1051	1199.9	Better	Fail	145	8633.6	Better	Pass
3840		1112	1171.4	Better	Fail				
3841		5950	257.2	Worse	Fail				
3851		11414	194.3	Worse	Fail	3838	576.0	Same	Fail
3965		3798	864.6	Same	Fail	88	17284.5	Better	Pass
3970	3779	127	8539.4	Better	Pass		100000.0	Better	Pass
3972		9886	159.4	Worse	Fail	18898	134.3	Worse	Fail
3973		679	1186.0	Better	Pass	77	4425.2	Better	Pass
3974		791	1354.1	Better	Pass	124	4642.0	Better	Pass
3975		1035	1187.0	Better	Fail	1730	1049.3	Better	Fail
3976		1095	1154.4	Better	Fail	1592	994.0	Better	Fail
3977		1131	1269.0	Better	Fail	3	57095.8	Better	Pass
3978		1331	1056.9	Better	Fail	459	3686.4	Better	Pass
3979		2701	748.4	Same	Fail	4460	260.6	Worse	Fail
3980		619	1410.8	Better	Pass	2340	844.2	Same	Fail
3981		598	1574.5	Better	Pass	222	2055.5	Better	Pass
3982		3303	433.3	Same	Fail	5432	247.4	Same	Fail
3983		1183	1105.4	Same	Fail	5199	245.2	Worse	Fail
3984		1029	1179.1	Better	Fail	3938	612.5	Same	Fail
3985		1175	1174.7	Better	Fail	412	1836.3	Same	Fail
3986		1198	1100.7	Better	Fail	2015	1054.4	Same	Fail
3987		2049	700.1	Same	Fail	1682	1015.4	Same	Fail
3996		739	1193.5	Better	Pass	3807	576.1	Same	Fail
3997		3810	352.6	Worse	Fail	7463	333.3	Worse	Fail
3998		4717	344.6	Worse	Fail	5009	422.5	Same	Fail
3999		3514	452.5	Same	Fail	7112	142.3	Worse	Fail
4000		10210	100.7	Worse	Fail	44448	26.1	Worse	Fail

* Cumulative amount of agent detected at 20 hr after dosing.

** Time to Accumulate 1000 ng (min)

Table 2. Battelle Module 2 Results: M8 Chemical Detection Paper, Liquid Agent

ICD No.	Alias ICD No.	Challenge Agent					
		HD		GD		VX	
		Date(s) Tested (Breakthroughs*, Mean Time, min)	Test Decision Relative to Standard	Date(s) Tested (Breakthroughs*, Mean Time, min)	Test Decision Relative to Standard	Date(s) Tested (Breakthroughs*, Mean Time, min)	Test Decision Relative to Standard
1511		11/28/01 (0, 360.0) 04/08/02 (0/8, 360.0) 01/08/03 (2, 300.7) 01/13/03 (0, 360)	PC** PC PC, Invalid PC	03/22/01 (6, 246.2) 05/11/01 (5, 177.7) 04/11/02 (8, 41.9)	PC PC PC	04/18/02 (6/8, 125.8)	PC
2701	3354	09/04/01 (4, 248.3)	Fail	09/05/01 (1, 326.0)	Pass	05/16/01 (3, 245.6)	Fail
3004	2289	03/05/01 (4, 246.4) 03/07/01 (0, 360.0) 03/12/01 (0, 360.0) 05/04/01 (0, 360.0) 09/04/01 (1, 322.3) 11/15/01 (2, 327.8)	Invalid PC PC PC PC Invalid	03/14/01 (5, 185.0) 09/05/01 (5, 170.9) 04/10/02 (3, 293.3)	PC PC PC	03/22/01 (8, 88.7) 05/16/01 (5, 192.8)	PC PC
3369		03/05/01 (2, 280.4) 03/12/01 (1, 320.1)	Invalid Pass	03/14/01 (0, 360.0)	Pass	03/22/01 (1, 321.0)	Pass
3371		03/05/01 (0, 360.0) 03/12/01 (0, 360.0)	Invalid Pass	03/14/01 (0, 360.0)	Pass	03/22/01 (1, 324.6)	Pass
3372		03/05/01 (1, 320.8) 03/12/01 (0, 360.0)	Invalid Pass	03/14/01 (0, 360.0)	Pass	03/22/01 (0, 360.0)	Pass
3453		03/05/01 (4, 202.4) 03/12/01 (0, 360.0)	Invalid Pass	05/11/01 (0, 360.0)	Pass	05/16/01 (1, 326.1)	Pass
3459		05/04/01 (2, 291.6) 03/05/01 (9, 35.6)	Fail Invalid				
3460		03/05/01 (1, 330.0) 05/04/01 (0, 360.0)	Invalid Pass	05/11/01 (9, 4.1)	Fail	05/16/01 (9, 34.2)	Fail

* out of nine replicates, unless noted otherwise.

** process control

Table 2. Module 2 Results (cont'd.)

ICD No.	Alias ICD No.	Challenge Agent					
		HD		GD		VX	
		Date(s) Tested (Breakthroughs*, Mean Time, min)	Test Decision Relative to Standard	Date(s) Tested (Breakthroughs*, Mean Time, min)	Test Decision Relative to Standard	Date(s) Tested (Breakthroughs*, Mean Time, min)	Test Decision Relative to Standard
3461		03/05/01 (1, 330.6) 03/12/01 (1, 321.0)	Invalid Pass	05/11/01 (9, 23.6)	Fail	05/16/01 (0, 360.0)	Pass
3519		03/05/01 (0, 360.0) 03/12/01 (0, 360.0)	Invalid Pass	03/14/01 (0, 360.0)	Pass	05/16/01 (2, 283.0)	Fail
3520		03/05/01 (2, 283.2) 03/12/01 (0, 360.0)	Invalid Pass	05/11/01 (0, 360.0)	Pass	05/16/01 (0, 360.0)	Pass
3521		03/07/01 (0, 360.0)	Pass	03/14/01 (0, 360.0)	Pass	03/22/01 (4, 216.4)	Fail
3522		03/07/01 (2, 284.7)	Fail	03/14/01 (0, 360.0)	Pass	03/22/01 (5, 170.4)	Fail
3523		03/07/01 (2, 281.6)	Fail	03/14/01 (1, 322.8)	Pass	03/22/01 (5, 186.6)	Fail
3524		03/07/01 (1, 321.6)	Pass	03/14/01 (2, 284.4)	Fail	03/22/01 (0, 360.0)	Pass
3673	3523	09/04/01 (0, 360.0)	Pass	09/05/01 (0, 360.0)	Pass		
3712		09/04/01 (0, 360.0)	Pass	09/05/01 (4, 282.1)	Fail		
3713		09/04/01 (0, 360.0)	Pass	09/05/01 (8, 126.4)	Fail		
3714		09/04/01 (0, 360.0)	Pass	09/05/01 (3, 306.0)	Fail		
3715		09/04/01 (0, 360.0)	Pass	09/05/01 (0, 360.0)	Pass		
3716		09/04/01 (0, 360.0)	Pass	09/05/01 (1, 336.5)	Pass		
3717		09/04/01 (0, 360.0)	Pass	09/05/01 (0, 360.0)	Pass		
3718		09/04/01 (0, 360.0)	Pass	09/05/01 (0, 360.0)	Pass		

* out of nine replicates, unless noted otherwise.

** process control

Table 2. Module 2 Results (cont'd.)

ICD No.	Alias ICD No.	Challenge Agent					
		HD		GD		VX	
		Date(s) Tested (Breakthroughs*, Mean Time, min)	Test Decision Relative to Standard	Date(s) Tested (Breakthroughs*, Mean Time, min)	Test Decision Relative to Standard	Date(s) Tested (Breakthroughs*, Mean Time, min)	Test Decision Relative to Standard
3768		11/15/01 (1, 320.4) 11/28/01 (0, 360.0)	Invalid Pass				
3769		11/15/01 (9, 44.0) 11/28/01 (8, 57.2)	Invalid Fail				
3770		11/15/01 (1, 320.7) 11/28/01 (1, 320.9)	Invalid Pass				
3771		11/15/01 (0, 360.0) 11/28/01 (0, 360.0)	Invalid Pass				
3773	3790	11/28/01 (0, 360.0)	Pass				
3782		11/28/01 (0, 360.0)	Pass				
3783		11/15/01 (0, 360.0) 11/28/01 (0, 360.0)	Invalid Pass				
3784		11/15/01 (2, 319.2) 11/28/01 (0, 360.0)	Invalid Pass				
3785		11/15/01 (0, 360.0) 11/28/01 (0, 360.0)	Invalid Pass				
3829		04/08/02 (0, 360.0)	Pass	04/10/02 (2, 235.2)	Fail	04/18/02 (2, 282.8)	Fail
3830	3772	04/08/02 (0, 360.0)	Pass	04/10/02 (0, 360.0)	Pass	04/18/02 (0, 360.0)	Pass
3831		04/08/02 (0, 360.0)	Pass	04/10/02 (2, 255.4)	Fail	04/18/02 (6, 208.1)	Fail
3832	3791	04/08/02 (1, 330.8)	Pass	04/10/02 (0, 360.0)	Pass	04/18/02 (0, 360.0)	Pass
3833		04/08/02 (0, 360.0)	Pass	04/10/02 (1, 293.3)	Pass	04/18/02 (0, 360.0)	Pass
3834		04/08/02 (0, 360.0)	Pass	04/10/02 (1, 291.2)	Pass	04/18/02 (0, 360.0)	Pass
4020		01/17/03 (1, 320.7)	Pass				

* out of nine replicates, unless noted otherwise.

** process control

Table 2. Module 2 Results (cont'd.)

ICD No.	Alias ICD No.	Challenge Agent					
		HD		GD		VX	
		Date(s) Tested (Breakthroughs*, Mean Time, min)	Test Decision Relative to Standard	Date(s) Tested (Breakthroughs*, Mean Time, min)	Test Decision Relative to Standard	Date(s) Tested (Breakthroughs*, Mean Time, min)	Test Decision Relative to Standard
4028		01/17/03 (2, 353.1)	Fail				
4029		01/17/03 (0, 360.0)	Pass				
4050		01/17/03 (0, 360.0)	Pass				
4052		01/17/03 (0, 360.0)	Pass				
4076		01/08/03 (1, 320.3) 01/13/03 (0/8, 360.0)	Invalid Pass				
4077		01/08/03 (0, 360.0) 01/13/03 (0, 360.0)	Invalid Pass				
4078		01/08/03 (0, 360.0) 01/13/03 (0, 360.0)	Invalid Pass				
4079		01/08/03 (1, 321.0) 01/13/03 (1, 320.7))	Invalid Pass				
4080		01/08/03 (0, 360.0) 01/13/03 (0, 360.0)	Invalid Pass				
4081		01/08/03 (1, 320.8) 01/13/03 (0, 360.0)	Invalid Pass				
4082		01/08/03 (2, 280.3) 01/13/03 (0, 360.0)	Invalid Pass				
4083		01/08/03 (1, 325.1) 01/13/03 (0, 360.0)	Invalid Pass				
4084		01/08/03 (1, 321.0) 01/13/03 (0, 360.0)	Invalid Pass				
4085		01/17/03 (1, 320.2)	Pass				
4086		01/17/03 (0, 360.0)	Pass				
4087		01/17/03 (1, 320.8)	Pass				

* out of nine replicates, unless noted otherwise.

** process control

Table 2. Module 2 Results (cont'd.)

Table 3. Battelle Module 3 Results: Candidate aTSP in Penetration Cell Liquid HD and GD Challenges

ICD No.	Challenge Agent							
	HD				GD			
	A _{20hr} *	T1000**	Candidate Performance Relative to Standard	Test Decision Relative to Standard	A _{20hr} *	T1000**	Candidate Performance Relative to Standard	Test Decision Relative to Standard
3004	2641	606.0	-	-	40313	49.3	-	-
3533	6002	376.5	Worse	Fail	34239	58.4	Same	Fail
3665	5578	421.6	Same	Fail	39780	43.2	Same	Fail
3668	2503	428.0	Worse	Fail	48903	24.1	Worse	Fail
3699	6004	192.9	Worse	Fail	38716	50.5	Same	Fail
3768	5142	441.4	Worse	Fail	6266	235.6	Better	Pass
3769	7290	156.1	Worse	Fail	57559	18.3	Worse	Fail
3770	5738	495.6	Same	Fail	43442	74.9	Same	Fail
3771	682	4776.0	Better	Pass	90	16293.6	Better	Pass
3772	7011	181.0	Worse	Fail	37	117849.4	Better	Pass
3782					23	92024.5	Better	Pass
3834	7248	164.6	Worse	Fail	154	161796.0	Same	Fail

* Cumulative amount of agent detected at 20 hr after dosing.

** Time to Accumulate 1000 ng (min)

Table 4. Battelle Module 5 Results: Lesion Area Ratio at Test Sites Pretreated and Challenged with 1 μ L HD per Site for 4 hr, Sites Occluded.

Set	ICD No.	n*	Lesion Area Ratio		p Value for Candidate vs ICD 3004 at Fixed Sites	p Value for Candidate vs ICD 3004 at Rotated Sites	Test Decision Relative to Standard
			Mean	STDs**			
1, Dosed 11/28/01 - 12/05/01	3768	24	0.14	0.34	<0.0001		Better
	3770	24	0.16	0.31	<0.0001		Better
	3771	24	0.46	0.73	0.1023		Same
	3772	24	0.45	0.43	0.7609		Same
	3004, rotated	24	0.57	0.46	0.9843		Same
	none, rotated	24	1.13	0.83			
	none, fixed	24	1.00	0.00			
	3004, fixed	24	0.57	0.39			
2, Dosed 12/10/01 - 12/18/01	3769	24	0.17	0.14	<0.0001		Better
	3790	24	0.25	0.24	0.0028		Better
	3791	24	0.38	0.26	0.9832		Same
	3792	24	0.50	0.40	0.6399		Same
	3793	24	0.74	0.55	0.0151		Worse
	none, rotated	24	0.98	0.37			
	none, fixed	24	1.00	0.00			
	3004, fixed	24	0.35	0.17			
3, Dosed 12/20/01 - 01/23/02	3533	23	0.41	0.34	0.8124		Same
	3665	23	0.37	0.31	0.2315		Same
	3668	23	0.24	0.18	0.0025		Better
	3699	23	0.66	0.43	0.6197		Same
	3782	23	0.32	0.28	0.0358		Better
	none, rotated	23	1.05	0.51			
	none, fixed	23	1.00	0.00			
	3004, fixed	23	0.45	0.24			
4, Dosed 07/02/02 - 07/10/02	3833	24	0.51	0.48	0.6355	>0.05	Same
	3834 Lot No. 020305-ARL	24	0.30	0.25	<0.0001	<0.05	Better
	3884	24	0.43	0.42	0.1462	>0.05	Same
	3970	24	0.25	0.20	<0.0001	<0.05	Better
	3004, rotated	24	0.49	0.23	0.9754		Same
	none, rotated	24	1.03	0.49			
	none, fixed	24	1.00	0.00			
	3004, fixed	24	0.57	0.35			
	5, 3973	22	0.30	0.18	0.9739	0.9929	Same

Set	ICD No.	n*	Lesion Area Ratio		p Value for Candidate vs ICD 3004 at Fixed Sites	p Value for Candidate vs ICD 3004 at Rotated Sites	Test Decision Relative to Standard
			Mean	STDs**			
Dosed 11/13/02 - 11/25/02	3725	17	0.50	0.49	0.4478	0.0527	Same
	3886	22	0.19	0.13	0.0040	0.0971	Same
	3887	22	0.23	0.18	0.0170	0.2559	Same
	3004, rotated	22	0.30	0.22			
	none, rotated	22	0.85	0.44			
	none, fixed	22	1.00	0.00			
	3004, fixed	22	0.39	0.38			
6, Dosed 11/15/02 - 11/21/02	3903	24	0.37	0.20	0.8713	0.9985	Same
	4020	24	0.16	0.09	0.0019	0.0002	Better
	4021	24	0.33	0.27	0.9612	0.6606	Same
	4022	24	0.29	0.22	0.8757	0.5014	Same
	3004, rotated	24	0.36	0.24			
	none, rotated	24	0.82	0.23			
	none, fixed	24	1.00	0.00			
	3004, fixed	24	0.34	0.29			
7, Dosed 11/18/02 - 11/20/02	4028	24	0.07	0.12	<0.0001	<0.0001	Better
	4029	24	0.12	0.10	<0.0001	<0.0001	Better
	4050	24	0.26	0.22	0.0421	0.0913	Same
	4051	24	0.26	0.19	0.0849	0.1693	Same
	3004, rotated	24	0.35	0.10			
	none, rotated	24	0.99	0.36			
	none, fixed	24	1.00	0.00			
	3004, fixed	24	0.38	0.13			
8, Dosed 11/26/02 - 12/05/02	4052	24	0.22	0.20	0.0020	0.0067	Better
	3834 Lot No. 020807-ARL	16	0.15	0.12	<0.0001	<0.0001	Better
	3834 Lot No. 021029-ARL	24	0.19	0.12	0.0007	0.0025	Better
	3773 Lot No. 021030-ARL	24	0.25	0.12	0.0637	0.1476	Same
	ICD 3004, rotated	24	0.38	0.28			
	none, rotated	24	0.93	0.48			
	none, fixed	24	1.00	0.00			
	ICD 3004, fixed	24	0.39	0.26			

Table 5. Battelle Module 6 Results: Lethality Rates Among Rabbits Pretreated and Challenged with 0.5 mg VX/kg for 4 hr, Sites Occluded, Set 1 Dosed 16-23 September 2002.

Pretreatment Material, ICD Number	# Dosed	# Dead					24-hr Lethality Rate	Pretreatment p Value: aTSP Relative to Untreated Controls	
		1 hr	2 hr	3 hr	4 hr	24 hr		ICD 3004	
3004	15	0	0	1	1	3	0.20	0.0014*	-
3792	14	0	1	2	2	6	0.43	0.0064*	0.2451
3833	14	0	0	0	2	4	0.29	0.0006*	0.6817
3834	8	0	0	0	0	0	0.00	0.0002*	0.2421
3886	8	0	0	0	0	2	0.25	0.0070*	1.0000
3887	8	0	0	0	0	1	0.13	0.0014*	0.6186
3903	8	0	0	0	0	1	0.13	0.0014*	0.6186
none	10	2	10	10	10	10	1.00	-	0.0014**

* Significantly different from the untreated controls at a Bonferroni-corrected decision level of $0.05/6 = 0.0083$.

** Significantly better than ICD 3004 at a Bonferroni-corrected decision level of $0.05/6 = 0.0083$.

Table 6. Battelle Module 6 Results: Lethality Rates Among Rabbits Pretreated and Challenged with 0.5 mg VX/kg for 4 hr, Sites Occluded, Set 2 Dosed 24 September - 10 October 2002.

Pretreatment Material, ICD Number	# Dosed	# Dead					24-hr Lethality Rate	Pretreatment p Value: aTSP Relative to	
		1 hr	2 hr	3 hr	4 hr	24 hr		Untreated Controls	ICD 3004
3004	24	0	1	3	4	5	0.21	0.0001*	-
3771	16	0	0	1	1	2	0.13	0.0001*	0.6808
3830	16	0	0	0	0	3	0.19	0.0001*	1.0000
3832	16	0	2	5	5	7	0.44	0.0008*	0.1658
3884	16	0	0	0	0	0	0.00	0.0001*	0.0712
4022	16	0	0	0	1	3	0.19	0.0001*	1.0000
4028	16	1	1	2	2	3	0.19	0.0001*	1.0000
none	16	7	16	16	16	16	1.00	-	0.0001**

* Significantly different from the untreated controls at a Bonferroni-corrected decision level of $0.05/6 = 0.0083$.

** Significantly better than ICD 3004 at a Bonferroni-corrected decision level of $0.05/6 = 0.0083$.

Table 7. Battelle Module 6 Results: Lethality Rates Among Rabbits Pretreated and Challenged with 0.5 mg VX/kg for 4 hr, Sites Occluded, Set 3 Dosed 21-28 October 2002.

Pretreatment Material, ICD Number	# Dosed	# Dead					24-hr Lethality Rate	Pretreatment p Value: aTSP Relative to Untreated Controls	
		1 hr	2 hr	3 hr	4 hr	24 hr		ICD 3004	
3004	21	1	2	3	3	3	0.14	<0.0001*	-
3829	18	0	0	0	2	2	0.11	<0.0001*	1.0000
3970	18	0	0	1	2	5	0.28	<0.0001*	0.4324
4020	16	0	1	1	1	1	0.06	<0.0001*	0.6184
4021	14	0	0	1	1	2	0.14	<0.0001*	1.0000
4029	14	0	0	0	0	0	0.00	<0.0001*	0.2588
none	14	11	14	14	14	14	1.00	-	<0.0001**

* Significantly different from the untreated controls at a Bonferroni-corrected decision level of $0.05/6 = 0.0083$.

** Significantly better than ICD 3004 at a Bonferroni-corrected decision level of $0.05/6 = 0.0083$.

Table 8. Battelle Module 6 Results: Lethality Rates Among Rabbits Pretreated and Challenged with 0.5 mg VX/kg for 4 hr, Sites Occluded, Set 4 Dosed 21 October - 12 November 2002.

Pretreatment Material, ICD Number	#Dosed	# Dead					24-hr Lethality Rate	Pretreatment p Value: aTSP Relative to	
		1 hr	2 hr	3 hr	4 hr	24 hr		Untreated Controls	ICD 3004
3004	12	0	0	0	1	3	0.25	0.0014*	-
3773	16	0	0	0	0	1	0.06	<0.0001*	0.0672
4050	12	0	0	0	0	1	0.08	0.0001*	0.5901
4051	12	0	0	0	1	1	0.08	0.0001*	0.5901
4052	12	0	0	0	1	2	0.17	0.0007*	1.0000
none	8	8	8	8	8	8	1.00	-	0.0014**

* Significantly different from the untreated controls at a Bonferroni-corrected decision level of $0.05/6 = 0.0083$.

** Significantly better than ICD 3004 at a Bonferroni-corrected decision level of $0.05/6 = 0.0083$.

Table 9. Battelle Module 7 Results: Lethality Rates Among Rabbits Pretreated and Challenged with Two Vapor Caps Each Dosed with 28 µL GD/kg for 4 hr, Set 3 Dosed 10-25 April 2002.

Pretreatment Material, ICD Number	# Dosed	# Dead					24-hr Lethality Rate	Pretreatment p Value: aTSP Relative to	
		1 hr	2 hr	3 hr	4 hr	24 hr		Untreated Controls	ICD 3004
3004	12	1	6	9	9	11	0.92	1.0000	-
3829	13	0	1	1	1	2	0.15	0.0002*	0.0002**
3830	6	0	0	0	0	0	0.00	0.0003*	0.0004**
3831	6	0	0	0	2	4	0.67	0.1648	0.2451
3832	10	0	0	1	2	3	0.30	0.0040*	0.0062**
3833	6	0	0	0	0	0	0.00	0.0003*	0.0004**
3834	6	0	0	0	0	0	0.00	0.0003*	0.0004**
none	8	2	5	6	7	8	1.00	-	1.0000

* Significantly different from the untreated controls at a Bonferroni-corrected decision level of $0.05/6 = 0.0083$.

** Significantly better than ICD 3004 at a Bonferroni-corrected decision level of $0.05/6 = 0.0083$.

Table 10. Battelle Module 7 Results: Lethality Rates Among Rabbits Pretreated and Challenged with Two Vapor Caps Each Dosed with 28 µL GD/kg for 4 hr, Set 4 Dosed 30 April - 29 May 2002.

Pretreatment Material, ICD Number	# Dosed	# Dead					24-hr Lethality Rate	Pretreatment p Value: aTSP Relative to Untreated Controls	
		1 hr	2 hr	3 hr	4 hr	24 hr		ICD 3004	
3004	15	0	8	12	13	15	1.00	1.0000	-
3603	6	0	1	4	5	6	1.00	0.1409	1.0000
3725	10	0	0	3	4	5	0.50	0.0743	0.0047**
3771	15	0	0	1	3	6	0.40	0.0801	0.0011**
3773	6	0	0	1	1	1	0.17	0.0152	0.0020**
3792	6	0	0	0	0	0	0.00	0.0152	0.0002**
3884	6	0	0	0	0	0	0.00	1.0000	0.0002**
none	10	3	8	8	8	9	0.90	-	1.0000

* Significantly different from the untreated controls at a Bonferroni-corrected decision level of $0.05/6 = 0.0083$.

** Significantly better than ICD 3004 at a Bonferroni-corrected decision level of $0.05/6 = 0.0083$.

Table 11. Battelle Module 7 Results: Lethality Rates Among Rabbits Pretreated and Challenged with Two Vapor Caps Each Dosed with 28 µL GD/kg for 4 hr, Set 5 Dosed 29 May - 12 June 2003.

Pretreatment Material, ICD Number	# Dosed	# Dead					24-hr Lethality Rate	Pretreatment p Value: aTSP Relative to	
		1 hr	2 hr	3 hr	4 hr	24 hr		Untreated Controls	ICD 3004
3004	9	1	3	7	7	9	1.00	1.0000	-
3886	4	0	0	0	0	0	0.00	0.0048*	0.0014**
3905	6	0	1	2	4	5	0.83	1.0000	0.4000
3906	6	0	0	1	2	5	0.83	1.0000	0.4000
3907	6	0	0	4	5	6	1.00	1.0000	1.0000
3908	6	0	0	1	2	5	0.83	1.0000	0.4000
3909	6	0	0	2	2	6	1.00	1.0000	1.0000
none	6	1	5	5	5	6	1.00	-	1.0000

* Significantly different from the untreated controls at a Bonferroni-corrected decision level of $0.05/6 = 0.0083$.

** Significantly better than ICD 3004 at a Bonferroni-corrected decision level of $0.05/6 = 0.0083$.

Table 12. Battelle Module 7 Results: Lethality Rates Among Rabbits Pretreated and Challenged with Two Vapor Caps Each Dosed with 28 µL GD/kg for 4 hr, Set 6 Dosed 11 August - 12 September 2003.

Pretreatment Material, ICD Number	# Dosed	# Dead					24-hr Lethality Rate	Pretreatment p Value: aTSP Relative to	
		1 hr	2 hr	3 hr	4 hr	24 hr		Untreated Controls	ICD 3004
3004	23	0	2	10	13	21	0.91	1.0000	-
4020									
Lot No.	10	0	0	0	1	2	0.20	0.0002*	0.0001**
020828-ARL									
4028									
Lot No.	24	0	4	11	12	18	0.75	0.2097	0.2448
020904-ARL									
4029									
Lot No.	10	0	0	1	2	2	0.20	0.0002*	0.0001**
020904-ARL									
4050									
Lot No.	13	0	0	1	3	6	0.46	0.0097	0.0049**
020906-ARL									
4051									
Lot No.	8	0	0	0	0	0	0.00	<0.0001*	0.0000**
020906-ARL									
4052									
Lot No.	10	0	0	0	1	2	0.20	0.0002*	0.0001**
020906-ARL									
none	16	3	8	12	15	15	0.94	-	1.0000

* Significantly different from the untreated controls at a Bonferroni-corrected decision level of $0.05/6 = 0.0083$.

** Significantly better than ICD 3004 at a Bonferroni-corrected decision level of $0.05/6 = 0.0083$.

Table 13. Battelle Module 7 Results: Lethality Rates Among Rabbits Pretreated and Challenged with Two Vapor Caps Each Dosed with 28 µL GD/kg for 4 hr, Set 7 Dosed 6 October - 25 November 2003.

Pretreatment Material, ICD Number	# Dosed	# Dead					24-hr Lethality Rate	Pretreatment p Value: aTSP Relative to	
		1 hr	2 hr	3 hr	4 hr	24 hr		Untreated Controls	ICD 3004
3004	15	0	1	3	4	10	0.67	0.1181	-
4020 Lot No. 02T-362	11	0	0	0	0	0	0.00	<0.0001*	0.0007**
4029 Lot No. 02T-272	11	0	0	0	0	0	0.00	<0.0001*	0.0007**
4050 Lot No. 02T-297	24	0	1	1	2	4	0.17	<0.0001*	0.0024**
4052 Lot No. 02T-299	11	0	0	1	1	1	0.09	0.0001*	0.0052**
None	9	1	2	4	5	9	1.00	-	0.1181

* Significantly different from the untreated controls at a Bonferroni-corrected decision level of $0.05/6 = 0.0083$.

** Significantly better than ICD 3004 at a Bonferroni-corrected decision level of $0.05/6 = 0.0083$.

Table 14. Battelle Module 7 Results: Lethality Rates Among Rabbits Pretreated and Challenged with Two Vapor Caps Each Dosed with 28 µL GD/kg for 4 hr, Set 8 Dosed 31 August 2004.

Pretreatment Material, ICD Number	# Dosed	# Dead					24-hr Lethality Rate	Pretreatment p Value: aTSP Relative to	
		1 hr	2 hr	3 hr	4 hr	24 hr		Untreated Controls	ICD 3004
3004	3	0	0	2	2	2	0.67	1.0000	-
4212	24	0	1	3	12	17	0.71	1.0000	1.0000
None	2	0	1	1	1	2	1.00	-	1.0000

* Significantly different from the untreated controls at a Bonferroni-corrected decision level of $0.05/6 = 0.0083$.

** Significantly better than ICD 3004 at a Bonferroni-corrected decision level of $0.05/6 = 0.0083$.

Table 15. Battelle Module 9 Results: Lethality Rates Among Guinea Pigs Pretreated and Challenged with 100 mg GD/kg for 2 hr, Set 1 Dosed 12 May - 28 July 2003.

Pretreatment Material, ICD Number	# Dosed	# Dead					24-hr Lethality Rate	Pretreatment p Value: aTSP Relative to	
		1 hr	2 hr	3 hr	4 hr	24 hr		Untreated Controls	ICD 3004
3004	36	0	3	3	3	22	0.61	0.0154	-
3834	24	0	0	0	0	7	0.29	<0.0001*	0.0193
4020	24	1	2	2	2	5	0.21	<0.0001*	0.0033**
4028	23	0	1	1	1	15	0.65	0.0363	0.7893
4029	10	0	0	0	0	0	0.00	<0.0001*	0.0006**
4050	22	0	1	1	1	7	0.32	<0.0001*	0.0570
4051	24	0	1	1	1	7	0.29	<0.0001*	0.0193
4052	21	0	0	0	0	7	0.33	0.0001*	0.0570
None	24	2	14	14	14	22	0.92	-	0.0154

* Significantly different from the untreated controls at a Bonferroni-corrected decision level of $0.05/6 = 0.0083$.

** Significantly better than ICD 3004 at a Bonferroni-corrected decision level of $0.05/6 = 0.0083$.

Table 16. Summary of aTSP candidate formulations (order by ICD number).

ICD #	Percent Base Oil (PFPE = Y25)	Percent Teflon (PTFE = F5A)	Compound (%, ICD#, if any)	Other added compounds (%, ICD# if any)	PI/Supplier
1511			Fomblin Y Grease RT-15		Ausimont
2289	50% PFPE	50.0%	Note: 50% Fomblin Y25; 50% Poly F5A		McCreery
2373			50% TEFLON MP1200; 50% KRYTOX GPL102		McCreery
2478			POLYMIST F5A		Ausimont
2650	90% Fomblin (ICD#1511)		S-330 (10%)		Braue
2701	54% PFPE	36.0%	S-330 (10%)		Braue
2701	53.6%	35.8%	S-330 (10.7%)		Braue
2701	53.6%	35.8%	S-330 (10.7%)		Braue
2702	50% Surfactant - Light (ICD#2853)	40.0%	S330 (Monsanto, 10%)		Braue
2703			S330 (Monsanto)		Monsanto
2730	86% Fomblin (ICD#1511)		S330 (Monsanto, 9.5%)	4% Shark liver oil	Arroyo
2835	All Guard 5000				All Guard
2836	31.5% Petrolatum and 13.5% Fomblin HC/04		S-330 (10%)	Sorbitan Sterate (4.5%), Water (40.5%),	SRI, Kwong
2837			Carogen #C-0915 (N-dodecanoyl-2-oxazolidone)		Carogen
2839	Fomblin (ICD#1511)		MnO ₂		Novak Aldrich
2840	Fomblin (ICD#1511)		MnO ₂	16-DOXYL	Novak Aldrich
2847	Fomblin (ICD#1511) 45%	45.0%	Butanedione monoxime (10%)		Novak Aldrich
2848			H ₅ PV ₂ Mo ₁₀ O ₄₀		MAJ Weir
2849	Proderm				Proderm

ICD #	Percent Base Oil (PFPE = Y25)	Percent Teflon (PTFE = F5A)	Compound (% , ICD#, if any)	Other added compounds (% , ICD# if any)	PI/Supplier
2850	54% PFPE	36.0%	2,3 Butanedione Monoxime (10%, Aldrich)		Braue
2851	40% Surfactant - Light (ICD#2853)	40.0%	DLC 8(fine), Mg ₂ NiH ₂ + propylene glycol butyl ether (10%, 2942)	10% 2289 mix	Mainstream
2851	Fomblin (ICD#1511) 30%	45.0%	Oxime (Sigma #B-0753)		Aldrich
2852	50% PFPE	25.0%	Diacetyl Monoxime (25%)		Braue
2853			Light PFPE Surfactant,		Dupont,
2854			Medium PFPE Surfactant,		Dupont,
2859	SyDerma				MAJ Weir
2861	45% PFPE (Y25)	45% F5A	Surfactant - Light (10%, ICD#2853)		Ausimont
2862	45% PFPE	45.0%	Surfactant - Medium (10%, ICD#2854)		Ausimont
2863	40% PFPE	40.0%	Surfactant - Medium (20%, ICD#2854)		Ausimont
2864	45% PFPE	45.0%	Surfactant - Heavy (10%, ICD#2855)		Ausimont
2865	40% PFPE	40.0%	Surfactant - Heavy (20%, ICD#2855)		Ausimont
2866	40% PFPE	40.0%	Surfactant - Light (20%, ICD#2853)		Ausimont
2867	35% PFPE	35.0%	Surfactant - Light (30%, ICD#2853)		Ausimont
2868	25% PFPE	25.0%	Surfactant - Light (50%, ICD#2853)		Ausimont
2869	35% PFPE	35.0%	Surfactant - Medium (30%, ICD#2854)		Ausimont
2870	25% PFPE	25.0%	Surfactant - Medium (50%, ICD#2854)		Ausimont
2871	35% PFPE	35.0%	Surfactant - Heavy (30%, ICD#2855)		Ausimont
2872	25%PFPE	25.0%	Surfactant - Heavy (50%, ICD#2855)		Ausimont
2873	50% Surfactant - Light (ICD#2853)	50% ICD#2496			Ausimont
2874	50% Surfactant -	50% ICD#2479			Ausimont

ICD #	Percent Base Oil (PFPE = Y25)	Percent Teflon (PTFE = F5A)	Compound (% , ICD#, if any)	Other added compounds (% , ICD# if any)	PI/Supplier
	Light (ICD#2853)				
2875	50% Surfactant - Light (ICD#2853)	50% MP1200			Ausimont
2876	50% Surfactant - Light (ICD#2853)	50% ICD#2478			Ausimont
2877	42.5 PFPE	42.5%	2,3 Butanedione Monoxime (5%)	Surfactant - Light (10%, ICD#2853)	CPT Novak
2878	40% PFPE	40.0%		Surfactant - Light (10%, ICD#2853)	Ausimont
2879	45% PFPE	45.0%	Canadian Decon Solution (AUG 11, 1990 Sample) (10%)		Braue
2880	50% PFPE	50.0%	Note: 50% F5A (Lot#710546); 50% Y25 (Lot#VT250)		Braue
2881	50% PFPE	50.0%	Note: 50% F5A (Lot#480324); 50% Y25 (Lot#VT250)		Braue
2882	50% PFPE	50.0%	Note: 50% F5A (Lot#450230); 50% Y25 (Lot#VT250)		Braue
2883	50% PFPE	50.0%	Note: 50% F5A (Lot#630439); 50% Y25 (Lot#VT250)		Braue
2884	40% PFPE	40.0%	2,3 Naphthacyanine (10%)	Surfactant - Light (10%, ICD#2853)	CPT Novak
2885	40% PFPE	40.0%	Iodobenzene Diacetate (10%)	Surfactant - Light (10%, ICD#2853)	Aldrich
2886	40% PFPE	40.0%	Poly (Bisphenol A carbonate)	Surfactant - Light (10%, ICD#2853)	Aldrich
2887	49.5% Surfactant - Light (ICD#2853)	49.5%		1% Water	MAJ Weir
2888	47.5% Surfactant - Light (ICD#2853)	47.5%		5% Water	MAJ Weir
2889	49.5% Surfactant - Light (ICD#2853)	49.5%	1% 1.25m Potassium (2,3 Butanedione monoximate)		CPT Novak
2890	47.5% Surfactant -	47.5%	5% 1.25m Potassium (2,3 Butanedione monoximate)		CPT Novak

ICD #	Percent Base Oil (PFPE = Y25)	Percent Teflon (PTFE = F5A)	Compound (% , ICD#, if any)	Other added compounds (% , ICD# if any)	PI/Supplier
	Light (ICD#2853)				
2891	45% Surfactant - Light (ICD#2853)	45.0%	10% 1.25m Potassium (2,3 Butanedione monoximate)		CPT Novak
2892	40% Surfactant - Light (ICD#2853)	40.0%	10% 1.25m Potassium (2,3 Butanedione monoximate)	10% Water	CPT Novak
2893	47.5% Surfactant - Light (ICD#2853)	47.5%	5% 1.25m solution of 2,3 Butanedione monoxime		CPT Novak
2894	Syderma		2,3 Butanedione Monoxime (1%)		CPT Novak
2895	Syderma		2,3 Butanedione Monoxime (5%)		CPT Novak
2896	Syderma		2,3 Butanedione Monoxime (10%)		CPT Novak
2897	50% PFPE	50.0%	Note: 50% F5A (Lot#630439); 50% Y25 (Lot#VT590)		Braue
2898	50% PFPE	50.0%	Note: 50% Y25 (Lot#VT590); 50% F5A (Lot#480324)		Braue
2899	50% PFPE	50.0%	Note: 50% Y25 (Lot#VT590); 50% F5A (Lot#450230)		Braue
2900	50% PFPE	50.0%	Note: 50% Y25 (Lot#VT590); 50% F5A (Lot#710546)		Braue
2901	50% PFPE	50.0%	Note: 50% Y25 (Lot#VT590); 50% F5A (Lot#710546 (Thermally Treated)		Braue
2902	50% PFPE	50.0%	Iodobenzene Diacetate (ICD#3254, 9.99%)	9.99% ICD#2853 (light surfactant)	Aldrich
2904	Syderma (ICD#2859)	0.0%	1.25 m basic Butanedione (10%)	KOH	CPT Novak
2905	40% Surfactant-light (ICD#2853)	40.0%	Iodobenzene diacetate (10%), 1.25m basic Butanedione (10%)		Aldrich
2906	45% Surfactant - Heavy (ICD#2855)	45.0%		10% Water	Ausimont

ICD #	Percent Base Oil (PFPE = Y25)	Percent Teflon (PTFE = F5A)	Compound (% , ICD#, if any)	Other added compounds (% , ICD# if any)	PI/Supplier
2907	45% Surfactant - Medium (ICD#2854)	45.0%		10% Water	Ausimont
2908	Syderma (ICD#2859)		Sucrose (10%)		Syderma
2909	40% Surfactant - Light (ICD#2853)	40.0%	Sucrose (10%)	10% Water	Ausimont
2910	Syderma (ICD#2859)		Heptane Sulfonic acid (10%)		Syderma
2911	40% Surfactant - Light (ICD#2853)	40.0%	Heptane Sulfonic acid (10%)	10% Water	Aldrich
2912	Syderma (ICD#2859)		Adenosine Triphosphate (10%)		Syderma
2913	45% Surfactant - Light (ICD#2853)	45.0%	Adenosine Triphosphate (10%)		Aldrich
2914	50% PFPE	50.0%	Note: 50% Y25 (Lot#VT590); 50% F5A (Lot#480324)		Braue
2915	50% PFPE	50.0%	Note: 50% Y25 (Lot#VT590); 50% F5A (Lot#480324)		Braue
2916	100% PFPE		Note: 100% Fomblin Y25 (Lot#VT590)		Braue
2917		100.0%	Note: 100% Polymist Teflon F5A (Lot#480324)		Braue
2918	Foam Glove				Braue
2919	40% Surfactant - Light (ICD#2853)	40.0%		20% Water	Ausimont
2920	40% Surfactant - Medium (ICD#2854)	40.0%		20% Water	Ausimont
2921	40% Surfactant - Heavy (ICD#2855)	40.0%		20% Water	Ausimont
2924		100.0%	Note: 100% Polymist Teflon F5A (Lot#6N0522)		Ausimont

ICD #	Percent Base Oil (PFPE = Y25)	Percent Teflon (PTFE = F5A)	Compound (% , ICD#, if any)	Other added compounds (% , ICD# if any)	PI/Supplier
2925		100.0%	Note: 100% Polymist Teflon F5A (Lot#730526)		Ausimont
2926	50% PFPE	50.0%	Note: 50% Y25 (Lot#VT590); 50% F5A (Lot#480324)		Braue
2927	50% PFPE	50.0%	Note: 50% Y25 (Lot#VT590); 50% F5A (Lot#480324)		Braue
2928	50% PFPE	50.0%	Note: 50% Y25 (Lot#VT590); 50% F5A (Lot#480324)		Braue
2929	50% PFPE	50.0%	Note: 50% Y25 (Lot#VT590); 50% F5A (Lot#480324)		Braue
2930	50% PFPE	50.0%	Note: 50% Y25 (Lot#VT590); 50% F5A (Lot#480324)		Braue
2931	50% PFPE	50.0%	Note: 50% Y25 (Lot#VT590); 50% F5A (Lot#480324)		Braue
2932	50% PFPE	50.0%	Note: 50% Y25 (Lot#VT590); 50% F5A (Lot#480324)		Braue
2933	50% PFPE	50.0%	Note: 50% Y25 (Lot#VT590); 50% F5A (Lot#480324)		Braue
2936	40% Surfactant - Light (ICD#2853)	40.0%	DNA from Herring Test	10% Water	CPT Novak
2937	40% Surfactant - Light (ICD#2853)	40.0%	DNA from Salmon Test	10% Water	CPT Novak
2944	40% Surfactant - Light (ICD#2853)	40.0%	TiFeMn(Fine) (10%, ICD#2939)	10% ICD#2289 base cream	Mainstream
2945	35% Surfactant - Light (ICD#2853)	35.0%	TiFeMn(Fine) (10%, ICD#2939)	10% Water, 10% ICD#2289 base	Mainstream
2946	SPF 15 PABA free, water proof Sunblock		Vitamin E	Aloe	Arroyo
2947	SPF 15 Sweatproof, waterproof, UVA/UVB				Braue

ICD #	Percent Base Oil (PFPE = Y25)	Percent Teflon (PTFE = F5A)	Compound (% , ICD#, if any)	Other added compounds (% , ICD# if any)	PI/Supplier
	Sunblook, Active				
2948	40% Surfactant - Light (ICD#2853)	40.0%	CaNi-8(fine) CaNi ₅ H ₃ + perfluoropropene reaction product coating (10%, 2940)	10% ICD#2289 Mix	Mainstream
2949	35% Surfactant - Light (ICD#2853)	35.0%	CaNi-8(fine) CaNi ₅ H ₃ + perfluoropropene reaction product coating (10%, 2940)	10% ICD#2289 Mix, 10% Water	Mainstream
2950	40% Surfactant - Light (ICD#2853)	40.0%	CaNi-H(fine), CaNi ₅ H ₃ powder (10%, 2941)	10% ICD#2289 mix	Mainstream
2951	40% Surfactant - Light (ICD#2853)	40.0%	DLC 8(fine), Mg ₂ NiH ₂ + propylene glycol butyl ether (10%, 2942)	10% ICD#2289 mix	Mainstream
2952	35% Surfactant - Light (ICD#2853)	35.0%	DLC 8(fine), Mg ₂ NiH ₂ + propylene glycol butyl ether (10%, 2942)	10% ICD#2289 Mix, 10% Water	Mainstream
2953	60% Surfactant - Light (ICD#2853)	30.0%	MgNi(fine) slightly hydrided Mg ₂ Ni powder (10%, 2943)		Mainstream
2954	50% Surfactant - Light (ICD#2853)	40.0%	MgNi(fine) slightly hydrided Mg ₂ Ni powder (10%, 2943)		Mainstream
2956	50% 2916	50% 2917	50% 2916 (rec'd 4-Mar-97); 50% 2917 (rec'd 4-Mar-97)		Braue
2957	50% 2916	50% 2917	50% 2916 (rec'd 4-Mar-97); 50% 2917 (rec'd 4-Mar-97)		Braue
2958	50% 2916	50% 2917	50% 2916 (rec'd 4-Mar-97); 50% 2917 (rec'd 9-May-97)		Braue
2959	100% PFPE		Note: 100% Fomblin Y25 (Lot#0306RG)		Ausimont
2960	100% PFPE		Note: 100% Fomblin Y25 (Lot#1419RG)		Ausimont
2961	50% 2916	50% 2917	50% 2916 (rec'd 4-Mar-97); 50% 2917 (rec'd 9-May-97)		Braue
2962			Nanocrystalline MgO		Braue

ICD #	Percent Base Oil (PFPE = Y25)	Percent Teflon (PTFE = F5A)	Compound (% , ICD#, if any)	Other added compounds (% , ICD# if any)	PI/Supplier
2963			Zinc Oxide		Braue
2972	90% 2916		S-330 (10%)		Monsanto
2984			HBR technologies "BASE" compound		HBR Technologies
2985	66% 2984		Butanol (33%)		Aldrich
2986	98% 2984		Hydroxylamine (2%)		Aldrich
2987	99% 2984		Zinc chloride (10 mM)		Aldrich
2988	99% 2984		2-pyridine Aldoxime Methchloride (15mg/ml)		Aldrich
2989	99% 2984		2-pyridine Aldoxime Methchloride (15mg/ml)	Zinc chloride (10 mM)	Aldrich
2991			TSP001-0298		McKesson
2992			TSP002-0298		McKesson
2993			TSP003-0298		McKesson
2994			Permethrin Technical 91.6%		Gharda Chemicals Limited
3003			TSP004		McKesson
3004			TSP005		McKesson
3005			TSP006		McKesson
3051	95% 2289		$K_5Co(III)W_{12}O_4$		Hill, Emory U
3053			$K_6 Co_{II} W_{12} O_{40}$		Hill, Emory U
3056	90% 1511		HTH (10%)		Aldrich
3057	50% Fomblin Y25 (ICD#2960)	20.0%	HTH (10%)	10% Surfactant - Light (ICD#2853), 10% Water	Aldrich
3058	50% Fomblin Y25 (ICD#2960)	20.0%	HTH (10%)	10% Surfactant - Light (ICD#2853), 10% Water	Aldrich
3059	90% 1511		Chloramine T (10%)		Aldrich

ICD #	Percent Base Oil (PFPE = Y25)	Percent Teflon (PTFE = F5A)	Compound (% , ICD#, if any)	Other added compounds (% , ICD# if any)	PI/Supplier
3060	90% 1511		Chloramine B (10%)		Aldrich
3061	50% Fomblin Y25 (ICD#2916)	20.0%	Lyophilized OPAH enzyme (10%)	10% Surfactant - Light (ICD#2853), 10% Water	Broomfield
3064			Cetearyl Alcohol		Braue
3065			Cetyl Stearyl Alcohol		Braue
3066			PEG-82 Glyceryl Monotallowate		Braue
3067			PEG-82 Glyceryl Monotallowate		Braue
3068			N,N-diethyl-m-toluamide; product code #207320		Braue
3069			Diazolidinyl Urea		Braue
3070			Polyoxyethylene 400		Braue
3071			Glycereth-7		Braue
3072			Smectite Clay		Braue
3073			Prop Glycol Dicaprylate/dicaprate; batch #64117		Braue
3074			Lexemul AS; batch #63111		Braue
3075			Silicon Dioxide Crystalline Free		Braue
3076			Hydroxyethylcellulose		Braue
3077			R12-100 RY92398 Dendritic polymer w/trisubstituted ethanolamine component		Yin, ARL
3107	50% Fomblin y25 (ICD#2916)	40.0%	MgNi(fine) slightly hydrided Mg ₂ Ni powder (10%, 2943)		Mainstream
3108	50% Fomblin y25 (ICD#2916)	40.0%	DLC 8(fine), Mg ₂ NiH ₂ + Propylene Glycol Butyl Ether (10%, 2942)		Mainstream
3109	50% Fomblin y25 (ICD#2916)	40.0%	TiFeMn(Fine) with Methylmethacrylate (10%, 2938)		Mainstream
3109	49.9% Fomblin y25 (ICD#2959)	40.0%	TiFeMn(Fine) with Methylmethacrylate (9.99%, 2938)		Mainstream

ICD #	Percent Base Oil (PFPE = Y25)	Percent Teflon (PTFE = F5A)	Compound (% , ICD#, if any)	Other added compounds (% , ICD# if any)	PI/Supplier
3110	50% Fomblin y25 (ICD#2916)	40.0%	CaNi-8(fine) CaNi ₅ H ₃ + Perfluoropropene Reaction Product Coating (10%, 2940)		Mainstream
3111	50% Fomblin y25 (ICD#2916)	40.0%	TiFeMn(Fine) (10%, 2939)		Mainstream
3112	50% Fomblin y25 (ICD#2916)	40.0%	CaNi-H(fine), CaNi ₅ H ₃ powder (10%, 2941)		Mainstream
3113	50% Fomblin y25 (ICD#2916)	40.0%	Nanocrystalline MgO (10%, 2962)		Nantek
3114	50% Fomblin y25 (ICD#2916)	40.0%	Zinc oxide (10%, 2963)		Nantek
3115	50% Fomblin y25 (ICD#2916)	40.0%	K ₅ Co(III)W ₁₂ O ₄₀ (ICD#3481, 10%)		Hill, Emory U
3116	90% ICD#2289		RY92398 Dendritic Polymer with Ethanolamine Active Component (2%, ICD#3077)	8% Water	Yin, ARL
3119			4.12% #3073; 3.86% #3071; 3.76% #3063; 3.76% #3065; 2.82% #3066; 2.80% #3075; 2.65% #3074; 1.67% #3070; 1.20% #3072; 1.11% #3067; 0.85% #3076; 0.41% #3069	70.98% Water	Braue
3121	40% 2289	40.0%	30 wt% Aqueous Solution of RY92398 Dendritic Polymer with Ethanolamine Active Component (20%, ICD#3077)		Yin, ARL
3122			from MAJ Vessley		MAJ Vessley
3123			98% Hexadecyl Hexadecanote		Braue
3124	45.0%	45.0%	Dendritic Polymer (2%, 3077)		Yin, ARL
3125			4.07% #3073; 3.82% #3071; 3.72% #3063; 3.72% #3065; 2.79% #3066; 2.77% #3075; 2.62% #3074; 1.66% #3070; 1.18% #3072;	70.20% Water	Braue

ICD #	Percent Base Oil (PFPE = Y25)	Percent Teflon (PTFE = F5A)	Compound (% , ICD#, if any)	Other added compounds (% , ICD# if any)	PI/Supplier
			1.10% #3067; 0.85% #3076; 0.41% #3069; 1.10% #3123		
3126	40.0%	40.0%	Dendretic Polymer (3077, 2.00%)	Water (18.0%)	Yin, ARL
3127	62.0%	31.0% (ICD#2478)	MgO Nanoparticles from Nantek (7.00%, ICD#2962)		Nantek
3128	62.0%	31.0% (ICD#2478)	ZnO Nanoparticles from Nantek (7.00%, ICD#2963)		Nantek
3129	50% Fomblin y25 (ICD#2916)	40% 2917	10% ICD3293 (XE555, M291 SDK resin)		Braue
3148			Copolymer 25% VBC; 75% 2-ethylhexyl methacrylate; TMA quaternized; solid content: 0.0691 g/ml;[N+]=0.1117M IBA		Oklahoma State Univ
3149	45.5%	45.5%	(ICD#2289, 9%)		Braue
3150	40.0%	30.0%	10% ICD3293 (XE555, M291 SDK resin)	Water(10%), 2853 (10%)	USAMRICD
3151	62.5%	30.0%	7.5% ICD3293 (XE555, M291 SDK resin)		USAMRICD
3151	62.6%	29.9%	7.5% ICD3293 (XE555, M291 SDK resin)		USAMRICD
3152	50% 2289	45.0%	HPV ₂ W ₁₀ O ₄₀ POM (5%, ICD #3154)		Hill, Emory U
3153	50.0%	45.0%	HPV ₂ MoO ₄₀ x Water (ICD#3155, 5%)		Hill, Emory U
3154			HPV ₂ W ₁₀ O ₄₀ x Water		Hill, Emory U
3155			HPV ₂ Mo ₁₀ O ₄₀ x Water		Hill, Emory U
3156	45.0%	45.0%	Dendretic Polymer (3077, 1%)	Water (9%)	Yin, ARL
3157	45.0%	45.0%	Dendretic Polymer (3077, 0.5%)	Water (9.5%)	Yin, ARL
3158	45.0%	45.0%	Dendretic Polymer (3077, 0.1%)	Water (9.9%)	Yin, ARL
3159	45.0%	45.0%	Dendretic Polymer (3077, 0.1%)	Water (9.9%)	Yin, ARL
3167			60% PhB/40% MP		Shea, UCI Berkley

ICD #	Percent Base Oil (PFPE = Y25)	Percent Teflon (PTFE = F5A)	Compound (% , ICD#, if any)	Other added compounds (% , ICD# if any)	PI/Supplier
3168			60% PhB/40% DS		Shea, UCI Berkley
3169			0.0025 M Methylnicotinate	Water	Braue
3170			0.25 M Methylnicotinate	Water	Braue
3171			Methylnicotinate 99% (M5,920-3 [93-60-7])		Braue
3172	57.8%	38.1%	Polysilsesquioxane with 40% MPTES (SH groups) incorporated (ICD#3167, 4.08%)		Shea, UCI Berkley
3173	58.0%	38.0%	Polysilsesquioxane with 60% MPTES (SH groups) incorporated (ICD#3301, 4.06%)		Shea, UCI Berkley
3189	58.2%	38.0%	Polysilsesquioxane with 80% MPTES (SH groups) incorporated (ICD#3302, 3.83%)		Shea, UCI Berkley
3190	57.6%	37.9%	polysilsesquioxane with 40% TESDS (SS groups) incorporated (ICD#3168, 4.48%)		Shea, UCI Berkley
3191	58.0%	37.8%	Polysilsesquioxane with 60% TESDS (SS groups) incorporated (ICD#3303, 4.20%)		Shea, UCI Berkley
3192	58.2%	37.9%	Polysilsesquioxane with 80% TESDS (SS groups) incorporated (ICD#3304, 3.92%)		Shea, UCI Berkley
3200	50.0%	40.0%	Dendritic Polymer (ICD#3077, 1%); S330 (ICD#2703, 5%)	Water (4%)	Yin, ARL
3201	50.0%	40.0%	OPAA Dried Enzyme (10%)		Broomfield
3202	50.0%	35.0%	OPAA Dried Enzyme (5%)	ICD#2853 (5%), Water (5%)	Broomfield
3203	50.0%	40.0%	OPAA Dried Enzyme (5%)	ICD#2853 (5%)	Broomfield
3204	50.0%	40.0%	OPAA Wet Enzyme (10%, ICD)		Broomfield
3205	50.0%	35.0%	OPAA Wet Enzyme (5%, ICD)	ICD#2853 (5%), Water (5%)	Broomfield
3206	50.0%	40.0%	OPAA Wet Enzyme (5%, ICD)	ICD#2853 (5%)	Broomfield

ICD #	Percent Base Oil (PFPE = Y25)	Percent Teflon (PTFE = F5A)	Compound (% , ICD#, if any)	Other added compounds (% , ICD# if any)	PI/Supplier
3207	50.0%	40.0%	OPAA Dried Enzyme (5%)	Water (5%)	Broomfield
3209	45.0%	30.0%	OPAA Dried Enzyme (5%)	ICD#2853 (10%), Water (10%)	Broomfield
3210	35.0%	30.0%	OPAA Dried Enzyme (5%)	ICD#2853 (15%), Water (15%)	Broomfield
3211	43.4%	43.4%	Dendretic Polymer (1.7%, 3077)	Water (15.6%)	Yin, ARL
3212			Dendretic Polymer w/perfluoroalkyl end groups 17F-PEOX 20/100		Yin, ARL
3213			Dendritic Polymer w/perfluoroaryl end groups 5F-PEOX 20/100		Yin, ARL
3214	47.3%	47.3%	Dendretic Polymer (0.540%, ICD#3077)	CuSO4 (0.0800%), Water (4.69%)	Yin, ARL
3215	46.7%	46.7%	Dendretic Polymer with perfluoroalkyl endgroup (1.33%, ICD#3212)	Water (5.33%)	Yin, ARL
3216	46.5%	46.5%	Dendretic Polymer with perfluoroaryl endgroup (1.40%, ICD#3213)	Water (5.59%)	Yin, ARL
3217	45.0%	45.0%	Dendretic Polymer (1.49%, ICD#3077)	CuSO4 (0.0500%), Water (8.50%)	Yin, ARL
3218	40.0%	40.0%	Dendretic Polymer (10.0%, ICD#3077)	Water (10.0%)	Yin, ARL
3219	44.3%	44.3%	Dendretic Polymer with perfluoroaryl endgroup (1.41%, ICD#3213)	CuSO4 (0.880%), Water (9.17%)	Yin, ARL
3220	47.2%	47.2%	Dendretic Polymer with perfluoroalkyl endgroup (0.749%, ICD#3212)	CuSO4 (0.375%), Water (4.49%)	Yin, ARL
3222			2% O-Iodosobenzoate anion; 5% Latex Copolymer (75% butyl methacrylate; 25% chloromethylstyrene)		Braue
3223			O-iodosobenzoate anion w/latex copolymer (14.3%, ICD #3222); 71.4%, ICD#3004	Light surfactant - ICD#2853 (14.3%)	Braue
3224			Triosyn T50 Beads		
3225			Triosyn T40 Beads		
3226			Triosyn T50 Fragments		

ICD #	Percent Base Oil (PFPE = Y25)	Percent Teflon (PTFE = F5A)	Compound (% , ICD#, if any)	Other added compounds (% , ICD# if any)	PI/Supplier
3227	51.1%	38.0%	Dendretic Polymer with Perfluoralkyl endgroup (1.30%, ICD#3212), S330 (ICD 2703, 4.35%)	Water (5.22%)	Yin, ARL
3236	45.1%	45.6%	Iodine releasing polymer (4.56%, ICD#3226)	Water (4.78%)	Biotech
3237	45.0%	42.5%	Iodine releasing polymer (10.0%, ICD#3226)	Water (2.50%)	Biotech
3238			Dendretic Polymer with Perfluoralkyl endgroup		Yin, ARL
3241			Dendretic Polymer with Perfluoraryl endgroup		Yin, ARL
3244	55.0%	30.0%	Dendretic Polymer with Perfluoroaryl endgroup (0.999%, ICD#3213), S330 (10.0%, ICD#2703)	Water (3.99%)	Yin, ARL
3245	55.0%	30.0%	Dendretic Polymer with Perfluoroalkyl Endgroup (1.02%, ICD#3212), S330 (9.985%, ICD#2703)	Water (4.07%)	Yin, ARL
3246	46.7%	46.7%	Dendretic Polymer (1.33%, ICD#3077)	Water (5.31%)	Yin, ARL
3247	46.7%	46.7%	Dendretic Polymer with Perfluoralkyl endgroup (1.33%, ICD# 3241)	Water (5.31%)	Yin, ARL
3248	46.7%	46.7%	Dendretic Polymer with Perfluoroaryl endgroup (1.33%, ICD# 3238)	Water (5.31%)	Yin, ARL
3249	54.9%	30.1%	Dendretic Polymer with Perfluoroaryl endgroup (0.998%, ICD# 3241), S330 (10.0%, ICD 2703)	Water (3.99%)	Yin, ARL
3250	54.9%	30.0%	Dendretic Polymer with Perfluoroaryl endgroup (1.00%, ICD# 3238), S330 (10.0%, ICD 2703)	Water (4.00%)	Yin, ARL
3251	50.0%	36.4%	(9.09% ICD#3254) Iodobenzendiacetate (0.909% ICD#3077)	Water (3.64%)	Yin, ARL
3252	50.0%	36.3%	(9.07% ICD#3254) Iodobenzendiacetate (0.926% ICD#3238)	Water (3.70%)	Yin, ARL
3253	50.0%	36.4%	Dendretic Polymer with Perfluoroaryl endgroup (ICD#3241, 0.911%), IBDA (ICD 3254, 8.9%)	Water (3.64%)	Yin, ARL
3254			Iodobenzene Diacetate (98%) C6H5I(O2CCH3)2 Aldrich Chemical		Aldrich

ICD #	Percent Base Oil (PFPE = Y25)	Percent Teflon (PTFE = F5A)	Compound (% , ICD#, if any)	Other added compounds (% , ICD# if any)	PI/Supplier
			Company Lot#01008MQ CAT#17872-1		
3258			3+M1 (ZrNi0.95M0.05 + Methyl Methacrylate)		Mainstream
3259			A3+M3 (ZrNi0.95M0.05 + 2(dimethylamino)ethyl methacrylate)		Mainstream
3265	47.2%	42.5%	A1+M1 (TiFe0.9Mn0.1 + Methyl Methacrylate) (9.33%, ICD#3257)	Water (1.00%)	Mainstream
3266	47.1%	42.3%	A3+M1 (ZrNi0.95M0.05 + Methyl Methacrylate) (9.67%, ICD#3258)	Water (0.996%)	Mainstream
3267	46.5%	42.4%	A3+M3 (ZrNi0.95M0.05 + 2(dimethylamino)ethyl methacrylate)(10.1%, ICD#3259)	Water (1.00%)	Mainstream
3268	46.8%	42.6%	A1 + M4 (TiFe0.9Mn0.1 + Styrene) (9.53%, ICD#3264)	Water (1.09%)	Mainstream
3269		100.0%	Note: Teflon Powder F5A; Lot#730562		Ausimont
3270	47.7%	46.0%	5F-PZOX 20/100, Protected Dendretic Polymer with Perfluoroaryl endgroup (1.31% ICD#3242)	Water (5.23%)	Yin, ARL
3271	46.6%	46.6%	5F-PZOX 20/100, Deprotected Dendretic Polymer with Perfluoroaryl endgroup (1.40% ICD#3243)	Water (5.46%)	Yin, ARL
3272	46.7%	46.7%	17F-PZOX 20/100, Deprotected Dendretic Polymer with Perfluoroalkyl endgroup (1.33% ICD#3240)	Water (5.33%)	Yin, ARL
3273	46.7%	46.7%	17F-PZOX 20/100, Protected Dendretic Polymer with Perfluoroaryl endgroup (1.33% ICD#3239)	Water (5.33%)	Yin, ARL
3274			K ₇ PW ₁₀ Ti ₂ O ₄₀		Eltron
3275			H ₅ PMo ₁₀ V ₂ O ₄₀		Eltron
3276			H ₅ PV ₂ Mo ₁₀ O ₄₀		Eltron

ICD #	Percent Base Oil (PFPE = Y25)	Percent Teflon (PTFE = F5A)	Compound (% , ICD#, if any)	Other added compounds (% , ICD# if any)	PI/Supplier
3277	49.0%	49.0%	K ₇ PW ₁₀ Ti ₂ O ₄₀ , x water; (2.00%, ICD#3274)		Eltron
3278	48.0%	48.0%	H ₂ PV ₂ Mo ₁₀ O ₄₀ , x water; (4.00%, ICD#3275)		Eltron
3279	43.2%	43.2%	K ₅ Co(III)W ₁₀ O ₄₀ , (ICD#3281, 13.5%)		Hill, Emory U
3280	47.6%	47.6%	H ₅ PV ₂ Mo ₁₀ O ₄₀ on CeO ₂ (4.75%, ICD#3276)		Eltron
3281			Liqui-Char-Vet Aqueous Suspension Activated Charcoal, USP		WRAIR
3284	54.0%	36.0%	IBA, 10%		Aldrich
3289	44.0%	44.0%	Dendretic Polymer (ICD#3077, 1.95%)	Water (7.80%), Na ₂ CO ₃ (2.44%)	Yin, ARL
3290	42.9%	42.8%	Dendretic Polymer with Perfluoroaryl endgroup (ICD#3241, 1.92%)	Water (7.68%), Na ₂ CO ₃ (4.75%)	Yin, ARL
3291	43.1%	42.3%	Dendretic Polymer with Perfluoroaryl endgroup (ICD#3238, 1.99%)	Water (7.95%), Na ₂ CO ₃ (4.69%)	Yin, ARL
3292	42.6%	42.8%		Water (9.84%), Na ₂ CO ₃ (4.75%)	Aldrich
3293			XE555 (M291 SDK Resin)		Rohm and Haas
3294	49.6%	40.2%	A1+M1 (TiFe0.9Mn0.1 + Methyl Methacrylate) (10.3%, ICD#3257)		Mainstream
3295	49.8%	41.0%	A1 + M4 (TiFe0.9Mn0.1 + Styrene) (9.21%, ICD#3264)		Mainstream
3296	49.8%	40.2%	A3+M1 (ZrNi0.95M0.05 + Methyl Methacrylate) (10.0%, ICD#3258)	.	Mainstream
3297	50.0%	39.9%	A3+M3 (ZrNi0.95M0.05 + 2(dimethylamino)ethyl methacrylate)(10.2%, ICD#3259)		Mainstream
3298			K ₅ Co(III) ₁₂ O ₄₀		Hill, Emory U
3299	74.8% base cream (ICD#3004)		Dendretic Polymer with Perfluoroaryl endgroup (ICD#3241, 0.998%), IBDA (ICD#3254, 9.98%)	Light Surfactant (10.2% 2853), Water (3.99%)	Yin, ARL
3300	53.2%	34.0%	Dendretic Polymer with Perfluoroaryl endgroup (ICD#3238, 0.851%), ICD3293 (XE555, M291 SDK resin, 8.5%)	Water (3.40%)	Yin, ARL

ICD #	Percent Base Oil (PFPE = Y25)	Percent Teflon (PTFE = F5A)	Compound (% , ICD#, if any)	Other added compounds (% , ICD# if any)	PI/Supplier
3301			40% PhB/60% MP		Shea, UCI Berkley
3302			20% PhB/80% MP		Shea, UCI Berkley
3303			40% PhB/60% DS		Shea, UCI Berkley
3304			20% PhB/80% DS		Shea, UCI Berkley
3305	57.3%	40.0%	Polysilsesquioxane containing 60% PhB/40% MPTES (ICD#3167, 2.65%)		Shea, UCI Berkley
3306			Trivorex		
3308	54.0%	37.5%	10% w/w H ₅ PV ₂ Mo ₁₀ O ₄₀ on Activated Carbon (ICD#3275, 8.50%)	Activated Carbon Darco G-60 70-230 mesh, 60 A	CPT Hobson (new prep)
3309	50.0%	40.5%	Trivorex (ICD#3306, 9.57%)		Trivorex
3310	95.1%	0.0%	S-330 (ICD#2703, 4.87%)		Monsanto
3311	94.4%	0.0%	XE555, M291 SDK resin (ICD3293 , 5.6%)		Braue
3312	93.5%	0.0%	DP (ICD#3077, 1.30%)	Water (5.21%)	Yin, ARL
3313	93.5%	0.0%	DP w/Perfluoroalkyl (ICD#3238, 1.31%)	Water (5.23%)	Yin, ARL
3314	96.4%	0.0%	Polysilsesquioxane with Alkylthiol (3.55%, ICD#3167)		Shea, U CA Berkley
3315	79.9%	0.0%	Iodobenzene Diacetate (10.0%, ICD#3254)	Light surfactant (10.1% ICD#2853)	Aldrich
3316	95.0%	0.0%	H ₅ PV ₂ Mo ₁₀ O ₄₀ (5.03%, ICD#3275)		Eltron
3317	90.1%	0.0%	Ti/Mn Alloy (9.93%, ICD#2157)		Mainstream
3318	93.5%	0.0%	Dendritic Polymer w/Perfluoroaryl (ICD#3241, 1.30%)	Water (5.21%)	Yin, ARL
3319	?	?	73% Perfluoroalkylether; 18% PTFE	received from METTS	METTS
3320	49.2%	49.7%	H ₅ PV ₂ Mo ₁₀ O ₄₀ (1.14%, ICD#3275)		Eltron
3321	53.8%	37.5%	Activated Carbon (8.75%)		CPT Hobson (new prep)

ICD #	Percent Base Oil (PFPE = Y25)	Percent Teflon (PTFE = F5A)	Compound (% , ICD#, if any)	Other added compounds (% , ICD# if any)	PI/Supplier
3322			Activated Carbon (DARCO G-60, 100 Mesh)		CPT Hobson
3323			CLECS		Altus
3327				Antigas No. 7 Lot#ZA270899	Porton Down
3328	45.7%	45.7%	5% MgO		Nantek
3329	47.5%	47.5%	5% ZnO		Nantek
3330	48.8%	48.8%	2.5% CaO		Nantek
3331	45.7%	45.7%	5% TiO		Nantek
3332	49.0%	49.0%	2% MgO		Nantek
3333	49.0%	49.0%	2% ZnO		Nantek
3334	49.0%	49.0%	2% CaO		Nantek
3335	48.8%	48.8%	2.5% MgO		Nantek
3336	52.0%	40.0%	OPAA Crystals (1%)	Polyethylene oxide (300K), Glycodeoxycholic acid sodium salt, polyvinyl alcohol (water content 7.1%), Tyloxapol, isopropanol, 20 mM HEPES pH 7.2 and Tris(2-carboxyethyl)phosphine hydrochloride	Altus
3337	52.0%	40.0%	OPAA Crystals (1%)	Polyethylene oxide (100K), Glycodeoxycholic acid sodium salt, polyvinyl alcohol (water content 8.2%), Tyloxapol, isopropanol, 20 mM HEPES pH 7.2 and Tris(2-carboxyethyl)phosphine hydrochloride	Altus

ICD #	Percent Base Oil (PFPE = Y25)	Percent Teflon (PTFE = F5A)	Compound (% , ICD#, if any)	Other added compounds (% , ICD# if any)	PI/Supplier
3338	52.0%	40.0%	OPAA Crystals (1%)	Glycodeoxycholic acid sodium salt, Polyvinyl alcohol (water content 7.7%), Tyloxapol, isopropanol, 20 mM HEPES pH 7.2 and Tris(2-carboxyethyl)phosphine hydrochloride	Altus
3339	52.0%	40.0%	OPAA Crystals (1%)	Polyethylene oxide (100K), Glycodeoxycholic acid sodium salt (water content 7.7%), Tyloxapol, isopropanol, 20 mM HEPES pH 7.2 and Tris(2-carboxyethyl)phosphine hydrochloride	Altus
3340	52.0%	40.0%	OPAA CLEC (1%)	Polyethylene oxide (100K), Glycodeoxycholic acid sodium salt, (water content 23.26%), Tyloxapol, isopropanol, 20 mM HEPES pH 7.2 and Tris(2-carboxyethyl)phosphine hydrochloride	Altus
3341			Polymer 5F-PZOX/PEI 100-20 + Quat (100%)		CPT Hobson
3342			Polymer 5F-PZOX/PEI 100-20 + Quat (50%) + G (50%)		CPT Hobson
3343			Polymer 5F-PZOX/PEI 100-20 + G (100%)		CPT Hobson
3344			Polymer 17F-PZOX/PEI 100-20 + G (100%)		CPT Hobson
3345			Polymer C12-PZOX/PEI 100-20 + Q (100%)		CPT Hobson
3346			Polymer C12-PZOX/PEI 100-20 + G (50%) + Q (50%)		CPT Hobson

ICD #	Percent Base Oil (PFPE = Y25)	Percent Teflon (PTFE = F5A)	Compound (% , ICD#, if any)	Other added compounds (% , ICD# if any)	PI/Supplier
3347	47.7%	45.8%	New Dendritic Polymer with Perfluoroaryl endgroup (1.30% ICD#3343)	Water (5.21%)	Yin, ARL
3348	47.7%	45.8%	New Dendritic Polymer with Perfluoroaryl endgroup (1.33% ICD#3344)	Water (5.31%)	Yin, ARL
3349	55.0%	30.0%	New Dendritic Polymer with Perfluoroaryl endgroup (1.00% ICD#3343), S330 (10.0%, ICD 2703)	Water (4.00%)	Yin, ARL
3350	55.5%	29.7%	New Dendritic Polymer with Perfluoroaryl endgroup (0.9899% ICD#3342), S330 (9.899%, ICD#2703)	Water (3.96%)	Yin, ARL
3351			Nanocrystalline CaO		CPT Hobson
3352			Nanocrystalline MgO		CPT Hobson
3353	47.5%	47.5%	[NaPOM]TiO ₂ (5%)		Nantek
3354	54.2%	35.6%	S-330 (9.95%, ICD#2703)		CPT Hobson (new prep)
3358	60.4%	35.0%	TSR10/M Catalyst (aq) (1.6%)	Light Surfactant (ICD#2853, 3.0 %)	Biopraxis
3359	62.4%	35.8%	TF01/F Catalyst (dry/air), (1.8%)		Biopraxis
3360	60.4%	35.0%	FSX01/M Catalyst (aq) (3.0%)	Light Surfactant (ICD#2853, 3.0 %)	Biopraxis
3361	62.5%	32.9%	MMO01/M Catalyst (aq) (1.6%)	Light Surfactant (ICD#2853, 3.1 %)	Biopraxis
3362	58.5%	35.6%	TSR05/M Catalyst (aq) (1.50%, ICD#3545)	Light Surfactant (ICD#2853, 4.40%)	Biopraxis
3363			53.4% Sucrose; 35.6% Polymer (C-18); 2.7% OPAA; 7.1% OPH; 1.2% Bistrispropane (BTP) Buffer		Braue
3364	46.5%	46.7%	Dendritic Polymer with C18 endgroup (1.34%, ICD#3077)	Water (5.37%)	Yin, ARL

ICD #	Percent Base Oil (PFPE = Y25)	Percent Teflon (PTFE = F5A)	Compound (% , ICD#, if any)	Other added compounds (% , ICD# if any)	PI/Supplier
3365	45.1%	44.9%	New Dendritic Polymer with Perfluoroalkyl endgroup (2.00% ICD#3344)	Water (8.00%)	Yin, ARL
3366	40.0%	40.0%	IBDA (10.0%, ICD 3254)	Light Surfactant (10.0%, ICD 2853)	Aldrich
3367	49.7%	40.5%	A1+M1 (TiFe0.9Mn0.1 + Methyl Methacrylate) (9.89%, ICD#3257)		Mainstream
3368	45.2%	45.0%	New Dendritic Polymer with Perfluoroaryl endgroup (1.95% ICD#3343)	Water (7.81%)	Yin, ARL
3369	43.8%	43.8%	New Dendritic Polymer with Perfluoroaryl endgroup and quat function (1.24%, ICD#3341)	Water (4.95%)	Yin, ARL
3370	43.8%	43.8%	New Dendritic Polymer with Perfluoroaryl endgroup and quat +EtAmine function (1.24%, ICD#3342)	Water (4.95%)	Yin, ARL
3371	44.1%	44.1%	New Dendritic Polymer with Perfluoroalkyl endgroup and quat function (1.18%, ICD#3345)	Water (4.74%)	Yin, ARL
3372	44.3%	44.3%	New Dendritic Polymer with Perfluoroaryl endgroup and quat +EtAmine function (1.14%, ICD#3346)	Water (4.55%)	Yin, ARL
3373			5% [TEA]AuCl ₂ by weight in 95% Cu(NO ₃) ₂		CPT Hobson
3374			10% [TEA]AuCl ₂ by weight in 90% Cu(NO ₃) ₂		CPT Hobson
3375			9.95% [TEA]AuCl ₂ by weight in 89.95% Cu(NO ₃) ₂ ; 0.05% DMSO		CPT Hobson
3376			20% [TEA]AuCl ₂ by weight in 80% Cu(NO ₃) ₂		CPT Hobson
3377	47.8%	47.7%	5% [TEA]AuCl ₂ by weight in 95% Cu(NO ₃) ₂ : (ICD#3373, 4.50%)		Hill, Emory
3378	47.3%	47.4%	10% [TEA]AuCl ₂ by weight in 90% Cu(NO ₃) ₂ : (ICD#3374, 5.23%)		Hill, Emory

ICD #	Percent Base Oil (PFPE = Y25)	Percent Teflon (PTFE = F5A)	Compound (% , ICD#, if any)	Other added compounds (% , ICD# if any)	PI/Supplier
3379	47.5%	47.2%	9.95% [TEA]AuCl ₂ by weight in 89.95% Cu(NO ₃) ₂ , 0.05% DMSO: (5.38% ICD#3375)		Hill, Emory
3380	47.5%	47.3%	20% [TEA]AuCl ₂ by weight in 80 % Cu(NO ₃) ₂ : (5.25%, ICD#3376)		Hill, Emory
3381	57.0%	30.0%	TMO01/M Catalyst (aq) (4.49%, ICD#3546)	Light Surfactant (ICD#2853, 8.53%)	Biopraxis
3447			Insect Repellent AI3-37220		Braue
3448	47.6%	45.2%	MgO (new) nanoparticles from Nantek (7.22%, ICD#3352)		Nantek
3449	61.1%	32.6%	AP-CaO (6.2%, 3351)		Nantek
3450	51.1%	43.6%	Phenyl bridged polysilsequioxane (5.34%)		Shea, UCI Berkley
3451	45.6%	44.5%	Dendritic Polymer with Perfluoroaryl (1.97%, ICD#3343)	7.91% Water	Yin, ARL
3452	45.8%	44.4%	Dendritic Polymer with Perfluoroaryl (3.88%, ICD#3343)	5.94% Water	Yin, ARL
3453	53.1%	40.6%	Dendritic Polymer with Perfluoroaryl (3.75%, ICD#3343)	2.50% Water	Yin, ARL
3453	53.0%	40.7%	Dendritic Polymer with Perfluoroaryl (3.81%, ICD#3343)	2.50% Water	Yin, ARL
3454	54.2%	37.5%	Dendritic Polymer with Perfluoroaryl (6.66%, ICD#3343)	1.67% Water	Yin, ARL
3454	53.9%	37.7%	Dendritic Polymer with Perfluoroaryl (6.71%, ICD#3343)	1.74% Water	Yin, ARL
3455	45.0%	45.0%	Dendritic Polymer with Perfluoroaryl (0.988%, ICD#3343)	7.99% Water; 1.03% ICD#2853	Yin, ARL
3456	45.4%	44.7%	Dendritic Polymer with Perfluoroaryl (3.00%, ICD#3343)	5.92% Water; 0.987% ICD#2853	Yin, ARL
3457	46.2%	44.0%	Dendritic Polymer with Perfluoroaryl (1.01%, ICD#3343)	5.83% Water; 2.93% ICD#2853	Yin, ARL
3458	51.7%	41.5%	Dendritic Polymer with Perfluoroaryl (2.04%, ICD#3343)	2.72% Water; 2.09% ICD#2853	Yin, ARL

ICD #	Percent Base Oil (PFPE = Y25)	Percent Teflon (PTFE = F5A)	Compound (% , ICD#, if any)	Other added compounds (% , ICD# if any)	PI/Supplier
3459	46.3%	43.7%	Dendritic Polymer with Perfluoroaryl (2.92%, ICD#3343)	3.17% Water; 3.86% ICD#2853	Yin, ARL
3460	45.0%	45.0%	Dendritic Polymer with Perfluoroaryl (1.01%, ICD#3343)	2.99% Water; 5.99% ICD#2853	Yin, ARL
3460	44.7%	44.7%	Dendritic Polymer with Perfluoroaryl (1.19%, ICD#3343)	3.18% Water, 6.16% ICD#2853	Yin, ARL
3461	45.7%	44.3%	Dendritic Polymer with Perfluoroaryl (4.91%, ICD#3344)	3.05% Water; 2.05% ICD#2853	Yin, ARL
3461	45.5%	44.5%	Dendritic Polymer with Perfluoroaryl (4.92%, ICD#3344)	3.02% Water; 2.01% ICD#2853	Yin, ARL
3462	59.4%	33.2%	Dendritic Polymer with Perfluoroaryl (5.18%, ICD#3344)	0.744% Water; 1.48% ICD#2853	Yin, ARL
3463	45.4%	44.6%	Dendritic Polymer with Perfluoroaryl (4.96%, ICD#3344)	1.09% Water; 3.96% ICD#2853	Yin, ARL
3464	45.2%	44.6%	Dendritic Polymer with Perfluoroaryl (2.01%, ICD#3344)	1.23% Water; 7.01% ICD#2853	Yin, ARL
3465	45.1%	44.9%	Dendritic Polymer with Perfluoroaryl (5.02%, ICD#3343)	5.00% ICD#2853	Yin, ARL
3466			TiO ₂ LH2-65		Nantek
3467			APCaO JCW1-2		Nantek
3468			APMgO #285		Nantek
3469			ZnO LH2-85		Nantek
3470	38.1%	42.9%	Lupasol (9.7%)	Fluorolink 7004 (1.9 %), Water (7.4%)	TDA
3471	26.5%	49.2%	Lupasol (15.1%)	Fluorolink 7004 (3.1%), Water (6.1%)	TDA
3479	50.0%	50.0%	ICD#2289 prepared by extruder		Yin, ARL
3481			K ₅ Co(III)W ₁₀ O ₄₀		Hill, Emory
3486			Potassium O,O'-Diocetylphosphorodithioate		CPT Hobson

ICD #	Percent Base Oil (PFPE = Y25)	Percent Teflon (PTFE = F5A)	Compound (% , ICD#, if any)	Other added compounds (% , ICD# if any)	PI/Supplier
3487			Dithiophosphoric acid O,O'-dioctyl ester		CPT Hobson
3488	49.2%	45.6%	Potassium O,O'-Diocetylphosphorodithioate (ICD#3486, 5.21%)		CPT Hobson (new prep)
3493			20% TEAAuCl ₂ /20% CuSO ₄ /TBANO ₃ non POM compound		Hill, Emory
3496	44.5%	44.5%	Dendritic Polymer with Perfluoroaryl (1%, ICD#3344) prepared by extruder at ARL	Trace Water	Yin, ARL
3510			APMgO		Nantek
3511			[Ag ₅ PV ₂ Mo ₁₀ O ₄₀]APMgO		Nantek
3512			ZnO		Nantek
3513			[Ag ₅ PV ₂ Mo ₁₀ O ₄₀]ZnO		Nantek
3514			APTiO ₂		Nantek
3515			[Ag ₅ PV ₂ Mo ₁₀ O ₄₀]APTiO ₂		Nantek
3516	50.0%	45.0%	5.00%, ICD#3493		Hill, Emory
3517	45.0%	45.0%	1. REF #DQD 110100: 1% perfluoroalkyl dendrimer (17F-PEOX similar to ICD#3344) prepared by extruder	9% Water	Yin, ARL
3518	45.0%	45.0%	1. REF#DQD 101600: 1% perfluoroaryl dendrimer (17F-PEOX similar to ICD#3343) prepared by extruder	9% Water	Yin, ARL
3519	51.5%	46.1%	Aerogel prepared Magnesium oxide (AP-MgO) (2.40%, ICD#3510)		Nantek
3520	49.7%	47.8%	Aerogel prepared Magnesium oxide (AP-MgO)/Ag ₅ Pv ₂ Mo ₁₀ O ₄₀ (POM) (2.48%, ICD#3511)		Nantek
3520	49.7%	47.8%	Aerogel prepared Magnesium oxide (AP-MgO)/Ag ₅ Pv ₂ Mo ₁₀ O ₄₀ (POM) (2.56%, ICD#3511)		Nantek
3520	49.7%	47.8%	Aerogel prepared Magnesium oxide (AP-		Nantek

ICD #	Percent Base Oil (PFPE = Y25)	Percent Teflon (PTFE = F5A)	Compound (% , ICD#, if any)	Other added compounds (% , ICD# if any)	PI/Supplier
			MgO)/Ag ₅ Pv ₂ Mo ₁₀ O ₄₀ (POM) (2.56%, ICD#3511)		
3521	49.8%	47.6%	Zinc oxide (2.55%, ICD#3512)		Nantek
3522	50.1%	47.5%	Zinc oxide (ZnO))/Ag ₅ Pv ₂ Mo ₁₀ O ₄₀ (POM) (2.50%, ICD#3513)		Nantek
3523	50.0%	47.5%	Aerogel prepared Titanium oxide (AP-TiO ₂) (2.51%, ICD#3514)		Nantek
3524	49.8%	47.6%	Aerogel prepared Titanium oxide (AP-TiO ₂)/Ag ₅ Pv ₂ Mo ₁₀ O ₄₀ (POM) (2.55%, ICD#3515)		Nantek
3525	50.0%	47.5%	Al ₂ O ₃ (5um) (2.54%, ICD#3480)		A Ternay
3526	50.0%	47.5%	Al ₂ O ₃ (I30020) (2.53%, ICD#3494)		A Ternay
3530	50.1%	48.9%	40% DS/60% PhB (1.00%, ICD#3168)		Shea, UCI Berkley
3531	50.5%	49.4%	60% DS/40% PhB (1.11%, ICD#3303)		Shea, UCI Berkley
3532	50.0%	48.8%	80% DS/20% PhB (1.17%, ICD#3304)		Shea, UCI Berkley
3533	50.0%	47.5%	Silica Gel (SiO ₂) (2.50%)		Shea, UCI Berkley
3534			Silica Gel (SiO ₂)		Shea, UCI Berkley
3539			100% Ph-B THF/solvent procedure		Shea, UCI Berkley
3540			100% Ph-B EtOH/Water procedure		Shea, UCI Berkley
3541			40% MP/Ph-B		Shea, UCI Berkley
3542			40% MP/Ph-B		Shea, UCI Berkley
3543			40% MP/Ph-B		Shea, UCI Berkley
3544			TSR05M Extracellular precipitate (Manganese Sulfide) Solid		Biopraxis
3545			TSR05M Extracellular precipitate (Manganese Sulfide) Aqueous Suspension		Biopraxis
3546			TM001/M Extracellular precipitate (Manganese Oxide) Solid		Biopraxis

ICD #	Percent Base Oil (PFPE = Y25)	Percent Teflon (PTFE = F5A)	Compound (% , ICD#, if any)	Other added compounds (% , ICD# if any)	PI/Supplier
3547			TM001/M Extracellular precipitate (Manganese Oxide) Aqueous Suspension		Biopraxis
3548	51.1%	43.6%	100% PhB/THF (5.32%, ICD#3539)		Shea, UCI Berkley
3549	51.1%	43.6%	100% PhB/EtOH (5.34%, ICD#3540)		Shea, UCI Berkley
3550	51.1%	43.6%	40% MP/ PhB (5.33%, ICD#3541)		Shea, UCI Berkley
3551	51.1%	43.6%	40% MP/ PhB (5.32%, ICD#3542)		Shea, UCI Berkley
3552	51.1%	43.6%	40% MP/ PhB (5.34%, ICD#3543)		Shea, UCI Berkley
3552	51.0%	43.6%	40% MP/ PhB (5.38%, ICD#3543)		Shea, UCI Berkley
3553	48.3%	44.8%	TSR05/M catalyst (2.48%, ICD#3544)	Surfactant - Light (2.31%, ICD#2853), water (2.12%)	Biopraxis
3554	48.2%	44.9%	TM001/M catalyst (2.70%, ICD#3546)	Surfactant - Light (2.13%, ICD#2853), water (2.12%)	Biopraxis
3555	51.1%	47.6%	TSR05/M catalyst (1.34%, ICD#3544)		Biopraxis
3556	50.6%	46.8%	TM001/M catalyst (2.56%, ICD#3546)		Biopraxis
3557	48.0%	44.9%	TSR05/M catalyst (aq) (5.03%, ICD#3545)	Surfactant - Light (2.00%, ICD#2853)	Biopraxis
3558	49.0%	44.0%	TM001/M catalyst (aq) (4.90%, ICD#3547)	Surfactant - Light (2.00%, ICD#2853)	Biopraxis
3564			Impran		
3565	46.7%	45.5%	MSR05/F catalyst (2.38%, ICD#3577)	Surfactant - Light (2.51%, ICD#2853), water (2.89%)	Biopraxis
3566	45.5%	46.3%	MSR09/F catalyst (3.06%, ICD#3581)	surfactant - Light (3.10%, ICD#2853), water (2.12%)	Biopraxis
3567	46.0%	47.0%	TSR02/M catalyst (1.98%, ICD#3583)	Surfactant - Light (2.35%, ICD#2853), water (2.67%)	Biopraxis

ICD #	Percent Base Oil (PFPE = Y25)	Percent Teflon (PTFE = F5A)	Compound (% , ICD#, if any)	Other added compounds (% , ICD# if any)	PI/Supplier
3568	46.7%	46.4%	MSR03/F catalyst (2.13%, ICD#3579)	surfactant - Light (2.34%, ICD#2853), water (2.00%)	Biopraxis
3569	47.2%	45.9%	TFR03/F1 catalyst (2.44%, ICD#3575)	Surfactant - Light (2.28%, ICD#2853), water (2.24%)	Biopraxis
3570	49.7%	43.4%	MSR05/F catalyst (aq) (4.86%, ICD#3578)	Surfactant - Light (1.97%, ICD#2853)	Biopraxis
3571	48.1%	44.9%	MSR09/F catalyst (aq) (4.94%, ICD#3582)	Surfactant - Light (2.07%, ICD#2853)	Biopraxis
3572	48.2%	44.8%	TSR02/M catalyst (aq) (4.97%, ICD#3584)	Surfactant - Light (2.11%, ICD#2853)	Biopraxis
3573	55.2%	38.8%	MSR03/F catalyst (aq) (4.24%, ICD#3580)	Surfactant - Light (1.83%, ICD#2853)	Biopraxis
3574	48.1%	44.9%	TFR03/F1 catalyst (aq) (4.98%, 3576)	Surfactant - Light (2.03%, ICD#2853)	Biopraxis
3575			TFR03/F1 extracellular precipitate		Biopraxis
3576			TFR03/F1 extracellular precipitate		Biopraxis
3577			MSR05/F extracellular precipitate		Biopraxis
3578			MSR05/F extracellular precipitate		Biopraxis
3579			MSR03/F extracellular precipitate		Biopraxis
3580			MSR03/F extracellular precipitate		Biopraxis
3581			MSR09/F extracellular precipitate		Biopraxis
3582			MSR09/F extracellular precipitate		Biopraxis
3583			TSR02/M extracellular precipitate		Biopraxis
3584			TSR02/M extracellular precipitate		Biopraxis
3585	47.5%	47.4%	Impran (5.09%, ICD#3564)		Russian material
3587	45.0%	44.9%	Potassium dithiophosphate O,O'-dibutyl ester (1.00%,		Organic Synthesis Laboratory

ICD #	Percent Base Oil (PFPE = Y25)	Percent Teflon (PTFE = F5A)	Compound (% , ICD#, if any)	Other added compounds (% , ICD# if any)	PI/Supplier
			ICD#3586)		
3598	50.6%	42.6%	TFR03/M (2.61%, ICD#3592)	Surfactant - Light (2.15%, ICD#2853), water (2.01%)	Biopraxis
3599	55.2%	38.6%	TFR03/M(aq) (4.34%, ICD#3593)	Surfactant - Light (1.88%, ICD#2853)	Biopraxis
3600	47.3%	44.2%	MSR06/F (3.12%, ICD#3594)	Surfactant - Light (2.00%, ICD#2853), water (3.37%)	Biopraxis
3601	48.4%	44.6%	MSR06/F(aq) (4.97%, ICD#3595)	Surfactant - Light (2.03%, ICD#2853)	Biopraxis
3602	50.3%	43.2%	TFO01/F5 (2.46%, ICD#3596)	Surfactant - Light (2.14%, ICD#2853), water (1.96%)	Biopraxis
3603	48.0%	44.8%	TFO01/F5(aq) (5.08%, ICD#3597)	Surfactant - Light (2.07%, ICD#2853)	Biopraxis
3604			Diethanolamine modified (DEAM). Cross-linked Polystyrene/divinylbenzene copolymer modified with 1.2 mmol/g diethanolamine.		Univ of Bath
3605			Diethanolamine modified (DEAM). Cross-linked polystyrene/divinylbenzene copolymer modified with 1.5 mmol/g diethanolamine.		Univ of Bath
3606			Diethanolamine modified (DEAM). Cross-linked Polystyrene/divinylbenzene copolymer modified with 1.0 mmol/g diethanolamine.		Univ of Bath
3607			Dendritic Polymer (C12-20-100)+G		Yin, ARL
3608			Dendritic Polymer (5F-pZOX/PZI)		Yin, ARL
3609	60.0%	40.0%	DD010901B		Yin, ARL
3610	55.0%	45.0%	DD010901A		Yin, ARL

ICD #	Percent Base Oil (PFPE = Y25)	Percent Teflon (PTFE = F5A)	Compound (% , ICD#, if any)	Other added compounds (% , ICD# if any)	PI/Supplier
3611	50.0%	40.0%	ICD#3608 (DD01180, 15F-PZOX/PZI) 2%	Water 8%	Yin, ARL
3612	50.0%	40.0%	ICD#3607 (DD012301A, C12-20-100+G) 2%	Water 8%	Yin, ARL
3613	54.0%	36.0%	DD012301A (C12-20-100)+G (2%)	Water 8%	Yin, ARL
3622	49.5%	38.1%	OPAA-2 0.95%	Tyloxapol (1.9%), Polyethyethylene oxide (300K M. W., 0.18%), Glycodeoxycholic Acis Sodium Salt (0.09%), 10% polyvinyl alcohol (1.85%), 20 nM MOPS (3.69%), Isopropanol (3.69%)	Altus
3623	49.5%	38.1%	OPAA-2 0.95%	Tyloxapol (1.9%), Polyethyethylene oxide (600K M. W., 0.18%), Glycodeoxycholic Acis Sodium Salt (0.09%), 10% polyvinyl alcohol (1.85%), 20 nM MOPS (3.69%), Isopropanol (3.69%)	Altus
3624	49.5%	38.1%	OPAA-2 0.95%	Tyloxapol (1.9%), Polyethyethylene oxide (900K M. W., 0.18%), Glycodeoxycholic Acis Sodium Salt (0.09%), 10% polyvinyl alcohol (1.85%), 20 nM MOPS (3.69%), Isopropanol (3.69%)	Altus
3625	49.5%	38.1%	OPAA-2 0.95%	Polyethyethylene oxide (100K M. W., 0.18%), Glycodeoxycholic Acis Sodium Salt (0.09%), 10% polyvinyl alcohol (1.85%), 20 nM	Altus

ICD #	Percent Base Oil (PFPE = Y25)	Percent Teflon (PTFE = F5A)	Compound (% , ICD#, if any)	Other added compounds (% , ICD# if any)	PI/Supplier
				MOPS (3.69%), Isopropanol (0.92%), water (2.77%)	
3626	49.5%	38.1%	OPAA-2 0.95%	Polyethyethylene oxide (100K M. W., 0.19%), Glycodeoxycholic Acis Sodium Salt (0.09%), 10% polyvinyl alcohol (1.88%), 20 nM MOPS (3.76%), Isopropanol (0.94%), water (2.63%), 25% Jeffamine T-4.3 (0.01%)	Altus
3627	49.5%	38.1%	OPAA-2 0.95%	Polyethyethylene oxide (100K M. W., 0.19%), Glycodeoxycholic Acis Sodium Salt (0.10%), 10% polyvinyl alcohol (1.91%), 20 nM MOPS (3.83%), Isopropanol (0.96%), water (2.49%), 25% Jeffamine T-4.3 (0.03%)	Altus
3628			APMgO		Nantek
3629			[2Mol % CeCuNO ₃]TiO ₂		Nantek
3630	49.2%	46.4%	PS/DVB 1.19 mmol/g DEAM (2.45%, ICD#3604)	Water (0.983%), surfactant - light (0.995%, ICD#2853)	James, Univ of Bath
3631	47.9%	47.8%	PS/DVB 1.54 mmol/g DEAM (2.38%, ICD#3605)	Water (0.954%), surfactant - light (0.954%, ICD#2853)	James, Univ of Bath
3632	49.2%	46.6%	PS/DVB 0.98 mmol/g DEAM (2.33%, ICD#3606)	Water (0.932%), surfactant - light (0.932%, ICD#2853)	James, Univ of Bath
3633	50.0%	47.5%	[2Mol % CeCuNO ₃] on AP-TiO ₂ (2.50%, ICD#3629)		Nantek

ICD #	Percent Base Oil (PFPE = Y25)	Percent Teflon (PTFE = F5A)	Compound (% , ICD#, if any)	Other added compounds (% , ICD# if any)	PI/Supplier
3634	50.2%	47.3%	ApMgO (2.49%, ICD#3628)		Nantek
3635			(CH ₃) ₃ V ₆ O ₁₉ /CeO ₂		Hill, Emory U
3649			Na ₅ PV ₂ Mo ₁₀ O ₄₀		Hill, Emory U
3650			AgNO ₃		Hill, Emory U
3651			Ag ₅ PV ₂ Mo ₁₀ O ₄₀		Hill, Emory U
3655			Zn 95% Pd 5% Alloy		Zamani, WRAIR
3656			Zn 90% Pd 10% Alloy		Zamani, WRAIR
3657			Zn 80% Pd 20% Alloy		Zamani, WRAIR
3658			Petrolatum ?%; mineral oil ?%; ceresin ?%; lanolin alcohol ?%		Zamani, WRAIR
3660			Zn 80% Pd 20% alloy (49.5%, ICD#3657); (50.5%, ICD#3658)		Zamani, WRAIR
3661			10%[Na ₅ PV ₂ Mo ₁₀ O ₄₀]TiO ₂		Hill, Emory U
3662			10%[Na ₅ PV ₂ Mo ₁₀ O ₄₀]MgO		Hill, Emory U
3663			Aerogel prepared Titanium oxide (AP-TiO ₂)		CPT Hobson
3664	52.6%	44.9%	10%[Na ₅ PV ₂ Mo ₁₀ O ₄₀]TiO ₂ (2.50%, ICD#3661)		Nantek
3665	52.5%	45.0%	10%[Na ₅ PV ₂ Mo ₁₀ O ₄₀]MgO (2.50%, ICD#3662)		Nantek
3666	52.8%	44.7%	Na ₅ PV ₂ Mo ₁₀ O ₄₀ (2.48%, ICD#3649)		Nantek
3667	48.4%	40.6%	Ag ₅ PV ₂ Mo ₁₀ O ₄₀ (2.31%, ICD#3651)		Nantek
3668	52.5%	45.0%	AgNO ₃ (2.49%, ICD#3650)		Nantek
3669	52.6%	44.9%	(CH ₃) ₃ V ₆ O ₁₉ /CeO ₂ (2.49%, ICD#3635)		Hill, Emory U
3670	51.2%	47.3%	Pd (5%)/Zn from Zamani, WRAIR (1.55%, ICD#3655)		Zamani, WRAIR
3671	51.4%	47.1%	Pd (10%)/Zn from Zamani, WRAIR (1.50%, ICD#3656)		Zamani, WRAIR

ICD #	Percent Base Oil (PFPE = Y25)	Percent Teflon (PTFE = F5A)	Compound (% , ICD#, if any)	Other added compounds (% , ICD# if any)	PI/Supplier
3672	50.5%	48.0%	Pd (20%)/Zn from Zamani, WRAIR (1.5%, 3657)		Zamani, WRAIR
3673	50.1%	47.4%	Aerogel prepared Titanium oxide (AP-TiO ₂) (2.51%, ICD#3663)		Nantek
3692			60% TBAN ₀₃ ; 20% TEAAuC ₁₂ ; 20% CuSO ₄		Hill, Emory U
3693	47.5%	47.5%	Green Powder; (ICD#3692, 4.5%)		Hill, Emory U
3696			6.5% H ₅ PV ₂ Mo ₁₀ O ₄₀ , 93.5% Celite		Hill, Emory U
3697			6.6% H ₅ PV ₂ Mo ₁₀ O ₄₀ , 93.4% Silica gel		Hill, Emory U
3698	54.0%	37.5%	6.5% H ₅ PV ₂ Mo ₁₀ O ₄₀ on 93.5% Celite (ICD#3696, 8.5%)		CPT Hobson
3699	54.0%	37.5%	6.6% H ₅ PV ₂ Mo ₁₀ O ₄₀ , 93.4% Silica Gel (ICD#3697, 8.5%)		CPT Hobson
3700			Nanoscale CeO ₂		Nantek
3704			5wt% H ₅ PV ₂ Mo ₁₀ O ₄₀ (ICD#2848) on CeO ₂ (ICD#3700)		Nantek
3705			5wt% Na ₅ PV ₂ Mo ₁₀ O ₄₀ (ICD#3649) on CeO ₂ (ICD#3700)		Nantek
3706			5wt% Ag ₅ PV ₂ Mo ₁₀ O ₄₀ (ICD#3651) on CeO ₂ (ICD#3700)		Nantek
3707			42% Cu(CIO) ₂ x 6Water; 40% POM; 18% Cu(NO ₃) x 2.5Water		Nantek
3708	50.1%	46.9%	Nanoscale CeO ₂ (ICD#3700, 3.00%)		Nantek
3709	50.0%	47.0%	5wt% H ₅ PV ₂ Mo ₁₀ O ₄₀ (ICD#2848) on CeO ₂ (ICD#3700) (ICD#3704, 3.00%)		Nantek
3710	50.0%	47.0%	5wt% Na ₅ PV ₂ Mo ₁₀ O ₄₀ (ICD#3649) on CeO ₂ (ICD#3700) (ICD#3705, 3.00%)		Nantek
3711	50.0%	47.0%	5wt% Ag ₅ PV ₂ Mo ₁₀ O ₄₀ (ICD#3651) on CeO ₂ (ICD#3700) (ICD#3706, 3.00%)		Nantek
3712	47.8%	32.1%	Lupasol P (polyethylene imine) (ICD#3720, 9.48%)	Fluorolink 7004 (ICD#3719,	CPT Hobson

ICD #	Percent Base Oil (PFPE = Y25)	Percent Teflon (PTFE = F5A)	Compound (% , ICD#, if any)	Other added compounds (% , ICD# if any)	PI/Supplier
				2.71%), Water (7.93%)	
3713	48.3%	32.2%	Lupasol P (polyethylene imine) (ICD#3720, 6.96%)	Fluorolink 7004 (ICD#3719, 2.58%), Water (9.94%)	CPT Hobson
3714	59.8%	14.9%	Lupasol P (polyethylene imine) (ICD#3720, 19.9%)	Fluorolink 7004 (ICD#3719, 2.19 %), Water (3.18%)	CPT Hobson
3715	45.0%	21.0%	Lupasol P (polyethylene imine) (ICD#3720, 25.0%)	Fluorolink 7004 (ICD#3719, 2.00%), Water (7.00%)	CPT Hobson
3716	43.1%	24.9%	Lupasol P (polyethylene imine) (ICD#3720, 25.0%)	Fluorolink 7004 (ICD#3719, 1.99%), Water (4.97%)	CPT Hobson
3717	39.9%	29.9%	Lupasol P (polyethylene imine) (ICD#3720, 25.0%)	Fluorolink 7004 (ICD#3719, 2.00%), Water (3.19%)	CPT Hobson
3718	34.9%	29.9%	Lupasol P (polyethylene imine) (ICD#3720, 25.0%)	Fluorolink 7004 (ICD#3719, 2.00%), Water (8.18%)	CPT Hobson
3719			Fluorolink 7004, 1, Propene, 1,1,2,3,3,3-hexafluoro-, telomers with chlorotrifluoroethene, oxidized, reduced, ethyl ester, hydrolyzed, CAS #220182-27-4.		Ausimont USA, Inc
3720			Lupasol P, a 50:50 wt % mixture of water and aziridine, homopolymer, CAS #9002-98-6.		BASF Corp
3724	55.0%	25.0%	Lupasol P (polyethylene imine) modified by C18 (ICD#3723, 10%)	Water (10%)	Yin, ARL
3725	40.0%	40.0%	Lupasol P (polyethylene imine) modified by C18 (ICD#3723, 10%)	Water (10%)	Yin, ARL
3726	55.0%	25.0%	C18 PEOX 20/100 + G (ICD#3077, 10%)	Water (10%)	Yin, ARL
3727	40.0%	40.0%	C18 PEOX 20/100 + G (ICD#3077, 10%)	Water (10%)	Yin, ARL
3728	55.0%	25.0%	Lupasol P (polyethylene imine) (ICD#3720, 20%)		Yin, ARL

ICD #	Percent Base Oil (PFPE = Y25)	Percent Teflon (PTFE = F5A)	Compound (% , ICD#, if any)	Other added compounds (% , ICD# if any)	PI/Supplier
3729	40.0%	40.0%	Lupasol P (polyethylene imine) (ICD#3720, 20%)		Yin, ARL
3730			Fluorolink 7005, a perfluoropolyether derivative (PFPE-CONH-(CH ₂) ₃ -(OCH ₂ CH ₃) ₁₈ -CH ₃) from Ausimont, CAS# not assigned		Ausimont USA, Inc
3731			Lupasol SC 61B, hydroxyethylated polyethylenimine, Product ID#NLE 555415.		BASF Corp
3732			Lupasol WF (water free), polyethylenimine, (CH ₂ -CH ₂ -NH-) _x Product ID# NLE 187702, CAS# 9002-98-6.		BASF Corp
3733			Lupasol G20 water free, polyethylenimine, Product ID#NLE 555415, CAS# 25987-06-8.		BASF Corp
3735	47.7%	47.3%	Au/Cu (ICD#3374; 5.00%)		CPT Hobson
3736	50.2%	45.7%	ICD#3692; 4.20%		CPT Hobson
3737	47.70%	47.30%	Cu(ClO ₄) ₂ x 6Water, Cu(NO ₃) ₂ x 2.5 Water POM 40% [TBA salt of Cu(OH ₂)Fe ₂ (P ₂ W ₁₅ O ₅₆)(P ₂ Cu ₂ (OH ₂) ₂ W ₁₃ O ₅₂) ⁻¹⁶]. (3707, 5.0%)		CPT Hobson
3742	38.0%	33.0%	Lupasol P (polyethylene imine) (ICD#3720, 26%)	Fluorolink 7004 (ICD#3719, 3%)	Yin, ARL
3743	38.0%	33.0%	Lupasol P (polyethylene imine) (ICD#3720, 26%)	Fluorolink 7005 (ICD#3730, 3%)	Yin, ARL
3744	55.0%	25.0%	C18 PEOX 20/100 + G (ICD#3077, 10%)	0.05 M, LaCl ₃ in Water (10%)	Yin, ARL
3745	38.0%	33.0%	0.05 M, LaCl ₃ in Water (26%)	Fluorolink 7005 (ICD#3730, 3%)	Yin, ARL
3746	40.0%	45.1%	Lupasol SC (ICD#3731, 10.0%)	Fluorolink 7004 (ICD#3719, 2.00%), water (2.93%)	CPT Hobson
3747	39.8%	39.8%	Lupasol SC (ICD#3731, 10.0%)	Fluorolink 7004 (ICD#3719, 2.19%), water (8.35%)	CPT Hobson
3748	39.9%	39.9%	Lupasol SC (ICD#3731, 10.0%)	Fluorolink 7005 (ICD#3730, 3%)	CPT Hobson

ICD #	Percent Base Oil (PFPE = Y25)	Percent Teflon (PTFE = F5A)	Compound (% , ICD#, if any)	Other added compounds (% , ICD# if any)	PI/Supplier
				1.00%), water (9.18%)	
3749	35.4%	43.7%	Lupasol SC (ICD#3731, 14.9%)	Fluorolink 7005 (ICD#3730, 1.01%), water (4.97%)	CPT Hobson
3750	34.0%	44.0%	Lupasol SC (ICD#3731, 15.0%)	Fluorolink 7004 (ICD#3719, 2.00%), water (5.00%)	CPT Hobson
3751	40.0%	39.8%	Lupasol G20 (ICD#3733, 10.0%)	Fluorolink 7004 (ICD#3719, 1.99%), water (8.17%)	CPT Hobson
3752	39.9%	42.9%	Lupasol G20 (ICD#3733, 10.0%)	Fluorolink 7004 (ICD#3719, 2.00%), water (5.19%)	CPT Hobson
3753	39.9%	42.9%	Lupasol G20 (ICD#3733, 10.0%)	Fluorolink 7005 (ICD#3730, 1.04%), water (6.19%)	CPT Hobson
3754	36.0%	43.0%	Lupasol G20 (ICD#3733, 15.0%)	Fluorolink 7005 (ICD#3730, 1.04%), water (5.00%)	CPT Hobson
3755	39.9%	39.9%	Lupasol Water Free (ICD#3732, 10.0%)	Fluorolink 7004 (ICD#3719, 2.00%), water (8.18%)	CPT Hobson
3756	39.9%	34.9%	Lupasol Water Free (ICD#3732, 10.0%)	Fluorolink 7004 (ICD#3719, 2.00%), water (13.2%)	CPT Hobson
3757	40.0%	35.0%	Lupasol Water Free (ICD#3732, 10.0%)	Fluorolink 7005 (ICD#3730, 1.08%), water (13.8%)	CPT Hobson
3758	44.0%	35.0%	Lupasol Water Free (ICD#3732, 15.0%)	Fluorolink 7005 (ICD#3730, 1.00%), water (5.00%)	CPT Hobson
3759	43.5%	35.6%	Lupasol P (polyethylene imine) (ICD#3720, 14.8%)	Fluorolink 7005 (ICD#3730, 0.988%), water (5.14%)	CPT Hobson
3760	43.8%	36.2%	Lupasol P (polyethylene imine) (ICD#3720, 19.0%)	Fluorolink 7005 (ICD#3730, 0.952%)	CPT Hobson

ICD #	Percent Base Oil (PFPE = Y25)	Percent Teflon (PTFE = F5A)	Compound (% , ICD#, if any)	Other added compounds (% , ICD# if any)	PI/Supplier
3766			Lupasol FG, ethylenediamine-ethylenimine copolymer, (C ₂ H ₈ N ₂ .C ₂ H ₅ N)X Product#NCS 971991, CAS#25987-06-8.		BASF Corp.
3767			PAA-HCL-3L, 50.4 wt % aqueous solution of homopolymer of 2-propen-1-amine hydrochloride, CAS #71550-12-4.		CPT Hobson
3768	41.8%	49.1%	S-330 (ICD#2703, 9.91%)		Yin, ARL
3769	40.0%	40.0%	IBDA (ICD#3254; 10%)	Light Surfactant (ICD#3719; 10%)	Yin, ARL
3770	62.5%	30.0%	ICD3293 (XE555, M291 SDK resin) 7.5%		Yin, ARL
3771	38.0%	33.0%	Lupasol P (ICD#3720; 26%)	Fluorolink 7004 (ICD#3719, 3.00%)	Yin, ARL
3772	38.0%	33.0%	Lupasol G20 (ICD#3733; 26%)	Fluorolink 7005 (ICD#3730, 3.00%)	Yin, ARL
3773	38.0%	33.0%	Lupasol G20 (ICD#3733; 26%)	Fluorolink 7004 (ICD#3719, 3.00%)	Yin, ARL
3774	38.0%	33.0%	Lupasol SC (ICD#3731; 26%)	Fluorolink 7004 (ICD#3719, 3.00%)	Yin, ARL
3775	38.0%	33.0%	Lupasol SC (ICD#3731; 26%)	Fluorolink 7005 (ICD#3730, 3.00%)	Yin, ARL
3778	38.0%	32.9%	Lupasol WF (ICD#3732, 26.1%)	Fluorolink 7005 (ICD#3730, 2.89%)	CPT Hobson
3779	37.9%	33.0%	Lupasol WF (ICD#3732, 26.1%)	Fluorolink 7004 (ICD#3719, 2.99%)	CPT Hobson
3780	38.0%	32.9%	Lupasol FG (ICD#3766, 26.0%)	Fluorolink 7005 (ICD#3730, 3.09%)	CPT Hobson
3781	37.9%	33.0%	Lupasol FG (ICD#3766, 26.1%)	Fluorolink 7004 (ICD#3719, 3.04%)	CPT Hobson
3782	38.0%	32.9%	Lupasol FG (ICD#3766, 13.0%); Lupasol WF (ICD#3732, 13.1%)	Fluorolink 7004 (ICD#3719, 1.50%); Fluorolink 7005 (ICD#3730, 1.50%)	CPT Hobson

ICD #	Percent Base Oil (PFPE = Y25)	Percent Teflon (PTFE = F5A)	Compound (% , ICD#, if any)	Other added compounds (% , ICD# if any)	PI/Supplier
3786	38.0%	32.9%	Lupasol Water Free (ICD#3732, 26.1%)	Fluorolink 7005 (ICD#3730, 3.04%)	CPT Hobson
3787	37.9%	33.0%	Lupasol Water Free (ICD#3732, 26.0%)	Fluorolink 7004 (ICD#3719, 3.00%)	CPT Hobson
3790	38.0%	33.0%	Lupasol G20 (ICD#3733; 26%)	Fluorolink 7004 (ICD#3719, 3.0%)	Yin, ARL
3791	38.0%	33.0%	Lupasol WF (ICD#3732, 26%)	Fluorolink 7005 (ICD#3730, 3.0%)	Yin, ARL
3792	38.0%	33.0%	Lupasol FG (ICD#3766, 26%)	Fluorolink 7005 (ICD#3730, 3.0%)	Yin, ARL
3793	34.5%	30.0%	Lupasol P (ICD#3720; 23.6%)	Fluorolink 7005 (ICD#3730, 2.7%); Water (9.0%)	Yin, ARL
3808	49.1%	45.0%	Dytek EP (4.91%)	Fluorolink 7005 (ICD#3730, 1.00%)	CPT Hobson
3809	37.9%	33.1%	Lupasol WF (ICD#3732, 21.02%); Dytek EP (5.03%)	Fluorolink 7005 (ICD#3730, 3.02%)	CPT Hobson
3810	48.9%	45.0%	Dytek EP (5.05%)	Fluorolink 7004 (ICD#3719, 1.06%)	CPT Hobson
3811	37.8%	33.0%	Lupasol FG (ICD#3766, 21.13%); Dytek EP (5.03%)	Fluorolink 7005 (ICD#3730, 3.04%)	CPT Hobson
3815			Cu(II); Otf; NO ₃		Hill, Emory
3816			POM; CU(II); Otf; NO ₃		Hill, Emory
3817			POM; CU(II); Otf; NO ₃ (different POM)		Hill, Emory
3818	47.5%	47.3%	NO1-51-2 (ICD#3815; 5.22%)		CPT Hobson
3819	47.5%	47.4%	NO2-51-2 (ICD#3816; 5.08%)		CPT Hobson
3820	47.6%	47.4%	NO4-53-2 (ICD#3817; 5.02%)		CPT Hobson
3821	54.7%	40.9%	Polymer ID: FPD#6 (ICD#3822; 4.42%)		CPT Hobson
3822			FDP#6		Univ of CA, Berkley

ICD #	Percent Base Oil (PFPE = Y25)	Percent Teflon (PTFE = F5A)	Compound (% , ICD#, if any)	Other added compounds (% , ICD# if any)	PI/Supplier
3823			Lupasol FG + 10% C12		BASF Corp.
3824			Lupasol WF + 10% C12		BASF Corp.
3825	39.9%	38.3%	Lupasol FG + 10% C12 (ICD#3823, 20.46%)	Fluorolink 7004 (ICD#3719, 1.34%)	BASF Corp.
3826	39.3%	38.6%	Lupasol FG + 10% C12 (ICD#3823, 21.00%)	Fluorolink 7005 (ICD#3730, 1.17%)	BASF Corp.
3827	39.4%	39.2%	Lupasol WF + 10% C12 (ICD#3824, 19.61%)	Fluorolink 7004 (ICD#3719, 1.77%)	BASF Corp.
3828	40.5%	38.8%	Lupasol WF + 10% C12 (ICD#3824, 19.42%)	Fluorolink 7005 (ICD#3730, 1.26%)	BASF Corp.
3829	38.0%	33.0%	Lupasol P (ICD#3720, 26%)	Fluorolink 7005 (ICD#3730, 3%)	BASF Corp.
3830	38.0%	33.0%	Lupasol G20 (ICD#3733, 26%)	Fluorolink 7005 (ICD#3730, 3%)	BASF Corp.
3831	38.0%	33.0%	Lupasol SC (ICD#3731, 26%)	Fluorolink 7005 (ICD#3730, 3%)	BASF Corp.
3832	38.0%	33.0%	Lupasol WF (ICD#3732, 26%)	Fluorolink 7005 (ICD#3730, 3%)	BASF Corp.
3833	38.0%	33.0%	Lupasol FG (ICD#3766, 26%)	Fluorolink 7004 (ICD#3719, 3%)	BASF Corp.
3834	38.0%	33.0%	Lupasol FG (ICD#3766, 13%); Lupasol WF (ICD#3732, 13%)	Fluorolink 7005 (ICD#3730, 1.5%); Fluorolink 7004 (ICD#3719, 1.5%)	BASF Corp.
3835	38.4%	32.7%	Lupasol WF (ICD#3732, 12.73%); Lupasol FG (ICD#3766, 13.13%)	Fluorolink 7005 (ICD#3730, 3.02%)	BASF Corp.
3836	37.8%	32.7%	Lupasol WF (ICD#3732, 13.12%); Lupasol G20 (ICD#3733, 13.32%)	Fluorolink 7005 (ICD#3730, 3.01%)	BASF Corp.
3837	37.9%	32.8%	Lupasol WF (ICD#3732, 13.16%); Lupasol SC (ICD#3731, 13.06%)	Fluorolink 7005 (ICD#3730, 3.08%)	BASF Corp.
3838	38.2%	32.5%	Lupasol WF (ICD#3732, 13.08%); Lupasol P (ICD#3720, 13.13%)	Fluorolink 7005 (ICD#3730, 3.04%)	BASF Corp.
3839	37.9%	32.8%	Lupasol P (ICD#3720, 13.16%);	Fluorolink 7005 (ICD#3730, 3.04%)	BASF Corp.

ICD #	Percent Base Oil (PFPE = Y25)	Percent Teflon (PTFE = F5A)	Compound (% , ICD#, if any)	Other added compounds (% , ICD# if any)	PI/Supplier
			Lupasol FG (ICD#3766, 13.07%)	3.08%	
3840	37.5%	32.8%	Lupasol P (ICD#3720, 13.55%); Lupasol G20 (ICD#3733, 13.06%)	Fluorolink 7005 (ICD#3730, 3.07%)	BASF Corp.
3841	37.9%	32.9%	Lupasol P (ICD#3720, 13.24%); Lupasol SC (ICD#3731, 12.99%)	Fluorolink 7005 (ICD#3730, 2.97%)	BASF Corp.
3842	37.8%	32.8%	Lupasol FG (ICD#3766, 13.39%); Lupasol SC (ICD#3731, 12.89%)	Fluorolink 7005 (ICD#3730, 3.07%)	BASF Corp.
3843	37.7%	32.9%	Lupasol SC (ICD#3731, 13.04%); Lupasol G20 (ICD#3733, 13.14%)	Fluorolink 7005 (ICD#3730, 3.22%)	BASF Corp.
3844	38.0%	33.0%	Lupasol G20 (ICD#3733, 13%); Lupasol FG (ICD#3766, 13%)	Fluorolink 7005 (ICD#3730, 3.0%)	BASF Corp.
3850			60% 1,4-bis(9triethoxysilyl)benzene; 40% 3-aminopropyltriethoxysilane		Shea, UCI Berkley
3851	47.4%	47.2%	bridged polysilsesquioxane of 60% PhB and 40% APTES (ICD#3850; 5.36%)		Shea, UCI Berkley
3852			Lupasol LU 321, a 15:80:5 wt % mixture of formamide polymer (Product ID# NLE 073991) water, and sodium formate.		BASF Corp.
3853	30.8%	45.7%	Lupasol LU 321 (ICD#3852, 16.98%)	Fluorolink 7005 (ICD#3730, 2.41%); water (4.10%)	BASF Corp.
3854	34.8%	39.6%	Lupasol LU 321 (ICD#3852, 22.96%)	Fluorolink 7005 (ICD#3730, 2.64%)	BASF Corp.
3855	38.3%	35.4%	Lupasol LU 321 (ICD#3852, 20.11%)	Fluorolink 7004 (ICD#3719, 1.05%); water (5.12%)	BASF Corp.
3856	37.9%	35.2%	Lupasol LU 321 (ICD#3852, 25.18%)	Fluorolink 7004 (ICD#3719, 1.74%)	BASF Corp.

ICD #	Percent Base Oil (PFPE = Y25)	Percent Teflon (PTFE = F5A)	Compound (% , ICD#, if any)	Other added compounds (% , ICD# if any)	PI/Supplier
3857	38.0%	32.9%	Lupasol LU 321 (ICD#3852, 13.04%); Lupasol G20 (ICD#3733, 13.04%)	Fluorolink 7005 (ICD#3730, 2.97%)	BASF Corp.
3858	38.2%	32.9%	Lupasol LU 321 (ICD#3852, 13.05%); Lupasol WF (ICD#3732, 12.81%)	Fluorolink 7005 (ICD#3730, 3.10%)	BASF Corp.
3859	33.5%	40.9%	Lupasol LU 321 (ICD#3852, 11.32%); Lupasol SC (ICD#3731, 11.63%)	Fluorolink 7005 (ICD#3730, 2.66%)	BASF Corp.
3860	35.2%	37.7%	Lupasol LU 321 (ICD#3852, 12.22%); Lupasol P (ICD#3720, 12.13%)	Fluorolink 7005 (ICD#3730, 2.78%)	BASF Corp.
3861	35.6%	36.6%	Lupasol LU 321 (ICD#3852, 12.32%); Lupasol FG (ICD#3766, 12.37%)	Fluorolink 7005 (ICD#3730, 3.14%)	BASF Corp.
3863			Dytek EP, 1,3-pentanediamine, CAS# 589-37-7.		Dytek
3868			PAA-10C, 10.3 wt % aqueous solution of homopolymer of 2-propen-1-amine, CAS#30551-89-4		NittoBoseki Co, Ltd
3871	33.7%	40.7%	ICD#3867 (22.64%)	Fluorolink 7004 (ICD#3719, 2.93%)	CPT Hobson
3872	37.8%	32.9%	ICD#3867 (26.09%)	Fluorolink 7005 (ICD#3730, 3.18%)	CPT Hobson
3873	28.2%	52.1%	ICD#3868 (18.86%)	Fluorolink 7004 (ICD#3719, 0.76%)	CPT Hobson
3874	25.4%	54.9%	ICD#3868 (17.63%)	Fluorolink 7005 (ICD#3730, 2.07%)	CPT Hobson
3875	34.0%	39.7%	ICD#3867 (11.64%) ICD#3868 (11.95%)	Fluorolink 7005 (ICD#3730, 2.76%)	CPT Hobson
3877			[2Mol % AgNO ₃]AP-TiO ₂		CPT Hobson
3878			[10%[Na ₅ PV ₂ Mo ₁₀ O ₄₀]AP-TiO ₂		CPT Hobson
3879			[2Mol % CeNO ₃] ₃ /Cu(NO ₃) ₂]AP-TiO ₂		CPT Hobson

ICD #	Percent Base Oil (PFPE = Y25)	Percent Teflon (PTFE = F5A)	Compound (% , ICD#, if any)	Other added compounds (% , ICD# if any)	PI/Supplier
3880			AP-MgO		CPT Hobson
3882			Cu(Krytox) ₂		METTS
3883			Styrene/divinylbenzene sulfonate(METSS)		METTS
3884	37.8%	32.7%	Lupasol WF (ICD#3732, 13.12%); Lupasol G20 (ICD#3733, 13.32%)	Fluorolink 7005 (ICD#3730, 3.01%)	Yin, ARL
3885	37.9%	32.8%	Lupasol WF (ICD#3732, 13.16%); Lupasol SC (ICD#3731, 13.06%)	Fluorolink 7005 (ICD#3730, 3.08%)	Yin, ARL
3886	37.9%	32.8%	Lupasol P (ICD#3720, 13.16%); Lupasol FG (ICD#3766, 13.07%)	Fluorolink 7005 (ICD#3730, 3.08%)	Yin, ARL
3887	37.5%	32.8%	Lupasol P (ICD#3720, 13.55%); Lupasol G20 (ICD 3733, 13.06%)	Fluorolink 7005 (ICD#3730, 3.07%)	Yin, ARL
3889			TFO01/FD aq		Biopraxis
3890			TFO01/FS aq		Biopraxis
3891			TFO01/FC aq		Biopraxis
3892			TFO01/MS aq		Biopraxis
3893			TFO01/FD		Biopraxis
3894			TFO01/FS		Biopraxis
3895			TFO01/FC		Biopraxis
3896			TFO01/MS		Biopraxis
3898	58.5%	35.6%	TSR05/M catalyst (1.50%, ICD#3544)	Light Surfactant (ICD#2853, 4.40%)	Biopraxis
3899	57.0%	30.0%	TMO01/M catalyst (4.49%, ICD#3546)	Light Surfactant (ICD#2853, 8.53%)	Biopraxis
3900	37.9%	32.9%	Lupasol P (ICD#3720, 13.24%); Lupasol SC (ICD#3731, 12.99%)	Fluorolink 7005 (ICD#3730, 2.97%)	Yin, ARL

ICD #	Percent Base Oil (PFPE = Y25)	Percent Teflon (PTFE = F5A)	Compound (% , ICD#, if any)	Other added compounds (% , ICD# if any)	PI/Supplier
3901	37.8%	32.8%	Lupasol FG (ICD#3766, 13.39%); Lupasol SC (ICD#3731, 12.89%)	Fluorolink 7005 (ICD#3730, 3.07%)	Yin, ARL
3902	37.7%	32.9%	Lupasol SC (ICD#3731, 13.04%); Lupasol G20 (ICD#3733, 13.14%)	Fluorolink 7005 (ICD#3730, 3.22%)	Yin, ARL
3903	34.1%	40.1%	Lupasol G20 (ICD#3733, 11.44%); Lupasol FG (ICD#3766, 11.66%)	Fluorolink 7005 (ICD#3730, 2.68%)	Yin, ARL
3905	50.0%	45.0%	[10%[Na ₅ PV ₂ Mo ₁₀ O ₄₀]AP-TiO ₂ (ICD#3878, 5.0%)		Yin, ARL
3906	50.0%	45.0%	AP-MgO (Lot#01-009) (ICD#3880, 5.0%)		Yin, ARL
3907	50.0%	47.5%	[2Mol % Ce(NO ₃) ₃ /Cu(NO ₃) ₂]AP-TiO ₂ (ICD#3879, 2.5%)		Yin, ARL
3908	50.2%	47.3%	AP-MgO (Lot#01-009) (ICD#3880, 2.5%)		Yin, ARL
3909	52.6%	44.9%	[10%[Na ₅ PV ₂ Mo ₁₀ O ₄₀]AP-TiO ₂ (ICD#3878, 2.5%)		Yin, ARL
3910	49.2%	45.4%	TFO01/FD (ICD#3893, 2.65%)	Light Surfactant (ICD#2853, 2.79%)	CPT Hobson
3911	49.1%	45.3%	TFO01/FD (ICD#3893, 3.52%)	Light Surfactant (ICD#2853, 2.13%)	CPT Hobson
3912	49.8%	43.2%	TFO01/FD (ICD#3893, 5.06%)	Light Surfactant (ICD#2853, 2.00%)	CPT Hobson
3913	49.5%	41.7%	TFO01/FD (ICD#3893, 6.93%)	Light Surfactant (ICD#2853, 1.89%)	CPT Hobson
3914	48.1%	40.2%	TFO01/FD (ICD#3893, 9.55%)	Light Surfactant (ICD#2853, 2.21%)	CPT Hobson
3915	49.6%	45.5%	TFO01/FS (ICD#3894, 2.62%)	Light Surfactant (ICD#2853, 2.32%)	CPT Hobson
3916	48.8%	45.4%	TFO01/FS (ICD#3894, 3.62%)	Light Surfactant (ICD#2853, 2.14%)	CPT Hobson
3917	48.5%	46.0%	TFO01/FS (ICD#3894, 3.89%)	Light Surfactant (ICD#2853, 1.67%)	CPT Hobson
3918	47.8%	43.1%	TFO01/FS (ICD#3894, 6.93%)	Light Surfactant (ICD#2853, 1.67%)	CPT Hobson

ICD #	Percent Base Oil (PFPE = Y25)	Percent Teflon (PTFE = F5A)	Compound (% , ICD#, if any)	Other added compounds (% , ICD# if any)	PI/Supplier
				2.10%)	
3919	47.7%	40.6%	TFO01/FS (ICD#3894, 9.72%)	Light Surfactant (ICD#2853, 1.94%)	CPT Hobson
3920	49.6%	45.3%	TFO01/FC (ICD#3895, 2.73%)	Light Surfactant (ICD#2853, 1.94%)	CPT Hobson
3921	50.8%	43.6%	TFO01/FC (ICD#3895, 3.67%)	Light Surfactant (ICD#2853, 2.03%)	CPT Hobson
3922	50.6%	42.4%	TFO01/FC (ICD#3895, 4.88%)	Light Surfactant (ICD#2853, 2.04%)	CPT Hobson
3923	50.1%	41.1%	TFO01/FC (ICD#3895, 6.63%)	Light Surfactant (ICD#2853, 2.15%)	CPT Hobson
3924	46.9%	42.6%	TFO01/FC (ICD#3895, 8.70%)	Light Surfactant (ICD#2853, 1.75%)	CPT Hobson
3925	55.7%	50.3%	TFO01/MS (ICD#3896, 2.55%)	Light Surfactant (ICD#2853, 2.16%)	CPT Hobson
3926	49.4%	44.6%	TFO01/MS (ICD#3896, 3.64%)	Light Surfactant (ICD#2853, 2.31%)	CPT Hobson
3927	48.1%	44.4%	TFO01/MS (ICD#3896, 5.08%)	Light Surfactant (ICD#2853, 2.39%)	CPT Hobson
3928	47.0%	43.6%	TFO01/MS (ICD#3896, 7.34%)	Light Surfactant (ICD#2853, 2.10%)	CPT Hobson
3929	49.5%	39.2%	TFO01/MS (ICD#3896, 9.31%)	Light Surfactant (ICD#2853, 2.07%)	CPT Hobson
3930	43.2%	45.1%	TFO01/FD aq (ICD#3889, 9.70%)	Light Surfactant (ICD#2853, 2.05%)	CPT Hobson
3931	43.3%	45.5%	TFO01/FS aq (ICD#3890, 9.44%)	Light Surfactant (ICD#2853, 1.83%)	CPT Hobson
3932	42.6%	46.1%	TFO01/FC aq (ICD#3891, 9.50%)	Light Surfactant (ICD#2853, 1.87%)	CPT Hobson
3933	45.0%	42.9%	TFO01/MS aq (ICD#3892, 9.90%)	Light Surfactant (ICD#2853, 2.20%)	CPT Hobson
3934			TMO01/MC		Biopraxis

ICD #	Percent Base Oil (PFPE = Y25)	Percent Teflon (PTFE = F5A	Compound (%, ICD#, if any)	Other added compounds (%, ICD# if any)	PI/Suppli er
3935			TSR02/MC		Biopraxis
3936			TSR02/MF		Biopraxis
3937			MSR06/FL		Biopraxis
3938			TMO01/MG		Biopraxis
3939			MSR05/FL		Biopraxis
3940			MSR03/MF		Biopraxis
3941			MSR03/MLA		Biopraxis
3942			MSR03/FL		Biopraxis
3943			MSR06/ML		Biopraxis
3944			MSR03/MX		Biopraxis
3945			MSR05/ML		Biopraxis
3946			MSR03/MLB		Biopraxis
3947			TSR02/MX		Biopraxis
3948			TSR02/MX aq		Biopraxis
3949			MSR03/MX aq		Biopraxis
3950			MSR03/FL aq		Biopraxis
3951			MSR05/FL aq		Biopraxis
3952			MSR03/MF aq		Biopraxis
3953			TSR02/MF aq		Biopraxis
3954			TSR02/ML aq		Biopraxis
3955			MSR06/FL aq		Biopraxis
3956			TMO01/MG aq		Biopraxis
3957			TMO01/MC aq		Biopraxis

ICD #	Percent Base Oil (PFPE = Y25)	Percent Teflon (PTFE = F5A)	Compound (% , ICD#, if any)	Other added compounds (% , ICD# if any)	PI/Supplier
3958			MSR03/MLA aq		Biopraxis
3959			MSR06/ML aq		Biopraxis
3960			MSR05/ML aq		Biopraxis
3961			MSR03/MLB aq		Biopraxis
3963	52.5%	45.0%	Styrene/divinylbenzene sulfonate(METSS) (ICD#3883, 2.5%)		Yin, ARL
3964	47.9%	47.9%	Cu(Krytox) ₂ (ICD#3882, 4.2%)		Yin, ARL
3965	52.5%	45.0%	[2Mol % AgNO ₃]AP-TiO ₂ (ICD#3877, 2.5%)		Yin, ARL
3970	37.9%	33.0%	Lupasol WF (ICD#3732, 26.1%)	Fluorolink 7004 (ICD#3719, 3.00%)	Yin, ARL
3971	37.9%	35.2%	Lupasol LU 321 (ICD#3852, 25.17%)	Fluorolink 7004 (ICD#3719, 1.74%)	Yin, ARL
3972	34.8%	39.6%	Lupasol LU 321 (ICD#3852, 22.97%)	Fluorolink 7005 (ICD#3730, 2.69%)	Yin, ARL
3973	52.5%	45.0%	10%[Na ₅ PV ₂ Mo ₁₀ O ₄₀]MgO (ICD#3662, 2.50%)		Yin, ARL
3974	46.5%	48.1%	TMO01/MC (ICD#3934, 3.29%)	Light Surfactant (ICD#2853, 2.10%)	CPT Hobson
3975	47.0%	48.4%	TSR02/MC (ICD#3935, 2.52%)	Light Surfactant (ICD#2853, 2.52%)	CPT Hobson
3976	47.0%	48.5%	TSR02/MF(ICD#3936, 2.52%)	Light Surfactant (ICD#2853, 2.52%)	CPT Hobson
3977	47.5%	48.2%	MSR06/FL (ICD#3937, 2.43%)	Light Surfactant (ICD#2853, 2.43%)	CPT Hobson
3978	47.0%	48.5%	TMO01/MG (ICD#3938, 2.52%)	Light Surfactant (ICD#2853, 2.02%)	CPT Hobson
3979	47.3%	48.2%	MSR05/FL (ICD#3939, 2.51%)	Light Surfactant (ICD#2853, 2.02%)	CPT Hobson
3980	47.0%	48.5%	MSR03/MF (ICD#3940, 2.52%)	Light Surfactant (ICD#2853, 2.05%)	CPT Hobson
3981	46.9%	48.3%	MSR03/MLA (ICD#3941, 2.81%)	Light Surfactant (ICD#2853,	CPT Hobson

ICD #	Percent Base Oil (PFPE = Y25)	Percent Teflon (PTFE = F5A)	Compound (% , ICD#, if any)	Other added compounds (% , ICD# if any)	PI/Supplier
				2.08%)	
3982	50.1%	45.5%	MSR03/FL (ICD#3942, 2.39%)	Light Surfactant (ICD#2853, 1.96%)	CPT Hobson
3983	48.3%	51.0%	MSR06/ML (ICD#3943, 2.81%)	Light Surfactant (ICD#2853, 2.02%)	CPT Hobson
3984	46.9%	48.4%	MSR03/MX (ICD#3944, 2.57%)	Light Surfactant (ICD#2853, 2.06%)	CPT Hobson
3985	46.9%	48.4%	MSR05/ML (ICD#3945, 2.59%)	Light Surfactant (ICD#2853, 2.13%)	CPT Hobson
3986	47.2%	48.2%	MSR03/MLB (ICD#3946, 2.53%)	Light Surfactant (ICD#2853, 2.03%)	CPT Hobson
3987	46.9%	48.3%	TSR02/MX (ICD#3947, 2.51%)	Light Surfactant (ICD#2853, 2.31%)	CPT Hobson
3993	54.0%	37.5%	H5P/Silica (ICD#3697, 8.50%)		Yin, ARL
3994	38.2%	32.5%	Lupasol WF (ICD#3732, 13.08%); Lupasol P (ICD#3720, 13.13%)	Fluorolink 7005 (ICD#3730, 3.09%)	Yin, ARL
3995			Phenyl Bridge Polysilsesquioxane		Shea, UCI Berkley
3996	50.0%	48.0%	(ICD#3816, 2.00%)		Yin, ARL
3997	33.7%	40.7%	(ICD#3867, 22.64%)	Fluorolink 7004 (ICD#3719, 2.95%)	Yin, ARL
3998	37.4%	33.6%	(ICD#3867, 25.83%)	Fluorolink 7005 (ICD#3730, 3.16%)	Yin, ARL
3999	28.2%	52.1%	(ICD#3868, 18.88%)	Fluorolink 7004 (ICD#3719, 0.76%)	Yin, ARL
4000	25.4%	54.9%	(ICD#3868, 17.62%)	Fluorolink 7005 (ICD#3730, 2.07%)	Yin, ARL
4006	45.0%	50.6%	TSR02/MX aq (ICD#3948, 2.42%)	Light Surfactant (ICD#2853, 1.96%)	CPT Hobson
4007	42.7%	53.2%	MSR03/MX aq (ICD#3949, 2.29%)	Light Surfactant (ICD#2853, 1.86%)	CPT Hobson

ICD #	Percent Base Oil (PFPE = Y25)	Percent Teflon (PTFE = F5A)	Compound (% , ICD#, if any)	Other added compounds (% , ICD# if any)	PI/Supplier
4008	41.2%	54.8%	MSR03/FL aq (ICD#3950, 2.20%)	Light Surfactant (ICD#2853, 1.78%)	CPT Hobson
4009	45.5%	50.1%	MSR05/FL aq (ICD#3951, 2.44%)	Light Surfactant (ICD#2853, 2.01%)	CPT Hobson
4010	44.7%	50.9%	MSR03/MF aq (ICD#3952, 2.39%)	Light Surfactant (ICD#2853, 1.96%)	CPT Hobson
4011	44.6%	51.1%	TSR02/MF aq (ICD#3953, 2.40%)	Light Surfactant (ICD#2853, 1.97%)	CPT Hobson
4012	46.8%	48.7%	TSR02/ML aq (ICD#3954, 2.51%)	Light Surfactant (ICD#2853, 2.05%)	CPT Hobson
4013	44.5%	51.1%	MSR06/FL aq (ICD#3955, 2.40%)	Light Surfactant (ICD#2853, 2.00%)	CPT Hobson
4014	44.2%	51.4%	TMO01/MG aq (ICD#3956, 2.39%)	Light Surfactant (ICD#2853, 2.00%)	CPT Hobson
4015	45.6%	49.9%	TMO01/MC aq (ICD#3957, 2.45%)	Light Surfactant (ICD#2853, 2.03%)	CPT Hobson
4016	46.7%	48.4%	MSR03/MLA aq (ICD#3958, 2.51%)	Light Surfactant (ICD#2853, 2.06%)	CPT Hobson
4017	46.2%	49.3%	MSR06/ML aq (ICD#3959, 2.49%)	Light Surfactant (ICD#2853, 2.07%)	CPT Hobson
4018	46.3%	49.2%	MSR05/ML aq (ICD#3960, 2.48%)	Light Surfactant (ICD#2853, 2.07%)	CPT Hobson
4019	46.3%	49.2%	MSR03/MLB aq (ICD#3961, 2.50%)	Light Surfactant (ICD#2853, 2.05%)	CPT Hobson
4020	37.6%	32.9%	Lupasol P (ICD#3720, 13.52%); Lupasol G (ICD#3733, 13.08%)	Fluorolink 7005 (ICD#3730, 1.50%); Fluorolink 7004 (ICD#3719, 1.50%)	Yin, ARL
4021	38.3%	32.6%	Lupasol P (ICD#3720, 13.10%); Lupasol WF (ICD#3732, 13.09%)	Fluorolink 7005 (ICD#3730, 3.04%)	Yin, ARL
4022	38.5%	32.7%	Lupasol WF (ICD#3732, 12.75%); Lupasol FG (ICD#3766, 13.15%)	Fluorolink 7005 (ICD#3730, 3.03%)	Yin, ARL

ICD #	Percent Base Oil (PFPE = Y25)	Percent Teflon (PTFE = F5A)	Compound (% , ICD#, if any)	Other added compounds (% , ICD# if any)	PI/Supplier
4023	50.0%	47.0%	[5wt% Ag ₅ PV ₂ Mo ₁₀ O ₄₀]CeO ₂ (ICD#4025, 3.00%)		Yin, ARL
4024			[5wt% Na ₅ PV ₂ Mo ₁₀ O ₄₀]CeO ₂		Hill, Emory
4025			[5wt% Ag ₅ PV ₂ Mo ₁₀ O ₄₀]CeO ₂		Hill, Emory
4026	50.0%	47.0%	[5wt% Na ₅ PV ₂ Mo ₁₀ O ₄₀]CeO ₂ (ICD#4024, 3.00%)		Yin, ARL
4027	50.0%	47.0%	(ICD#3995; 3.00%)		Yin, ARL
4028	54.0%	36.0%	S-330 (ICD#2703, 10.0%)		Yin, ARL
4029	37.9%	32.8%	Lupasol P (ICD#3720, 13.17%); Lupasol FG (ICD#3766, 13.07%)	Fluorolink 7005 (ICD#3730, 1.50%); Fluorolink 7004 (ICD#3719, 1.50%)	Yin, ARL
4032	43.9%	41.6%	Lupasol G20 (ICD#3733, 13.02%)	Fluorolink 7005 (ICD#3730, 1.50%)	CPT Hobson
4033	46.8%	46.0%	Lupasol G20 (ICD#3733, 6.48%)	Fluorolink 7005 (ICD#3730, 0.75%)	CPT Hobson
4034	44.0%	41.5%	Lupasol WF (ICD#3732, 13.02%)	Fluorolink 7005 (ICD#3730, 1.50%)	CPT Hobson
4035	47.3%	45.5%	Lupasol WF (ICD#3732, 6.45%)	Fluorolink 7005 (ICD#3730, 0.74%)	CPT Hobson
4036	43.4%	40.6%	Lupasol G20 (ICD#3733; 14.34%)	Fluorolink 7004 (ICD#3719, 1.65%)	CPT Hobson
4037	46.7%	45.2%	Lupasol G20 (ICD#3733; 7.22%)	Fluorolink 7004 (ICD#3719, 0.83%)	CPT Hobson
4038	44.0%	41.5%	Lupasol FG (ICD#3766, 13.00%)	Fluorolink 7004 (ICD#3719, 1.50%)	CPT Hobson
4039	47.1%	45.6%	Lupasol FG (ICD#3766, 6.51%)	Fluorolink 7004 (ICD#3719, 0.75%)	CPT Hobson
4040	44.1%	41.4%	Lupasol FG (ICD#3766, 13.01%)	Fluorolink 7005 (ICD#3730, 1.50%)	CPT Hobson
4041	47.0%	45.7%	Lupasol FG (ICD#3766, 6.53%)	Fluorolink 7005 (ICD#3730, 1.50%)	CPT Hobson

ICD #	Percent Base Oil (PFPE = Y25)	Percent Teflon (PTFE = F5A)	Compound (% , ICD#, if any)	Other added compounds (% , ICD# if any)	PI/Supplier
				0.75%)	
4042	44.0%	41.5%	Lupasol FG (ICD#3766, 6.50%); Lupasol WF (ICD#3732, 6.50%)	Fluorolink 7005 (ICD#3730, 0.75%); Fluorolink 7004 (ICD#3719, 0.75%)	CPT Hobson
4043	48.7%	47.2%	Lupasol FG (ICD#3766, 3.36%); Lupasol WF (ICD#3732, 3.36%)	Fluorolink 7005 (ICD#3730, 0.39%); Fluorolink 7004 (ICD#3719, 0.39%)	CPT Hobson
4044	44.9%	40.7%	Lupasol P (ICD#3720, 12.94%)	Fluorolink 7005 (ICD#3730, 1.49%)	CPT Hobson
4045	48.0%	44.8%	Lupasol P (ICD#3720, 6.39%)	Fluorolink 7005 (ICD#3730, 0.74%)	CPT Hobson
4046	50.7%	32.6%	Lupasol WF (ICD#3732, 14.97%)	Fluorolink 7004 (ICD#3719, 1.77%)	CPT Hobson
4047	47.9%	36.0%	Lupasol P (ICD#3720; 14.14%)	Fluorolink 7004 (ICD#3719, 1.99%)	CPT Hobson
4048	50.3%	41.4%	Lupasol WF (ICD#3732, 7.45%)	Fluorolink 7004 (ICD#3719, 0.88%)	CPT Hobson
4049	49.0%	42.9%	Lupasol P (ICD#3720; 7.07%)	Fluorolink 7004 (ICD#3719, 0.99%)	CPT Hobson
4050	38.2%	32.5%	Lupasol P (ICD#3720, 13.14%); Lupasol WF (ICD#3732, 13.09%)	Fluorolink 7005 (ICD#3730, 1.50%); Fluorolink 7004 (ICD#3719, 1.50%)	Yin, ARL
4051	37.8%	32.7%	Lupasol G20 (ICD#3733, 13.33%); Lupasol FG (ICD#3766, 13.13%)	Fluorolink 7005 (ICD#3730, 1.50%); Fluorolink 7004 (ICD#3719, 1.50%)	Yin, ARL
4052	37.8%	32.7%	Lupasol G20 (ICD#3733, 13.33%); Lupasol WF (ICD#3732, 13.13%)	Fluorolink 7005 (ICD#3730, 1.50%); Fluorolink 7004 (ICD#3719, 1.50%)	Yin, ARL

ICD #	Percent Base Oil (PFPE = Y25)	Percent Teflon (PTFE = F5A)	Compound (% , ICD#, if any)	Other added compounds (% , ICD# if any)	PI/Supplier
4069			50mM Minocycline in PEG ointment USP + 2% DMSO (w/w)		J Nicholson
4071			50mM Doxycycline in PEG ointment USP + 2% DMSO (w/w)		J Nicholson
4072			8mM Doxycycline in DMSO		J Nicholson
4088			8.93% NanoActive TiO ₂		Nantek
4089			2.27% (AgNO ₃ , AgNO ₃ coated NanoActive TiO ₂)		Nantek
4090			2.29% (physical mixture: Cu/Cu, FePOM, NanoActive TiO ₂)		Nantek
4091			4.55% NanoActive SiO ₂		Nantek
4132			Formulation unknown		METSS Corp
4133			Formulation unknown		METSS Corp
4134			Cu (krytox) ₂		METSS Corp
4135			Formulation unknown		METSS Corp
4136			Formulation unknown		Philip Bartram, APG-EA
4142	65.0%	14.0%	ICD#4136, 7.0%; ICD#3663, 7.0%	S-330 (ICD#2703, 7.0%)	Braue
4143	66.0%	20.0%	ICD#4136, 7.0%	S-330 (ICD#2703, 7.0%)	Braue
4144	17.0%	17.0%	ICD#3003 53.0%; ICD#3663 8.0%	S-330 (ICD#2703, 5.0%)	Braue
4145	65.0%	15.0%	ICD#4136, 5.0%	S-330 (ICD#2703, 15.0%)	Braue
4146	65.0%	20.0%	ICD#3663, 5.0%	S-330 (ICD#2703, 10.0%)	Braue
4148			NanoActive Titanium Oxide		Nantek
4149	60.0%	20.0%	ICD#4136, 10.0%	S-330 (ICD#2703, 10.0%)	Braue

ICD #	Percent Base Oil (PFPE = Y25)	Percent Teflon (PTFE = F5A)	Compound (% , ICD#, if any)	Other added compounds (% , ICD# if any)	PI/Supplier
4150	66.0%	20.0%	ICD#4136, 7.0%	S-330 (ICD#2703, 7.0%)	Braue
4151	60.0%	22.0%	ICD#3663, 16.0%	S-330 (ICD#2703, 2.0%)	Braue
4152	70.0%	13.0%	ICD#4136, 14.0%	S-330 (ICD#2703, 3.0%)	Braue
4153	60.0%	35.0%	ICD#4136, 4.0%	S-330 (ICD#2703, 1.0%)	Braue
4154	64.0%	18.0%	ICD#4136, 9.0%	S-330 (ICD#2703, 9.0%)	Braue
4155	60.0%	20.0%	ICD#3663, 10.0%	S-330 (ICD#2703, 10.0%)	Braue
4156	70.0%	10.0%	ICD#4136, 10.0%	S-330 (ICD#2703, 10.0%)	Braue
4158	68.0%		ICD#3003 11.0%; ICD#4136 18.0%	S-330 (ICD#2703, 3.0%)	Braue
4159	60.0%	20.0%	ICD#4148, 10.0%	S-330 (ICD#2703, 10.0%)	Braue
4160	64.0%	20.0%	ICD#4136, 8.0%	S-330 (ICD#2703, 8.0%)	Braue
4161	64.0%	20.0%	ICD#4136, 6.0%	S-330 (ICD#2703, 10.0%)	Braue
4162			Formulation unknown		
4163			Formulation unknown		
4164	60.0%	20.0%	ICD#4162, 10.0%	S-330 (ICD#2703, 10.0%)	Braue
4165	60.0%	20.0%	ICD#4163, 10.0%	S-330 (ICD#2703, 10.0%)	Braue
4166	54.5%	27.3%	ICD#4162, 18.2%		Braue
4167	54.3%	36.6%	ICD#4162, 9.0%		Braue
4168	60.0%	20.0%	ICD#4163, 20.0%		Braue

ICD #	Percent Base Oil (PFPE = Y25)	Percent Teflon (PTFE = F5A)	Compound (% , ICD#, if any)	Other added compounds (% , ICD# if any)	PI/Supplier
4169	50.0%	47.5%	ICD#4148, 2.5%		Braue
4170	60.0%	20.0%	ICD#4132, 10.0%	S-330 (ICD#2703, 10.0%)	Braue
4171	60.0%	10.0%	ICD#4132, 10.0%	S-330 (ICD#2703, 20.0%)	Braue
4172	55.0%	25.0%	ICD#4132, 10.0%	S-330 (ICD#2703, 10.0%)	Braue
4173	55.0%	25.0%	ICD#4133, 10.0%	S-330 (ICD#2703, 10.0%)	Braue
4174	56.0%	22.0%	ICD#4132, 11.0%	S-330 (ICD#2703, 11.0%)	Braue
4175	60.0%	20.0%	ICD#4133, 10.0%	S-330 (ICD#2703, 10.0%)	Braue
4176			ICD#3003 90.0%; ICD#4133 10.0%		Braue
4177			ICD#3003 90.0%; ICD#4132 10.0%		Braue
4178	50.4%	24.7%	ICD#3447, 12.4%	S-330 (ICD#2703, 12.4%)	Braue
4179	57.0%	14.0%	ICD#4133, 19.0%		Braue
4180	71.0%	26.0%	ICD#4133, 13.0%		Braue
4181	40.0%	30.0%	ICD#4134, 20.0%	S-330 (ICD#2703, 10.0%)	Braue
4182	40.0%	30.0%	ICD#4135, 20.0%	S-330 (ICD#2703, 10.0%)	Braue
4183	22.0%	22.0%	ICD#4134, 45.0%	S-330 (ICD#2703, 11.0%)	Braue
4184	22.0%	22.0%	ICD#4135, 45.0%	S-330 (ICD#2703, 11.0%)	Braue
4188	20.0%	25.0%	ICD#4134, 40.0%	S-330 (ICD#2703, 15.0%)	Braue
4189	13.0%	20.0%	ICD#4134, 47.0%	S-330 (ICD#2703, 20.0%)	Braue

ICD #	Percent Base Oil (PFPE = Y25)	Percent Teflon (PTFE = F5A)	Compound (% , ICD# , if any)	Other added compounds (% , ICD# if any)	PI/Suppli er
4204	20.0%	20.0%	ICD#4134, 40.0%	S-330 (ICD#2703, 20.0%)	Braue
4205	29.0%	49.0%	ICD#4134, 22.0%		Braue
4206	21.0%	17.0%	ICD#4134, 45.0%	S-330 (ICD#2703, 17.0%)	Braue
4207	18.0%	20.0%	ICD#4134, 45.0%	S-330 (ICD#2703, 17.0%)	Braue
4208	18.0%	20.0%	ICD#4134, 45.0%	S-330 (ICD#2703, 17.0%)	Braue
4209	40.0%	20.0%	ICD#4134, 20.0%	S-330 (ICD#2703, 20.0%)	Braue
4210	15.0%	20.0%	ICD#4134, 45.0%	S-330 (ICD#2703, 20.0%)	Braue
4211	13.0%	20.0%	ICD#4134, 47.0%	S-330 (ICD#2703, 20.0%)	Braue
4212	18.0%	20.0%	ICD#4134, 45.0%	S-330 (ICD#2703, 17.0%)	Braue

Table 17. Summary of penetration cell results for HD vapor at the USAMRICD. The table provides the time in minutes (with standard deviation) that it took for 1000 ng of HD vapor to break through candidate formulation. The table also provides the total ng (with standard deviation) of HD that breaks through the candidate formulation in 20 hours. The candidate formulations were spread at a thickness of 0.15 mm. The listed values are calculated by interpolation or extrapolation of the raw data generated from the MINICAMS analysis.

Date	Active	ICD #	T1000 min Avg	T1000 STD	ng in 20 h Avg	ng in 20 h STD
19980416	S-330	2650	54278	28806	10.8	3.6
19980420	S-330	2650	39736	11425	31.4	24.1
19980421	S-330	2701	31145	20206	18.8	6.9
19980422	S-330	2701	48099	28150	11	2.8
19980617	S-330	2701	NA	NA	65.5	21
19980624	S-330	2701	NA	NA	16.4	3.1
20020423	10% S-330	2701	58584	31794	6.43	6.24
20020508	10% S-330	2701	1058	56.9	1329	133
20020514	10% S-330	2701	1074	535	1782	984
19980512	Iodobenzene Diacetate	2902	39047	24679	14.4	6.1
19980513	Iodobenzene Diacetate	2902	89289	10598	4	1.9
19980610	Mg/Ni	2954	NA	NA	4673	69.6
19980505	None	3004	NA	NA	2789	176
19980506	None	3004	NA	NA	2259	178
19980506	None	3004	NA	NA	2439	209
19990727	None	3004	587	579	3516	211
19990908	None	3004	447	86.6	7811	444
19990915	None	3004	539	47.1	3949	309
20010523	None	3004	161	8.00	8147	376
20010530	None	3004	165	11.0	8013	514
20010612	None	3004	155	9.87	8154	431
20010621	None	3004	500	53.2	3666	235
20020131	None	3004	506	219	3404	983
20020306	None	3004	270	30.9	5352	251
20020326	None	3004	482	51.5	2856	95.1
20020603	None	3004	543	21.8	3864	196
19980608	K5Co(III)W12O4	3051	856	47.6	1943	116
19981109	Mg/Ni	3107	747	138	2915	521
19990111	Mg ₂ NiH ₂	3108	866	145	2989	386
19981117	TiFeMn	3109	921	303	1944	1166
19981130	CaNi ₅ H ₃	3110	620	95	3562	275
19981102	TiFeMn	3111	NA	NA	2416	103

Date	Active	ICD #	T1000 min Avg	T1000 STD	ng in 20 h Avg	ng in 20 h STD
19990114	TiFeMn	3111	555	145	4365	456
19981201	CaNi ₅ H ₃	3112	705	106	3081	364
19981027	K ₅ Co(III)W ₁₂ O ₄₀	3115	NA	NA	2151	229
19981103	K ₅ Co(III)W ₁₂ O ₄₀	3115	944	103	1751	274
19981015	ethanolamine	3116	783	174	2589	152
19981028	ethanolamine	3121	NA	NA	1902	520
19990119	dendritic polymer	3126	2290	775	257	230
19990121	MgO	3127	299	55	NA	NA
19990120	ZnO	3128	258	60	NA	NA
19990923	ZnO	3128	137	5.8	11833	687
19981208	None	3149	497	148	3919	1555
19981214	Ambergard XE555	3150	260	47	7193	491
19990113	Ambergard XE555	3151	965	368	1454	1254
19991013	Ambergard XE555	3151	3560	2034	130	84.4
19981207	HPV ₂ MoO ₄₀ *10H ₂ O	3152	869	148	1835	355
19981202	HPV ₂ MoO ₄₀ *10H ₂ O	3153	675	118	2788	410
19990901	polysilsesquioxane	3172	2409	516	307	115
19990902	polysilsesquioxane	3173	664	62	3608	239.6
19990927	polysilsesquioxane	3189			2849	233.1
19990928	polysilsesquioxane	3190	2901	2042	496	348.2
19990929	polysilsesquioxane	3191	18216	9368	56	21.8
19990930	polysilsesquioxane	3192	1848	1452	1369	1318
19990315	dendritic polymer	3215	1568	482	733	426
19990323	dendritic polymer	3215	NA	NA	1293	580
19990316	dendritic polymer	3216	1549	394	507	394
19990621	Iodine	3226	406	90	4821	388
19990413	dendritic polymer	3227	60418	62719	15.6	15.4
19990920	dendritic polymer	3227	708	24	2877	218
19990623	Iodine	3237	485	87.9	3919	173
19990422	dendritic polymer	3244	25769	25333	183	224
19990402	dendritic polymer	3245	144315	133236	9.6	3.5
19990428	dendritic polymer	3246	593	108	2639	282
19990504	dendritic polymer	3248	914	74.2	1784	128
19990507	IBDA/dendritic polymer	3251	14723	9032	15.6	3.5
19990510	IBDA	3252	13385	12501	229	318
19990512	IBDA/dendritic polymer	3253	2035	584	224	106
19990624	TiFeO	3265	467	30	4335	143.8

Date	Active	ICD #	T1000 min Avg	T1000 STD	ng in 20 h Avg	ng in 20 h STD
19990802	ZrNiO	3266	703	150	3010	679
19990803	ZrNiO	3267	974	484	1162	389.8
19990804	TiFeO	3268	693	62	3002	209.9
19990805	dendritic polymer	3270	787	187	1923	1259
19990818	dendritic polymer	3271	881	175	2093	598
19990819	dendritic polymer	3272	552	108	4039	754
19990823	dendritic polymer	3273	787	85	2117	971
19990824	K ₇ PW ₁₀ Ti ₂ O ₄₀	3277	629	55	3387	226
19990825	H ₂ PV ₂ Mo ₁₀ O ₄₀	3278	651	117	3191	530
19990826	K ₅ Co(III)W ₁₂ O ₄₀	3279	685	146	3009	502
19990825	HPV ₂ MoO ₄₀ *10H ₂ O	3280	NA	NA	133	65.4
20010627	None	3658	6666	14601	7792	4227
20010619	Zn/Pd alloy	3660	129	3.29	9561	45.4
20010710	Zn/Pd alloy	3670	608	138.8	3440	589
20010802	Zn/Pd alloy	3671	720	52.3	2696	160
20020529	none	Petroleum jelly	427	30.2	3777	137

Table 18. Summary of results in the weanling pig HD vapor model. The data are order by chronological date. The table provides references for the dates of experiments, laboratory notebook numbers, pages in the notebook, weanling pig animal numbers, ICD numbers of candidate formulations, the thickness of applied TSP or aTSP, the duration time of the saturated HD vapor cup exposure (1.4 mg/L), the mean a* erythema values from reflectance color meter measurements with the corresponding standard error of the mean and standard deviation (N-1 formula), and the percent of positive control ([mean a* for candidate/mean a* for positive control] * 100). The smaller the percent of control value, the better protection the candidate formulation provided.

Dates	Notebook	Page #	Pig #	ICD #	aTSP Thickness	HD Vapor Exposure	Erythema Mean a* value	Erythema a* SEM	Erythema a* STDEV	% of Control
16-Jul-96	021-96	65-119	51-56	PC	None	15 min	7.71	1.26	3.1	100
			51-56	2289	0.2	15 min	4.16	0.69	1.7	54.0
			51-56	2701	0.1	15 min	0.98	0.26	0.6	12.7
			51-56	2701	0.1	30 min	1.98	0.51	1.2	25.7
			51-56	2701	0.1	45 min	3.90	0.78	1.91	50.58
			51-56	2701	0.1	60 min	5.97	0.96	2.35	77.43
16-Jul-96	021-96	120-155	57-62	PC	None	15 min	7.87	0.36	0.88	100.00
			57-62	2289	0.2	15 min	3.57	0.61	1.48	45.36
			57-62	1511	0.2	15 min	8.49	1.43	3.50	107.88
			57-62	2373	0.2	15 min	11.00	0.26	0.63	139.77
			57-62	2835	0.2	15 min	11.07	0.77	1.88	140.66
			57-62	2837	0.2	15 min	5.84	0.47	1.15	74.21
7-Oct-96	048-96	31-66	63-68	PC	None	15 min	8.51	0.91	2.23	100.00
			63-68	2289	0.2	15 min	5.42	1.05	2.57	63.69
			63-68	2837+2289	0.2	15 min	5.56	0.54	1.34	65.33
			63-68	2837+2289	0.1	15 min	8.66	0.91	2.23	101.76
			63-68	2837+2289	0.2	30 min	9.60	0.99	2.43	112.81
				2837+2289	0.1	30 min	10.70	0.65	1.59	125.73
23-Oct-96	048-96	68-106	69-74	PC	None	15 min	5.50	1.04	2.55	100.00
			69-74	2289	0.2	15 min	6.66	0.94	2.31	121.09
			69-74	2730	0.1	15 min	2.48	0.58	1.43	45.09

Dates	Notebook	Page #	Pig #	ICD #	aTSP Thickness	HD Vapor	Erythema Mean a*	Erythema a* SEM	Erythema a* STDEV	% of Control
			69-74	2730	0.1	30 min	4.65	0.77	1.88	84.55
			69-74	2730	0.1	45 min	5.55	0.57	1.39	100.91
			69-74	2730	0.1	60 min	7.48	0.61	1.50	136.00
20-Nov-96	076-96	3-15	75-81	PC	None	15 min	7.95	0.67	1.64	100.00
			75-81	2289	0.2	15 min	8.53	0.57	1.39	107.30
			75-81	2850	0.1	15 min	10.58	0.58	1.42	133.08
			75-81	2850	0.1	30 min	11.29	0.70	1.72	142.01
			75-81	2850	0.1	45 min	10.74	0.73	1.78	135.09
			75-81	2850	0.1	60 min	10.14	0.87	2.12	127.55
18-Dec-96	076-96	5, 16-46	82-87	PC	None	15 min	6.85	0.42	1.02	100.00
			82-87	2289	0.2	15 min	7.12	0.33	0.81	103.94
			82-87	2836	0.1	15 min	2.52	0.54	1.32	36.79
			82-87	2836	0.1	30 min	5.42	0.82	2.02	79.12
			82-87	2836	0.1	45 min	8.77	0.51	1.24	128.03
			82-87	2836	0.1	60 min	9.67	0.60	1.48	141.17
18-Dec-96	076-96	49	88	PC	None	15 min	9.19			100.00
				2289	0.2	15 min	7.76			84.44
				PC	None	15 min	9.78			100.00
				2289	0.2	15 min	7.82			79.96
				PC	None	15 min	8.37			100.00
				2289	0.2	15 min	7.44			88.89
1/7/1997	076-96	71-104	89-94	PC	none	15 min	4.72	0.57	1.40	100.00
				old 2289	0.2	15 min	2.75	0.49	1.21	58.26
				new 2289	0.2	15 min	5.82	0.61	1.49	123.31
22-Jan-97	076-96	105-129	95-98	PC	none	15 min	5.79	0.90	1.80	100.00
				2289 (R1)	0.2	15 min	7.66	0.78	1.55	132.30
				2289 (R2)	0.2	15 min	8.07	0.22	0.44	139.38
				2289 (P1)	0.2	15 min	8.85	0.40	0.81	152.85
				2289	0.2	15 min	7.62	0.56	1.11	131.61

Dates	Notebook	Page #	Pig #	ICD #	aTSP Thickness	HD Vapor	Erythema Mean a*	Erythema a* SEM	Erythema a* STDEV	% of Control
				(Iowa)						
				1511	0.2	15 min	8.73	0.36	0.73	150.78
4-Feb-97	076-96	130-141	99-100	PC	none	15 min	5.70	0.58	1.15	100.00
				2289 (A)	0.2	15 min	9.91	0.61	1.22	173.86
				2289 (B)	0.2	15 min	9.96	0.70	1.40	174.74
18-Mar-97	011-97	6-37	103-108	PC	None	15 min	6.10	0.97	2.38	100.00
				2650	0.1	30 min	1.23	0.99	2.43	20.16
				2880	0.2	15 min	6.61	0.94	2.30	108.36
				2881	0.2	15 min	6.86	0.83	2.03	112.46
				2882	0.2	15 min	7.18	0.51	1.26	117.70
				2883	0.2	15 min	7.60	0.58	1.42	124.59
25-Mar-97	011-97	38-68	109-114	PC	None	15 min	3.79	0.82	2.02	100.00
				2650	0.1	30 min	0.54	0.18	0.44	14.25
				2897	0.2	15 min	5.97	0.88	2.14	157.52
				2898	0.2	15 min	1.64	0.53	1.30	43.27
				2900	0.2	15 min	5.88	0.49	1.19	155.15
				2901	0.2	15 min	5.71	2.04	0.83	150.66
16-Apr-97	011-97	81-111	115-120	PC	None	15 min	5.10	1.54	3.78	100.00
				2650	0.1	30 min	0.59	0.50	1.23	11.57
				2881	0.2	15 min	6.50	1.20	2.94	127.45
				2898	0.2	15 min	2.75	1.12	2.74	53.92
				2914	0.2	15 min	6.76	0.99	2.42	132.55
				2915	0.2	15 min	7.68	1.27	3.12	150.59

- NOTES:
1. Pigs 63-68: ICD 2837 was applied as a 2% (w/v) ethanol solution at the rate of 25 µl per 0.5 cm² and allowed to dry for 2 hr.
 2. Pigs 95-98: 2289 (R1) = F5A lot # 140089 Y25 lot #0306RG; 2289 (R2) = F5A lot # 5N0414 Y25 lot #0306RG; 2289 (P1) = F5A lot # 140089 Y25 lot #5167 with 20% lot #0306RG.
 3. Pigs 99-100: 2289 (A) = F5A lot # 710537 Y25 lot #VT590; 2289 (B) = Prepared by Dr Lou lot # WRAST02/16-2.
 4. Pigs 109-114: ICD 2897- 2901 are all like 2289 using different lots of F5A.
 5. Pigs 115-120: All TSP formulations like 2289 using same F5A lot # 480324, except mixed differently.

Table 19a. Summary of results in the haired guinea pig and weanling pig HD vapor model. All animals were weanling pigs except for the first four experiments dated 12 Feb 97, 19 Feb 97, 4 Mar 97, and 11 Mar 97. The table provides references for the dates of experiments, weanling pig animal numbers, ICD numbers of candidate formulations, the thickness of applied TSP or aTSP, the duration time of the saturated HD vapor cup exposure (1.4 mg/L), the mean a* erythema values from reflectance color meter measurements with the corresponding standard error of the mean, and the percent of positive control ([mean a* for candidate/mean a* for positive control] * 100), the mean histology score with corresponding standard error of the mean, and the percent of positive control ([mean histology score for candidate/mean histology score for positive control] * 100). The smaller the percent of control value, the better protection the candidate formulation provided. Based on statistical analysis of either the erythema data or the histology data, there is a column stating whether the candidate formulation passed the screen (meaning it provided significant protection compared to positive control animals) failed the screen (meaning it provided equivalent protection compared to positive control animals), or failed worse (meaning it produced significantly worse damage compared to positive control animals).

DATE Experiment Started	PIG #	ICD #	aTSP Thickness	HD Vapor Exposure		Erythema Mean a* Value	Erythema Mean a* SEM	Percent of Control	P/F/W		Histo- logy Mean SCORE	Histo- logy SEM	Percent of Control	P/F/W
12-Feb-97	258-265	PC	None	5 min		5.86	0.84	100.00						
	GP	1511	0.1	5 min		4.03	0.85	68.77	F					
		2289	0.1	5 min		4.74	0.65	80.89	F					
		NC	0.1	5 min		-0.16	0.32	-2.73						
19-Feb-97	266-273	PC	None	5 min		5.47	0.59	100.00						
	GP	1511	0.1	5 min		2.69	0.44	49.18	P					
		2289	0.1	5 min		2.93	0.60	53.56	P					
		NC	0.1	5 min		-0.26	0.66	-4.75						
4-Mar-97	274-281	PC	None	5 min		5.36	0.62	100.00						
	GP	1511	0.1	5 min		2.39	0.56	44.59	P					

DATE Experiment Started	PIG #	ICD #	aTSP Thickness	HD Vapor Exposure		Erythema Mean a* Value	Erythema Mean a* SEM	Percent of Control	P/F/W		Histo- logy Mean SCORE	Histo- logy SEM	Percent of Control	P/F/W
		2883	0.1	5 min		2.71	0.48	50.56	P					
		NC	0.1	5 min		-0.84	0.33	-15.67						
11-Mar-97	282-289	PC	None	5 min		3.89	0.54	100.00						
	GP	1511	0.1	5 min		2.11	0.55	54.24	P					
		2883	0.1	5 min		2.19	0.60	56.30	P					
		NC	0.1	5 min		-1.43	0.41	-36.76						
13-May-97	121-126	PC	None	15 min		5.44	0.74	100.00						
		2650	0.1	30 min		1.19	0.26	21.88	P					
		2927	0.2	15 min		7.90	0.61	145.22	F/W					
		2928	0.2	15 min		8.56	0.62	157.35	F/W					
		2930	0.2	15 min		8.08	0.50	148.53	F/W					
		2933	0.2	15 min		8.32	0.43	152.94	F/W					
20-May-97	127-132	PC	None	15 min		6.10	1.49	100.00						
		2650	0.1	30 min		0.85	0.48	13.93	P					
		2926	0.2	15 min		1.09	0.22	17.87	P					
		2929	0.2	15 min		5.99	1.13	98.20	F					
		2931	0.2	15 min		8.16	1.14	133.77	F					
		2932	0.2	15 min		8.30	1.16	136.07	F					
12-Aug-97	133-138	PC	None	15 min		3.28	1.02	100.00						
		2650	0.1	30 min		0.23	0.41	7.01	P					
		2956	0.2	15 min		4.53	0.93	138.11	F					
		2957	0.2	15 min		1.83	0.56	55.79	F					
		2958	0.2	15 min		5.98	0.74	182.32	F/W					
		2926	0.2	15 min		1.16	0.51	35.37	P					

DATE Experiment Started	PIG #	ICD #	aTSP Thickness	HD Vapor Exposure		Erythema Mean a* Value	Erythema Mean a* SEM	Percent of Control	P/F/W		Histo- logy Mean SCORE	Histo- logy SEM	Percent of Control	P/F/W
14-Apr-98	139-144	PC	None	15 min		5.97	0.88	100.00						
		2650	0.1	30 min		1.24	0.24	20.77	P					
		2902	0.1	15 min-30 min		1.63	0.31	27.30	P					
		2951	0.1	15 min-30 min		8.80	0.95	147.40	F					
		2954	0.1	15 min-30 min		7.98	0.90	133.67	F					
		3051	0.1	15 min-30 min		11.28	0.75	188.94	F/W					
5-May-98	145-150	PC	None	15 min		5.01	1.27	100.00						
		2650	0.1	30 min		0.87	0.82	17.37	P					
		2902	0.1	15 min		1.60	1.03	31.94	P					
		2902	0.1	30 min		3.35	1.28	66.87	F					
		2902	0.1	45 min		6.73	1.16	134.33	F					
		2902	0.1	60 min		7.69	0.95	153.49	F					
17-Feb-99	151-154	PC	None	15 min		1.48	0.33	100.00						
		2650	0.1	30 min		0.03	0.23	2.03	P					
		3126	0.1	15 min		8.72	0.27	589.19	F/W					
		3126	0.1	30 min		9.09	0.46	614.19	F/W					
		3126	0.1	45 min		10.15	0.43	685.81	F/W					
		3126	0.1	60 min		9.86	0.45	666.22	F/W					
23-Feb-99	155-156	PC	None	0 min		1.30	0.51	100.00						
		PC	None	10 min		3.59	1.72	275.88						
		PC	None	15 min		8.58	0.64	659.34						
		PC	None	20 min		9.75	0.65	749.25						
		PC	None	25 min		9.12	0.33	700.84						

DATE Experiment Started	PIG #	ICD #	aTSP Thickness	HD Vapor Exposure		Erythema Mean a* Value	Erythema Mean a* SEM	Percent of Control	P/F/W		Histo- logy Mean SCORE	Histo- logy SEM	Percent of Control	P/F/W
		PC	None	30 min		9.66	0.49	742.33						
23-Mar-99	163-164	PC	None	15 min		5.33	3.11	100.00						
		2650	0.1	30 min		1.21	0.25	22.78	P					
		3215	0.1	15 min		12.34	0.37	231.60	F/W					
		3215	0.1	30 min		12.88	0.32	241.85	F/W					
		3215	0.1	45 min		12.66	0.37	237.63	F/W					
		3215	0.1	60 min		11.94	0.96	224.11	F/W					
24-Mar-99	165-166	PC	None	15 min		3.15	0.214	100.00						
		2650	0.1	30 min		0.70	0.16	22.17	P					
		3216	0.1	15 min		10.01	1.256	318.07	F/W					
		3216	0.1	30 min		11.93	0.374	379.00	F/W					
		3216	0.1	45 min		12.08	1.084	383.61	F/W					
		3216	0.1	60 min		11.80	0.415	374.71	F/W					
6-Apr-99	167-172	PC	None	15 min		5.58	1.00	100.00						
		2650	0.1	30 min		1.73	0.36	30.97	P					
		3227	0.1	15 min		6.39	1.56	114.44	F					
		3227	0.1	30 min		8.26	1.35	147.99	F					
		3227	0.1	45 min		8.82	1.11	158.06	F					
		3227	0.1	60 min		9.08	1.03	162.74	F/W					
14-Apr-99	173-178	PC	None	15 min		5.60	1.70	100.00						
		2650	0.1	30 min		1.80	0.60	32.16	P					
		3245	0.1	15 min		3.62	0.77	64.64	F					
		3245	0.1	30 min		5.07	1.10	90.54	F					
		3245	0.1	45 min		5.91	0.99	105.54	F					
		3245	0.1	60 min		6.77	1.42	120.89	F					

DATE Experiment Started	PIG #	ICD #	aTSP Thickness	HD Vapor Exposure		Erythema Mean a* Value	Erythema Mean a* SEM	Percent of Control	P/F/W		Histo- logy Mean SCORE	Histo- logy SEM	Percent of Control	P/F/W
20-Apr-99	179-184	PC	None	15 min		3.26	0.39	100.00						
		2650	0.1	30 min		1.40	0.36	42.94	F					
		3244	0.1	15 min		1.16	0.39	35.58	F					
		3244	0.1	30 min		1.92	0.43	58.90	F					
		3244	0.1	45 min		4.14	1.04	126.99	F					
		3244	0.1	60 min		6.00	0.70	184.05	F/W					
11-Mar-99	161-162	PC	None	15 min		5.85	1.40	100.00						
27-Apr-99	185-188	DEET	0.15	15 min		7.16	1.21	122.48	F					
		DEET+2701	0.1	15 min		1.95	0.61	33.39	P					
		DEET+2701	0.1	30 min		2.31	0.94	39.43	P					
		DEET+2701	0.1	45 min		4.16	1.12	71.09	F					
		DEET+2701	0.1	60 min		7.12	1.19	121.76	F					
4-May-99	189-192	PC	None	15 min		2.93	0.70	100.00						
6-May-99	193-194	2650	0.1	30 min		0.54	0.25	18.33	F					
		3004	0.1	15 min		4.53	1.87	154.64	F					
		DEET+3004	0.1	15 min		3.57	0.80	121.84	F					
		DEET+3249	0.1	15 min		1.32	0.24	45.05	F					
		DEET+3250	0.1	15 min		1.88	0.50	64.06	F					
10-Aug-99	195-200	PC	None	15 min		5.12	1.10	100.00						
		2650	0.1	30 min		1.21	0.37	23.66	P					
		3251	0.1	15 min		9.61	0.44	187.64	F/W					
		3252	0.1	15 min		10.16	0.17	198.38	F/W					
		3253	0.1	15 min		9.55	0.77	186.49	F/W					
		3284	0.1	15 min		8.90	0.84	173.69	F/W					

DATE Experiment Started	PIG #	ICD #	aTSP Thickness	HD Vapor Exposure		Erythema Mean a* Value	Erythema Mean a* SEM	Percent of Control	P/F/W		Histo- logy Mean SCORE	Histo- logy SEM	Percent of Control	P/F/W
31-Aug-99	201-206	PC	None	15 min		3.86	1.31	100.00						
		2650	0.1	30 min		0.15	0.40	3.91	P					
		2902	0.1	15 min		2.42	1.01	62.72	F					
		3151	0.1	15 min		-0.16	0.46	-4.04	P					
		3109	0.1	15 min		7.73	0.93	200.18	F/W					
		3290	0.1	15 min		6.53	1.05	169.27	F/W					
8-Sep-99	207-212	PC	None	15 min		7.93	1.38	100.00						
		2650	0.1	30 min		1.64	0.40	20.68	P					
		3247	0.2	15 min		10.11	0.77	127.43	F					
		3248	0.2	15 min		9.85	0.66	124.21	F					
		3299	0.2	15 min		2.81	0.75	35.37	P					
		3300	0.2	15 min		0.50	0.37	6.34	P					
28-Sep-99	213, 215,	PC	None	15 min		4.99	1.05	100.00						
	And 216	2650	0.1	30 min		0.28	0.57	5.61	P					
		3305	0.1	15 min		5.62	1.35	112.63	F					
		3280	0.1	15 min		8.66	0.86	173.55	F/W					
		3294	0.1	15 min		8.45	1.63	169.34	F/W					
		3289	0.1	15 min		8.51	1.15	170.54	F/W					
30-Sep-99	217-218	PC	None	15 min		4.09	2.26	100.00						
		2650	0.1	30 min		-0.45	0.70	-11.11	F					
		3305	0.2	15 min		-0.17	0.97	-4.09	F					
		3280	0.2	15 min		2.91	0.81	71.20	F					
		3294	0.2	15 min		6.35	1.59	155.44	F					
		3289	0.2	15 min		5.48	0.28	134.16	F					

DATE Experiment Started	PIG #	ICD #	aTSP Thickness	HD Vapor Exposure		Erythema Mean a* Value	Erythema Mean a* SEM	Percent of Control	P/F/W		Histo- logy Mean SCORE	Histo- logy SEM	Percent of Control	P/F/W
2-Nov-99	219-224	PC		15 min		need to redo analysis								
		2650	0.1	30 min										
		3299	0.1	15 min										
		3300	0.1	15 min										
		3172	0.1	15 min										
		3308	0.1	15 min										
16-Nov-99	225-230	PC		15 min		5.71	1.71	100.00						
		2650	0.1	30 min		0.85	0.37	14.92	P					
		3151	0.1	15 min		0.76	0.48	13.29	P					
		3151	0.1	30 min		5.35	1.12	93.70	F					
		3151	0.1	45 min		8.47	0.78	148.34	F					
		3151	0.1	60 min		8.58	1.07	150.26	F					
17-Jan-01	237-242	PC	None	30 min		1.98	1.09	100.00			1.17	0.45	100.00	
		2650	0.1	30 min		-0.17	0.36	-8.59	F		0.21	0.10	17.95	F
		3004	0.1 normal cleaning	15 min		6.80	1.30	343.43	F/W		4.71	0.80	402.56	F/W
		3004	0.1 special cleaning	15 min		7.04	1.01	355.56	F/W		4.46	0.74	381.20	F/W
		3004	0.2 normal cleaning	15 min		6.90	0.81	348.48	F/W		4.33	0.46	370.09	F/W

DATE Experiment Started	PIG #	ICD #	aTSP Thickness	HD Vapor Exposure		Erythema Mean a* Value	Erythema Mean a* SEM	Percent of Control	P/F/W		Histo- logy Mean SCORE	Histo- logy SEM	Percent of Control	P/F/W
		3004	0.2 special cleaning	15 min		6.53	1.08	329.80	F/W		4.33	0.74	370.09	F/W
6-Feb-01	243-248	PC	None	15 min		4.89	0.42	100.00			2.25	0.39	100.00	
		2650	0.1	30 min		0.23	0.56	4.70	P		0.00	0.00	0.00	P
		3004	0.1	30 min		8.73	0.25	178.53	F/W		7.33	0.27	325.78	F/W
		3450	0.1	30 min		6.04	0.57	123.52	F		4.25	0.63	188.89	F/W
		3454	0.1	30 min		6.49	0.50	132.72	F		4.00	0.46	177.78	F/W
		3520	0.1	30 min		4.82	0.68	98.57	F		2.38	0.49	105.78	F
13-Feb-01	249-254	PC	None	15 min		6.85	1.20	100.00			2.83	0.42	100.00	
		2650	0.1	30 min		0.40	0.53	5.84	P		0.08	0.08	2.83	P
		3378	0.1	30 min		7.31	0.63	106.72	F		6.63	0.69	234.28	F/W
		3380	0.1	30 min		7.58	0.42	110.66	F		5.79	0.40	204.59	F/W
		3519	0.1	30 min		7.14	0.62	104.23	F		4.92	0.76	173.85	F/W
		3523	0.1	30 min		7.49	0.50	109.34	F		5.21	0.72	184.10	F/W
21-Feb-01	255-260	PC	None	15 min		6.29	0.95	100.00			2.29	0.69	100.00	
		2650	0.1	30 min		0.22	0.23	3.50	P		0.00	0.00	0.00	P
		3369	0.1	30 min		8.09	0.86	128.62	F		7.21	0.60	314.85	F/W
		3379	0.1	30 min		7.83	0.66	124.48	F		7.13	0.33	311.35	F/W
		3479	0.1	30 min		9.21	0.72	146.42	F/W		7.96	0.04	347.60	F/W
		3551	0.1	30 min		8.01	0.64	127.34	F		5.33	0.45	232.75	F/W
20-Mar-01	261-266	PC	None	15 min		8.05	0.58	100.00			3.92	0.48	100.00	
		2650	0.15	30 min		0.26	0.33	3.23	P		0.21	0.21	5.36	P
		3524	0.15	30 min		8.45	0.84	104.97	F		5.63	0.59	143.62	F

DATE Experiment Started	PIG #	ICD #	aTSP Thickness	HD Vapor Exposure		Erythema Mean a* Value	Erythema Mean a* SEM	Percent of Control	P/F/W		Histo- logy Mean SCORE	Histo- logy SEM	Percent of Control	P/F/W
		3552	0.15	30 min		7.54	1.21	93.66	F		4.83	0.90	123.21	F
		3553	0.15	30 min		9.05	0.32	112.42	F		7.54	0.29	192.35	F/W
		3585	0.15	30 min		9.45	0.45	117.39	F		7.13	0.51	181.89	F/W
3-Apr-01	267-272	PC	None	15 min		5.89	0.65	100.00			2.71	0.41	100.00	
		2650	0.15	30 min		0.22	0.06	3.74	P		0.04	0.04	1.48	P
		2701	0.15	30 min		0.23	0.13	3.90	P		0.08	0.05	2.95	P
		3454	0.15	30 min		9.12	0.80	154.84	F/W		7.33	0.24	270.48	F/W
		3520	0.15	30 min		5.77	1.02	97.96	F		4.38	0.78	161.62	F
		3523	0.15	30 min		6.90	0.58	117.15	F		5.58	0.76	205.90	F/W
24-Apr-01	273-278	PC	None	15 min		8.05	0.93	100.00			4.17	0.95	100.00	
		2650	0.15	30 min		0.79	0.42	9.81	P		0.08	0.08	1.92	P
		3300	0.15	30 min		3.01	0.86	37.39	P		1.17	0.69	28.06	P
		3610	0.15	30 min		9.34	1.02	116.02	F		6.88	0.46	164.99	F/W
		3611	0.15	30 min		9.94	0.56	123.48	F		8.00	0.00	191.85	F/W
		3633	0.15	30 min		9.13	0.65	113.42	F		6.08	0.43	145.80	F/W
8-May-01	279-284	PC	None	15 min		11.01	0.45	100.00			5.92	0.49	100.00	
		2650	0.15	30 min		1.62	0.35	14.71	P		0.00	0.00	0.00	P
		3004	0.15	30 min		11.24	0.52	102.09	F		7.38	0.40	124.66	F
		3530	0.15	30 min		10.87	0.28	98.73	F		6.71	0.33	113.34	F
		3531	0.15	30 min		10.27	0.52	93.28	F		5.96	0.77	100.68	F
		3533	0.15	30 min		8.02	0.64	72.84	P		4.04	0.93	68.24	F
22-May-01	285-290	PC	None	15 min		5.27	1.64	100.00			2.38	0.90	100.00	
		PC	None	30 min		9.68	0.70	100.00			6.00	0.86	100.00	
		1511	0.2	15 min		8.25	1.60	156.55	F		4.54	0.97	190.76	F/W
		1511	0.2	30 min		10.37	0.63	107.13	F		7.04	0.62	117.33	F
		3004	0.2	15 min		8.68	1.08	164.71	F/W		5.33	0.81	223.95	F/W

DATE Experiment Started	PIG #	ICD #	aTSP Thickness	HD Vapor Exposure		Erythema Mean a* Value	Erythema Mean a* SEM	Percent of Control	P/F/W		Histo- logy Mean SCORE	Histo- logy SEM	Percent of Control	P/F/W
		3004	0.2	30 min		10.04	0.36	103.72	F		7.46	0.28	124.33	F
12-Jun-01	291-296	PC	None	30 min		8.52	0.50	100.00			7.58	0.27	100.00	
		2650	0.15	30 min		0.83	0.47	9.74	P		0.38	0.24	5.01	P
		3151	0.15	30 min		2.71	0.87	31.81	P		2.67	0.52	35.22	P
		3370	0.15	30 min		8.46	0.82	99.30	F		7.67	0.33	101.19	F
		3470	0.15	30 min		4.91	0.99	57.63	P		2.75	0.55	36.28	P
		3471	0.15	30 min		5.48	1.29	64.32	F		2.79	0.46	36.81	P
26-Jun-01	297-302	PC	None	30 min		9.10	0.44	100.00			5.38	0.56	100.00	
		2650	0.15	30 min		0.63	0.25	6.92	P		0.00	0.00	0.00	P
		3667	0.15	30 min		9.17	0.30	100.77	F		5.63	0.51	104.65	F
		3664	0.15	30 min		8.66	0.43	95.16	F		5.92	0.57	110.04	F
		3665	0.15	30 min		7.03	0.54	77.25	P		4.33	0.63	80.48	F
		3532	0.15	30 min		8.67	0.47	95.27	F		5.29	0.28	98.33	F
25-Jul-01	303-308	PC	None	30 min		8.91	0.65	100.00			5.13	0.65	100.00	
		2650	0.15	30 min		0.52	0.24	5.84	P		0.04	0.04	0.78	P
		3548	0.15	30 min		6.81	0.94	76.43	F		3.63	0.64	70.76	F
		3549	0.15	30 min		8.51	0.72	95.51	F		5.50	0.74	107.21	F
		3551	0.15	30 min		6.91	1.25	77.55	F		3.71	0.55	72.32	F
		3630	0.15	30 min		9.70	0.42	108.87	F		7.63	0.23	148.73	F/W
7-Aug-01	309-314	PC	None	30 min		9.31	0.62	100.00			6.25	0.83	100.00	
		2650	0.15	30 min		0.11	0.27	1.18	P		0.00	0.00	0.00	P
		2902	0.15	30 min		4.75	1.23	51.02	P		2.75	0.63	44.00	P
		3600	0.15	30 min		10.06	0.13	108.06	F		7.17	0.23	114.72	F
		3631	0.15	30 min		9.54	0.50	102.47	F		7.63	0.28	122.08	F
		3668	0.15	30 min		9.62	0.55	103.33	F		6.54	0.56	104.64	F

DATE Experiment Started	PIG #	ICD #	aTSP Thickness	HD Vapor Exposure		Erythema Mean a* Value	Erythema Mean a* SEM	Percent of Control	P/F/W		Histo- logy Mean SCORE	Histo- logy SEM	Percent of Control	P/F/W
4-Sep-01	315-320	PC	None	30 min		6.50	1.03	100.00			3.04	0.62	100.00	
		2650	0.15	30 min		5.19	0.62	79.85	F		2.63	0.70	86.51	F
		3709	0.15	30 min		8.86	0.65	136.31	F		5.67	0.74	186.51	F/W
		3666	0.15	30 min		9.82	0.34	151.08	F/W		6.88	0.75	226.32	F/W
		3378	0.15	30 min		7.51	0.93	115.54	F		5.25	0.61	172.70	F/W
		3718	0.15	30 min		0.07	0.70	1.08	P		0.08	0.08	2.63	P
18-Sep-01	321-326	PC	None	30 min		9.71	0.55	100.00			6.54	0.60	100.00	
		3718	0.15	30 min		2.26	0.56	23.27	P		0.96	0.58	14.68	P
		PC	None	45 min		10.41	0.56	100.00			6.33	0.84	100.00	
		3718	0.15	45 min		4.61	0.40	44.28	P		2.00	0.77	31.60	P
		PC	None	60 min		10.12	0.47	100.00			7.17	0.55	100.00	
		3718	0.15	60 min		7.68	1.22	75.89	P		0.83	0.52	11.58	P
2-Oct-01	327-330	PC	None	30 min		9.44	0.49	100.00			6.25	0.90	100.00	
		2650	0.15	30 min		0.86	0.42	9.11	P		0.00	0.00	0.00	P
		3724	0.15	30 min		9.46	0.50	100.21	F		8.00	0.00	128.00	F/W
		3726	0.15	30 min		9.13	0.66	96.72	F		8.00	0.00	128.00	F/W
		3728	0.15	30 min		8.81	0.87	93.33	F		7.56	0.30	120.96	F/W
		3729	0.15	30 min		9.05	0.96	95.87	F		6.06	1.05	96.96	F
4-Oct-01	331-332	PC	None	30 min		9.19	0.70	100.00			4.25	0.50	100.00	
		2650	0.15	30 min		0.08	0.67	0.87	P		0.00	0.00	0.00	P
		3725	0.15	30 min		7.98	1.26	86.83	F		6.63	0.63	156.00	F/W
		3727	0.15	30 min		8.84	0.58	96.19	F		7.50	0.25	176.47	F/W
		3742	0.15	30 min		-0.84	0.42	-9.14	P		0.13	0.13	3.06	P
		3743	0.15	30 min		2.70	0.58	29.38	P		0.75	0.75	17.65	P
16-Oct-01	333-338	PC	None	30 min		8.17	1.03	100.00			4.63	1.10	100.00	

DATE Experiment Started	PIG #	ICD #	aTSP Thickness	HD Vapor Exposure		Erythema Mean a* Value	Erythema Mean a* SEM	Percent of Control	P/F/W		Histo- logy Mean SCORE	Histo- logy SEM	Percent of Control	P/F/W
		2650	0.15	30 min		0.50	0.14	6.12	P		0.04	0.04	0.86	P
		3564	0.15	30 min		6.22	1.65	76.13	F		2.71	0.90	58.53	F
		3698	0.15	30 min		9.56	0.42	117.01	F		7.29	0.61	157.45	F/W
		3742	0.15	30 min		3.22	1.07	39.41	P		1.42	0.55	30.67	P
		3743	0.15	30 min		3.72	1.08	45.53	P		1.25	0.53	27.00	P
30-Oct-01	339-344	PC	None	30 min		8.67	0.54	100.00			3.38	0.45	100.00	
		2650	0.15	30 min		0.82	0.27	9.46	P		0.00	0.00	0.00	P
		3603	0.15	30 min		10.23	0.26	117.99	F		7.96	0.04	235.50	F/W
		3699	0.15	30 min		4.39	1.26	50.63	P		1.54	6.00	45.56	P
		3744	0.15	30 min		9.96	0.21	114.88	F		5.71	0.50	168.93	F/W
		3745	0.15	30 min		9.91	0.42	114.30	F		5.57	0.36	164.79	F/W
13-Nov-01	345-350	PC	None	30 min		7.76	1.30	100.00			3.71	0.96	100.00	
		2650	0.15	30 min		1.17	0.18	15.08	P		0.17	0.17	4.58	P
		3710	0.15	30 min		9.24	0.52	119.07	F		6.67	0.75	179.78	F/W
		3711	0.15	30 min		9.67	0.42	124.61	F		6.38	0.65	171.97	F/W
		3770	0.15	30 min		4.07	1.51	52.45	P		1.51	0.81	40.70	P
		3772	0.15	30 min		2.10	0.54	27.06	P		0.04	0.04	1.08	P
27-Nov-01	351-356	PC	None	30 min		9.41	0.76	100.00			5.13	0.75	100.00	
		2650	0.15	30 min		1.32	0.32	14.03	P		0.00	0.00	0.00	P
		3773	0.15	30 min		1.58	0.36	16.79	P		0.21	0.10	4.09	P
		3778	0.15	30 min		2.70	0.32	28.69	P		0.46	0.23	8.97	P
		3780	0.15	30 min		2.69	0.48	28.59	P		0.29	0.20	5.65	P
		3782	0.15	30 min		1.60	0.46	17.00	P		0.08	0.08	1.56	P
8-Jan-02	357-362	PC	None	30 min		9.25	1.11	100.00			5.17	0.73	100.00	
		2650	0.15	30 min		1.71	0.40	18.49	P		0.21	0.14	4.06	P
		3809	0.15	30 min		8.36	1.36	90.38	F		3.88	0.86	75.05	F

DATE Experiment Started	PIG #	ICD #	aTSP Thickness	HD Vapor Exposure		Erythema Mean a* Value	Erythema Mean a* SEM	Percent of Control	P/F/W		Histo- logy Mean SCORE	Histo- logy SEM	Percent of Control	P/F/W
		3770	0.15	30 min		6.41	0.98	69.30	F		3.42	0.91	66.15	F
		3779	0.15	30 min		3.83	0.90	41.41	P		1.88	0.59	36.36	P
		3781	0.15	30 min		3.77	0.91	40.76	P		1.54	0.55	29.79	P
22-Jan-02	363-368	PC	None	30 min		9.33	0.65	100.00			4.83	0.76	100.00	
		3773	0.15	30 min		1.69	0.46	18.11	P		0.17	0.17	3.52	P
		PC	0.15	45 min		9.51	0.75	100.00			7.00	0.53	100.00	
		3773	0.15	45 min		3.46	0.84	36.38	P		1.21	0.42	17.29	P
		PC	0.15	60 min		9.62	0.64	100.00			7.71	0.14	100.00	
		3773	0.15	60 min		4.74	1.02	49.27	P		2.04	0.53	26.46	P
5-Feb-02	369-374	PC	None	30 min		8.46	1.19	100.00						
7-Feb-02		3782	0.15	30 min		0.84	0.25	9.93	P					
		3782	0.15	45 min		1.47	0.37	17.38	P					
		3782	0.15	60 min		2.70	0.33	31.91	P					
		3782	0.15	75 min		3.25	0.64	38.42	P					
		3782	0.15	90 min		4.28	0.87	50.59	P					
26-Feb-02	375-380	PC	None	30 min		9.46	0.40	100.00			5.04	1.08	100.00	
		2701	0.15	30 min		1.44	0.39	15.22	P		1.46	0.83	28.97	P
		2701	0.15	45 min		2.82	0.32	29.81	P		0.83	0.31	16.47	P
		2701	0.15	60 min		4.89	0.75	51.69	P		1.46	0.55	28.97	P
		2701	0.15	75 min		6.31	0.39	66.70	P		2.33	0.27	46.23	F
		2701	0.15	90 min		7.30	0.58	77.17	P		3.79	0.30	75.20	F
11-Mar-02	381-386	PC	None	30 min		8.83	0.51	100.00			6.08	0.57	100.00	
		2650	0.15	30 min		0.58	0.33	6.57	P		1.33	0.84	21.88	P
		3818	0.15	30 min		9.34	0.72	105.78	F		7.08	0.63	116.45	F
		3819	0.15	30 min		9.17	0.58	103.85	F		7.17	0.54	117.93	F
		3820	0.15	30 min		9.12	0.71	103.28	F		6.88	0.56	113.16	F

DATE Experiment Started	PIG #	ICD #	aTSP Thickness	HD Vapor Exposure		Erythema Mean a* Value	Erythema Mean a* SEM	Percent of Control	P/F/W		Histo- logy Mean SCORE	Histo- logy SEM	Percent of Control	P/F/W
		3821	0.15	30 min		8.30	0.45	94.00	F		5.79	0.53	95.23	F
3-Apr-02	387-392	PC	None	30 min		8.67	0.39	100.00			6.54	0.68	100.00	
		3829	0.15	30 min		6.50	0.87	74.97	P		4.08	0.80	62.39	P
		3829	0.15	45 min		6.97	0.69	80.39	F		5.54	1.02	84.71	F
		3829	0.15	60 min		7.71	0.22	88.93	F		6.67	0.68	101.99	F
		3829	0.15	75 min		8.14	0.32	93.89	F		7.29	0.43	111.47	F
		3829	0.15	90 min		7.69	0.39	88.70	F		7.83	0.12	119.72	F
16-Apr-02	393-398	PC	None	30 min		10.27	0.35	100.00			5.54	0.71	100.00	
		2650	0.15	30 min		1.73	0.31	16.85	P		0.25	0.25	4.51	P
		3829	0.15	30 min		6.40	1.09	62.32	P		2.13	0.80	38.45	P
		3830	0.15	30 min		4.02	0.81	39.14	P		0.96	0.28	17.33	P
		3831	0.15	30 min		8.54	0.76	83.15	F		3.67	0.55	66.25	F
		3832	0.15	30 min		2.68	0.62	26.10	P		0.58	0.32	10.47	P
30-Apr-02	399-403	PC	None	30 min		8.30	0.44	100.00			4.70	0.73	100.00	
		2650	0.15	30 min		1.06	0.41	12.77	P		0.10	0.10	2.13	P
		3771	0.15	30 min		2.10	0.61	25.30	P		0.35	0.22	7.45	P
		3833	0.15	30 min		1.32	0.56	15.90	P		0.15	0.15	3.19	P
		3834	0.15	30 min		0.97	0.47	11.69	P		0.00	0.00	0.00	P
		3884	0.15	30 min		2.03	0.89	24.46	P		0.45	0.23	9.57	P
21-May-02	404-409	PC	None	30 min		7.93	1.20	100.00			4.29	0.96	100.00	
		2650	0.15	30 min		1.17	0.39	14.75	P		0.46	0.31	10.72	P
		3885	0.15	30 min		4.80	1.11	60.53	F		1.50	0.60	34.97	P
		3886	0.15	30 min		4.01	1.47	50.57	F		1.38	0.69	32.17	P
		3887	0.15	30 min		3.84	1.21	48.42	F		1.33	0.90	31.00	P
		3900	0.15	30 min		5.13	1.70	64.69	F		2.04	0.75	47.55	F

DATE Experiment Started	PIG #	ICD #	aTSP Thickness	HD Vapor Exposure		Erythema Mean a* Value	Erythema Mean a* SEM	Percent of Control	P/F/W		Histo- logy Mean SCORE	Histo- logy SEM	Percent of Control	P/F/W
11-Jun-02	410-415	PC	None	30 min		11.27	0.94	100.00			7.83	0.12	100.00	
		2650	0.15	30 min		3.40	1.09	30.17	P		1.04	0.22	13.28	P
		3901	0.15	30 min		8.02	0.50	71.16	P		3.58	0.41	45.72	P
		3902	0.15	30 min		7.57	0.57	67.17	P		3.33	0.50	42.53	P
		3903	0.15	30 min		5.64	1.04	50.04	P		2.58	0.63	32.95	P
		3905	0.15	30 min		10.98	0.98	97.43	F		7.21	0.43	92.08	F
25-Jun-02	416-421	PC	None	30 min		10.33	0.78	100.00			6.79	0.30	100.00	
		2650	0.15	30 min		0.53	0.31	5.13	P		0.08	0.08	1.18	P
		3885	0.15	30 min		7.18	1.32	69.51	P		2.71	0.75	39.91	P
		3886	0.15	30 min		4.66	1.12	45.11	P		1.25	0.38	18.41	P
		3887	0.15	30 min		4.96	0.90	48.02	P		1.42	0.33	20.91	P
		3900	0.15	30 min		8.23	0.99	79.67	F		4.04	0.55	59.50	P
10-Jul-02	422-427	PC	None	30 min		8.82	0.93	100.00			5.17	0.84	100.00	
		3833	0.15	30 min		1.95	0.26	22.11	P		0.54	0.23	10.44	P
		3833	0.15	45 min		6.34	1.02	71.88	F		2.46	0.87	47.58	P
		3833	0.15	60 min		7.84	0.89	88.89	F		3.46	1.14	66.92	F
		3833	0.15	75 min		9.06	0.90	102.72	F		5.00	0.80	96.71	F
		3833	0.15	90 min		10.13	0.53	114.85	F		6.13	0.64	118.57	F
6-Aug-02	428-433	PC	None	30 min		7.25	0.97	100.00			3.85	0.32	100.00	
		3792	0.15	30 min		1.02	0.77	14.07	P		0.50	0.22	12.99	P
		3792	0.15	45 min		1.23	0.65	16.97	P		0.10	0.10	2.60	P
	Note: animal #431 omitted from summary	3792	0.15	60 min		2.02	0.29	27.86	P		1.10	0.41	28.57	P

DATE Experiment Started	PIG #	ICD #	aTSP Thickness	HD Vapor Exposure		Erythema Mean a* Value	Erythema Mean a* SEM	Percent of Control	P/F/W		Histo- logy Mean SCORE	Histo- logy SEM	Percent of Control	P/F/W
		3792	0.15	75 min		4.94	0.87	68.14	P		2.25	0.38	58.44	P
		3792	0.15	90 min		7.19	0.88	99.17	F		3.65	0.56	94.81	F
27-Aug-02	434-439	PC	None	30 min		8.30	0.85	100.00			7.75	0.20	100.00	
		2650	0.15	30 min		4.64	0.48	55.90	P		3.17	0.82	40.90	P
		3004	0.15	30 min		8.76	0.75	105.54	F		7.75	0.25	100.00	F
		3771	0.15	30 min		4.86	0.42	58.55	P		3.08	0.62	39.74	P
		3832	0.15	30 min		8.61	0.33	103.73	F		5.67	0.56	73.16	P
		3834	0.15	30 min		7.83	0.92	94.34	F		5.71	0.65	73.68	P
10-Sep-02	440-445	PC	None	30 min		8.73	0.36	100.00			6.04	0.78	100.00	
		2650	0.15	30 min		1.79	0.62	20.50	P		0.71	0.61	11.75	P
		4020	0.15	30 min		1.02	0.90	11.68	P		0.63	0.53	10.43	P
		4021	0.15	30 min		3.06	1.29	35.05	P		1.54	0.79	25.50	P
		4022	0.15	30 min		3.76	1.12	43.07	P		1.08	0.49	17.88	P
		4028	0.15	30 min		1.45	0.71	16.61	P		0.71	0.47	11.75	P
24-Sep-02	446-451	PC	None	30 min		9.05	0.56	100.00			7.08	0.34	100.00	
26-Sep-02		2650	0.15	30 min		0.58	0.34	6.41	P		0.25	0.11	3.53	P
		4042	0.15	30 min		5.42	1.13	59.89	P		3.83	0.99	54.10	P
		4050	0.15	30 min		1.17	0.50	12.93	P		0.92	0.23	12.99	P
		4051	0.15	30 min		1.53	0.70	16.91	P		0.38	0.13	5.37	P
		4052	0.15	30 min		0.98	0.69	10.83	P		0.88	0.27	12.43	P
8-Oct-02	452-457	PC	None	30 min		10.26	1.04	100.00			5.71	0.78	100.00	
		2650	0.15	30 min		2.69	0.40	26.22	P		0.38	0.29	6.65	P
		4029	0.15	30 min		2.61	0.60	25.44	P		0.58	0.25	10.16	P
		4036	0.15	30 min		5.02	1.19	48.93	P		1.75	0.80	30.65	P
		4038	0.15	30 min		5.73	0.95	55.85	P		2.50	0.83	43.78	P
		4047	0.15	30 min		4.69	0.95	45.71	P		1.38	0.48	24.17	P

DATE Experiment Started	PIG #	ICD #	aTSP Thickness	HD Vapor Exposure		Erythema Mean a* Value	Erythema Mean a* SEM	Percent of Control	P/F/W		Histo- logy Mean SCORE	Histo- logy SEM	Percent of Control	P/F/W
29-Oct-02	458-463	PC	None	30 min		8.96	0.57	100.00			5.58	0.76	100.00	
		2650	0.15	30 min		0.75	0.35	8.37	P		0.08	0.08	1.43	P
		4032	0.15	30 min		4.80	0.61	53.57	P		1.25	0.48	22.40	P
		4040	0.15	30 min		6.79	0.82	75.78	F		2.25	0.58	40.32	P
		4044	0.15	30 min		6.13	0.58	68.42	P		2.83	0.45	50.72	P
		4046	0.15	30 min		1.23	0.41	13.73	P		0.83	0.47	14.87	P
19-Nov-02	464-469	PC	None	30 min		9.88	0.50	100.00			7.79	0.10	100.00	
		2650	0.15	30 min		2.38	0.51	24.09	P		0.75	0.35	9.63	P
		4034	0.15	30 min		5.82	0.58	58.91	P		3.54	0.68	45.44	P
		4039	0.15	30 min		8.95	0.24	90.59	F		7.00	0.50	89.86	F
		4043	0.15	30 min		8.84	0.48	89.47	F		6.21	0.62	79.72	F
		4049	0.15	30 min		8.13	0.58	82.29	P		4.25	0.38	54.56	P
3-Dec-02	470-475	PC	None	30 min		8.67	0.89	100.00			6.13	0.72	100.00	
		2650	0.15	30 min		1.53	1.05	17.65	P		0.83	0.29	13.54	P
		4033	0.15	30 min		8.72	0.94	100.58	F		5.79	0.88	94.45	F
		4037	0.15	30 min		7.77	1.24	89.62	F		4.88	0.63	79.61	F
		4041	0.15	30 min		9.33	0.47	107.61	F		6.88	0.39	112.23	F
		4048	0.15	30 min		5.53	0.56	63.78	P		2.42	0.53	39.48	P
21-Jan-03	476-481	PC	None	30 min		9.22	0.29	100.00			6.42	0.31	100.00	
		2650	0.15	30 min		1.88	0.44	20.39	P		0.25	0.11	3.89	P
		3834Y	0.15	30 min		1.71	0.40	18.55	P		0.58	0.25	9.03	P
		3834Z	0.15	30 min		2.23	0.41	24.19	P		0.63	0.28	9.81	P
		4035	0.15	30 min		8.75	0.54	94.90	F		5.71	0.58	88.94	F
		4045	0.15	30 min		8.18	0.48	88.72	F		6.75	0.59	105.14	F

DATE Experiment Started	PIG #	ICD #	aTSP Thickness	HD Vapor Exposure		Erythema Mean a* Value	Erythema Mean a* SEM	Percent of Control	P/F/W		Histo- logy Mean SCORE	Histo- logy SEM	Percent of Control	P/F/W
4-Feb-03	482-487	PC	None	30 min		8.18	0.41	100.00			3.88	0.88	100.00	
		2650	0.15	30 min		1.16	0.16	14.18	P		0.00	0.00	0.00	P
		4088	0.15	30 min		4.00	0.64	48.90	P		1.58	0.54	40.72	P
		4089	0.15	30 min		8.50	0.52	103.91	F		5.38	0.63	138.66	F
		4090	0.15	30 min		8.43	0.50	103.06	F		5.67	0.54	146.13	F/W
		4091	0.15	30 min		6.54	0.75	79.95	F		3.92	0.55	101.03	F
19-Feb-03	488-493	PC	None	15 min		2.82	0.62	100.00			0.58	0.23	100.00	
		4083	0.1	15 min		8.85	0.57	313.83	F/W		5.10	0.41	879.31	F/W
		4083	0.2	15 min		8.63	0.72	306.03	F/W		5.38	0.37	927.59	F/W
		PC	0.15	30 min		8.34	0.89	100.00			3.79	0.62	100.00	
		4083	0.1	30 min		9.22	0.85	110.55	F		7.50	0.23	197.89	F/W
		4083	0.2	30 min		8.67	0.93	103.96	F		7.92	0.05	208.97	F/W
11-Mar-03	494-497	PC	None	30 min		2.67	0.79	100.00			1.50	0.65	100.00	
		4029	0.15	30 min		-0.23	0.30	-8.61	P		0.00	0.00	0.00	P
		4029	0.15	45 min		0.67	0.32	25.09	F		0.63	0.16	42.00	F
		4029	0.15	60 min		1.16	0.61	43.45	F		0.69	0.43	46.00	F
		4029	0.15	75 min		2.73	0.84	102.25	F		2.19	0.12	146.00	F
		4029	0.15	90 min		2.38	0.91	89.14	F		2.13	0.31	142.00	F
13-Mar-03	498-499	PC	None	25 min		1.96	1.16	100.00			1.00	0.25	100.00	
		4029	0.15	30 min		4.19	0.73	213.78			1.75	0.50	175.00	
		4029	0.15	35 min		5.84	0.68	297.96			4.25	0.25	425.00	
		4029	0.15	40 min		6.72	1.08	342.86			5.00	0.75	500.00	
		4029	0.15	45 min		7.76	1.10	395.92			5.50	0.50	550.00	
		4029	0.15	50 min		7.52	1.57	383.67			5.63	0.38	563.00	
25-Mar-03	500-505	PC	None	25 min		8.31	0.99	100.00			4.54	0.76	100.00	

DATE Experiment Started	PIG #	ICD #	aTSP Thickness	HD Vapor Exposure		Erythema Mean a* Value	Erythema Mean a* SEM	Percent of Control	P/F/W		Histo- logy Mean SCORE	Histo- logy SEM	Percent of Control	P/F/W
		None	None	30 min		9.38	0.68	112.88	F		5.54	0.72	122.03	F
		None	None	35 min		9.75	0.58	117.33	F		5.58	0.24	122.91	F
		None	None	40 min		9.69	0.67	116.61	F		7.29	0.28	160.57	F/W
		None	None	45 min		9.74	0.64	117.21	F		7.50	0.26	165.20	F/W
		None	None	50 min		9.52	0.63	114.56	F		7.21	0.50	158.81	F/W
8-Apr-03	506-511	PC	None	30 min		7.58	0.68	100.00			5.33	0.52	100.00	
		4028	0.15	30 min		0.74	0.27	9.76	P		0.33	0.24	6.19	P
		4028	0.15	45 min		1.74	0.53	22.96	P		0.96	0.38	18.01	P
		4028	0.15	60 min		3.79	0.78	50.00	P		2.42	0.49	45.40	P
		4028	0.15	75 min		6.37	0.75	84.04	F		3.83	0.52	71.86	F
		4028	0.15	90 min		6.46	1.00	85.22	F		4.29	0.60	80.49	F
22-Apr-03	512-517	PC	None	30 min		7.08	0.90	100.00			4.06	0.72	100.00	
		3834	0.15	30 min		2.94	1.18	41.53	P		2.19	0.68	53.94	F
		3834	0.15	45 min		3.08	0.95	43.50	P		1.50	0.43	36.95	F
	Note: animals #512 and #513 omitted from summary													
		3834	0.15	60 min		3.70	0.80	52.26	P		2.00	0.86	49.26	F
		3834	0.15	75 min		4.44	0.61	62.71	F		2.75	0.40	67.73	F
		3834	0.15	90 min		6.21	0.67	87.71	F		4.13	0.72	101.72	F
6-May-03	518-523	PC	None	30 min		8.11	0.66	100.00			4.67	0.56	100.00	
		4029	0.15	30 min		0.35	0.40	4.32	P		0.29	0.19	6.21	P
		4029	0.15	45 min		1.33	0.55	16.40	P		0.63	0.17	13.49	P
		4029	0.15	60 min		2.86	0.89	35.27	P		2.04	0.76	43.68	P
		4029	0.15	75 min		4.35	1.24	53.64	P		2.75	0.84	58.89	F
		4029	0.15	90 min		5.70	0.54	70.28	F		4.29	0.88	91.86	F

DATE Experiment Started	PIG #	ICD #	aTSP Thickness	HD Vapor Exposure		Erythema Mean a* Value	Erythema Mean a* SEM	Percent of Control	P/F/W		Histo- logy Mean SCORE	Histo- logy SEM	Percent of Control	P/F/W
20-May-03	524-529	PC	None	30 min		7.64	0.58	100.00			5.83	0.31	100.00	
		4020	0.15	30 min		0.76	0.26	9.95	P		0.08	0.08	1.37	P
22-May-03		4020	0.15	45 min		1.25	0.13	16.36	P		0.71	0.15	12.18	P
		4020	0.15	60 min		1.94	0.50	25.39	P		1.50	0.50	25.73	P
		4020	0.15	75 min		3.16	0.79	41.36	P		2.46	0.73	42.20	P
		4020	0.15	90 min		4.50	0.78	58.90	P		4.38	0.73	75.13	F
10-Jun-03	530-535	PC	None	30 min		8.83	1.10	100.00			4.10	1.15	100.00	
		4029	0.15	30 min		1.08	0.35	12.23	P		0.10	0.10	2.44	P
		4029	0.15	45 min		2.13	0.55	24.12	P		0.65	0.29	15.85	P
Note: animal #533 omitted from summary														
		4029	0.15	60 min		3.20	1.17	36.24	P		1.40	0.49	34.15	P
		4029	0.15	75 min		4.85	0.79	54.93	P		2.50	0.56	60.98	F
		4029	0.15	90 min		6.28	1.33	71.12	P		3.10	0.82	75.61	F
24-Jun-03	536-541	PC	None	30 min		9.33	0.37	100.00			6.46	0.22	100.00	
		4051	0.15	30 min		0.43	0.26	4.61	P		0.00	0.00	0.00	P
		4051	0.15	45 min		1.76	0.84	18.86	P		0.67	0.47	10.37	P
		4051	0.15	60 min		3.92	1.12	42.02	P		2.25	0.53	34.83	P
		4051	0.15	75 min		5.09	1.04	54.56	P		3.29	0.48	50.93	P
		4051	0.15	90 min		6.87	0.60	73.63	P		4.38	0.15	67.80	P
8-Jul-03	542	PC	None	10 min		NA	NA							
		None	None	15 min		NA	NA							
		None	None	30 min		NA	NA							
		None	None	45 min		NA	NA							

DATE Experiment Started	PIG #	ICD #	aTSP Thickness	HD Vapor Exposure		Erythema Mean a* Value	Erythema Mean a* SEM	Percent of Control	P/F/W		Histo- logy Mean SCORE	Histo- logy SEM	Percent of Control	P/F/W
15-Jul-03	543-548	PC	None	30 min		9.91	0.81	100.00			4.85	0.10	100.00	
		4052	0.15	30 min		1.18	0.36	11.91	P		0.25	0.25	5.15	P
		4052	0.15	45 min		0.30	0.37	3.03	P		0.00	0.00	0.00	P
Note: animal #546 omitted from summary														
		4052	0.15	60 min		1.23	0.64	12.41	P		0.45	0.20	9.28	P
		4052	0.15	75 min		3.06	0.72	30.88	P		1.90	0.50	39.18	P
		4052	0.15	90 min		3.94	1.32	39.76	P		2.25	0.40	46.39	P
29-Jul-03	549-554	PC	None	30 min		7.47	1.19	100.00			4.13	0.80	100.00	
		2650	0.15	30 min		0.75	0.35	10.04	P		0.00	0.00	0.00	P
		3004	0.15	30 min		10.36	0.49	138.69	F/W		7.79	0.21	188.62	F/W
		3834	0.15	30 min		0.82	0.59	10.98	P		0.54	0.36	13.08	P
		4020	0.15	30 min		1.53	0.74	20.48	P		0.33	0.17	7.99	P
		4028	0.15	30 min		1.10	0.88	14.73	P		0.21	0.14	5.08	P
12-Aug-03	555-560	PC	None	30 min		8.79	0.51	100.00			6.54	0.59	100.00	
		2650	0.15	30 min		1.91	0.51	21.73	P		1.04	0.36	15.90	P
		4029	0.15	30 min		2.27	0.48	25.82	P		1.38	0.39	21.10	P
		4050	0.15	30 min		2.60	0.77	29.58	P		1.42	0.48	21.71	P
		4051	0.15	30 min		2.10	0.75	23.89	P		1.13	0.39	17.28	P
		4052	0.15	30 min		1.56	0.35	17.75	P		1.00	0.46	15.29	P
16-Sep-03	561-566	PC	None	30 min		9.02	0.56	100.00			5.25	0.71	100.00	
		3834	0.15	30 min		1.45	0.52	16.08	P		0.00	0.00	0.00	P
		3834	0.15	45 min		2.10	0.23	23.28	P		0.13	0.09	2.48	P

DATE Experiment Started	PIG #	ICD #	aTSP Thickness	HD Vapor Exposure		Erythema Mean a* Value	Erythema Mean a* SEM	Percent of Control	P/F/W		Histo- logy Mean SCORE	Histo- logy SEM	Percent of Control	P/F/W
		3834	0.15	60 min		3.12	0.51	34.59	P		0.92	0.35	17.52	P
		3834	0.15	75 min		5.80	1.09	64.30	P		2.13	0.49	40.57	P
		3834	0.15	90 min		7.43	0.69	82.37	F		4.00	0.41	76.19	F
23-Mar-04	567-572	PC	None	30 min		8.66	0.84	100.00			6.83	0.40	100.00	
		4212	0.15	30 min		0.43	0.51	4.97	P		0.33	0.21	4.83	P
		4212	0.15	45 min		0.60	0.38	6.93	P		0.50	0.26	7.32	P
		4212	0.15	60 min		1.52	0.60	17.55	P		0.71	0.18	10.40	P
		4212	0.15	75 min		2.48	0.64	28.64	P		1.58	0.50	23.13	P
		4212	0.15	90 min		3.65	0.59	42.15	P		2.58	0.44	37.77	P

Table 19b. Summary of results for the weanling pig HD vapor model at the USAMRICD. The data are order by ICD number for easy reference to Table 19a. The table provides references for the dates of experiments, ICD numbers of candidate formulations, the thickness of applied TSP or aTSP, the duration time of the saturated HD vapor cup exposure (1.4 mg/L), and the percent of positive control ([mean a* for candidate/mean a* for positive control] * 100), and the percent of positive control ([mean histology score for candidate/mean histology score for positive control] * 100). The smaller the % of control value, the better protection the candidate formulation provided. Based on statistical analysis of either the erythema data or the histology data, there is a column stating whether the candidate formulation passed the screen (meaning it provided significant protection compared to positive control animals) failed the screen (meaning it provided equivalent protection compared to positive control animals), or failed worse (meaning it produced significantly worse damage compared to positive control animals).

DATE	ICD #	THICKNESS mm	Exposure Time, min	Erythema		Histology	
				Percent of Control	P/F/W	Percent of Control	P/F/W
22-May-01	1511	0.2	15 min	157	F	190.76	F/W
22-May-01	1511	0.2	30 min	107	F	117.33	F
13-May-97	2650	0.1	30 min	22	P		
20-May-97	2650	0.1	30 min	14	P		
12-Aug-97	2650	0.1	30 min	7	P		
14-Apr-98	2650	0.1	30 min	21	P		
5-May-98	2650	0.1	30 min	17	P		
17-Feb-99	2650	0.1	30 min	2	P		
23-Mar-99	2650	0.1	30 min	23	P		
24-Mar-99	2650	0.1	30 min	22	P		
6-Apr-99	2650	0.1	30 min	31	P		
14-Apr-99	2650	0.1	30 min	32	P		
20-Apr-99	2650	0.1	30 min	43	F		
6-May-99	2650	0.1	30 min	18	F		
10-Aug-99	2650	0.1	30 min	24	P		
31-Aug-99	2650	0.1	30 min	4	P		
8-Sep-99	2650	0.1	30 min	21	P		
28-Sep-99	2650	0.1	30 min	6	P		
30-Sep-99	2650	0.1	30 min	-11	F		
16-Nov-99	2650	0.1	30 min	15	P		

					Erythema			Histology	
DATE	ICD #	THICKNESS mm	Exposure Time, min		Percent of Control	P/F/W		Percent of Control	P/F/W
17-Jan-01	2650	0.1	30 min		-9	F		17.95	F
6-Feb-01	2650	0.1	30 min		5	P		0.00	P
13-Feb-01	2650	0.1	30 min		6	P		2.83	P
21-Feb-01	2650	0.1	30 min		3	P		0.00	P
20-Mar-01	2650	0.15	30 min		3	P		5.36	P
3-Apr-01	2650	0.15	30 min		4	P		1.48	P
24-Apr-01	2650	0.15	30 min		10	P		1.92	P
8-May-01	2650	0.15	30 min		15	P		0.00	P
12-Jun-01	2650	0.15	30 min		10	P		5.01	P
26-Jun-01	2650	0.15	30 min		7	P		0.00	P
25-Jul-01	2650	0.15	30 min		6	P		0.78	P
7-Aug-01	2650	0.15	30 min		1	P		0.00	P
4-Sep-01	2650	0.15	30 min		80	F		86.51	F
2-Oct-01	2650	0.15	30 min		9	P		0.00	P
4-Oct-01	2650	0.15	30 min		1	P		0.00	P
16-Oct-01	2650	0.15	30 min		6	P		0.86	P
30-Oct-01	2650	0.15	30 min		9	P		0.00	P
14-Nov-01	2650	0.15	30 min		15	P		4.58	P
27-Nov-01	2650	0.15	30 min		14	P		0.00	P
8-Jan-02	2650	0.15	30 min		18	P		4.06	P
11-Mar-02	2650	0.15	30 min		7	P		21.88	P
16-Apr-02	2650	0.15	30 min		17	P		4.51	P
30-Apr-02	2650	0.15	30 min		13	P		2.13	P
21-May-02	2650	0.15	30 min		15	P		10.72	P
11-Jun-02	2650	0.15	30 min		30	P		13.28	P
25-Jun-02	2650	0.15	30 min		5	P		1.18	P
27-Aug-02	2650	0.15	30 min		56	P		40.90	P
10-Sep-02	2650	0.15	30 min		21	P		11.75	P
26-Sep-02	2650	0.15	30 min		6	P		3.53	P
8-Oct-02	2650	0.15	30 min		26	P		6.65	P
29-Oct-02	2650	0.15	30 min		8	P		1.43	P
19-Nov-02	2650	0.15	30 min		24	P		9.63	P
3-Dec-02	2650	0.15	30 min		18	P		13.54	P

					Erythema			Histology	
DATE	ICD #	THICKNESS mm	Exposure Time, min		Percent of Control	P/F/W		Percent of Control	P/F/W
21-Jan-03	2650	0.15	30 min		20	P		3.89	P
4-Feb-03	2650	0.15	30 min		14	P		0.00	P
29-Jul-03	2650	0.15	30 min		10	P		0.00	P
12-Aug-03	2650	0.15	30 min		22	P		15.90	P
3-Apr-01	2701	0.15	30 min		4	P		2.95	P
26-Feb-02	2701	0.15	30 min		15	P		28.97	P
26-Feb-02	2701	0.15	45 min		30	P		16.47	P
26-Feb-02	2701	0.15	60 min		52	P		28.97	P
26-Feb-02	2701	0.15	75 min		67	P		46.23	F
26-Feb-02	2701	0.15	90 min		77	P		75.20	F
5-May-98	2902	0.1	15 min		32	P			
31-Aug-99	2902	0.1	15 min		63	F			
14-Apr-98	2902	0.1	15 min-30 min		27	P			
5-May-98	2902	0.1	30 min		67	F			
5-May-98	2902	0.1	45 min		134	F			
5-May-98	2902	0.1	60 min		153	F			
7-Aug-01	2902	0.15	30 min		51	P		44.00	P
20-May-97	2926	0.2	15 min		18	P			
12-Aug-97	2926	0.2	15 min		35	P			
13-May-97	2927	0.2	15 min		145	F/W			
13-May-97	2928	0.2	15 min		157	F/W			
20-May-97	2929	0.2	15 min		98	F			
13-May-97	2930	0.2	15 min		149	F/W			
20-May-97	2931	0.2	15 min		134	F			
20-May-97	2932	0.2	15 min		136	F			
13-May-97	2933	0.2	15 min		153	F/W			
14-Apr-98	2951	0.1	15 min-30 min		147	F			
14-Apr-98	2954	0.1	15 min-30 min		134	F			
12-Aug-97	2956	0.2	15 min		138	F			
12-Aug-97	2957	0.2	15 min		56	F			
12-Aug-97	2958	0.2	15 min		182	F/W			

					Erythema			Histology	
DATE	ICD #	THICKNESS mm	Exposure Time, min		Percent of Control	P/F/W		Percent of Control	P/F/W
6-May-99	3004	0.1	15 min		155	F			
6-Feb-01	3004	0.1	30 min		179	F/W		325.78	F/W
8-May-01	3004	0.15	30 min		102	F		124.66	F
27-Aug-02	3004	0.15	30 min		106	F		100.00	F
29-Jul-03	3004	0.15	30 min		139	F/W		188.62	F/W
22-May-01	3004	0.2	15 min		165	F/W		223.95	F/W
22-May-01	3004	0.2	30 min		104	F		124.33	F
17-Jan-01	3004	0.1 normal cleaning	15 min		343	F/W		402.56	F/W
17-Jan-01	3004	0.1 special cleaning	15 min		356	F/W		381.20	F/W
17-Jan-01	3004	0.2 normal cleaning	15 min		348	F/W		370.09	F/W
17-Jan-01	3004	0.2 special cleaning	15 min		330	F/W		370.09	F/W
14-Apr-98	3051	0.1	15 min - 30 min		189	F/W			
31-Aug-99	3109	0.1	15 min		200	F/W			
17-Feb-99	3126	0.1	15 min		589	F/W			
17-Feb-99	3126	0.1	30 min		614	F/W			
17-Feb-99	3126	0.1	45 min		686	F/W			
17-Feb-99	3126	0.1	60 min		666	F/W			
31-Aug-99	3151	0.1	15 min		-4	P			
16-Nov-99	3151	0.1	15 min		13	P			
16-Nov-99	3151	0.1	30 min		94	F			
16-Nov-99	3151	0.1	45 min		148	F			
16-Nov-99	3151	0.1	60 min		150	F			
12-Jun-01	3151	0.15	30 min		32	P		35.22	P
23-Mar-99	3215	0.1	15 min		232	F/W			
23-Mar-99	3215	0.1	30 min		242	F/W			

					Erythema		Histology	
DATE	ICD #	THICKNESS mm	Exposure Time, min		Percent of Control	P/F/W	Percent of Control	P/F/W
23-Mar-99	3215	0.1	45 min		238	F/W		
23-Mar-99	3215	0.1	60 min		224	F/W		
24-Mar-99	3216	0.1	15 min		318	F/W		
24-Mar-99	3216	0.1	30 min		379	F/W		
24-Mar-99	3216	0.1	45 min		384	F/W		
24-Mar-99	3216	0.1	60 min		375	F/W		
6-Apr-99	3227	0.1	15 min		114	F		
6-Apr-99	3227	0.1	30 min		148	F		
6-Apr-99	3227	0.1	45 min		158	F		
6-Apr-99	3227	0.1	60 min		163	F/W		
20-Apr-99	3244	0.1	15 min		36	F		
20-Apr-99	3244	0.1	30 min		59	F		
20-Apr-99	3244	0.1	45 min		127	F		
20-Apr-99	3244	0.1	60 min		184	F/W		
14-Apr-99	3245	0.1	15 min		65	F		
14-Apr-99	3245	0.1	30 min		91	F		
14-Apr-99	3245	0.1	45 min		106	F		
14-Apr-99	3245	0.1	60 min		121	F		
8-Sep-99	3247	0.2	15 min		127	F		
8-Sep-99	3248	0.2	15 min		124	F		
10-Aug-99	3251	0.1	15 min		188	F/W		
10-Aug-99	3252	0.1	15 min		198	F/W		
10-Aug-99	3253	0.1	15 min		186	F/W		
28-Sep-99	3280	0.1	15 min		174	F/W		
30-Sep-99	3280	0.2	15 min		71	F		
10-Aug-99	3284	0.1	15 min		174	F/W		
28-Sep-99	3289	0.1	15 min		171	F/W		
30-Sep-99	3289	0.2	15 min		134	F		
31-Aug-99	3290	0.1	15 min		169	F/W		
28-Sep-99	3294	0.1	15 min		169	F/W		
30-Sep-99	3294	0.2	15 min		155	F		
8-Sep-99	3299	0.2	15 min		35	P		
24-Apr-01	3300	0.15	30 min		37	P	28.06	P

					Erythema			Histology	
DATE	ICD #	THICKNESS mm	Exposure Time, min		Percent of Control	P/F/W		Percent of Control	P/F/W
8-Sep-99	3300	0.2	15 min		6	P			
28-Sep-99	3305	0.1	15 min		113	F			
30-Sep-99	3305	0.2	15 min		-4	F			
21-Feb-01	3369	0.1	30 min		129	F		314.85	F/W
12-Jun-01	3370	0.15	30 min		99	F		101.19	F
13-Feb-01	3378	0.1	30 min		107	F		234.28	F/W
4-Sep-01	3378	0.15	30 min		116	F		172.70	F/W
21-Feb-01	3379	0.1	30 min		124	F		311.35	F/W
13-Feb-01	3380	0.1	30 min		111	F		204.59	F/W
6-Feb-01	3450	0.1	30 min		124	F		188.89	F/W
6-Feb-01	3454	0.1	30 min		133	F		177.78	F/W
3-Apr-01	3454	0.15	30 min		155	F/W		270.48	F/W
12-Jun-01	3470	0.15	30 min		58	P		36.28	P
12-Jun-01	3471	0.15	30 min		64	F		36.81	P
21-Feb-01	3479	0.1	30 min		146	F/W		347.60	F/W
13-Feb-01	3519	0.1	30 min		104	F		173.85	F/W
6-Feb-01	3520	0.1	30 min		99	F		105.78	F
3-Apr-01	3520	0.15	30 min		98	F		161.62	F
13-Feb-01	3523	0.1	30 min		109	F		184.10	F/W
3-Apr-01	3523	0.15	30 min		117	F		205.90	F/W
20-Mar-01	3524	0.15	30 min		105	F		143.62	F
8-May-01	3530	0.15	30 min		99	F		113.34	F
8-May-01	3531	0.15	30 min		93	F		100.68	F
26-Jun-01	3532	0.15	30 min		95	F		98.33	F
8-May-01	3533	0.15	30 min		73	P		68.24	F
25-Jul-01	3548	0.15	30 min		76	F		70.76	F
25-Jul-01	3549	0.15	30 min		96	F		107.21	F
21-Feb-01	3551	0.1	30 min		127	F		232.75	F/W
25-Jul-01	3551	0.15	30 min		78	F		72.32	F
20-Mar-01	3552	0.15	30 min		94	F		123.21	F
20-Mar-01	3553	0.15	30 min		112	F		192.35	F/W
16-Oct-01	3564	0.15	30 min		76	F		58.53	F
20-Mar-01	3585	0.15	30 min		117	F		181.89	F/W

					Erythema			Histology	
DATE	ICD #	THICKNESS mm	Exposure Time, min		Percent of Control	P/F/W		Percent of Control	P/F/W
7-Aug-01	3600	0.15	30 min		108	F		114.72	F
30-Oct-01	3603	0.15	30 min		118	F		235.50	F/W
24-Apr-01	3610	0.15	30 min		116	F		164.99	F/W
24-Apr-01	3611	0.15	30 min		123	F		191.85	F/W
25-Jul-01	3630	0.15	30 min		109	F		148.73	F/W
7-Aug-01	3631	0.15	30 min		102	F		122.08	F
24-Apr-01	3633	0.15	30 min		113	F		145.80	F/W
26-Jun-01	3664	0.15	30 min		95	F		110.04	F
26-Jun-01	3665	0.15	30 min		77	P		80.48	F
4-Sep-01	3666	0.15	30 min		151	F/W		226.32	F/W
26-Jun-01	3667	0.15	30 min		101	F		104.65	F
7-Aug-01	3668	0.15	30 min		103	F		104.64	F
16-Oct-01	3698	0.15	30 min		117	F		157.45	F/W
30-Oct-01	3699	0.15	30 min		51	P		45.56	P
4-Sep-01	3709	0.15	30 min		136	F		186.51	F/W
15-Nov-01	3710	0.15	30 min		119	F		179.78	F/W
16-Nov-01	3711	0.15	30 min		125	F		171.97	F/W
4-Sep-01	3718	0.15	30 min		1	P		2.63	P
18-Sep-01	3718	0.15	30 min		23	P		14.68	P
18-Sep-01	3718	0.15	45 min		47	P		30.58	P
18-Sep-01	3718	0.15	60 min		79	P		12.69	P
2-Oct-01	3724	0.15	30 min		100	F		128.00	F/W
4-Oct-01	3725	0.15	30 min		87	F		156.00	F/W
2-Oct-01	3726	0.15	30 min		97	F		128.00	F/W
4-Oct-01	3727	0.15	30 min		96	F		176.47	F/W
2-Oct-01	3728	0.15	30 min		93	F		120.96	F/W
2-Oct-01	3729	0.15	30 min		96	F		96.96	F
4-Oct-01	3742	0.15	30 min		-9	P		3.06	P
16-Oct-01	3742	0.15	30 min		39	P		30.67	P
4-Oct-01	3743	0.15	30 min		29	P		17.65	P
16-Oct-01	3743	0.15	30 min		46	P		27.00	P
30-Oct-01	3744	0.15	30 min		115	F		168.93	F/W
30-Oct-01	3745	0.15	30 min		114	F		164.79	F/W

					Erythema			Histology	
DATE	ICD #	THICKNESS mm	Exposure Time, min		Percent of Control	P/F/W		Percent of Control	P/F/W
17-Nov-01	3770	0.15	30 min		52	P		40.70	P
8-Jan-02	3770	0.15	30 min		69	F		66.15	F
30-Apr-02	3771	0.15	30 min		25	P		7.45	P
27-Aug-02	3771	0.15	30 min		59	P		39.74	P
18-Nov-01	3772	0.15	30 min		27	P		1.08	P
27-Nov-01	3773	0.15	30 min		17	P		4.09	P
22-Jan-02	3773	0.15	30 min		18	P		3.52	P
22-Jan-02	3773	0.15	45 min		37	P		25.05	P
22-Jan-02	3773	0.15	60 min		51	P		42.24	P
27-Nov-01	3778	0.15	30 min		29	P		8.97	P
8-Jan-02	3779	0.15	30 min		41	P		36.36	P
27-Nov-01	3780	0.15	30 min		29	P		5.65	P
8-Jan-02	3781	0.15	30 min		41	P		29.79	P
27-Nov-01	3782	0.15	30 min		17	P		1.56	P
7-Feb-02	3782	0.15	30 min		10	P			
7-Feb-02	3782	0.15	45 min		17	P			
7-Feb-02	3782	0.15	60 min		32	P			
7-Feb-02	3782	0.15	75 min		38	P			
7-Feb-02	3782	0.15	90 min		51	P			
6-Aug-02	3792	0.15	30 min		14	P		12.99	P
6-Aug-02	3792	0.15	45 min		17	P		2.60	P
6-Aug-02	3792	0.15	60 min		28	P		28.57	P
6-Aug-02	3792	0.15	75 min		68	P		58.44	P
6-Aug-02	3792	0.15	90 min		99	F		94.81	F
8-Jan-02	3809	0.15	30 min		90	F		75.05	F
11-Mar-02	3818	0.15	30 min		106	F		116.45	F
11-Mar-02	3819	0.15	30 min		104	F		117.93	F
11-Mar-02	3820	0.15	30 min		103	F		113.16	F
11-Mar-02	3821	0.15	30 min		94	F		95.23	F
3-Apr-02	3829	0.15	30 min		75	P		62.39	P
16-Apr-02	3829	0.15	30 min		62	P		38.45	P
3-Apr-02	3829	0.15	45 min		80	F		84.71	F
3-Apr-02	3829	0.15	60 min		89	F		101.99	F

					Erythema			Histology	
DATE	ICD #	THICKNESS mm	Exposure Time, min		Percent of Control	P/F/W		Percent of Control	P/F/W
3-Apr-02	3829	0.15	75 min		94	F		111.47	F
3-Apr-02	3829	0.15	90 min		89	F		119.72	F
16-Apr-02	3830	0.15	30 min		39	P		17.33	P
16-Apr-02	3831	0.15	30 min		83	F		66.25	F
16-Apr-02	3832	0.15	30 min		26	P		10.47	P
27-Aug-02	3832	0.15	30 min		104	F		73.16	P
30-Apr-02	3833	0.15	30 min		16	P		3.19	P
10-Jul-02	3833	0.15	30 min		22	P		10.44	P
10-Jul-02	3833	0.15	45 min		72	F		47.58	P
10-Jul-02	3833	0.15	60 min		89	F		66.92	F
10-Jul-02	3833	0.15	75 min		103	F		96.71	F
10-Jul-02	3833	0.15	90 min		115	F		118.57	F
30-Apr-02	3834	0.15	30 min		12	P		0.00	P
27-Aug-02	3834	0.15	30 min		94	F		73.68	P
22-Apr-03	3834	0.15	30 min		42	P		53.94	F
29-Jul-03	3834	0.15	30 min		11	P		13.08	P
16-Sep-03	3834	0.15	30 min		16	P		0.00	P
22-Apr-03	3834	0.15	45 min		44	P		36.95	F
16-Sep-03	3834	0.15	45 min		23	P		2.48	P
22-Apr-03	3834	0.15	60 min		52	P		49.26	F
16-Sep-03	3834	0.15	60 min		35	P		17.52	P
22-Apr-03	3834	0.15	75 min		63	F		67.73	F
16-Sep-03	3834	0.15	75 min		64	P		40.57	P
22-Apr-03	3834	0.15	90 min		88	F		101.72	F
16-Sep-03	3834	0.15	90 min		82	F		76.19	F
30-Apr-02	3884	0.15	30 min		24	P		9.57	P
21-May-02	3885	0.15	30 min		61	F		34.97	P
25-Jun-02	3885	0.15	30 min		70	P		39.91	P
21-May-02	3886	0.15	30 min		51	F		32.17	P
25-Jun-02	3886	0.15	30 min		45	P		18.41	P
21-May-02	3887	0.15	30 min		48	F		31.00	P
25-Jun-02	3887	0.15	30 min		48	P		20.91	P
21-May-02	3900	0.15	30 min		65	F		47.55	F

					Erythema			Histology	
DATE	ICD #	THICKNESS mm	Exposure Time, min		Percent of Control	P/F/W		Percent of Control	P/F/W
25-Jun-02	3900	0.15	30 min		80	F		59.50	P
11-Jun-02	3901	0.15	30 min		71	P		45.72	P
11-Jun-02	3902	0.15	30 min		67	P		42.53	P
11-Jun-02	3903	0.15	30 min		50	P		32.95	P
11-Jun-02	3905	0.15	30 min		97	F		92.08	F
10-Sep-02	4020	0.15	30 min		12	P		10.43	P
22-May-03	4020	0.15	30 min		10	P		1.37	P
29-Jul-03	4020	0.15	30 min		20	P		7.99	P
22-May-03	4020	0.15	45 min		16	P		12.18	P
22-May-03	4020	0.15	60 min		25	P		25.73	P
22-May-03	4020	0.15	75 min		41	P		42.20	P
22-May-03	4020	0.15	90 min		59	P		75.13	F
10-Sep-02	4021	0.15	30 min		35	P		25.50	P
10-Sep-02	4022	0.15	30 min		43	P		17.88	P
10-Sep-02	4028	0.15	30 min		17	P		11.75	P
8-Apr-03	4028	0.15	30 min		10	P		6.19	P
29-Jul-03	4028	0.15	30 min		15	P		5.08	P
8-Apr-03	4028	0.15	45 min		23	P		18.01	P
8-Apr-03	4028	0.15	60 min		50	P		45.40	P
8-Apr-03	4028	0.15	75 min		84	F		71.86	F
8-Apr-03	4028	0.15	90 min		85	F		80.49	F
8-Oct-02	4029	0.15	30 min		25	P		10.16	P
11-Mar-03	4029	0.15	30 min		-9	P		0.00	P
13-Mar-03	4029	0.15	30 min		214			175.00	
6-May-03	4029	0.15	30 min		4	P		6.21	P
10-Jun-03	4029	0.15	30 min		12	P		2.44	P
12-Aug-03	4029	0.15	30 min		26	P		21.10	P
13-Mar-03	4029	0.15	35 min		298			425.00	
13-Mar-03	4029	0.15	40 min		343			500.00	
11-Mar-03	4029	0.15	45 min		25	F		42.00	F
13-Mar-03	4029	0.15	45 min		396			550.00	
6-May-03	4029	0.15	45 min		16	P		13.49	P
10-Jun-03	4029	0.15	45 min		24	P		15.85	P

					Erythema			Histology	
DATE	ICD #	THICKNESS mm	Exposure Time, min		Percent of Control	P/F/W		Percent of Control	P/F/W
13-Mar-03	4029	0.15	50 min		384			563.00	
11-Mar-03	4029	0.15	60 min		43	F		46.00	F
6-May-03	4029	0.15	60 min		35	P		43.68	P
10-Jun-03	4029	0.15	60 min		36	P		34.15	P
11-Mar-03	4029	0.15	75 min		102	F		146.00	F
6-May-03	4029	0.15	75 min		54	P		58.89	F
10-Jun-03	4029	0.15	75 min		55	P		60.98	F
11-Mar-03	4029	0.15	90 min		89	F		142.00	F
6-May-03	4029	0.15	90 min		70	F		91.86	F
10-Jun-03	4029	0.15	90 min		71	P		75.61	F
29-Oct-02	4032	0.15	30 min		54	P		22.40	P
3-Dec-02	4033	0.15	30 min		101	F		94.45	F
19-Nov-02	4034	0.15	30 min		59	P		45.44	P
21-Jan-03	4035	0.15	30 min		95	F		88.94	F
8-Oct-02	4036	0.15	30 min		49	P		30.65	P
3-Dec-02	4037	0.15	30 min		90	F		79.61	F
8-Oct-02	4038	0.15	30 min		56	P		43.78	P
19-Nov-02	4039	0.15	30 min		91	F		89.86	F
29-Oct-02	4040	0.15	30 min		76	F		40.32	P
3-Dec-02	4041	0.15	30 min		108	F		112.23	F
26-Sep-02	4042	0.15	30 min		60	P		54.10	P
19-Nov-02	4043	0.15	30 min		89	F		79.72	F
29-Oct-02	4044	0.15	30 min		68	P		50.72	P
21-Jan-03	4045	0.15	30 min		89	F		105.14	F
29-Oct-02	4046	0.15	30 min		14	P		14.87	P
8-Oct-02	4047	0.15	30 min		46	P		24.17	P
3-Dec-02	4048	0.15	30 min		64	P		39.48	P
19-Nov-02	4049	0.15	30 min		82	P		54.56	P
26-Sep-02	4050	0.15	30 min		13	P		12.99	P
12-Aug-03	4050	0.15	30 min		30	P		21.71	P
26-Sep-02	4051	0.15	30 min		17	P		5.37	P
24-Jun-03	4051	0.15	30 min		5	P		0.00	P
12-Aug-03	4051	0.15	30 min		24	P		17.28	P

					Erythema			Histology	
DATE	ICD #	THICKNESS mm	Exposure Time, min		Percent of Control	P/F/W		Percent of Control	P/F/W
24-Jun-03	4051	0.15	45 min		19	P		10.37	P
24-Jun-03	4051	0.15	60 min		42	P		34.83	P
24-Jun-03	4051	0.15	75 min		55	P		50.93	P
24-Jun-03	4051	0.15	90 min		74	P		67.80	P
26-Sep-02	4052	0.15	30 min		11	P		12.43	P
15-Jul-03	4052	0.15	30 min		12	P		5.15	P
12-Aug-03	4052	0.15	30 min		18	P		15.29	P
15-Jul-03	4052	0.15	45 min		3	P		0.00	P
15-Jul-03	4052	0.15	60 min		12	P		9.28	P
15-Jul-03	4052	0.15	75 min		31	P		39.18	P
15-Jul-03	4052	0.15	90 min		40	P		46.39	P
19-Feb-03	4083	0.1	15 min		314	F/W		879.31	F/W
19-Feb-03	4083	0.1	30 min		111	F		197.89	F/W
19-Feb-03	4083	0.2	15 min		306	F/W		927.59	F/W
19-Feb-03	4083	0.2	30 min		104	F		208.97	F/W
4-Feb-03	4088	0.15	30 min		49	P		40.72	P
4-Feb-03	4089	0.15	30 min		104	F		138.66	F
4-Feb-03	4090	0.15	30 min		103	F		146.13	F/W
4-Feb-03	4091	0.15	30 min		80	F		101.03	F
23-Mar-04	4212	0.15	30 min		5	P		4.83	P
23-Mar-04	4212	0.15	45 min		7	P		7.32	P
23-Mar-04	4212	0.15	60 min		18	P		10.40	P
23-Mar-04	4212	0.15	75 min		29	P		23.13	P
23-Mar-04	4212	0.15	90 min		42	P		37.77	P
21-Jan-03	3834Y	0.15	30 min		19	P		9.03	P
21-Jan-03	3834Z	0.15	30 min		24	P		9.81	P
27-Apr-99	DEET	0.15	15 min		122	F			
27-Apr-99	DEET+2701	0.1	15 min		33	P			
27-Apr-99	DEET+2701	0.1	30 min		39	P			
27-Apr-99	DEET+2701	0.1	45 min		71	F			
27-Apr-99	DEET+2701	0.1	60 min		122	F			
6-May-99	DEET+3004	0.1	15 min		122	F			
6-May-99	DEET+3249	0.1	15 min		45	F			

					Erythema		Histology	
DATE	ICD #	THICKNESS mm	Exposure Time, min		Percent of Control	P/F/W	Percent of Control	P/F/W
6-May-99	DEET+3250	0.1	15 min		64	F		

Table 20. Summary of wash and wipe test results at the USAMRICD. Experiments were conducted on 19 September 2002 (Notebook #032-02, pp.127-131). Experiments used weanling pigs 446, 447, 449, and 450. Exposure tabs were placed in five columns of nine rows down the ventral surface. The scoring ranges for the wash and wipe tests were 0 to 4 and 0 to 3, respectively. A higher score indicated that more aTSP remained on the skin after the wash or wipe procedure. Complete details of the composition of the candidate formulations are listed in Table 16.

ICD #	Active Moiety	aTSP Pre-Wash Drying Time & Pig Position (right or left of midline)						Wipe	Comments
		15 min-right	15 min-left	15 min-AVG	60 min-right	60 min-left	60 min-AVG		
3004	SERPACWA	4	4	4	4	4	4	2	
3771	Lup P, FL7004	4	4	4	4	4	4	3	
3773	Lup G20, FL7004	1	2	1.5	0	1	0.5	3	
3792	Lup FG, FL7005	0	0	0	1	1	1	0	
3829	Lup P, FL7005	4	4	4	2	2	2	3	
3830	Lup G20, FL7005	3	4	3.5	2	3	2.5	0	
3830	Lup G20, FL7005	2	2	2	1	2	1.5	0	
3832	Lup WF, FL7005	2	4	3	4	3	3.5	2	
3833	Lup FG, FL7004	0	0	0	0	0	0	1	
3834	Lup FG/WF, FL7004/05	2	4	3	1	2	1.5	3	
3884	Lup WF/G20, FL7005	4	4	4	4	4	4	0	
3886	Lup P/FG, FL7005	2	2	2	4	4	4	1	
3887	Lup P/G20, FL7005	4	4	4	2	4	3	0	
3903	Lup G20/FG, FL7005	2	2	2	2	1	1.5	1	
3970	Lup WF, FL7004	3	4	3.5	4	2	3	3	
4020	Lup P/G20/04/05	4	3	3.5	4	2	3	3	
4021	Lup P/WF/05	4	3	3.5	4	4	4	2	hard to spread
4022	Lup FG/WF/05	4	3	3.5	4	4	4	1	
4028	S-330	4	4	4	4	4	4	3	
4029	Lup P/FG/04/05	2	3	2.5	4	4	4	3	
4032	Lup G20, FL7005	3	2	2.5	0	3	1.5	1	

		aTSP Pre-Wash Drying Time & Pig Position (right or left of midline)											
ICD #	Active Moiety	15 min-right	15 min-left		15 min-AVG		60 min-right	60 min-left		60 min-AVG		Wipe	Comments
4033	Lup G20, FL7005	2	3		2.5		3	2		2.5		2	
4034	Lup WF, FL7005	4	4		4		3	4		3.5		2	hard to spread
4035	Lup WF, FL7005	4	4		4		3	4		3.5		3	
4036	Lup G20, FL7004	2	1		1.5		1			1		2	
4037	Lup G20, FL7004	3	4		3.5		3	4		3.5		2	
4038	Lup FG, FL7004	3	4		3.5		4	2		3		3	flakes during wiping
4039	Lup FG, FL7004	3	2		2.5		3	2		2.5		3	
4040	Lup FG, FL7005	3	3		3		2	2		2		0	
4041	Lup FG, FL7005	3	4		3.5		3	3		3		0	
4042	Lup FG/WF, FL7004/05	2	2		2		2	4		3		2	
4043	Lup FG/WF, FL7004/05	1	2		1.5		2	2		2		2	flakes during wiping
4044	Lup P, FL7005	4	4		4		4	4		4		2	
4045	Lup P, FL7005	4	4		4		4	4		4		3	
4046	Lup WF,FL7004	4	4		4		4	3		3.5		3	hard to spread
4047	Lup P, FL7004	4	4		4		4	4		4		3	
4048	Lup WF,FL7004	4	1		2.5		4	3		3.5		2	spreads poorly; crumbles
4049	Lup P, FL7004	4	4		4		4	4		4		2	balls up during wiping

Table 21. Summary of wash and wipe test results at the USAMRICD. Experiments conducted on 6 December 2002 (Notebook #069-02, pp.2-8). Experiments used weanling pigs 474 and 475. The exposure tabs were applied in three columns of six rows. The scoring ranges for the wash test and wipe tests were 0 to 4 and 0 to 3, respectively. A higher score indicated that more aTSP remained on the skin after the wash or wipe procedure. A plus sign (+) alongside a visual score indicated that the aTSP was slightly better than the given visual score, but was not effective enough to be given a score of one rank higher. Complete details of the composition of the candidate formulations are listed in Table 16.

		aTSP Pre-Wash Drying Time & Pig Position (right or left of midline)								
ICD #	Active Moiety	15 min right	15 min left	15 min AVG	15 min Wipe	60 min right	60 min left	60 min AVG	60 min Wipe	Comments
4020	Lup P/G20/04/05	1+	3+	2+	2+	2	4	3	3	
4021	Lup P/WF/05	3+	2	2+	2+	3	4	3+	2+	
4029	Lup P/FG/04/05	0	1+	0+	2+	4	2+	3	3	
4050	Lup P/WF/04/05	3+	4	3+	3	4	4	4	3+	
4051	Lup G20/FG/04/05	0	0	0	1+	1+	1+	1+	3	
4052	Lup G20/FW/04/05	1+	2	1+	3	3+	3+	3+	3	

Table 22. Summary of wipe test results at the USAMRICD. Experiments conducted on 6-7 February 2003 (Notebook #069-02, pp.75-79). Experiments used weanling pigs 484, 485, and 486. Exposure tabs were placed in two columns of four rows down the ventral surface. The scoring range for the wipe test was 0 to 3. A higher score indicated that more aTSP remained on the skin after the wipe procedure. Complete details of the composition of the candidate formulations are listed in Table 16.

		15 Min Wipe-Non Normalized				
ICD#	Active Moiety		Near Midline	Far Midline		Average
3004	None		2	1.5		1.75
3771	Lup P, FL-7004		3	3		3
3773	Lup G20, FL-7004		2	2		2
3779	Lup WF, FL-7004		3	3		3
3792	Lup FG, FL-7005		1	1		1
3829	Lup P, FL-7005		3	3		3
3830	Lup G20, FL-7005		1.5	1.5		1.5
3832	Lup WF, FL-7005		2.5	2.5		2.5
3833	Lup FG, FL-7004		2	2.5		2.25
3834	Lup WF/G20, FL-7004/7005		3	3		3
3884	Lup WF/G20, FL-7005		1.5	2		1.75
3886	Lup P/FG, FL-7005		2	2		2
3887	Lup P/G20, FL-7005		2	2		2
3903	Lup FG/G20, FL-7005		1.5	1.5		1.5
4022	Lup WF/FG, FL-7005		1.5	1.5		1.5
4028	S-330		2	2.5		2.25
4088	Nano TiO ₂		2	2		2

Table 23. Summary of the initial safety screening for acute eye and skin irritation in rabbits for lead candidate aTSP formulations. The evaluations were performed at the USACHPPM. Full reports are available in Appendix B. The only tested aTSP formulation that showed any sign of toxicity was ICD 3833 which contained the 26% Lupasol FG, 3% Fluorolink 7004, 38% Fomblin Y25, and 33% F5A PTFE. ICD 3833 produced moderate irritation in the rabbit eye which was resolved within 72 hours. In humans, ICD 3833 should be used with caution around the eyes and mucosa.

ICD No.	Eye Irritation	Skin Irritation	Toxicology Study No.	Date
2701	None	None	85-2594-99	September 1999
3151	None	None	85-MA-6631-01	September 2001
3247	None	None	85-2594-99	September 1999
3248	None	None	85-2594-99	September 1999
3249	None	None	85-2594-99	September 1999
3308	None	None	85-MA-6631-01	September 2001
3471	None	None	85-MA-6631-01	September 2001
3533	None	None	85-MA-6631-01	September 2001
3551	None	None	85-MA-6631-01	September 2001
3665	None	None	85-MA-6631-01	September 2001
3673	None	None	85-MA-6631-01	September 2001
3792	None	None	85-XC-5154-02	Jun-Jul 2002
3829	None	None	85-XC-5154-02	Jun-Jul 2002
3830	None	None	85-XC-5154-02	Jun-Jul 2002
3831	None	None	85-XC-5154-02	Jun-Jul 2002
3832	None	None	85-XC-5154-02	Jun-Jul 2002
3833	Moderate	None	85-XC-5154-02	Jun-Jul 2002
3834	None	None	85-XC-5154-02	Jun-Jul 2002
4020	None	None	85-XC-01FA-03	July 2003
4029	None	None	85-XC-01FA-03	July 2003
4050	None	None	85-XC-01FA-03	July 2003
4051	None	None	85-XC-01FA-03	July 2003
4052	None	None	85-XC-01FA-03	July 2003

Table 24. Summary of *in vivo* and *in vitro* DTN data for the most promising aTSP candidate formulations. The data was organized into a complete matrix of values for each test compound's result on a damage/undesirable measure. The results were expressed as percentages of the same measurement for SERPACWA. Therefore, lower percentage scores indicate BETTER performance. Data in red with white field has been estimated by averaging individual components.

WEIGHTS:		8	5	7	3	2	2	2	2	5
CODE:		HDV	HDL	VXL	GDV	HDL SPME	GDL SPME	VXL SPME	WASH	WIPE
ICD No.	Active	Percent of PC for Pig HDV (30min)	LAR(%) for Rabbit HDL	24hr. Lethality (.5mg) Rabbit VXL	24hr. Lethality (2 caps) Rabbit GDV	HS-SPME % SERPA CWA HDL	HS-SPME % SERPA CWA GDL	HS-SPME % SERPA CWA VXL	Normalized Wash Test	Normalized Wipe Test
3771	Lupasol P,FL/04	25.1	45.9	12.5	60.0	89.8	8.6	70.4	1.0	1.0
3772\3830	Lupasol G20, FL05	30.8	45.3	18.8	1.0	31.6	1.0	74.1	37.5	75.0
3773\3790	Lupasol G20, FL04	16.3	25.2	25.0	16.7	34.8	1.0	65.7	75.0	17.2
3791\3832	Lupasol WF, FL05	26.1	37.7	43.8	30.0	25.2	1.4	61.4	18.8	24.9
3780\3792	Lupasol FG, FL05	28.1	50.5	42.9	1.0	27.3	1.0	12.7	87.5	83.4
3829	Lupasol P, FL05	61.7	45.9	6.3	15.4	89.8	8.6	70.4	25.5	1.0
3833	Lupasol FG, FL04	15.7	51.0	28.6	1.0	22.3	1.0	31.4	100.0	45.5
3834	Lupasol FG/WF, FL04/05	11.6	30.0	1.0	1.0	18.4	1.0	18.8	43.8	1.0
3884	Lupasol G20/WF, FL04/05	23.5	43.0	1.0	1.0	19.4	1.0	25.2	1.0	70.8
3886	Lupasol P/FG, FL05	46.9	18.9	25.0	1.0	27.3	1.0	12.7	25.5	49.7
3887	Lupasol P/G20, FL05	48.3	23.3	12.5	7.8	33.2	1.0	40.0	13.0	66.7
3903	Lupasol G20/FG, FL05	50.5	37.0	12.5	1.0	25.1	1.0	16.4	56.3	58.0
3779\3970	Lupasol WF, FL04	43.3	25.0	31.3	30.0	57.9	11.0	86.8	18.8	1.0
4020	Lupasol P/G20, FL04/05	12.4	16.1	1.0	7.8	33.2	1.0	40.0	89.6	8.9
4021	Lupasol P/WF, FL05	35.9	33.2	8.3	58.0	4.0	4.0	9.0	13.3	16.7
4022	Lupasol FG/WF, FL05	43.4	28.6	18.8	1.0	18.4	1.0	18.8	6.8	58.0
4028	S-330	17.1	6.9	18.8	100.0	0.0	100.0	100.0	1.0	13.0
4029	Lupasol P/FG, FL04/05	25.5	11.8	1.0	1.0	27.3	1.0	12.7	43.2	8.9
4050	Lupasol P/WF, FL04/05	13.4	26.2	1.0	58.0	4.0	4.0	9.0	41.7	1.0
4051	Lupasol G20/FG, FL04/05	18.6	25.9	1.0	1.0	25.1	1.0	16.4	48.2	25.5
4052	Lupasol G20/WF, FL04/05	10.2	22.0	16.7	15.0	19.4	1.0	25.2	59.1	1.0
3004	SERPAWCA	102.0	40.8	13.0	97.2	100.0	100.0	100.0	1.0	37.3

Table 25. Summary of normalized weighted scores (higher is better). To make higher scores indicate better performance, the raw data percentages were subtracted from 100. The adjusted scores were multiplied by the appropriate normalized weighting factor (weighting factor divided by total of all the weighing factors, 36) to generate the normalized weighted scores reported in this table.

		Weighted Normalized Scores (higher is better)								
ICD No.	Active	HDV	HDL	VXL	GDV	HDLspme	GDLspme	VXLspme	WASH	WIPE
		Perc ent of PC for Pig HDV (30min)	LAR(%) for Rabbit HDL	24hr. Lethality (.5mg) Rabbit VXL	24hr. Lethality (2 caps) Rabbit GDV	HS-SPME % SERPACWA HDL	HS-SPME % SERPACWA GDL	HS-SPME % SERPACWA VXL	Normalized Wash Test	Normalized Wipe Test
3771	Lupasol P,FL/04	16.6	7.5	17.0	3.3	0.6	5.1	1.6	5.6	13.9
3772\3830	Lupasol G20, FL05	15.4	7.6	15.8	8.3	3.8	5.6	1.4	3.5	3.5
3773\3790	Lupasol G20, FL04	18.6	10.4	14.6	6.9	3.6	5.6	1.9	1.4	11.5
3791\3832	Lupasol WF, FL05	16.4	8.7	10.9	5.8	4.2	5.5	2.1	4.5	10.4
3780\3792	Lupasol FG, FL05	16.0	6.9	11.1	8.3	4.0	5.6	4.9	0.7	2.3
3829	Lupasol P, FL05	8.5	7.5	18.2	7.1	0.6	5.1	1.6	4.1	13.9
3833	Lupasol FG, FL04	18.7	6.8	13.9	8.3	4.3	5.6	3.8	0.0	7.6
3834	Lupasol FG/WF, FL04/05	19.6	9.7	19.4	8.3	4.5	5.6	4.5	3.1	13.9
3884	Lupasol G20/WF, FL04/05	17.0	7.9	19.4	8.3	4.5	5.6	4.2	5.6	4.1
3886	Lupasol P/FG, FL05	11.8	11.3	14.6	8.3	2.3	5.3	3.2	4.1	7.0
3887	Lupasol P/G20, FL05	11.5	10.7	17.0	7.7	3.7	5.6	3.3	4.8	4.6
3903	Lupasol G20/FG, FL05	11.0	8.8	17.0	8.3	4.2	5.6	4.6	2.4	5.8
3779\3970	Lupasol WF, FL04	12.6	10.4	13.4	5.8	2.3	4.9	0.7	4.5	13.9
4020	Lupasol P/G20, FL04/05	19.5	11.7	19.4	6.4	2.9	5.4	2.1	0.6	12.7
4021	Lupasol P/WF, FL05	14.2	9.3	17.8	6.4	2.4	5.3	1.9	4.8	11.6
4022	Lupasol FG/WF, FL05	12.6	9.9	15.8	7.1	4.1	5.5	3.5	5.2	5.8
4028	S-330	18.4	12.9	15.8	0.0	5.6	0.0	0.0	5.6	12.1
4029	Lupasol P/FG, FL04/05	16.6	12.3	19.4	7.1	3.0	5.4	3.8	3.2	12.7
4050	Lupasol P/WF, FL04/05	19.2	10.3	19.4	5.4	2.4	5.2	1.5	3.2	13.9
4051	Lupasol G20/FG, FL04/05	18.1	10.3	19.4	8.0	4.0	5.6	3.3	2.9	10.3
4052	Lupasol G20/WF, FL04/05	20.0	10.8	16.2	7.4	3.7	5.4	2.1	2.3	13.9
3004.0000	SERPAWCA	-0.4	8.2	16.9	0.2	0.0	0.0	0.0	5.6	8.7

Table 26. Summary of compound rankings based on individual measures listed in Table 24.

ICD No.	Active	Percent of PC for Pig HDV (30min)	LAR (%) for Rabbit HDL	24hr. Lethality (.5mg) Rabbit VXL	24hr. Lethality (2 caps) Rabbit GDV	HS-SPME % SERPA CWA HDL	HS-SPME % SERPA CWA GDL	HS-SPME % SERPA CWA VXL	Normalized Wash Test	Normalized Wipe Test
3771	Lupasol P,FL/04	10	20	10	20	21	19	17	3	4
3772\3830	Lupasol G20, FL05	14	18	15	4	10	5	19	12	21
3773\3790	Lupasol G20, FL04	6	8	18	14	13	5	14	19	11
3791\3832	Lupasol WF, FL05	12	15	22	18	6	11	11	9	12
3780\3792	Lupasol FG, FL05	13	21	21	4	8	5	1	20	22
3829	Lupasol P, FL05	21	20	7	13	21	19	17	11	4
3833	Lupasol FG, FL04	5	22	19	4	4	5	5	22	15
3834	Lupasol FG/WF, FL04/05	2	12	4	4	2	5	3	15	4
3884	Lupasol G20/WF, FL04/05	9	17	4	4	3	5	4	3	20
3886	Lupasol P/FG, FL05	18	4	18	4	19	15	10	11	16
3887	Lupasol P/G20, FL05	19	6	10	9	11	5	8	6	19
3903	Lupasol G20/FG, FL05	20	14	10	4	5	5	2	17	18
3779\3970	Lupasol WF, FL04	16	7	20	18	18	20	20	9	4
4020	Lupasol P/G20, FL04/05	3	3	4	16	15	12	13	21	8
4021	Lupasol P/WF, FL05	15	13	8	15	16	16	15	7	10
4022	Lupasol FG/WF, FL05	17	11	15	11	7	10	7	5	18
4028	S-330	7	1	15	22	1	22	22	3	9
4029	Lupasol P/FG, FL04/05	11	2	4	12	14	14	6	14	8
4050	Lupasol P/WF, FL04/05	4	10	4	19	17	17	18	13	4
4051	Lupasol G20/FG, FL04/05	8	9	4	8	9	5	9	16	13
4052	Lupasol G20/WF, FL04/05	1	5	13	10	12	13	13	18	4
3004	SERPAWCA	22	16	12	21	22	22	22	3	14

Table 27. Summary of normalized weighted rank scores (higher is better). To make higher scores indicate better performance, the rank number was subtracted from the 23 (the total number of compounds plus 1). The adjusted scores were multiplied by the appropriate normalized weighting factor (weighting factor divided by total of all the weighing factors, 36) to generate the normalized weighted scores reported in this table.

ICD No.	Active	Weighted Normalized Rank Scores (higher is better)								
		HDV	HDL	VXL	GDV	HDL SPME	GDL SPME	VXL SPME	WASH	WIPE
		Perce nt of PC for Pig HDV (30min)	LAR(%) for Rabbit HDL	24hr. Lethality (.5mg) Rabbit VXL	24hr. Lethality (2 caps) Rabbit GDV	HS- SPME % SERPA CWA HDL	HS- SPME % SERPA CWA GDL	HS- SPME % SERPA CWA VXL	Norma lized Wash Test	Normal ized Wipe Test
3771	Lupasol P,FL/04	2.9	0.5	2.5	0.3	0.1	0.3	0.4	1.1	2.7
3772\3830	Lupasol G20, FL05	2.0	0.7	1.6	1.6	0.7	1.0	0.2	0.6	0.3
3773\3790	Lupasol G20, FL04	3.8	2.1	1.1	0.8	0.6	1.0	0.5	0.2	1.7
3791\3832	Lupasol WF, FL05	2.4	1.1	0.2	0.5	0.9	0.7	0.7	0.8	1.5
3780\3792	Lupasol FG, FL05	2.2	0.3	0.4	1.6	0.8	1.0	1.2	0.2	0.1
3829	Lupasol P, FL05	0.4	0.5	3.1	0.8	0.1	0.3	0.4	0.7	2.7
3833	Lupasol FG, FL04	4.0	0.1	0.8	1.6	1.1	1.0	1.0	0.1	1.1
3834	Lupasol FG/WF, FL04/05	4.7	1.5	3.8	1.6	1.2	1.0	1.1	0.4	2.7
3884	Lupasol G20/WF, FL04/05	3.1	0.8	3.8	1.6	1.1	1.0	1.1	1.1	0.4
3886	Lupasol P/FG, FL05	1.1	2.6	1.1	1.6	0.2	0.4	0.7	0.7	1.0
3887	Lupasol P/G20, FL05	0.9	2.4	2.5	1.2	0.7	1.0	0.8	0.9	0.6
3903	Lupasol G20/FG, FL05	0.7	1.3	2.5	1.6	1.0	1.0	1.2	0.3	0.8
3779\3970	Lupasol WF, FL04	1.6	2.2	0.6	0.5	0.3	0.2	0.2	0.8	2.7
4020	Lupasol P/G20, FL04/05	4.4	2.8	3.8	0.6	0.4	0.6	0.6	0.1	2.2
4021	Lupasol P/WF, FL05	1.8	1.4	2.9	0.7	0.4	0.4	0.4	0.9	1.8
4022	Lupasol FG/WF, FL05	1.3	1.7	1.6	1.0	0.9	0.7	0.9	1.0	0.8
4028	S-330	3.6	3.1	1.6	0.1	1.2	0.1	0.1	1.1	1.9
4029	Lupasol P/FG, FL04/05	2.7	2.9	3.8	0.9	0.5	0.5	0.9	0.5	2.2
4050	Lupasol P/WF, FL04/05	4.2	1.8	3.8	0.3	0.3	0.3	0.3	0.6	2.7
4051	Lupasol G20/FG, FL04/05	3.3	1.9	3.8	1.3	0.8	1.0	0.8	0.4	1.4
4052	Lupasol G20/WF, FL04/05	4.9	2.5	1.9	1.1	0.6	0.6	0.6	0.3	2.7
3004	SERPAWCA	0.2	1.0	2.1	0.2	0.1	0.1	0.1	1.1	1.3

Table 28. Summary of the normalized numerical rankings for groups of measures based on the combined measures. Rankings are given for weighted and unweighted data and *in vivo* and *in vitro* experiments. Note that the highest rank the compound can receive is a 1; the lowest is 22. The table is ordered by the overall best average ranking considering all the different groups measures.

		COMPUTED ON PERCENTAGES						COMPUTED ON INDIVIDUAL RANKS						Overall
		Weighted			Un-weighted			Weighted			Un-weighted			
ICD No.	Active	ALL	In Vivo	Physical	ALL	In Vivo	Physical	ALL	In Vivo	Physical	ALL	In Vivo	Physical	
3834	polymer C/D/04/05	1	2	3	1	3	3	1	2	2	1	3	3	2.08
4029	polymer A/C/04/05	2	3	5	2	2	4	4	3	5	2	2	5.5	3.29
4050	polymer A/D/04/05	3	7	1	3	13	2	2	5	1	3	7	1	4.00
4052	polymer BD/04//05	4	5	4	5	5	6	5	6	3	4	5	5.5	4.79
4051	polymer B/C/04/05	6	4	6	4	4	8	6	4	9	5	4	9	5.75
4020	polymer A/B/04/05	5	1	10	10	1	14	3	1	14	7	1	16	6.92
3884	polymer B/D/05	8	6	15	6	6	9	7	7	13	6	6	7	8.00
4021	polymer A/D/05	7	16	2	7	18	1	9	11	4	9	16	2	8.50
4022	polymer C/D/05	10	13	11	8	8	5	12	15	8	8	12	4	9.50
3886	polymer A/C/05	11	14	12	9	9	7	13	13	10	10	8.5	8	10.38
3773\3790	polymer B/04	9	8	14	14	7	16	10	9	18	15	10.5	20	12.54
4028	S-330	13	10	16	21	20	20	8	8	7	11	8.5	10	12.71
3887	polymer A/B/05	15	12	18	11	10	11	14	10	19	13	10.5	13.5	13.08
3771	polymer A/04	12	17	7	17	21	13	11	14	6	16	17.5	13.5	13.75
3903	polymer B/C/05	18	15	17	12	14	12	16	16	16	12	13	11	14.33
3833	polymer C/04	14	9	19	15	12	18	15	12	17	14	14	15	14.50
3791\3832	polymer D/05	17	20	8	13	19	10	19	21	15	18	21	12	16.08
3779\3970	polymer D/04	16	19	9	16	17	15	17	18	12	20	17.5	19	16.29
3829	polymer A/05	19	21	13	19	16	17	18	19	11	21	20	18	17.67
3772\3830	polymer B/05	20	11	20	18	11	21	20	17	22	18	15	21	17.83
3780\3792	polymer C/05	21	18	21	20	15	19	21	20	20	18	19	17	19.08
3004	SERPAWCA	22	22	22	22	22	22	22	22	21	22	22	22	21.92

Table 29. Compound Rankings on Combined Measures

		COMPUTED ON PERCENTAGES						COMPUTED ON INDIVIDUAL RANKS						
		Weighted			Un-weighted			Weighted			Un-weighted			
ICD No.	Active	ALL	In Vivo	Physical	ALL	In Vivo	Physical	ALL	In Vivo	Physical	ALL	In Vivo	Physical	Overall
3834	Lupasol FG/WF, FL04/05	1	1	1	1	1	1	1	2	1	1	1	1	1.1
4029	Lupasol P/FG, FL04/05	2	4	2	3	4	5	4	5	6	4	4	10	4.3
4051	Lupasol G20/FG, FL04/05	3	3	8	4	2	6	5	4	8	3	4	8	4.8
4052	Lupasol G20/WF, FL04/05	4	5	3	5	5	9	3	3	2	5	5	12	5.1
3884	Lupasol G20/WF, FL04/05	7	7	13	2	6	2	7	7	3	2	6	2	5.3
4020	Lupasol P/G20, FL04/05	5	2	14	11	3	18	2	1	18	7	2	17	8.3
4050	Lupasol P/WF, FL04/05	6	6	7	8	7	13	6	6	12	12	7	18	9.0
3887	Lupasol P/G20, FL05	14	13	17	7	10	7	10	10	15	6	9	6	10.3
4022	Lupasol FG/WF, FL05	12	15	11	6	15	3	15	17	10	10	16	4	11.0
3773\3790	Lupasol G20, FL04	8	8	12	14	8	15	9	9	16	13	11	14	11.4
3903	Lupasol G20/FG, FL05	18	16	16	9	13	8	14	15	10	8	12	4	11.8
4021	Lupasol P/WF, FL05	9	9	9	10	14	10	13	11	17	16	15	15	12.3
4028	S-330	11	11	15	21	20	20	8	8	7	10	10	10	12.5
3833	Lupasol FG, FL04	13	10	19	15	12	17	12	12	11	11	13	7	12.7
3771	Lupasol P,FL/04	10	17	4	17	21	11	11	14	6	19	18	13	13.4
3791\3832	Lupasol WF, FL05	16	20	5	12	19	4	19	21	4	16	21	5	13.5
3886	Lupasol P/FG, FL05	17	14	18	13	9	14	16	13	20	14	8	21	14.8
3779\3970	Lupasol WF, FL04	15	19	6	16	18	12	18	19	14	21	20	20	16.5
3772\3830	Lupasol G20, FL05	20	12	20	18	11	21	20	16	21	18	15	16	17.3
3829	Lupasol P, FL05	19	21	10	19	17	16	17	18	13	20	20	19	17.4
3780\3792	Lupasol FG, FL05	21	18	21	20	16	19	21	20	19	16	17	11	18.3
3004	SERPAWCA	22	22	22	22	22	22	22	22	22	22	22	22	22.0

APPENDIX A: aTSP PUBLICATIONS

aTSP Peer Review Publications

- Braue, EH Jr. and Pannella, MG "Topical Protectant Evaluation By FT-IR Spectroscopy," Appl. Spectrosc., 44, 1061-1063, 1990.
- Braue, EH Jr., Mershon, MM, Wade, JV, and Litchfield, MR, "In Vivo Assessment of Vesicant Skin Injury Using a Minolta Chroma Meter," J. Soc. Cosmet. Chem., 41, 259-265, 1990.
- Braue, EH, Jr., Koplovitz, I, Mitcheltree, LW, Clayson, ET, Litchfield, MR, and Bangledorf, CR, "Characterization of the Sulfur Mustard Vapor Induced Cutaneous Lesions on Hairless Guinea Pigs," Toxicology Methods 2, 242-254, 1992.
- Braue, EH, Jr., Litchfield, MR, Bangledorf, CR, and Rieder, RG, "FT-IR/ATR Evaluation of topical skin protectants useful for sulfur mustard and related compounds," SPIE, 1575, 311-312, 1992.
- Braue, EH Jr., Nalls, CR, Way, RA, Zallnick, JE, Rieder, RG, and Mitcheltree, LW, "Nikolsky's Sign—A novel way to evaluate damage at the dermal-epidermal junction," Skin Res Tech 3, 245-251, 1997.
- Braue, EH Jr., Nalls, CR, Way, RA, Zallnick, JE, Rieder, RG, Lee, RB, and Mitcheltree, LW, "Characterization of the sulfur mustard vapor induced cutaneous lesions on haired guinea pigs," Skin Res Tech, 4, 99-108, 1998.
- Braue, EH Jr., "Development of a Reactive Topical Skin Protectant," J Appl Toxicol, 19, S47-53, 1999.
- Braue, EH, Jr, Hanssen, KA, Doxzon, BF, Lumpkin, HL and Clarkson, ED, Efficacy Studies of RSDL, M291 SDK, 0.5% Bleach, 1% Soapy Water and SERPACWA, Part 1: Guinea Pigs Challenged with VX. **Cutan Ocul Toxicol, 30 (1):** 15-28, 2011.
- Braue, EH, Jr, Hanssen, KA, Doxzon, BF, Lumpkin, HL and Clarkson, ED, Efficacy Studies of RSDL, M291 SDK, 0.5% Bleach, 1% Soapy Water and SERPACWA, Part 2: Guinea Pigs Challenged with Soman. **Cutan Ocul Toxicol, 30 (1):** 29-37, 2011.
- Bryant, MA and **Braue EH, Jr.**, "Comparison of Fixation and Processing Methods for Hairless Guinea Pig Skin Following Sulfur Mustard Exposure," Toxicology Methods, 2, 87-100, 1992.
- Graham, JS, Bryant, MA, and Braue, EH Jr., "Effect of Sulfur Mustard on Mast Cells in Hairless Guinea Pig Skin," J. Toxicol.-Cut. & Ocular Toxicol., **13(1)**, 47-54, 1994.

Hobson, ST, Lehnert, EK, and Braue, EH Jr., "The U. S. Army Reactive Topical Skin Protectant (rTSP): Challenges and Successes," *MRS Symposium Series CC: Hybrid Organic Inorganic Materials* [Online], 628, CC10.8.1-CC10.8.8, 2000.

Hobson, ST, and Braue, EH Jr., Development of multifunctional perfluorinated polymer blends as an active barrier cream against chemical warfare agents. "*Polymeric Materials: Science & Engineering*," 84, 80, 2001.

Mershon, MM, Wade, JV, Mitcheltree, LW, Petralli, JP, and Braue, EH Jr., "Hairless Guinea Pig Bioassay Model for Vesicant Vapor Exposures," *Fundam. Appl. Toxicol.* 15, 622-630, 1990.

Snider, TH, Matthews, MC, and Braue, EH Jr., "A model for assessing efficacy of topical skin protectants against sulfur mustard vapor using hairless guinea pigs," *J Appl Toxicol*, 19, S55-58, 1999.

aTSP Patents

Braue, EH Jr., Hobson, ST, and Mershon, MM, Active Topical Skin Protectants, Provisional Patent Application No. 60/209,337 filed June 2, 2000.

Braue, EH Jr., Hobson, ST, Govardhan, C, and Khalaf, N, Active Topical Skin Protectants Containing OPAA Enzymes and CLECs, U.S. Patent No. 6,410,604, June 25, 2002.

Braue, EH Jr., Hobson, ST, Hill, CL, Boring, E, and Rhule, J, Active Topical Skin Protectants Using Polyoxometalates and/or Coinage Metal Complexes, U.S. Patent No. 6,414,039, July 2, 2002.

Braue, EH Jr., Hobson, ST, White, J, and Bley, R, Active Topical Skin Protectants Using Polyoxometallates, U.S. Patent No. 6,420,434, July 16, 2002.

Braue, EH Jr., Hobson, ST and Lehnert, EK, Active Topical Skin Protectants, U.S. Patent No. 6,472,437, October 27, 2002.

Braue, EH Jr., Mershon, MM, Braue, CR, and Way, RA, Active Topical Skin Protectants Containing S-330, U.S. Patent No. 6,472,438, October 29, 2002.

Braue, EH Jr., Hobson, ST, Boecker, JD, and Smith, BM, Active Topical Skin Protectants Containing Amines, Polyalkenimines and/or Derivatives, U.S. Patent No. 7,976,832, July 12, 2011.

Hill, CL, Xu, L, Rhule, JT, Boring, EA, Hobson, ST, and Braue, EH Jr, Polyoxometalate Materials, Metal-Containing Materials, and Methods of Use Thereof, U.S. Patent No. 6,723,349, April 20, 2004.

Hobson, ST, Braue, EH Jr., Lehnert, EK, Klabunde, KJ, Koper, OP, and Decker, S, Active Topical Skin Protectants Using Reactive Nanoparticles, U.S. Patent No. 6,403,653, June 11, 2002.

Hobson, ST, Braue, EH Jr., Lehnert, EK, Klabunde, KJ, Decker, S, Hill, CL, Rhule, J, Boring, E, and Koper, O, Active Topical Skin Protectants Using Combinations of Reactive Nanoparticles and Polyoxometalates or Metal Salts, U.S. Patent No. 6,410,603, June 25, 2002.

Hobson, ST, Braue, EH Jr., and Shea, K, Active Topical Skin Protectants Using Organic Inorganic Polysilsesquioxane Materials, U.S. Patent No. 6,417,236, July 9, 2002.

Hobson, ST, Braue, EH Jr., and Back, D, Active Topical Skin Protectants Using Polymer Coated Metal Alloys, U.S. Patent No. 6,437,005, August 20, 2002.

aTSP GOVERNMENT PUBLICATIONS

Arroyo, CM, Sankovich, JM, Kahler, DW, Burman, DL, and Braue, EH Jr., "Application of EPR and NMR to the analysis of phosphovanadomolybdate polyoxometalate, $H_5PV_2Mo_{10}O_{40}$, reacting with chloroethyl sulfides (H-MG and HD)," Proceedings of the U. S. Army 2002 Medical Defense Bioscience Review, USAMRICD, Aberdeen Proving Ground, MD, 2002 (on CD ROM).

Braue, EH Jr., Mershon, MM, Wade, JV, and Litchfield, MR, "In Vivo Assessment of Vesicant Skin Injury Using a Minolta Chroma Meter, Proceedings of the 1989 Medical Defense Bioscience Review, U.S. Army Medical Research Institute of Chemical Defense, pp. 577-583, 1989. AD B139550.

Braue, EH Jr. and Pannella, MG, "Topical Protectant Evaluation by FT-IR Spectroscopy," Proceedings of the 1989 Medical Defense Bioscience Review, U.S. Army Medical Research Institute of Chemical Defense, pp. 615-617, 1989. AD B139550.

Braue, EH Jr., Mershon, MM, Larsen, T, Mitcheltree, LW, Litchfield, MR, and Bangledorf, CR, "Fluid-Filled Blisters Observed on Hairless Guinea Pigs Following Vapor Exposure to Sulfur Mustard (HD). Proceedings of TTCP, TPI Meeting, July 1990 in Porton-Down, England, ICD No. A90-045a.

Braue, EH Jr., Mershon, MM, Larsen, T, Mitcheltree, LW, Clayson, ET, Litchfield, MR, and Bangledorf, CR, "The Hairless Guinea Pig as an *in vivo* Model for the Assessment of Antivesicant Compounds. Proceedings of the RSG-3 Meeting, April 1991 in Grenoble, France, ICD No. A91-022.

Braue, EH Jr., Mershon, MM, Larsen, T, Mitcheltree, LW, Clayson, ET, Litchfield, MR, and Bangledorf, CR, "Assessment of Antivesicant Compounds using the Hairless Guinea Pig." Proceedings of the 1991 Medical Defense Bioscience Review, U.S. Army Medical Research Institute of Chemical Defense, pp. 9-16, 1991. AD B158588.

Braue, EH Jr., Bangledorf, CR, and Rieder, RG, "New methods for evaluating skin injury from sulfur mustard in the hairless guinea pig," Proceedings of the 1993 Medical Defense Bioscience Review, U.S. Army Medical Research Institute of Chemical Defense. Vol No. 3, pp. 105-111, 1993. AD A275667.

Braue, EH Jr., Nalls, CR, Way, RA, Zallnick, JE, Rieder, RG, and Mitcheltree, LW "The haired guinea pig as a vesicant animal model," Proceedings of the 1996 Medical Defense Bioscience Review, U.S. Army Medical Research Institute of Chemical Defense. Vol No. II, pp 685-694, 1996. AD A321841.

Braue, EH Jr., "Development of a Reactive Topical Skin Protectant," Proceedings of the 1998 Medical Defense Bioscience Review, U.S. Army Medical Research Institute of Chemical Defense, APG, MD.

Braue, EH Jr., Hobson, ST, Lehnert, EK, Lewis, N, Nalls-Braue, CR, Doxzon, BF, Simons, RT, DiLeonardi, PA, Nohe, TL, and Graham, JS, "Progress in Developing an Active Topical Skin Protectant," Proceedings of the 22nd Army Science Conference, 11-13 December 2000, Baltimore, MD, pp. 369-374.

Braue, EH Jr., Hobson, ST, Lehnert, EK, Lewis, N, Nalls, CR, Doxzon, BF, Simons, RT, DiLeonardi, PA, Knickman, JK, Stone, JA, Nohe, TL, and Graham, JS, "Progress in Developing a Reactive Topical Skin Protectant," Proceedings of the U. S. Army 2000 Medical Defense Bioscience Review, Vol III, USAMRICD, pp. 949-956.

Braue, EH Jr, Hobson, ST, Lehnert, EK, Lewis, N, Nalls-Braue, CR, Doxzon, BF, Simons, RT, DiLeonardi, PA, Nohe, TL, and Graham, JS, "Progress in Developing an Active Topical Skin Protectant," Proceedings of the 2001 Scientific Conference on Chemical and Biological Defense Research, 6-8 March 2001, Hunt Valley, MD.

Braue, EH Jr., Hanssen, KA, Doxzon, BF, Lumpkin, HL, and Clarkson, E, Evaluation of RSDL, M291 SDK, 0.5% Bleach, 1% Soapy Water, and SERPACWA; Part 1: Challenge with VX, USAMRICD-TR-09-01. U.S. Army Medical Research Institute of Chemical Defense, Aberdeen Proving Ground, MD, June 2009.

Braue, EH Jr., Hanssen, KA, Doxzon, BF, Lumpkin, HL, and Clarkson, E, Evaluation of RSDL, M291 SDK, 0.5% Bleach, 1% Soapy Water, and SERPACWA; Part 2: Challenge with GD, USAMRICD-TR-10-04. U.S. Army Medical Research Institute of Chemical Defense, Aberdeen Proving Ground, MD, June 2010.

Braue, EH Jr., Hanssen, KA, Doxzon, BF, Lumpkin, HL, and Clarkson, E, (U) Evaluation of RSDL, M291 SDK, 0.5% Bleach, 1% Soapy Water, and SERPACWA; Challenge with toxic compounds. USAMRICD-TR-12-03. U.S. Army Medical Research Institute of Chemical Defense, Aberdeen Proving Ground, MD, March 2012 (classified report).

Braue, EH Jr., Hanssen, KA, Doxzon, BF, Lumpkin, HL, and Clarkson, E, Efficacy studies OF RSDL, M291 SDK, 0.5% BLEACH, 1% SOAPY WATER AND SERPACWA; PART 3: Challenge with EA6033, USAMRICD-TR-14-03. U.S. Army Medical Research Institute of Chemical Defense, Aberdeen Proving Ground, MD, June 2014 (classified report).

Braue, EH Jr., Smith, KH, Doxzon, BF, Lumpkin, HL, Devorak, JL, and Stevenson, RS, Evaluation of RSDL, M291 SDK, 0.5% Bleach, 1% Soapy Water, and SERPACWA; Part 4: Challenge with EA6030, USAMRICD-TR-XXX. U.S. Army Medical Research Institute of Chemical Defense, Aberdeen Proving Ground, MD, June 2015 (classified report).

Braue, EH Jr., Smith, KH, Doxzon, BF, Lumpkin, HL, Devorak, JL, and Stevenson, RS, Evaluation of RSDL, M291 SDK, 0.5% Bleach, 1% Soapy Water, and SERPACWA; Part 5: Challenge with EA6032, USAMRICD-TR-XXX. U.S. Army Medical Research Institute of Chemical Defense, Aberdeen Proving Ground, MD, June 2015 (classified report).

Braue, EH Jr., Smith, KH, Doxzon, BF, Lumpkin, HL, JL, and Stevenson, RS, Evaluation of RSDL, M291 SDK, 0.5% Bleach, 1% Soapy Water, and SERPACWA; Part 6: Challenge with EA6039, USAMRICD-TR-XXX. U.S. Army Medical Research Institute of Chemical Defense, Aberdeen Proving Ground, MD, June 2015 (classified report).

Braue, EH Jr., Smith, KH, Doxzon, BF, Lumpkin, HL, JL, and Stevenson, RS, Evaluation of RSDL, M291 SDK, 0.5% Bleach, 1% Soapy Water, and SERPACWA; Part 7: Challenge with EA5488, USAMRICD-TR-XXX. U.S. Army Medical Research Institute of Chemical Defense, Aberdeen Proving Ground, MD, June 2015 (classified report).

Braue, EH Jr., Smith, KH, Doxzon, BF, Devorak, JL, Stevenson, RS, and Lumpkin, HL, Evaluation of RSDL, M291 SDK, 0.5% Bleach, 1% Soapy Water, and SERPACWA; Part 8: Challenge with EA6053, USAMRICD-TR-XXX. U.S. Army Medical Research Institute of Chemical Defense, Aberdeen Proving Ground, MD, June 2015 (classified report).

Braue, EH Jr., Smith, KH, Doxzon, BF, Lumpkin, HL, Devorak, JL, and Stevenson, RS, Evaluation of RSDL, M291 SDK, 0.5% Bleach, 1% Soapy Water, and SERPACWA; Part 9: Challenge with EA6072, USAMRICD-TR-XXX. U.S. Army Medical Research Institute of Chemical Defense, Aberdeen Proving Ground, MD, June 2015 (classified report).

Braue, EH Jr., Devorak, JL, Doxzon, BF, Lumpkin, HL, and Azeke, JI, Evaluation of RSDL, M291 SDK, 0.5% Bleach, 1% Soapy Water, and SERPACWA; Part 10: Challenge with EA6048, USAMRICD-TR-XXX. U.S. Army Medical Research Institute of Chemical Defense, Aberdeen Proving Ground, MD, June 2015 (classified report).

- Braue, EH Jr., Doxzon, BF, Lumpkin, HL, Smith, KH, Devorak, JL, and Stevenson, RS, Evaluation of RSDL, M291 SDK, 0.5% Bleach, 1% Soapy Water, and SERPACWA; Part 11: Challenge with EA4243 (VR, Russian VX), USAMRICD-TR-16-01. U.S. Army Medical Research Institute of Chemical Defense, Aberdeen Proving Ground, MD, January 2016.
- Braue, EH Jr., Doxzon, BF, Lumpkin, HL, Smith, KH, Devorak, JL, and Stevenson, RS, Evaluation of RSDL, M291 SDK, 0.5% Bleach, 1% Soapy Water, and SERPACWA; Part 12: Challenge with EA1212 (GF, cyclosarin, USAMRICD-TR-16-02. U.S. Army Medical Research Institute of Chemical Defense, Aberdeen Proving Ground, MD, January 2016.
- Govardhan, CP, Khalaf, N, and Braue, EH Jr., "Reactive topical skin formulations with crystals of the organophosphorus acid anhydrolase enzyme (OPAA-2)," Proceedings of the U. S. Army 2000 Medical Defense Bioscience Review, Vol III, USAMRICD, pp. 967-973.
- Grow, AE and Braue, EH Jr., "Catalysts for use in reactive topical skin protectants," Proceedings of the U. S. Army 2000 Medical Defense Bioscience Review, Vol III, USAMRICD, p. 977.
- Grow, AE and Braue, EH Jr, "Microcatalysts as active moieties for topical skin protectants," Proceedings of the U. S. Army 2002 Medical Defense Bioscience Review, USAMRICD, Aberdeen Proving Ground, MD, 2002 (on CD ROM).
- Hobson ST and Braue, EH Jr. "Active topical skin protectants: swiftly moving towards the goal of protecting the warfighter against chemical warfare agents," Proceedings of the U. S. Army 2002 Medical Defense Bioscience Review, USAMRICD, Aberdeen Proving Ground, MD, 2002 (on CD ROM).
- Hoffman, TL, Snider, TH, Matthews, MC, and Braue, EH, Jr., Assessment of Active Topical Skin Protectants Against Challenges with Sulfur Mustard, Soman, or VX, Proceedings of the U. S. Army 2004 Medical Defense Bioscience Review, USAMRICD, Aberdeen Proving Ground, MD, 2004 (on CD ROM).
- Kurt, EM and Braue, EH Jr., "Skin Adsorption Pharmacology of Topical Skin Protectant ICD #2289," USAMRICD-TR-97-03, USAMRICD, APG, MD, June 1997.
- Snider, H, Matthews, MC, and Braue, EH Jr., "A model for assessing efficacy of topical skin protectants against sulfur mustard vapor using hairless guinea pigs," Proceedings of the 1998 Medical Defense Bioscience Review, U.S. Army Medical Research Institute of Chemical Defense, APG, MD.

Snider, TH, Matthews, MC and Braue, EH Jr., "Efficacy Evaluation of Reactive Topical Skin Protectants Against Nerve Agent Vapors," Proceedings of the U. S. Army 2000 Medical Defense Bioscience Review, Vol III, USAMRICD, pp. 1025-1031.

Snider, TH, Matthews, MC, and Braue, EH Jr., "Teflon disks improve the lesion area of candidate active topical skin protectants against sulfur mustard," Proceedings of the U. S. Army 2002 Medical Defense Bioscience Review, USAMRICD, Aberdeen Proving Ground, MD, 2002 (on CD ROM).

Snider, TH, Matthews, MC and Braue, EH Jr., "Multi-tiered screening of reactive topical skin protectant candidates against chemical agents," Proceedings of the U. S. Army 2002 Medical Defense Bioscience Review, USAMRICD, Aberdeen Proving Ground, MD, 2002 (on CD ROM).

Snider, TH, Wilhelm, CM, Matthews, MC, and LeClaire, RD. Efficacy aTSP Decision Tree Network (DTN) Screening. Ft. Detrick, Md.: U.S. Army Medical Research and Materiel Command;. Battelle Memorial Institute Contract No. DAMD17-99-D 0010, Final report, Task 003, July 2005.

Yin, R, DeSchepper, D, Qin, D, Piehler, L, Durst, HD, Hobson, S, and Braue, E, "Nanoreactor-based reactive topical skin protective creams," Proceedings of the U. S. Army 2002 Medical Defense Bioscience Review, USAMRICD, Aberdeen Proving Ground, MD, 2002 (on CD ROM).

aTSP BOOK CHAPTERS

Braue, EH Jr., and Hobson, ST, "Nanomaterials as active components in chemical warfare agent barrier creams." In A.W. Miziolek, S. Karna, J.M. Mauro, and R.A. Vaia eds. Defense Applications of Nanomaterials, ACS Symposium Series Book, Feb 2005 (invited submission).

Braue, EH Jr., Doxzon, BF, Lumpkin, BF, Hanssen, KA, and Graham, JS, "Military perspectives in chemical penetration retardation." In E.W. Smith and H.I. Maibach, eds., Percutaneous Penetration Enhancers-Volume 2, CRC Press, 2008, pp. 611-625. (invited submission).

Braue, EH Jr., Boardman, CH, and Hurst, CG, "Decontamination." In F.R. Sidell, E.T. Takafuji, and D.R. Franz, eds., Textbook of Military Medicine, Medical aspects of Chemical Warfare, Office of The Surgeon General, U.S. Army, 2008, pp.527-557.

Lukey, BJ, Slife, HF Jr., Clarkson, E, Hurst, CG, and Braue, EH Jr (corresponding author), "Chemical warfare agent decontamination from skin," In J.A. Romano Jr., B.J. Lukey, and H. Salem, eds., 2nd Edition of Chemical Warfare Agents: Chemistry, Pharmacology, Toxicology, and Therapeutics, CRC Press, 2008, pp. 611-625.

APPENDIX B: Contracts supporting the aTSP Program

Broad Agency Announcements (BAA) Final Report from Southern Research Institute

Award Number: DAMD17-3-C-3186

AD A 326413

CONTRACT NUMBER DAMD17-93-C-3186

TITLE: Antivesication by Simultaneous Prophylaxis and
Detoxification

PRINCIPAL INVESTIGATOR: Cecil D. Kwong, Ph.D.

CONTRACTING ORGANIZATION: Southern Research Institute
Birmingham, Alabama 35255-5305

REPORT DATE: December 1996

TYPE OF REPORT: Final

PREPARED FOR: Commander
U.S. Army Medical Research and Materiel Command
Fort Detrick, Frederick, Maryland 21702-5012

DISTRIBUTION STATEMENT: Approved for public release;
distribution unlimited

The views, opinions and/or findings contained in this report are those of the author(s) and should not be construed as an official Department of the Army position, policy or decision unless so designated by other documentation.

REPORT DOCUMENTATION PAGE			Form Approved OMB No. 0704-0188	
Public reporting burden for this collection of information is estimated to average 1 hour per response, including the time for reviewing instructions, searching existing data sources, gathering and maintaining the data needed, and completing and reviewing the collection of information. Send comments regarding this burden estimate or any other aspect of this collection of information, including suggestions for reducing this burden, to Washington Headquarters Services, Directorate for Information Operations and Reports, 1215 Jefferson Davis Highway, Suite 1204, Arlington, VA 22202-4302, and to the Office of Management and Budget, Paperwork Reduction Project (0704-0188), Washington, DC 20503.				
1. AGENCY USE ONLY (Leave blank)	2. REPORT DATE December 1996	3. REPORT TYPE AND DATES COVERED Final (13 Dec 93 - 12 Nov 96)		
4. TITLE AND SUBTITLE Antivesication by Simultaneous Prophylaxis and Detoxification		5. FUNDING NUMBERS DAMD17-93-C-3186		
6. AUTHOR(S) Cecil D. Kwong, Ph.D.				
7. PERFORMING ORGANIZATION NAME(S) AND ADDRESS(ES) Southern Research Institute Birmingham, Alabama 35255-5305		8. PERFORMING ORGANIZATION REPORT NUMBER		
9. SPONSORING/MONITORING AGENCY NAME(S) AND ADDRESS(ES) Commander U.S. Army Medical Research and Materiel Command Fort Detrick, Frederick, MD 21702-5012		10. SPONSORING/MONITORING AGENCY REPORT NUMBER		
11. SUPPLEMENTARY NOTES				
12a. DISTRIBUTION / AVAILABILITY STATEMENT Approved for public release; distribution unlimited		12b. DISTRIBUTION CODE		
13. ABSTRACT (Maximum 200) Our project DAMD 17-93-C-3186 entitled "Antivesication by Simultaneous Prophylaxis and Detoxification" has been directed toward the development of a new topically applied pretreatment that will prevent or minimize the vesication caused by exposure to sulfur mustard (HD). The target formulation for our current work is one that would be efficacious against CEES (2-chloroethylethyl sulfide) by providing a barrier to agent penetration while simultaneously detoxifying the agent via chemical reaction. Our efforts have included the identification and/or synthesis of candidate reactive materials and formulation bases, the development of prototype formulations comprised of reactive materials in various base creams, and the development of screening methods to determine the CWA efficacy of our formulations and formulation components.				
14. SUBJECT TERMS Chloroethylethylsulfide, CEES, mustard, barrier, reactive barrier, detoxification, antivesication, S-330, oxidant, perfluoroalkylpolyether, teflon powder, FOMBLIN, polysiloxane, N-halo oxidant, polyquaternium, PEG, HD		15. NUMBER OF PAGES 329		16. PRICE CODE
17. SECURITY CLASSIFICATION OF REPORT Unclassified	18. SECURITY CLASSIFICATION OF THIS PAGE Unclassified	19. SECURITY CLASSIFICATION OF ABSTRACT Unclassified	20. LIMITATION OF ABSTRACT Unlimited	

FOREWORD

Opinions, interpretations, conclusions and recommendations are those of the author and are not necessarily endorsed by the U.S. Army.

____ Where copyrighted material is quoted, permission has been obtained to use such material.

____ Where material from documents designated for limited distribution is quoted, permission has been obtained to use the material.

~~CDC~~ Citations of commercial organizations and trade names in this report do not constitute an official Department of Army endorsement or approval of the products or services of these organizations.

____ In conducting research using animals, the investigator(s) adhered to the "Guide for the Care and Use of Laboratory Animals," prepared by the Committee on Care and use of Laboratory Animals of the Institute of Laboratory Resources, National Research Council (NIH Publication No. 86-23, Revised 1985).

____ For the protection of human subjects, the investigator(s) adhered to policies of applicable Federal Law 45 CFR 46.

____ In conducting research utilizing recombinant DNA technology, the investigator(s) adhered to current guidelines promulgated by the National Institutes of Health.

____ In the conduct of research utilizing recombinant DNA, the investigator(s) adhered to the NIH Guidelines for Research Involving Recombinant DNA Molecules.

____ In the conduct of research involving hazardous organisms, the investigator(s) adhered to the CDC-NIH Guide for Biosafety in Microbiological and Biomedical Laboratories.

Cecile D. Kwong
PI - Signature

12/12/96
Date

TABLE OF CONTENTS

Page No.

SCIENTIFIC PROGRESS

1.	Introduction	1
2.	Body	5
2.1	Preparation of Polymers and Other Potential SM-Reactive Components ..	26
2.1.1	Preparation of Polymers with Ion-Attached Detoxicants	26
2.1.2	Synthesis of Polymers with Covalently Attached Detoxicants	28
2.2	Formulation	33
2.2.1	Preparation of Formulations Containing Polymers with Reactive Counterions	33
2.2.2	Preliminary Cyclodextrin-Containing Formulations	39
2.2.3	PEG-based Formulations Containing Various Nucleophiles	40
2.2.4	Preliminary Perfluoro Alkylpolyether-Containing Formulations	44
2.2.5	Methyl Cellulose-thickened Polyquaternium Solutions	46
2.2.6	Preliminary Efforts to Prepare Dr. Hackley's FOMBLIN A-based Formulations	47
2.2.7	Commercial Barrier Creams	48
2.2.8	Microemulsions	49
2.2.9	Modifications of a FOMBLIN-based Skin Protective Compositions	52
2.2.10	Ringin Gel Microemulsions	58
2.2.11	Modified Polyethyleneimine-based Burn Ointment	60
2.2.12	Modified Formulations from Commercial Supplier Literature	61

2.3	Reactivity and Barrier Evaluations	64
2.3.1	Overview	64
2.3.2	Reactivity Tests	69
2.3.2.1	Reactivity-Test Procedure	69
2.3.2.2	Results of Reactivity Tests	70
2.3.2.2.1	Midterm Results	70
2.3.2.2.2	Post-Midterm Results	73
2.3.2.2.3	Summary of Reactivity Test Results	75
2.3.3	Barrier Tests	75
2.3.3.1	Permeation-Test Apparatus	76
2.3.3.2	Barrier-Test Procedure	81
2.3.3.3	Results of Barrier Tests	82
2.3.3.3.1	Midterm Results	82
2.3.3.3.2	Post-Midterm Results	86
3.	Conclusions	97
4.	References	98

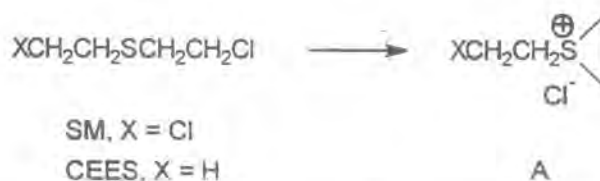
APPENDICES

SCIENTIFIC PROGRESS

1. Introduction

The overall objective of this project has been to develop a new topically applied pretreatment that will prevent or minimize the vesication caused by exposure to chemical-warfare agents such as sulfur mustard (SM). Our target formulation has been an effective lotion or cream that has minimal side effects, does not interfere with standard battlefield medical procedures, and is stable and easily stored. As envisioned, our formulation would provide a barrier to agent penetration while simultaneously detoxifying the agent via chemical reaction. The barrier to agent penetration would be presented by an appropriate film-forming polymer such as those used in commercially available topical formulations (sunscreens, barrier creams, etc.). The detoxicants would be supplied in the formulation as reactive counterions of cationic or anionic polymers, as reactive groups covalently attached to an appropriate polymeric support, or as added reactive components.

Our study was directed toward the following areas: (1) the identification, synthesis, modification, and evaluation of potential formulation components with efficacy against CEES (2-chloroethylethyl sulfide); (2) the development of preliminary formulations containing reactive components that had been identified both from our evaluations and from the literature; and (3) the development of appropriate methods for evaluating the reactivity and barrier efficacies of potential components and preliminary formulations. Our selection of CEES-reactive materials from the literature¹ included: nucleophiles capable of reacting with CEES or the cyclic ethylene sulfonium intermediate (A) common in CEES chemistry; oxidizing agents that convert the sulfur of CEES to its less toxic sulfoxide form; and alkylating agents that convert the sulfur of CEES to a sulfonium.

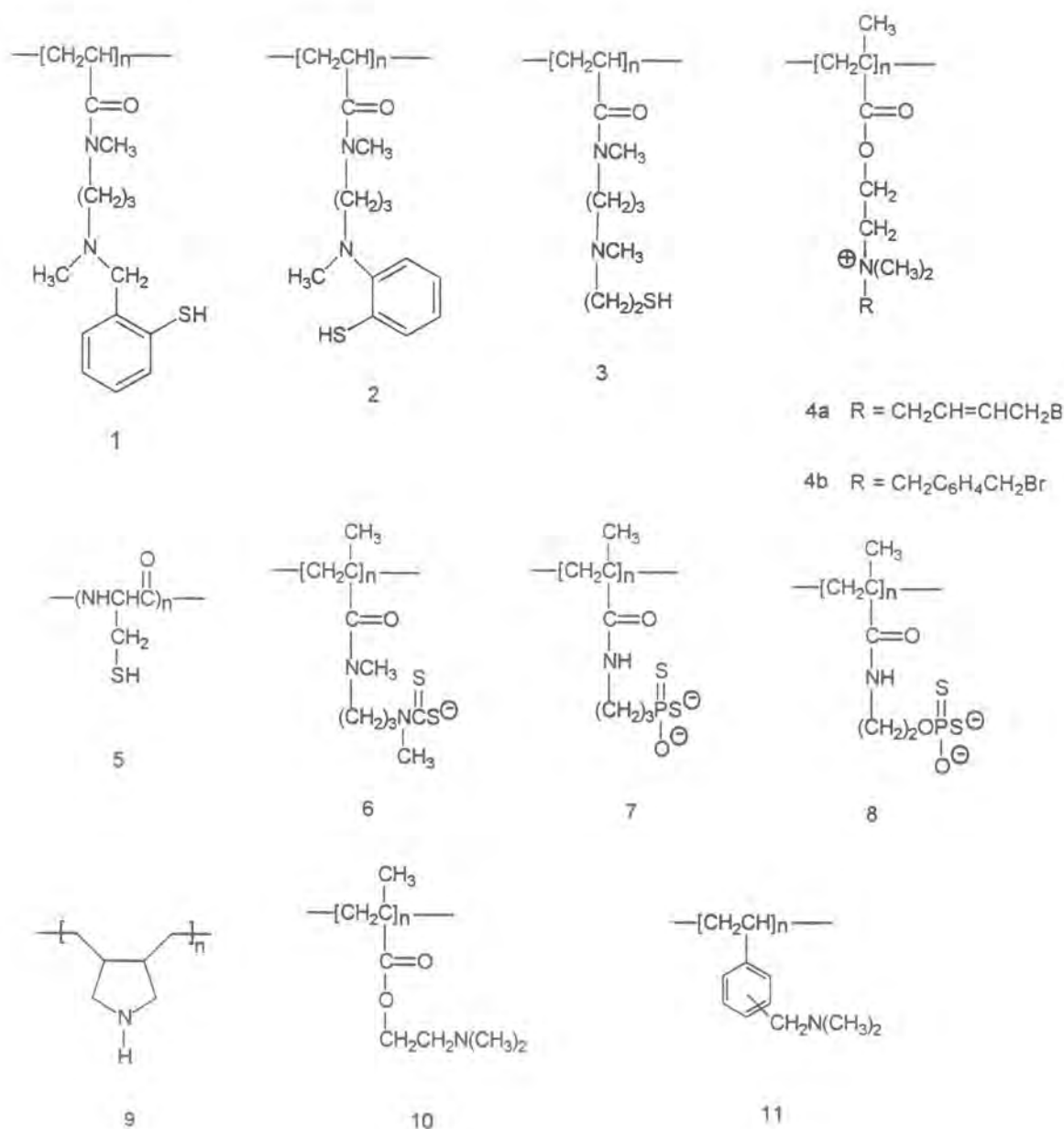


For our preliminary efforts, we decided to avoid lipophilic film-forming components because of the well known oil solubility of SM and CEES. While lipophilic films would repel water effectively and would be less readily washed off the skin (properties that are useful in consumer products like sunscreens), these films might also expedite the dissolution and transport of SM and CEES to and through the skin. Therefore, we initially focused on the development of reactive detoxicant-containing gels or creams with **high water content**. We anticipated that the film-forming polymers (*e.g.*, polyquaterniums, polyacrylates, hydroxyethyl cellulose, etc.) of these formulations would

repel oil-like substances either by the high concentration of charged quaternary or carboxylate groups or by the high degree of hydration inherent with these charged polymers. We also hoped that the high degree of hydration for these charged polymers might also facilitate the reactivity of our included detoxicants with SM and CEES. (We were also hopeful that the polyquaterniums could enhance reactivity with CEES by either a phase-transfer catalysis (PTC) or ion-exchange mechanism since quaternary compounds are prominent in these methodologies.) We first prepared formulations with some commercially available polycationic and polyanionic polymers commonly found in topically applied formulations to determine if the film provided by these materials would protect against SM or CEES exposure. Since we also wanted to determine if these polymeric films could be modified to deliver detoxicants as reactive counterions, and therefore, we selected and modified three candidate polyquaternium components by ion-exchanging their Cl^- counterions with some known SM- and CEES-reactive counterions, and we incorporated these modified polyquaterniums into our preliminary formulation.

Our second approach was to modify known high water content sunscreen or barrier cream formulations by adding polymerically bound SM- or CEES-reactives. Our pursuit of this approach was slow, because it required the synthesis of target polymers 1-11. The cationic targets were designed primarily as sources/deliverers of the CEES-reactive functionalities. The benzyl- and allyl bromide-containing targets were designed to mimic alkyl halides such as methyl iodide that can irreversibly alkylate the sulfur atom of SM and CEES to a sulfonium form that is incapable of alkylating key cellular targets.

Our overall approach was then modified after the reactive barrier evaluation of examples of our preliminary, high water content polymer-based formulations showed low efficacies. These results led us to suspect that the applied CEES must be "floating" on the surface of our formulations. Thus, the CEES was only surface contacting the detoxicant-containing phase of our formulations, and as a result, our formulation was only providing a barrier, and the detoxification of CEES by direct reaction was minimal. Therefore, we shifted our investigation to formulations and formulation components (*e.g.*, cosolvents, emulsifiers, etc.) that could increase the potential for CEES-detoxification by promoting the dissolution of CEES into a barrier formulation (relative to skin) containing a CEES-reactive component. Since cyclodextrins were known to solubilize compounds that are normally insoluble in water, we wanted to determine if they had any utility in our research. We also looked into the potential application of polyethylene glycols (PEGs) since they are also commonly used solubilizers. The PEGs were also of interest because they were known to be very effective crown ether-like mimics in phase transfer catalyst systems for reactions including the formation of esters by the nucleophilic displacements of alkyl halides by benzoates and some other not especially nucleophilic carboxylates.² A search of the literature for PEG-containing formulations led to our finding a PEG-based ointment that provides protection against organophosphate poisoning³ and another reactive



PEG-based formulation with SM efficacy.⁴ We reproduced three of the formulations from the second of these references for use as standards (since the references also showed their efficacy data) and for evaluating our analytical methodologies.

Since the efficacy of the PEG-based formulations could be due to the participation of a phase-transfer catalysis mechanism, we also considered other potential phase-transfer catalysts, including modified versions of our emulsifying, film-forming polyquaterniums. We also studied microemulsions and other gel-type formulations that contained CEES-solubilizing phases.

We also investigated formulations based on the barrier-providing perfluoro alkylpolyethers, especially after Dr. Hackley's fifth quarter site visit. While discussing his other projects directed toward protective formulations, Dr. Hackley told us about some effective formulations (comprised of perfluoro alkylpolyether and teflon powder, with and without an oxidizing agent (S-330 = 1,3,4,6-tetrachloro-7,8-diphenyl-2,5-diiminoglycoluril) that were to be the benchmark for our work. We were also encouraged to develop other perfluoro alkylpolyether-based formulations, including variations of his active formulation. With this directive, we searched the literature for other perfluoro alkylpolyether-containing formulations, alternate oxidants, and other stable oxidant-containing formulations (*e.g.*, thickened bleaches and acne formulations). We also began pursuing the use of oxidizing agents instead of nucleophiles as our formulation reactives, and we expanded our investigations of barrier cream-type formulations to include formulations based on the commonly used polysiloxanes, polyethyleneimines, and petrolatum.

Our efforts have resulted in some promising compositions that appear to be more efficacious than the benchmark formulation. Of these, the most studied is comprised of FOMBLIN HC/04 perfluoro alkylpolyether oil, petrolatum, sorbitan stearate, water, and 1,3,4,6-tetrachloro-7,8-diphenyl-2,5-diiminoglycoluril (S-330). Efficacious variations of this formulation contain: the higher molecular weight perfluoro alkylpolyethers FOMBLIN HC/25 or HC/R instead of HC/04; the polysiloxane combination of DOW 200 (1000 cSt) and DOW 593 instead of FOMBLIN HC/04; or no barrier-providing polymer at all. Since the essential formulation component appeared to be the stable and reactive oxidant, S-330, we also prepared variations in which some other N-halo oxidants were used instead of S-330, and we obtained efficacious formulations with 1,3-dichloro-5,5-dimethylhydantoin. While our efforts have not resulted in a final product (potential shelf life stability problems not yet fully determined), we have clearly developed a preliminary product that could lead to an ointment to prevent the vesication caused by exposure to SM.

Finally, we want to emphasize that an essential part of our work has been the development of methods for determining the efficacies (either reactive or barrier reactive) of our formulations or formulation components against CEES. The reactive barrier efficacy of our formulation was determined by using an automated permeation test system. This system was originally developed for conducting permeation and penetration tests of air-permeable and air-impermeable materials with chemical-warfare agents (CWAs) and agent simulants by the Southern Research Institute Physical Chemistry Group under prior contracts for the Department of Defense. As has been reported in earlier reports and will be described fully later in this report, our current primary system is based on a Minicams that monitors the concentration of CEES in an air stream that flows through or past thin, circular silicone rubber specimens mounted in a stainless steel partition cell that have been challenged with agent vapor.

2. Body

This section briefly describes all of our activities during each quarter. A more detailed description of the "Reactivity and Barrier Evaluations" is given in Section 2.3.

Our first quarter activities included the ion-exchanging of various commercially available cationic polymers with a number of known SM-reactive counterions. Our initially targeted polyquaterniums included Merquat 100 (polydiallyldimethylammonium chloride), Polycare 133 (polymethacrylamidopropyltrimethylammonium chloride), and the quaternium-containing polyurea Mirapol A-15. Our selected counterions included thiosulfate, ethane dithiophosphonate, histidine, cysteine, 2-mercaptobenzoic acid, mercaptopyruvic acid, diethyldithiocarbamic acid, thiocetic acid (reduced form), and thioglycolic acid.

We also began acquiring materials that would be used in the synthesis of polymers with covalently attached reactive side chains, and we obtained and investigated ingredients that could be used in preparing our reactive polymer-containing formulations. Our analytical activities during this quarter included the assembly of our experimental apparatus and the performance of preliminary studies to establish our test methods and provide feedback for our formulation efforts.

During the second quarter, we investigated several formulations that could accommodate our first quarter's counterion-exchanged cationic polymers. As a result of these efforts, we found that we could prepare stable, quaternary salt containing emulsions using a formulation containing cetyl dimethicone copolyol, polyglyceryl-4-isostearate, hexyl laurate, light mineral oil, caprylic/caprylic triglycerides, isopropyl myristate, water, and NaCl. While determining the compatibility of this base formulation with polycationics commonly used in commercial products, we found stable emulsions were obtained even when some of the water phase was replaced with varying amounts ranging from 2-50% of Merquat 100 (obtained as a 40% aqueous solution in its chloride form) or 40% Polycare 133 (obtained as a 50% aqueous solution in its chloride form). We also determined that thioglycolate, histidine, and sodium thiosulfate were also compatible additives to these base formulations.

We continued with our efforts to synthesize our targeted monomers and polymers with covalently attached reactive detoxicants. Our efforts included a synthesis of poly(L-cysteine) 5.¹⁸ Unfortunately, our isolated yields were much lower than the reported yield.

We also began looking for agents that could help to increase the potential for SM-detoxification by increasing the dissolution of SM. One compound class that seemed potentially applicable was the cyclodextrins, which are cyclic oligosaccharides containing

a minimum of 6 D-(+)-glucopyranose units attached by $\alpha(1-4)$ glucosidic bonds. The three natural cyclodextrins, α , β , and γ , contain 6, 7, and 8 glucose units, respectively, and exhibit 14, 2 and 23 g/100 mL water solubility, respectively. Their different complexing abilities are attributed to the size of their nonpolar cavities and their hydrophilic outer surfaces. Cyclodextrins form inclusion complexes with hydrophobic molecules by entrapping these substances in their inner cavity. In general, the β and γ cyclodextrins can accommodate the larger hydrophobic molecules because of their larger internal cavities.⁵ To preliminarily determine if any of the cyclodextrins could be of use to us, we prepared the following samples: (1) a 5:8:7 mixture of α , β and γ cyclodextrins (11.57 g/L; 0.01 M); (2) a water-in-oil formulation containing this cyclodextrin mixture at a level of 80%; (3) a water-in-oil emulsion formulation containing 30% by weight hydroxypropyl β -cyclodextrin; and (4) a Carbopol 940 thickened aqueous gel containing 28.6% hydroxypropyl β -cyclodextrin by weight.

Our second quarter analytical activities were directed toward the reactivity and barrier testing of a series of candidate formulations. We also made a number of improvements to our experimental methods that were suggested by our earlier preliminary studies.

Our third quarter synthesis activities were focused on the preparation of our targeted monomers and polymers with covalently attached reactive detoxicants. Our efforts to make target polymers 1, 2, and 3 were hindered by the difficulty of synthesizing the side chains of these compounds.

During the third quarter, more of our efforts were directed toward explaining the lackluster evaluation results for our preliminary formulations. One of our original premises regarding the polyanionic and polycationic film-forming components was that the reactive counterions present in these films should be reactive with SM. We had even further postulated that charged film-forming polymers components might also facilitate SM attack via a phase-transfer catalysis (PTC) or an ion-exchange mechanism. Therefore, we were surprised when our formulations containing Merquat 100 polymer exchanged with known SM-reactives (*e.g.*, thiosulfate, glycine, etc.) showed minimal decreases in permeation rate and minimal reactivities. As a result, we also began considering modifications to the overall strategy.

From our earlier perusal of the SM chemistry literature, we knew that the development of our target formulation would require the balancing of a number of critical parameters. We knew that SM is only sparingly soluble in water and that hydrolysis and physiologically relevant alkylation reactions occur only with the dissolved SM.¹ Also, we knew that SM hydrolysis is retarded by added chloride, is not pH dependent, may or may not be altered by metal ions such as Ag^+ , Cu^{2+} , Mn^{2+} , Mg^{2+} , Ca^{2+} , Ni^{2+} , and Fe^{3+} , and

the reactions of SM are markedly retarded in solvents less polar than water.¹ We were aware that the micro environment can affect the reactivity of SM, as illustrated by the finding that the presence of detergent micelles can significantly retard the disappearance of SM. For example, the rate of SM hydrolysis in 5% lauryldimethylbenzylammonium chloride is ~5% of that in water, while the solubility of SM is increased tenfold.¹ (These hydrolysis results can be partially explained by the Cl⁻, and by reports that soluble alkyltrimethylammonium salts often are found not to be effective PTCs because they promote the formation of stable aqueous emulsions.⁶⁻⁹)

We also continued to investigate the possible participation of a PTC or an ion-exchange mechanism in our proposed formulations. The literature on phase-transfer catalysts included numerous examples of quaternary salt-based PTCs, and since quaternary salts had been our originally targeted polymers, we focused on the applicability of these catalysts. A brief survey immediately indicated that the *R* groups on the quaternary salt were highly influential on the performance of the catalyst system. For example, tetramethylammonium-based PTCs have poor catalytic activity, especially when compared to the quaternary salts with larger alkyls (*e.g.*, tetrabutylammonium). Similarly affected activities were illustrated by the poor activity of the polystyrene-divinylbenzene (DVB) anchored trimethylammonium resin Bio-Rad AG 1-X2 *vs.* the much better activity of a similar polystyrene-DVB anchored tributylammonium resin.¹⁰ Another effective catalyst configuration included a lengthened alkyl spacer between the support and the ammonium group.¹¹ Presumably, these results showed the dependence of catalytic activity on the greater lipophilicity imparted by the alkyl chains, perhaps by allowing organic reactants to be more soluble in the solutions containing these quaternary salts, thereby improving the capacity for reaction. To preliminarily determine if a polyquat-based PTC could be useful in our formulation, we obtained some samples of some commercially available PTCs (*e.g.*, tetrabutylammonium hydroxide and Adogen 464 (methyltrialkyl(C₈-C₁₀)ammonium chloride) as candidate to evaluate.

Our examination of the PTC literature also identified some other PTC classes as potential components for our formulations, including phosphonium salts and polyethylene glycols (PEGs). Besides having comparable activities, these alternate classes were also known to be more stable than the quaternary ammonium salts, since they do not undergo Hoffmann elimination degradation. Of these alternate classes, the PEGs seemed to be an especially promising candidate class because of their known effectiveness in catalyzing reactions including nucleophilic displacements of alkyl halides.² These catalysts act by a crown ether-like mechanism and complex the cations of reactive salts, thus providing accessible anions for nucleophilic attack. Since the PEGs are commonly used in topical and other "skin contact" formulations, and since they are also nontoxic, inexpensive, and readily available from commercial sources, they appeared to be ideal candidate components for our formulations. Further support for the use of PEGs was a PEG-based

ointment that was reported to provide protection against organophosphate poisoning.³ This ointment was based on a mixture of PEGs [mwt. (rel. amt. by wt.): 400(3)/800(1)/10,000(1)/20,000(3) containing various amines, hydroxide, or alkali oximates as the reactive nucleophiles.

The literature-reported PEG-type PTCs included various molecular weight PEGs, PEG ethers, amine-capped PEGs, HS-capped PEGs, and polymerically bound PEGs (*e.g.*, polyvinylbenzyl-bound). This last group of potentially applicable PTCs were especially interesting since they wherein effect, polymerically bound crown ethers. To further determine if any of these PEGs could be viable components for our formulations, we obtained a number of commercially available PEGs, and these were blended with SM-reactive alkali salts such as those in the previously described ointment.

We also tried to explain the low reactivities of our early formulations, if our polycationic or polyanionic formulation components were acting by an ion-exchange mechanism, and if so, could this mechanism be exploited to improve the lackluster performances of our early formulations. We also wanted to determine if the reduced water content of our formulations was affecting the reactivity of our nucleophilic components since the literature clearly showed that SM reactions were markedly retarded in solvents less polar than water. This decreased SM reactivity in less polar solvents could be due to decreased dissociation of the ion pairs in these solutions, thus limiting the availability of the nucleophilic counterions for SM attack. Still, we felt that the water content of our formulations should have been sufficient to allow some dissociation, and therefore, some reactivity should have been observed.

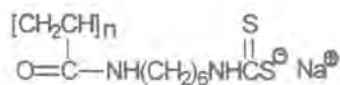
The relative selectivities of various counterions for quaternary salt-based ion-exchange resins are well established, at least for the many commercial polystyrene-DVB anchored trimethylquaternary salts. Table 1, from the **1993 BioRad Life Science Research Products Catalog**, shows the relative selectivities of various counterions for BioRad AG-1-X8, a strongly basic anion exchange resin comprised of trimethylquaternary ammonium functional groups covalently attached to a styrene-divinylbenzene copolymer. According to this table, OH⁻ is the most readily exchanged anion, easily exchanging with all of the anions listed below it on the table (including Cl⁻). Since many of our selected nucleophiles could be expected to be lower than Cl⁻ on the table, their affinities to the resin would be expected to be greater than that of Cl⁻, and ion exchange would be expected to occur at a much slower rate, even under optimal conditions. Therefore, if an ion-exchange mechanism participates in our polycation-based formulation, our chances for a successful formulation may be improved by using the more easily exchanged anions such as OH⁻, phosphate, or acetate. To pursue this premise, the OH⁻, phosphate, and acetate-exchanged forms of Merquat 100 were prepared.

**Table 1. Relative Selectivities of Various Counterions on AG Resins
(BioRad 1993 Life Science Research Products Catalog)**

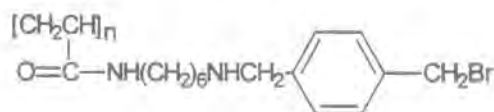
Counterion	Rel. Selectivity	Counterion	Rel. Selectivity
OH ⁻	1.0	Sulfite	27
F ⁻	1.6	Cyanide	28
Propionate	2.6	Bromide	50
Acetate	3.2	Nitrate	65
Formate	4.6	Chlorate	74
Phosphate	5.0	Sulfate	85
Iodate	5.5	Phenate	110
Carbonate	6.0	Iodide	175
Chloride	22	Citrate	220
Nitrite	24	Salicylate	450
Bromate	27	Benzenesulfonate	500

Due to the emphasis on synthesis and formulation only a limited amount of reactivity and barrier evaluation was conducted during this quarter. Most of our analytical effort was directed toward repeating earlier tests that had given anomalous results. We also manually checked the data acquisition and computer calculations of the new Minicams system that was acquired for this project.

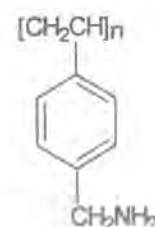
During the fourth quarter, we completed the synthesis of originally targeted polymers **4b** and **9**, and we obtained samples of commercially available **10** and **11**. Polymers **12-14** were designed and synthesized as new targets. Target **12** was designed as a more easily obtained analog of original target **6** while polymer **13** was designed as an easily obtained analog of **4b**. Polymer targets **9-12** and **14** contain covalently-attached nucleophilic groups while polymers **4b** and **13** contain reactive benzyl bromides that may be alkylated by the sulfurs of CEES and SM. Aminomethylpolystyrene **14** was prepared both as a target and an intermediate for some other targets that will be shown in a later scheme. We also continued to pursue the synthesis of our other monomers and polymers with covalently attached reactive detoxicants, and we shifted some of our efforts toward duplicating and modifying the agent-reactive PEG-based formulations in the literature.



12



13



14

For our formulation efforts, we continued to search the literature for other PEG-based protective ointments and found an SM-reactive skin decontaminating lotion based on a mixture of PEG monomethyl ethers (MPEGs) with an average mwt. of 550. The simplicity of the formulations in this reference and the direct relation of these formulations to our work suggested that we should copy some of them as standards. Therefore, we attempted to reproduce the active formulations containing the readily available potassium salts of acetone monoxime, 2,3-butanedione monoxime, and phenol. We also prepared some modified formulations in which these salts were replaced with other SM-reactive nucleophiles from the Papirmeister list of SM competitive factors.¹ Other modified formulations were prepared using commercially available amine-capped PEGs, HS-capped PEG, and other HS-capped polyols. We also prepared related versions in which the reactant and water proportions were varied, and other versions using different PEGs and PEG ethers.

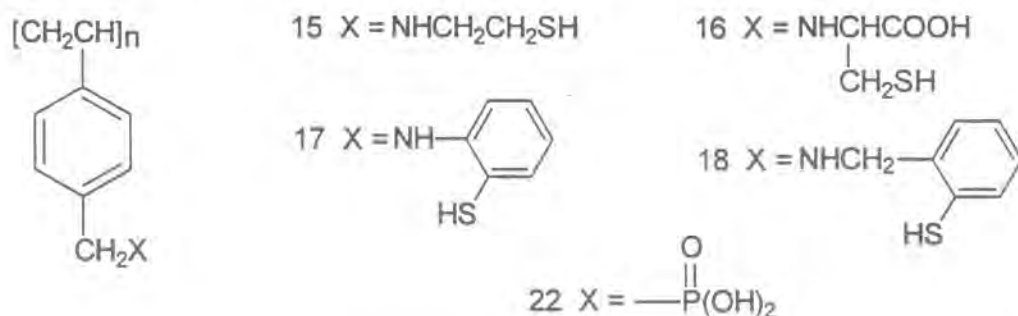
To preliminarily determine if a quaternary ammonium-based PTC could be useful in our formulation and if an ion-exchange mechanism may actually be participating in our formulations, we prepared samples containing the commercially available PTC (a 40% solution of tetrabutylammonium hydroxide in water and a tetrabutylammonium hydroxide-sodium hydroxide solution), and 5% solutions of both OH⁻ and acetate exchanged Merquat 100. We also began the synthesis of a polystyrene-DVB anchored tributylammonium resin¹⁰ and a variant that included a lengthened alkyl spacer between the support and the ammonium groups¹¹ since these catalysts were known to be more effective catalysts than the corresponding polystyrene-DVB anchored trimethylammonium resin. Finally, in an attempt to correlate our results with the SM competition factors, we also prepared 0.3 *N* and 3.0 *N* solutions of NaOH, 0.3 *N* and 3.0 *N* solutions of NaOH with tetrabutylammonium hydroxide, a 2% solution of KOH in MPEG (avg. mwt. 550), and a number of phosphate buffer solutions of varying pHs.

Our analytical activities during the fourth quarter included the performance of reactivity tests on solutions containing reactive chemical species that could be used in our protective formulations.

During the fifth quarter, we began shifting our efforts away from synthesis and more toward formulation. This shift was prompted primarily by our analysis of the very limited SM reactivity shown by our preliminary formulation. The reactants in these formulations included small molecule reactants with known SM-reactive functional groups. These small molecule compounds should have been the most reactive forms for compounds containing these functionalities, and they were expected to be more reactive than the corresponding polymerically bound forms that we had targeted. The low reactivities and efficacies of our preliminary formulations indicated that success in developing an effective antivesicating formulation was going to depend on balancing the barrier properties of the

formulation vs. the capacity of the formulation to solubilize both CEES and any reactants. Thus, formulation, not synthesis, appeared to be the key to our success. Additional impetus for this shift was obtained during Dr. Hackley's site visit. While telling us about his other antivesication work and while discussing the progress and future directions of our project, he also expressed his reservations in the reliance of our approaches on the nucleophilic attack of CEES by our various formulation components, since historically, such an approach had not been successful. He then showed us his best formulation which was comprised of a perfluoro alkylpolyether, teflon powder, and an oxidant (S-330 or 1,3,4,6-tetrachloro-7,8-diphenyl-2,5-diiminoglycoluril). Dr. Hackley indicated that his formulation was to be our benchmark, and that our goal would be to make a better formulation than his. Therefore, we began an extensive search of the literature for perfluoro alkylpolyether-containing formulations and oxidant-containing formulations that would be appropriate and adaptable to our needs.

However, we were still committed to preparing as many of the targeted polymers (or more easily obtained analogs) as possible, and therefore, our activities during this quarter still included the synthesis or procurement of the following addition products of Merrifield polymer [poly(vinylbenzyl chloride)] with cysteine (**15**), cysteamine (**16**), 2-aminobenzenethiol (**17**), and 2-aminobenzylmercaptan (**18**), and polystyrene-bound phosphonic acid **22**. While some of these were not among our originally targeted polymers, **15-18** were all designed as polymers with covalently attached reactants (*e.g.* sulfhydryl, amino, and carboxylate groups). Phosphonic acid **22** was targeted because of its potential reactivity with CEES and because of its potential for catalyzing the reaction of CEES with other nucleophiles.



For our formulation efforts, we continued to investigate the agent-reactive PEG-based formulations⁴ from the literature that were originally prepared as standards. We also prepared a number of analogous formulations in which the reactant proportions were changed in an attempt to match other formulations within the Purdon reference. The evaluation results from our earlier attempts were inconsistent with the reported results, and therefore, we wanted to determine if our interpretation of the reported experimental

methods had been incorrect. We also prepared analogous formulations by using an uncapped PEG (with the same average mwt. of 550) in the reactant concentrations that we originally investigated.

We began directing our efforts toward the preparation, evaluation, and modification of literature-reported base formulations such as those used in sunscreens and barrier creams. For these preliminary efforts, we wanted to use commercially available components, and we obtained samples and formulation information regarding a number of these products. Further justification for this approach was that in most cases, we were able to select commercial products that contained our targeted functionalities in forms that were similar or equivalent to our targets. Furthermore, we anticipated that the data obtained from the evaluation of preliminary formulations would indicate which of our synthesis targets should be further pursued. Examples of our selected commercial products include: carboxylate and phosphate-containing alkylamido alkylamines (mild amphoteric detergents found in hair conditioners and shampoos); fatty acid mono- and diphosphates (*e.g.*, DEA-oleth-3 phosphate, DEA-oleth-10 phosphate, C₁₂₋₁₅areth-2 phosphate, cetareth-4 phosphate, nonoxynol-9 phosphate); protein derivatives (conditioning agents for hair and skin products prepared from animal or vegetable proteins by partial enzymatic or chemical hydrolysis; *e.g.* hydrolyzed elastin and TEA-oleoyl hydrolyzed animal protein); Quaternary ammonium compounds (often used as substantivity agents and antimicrobial agents; *e.g.*, Merquat 100, Polycare 133, Mirapol A-15; Ucare JR Polyquaternium celluloses), and other substantivity agents (Dimethicone and other polysiloxanes, FOMBLIN and other perfluoropolyethers, polyethyleneimines).

In our investigation of barrier-providing formulations based on perfluoro alkylpolyethers (*e.g.* FOMBLINs HC/04, HC/25, and HC/R, Brooks/Montefluos), the first example that we prepared was a FOMBLIN HC/04-based barrier-providing gel which reportedly applied the perfluoroether as a semi-occlusive, vapor restrictive layer that allowed skin respiration. This formulation was prepared both as a test formulation and a base formulation to which we would attempt to add various reactive additives.

We also investigated polysiloxane-based barrier creams. We obtained two different grades of Dimethicone and some other newly developed polysiloxanes from Dow Corning. From the formulation information also received from DOW, and we selected and investigated a number of their suggested formulations as potential base formulations. To these silicone-based formulations, we attempted to add some lipophilic nucleophiles to determine if such additives could sequester and facilitate the detoxification of CEES.

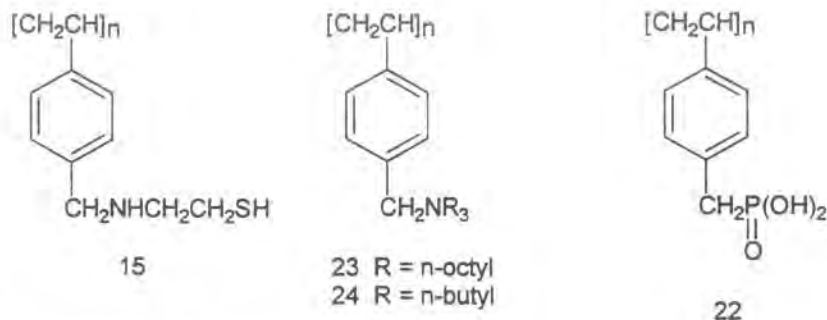
We also began looking into formulations based on polyethyleneimines (PEIs). We wanted to determine if solutions of this material were also nucleophilic to CEES or if nucleophilic agents such as cysteine, cystine, etc. could be incorporated into a PEI

formulation to increase any CEES reactivity without decreasing the substantivity enhancement provided by this material.

We also obtained three consumer products which contained components that either could be reactive with SM and CEES or could provide a barrier against these agents. These products were two toothpastes (Colgate Clear Blue Winterfresh Gel and Arm & Hammer Peroxicare) and a zinc oxide ointment (Desitin). Dr. Comber had suggested that toothpastes be evaluated because of the reactive components that are often incorporated in these products, and accordingly, we selected the Colgate and Arm & Hammer products as our candidate toothpastes after scrutinizing the compositions presented on their packaging. The Colgate product contains tetrasodium pyrophosphate and sodium fluoride as potentially reactive components in a base of PEG-12, sorbitol, glycerine, water, sodium lauryl sulfate, cellulose gum, and hydrated silica. The Arm & Hammer product contains sodium carbonate peroxide, sodium bicarbonate, and sodium fluoride as reactants in a base of PEG-8, Poloxamer 338, silica, water, sodium lauroyl sarcosinate, and sodium lauryl sulfate. The well known Desitin ointment (diaper rash treatment) was selected as our zinc oxide-based candidate to determine if such an ointment could prevent CEES penetration, and if it would be a modifiable base formulation.

Our analytical results again included the performance of reactivity tests on solutions containing reactive chemical species that could be used in our protective formulations. We also performed barrier efficacy tests on many of our preliminary formulations and formulation components to determine their efficacies and to establish this method. More significantly, we began modifying our barrier testing apparatus so that we would be able to challenge our formulations with CEES vapor rather than droplets. These modifications were made according to suggestions by Dr. Hackley during his site visit.

During the sixth quarter, we continued to direct our synthesis efforts toward the target polymers with covalently attached reactive groups. As a result, we synthesized the following targeted addition products of Merrifield polymer or poly(vinylbenzyl chloride): cysteamine adduct **15**; tri-*n*-octylamine adduct **23**; and tri-*n*-butylamine adduct **24**; and polystyrene-bound phosphonic acid **22**. Cysteamine adduct **15** was prepared as a target polymer with covalently attached reactant/nucleophile, while trialkylamine adducts **23** and **24** were prepared as polymerically-bound quaternary salts. Phosphonic acid **22** was targeted because it could be reactive with CEES or it could facilitate the reaction of CEES with other nucleophiles, possibly by catalyzing the formation of the sulfonium intermediates of CEES.



We continued to investigate the agent-reactive polyethyleneglycol (PEG) formulations from the literature.⁴ We had previously attempted to reproduce and test Purdon's polyethylene glycol methyl ether (MPEG 550) based formulations containing the potassium salts of acetone oxime, 2,3-butanedione monoxime, and phenol, but our reactivity results were inconsistent and much lower than the reported results. At the end of the fifth quarter, we prepared some similar formulations in another attempt to match the reactant proportions of the Purdon formulations. The evaluation of these formulations showed that solutions prepared with a 13X excess of KOH relative to the oxime or phenol components (0.0009 mol KOH/g formulation vs. 0.000069 mol oxime, etc./g formulation) exhibited marked reactivity towards CEES. To determine the reactivity contribution of the individual components of these formulations, we prepared a MPEG 550 solution containing 0.0009 mol/g KOH (the same concentration of KOH as in the active solutions) and another solution containing only the MPEG 550. Later efforts included two MPEG formulations in which the reactive oximate and KOH were replaced with DEA-oleth-3-phosphate. These versions were prepared to see if the previously demonstrated reactivity of the phosphate group (in our phosphate buffer reactivity evaluations) could also be supplied by a phosphate-containing commercial product. One of these MPEG 550 solutions contained the DEA-oleth-3-phosphate in the same concentration as the oximates, etc. while the other was a 1:1 mixture of the DEA-oleth-3-phosphate and MPEG 550.

We also continued our study of solutions of poly(diallyldimethylammonium) hydroxide and acetate (the hydroxide and acetate exchanged forms of Merquat 100) since we had seen significant reactivity for these ion-exchanged cationic polymers with CEES. We prepared a more concentrated solution (20%) of Merquat 100 (OH⁻) and a methyl cellulose-thickened solution of 5% Merquat 100 (OH⁻). We also prepared OH-exchanged forms of Polycare 133 and Mirapol A-15, and we evaluated 5% solutions of these materials.

We reinvestigated an earlier formulation that was based on nonionic silicone emulsifiers/emulsion stabilizers which we had been found to be able to tolerate high levels of polycationic emulsifiers. In this reinvestigation, we used hydroxy- or acetate-exchanged

forms of the polycationic emulsifiers, and we replaced the NaCl with other alkali salts to determine if replacing these chloride sources as well as the NaCl would result in efficacious formulations.

We continued to study compositions based on other polydialkylsiloxanes (e.g. Dimethicone). We tried more of the formulations presented in Dow's literature as potential base formulations to which we could add reactive components.

We also prepared some polyethyleneimine (PEI) containing solutions to determine if solutions of this material could also be nucleophilic to CEES or if a nucleophilic agent such as cysteine, cystine, etc. could be incorporated into a PEI formulation. We prepared three cysteine-containing aqueous solutions (1:2, 1:1, and 1:0.5 Cys/PEI). We also attempted to mimic the reactive PEG-based formulations and prepared a PEI solution containing acetoneoxime (1:1:3 PEI/acetoneoxime/water).

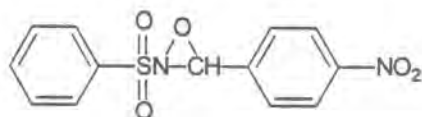
Our efforts to prepare barrier-providing formulations based on perfluoropolyethers (e.g. FOMBLIN) were limited to continued studies of the FOMBLIN gel base studied last quarter. We attempted two modifications of the perfluoropolyether gel base in which the triethanolamine component was replaced with the SM-reactive ethanolamine or with a polyethyleneimine. Unfortunately, we did not obtain a stable emulsion with either attempt. We also determined that the perfluoropolyether gel base was not compatible with the polyethylene glycol methyl ether component of the MPEG 550 formulations.

During this quarter, our efforts to investigate Dr. Hackley's perfluoro alkylpolyether/teflon powder formulation were slowed by a lack of information regarding the exact components that had been used to make these formulations. We obtained three grades of polytetrafluoroethylene powders from Dupont, anticipating that one of these should be applicable to the reproduction and modification of Dr. Hackley's perfluoropolyether formulations since Dr. Hackley had indicated that a teflon powder had been used to thicken his formulations.

We also continued our search for new components for our formulations. We began preliminary investigations into the use of reactive metals as catalytic agents or reactive components for our formulations. We also reevaluated neat samples of some previously evaluated candidate components: Glycol dimercaptopropionate (GDMP); trimethylolpropane tris-3-mercaptopropionate (TMOPT); pentaerythritol tetra-3-mercaptopropionate (PETTMP); and polyoxyalkylene diamine (POAD). These materials had all been previously evaluated as potential reactive components in the MPEG 550 formulations, and as such, they had been evaluated at low concentrations. Since we wanted to consider them as potential PEG alternatives, we also wanted to determine if high concentrations of these materials would show any reactivity to CEES.

This quarter's analytical efforts were directed toward the completion of a modified barrier testing apparatus that would allow us to challenge our formulations with CEES vapor rather than droplets. We also investigated a silicone rubber as the membrane for our barrier testing. This membrane initially seemed to offer the advantages of allowing a more consistent, level application of the reactive component-containing compositions. However, we found that continued testing frequently gave anomalous results, and therefore, we also directed significant effort toward determining the cause for these anomalies.

During the seventh quarter, our synthesis efforts were directed away from our target polymers and toward the preparation of new reactants. One of these new reactants was *N*-sulfonyloxaziridine oxidizing agent **25**^{19,20}. *N*-Sulfonyloxaziridines were reported to react very rapidly with SM in CDCl₃ at room temperature,²¹ and therefore, these oxidants were selected as candidate reactants for our formulations. We also pursued the preparation of oxygenated unconjugated unsaturated fatty acid esters such as peroxidized ethyl linoleate, since these fatty acids were reported to oxidize sulfides.²² To preliminarily investigate this approach, we obtained some ethyl linoleate and oxygenated this material by bubbling dry oxygen through at room temperature while irradiating with a 50-watt tungsten lamp, as described in the reference.



25

Our formulating activities were directed mainly toward the modification of our efficacious preliminary formulations. We attempted to add Teflon powder, S-330, benzoyl peroxide, 5% sodium hypochlorite solution (household bleach), and copper, zinc, and iron metals to our FOMBLIN HC/04 gel base, and we found that only the addition of household bleach gave a clear or homogeneous solution. However, this solution darkened with time, suggesting the need for stabilization of this formulation. We attempted to thicken our polyethylene glycol methyl ether (MPEG 550)/potassium hydroxide (KOH) formulation with a higher molecular weight MPEG (mwt. = 2000) and found that the higher molecular weight MPEG was not soluble, thus suggesting that a mixture of PEGs of varying higher molecular weights might be the preferred approach. We prepared methyl-, hydroxyethyl-, hydroxypropyl-, and sodium carboxymethyl cellulose-thickened solutions of Mirapol A-15 (OH⁻-exchanged), Polycare 133 (OH⁻-exchanged), and Merquat 100 (OH⁻-exchanged) and found combinations that resulted in clear or homogeneous thickened solutions. For example, suitable "gels" were obtained with 5% solutions of Mirapol A-15 (OH⁻-exchanged) containing 1% and 3% hydroxyethyl cellulose or 3%

methyl cellulose; and a 5% solution of Polycare 133 (OH⁻-exchanged) containing 3% methyl cellulose. On the other hand, a free flowing solution was obtained when we tried to thicken a 5% solution of Mirapol A-15 (OH⁻-exchanged) with 1% hydroxypropyl cellulose, and our attempt to thicken the solution by increasing the hydroxypropyl cellulose content to 3% resulted in a 2-layer mixture that gradually became homogeneous only after a couple of weeks. Our efforts to thicken a 5% solution of Mirapol A-15 (OH⁻-exchanged) with sodium carboxymethyl cellulose showed that this cellulose was not soluble.

We also prepared inhouse versions of Dr. Hackley's FOMBLIN A/teflon powder and FOMBLIN A/teflon powder/S-330 oxidant formulations. Prior to Dr. Hackley's site visits, we had obtained samples of FOMBLIN HC/04 and FOMBLIN HC/25. During Dr. Hackley's first site visit, he indicated that his FOMBLIN A/teflon powder and FOMBLIN A/teflon powder/S-330 oxidant formulations were to be our benchmark formulations, and he also gave us ~10 g samples of these materials. Larger quantities were not supplied because he thought that we should be able to find similar commercial products very easily. However, after calling a number of local drug stores, safety equipment suppliers, etc., we were unable to find any topically applied formulations containing FOMBLIN A. Subsequent calls to Brooks Industries and Ausimont S.p.A. (the U.S. distributors of cosmetic grade FOMBLIN and industrial grade FOMBLINs including FOMBLIN A, respectively) helped us to determine that the only commercially available products containing FOMBLIN A were the Blue Coral car waxes. We also learned that FOMBLIN A is prepared exclusively for Blue Coral. Since neither the two available Blue Coral car waxes resembled Dr. Hackley's benchmark formulation and since our supply of the FOMBLIN A/teflon powder formulation had been depleted by our reactivity and barrier evaluations (leaving us with none for direct comparison with our formulations or for modification), we were very interested in preparing some batches of the FOMBLIN/teflon powder formulations from FOMBLIN HC/25 and some Dupont Teflon powder (mp 1200) that we had previously obtained. Combining these components in the 72/28 proportions previously given to us by Dr. Hackley resulted in a white creamy lotion that resembled but did not have as thick a consistency as Dr. Hackley's FOMBLIN A formulations. We also prepared an inhouse sample of our FOMBLIN HC/25 / Dupont Teflon powder (mp 1200) formulation with the S-330 in the recommended proportions, and again, our product was thinner than Dr. Hackley's and was more lotion-like in consistency.

We obtained two commercially available barrier creams to see if their compositions provided an efficacious barrier against CEES: Kerodex 71 (Whitehall Laboratories Inc.), a cream containing calcium carbonate, cetearyl alcohol, cetrimonium bromide, cetyl alcohol, iron oxide, isopropyl alcohol, kaolin, methylparaben, mineral oil, paraffin, petrolatum, propylparaben, sodium hexametaphosphate, sodium lauryl sulfate, water, and zinc oxide; and DermaPlus, which contains dimethicone, polyvinylpyrrolidone, triethanolamine, isopropyl myristate, water, isobutane, stearic acid, coconut acid, glycerin,

propane, cetyl alcohol, cetearyl alcohol, cetareth-20, triclosan, methyl paraben, tetrasodium EDTA, hydroxyethyl cellulose, aloe vera gel, tocopherol acetate, lanolin, and polyparaben.

We also prepared some 0.1 M phosphate buffer solutions (pH 5.1) containing copper, zinc, and iron in an attempt to determine if the inclusion of these metals would affect the reactivity of the buffer solution.

We investigated microemulsions based on work by Menger *et al* that demonstrated the CEES decontaminating efficacy of sodium hypochlorite-containing microemulsions that use low molecular weight alcohols as cosurfactants.²³⁻²⁵ We were interested in determining if a similar microemulsion approach could be used in the pursuit of our formulation, and therefore, we prepared the following microemulsion formulations to get some experience.

- (1) 3% cyclohexane / 82% water / 5% sodium dodecyl sulfate / 10% butanol
- (2) 4% *n*-hexadecane / 60% water / 24% Brij 97($\text{CH}_3(\text{CH}_2)\text{CH}=\text{CH}(\text{CH}_2)_8(\text{OCH}_2\text{CH}_2)_{10}\text{OH}$) / 12% 1-butanol
- (3) 24% heptane / 56% water / 8% sodium dioctylsulfosuccinate / 12% 1-butanol

We then added bleach to these microemulsions as described by Menger, and we obtained clear, free-flowing solutions in all cases. We also prepared solutions in which we added 5% sodium acetate, 5% potassium phosphate dibasic, and 3.2% and 10% solutions of sodium thiosulfate to the Brij 97-containing microemulsion, and in all cases, we again obtained clear solutions. An attempt to include the S-330 additive (of Dr. Hackley's FOMBLIN-containing formulations) resulted in a cloudy mixture while the substitution of ethanolamine for the 1-butanol in the Brij-97-containing formulation gave a clear solution. We also attempted to modify the following quaternary ammonium salt-based microemulsions by adding our cationic emulsifiers (Mirapol A-15, Merquat 100, and Polycare 133) to the composition. Unfortunately, we obtained two-phase solutions with each of these attempts.

4% hexadecane / 66% water / 18% cetyltrimethylammonium chloride (CTAC) / 18% 1-butanol

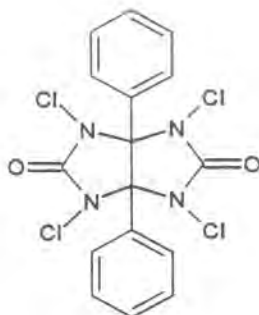
Next, we attempted to thicken and to improve the short shelf life of the hypochlorite-containing microemulsions by using clay stabilizers such as the Van Gel O (magnesium aluminum silicate) used in the commercially available Clorox gel. Our preliminary attempt to add Van Gel O to our microemulsions did not give homogeneous solutions, and therefore, we obtained some patents describing the preparation of

hypochlorite-containing gels.²⁶⁻²⁸ According to these patents, the thickened hypochlorite-containing formulation results from the combination of the following ingredients: (a) a colloidal alumina thickener with $< 1\mu$ average particle size; (b) an electrolyte/buffer; © a surfactant system including two surfactant components - one being a fatty acid anionic surfactant and the other being a bleach-stable surfactant or mixed surfactant; (d) a bleach; and (e) an abrasive with an average particle size of $1-400\mu$. The gel-like consistency was stated to result from the interaction of the clay and anionic surfactants. We attempted to repeat the work in these patents, and we also attempted some variations that contained less hypochlorite than those in the patent. We also continued to investigate the compositions and applicability of other oxidant-containing formulations.

During this quarter, we prepared samples of our preliminary formulations for Dr. Hackley including the FOMBLIN-based gel, 5% aqueous solution of OH-exchanged Mirapol A-15 thickened with hydroxyethyl cellulose, our cetyldimethicone copolyol-based emulsion containing 5% aqueous OH-exchanged Merquat 100 and sodium acetate, and our cetyldimethicone copolyol-based emulsion containing 5% aqueous OH-exchanged Merquat 100 and potassium phosphate dibasic. We also continued to search the literature for alternate detoxifying approaches and potential reactive components.

Our seventh quarter analytical efforts included the performance of additional reactivity tests and barrier tests with CEES to support the synthesis and formulation efforts. We continued to work on the modification of our permeation test procedure for our barrier evaluations so that the challenge to each test sample would be saturated CEES vapor rather than liquid CEES droplets. We also conducted a series of tests to evaluate and characterize the effects of switching to a vapor challenge in the barrier tests and found this method of agent challenge to be advantageous for this study. We determined that silicone rubber was suitable for use as the substrate material for these vapor-challenge tests. We also had to direct some of our effort toward identifying the source of anomalous results that we continued to encounter in our evaluations.

During the eighth quarter, we completed our syntheses of the oxidizing agents mentioned in our last quarterly report: *N*-sulfonyloxaziridine oxidizing agent **25**^{19,20} and peroxidized ethyl linoleate²² (since such fatty acids were reported to oxidize sulfides). We also began preparing some S-330 oxidizing agent (1,3,4,6-tetrachloro-7,8-diphenyl-2,5-diiminoglycoluril²⁹ **26**) since our supply of this component was dwindling. We also obtained a sample of chloramine T as a potential alternate oxidizing component.



26

Our formulating activities included the modification of our efficacious preliminary formulations and the investigation of other candidate formulations including a number of creams, gels, and microemulsions. Also included in our activities was the acquisition of materials and components for these formulations.

We prepared another phosphate buffer-containing Menger-type microemulsion as a continuation of our studies of these systems. An attempt to prepare a Clorox-loaded FOMBLIN gel base resulted in a runny mixture that was unacceptable.

In our search of the literature for perfluoroether-containing formulations, we found a FOMBLIN-containing protective composition³⁰ comprised of FOMBLIN HC/04, petrolatum, sorbitan stearate, and water. We attempted to prepare reactive-containing variations by adding 2.5% loadings of S-330, our synthesized oxaziridine oxidant **25**, or bleach to modifications of this formulation, and we obtained an acceptable candidate from the addition of the S-330.

We also continued to study Clorox-containing, thickened bathroom cleaners since bleach is stable in these formulations. (The instability of bleach is the major weakness of the Menger-type and other bleach-containing microemulsions.) In our last report, we mentioned that we hoped to thicken and to improve the short shelf life of hypochlorite-containing microemulsions with the clay stabilizers such as the Van Gel O (magnesium aluminum silicate) that are used in commercially available bathroom cleaners such as Clorox gel. Since our preliminary attempts to add magnesium aluminum silicate to our microemulsions did not give homogeneous solutions, we attempted to prepare a thickened formulation with magnesium aluminum silicate samples from other commercial sources. Unfortunately, we continued to obtain compositions with consistencies ranging from runny lotions to thick pastes, and since none of these "felt" good on the skin, none of these were considered to be candidates.

We pursued ringing gel microemulsions in an attempt to determine if the reactivity and efficacy of the free-flowing microemulsions would be impeded in thickened microemulsions. We prepared a mineral oil-containing ringing gel microemulsion based on technical literature from Croda. We also attempted a number of variations containing oxidized ethyl linoleate, potassium phosphate dibasic, and chloramine T, but we obtained an acceptable ringing gel microemulsion only with the mixture containing the oxidized ethyl linoleate.

We also attempted to prepare a silicone oil-containing ringing gel microemulsion based on technical literature from Croda. Unfortunately, this attempt was unsuccessful because one of the components refused to dissolve in the mixture. Our attempts to prepare a dimethicone-based protective hand lotion and variations containing oxidized ethyl linoleate similarly resulted in nonhomogeneous mixtures.

A modification of a burn ointment based on gelatin and polyethyleneimine³¹ was attempted since the reference composition already contained both proteins and amines with potential reactivity with CEES. One attempted variation was the preparation of mixtures containing various amounts of FOMBLIN HC/04, but unfortunately, these efforts resulted in unacceptable nonhomogeneous mixtures.

We prepared some antiperspirant stick formulations to gain some experience with these acid-containing formulations. We also attempted to prepare a hand & body lotion based on Dow 245 (cyclomethicone) as well as variations of this lotion that incorporated oxidized ethyl linoleate. Unfortunately, a major component in these formulations remained insoluble throughout all of our attempts. A subsequent attempt of a hand & body lotion based on Dow 580 wax and variations containing oxidized ethyl linoleate gave white creamy lotions. We also preliminarily investigated a sunscreen lotion based on a cationic cellulosic polymer, a style/setting Gel based on hydroxypropyl guar and containing Polycare 133 (OH-exchanged), a cetyl dimethicone-based skin moisturizer, a hydrolyzed silk & elastin-based facial firming gel, a polysiloxane-based clear sunscreen oil, a polysiloxane-based clear styling gel, a polysiloxane-based conditioning setting gel. All of these gave homogeneous gels, creams, lotions, etc. that could be appropriate vehicles for our reactive components. Our attempt to prepare a cold cream based on Dow Q2-5200 (dimethicone copolyol) and variations of this cold cream containing oxidized ethyl linoleate were unsuccessful, and we consistently obtained two-phase solutions. Finally, we also obtained two commercial products: a sulfur-containing antidandruff hair and scalp conditioner and a benzoyl peroxide-containing acne medication.

During this quarter no reactivity tests were conducted, because our efforts were directed toward conducting barrier tests with our candidate formulations. However, we experienced a series of unanticipated experimental problems with the Minicams-based

permeation test system. The problems created a number of delays and produced test results that were unacceptable. As a result of our efforts, we were able to correct a number of different instrumental problems that had been difficult to isolate. Because of difficulty with one line (out of four) in the permeation test system, we completely disassembled, cleaned, and re-assembled the entire permeation test system. While this action appeared to fix the problem with the malfunctioning permeation test line, the correction was only temporary, and this problem quickly reoccurred. Therefore, a significant amount of time was again spent trying to locate and fix the problem with the system. Furthermore, while trouble-shooting the apparatus, the Minicams pump failed, and we had to order a new pump, thus creating another delay in the barrier testing. After we received the new pump, the permeation test data were unacceptably (and strangely) noisy, and thus, we had to continue to investigate the test system for the source of the poor system performance. We checked the performance of the temperature-control apparatus, the flow-control system and its components, the stream-selection valve and its operation, the Minicams software for possible "bugs," and our calibration procedures for problems. We finally determined that there was a very small but significant amount of contamination in the permeation test lines that erratically affected the flows from the test cell and blocked the transport of CEES that permeated the test samples. This contamination was likely fine debris from the test samples or from the air stream flowing through the lower compartments of the test-cell chambers. At the end of the reporting period, the Minicams-based permeation test system was finally operating as before and we began acquiring meaningful barrier test results. We also installed very fine mesh stainless-steel screens in the flow lines immediately downstream of the test cell to collect any fine dust that may be pulled into the system during the loading and unloading of test samples. These screens can be removed and cleaned between tests.

Because of the chronic problems with the Minicams-based permeation test system and the resulting delays in the barrier testing, we also began setting up a second permeation system both as a backup and to increase the rate of testing. The second system is older, ACAMS based, and is not computer controlled with automated data collection and analysis, but some side-by-side testing with the Minicams system shows that it provides permeation data that are similar to those produced by the Minicams system (as it should if there are no systematic errors in the testing method). This system was then interfaced to a computer and set up with an available commercial data-acquisition software package to allow the reduction of data using the same commercial spreadsheet software that we use to reduce the raw permeation data from the Minicams.

Our synthesis efforts for the ninth and tenth quarters were limited to completing our preparation and resynthesizing additional quantities of S-330 oxidizing agent (1,3,4,6-tetrachloro-7,8-diphenyl-2,5-diiminoglycoluril²⁹). Formulation activities were the main focus of these final quarters, and they included the modification of our efficacious

preliminary formulations, the investigation of other candidate formulations including a number of creams, gels, and microemulsions, and a continued search for alternative oxidants for our formulations (since we have no supplier for the S-330).

During these quarters, we continued to modify our preliminary formulations and to investigate new potential base formulations. Our efforts were primarily focused on preparing additional quantities of some preliminary formulations that our early tests had shown to have good barrier and reactivity efficacy against CEES: 2.5%, 5%, and 10% S-330-loaded versions of a FOMBLIN-containing skin protective composition comprised of FOMBLIN HC/04 (7.5 g), petrolatum (17.5 g), sorbitan stearate (2.5 g), and water (22.5%); a burn ointment³¹ comprised of Crodyne BY-19 gelatin (5 g), Corcat P-600 polyethyleneimine (15 g), and water (30 g) that was considered and pursued since its protein and amine components would have potential reactivity with CEES; and a microemulsion comprised of Brij 97 (24 g), hexadecane (4 g), ethanolamine (12 g), and water (60 g).

We attempted to prepare reactive-containing variations of our FOMBLIN-containing formulation by adding 2.5% loadings of our previously reported synthesized oxaziridine oxidant **25**, oxidized ethyl linoleate, bleach, potassium *p*-toluenethiosulfonate, sodium phosphate, or sodium thiosulfate. We obtained acceptable, stable homogenous candidates from the addition of the oxidized ethyl linoleate, bleach, and sodium phosphate. We also attempted to prepare some more substantive variations of the FOMBLIN/petrolatum/sorbitan stearate/water composition by adding Merquat 100 (Cl form, Calgon, Polyquaternium 6 = poly(diallyldimethylammonium chloride) or UCare JR-30M (Amerchol, Polyquaternium 10 = quaternized cellulose).

Because of the low viscosity of the ethanolamine-containing microemulsion, we also attempted to prepare variations that were thickened by a number of emulsion thickeners including: Acryloid K-125 (Rohm & Haas, polyacrylate); Pemulen TR-1 (BF Goodrich, Acrylates C10-30 Alkyl Acrylate crosspolymer); Carbopol 1342 (BF Goodrich, Acrylates/C10-30 Alkyl acrylate crosspolymer); UCare JR-30M (Amerchol, Polyquaternium 10 = quaternized cellulose); and pectin (Ball, polysaccharide). Stable homogeneous solutions were obtained with Pemulen TR-1 and Carbopol 1342.

We also attempted some variations of the gelatin-PEI-based burn ointment³¹ [comprised of Crodyne BY-19 gelatin (5 g), Corcat P-600 polyethyleneimine (15 g), and water (30 g)]. Since earlier attempts to incorporate FOMBLIN in this formulation were unsuccessful, we attempted to incorporate sodium thiosulfate, sodium acetate, potassium phosphate, sodium oximate, acetic acid, phosphoric acid, peracetic acid, and ammonium persulfate solutions into this base composition. We obtained clear gels from the addition

of acetic acid and phosphoric acid, while a cloudy gel was obtained from the addition of ammonium persulfate.

We also prepared a new batch of a FOMBLIN/teflon powder/S-330 formulation that presumably was similar to the benchmark formulation provided to us by Dr. Hackley. Dr. Hackley had previously given us a sample of his FOMBLIN/teflon powder formulation, and to a portion of this formulation, we added S-330 to give a formulation that was 10% S-330. (In one of his meetings with us, he had indicated that the benchmark composition contained this proportional amount of the S-330.) We prepared our composition from the formulation supplied by Dr. Hackley rather than trying to match the indicated composition of the benchmark formulation [FOMBLIN (54), teflon powder (36), and S-330 (10)] because we lacked information regarding the sources and grades of the FOMBLIN and teflon powder for Dr. Hackley's formulation. Our resulting formulation was a white cream while Dr. Hackley's formulation was a thicker, olive green cream, and thus, our version did not appear to match his formulation very closely. (However, evaluations showed that our version was more efficacious than Dr. Hackley's.)

During the tenth quarter, we continued to modify our preliminary formulations and to investigate new potential base formulations. Our focus was directed toward the modification of our efficacious preliminary FOMBLIN-containing skin protective composition comprised of FOMBLIN HC/04 (7.5 g), petrolatum (17.5 g), sorbitan stearate (2.5 g), and water (22.5%) containing 2.5%, 5%, and 10% of the oxidant S-330 (1,3,4,6-tetrachloro-7,8-diphenyl-2,5-diiminoglycoluril). To determine if the performance of the formulation could be enhanced with a higher molecular weight FOMBLIN/barrier polymer component, we replaced the FOMBLIN HC/04 with the higher molecular weight perfluoro alkylpolyethers FOMBLIN HC/25 and HC/R. We also prepared a version of our formulation in which the FOMBLIN HC/04 was replaced with DOW 200 and DOW 593 polysiloxanes, and we prepared another in which the FOMBLIN HC/04 was eliminated from the formulation. We also increased the proportion of S-330 from 10% to 12.3%, and we prepared versions in which SRI-prepared S-330 was used in place of the S-330 originally provided by Dr. Hackley. We also tried to incorporate other commercially available oxidants and reactants instead of the S-330 (*e.g.* 3-bromo-4,4-dimethyl-2-oxazolidinone = BDO; chloramine T; 1,3-dichloro-5,5-dimethylhydantoin; HTH calcium hypochlorite, and benzoyl peroxide, and obtained an active formulation with the 1,3-dichloro-5,5-dimethylhydantoin). We also attempted to prepare more skin substantive variations by adding Merquat 100 (Cl⁻ form, Calgon, Polyquaternium 6 = poly(diallyldimethylammonium chloride)) or UCare JR-30M (Amerchol, Polyquaternium 10 = quaternized cellulose) to the FOMBLIN/petrolatum/sorbitan stearate/water composition.

We also continued to investigate our burn ointment composition³¹ [Crodyne BY-19 gelatin (5 g), Corcat P-600 polyethyleneimine (15 g), and water (30 g)] that had preliminarily shown some promise. We prepared variations in which we attempted to add the CEES-reactive nucleophiles including sodium acetate, sodium phosphate, sodium oximate, etc. to this base composition.

Analytically, we continued to experience problems with the Minicams. However, because of the backup ACAMS system whose setup was completed during the ninth quarter, we were able to continue barrier testing our formulations through these quarters. Furthermore, we were finally able to determine that our software was also a culprit in the continuing difficulties.

In the closing quarters of this project, we focused most of our efforts on the preparation of the final report. Our laboratory efforts were aided by a granted extension that allowed us to run some efficacy confirmatory tests based on information relayed to us by Drs. Hackley and Braue at the 1996 Medical Defense Bioscience Review. At this meeting, we learned more of the details regarding the methods used by Dr. Hackley's lab to determine the efficacy of the FOMBLIN/teflon powder/S-330 formulation. Most significantly, we learned that M-8 paper was being used to determine the efficacies of both their and our formulations. With this information, we modified our test apparatus and reevaluated both Dr. Hackley's and our formulations by placing some M-8 paper between our formulation and the test cell silicone membrane. We also retested some of our S-330-containing formulations to get more information regarding the shelf-life stability of our formulations.

2.1 Preparation of Polymers and Other Potential SM-Reactive Components

Details of our ion-exchange and synthesis activities are presented in the following sections.

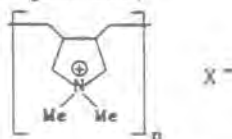
2.1.1. Preparation of Polymers with Ion-attached Detoxicants

During the first quarter, we began work with the cationic and anionic polymers shown below. They included three cationic quaternary ammonium chloride polymers (Merquat 100, Mirapol A-15, and Polycare 133) and two anionic polymers (polyacrylic acid and poly(vinylbenzenesulfonic acid)). Our first activity with the Merquat 100 and Mirapol A-15 was to determine the number of reactive sites per gram of these polymers. A gram of each was dissolved in water, and then, enough silver nitrate solution was then added to precipitate all of the chloride associated with polymer. The silver chloride was centrifuged and dried, and the number of exchange sites for a given weight of polymer was then calculated from the obtained weight of silver chloride. For Merquat 100, this value was found to be 2.83 mmol/gram of polymer solution (40% solids), while the value for Mirapol A-15 was found to be 5.16 mmol/gram of polymer solution (50% solids). These values were determined to estimate the required amount of the acid counterions to titrate the hydroxide forms of these polymers.

We then ion-exchanged larger amounts of Merquat 100 to its hydroxide form, and we titrated with histidine hydrochloride, cysteine, and 2-mercaptobenzoic acid to obtain the respective salts of the Merquat polymer. To convert Merquat 100 to its thiosulfate-exchanged form, we first converted the chloride form of IRA 400 ion-exchange resin (Sigma) to its thiosulfate form by batch-washing with sodium thiosulfate, and we then used this resin to convert Merquat 100 (OH^-) to its thiosulfate exchanged form. We similarly generated a thioglycolate-exchanged Merquat 100 which had been targeted because of thioglycolate's high SM-reactivity competition factor for SM.¹

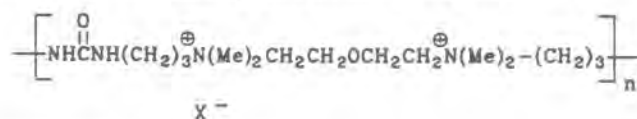
Polyquaternium compounds with anionic counterion detoxicants

Polypyrrolidinium Compounds (Merquat 100)

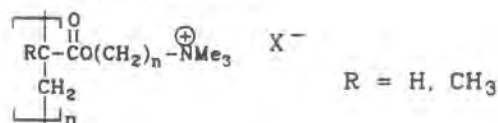


X^- = thiosulfate, ethane dithiophosphonate, the carboxylate salts of 2-mercaptobenzoic acid, cysteine, homocysteine, mercaptopyruvic acid, diethyldithiocarbamic acid, mercaptomalonic acid, histidine, thioctic acid (reduced form), 1-thiogluconic acid, and thioglycolic acid.

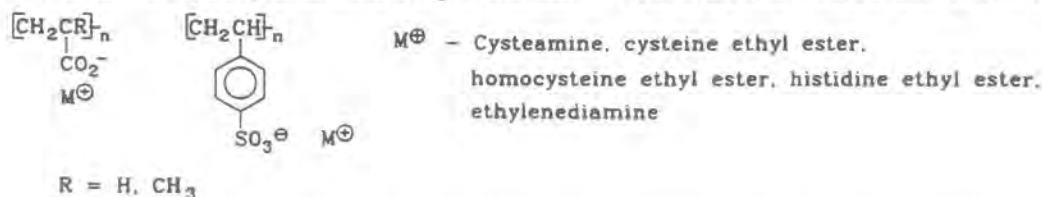
Quaternary ammonium salt-containing polyurea (Mirapol A-15)



Polyquaternium Acrylamides (Polycare 133)



Polyanionics - Polyacrylates and Polysulfonates - with cationic counterion detoxicants

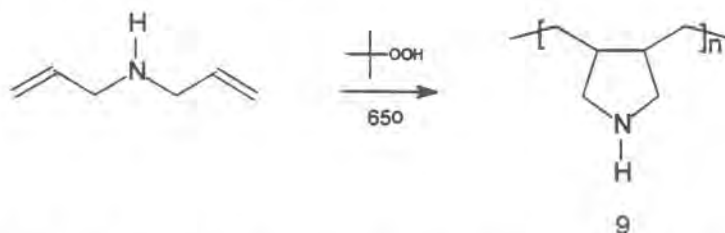


We were unsuccessful in our efforts to prepare two of our targeted salts: the diethyldithiocarbamate and reduced thioctic acid salts of Merquat 100. A usable form of the diethyldithiocarbamate exchanged polymer could not be obtained because the addition of the diethyldithiocarbamate counterion to a Merquat 100 (OH⁻) solution caused the precipitation of an insoluble material. Our efforts to prepare the reduced thioctic acid salt of Merquat 100 were unsuccessful because we were unable to reduce thioctic acid¹² in an acceptable yield.

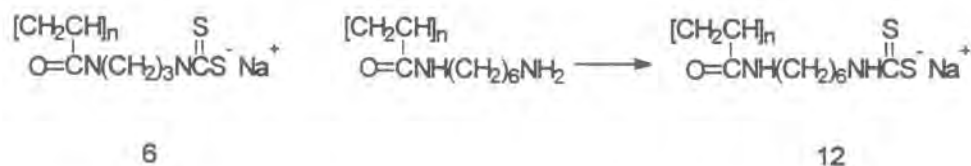
Other successful ion-exchange activity included the generation of the cysteine, histidine, and hydroxide forms of Mirapol A-15, and the preparation of the cysteine and hydroxide forms of Polycare 133. The hydroxide forms of the Mirapol A-15 and Polycare 133 polymers were prepared on scales that would allow the preparation of other exchanged forms of these polymers. However, we limited the number of these exchanged forms that we prepared because we felt that we already had a sufficient number of polymers to proceed with our formulating activities and with reactivity and barrier evaluations, at least in these preliminary stages. We were anxious to begin confronting and addressing the formulating challenges associated with these types of polymers and to explore some of the problems that may be associated with their *in vitro* evaluations. We also felt that at this time, more attention should be paid to the other proposed class of targets, especially the synthesized polymers with reactive, covalently attached side chains containing SM-reactive functionalities.

2.1.2. Synthesis of Polymers with Covalently Attached Detoxicants

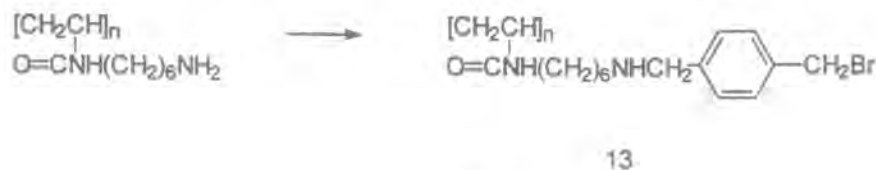
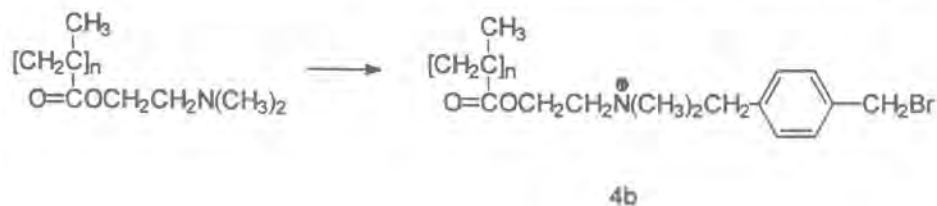
Polymer **9** was prepared by treating diallylamine hydrochloride in water with *t*-butylhydroperoxide at 65°C.¹³ The resulting thickened brown solution was evaporated under vacuum to give a very viscous brown solid.



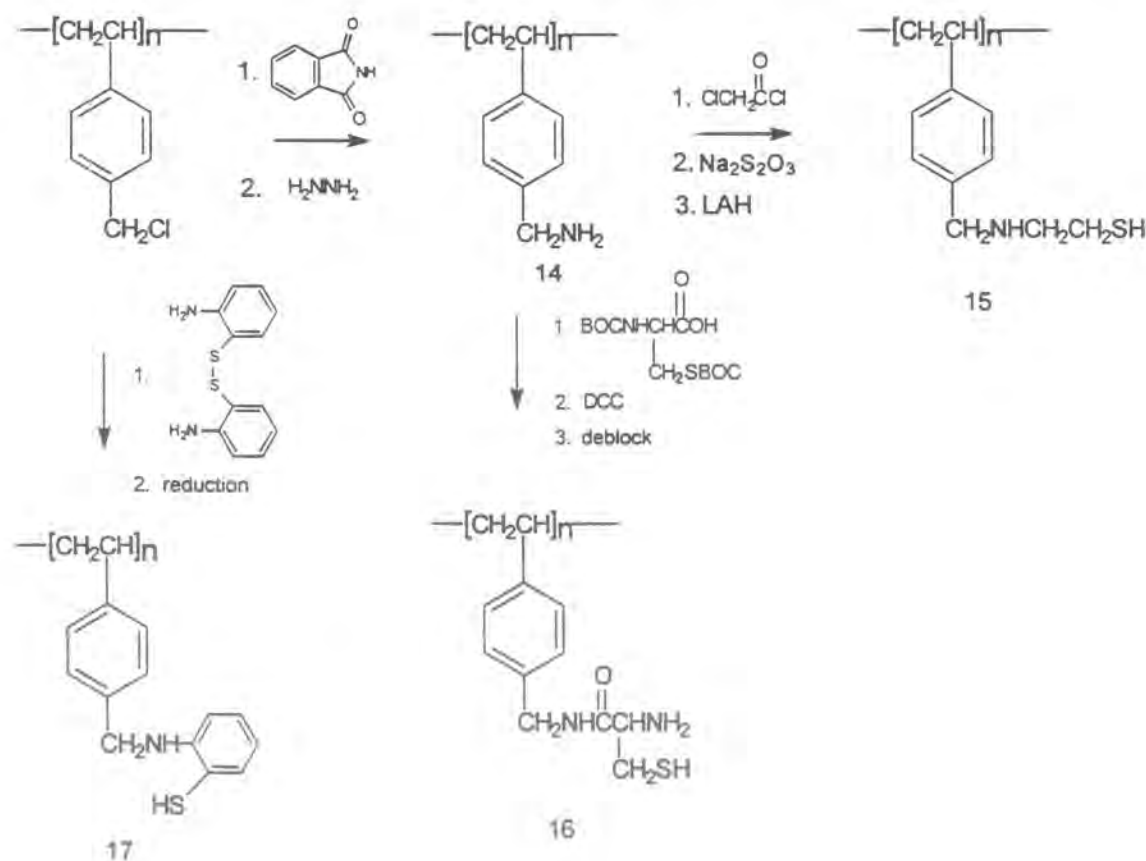
For target **12**, we chose to derivatize/modify a commercially available polymer instead of preparing a monomer that would unambiguously lead to the synthesis of originally targeted polymer **6**, because by doing so, we would be able to obtain this and related targets much quicker and easier. Polymer **12** was prepared by treating commercially available 6-aminohexylamide gel (Aldrich) with carbon disulfide and sodium hydroxide. The formation of the desired product was determined by comparing the infrared spectra (IR) of the starting material and product.



A similar method was used to prepare targets **4b** and **13**. Chloroform solutions of the desired backbone polymers (polydimethylaminoethylmethacrylate and 1-aminohexylamide gel) were added slowly to chloroform solutions of α,α' -dibromo-*p*-xylene with stirring, and the reaction mixtures were further stirred for 2-3 days at room temperature. The resulting solids were filtered, dried under vacuum, and analyzed by IR.

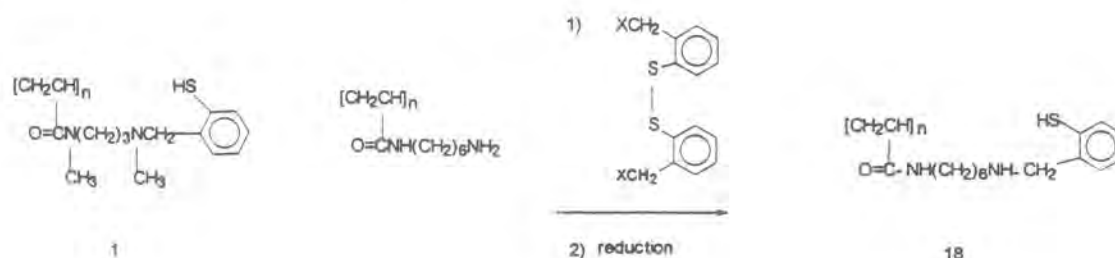


The following procedure was used to prepare aminomethylpolystyrene **14**.¹⁴ Merrifield Polymer (chloromethylated polystyrene-divinylbenzene beads, Fluka, 4.3 mmol Cl/g resin) was heated at 100°C and treated with potassium phthalimide in DMF under nitrogen. After stirring at 100°C overnight, the mixture was cooled, filtered, washed with distilled water and methanol, and dried under reduced pressure to give the phthalimido polymer. This intermediate was then suspended in boiling absolute ethanol and 98% aqueous hydrazine monohydrate was added with stirring, and the resulting mixture was refluxed for 10 h. Filtration, washing with ethanol, 0.2 N sodium hydroxide, distilled water, and anhydrous methanol followed by vacuum drying, gave the desired aminomethylpolystyrene. As mentioned previously, this polymeric material was prepared both as a potential detoxicant and as an intermediate in the preparation of targets such as **15-17**. For example, our approach to mercaptoethylaminomethylpolystyrene **15** paralleled a preparation for some aminoalkanethiol derivatized tryptamines.¹⁵ Aminomethylpolystyrene was treated first with chloroacetylchloride, and the resulting amide was treated with an alkali thiosulfate. Reduction of resulting adduct with lithium aluminum hydride then gave the desired mercaptoethylaminomethylpolystyrene **15**. For the preparation of the cysteine addition product **16**, our examination of the peptide chemistry literature suggested that we could pursue the addition of either *N,S*-di-BOC-cysteine¹⁶ or the formylthiazolidine of cysteine¹⁷ to the aminomethylpolystyrene under carbodiimide

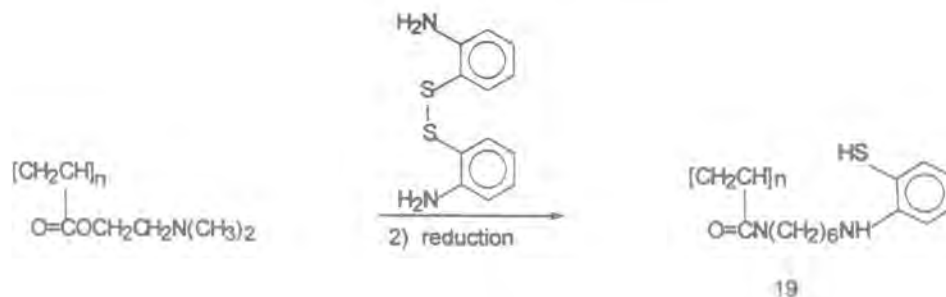


conditions followed by the appropriate deprotection conditions. Polymer **17** was targeted as a variation of our original target **1**. We anticipated that we should be able to prepare this target by adding 2-aminophenyldisulfide to Merrifield polymer (chloromethyl-polystyrene) followed by disulfide reduction.

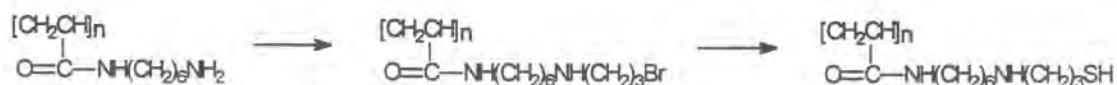
We modified our approach to a target **1** type polymer so that target **18** could be obtained from commercially available 1-aminohexylamide gel, instead of pursuing a longer route that would require the preparation of the corresponding monomer for **1**. (Our original approach to **1** was to add the appropriate halo- or tosylmethylbenzene disulfide to the 1-aminohexylamide gel followed by reduction of the disulfide of the addition product.) However, this target and approach modification was not successful, because we were unable to prepare 2-hydroxymethylbenzenedisulfide either from thiosalicylic acid or by dimerizing 2-mercaptobenzyl alcohol. A closer inspection of the literature showed that other investigators also had difficulties in their efforts to dimerize 2-mercaptobenzyl alcohol. We then considered other alternate approaches to a mercaptobenzyl-containing polymer, including the further modification of our target so that a different polymer backbone such as polystyrene would be used. By doing so, any problems or limitations due to the lability of the acrylamide bond could be avoided.



We also redesigned both the target and the approach to a 2-aminothiophenol-containing target **2**. Instead of pursuing **2**, we targeted **19** and planned to prepare it by adding 2-aminophenyldisulfide to a synthesized haloalkylene polyacrylamide followed by reduction of the disulfide. We also planned to prepare a structurally similar product by the Mannich reaction of 1-aminohexylamide gel with 2-aminophenyldisulfide.



As for the remaining targets (3, 4a, 7, and 8) from our original list, we pursued the more easily obtained target 20 (instead of preparing the monomer for target 3) by first monoalkylating 1-aminoethylamide gel with 1,3-dibromopropane and then introducing the mercapto group with potassium acetate or thiosulfate. Although some preliminary work was also directed toward the preparation of an acrylamide-1,4-dibromo-2-butene adduct as a monomer for polymer 4a, most of our effort toward a 4a-type target was directed to the more easily obtained target resulting from the addition of 1,4-dibromo-2-butene to commercially available poly(dimethylaminoethyl-methacrylate), similar to the preparation of target 4b.

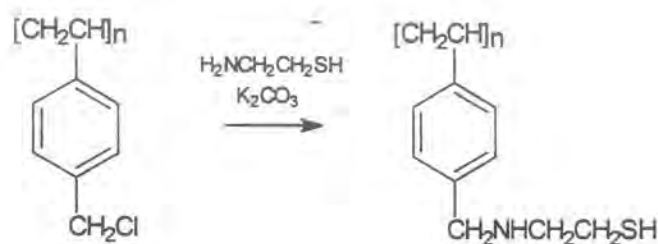


20

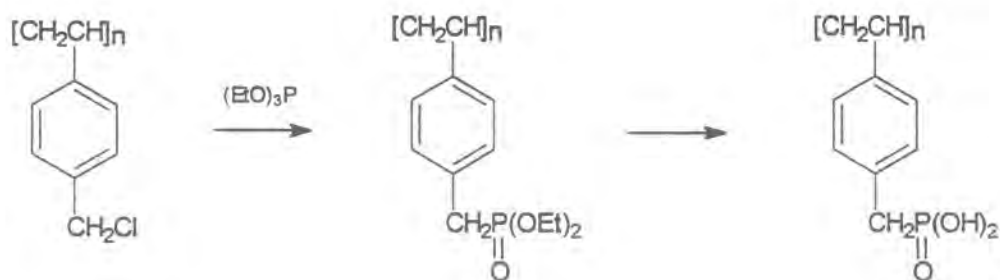
Our continued efforts to synthesize polycysteine¹⁸ 5 were abandoned due to low yields and the expense of the reagents. We chose instead to direct our efforts to our previously discussed aminomethylpolystyrene-cysteine adduct, since this form is favored by projected cost, difficulty of synthesis, and the availabilities of both amine and thiol groups as reactives in the final product vs. only thiol in polycysteine.

Only preliminary literature searches were performed for 7 and 8. While the dithiophosphonate and dithiophosphate groups of 7 and 8 appeared to be attractive candidates because of their high competitive factors (both were > 100,000), we decided that their syntheses was not straightforward and that we should instead pursue our new directions, especially the FOMBLIN perfluoro alkylpolyether-containing and oxidant-containing formulations.

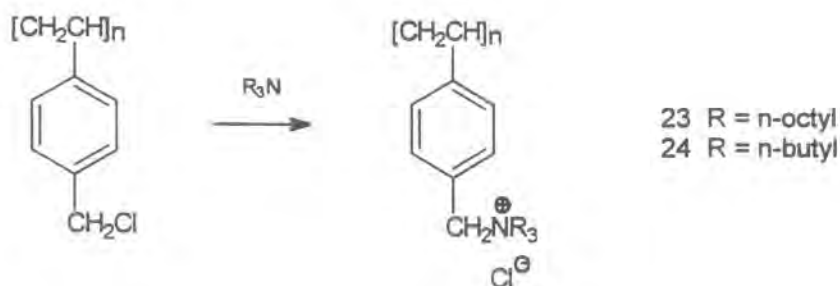
The preparation for aminomethylpolystyrene¹⁴ 14 was modified for preparing the cysteamine adduct 21 of Merrifield polymer and polystyrene-bound phosphonic acid 22. Merrifield Polymer (chloromethylated polystyrene-divinylbenzene beads, Fluka, 4.3 mmol Cl/g resin) was heated at 80-140°C for 24-28 h with potassium carbonate and cysteamine in DMF under nitrogen. After stirring overnight, the mixture was cooled, filtered, washed with distilled water and methanol, and dried under reduced pressure to give the modified polymers, based on the disappearance of the CH₂-Cl peak in the IR. The phosphonic acid diester precursors to 22 were prepared by refluxing either Merrifield polymer or poly(vinylbenzyl chloride) and triethylphosphite in diethylene glycol diethyl ether for 8 h. Hydrolysis of these intermediates by treatment with bromotrimethylsilane gave the phosphonic acid target. Trialkylamine adducts 23 and 24 were also prepared from Merrifield polymer by the respective additions of tri-*n*-octylamine and tri-*n*-butylamine.



21



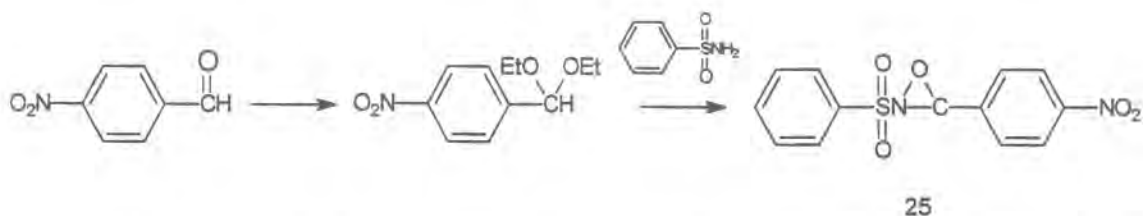
22



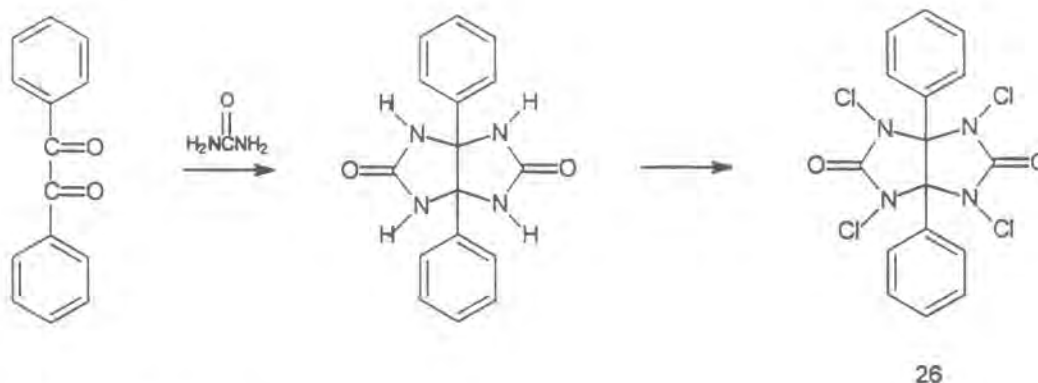
23 R = n-octyl

24 R = n-butyl

Our synthesis of *N*-sulfonyl-oxaziridine oxidizing agent **25** followed the literature.¹⁹⁻²¹ We first prepared the diethylacetal of *p*-nitrobenzaldehyde by refluxing *p*-nitrobenzaldehyde with ethanol and a catalytic amount of sulfuric acid followed by chromatographic purification of the product mixture (since this reaction does not go to completion). Next, equimolar amounts of benzenesulfonamide and the diethylacetal of *p*-nitrobenzaldehyde were heated in a 150-180°C oil bath until ethanol ceased to distill. The resulting sulfonimine adduct was then converted to the *N*-sulfonyloxaziridine **25** by treating a $\text{CHCl}_3/\text{NaHCO}_3/\text{H}_2\text{O}$ solution of the sulfonimine adduct with *m*-chloroperbenzoic acid at 0°C.



We prepared an oxygenated/oxidized unsaturated fatty acid ester by bubbling dry oxygen through ethyl linoleate at room temperature with irradiation with a 50-watt tungsten lamp.²² We also prepared multiple batches of S-330 oxidizing agent **26** (1,3,4,6-tetrachloro-7,8-diphenyl-2,5-diiminoglycoluril²⁹) as described in the literature by refluxing benzil with urea in benzene with a catalytic amount of acid, followed by treatment of an aqueous slurry of the resulting diphenylglycoluril with NaOCl and enough HCl to keep the pH in the 7-8 range.



2.2. Formulation

The following sections give details primarily for the evaluated formulations.

2.2.1. Preparation of Formulations Containing Polymers with Reactive Counterions

The following polyacrylic acid (Carbopol 940)-based formulation was pursued as a potential delivery system for our counterion-exchanged polyquaterniums (Merquat 100). An insoluble complex immediately formed upon addition of the polyquaternium component.

H868-2

Water, D.I.	85 g
Gaffix VC-713	3.5 g
Merquat 100	1.0 g

Isopropanol	10.0 g
Carbopol 940	0.5 g
Triethanolamine	to pH 6

[Gaffix VC-713 Polymer is an ISP/GAF product comprised of the polymer of 2-propenoic acid, 2-methyl-2-dimethylaminoethyl ester with the polymers of 1-ethenylhexahydro-2H-azepin-2-one and 1-ethenyl-2-pyrrolidinone, and ethanol.]

Formulations containing cellulose-based polymeric thickeners were pursued because these thickened aqueous formulations are known to tolerate heavy concentrations of polycationics. Our challenge was to find appropriate emulsifiers that would allow a small oil phase for cream or lotion generation. The following formulation using the histidine- exchanged Merquat 100 gave a light yellow lotion.

Water	88 g
Glycerin	2.0 g
Hydroxyethyl Cellulose	0.5 g
Triethanolamine	0.5 g
Merquat (Histidine)	8.7 g
Glycol Stearate	2.75 g
Stearic Acid	2.5 g
Mineral Oil	2.0 g
Preservative	0.75 g
Acetylated lanolin	0.5 g
Cetyl alcohol	0.25 g

A similar white lotion was obtained by repeating the formulation with cysteine-exchanged Merquat.

The following emulsion creams were found to tolerate high concentrations of polycationics and included emulsifiers that would allow an oil phase for cream or lotion generation. To determine the compatibility of this base formulation with polycationics such as the polypyrrolidiniums, seven variations were prepared by replacing some part of the water phase with a polycationic. All of these formulations were stable.

H868-7 (Emulsion/cream with 5% Merquat 100, thus loading this emulsion with 2% of the polypyrrolidinium component since Merquat 100 is a 40% solution of this polyquat.)

Water Phase

D. I. Water	74 g
NaCl	0.8 g
Merquat 100	5 g

Oil Phase

Cetyl Dimethicone Copolyol (and)	
Polyglyceryl-4-Isostearate (and)	
Hexyl Laurate (Abil WE-09)	5 g
Light Mineral Oil	5 g
Caprylic/Caprylic Triglycerides	
(Tegosoft CT)	5 g
Isopropyl Myristate (Tegosoft M)	5 g

[Mixing instructions: All the ingredients of the oil phase were combined with each other and all the ingredients of the water phase were combined. Then, the water phase was added slowly with gentle mixing to the oil phase at room temperature to produce the emulsion. The emulsion was homogenized for approximately three minutes to produce a thick cream.]

H868-8 (Variation with 50% Merquat 100, thus loading this emulsion with 20% of the polypyrrolidinium component.)

Water Phase

D. I. Water	31 g
NaCl	0.8 g
Merquat 100	50 g

Oil Phase

Cetyl Dimethicone Copolyol (and)	
Polyglyceryl-4-Isostearate (and)	
Hexyl Laurate (Abil WE-09)	5 g
Light Mineral Oil	4 g
Caprylic/Caprylic Triglycerides	
(Tegosoft CT)	4 g
Isopropyl Myristate (Tegosoft M)	4 g

[Mixing instructions: Same as H868-7.]

H868-10 (Variation with 40% Polycare 133, thus loading this emulsion with 20% of the polyquaternium component since Polycare 133 is a 50% aqueous solution of polymethacrylamidopropyltrimethylammonium chloride.)

Water Phase

D. I. Water	39 g
NaCl	0.8 g
Polycare 133	40 g

Oil Phase

Cetyl Dimethicone Copolyol (and)	
Polyglyceryl-4-Isostearate (and)	
Hexyl Laurate (Abil WE-09)	5 g
Light Mineral Oil	5 g
Caprylic/Caprylic Triglycerides	
(Tegosoft CT)	5 g
Isopropyl Myristate (Tegosoft M)	5 g

[Mixing instructions: Same as H868-7.]

H868-11 (Variation with 20% Merquat 100 with thioglycolate counterion.)

Water Phase

D. I. Water	18.7 g
NaCl	0.8 g
Merquat 100	
(thioglycolate exchanged, 25% solution)	60.5 g

Oil Phase

Cetyl Dimethicone Copolyol (and)	
Polyglyceryl-4-Isostearate (and)	
Hexyl Laurate (Abil WE-09)	5 g
Light Mineral Oil	5 g
Caprylic/Caprylic Triglycerides	
(Tegosoft CT)	5 g
Isopropyl Myristate (Tegosoft M)	5 g

[Mixing instructions: Same as H868-7.]

H868-13 (Polycationic-containing emulsions based on the non-ionic silicone-based emulsifier, ABIL WE-09 from Goldschmidt Chemical Corporation.)

Water Phase

D. I. Water	80 g
NaCl	0.8 g

Oil Phase

Cetyl Dimethicone Copolyol (and)	
Polyglyceryl-4-Isostearate (and)	
Hexyl Laurate (Abil WE-09)	5 g
Light Mineral Oil	5 g

Caprylic/Caprylic Triglycerides (Tegosoft CT)	5 g
Isopropyl Myristate (Tegosoft M)	5 g

[Mixing instructions: Same as H868-7.]

H868-14 (Variation with 7.4% Merquat with histidine as the counterion.)

Water Phase

D. I. Water	17.9 g
NaCl	0.8 g
Merquat 100 (histidine exchanged, 30% solution)	61.3 g

Oil Phase

Cetyl Dimethicone Copolyol (and) Polyglyceryl-4-Isostearate (and) Hexyl Laurate (Abil WE-09)	5 g
Light Mineral Oil	5 g
Caprylic/Caprylic Triglycerides (Tegosoft CT)	5 g
Isopropyl Myristate (Tegosoft M)	5 g

[Mixing instructions: Same as H868-7.]

H868-15 (Variation with 18.8% Merquat 100 with thiosulfate as the counterion.)

Water Phase

NaCl	0.8 g
Merquat 100 (thiosulfate exchanged)	0.0 g

Oil Phase

Cetyl Dimethicone Copolyol (and) Polyglyceryl-4-Isostearate (and) Hexyl Laurate (Abil WE-09)	2.5 g
Light Mineral Oil	2.5 g
Caprylic/Caprylic Triglycerides (Tegosoft CT)	2.5 g
Isopropyl Myristate (Tegosoft M)	2.5 g

[Mixing instructions: Same as H868-7.]

Our interest in these emulsion formulations lessened after our preliminary reactivity tests showed that they had little to no effect on CEES. However, later in the project, we determined that solutions of OH^- , acetate, etc. exchanged polyquaternium emulsifiers Merquat 100, Polycare 133, and Mirapol A-15 were effective in hydrolyzing CEES, especially when all chloride ion sources were removed. Therefore, we decided that we should investigate these H868-13 emulsion formulations once again using the ion-exchanged emulsifiers and eliminating all chloride sources in the formulation. As a result, the following were prepared.

I194-7-A

Water Phase

D. I. Water	73.6 g
NaBr	1.41 g
5% Aqueous OH^- -exchanged Merquat 100	5 g

Oil Phase

Cetyl Dimethicone Copolyol (and)	
Polyglyceryl-4-Isostearate (and)	
Hexyl Laurate (Abil WE-09)	5 g
Light Mineral Oil	5 g
Caprylic/Caprylic Triglycerides	
(Tegosoft CT)	5 g
Isopropyl Myristate (Tegosoft M)	5 g

I194-7-B

Water Phase

D. I. Water	73.9 g
Sodium Acetate	1.12 g
5% Aqueous OH^- -exchanged Merquat 100	5 g

Oil Phase

Cetyl Dimethicone Copolyol (and)	
Polyglyceryl-4-Isostearate (and)	
Hexyl Laurate (Abil WE-09)	5 g
Light Mineral Oil	5 g
Caprylic/Caprylic Triglycerides	
(Tegosoft CT)	5 g
Isopropyl Myristate (Tegosoft M)	5 g

I194-7-C

Water Phase

D. I. Water	68.9 g
Tetrasodiumpyrophosphate	6.11 g
5% Aqueous OH ⁻ -exchanged Merquat 100	5 g

Oil Phase

Cetyl Dimethicone Copolyol (and) Polyglyceryl-4-Isostearate (and) Hexyl Laurate (Abil WE-09)	5 g
Light Mineral Oil	5 g
Caprylic/Caprylic Triglycerides (Tegosoft CT)	5 g
Isopropyl Myristate (Tegosoft M)	5 g

I194-7-D

Water Phase

D. I. Water	72.62 g
Potassium phosphate dibasic	2.38 g
5% Aqueous OH ⁻ -exchanged Merquat 100	5 g

Oil Phase

Cetyl Dimethicone Copolyol (and) Polyglyceryl-4-Isostearate (and) Hexyl Laurate (Abil WE-09)	5 g
Light Mineral Oil	5 g
Caprylic/Caprylic Triglycerides (Tegosoft CT)	5 g
Isopropyl Myristate (Tegosoft M)	5 g

2.2.2. Preliminary Cyclodextrin-Containing Formulations

H868-16

5:8:7 mixture of α , β and γ cyclodextrins (11.57 g/L; 0.01 M)

H868-17

water-in-oil formulation containing the H868-16 mixture at a level of 80% of the formulation

H868-18

water-in-oil emulsion formulation containing 30% by weight hydroxypropyl β -cyclodextrin

H868-20

Carbopol 940 thickened aqueous gel containing 28.6% hydroxypropyl β -cyclodextrin by weight

2.2.3. PEG-based Formulations Containing Various Nucleophiles

Our efforts to copy and modify the reactive polyethylene glycol-based formulations^{3,4} from the literature resulted in the preparation of a number of formulations. Three of the formulations from the second reference were prepared as standards for our work and for our analytical methodologies. Approximately 1.25 *M* solutions were prepared by mixing appropriate amounts of the potassium salts of acetone monoxime, 2,3-butanedione monoxime, and phenol into commercially obtained polyethylene glycol monomethyl ether (MPEG, Aldrich, avg. mwt. 550). Alternate nucleophiles that were incorporated to give acceptable modified formulations included sodium diethyldithiocarbamate, glycoldimercaptopropionate (Hampshire Chemical Corporation), the tris-mercaptopropionate of trimethylolpropane (Hampshire Chemical Corporation), the tetra-3-mercaptopropionate of pentaerythritol (PTM-20, Hampshire Chemical Corporation), polyoxyalkylenediamine (Huntsman), and potassium *p*-toluenethiosulfonate (Aldrich). We also prepared two variations in which the polyethylene glycol methyl ether 550 (MPEG 550) of the original oximate and phenolate solutions was replaced with a mixture of polyethylene glycols (mwt. 400 and 600) that were proportionally combined to give a PEG blend with a molecular weight of 550. Other similar formulations were then prepared because the evaluations of our first three ~1.25 *M* formulation "standards" (0.0009 mol actives/g formulation) gave data that were inconsistent with the reported results. (The actual compositions of the originally selected formulations from this reference were presented somewhat ambiguously so that we were not certain that we had really reproduced the exact formulations.) These formulations included a batch that contained only 0.000069 mol actives/g of formulation while another batch inadvertently contained 0.0009 mol KOH/g formulation and 0.000069 mol of the other active/g formulation. Interestingly, the formulations containing 0.000069 mol active/formulation and 0.0009 mol KOH/g formulations showed good reactivity results. The following is a listing of all of our PEG-based formulations.

H823-111A

2,3-butanedione monoxime (3.1 g), 50% KOH soln (3.22 g), polyethylene glycol monomethyl ether, avg. mwt. 550 = MPEG 550 (27 g); (0.0009 mol actives/g formulation)

H823-111B

acetone monoxime (2.3 g), 50% KOH soln (3.22 g), MPEG 550 (27 g); (0.0009 mol actives/g formulation)

H823-111C

2,3-butanedione monoxime (3.1 g), 50% KOH soln (3.22 g), mixture of polyethylene glycols with avg. mwts. of 350 and 750 to give an avg. mwt. of 550 (27 g); (0.0009 mol actives/g formulation)

H823-111D

acetone monoxime (2.3 g), 50% KOH soln (3.22 g), mixture of polyethylene glycols with avg. mwts. of 350 and 750 to give an avg. mwt. of 550 (27 g); (0.0009 mol actives/g formulation)

H823-111E

phenol (2.94 g), 50% KOH soln (3.22 g), MPEG 550 (27 g); (0.0009 mol actives/g formulation)

H823-111G

sodium diethyldithiocarbamate (7 g), MPEG 550 (27 g); (0.0009 mol actives/g formulation)

H823-111K

glycol dimercaptopropionate (GDMP, 7.4 g), MPEG 550 (27 g); (0.0009 mol actives/g formulation)

H823-111L

trimethylolpropane tris 3-mercaptopropionate (TMOPT, 10.2 g) (3.26 g), MPEG 550 (27 g); (0.0008 mol actives/g formulation)

H823-111M

pentaerythritol tetra-3-mercaptopropionate (PETTMP, 15.3 g), MPEG 550 (27 g); (0.0007 mol actives/g formulation)

H823-111N

polyoxyalkylenediamine (POAD, 28.1 g), MPEG 550 (27 g); (0.0005 mol/g formulation)

H823-116A

p-toluenethiosulfonic acid, K salt (7.06 g), MPEG 550 (27 g); (0.0009 mol actives /g formulation)

H823-116B

MPEG 550 (neat)

H823-123A

2,3-butanedione monoxime (3.1 g), 50% KOH soln (3.22 g), 3:1 mixture of polyethylene glycols with avg. mwts. of 400 and 600 to give an avg. mwt. of 550 (27 g); (0.0009 mol actives/g formulation)

H823-123B

acetone oxime (2.3 g), 50% KOH soln (3.22 g), 3:1 mixture of polyethylene glycols with avg. mwts. of 400 and 600 to give an avg. mwt. of 550 (27 g); (0.0009 mol actives/g formulation)

H823-123C

phenol (2.94 g), 50% KOH soln (3.22 g), 3:1 mixture of polyethylene glycols with avg. mwts. of 400 and 600 to give an avg. mwt. of 550 (27 g); (0.0009 mol actives/g formulation)

H823-123E

sodium diethyldithiocarbamate (7 g), 50% KOH soln (3.22 g), 3:1 mixture of polyethylene glycols with avg. mwts. of 400 and 600 to give an avg. mwt. of 550 (27 g); (0.0009 mol actives/g formulation)

H823-111A2

2,3-butanedione monoxime (0.21 g, 0.000069 mol/g formulation), 50% KOH soln (3.22 g, 0.0009 mol/g formulation), polyethylene glycol monomethyl ether, avg. mwt. 550 = MPEG 550 (27 g)

H823-111B2

acetone oxime (0.15 g, 0.000069 mol/g formulation), 50% KOH soln (3.22 g, 0.0009 mol/g formulation), MPEG 550 (27 g)

H823-111E2

phenol (0.2 g, 0.000069 mol/g formulation), 50% KOH soln (3.22 g, 0.0009 mol/g formulation), MPEG 550 (27 g)

H823-123I

3:1 mixture of polyethylene glycols with avg. mwts. of 400 and 600 to give an avg. mwt. of 550

H823-123J

p-toluenethiosulfonic acid, K salt, (0.0009 mol/g formulation), 3:1 mixture of polyethylene glycols with avg. mwts. of 400 and 600 to give an avg. mwt. of 550 (27 g)

H823-123K

glycol dimercaptopropionate (GDMP, 7.4 g, 0.0009 mol/g formulation), 3:1 mixture of polyethylene glycols with avg. mwts. of 400 and 600 to give an avg. mwt. of 550 (27 g)

H823-123L

trimethylolpropane tris 3-mercaptopropionate (TMOPT, 10.2 g, 0.0008 mol/g formulation), 3:1 mixture of polyethylene glycols with avg. mwts. of 400 and 600 to give an avg. mwt. of 550 (27 g)

H823-123M

pentaerythritol tetra-3-mercaptopropionate (PETTMP, 15.3 g, 0.0007 mol/g formulation), 3:1 mixture of polyethylene glycols with avg. mwts. of 400 and 600 to give an avg. mwt. of 550 (27 g)

H823-123N

polyoxyalkylenediamine (POAD, 27 g, 0.0005 mol actives/g formulation), MPEG 550 (27 g)

H823-111A3

butanedione monoxime (0.21 g, 0.000069 mol/g formulation), 50% KOH soln (0.22 g, 0.0006 mol/g formulation), MPEG 550 (27 g)

H823-111B3

acetone oxime (0.15 g, 0.000069 mol/g formulation), 50% KOH soln (0.22 g, 0.0006 mol/g formulation), MPEG 550 (27 g)

H823-116D

50% KOH (3.32 g, 0.0009 mol KOH/g formulation), MPEG 550 (27 g)

2.2.4 Preliminary Perfluoro Alkylpolyether-Containing Formulations

In our investigation of barrier-providing formulations containing perfluoro alkylpolyethers (*e.g.* FOMBLINs HC/04, Brooks/Montefluos), the following FOMBLIN HC/04-based barrier-providing gel was prepared. This gel was reported to apply the perfluoroether as a semi-occlusive, vapor restrictive layer that allowed skin respiration, and therefore, it was prepared both as a test formulation and as a base formulation to which we would attempt to add various reactive additives. We also prepared a version substituting for the FOMBLIN HC/04 with the higher molecular weight FOMBLIN HC/25 and FOMBLIN HC/R, and we attempted version which attempted to replace the triethanolamine with more CEES-reactive ethanolamine or a polyethyleneimine. Unfortunately, the triethanolamine and polyethyleneimine attempts did not give acceptable formulations.

H823-144A (FOMBLIN HC/04-based gel, Brooks Industries, Inc.)

<u>Ingredients</u>	<u>Nomenclature</u>	<u>%</u>
Demineralized Water	Water	QS

Carbopol 1342	Acrylate/C ₁₀₋₃₀ Alkyl Acrylate Crosspolymer	0.10
FOMBLIN HC/04	Perfluoropolymethylisopropyl Ether	0.50
Glycerin	Glycerin	0.50
Standapol ES-2	Sodium Laureth Sulfate	0.02
Triethanolamine 99%	Triethanolamine	0.20
Nipasol M	Propylparaben	0.05
Nipagen M	Methylparaben	0.20

Mixing Instructions: The water and Carbopol 1342 were combined and heated to 40 °C. After complete solution, the heat was removed, and the methylparaben and propylparaben were added. The FOMBLIN, glycerin, and sodium laureth sulfate were combined, and the resulting white cream was added to the water-Carbopol, etc. solution. Triethanolamine was then added, giving a clear gel.

H823-144E (H823-144A prepared with higher molecular weight FOMBLIN HC/25)

<u>Ingredients</u>	<u>Nomenclature</u>	<u>%</u>
Demineralized Water	Water	QS
Carbopol 1342	Acrylate/C ₁₀₋₃₀ Alkyl Acrylate Crosspolymer	0.10
FOMBLIN HC/25	Perfluoropolymethylisopropyl Ether	0.50
Glycerin	Glycerin	0.50
Standapol ES-2	Sodium Laureth Sulfate	0.02
Triethanolamine 99%	Triethanolamine	0.20
Nipasol M	Propylparaben	0.05
Nipagen M	Methylparaben	0.20

We attempted to add Teflon powder, 1,3,4,6-tetrachloro-7,8-diphenyl-2,5-diiminoglycoluril (S-330), benzoyl peroxide, 5% sodium hypochlorite solution (household bleach), and copper, zinc, and iron metals to this FOMBLIN HC/04 gel base. We obtained an acceptable formulation (I194-19) only from the addition of household bleach. This solution darkened with time, suggesting the need for stabilization of this formulation.

I194-19

<u>Ingredients</u>	<u>Nomenclature</u>	<u>%</u>
Demineralized Water	Water	39.12
Carbopol 1342	Acrylate/C ₁₀₋₃₀ Alkyl Acrylate Crosspolymer	0.05
FOMBLIN HC/04	Perfluoropolymethylisopropyl Ether	0.25
Clorox	Bleach	10.00
Glycerin	Glycerin	0.25
Standapol ES-2	Sodium Laureth Sulfate	0.01
Triethanolamine 99%	Triethanolamine	0.10

Nipasol M	Propylparaben	0.025
Nipagen M	Methylparaben	0.10

Mixing Instructions: The Clorox and water were combined. Carbopol 1342 was added and heated to 40°C. After complete solution, the heat was removed, and the methyl paraben and propyl paraben were added. The FOMBLIN, glycerin, and sodium laureth sulfate were combined (giving a white cream) and then added to the Clorox/water, etc. solution. Triethanolamine was then added, giving a dark yellow, clear gel.

2.2.5 Preliminary Polyethyleneimine and Methyl Cellulose-thickened Solutions

In a preliminary attempt to see if polyethyleneimine (PEI) could provide substantivity as well as serve an anchor for CEES-reactive moieties, the following PEI-based mixtures were prepared by adding a cysteine solution to a commercially available PEI (Corcat P-12). Clear solutions were obtained with the following formulations.

H823-145A

Cysteine (dissolved in 7 mL of water)	0.5 g
Corcat P-600	2.0 g

H823-145B

Cysteine (dissolved in 7 mL of water)	0.5 g
Corcat P-600	1.0 g

H823-145C

Cysteine (dissolved in 7 mL of water)	0.5 g
Corcat P-600	0.5 g

During our study of gels and microemulsions as potential reactive vehicles, we prepared following preliminary thickened formulations in an attempt to incorporate the CEES reactivity of ion-exchanged polyquaternium emulsifiers in a thickened delivery system. We prepared methyl, hydroxyethyl, hydroxypropyl, and sodium carboxymethyl cellulose-thickened solutions of Mirapol A-15 (OH⁻-exchanged), Polycare 133 (OH⁻-

exchanged) containing 3 % methyl cellulose. On the other hand, a free flowing solution was obtained when we tried to thicken a 5 % solution of Mirapol A-15 (OH⁻-exchanged) with 1 % hydroxypropyl cellulose, and our attempt to thicken the solution by increasing the hydroxypropyl cellulose content to 3 % resulted in a 2-layer mixture that gradually became homogeneous only after a couple of weeks. Our efforts to thicken a 5 % solution of Mirapol A-15 (OH⁻-exchanged) with sodium carboxymethyl cellulose showed that this cellulose was not soluble.

I194-8-A

5 % Aqueous Solution of OH ⁻ -exchanged Mirapol A-15	10 g
Methyl cellulose	0.3 g

I194-8-B

5 % Aqueous Solution of OH ⁻ -exchanged Polycare 133	10 g
Methyl cellulose	0.3 g

I194-8-D

5 % Aqueous Solution of OH ⁻ -exchanged Mirapol A-15	10 g
Hydroxyethyl cellulose	0.1 g

I194-8-E

5 % Aqueous Solution of OH ⁻ -exchanged Mirapol A-15	10 g
Hydroxyethyl cellulose	0.3 g

I194-8-F

1 % Aqueous Solution of OH ⁻ -exchanged Mirapol A-15	10 g
Hydroxypropyl cellulose	0.1 g

I194-8-G

5 % Aqueous Solution of OH ⁻ -exchanged Mirapol A-15	10 g
Hydroxypropyl cellulose	0.3 g

2.2.6. Preliminary Efforts to Prepare Dr. Hackley's FOMBLIN A-based Formulation

We also pursued inhouse versions of Dr. Hackley's active formulations. During his first site visit, Dr. Hackley indicated that compositions comprised of FOMBLIN A and

teflon powder and FOMBLIN A, teflon powder, and an oxidant (S-330 = 1,3,4,6-tetrachloro-7,8-diphenyl-2,5-diiminoglycoluril) were to be our benchmark formulations, and he also gave us ~10 g samples of these materials. Larger quantities were not supplied because he thought that we should be able to find similar commercial products very easily. However, after calling a number of local drug stores, safety equipment suppliers, etc., we were unable to find any topically applied formulations containing FOMBLIN A. Calls to Brooks Industries and Ausimont S.p.A. (the U.S. distributors of cosmetic grade FOMBLIN and industrial grade FOMBLINs including FOMBLIN A, respectively) helped us to determine that the only commercially available products containing FOMBLIN A were the Blue Coral car waxes. We also learned that FOMBLIN A is prepared exclusively for Blue Coral. Since our supply of the FOMBLIN A/teflon powder formulation had been depleted by our reactivity and barrier evaluations (leaving us with none for direct comparison with our formulations or for modification), we decided to try to prepare formulation similar to Dr. Hackley's by following the composition information that he had provided.

Our starting materials for these efforts were FOMBLIN HC/25 and Dupont Teflon powder (mwt. 1200) that we had previously obtained. From the combination of FOMBLIN HC/25 and Dupont Teflon powder (mwt. 1200), we obtained a white creamy lotion (I194-11A) that resembled but did not have the thick consistency of Dr. Hackley's FOMBLIN A formulations. We also prepared the following oxidant-loaded versions: S-330 (0.1 g) was added to I194-11A (51.5 g) to give I194-11A1 as a white lotion; S-330 (0.26 g) was added to I194-11A (5 g) to give I194-11C as a white lotion; and ethyl linoleate (0.26 g) was added to I194-11A (5 g) to give I194-11D as a white lotion.

I194-11A

FOMBLIN HC/25	37 g
Dupont Teflon powder (mwt. 1200)	14.5 g

We also used the /teflon powder formulation (ICD #1511) supplied by Dr. Hackley to prepare a sample containing S-330 in the recommended 10% proportion.

I194-11F

ICD #1511	4.5 g
S-330	0.5 g

2.2.7. Commercial Barrier Creams

I194-13-1 (DermaPlus, Benchmark) and -2 (Kerodex, Whitehall Lab. Inc.) are two commercially available barrier creams that we tested to see if their compositions would

provide starting point formulations that could be modified for our purposes. Kerodex 71 is a petrolatum based cream containing calcium carbonate, cetearyl alcohol, cetrimonium bromide, cetyl alcohol, iron oxide, isopropyl alcohol, kaolin, methylparaben, mineral oil, paraffin, petrolatum, propylparaben, sodium hexametaphosphate, sodium lauryl sulfate, water, and zinc oxide. The DermaPlus contains dimethicone, polyvinylpyrrolidone, triethanolamine, isopropyl myristate, water, isobutane, stearic acid, coconut acid, glycerin, propane, cetyl alcohol, cetearyl alcohol, cetareth-20, triclosan, methyl paraben, tetrasodium EDTA, hydroxyethyl cellulose, aloe vera gel, tocopherol acetate, lanolin, and polyparaben.

2.2.8. Microemulsions

Our continued search of the literature for potential delivery formulations led us to recent work by F. Menger who reported a number of advantages (low cost, ease of preparation) and the decontaminating efficacy of hypochlorite-containing microemulsions in which low molecular weight alcohols are used as cosurfactants.²³⁻²⁵ We began studying Menger's microemulsions to determine if a similar approach could be used in our formulation, and we prepared the microemulsions I194-9A-C to get some experience with these formulations. When bleach was added to these microemulsion formulations, as described by Menger, we obtained clear, free-flowing solutions. However, these were not evaluated because of their consistencies and because of their reported short shelf life problem (rapid decrease in potency even after only 1 day). Before a similar microemulsion could be useful to us, we would need to prepare a stabilized version or to determine that a version with a different reactant would also be reactive with CEES. Therefore, we prepared a modification of I194-9A in which ethanolamine was substituted for 1-butanol giving a clear solution (I194-9D). We also prepared solutions in which we added 5% sodium acetate, 5% potassium phosphate dibasic, and 3.2% and 10% solutions of sodium thiosulfate to this microemulsion, and in all cases, we obtained clear solutions. Our attempt (I194-14F) to include the S-330 additive resulted in a cloudy mixture that cleared upon setting. Because of the low viscosity of the ethanolamine-containing microemulsion, we also attempted to thicken I194-9D with a number of emulsion thickeners including: Acryloid K-125 (Rohm & Haas, polyacrylate); Pemulen TR-1 (BF Goodrich, Acrylates C10-30 Alkyl Acrylate crosspolymer); Carbopol 1342 (BF Goodrich, Acrylates/C10-30 Alkyl acrylate crosspolymer); UCare JR-30M (Amerchol, Polyquaternium 10 = quaternized cellulose); and pectin (Ball, polysaccharide). Stable homogeneous solutions were obtained with Pemulen TR-1 and Carbopol 1342.

I194-9A

<i>n</i> -hexadecane	4%
water	60%
Brij 97 = $(\text{CH}_3(\text{CH}_2)_7\text{CH}=\text{CH}(\text{CH}_2)_8(\text{OCH}_2\text{CH}_2)_{10}\text{OH})$	24%
1-butanol	12%

I194-9B

cyclohexane	3%
water	82%
sodium dodecyl sulfate	5%
butanol	10%

I194-9C

heptane	24%
water	56%
sodium dioctylsulfosuccinate	8%
1-butanol	12%

I194-9D

<i>n</i> -hexadecane	4%
water	60%
Brij 97	24%
ethanolamine	12%

I194-10E

I194-9A	4.5 mL
5% Sodium acetate solution	0.16 g

I194-10F

I194-9A	4.5 mL
5% Potassium phosphate dibasic solution	0.27 g

I194-10G

I194-9A	1.5 mL
S-330	20 mg

I194-10H

I194-9A	4.5 mL
3.2% Sodium thiosulfate solution	0.38 g

I194-14F

<i>n</i> -hexadecane	0.4 g
water	6 g
Brij 97	2.4 g
butanol	1.2 g
S-330	20 mg

I194-75E (homogeneous, not as thick as 75D)

I194-9-D	5 mL
Pemulen TR-1	25 mg

I194-75G (homogeneous, thick gel)

I194-9-D	5 mL
Carbopol 1342	25 mg

We also prepared the following quaternary ammonium salt-based microemulsion (I194-14B). Our efforts to modify this formulation by substituting our polycationic emulsifiers (Mirapol A-15, Merquat 100, and Polycare 133) for the CTAC were unsuccessful, giving two-phase solutions in each of these attempts.

I194-14B

hexadecane	4%
water	60%
cetyltrimethylammonium chloride (CTAC)	18%
1-butanol	18%

We also attempted to thicken and improve the short shelf life of the bleach-containing microemulsions by using clay stabilizers such as the Van Gel O (magnesium aluminum silicate) that are used in commercially available bleach gels. Our preliminary attempts just to add Van Gel O to our microemulsions did not give homogeneous solutions. We then obtained copies of patents describing the preparation of hypochlorite-containing gels.²⁶⁻²⁸ These patents stated that a thickened hypochlorite-containing formulation results from the combination of the following ingredients: (a) colloidal alumina thickener with $< 1\mu$ average particle size; (b) electrolyte/buffer; (c) surfactant system including two surfactant components - one being a fatty acid anionic surfactant and the other being a bleach-stable surfactant or mixed surfactant; (d) bleach; and (e) abrasive with an average particle size of $1-400\mu$. The gel-like consistency is stated to result from the interaction of the clay and anionic surfactants. Therefore, to determine if such a combination (excluding abrasives) could be useful to us, we attempted to prepare selected formulations from the patent as well as similar variations containing lower amounts of hypochlorite. We

obtained a variety of compositions with consistencies ranging from runny lotions to thick pastes, none of which "felt" good on the skin, and therefore, none were considered to be candidate formulations.

2.2.9. Modifications of a FOMBLIN-based Skin Protective Composition

Our second efforts to develop a perfluoroether-containing formulation³⁰ were initiated by a FOMBLIN-containing protective skin protective composition in the literature. After reproducing the reported formulation (FOMBLIN HC/04, petrolatum, sorbitan stearate, and water), we prepared reactive-containing variations of this formulation by adding 2.5% loadings of S-330, our synthesized oxaziridine oxidant, and bleach to this formulation. After an acceptable candidate was obtained from the addition of the S-330, we prepared analogous formulations with higher concentrations of the S-330 and other reactants and organic oxidants. Among these were 2.5% loadings of S-330, SRI-synthesized S-330, our previously reported synthesized oxaziridine oxidant, oxidized ethyl linoleate, bleach, Chloramine T, 1,3-dichloro-5,5-dimethylhydantoin (DCDMH), potassium *p*-toluenethiosulfonate, sodium phosphate, and sodium thiosulfate to this - containing formulation. We obtained acceptable, stable homogenous candidates from the addition of S-330, SRI-synthesized S-330 the oxidized ethyl linoleate, sodium phosphate, Chloramine T, and DCDMH. Other attempted variations included versions containing polyquaterniums (Merquat, UCare JR-30M, etc.) as substantivity enhancers, versions with removed or reduced water content, with higher molecular weight FOMBLINs, with polysiloxanes instead of the FOMBLIN, or with no FOMBLIN. As will be discussed in the evaluation section, these formulation variations have also shown good efficacy against CEES.

I194-36A

Petrolatum	7.5 g
FOMBLIN HC/04	7.5 g
Sorbitan stearate	2.5 g
H ₂ O	22.5 g

Mixing Instructions: The petrolatum, FOMBLIN, and sorbitan stearate were combined and heated to 75 °C with stirring. The water was also heated to 75 °C before it was added to the petrolatum, etc. mixture with stirring followed by cooling to room temperature to give a thick white cream.

I194-36B (I194-36A with 2.5% S-330)

Petrolatum	17.5 g
FOMBLIN HC/04	7.5 g
Sorbitan stearate	2.5 g

S-330	1.325 g
H ₂ O	22.5 g

Mixing Instructions: The petrolatum, FOMBLIN, sorbitan stearate, and S-330 were combined and heated to 75 °C with stirring. The water was also heated to 75 °C before it was added to the petrolatum, etc. mixture with stirring followed by cooling to room temperature to give a thick pale yellow cream containing a small amount of unincorporated water.

I194-36C (I194-36A with 2.5% oxaziridine)

petrolatum [17.5 g], FOMBLIN HC/04 [7.5 g], sorbitan stearate [2.5 g], H₂O [22.5 g], oxaziridine oxidant [1.325 g] → nonhomogeneous mixture

I194-36D (I194-36A with bleach)

petrolatum [17.5 g], FOMBLIN HC/04 [7.5 g], sorbitan stearate [2.5 g], bleach [22.5 g] → nonhomogeneous mixture

I194-36E (I194-36A with 5% S-330)

petrolatum [8.75 g], FOMBLIN HC/04 [3.75 g], sorbitan stearate [1.25 g], S-330 [1.325 g], water [11.25 g] → beige cream

I194-36F (I194-36A with 10% S-330)

petrolatum [8.75 g], FOMBLIN HC/04 [3.75 g], sorbitan stearate [1.25 g], S-330 [2.65 g], water [11.25 g] → beige cream

I194-73A (I194-36A with 2.5% ethyl linoleate)

petrolatum [17.5 g], FOMBLIN HC/04 [7.5 g], sorbitan stearate [2.5 g], ethyl linoleate [1.325 g], H₂O [22.5 g] → white cream

I194-73B (I194-36A with 2.5% oxidized ethyl linoleate)

petrolatum [17.5 g], FOMBLIN HC/04 [7.5 g], sorbitan stearate [2.5 g], oxidized ethyl linoleate [1.325 g], H₂O [22.5 g] → white cream

I194-73C (I194-36A with 2.5% *p*-toluenethiosulfonic acid, potassium salt)

petrolatum [17.5 g], FOMBLIN HC/04 [7.5 g], sorbitan stearate [2.5 g], *p*-toluenethiosulfonic acid potassium salt [1.325 g], H₂O [22.5 g] → two phases

I194-73D (I194-36A with bleach)

petrolatum [17.5 g], FOMBLIN HC/04 [7.5 g], sorbitan stearate [2.5 g], bleach (35% aqueous bleach solution) [17.5 g] – beige cream

I194-73E (I194-36A with phosphate buffer solution)

petrolatum [17.5 g], FOMBLIN HC/04 [7.5 g], sorbitan stearate [2.5 g], 0.1 M sodium phosphate buffer [22.5 g] – off-white cream

I194-73F (I194-36A with 2.5% sodium thiosulfate)

petrolatum [17.5 g], FOMBLIN HC/04 [7.5 g], sorbitan stearate [2.5 g], 2.5% sodium thiosulfate [1.325 g] – white cream

I194-73G2 and G3 (I194-36A with 10% SRI-synthesized S-330)

petrolatum [8.25 g], FOMBLIN HC/04 [3.75 g], sorbitan stearate [1.25 g], SRI-synthesized S-330 [2.8 g] – beige cream

I194-74A (I194-36A with 1.5% Merquat (Cl⁻))

petrolatum [8.75 g], FOMBLIN HC/04 [3.75 g], sorbitan stearate [1.25 g], Merquat (Cl⁻) [1 g], H₂O [11.25 g] – thick white cream

I194-74B (I194-36A with 1% UCare JR-30M quaternized cellulosic emulsifier/thickener)

UCare JR-30M [0.25 g], petrolatum [8.75 g], FOMBLIN HC/04 [3.75 g], sorbitan stearate [1.25 g], H₂O [11.25 g] – thick white cream

I194-74C (I194-74A + 10% S-330 and 1.39% Merquat 100)

Petrolatum [8.75 g], FOMBLIN HC/04 [3.75 g], sorbitan stearate [1.25 g], 1.39% Merquat (Cl⁻) [1 g], H₂O [11.25 g], S-330 [2.8 g, 10% load] – thick beige cream

I194-74D (I194-74B + 10% S-330)

Petrolatum [8.75 g], FOMBLIN HC/04 [3.75 g], sorbitan stearate [1.25 g], H₂O [11.25 g], UCare JR-30M [0.25 g], S-330 [2.8 g] – thick beige cream

I194-80A (I194-36A with no water)

FOMBLIN HC/04 [3.75 g], petrolatum [8.75 g], sorbitan stearate [1.25 g] – off-white cream

I194-80B (I194-80A with Corcat P-600 PEI)

FOMBLIN HC/04 [3.75 g], petrolatum [8.75 g], sorbitan stearate [1.25 g], Corcat P-600 [11.25 g] – thick beige cream

I194-80C (I194-80A with 2.5% SRI-synthesized S-330)

FOMBLIN HC/04 [3.75 g], petrolatum [8.75 g], sorbitan stearate [1.25 g], SRI S-330 [0.66 g] – thick yellow cream

I194-80D (I194-36A with 2.5% Methylphenylsulfoxide as a potential oxidant)

FOMBLIN HC/04 [1.88 g], petrolatum [4.4 g], sorbitan stearate [0.625 g], methylphenylsulfoxide [0.33 g], water [5.63 g] – contained insolubles

I194-80E (I194-80D without water)

FOMBLIN HC/04 [1.88 g], petrolatum [4.4 g], sorbitan stearate [0.625 g], Methylphenylsulfoxide [0.33 g] – contained insoluble components

I194-80F (-80D with 2.5% Resorcinol sulfoxide as a potential oxidant)

FOMBLIN HC/04 [1.88 g], petrolatum [4.4 g], sorbitan stearate [0.625 g], Resorcinol sulfoxide [0.33 g] – contained insoluble components; H₂O [5.63 g] added – contained insoluble components

I194-81A (-80A with the agent-reactive composition Jordi gel/PNP)

FOMBLIN HC/04 [2.67 g], petrolatum [6.24 g], sorbitan stearate [0.89 g], Jordi gel/PNP [0.2 g] – stiff yellow cream

Jordi gel/PNP is an agent reactive composition developed by SRI under Contract DAAA15-92-C0087, "Development of a Basic Soldier Skills Decontaminating Kit".

I194-81B (-80A with 2.5% benzoyl peroxide)

FOMBLIN HC/04 [3.75 g], petrolatum [8.75 g], sorbitan stearate [1.25 g], benzoyl peroxide [0.66 g] – not soluble

I194-81C (-80A with 2.3% Chloramine T)

FOMBLIN HC/04 [6.25 g], petrolatum [14.6 g], sorbitan stearate [2.1 g], Chloramine T [1 g], EtOH [7.5 g], H₂O [11.25 g] – beige cream + some liquid

I194-81D (I194-36A with 10% SRI-synthesized S-330 and no FOMBLIN)

petrolatum [8.75 g], sorbitan stearate [1.25 g], H₂O [11.25 g], SRI S-330 [2.4 g] – pale yellow cream

I194-81E (I194-81D with 1% UCare JR-30M)

petrolatum [8.75 g], sorbitan stearate [1.25 g], SRI S-330 [2.4 g], UCare JR-30M [0.26 g] in H₂O [11.25 g] – pale yellow cream

I194-82A (I194-36A with 2.5% Iron and no water)

Iron powder [0.66 g], petrolatum [8.75 g], FOMBLIN HC/04 [3.75 g], sorbitan stearate [1.25 g] – iron not homogeneous in this mixture

I194-82B (I194-36A with 2.5% Chloramine T and no water)

Chloramine T [0.66 g], petrolatum [8.75 g], FOMBLIN HC/04 [3.75 g], sorbitan stearate [1.25 g] – beige ointment

I194-82C (Replacement of FOMBLIN HC/04 with Polysiloxanes)

petrolatum [8.75 g], Dow 200 (1000 cSt) [1.9 g], Dow 593 [1.9 g], sorbitan stearate [1.25 g], H₂O [11.25 g] – off white cream

I194-82D and D1 (-82C with 10% SRI S-330)

petrolatum [8.75 g], Dow 200 (1000 cSt) [1.9 g], Dow 593 [1.9 g], sorbitan stearate [1.25 g], SRI S-330 [2.4 g], H₂O [11.25 g] – off white cream

I194-82E (I194-36A higher mwt. FOMBLIN HC/25)

petrolatum [4.375 g], FOMBLIN HC/25 [1.875 g], sorbitan stearate [0.625 g], H₂O [5.625 g] – white cream

I194-85A (I194-36A with higher mwt. FOMBLIN and 10% SRI-synthesized S-330)

FOMBLIN HC/R [3.75 g], petrolatum [8.75 g], sorbitan stearate [1.25 g], SRI S-330 [2.8 g], H₂O [11.25 g] → stiff white cream

I194-85B (I194-36A or -85A with higher mwt. FOMBLIN HC/R and no SRI S-330)

FOMBLIN HC/R [3.75 g], petrolatum [8.75 g], sorbitan stearate [1.25 g], H₂O [11.25 g] → stiff cold cream

I194-85C (I194-36A with 12.3 % SRI-330)

FOMBLIN HC/04 [3.75 g], petrolatum [8.75 g], sorbitan stearate [1.25 g], SRI S-330 [3.5 g], H₂O [11.25 g] → stiff yellow cream

I194-85D (I194-36A with 10% S-330)

FOMBLIN HC/R [7.5 g], petrolatum [17.5 g], sorbitan stearate [2.5 g], S-330 [5.6 g], H₂O [22.5 g] → beige cold cream. Solid precipitated out of the mixture after 2 days. Mixture reheated and slowly cooled to give a stiff beige cream that precipitated out again.

I194-85E (I194-36A with 10% S-330)

FOMBLIN HC/R [3.75 g], petrolatum [8.75 g], sorbitan stearate [1.25 g], S-330 [2.8 g], H₂O [11.25 g] → stiff beige cream.

I194-87A (I194-36A with 5% BDO)

3-Bromo-4,4-dimethyl-2-oxazolidinone [1.4 g], petrolatum [8.75 g], FOMBLIN HC/04 [3.75 g], sorbitan stearate [1.25 g], H₂O [11.25 g] → mixture containing insolubles; small amount of chlorine gas released during preparation of mixture.

I194-87B (I194-36A with 10% BDO)

3-Bromo-4,4-dimethyl-2-oxazolidinone [2.8 g], petrolatum [8.75 g], FOMBLIN HC/04 [3.75 g], sorbitan stearate [1.25 g], H₂O [11.25 g] → mixture containing insolubles; Much chlorine gas released during preparation of mixture

I194-87C (I194-36A with 5% DCDMH)

1,3-Dichloro-5,5-dimethylhydantoin [1.4 g], petrolatum [8.75 g], FOMBLIN HC/04 [3.75 g], sorbitan stearate [1.25 g], H₂O [11.25 g] → stiff off-white cream

I194-87D (I194-36A with 10% DCDMH)

1,3-Dichloro-5,5-dimethylhydantoin [2.8 g], petrolatum [8.75 g], FOMBLIN HC/04 [3.75 g], sorbitan stearate [1.25 g], H₂O [11.25 g] – stiff off-white cream

I194-87G (I194-36A with 2.5% DCDMH)

1,3-Dichloro-5,5-dimethylhydantoin [0.53 g], petrolatum [8.75 g], FOMBLIN HC/04 [3.75 g], sorbitan stearate [1.25 g], H₂O [8 g] – stiff off-white cream

I194-89A (I194-87G with no FOMBLIN)

1,3-Dichloro-5,5-dimethylhydantoin [0.47 g], petrolatum [8.75 g], FOMBLIN HC/04 [3.75 g], sorbitan stearate [1.25 g] – stiff off-white cream, Clorox odor

I194-89B (I194-87G with polysiloxanes instead of FOMBLIN)

1,3-Dichloro-5,5-dimethylhydantoin [0.47 g], petrolatum [8.75 g], DOW 200 (1000cSt) [1.9 g], DOW 593 [1.9 g], sorbitan stearate [1.25 g], H₂O [8 g] – stiff off-white cream, Clorox odor

2.2.10. Ringing Gel Microemulsions

We also pursued ringing gel microemulsions in an attempt to determine if the reactivity and efficacy of the free-flowing microemulsions will be impeded in thickened microemulsions. We prepared a mineral oil-containing ringing gel microemulsion based on technical literature from Croda. We also attempted variations containing oxidized ethyl linoleate, potassium phosphate dibasic, chloramine T, and S-330, but we only obtained an acceptable ringing gel microemulsion with the mixture containing the oxidized ethyl linoleate.

I194-42-1 (Clear Gel, Croda)

H ₂ O	54 g
Propylene glycol	12 g
Crodofos N-3 Neutral (DEA Oleth 3-Phosphate)	2 g
Crodofos N-10 Neutral (DEA Oleth 10-Phosphate)	4 g
Volpo 5	4 g
Volpo 3	7 g
Mineral oil	17 g

I194-42-2

I194-42-1 with 2 g ethyl linoleate replacing 2 g mineral oil

I194-42-3

I194-42-1 with 3 g oxidized ethyl linoleate replacing 3 g mineral oil

I194-42-4

I194-42-1 with 1 g potassium phosphate dibasic in 53 g water – 2 phase mixture

I194-42-5

I194-42-1 with 2 g chloramine T, 52 g water – 2 phase mixture

I194-11E

5 g I194-42-1 with 20 mg S-330 – clear gel containing insolubles

We prepared a silicone oil-containing ringing gel microemulsion (I194-71A) based on technical literature from Croda. We also attempted to replace part of the mineral oil with various reactants including: ethyl linoleate – a cloudy gel (I194-42-2); and oxidized ethyl linoleate gave a nonhomogeneous pale yellow gel (I194-42-3). We also attempted to replace: 1 g of the water component with 1 g potassium phosphate dibasic (I194-42-4); and 2 g chloramine T hydrate – cloudy mixture (I194-42-5).

I194-71A (Croda Volatile Silicone Gel, ringing gel microemulsion)

Crodafos N-3 Neutral	7 g
Volpo 5	4 g
Volpo 3	7 g
Dow 345	10 g
Mineral oil	10 g
propylene glycol	10 g
H ₂ O	52 g

Mixing Instructions: Water and propylene glycol were combined and heated to 90-95°C. The Crodafos, Volpo, Dow 345, and mineral oil components were then combined and heated to 90-95°C. The water and propylene glycol mixture was then added to the other phase, resulting in a thick gel that was stirred manually and allowed to cool slowly to room temperature, giving a ringing gel.

2.2.11. Modified Polyethyleneimine-based Burn Ointment

Another composition with promising preliminary evaluation results was a burn ointment based on gelatin and polyethyleneimine.³¹ This ointment was especially attractive since it would contain both proteins and amines with potential reactivity with CEES. Furthermore an approximate reproduction of this formulation, I194-45A, showed efficacy against CEES, and therefore, we attempted to prepare a series of variations by adding different reactants to this composition including: 3% FOMBLIN HC/04; FOMBLIN and petrolatum; FOMBLIN, petrolatum, and glycerine; sodium thiosulfate (1-9%); 1% potassium phosphate dibasic; sodium acetate (3-4%) bleach; 3% S-330; 3% Chloramine T; 3% acetic acid; 3% phosphoric acid; 3% acetone oxime; 3% butanedione monoxime; 3% peracetic acid; and 3% ammonium persulfate. One-phase mixtures were obtained only from the addition of 1% sodium thiosulfate, 1% sodium acetate, 1% potassium phosphate dibasic, 3% acetic acid, 3% phosphoric acid, 3% acetone oxime, 3% butanedione monoxime, 3% peracetic acid, and 3% ammonium persulfate.

I194-45A

Crodyne BY-19	5 g
H ₂ O	30 g
Corcat P-600	15 g

I194-77C

PEI/Gelatin Burn Ointment I194-45A	99%
Sodium thiosulfate	1%

I194-77F (I194-45A PEI/Gelatin Burn Ointment with 1% Sodium acetate → clear, slightly thickened solution)

Part A

Crodyne BY-19	0.5 g
H ₂ O	2.25 g
Sodium acetate	0.05 g

Part B

Corcat P-600	1.5 g
H ₂ O	0.75 g

Mixing Instructions: Part A components were combined and heated to 45°C. Part B components were combined and heated to 45°C. Part B was added to Part A and stirred for 10 minutes and allowed to cool to room temperature.

Other formulations that were made similarly include:

I194-78C (PEI/gelatin Burn Ointment with 1 % Potassium phosphate dibasic)

Corcat P-600 [1.5 g], H₂O [0.75 g], Crodyne BY-19 [0.5 g], H₂O [2.25 g], Potassium phosphate dibasic [0.05 g] → slightly cloudy, slightly thickened solution

I194-79G (-79A PEI/gelatin Burn Ointment with 3 % Acetic acid)

Corcat P-600 [1.5 g], H₂O [0.75 g], Crodyne BY-19 [0.5 g], H₂O [2.25 g], HOAc [0.16 g] → clear gel

I194-79H (-79A PEI/gelatin Burn Ointment with 3 % Phosphoric acid)

Corcat P-600 [1.5 g], H₂O [0.75 g], Crodyne BY-19 [0.5 g], H₂O [2.25 g], phosphoric acid [0.16 g] → clear gel

I194-79I (-79A PEI/gelatin Burn Ointment with 3 % Acetone Oxime)

Corcat P-600 [1.5 g], H₂O [0.75 g], Crodyne BY-19 [0.5 g], H₂O [2.25 g], acetone oxime [0.16 g] → clear runny solution

I194-79J (-79A PEI/gelatin Burn Ointment with 3 % Butanedione monoxime)

Corcat P-600 [1.5 g], H₂O [0.75 g], Crodyne BY-19 [0.5 g], H₂O [2.25 g], butanedione monoxime [0.16 g] → clear, yellow runny solution

I194-79K (-79A PEI/gelatin Burn Ointment with 3 % Peracetic acid)

Corcat P-600 [1.5 g], H₂O [0.75 g], Crodyne BY-19 [0.5 g], H₂O [2.25 g], peracetic acid [0.16 g] → clear, yellow runny solution

I194-79L (-79A PEI/gelatin Burn Ointment with 3 % Ammonium persulfate)

Corcat P-600 [1.5 g], H₂O [0.75 g], Crodyne BY-19 [0.5 g], H₂O [2.25 g], ammonium persulfate [0.16 g] → slightly cloudy gel

2.2.12. Modified Formulations from Commercial Supplier Literature

The following antiperspirant stick formulations were prepared to allow us to gain some experience with these acid-containing formulations.

I194-46A

Stearyl alcohol [12 g], Carbowax PEG 1450 [2 g], PEG Distearate 6000 [3 g], NaOAc [10 g], Volatile silicone 7158 [23 g] – hard, waxy solid

I194-46B

Stearyl alcohol [12 g], Carbowax PEG 1450 [1 g], Carbowax PEG 1000 [1 g], PEG Distearate 6000 [3 g], NaOAc [10 g], Volatile silicone 7158 [23 g] – hard waxy solid

We also prepared the following hand & body lotion based on Dow 580 silicone wax. Variations containing ethyl linoleate and oxidized ethyl linoleate were also prepared.

I194-48A

Water [72.95 g], Carbomer 934 [0.15 g], glycerine [3 g], triethanolamine [0.9 g], propylene glycol [2 g], isopropyl myristate [3 g], mineral oil [5 g], Arlacel 165 [2.5 g], stearic acid [1.5 g], Dow 580 wax [5 g], petrolatum [4 g] – white creamy lotion

I194-48B (I194-48A with oxidized ethyl linoleate)

Water [72.95 g], Carbomer 934 [0.15 g], glycerine [3 g], triethanolamine [0.9 g], propylene glycol [2 g], oxidized ethyl linoleate (I194-38) [3 g], mineral oil [5 g], Arlacel 165 [2.5 g], stearic acid [1.5 g], Dow 580 wax [5 g], petrolatum [4 g] – white creamy lotion

I194-48C (I194-48A with ethyl linoleate)

Water [72.95 g], Carbomer 934 [0.15 g], glycerine [3 g], triethanolamine [0.9 g], propylene glycol [2 g], ethyl linoleate [3 g], mineral oil [5 g], Arlacel 165 [2.5 g], stearic acid [1.5 g], Dow 580 wax [5 g], petrolatum [4 g] – white creamy lotion

We investigated a sunscreen lotion containing a cationic cellulosic polymer; a style/setting Gel based on hydroxypropyl guar and containing Polycare 133 (OH-exchanged); a cetyl dimethicone-based skin moisturizer; a hydrolyzed silk & elastin-based facial firming gel; a polysiloxane-based clear sunscreen oil; a polysiloxane-based clear styling gel; a polysiloxane-based conditioning setting gel. In our preliminary investigations into these formulations on, all gave homogeneous gels, creams, lotions, etc. that could have been appropriate vehicles for our reactive components. Our attempt to prepare a cold cream based on Dow Q2-5200 and variations of this cold cream containing oxidized ethyl linoleate were unsuccessful and consistently gave two phase solutions. Two

other formulations were only preliminarily investigated: a protective hand cream by DOW; and a modification of a Chloramine T-containing protective ointment from the literature in which S-330 was used instead of Chloramine T.³²

I194-51-A (Sunscreen lotion)

UCare Polymer JR-30M [1 g], ethanol [48 g], water [48 g]

- thick colorless gel with lots of bubbles

I194-51-B (Sunscreen lotion)

[I194-51-A, 9.7 g], PABA [0.3 g]

- thick beige gel with lots of bubbles

I194-57-A (Style/Setting Gel, Rhone-Poulenc)

N-Hance HP 405 (hydroxypropyl guar) [2 g], H₂O [90 g], Glycerine [3 g], Polycare 133 [2 g], Volpo 20 [2 g], Abil B 8852 (dimethicone copolyol) [1 g] - cloudy gel with clear liquid on top

I194-58 (Moisturizer containing cetyl dimethicone, DOW)

H₂O [81 g], Carbomer 940 [1 g], glycerine [3 g], Dow 2502 [10 g], Stearic acid [3 g], Arlacel 165 [1.5 g], cetyl alcohol [0.5 g], triethanolamine [0.4 g] - white cream with a small amount of clear liquid on top than 57-A

I194-59 (Silk & Elastin Facial Firming Gel)

Propylene glycol [5 g], H₂O [51.6 g], Crolastin [0.5 g], Carbomer 940 [40 g, 2% soln], disodium EDTA [0.2 g], Crosilk 10,000 [2.5 g], triethanolamine [0.5 g] - clear brownish-yellow gel

I194-62 (Clear Sunscreen Oil, DOW)

DOW 344 [40 g], Dow 1401 [20 g], Dow 345 [16 g], diisopropyl adipate [10 g], Finsolv TN [10 g] - clear colorless solution

I194-63 (Clear Styling Gel, DOW)

Carbomer 934 [0.5 g], H₂O [90.3 g], triethanolamine [0.7 g], Emulphor EL-719 [1 g], Dow 1401 [0.5 g], PVP/VA E-735 [6 g], EtOH [1 g] → colorless gel; to be retried with organic oxidants

I194-64 (Conditioning Setting Gel)

Carbomer 940 [1 g], H₂O [86.5 g], Dowicil 200 [0.1 g], NaOH [9.4 g, 20% soln], Gaffix VC-713 [10 g], Dow 3225C [0.5 g], Dow 7224 [0.5 g] → colorless slightly cloudy gel

I194-70B (Modified Chloramide T Protective Ointment)

60% glyceryl triacetate, 25% S-330, 25% magnesium stearate → cream-like lotion

I194-67A (Polysiloxane-based Protective Hand Cream, DOW)

Dow 593 [2 g], Dow 200 (100 cST) [2 g], stearic acid [6 g], cetyl alcohol [1.5 g], mineral oil [2.2 g], isopropyl lanolate [0.5 g], H₂O [82.3 g], triethanolamine [1.5 g] → white cold cream

2.3. Reactivity and Barrier Evaluations

2.3.1. Overview

Under the research program, we experimentally determined the potential protective effectiveness of candidate formulations towards sulfur mustard by performing evaluations of the reactivity and the barrier properties of the formulations towards CEES, which is the compound that we used as a simulant for sulfur mustard. The main objective of the reactivity and barrier evaluations was to quantify the protection against CEES (or mustard) for candidate formulations and to provide feedback into the chemistry and formulation of an effective protective lotion or cream. This section of the Final Report describes and discusses the methods and results of the reactivity tests and barrier tests that we conducted during the project.

The experimental results obtained during the first year of the research program were documented in our revised Midterm Report dated July 11, 1995. The results of the reactivity and barrier tests that we reported in the Midterm Report are reported again in this comprehensive Final Report for comparison with the test results obtained since the Midterm Report. The following paragraphs summarize our efforts on the reactivity and barrier evaluations during the first year of the contract.

In our First Quarterly Report (dated March 24, 1994) we described the assembly of the experimental apparatus and the performance of some preliminary studies to establish test methods that would provide meaningful reactivity and barrier data for formulations with and without active ingredients. The preliminary studies were necessary at the beginning of the project to determine the best experimental apparatus and procedures to be used for the evaluations. Based on the preliminary studies, we made some modifications to the experimental methods for the reactivity tests and the barrier tests. The developed test methods are fully described in the following sections of this report.

We conducted additional reactivity tests and barrier tests in the second quarter of the project to evaluate a series of candidate formulations (and appropriate controls) that were prepared by the Organic Chemistry Group. We also made a few additional improvements to the experimental methods as needed.

During the third and fourth quarters of the project, we performed a limited number of reactivity and barrier evaluations because emphasis was placed primarily on the synthesis and formulation efforts. The reactivity tests were performed on solutions containing reactive chemical species of potential interest to our development of a protective lotion or cream. The barrier tests that we conducted during this period were mostly replicate tests to explain some earlier anomalous test results, but several tests were performed to determine barrier properties for some candidate formulation components and to provide data for comparison with the results of the reactivity tests with the same formulations. A few tests were also conducted to investigate some inconsistencies in the barrier test results.

The results of the reactivity tests conducted during the third and fourth quarters were previously reported in the Fourth Quarterly report and in the Midterm Report, but the results of the limited barrier tests were not reported because of apparent but unexplainable problems evidenced by the test data. That is, the data were considered to be unreliable. Because of the problems with the test data, we began to check the permeation test system for any problems with the various components, including the new Minicams permeation test system (CMS Research Corporation, Birmingham, AL) that we had procured at the beginning of the contract. No hardware problems that could account for the poor data were identified.

We also manually checked the data acquisition and computer calculations performed by the new Minicams permeation system. This was done to verify that the Minicams system produced valid permeation data. No problems with the Minicams software were found at that time, but we discovered later in the research program that the Minicams data-reduction software performed calculations differently under certain conditions (see below). This software behavior significantly affected the calculated permeation data in some cases and generated strange artifacts in the permeation rate curves. We later determined that we could "correct" the data for this previously unknown

software behavior, or more accurately, we determined that we could recalculate the permeation rate data and generate permeation rate curves that were more realistic and reliable for interpretation. Therefore, this final report includes the corrected results for a number of barrier tests that were conducted during the third and fourth quarters. It is important to note, however, that during the course of the research program, we did experience other problems with the permeation test system and test procedures that affected the permeation results, but many of these problems were caused by normal "wear-and-tear" on the test system or by unforeseen experimental problems caused by the test formulations themselves. The presentation of the test results in this report includes discussion of any other problems that we encountered and how they affected the test data. Overall, the Minicams-based permeation test system performed very well during the research program and provided reliable and useful data to support the formulation development efforts.

During the fifth reporting period, we performed additional reactivity tests with CEES to support the synthesis and formulation efforts. No barrier tests were performed during the reporting period. The reactivity tests were performed on solutions containing reactive chemical species of potential interest to our development of a protective lotion or cream. The solutions that we tested included phosphate buffers at different pH values, various solutions containing PEG 550 with KOH and other actives, other potentially active compounds, and several substituted Merquats. The most interesting solutions or formulations tested were PEG methyl-ether formulations containing KOH and butanedione oxime or acetone oxime, which exhibited marked reactivity towards CEES. Merquat hydroxide was also significantly reactive with CEES. Reactivity tests with different amounts of active were also conducted, but some of the test data were anomalous, and therefore, some of these tests were subsequently repeated.

In the sixth quarter of the project, we performed additional CEES reactivity tests to support the synthesis and formulation efforts. We also conducted reactivity tests and a limited number of barrier tests with a FOMBLIN cream and with the same FOMBLIN cream containing an active component. These particular FOMBLIN samples were supplied to us for evaluation by USAMRICD for evaluation. Based on the results of the barrier tests with the FOMBLIN samples (see Section 2.3.3.3.2) and on a recommendation from USAMRICD, we modified our permeation test procedure used for the barrier evaluations so that the challenge to each test sample would be saturated CEES vapor rather than liquid CEES droplets. We then conducted a series of tests to evaluate and characterize the effects of switching to a vapor challenge in the barrier tests and found this method of agent challenge to be advantageous for the study. We then conducted additional tests of the FOMBLIN samples using the vapor challenge. The reactivity and permeation data obtained during the sixth reporting period were very valuable in further focusing our development of a protective lotion or cream.

During the seventh reporting period, we performed additional reactivity tests and barrier tests with CEES to support the synthesis and formulation efforts. As described above, we had modified our permeation test procedure used for the barrier evaluations so that the challenge to each test sample would be saturated CEES vapor rather than liquid CEES droplets. We had also conducted a series of tests to evaluate and characterize the effects of switching to a vapor challenge in the barrier tests and had consequently decided to switch mostly to vapor challenges. The substrate used in the first vapor-challenge tests was neoprene. Earlier in the research program, we had attempted to use silicone rubber as the substrate for the barrier tests, but with the liquid-droplet challenge, the permeation rate was too high for the detection system. Based on the results of the vapor-challenge tests conducted during the sixth reporting period with neoprene, we decided to re-evaluate the use of silicone rubber as the substrate material and determined that we could use silicone instead of neoprene for the vapor-challenge tests. Silicone was more desirable than neoprene because it was more permeable. Section 2.3.3.3.2 describes the results of the vapor-challenge barrier tests that we conducted with silicone rubber as the substrate material in the seventh quarter and includes a discussion of the use of silicone as the substrate.

In the eighth quarter, we did not conduct any reactivity tests, but we attempted to continue the barrier testing of candidate formulations. However, we experienced a series of unanticipated problems with the permeation test system. The problems created a number of delays and produced test results that were unacceptable. Near the end of the reporting period, we were finally able to correct a number of different instrumental problems that were difficult to isolate before they could be remedied. Replacement of the stream-selection valve in the permeation test system appeared to have corrected the major problem with the test system. We then began collecting more reliable barrier test results, which are described in Section 2.3.3.3.2. Additional details of the instrumental problems that we experienced are described in Section 2.3.3.3.2.

We performed additional barrier tests with CEES during the ninth reporting period to support the synthesis and formulation efforts. No reactivity tests were conducted during the quarter.

Because of the technical problems described above with the Minicams-based permeation test system and because of the resulting delays in the barrier testing, we assembled a second permeation system to increase the rate of testing. The second system was an older, ACAMS-based system that was not computer controlled with automated data collection and analysis. Limited side-by-side testing with the Minicams system showed that it provided permeation data that were analogous to those produced by the Minicams system (as it should in the absence of systematic testing errors), and therefore, we connected a computer to the ACAMS via an analog-to-digital interface to allow collection of data from the older permeation test system. We also installed commercial data-acquisition software and programmed it to collect and store the permeation data in a form

that could be imported directly into a spreadsheet program. Spreadsheet macros were written to process the data and provide output in a format similar to that produced by the Minicams system. The older permeation system was then used as a second permeation system for the barrier tests.

During the tenth and last quarter of the research project, we conducted additional barrier tests on the most promising candidate formulations and on a few other new possible candidates. Some of these tests were conducted as replicates of earlier tests or to answer specific questions. Also during the last reporting period, we continued to have sporadic problems with the permeation test system. Strange "spikes" in the permeation rate curves, similar to (but not the same as) those caused by the worn stream-selection valve, were obtained for some tests. Although previously we had manually checked all calculations made by the Minicams software, we checked the software calculations again and discovered a potential problem that was magnified by the switch from neoprene to silicone as the substrate. We found that if the Minicams response was above (even slightly) the highest calibration point or below the lowest calibration point in the calibration curve, the software no longer used the calibration curve to calculate the amount of CEES detected. Instead, the software used a one-point calibration to calculate the amount of CEES. This method of calculating the amount of CEES as compared to using the calibration curve often gave significantly different results. This software operation was not documented in the manuals and literature supplied with the Minicams, but it was confirmed by CMS Corporation by telephone. CMS provided good justification for the calibration routine, but we found that it unrealistically affected many of our permeation rate curves. Therefore, we decided to correct the permeation data and rate curves using the fitted calibration curves.

Of course, it is always best when the range of the calibration curve covers the range of the detected amounts, and we were already using a calibration amount near the upper detection limit for the Minicams system. After discovering the software anomaly, we used the calculated calibration curves to correct all of the permeation rate curves where data points fell above the calibration range. These corrections were made as needed for all permeation data collected since the Midterm report. (The Midterm report included only tests using neoprene, and thus, the software exception was not as significant.) In most cases, these corrections merely removed the "spikes" from the curves, but in some cases, the curves changed in shape when the curves peaked above the highest calibration point. Because of the true shape of some curves, these curves actually did not exhibit any problems with the calculated amounts. Also, there was no obvious indication in the computer-generated output that we were significantly outside of the calibration range. The biggest indication of the problem was when the permeation data fluctuated around the highest calibration point and significant spikes resulted, which we initially attributed to recurring problems with the stream-selection valve. (Replacement of the stream-selection valve had significantly improved the test results but had not solved all of the problems; therefore, we looked for other possible explanations and found the software anomaly.)

To limit the effect of the software exception, we increased the range of our calibration data. We also increased the number of calibration points and cross checked the calibration of the four lines in the test system. These steps improved the calibration curves and limited the software problem from occurring. Still, we had to check, and correct as needed, all of the permeation data generated since switching from neoprene to silicone as the substrate material. The effort produced more reasonable permeation rate curves and also made some previously poor results meaningful. Overall, however, general trends in the barrier test data and the conclusions that we had previously made were not significantly affected. Specific differences are discussed in Section 2.3.3.3.2.

Table 2 lists the formulations (or solutions or suspensions) that we tested under the entire research project. Some of the formulations were tested to establish our test methods (apparatus and procedures), but most of the formulations were tested as part of the research-and-development effort. Table 2 lists for each formulation the identification number assigned by the Organic Chemistry Group, the identification number assigned by the Physical Chemistry Group, and a description of the formulation.

2.3.2. Reactivity Tests

2.3.2.1. Reactivity-Test Procedure

The experimental approach that we used to assess the relative reactivity of candidate formulations with CEES involved spiking an aliquot of CEES into each formulation followed by subsequent addition of a solvent to extract the residual CEES. The spike was physically mixed into the formulation by various methods. The extraction solvent was analyzed by a solid-sorbent-preconcentration/gas-chromatographic method. In this analysis method, an aliquot of the solution to be analyzed (*i.e.*, the extraction solvent) was spiked by syringe through an NO_x filter (triethanolamine on Chromosorb P) onto a solid-sorbent preconcentration tube (a glass tube packed with a solid sorbent) while air was pulled into and through the tube by a pump. The solvent mostly evaporated and passed through the sorbent bed, but the CEES was adsorbed by the sorbent. The CEES in the sorbent tube was subsequently quantified by thermally desorbing the tube in a specially modified injection port on the gas chromatograph (GC). Sorbent tubes were thermally desorbed ("blanked") and checked prior to use. A Hewlett Packard Model 5890A gas chromatograph equipped with a flame-photometric detector (FPD) and a sulfur-specific optical filter was used. The GC was optimized for CEES response and was calibrated daily as needed. We chose to use the solid-sorbent-preconcentration technique for increased sensitivity and to protect the GC from nonvolatile contaminants that may have extracted from the formulations.

The test procedure used for most of the reactivity tests conducted with neat CEES was as follows. 0.25 g of each test sample (*i.e.*, formulation) was weighed into a 1-dram septum vial and was capped. CEES (1 μ L) was spiked into the vial through the septum.

The sample/CEES mixture was stirred using one of several methods (see the next section). The vial and its contents were allowed to sit for the desired reaction time (typically 10 minutes). After the reaction period, 2 mL of hexane was added. The mixture was stirred for 30 sec. The vial was shaken for 15 sec every 5 min for 20 min (four times). The solvent layers (if any) were then allowed to separate. A 5- μ L aliquot of the hexane layer was added to 2 mL of hexane in another septum vial to dilute the CEES concentration before analysis. The dilution vial was shaken to ensure good mixing. A 5- μ L spike of the dilution solution was then spiked onto a solid-sorbent tube for analysis. From the analysis, the percent recovery was calculated.

For the controls, which were prepared and analyzed on each day of testing, 2 mL hexane was used as the test solution, which was "worked up" in an analogous manner to the test solutions. That is, the vial was vortex mixed, and 5 μ L was spiked into another sealed 1-dram vial with 2 mL hexane. This final hexane solution was analyzed in the same manner as the diluted extracts from the reaction solutions.

When we started conducting reactivity tests with NaOH solutions (starting with Test Set H874-78 in Appendix A), we further modified our test procedure to improve the accuracy and precision of the test method. The overall procedure was the same so that all of the reactivity data could still be compared, but we changed from injecting the CEES into the formulation or solution to injecting the CEES onto the inside wall of the vial containing the reaction mixture. We also modified the mixing times, but the relative amounts of formulation and CEES remained the same, and the same reaction time (10 min) was used.

While performing the reactivity tests of solutions listed in Table 2, we experienced several analytical complications that all produced "messy" chromatograms. We typically used the NO_x filters when spiking the solid sorbent tubes to prevent degradation of the CEES, but we also found that we needed to start filtering the air through charcoal filters because of contaminants in the laboratory air. We also found that the CEES standards were unstable, and therefore we started storing them in a refrigerator. Finally, the extracts from the test solutions also had contaminants. All of these contamination problems complicated the CEES analysis and contaminated the GC column, but we modified our analysis procedures to minimize these problems.

2.3.2.2. Results of Reactivity Tests

2.3.2.2.1 Midterm Results

The results of the reactivity tests as reported in the Midterm Report for this contract are given in Table A-1 in Appendix A. Table A-1 lists for each test the Test No., the solution, a description of the solution, the reaction time, the percent recovery, and the average recovery for each solution. A "-" in the table indicates that the sample could not

be analyzed for some reason. A "0" in the table indicates that no residual CEES was detected. The test data in Table A-1 are given in chronological order with control data preceding the corresponding tests conducted on the same day.

Table A-1 presents the principal results of the reactivity tests of several formulations with neat CEES. We also tested water (Milli-Q water) for comparison, and we ran numerous different controls to evaluate further our experimental method. We typically ran two types of control samples in which no formulation was used. In one set of controls, we spiked the neat CEES directly into 2 mL of hexane. In the other set of controls, we spiked the neat CEES directly onto the bottom of the glass vials. The vials were stirred and extracted in the same way as the formulations. Both sets of controls were diluted and analyzed like the formulations. The recovery in percent for each reactivity test is reported in Table A-1 along with the average recovery for each formulation or control tested on a given day. The recovery was calculated based on the measured concentration of the dilution solution, the dilution and sampling steps, and the mass of the starting spike of neat CEES.

The results in Table A-1 are given in the order tested so that controls are appropriately grouped with the formulations evaluated. Test Set H874-36 includes tests of the polyacrylic-acid formulations (H874-8-3 and H874-8-5) and the shave cream (H874-8-7). These test results show that CEES is reacted by these formulations. Also included in Test Set H874-36 are replicate tests with water in which we were able to recover an average of 4% of the CEES. The unstirred control (direct spike into hexane) and the stirred control showed that evaporation of CEES was probably important for the stirred control.

Because it was difficult to stir the CEES into some of the formulations, and because there was a potential to lose CEES by evaporation during stirring, we decided to evaluate different methods of stirring. Test Set H874-40 was designed to evaluate three different ways of stirring the formulations: (1) stirring the sample/CEES mixture by hand with a glass stirring rod (the method that we used initially); (2) stirring by an ultrasonic bath; and (3) stirring by inserting a short glass rod (3 cm long) into the formulation followed by mixing with a vortex mixer. These stirring methods were evaluated for controls, one of the polyacrylic formulations (H874-8-5), and the shave cream. The short glass rod plus the vortex mixer seemed to work as well as the hand stirring method but gave better recovery results from the empty vial controls. This appears to be because the cap did not have to be removed for mixing. We decided that we would use the short glass rod along with a vortex mixer for the rest of the tests.

The next set of reactivity tests, Test Set H874-45, was conducted to evaluate petrolatum as a control formulation and to determine extraction efficiencies. We were concerned that a low recovery may be an indication of a poor extraction rather than reaction. We determined that the recovery of petrolatum was similar to the recovery from

hexane. In an attempt to evaluate the extraction efficiency, we added CEES to water, analyzed the water directly, extracted CEES from the water using hexane, analyzed the hexane extract, and also analyzed the water after extraction by hexane. Unfortunately, the hydrolysis was too complete and all three analyses produced essentially the same very low recovery.

After Test Set H874-45, we observed that the recoveries for our CEES-in-hexane controls had been steadily dropping. We postulated that the neat CEES was slowly hydrolyzing, and therefore, we obtained a new bottle of CEES that gave us higher recoveries again as shown in Tests H874-49-1 through -3 and in Tests H874-51-1 through -3.

Test Set H874-51 was a set of tests to investigate whether the extracted CEES would be stable in the hexane. (That is, would hydrolysis be quenched by the extraction into hexane?) The results for these tests indicated that the CEES would be stable in the hexane after extraction.

The next two sets of tests given in Table A-1 (Test Sets H874-55 and H874-57) were conducted to assess the relative reactivity of candidate formulations that were indicated to have some reactivity towards CEES in the barrier tests. The α,β,γ -cyclodextrin, the 28.6% (w/w) hydroxypropyl β -cyclodextrin in Carbopol-940-thickened gel, the 20% (w/w) Merquat 100 plus thioglycolate, and the 5.4% (w/w) Merquat 100 plus histidine all showed similar and modest reactivities towards CEES when compared to the corresponding controls.

In several of the water tests, we also analyzed the water before and after extraction and the hexane extract for ethyl 2-hydroxyethyl sulfide (EHES)—the primary hydrolysis product of CEES. While some EHES was detected in some samples (water and hexane), it did not appear to be a major compound in the samples. Moreover, the analysis was only semi-quantitative because of the low gas-chromatographic response for EHES (with our setup) and because of overlapping chromatographic peaks. We also analyzed both layers of two sets of samples immediately after extraction and again one hour after extraction in an attempt to determine if the EHES concentration increased with time. We did not measure any meaningful data on EHES versus time and concluded that the analysis of EHES would not provide useful information.

Starting with Test Set H874-78-1, we began to evaluate the reactivity of hydroxide and other nucleophiles to provide information for the formulation work. The results of these reactivity tests show that all of the solutions with NaOH effectively reacted with the CEES, as expected. The solutions with 3 N NaOH showed less reactivity than the 0.3 N NaOH, which may indicate that the solubility or dissolution rate of CEES may have been affected by the NaOH concentration. The effect, if any, of the t-butyl ammonium hydroxide in the NaOH solutions was not readily apparent. The solution of t-butyl

ammonium hydroxide itself showed about the same reactivity as the 3 N NaOH. The 2% solution of KOH with 500 poly(ethylene glycol) methyl ether showed moderate reactivity towards CEES. The two 5% Merquat formulations tested (with and without HOAc) exhibited the same significant reactivity.

To summarize the reactivity tests conducted during the first year of the contract, we determined that aqueous-based formulations can be reactive, but the efficiency of mixing is very important. We also determined that for some formulations, we needed to increase the reaction time to evaluate a given formulation, while for other formulations, we needed to decrease the reaction time to make an evaluation. Of course, comparisons of formulations with similar reactivities must be made based on tests using the same reaction time. We also decided that because of the many analysis steps involved in the reactivity tests, we would limit reactivity testing to candidate formulations that exhibited significant reactivity in the barrier tests unless there was a specific reason to perform a reactivity test. That is, we decided to use the barrier tests for reactivity screening.

2.3.2.2.2 Post-Midterm Results

The results of the reactivity tests conducted after submitting the Midterm Report are given in Table D-1 in Appendix D, which lists for each test the Test No., the formulation identification numbers used by the Organic Chemistry Group and the Physical Chemistry Group, a description of the formulation, the reaction time, and the percent recovery of CEES after reaction. The average CEES recovery for each set of replicate tests is also given in Table D-1. A "--" for CEES recovery in the table indicates that the sample could not be analyzed because of an experimental problem. A "0" in the table indicates that no residual CEES was detected. The test data in Table D-1 are given in chronological order with control data preceding the corresponding tests conducted on the same day. A number of the formulations listed in Table ? were not tested because similar formulations showed low reactivity or because the barrier tests provided sufficient information.

As previously mentioned, the reactivity tests reported in Table D-1 were performed on solutions or formulations containing reactive chemical species of potential interest to our development of a protective lotion or cream. The solutions tested included phosphate buffers at different pH values, mixtures of PEG and KOH and with various actives, substituted Merquats, the FOMBLIN samples supplied by the U.S. Army, a proprietary chlorinating agent, fine metal dusts suspended in phosphate buffer (pH 5), FOMBLIN gel base, 5% Mirapol (OH) with 3% methyl cellulose, two Goldschmidt solutions with quat(OH), and other potentially active formulations or components. Some of the most interesting solutions or formulations tested were the PEG formulations containing KOH and various actives, some of which exhibited marked reactivity towards CEES. The Merquats, Mirapol, and Polycare were also significantly reactive with CEES. Reactivity tests with different amounts of active were also conducted, but the data from a few tests

were initially anomalous, and therefore, the corresponding tests were repeated. The results of all of the reactivity tests are described and discussed in more detail in the following paragraphs.

The reactivity tests with the phosphate buffers were conducted to investigate simply the pH dependence of the hydrolysis of CEES. As shown by the test results, CEES was effectively destroyed during the 10-min reaction time at all pH values tested. The least reaction was observed near neutral pH. Because the results were similar for the different pH values and because kinetic studies (reaction versus time) would be required to further investigate the effect of pH on the CEES hydrolysis, we decided not to continue the study of the phosphate buffers. Still, the test data indicated that phosphate could be an important component in a formulation.

The next formulations that we studied were the PEG-ME 550 formulations containing KOH and butanedione monoxime, acetone oxime, or phenol (see Test Series H874-94 and H874-96) at a concentration of 1.25 M (0.0009 moles of active per gram of formulation). These formulations were first prepared to be the same as those prepared and evaluated by Purdon (?). As shown in Table D-1, the reactivities of these formulations were low and were also lower than the reactivities reported by Purdon. Similar formulations using a mixture of PEG 400 and PEG 600 were also tested (see Test Series H874-104 and H874-106), and the test results were similar to the earlier results. We then re-prepared the PEG-ME formulations with a lower concentration of the actives and the same concentration of KOH (see Test Series H874-108 and H874-110), but to our surprise, the reactivity went up. For comparison, we also tested the reactivity of PEG-ME 550 (see Test Series H874-102) and PEG (400+600) (see Test Series H874-118) without any active component or KOH; both of these PEGs showed low reactivity. Because of the strange results, we repeated the reactivity tests of the butanedione monoxime and acetone oxime with KOH and PEG-ME 550 using various concentrations of the active (including no active) and KOH (see Test Series H874-122, H874-126, H874-128, and H874-138). The results were reproducible and indicated that the reactivity was high when the KOH concentration was high and the concentration of the active component was low or zero; that is, the active component actually inhibited the reaction of the CEES.

As reported in Table D-1, we also evaluated several other potential reactive components in PEG formulations and in neat form, and a few candidates were identified. Also reported in Table D-1 are the results of reactivity tests with the FOMBLIN samples provided by the U.S. Army. Neither the base FOMBLIN nor the FOMBLIN plus the active component (see Test Series H874-120) exhibited significant reactivity, although the FOMBLIN plus the active was slightly more reactive. The FOMBLIN HC/04 in a gel base showed a low recovery of CEES (Test Series H874-128), but it was unclear whether the low recovery was indicative of reaction or a physical recovery problem.

The most reactive formulations (other than basic solutions) that we investigated included the Merquat and Polycare. Test Series H874-110, H874-116, and H874-136 support these findings. Test Series H874-134 shows that Mirapol formulations are also quite reactive. These results were considered in our formulation efforts.

A sample of a proprietary chlorinating agent was obtained and evaluated as an example of a different class of lipophilic oxidants. The results of the reactivity tests in Table D-1 show that chlorination in water with this type of oxidizing agent is a viable reaction method. Unfortunately, additional samples of this agent were not available.

We evaluated the reactive potential of metal particles in phosphate buffer at pH 5. As shown in Table D-1, the solution containing copper was very reactive, but the zinc and iron suspensions were less reactive. Unfortunately, the reactivity of the copper suspension was not discernable from the reactivity of pH-5 phosphate buffer with no metal added (see above).

Both the FOMBLIN gel base and the 5% Mirapol (OH) with added methyl cellulose were very reactive with CEES. The two Goldschmidt formulations were reactive, but not as reactive as other formulations that we investigated.

2.3.2.2.3 Summary of Reactivity Test Results

Overall, the reactivity tests provided indications of candidate formulations and candidate formulation components that could be used in the formulation effort. These data showed that basic formulations could effectively decontaminate CEES (and presumably HD) by what appeared to be hydrolysis reactions. Some of the oxidizing agents also showed promise. Unfortunately, there were no strong indications in the data of catalytic reactions; that is, the reactions were all likely stoichiometric. However, the reactivity test data were very useful in helping to guide the development effort.

2.3.3. Barrier Tests

Under this research program, we conducted tests to assess the barrier properties of candidate formulations towards CEES. The barrier tests were permeation tests in which formulations were spread onto an appropriate supportive and permeable substrate and were then challenged by neat liquid CEES or by saturated CEES vapor. After the formulation was challenged, the permeation of CEES through the formulation and the substrate was measured as a function of time. In our First Quarterly Report for the contract, we described our initial experimental method for conducting barrier tests, and we also described the results of a number of preliminary barrier tests. During the second quarterly reporting period, we made some minor improvements to the test method (*i.e.*, apparatus and procedures) that were based on the results of the preliminary tests. We then proceeded with the evaluation of candidate formulations. Other minor improvements in

the test procedures were made over the course of the contract as noted below. The main purpose of the barrier tests was to determine the physical protection afforded by the candidate formulations, but the tests also provided limited information about the reactivity of the formulation towards CEES. In this section of the Final Report, we describe the experimental permeation method and the results of the principal barrier tests that we conducted.

2.3.3.1. Permeation-Test Apparatus

The principal permeation-test apparatus consisted of a multichamber stainless-steel test cell; a temperature-control box for the test cell; a Minicams permeation system (CMS Research Corporation, Birmingham, AL) consisting of a gas-stream-selection valve housed in a valve oven and a Minicams; and a flow-control system. Figure 1 shows a schematic diagram of the permeation test system. These components are described in more detail below. Later in the research program, we also used an older generation permeation test system to check the test results against those obtained using the Minicams-based permeation test system. The older system was based on the use of an ACAMS (Automatic Continuous Air Monitoring System) to sample and analyze the air streams containing CEES vapor. Both systems are described below.

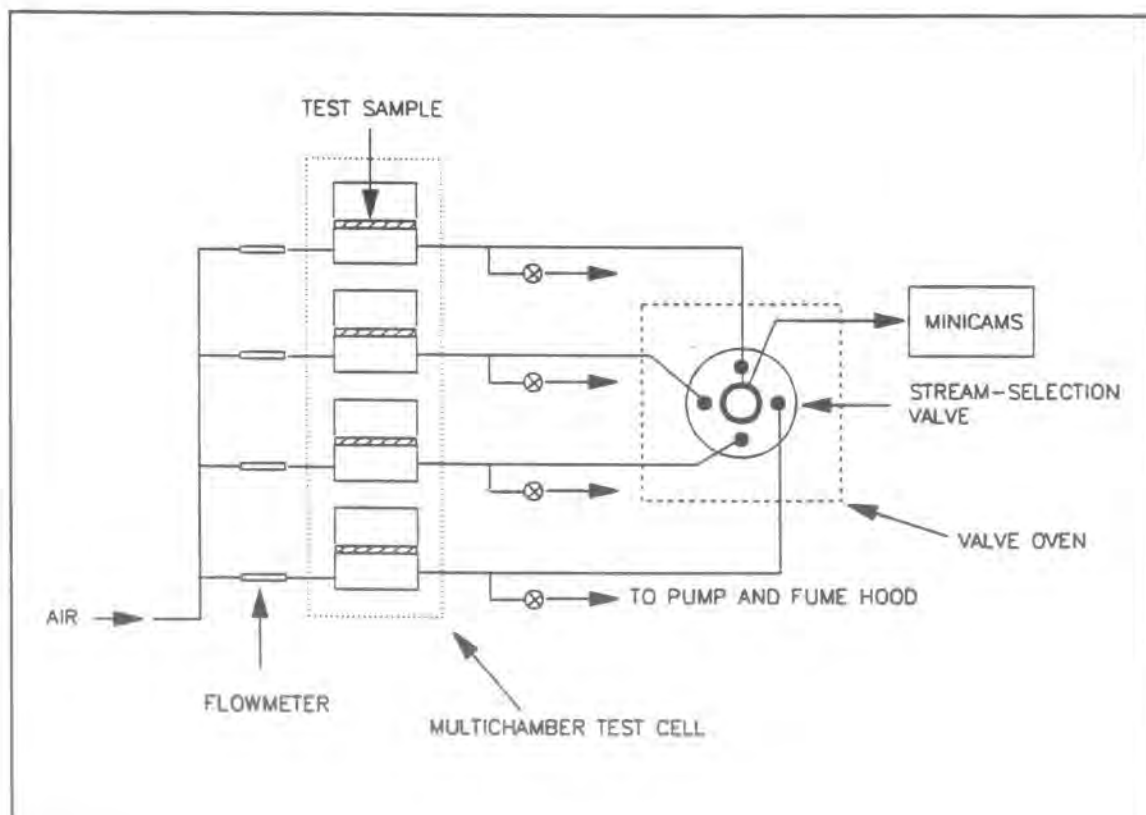


Figure 1 Schematic diagram of the permeation test system.

Test cell

The test cell was constructed of stainless steel and consisted of an array of four individual chambers. Four test samples were sealed in the four test-cell chambers. The test samples that we tested under the program consisted of an elastomer substrate (neoprene or silicone) covered with the test formulation (see below). The configuration of each test sample in the test cell divided each test-cell chamber into an upper compartment and a lower compartment as shown in Figure 2. The exposed upper surface area of each sample in the test cell was 10 cm². In liquid-droplet-challenge tests, droplets of CEES were placed on the upper surface of the test samples. In vapor-challenge tests, a single CEES droplet was placed in a recession in the top of a three-legged Teflon droplet stand that could be placed on the top of each test sample. The upper half of each test-cell chamber was sealed immediately after contamination to limit evaporation of the CEES droplets. (The test cells are designed so that air can optionally be flowed through the upper chambers to simulate the evaporation of CW-agent or agent-simulant drops in open air.) When the Teflon droplet stand was used, each test sample was only exposed to CEES vapor, which was presumed to reach saturation concentration in the sealed upper test-cell compartment. Air was passed through the bottom half of each chamber at a flow rate of 1 L/min to sweep any CEES that permeated through the test sample into the Minicams (or ACAMS) sampling-and-analysis system. The amount of CEES permeating the test sample versus time was measured.

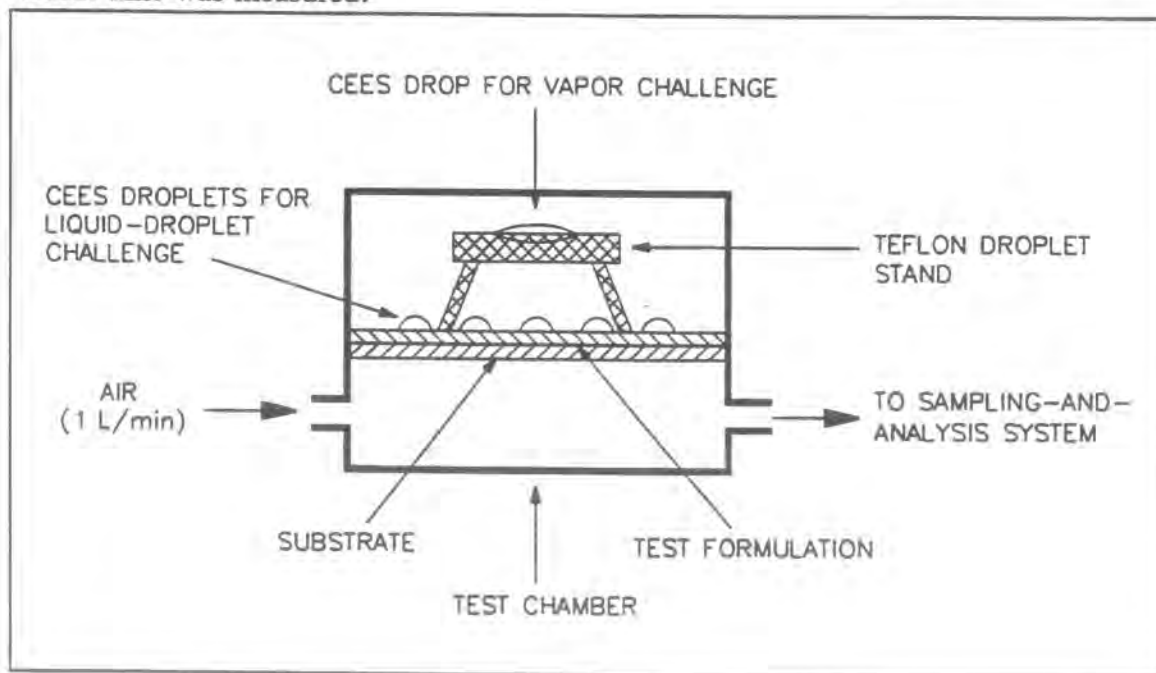


Figure 2 Configuration of the test sample in one chamber of the permeation test cell.

Temperature-control box

The temperature of the test cell was controlled with a modular heating-and-cooling unit previously designed and assembled at Southern Research Institute. The unit consisted of two aluminum plates, three cartridge heaters, an Omega temperature controller, and a pair of Melcor thermoelectric cooling modules. The thermoelectric cooling modules were sandwiched between the two aluminum plates, and the cartridge heaters were inserted into wells drilled in the upper aluminum plate. The test cell was placed on top of the upper aluminum plate, and both the test cell and the temperature-control unit were mounted in an insulated, rectangular box.

The thermoelectric cooling modules were supplied with a constant 1-amp current from an external constant-current source to continually cool the upper aluminum plate. The cooling of the upper plate was offset by heating from the cartridge heaters, which were proportionally controlled with an Omega temperature controller to maintain the temperature of the test cell. The tests were conducted at 77°F.

Gas-stream-selection valve

Any CEES that permeated through the material was entrained in the stream of air flowing through the lower test-cell chamber and was swept out of the test cell. A constant fraction of the air stream that exited from each lower chamber was periodically and automatically directed through a sixteen-position stream-selection valve into the Minicams or through a four-port stream-selection valve into the ACAMS in the older permeation system for analysis. The rotation of the stream-selection valve was triggered by and synchronized with the sampling cycle of the Minicams or ACAMS. The remainder of the CEES vapor stream was pumped into the external mechanical pump and vented into the chemical fume hood. The test cell, the gas-stream-selection valve, and the Minicams or ACAMS were interconnected with heat-traced 0.125-in.-OD Teflon tubing. Because the Minicams cycle was set at 5 min, the CEES permeation rate through a given material was determined once every 20 min (that is, every 4 x 5 min). The ACAMS cycle was set to 3.75 min; therefore, the CEES permeation rate through a given material was determined once every 15 min (that is, every 4 x 3.75 min).

Minicams

The Minicams (CMS Corporation, Birmingham, AL) is an automated gas chromatograph that continuously samples compounds from an air stream and determines the concentration of the specified compounds in the air stream as a function of time. The operation of the Minicams consists of a continuous series of alternating adsorption and desorption cycles. For this study, the adsorption (or sampling) cycle duration was set at 2.67 min, and the desorption (or purge) cycle duration was set at 2.33 min. Thus, each complete Minicams cycle lasted 5.00 min.

During the sampling period, a fraction of the effluent air from the bottom chamber of the test cell was pulled, by means of a mechanical pump, through a preconcentrator tube (a glass tube filled with Tenax solid sorbent). Any CEES vapor in the air stream was adsorbed on the solid sorbent in the preconcentrator tube. At the end of the sample period, the preconcentrator tube was heated to approximately 200 °C to desorb the collected CEES from the sorbent bed, and the desorbed CEES was swept into a chromatographic column. Following this desorption or purge cycle, the Minicams switched back to the sampling mode, and the alternating series of adsorption and desorption cycles continued. During each successive cycle, the CEES collected in the previous cycle eluted from the GC column and was detected by a flame-photometric detector (FPD). The detector response was output to a personal computer to collect the detector peak responses versus time. Operation of the Minicams was controlled by the computer.

For this study, a calibration curve for the Minicams was generated on the day of each test by injecting known amounts of CEES (in hexane) into one of the heat-traced Teflon sample lines leading from the test cell to the stream-selection valve. All four lines from the test cell were checked periodically for accurate response. A plot of the amount of agent injected versus the peak height yielded the calibration curve. A regression analysis was performed (by the computer) on the calibration data to find the equation of the calibration curve.

During the second half of the contract, we mostly switched from liquid-droplet challenges with neoprene rubber as the substrate to vapor challenges using silicone rubber as the substrate. During this phase of testing, we experienced recurring technical problems with the permeation test system that were determined to be a combination of problems including transfer-line contamination by dust particles (resolved by incorporating fine-mesh, stainless-steel screens in the lines to filter out dust particles), poor permeation-system performance because of a worn and misaligned stream-selection valve (resolved by replacing the stream-selection valve), and strange permeation rate data and curves that were finally attributed to a small undocumented routine in the Minicams software that used a one-point calibration (instead of the fitted calibration curve) to compute the amount of CEES detected whenever a data point fell above or below the calibration range. The latter difficulty was a fairly common occurrence when using silicone rubber as the substrate. That is, the amount of CEES detected was frequently just above the highest calibration amount, and thus, the software used another method of calculating the amount of CEES detected. This software exception caused many of the permeation rate curves to exhibit discontinuities. After discovering the exception in the Minicams software, we performed the calibration calculations independently of the Minicams software, recalculated the "disparate" points in the permeation rate data, and plotted corrected permeation rate curves.

Another important characteristic of the Minicams-based permeation system was that it was too sensitive in many of the permeation tests. That is, the amount of CEES detected approached the upper detection limit of the Minicams as it was configured, even after using a phosphorus filter instead of a sulfur filter (to limit the signal to the PMT) and after turning the PMT voltage down as much as feasible. The effect on the permeation rate curves was that they prematurely leveled off or that the curves reached a relatively flat plateau rather than a peak. That is, the apparent steady-state permeation rates in some tests may have been low and not equal to the true steady-state permeation rates, or the tops of some rising-and-falling curves were flattened. In most cases, however, the permeation rate data were still meaningful and could be used for comparative evaluation of the formulations. The ACAMS (see below) was not as sensitive as the Minicams and had a higher detection limit; therefore, the permeation rate curves generated using the ACAMS system were not instrumentally affected. The detection sensitivity of the Minicams was still desirable for cases of low permeation.

ACAMS

The ACAMS, a predecessor of the Minicams, is also an automated gas chromatograph that continuously samples compounds from an air stream and determines the concentration of the specified compounds in the air stream as a function of time. The operation of the ACAMS consists of a continuous series of alternating adsorption and desorption cycles. For this project, the adsorption (or sampling) cycle duration was set at 2.00 min, and the desorption (or purge) cycle duration was set at 1.75 min. Thus, each complete ACAMS cycle lasted 3.75 min.

During the sampling period, a fraction of the effluent air from the bottom chamber of the test cell was pulled, by means of a mechanical pump, through a preconcentrator tube (a glass tube filled with Tenax solid sorbent). Any CEES vapor in the air stream was adsorbed on the solid sorbent in the preconcentrator tube. At the end of the sample period, the preconcentrator tube was heated to approximately 200°C to desorb the collected CEES from the sorbent bed, and the desorbed CEES was swept into a chromatographic column. Following this desorption or purge cycle, the ACAMS switched back to the sampling mode, and the alternating series of adsorption and desorption cycles continued. During each successive cycle, the CEES collected in the previous cycle eluted from the GC column and was detected by a flame-photometric detector (FPD). The detector response was output to a strip-chart recorder to record the chromatogram and to a personal computer to collect the detector peak responses versus time. Operation of the ACAMS was self-controlled, but triggers were produced by the ACAMS and transmitted via an analog-to-digital converter to the computer so that the computer would know when to measure the detector peak responses.

For this study, a calibration curve for the ACAMS was generated on the day of each test by injecting a known amount of CEES (in hexane) into one of the heat-traced

Teflon sample lines leading from the test cell to the stream-selection valve. All four lines from the test cell were checked periodically for accurate response. A plot of the amount of agent injected versus the peak height yielded the calibration curve. A regression analysis was performed (by the computer) on the calibration data to find the equation of the calibration curve.

Flow-control system

The flow of air through the lower chambers of the test cell was regulated by mechanical pumps and metering valves and was monitored with a set of Gilmont rotameters. The flow of air into the Minicams or ACAMS was directed with the stream-selection valve. The rotameters, test cell, metering valves, stream-selection valve, pump, and Minicams or ACAMS were interconnected with 0.125-in.-OD Teflon TFE tubing. The Teflon sample lines from the test cell to the stream-selection valve and from the stream-selection valve to the Minicams were heat-traced to minimize the adsorption of CEES on the inner walls of the sample lines.

2.3.3.2. Barrier-Test Procedure

Each barrier test was a liquid-challenge or vapor-challenge permeation test in which the four-chamber permeation test cell was loaded with four identical elastomer samples. The upper surface of each of three of the four elastomer samples was coated with a candidate formulation. The fourth sample was left uncoated to provide a control sample. The formulation was deposited on the upper surface of the elastomer using a disposable 5-mL syringe. The formulation was then spread on the upper surface of the elastomer using a clean glass stirring rod. This method appeared to provide an adequate method for spreading the formulation for the purpose of comparative evaluation.

For the liquid-droplet-challenge tests, the upper surface of each of the four test samples was uniformly contaminated with droplets of CEES using a microliter syringe equipped with a repeating dispenser to give a contamination density of 10 g/m^2 ($10 \mu\text{L}/10 \text{ cm}^2$). Each test sample was contaminated with ten $1\text{-}\mu\text{L}$ droplets of CEES. For most of the vapor-challenge tests, a single $5\text{-}\mu\text{L}$ drop of CEES was deposited in a recession in the center of the top of the Teflon droplet stand, as previously described. In some of the preliminary vapor-challenge tests that we conducted, one $10\text{-}\mu\text{L}$ drop was used.

After the CEES contamination of the test samples, the top of the test cell was sealed, and air was flowed through the lower compartment of each test-cell chamber. The effluent air stream from the lower compartment of each test-cell chamber was periodically and automatically sampled and analyzed for permeated CEES vapor every 20 min (or every 15 min for the ACAMS-based system) for typically 1000 min. Some shorter and longer tests were conducted for specific reasons as discussed in Section 2.3.3.3.

For each permeation test using the Minicams-based permeation system, which typically involved four test samples, the Minicams permeation software computed a calibration curve from the calibration data; quantified the detector responses for CEES in each chromatogram; calculated the instantaneous permeation rate for each Minicams sampling cycle; and calculated the cumulative permeation from the start of the test to the end of each sampling cycle. The results of the test were output by the computer in tabular form. Each data table consisted of the data generated during each Minicams cycle over the duration of the test. For each Minicams cycle, the tabulated data consisted of the elapsed time, the sampling port, the volume of air sampled, the detector response (peak height), the amount of CEES detected (calculated from the peak height using the calibration curve), the instantaneous permeation rate, and the cumulative permeation from the start of the test to the end of the current Minicams cycle.

For each permeation test using the ACAMS-based permeation system, the appropriate electronic triggers and the peak heights were read via an analog-to-digital board in a personal computer and were then stored on disk. The raw data were then analyzed using commercial spreadsheet software and custom macros to process the calibration data and to generate the same types of data generated by the Minicams system.

As previously described, a synthetic elastomeric polymer (elastomer) was used as a substrate for the candidate formulations in the CEES permeation tests. We looked for an elastomer that would physically function as a substrate on which the formulations could be spread but would still allow the CEES to permeate it readily and provide little resistance to CEES permeation in comparison to the formulations. We initially evaluated three polymeric materials: polyethylene, silicone, and neoprene. Neoprene was found to be the best choice for the liquid-droplet-challenge tests, and silicone was found to be the best choice for the vapor-challenge tests.

2.3.3.3. Results of Barrier Tests

2.3.3.3.1. Midterm Results

Table B-1 in Appendix B lists the principal barrier tests that we conducted during the first year of the contract. These results were previously reported in the Midterm Report. The tests are listed in the order that they were conducted. Table B-1 gives for each test the test number, the substrate material (which was neoprene for all of the tests reported herein), the average substrate thickness in mils, the formulation description, the formulation number used by the Organic Chemistry Group, the formulation number used by the Physical Chemistry Group, the amount of formulation spread onto the substrate, the test duration, and the cumulative permeation for the test. The permeation data for each test listed in Table B-1 are plotted in the figures given in Appendix C. The plots are grouped by formulation for ease of comparison. The plots in each group are given in the order tested.

Please note that the barrier tests (and reactivity tests) conducted during the first year of the contract were mainly "screening" tests. That is, we were only interested in the semi-quantitative test results. For that reason, we do not report any average test results for comparison. In the case of the permeation-rate curves, there isn't a "best" quantitative value for comparison. Essentially three different values can be obtained from each curve - a breakthrough time, a cumulative permeation amount, and for some curves, a maximum or steady-state permeation rate. We did not calculate breakthrough times because breakthrough amounts can be defined differently for different purposes, and for this project, no particular breakthrough amounts were defined. Table B-1 in Appendix B gives for each permeation test the cumulative permeation amount corresponding to the test duration, but the test durations vary from test to test. Values of the steady-state permeation rates were also not reported for these curves because their values had only semiquantitative significance for our purposes. The real value of each of the curves reported in Appendix C was the approximate breakthrough time, the general shape of the curve, or whether or not reaction of the CEES was apparent as evidenced by a fall off of the curve after a maximum in the permeation-rate curve.

Although quantitative mean values with errors might be calculated from the permeation-test results, the actual values would not be very meaningful because of the fact that the permeation data measured under this program may not be quantitatively representative of the permeation of CEES (or HD) through a formulation spread onto skin. The physical differences are too significant. However, the permeation data generated under the research project are very useful for comparing the potential efficacy of various formulations. For comparative purposes, the testing conditions must be as reproducible as possible and must still have a link to realistic exposure conditions. Our tests were conducted with these principles in mind.

The first group of plots given in Appendix C (Figures C-1 through C-17) are for the samples of bare neoprene that were included in the testing as control samples. The permeation curves for the neoprene samples are all similar in overall shape (given a few small anomalies) with the noted exceptions that the maximum permeation rate jumps from about 150 ng/min/cm² to around 300 ng/min/cm² starting with Test H871-57-1. Starting with Test Run H871-57, we used a new supply of CEES for the testing after observing that the CEES had degraded to an extent (see Section 2.3.2.2). There are also three tests with anomalous maximum permeation rates--Tests H971-47-1, H871-69-1, and H871-87-1--that may indicate that there was an experimental problem. The permeation rates measured in all of the tests in Test Run H871-47 appeared to be low, while the permeation rates for all of the tests in Test Runs H871-69 and H871-87 were unusually high. We believe that there may have been problems with the calibration curves for these test runs. (There is one calibration curve per test run.) Still, the permeation data (which can be inherently variable) for neoprene are relatively consistent and provide a reference for evaluating the candidate formulations. Note that Tests H871-54-1 and H871-54-2 were run for over 8000 min; Test Run H871-54 was conducted for an extended period to determine some basic

information about the permeation tests. The results of Test Run H871-54 are discussed below.

Figures C-18 through C-21 show CEES permeation results for Milli-Q water on neoprene. Note that Tests H871-54-3 and H871-54-4 were run for over 8000 min (see below). The results for these tests are not consistent, but they all indicate from the reduced permeation rate or from the falling permeation rate at longer times that the CEES was probably hydrolyzed by the water during the test. The inconsistent results probably resulted from how the CEES droplets behaved when deposited on the surface of the water layer. The low steady-state permeation rates observed in two of the tests suggest that the CEES droplets may have "floated" on the surface of the water. Note that we had to use a much larger loading with water than with the other formulations. This was because the neoprene samples were slightly "bowl shaped" in the test cell, and therefore, more water was required to completely cover the surface of the substrate. The thicker formulations could be spread over the surface of the indented substrate samples.

Test Run H871-54 was conducted to determine how long a steady-state permeation rate would be measured for the bare neoprene and to determine how long CEES would "survive" in the presence of the water. We determined that the maximum steady-state permeation rate through the neoprene would be maintained for at least 2000 min, which is twice as long as we typically run the barrier tests. This fact suggests that if a drop is observed in the maximum steady-state permeation rate during the 1000 min of a typical test, then the CEES is probably reacting. The results for Milli-Q water are less clear, but they indicate that we should indeed expect a reduced maximum permeation rate or a fall in the permeation rate for formulations that are reactive towards CEES. It is important to note that if reaction is rapid, the first part of the permeation rate curve would also be significantly affected.

Tests H871-41-2 and H871-44-2 (Figures C-22 and -23) are tests of unneutralized (pH 3.5) 0.4% (w/w) polyacrylic acid in water. We believe that the results of Test H871-41-2 are representative of the formulation when it is spread evenly. Tests H871-41-3 and H871-44-3 (Figures C-24 and -25) are tests of neutralized (pH 6.5) 0.4% (w/w) polyacrylic acid in water. The differences are probably due to differences in how the formulation was spread on the neoprene. Regardless of the variability in the tests with the polyacrylic acid/water formulations, these formulations appear to provide a limited barrier towards CEES and also appear to facilitate the hydrolysis of CEES.

To have another reference formulation, we conducted a number of tests using petrolatum as the formulation. Figures C-26 through C-31 show the permeation results for petrolatum at two different loadings. The results for these tests are anomalous because the permeation rates were higher with the higher loading of petrolatum. As noted above, however, the reliability of Test Run H871-47 is suspect because of a poor calibration curve. Regardless of the apparent calibration problem, the petrolatum appears to provide

some additional barrier to CEES when spread on the neoprene in that the initial permeation by CEES is slowed.

Figures C-32 through C-43 present the permeation data for the various cyclodextrin formulations that we tested. The neat α,β,γ -cyclodextrin and the water-in-oil emulsion containing 80% (w/w) α,β,γ -cyclodextrin exhibited similar permeation properties, which can be described as limited barrier and reactivity properties. Test H871-69-2 showed an unusually high maximum permeation rate, but this was true for all of the tests in Test Run H871-69 as previously discussed. The water-in-oil emulsion containing 24% (w/w) hydroxypropyl β -cyclodextrin and the Carbopol-940-thickened aqueous gel containing 28.6% (w/w) hydroxypropyl β -cyclodextrin both exhibited some protective capability in that the approach to the steady-state permeation was slowed. It is unknown if this effect was because of reduced permeability or because of some reactivity.

Figures C-44 through C-64 present the results for the emulsion formulations that we prepared with polycationics. Figures C-44 through C-46 give the permeation data for the base formulation (the control), which provided some initial permeation resistance. The 2% (w/w) Merquat-100 formulation (Figures C-47 through C-49) showed permeation similar to the base formulation. The 20% (w/w) Merquat-100 formulation (Figures C-50 through C-52) and the 20% (w/w) Polycare-133 formulation (Figures C-53 through C-55) produced permeation data similar to the base formulation, but the Polycare-133 formulation showed somewhat greater resistance to permeation. (The permeation rates for Tests H871-87-2, -3, and -4 were unusually high as previously discussed.)

Figures C-56 through C-64 show the permeation data for the base emulsion plus polycationics containing reactive counterions. The 20% (w/w) Merquat-100 with thioglycolate yielded permeation data that were comparable to the base formulation and to the 20% (w/w) Merquat-100 formulation without the reactive counterion. Some tailing off of the permeation rate at longer times is indicative of some slow reaction. The 5.4% (w/w) Merquat with histidine and the 18.8% (w/w) Merquat with thiosulfate also showed similar permeation results to the base formulation with some indication of slow reaction. (The permeation rates for Tests H871-69-3 and -4 were unusually high as previously discussed.)

Overall, the permeation results from the first year of the research program showed that formulations could be developed to provide some reactivity and barrier properties towards CEES, but we did not observe a formulation that was very impermeable or that was very reactive. The results of these first tests, however, did give us important information needed to develop better formulations.

2.3.3.3.2 Post-Midterm Results

The results of the principal barrier tests that were conducted at Southern Research Institute after those reported in the Midterm report are given in Appendices E and F. Tables E-1 and E-2 in Appendix E respectively list the tests conducted using the Minicams-based permeation test system and the ACAMS-based permeation test system. Appendix F presents figures of the plotted permeation data. Following the Midterm report, we decided that it was better to present the results of the barrier tests by test run for relative comparison of the performance of the tested formulation(s) to the bare substrate material, which was always included as a control in each test run. This allows the permeation results in each test run to be interpreted relative to the corresponding bare-substrate control without being biased by the variability between test runs.

Tables E-1 and E-2 list the barrier tests in the order that they were conducted. Tables E-1 and E-2 give for each test the test number, the substrate material (which was neoprene or silicone), the average substrate thickness in mils, the formulation description, the formulation number used by the Organic Chemistry Group, the formulation number used by the Physical Chemistry Group, the amount of formulation spread onto the substrate, the challenge type (liquid-droplet challenge or vapor challenge and the amount of CEES for the challenge), the test duration, and the cumulative permeation for the test. Table E-1 also indicates whether the data were "corrected" for the software anomaly previously described. This correction was only made if needed. The plotted permeation data in Appendix F are grouped for purposes of discussion, which follows below.

As discussed in Section 2.3.1, we had conducted a limited number of barrier tests during the third and fourth quarters of the contract that we did not report in the Midterm report because the data were considered unacceptable at the time. However, after we later identified the Minicams software anomaly, we corrected the permeation data for these tests, and the data are presented in Figures F-1 through F-14. The results of these 14 tests provide additional information about some of the barrier formulations and components that we tested and are included here to supplement the Midterm test results.

Figure F-1 presents the results of additional tests of formulations D0603-139-1, -2, and -3 (see Figures C-47 through C-55 in Appendix C). The data in Figure F-1 show again that the Goldschmidt emulsion formulations with Merquat 100 were similar in their barrier properties to the base formulation (see Figures C-44, C-45, and C-46), which by itself exhibited a slower breakthrough than the bare neoprene. Although the earlier test results indicated that the Polycare-133 formulation exhibited slightly more resistance, this additional test didn't evidence this effect.

Figure F-2 gives the data for repeated tests of formulations D0603-139-7 (Goldschmidt emulsion containing Merquat 100 with thiosulfate) and D0603-139-9 (Goldschmidt emulsion containing cyclodextrin). (See Figures C-62 through C-64 for

D0603-139-7 and Figures C-35 through C-37 for D0603-139-9 in Appendix C.) The results of the tests in Figure F-2 showed again that the Merquat-100 formulation with the thiosulfate provided some additional protection versus the bare neoprene. The permeation curves in Figure F-2, however, showed very low maximum permeation rates, and therefore, we made new standards with new CEES and used new CEES to challenge the samples after Test-Run H871-96. Test-Run H871-107 (Figure F-3) shows a repeat of Test-Run H871-96. The results of these repeated tests were qualitatively analogous to the earlier test results.

Figure F-4 shows some additional tests to check the barrier properties of water on neoprene. Similar to earlier results, a layer of water prevented the penetration of CEES through the neoprene because of the low solubility of CEES in water or because of the hydrolysis of the CEES by the water. It is apparent that formulations containing water can improve the protection provided by lotions or creams.

Test-Run H871-90 (Figure F-5) was conducted to check the effect of adding 20% methyl iodide to petrolatum. Figure F-6 shows the results of barrier tests of the plain petrolatum. The methyl iodide had no significant effect on the barrier properties of the petrolatum, which does provide some protection by itself.

Figures F-7 through F-10 give the results of replicate tests of the following solutions: D0603-140-5 (0.3 N NaOH in water), D0603-140-6 (3 N NaOH and t-butyl ammonium hydroxide in water), and D0603-140-7 (0.3 N NaOH and t-butyl ammonium hydroxide in water). The results of these tests were inconsistent, probably because of the fact that the droplets placed on the surface of the solutions behaved very irregularly. Moreover, there was an undetermined experimental problem in Test-Runs H871-113 and H871-116 as evidenced by the unusually high permeation rates calculated for these two test runs. The results of the tests in Test-Run H871-119 (Figure F-9) appear to be the most reasonable based on previous results for plain water (see Figure F-4). The tests in Figures F-7 through F-10 show that the testing of solutions or liquids by the barrier test method that we used may not produce reliable data when liquid-droplet challenges are used. However, it is apparent that water-based, basic formulations can protect against CEES (and probably HD). The effect of the t-butyl ammonium hydroxide could not be assessed in these tests.

Because of the inconsistencies in the previously conducted tests, the system was checked for problems, and Test-Run H871-126 (Figure F-11) with four replicate neoprene samples was conducted to check the performance of the system before proceeding. The results of this test run showed no particular problems.

Figures F-12 through F-14 present the results of replicate barrier tests of the following formulations: D0603-140-8 (2% KOH, propylene glycol, and MPEG 500), D0603-140-9 (5% Merquat 100 (OH⁻) in H₂O), and D0603-140-10 (5% Merquat 100 and

HOAc in H₂O). The test results for these solutions were somewhat inconsistent, again likely because of the irregular behavior of the CEES droplets on the solution surfaces. However, the MPEG-500 formulation (D0603-140-8) showed similar positive barrier properties as evidenced by the slow rise in the permeation curves. The Merquat 100 solutions showed mixed results, but the reaction of CEES in the solutions was evident.

As previously described, all barrier tests conducted prior to the sixth reporting period were performed using a liquid-droplet CEES challenge consisting of ten 1- μ L droplets of neat CEES deposited in a regular pattern on the top of the test sample (supportive and permeable substrate covered with the test formulation or solution). After the formulation was challenged, the permeation of CEES through the formulation and the substrate was measured as a function of time. During the sixth quarter, we performed additional liquid-droplet permeation tests, but also, for reasons discussed below, we modified the test procedure so that the CEES challenge would be a saturated-vapor challenge rather than a droplet challenge, and therefore, most of the tests reported in Tables E-1 and E-2 were conducted using a vapor challenge. Our experimental methods for conducting the barrier tests were fully described in Sections 2.3.3.1 and 2.3.3.2.

To summarize the vapor-challenge barrier test method here, we fabricated small Teflon platforms that resided in the upper compartments of the sample chambers in the permeation test cell (which contained four separate sample chambers). Instead of placing 10 1- μ L droplets on the surface of each test sample in a regular pattern, we placed a single 5- μ L drop (or 10- μ L drop in early tests) of CEES on the Teflon platform inside each upper compartment. Because the upper compartment was sealed during each permeation test, the CEES droplet could be expected to evaporate inside the upper compartment until the concentration of CEES vapor reached its saturation vapor concentration. Based on ideal Fickian diffusion, permeation should be the same for a liquid challenge and for a saturated-vapor challenge (although deviations from ideal behavior are common).

The permeation data for the tests conducted during the sixth quarter are listed in Table E-1 and are plotted in Figures F-15 through F-22. The graphed permeation data by test run are grouped and presented as appropriate for discussion.

The tests presented in Figures F-15 and F-16 were conducted using the RT-15 Fomblin formulation and the ICD #2730 Fomblin plus active formulation that were given to us by Dr. Hackley of USAMRICD during his visit to the Institute on March 16, 1995. Each of Figures F-15 and F-16 show that the Fomblin and Fomblin plus active did not provide permeation resistance much different from the bare neoprene that was run for comparison. The formulation with active did exhibit more protection than the Fomblin without the active component. Also, there did not appear to be significant degradation of the CEES at longer times by the active in the Fomblin samples containing the active component.

Because of these test results, we developed the vapor-challenge procedure so that we could see if the contamination by liquid droplets was too severe for the formulations. Figure F-17 shows our first set of vapor-challenge tests with bare neoprene. The results were similar to our previous droplet-challenge tests except that breakthrough occurred later. (The curves in Figure F-17 show some noise that was attributed to an instrumental electronic problem that was corrected in subsequent tests.) Figure F-18 shows the results of repeated tests of the Fomblin and Fomblin plus active using the vapor challenge. The relative differences between the permeation rate curves in Figure F-18 for the vapor challenge of the Fomblin samples and for the bare neoprene are analogous to the relative differences between the rate curves in Figures F-15 and F-16 for the liquid-challenge tests of the same types of samples. The biggest difference between the liquid-challenge tests and the vapor-challenge tests was the delayed breakthrough in the vapor-challenge tests. The vapor-challenge tests also showed some noise in the curves and an apparent calibration problem (as evidenced by the very high permeation rates), but the relative differences are believed to be real.

To further characterize the vapor-challenge test method, we conducted additional tests with bare neoprene as shown in Figures F-19, F-20, and F-21. These tests also demonstrated the delayed breakthrough measured for the neoprene. The vapor-challenge curves also show a "two-phase" permeation behavior that could be explained by several different physicochemical effects.

For comparison with the results on the Fomblin samples and to further demonstrate the advantage of using the vapor challenge, Figure F-22 shows the results of barrier tests for two bare neoprene samples and two neoprene samples covered with water. The physical problems associated with contaminating a liquid with CEES droplets is bypassed with this approach. As shown, the water effectively prevented the permeation of CEES vapor through the neoprene substrate. Of course, the test-cell compartment was sealed and thereby prevented the water from evaporating; however, the test results show that an aqueous-based formulation that would not dry out would provide good protection.

The permeation data for the tests conducted during the seventh quarter of the project are listed in Table E-1 and are plotted in Figures F-23 through F-37 in Appendix F. The graphed permeation data by test run are grouped for purposes of discussion below.

The first three test runs presented in Figures F-23, F-24, and F-25 were conducted to evaluate silicone instead of neoprene as the substrate material for vapor-challenge tests and to check the effect of water on the surface of the silicone. As shown in Figures F-23 through F-25, CEES permeates silicone much faster than it permeates neoprene (see Figures F-19 through F-22 for comparison). This means that the silicone is much less of a barrier to CEES than is neoprene, and therefore, the permeation curve for each formulation evaluated is more representative of just the formulation (taking into account the steady-state permeation rate through the silicone). The first two test runs also included

a few tests with water on the silicone. The water slowed the initial breakthrough, but did not affect the permeation to a great extent, in contrast to its measured effect on neoprene (see Figure F-22). We did not pursue an explanation for the inconsistent effect of plain water on the permeation of CEES through the two different substrates, but the differences in the wetting behavior of water on the two substrates may have been a factor.

As previously described and shown in Table E-1, all of the permeation test runs consisted of tests of four samples -- typically one control sample and three replicates. However, for most of the tests conducted during the seventh reporting period, the fourth chamber in our test cell developed an apparent leak between the upper and lower compartments of the chamber resulting in high measured permeation rates for the fourth test reported for each test run. This problem began to appear in Test-Runs I215-7 (Figure F-23), I215-10 (Figure F-24), and I215-13 (Figure F-25), as shown by the highest permeation rate curve in each of these figures. This problem became very evident when we began testing formulations following Test-Run I215-13. Although the results for the fourth test-cell chamber are reported in Table E-1 for each test, the unreliable permeation curves are not shown in Figures F-26 through F-37 to prevent confusion. Near the end of the reporting period, we completely disassembled, cleaned, and re-assembled the entire permeation test system and fixed the problem with the fourth test-cell chamber.

The remainder of the formulations that we tested during the seventh reporting period all showed barrier properties better than the bare silicone (see Figures F-26 through F-37). The permeation results for the MPEG 550 with KOH (Figure F-26) also showed evidence of reactivity with the CEES as indicated by the fall off of the permeation rate curves. The MPEG 550 with KOAc and water (Figure F-35), however, was less of a barrier than the MPEG-550/KOH formulation and showed no apparent reactivity. The DermaPlus skin protectant (Figure F-36) also showed little improvement over the bare silicone.

For comparison with our formulations, we also re-tested the Fomblin plus active that was given to us by Dr. Hackley during his visit to the Institute on March 16, 1995. Figure F-31 shows the results for the Fomblin plus active on silicone. Several of our formulations exhibited protection in the barrier tests that was comparable to that of the ICD Fomblin plus active.

During the eighth reporting period, we attempted to continue to conduct barrier tests with candidate formulations. However, we experienced a series of unanticipated experimental problems with the Minicams-based permeation test system. The problems created a number of delays and produced test results that were mostly unacceptable. Near the end of the reporting period, we were finally able to correct a number of different instrumental problems that were difficult to isolate before they could be remedied. We then began collecting reliable barrier test results, and these results are given below.

Additional details of the instrumental problems that we experienced are described in the following paragraphs.

As reported above, we had difficulty with one line (out of four) in the permeation test system during the seventh reporting period. We also stated that we had completely disassembled, cleaned, and re-assembled the entire permeation test system and had apparently fixed the problem with the malfunctioning permeation test line. However, this problem quickly recurred, and we spent most of the eighth reporting period trying to locate and fix the problem with the system. While trouble-shooting the apparatus, the Minicams pump failed, and we had to order a new pump. This created another delay in the barrier testing. After we received the new pump, the permeation test data were unacceptably (and strangely) noisy, and thus, we had to continue to investigate the test system for the source of the poor performance.

We checked the performance of the temperature-control apparatus, the flow-control system and its components, the stream-selection valve and its operation, the Minicams software for possible "bugs", and our calibration procedures for problems. We also increased the number of calibration points used for each calibration curve during this period and started checking the calibration between the four lines of the permeation test cell; however, the change in the calibration procedures, while improving the test results, did not account for the major problems that we had experienced. We finally determined that there was a very small but significant amount of contamination collecting in the permeation test lines that erratically affected the flows from the test cell and blocked the transport of CEES that permeated the test samples. This contamination was likely fine debris from the test samples or from the air stream flowing through the lower compartments of the test-cell chambers. We again cleaned and replaced lines as needed and then installed stainless-steel screens of very fine mesh in the flow lines immediately downstream of the test cell to collect any dust that could be pulled into the system during the loading and unloading of test samples. These screens were then removed and cleaned periodically between tests. Finally, we determined that a single 5- μ L drop instead of a 10- μ L drop could be used in the vapor-challenge tests. At the end of the eighth reporting period, the Minicams-based permeation test system was finally operating as before, and we began acquiring more reliable barrier test results.

Regardless of the problems experienced with the permeation test system during the seventh and eighth quarters of the project, we did conduct several barrier tests with limited success during the eighth reporting period. The results of these tests were found to be more meaningful after the permeation rate data were corrected (as needed) for the software anomaly that we discovered later in the research program. The results of the tests conducted during the eighth reporting period, however, were still mostly unacceptable (even after the software calculation correction) because of the instrumental problems. Still, the following useful information could be extracted from several of the tests.

Formulations D0603-150-20 (20% Merquat (OH⁻) in water), D0603-150-23 (Abil WE-09, Tegasoft M, Tegasoft CT, mineral oil, Merquat 100 (OH⁻), H₂O, and Na₂P₂O₇·10H₂O), D0603-150-31 (Kerodex 71 skin protectant cream), D0603-150-32 (hydroxyethyl cellulose and Mirapol (OH⁻)), D0603-155-2 (H₂O, propylene glycol, Crodafo N-3 Neutral, Crodafo N-10 Neutral, Volpo 5, Volpo 3, and mineral oil), and D0603-155-7 (Sulfur 8 Medicated Light Formula (Antidandruff)) all exhibited little to no protective properties.

The following formulations, however, showed promise as protective formulations: D0603-150-21 (Abil WE-09, Tegasoft M, Tegasoft CT, mineral oil, Merquat 100 (OH⁻), H₂O, and NaBr), D0603-150-34 (petrolatum, H₂O, Fomblin HC/04, sorbitan stearate, and S330), D0603-150-35 (hand and body lotion based on DOW 580 wax with oxidized ethyl linoleate), D0603-155-1 (Brij-97, ethanolamine, H₂O, hexadecane), D0603-155-4 (Brij-97, butanol, H₂O, hexadecane, and S330), D0603-155-6 (Crodyne BY19, H₂O, and Corcat P-600), D0603-155-13 (Fomblin HC/04, petrolatum, H₂O, sorbitan stearate, and S330), and D0603-155-14 (Fomblin HC/04, petrolatum, H₂O, sorbitan stearate, and S330). Because of the encouraging test results for these formulations, several of these same formulations, fresh preparations of some of these formulations, and new, similar versions were subsequently tested after the permeation test system was operating properly again (see below).

Because of the problems with the Minicams-based permeation test system and the resulting delays in the barrier testing, we began setting up a second permeation system during the eighth reporting period to increase the rate of testing. The second system was older, ACAMS based, and was not computer controlled with automated data collection and analysis, but some side-by-side testing with the Minicams system showed that it provided permeation data that were similar to those produced by the Minicams system (as it should in the absence of systematic errors in the testing method). The ACAMS-based permeation test system was described in more detail in Section 2.3.3.1.

During the ninth reporting period, we measured very encouraging barrier test data for several new formulations. Figures F-38 through F-47 show the results of the barrier tests completed during the ninth reporting period. These figures are ordered in a manner to facilitate discussion of the results. All of these tests were vapor-challenge tests using a 5- μ L drop as the source of the saturated vapor in the sealed upper compartment of each test-cell chamber.

Figure F-38 shows the test results for the microemulsion formulation D0603-155-15 (Brij-97, H₂O, hexadecane, and ethanolamine). The formulation, when compared to the bare silicone, exhibits low barrier properties, but reaction (presumably hydrolysis) of the CEES is apparent at longer times.

Figure F-39 shows a test of a freshly prepared version (D0603-155-26) of the benchmark formulation (ICD #1511 with S330) provided by USAMRICD. As shown, the formulation displayed some initial barrier effect when compared to the bare silicone, and reaction was evident at longer times. This formulation was tested for comparison with other formulations.

Figures F-40 through F-46 show a series of comparative tests of a formulation with different loadings of S330. Figure F-40 shows the test results for a fresh preparation of the base formulation (D0603-155-16; Fomblin HC/04, petrolatum, sorbitan stearate, and H₂O) without S330. Little protection is afforded by the base formulation, although the steady-state permeation rate is slightly lower than for the bare silicone. Figures F-41, F-42, and F-43 show the test results for the formulation with 2.5% S330. Figure F-41 shows the permeation results for a fresh batch of the formulation, which shows some initial barrier properties and reaction at longer times. Figures F-42 and F-43 (replicate test runs) show the effects of approximately two months of shelf life on the formulation. The data for the older formulation show a reduction in the formulation's protective ability. Figures F-44 and F-45 show the results for 5% S330 in the same base formulation. Figure F-44 shows the results for a fresh batch, and Figure F-45 shows the data for a batch approximately two months after preparation. The 5% S330 formulations show considerably better protection than the 2.5% S330 preparations. Figure F-45, when compared to Figure F-44, shows again that shelf life does affect the formulation efficacy. Figure F-46 shows that 10% S330 significantly limits the permeation of CEES and that reaction is also apparent. All of these S330 formulations (including our inhouse preparation of the USAMRICD formulation) demonstrated protection as good as or better than the USAMRICD formulation as supplied to us.

Figure F-47 presents the barrier tests of a commercial burn ointment (D0603-155-18). This burn ointment also exhibited protective properties warranting additional study.

During the ninth reporting period, we also continued to set up the ACAMS-based permeation system by interfacing it to a computer and by setting up a commercial data-acquisition software package that we had available for use. Data reduction was performed using the same commercial spreadsheet software that we used to reduce the raw permeation data from the Minicams system. Preliminary testing showed that this second test system produced data similar to those produced by the Minicams permeation system.

Figures F-48 through F-81 show the results of the barrier tests conducted after the ninth reporting period through the end of the contract. The results of these tests, which primarily focused on the most promising formulations and components identified in earlier tests, are grouped by the formulation.

Figure F-48 shows a repeated test of the USAMRICD formulation (D0603-150-2; ICD #2730 Fomblin formulation with active). Comparison with earlier tests (see Figures

F-15, F-16, F-18, and F-31) shows that the activity of the formulation decreased over time.

Figure F-49 shows a test of another variation on previously tested formulations containing Merquat and Fomblin HC/04 (D0603-155-19; Merquat 100 (Cl⁻), petrolatum, H₂O, Fomblin HC/04, and sorbitan stearate). This formulation did not exhibit any significant barrier or reactivity properties.

Formulation D0603-155-20 (Ucare JR-30M, H₂O, Fomblin HC/04, petrolatum, and sorbitan stearate) also showed minimal barrier properties (Figure F-50).

Figure F-51 presents the barrier-test results for formulation D0603-155-21 (Merquat 100 (Cl⁻), petrolatum, H₂O, Fomblin HC/04, and sorbitan stearate with 10% S330 added). This formulation with the active showed significant reactivity towards CEES when compared to the base formulation D0603-155-19 (see Figure F-49).

Figure F-52 shows the permeation data for the D0603-155-22 (Ucare JR-30M, H₂O, Fomblin HC/04, petrolatum, and sorbitan stearate with S330), which is the same formulation as D0603-155-20 but with S330 added. The addition of S330 to this formulation, however, did not perform as well as when S330 was added to the base formulation D0603-155-19 to produce D0603-155-21 (see Figures F-49 and F-51).

Figures F-53, F-54, and F-55 show the permeation results for three variations of formulations containing Corcat P-600, H₂O, and Crodyne BY-19 with three different additives -- HOAc, phosphoric acid, and ammonium persulfate. None of these formulations exhibited any significant barrier properties.

Figures F-56 and F-57 show the test results for another preparation (D0603-155-31) of Fomblin HC/04, petrolatum, H₂O, and sorbitan stearate with S330. These results show again the positive efficacy of this formulation. Test-Run I409-82 (Figure F-57) was conducted almost two months after Test-Run I409-52 (Figure F-57), demonstrating the stability of the formulation over time.

Formulation D0603-155-32 (DOW 593, DOW 200, H₂O, stearic acid, cetyl alcohol, mineral oil, isopropyl lanolate, triethanolamine, and glycerine) exhibited promising barrier and reactivity properties (Figure F-58).

Discussions with USAMRICD personnel revealed that ICD's inhouse testing of ICD #1511 consisted of liquid-droplet challenges of the formulation spread onto M8 agent-detector paper. A color change in the detector paper would indicate that liquid agent penetrated the formulation and was adsorbed by the paper. We were told that ICD #1511 routinely passed this test, but our permeation results showed that CEES permeated the formulation. Of course the physicochemical behavior for penetration and permeation are

different and even though CEES liquid may not physically penetrate a formulation, CEES may permeate a formulation by the characteristic solution/diffusion process. To investigate the differences in test approaches and the resulting results, we conducted several tests of formulation D0603-155-33 (ICD #1511 from USAMRICD) under different conditions as described in the following paragraph.

Figures F-59 and F-60 show first the permeation of ICD #1511 on silicone by CEES vapor. The maximum permeation rates achieved in Test-Run I409-61 (Figure F-59) were uncharacteristically low, but the results in both Figures F-59 and F-60 show that the formulation provides little resistance to permeation by CEES vapor. Figure F-61 shows the permeation behavior when neoprene is the substrate. The breakthrough times are much longer because of the lower permeability of neoprene as compared to that of silicone. These test results do show a slight protection provided by ICD formulation at longer times. We then conducted a set of vapor-challenge tests of the ICD formulation on silicone with M8 paper between the silicone and the formulation; that is, the formulation was spread on the M8 paper, which was placed on top of the silicone substrate. As shown in Figure F-62, the CEES vapor easily permeated the formulation, the M8 paper, and the silicone. As expected, there was no observed color change in the M8 paper, which is known not to change color upon exposure to agent vapor. (We did verify that liquid CEES would change the color of the M8 paper.) Test-Run I409-100 (Figure F-63) was set up in a similar manner, but this time we used a liquid-droplet CEES challenge and neoprene as the substrate (because liquid-droplet challenges on silicone had already been determined to be experimentally unfeasible). In this test, the formulation appeared to provide some protection, as in Test I409-67 (Figure F-61), and the M8 paper itself appeared to slow the CEES penetration to an extent (probably because of adsorption by the paper itself). In contrast to the test results verbally provided by ICD, however, we did observe color changes in the M8 paper in the two test-cell chambers where M8 paper was used. The color changes consisted of red spots in the M8 paper corresponding to the locations beneath where the drops were deposited. These results were in contrast to those reported by ICD. It is possible, however, that our procedures for spreading the formulation on the samples and for the contamination of the samples varied enough from ICD's methods that different results could be obtained. The principal conclusion from this brief study of ICD #1511, however, is that CEES vapor can permeate the formulation, even if liquid CEES cannot penetrate it. Moreover, even if the testing method and the results differ between ICD and Southern, the test method that we used was chosen because of its sensitivity to permeant vapor and was appropriate for comparing the protection efficacy of various formulations, including the ICD #1511 (and the ICD #2730 formulation with active).

Figure F-64 shows the results of another preparation (D0603-155-34) of petrolatum, H₂O, Fomblin HC/04, and sorbitan stearate plus SRI S330 with different composition amounts than D0603-155-31 (see Figures F-56 and F-59). These two variations showed similar performance.

Figures F-65 and F-66 show the results for another variation on our Fomblin formulation using Fomblin HC/R instead of HC/04. The results are similar to those for the HC/04 formulations in that the base formulation without S330 (D0603-157-1; Figure F-66) shows no significant barrier properties, but the formulation with active (D0603-157-2; Figure F-65) shows significant reactivity.

Figure F-67 indicates that if the Fomblin is removed from the formulation, the protection is similar to that of the formulation with Fomblin. Figures F-68 and F-69 show that the effect of more than doubling the S330 amount in the formulation had limited effect on the permeation of the formulation by CEES vapor.

Replicate permeation results for D0603-157-7 (petrolatum, DOW 200, DOW 593, H₂O, and sorbitan stearate with SRI S330) show good reactivity with CEES vapor. The test results also show the stability of this formulation as evidenced by the fact that Test-Run I409-133 (Figure F-71) was conducted about two months after Test-Run I409-88 (Figure F-70).

Figures F-72 and F-73 show the test results for a Fomblin formulation containing dichlorodimethylhydantoin with approximately two months between the respective test runs. The activity of the formulation appeared to have decreased slightly with age. Another similar preparation (D0603-157-9) with twice the dichlorodimethylhydantoin showed very significant reactivity with CEES (Figure F-74).

Figures F-75 through F-79 show the barrier results for several additional formulations containing dichlorodimethylhydantoin. All of these formulations showed reactivity toward CEES, but none of these formulations performed as well as D0603-157-9.

Figure F-80 shows a new preparation of our Fomblin-based formulation with results similar to earlier data.

Figure F-81 shows tests of a Fomblin formulation with Jordigel/PnP added. This formulation exhibited no significant barrier properties.

As previously mentioned in this report, we also conducted barrier tests using an older ACAMS-based permeation system. Figures F-82 through F-97 show the results of these tests.

As a check of the ACAMS system, Figures F-82 and F-83 respectively show the permeation of CEES vapor through bare silicone and bare neoprene. The permeation data were consistent for each substrate material and were similar to results obtained with the Minicams system.

Figures F-84 and F-85 show the test results for a formulation of Brij-97, ethanolamine, H₂O, and hexadecane. As shown in the figures, this formulation did not provide much of a barrier, but it did evidence some reactivity with CEES.

Figures F-86 and F-87 show the permeation results for two similar formulations of Corcat P-600, H₂O, Crodyne BY-19, and either peracetic acid (D0603-155-29) or ammonium persulfate (D0603-155-30). Both formulations showed some reactivity with CEES at longer times, but provided little protection.

To compare with the permeation data obtained using the Minicams system, the tests in Figures F-88, F-89, and F-90 were conducted using the formulations provided by USAMRICD. Figure F-88 shows that ICD #1511 provides little protection from CEES vapor. Figures F-89 and F-90 show the results of liquid-droplet challenges of ICD #1511 spread directly on the silicone and also spread on M8 paper placed on top of the silicone to mimic the test method used by USAMRICD. The results of these tests showed that the formulation provided little protection. Moreover, the M8 paper changed color, indicating that liquid CEES penetrated the formulation. These results were similar to the analogous tests conducted with the Minicams system (discussed above).

Figures F-91, F-92, and F-93 show tests of several variations of the most promising formulations with S330 that we developed and tested under the research program. The test results show how formulation differences affect the permeation of CEES.

Figures F-94, F-95, and F-96 show tests of several variations of our most promising formulations with dichlorodimethylhydantoin. All of these formulations exhibited good reactivity towards CEES.

Figure F-97 shows a test run with a Fomblin formulation containing Jordigel/PnP added. This formulation exhibited no significant barrier properties.

3. Conclusions

Our investigations of reactive components and reactive-containing compositions have resulted in the development of some promising efficacious prototype formulations which appear to be more efficacious than the benchmarks provided by our Project Officer. Our most promising compositions are comprised of petrolatum, sorbitan stearate, and water with either of the N-halo oxidants 1,3,4,6-tetrachloro-7,8-diphenyl-2,5-diiminoglycoluril (S-330) or 1,3-dichloro-5,5-dimethylhydantoin, and optionally, with a barrier-providing polymer such as a perfluoro alkylpolyether (FOMBLIN HC/04, HC/25, or HC/R) or a polysiloxane. However, at this time, none of our prototypes have been investigated enough to be considered final products. Still, they clearly show a direction that could lead to an effective reactive topical skin protectant against vesication.

A significant component of our work has been the development of methods for determining the efficacies (either reactive or reactive barrier) of our formulations and formulation components. The reactive barrier efficacies of our formulations have been quantified by a method using either of two automated permeation test systems, one based on a Minicams and another based the well known ACAMS, both of which were specifically modified for our work. Both detection systems were used to monitor the concentration of CEES in an air stream that flows over the back sides of thin, circular agent-challenged rubber specimens mounted in a stainless steel partition cell. Modifications made during the course of this effort include the identification of silicone rubber as an appropriate specimen material for our tests. We also redesigned our test apparatus to allow the specimens to be challenged by CEES vapor rather than droplets. Our overall methodology was based on work originally performed by the Southern Research Institute Physical Chemistry Group under prior contracts for the Department of Defense in which permeation and penetration tests were conducted with chemical-warfare agents and agent simulants on air-permeable and air-impermeable materials.

4. References

1. B. Papirmeister, A. Feister, S. Robinson, R. Ford. **Medical Defense Against Mustard Gas**. p. 91.
2. G. E. Totten, N. A. Clinton, *Rev. Macromol. Chem. Phys.*, **1988**, C28, 293-337 and references within.
3. R. Reiner, K. Roßmann, C. van Hooidek, B. Ceulen, J. Bock., *Arzneim.-Forsch./Drug Res.*, **1982**, 32, 630.
4. J. Garfield Purdon, Proceedings of the 1991 U.S. Army Chemical Research, Development and Engineering Center Scientific conference on Chemical Defense Research 19-22 November 1991, 449-455.
5. M. Amann and G. Dressnandt, *Cosmetics & Toiletries*, **1993**, 108, 90-95.
6. D. Landini, A. Maia, F. Montanari, *JACS*, **1978**, 100, 2796;
7. *JCS Chem. Comm.*, **1977**, 112.
8. C. M. Starks, *JACS*, **1971**, 93, 195.
9. C. M. Starks, R. M. Owens, *JACS*, **1973**, 95, 3613.
10. H. Moinari, F. Montanari, S. Quici, P. Tundo, *JACS*, **1979**, 101(14), 3920-3927.

11. S. L. Regen, *Angew. Chem. Internat. Ed.*, **1979**, 18(6), 421-492.
12. K. J. Pratt, C. Carles, T. J. Carne, M. J. Danson, K. J. Stevenson, Detection of bacterial lipoic acid, *Biochem. J.*, **1989**, 258, 749-754.
13. G. B. Butler, A. Crawshaw, W. L. Miller, *JACS*, **1958**, 80, 3615-8.
14. N. M. Weinshenker, C. M. Shen, J. Y. Wong, *Org. Syn. Col. Vol. VI*, **1988**, p. 951.
15. N. N. Suvorov, L. K. Vinograd, M. V. Vasin, V. S. Minaeva, *Khim Geterotsikl. Soedin.* **1973**, 11, 1505-11.
16. M. Muraki, T. Mizoguchi, *Chem. Pharm. Bull.*, **19**, 1708 (1971).
17. M. Huche, M. Savignac, G. Pourcelot, *Nouv. J. Chim.*, **1981**, 5(2), 109-111.
18. A. Berger, J. Noguchi, E. Katchalski, *J. Am. Chem. Soc.*, **1956**, 78, 4483-4488.
19. F. A. Davis, R. H. Jenkins, Jr., S. G. Yocklovich, S. G., *Tetrahedron Lett.*, **1978**, 5171-5178.
20. F. A. Davis, J. M. Billmers, D. J. Gosciniak, J. C. Towson, R. D. Bach, *J. Org. Chem.*, **1986**, 51, 4240-4245.
21. Y.-C. Yang, L. L. Szafraniec, W. T. Beaudry, F. A. Davis, *J. Org. Chem.*, **1990**, 55, 3664-3666.
22. W. v. B. Robertson, J. L. Hartwell, S. Kornberg, *J. Am. Chem. Soc.*, **1944**, 66, 1894-1897.
23. F. M. Menger, A. R. Erlington, *J. Am. Chem. Soc.* **1991**, 113, 9621-9624.
24. F. M. Menger, *Angew. Chem. Int. Ed.*, **1991**, 30, 1086-1099.
25. F. M. Menger, A. R. Erlington, *J. Am. Chem. Soc.* **1990**, 112, 8201-8203.
26. C. K. Choy, F. I. Keen, *US 4,599,186*, **1986**.
27. C. K. Choy, F. I. Keen, *US 4,657,692*, **1987**.
28. C. K. Choy, F. I. Keen, A. Garabedian, C. J. Spurgeon, *US 4,695,394*, **1987**.

29. J. W. Williams. U.S. 2,649, 289, **1953**. D. Li, *Tongweisu*, **1991**, 4(2), 105-6, CA:117:902047.
30. A. Utsu, *Jpn. Kokai, Tokkyo Koho JP 04 49,213*, **1992**, CA 117:97118q.
31. D. G. Murray, *U.S.* 4,659,572, **1987**.
32. M. B. Sulzberger, A. Kanof, and R. L. Baer. *US* 2,630,399, **1953**. CA:47:6099d.4. Conclusion

Bibliography of Publications and Meeting Abstracts Resulting from This Effort

Cecil D. Kwong, Donald P. Segers, Robert C. Reynolds, Jackie W. Truss, Lowell D. Thomas-Updike, and Brennie E. Hackley, Jr. **Efforts Directed Toward the Development of a Reactive Topical Skin Protectant Against CEES.** 1996 Medical Defense Bioscience Review, Baltimore, MD, May 12-16, 1996.

Efforts Directed Toward the Development of a Reactive Topical Skin Protectant Against CEES

*Cecil D. Kwong,¹ Donald P. Segers,¹ Robert C. Reynolds,¹
Jackie W. Truss,¹ Lowell D. Thomas-Updike,¹ and Brennie E. Hackley, Jr.²*

¹Southern Research Institute, Birmingham, Alabama

²U. S. Army Medical Research Institute, Aberdeen Proving Ground

Our project DAMD 17-93-C-3186 entitled "Antivesication by Simultaneous Prophylaxis and Detoxification" has been directed toward the development of a new topically applied pretreatment that will prevent or minimize the vesication caused by exposure to sulfur mustard (HD). The target formulation for our current work is one that would be efficacious against CEES (2-chloroethylethyl sulfide) by providing a barrier to agent penetration while simultaneously detoxifying the agent via chemical reaction. Our efforts have included the identification and/or synthesis of candidate reactive materials and formulation bases, the development of prototype formulations comprised of reactive materials in various base creams, and the development of screening methods to determine the CWA efficacy of our formulations and formulation components.

This research was funded by U. S. Army Medical Research Institute of Chemical Defense under Contract DAMD17-93-C-3186.

Presented at the "1996 Medical Defense Bioscience Review" in Baltimore on May 12-16, 1996.

List of All Personnel Receiving Pay from the Negotiated Effort

Synthesis and Formulation Personnel

Robert N. Comber (Original Project PI)
Cecil D. Kwong, PI
Robert C. Reynolds, Co-PI
Jackie W. Truss

Reactivity and Barrier Reactivity Evaluation Personnel

Donald P. Segers
Lowell D. Updike
Reuben B. Watkins
Amie E. Gabriel
Jeffery N. Smith
Ralph Spafford
Thomas E. Gullo
Stephen Wildeman

Analytical Chemistry and Spectroscopy

William C. Coburn Jr.
James M. Riordan
Gregory A. Rener
Christine Richards

Glassware

Joan C. Bearden
Willie Johnson
Albert Moody

Others

Thomas D. Stringfellow, Reproduction
Larry N. Wilson, Microbiology
Charles M. Shaefer, Machine Shop

BAA final report from Biopraxis, Inc.*

Award Number: DAMD17-98-C-8028

***Note: Distribution of the details of this project are limited, so only the first few pages are listed.**

Award Number: DAMD17-98-C-8028

TITLE: Microcatalysts for Use in Reactive Topical Skin
Protectants

PRINCIPAL INVESTIGATOR: Ann E. Grow.0

CONTRACTING ORGANIZATION: Biopraxis, Incorporated
San Diego, California 92191

REPORT DATE: April 2000

TYPE OF REPORT: Final

PREPARED FOR: U.S. Army Medical Research and Materiel Command Fort
Detrick, Maryland 21702-5012

DISTRIBUTION STATEMENT: Distribution authorized to U.S. Government
agencies only (proprietary information, Apr 00). Other requests for this
document shall be referred to U.S. Army Medical Research and Materiel
Command, 504 Scott Street, Fort Detrick, Maryland 21702-5012.

The views, opinions and/or findings contained in this report are those of
the author(s) and should not be construed as an official Department of the
Army position, policy or decision unless so designated by other
documentation.

NOTICE

USING GOVERNMENT DRAWINGS, SPECIFICATIONS, OR OTHER DATA INCLUDED IN THIS DOCUMENT FOR ANY PURPOSE OTHER THAN GOVERNMENT PROCUREMENT DOES NOT IN ANY WAY

OBLIGATE THE U.S. GOVERNMENT. THE FACT THAT THE GOVERNMENT FORMULATED OR SUPPLIED THE DRAWINGS, SPECIFICATIONS, OR OTHER DATA DOES NOT LICENSE THE HOLDER OR ANY OTHER PERSON OR CORPORATION; OR CONVEY ANY RIGHTS OR PERMISSION TO MANUFACTURE, USE, OR SELL ANY PATENTED INVENTION THAT MAY RELATE TO THEM.

LIMITED RIGHTS LEGEND

Award Number: DAMD17-98-C-8028

Organization: Biopraxis, Incorporated Location of
Limited Rights Data (Pages):

Those portions of the technical data contained in this report marked as limited rights data shall not, without the written permission of the above contractor, be (a) released or disclosed outside the government, (b) used by the Government for manufacture or, in the case of computer software documentation, for preparing the same or similar computer software, or (c) used by a party other than the Government, except that the Government may release or disclose technical data to persons outside the Government, or permit the use of technical data by such persons, if (i) such release, disclosure, or use is necessary for emergency repair or overhaul or (ii) is a release or disclosure of technical data (other than detailed manufacturing or process data) to, or use of such data by, a foreign government that is in the interest of the Government and is required for evaluation or informational purposes, provided in either case that such release, disclosure or use is made subject to a prohibition that the person to whom the data is released or disclosed may not further use, release or disclose such data, and the contractor or subcontractor or subcontractor asserting the restriction is notified of such release, disclosure or use. This legend, together with the indications of the portions of this data which are subject to such limitations, shall be included on any reproduction hereof which includes any part of the portions subject to such limitations.

THIS TECHNICAL REPORT HAS BEEN REVIEWED AND IS APPROVED FOR PUBLICATION.

REPORT DOCUMENTATION PAGE			Form Approved OMB No. 074-0188	
Public reporting burden for this collection of information is estimated to average 1 hour per response, including the time for reviewing instructions, searching existing data sources, gathering and maintaining the data needed, and completing and reviewing this collection of information. Send comments regarding this burden estimate or any other aspect of this collection of information, including suggestions for reducing this burden to Washington Headquarters Services, Directorate for Information Operations and Reports, 1215 Jefferson Davis Highway, Suite 1204, Arlington, VA 22202-4302, and to the Office of Management and Budget, Paperwork Reduction Project (10704-0188), Washington, DC 20503				
1. AGENCY USE ONLY (Leave blank)		2. REPORT DATE April 2000	3. REPORT TYPE AND DATES COVERED Final (23 Mar 98 - 22 Mar 00)	
4. TITLE AND SUBTITLE Microcatalysts for Use in Reactive Topical Skin Protectants			5. FUNDING NUMBERS DAMD17-98-C-8028	
6. AUTHORS) Ann E. Grow				
7. PERFORMING ORGANIZATION NAMES) AND ADDRESSES) Biopraxis, Incorporated San Diego, California 92191 E-MAIL: agrow@biopraxis.com			8. PERFORMING ORGANIZATION	
9. SPONSORING / MONITORING AGENCY NAME(S) AND ADDRESS(ES) U.S. Army Medical Research and Materiel Command Fort Detrick, Maryland 21702-5012			10. SPONSORING / MONITORING AGENCY REPORT NUMBER	
11. SUPPLEMENTARY NOTES				
12a. DISTRIBUTION / AVAILABILITY STATEMENT Distribution authorized to U.S. Government agencies only (proprietary information, Apr 00). Other requests for this document shall be referred to U.S. Army Medical Research and Materiel Command, 504 Scott Street, Fort Detrick, Maryland 21702-5012.			12b. DISTRIBUTION CODE	
13. ABSTRACT (Maximum 200 Words) Biopraxis is developing a new, economical approach for producing catalysts under ambient conditions, with high yield and low waste, from inexpensive precursors. The objective of the reactive Topical Skin Protectant (rTSP) program is to demonstrate the feasibility of using this technology to produce inexpensive catalysts suitable for protecting the U.S. Armed Forces against chemical warfare agents. In vial tests with diisopropyl fluorophosphate (DFP) and chloroethyl ethyl sulfide (CEES), more than half of the 80 catalysts screened were effective against one or both simulants. Twenty-two were screened as rTSP formulations against DFP; all but three were effective. GC analyses showed that the various catalysts produced different reaction products, including unsaturated and/or halogenated products. Five of the six formulations tested against GD by USAMRICD showed superior efficacy in comparison with the non-reactive TSP. While the non-reactive TSP reaches breakthrough in -5.1 hours, and allows a cumulative penetration of -10,000ng GD in 20 hours, the best rTSP formulations resisted breakthrough for 22.6 and 20.0 hours, and permitted only 360ng and 970ng GD, respectively, to penetrate during the first 20 hours. There are many ways to improve performance even further.				
14. SUBJECT TERMS Catalysts, chemical warfare agents, protective skin cream, DFP, CEES			15. NUMBER OF PAGES	
			16. PRICE CODE	
17. SECURITY CLASSIFICATION OF REPORT Unclassified	18. SECURITY CLASSIFICATION OF THIS PAGE Unclassified	19. SECURITY CLASSIFICATION OF ABSTRACT Unclassified	20. LIMITATION OF ABSTRACT Unlimited_	

FOREWORD

Opinions, interpretations, conclusions and recommendations are those of the author and are not necessarily endorsed by the U.S. Army.

Where copyrighted material is quoted, permission has been obtained to use such material.

Where material from documents designated for limited distribution is quoted, permission has been obtained to use the material.

Citations of commercial organizations and trade names in this report do not constitute an official Department of Army endorsement or approval of the products or services of these organizations.

N/A In conducting research using animals, the investigator(s) adhered to the "Guide for the Care and Use of Laboratory Animals," prepared by the Committee on Care and use of Laboratory Animals of the Institute of Laboratory Resources, national Research Council (NIH Publication No. 86-23, Revised 1985).

N/A^A For the protection of human subjects, the investigator(s) adhered to policies of applicable Federal Law 45 CFR 46.

N/A In conducting research utilizing recombinant DNA technology, the investigator(s) adhered to current guidelines promulgated by the National Institutes of Health.

N/A In the conduct of research utilizing recombinant DNA, the investigator(s) adhered to the NIH Guidelines for Research Involving Recombinant DNA Molecules.

N/A In the conduct of research involving hazardous organisms, the investigator(s) adhered to the CDC-NIH Guide for Biosafety in Microbiological and Biomedical Laboratories.


PI - Signature 0 3///40
ate

TABLE OF CONTENTS

Cover	
SF 298	ii
Foreword	iii
Table of Contents	iv
Introduction	1
Body	1
Task 1 — Assessment of Reactivity Against Simulants	3
Task 2 — Determination of Formulation Efficacy	
Government Testing	16
Key Research Accomplishments	19
Reportable Outcomes	19
Conclusions	20
Table 1 — USAMRICD Penetration Cell Test Results	17
Appendices	21

BAA Final report from Biopraxis, Inc

Award Number: DAMD17-01-C-0057

TITLE: Reactive Topical Skin Protectant

PRINCIPAL INVESTIGATOR: Ann E. Grow

CONTRACTING ORGANIZATION: Biopraxis, Incorporated
San Diego, California 92191-0078

REPORT DATE: June 2004

TYPE OF REPORT: Final

PREPARED FOR: U.S. Army Medical Research and Materiel Command Fort
Detrick, Maryland 21702-5012

DISTRIBUTION STATEMENT: Approved for Public Release;
Distribution Unlimited

The views, opinions and/or findings contained in this report are those of the author(s) and should not be construed as an official Department of the Army position, policy or decision unless so designated by other documentation.

[20050415 060

REPORT DOCUMENTATION PAGE			<i>Form Approved</i> <i>OMB No. 074-0188</i>	
Public reporting burden for this collection of information is estimated to average 1 hour per response, including the time for reviewing instructions, searching existing data sources, gathering and maintaining the data needed, and completing and reviewing this collection of information. Send comments regarding this burden estimate or any other aspect of this collection of information, including suggestions for reducing this burden to Washington Headquarters Services, Directorate for Information Operations and Reports, 1215 Jefferson Davis Highway, Suite 1204, Arlington, VA 22202-4302, and to the Office of Management and Budget, Paperwork Reduction Project (0704-0188), Washington, DC 20503				
1. AGENCY USE ONLY (Leave blank)		2. REPORT DATE June 2004	3. REPORT TYPE AND DATES COVERED Final (22 Oct 2001 - 1 Mar 2004)	
4. TITLE AND SUBTITLE Reactive Topical Skin Protectant			5. FUNDING NUMBERS DAMD17-01-C -0057	
6. AUTHOR(S) Ann E. Grow				
7. PERFORMING ORGANIZATION NAME(S) AND ADDRESS(ES) Biopraxis, Incorporated San Diego, California 92191-007 <i>E-Mail:</i> agrow@biopraxis.com			8. PERFORMING ORGANIZATION REPORT NUMBER	
9. SPONSORING / MONITORING AGENCY NAME(S) AND ADDRESS(ES) U.S. Army Medical Research and Materiel Command Fort Detrick, Maryland 21702-5012			10. SPONSORING / MONITORING AGENCY REPORT NUMBER	
11. SUPPLEMENTARY NOTES				
12a. DISTRIBUTION / AVAILABILITY STATEMENT Approved for Public Release; Distribution Unlimited				12b. DISTRIBUTION CODE
13. ABSTRACT (Maximum 200 Words) Biopraxis is developing a method for production of novel catalysts from inexpensive precursors, at high yield, under mild conditions. Under an earlier program, Biopraxis demonstrated that catalysts produced by this method can effectively neutralize the agent simulants diisopropyl fluorophosphate (DFP) and 2-chloroethyl ethyl sulfide (CEES). Government testing identified a formulation that exhibited excellent efficacy against both GD and HD, reducing nerve agent penetration by 93.1% and mustard penetration by 81.5% in comparison with the non-reactive TSP. Accordingly, the Government awarded a follow-on program. The program was cut short due to funds being diverted for the Iraq war. The best formulation that had been identified by that time did not allow any detectable GD penetration in 20hours (99.96% reduction) and was projected to take more than 950 hours to reach breakthrough (a 16,502% increase). This same formulation also showed excellent efficacy against HD; i.e., a 217% increase in the time to breakthrough, and a 59% reduction in penetration by 20hours, in comparison with the non-reactive TSP. Since the catalysts are solid particulates, formulations, may contain mixtures of catalysts that are superior for decontaminating different agents.				
14. SUBJECT TERMS Catalysts, protective skin cream, DFP, CEES, GD, HD				15. NUMBER OF PAGES 16
				16. PRICE CODE
17. SECURITY CLASSIFICATION OF REPORT Unclassified	18. SECURITY CLASSIFICATION OF THIS PAGE Unclassified	19. SECURITY CLASSIFICATION OF ABSTRACT Unclassified	20. LIMITATION OF ABSTRACT Unlimited	

Table of Contents

Cover.....	
SF 298	2
Table of Contents.....	3
I n t r o d u c t i o n	4
Body.....	4
Key Research Accomplishments	15
Reportable Outcomes	16
Conclusions.....	16

INTRODUCTION

Biopraxis is developing a method for production of novel catalysts from inexpensive precursors, at high yield, under mild conditions. Under the first "reactive Topical Skin Protectant (rTSP)" program, Biopraxis demonstrated that catalysts produced by this method can effectively neutralize chemical warfare agents. Catalysts were prepared and screened against the vapors of the chemical warfare (CW) simulants diisopropyl fluorophosphate (DFP) and 2-chloroethyl ethyl sulfide (CEES) in simple vial tests. More than three dozen catalysts were found to be effective at degrading the simulants. Select catalysts that performed well against one or both of the simulants were then prepared as formulations comprising the catalyst mixed with the non-reactive Topical Skin Protectant (TSP) oil, thickener, and (for moist catalyst preparations) surfactant; and then tested against a DFP vapor challenge using a modification of the penetration cell protocol developed by USAMRICD. Of the 22 catalysts screened in formulations, at least 18 appeared promising for protection against DFP. Gas chromatographic analyses of the vapors penetrating the rTSP formulations confirmed that the different catalysts produced a range of different reaction products.

Formulations submitted to the Government for testing against GD exhibited superior efficacy in comparison with the non-reactive TSP (13004). The Government subsequently placed a purchase order to acquire batches of several catalysts for more extensive Government testing. The most promising formulation (13600) that had been identified by early July 2001 showed substantially superior efficacy against both HD and GD. While 13004 reached GD breakthrough (time to 1,000 ng total penetration) at 346+68 min and allowed 6,672+865 ng to penetrate over 20 hr, 13600 did not reach breakthrough until 2,086+1349 min and allowed only 461+648 ng to penetrate by 20 hr. While 13004 reached HD breakthrough at 586+46 min, and allowed 2,758+299 ng to penetrate over 20 hr, 13600 did not reach breakthrough until 1,704+548 min and allowed only 510+368 ng penetration by 20 hr.

Accordingly, the Government awarded a follow-on rTSP program. Under this second program, Biopraxis proposed to test additional novel catalysts against CW agent simulants, characterize the catalysts, and provide select samples for Government testing.

BODY

The catalysts studied on this USAMRICD program were originally developed for use in treating environmental pollutants. Biopraxis proposed to use data on pollutant treatment efficacy, coupled with tests of select catalysts against CW agent simulants, to identify promising catalysts for Government formulation tests with surety materiel.

Catalyst Selection

Biopraxis catalogues all catalysts and their properties in an extensive database. This database contains all data collected during the first rTSP project and Government surety materiel test results, as well as data on environmental remediation. At the beginning of the follow-on rTSP program, the database was re-analyzed in an effort to determine what production parameters might yield catalysts that are effective against CW agents.

Catalysts have been produced under both oxygen and nitrogen environments. Analysis of the database suggested that oxygen-based techniques might hold great promise for production of catalysts for degrading CW agents, particularly from the perspective of future production-scale efforts, in that production costs are expected to be even lower than for catalysts produced under nitrogen. In addition, catalysts produced under oxygen are less likely to be oxidized when exposed to the atmosphere than those produced under nitrogen, and the resulting skin cream therefore easier to produce, package, and store. However, little work had been done on these catalysts under the

earlier rTSP work. Of the ten catalysts sent for Government GD/HD testing under the purchase order, only two were produced under oxygen. One of these (TF001/F_s) performed well against both GD and HD, and another (TM001/M) performed exceptionally well against GD. In addition, several catalysts produced under oxygen had performed well against DFP in vial or flow cell tests at Biopraxis, but had not yet been tested in Government GD/HD tests.

On the environmental remediation studies, Biopraxis had identified two other production parameters that can significantly impact the properties of the catalyst. The available data suggested there may have been similar phenomena occurring with catalysts in the rTSP program. Because experiments with agent simulants had not been specifically designed to address the impact of these parameters, the data were often scattered and incomplete. However, in some cases, the production parameters that produced catalysts that were more effective in DFP and CEES vapor test results were the same as those that produced superior catalysts against environmental pollutants.

Accordingly, most of the work on the current rTSP program concentrated on catalysts produced under oxygen; and explored the impact of the other production parameters on simulant treatment efficacy, using the production methods developed elsewhere. During catalyst production, two alternatives for each of the two key production parameters were used, resulting in a matrix of four 'recipes' for each type of catalyst. Three catalysts were chosen for use in studies to evaluate the impact of tailoring these production parameters, i.e.:

- TF001/F_s — This catalyst performed very well against GD (81.3% reduction in agent penetration over 20 hours' exposure to vapor, in comparison with 13004) and moderately well against HD (56.4% reduction) in Government testing after the initial Biopraxis rTSP program; and also performed well against DFP and CEES in Biopraxis vial tests during the initial rTSP program. Production parameter alternatives were "F" vs "FM" and "C" vs "D".
- TM001/M — This catalyst performed very well against GD (83.8% reduction) and moderately well against HD (41.9% reduction) in Government testing after the initial Biopraxis rTSP program; and performed well against DFP in vial tests and flow cells at Biopraxis. Production parameter alternatives were "M" vs "MF" and "G" vs "C".
- MM001/M — This catalyst did well against DFP in vial tests and Reifenrath formulation tests at Biopraxis, but performed only moderately well in Government tests against GD (10.9% reduction, using a formulation prepared by Biopraxis on the initial rTSP program). Production parameter alternatives were "M" vs "MF" and "G" vs "C".

The initial production run was done on a small (100 mL) scale, to produce enough material for in-house vial tests against DFP and CEES. The most effective catalysts were then to be produced on a larger (2 L) scale to provide samples for Government testing (see below).

Surprisingly, the MM001/MG recipe did not produce any catalyst. This may have been due to some sort of contamination, or possibly an inadvertent failure to include all of the necessary ingredients. It was also disappointing, since the combination of M and G was highly effective at producing catalysts in the TM001 matrix; i.e., high percentages of both DFP and CEES were removed / destroyed during simulant testing. The other recipes produced the expected yield of catalyst, and were characterized and screened against simulants.

Catalyst Characterization

Studies on environmental remediation had found, surprisingly, that a single production run could yield more than one type of particle (e.g., the particles were visibly different from each other when examined under the microscope), and that the different particles in a single run have different catalytic properties. Therefore, the efficacy of the rTSP formulation might be optimized by

maximizing the proportion of a given type of particle incorporated into the skin cream. This could be accomplished by developing methods for separating the particle types after production and only incorporating the most active particles into the rTSP. Alternatively, production of a particular particle-type might be maximized by altering the production parameters. (Preliminary studies on environmental remediation indicate the latter alternative may indeed be feasible.) In addition, future catalyst bulk-scale production will require analytical methods to assess catalyst quality.

Therefore, the catalysts were subjected to a series of analyses, using techniques that enabled data to be collected from individual particles in mixtures (e.g., light microscopy, Raman microscopy, scanning electron microscopy, etc.) These analyses reveal information on the proprietary nature of the catalysts, and are not included in this report.

Catalyst Testing with Simulants

The catalysts are produced in water and are highly porous (i.e., each particle contains an exceptionally large reservoir of water.) Earlier studies indicated that they could be freeze-dried and still exhibit catalytic activity (although in some instances, the range of environmental pollutants against which they were effective was altered.) Dried catalysts were easier to screen against simulants, since water vapor could have an affect in and of itself (e.g., hydrolyze the CEES). Accordingly, freeze-dried catalysts were tested for efficacy against DFP and CEES in simple vial tests. 3.0 ± 0.1 mg catalyst was placed into a 10 mL gas-tight, PTFE/silicon septum vial, along with either 2.5 pL of CEES or 2.0 pL DFP on a cellulose paper filter, and incubated at 20°C for 24 hr. Standards ranged from 0.1 - 2.0 pL DFP, or 0.1 - 2.5pL CEES, on cellulose paper filters. Samples, catalyst-only controls, and standards were all run in triplicate. After incubation, a 10 cc gas-tight syringe was used to pull a 1 mL vapor sample from each vial, and the vapor was injected directly into the GC. The syringe was flushed with compressed air between injections. Analyses were done on a Buck Scientific 910 GC equipped with an Alltech AT-5 (30m) column, and flame ionization (FID), photoionization (PID), and dry electrolytic conductivity (DELCD) detectors. The DELCD is sensitive to halogenated compounds, while the PID is sensitive to unsaturated compounds. The FID hydrogen gas was set at a flow rate of 25 mL/min. Both the FID and PID were run at 150°C, and the DELCD at 1200°C. The chromatographic grade helium carrier gas was set at 6 psi. The column-oven temperature was ramped from 40°C to 170°C over 10 min when analyzing DFP, and from 40°C to 200°C over 10 min when analyzing CEES.

In most cases, the production parameters had a significant impact on catalyst efficacy against DFP and CEES (Table 1.) The pattern of these effects was often similar for the two simulants; i.e., catalysts that were effective against DFP also tended to be effective against CEES.

For the TM001 matrix, the most effective catalyst against both DFP and CEES was produced when M and G were the key production parameters. This combination produced a catalyst that removed and/or destroyed 653.0 ± 27.5 mg DFP / g catalyst, representing $92.3 \pm 0.5\%$ of the DFP added to the vial (Figure 1). This same catalyst removed and/or destroyed 594.7 ± 100.0 mg CEES / g catalyst, representing $83.0 \pm 12.5\%$ of the CEES added to the vial (Figure 2). It was interesting to note the trends in efficacy for this catalyst against DFP. With either M or M_F, catalysts produced with G outperformed those produced with C; and with either G or C, those produced with M outperformed those produced with M_F. Although such definite matrix patterns were not seen in the results for CEES, the catalyst that performed best against DFP also exhibited superior efficacy against CEES.

The results of this matrix was particularly interesting, since TM001/MC was the recipe used to prepare the catalyst that performed very well against GD (ICD3554 yielded an 83.8% reduction in GD penetration) and moderately well against HD (41.9% reduction) in earlier Government tests. If simulant vial testing could be used to predict formulation efficacy against surety material, the new TM001/MG recipe should yield a catalyst with superior performance against both chemical

warfare agents.

Table 1. Results of Simulant Tests with Freeze-Dried Catalysts
(Italics indicate recipes previously tested by the Government)

<i>Catalyst</i>	Percent <i>DFP removed/destroyed</i>	Percent <i>CEES removed/destroyed</i> I
TF001/FC	98.5 ± 2.5%	84.5 ± 14.0%
TF001/FD	29.9 ± 51.8%	57.2 ± 38.3%
TF001/F _m C	33.3 ± 57.6%	51.1 ± 26.4%
TF001/F _m D	52.9 ± 50.2%	77.4 ± 25.1%
TM001/MG	92.3 ± 0.5%	83.0 ± 12.5%
<i>TM001/MC</i>	74.0 ± 9.0%	20.8 ± 36.0%
TM001/M _F G	84.4 ± 6.3%	65.1 ± 15.2%
TM001/M _F C	65.1 ± 0.6%	66.8 ± 45.1%
<i>MMON/MC</i>	44.1 ± 45.1%	47.7 ± 24.1%
MM001/M _F G	39.2 ± 36.5%	45.5 ± 28.9%
MM001/M _F C	28.5 ± 27.1%	19.1 ± 10.6%
MSR03/FL	99.9 ± 0.05%	
MSR03/MF	52.8 ± 6.9%	
MSR03/ML	27.3 ± 62.8%	
MSR06/ML	85.0 ± 21.2%	
MSR06/FL	80.1 ± 22.6%	

The vial test results for TF001 showed the most effective catalyst against DFP and CEES was produced with F and C as the key production parameters. The resulting catalyst removed/destroyed 688.8 ± 24.4 mg DFP / g catalyst (98.5 ± 2.5% DFP removed/destroyed; Figure 3). This was one of the few vial tests in which breakdown products could be detected. This same catalyst was also the most effective against CEES, removing/destroying 569.5 ± 65.3 mg CEES / g catalyst (85.4 ± 14.0% CEES removed/destroyed; Figure 4). When comparing Figures 3 and 4, it was apparent that although the exact ratios are different, the overall trends within the matrices were similar for DFP and CEES.

A variation on the TF001/FD recipe was used to prepare the TF001/F_s catalyst that was effective against both GD (81.3% reduction) and HD (56.4% reduction) in earlier Government penetration cell tests. TF001/F_s removed/destroyed 83% of the DFP and 66% of the CEES in earlier vial tests. If the simulant vial test results could be used to predict surety material formulation results, TF001/FC might provide even better performance against CW agents.

Overall, MM001 catalysts performed only moderately well compared to those in the TM001 and

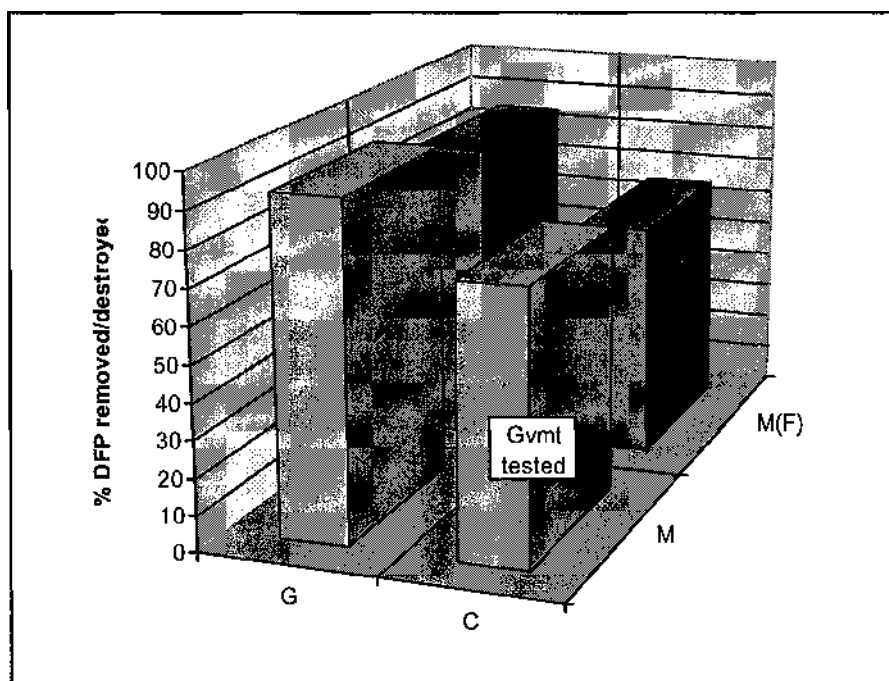


Figure 1: TM001 vial tests against DFP

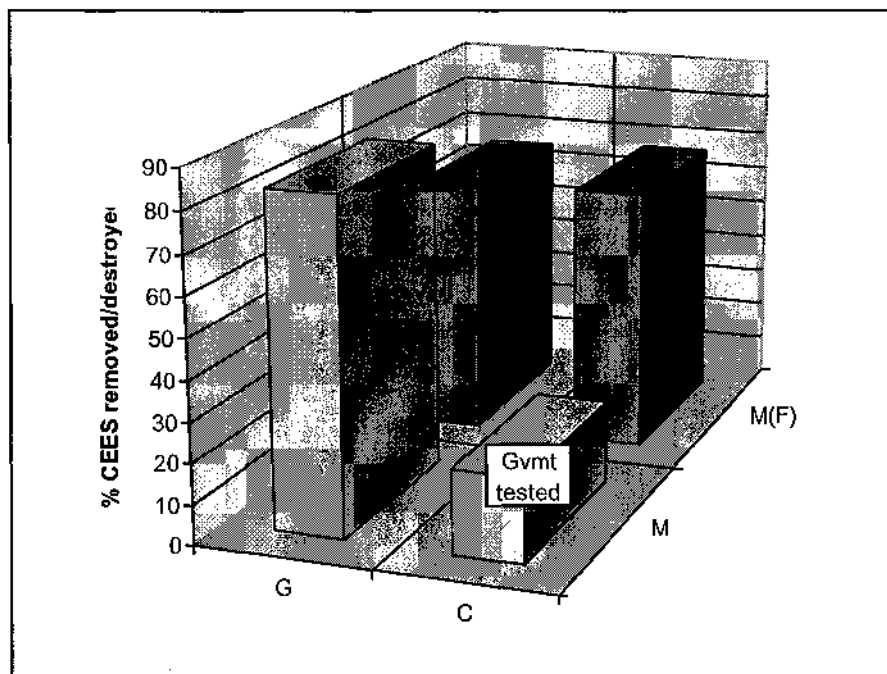


Figure 2: TM001 vial tests against CEES

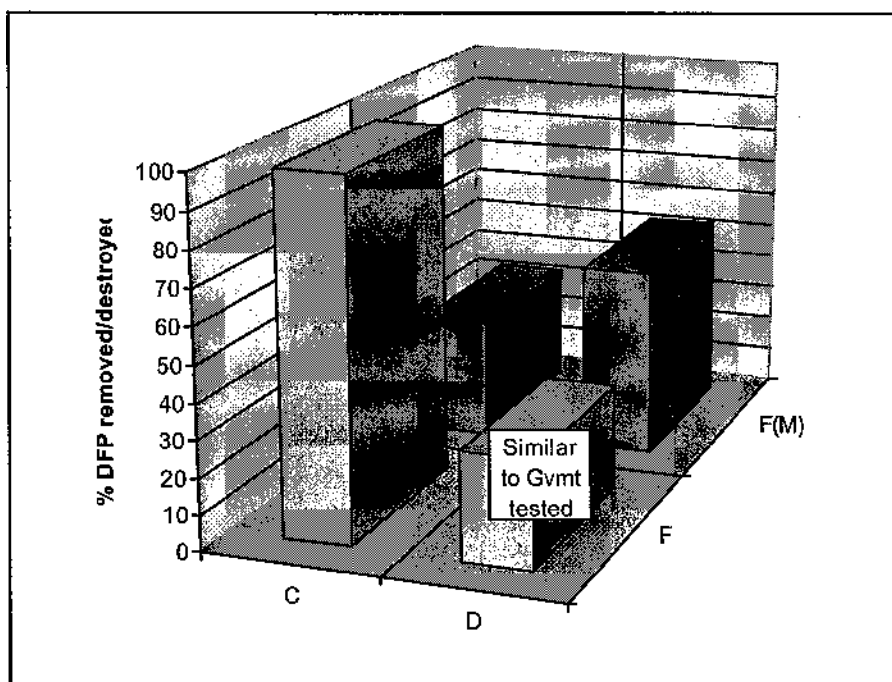


Figure 3: TF001 vial tests against DFP

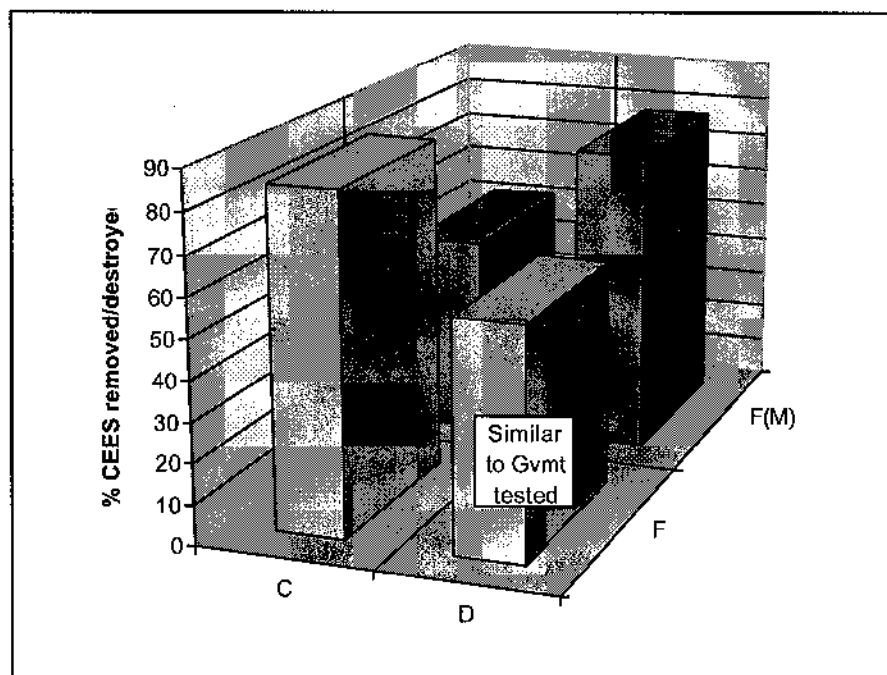


Figure 4: TF001 vial tests against CEES

TF001 matrices. The most effective MM001 catalyst removed/destroyed 292.2 ± 289.7 mg DFP / g catalyst, or $44.1 \pm 45.1\%$ of the DFP placed in the vial (Figure 5). This same catalyst removed/ destroyed 333.6 ± 171.7 mg CEES / g catalyst, or $47.7 \pm 24.1\%$ of the CEES in the vial (Figure 6). However, like the other catalyst matrices, MM001 catalysts also exhibited similar patterns in efficacy against DFP and CEES (compare Figures 5 and 6), with the exception that, as noted above, the combination of M and G did not produce any catalyst at all. This was an unexpected result, since the MM001/MG recipe is very similar to the MM001/MC recipe; and since switching from the TM001/MC to the TM001/MG recipe not only produced a catalyst, but yielded a superior one.

The MM001/MC recipe was used to prepare the formulation that yielded 10.9% GD reduction in earlier Government tests (ICD3361). Since tailoring the MM001 recipe did not appear to have produced a more effective catalyst, the MM001 series was dropped from the Government test program.

In order to provide as many samples to the Government for testing as possible, the simulant test matrix with the MSR03 and MSR06 catalyst series against DFP was incomplete, and studies were not done with CEES. MSR03/FL performed moderately well in earlier Government tests (65.3% reduction in GD penetration, and 53.2% reduction in HD penetration.) Substituting M for F, and substituting F for L, can produce superior and/or very unusual catalysts. DFP tests, however, indicated that the original 'recipe' produced the best catalyst, with essentially all DFP removed / destroyed during the test period, whereas MSR03/MF and MSR03/ML did not do nearly as well (52.8 and 27.3% DFP removed / destroyed, respectively.) MSR06/FL performed extremely well in earlier Government tests (93.1% reduction of GD penetration, and 81.5% reduction of HD penetration); and environmental remediation studies found that substituting M for F could produce a catalyst that is superior for other applications. MSR06/ML may have performed marginally better against DFP, although the difference was not statistically significant.

Catalyst Selection and Production for Government Testing

Three catalysts were used in earlier Government weanling pig tests, in formulations ICD3603 (based on TF001/F.), ICD3553 (based on TSR06/M), and ICD3600 (based on MSR06/F). Despite very promising penetration cell tests, none of these formulations appeared to be effective in the weanling pig tests.

The formulations used in the weanling pig tests were prepared under air and stored under air for as long as nine months. It is highly likely that the catalysts were oxidized during the prolonged storage under adverse conditions. Biopraxis requested that the Government (a) retest the air-stored formulations by the Reifenrath protocol, to confirm that their efficacy was degraded, and then (b) conduct new animal tests using freshly-prepared formulations, if the penetration cell tests indicate that the stored formulations are no longer effective. The Government testing was halted, due to lack of funds (monies were diverted to support the war in Iraq) before this could be done.

It should be noted that analysis of the results from Government surety tests should take into account when the Government prepared the formulation, whether it was prepared under air, and how long it was stored (and under what conditions) before tests were conducted. However, this information has not been made available to Biopraxis and therefore could not be included in this report.

Six catalysts were chosen from the modified production experiments; in addition, nine were chosen based on results from environmental remediation studies that indicated new and unusual catalysts had been developed.

Three pairs of catalysts were prepared from recipes in which catalysts are produced under oxygen,

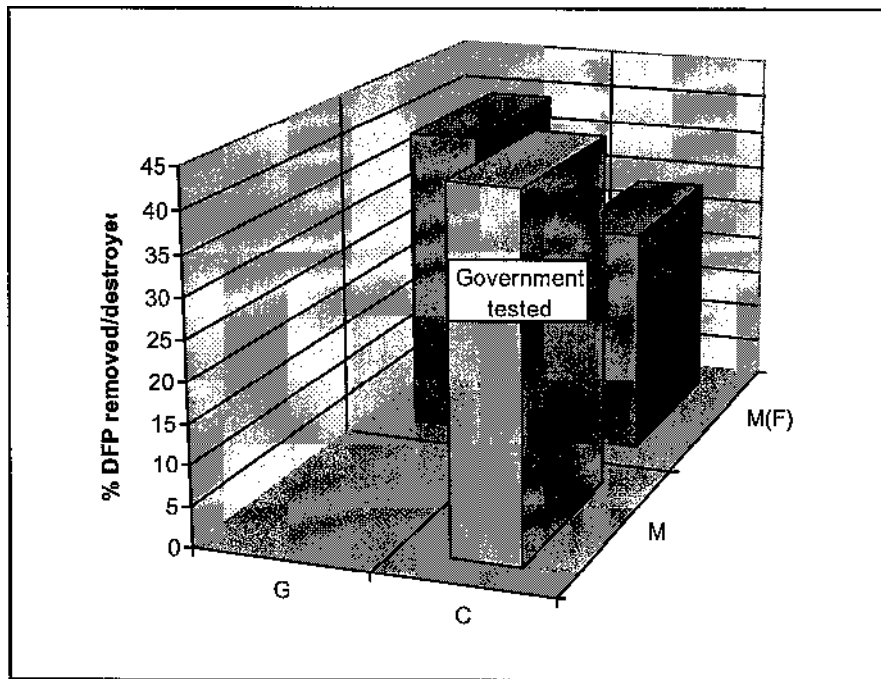


Figure 5: 1VEVI001 vial tests against DFP

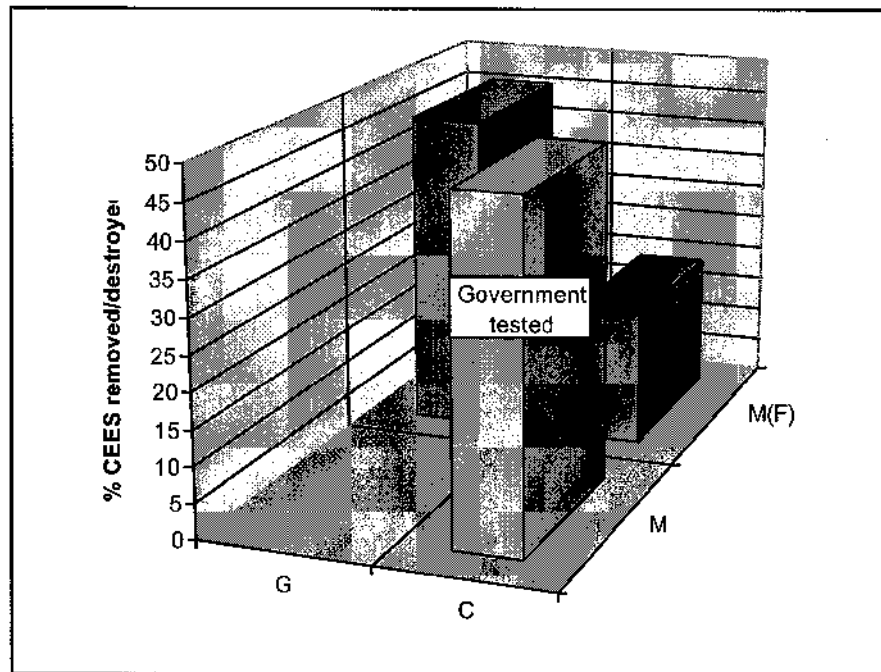


Figure 6: MM001 vial tests against CEES

•
i.e., one that was sent to the Government previously and performed well, matched against one produced by a modified recipe that appeared to be more effective against simulants. These included:

- TM001/MC and TM001/MG

TM001/MC performed very well against GD and moderately well against HD in earlier Government penetration cell tests, and performed well against DFP in vial tests and penetration cell tests at Biopraxis. TM001/MG exhibited greater efficacy against DFP and substantially great efficacy against CEES in recent vial tests.

- TF001/FC and TF001/FD

TF001/F_s performed very well against GD (81.3% reduction) and moderately well against HD (56.4% reduction) in earlier Government testing; and also performed well against DFP and CEES in earlier Biopraxis vial tests. TF001/FD was substantially better at removing/degrading both DFP and CEES than TF001/FD, which is a variation of the TF001/F, recipe.

- TF001/F_s and TF001/M,

As noted above, TF001/F_s did very well in earlier Government tests. Studies on environmental remediation have found that substituting M for F can produce more reactive material.

Another nine catalysts were chosen on the basis of environmental remediation studies. As mentioned earlier, these studies identified some key production parameters that produced superior catalysts under nitrogen. Some of the catalysts that performed well in earlier Government tests were modified using these new recipes, which appeared to produce catalysts with interesting properties. Due to timing and funding constraints, the "new, improved" version(s), as well as a fresh batch of the original catalyst, were provided to USAMRICD without simulant testing. (Aliquots of each sample were retained at Biopraxis, and some limited DFP testing, as reported above, was done after the samples had been sent to the Government.) The catalysts that were provided included:

- MSR06/FL and MSR06/ML

MSR06/FL performed extremely well in earlier Government tests (93.1% reduction of GD penetration, and 81.5% reduction of HD penetration.) Environmental remediation studies found that substituting M for F could produce a catalyst that is superior for other applications.

- MSR03/ML, MSR03/FL, and MSR03/MF

MSR03/FL performed moderately well in earlier Government tests (65.3% reduction in GD penetration, and 53.2% reduction in HD penetration.) As noted above, substituting M for F can produce a catalyst that is superior for other applications. In addition, substituting F for L can produce very unusual catalysts.

- TSR02/MF and TSR02/ML

TSR02/MF performed moderately well in earlier Government tests (56.5% reduction in GD penetration, and 52.6% reduction in HD penetration.) Substituting L for F can produce a catalyst that is superior for other applications.

- MSR05/FL and MSR05/ML

- MSR05/FL performed moderately well in earlier Government tests (51.8% reduction in GD penetration, and 53.8% reduction in HD penetration.) As noted above, substituting M for F can produce a catalyst that is superior for other applications.

Two-liter samples of all of these catalysts were prepared and sent to the Government for testing with surety materiel.

Government Testing with Surety Materiel

As noted above, Government testing was cut short by the diversion of funds to support the war in Iraq. The two TF001 series of catalysts were not tested at all. A single formulation of the other catalysts was tested against HD and/or GD in vapor penetration cells. The results were compared against Government ICD# 3004 (TSP) which had a time to breakthrough (1,000 ng) for HD of 586 ± 87 minutes, and a total penetration at 20 h of 2758 ± 299 ng HD; and a time to breakthrough (1,000 ng) for GD of 346 ± 68 minutes, and a total penetration at 20 h of 6672 ± 865 ng GD.

As above, it should be remembered that preparation and storage under air may adversely affect formulations containing catalysts prepared under nitrogen. Biopraxis has found that these catalysts are stable for years if kept under nitrogen; and a skin cream could be prepared and sealed into tubes under anoxic conditions. Information on formulation preparation and storage, and the length of time the formulation was stored prior to testing, was not provided to Biopraxis, and therefore could not be considered in the following analyses. Moreover, the methods used to prepare a given formulation (e.g., the percentage of each component, whether moist or freeze-dried catalyst was used, and the method used to mix all the components together) can have a significant impact on how well the formulation performs; a poorly mixed formulation may break through immediately even if the catalyst itself is highly effective against the agent. Accordingly, the results given below reflect the *minimum* performance that a given catalyst may yield.

• TM001/MC and TM001/MG:

In earlier Government vapor penetration cell tests, TM001/MC performed very well against GD (1182 ± 148 minutes to breakthrough, a 342% increase over TSP, and 1081 ± 444 total ng penetration in 20 h, a 84% reduction in comparison with TSP) and moderately well against HD (944 ± 140 minutes to breakthrough, a 161% increase in over TSP, and 1601 ± 329 ng penetration in 20 h, a 42% reduction in comparison with TSP).

The formulation that was prepared this time was tested against GD and HD vapors again. It did even better, taking $4,642 \pm 2,389$ minutes to breakthrough (an increase of 1,342% in comparison with TSP), and 124 ± 121 total ng at 20 h (a reduction of 98%). It should be noted that the data from three of the five cells clustered together, with an average of 6,372 minutes to breakthrough (1,842% increase), and 36 ng penetration at 20 h (99.5% reduction), while the other two averaged 2,046 minutes and 256 ng, respectively. I.e., the catalyst would yield even better performance if the formulation were mixed/spread consistently.

TM001/MG exhibited greater efficacy against DFP and substantially great efficacy against CEES in vial tests. It was tested as a single formulation, against GD, by the Government. The results were excellent, i.e., $3,686 \pm 3,194$ minutes to breakthrough, an increase of 1,065%; and 459 ± 395 ng penetration in 20 h, a reduction of 93% in comparison with non-reactive TSP (13004). Individual cell data were not provided; but the very large standard deviations indicate that several cells did far better than the average. The Government did not test the formulation against HD.

• MSR06/FL and MSR06/ML:

In earlier Government tests, MSR06/FL performed extremely well (93.1% reduction of GD penetration, and 81.5% reduction of HD penetration.) The formulation that was prepared this time

was tested against GD and HD vapors again. Performance against GD was extraordinary; i.e., 57,096+44,512 minutes to breakthrough (16,502% increase) and 3+4 ng penetration at 20 h (99.96% reduction). Performance against HD was good; i.e., 1,269+477 minutes to breakthrough (217% increase) and 1,131+734 ng penetration by 20 h (59% reduction.)

Environmental remediation studies found that substituting M for F could produce a catalyst that is superior for other applications. MSR06/ML had been tested against DFP (after the catalyst was submitted to the Government), but was tested against HD only by the Government. It did well in comparison with 13004 (1,105+370 minutes to breakthrough, a 189% increase; and 1,183+663 ng penetration by 20 h, a 57% reduction), but not as well as hoped.

- MSR03/ML, MSR03/FL, and MSR03/MF:

MSR03/FL performed moderately well in earlier Government tests (65.3% reduction in GD penetration, and 53.2% reduction in HD penetration.) Substituting M for F can produce a catalyst that is superior for other applications. In addition, substituting F for L can produce very unusual catalysts. These catalysts were screened against DFP only, after samples had been sent to the Government for evaluation. MSR03/FL did very well against DFP; the others were not nearly as effective.

The Government spreadsheet reports having made formulations from five MSR03 catalysts, three of which were given codes that do not match the codes provided to the Government. It is therefore difficult to determine which catalysts were actually tested as formulations and how their performance matched expectations.

Apparently, MSR03/FL was not tested against surety materiel.

MSR03/ML was apparently tested against HD only. It did well in comparison with 13004; i.e., 1,411+349 minutes to breakthrough (241% increase) and 619+108 ng penetration by 20 h (78% reduction.)

"MSR03/MLA" was screened against both HD and GD. It did very well against GD; time to breakthrough was 2,055+688 minutes (594% increase) and total penetration by 20 h was 222+85 ng (97% reduction.) This formulation also yielded the best performance against HD of those tested on this program; i.e., time to breakthrough of 1,571+98 minutes (268% increase) and total penetration at 20 h or 598+70 (78% reduction.)

"MSR03/MX" and "MSR03/MLB" were screened against HD. "MSR03/MX" did well, increasing the time to breakthrough by 201% (1,179+94 minutes) and reducing total penetration at 20 h by 63% (1,029+176 ng), which was better than MSR03/FL in the earlier Government tests, although not as well as some other catalysts that were studied on this program. "MSR03/MLB" exhibited a similar efficacy against HD, increasing time to breakthrough by 188% (1,101+80) and reducing penetration by 57% (1,198+158 ng.)

- TSR02/MF and TSR02/ML:

TSR02/MF performed moderately well in earlier Government tests (56.5% reduction in GD penetration, and 52.6% reduction in HD penetration.) The new formulation made with this catalyst was tested against HD only. It exhibited a similar efficacy this time, increasing time to breakthrough by 197% (1,154+104 minutes) and reducing penetration at 20 h by 60% (1,095+204 ng.)

Substituting L for F can produce a catalyst that is superior for other applications. Due to time and funding constraints, TSR02/ML was not tested against simulants. The Government spreadsheet

does not show a TSR02/ML but does list a "TSR02/MC", which is presumably a typographical error. This catalyst was screened against HD, and its performance was very similar to that of TSR02/MF; i.e., it increased time to breakthrough by 203% (1,187+118 minutes) and reduced penetration by 62% (1,035+217 ng.)

- **MSR05/FL and MSR05/ML:**

MSR05/FL performed moderately well in earlier tests (51.8% reduction in GD penetration, and 53.8% reduction in HD penetration.) It was not tested by the Government on this program.

As noted above, substituting M for F can produce a catalyst that is superior for other applications. MSR05/ML was screened against both GD and HD. It increased the time to breakthrough for GD by 531% (1,836+1,212 minutes) in comparison with 13004 and reduced penetration by 94% (412+445 ng.) It also the time to breakthrough for HD by 201% (1,175+325 minutes) in comparison with 13004 and reduced penetration by 57% (1,175+594 ng.) I.e., the new catalyst recipe significantly improved performance against GD, while retaining its efficacy against HD.

In short, all of the formulations tested against surety materiel by the Government had substantially improved efficacy against GD and/or HD, in comparison with the non-reactive TSP. Some were extraordinary; e.g., MSR06/FL, which did not allow any detectable GD penetration for 20 h and was projected to take more than 950 hours (40 days) to reach breakthrough. This same formulation also showed excellent efficacy against HD.

It should be noted that, since these catalysts are solid particulates, catalysts with different chemistries do not interact with each other. Therefore, a mixture of different catalysts may be used to produce a superior skin cream formulation. Environmental remediation and earlier rTSP studies showed that the results obtained with mixtures were often synergistic rather than additive; i.e., were much more effective than might be predicted on the basis of single-catalyst tests.

KEY RESEARCH ACCOMPLISHMENTS

- Catalyst production parameters that were shown to improve performance against pollutants on environmental remediation programs were explored for their ability to improve performance against CW agents. As far as can be determined from the limited testing that was done, catalyst performance can be predicted on the basis of simulant testing, and can be improved by "tweaking" the catalyst production parameters.
- Fifteen catalysts were prepared for Government surety materiel testing. All of the formulations that were screened showed substantially superior performance against GD and/or HD, in comparison with the non-reactive TSP.
- The most effective formulation against GD, made with MSR06/FL catalyst, did not allow any detectable GD penetration for 20 h and was projected to take more than 950 hours (40 days) to reach breakthrough. This same formulation also showed excellent efficacy against HD.
- The most effective formulation against HD, made with "MSR03/MLA" catalyst, increased the time to breakthrough by 268%, in comparison with the non-reactive TSP (i.e., did not reach breakthrough for more than 26 h), and reduced penetration by 78% (i.e., allowed only 598 ng to penetrate in 20 h.) It also did very well against GD; time to breakthrough was increased by 594% to more than 34 h, and total penetration was reduced by 97% to only 222 ng in 20 h.

REPORTABLE OUTCOMES

- 'Microcatalysts as Active Moieties for Topical Skin Protectants,' Ann E. Grow, Biopraxis, Inc., and Ernest H. Braue, Jr., USAMRICD, presented at the U.S. Army Medical Research and Materiel Command (*USAMRMC Bioscience 2002 Medical Defense Review*).
- Funding for the rTSP development program area was halted in order to conserve Government monies for the war in Iraq.

CONCLUSIONS

The concept of applying a topical protectant to vulnerable skin surfaces before entry into a chemical combat arena has been proposed as a means of protecting troops from percutaneous chemical warfare agent toxicity since these weapons were first used during World War I. Topical protectants would augment the protection afforded by the protective overgarments or, ideally, redefine the circumstances requiring Mission Oriented Protective Posture (MOPP) levels. The rapid action of vesicating agents such as sulfur mustard and lewisite suggests that a preexposure skin protection system, or a contamination avoidance approach, offers the best opportunity to prevent the serious consequences of the percutaneous toxicity of blistering agents. A skin protectant also reduces the risk of exposure to organophosphorus agents which, unlike vesicants, are lethal in droplet amounts. In addition, the development of improved prophylactics for CW agents can deter their use by the enemy, and increase the warfighter's capability to sustain his operational tempo.

The U.S. Army Chemical School has developed a topical skin protectant (TSP) against CW agents (now called "SERPACWA") that extends the protection afforded by MOPP and allows a longer window for decontamination. However, since it is a non-reactive barrier cream, it does not completely remove the possibility for contamination and, therefore, decontamination is still required. In addition, it does not provide very good protection against mustard vapor. In order to overcome these deficiencies, there is a clear need for a next generation TSP that contains a reactive component that will decontaminate CW agents as well as protect against nerve and mustard vapors.

The work that has been done to date has been extremely successful. Vial screening tests identified many, diverse catalysts that showed efficacy against DFP and/or CEES. Catalyst production parameters that can be "tweaked" to improve performance have been identified. Government formulation testing against surety materiel has identified many catalysts that exhibit excellent efficacy against GD and/or HD. Several methods can be used to enhance performance even further, notably the use of catalyst mixtures and optimizing the composition of the formulation. Many promising, new catalysts remain to be screened. Since the precursors are inexpensive and the simple production method offers a high yield under ambient conditions, the costs for producing the catalysts in bulk are expected to be very low.

SBIR final report from Nantek, Inc, Phase II

Award Number: DAMD17-97-C-7016

AD _____

Award Number: DAMD17-97-C-7016

TITLE: Development of Reactive Topical Skin Protectants Against
Sulfur Mustard and Nerve Agents

PRINCIPAL INVESTIGATOR: Kenneth J. Klabunde, Ph.D.

CONTRACTING ORGANIZATION: Nantek, Incorporated
Manhattan, Kansas 65502

REPORT DATE: July 2000

TYPE OF REPORT: Final, Phase II

PREPARED FOR: U.S. Army Medical Research and Materiel Command
Fort Detrick, Maryland 21702-5012

DISTRIBUTION STATEMENT: Distribution authorized to U.S.
Government agencies only (specific authority). Other requests
for this document shall be referred to U.S. Army Medical
Research and Materiel Command, 504 Scott Street, Fort Detrick,
Maryland 21702-5012.

The views, opinions and/or findings contained in this report are
those of the author(s) and should not be construed as an official
Department of the Army position, policy or decision unless so
designated by other documentation.

NOTICE

USING GOVERNMENT DRAWINGS, SPECIFICATIONS, OR OTHER DATA INCLUDED IN THIS DOCUMENT FOR ANY PURPOSE OTHER THAN GOVERNMENT PROCUREMENT DOES NOT IN ANY WAY OBLIGATE THE US GOVERNMENT. THE FACT THAT THE GOVERNMENT FORMULATED OR SUPPLIED THE DRAWINGS, SPECIFICATIONS, OR OTHER DATA DOES NOT LICENSE THE HOLDER OR ANY OTHER PERSON OR CORPORATION; OR CONVEY ANY RIGHTS OR PERMISSION TO MANUFACTURE, USE, OR SELL ANY PATENTED INVENTION THAT MAY RELATE TO THEM.

SBIR DATA RIGHTS LEGEND

Contract: DAMD17-97-C-7016
Contractor: Nantek, Incorporated

For a period of five (5) years after completion of the project from which the data was generated, the Government's rights to use, modify, reproduce, release, perform, display, or disclose any technical data or computer software contained in this report are restricted as provided in paragraph (b)(4) of the Rights in Noncommercial Technical Data and Computer Software Small Business Innovative Research (SBIR) Program clause contained in the above-identified contract [DFARS 252.227-7018(Jun. 1995)]. No restrictions apply after expiration of that period. Any reproduction of technical data, computer software, or portions thereof marked as SBIR data must also reproduce those markings and this legend.

This technical report has been reviewed and is accepted under the provisions of the Small Business Innovation Research Program.

This report is published in the interest of scientific and technical information exchange and does not constitute approval or disapproval of its ideas or findings.

Do not return copies of this report unless contractual obligations or notice on a specific document requires its return.

REPORT DOCUMENTATION PAGE

Form Approved
OMB No. 074-0188

Public reporting burden for this collection of information is estimated to average 1 hour per response, including the time for reviewing instructions, searching existing data sources, gathering and maintaining the data needed, and completing and reviewing this collection of information. Send comments regarding this burden estimate or any other aspect of this collection of information, including suggestions for reducing this burden to Washington Headquarters Services, Directorate for Information Operations and Reports, 1215 Jefferson Davis Highway, Suite 1204, Arlington, VA 22202-4302, and to the Office of Management and Budget, Paperwork Reduction Project (0704-0188), Washington, DC 20503

1. AGENCY USE ONLY (Leave blank)		2. REPORT DATE July 2000	3. REPORT TYPE AND DATES COVERED Final, Phase II(1 Jul 98 -30 Jun 00)	
4. TITLE AND SUBTITLE Development of Reactive Topical Skin Protectants Against Sulfur Mustard and Nerve Agents			5. FUNDING NUMBERS DAMD17-97-C-7016	
6. AUTHOR(S) Kenneth J. Klabunde, Ph.D.				
7. PERFORMING ORGANIZATION NAME(S) AND ADDRESS(ES) Nantek, Incorporated Manhattan, Kansas 65502 E-MAIL: kenjk@ksu.edu			8. PERFORMING ORGANIZATION REPORT NUMBER	
9. SPONSORING / MONITORING AGENCY NAME(S) AND ADDRESS(ES) U.S. Army Medical Research and Materiel Command Fort Detrick, Maryland 21702-5012			10. SPONSORING / MONITORING AGENCY REPORT NUMBER	
11. SUPPLEMENTARY NOTES				
12a. DISTRIBUTION / AVAILABILITY STATEMENT Distribution authorized to U.S. Government agencies only (specific authority). Other requests for this document shall be referred to U.S. Army Medical Research and Materiel Command, 504 Scott Street, Fort Detrick, Maryland 21702-5012.				12b. DISTRIBUTION CODE
<p>13. ABSTRACT (Maximum 200 Words)</p> <p>Research has been conducted regarding the development of a topical skin protectant containing reactive nanoparticles. Such a protectant cream will be able to detoxify multiple types of chemical warfare agents, which will enhance the effectiveness of the current technology.</p> <p>Nanoparticle formulations of simple metal oxides have been identified as the best agents for detoxification of CW simulants such as 2-chloroethyl ethyl sulfide, diisopropyl fluorophosphonate, paraoxon, and diethyl phenylthiomethylphosphonate. These chemicals are simulants for sulfur mustard, VX and G-agents. In the case of 2-CEES detoxification, the two major products are identified: ethyl vinyl sulfide and 2-(ethylthio)-ethanol. All of the phosphonate simulants undergo hydrolysis upon reaction with the nanoparticles.</p> <p>A number of enhancements for the synthesis of reactive nanoparticles have been developed. These enhancements have effectively doubled the specific surface area of the nanoparticles with corresponding increases in chemical reactivity.</p> <p>Work has also shown that nanocrystalline MgO and CaO are very good reagents for the decomposition of real CW agents such as VX, GD and HD. This research found that the MgO and CaO are highly reactive toward the three CW agents and that only the physical processes of liquid spreading and evaporation limit the reaction.</p>				
14. SUBJECT TERMS Chemical Defense, Topical Skin Protectant				15. NUMBER OF PAGES 125 / 26
				16. PRICE CODE
17. SECURITY CLASSIFICATION OF REPORT Unclassified	18. SECURITY CLASSIFICATION OF THIS PAGE Unclassified	19. SECURITY CLASSIFICATION OF ABSTRACT Unclassified	20. LIMITATION OF ABSTRACT Unlimited	

FOREWORD

Opinions, interpretations, conclusions and recommendations are those of the author and are not necessarily endorsed by the U.S. Army.

NA N/A Where copyrighted material is quoted, permission has been obtained to use such material.

N/A Where material from documents designated for limited distribution is quoted, permission has been obtained to use the material.

NA N/A Citations of commercial organizations and trade names in this report do not constitute an official Department of Army endorsement or approval of the products or services of these organizations.

N/A In conducting research using animals, the investigator(s) adhered to the "Guide for the Care and Use of Laboratory Animals," prepared by the Committee on Care and use of Laboratory Animals of the Institute of Laboratory Resources, national Research Council (NIH Publication No. 86-23, Revised 1985).

N/A For the protection of human subjects, the investigator(s) adhered to policies of applicable Federal Law 45 CFR 46.

N/A In conducting research utilizing recombinant DNA technology, the investigator(s) adhered to current guidelines promulgated by the National Institutes of Health.

N/A In the conduct of research utilizing recombinant DNA, the investigator(s) adhered to the NIH Guidelines for Research Involving Recombinant DNA Molecules.

N/A In the conduct of research involving hazardous organisms, the investigator(s) adhered to the CDC-NIH Guide for Biosafety in Microbiological and Biomedical Laboratories.

Tony Lau

PI - Signature

Date

Table of Contents

Front Cover	1
Report Documentation Page	2
Foreword	3
Table of Contents	4
Introduction	5
Project Results	6
Task 1. Novel Adsorbent Synthesis	7
Task 2. Investigation of Alternative Synthesis Approaches	10
Task 3. High Efficiency DAT Test Development	13
Task 4. DAT Characterization Using Warfare Simulants	17
Task 5. Comparison with Activated Carbon	22
Task 6. Destructive Adsorption of Paraoxon with Improved AP-MgO	24
Task 7. Comparative Studies with Activated Carbon	26
Task 8. Compatibility and Stability of RNPs in TSP Cream	32
Task 9. Solid Product Analysis	35
Task 10. Studies with Real Chemical Warfare Agents	37
Task 11. Formulation Development	41
Task 12. Final Formulation Selection	43
Task 13. Final Formulation Testing with Simulants	43
Task 14. Real Agent Testing of Nanoparticle rTSPs	53
Task 16. Economic Study of Scaled-up Production	57
Key Research Accomplishments	59
Reportable Outcomes	60
Conclusions	62
References	64
Index of Figures	65
Index of Tables	66
Appendices	67
List of Personnel Receiving Pay From This Research Effort	68

Introduction

The objective of this Phase II work is to develop a reactive nanoparticle technology to be incorporated into a reactive topical skin protectant (rTSP). The reactive topical skin protectant that is to be used to provide a secondary barrier capable of protecting military personnel from multiple forms of chemical warfare agents (HD, G-agents, VX). While a topical skin protectant has previously been developed which provides barrier protection, there is great interest in incorporating materials into the cream that will chemically decompose CW agents and thus provide additional protection for military personnel. Nantek's approach is to formulate highly reactive nanoparticles (RNPs) of metal oxides that behave as destructive adsorbents and to incorporate these RNPs into the current topical barrier cream. The objective of this work is to find the best synthetic methods and formulations of the RNP materials and test their destructive adsorption capabilities with chemical warfare (CW) simulants and later with actual chemical warfare agents.

In developing novel materials for reactive topical skin protectants there are several key items that need to be considered:

- 1) The active ingredient must be a non-toxic powder that can be blended with and remain suspended in the cream matrix.
- 2) It must destroy CW agents at acceptable rates under ambient temperature and high humidity.
- 3) It must be chemically compatible with the base skin cream and thereby retain its reactivity and stability within the TSP.
- 4) It must have a limited potential for irritation due to its close contact with human skin.
- 5) It must have a long shelf life.

The objective of this Phase II SBIR project was to demonstrate the feasibility of using reactive nanoparticle destructive adsorbents as the active ingredient for a reactive topical skin protectant against mustard gas and nerve agents. To meet this objective four major tasks were conducted:

- 1) Synthesis and examination of a broad array of nanoparticles under near ambient conditions to identify the best RNPs for incorporation into the base TSP.
- 2) Examine the compatibility of the RNPs in the base TSP. This focused on the suspension stability and the chemical compatibility of the nanoparticles with the other components of the base skin cream.
- 3) The performance of the nanoparticle destructive adsorbents was confirmed with real chemical warfare agents through limited laboratory tests conducted with a qualified independent laboratory.
- 4) Prototype rTSP systems incorporating RNP's were formulated and the reaction efficacy of the adsorbents evaluated on a preliminary basis.

Project Results

A great number of advances in RNP technology were accomplished during the Phase II project. All of these enhanced the development of a rTSP for the U.S. Army that is capable of detoxifying multiple types of CW agents.

Among the many important results were advances made in the synthesis of RNPs. During the project, many difficulties in the synthesis and mass production of RNPs have been conquered. These breakthroughs have also resulted in significant increases in the reactivity of the RNPs. For example, the specific surface area of one of our main RNPs, magnesium oxide (MgO) has been effectively doubled. This is important since the destructive adsorption of CW simulants are enhanced by the very high surface area and unique surface morphology of the RNPs. As important as the increased surface reactivity is the reduction of manufacturing costs. Enhancements to the large-scale production of this particular nanoparticle have significantly dropped the cost of the nanoparticles.

Another technical achievement has been the synthesis of new RNP materials such as nanocrystalline zinc oxide (ZnO) and iron oxide (Fe_2O_3) that are promising materials as destructive adsorbents. These new materials have shown efficacy for the detoxification of CW agent simulants and are known to be non-toxic. The "state-of-the-art" for these materials has been advanced to the point that Nantek, Inc. has successfully acquired a patent for both of these new RNP materials.

Work has shown that many types of these simple metal oxide nanoparticles are capable of decomposing CW agent simulants such as 2-chloroethyl ethyl sulfide (2-CEES or half mustard), paraoxon, diisopropyl fluorophosphonate (DFP), and diethyl phenylthiomethylphosphonate (DEPTMP). 2-CEES is a simulant of sulfur mustard and paraoxon is an insecticide with a molecular structure resembling VX. DFP is a simulant for the G-agents and DEPTMP was used as a sulfonated simulant of VX. The decomposition of 2-CEES by the nanoparticles proceeds via a dehydrochlorination. The two major products are ethyl vinyl sulfide ($\text{CH}_3\text{CH}_2\text{SCHCH}_2$) and 2-(ethylthio)-ethanol ($\text{CH}_3\text{CH}_2\text{SCH}_2\text{CH}_2\text{OH}$). For the phosphonated simulants, the decomposition proceeds via hydrolysis over the basic solid materials. For example, the nanoparticles decompose paraoxon to p-nitrophenol and diethyl phosphite. The RNPs are very good adsorbents and very strongly bind the CW simulants and the detoxified reaction products. This is an important consideration for materials to be included in a rTSP.

Research has been completed regarding tests to examine the compatibility and stability of the RNPs mixed in the TSP. Results have shown that the TSP does not degrade the RNPs and that the RNP/TSP can be stored for long times without deterioration of the RNPs. This indicates that it is possible to stockpile the RNP/TSP mixtures without worry about loss of efficacy. Also, it allows the protective cream to be mixed prior to application alleviating the need for mixing components on the battlefield by combat personnel.

Nantek has participated in collaboration with researchers at U.S. Army ERDEC-Aberdeen Proving Ground to test the capability of nanocrystalline MgO and CaO to decompose the real CW agents VX, GD and HD. This research found that both nanoparticle oxides were highly reactive toward the three CW agents but that the reaction is limited by the physical processes of liquid spreading and evaporation.

Research has been conducted to evaluate the nanoparticle containing TSPs in their efficacy in retarding the diffusion of real agents through the rTSP. While these results do

not indicate significant enhancement in the barrier properties of the material, they did indicate several simple problems that can be overcome through additional formulation testing.

A more detailed discussion of the research accomplishments for the approved Statement of Work is discussed in the following sections.

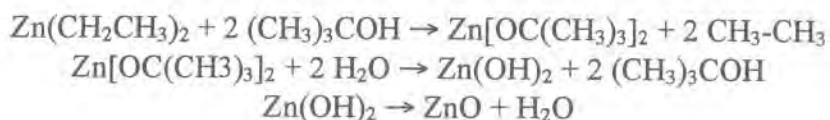
Task 1: Novel Adsorbent Synthesis

One of the best choices for an additive to a topical skin cream is zinc oxide since it is non-toxic and even has beneficial effects to the skin. Therefore, a major effort was placed on preparing high-surface-area zinc oxides. A large number of synthetic approaches were attempted and a description of the two most successful methods is given below. The work performed on these syntheses has led to a patent issued to Nantek, Inc. Since the work has led to a patent, the work is described in some detail.

Preparation of nanocrystalline zinc oxide from diethyl zinc.

The preparation consists of three main steps:

- A. Synthesis of the Zinc Oxide Powder
- B. Isolation of the Zinc Oxide Powder
- C. Thermal treatment of the Zinc Oxide Powder



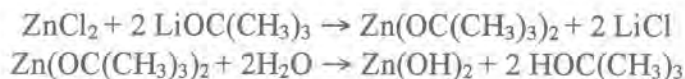
A. Synthesis of the zinc oxide powder. The starting materials were commercially available and used without further purification. In an argon filled inert atmosphere glove box 20-ml (0.020 mole) of 1.0 M diethyl zinc in hexanes was added to a 250-ml round bottom flask. The flask was removed from the glove box, placed under a head of argon gas, set on a stir plate and cooled to 0°C with an ice bath. Next a solution of 2.9-g (0.040 mole) t-butanol in 30-ml hexanes was added to the cooled diethyl zinc solution via syringe. This solution was added over a 5-10 minute time span so that the release of ethane was not extremely violent. Once this solution was completely added the ice bath was removed and the reaction warmed to room temperature (about 25°C). The reaction then continued stirring at room temperature for two hours. During this time the reaction mixture remained a clear colorless solution. Next, a solution of 0.72-ml (0.040 mole) water in 70-ml absolute ethanol was added to the reaction mixture. This solution was added drop-wise to the flask via syringe, which took 20-30 minutes. Once this solution was completely added the reaction was allowed to stir for an additional 2 hours. At this point the zinc oxide slowly formed a white colloidal solution.

B. Isolation of the zinc oxide powder. After the reaction was complete the argon line was removed and the reaction mixture was poured into a Schlenk tube (including a stir bar) and connected to a vacuum line equipped with a liquid nitrogen trap. While stirring at 25°C all of the solvent was evaporatively transferred from the Schlenk tube to the nitrogen trap leaving a dry, white zinc oxide powder.

C. Thermal treatment of the zinc oxide powder. The dry, white powder was placed into another Schlenk tube. This was then connected to a flow of argon and surrounded by a ceramic oven. The furnace was controlled by a temperature controller. The temperature was slowly raised from room temperature to 90°C where it remained for 4 hours. Next the temperature was slowly raised from 90°C to 250°C where it remained for an additional two hours. After the heat treatment was complete the Schlenk tube was allowed to cool to room temperature. The zinc oxide powder remained white during the heat treatment. It was found that this thermal treatment could also be carried out under vacuum with similar results. The percent yield for the ZnO was 85%.

Synthesis of nanocrystalline zinc oxide from zinc chloride

This second method for the preparation of nanocrystalline ZnO was carried out using zinc chloride and potassium tert-butoxide with heptane addition.



In a 250-mL round bottom flask with screw cap 2.73-g of ZnCl₂ in 125-mL of 2-propanol was dissolved with vigorous stirring. To a second 250-mL screw cap flask, 3.202-g of lithium t-butoxide and 125-mL of 2-propanol were added, which formed a thick gel. The second solution was added to the first and vigorously stirred for one hour. Next the solution was centrifuged and decanted. The resulting zinc alkoxide was then washed with 100-mL of 2-propanol. The zinc alkoxide was redispersed in 125-mL of 2-propanol and 3-mL of water was added drop wise with vigorous stirring for an additional 30 minutes. Then the solution was centrifuged and the solvent decanted. Next the zinc oxide was isolated and dried under vacuum. The surface area of the dried powder was 158 m²/g. Following drying, the powder underwent a heat treatment under flow of nitrogen for 20 seconds at 250°C. The specific surface area of the powder after heat treatment was 200 m²/g.

Characterization of the nanocrystalline zinc oxides

Elemental Analysis

Elemental analysis was conducted by Galbraith Laboratories and the results are shown in Table 1. In each analysis the percent by weight of zinc, carbon, and hydrogen was determined. The data shows that the zinc content was low and that the carbon, hydrogen, and oxygen content were high. This is due to the adsorbance of atmospheric contaminants such as CO₂ and H₂O, which form surface carbonates and hydroxyl groups. The percentage of ZnO in the sol-gel samples (denoted SG-ZnO) was found to be 86%. This is significantly lower than the commercial brands which generally claim to be 99% pure ZnO.

Table 1: Elemental analysis of zinc oxide.

Element	Found % from Et ₂ Zn	Found % from ZnCl ₂	Calculated % for ZnO	Calculated % for Zn(OH) ₂
Zinc	68.36	64.95	80.3	65.14
Carbon	0.71	2.36	0	-
Hydrogen	0.60	2.03	0	2.03
Oxygen (by difference)	30.33	30.66	19.7	32.54

X-ray Powder Diffraction and Specific Surface Areas

Powder x-ray diffraction studies were employed using a Scintag XDS 2000 spectrometer. Cu-K_α radiation was the light source used with an applied voltage of 40 KV and current of 40-mA. Two-theta angles ranged from 20° to 85° at a rate of 2° per minute. XRD was used to study the sol-gel zinc oxide samples as well as two commercial zinc oxide samples.

The diffraction patterns confirm that the SG-ZnO samples were ZnO but that they were less crystalline than the commercial ZnO samples. The SG-ZnO samples have much broader and less intense peaks than the commercial ZnO samples (Figure 1). This is due to an effect known as particle size broadening¹. Particle size broadening results when the sample is made up of very small crystallites. When the crystallite is small, smaller than 10-nm, the ability to obtain sharp diffraction peaks is lost.

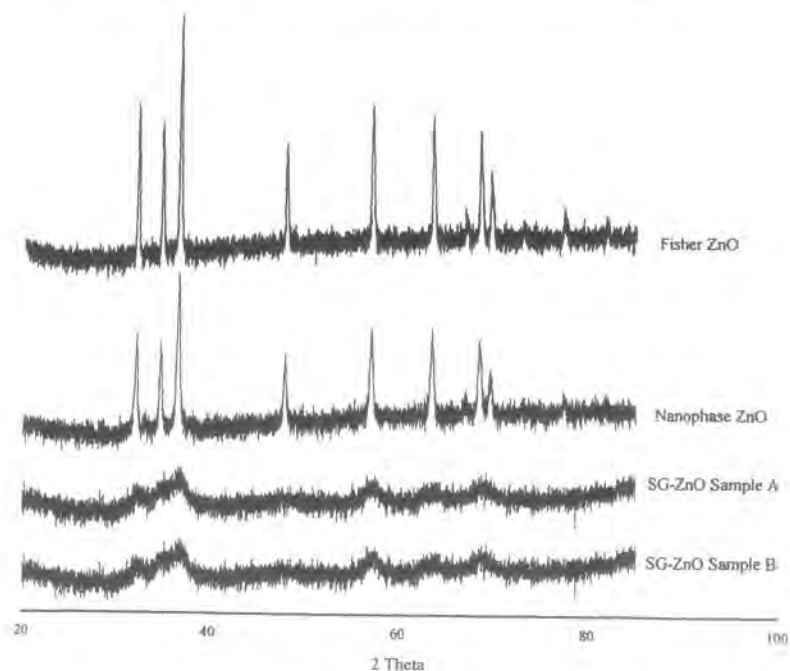


Figure 1: XRD of commercial and Nantek zinc oxides

These results show that the SG-ZnO has a significantly smaller crystallite size than the commercial ZnO samples (Table 2).

Table 2: Crystallite sizes and specific surface areas for various ZnO samples

Sample	Crystallite Size	Surface Area
*Fisher ZnO	42.1 nm	3 m ² /g
*Nanophase ZnO	32.3 nm	18 m ² /g
SG- ZnO Sample A	3.6 nm	108 m ² /g
SG- ZnO Sample B	4.2 nm	110 m ² /g
ZnO from ZnCl ₂	4.5 nm	173 m ² /g

* Commercial ZnO samples were heat treated in the same manner as the SG-ZnO samples.

Task 2: Investigation of Alternative Synthesis Approaches

At the beginning of this Phase II project, two synthetic approaches were used for preparation of high surface area metal oxides. These methods had been developed at Dr. Kenneth Klabunde's chemical laboratory at Kansas State University and had been "scaled-up" to a large batch scale reaction producing approximately 100-g of material per day.

The first of these two synthetic methods was dubbed the "CP" process for conventional preparation. This is the easier of the two methods but the surface area, and thus the chemical reactivity, of the material is lower than the second process. The second process was named the "AP" process since the material was produced via an aerogel preparation. This method produces a more reactive product but is more difficult to produce. These two methods were applicable to most of the nanoparticle metal oxides that Nantek, Inc. produced at the beginning of the Phase II project. A list of the nanoparticle oxides examined for use in a rTSP is given below.

Table 3: Examples of nanoparticles examined and their designations.

Sample	Designation
Commercial magnesium oxide (reference)	CM-MgO
Conventionally prepared magnesium oxide	CP-MgO
Autoclave prepared magnesium oxide	AP-MgO
Iron oxide coated autoclave prepared MgO	[Fe ₂ O ₃]AP-MgO
Commercial calcium oxide (reference)	CM-CaO
Conventionally prepared calcium oxide	CP-CaO
Autoclave prepared calcium oxide	AP-CaO
Iron oxide coated conventionally prepared CaO	[Fe ₂ O ₃]CP-CaO
Iron oxide coated autoclave prepared CaO	[Fe ₂ O ₃]AP-CaO
Sol-gel Zinc oxide	SG-ZnO
Commercial zinc oxide (reference)	CM-ZnO
Conventionally prepared zinc oxide	CP-ZnO
Autoclave prepared titanium dioxide	AP-TiO ₂

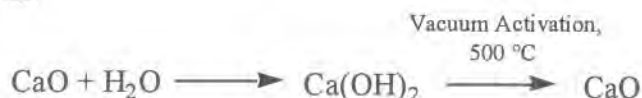
The work to find alternative routes to these processes have not only markedly increased the reactivity of the RNPs but also *significantly* decreased the cost of production (see Task 16). These new synthetic approaches have resulted in doubling, and in some cases tripling, the available surface area for reaction. As a consequence, the

amounts of simulant materials that are decomposed have risen accordingly. Another plus is that these new methods are applicable to all of our RNP materials.

Review of initial synthetic methods

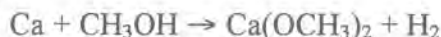
The following is a brief discussion of the synthetic methods that Nantek, Inc. used to make the metal oxide materials at the beginning of the Phase II project. The modifications to these synthetic methods will be described in the following sections.

The first method used at the start of the Phase II project was termed a “conventional process (CP)” which starts with commercial metal oxide that is hydrolyzed, dried, and activated under vacuum.



This method produces calcium oxide with a surface area of about 100 m²/g, and magnesium oxide with a surface area of 250 m²/g. For comparison, surface areas of commercial samples are 10 and 30 m²/g for calcium and magnesium oxides respectively.

The second synthetic method was termed “aerogel process (AP)” and starts with zero valent metal and methanol.



The obtained metal methoxide is hydrolyzed in an organic solvent (toluene) to form a metal hydroxide sol-gel. Next the sol-gel is supercritically dried in an autoclave to remove the organic solvent preserving at the same time the high porosity and surface area of the precursor material.



The last step is activation of the hydroxide, which is done overnight under vacuum at 500°C.



The brief description of the synthesis of the CP-CaO and AP-MgO are generally applicable to each of the nanoparticle metal oxides examined in the project. However, minor modifications are made for each metal oxide that was synthesized.

Description of new techniques applied to the synthesis of RNP materials

To simplify the large-scale process for the preparation of reactive nanoparticles three major modifications have been employed. Also, in order to facilitate large-scale production it was important to move from a batch-wise synthesis to a continuous process. The new techniques are high temperature alkoxide formation, replacement of the supercritical drying step with spray drying, and flow-activation of the metal hydroxide precursors. Each of these process modifications is described below.

These developments represent the current state of production for reactive nanoparticles. The combination of these three production advances has increased the SSA of the MgO nanoparticles from 250 to 720 m²/g. We have also seen corresponding increases in chemical reactivity with these and other samples.

High temperature alkoxide formation

The first major advance in the scaled-up synthesis of the nanoparticles was heating the reaction mixture during the formation of the metal alkoxide. Figure 2 shows the

increase in specific surface area (SSA) for three different magnesium oxide samples as a function of reaction temperature during methoxide formation. The graph clearly shows that the specific surface area of the final MgO product increases as the temperature of the initial reaction is raised. There is an optimal temperature for methoxide formation at 80°C. Above this point the SSA decreases.

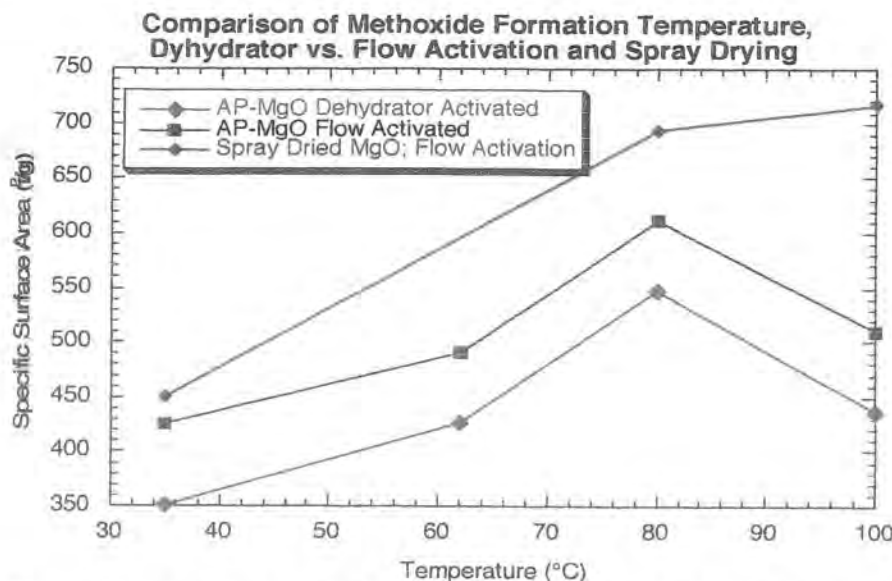


Figure 2: Increase in surface area of AP-MgO samples as a function of methoxide temperature.

Replacement of the hypercritical drying step by spray drying

The second improvement to the synthetic methods for nanoparticle production was to remove the supercritical drying step by using either microwave drying, carbon dioxide supercritical drying, or spray drying. Several sets of experiments were carried out where calcium hydroxide sol-gel was placed in the microwave and the solvent removed by microwave drying. The powder was then activated under vacuum at 500°C. The results were not very encouraging since the surface areas of such prepared calcium oxide were lower (about 70 m²/g) than samples prepared in the autoclave (120 m²/g). Similar results were found with magnesium oxide. Parameters such as heating time, power applied, and amount of the sample being used were varied.

Another, and very successful, method developed to bypass the hypercritical drying step was the implementation of spray drying to the process. In this method, the Mg(OH)₂ sol-gel is spray dried to rapidly remove solvent and form Mg(OH)₂ nanoparticles. The samples are spray dried using nitrogen gas as a carrier gas and the temperatures of the head unit are typically less than 130°C, which helps to eliminate sintering of the particles. When this method was combined with another advance, flow activation (described below), the surface area of magnesium oxide was increased from 250 m²/g to over 750 m²/g under select conditions. Engineers at Nantek have recently designed and built a bench-top unit that combines the spray drying and flow activation processes into a single unit. With un-optimized operating conditions, the unit is routinely capable of producing MgO with specific surface areas over 500 m²/g with a corresponding crystallite size of 3-

5 nm. With these samples we have observed an increase in reactivity for the decomposition of CW simulants. This method has been used to produce ZnO nanoparticles with an increase in specific surface area from 150 m²/g to 210 m²/g.

Flow activation of the metal hydroxide precursors

The final simplification of the synthetic process was to use flow activation of the hydroxide, instead of vacuum activation. This was a very important breakthrough in the synthesis of the nanoparticle metals oxides since it allows for a continuous activation process. With vacuum activation, the final metal oxides could only be made in a batch-wise fashion and from a very slow and tedious process. For these flow-activation experiments a simple tube furnace was used. The metal hydroxide powder was placed in a quartz boat, and hot nitrogen gas (150-650°C) was flowed over the sample. The activation times and temperatures were varied for each material in order to achieve the highest surface areas.

In general it can be concluded that flow activation works very well for all magnesium oxide samples and for aerogel prepared calcium oxide. However, it did not work well for the conventionally prepared CaO. The beneficial effect of the flow treatment can be explained as follows. High temperature flow “shocks” the hydroxide groups and adsorbed water/carbon dioxide out of existing crystals and removes them before they can recombine elsewhere. This effect is similar to the role of the vacuum in the dehydrator activation method. The result is an oxide that has been “flaked off” and has pores blasted through it as the steam escaped. The high temperature has the negative effect of sintering the sample and needs to be as low as possible. The ideal situation would be to build a reactor that delivers a sufficient amount of heat to convert the sample quickly but then removes the sample and cools it immediately. Flow activation is very sensitive to heat transfer effects which change with mass, temperature and time. Flow activation may be preserving or enhancing active sites at the surface of the nanoparticles.

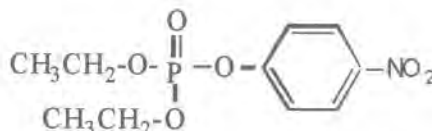
Task 3: High Efficiency Destructive Adsorption Technology (DAT) Test Development.

Because of the highly toxic nature of CW agents, a large portion of the screening and evaluation of the reactive nanoparticles was performed with simulant compounds. During the project four main tests were developed and used to compare the reactivity of the nanoparticle metal oxides towards decomposition of warfare simulants. The simulants used during the project were paraoxon, 2-chloroethyl-ethyl sulfide (2-CEES), diisopropyl fluorophosphonate (DFP) and diethyl phenylthiomethylphosphonate (DEPTMP). Paraoxon was used as a simulant of VX agent, 2-CEES as a simulant of mustard gas, DFP as a simulant of the G-agents, and DEPTMP as a sulfur containing simulant of VX. The general experimental parameters for each of these tests are given below.

Paraoxon destructive adsorption

In these studies 0.1-g metal oxide was placed in a round bottom flask, equipped with a magnetic stirrer, and 100-mL of pentane added. The solution was then purged with nitrogen to remove any moisture and 4.5-μL of paraoxon added. The disappearance of paraoxon was studied by UV-Vis spectroscopy. Paraoxon gives a very distinctive peak at

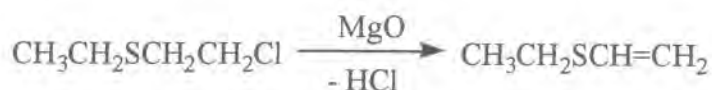
272-nm and the disappearance of this peak indicates adsorption from solution. In some cases it is possible to see p-nitrophenol, a decomposition product, which gives a distinct spectral feature at 220-nm. However, in most cases, the product is also adsorbed on the surface of the metal oxide, and it cannot be seen in UV-Vis of the solution. The data was taken at 2, 5, 10, 15, 20 minutes and then at 20 minute intervals to 2 hrs. After overnight reaction the solid product was separated, dried and studied by transmission IR spectroscopy.



For solid state ^{31}P NMR analysis the pentane solvent was gently vacuum evacuated to yield the dry powder sample for the analysis. The NMR analysis was performed at Spectral Data Systems in Champaign, Illinois.

2-CEES (2-chloroethyl ethyl sulfide) destructive adsorption

The purpose of these studies was to investigate our samples' reactivity with 2-chloroethyl ethyl sulfide (2-CEES), an analog of mustard agent, at room temperature. For example, an experiment with magnesium oxide and 2-CEES would result in the following reactions:



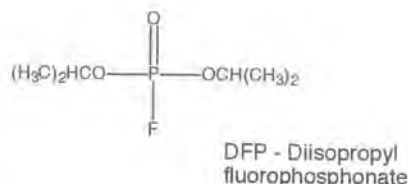
In the previous reactions, magnesium oxide may be substituted with calcium oxide, aluminum oxide, zinc oxide and various transition metal coated oxides. Metal-coated oxides refer to a monolayer coating of iron oxide or vanadium oxide onto the magnesium oxide (e.g., $[\text{Fe}_2\text{O}_3]\text{MgO}$). One of the products to the reaction between 2-CEES and RNP is ethyl vinyl sulfide that gives a characteristic peak at 1585 cm^{-1} in the IR region of the spectrum.

Our samples were examined by FT-IR using a modified gas cell having KBr windows. The cell is modified by connecting a glass flask with stopcock to the bottom of the gas phase IR cell. A joint is attached at the top so the cell can be evacuated on a glass vacuum line. 100-mg of RNP sample was placed in the flask and connected to the gas phase IR cell (10^{-3} Torr). This gas cell with bulb was then placed on the vacuum line and slowly evacuated. The cell was removed from the vacuum line (while maintaining a vacuum inside) and 14 microliters of 2-CEES injected through the stopcock of the glass flask. The cell was placed in the beam of the FT-IR and the intensity of the vinyl peak measured at the following time intervals (in minutes): 2, 5, 10, 15, 30, 45, 60, 90, 120, 150, 180, 210, 240, 270, 300. The greater the increase in this peak, the greater the conversion of the mustard simulant to the ethyl vinyl sulfide product.

Diisopropyl fluorophosphonate (DFP) destructive adsorption

In a typical experiment, the particular nanoparticle adsorbent ($\sim 0.1\text{-g}$) was weighed into a vapor phase IR cell that could be connected to a vacuum line. Prior to adsorption, the adsorbents were evacuated at room temperature for $\sim 15\text{-}30 \text{ min}$ ($\sim 10^{-4} \text{ torr}$). After

this treatment, a background spectrum was recorded. Subsequently, DFP was introduced (9 μ L, ~ 5 % by wt.) into the sample cell and the IR spectra of the vapor phase was recorded after 1 h. In order to assess the structure of the adsorbed species, reaction with DFP was carried out as described below and the DFP adsorbed on the solid was isolated and analyzed.

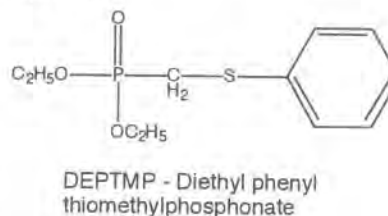


In a representative experiment, a 250-mL single necked flask provided with a serum cap, stir bar and a magnetic stirrer were charged with dry pentane (200-mL). To the above was sequentially added, the solid adsorbent (0.2-g) and DFP (9 μ L, ~ 5% by wt.). After an hour at room temperature, stirring was stopped, the solvent decanted off and the solid dried overnight under vacuum and analyzed by IR and solid-state ^{31}P NMR.

Diethyl phenylthiomethylphosphonate (DEPTMP) destructive adsorption

In a typical experiment, a 250-mL single necked flask provided with a serum cap, stir bar and a magnetic stirrer were charged with dry pentane (200-mL). To the above was sequentially added the solid adsorbent (0.2-g) and DEPTMP (9- μ L, ~ 5% by wt.). After an hour at room temperature, stirring was stopped and the clear liquid phase was analyzed by UV-VIS for quantitation of the residual DEPTMP. Subsequently, all the solvent was decanted off and the solid was dried overnight under vacuum and analyzed by FT-IR and NMR to assess the structure of the adsorbed species.

Samples for FT-IR analysis were prepared by grinding a sample of the dried solid (1 to 3-mg) with anhydrous KBr (100-mg). Pellets were made with a standard pellet press. Spectra of neat liquid were obtained by spreading a thin film of the liquid between a pair of salt plates. ^{31}P NMR spectra were obtained by Spectral Data Systems with a Tecmag 270 MHz



spectrometer equipped with a Doty Scientific 7-mm high speed CP-MAS probe, using direct excitation and high power proton decoupling. The observation frequency for ^{31}P was 109.55 MHz. Samples were packed in a sapphire rotor with kel-F end caps and typically spun at 4700 Hz. Chemical shifts were referenced to external 85% H_3PO_4 (0 ppm).

Tests involving RNP contained topical skin cream

These tests were designed to analyze the efficacy of topical skin cream containing RNPs for detoxifying CW simulant challenges. Two analytical methods were developed for use in testing of the TSP mixtures. The first was a penetration cup cell that emulates a MINI-CAM system. The second was a FT-IR method using an attenuated total reflectance attachment for FT-IR⁷.

Penetration cup experiments

This analytical method used a small glass penetration cup as the basis for the experiment. Basically it was a modification of a skin permeation test. As shown in Figure 3, a nitrocellulose filter with a small layer (about 0.15 mm thick) of skin cream and nanoparticle formulation was placed between the two parts of the penetration cell

Next the cell was assembled by attaching a thermal desorption tube (Tenax or Chromosorb) to the side port of the cell. If necessary, the cell was attached to a vacuum to "pull" the products onto the adsorption tube. After adsorbing the products onto the tube, the tube was transferred to a Dynatherm thermal desorption unit to release the products. The desorbed products were then sent to a GC/MS system by way of a heated transfer line for analysis. While this method seems simple to perform, many problems were encountered with its use and it was ultimately discarded.

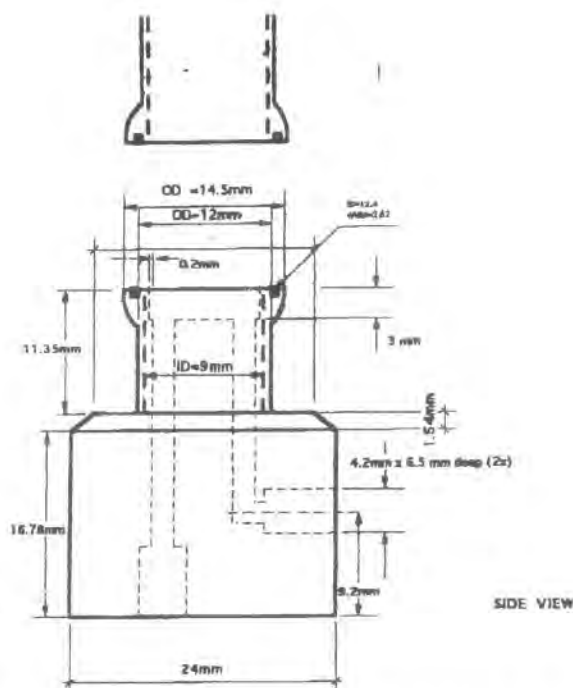


Figure 3: Schematic diagram of penetration cup cell used for testing the efficacy of RNP containing skin creams against CW simulant challenges.

Topical protectant evaluation by FT-IR spectroscopy

Also used was a horizontal attenuated total reflectance accessory (ATR) for our laboratory FT-IR in order to provide a second analysis of the topical skin protectants incorporating our reactive nanoparticles. In 1990, Braue and Pannella⁷ reported the development of a unique analytical method for evaluating the effectiveness of topical protectants against penetration by chemical agents using an FT-IR and the horizontal attenuated total reflectance (ATR) accessory. A template was designed which allowed a uniform-thickness layer of topical protectant (0.05 to 0.15 mm) to be applied to the surface of the ATR crystal. A chemical challenge was applied to the template filled with topical protectant, and spectra were recorded with the FT-IR spectrometer. Analysis of the recorded spectra identified how much time was required for the simulant challenge to break through the topical protectant barrier.

Initial sulfur mustard (HD) and nerve agent (VX) DAT experiments

The initial VX and HD tests performed at the Midwest Research Institute followed the similar experimental protocols. Namely, 0.1-g of AP-MgO or [Fe₂O₃]AP-CAO was

This report contains company proprietary information that could be the subject of patent applications. As such it is intended for use by the U.S. Department of Army for contract monitoring and is not intended for public dissemination without prior written approval of an officer of Nantek, Inc.

weighted, placed in an Erlenmeyer flask and covered with parafilm (several flasks were prepared at the same time). Then, 100-mL of organic solvent (CH_2Cl_2) was added to each flask. Next, 4 or 20- μL of HD or VX was added and the start time recorded. After 2 hours, analysis for agent was performed by gas chromatography with a flame photoionization detector (GC/FPD). Samples were also extracted after 6 hours and analyzed.

For the HD experiments, two methods were used: the same method described above for VX and a dry method where 4- μL of HD was injected directly onto dry AP-MgO or $[\text{Fe}_2\text{O}_3]\text{AP-CaO}$. After 6 h, the used metal oxide sample was extracted with an organic solvent (CH_2Cl_2) and analyzed via GC/FPD.

Task 4: Destructive Adsorption Technology (DAT) Characterization Using Chemical Warfare Simulants

The following is a summary of the paper titled "Development of Reactive Topical Skin Protectants against Sulfur Mustard and Nerve Agents"⁴ and other additional studies. The full paper is given as an attachment to this report.

Reactive nanoparticles provide a clear advantage over other competing decontamination technologies such as activated carbon adsorbents and highly caustic solutions. Other decontaminants used primarily for surface decontamination such as DS2, ozone, and ethanol-NaOH-ammonia solutions⁴⁻⁶, are highly toxic for skin exposure and would not be compatible with the proposed base skin cream. Activated carbon, a possible solid adsorbent, has the disadvantages that it does not destroy the toxic agent but merely "holds it" by weak adsorption forces and clean-up / disposal of the contaminated carbon is difficult because the hazardous material is only adsorbed and still highly toxic.

Caustic sorbents are obviously unsuitable for this application, posing a significant hazard for humans. In fact, the solutions used for such purposes are so highly caustic that they corrode metals, pain and wood.

Thus, new materials or adsorbents offering rapid kinetics yet are suitable from a safety and cost standpoint need to be developed that can protect skin from exposure to highly toxic nerve agents when combined with a suitable barrier base cream. The unique nanoparticle adsorbents under development by Nantek offer significant potential in meeting these difficult technical and economic challenges.

Several unique nanoparticles were developed during this work that are believed to be possible candidates for the reactive topical skin cream. These included oxides of magnesium, titanium, calcium, zinc, nickel and copper, and composite samples consisting of transition metal oxide-coated nanoparticles. The rationale behind the synthesis of the transition metal oxide-coated nanoparticles is that dramatic increases in reactivity of the nanoparticles has been observed with the destructive adsorption of chemicals such as carbon tetrachloride and acid gases by the metal oxide nanoparticles⁷⁻¹⁰. Extensive testing of the destructive adsorbent performance of a broad array of nanoparticle samples was conducted. These tests were conducted using simulants of nerve agents such as paraoxon and 2-CEES (the one armed mustard).

Decomposition of paraoxon on various metal oxides

In addition to the UV-Vis spectra analysis, adsorption of the paraoxon was readily visible on most of the white powder samples due to the change in the color of the powder from white to bright yellow. The p-nitrophenol anion is an intense, bright yellow color and this observation coupled with IR data strongly suggests that the anion was formed very quickly on the surface of the nanoparticle adsorbents.

Table 4 presents the samples studied at the initial phases of the research. The objective was to screen as many nanoparticle formulations as possible before focusing on a select few for further investigation. Figure 4 shows the results of paraoxon adsorption on various magnesium oxide samples. All samples in the figure used 100-mg of powder with the exception of the sample labeled AP-MgO (0.05-g) which used 50-mg of material. While all of the materials seemed to destructively adsorb the paraoxon at roughly the same extent, the samples based on AP-MgO were able to remove the paraoxon from solution at a much faster rate than those based on CP-MgO. This exceptional performance has been repeated in many test trials and is due to the AP-materials very high surface area. The iron oxide coated material also performed well. The amount of iron oxide was 1% by weight of the sample. While the CP-MgO materials did not perform as well as the AP-MgO samples, it important to note that they provided exceptional adsorptive properties nonetheless.

Table 4: Samples studies for paraoxon decomposition.

Sample	Designation	Specific Surface Area (m ² /g)
Autoclave prepared magnesium oxide	AP-MgO	562
Conventionally prepared magnesium oxide	CP-MgO	340
Iron oxide coated autoclave prepared MgO	[Fe ₂ O ₃]AP-MgO	360
Autoclave prepared calcium oxide	AP-CaO	112
Iron oxide coated autoclave prepared CaO	[Fe ₂ O ₃]AP-CaO	100
Conventionally prepared calcium oxide	CP-CaO	110
Iron oxide coated conventionally prepared CaO	[Fe ₂ O ₃]CP-CaO	68
Zinc oxide (i)	ZnO (i)	53
Zinc oxide (ii)	ZnO (ii)	70
Zinc oxide (iii)	ZnO (iii)	75
Commercial zinc oxide	CM-ZnO	24
Conventionally prepared zinc oxide	CP-ZnO	20
Titanium dioxide-activated at 200°C	TiO ₂ (act.)	42
Titanium dioxide- not activated	TiO ₂ (not act.)	44
Autoclave prepared titanium dioxide	AP-TiO ₂	127

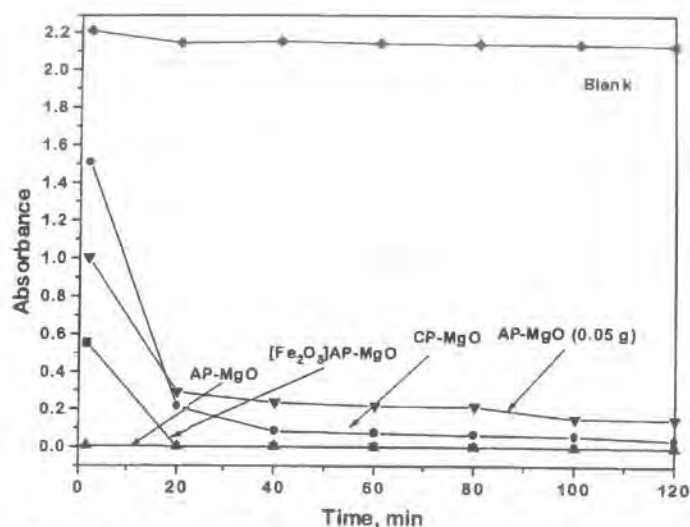


Figure 4: Rate of disappearance of paraoxon (4.5-μL) on magnesium oxide samples. Lower intensity indicates more destructive adsorption of paraoxon.

The data obtained for calcium oxide are shown in Figure 5. The iron oxide coating enhances the performance for both conventional and autoclave-prepared calcium oxide. For the iron-coated AP-CaO sample, only about 10% of the paraoxon was present after 2 hours of reaction (based on the height of the paraoxon peak). The CP-CaO did not behave as well, even though its surface area was comparable to AP-CaO. However, when iron oxide was present, the surface area of CP-CaO decreased (from 110 to 68 m²/g) but the amount of adsorbed paraoxon was much higher. The iron oxide coating either enhances the intrinsic surface reactivity and / or it protects the core CaO particles from adventitious water, thus enhancing destructive adsorbent activity over the uncoated samples.

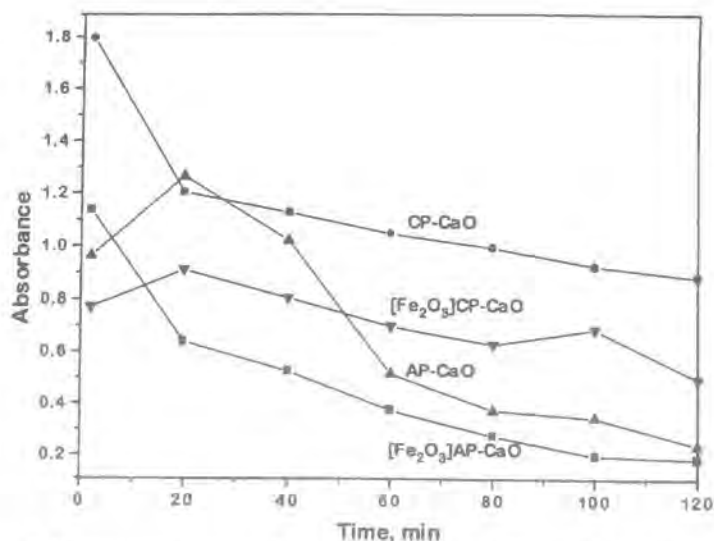


Figure 5: Rate of disappearance of paraoxon (4.5-μL) on calcium oxide samples (0.1-g). Lower intensity indicates more destructive adsorption of paraoxon.

Figure 6 provides data for the best oxides from each of the groups tested for the decomposition of paraoxon, as well as the blank test. Additionally, Table 5 gives a summary of the paraoxon decomposition after 2 and 20 hours exposure. Magnesium and calcium oxides, both coated and uncoated, were very active with essentially total disappearance of paraoxon within the 20-h exposure period. For a majority of the samples, decomposition occurred very rapidly with near-complete disappearance within the first 2-h of testing. Most notably, complete disappearance of the paraoxon was observed before the initial reading at 2 minutes for the AP-MgO material. High surface area ZnO and TiO₂ also performed very well for paraoxon decomposition.

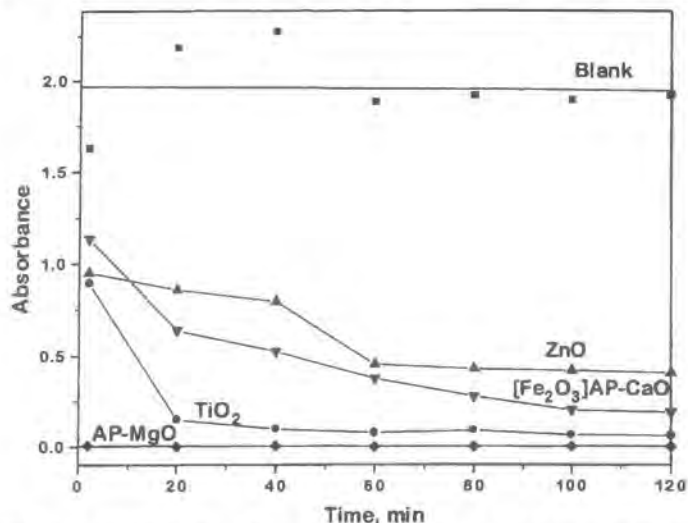


Figure 6: Rate of disappearance of paraoxon (4.5-μL) on various metal oxide samples (0.1-g). Lower intensity indicates more destructive adsorption of paraoxon.

Table 5: Decomposition of paraoxon on various metal oxides.

Sample	Specific Surface Area (m ² /g)	Peak Intensity-2hr $\lambda_{\text{max}} = 272\text{-nm}$	Peak Intensity-20hr $\lambda_{\text{max}} = 272\text{-nm}$
Blank-Reference	-	1.918	1.935
AP-MgO	562	0	0
CP-MgO	340	0.071	0
[Fe ₂ O ₃]AP-MgO	360	0	0
AP-CaO	112	0.240	0
[Fe ₂ O ₃]AP-CaO	100	0.189	0
CP-CaO	110	0.887	0.044
[Fe ₂ O ₃]CP-CaO	68	0.487	0
ZnO (I)	53	0.406	0.229
ZnO (iii)	75	0.496	-
CM-ZnO	24	1.739	2.432
CP-ZnO	20	1.473	0.918
TiO ₂ (activated)	42	1.412	1.297
TiO ₂ (not activated)	44	1.172	1.309
AP-TiO ₂	127	0	0

Comparison of vacuum and flow activated samples

Paraoxon tests for AP-CaO show the vacuum activated sample was better than flow activated one, as shown in Figure 7. The surface area of the flow-activated sample was somewhat higher (152 vs. 142 m²/g). However, the sample had much more carbonate on the surface, which could cause blocking of the reactive sites and thus lower reactivity. In case of CP-CaO, the surface area of flow activated sample was lower compared to the vacuum activated one (67 vs. 106 m²/g) and the reactivity with paraoxon was also lower.

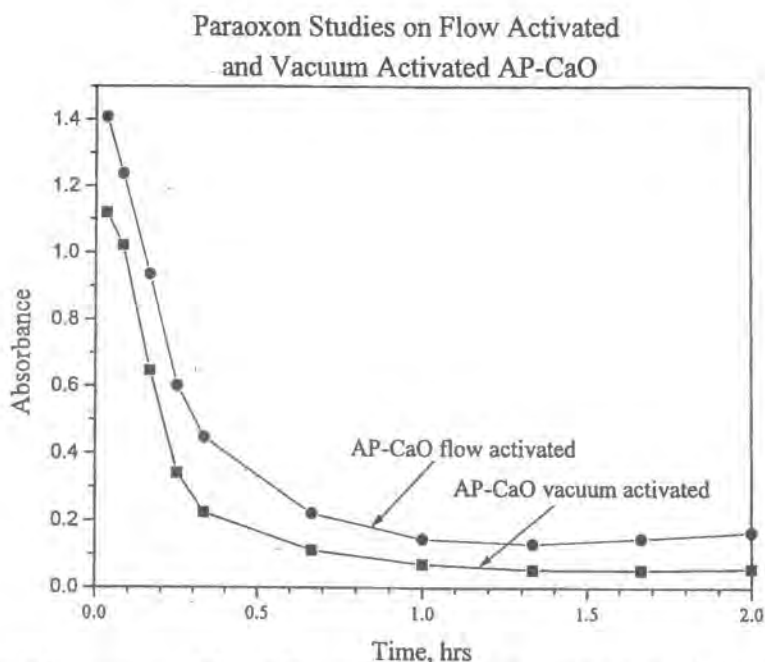


Figure 7: Reactivity comparison of vacuum and flow activated AP-CaO.

For AP-MgO, both activation methods worked very well, however, the flow-activated sample outperformed the vacuum activated sample to a small degree. The results of this test are shown in Figure 8.

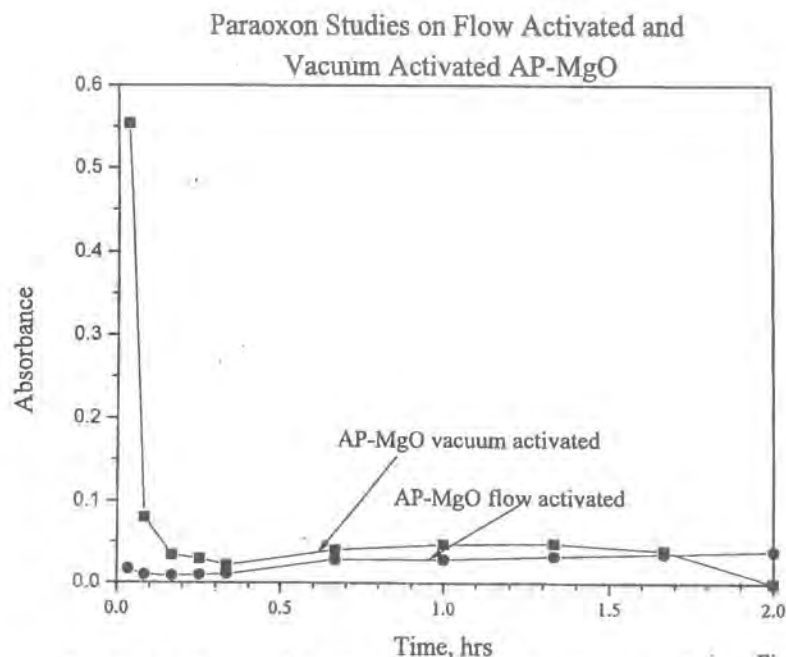


Figure 8: Reactivity comparison of vacuum and flow activated AP-MgO.

It can be concluded that the flow activation works very well for autoclave prepared magnesium oxide and it works reasonably well for autoclave prepared calcium oxide.

Task 5: Adsorption of Simulants Using Activated Carbon.

As a benchmark comparison with a known adsorbent, studies were conducted with several different types of activated carbon. While activated carbons are great adsorbents, it must be kept in mind that they do not decompose the simulant materials that they adsorb. *In contrast to this, reactive nanoparticle materials are capable of adsorbing large amounts of materials and chemically decomposing the adsorbed species to benign materials. For example, the decomposition products for the insecticide paraoxon on the reactive nanoparticle MgO are p-nitrophenol and diethyl phosphite.*

Figure 9 shows the results for some of these tests in which AP-MgO greatly outperforms the activated carbons, some of which possess a surface area that approaches double that of the RNP. Also, it is important to note the rapid kinetics of the destructive adsorption with the RNP compared to the activated carbons. This is another very important factor that favors the use of RNPs as a detoxifying agent in TSP. It is necessary that the RNP/TSP rapidly “deactivate” any CW challenge brought against it.

The activated carbon samples were (in increasing order of specific surface area): Darco (616 m²/g), Norit (872 m²/g), Amborsorb (1024 m²/g), and coconut shell (1062 m²/g). The same test conditions were used for the activated carbon samples as for the nanoparticles. The activated carbon samples performed well as expected. After about 1 hour a large portion of the paraoxon had been adsorbed from solution. There are several key features that are addressed here when comparing the activated carbons with AP-MgO. First, it should be noted that even though AP-MgO has a much lower specific surface area, it is a much better adsorbent. In fact, the data in this graph are normalized for mass not surface area. This means that MgO competes even better on a m²/g basis. A

second point is that the magnesium oxide is capable of adsorbing a larger amount of paraoxon per unit mass than the activated carbon. Third, and perhaps most important, the kinetics of the adsorption are much faster for the MgO than the other samples. A final difference in the two types of adsorbents is that the MgO does actually decompose the paraoxon into p-nitrophenol and phosphate(s) that remain strongly adsorbed to the surface of the nanoparticle. The activated carbon samples are not capable of destroying the paraoxon

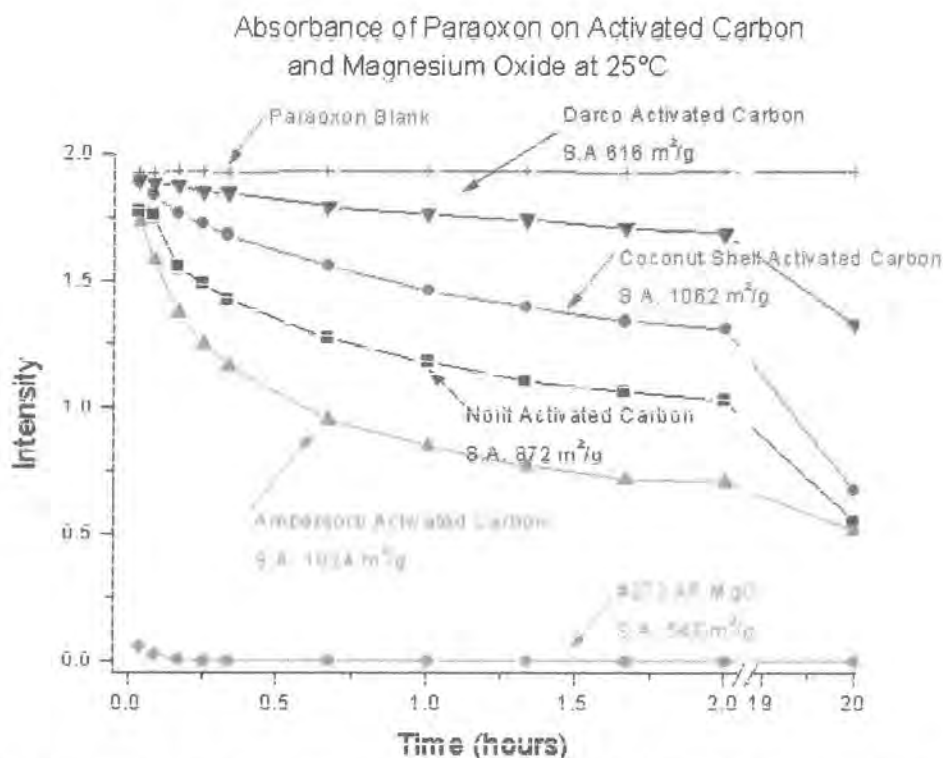


Figure 9: Comparison of activated carbon and AP-MgO for the destructive adsorbance of paraoxon.

To summarize, Nantek's AP-MgO reactant adsorbs significantly more paraoxon than activated carbon. This finding was not necessarily expected because the activated carbon materials with their high surface areas and large pore volumes are recognized for their adsorbent capability. It has been shown that the high surface area metal oxide materials do indeed destroy the highly toxic substances through the formation of reaction by-products, including p-nitrophenol for paraoxon decomposition and ethyl vinyl sulfide for 2-CEES.

Two tests were conducted for the adsorption of 2-CEES with activated carbon. In the first experiment 14-μL of 2-CEES was used and in the second one 50-μL, each experiment contained 0.1-g of activated carbon. No peaks were found in the vapor phase IR when 14-μL of 2-CEES were used (not even peaks of 2-CEES). Probably, 2-CEES was completely adsorbed by activated carbon, without actual decomposition. With 50 μL, some vinyl sulfide was seen, but the amount corresponded to impurities in 2-CEES, which was proved with a blank test, when no adsorbent was present.

Task 6: Destructive Adsorption of Paraaxon with Improved AP-MgO.

Tests have been conducted with the improved AP-MgO in regard to paraoxon destructive adsorption. It has been shown that the increased surface area of the spray dried MgO has led to a subsequent increase in the amount of paraoxon that the RNP is capable of decomposing. In these experiments, the amount of paraoxon was increased while the mass of RNP was held constant. Figure 10 shows the disappearance of paraoxon from the solution as a function of time for amounts of paraoxon ranging from 9 to 50- μ L.

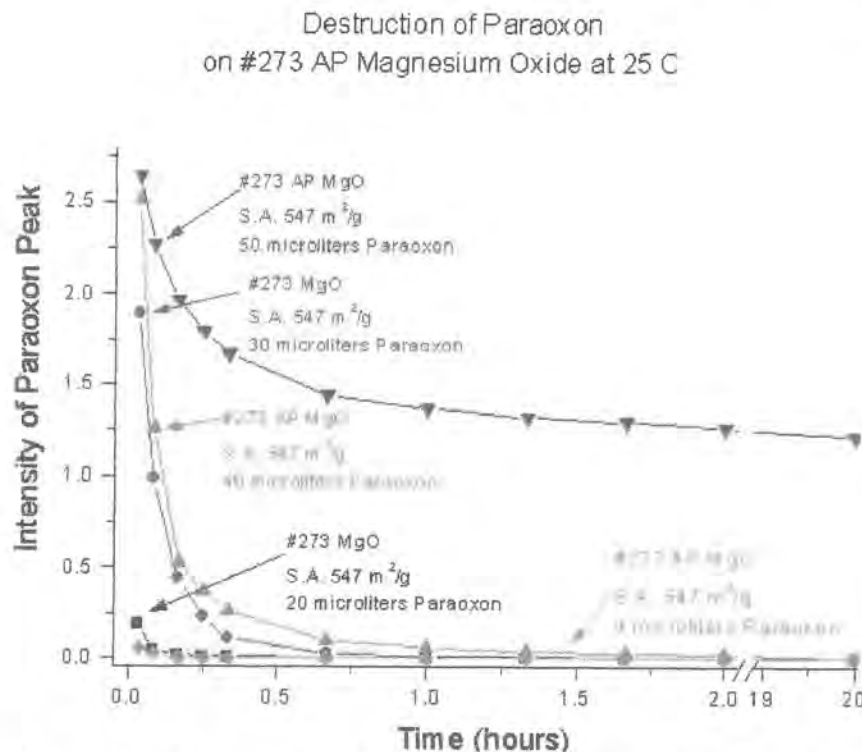


Figure 10: Destructive adsorption of paraoxon with spray dried MgO.

Note the rapid kinetics of the destructive adsorption of paraoxon over the RNP. Also note the large amounts of paraoxon that the material destructively adsorbs.

Destructive adsorption of paraoxon with nanocrystalline zinc oxide

The destructive adsorption of paraoxon was carried out to compare the abilities to not only adsorb, but to also destroy this VX simulant. These experiments were conducted with two commercial brands of ZnO, and the prepared SG-ZnO. 100-mg of ZnO was placed into a round bottom flask that had been flushed with argon. Next, 100-mL dry pentane was added to the flask and stirred. Then 3- μ L of paraoxon was added to the flask and ultraviolet/visible spectroscopy was used to monitor the disappearance of paraoxon from solution. Paraaxon gives a characteristic absorption in the UV-Vis region of the spectrum at 272-nm. This reaction was monitored every 20 minutes for 3 hours, and then a final data point acquired at 20 hours. The powder was then filtered and infrared spectroscopy was then used to identify the adsorbed species.

The results from UV/VIS show that the prepared ZnO destroyed more of the paraoxon than the commercial ZnO samples did (Tables 6 and 7). Figure 11 shows the absorbance of the paraoxon band declining over the time of the reaction.

The results from the IR show that the SG-ZnO samples have many new species adsorbed to the powder, whereas the commercial ZnO has little if any new species adsorbed. Figure 12 shows the solid pellet IR spectra taken following the reaction with paraoxon. When compared to less reactive, commercial ZnO it can be seen that there are many new bands seen on the prepared samples between the regions of 800-1500 cm^{-1} .

Also, a larger amount of paraoxon (4.5- μL) was used for destructive adsorption studies on various ZnO samples. The best sample (fastest adsorption) was zinc oxide prepared from zinc chloride (173 m^2/g), followed by ZnO prepared from diethyl zinc. All these samples were vastly superior to any of the commercial samples.

Table 6: Decomposition of paraoxon on ZnO after 20 hrs

Sample	% Paraoxon Destructively Adsorbed in 20 hours
Fisher ZnO	28%
Nanophase ZnO	45%
SG-ZnO Sample C	96%
SG-ZnO Sample D	100%
ZnO from ZnCl_2	100%

Table 7: Molar ratio of paraoxon destroyed vs. ZnO after 20-hrs decomposition

Sample	Molar Ratio
Fisher ZnO	1 mole Paraoxon : 333 moles ZnO
Nanophase ZnO	1 mole Paraoxon : 201 moles ZnO
SG-ZnO Sample C	1 mole Paraoxon : 95 moles ZnO
SG-ZnO Sample D	1 mole Paraoxon : 86 moles ZnO
ZnO from ZnCl_2	1 mole Paraoxon : 57 moles ZnO

* Theoretical Molar Ratio = 1 mole paraoxon : 6 moles ZnO

Crystallites of 4 nm have 30% of the ZnO at their surface and 70% in the bulk. If it takes 2 ZnO to react to 1 paraoxon, then this would result in the 1:6 ratio⁹. This indicates that a larger amount of paraoxon, or other phosphate organic compound, can be destructively adsorbed in large amounts simply due to the relatively large amount of surface that is available on the nanoparticle for reaction and decomposition.

The resulting powders were then extracted with methylene chloride and the extracts studied by IR to see if any of the adsorbed species could be removed. The IR spectra did not contain any bands attributable to paraoxon confirming that the species are strongly adsorbed to the ZnO surface.

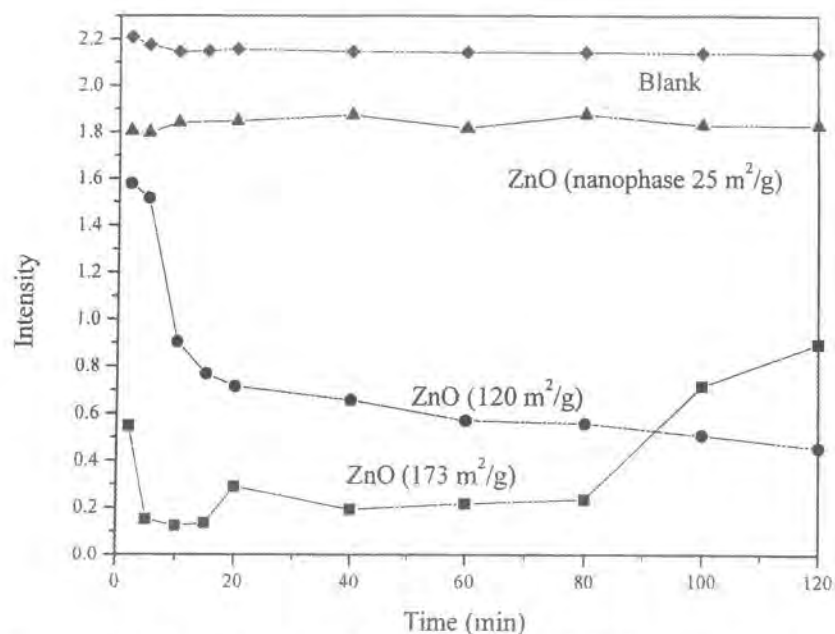


Figure 11: Destructive adsorbance of paraoxon by RNP-ZnO from pentane solution. Lower intensity indicates larger destructive adsorption.

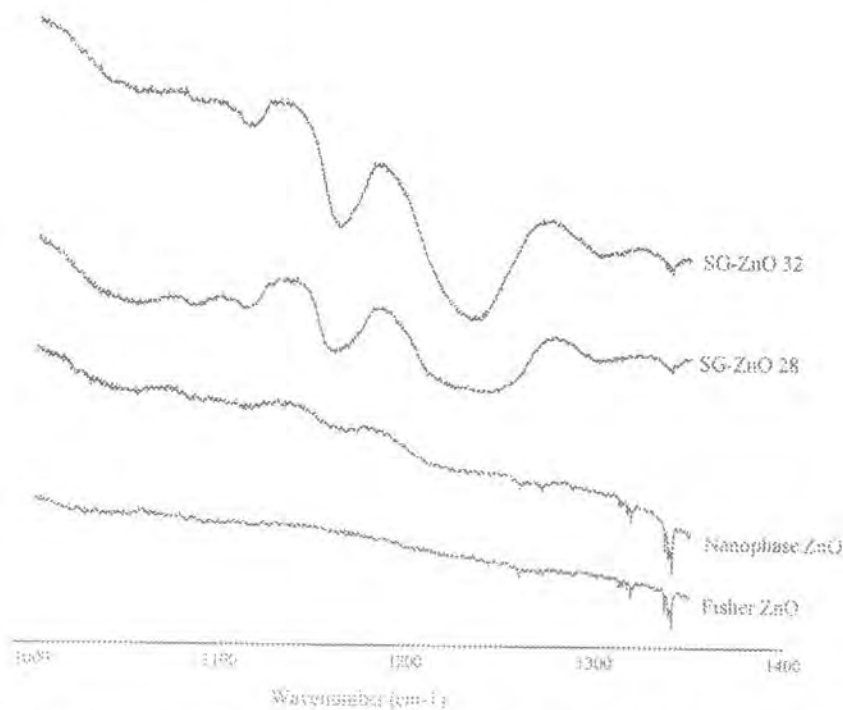


Figure 12: Solid state FT-IR of RNP-ZnO samples after the destructive adsorption of paraoxon.

Decomposition of 2-chloroethyl ethyl sulfide on nanoparticle metal oxides

For these experiments, the samples that exhibited the best adsorbent activity in the paraoxon studies were used to examine the dehydrochlorination of 2-chloroethyl-ethyl sulfide. This process is monitored by observing the growth of the characteristic vinyl peak for the ethyl vinyl sulfide decomposition product in the IR. It is necessary to observe the product of the reaction because the disappearance of 2-CEES cannot be monitored directly due to the majority of the peaks of 2-CEES superimposing the peaks of ethyl vinyl sulfide. The only significant difference between the 2-CEES spectrum and the ethyl vinyl sulfide spectrum is the peak at 1595 cm^{-1} that is attributed to the double bond of the vinyl compound. The observation of this peak growth was used as a fingerprint in the decomposition of 2-CEES. Some typical test results are shown in Figure 13 for several variations of calcium, magnesium and zinc oxides. It should be noted that the 2-CEES decomposition tests measure a decomposition product and, therefore, increased intensity versus time suggests greater decomposition activity.

It is particularly interesting that the CaO samples are very reactive, especially the iron oxide-coated sample, $[\text{Fe}_2\text{O}_3]\text{AP-CaO}$. Also note that SG-ZnO(iii) produced with a minimal amount of water is superior to ZnO(i). Titanium dioxide, neither commercial nor autoclave-prepared, showed strong activity towards 2-CEES despite the fact that it was very reactive when exposed to paraoxon.

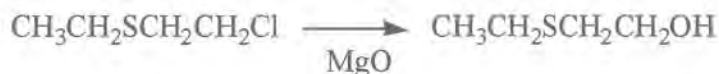
A rather peculiar result is that the best sample for paraoxon destructive adsorption (AP-MgO) behaved unexpectedly in the 2-CEES reaction. In a very short time, ethyl vinyl sulfide appeared in the spectrum, but it did not increase over time as with the other samples tested. Recall that the surface area of AP-MgO is very high ($>500\text{ m}^2/\text{g}$). It is suspected that this curious result is due to the establishment of a rapid equilibrium where 2-CEES is destroyed, but the ethyl vinyl sulfide is also largely adsorbed on the AP-MgO surface. Results from extraction experiments to determine the ratio of 2-CEES starting material to ethyl vinyl sulfide product indicate that $>85\%$ of the total 2-CEES is decomposed. Complete destruction may be inhibited by back-adsorption of the ethyl vinyl sulfide onto the MgO surface.

Similar behavior was observed for the CP-MgO samples, but to a lesser extent. In other words, back-adsorption of ethyl vinyl sulfide occurred at a lower rate than that observed during the AP-MgO experiments. This is possibly due to the lower surface area of the CP-MgO material.

Additional samples that were studied are: CP-MgO, $[\text{V}_2\text{O}_5]\text{CP-MgO}$, $[\text{Fe}_2\text{O}_3]\text{CP-MgO}$, $[\text{Fe}(\text{NO}_3)_2]\text{CP-MgO}$, $[\text{V}_2\text{O}_5]\text{AP-MgO}$, $[\text{Fe}_2\text{O}_3]\text{AP-MgO}$, $[\text{V}_2\text{O}_5]\text{CP-CaO}$, $[\text{V}_2\text{O}_5]\text{CP-CaO}$, $[\text{Fe}(\text{NO}_3)_2]\text{CP-CaO}$. These "core/shell" RNPs yielded results that were generally the same as the sample described previously.

Additional analytical tests have been performed to elucidate the reaction products, especially those that remain bound to the surface of the RNP. The first of these has been to make pellets of the samples after reaction with 2-CEES and examining the solid product by FT-IR. Attempts have also been made to quantitate the amount of 2-CEES decomposed but the results from these experiments have been difficult to accurately determine. However, data has been accumulated that indicates that there may be a second mechanism for 2-CEES decomposition, that of hydrolysis of the simulant.

The reaction proceeds as follows:



The product of this reaction is 2-(ethylthio)-ethanol. The presence of this product was studied by FT-IR comparing the neat $\text{CH}_3\text{CH}_2\text{SCH}_2\text{CH}_2\text{OH}$ with the solid product after reaction with 2-CEES.

Both the dehydrochlorination and hydrolysis products have been identified by supplementary analytical methods (GC/MS) for the reaction between 2-CEES and RNPs. In addition, the products from real agent tests (HD) with MgO indication detoxification via both of these mechanisms.

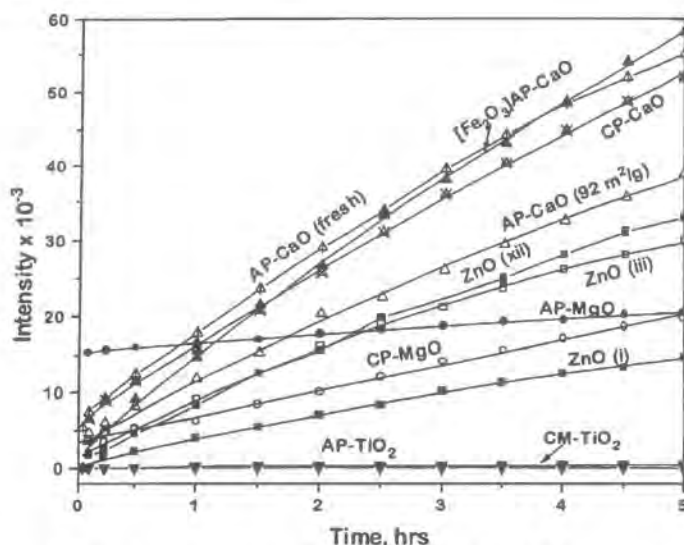


Figure 13: Appearance of ethyl vinyl sulfide during 2-CEES decomposition on various metal oxides. Higher intensity indicates more destructive adsorption of 2-CEES.

Reactions of the nanoparticle in the TSP

As expected, the rate of reaction was slower when reactants were embedded in the topical skin protectant. Nonetheless, a decrease in the paraoxon peak intensity was observed when analyzed in an analogous manner to the neat nanoparticle oxides. Preliminary results for the destructive adsorption of the simulant 2-CEES were also very encouraging. As with paraoxon, the adsorbent / cream mixture reacted with the simulant albeit at a slower rate than observed during the earlier adsorbent studies. Obviously the cream is forming a barrier for the nerve agents, thus slowing the availability of the simulant to the adsorbent surface sites. Figure 14 shows the comparison of the formation of the decomposition product, ethyl vinyl sulfide, for calcium and magnesium oxide adsorbents with and without the addition of the base TSP.

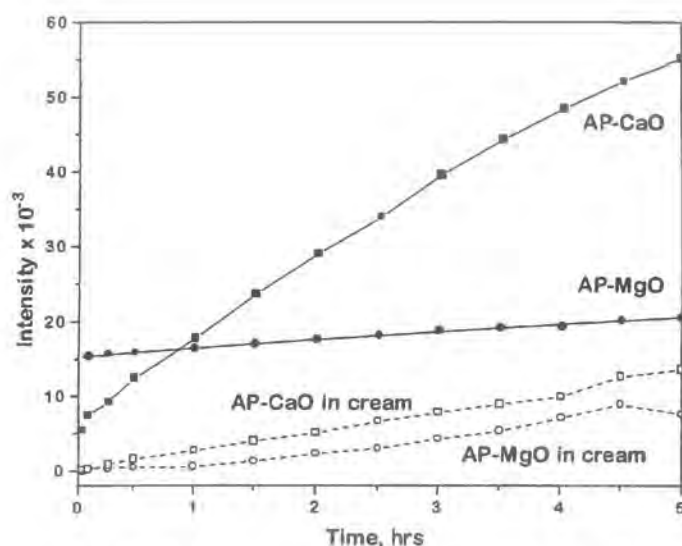


Figure 14: Appearance of ethyl vinyl sulfide during reaction of 2-CEES on metal oxides with and without the base cream. Higher intensity indicates more destructive adsorption of 2-CEES.

Note that while the formation of the dehydrochlorination product was attenuated, it definitely occurs even when the nanoparticles are included in the base TSP cream. This is not necessarily an indication that the reaction with the MgO is adversely affected. It may simply be due to slow diffusion of simulant into, and product out of, the cream.

Initial experiments analyzing the adsorption and decomposition of HD and VX with metal oxide nanoparticles

Early experiments with real CW agents showed that AP-MgO destructively adsorbed VX completely at 4 and 20- μ L tests. Note that the procedure used is described on pages 16-17. Using organic solvents (CH_2Cl_2) as an extraction medium, no VX was extracted from the used AP-MgO sample. $[\text{Fe}_2\text{O}_3]\text{AP-CaO}$ also completely adsorbed 4- μ L of VX. However, when 20- μ L was used about 60% of the VX remained after 6 hours.

Experiments with mustard indicated that some of the HD had been adsorbed / destroyed, but not all of it. The AP-MgO behaved the best with about 50% decomposition within 6 hours. However, the HD experiments were inconclusive owing to the wide variability and significant analytical noise.

These studies demonstrate two important things: better formulations of nanoparticle metal oxides are needed for HD decomposition, although AP-MgO behaved exceptionally well for VX destructive adsorption; and the simulants that were chosen, proved to be reasonable for the destructive adsorption reactions with VX and HD chemical warfare agents. In fact, paraoxon and VX destructive adsorption tracked very well with each other for the 4- μ L and 20- μ L experiments. Additionally, recent work with 2-CEES has shown that results are similar to HD, i.e. partial (85%) destruction over 6 hours was observed.

It should be emphasized that these initial tests used comparatively large amounts of simulants or real agents. These are very demanding tests and the fact that some HD was not destroyed should not be discouraging.

Other destructive adsorbent studies

In past research involving the dehalogenation of organic solvents, it was discovered that small amounts of transition metal oxides such as Fe_2O_3 and V_2O_5 are useful in “catalyzing” the surface of the RNPs such that they are capable of dechlorinating large amounts of materials⁷⁻¹⁰. The use of core shell materials such as $[\text{Fe}_2\text{O}_3]\text{CP-CaO}$ and $[\text{V}_2\text{O}_5]\text{AP-MgO}$ were described in the previous sections. Due to the success of some of these nanoparticles, Nantek embarked on studies to investigate the use of other types of “core/shell” nanoparticles for the detoxification of large amounts of CW.

$[\text{CaO}]\text{AP-MgO}$

The rationale behind combining these two metal oxides was to exploit the higher specific surface area of the MgO and the high reactivity of CaO although has been found that nanoparticles of both species are effective in the destruction of CW agents. While CaO is a stronger solid Lewis base than MgO the nanoparticle form of this metal oxide possesses a much lower specific surface area. Thus, if small amounts of CaO were coated over the surface of the MgO it may be able to disperse the CaO over the surface of the MgO and increase the reactivity of the combined oxide materials. The variations of synthesizing these “core/shell” RNPs were made by adding nanocrystalline MgO or $\text{Mg}(\text{OH})_2$ to a solution of $\text{Ca}(\text{OCH}_3)_2$ before and after the addition of water for hydrolysis to $\text{Ca}(\text{OH})_2$ sol-gel. Completion of the synthesis and activation of CaO yielded the desired nanocrystalline $[\text{CaO}]\text{AP-MgO}$ as confirmed by powder X-ray diffraction.

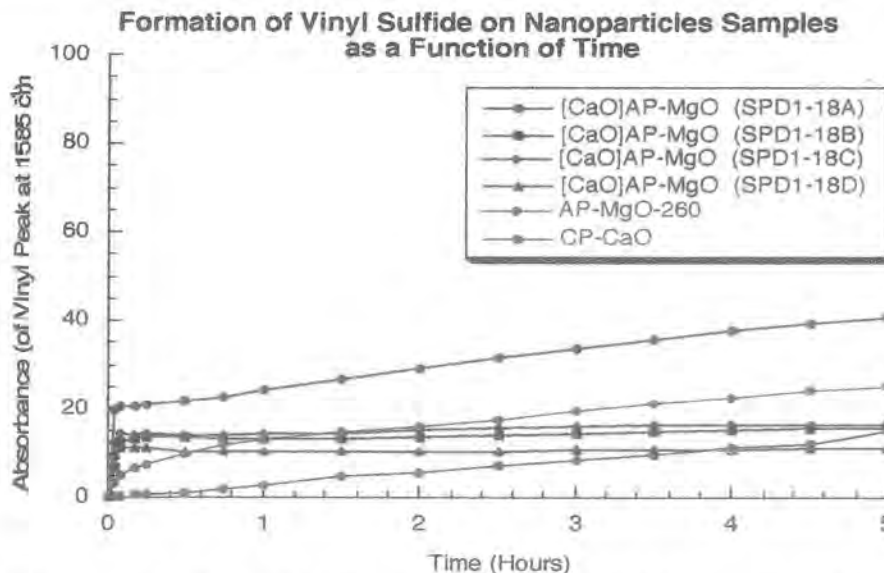


Figure 15: Formation of ethyl vinyl sulfide on $[\text{CaO}]\text{MgO}$ nanoparticle samples as a function of time.

Figure 15 shows the formation of ethyl vinyl sulfide (the dehydrochlorination product) from the reaction of 2-CEES with several $[\text{CaO}]\text{AP-MgO}$ formulations. Ethyl vinyl sulfide displays a very distinct $\text{C}=\text{C}$ absorption at 1585 cm^{-1} which is used to monitor the formation of product. It should be noted that these experiments monitor the

products in the vapor phase above the RNP reagent. It does not account for the amount of product that remains strongly adsorbed to the surface of the RNP. The higher the line of the data represents a greater extent of reaction. Two additional destructive adsorbents are displayed for comparison. These are AP-MgO, and CP-CaO. With the exception of one [CaO]MgO sample, it is seen that the new [CaO]AP-MgO formulations are intermediate in 2-CEES decomposition between AP-MgO and CP-MgO.

The synthesis and CW simulant testing of other “core/shell” RNPs has also been completed. These other RNPs include [TiO₂]AP-MgO, [ZnO]AP-MgO, [V₂O₅]AP-MgO and [Fe₂O₃]AP-MgO. The rationale of using these samples was to improve the efficacy of the best RNP – AP-MgO. These new materials worked well for the destructive adsorption of paraoxon although they were not as efficient as magnesium oxide alone (Figure 16).

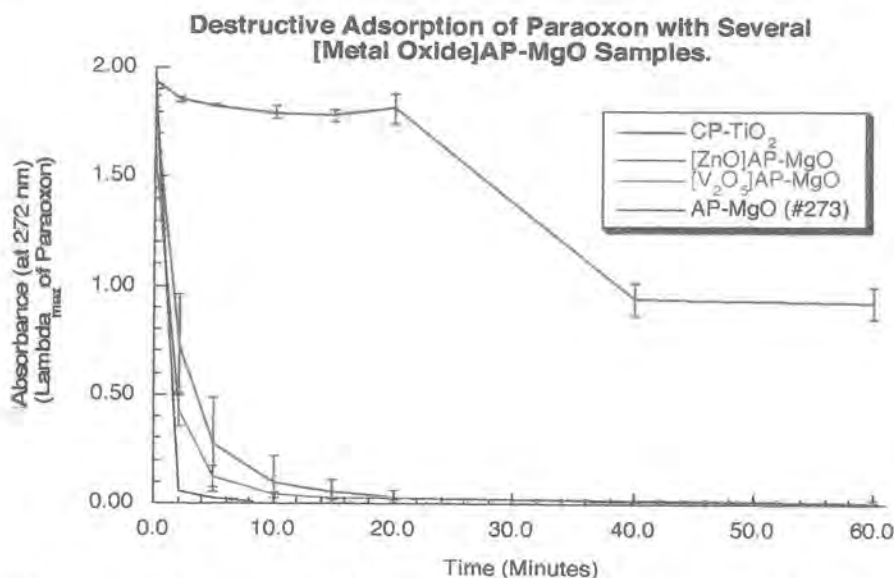


Figure 16: Destructive adsorption of paraoxon with “core/shell” RNP materials

Selection of the most suitable reactive nanoparticles for use as destructive adsorbent materials

The best formulations appear to be AP-MgO, [Fe₂O₃]AP-CaO, and CP-CaO. At this time AP-MgO alone or in combination with different metal oxide coatings appears to be the most suitable reactive adsorbent for the topical skin cream application. Based on the paraoxon and 2-CEES decomposition studies, iron oxide coated CaO, coated and uncoated MgO, and high surface area ZnO provide the most significant promise for a reactive adsorbent in the rTSP. The Fe₂O₃ coating provides enhanced reaction, possibly due to a catalytic effect and / or the prevention of hydroxylation of the oxide powders.

Autoclave-prepared MgO samples showed remarkable performance. These particles are the highest surface area samples tested, with a surface area of >500 m²/g. For the paraoxon studies the AP-MgO nearly instantaneously destructively adsorbed all of the paraoxon before the first reading at 2 minutes after exposure. For the 2-CEES experiments, it appears that the oxide reached a rapid equilibrium in about 5 minutes

where much of the 2-CEES was destroyed but the ethyl vinyl sulfide was also absorbed on the particle surface.

Task 8: Compatibility and Stability of RNPs in TSP cream

The purpose of this task was to evaluate the stability of the RNPs in the TSP cream. Two tests were conducted for this purpose. The first was to place RNPs into the TSP and store the mixture in a closed container under a N_2 atmosphere. Multiple samples were prepared and evaluated via powder X-ray diffraction (XRD) at time intervals extending to 6 months. These experiments are designed to test the compatibility of the RNPs with the TSP during long-term storage, for example, in an enclosed tube. The second set of experiments involved placing the RNPs in the base TSP and exposing the samples to low and high humidity environments in a set of controlled humidity cabinets. Low humidity was defined as 21% relative humidity and 75°F while high humidity was designated 65% relative humidity and 74°F. The purpose of these experiments is to examine the effect of humidity on the RNPs while they were contained in the TSP.

Experiments for affect of humidity RNP materials (without TSP)

A number of preliminary experiments were conducted on various RNP samples that are considered as candidates for inclusion in TSP. These experiments involved exposure to humidity in the humidity cabinet for periods up to six months. Samples included CP-CaO, AP-CaO, CP-MgO, AP-MgO, 2% $[Fe_2O_3]$ CP-CaO, 2% $[Fe_2O_3]$ AP-CaO, 10% $[Fe_2O_3]$ AP-CaO, 2 % $[Fe_2O_3]$ CP-MgO, Spray Dried MgO, $[TiO_2]$ AP-MgO, $[ZnO]$ AP-MgO, and ZnO.

Rather than discuss each of the samples on an individual basis, it is sufficient to note that, based on the results from the initial tests, it was decided that further tests with AP-MgO mixed with the TSP would be conducted. The results from these tests are discussed below.

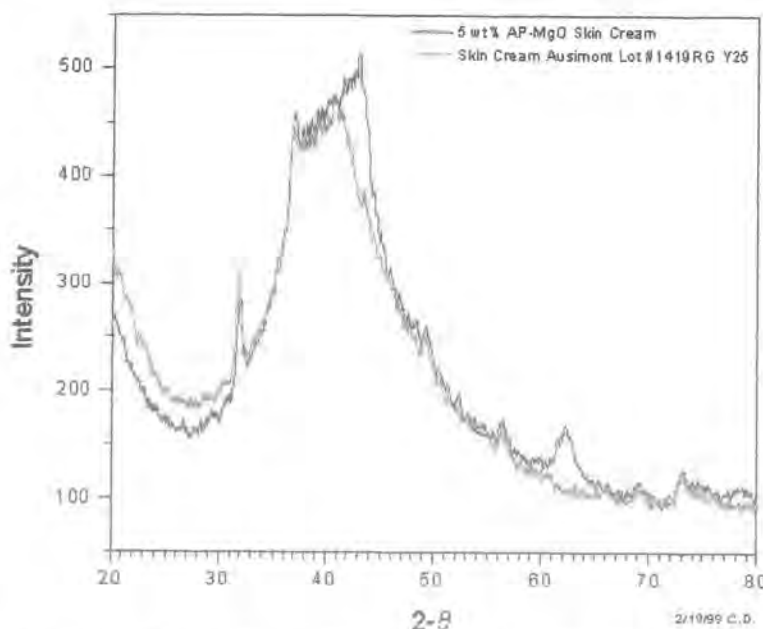


Figure 17: Overlay of the X-ray diffraction patterns for base TSP and TSP containing AP-MgO.

The small amount of MgO nanoparticles (5 % by mass) introduced into the sample is sufficient to show the major diffraction peaks for MgO at 43° and 62° of 2-theta. The MgO peak at 43° 2-theta appears as a definite shoulder to the main peak in the diffraction pattern of the neat base cream. The depletion of the signal intensity at these two positions is used as a measure of the conversion of the MgO in the cream to $\text{Mg}(\text{OH})_2$ or other decomposition product. The evolution of these two MgO peaks when the nanoparticle is included into the TSP is shown in Figure 17.

Figure 18 shows the XRD pattern for several 5-wt. percent loading of AP-MgO in the TSP as a function of time. A pattern for TSP alone and a control in which freshly mixed (minutes before XRD acquisition) RNP/TSP are included for reference. The figure also shows samples of MgO/TSP that were stored under nitrogen for intermittent periods of up to 3 months emulating the long-term storage conditions of the RNP/TSP. It is seen that there is no change in the diffraction pattern of these samples relative to that of the control. This indicates two facts. First, the TSP is compatible with the RNP and will not “breakdown” the added active materials of the mixture. Second, the RNPs remains intact (and chemically active) in the TSP for extended periods of time. There is no reason to believe that the RNP/TSP mixture would not remain stable and active for periods of one or more years. This indicates that the RNP/TSP mixture would have an extended shelf life, which is an important consideration for these CW detoxicants.

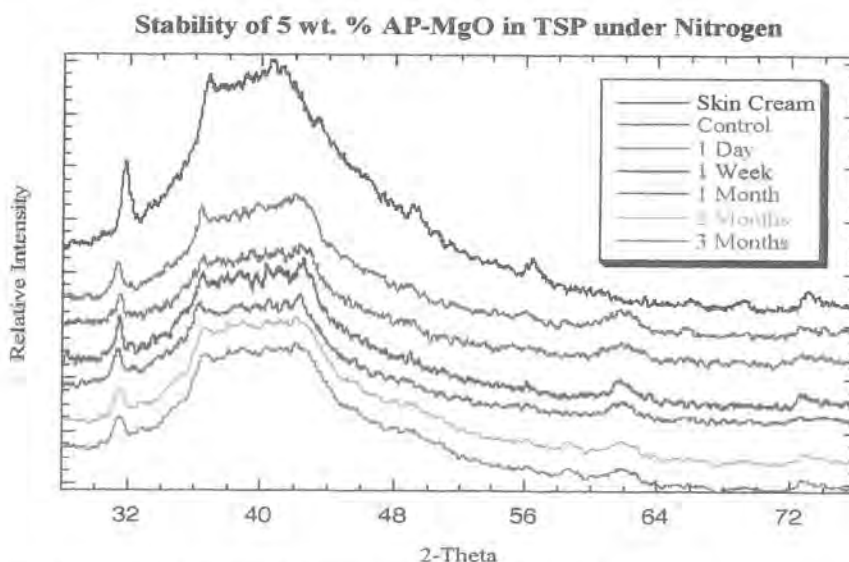


Figure 18: Stability of AP-MgO/TSP as a function of time under storage conditions.

The stability of the RNPs in the TSP when exposed to atmospheric moisture was also examined. These experiments were meant to emulate the moist conditions of the creams when applied by soldiers under field use conditions. These tests were performed in a humidity cabinet in which a constant relative humidity and temperature was maintained. It is known that MgO will convert to $\text{Mg}(\text{OH})_2$ over a period of a few days when exposed to high humidity. However, it is stable under conditions of low humidity for long periods of time, over 6 months. There seems to be a “conversion barrier” at 60 % relative humidity. Below this threshold the MgO is stable for long periods of time, above this

limit the MgO slowly converts to the hydroxide. It should be noted that tests have shown that $\text{Mg}(\text{OH})_2$ is also active for the destructive adsorption for CW simulants.

Figure 19 shows diffraction patterns for AP-MgO/TSP exposed to low humidity conditions (21 % RH at 75°C) for periods up to 2 months. It is readily seen that there was little to no conversion of the MgO to hydroxide even for extended exposure.

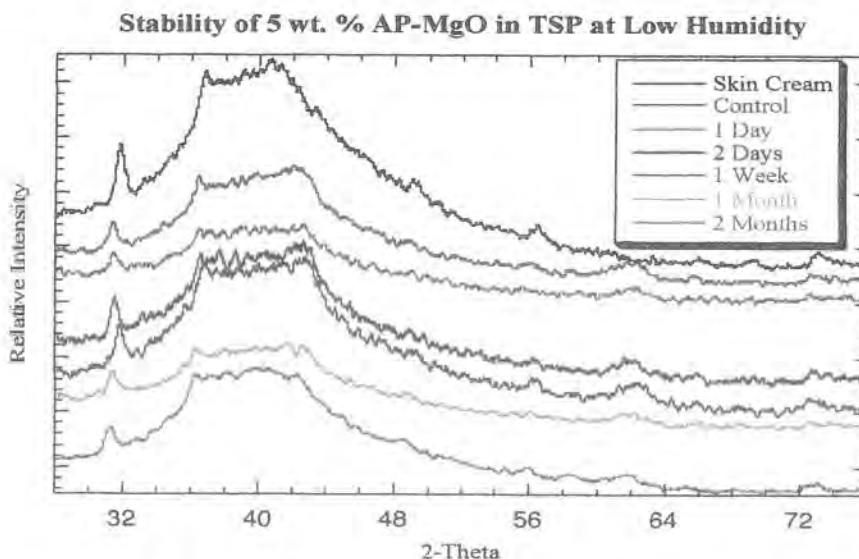


Figure 19: Stability of AP-MgO/TSP as a function of time under low humidity conditions.

The patterns for AP-MgO/TSP under high humidity (64 % RH at 74°C) are displayed in Figure 20. This information shows that the AP-MgO is stable to the effects of high humidity for periods up to one week. This is an interesting discovery. From previous humidity experiments for AP-MgO/TSP exposed to high humidity conditions in the absence of TSP it is known that the RNP converts to $\text{Mg}(\text{OH})_2$ after 1-2 days. The data collected here shows that the MgO is stable for up to one week under identical conditions. This indicates that the TSP provides protection for the MgO extending up to one week.

These results are important indicators that the MgO/TSP will remain active for extended periods of time under high humidity conditions. This is an important characteristic of the mixed TSP. Since it simulates the conditions under battledress overgarments this indicates that moisture will not interfere with the activity of the mixture.

In other experiments the effect of small amounts of transition metal oxides were loaded onto the surface of the AP-MgO and tested under identical humidity conditions. These samples included $[\text{CaO}]\text{AP-MgO}$, $[\text{ZnO}]\text{AP-MgO}$ coated material. The rationale of these experiments was that the coating oxide will either provide a protective layer on the MgO or act as a "sacrificial" component to inhibit the conversion of MgO to $\text{Mg}(\text{OH})_2$. The samples did not enhance the resistance to moisture.

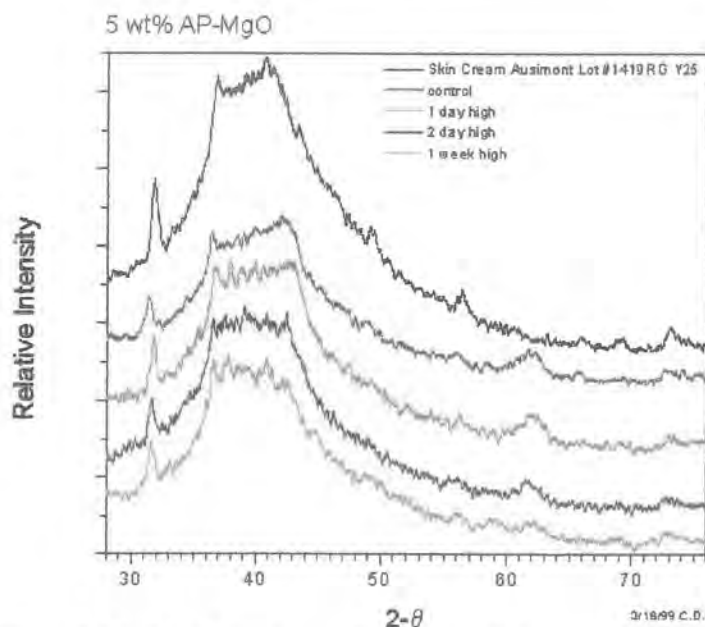


Figure 20: Stability of AP-MgO/TSP as a function of time under high humidity conditions.

Task 9: Solid product analysis of the chemical surface species.

Extraction of products from the reaction of MgO with 2-CEES

It is known that MgO and the other RNPs that are used as destructive adsorbents very strongly bind many organic molecules to their surfaces. Thus, we have been interested in identifying the bound products from the reactions that we have been studying.

In the case of 2-CEES reactions, the solid products after reaction were retained for further study via GC/MS. To do this, the solid product (100-mg) was placed in a 10-mL round bottom flask with 1-mL of solvent and a stirbar. The flask was capped and the mixture stirred for 30 minutes. Next the stirring was stopped and the solids in the mixture were allowed to settle before a 1-μL aliquot was obtained for GC/MS analysis. In the attempt to quantitate the amounts of the products for the reactions, a blank sample of 1-mL solvent was placed in a 10-mL round bottom flask and 14-μL of 2-CEES added under identical conditions to that used for the extract samples. 14-μL was the amount of that was used for the FT-IR experiments. A 1-mL aliquot of the 2-CEES solution was then obtained and injected in an analogous manner as for the extract samples. Similar procedures were performed for the products detected from the GC/MS analysis of the extracts.

Extraction of the MgO solid after reaction with 2-CEES indicated two products. The products were 2-(ethylthio)-ethanol ($\text{CH}_3\text{CH}_2\text{SCH}_2\text{CH}_2\text{OH}$) and ethyl vinyl sulfide ($\text{CH}_3\text{CH}_2\text{SCH}=\text{CH}_2$). Also observed in the extract was residual 2-CEES. The percentages of the three compounds based on the total amount of sulfur species extracted were 2-(ethylthio)-ethanol 44.2%, ethyl vinyl sulfide 41.6 %, and 14.2 % residual 2-CEES. It should be noted that, even under the best conditions, only about 1/3 of the original 2-CEES was accounted for by this method. In other words, with the best solvent extract, approximately 2/3 of the sulfur species remained on the surface of the RNP. The

products for the reaction were so strongly bound to the surface of the MgO that they were very difficult to extract. Many solvents were used in the attempt to extract the surface species (THF, benzene, DMSO, CCl₄, CH₂Cl₂, CHCl₃, H₂O, alcohols, ethers, alkanes, acetone, acetonitrile and others). Of all of the solvents, DMF (dimethyl formamide) proved to be the best extract for these experiments. The extraction with other solvents typically remove much less than 33 % of the sulfur species introduced to the RNP sample. Figure 21 displays a typical GC/MS spectrum for the extraction of an AP-MgO sample with DMF. The mass spectrum shown is for the 2-(ethylthio)-ethanol peak in the gas chromatogram. 2-(ethylthio)-ethanol is identified in the mass spectrum by a molecular ion peak at 106 m/e, another intense peak at 75 m/e, a fragment centered around 47 m/e and finally a smaller fragmentation pattern centered around 61 m/e.

Attempts at using other methods such as a simple headspace analysis (HS-GC/MS) and thermal desorption (TD-GC/MS) were made without success.

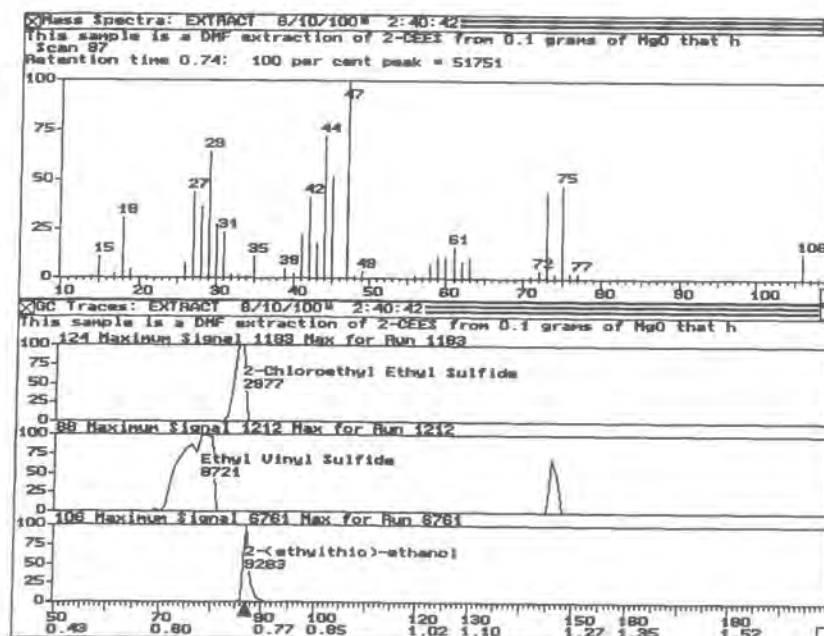


Figure 21: GC/MS of extracted products from reaction of 2-CEES and AP-MgO.

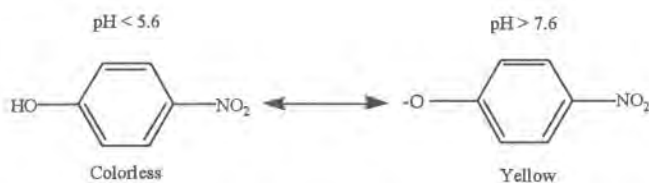
Determination of the Products from the Reaction of Paraoxon and AP-MgO

Attempts were made to extract and analyze the products from the reaction of RNP and the simulant paraoxon via GC/MS in an analogous manner as that described for 2-CEES. However, reproducible analyses were not obtained. Therefore, an alternative analysis was successfully developed.

The determination of the total amount of p-nitrophenol, a product of the decomposition of paraoxon with AP-MgO was performed. This method allowed the determination of the extent of reaction with consideration of species that remain adsorbed to the surface of the AP-MgO. By dissolving the MgO formulation with a dilute acid followed by neutralization with a weak base, all of the adsorbed species related to the reaction between paraoxon and MgO can be forced into solution for analysis. As a blank trial, the entire analysis was performed with paraoxon in the absence of MgO. This indicated that the paraoxon was not decomposed during the analytical procedure. After

This report contains company proprietary information that could be the subject of patent applications. As such it is intended for use by the U.S. Department of Army for contract monitoring and is not intended for public dissemination without prior written approval of an officer of Nantek, Inc.

the preparation of the samples was completed, the UV-Vis spectra were obtained for the MgO solutions after the reaction with paraoxon. There are two primary species in the solution that was observed in the UV-Vis, residual paraoxon and the p-nitrophenol product. At pH above 7.6 the p-nitrophenol exists as an anion which introduces an intense yellow color to the solution.



While each of these species gives rise to several absorptions in the UV-Vis region, paraoxon has a characteristic λ_{max} at 274-nm while the p-nitrophenol anion has a strong, characteristic adsorption at 400-nm. The absorptions at these wavelengths were used to determine the amount of each species by comparison with calibration curves generated from standard solutions. The data presented below are the average of three experiments.

Table 8: Decomposition of paraoxon by various RNP samples.

<u>Sample</u>	<u>Amount of paraoxon converted to p-nitrophenol (%)</u>
[Fe ₂ O ₃]AP-MgO	65.3
[CaO]AP-MgO	68.5
[ZnO]AP-MgO	69.3
[TiO ₂]AP-MgO	71.1
AP-MgO	85.9
AP-MgO after THF treatment	84.2

It seems that the presence of “shell” oxides actually hinders the destructive adsorption of the paraoxon on the MgO. This has been observed for systems with other “core/shell” materials. This is easily explained when it is considered that the presence of the shell materials is effectively “blocking” some of the active sites on the surface of the RNP. The purpose of the “shell” oxides is to promote a surface “catalytic” regeneration of the RNP. It has been shown that certain transition metal oxides are capable of greatly enhancing the destructive adsorption of certain molecules on RNPs⁷⁻¹⁰. Some shell oxides enhance the reactions to the point that the RNPs are stoichiometric reagents. Examples include chlorinated hydrocarbons and acid gases.

Task 10: Studies with chemical warfare agent challenges.

Studies of the reaction of MgO with chemical warfare agent challenges.

The following is a summary of the paper titled “Reactions of VX, GD, and HD with Nanosize MgO”⁴. The full paper is given as an attachment to this report.

Identification of products and kinetics of reactions between VX, GD, HD and MgO⁴

The room-temperature reactions of the chemical warfare agents VX (O-ethyl S-2-(diisopropylamino)ethyl methylphosphonothioate), GD (3,3-dimethyl-2-butyl

methylphosphonofluoridate, or Soman), and HD (2,2'-dichloroethyl sulfide, or mustard) with nanosize MgO were studied using solid-state MAS NMR. All three agents hydrolyze on the surface of the very reactive MgO nanoparticles. VX yields ethyl methylphosphonic acid (EMPA) and methylphosphonic acid (MPA), but no toxic S-(2-diisopropylamino)ethyl methylphosphonothioate (EA-2192). GD forms both GD-acid and MPA. For HD, in addition to hydrolysis to thiodiglycol, about 50% elimination to divinyl sulfide occurs. The reaction kinetics for all three agents are characterized by a fast initial reaction followed by gradual slowing to a steady-state reaction with first-order behavior. The fast reaction is consistent with liquid spreading through the porous nanoparticle aggregates. The steady-state reaction is identified as a gas-phase reaction, mediated by evaporation, once the liquid achieves its volume in the smallest available pores.

In the case of GD, the reaction with the MgO occurs through surface hydroxyl or surface adsorbed water. Two products for the reaction were observed. The major product was GD-acid (pinocolyl methyl phonic acid, 25.7 ppm) with a small amount of methylphosphonic acid (18.5 ppm) formed as a secondary product (see Figure 22). The ratio of the two products are about 4:1.

³¹P MAS NMR indicated that VX was hydrolyzed by surface hydroxyls or surface adsorbed water to form two products: ethyl methylphosphonic acid (25.2 ppm) or methylphosphonic acid (19.8 ppm). Surprisingly, the known product from hydrolysis in aqueous solution, toxic EA-2192, was not observed. A peak at 40 ppm would indicate this compound if it were present (see Figure 22).

Experiments with the destructive adsorption of HD on MgO showed the formation of three products - one from hydrolysis and two from elimination of HCl. These were thiodiglycol (broad peaks at 60.5 and 33.4 ppm), vinyl HD (132.8, 110.0, 44.7 and 35.4 ppm), and divinyl HD (131.2 and 113.1 ppm) (see Figure 22). Since the vinyl HD undergoes a second elimination, the final ratio of products is about 50 % thiodiglycol and 50 % divinyl HD.

Reaction between all three agents and MgO reveal very strong interaction between the products and adsorbent indicating the "strong adsorptive" nature of the RNP. A key finding was that reaction occurred very rapidly upon contact, but the overall rate was controlled by material transfer. Details and discussion of these experiments can be found in the attachment "Reactions of VX, GD, and HD with Nanosize MgO".

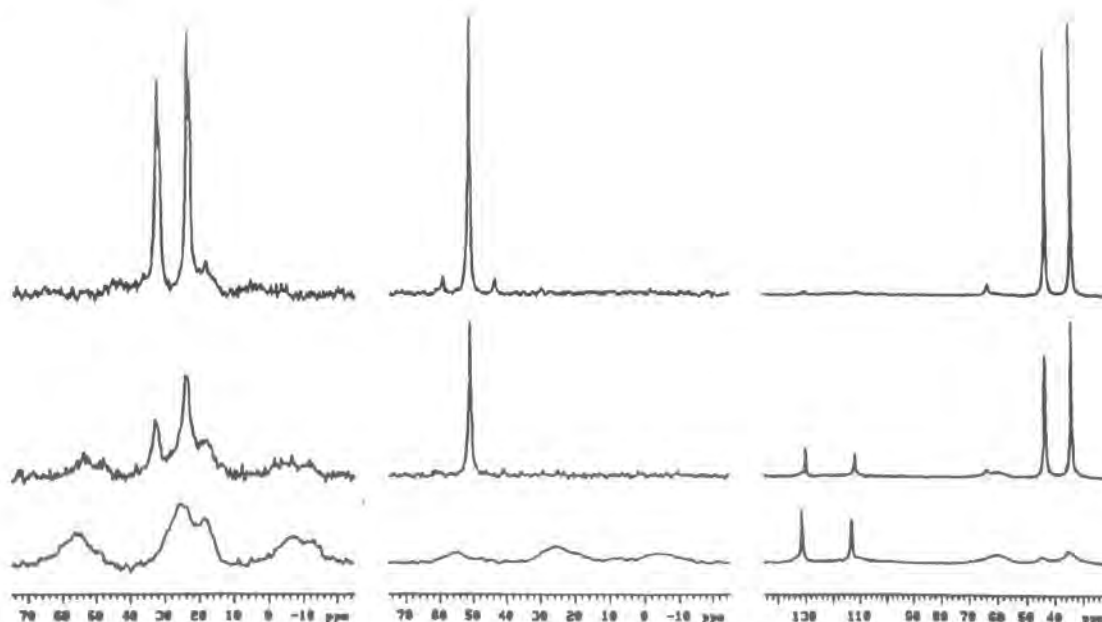


Figure 22: MAS NMR spectra obtained for agents added to AP-MgO: (left) GD (top to bottom) t=9.5 min, 1.0 h, and 23 h; (middle) VX at t= 8.5 min, 24 h, and 3 months; (right) HD at t=9.5 min, 3.8 h, and 1 week.

Studies of the reaction of nanocrystalline CaO and Ca(OH)₂ with chemical warfare agent challenges.

The following is a summary of the paper titled "Reactions of VX, GD, and HD with Nanosize CaO: Autocatalytic Dehydrohalogenation of HD"¹¹. The full paper is given as an attachment to this report.

Identification of products and kinetics of reactions between VX, GD, HD and CaO¹¹

Room-temperature reactions of the chemical warfare agents VX, GD, and HD with nanosize CaO (AP-CaO) and HD with commercial CaO were studied using solid-state MAS NMR. VX and GD hydrolyze to yield surface-bound complexes of nontoxic ethyl methylphosphonate and pinacolyl methyl phosphonate, respectively. It is significant to note that toxic EA-2192 is **not** formed during the basic hydrolysis of VX over the nanoparticles. The kinetics are characterized by an initial fast reaction followed by a slower, diffusion-limited reaction. Similar behavior was observed for HD on either dried or hydrated AP-CaO and CaO. On partially hydrated AP-CaO (but not CaO), an unusually fast steady-state elimination of HCl occurs after an induction period. This behavior is attributed to acid-catalyzed surface reconstruction (to regenerate fresh surface) and the formation of CaCl₂, which is known to be more reactive than CaO. The product distribution for HD is about 80 % divinyl sulfide and 20 % thiodiglycol and/or sulfonium ions, which apparently reside as surface alkoxides. Such kinetic behavior was not evident for the common mustard simulant 2-chloroethyl ethyl sulfide (CEES) on partially hydrated AP-CaO, which exhibited only the typical fast/diffusion-limited reaction.

³¹P MAS NMR of GD added to AP-CaO (see Figure 23) initially shows two doubles (J_{pf}=1049 Hz) are apparent for the GD isomers centered at circa 28.1 ppm. Over time,

This report contains company proprietary information that could be the subject of patent applications. As such it is intended for use by the U.S. Department of Army for contract monitoring and is not intended for public dissemination without prior written approval of an officer of Nantek, Inc.

hydrolysis cleaves the P-F bond and the sharp doublets are replaced by a broad singlet for PMPA at 24.3 ppm. The broadness of the PMPA peak and the presence of intense spinning sidebands are indicative of surface binding of this product. No further hydrolysis of pinacolyl methyl phosphonic acid (PMPA) to methylphosphonic acid (MPA) was observed during the 24-h observation period. The reaction profile is shown in Figure 24. After a fast, initial reaction, a steady-state half-life of 4.5 h was observed.

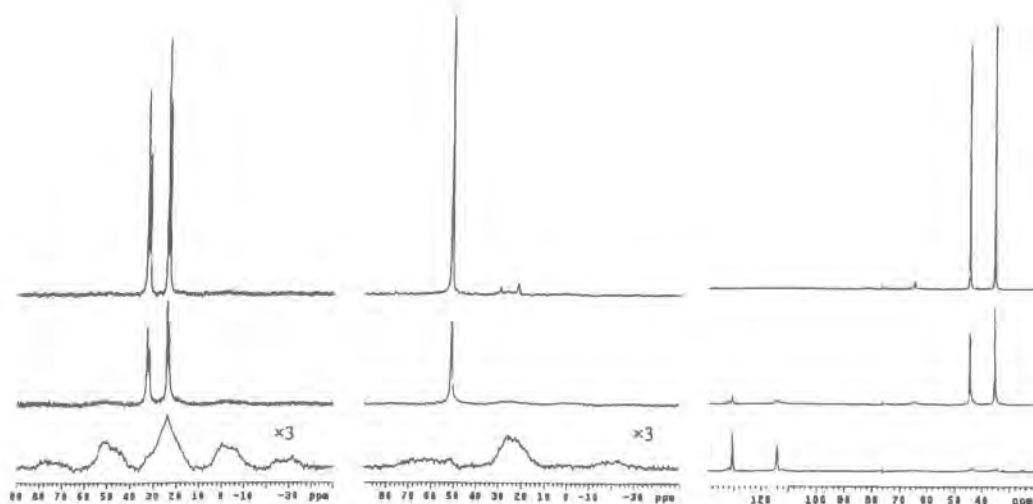


Figure 23: MAS NMR spectra obtained for agents added to fresh, “as received” AP-CaO: (left) GD (top to bottom) t=8.5 min, 1.9 h, and 25 h; (middle) VX at t= 8.5 min, 48 h, and 21 days; (right) ¹³C-HD at t=7.5 min, 6.8 h, and 70 h.

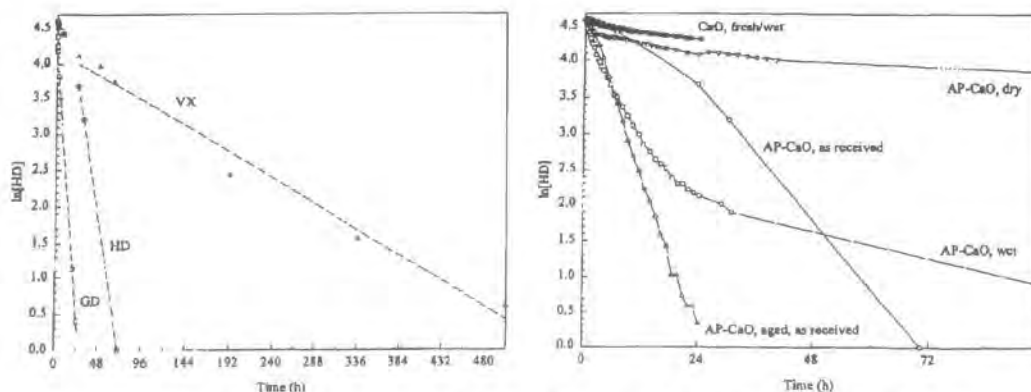


Figure 24: Reaction profiles for (left) GD, VX, and ¹³C-HD liquid on fresh, “as received” AP-CaO and (right) HD and ¹³C-HD on AP-CaO and CaO.

In the case of VX, the neat agent yields a sharp peak at 51.1 ppm (see Figure 23). Gradually, VX hydrolyzes to EMPA which emerges as a broad band at 25.0 ppm. Spinning sidebands are also apparent for this surface-bound species. No peak is evident for toxic EA-2192, which would occur near 40 ppm. The reaction profile in Figure 24 shows the same behavior exhibited by GD, except that the steady-state reaction is much slower, with a half-life of 93 hours.

hydrolysis cleaves the P-F bond and the sharp doublets are replaced by a broad singlet for PMPA at 24.3 ppm. The broadness of the PMPA peak and the presence of intense spinning sidebands are indicative of surface binding of this product. No further hydrolysis of pinacolyl methyl phosphonic acid (PMPA) to methylphosphonic acid (MPA) was observed during the 24-h observation period. The reaction profile is shown in Figure 24. After a fast, initial reaction, a steady-state half-life of 4.5 h was observed.

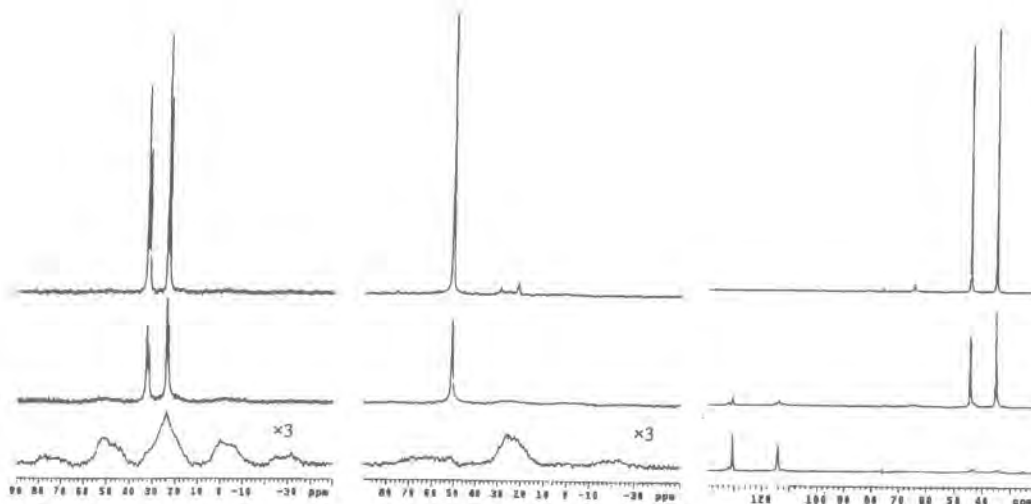


Figure 23: MAS NMR spectra obtained for agents added to fresh, "as received" AP-CaO: (left) GD (top to bottom) $t=8.5$ min, 1.9 h, and 25 h; (middle) VX at $t=8.5$ min, 48 h, and 21 days; (right) ¹³C-HD at $t=7.5$ min, 6.8 h, and 70 h.

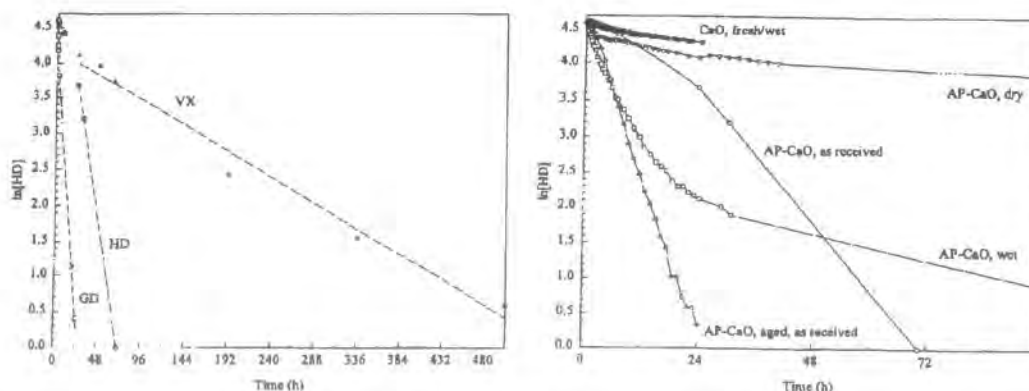


Figure 24: Reaction profiles for (left) GD, VX, and ¹³C-HD liquid on fresh, "as received" AP-CaO and (right) HD and ¹³C-HD on AP-CaO and CaO.

In the case of VX, the neat agent yields a sharp peak at 51.1 ppm (see Figure 23). Gradually, VX hydrolyzes to EMPA which emerges as a broad band at 25.0 ppm. Spinning sidebands are also apparent for this surface-bound species. No peak is evident for toxic EA-2192, which would occur near 40 ppm. The reaction profile in Figure 24 shows the same behavior exhibited by GD, except that the steady-state reaction is much slower, with a half-life of 93 hours.

The ^{13}C MAS NMR for ^{13}C labeled HD show peaks at 44.5 and 35.3 ppm. Over time sharp peaks appear for the elimination products at 130.6 and 114.2 ppm (divinyl sulfide) and 132.0, 112.3, 43.4, and 34.4 ppm (chloroethyl vinyl sulfide), and broad peaks emerge for the hydrolysis product at ca. 61 and 33 ppm (thiodiglycol). The broadness of the thiodiglycol product peaks is indicative of surface binding. The products indicate the reaction proceeds via 80% elimination and 20% hydrolysis. Minor amounts of sulfonium ions derived from the hydrolysis products were also detected, and these are included in the calculation of the elimination / hydrolysis distribution. The reaction profile is shown in Figure 24, which exhibits an induction period of 5 h followed by a rather fast steady-state reaction with a half-life of 8.7 h. These results are summarized in Table 9. Figure 24 also shows the reaction profiles for several different AP-CaO samples with HD.

Table 9: HD and CEES Reactions on AP-CaO and CaO.

Compound/Material/Hydration	NMR Method	Induction Period	Initial Half-life	Steady-State Half-life	Elimination/Hydrolysis
HD/AP-CaO/"as received"	^{13}C	5 h	8.7 h	8.7 h	80/20
HD/AP-CaO/ aged "as received"	^{13}C	1 h	3.5 h	3.5 h	80/20
HD/AP-CaO/"wet"	^{13}C	None	3.1 h	> 46 h	80/20
HD/AP-CaO/"dried"	^1H	None	4.0 h	> 11 days	5/95
HD/CaO/"as received"	^1H	40 min	31 h	> 49 days	80/20
HD/CaO/"wet"	^{13}C	None	9.1 h	> 49 days	60/40
CEES/AP-CaO/aged "as received"	^1H	None	<12 min	> 135 h	5/95
CEES/AP-CaO/"dried"	^1H	None	1.7 h	> 156 h	30/70

All three CW agents show similar kinetic behavior on the AP-CaO. First, a fast reaction due to liquid spreading over the solid sorbent followed by a slower, steady-state reaction mediated by evaporation. Such reactions are mediated by the evaporation rate or vapor pressure⁴. GD has a much higher vapor pressure than VX (0.4 vs 0.0007 mm Hg), and thus a much faster steady-state reaction (half-life 4.5h) compared to VX (93 h). For HD on partially hydrated AP-CaO, the presence of an induction period, the absence of a diffusion-limited reaction, and a predominant dehydrohalogenation reaction strongly suggests an autocatalytic surface reaction. Details and discussion of these experiments can be found in the attachment "Reactions of VX, GD, and HD with Nanosize CaO: Autocatalytic Dehydrohalogenation of HD".

Task 11. Formulation Development and Prototype Screening

Viscosity studies

The purpose of the viscosity studies was to examine the modification of the TSP flow characteristics when small amounts of reactive nanoparticles are incorporated into the samples. In these experiments, the RNP was added to the already mixed skin cream.

An important physical characteristic of fluids is their viscosity behavior under different shear and thermal conditions. Many protective lotions and creams are fluids that can be categorized as suspension or emulsions. Others may be simple solutions of different oils. Shear and temperature can affect the structure and homogeneity of both emulsions and suspensions. In a protective cream or lotion this structure can affect the performance of the product. Measurements of the viscosity of a protectant cream or lotion over a range of shear rates and at different temperatures can provide valuable

information relative to the ultimate performance of the material. This is true even if the protective lotion is a simple solution, and not a more complex emulsion or suspension.

For these experiments, premixed skin cream from USAMRICD was used as received by Nantek, Inc. To these creams small amounts of the nanoparticle samples were added and mixed by hand in the desired amount (i.e. either 1 or 2% of RNP on a wt./wt. basis with the TSP). Untreated TSP from the same shipment was used as the reference.

The experiments were performed at the Battelle Polymer Center in Columbus, Ohio. A Haake-7 Viscometer with a controlled temperature bath was used to obtain the viscosity data. The RNP/TSPs were analyzed using a standard operating procedure developed for viscosity measurements of skin protectants.

Samples were run at 10, 20, 30 and 40°C from 0 s⁻¹ increasing to 20 s⁻¹ in a 30 second linear ramp. As noticed in previous testing of TSP materials, slippage between the cone and plate occurred. Duplicates of each sample were run and the averages of the final data point are represented in the table below (viscosity in Poise). All of the samples containing nanoparticles added in the manner stated above were slightly more viscous than the TSP reference material.

Table 10: Viscosity of TSPs containing nanoparticles.^a

Temperature	TSP-Ref. (Poise)	1% MgO ^b (Poise)	2% MgO ^b (Poise)	1% ZnO ^b (Poise)	2% ZnO ^b (Poise)
10°C	1750	4250	4500	2500	3750
20°C	1250	3000	3250	1750	3250
30°C	750	1025	2000	750	825
40°C	450	425	1000	450	450

^aThe larger the value (Poise) represents a “tackier” cream

^bThe nanoparticles were added to the TSP as a percentage on a wt/wt basis.

The data from the viscosity studies highlights a problem initially encountered when the nanoparticles were incorporated into the base TSP cream. When the nanoparticles are added to the TSP base cream, even in the very small amounts used for the viscosity tests, the cream becomes “tacky” and loses its flow characteristics. This is due to two factors. First it is very difficult to get a good dispersion of the fine nanoparticle powders into the premixed TSP cream. These samples were made manually and it is assumed with confidence that strong mechanical stirring would lead to a better dispersion. There is another simple way to get around the dispersion problem (unfortunately this was uncovered after the viscosity tests were completed). This was to mix the nanoparticles with the powder component of the TSP to the desired amount and then to add the liquid component of the TSP before mixing. Through visual observation it was evident that this method definitely helps with the dispersion of the nanoparticles into the rTSP.

A second closely related problem was encountered when larger amounts of nanoparticles were introduced into the rTSP. When amount of 5% or greater were added the rTSPs had a tendency to dry out. Evidently the additional amount of nanoparticle powder introduced was enough to offset the balance between the liquid and solid components of the rTSP and they “dried up”. The obvious solution to this problem was to simply increase the liquids content of the TSP. Again, this problem was not encountered until after the completion of the viscosity tests. Unfortunately, the project

budget had not allocated additional funds for additional viscosity tests at Battelle. However, Nantek has very recently acquired a viscometer and will start examining the viscosity of these more recent formulations through internal funding.

Task 12: Final Formulation Selection

Based on the accumulated data for both simulant and real agent decomposition, we have selected AP-MgO as the nanoparticle of choice for the final development of the rTSP containing reactive nanoparticle technology. Another important consideration was that MgO is among the easiest of the nanoparticle materials that can be made on a large scale at a reasonable cost. Therefore the remaining experiments focused on AP-MgO. The following is a description of some final tests with simulants before moving into descriptions of the initial tests for the destructive adsorption of real agents with MgO containing rTSPs.

In addition, some of the real agent tests were performed with other promising metal oxides such as CaO, ZnO and TiO₂.

Task 13: Final Formulation Testing With Simulants.

Destructive adsorption of diethyl phenylthiomethylphosphonate (DEPTMP).

The objective of this research was two-fold. The first objective was to determine the efficacy of various reagents in adsorbing diethyl phenylthiomethylphosphonate (DEPTMP). The second objective was to determine the structure of the adsorbed species.

Procedure

Adsorbents examined in this study included aerogel prepared magnesium oxide (AP-MgO), conventionally prepared magnesium oxide (CP-MgO), commercially available magnesium oxide (CM-MgO), activated carbons (AC) from norite (AC-NO), Darco (AC-DA), coconut shell (AC-CO), and Amborsorb (AM).

In a typical experiment, a 250-mL single necked flask provided with a serum cap, stir bar and a magnetic stirrer were charged with dry pentane (200-mL). To the above was sequentially added the solid adsorbent (0.2-g) and DEPTMP (9-μL, ~ 5% by wt.). After an hour at room temperature, stirring was stopped and the clear liquid phase was analyzed by UV-VIS for quantitation of the residual DEPTMP. Subsequently, all the solvent was decanted off and the solid was dried overnight under vacuum and analyzed by FT-IR and NMR to assess the structure of the adsorbed species.

Samples for FT-IR analysis were prepared by grinding a sample of the dried solid (1 to 3-mg) with anhydrous KBr (100-mg). Pellets were made with a standard pellet press. Spectra of neat liquid were obtained by spreading a thin film of the liquid between a pair of salt plates. ³¹P NMR spectra were obtained using a Tecmag 270 MHz spectrometer equipped with a Doty Scientific 7-mm high speed CP-MAS probe, using direct excitation and high power proton decoupling. The observation frequency for ³¹P was 109.55 MHz. Samples were packed in a sapphire rotor with kel-F end caps and typically spun at 4700 Hz. Chemical shifts were referenced to external 85% H₃PO₄ (0 ppm).

Results and Discussion

The UV-VIS spectrum of DEPTMP in pentane contains two absorption bands centered about 209 and 256-nm. Adsorption of DEPTMP by the solid adsorbent should result in a reduction of its concentration in the liquid phase and hence a decrease in the intensity of its absorption peaks. First, a calibration curve was constructed by measuring absorptions of a series of solutions of pentane containing known amounts of DEPTMP. Then, samples of the liquid phase derived from reactions using DEPTMP/adsorbent were analyzed by UV-VIS after 1-hour reaction time. Using the calibration curve the amount of unadsorbed DEPTMP left in the liquid phase of these reactions was then calculated. Conversely, the amount of DEPTMP adsorbed can be calculated. Table 11 summarizes the results of the UV-Vis analysis of the liquid phase derived from DEPTMP and various adsorbents.

From the table below, it is clear that AP-MgO is superior to all other adsorbents and its ability to adsorb various reagents is attributed to its unique morphology and high surface area¹. Since near complete reaction was observed only with AP-MgO, we chose to examine the structure of the adsorbed species with this adsorbent.

Table 11: Amount of adsorbed DEPTMP as determined by UV-Vis analysis

Adsorbent	DEPTMP Adsorbed (%) ^a
CM-MgO	17
CP-MgO	74
AP-MgO	96
AC-DA ^b	24
AC-NO	35
AC-CO	28
AM	59

^aAverage of 3-4 determinations.

^bUse of crushed AC-DA resulted in 47% adsorbed DEPTMP.

Figure 25 shows the IR spectra of neat DEPTMP (A) and that of AP-MgO adsorbed DEPTMP (B & C). Since the IR absorption peaks due to 5% by wt. adsorbed DEPTMP were somewhat weak (B), another sample was prepared for the IR studies by carrying out a reaction in which a large excess of DEPTMP was treated with AP-MgO in pentane. After an hour reaction time, the excess reagent was removed by repeated washing with pentane until the liquid phase showed no more DEPTMP via UV-Vis analysis. The IR spectrum of this sample (C) shows more intense peaks.

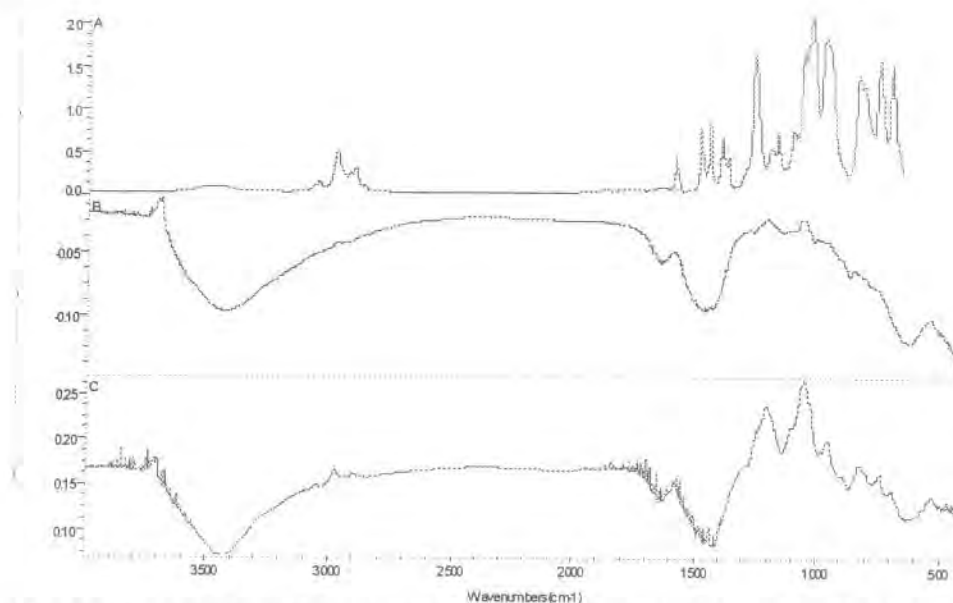


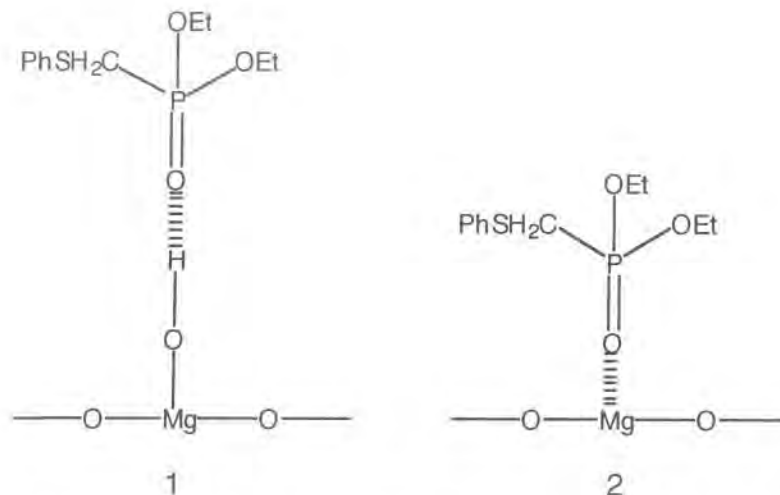
Figure 25: FT-IR spectra of neat DEPTMP (A), DEPTMP (5% by wt.)/AP-MgO (B) and DEPTMP (excess)/AP-MgO (C).

There is an appreciable amount of literature on the use of various IR techniques to explore the process of adsorption of phosphonates by inorganic oxides¹³⁻¹⁷. From this it appears that 1300-1000 cm⁻¹ region in the IR yields the most direct information about the nature of adsorbed species.

The following points emerge from a close examination of Figure 25.

- 1) Peaks in B and C appear broadened.
- 2) There is a negative absorption band in the 3700 to 3000 cm⁻¹ region.
- 3) The alkyl and aryl C-H bands (3100-2800 cm⁻¹) did not change much upon adsorption.
- 4) The $\nu_{P=O}$ band of DEPTMP shifted from 1250 to 1206 cm⁻¹ ($\Delta\nu = -44$ cm⁻¹).
- 5) The $\nu_{C-O(P)}$ band did not shift much (1048 \rightarrow 1049 cm⁻¹).
- 6) Other IR bands appear weaker upon adsorption.

These results indicate that the P=O bond is significantly perturbed upon adsorption. However, C-O stretch is not affected which suggests that adsorption does not involve the C-O(P) moiety. Thus, the initial adsorption might involve structures such as (1) and / or (2).



The AP-MgO used in this study showed a slight negative band in the 3500-3000 cm⁻¹ region while the DEPTMP adsorbed sample (Figure 25) shows a much larger negative band. This is in contrast to what was reported in the literature with some other reagents such as sarin¹³ and dimethyl methylphosphonate¹⁶. With these reagents, a broad band was observed in the 3550-2500 cm⁻¹ after adsorption and it was attributed to the generation of surface hydroxyl groups by the reagent decomposition. From the IR results it appears that at room temperature DEPTMP is mostly adsorbed by AP-MgO. In order to verify whether a simple adsorption or a hydrolytic decomposition of DEPTMP occurs, the solid sample from the adsorption reaction was analyzed by NMR.

Figure 26 shows the solid state ³¹P MAS NMR spectrum of DEPTMP adsorbed on AP-MgO (5% by wt.). It displays two major peaks centered about δ 24.2 and 15.7 ppm and a set of two smaller peaks. The latter are attributed to spinning side bands. From a literature survey¹⁸, δ value ranges from 29.6-32.6 ppm for derivatives of type (EtO)₂P(O)R wherein R is CH₃, Et, or butyl. Thus, it appears that the signals observed in the DEPTMP/AP-MgO sample are probably due to products that contain a more shielded phosphorous nucleus.

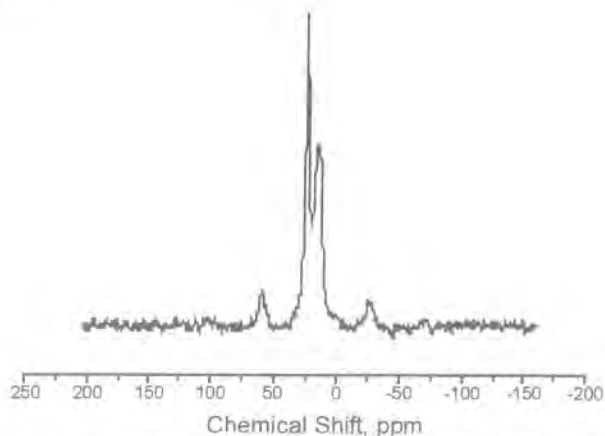
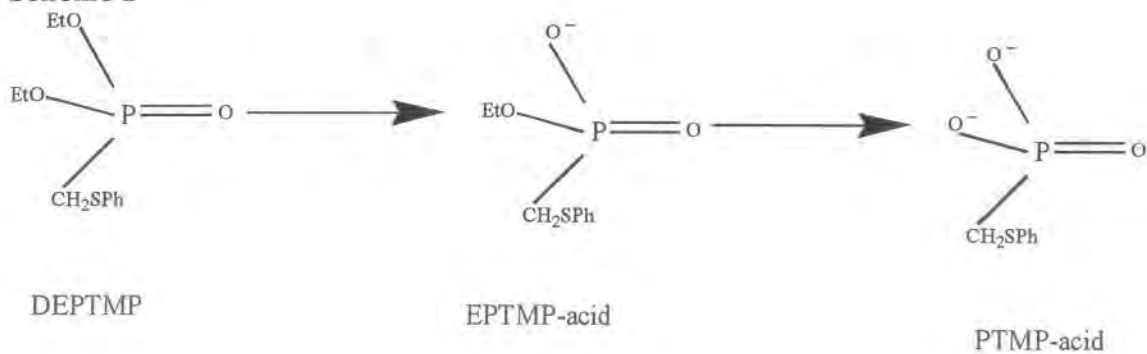


Figure 26: ³¹P NMR spectrum of DEPTMP (5% by wt.)/AP-MgO.

Based on the work of Wagner *et al.*¹, the major peaks are attributed to ethyl phenylthiomethyl phosphonic acid (EPTMP, δ 24.2 ppm) and phenylthiomethyl phosphonic acid (PTMP, δ 15.7 ppm). Due to the basic nature of magnesium oxide, we prefer to show the adsorbed species as the corresponding anions (Scheme 1).

Scheme 1



To summarize, ³¹P NMR results indicate that the ethoxy groups of DEPTMP are hydrolyzed by surface hydroxyls and/or physisorbed water in AP-MgO to produce a mixture of mono- and di-anionic species. The P=O group in these structures probably remain adsorbed as evidenced by IR. Even though the ethoxy groups were hydrolyzed, the C-O stretching value remained the same. This is likely because the IR stretching absorption values for CH₂O(P) and CH₂O(Mg) are not appreciably different.

Destructive adsorption of diisopropyl fluorophosphonate with AP-MgO.

The objective of this research was two-fold. The first was to determine the efficacy of various reagents in adsorbing diisopropyl fluorophosphate (DFP). The second was to determine the structure of the adsorbed species.

Procedure

Adsorbents examined in this study included: aerogel prepared magnesium oxide (AP-MgO), conventionally prepared magnesium oxide (CP-MgO), and commercially available magnesium oxide (CM-MgO).

In a typical experiment, the particular adsorbent (~0.1-g) was weighed into a vapor phase IR cell that could be connected to a vacuum line. Prior to adsorption, the adsorbents were evacuated at room temperature for ~15-30 min (~10⁻⁴ torr). After this treatment, a background spectrum was recorded. Subsequently, DFP was introduced (9 μL, ~5 % by wt.) into the sample cell and the IR spectra of the vapor phase was recorded after 1 h. In order to assess the structure of the adsorbed species, reaction with DFP was carried out as described below and the DFP adsorbed on the solid was isolated and analyzed.

In a representative experiment, a 250-mL single necked flask provided with a serum cap, stir bar and a magnetic stirrer was charged with dry pentane (200-mL). To the above was added sequentially, the solid adsorbent (0.2-g) and DFP (9 μL, ~5% by wt.). After an hour at room temperature, stirring was stopped, the solvent decanted off and the solid dried overnight under vacuum and analyzed by IR and solid state NMR.

Results and Discussion

The vapor phase IR spectra of neat DFP and that of the ones derived from CP-, CM-, and AP-MgO samples are shown in Figure 27. It is clear that the DFP reacted completely with AP-MgO as evidenced by absence of all IR absorptions (D). In contrast, CP-MgO (B) and CM-MgO (C) samples showed absorptions due to DFP in the vapor phase confirming their poor adsorption quality. Under the conditions of evacuation employed in our study, we observed only partial vaporization of DFP into the vapor phase. As a result, we were able to make only qualitative and not quantitative evaluation of the extent of reaction of DFP with different MgO samples.

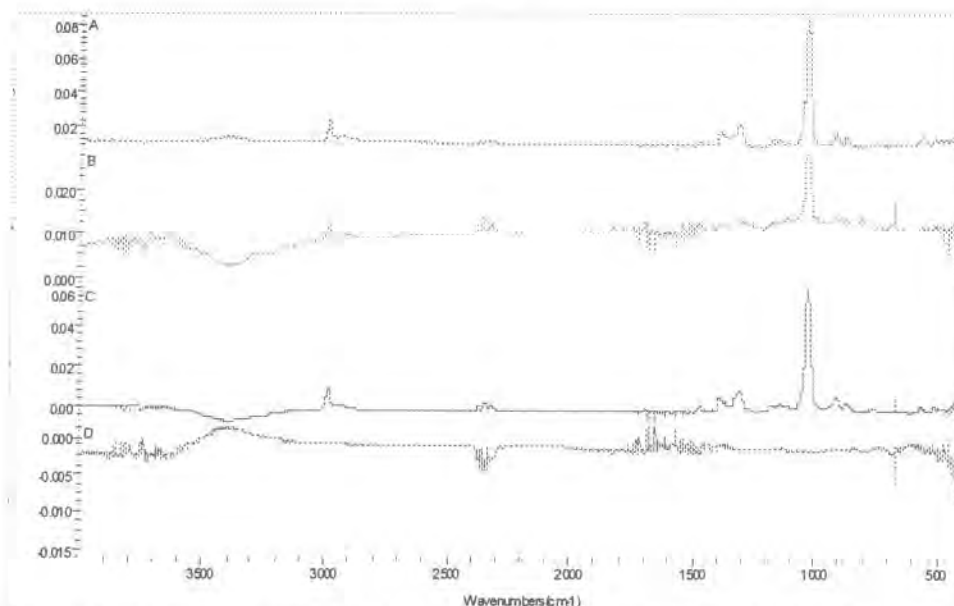


Figure 27: FT-IR vapor phase spectra of neat DFP (A), DFP/CP-MgO (B), DFP/CM-MgO (C), and DFP/AP-MgO (D)

Figure 28 shows the IR spectra of neat liquid DFP and that of DFP adsorbed AP-MgO sample. The following points are note-worthy about these spectra:

- 1) A broad absorption band was observed in the $3700\text{--}3000\text{ cm}^{-1}$ region after reaction.
- 2) The alkyl C-H stretch region ($3100\text{--}2800\text{ cm}^{-1}$) did not change much upon adsorption.
- 3) The $\nu_{\text{P=O}}$ band of DFP shifted from 1298 cm^{-1} to 1260 cm^{-1} ($\Delta\nu = -38\text{ cm}^{-1}$) and appeared as a rather weak band.
- 4) A slightly more intense band was observed around 1209 cm^{-1} .
- 5) The $\nu_{\text{C-O(p)}}$ band did not shift (1016 cm^{-1}).
- 6) Characteristic absorptions ($1177, 1141$ and 1110 cm^{-1}) due to "rocking vibration" mode of methyl group of isopropyl units were still observed without appreciable shift compared to neat DFP.
- 7) Prominent additional bands are seen in the $1100\text{--}990\text{ cm}^{-1}$ region: an intense peak at 1079 cm^{-1} and a broad absorption at 992 cm^{-1} .

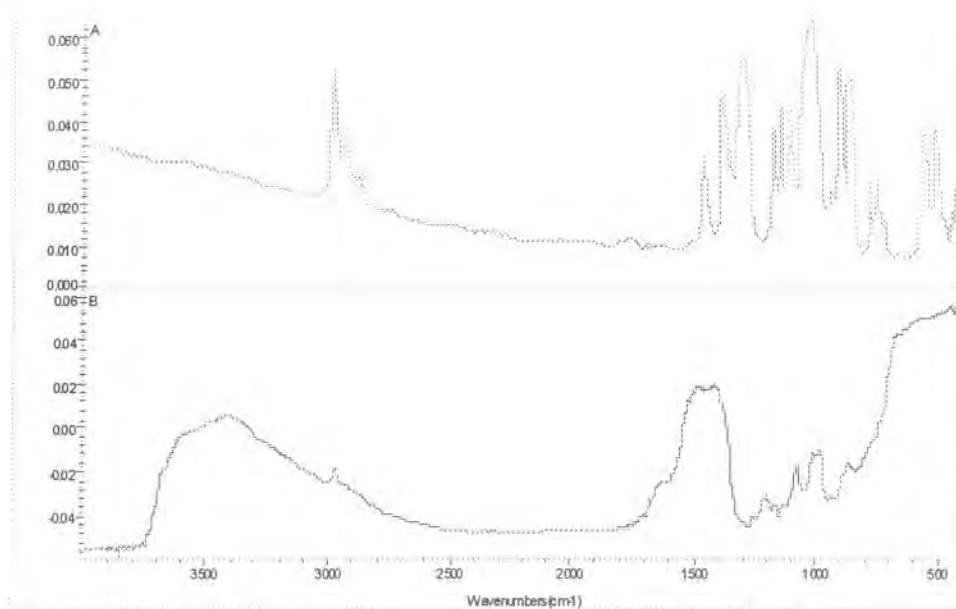
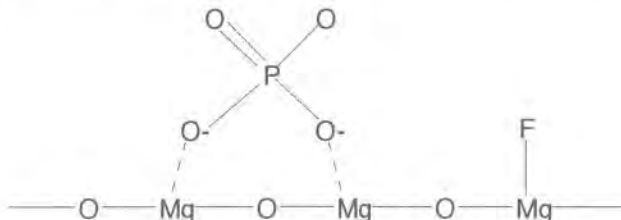


Figure 28: FT-IR Spectra of neat DFP (A) and DFP/AP-MgO (B)

We assign the pair of new peaks (1079 & 992 cm⁻¹) to the bridged “O-P-O” species as shown below. Existence of such structures has been proposed with dimethyl methylphosphonate/AP-MgO¹⁶, sarin and its related compounds adsorbed on alumina or magnesium oxide¹³.



More direct evidence for the existence of PO₄³⁻ in the DFP impregnated AP-MgO sample comes from its ³¹P NMR spectrum (Figure 29). In this spectrum a major peak centered about δ -0.76 ppm and two sets of minor peaks were seen. The latter are attributed to spinning side bands.

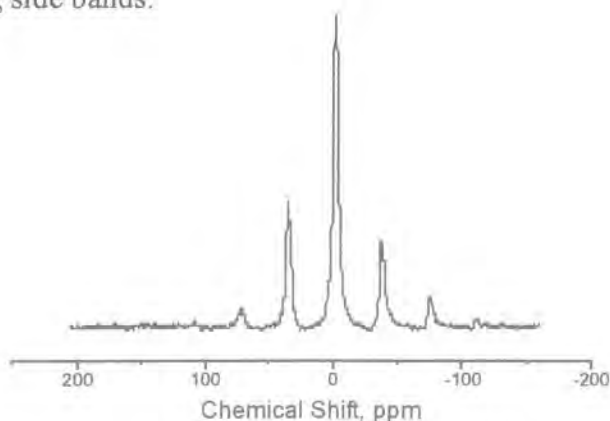


Figure 29: ³¹P NMR Spectrum of DFP (5% by wt.)/AP-MgO

It should be noted that ^{31}P NMR of neat DFP¹⁹ shows a peak centered around δ 11.2 ppm. The appreciable upfield shift observed with the adsorbed sample indicates a highly shielded phosphorus nucleus such as a phosphate anion (PO_4^{3-}), a product derived *via* complete hydrolysis of DFP by surface hydroxyls and/or physisorbed water in AP-MgO (Scheme 2).



Scheme 2

In conclusion, IR and ^{31}P NMR results clearly show existence of PO_4^{3-} as the major phosphorus species in the DFP/AP-MgO system. As with DEPTMP, the P=O group remains adsorbed onto MgO, probably in several slightly different environments, as evidenced by absorptions at 1260 and 1209 cm^{-1} . Also, the absorption values for CH-O(P) stretch remains the same before and after adsorption.

Destructive adsorption of paraoxon with AP-MgO.

The objective was to determine the structure of the adsorbed species derived from paraoxon and AP-MgO.

Procedure

In a typical experiment, a 250-mL single necked flask provided with a serum cap, stir bar and a magnetic stirrer charged with dry pentane (200-mL). To the above was sequentially added, AP-MgO (0.2-g) and paraoxon (9 μL , ~ 5% by wt.). After an hour at room temperature, stirring was stopped, all the solvent was decanted off and the solid was dried overnight under vacuum and analyzed by IR and NMR to assess the structure of the adsorbed species. Also, the above experiment was repeated with 4-nitrophenol (4-NP) in the place of paraoxon.

Results

Figure 30 shows the IR spectra of neat paraoxon (A), AP-MgO adsorbed paraoxon (B) and AP-MgO adsorbed 4-nitrophenol (4-NP, C). The following points are noteworthy:

The IR spectrum of paraoxon adsorbed AP-MgO looks very similar to 4-NP adsorbed AP-MgO except for broadening around 1500-1400 and 1100-1000 cm^{-1} region. Very weak peaks were observed in the 1290-1200 cm^{-1} region indicating the absence of either intact or adsorbed P=O bond.

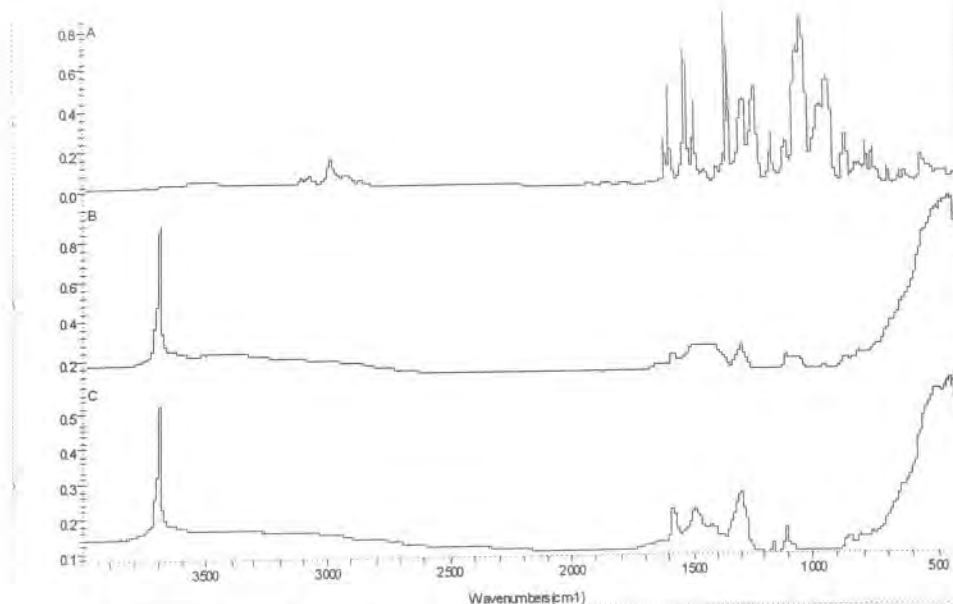


Figure 30: FT-IR spectra of neat paraoxon (A), paraoxon/AP-MgO (B) and 4-nitrophenol/AP-MgO (C)

The ^{31}P MAS spectra of paraoxon impregnated AP-MgO sample is shown in Figure 31. It displays a large peak centered on δ 0 ppm and two sets of two smaller peaks. The latter are attributed to spinning side bands.

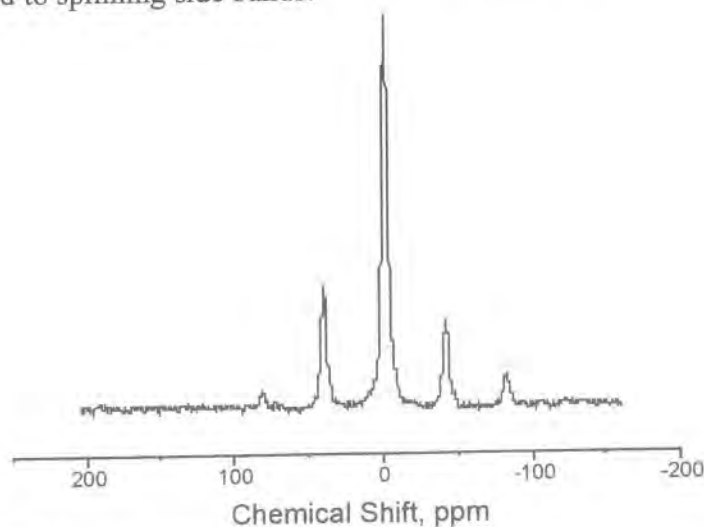
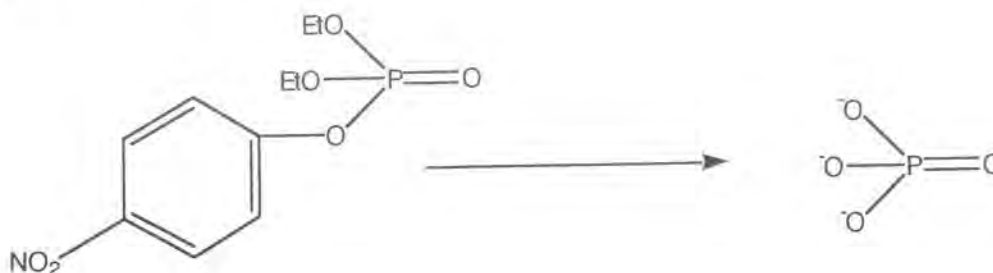


Figure 31: ^{31}P NMR Spectrum of Paraoxon/AP-MgO

On the basis of the chemical shift of the largest peak, we assign it to phosphate anion (PO_4^{3-}), a product derived *via* complete hydrolysis of paraoxon by surface hydroxyls and/or physisorbed water in AP-MgO (Scheme 3).



Scheme 3

From the above, it appears that treatment of AP-MgO with DFP or paraoxon results in the formation of PO_4^{3-} as the hydrolyzed product. Even though ^{31}P NMR of both samples look very similar, their IR spectra are quite different. For example, DFP shows strong absorptions for O-P-O, C-O moieties and somewhat weaker P=O stretching absorptions. In contrast, AP-MgO adsorbed paraoxon does not show any of these distinct bands. We believe that this is probably because of interference due to strong absorptions from aromatic C=C, NO_2 and phenolic C-O moieties of 4-nitrophenol, a by-product in the paraoxon reaction. To further ascertain the identities of the by-products in the paraoxon reaction we have examined the ^{13}C NMR spectrum of paraoxon impregnated AP-MgO. This sample exhibited 2 major peaks centered around δ 13.6 ppm and δ 60.5 ppm, respectively, and these are assigned to the methyl and the methylene carbons in ethanol, one of the products derived from hydrolysis of paraoxon. In addition, a set of four peaks was observed in the region δ 119-180 ppm and these are assigned to the aromatic carbons of the other hydrolysis product derived from paraoxon, namely 4-nitrophenol. The smaller peaks seen in the upfield region of the spectrum and the peak at δ 168.3 ppm are due to carbonaceous impurities present in the AP-MgO itself.

Conclusions

In conclusion, it appears that alkoxy groups of the phosphonate compounds examined in this study are easily hydrolyzed by AP-MgO. Reasonably good leaving groups such as fluoro of DFP or nitrophenol of paraoxon are cleaved while the alkylthio group of DEPTMP appears to stay intact. IR spectra of these reagents adsorbed AP-MgO seem to indicate initial adsorption proceeding *via* coordination of the P=O group to Mg followed by hydrolytic cleavage of the alkoxy as well as the reactive groups.

Destructive Adsorption of paraoxon and CEES by MgO contained in TSP.

To this point, it has been very difficult to assess the destructive adsorption capacity of nanocrystalline MgO and CaO while they are contained in the topical skin protectant (TSP). Initial efforts emulated a laboratory chemical agent monitoring system (CAMS) by using small, glass penetration cups that were coupled to thermal desorption tubes. The adsorbates were then thermally desorbed and transferred to a GC/MS for analysis. Unfortunately, it has been difficult to use this method to analyze the decomposition reaction(s).

Despite these analytical problems it is believed that the simulants are capable of penetrating through the TSP and accessing the MgO. This is indicated by two pieces of data. The first is the observation of a characteristic color change of MgO when acetone is used in the experiments described instead of simulant. From previous work it was known

that the strong binding of acetone to MgO produces a distinct orange color. This color change is readily observed when small amounts of acetone are deposited onto the MgO/rTSP mixtures. In addition, the detection of the oxidation product of CEES with a nanoparticle MgO/polyoxometalate formula contained in the TSP has been observed (Figure 32), indicating the ability of the simulants to access the reactive nanoparticles while contained in the TSP.

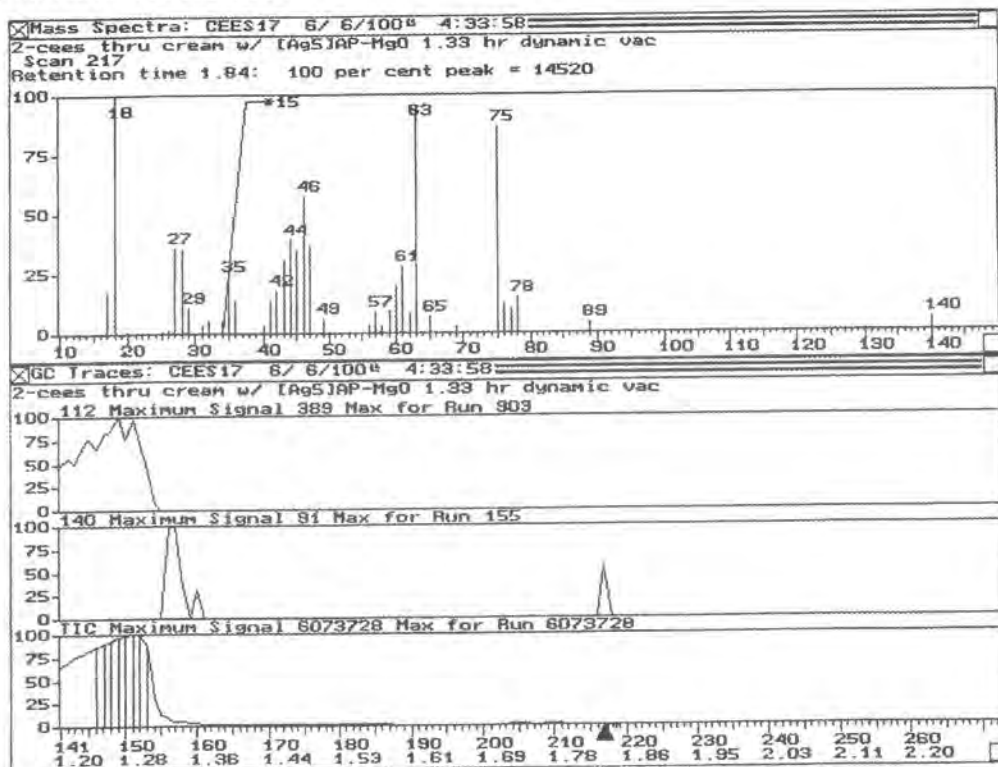


Figure 32: GC/MS of the formation of 2-chloroethyl-ethyl sulfoxide by a nanoparticle MgO formulation while incorporated in TSP.

Task 14: Real Agent Testing of Nanoparticle rTSPs

Nanoparticle rTSP tests with GD and HD at the Midwest Research Institute

The following is from a report on the results of a proof-of-principle testing of a series of reactive Topical Skin Protectants that contained the most promising reactive nanoparticle oxides. The work was performed at the Midwest Research Institute in Kansas City, Missouri. The tests were designed to examine the resistance to penetration of the rTSPs by the chemical agents GD and HD. A static liquid challenge/vapor permeation test was used for GD testing and a static vapor challenge/vapor permeation test was used for HD testing.

The tests used standard permeation cells for testing materials against real agent challenges. These cells were 2.5 inches in diameter. Many of the difficulties encountered during the tests were related to the scale-up in the test area from 7/16-inch diameter (0.15 in²) for the small permeation cells to 2.5-inch diameter (4.9 in²)—a 33-fold increase in surface area—for the large cells. The agent loading *per unit area* for the larger test surfaces is about 30% of that for the smaller surface area cells. However, the *total amount* of agent is about 10 times that used for the smaller surface area. TSP formulations were applied at a known thickness (0.15-mm) on nitrocellulose filter

This report contains company proprietary information that could be the subject of patent applications. As such it is intended for use by the U.S. Department of Army for contract monitoring and is not intended for public dissemination without prior written approval of an officer of Nantek, Inc.

supports sized for the large permeation cells. Static liquid GD challenge involved direct application of neat GD to the TSP preparations. The tops of the cells were sealed to contain the agent. A stream of dry nitrogen swept the underside of the test assembly and collected volatile permeated components onto individual sorbent tubes. The static vapor HD challenge involved suspending a HD-saturated pad above each TSP preparation. The tops of the cells were sealed to contain the agent and volatile permeated components were collected on individual sorbent tubes.

At the end of the collection period, the sorbent tubes were disassembled and the sorbent packs separated and extracted. The extracts were analyzed by full scan GC/MS for permeated agent. Retention time and specific ion plots were used to identify permeated agent. Quantitation of agent was by comparison of the response of GD or HD found in the samples with a calibration curve. Mass spectra were collected of GD, HD, and non-agent components. The number varied with the samples. Non-agent components were not identified. A detailed description of the sample preparation and the experimental procedure are given in the attached report.

Overall, the TSP formulations retained the majority of GD. The 2.0% AP-MgO formulation produced the lowest breakthrough (0.76%). This was for a single sample however. The duplicate was lost due to a very large liquid GD breakthrough. The highest GD breakthrough was 2.2% (average of duplicates) from the 2.0% TiO₂ formulation as given in Table 12.

On completion of the GD exposure, the TSP surfaces containing nanoparticles exhibited numerous cracks and fissures. Some areas where agent had been applied were transparent. The nitrocellulose filter was intact, but the filter/TSP layers had been rendered transparent. Agent decomposition reactions using standard decontamination solutions are highly exothermic. Whether or not the reaction of the agents with the nanoparticles is exothermic is unknown. However, the appearance of the test layers after 20-hours would suggest an exothermic reaction. Heat from the reaction may have contributed to the surface fracturing of the TSP formulations. As the fissures formed in the TSP coatings, it is likely that micro fissures not detectable by visual inspection were formed in the nitrocellulose support as well. Two of the samples had small holes at the completion of testing that were not present at the start of the test. This would result in large breakthrough of the GD that resulted in condensation of neat agent within the sorbent collection tubes. A photograph of the post-test appearance of two of the test cells is shown in the attached report.

Table 12: GD Static Liquid Challenge of TSP: Permeation Results

Duplicates of each TSP were prepared and tested. GD-1 and GD-2 are the two isomers detected by the analysis method. Agent weight is based on literature density of 1.02 g/mL. Permeation is based on a 2.5-inch (6.35-cm) diameter test swatch.

Sample name	Amount spiked (μL—mg)	Analysis file name	Appearance after 20 hr	GD found (mg)	Permeation (μg/cm ²)	Percent breakthrough
Nitrocellulose filter blank	—	06200004 ¹	no change	0.00	0.00	0.00%
TSP Blank	—	06200005 ²	no change	0.00	0.00	0.00%
2.0 %APMgO GD 1	94-96	06280004	"cracked," transparent filter	0.64	20.11	0.66%
2.0% APMgO GD 2		06280004	"cracked," transparent filter	0.73	22.97	0.76%
Average				Duplicate lost due to Safety Hazard		
5.0% APMgO GD 1	94-96	06280005	"cracked," transparent filter	1.15	36.27	1.20%
5.0% APMgO GD 1	94-96	06280006	"cracked"	1.41	44.59	1.47%
Average				1.28	40.43	1.33%
5.0% APMgO GD 2	94-96	06280005	"cracked," transparent filter	1.43	45.14	1.49%
5.0% APMgO GD 2	94-96	06280006	"cracked"	2.03	64.04	2.11%
Average				1.73	54.59	1.80%
2.0% APCaO GD 1	94-96	06280007	"cracked," transparent filter, small holes	1.15	36.21	1.19%
2.0% APCaO GD 1	94-96	06280008	"cracked," transparent filter, small holes	1.02	32.32	1.07%
Average				1.08	34.27	1.13%
2.0% APCaO GD 2	94-96	06280007	"cracked," transparent filter, small hole	1.25	39.49	1.30%
2.0% APCaO GD 2	94-96	06280008	"cracked," transparent filter, small hole	1.24	39.19	1.29%
Average				1.25	39.34	1.30%
5.0% TiO ₂ GD 1	94-96	06280009	"cracked," transparent filter	1.84	58.02	1.91%
5.0% TiO ₂ GD 1	94-96	06280010	"cracked," transparent filter	2.09	65.92	2.17%
Average				1.96	61.97	2.04%
5.0% TiO ₂ GD 2	94-96	06280009	"cracked," transparent filter	2.01	63.49	2.09%
5.0% TiO ₂ GD 2	94-96	06280010	"cracked," transparent filter	2.25	71.20	2.35%
Average				2.13	67.35	2.22%
2.0% ZnO GD 1	94-96	06280011	"cracked," transparent filter	1.18	37.30	1.23%
2.0% ZnO GD 1	94-96	06280012	"cracked," transparent filter	2.16	68.29	2.25%
Average				1.67	52.80	1.74%
2.0% ZnO GD 2	94-96	06280011	"cracked," transparent filter	1.16	36.51	1.20%
2.0% ZnO GD 2	94-96	06280012	"cracked," transparent filter	1.95	61.67	2.03%
Average				1.55	49.09	1.62%

The TSP formulations also performed reasonably well with HD vapor. The TSP without nanoparticles (single sample) exposed to the HD vapor experienced a 1.48% breakthrough. The lowest breakthrough experienced by the TSP containing nanoparticles was 1.44% for the 5.0% TiO₂ formulation. The highest HD breakthrough, 4.8%, was experienced by the 5.0% AP-MgO. This formulation also produced the highest GD breakthrough.

Table 13: HD Static Liquid Challenge of TSP: Permeation Results

Agent weight is based on literature density of 1.27 g/mL. Permeation is based on a 2.5-inch (6.35-cm) diameter test swatch.

Sample name	Amount Spiked (μL—mg)	Analysis file name	Appearance after 20 hr	HD found (mg)	Permeation μg/cm ²	Percent breakthrough
Nitrocellulose filter blank	-	07100009	no change	0.00	0.00	0.00%
TSP Blank	76-97	07100010	no change	1.43	45.20	1.48%
2.0 %AP-MgO HD 1	76-97	07100011	no change	3.16	99.88	3.26%
2.0% AP-MgO HD 2	76-97	07100012	no change	3.51	110.94	3.62%
		<i>Average</i>		3.34	105.41	3.44%
5.0% AP-MgO HD 1	76-97	07100013	no change	4.66	147.15	4.80%
5.0% AP-MgO HD 2	76-97	07100014	no change	3.71	117.26	3.83%
		<i>Average</i>				4.32
2.0% AP-CaO HD 1	76-97	07100015	no change	3.50	110.57	3.61%
2.0% AP-CaO HD 2	76-97	07100016	no change	1.87	58.93	1.92%
		<i>Average</i>		2.69	84.75	2.77%
5.0% TiO ₂ HD 1	76-97	07100017	no change	1.39	43.99	1.44%
5.0% TiO ₂ HD 2	76-97	07100018	no change	3.48	110.03	3.59%
		<i>Average</i>		2.44	77.01	2.52%
2.0% ZnO HD 1	76-97	07100020	no change	3.24	102.25	3.34%
2.0% ZnO HD 2	76-97	07100021	no change	3.00	94.78	3.09%
		<i>Average</i>		3.12	98.52	3.22%

The rTSP formulations containing nanoparticles commonly thickened (became “pasty”) over time even when sealed in airtight containers. Thickening of the rTSPs resulted in reduced spreadability. Adding increments of the oil component of the TSP solved this problem. In some cases rather large aliquots of additional oil component were added, particularly for the MgO and CaO samples. While the rTSP samples containing TiO₂ and ZnO did exhibit thickening, they did not require the large amounts of additional oil in order to overcome the problem with tackiness.

This problem with the nanoparticle rTSPs was also evident with the samples sent for viscosity testing. The problem seems to be more prevalent for samples containing MgO and CaO than for those with TiO₂ and ZnO. The problem is that the MgO and CaO are soaking up the oil over large periods of time and these formulations are drying out and

becoming more and more tacky. It does not seem that the MgO and CaO are reacting with the oil (see Task 8) but are simply adsorbing the oil component. Also it has been noted that the thickening occurs to a larger extent when larger amounts (moving from 2 to 5 or 10%) of nanoparticles are included into the rTSP. While both TiO₂ and ZnO do exhibit the thickening that MgO displays, it occurs to a much smaller degree.

The increased surface area coupled with the quick-drying feature of the TSP formulations caused difficulties in obtaining an evenly spread testing surface. The TSP formulations also contained granules and aggregates in varying sizes. Neither Nantek nor MRI personnel were able to break up the aggregates with the mixing tools used to add the oil. These granules further complicated spreading of the TSP by generating uneven surfaces. The granules caused streaking in the TSP coating. These streaks resulted in uneven coating thicknesses.

The problems encountered during these initial tests illustrate some the simple formulation issues that need to be overcome in order to generate a successful rTSP based on reactive nanoparticles. It seems that optimizing the procedure in which the nanoparticles are added to the base skin cream can make major improvements to the efficacy of the rTSPs. It is evident that the reactive nanoparticles are capable of destructive adsorption of a large number (and types) of CW agents and simulants. The difficulties to this point have been related with changes in the texture of the rTSP caused by the added nanoparticles.

Task 15: Economic study of scaled-up production of the adsorbents and adsorbent cream product

The following is a summary of plant designs and cost estimations for the scale-up production of nanoparticle metal oxides.

Pilot plant production of sol-gel prepared AP-MgO

Two stirred tank reactors are operated at room temperature for both the preparation of Mg(OCH₃)₂ and Mg(OH)₂. One variation under consideration is to operate the reactors at 80°C for the formation of Mg(OCH₃)₂ in order to speed up the reaction (high temperature methoxide formation). The reactors are initially being operated as batch reactors, but will be switched to a continuous mode as the feedthrough parameters are optimized. To start the process methanol, toluene and magnesium metal will be introduced into the reactor and allowed to mix. The total time of reaction is estimated to be 12 hours at room temperature. Once the reactions are complete the reactor will be drained and the sol-gel precursor fed to the spray dryer. The rate of draining will be dependent on the capacity of the spray dryer (3-5 liters per hour). Once out of the spray dryer the Mg(OH)₂ powder will be sent to a plug flow reactor for conversion to MgO. The plug flow reactor is operated at 550°C. Nitrogen is used to pneumatically transfer the Mg(OH)₂ powder through about 10-ft of copper tubing. The final MgO powder is then collected in a bag filter. The solvent from the spray dryer will be condensed and, in the future, recycled back to the reactors.

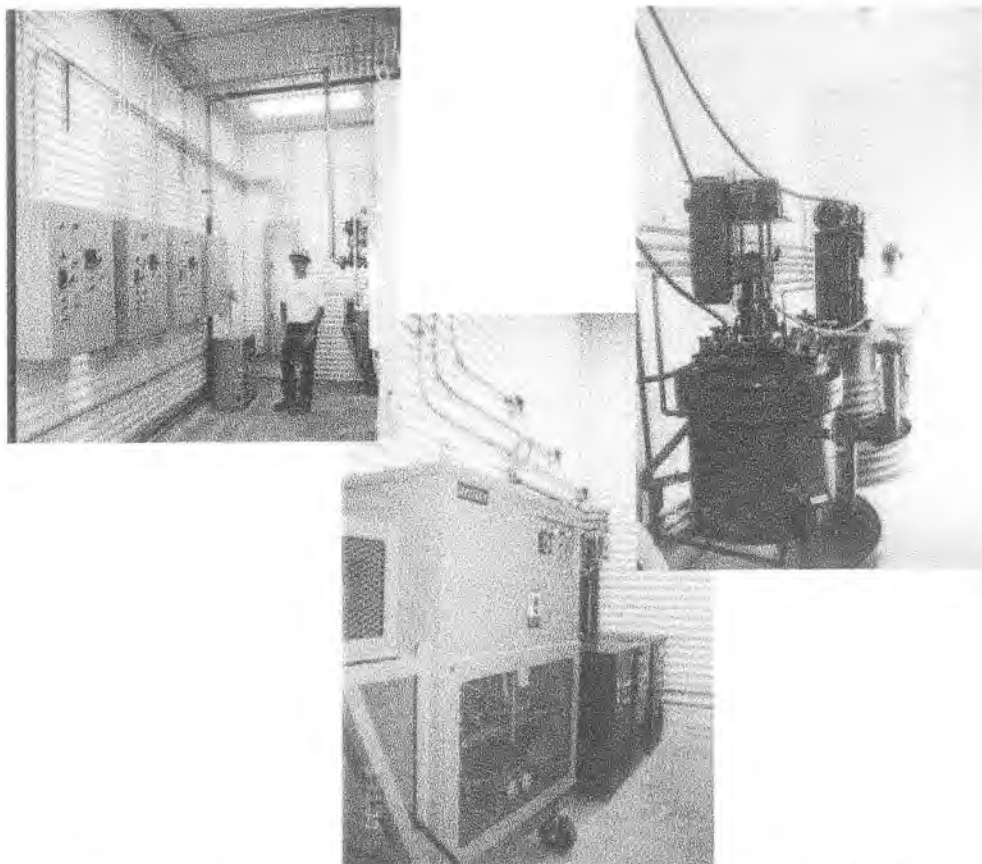


Figure 33: Photographs of the pilot-scale production plant for AP-MgO.

Description of Pilot Plant Scale, Continuous production of CP-MgO

In this process, two stirred tanks are heated to 90°C and continuously fed with metal oxide and water at the required rate of production. The rate of production in a pilot scale plant would approach 100-kg per hour. The retention time for the reaction to hydroxide would be controlled by the vessel size. The resulting thick slurry of hydroxide material would then be fed to a continuous belt filter to remove water to at least 50% solids content. Next, this cake would be sent through a continuous tray dryer that would lower the water content to below 0.5%. Finally, the exiting dried hydroxide material would be ground and directly fed to a belt furnace under a minimal flow of nitrogen in order to convert the hydroxide to the final metal oxide product.

Initial cost estimates for the large-scale production of reactive nanoparticles.

Nantek, Inc. has manufactured CP-MgO on a small scale via the process described above and tested the product material for the destructive adsorption of paraoxon and 2-CEES. This material behaved as well as material produced via the AP-MgO process. This illustrates that the method generates highly reactive materials that are competitive with the more expensive AP process.

With the completion of the pilot scale production plants drawing near, Nantek engineers have been examining the economics of full-scale plant production of nanoparticle metal oxides. Initial indication is that the AP materials can be produced at

costs less than \$100 per kg depending on the type of metal oxide and the exact process used to make the final product (please note that many are less than \$50 / kg). At full scale, such a plant would be capable of producing 20-kg per hour. For CP materials the cost is estimated to be much lower. The costs for CP materials are estimated at less than \$20 per kg (many are much less). For this type of plant, full-scale production would be capable of producing 100-kg per hour. While there are reactivity differences in the two types of materials produced they are small and need to be balanced by the cost of manufacture.

Key Research Accomplishments

This Phase II project has led to the following key research accomplishments:

- 1) Development of a new, patented synthetic method for producing nanocrystalline zinc oxide.
- 2) Discovery that elevated temperatures during metal alkoxide formation lead to increases in the surface area of the final metal oxide product.
- 3) Found that the cumbersome hypercritical activation step in the synthesis of RNPs can be circumvented by use of spray drying techniques.
- 4) Established that flow activation of the samples can replace vacuum activation in the larger scale production process.
- 5) Dramatic increases in the surface area and reactivity of MgO (and other RNPs) have been made through the combination of the advanced synthetic methods described above.
- 6) Determined that nanocrystalline ZnO is capable of detoxifying CW simulants such as paraoxon and 2-CEES on levels that are comparable to MgO, CaO and TiO₂.
- 7) Identified ethyl vinyl sulfide and 2-(ethylthio)-ethanol as two products from the reaction of 2-CEES and the RNPs.
- 8) Detected p-nitrophenol and surface bound phosphates as the major products from the reaction of paraoxon with RNPs.
- 9) Have identified and are implementing several analytical methods for the evaluation of select RNPs for detoxification of CW simulants while contained in TSP.
- 10) Determined that RNPs have good resistance to moisture when incorporated into the TSP.

- 11) Determined that AP-MgO is a very good destructive adsorbent for detoxifying the CW agents VX, GD, and HD.
- 12) Determined that AP-CaO and hydrated CaO are good destructive adsorbent for detoxifying VX, GD, and HD.
- 13) Thoroughly examined the hydrolysis products from the decomposition of paraoxon, DFP, and DEPTMP over AP-MgO.
- 14) Performed HD agent tests with RNP/rTSPs and determined several simple formulation problems that need to be addressed.
- 15) Examined the effects of several RNPs on the viscosity of the base TSP.
- 16) During the time frame of the Phase II project major advances have been made in scaling up the production of reactive nanoparticles. Recently Nantek completed the construction of a pilot-scale production plant for AP-MgO nanoparticles. This work greatly enhanced the reactivity of the nanoparticles and significantly decreased their cost.

Reportable Outcomes

Work from this project has directly or partially led to the following patents, publications and conference presentations:

Patents

U.S. Patent No. 6,057,488 entitled *NANOPARTICLES FOR THE DESTRUCTIVE SORPTION OF BIOLOGICAL AND CHEMICAL CONTAMINANTS*, Klabunde *et al.*, filed 09/15/98, issued 05/02/00

U.S. Patent No. 5,990,373 entitled *NANOMETER SIZED METAL OXIDE PARTICLES FOR AMBIENT TEMPERATURE ADSORPTION OF TOXIC CHEMICALS*, Klabunde *et al.*, filed 11/05/99, issued 11/23/00

U.S. Patent Application entitled *SYNTHESIS AND PROPERTIES OF NANOCRYSTALS OF ZINC OXIDE AND IRON OXIDE*, Klabunde *et al.* Filed June, 1999.

Publications

"Reactions of VX, GD, and HD with Nanosize MgO" Wagner, G. W.; Bertram, P. W.; Koper, O.; Klabunde, K.J. *J. Phys. Chem.*, **1999** *103*(16), 3225.

"Development of Reactive Topical Skin Protectants against Sulfur Mustard and Nerve Agents" Koper, O.; Lucas, E.; and Klabunde, K.J. *J. Appl. Toxicol.* **1999**, *19*, S59.

"Reactions of VX, GD, HD with Nanosize CaO: Autocatalytic Dehydrohalogenation of HD" Wagner, G.W.; Koper, O. B.; Lucas, E.; Decker, S.; Klabunde, K.J. *J. Phys. Chem. B* **2000**, *104*, 5118.

"Nanocrystals as Destructive Adsorbents for Military Warfare Agents and Their Simulants at Ambient Temperatures: Paraoxon and VX" Koper, O.; Mohs, C.; Pates, S.; Sigel, M.J.; Nichols, D.; and Klabunde, K.J *in preparation*.

Conference Presentations

"Nanocrystals as Destructive Adsorbents for Chemical Agents and Toxic Airborne Substances" by Olga Koper, Stephanie Pates, Jake Sigel, Shawn Decker, and Ken Klabunde at the workshop "Chemical Techniques for Decontamination of CB Warfare Agents" at the Decontamination Conference '99 (DECON 99) held in Nashville, Tennessee on June 8-10.

"Nanocrystals as Adsorbents for Chemical Agents and Air Pollutants" by Olga Koper, Stephanie Pates, and Ken Klabunde at the Scientific Conference on Chemical and Biological Defense Research at the Aberdeen Proving Ground, Maryland on November 17-20, 1998.

"Synthesis and Properties of Nanoscale Metal Oxides" by Olga Koper and Kenneth Klabunde at the 216th American Chemical Society National Meeting in Boston, Massachusetts August 23-27, 1998.

"Nanoparticles in Decontamination of CW Agents and Their Mimics" by Ken Klabunde presented as an invited lecture in the symposium sponsored by the Colloid and Surface Science Division. Symposium was at the 217th American Chemical Society National Meeting in Anaheim, California March 21-25, 1999.

"Metal Oxide Nanoparticles for the Decomposition of Chemical and Biological Warfare Agents" by Kenneth Klabunde at the International Workshop on Decontamination in a Chemical or Biological Warfare Environment, September 7-9, 1999. The meeting was sponsored by the Chemical and Biological Defence Establishment Porton Down and the U.S. Army.

"Metal Oxide Nanoparticles as Countermeasures against Chemical and Biological Threats" by Olga Koper, Shawn Decker, Slawomir Winecki, Jennifer John, Laura Hladky, Michael Sigel, David Jones, Heather Picolet, Shyamala Rajagopalan, Craig Hill and Kenneth Klabunde at the Decontamination Conference 2000 (DECON 2000) held in Salt Lake City, Utah on May 23-25, 2000.

"Addition of Reactive Nanoparticles to a Topical Skin Protectant to Enhance its Protective Properties" by Stephanie Pates, Jennifer John, Laura Hladky, Michael Sigel, David Jones, Shyamala Rajagopalan, Shawn Decker, Olga Koper, and Kenneth Klabunde at the 2000 Medical Defense Bioscience Review sponsored by the U.S. Army Medical Research and Materiel Command (USAMRMC) in Hunt Valley, MD June 4-9, 2000.

Conclusions

During the course of the Project a large number of advances for the incorporation or reactive nanoparticles into a reactive Topical Skin Protectant have been made. One of first was the synthesis of new nanoparticle metal oxides such as zinc oxide, titanium dioxide, and iron oxide. The new nanoparticle formulations of ZnO and TiO₂ are nearly as reactive as magnesium oxide that is considered one of Nantek's best materials for destructive adsorption of simulant and real agent challenges. This work has led Nantek to apply for a patent for the composition of matter relating to nanoparticle zinc oxide and iron oxide.

Many breakthroughs in the large-scale synthesis of magnesium oxide nanoparticles have been achieved during the first year of this project. These advances have led to a significant increase in the surface area of the reactive nanoparticles and thus the chemical reactivity. The development of these advances has also brought about significant reduction in the cost to manufacture these unique detoxification materials. These techniques are now being applied to our other reactive nanoparticle materials with equal success.

A large amount of work has shown that reactive nanoparticles based on MgO, CaO, ZnO and TiO₂ are quite effective for the destructive adsorption of simulants and real CW agents. In the case of phosphorus based simulants such as paraoxon, diisopropyl fluorophosphonate and diethyl phenylthiomethyl phosphate the decomposition is nearly complete. The mechanism of decomposition for these materials was via hydrolysis. For the mustard simulant 2-CEES the decomposition occurs via two mechanisms: the first and major one is dehydrochlorination to form ethyl vinyl sulfide and the second is via hydrolysis to form 2-(ethylthio)-ethanol.

Research with real agents (VX, GD, HD) show that both nanoparticle MgO and CaO are very effective decomposition agents. All three agents hydrolyze on the surface of the very reactive MgO and CaO nanoparticles. VX yielded ethyl methylphosphonic acid (EMPA) and methylphosphonic acid (MPA), but *no toxic* S-(2-diisopropylamino)ethyl methylphosphonothioate (EA-2192). GD formed both GD-acid and MPA. For HD, in addition to hydrolysis to thiodiglycol, about 50% elimination to divinyl sulfide occurs. The reaction kinetics for all three agents are characterized by a fast initial reaction followed by gradual slowing to a steady-state reaction with first-order behavior. The fast reaction is consistent with liquid spreading through the porous nanoparticle aggregates. The steady-state reaction is identified as a gas-phase reaction, mediated by evaporation, once the liquid achieves its volume in the smallest available pores.

Research shows that the RNPs and TSP are compatible with one another. Results show that the RNP/TSP can be stored for long times without deterioration of the RNPs. It has also been shown that the RNPs are not affected by moisture over short periods of time (days to weeks). This is an important consideration for a rTSP that is applied in the wet environment underneath a military MOPP uniform.

Initial research of rTSPs based on reactive nanoparticles has been encouraging. Initially, the nanoparticles of choice for this application were MgO and CaO. During the real agent testing of rTSPs it was determined that ZnO and TiO₂ may actually be better choices due to the relative ease of incorporating these materials into the base skin cream. While the data accumulated from the real agent permeation testing has not shown significant improvements in the efficacy of the protective nanoparticle creams, the

resolution of simple problems regarding the incorporation of the nanoparticles into the base TSP should yield a product that provides enhanced barrier protection.

Many of the requirements for a successful rTSP defined in the introduction have been met by the use of reactive nanoparticles.

- 1) All of the reactive nanoparticles examined in this study are non-toxic to humans.
- 2) The reactive nanoparticles **destroy** the three major types of CW agents – VX, GD and HD.
- 3) The nanoparticles are not known skin irritants (for example, ZnO is a common component of foot powders. ZnO and TiO₂ are both common components of sunscreens).
- 4) The nanoparticles do have a long shelf life that is needed for rTSPs that would likely be stored over periods of years to decades.

The fifth item, chemical compatibility between the nanoparticles and retention of the nanoparticle reactivity are less clearly achieved. The stability studies show that the nanoparticles are not adversely affected by the components of the base TSP material. However, problems have been encountered with the best way to incorporate the nanoparticles into the rTSP. This does not seem to be a major problem and could most likely be overcome by mechanical stirring and better formulation procedures.

Based on the successful decontamination of real agents by powder samples of MgO and CaO nanoparticles it is strongly recommended that work on more efficient ways to incorporate the nanoparticles into the base cream be investigated. At this point, the only major obstacle remaining for the use of nanoparticles in a reactive Topical Skin Protectant is to overcome the simple issue of how to most effectively incorporate the nanoparticles into the base cream.

References

1. "The powder method in x-ray crystallography" Azafoff and Buerger; McGraw-Hill Book Company, 1958, New York, Ch. 16.
2. Braue, E. H.; Pannella, M. G. *Appl. Spectroscopy*, **1990**, *44*(6), 1061.
3. Wagner, G. W.; Bartram, P. W.; Koper, O.; Klabunde, K.J. *J. Phys. Chem.*, **1999** *103*(16), 3225.
4. Yang, Y.C.; Baker, J.A.; Ward, J.R. *Chem. Rev.* **1992**, *92*, 1729.
5. Koper, O.; Lagadic, I.; Volodin, A.; Klabunde, K. *J. Chem. Mater.*, **1997**, *9*(11), 2468.
6. Mohs, C.; Klabunde, K. in "Chemistry of Advanced Materials: An Overview" Ed. by L.V. Interrante and M.J. Hampden-Smith, pp 271-327. Wiley-VCH, Berlin (1988).
7. Klabunde, K. J.; Stark, J.; Koper, O.; Mohs, C.; Park, D.; Decker, S.; Jiang, Y.; Lagadic, I.; Zhang, D. *J. Phys. Chem.*, **100**, *30*, 12142.
8. Koper, O.; Li, Y.; Klabunde, K. *J. Chem. Mater.*, **1993**, *5*(4), 500.
9. Koper, O.; Lagadic, I.; Volodin, A.; Klabunde, K. *J. Chem. Mater.*, **1997**, *9*(11), 2468.
10. Decker, S.; Klabunde, K.J. *J. Phys. Chem.*, **1996**, *118*(49), 12465.
11. Wagner, G.W.; Koper, O. B.; Lucas, E.; Decker, S.; Klabunde, K.J. *J. Phys. Chem. B* **2000**, *104*, 5118.
12. Wagner, G. W.; Bartram, P. W. Unpublished results.
13. Kuiper, A. E. T.; van Bokhoven, J. J. G. M.; Medema, J. *J. Catal.* **1976**, *43*, 154.
14. Lin, S. T.; Klabunde, K. *Langmuir*, **1985**, *1*, 600.
15. Li, Y.-X.; Klabunde, K. *Langmuir*, **1991**, *7*, 1388.
16. Li, Y.-X.; Schlup, J. R. Klabunde, K. *J. Langmuir*, **1991**, *7*, 1394.
17. Mitchell, M. B.; Sheinker, V.N.; Mintz, E. A. *J. Phys. Chem. B.* **1997**, *101*, 11192.
18. *Phosphorous-31 NMR: Principles and Applications*. Edited by David G. Gorenstein. **1984**, Chap. 18, 549, Academic Press, Inc. Orlando, Florida.
19. Reddy, G.S.; Schmutzler, R. Z. *Naturforsch. Part B.* **1970**, *25*, 1199.

Index of Figures

FIGURE 1: XRD OF COMMERCIAL AND NANTEK ZINC OXIDES.....	9
FIGURE 2: INCREASE IN SURFACE AREA OF AP-MGO SAMPLES AS A FUNCTION OF METHOXIDE TEMPERATURE.....	12
FIGURE 3: SCHEMATIC DIAGRAM OF PENETRATION CUP CELL USED FOR TESTING THE EFFICACY OF RNP CONTAINING SKIN CREAMS AGAINST CW SIMULANT CHALLENGES.....	16
FIGURE 4: RATE OF DISAPPEARANCE OF PARAOXON (4.5- μ L) ON MAGNESIUM OXIDE SAMPLES. LOWER INTENSITY INDICATES MORE DESTRUCTIVE ADSORPTION OF PARAOXON.....	19
FIGURE 5: RATE OF DISAPPEARANCE OF PARAOXON (4.5- μ L) ON CALCIUM OXIDE SAMPLES (0.1-G). LOWER INTENSITY INDICATES MORE DESTRUCTIVE ADSORPTION OF PARAOXON.....	19
FIGURE 6: RATE OF DISAPPEARANCE OF PARAOXON (4.5- μ L) ON VARIOUS METAL OXIDE SAMPLES (0.1-g). LOWER INTENSITY INDICATES MORE DESTRUCTIVE ADSORPTION OF PARAOXON.....	20
FIGURE 7: REACTIVITY COMPARISON OF VACUUM AND FLOW ACTIVATED AP-CAO.....	21
FIGURE 8: REACTIVITY COMPARISON OF VACUUM AND FLOW ACTIVATED AP-MGO.....	22
FIGURE 9: COMPARISON OF ACTIVATED CARBON AND AP-MGO FOR THE DESTRUCTIVE ABSORBANCE OF PARAOXON.....	23
FIGURE 10: DESTRUCTIVE ADSORPTION OF PARAOXON WITH SPRAY DRIED MGO.....	24
FIGURE 11: DESTRUCTIVE ADSORBANCE OF PARAOXON BY RNP-ZNO FROM PENTANE SOLUTION. LOWER INTENSITY INDICATES LARGER DESTRUCTIVE ADSORPTION.....	26
FIGURE 12: SOLID STATE FT-IR OF RNP-ZNO SAMPLES AFTER THE DESTRUCTIVE ADSORPTION OF PARAOXON.....	26
FIGURE 13: APPEARANCE OF ETHYL VINYL SULFIDE DURING 2-CEES DECOMPOSITION ON VARIOUS METAL OXIDES. HIGHER INTENSITY INDICATES MORE DESTRUCTIVE ADSORPTION OF 2-CEES.....	28
FIGURE 14: APPEARANCE OF ETHYL VINYL SULFIDE DURING REACTION OF 2-CEES ON METAL OXIDES WITH AND WITHOUT THE BASE CREAM. HIGHER INTENSITY INDICATES MORE DESTRUCTIVE ADSORPTION OF 2-CEES.....	29
FIGURE 15: FORMATION OF ETHYL VINYL SULFIDE ON [CAO]MGO NANOPARTICLE SAMPLES AS A FUNCTION OF TIME.....	30
FIGURE 16: DESTRUCTIVE ADSORPTION OF PARAOXON WITH "CORE/SHELL" RNP MATERIALS.....	31
FIGURE 17: OVERLAY OF THE X-RAY DIFFRACTION PATTERNS FOR BASE TSP AND TSP CONTAINING AP-MGO.....	32
FIGURE 18: STABILITY OF AP-MGO/TSP AS A FUNCTION OF TIME UNDER STORAGE CONDITIONS.....	33
FIGURE 19: STABILITY OF AP-MGO/TSP AS A FUNCTION OF TIME UNDER LOW HUMIDITY CONDITIONS.....	34
FIGURE 20: STABILITY OF AP-MGO/TSP AS A FUNCTION OF TIME UNDER HIGH HUMIDITY CONDITIONS.....	35
FIGURE 21: GC/MS OF EXTRACTED PRODUCTS FROM REACTION OF 2-CEES AND AP-MGO.....	36
FIGURE 22: MAS NMR SPECTRA OBTAINED FOR AGENTS ADDED TO AP-MGO: (LEFT) GD (TOP TO BOTTOM) T=9.5 MIN, 1.0 H, AND 23 H; (MIDDLE) VX AT T= 8.5 MIN, 24 H, AND 3 MONTHS; (RIGHT) HD AT T=9.5 MIN, 3.8 H, AND 1 WEEK.....	39
FIGURE 23: MAS NMR SPECTRA OBTAINED FOR AGENTS ADDED TO FRESH, "AS RECEIVED" AP-CAO: (LEFT) GD (TOP TO BOTTOM) T=8.5 MIN, 1.9 H, AND 25 H; (MIDDLE) VX AT T= 8.5 MIN, 48 H, AND 21 DAYS; (RIGHT) ^{13}C -HD AT T=7.5 MIN, 6.8 H, AND 70 H.....	40
FIGURE 24: REACTION PROFILES FOR (LEFT) GD, VX, AND ^{13}C -HD LIQUID ON FRESH, "AS RECEIVED" AP-CAO AND (RIGHT) HD AND ^{13}C -HD ON AP-CAO AND CAO.....	40
FIGURE 25: FT-IR SPECTRA OF NEAT DEPTMP (A), DEPTMP (5% BY WT.)/AP-MGO (B) AND DEPTMP (EXCESS)/AP-MGO (C).....	45
FIGURE 26: ^{31}P NMR SPECTRUM OF DEPTMP (5% BY WT.)/AP-MGO.....	46
FIGURE 27: FT-IR VAPOR PHASE SPECTRA OF NEAT DFP (A), DFP/CP-MGO (B), DFP/CM-MGO (C), AND DFP/AP-MGO (D).....	48
FIGURE 28: FT-IR SPECTRA OF NEAT DFP (A) AND DFP/AP-MGO (B).....	49
FIGURE 29: ^{31}P NMR SPECTRUM OF DFP (5% BY WT.)/AP-MGO.....	49
FIGURE 30: FT-IR SPECTRA OF NEAT PARAOXON (A), PARAOXON/AP-MGO (B) AND 4-NITROPHENOL/AP-MGO (C).....	51
FIGURE 31: ^{31}P NMR SPECTRUM OF PARAOXON/AP-MGO.....	51
FIGURE 32: GC/MS OF THE FORMATION OF 2-CHLOROETHYL-ETHYL SULFOXIDE BY A NANOPARTICLE MGO FORMULATION WHILE INCORPORATED IN TSP.....	53

FIGURE 33: PHOTOGRAPHS OF THE PILOT-SCALE PRODUCTION PLANT FOR AP-MGO.....	58
--	----

Index of Tables

TABLE 1: ELEMENTAL ANALYSIS OF ZINC OXIDE.....	9
TABLE 2: CRYSTALLITE SIZES AND SPECIFIC SURFACE AREAS FOR VARIOUS ZNO SAMPLES.....	10
TABLE 3: EXAMPLES OF NANOPARTICLES EXAMINED AND THEIR DESIGNATIONS.....	10
TABLE 4: SAMPLES STUDIES FOR PARAOXON DECOMPOSITION.....	18
TABLE 5: DECOMPOSITION OF PARAOXON ON VARIOUS METAL OXIDES.....	20
TABLE 6: DECOMPOSITION OF PARAOXON ON ZNO AFTER 20 HRS.....	25
TABLE 7: MOLAR RATIO OF PARAOXON DESTROYED VS. ZNO AFTER 20-HRS DECOMPOSITION.....	25
TABLE 8: DECOMPOSITION OF PARAOXON BY VARIOUS RNP SAMPLES.....	37
TABLE 9: HD AND CEES REACTIONS ON AP-CAO AND CAO.....	41
TABLE 10: VISCOSITY OF TSPs CONTAINING NANOPARTICLES. ^A	42
TABLE 11: AMOUNT OF ADSORBED DEPTMP AS DETERMINED BY UV-VIS ANALYSIS.....	44
TABLE 12: GD STATIC LIQUID CHALLENGE OF TSP: PERMEATION RESULTS.....	55
TABLE 13: HD STATIC LIQUID CHALLENGE OF TSP: PERMEATION RESULTS.....	56

Appendices

Please find the following attachments

1. "Reactions of VX, GD, and HD with Nanosize MgO" Wagner, G. W.; Bertram, P. W.; Koper, O.; Klabunde, K.J. *J. Phys. Chem.*, **1999** 103(16), 3225.
2. "Reactions of VX, GD, HD with Nanosize CaO: Autocatalytic Dehydrohalogenation of HD" Wagner, G.W.; Koper, O. B.; Lucas, E.; Decker, S.; Klabunde, K.J. *J. Phys. Chem. B* 2000, 104, 5118.
3. "Development of Reactive Topical Skin Protectants against Sulfur Mustard and Nerve Agents" Koper, O.; Lucas, E.; and Klabunde, K.J. *J. Appl. Toxic.* 1999, 19, S59
4. "Permeation of Chemical Agents" MRI Project No. 310086, August 2, 2000.

List of Personnel Receiving Pay From This Research Effort

Dr. Kenneth Klabunde – Principal Investigator
Dr. Olga Koper - Senior Scientist
Dr. Shawn Decker – Project Scientist
Dr. Shyamala Rajagopalan – Staff Scientist
Stephanie Pates – Chemist
Michael Sigel – Chemist
Jennifer John – Chemist
Laura Hladky – Chemist
David Jones – Chemical Engineer

Reactions of VX, GD, and HD with Nanosize MgO

George W. Wagner,^{*,†} Philip W. Bartram,[‡] Olga Koper,[§] and Kenneth J. Klabunde[§]*Geo-Centers, Inc., Gunpowder Branch Box 68, Aberdeen Proving Ground, Maryland 21010, Research and Technology Directorate, U.S. Army ERDEC, Aberdeen Proving Ground, Maryland 21010, and Department of Chemistry, Kansas State University and Nantek, Inc., 1500 Hayes Drive, Manhattan, Kansas 66502**Received: December 9, 1998; In Final Form: February 16, 1999*

The room-temperature reactions of the chemical warfare agents VX (*O*-ethyl *S*-2-(diisopropylamino)ethyl methylphosphonothioate), GD (3,3-dimethyl-2-butyl methylphosphonofluoridate, or Soman), and HD (2,2'-dichloroethyl sulfide, or mustard) with nanosize MgO have been studied using solid-state MAS NMR. All three agents hydrolyze on the surface of the very reactive MgO nanoparticles. VX yields ethyl methylphosphonic acid (EMPA) and methylphosphonic acid (MPA), but no toxic *S*-(2-diisopropylamino)ethyl methylphosphonothioate (EA-2192). GD forms both GD-acid and MPA. For HD, in addition to hydrolysis to thiodiglycol, about 50% elimination to divinyl sulfide occurs. The reaction kinetics for all three agents are characterized by a fast initial reaction followed by gradual slowing to a steady-state reaction with first-order behavior. The fast reaction is consistent with liquid spreading through the porous nanoparticle aggregates. The steady-state reaction is identified as a gas-phase reaction, mediated by evaporation, once the liquid achieves its volume in the smallest available pores.

Introduction

Nanosize inorganic oxide particles such as MgO are currently under consideration as reactive adsorbents for the decontamination of chemical warfare agents.¹ Although conventional MgO,² and other inorganic oxides such as alumina,³ possess reactivity toward CWA simulants, such reactivity is anticipated to be enhanced in nanosize particles.⁴ The increased reactivity is due not only to the larger surface area of smaller particles, but also to the greater amount of highly reactive edge and corner "defect" sites. Additionally, unusual lattice planes, also possessing greater reactivity, are stabilized and exposed in nanosize particles.

In this study, solid-state MAS NMR is used to examine the room-temperature reactions of neat VX, GD and HD liquid with nanosize MgO particles *in situ*. VX and GD (also called Soman) are "nerve" agents, whereas HD (mustard) is a "blister" agent.^{1a}

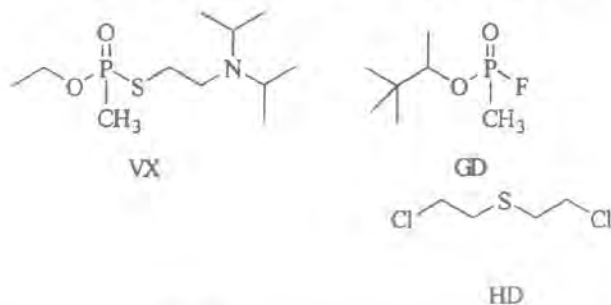
brief exposure to humid air occurred. Thus, the extent of surface hydration is uncertain. To enhance sensitivity, ¹³C-labeled HD (HD*)⁵ was used. The HD* contained about 8% CH₃C(O)OCH₂-CH₂SCH₂CH₂Cl as an impurity. GD and VX were >95% pure.

NMR. ³¹P and ¹³C MAS NMR spectra were obtained using a Varian Unityplus 300 NMR spectrometer equipped with a Doty Scientific 7 mm high-speed VT-MAS probe, using direct excitation (i.e., no CP) and high-power proton decoupling. The observation frequencies for ³¹P and ¹³C were 121 and 75 MHz, respectively. Samples were packed in double O-ring sealed macor rotors (Doty Scientific) and typically spun at 3000 Hz. Chemical shifts were referenced to external 85% H₃PO₄ (0 ppm) and TMS (0 ppm).

Reaction Procedure. Caution: These experiments should only be performed by trained personnel using applicable safety procedures. In a typical run, 5 wt % neat, liquid agent (5–6 μL) was added via syringe to the center of a column of AP-MgO (ca. 100 mg) contained in the NMR rotor. The rotor was then sealed with the double O-ring cap. MAS NMR spectra were obtained periodically to monitor the reaction *in situ*.

Results

GD. Selected ³¹P MAS NMR spectra obtained for 6 μL of GD added to 106 mg of AP-MgO are shown in the left column of Figure 1. In the top spectrum, the intense doublet centered at 28.5 ppm is due to GD, demonstrating the strong coupling between phosphorus and the directly bonded fluorine (*J*_{PF} = 1039 Hz). Sufficient resolution is achieved to observe secondary splitting of the doublet due to the different GD isomers. As the GD is hydrolyzed by surface hydroxyls and/or physisorbed water on the MgO, broad peaks emerge for GD-acid (pinacolyl methylphosphonic acid, 25.7 ppm) and methylphosphonic acid (MPA, 18.5 ppm). The major product is GD-acid, with about 18% MPA forming. As depicted in Scheme 1, GD-acid and MPA are most certainly in the ionized form due to the basic nature of the MgO surface. Indeed, the broad nature of their



Experimental Section

Materials. Nanosize MgO (aerogel-prepared, AP-MgO) was prepared as previously described and used as received.^{4a} The surface area was 344 m²/g. Samples were manipulated in air and

^{*} Geo-Centers, Inc. Tel: (410) 436-8468. Fax: (410) 436-3764. E-mail: gwwagner@cbdc.com.apgea.army.mil

[†] U.S. Army ERDEC.

[‡] Kansas State University and Nantek, Inc.

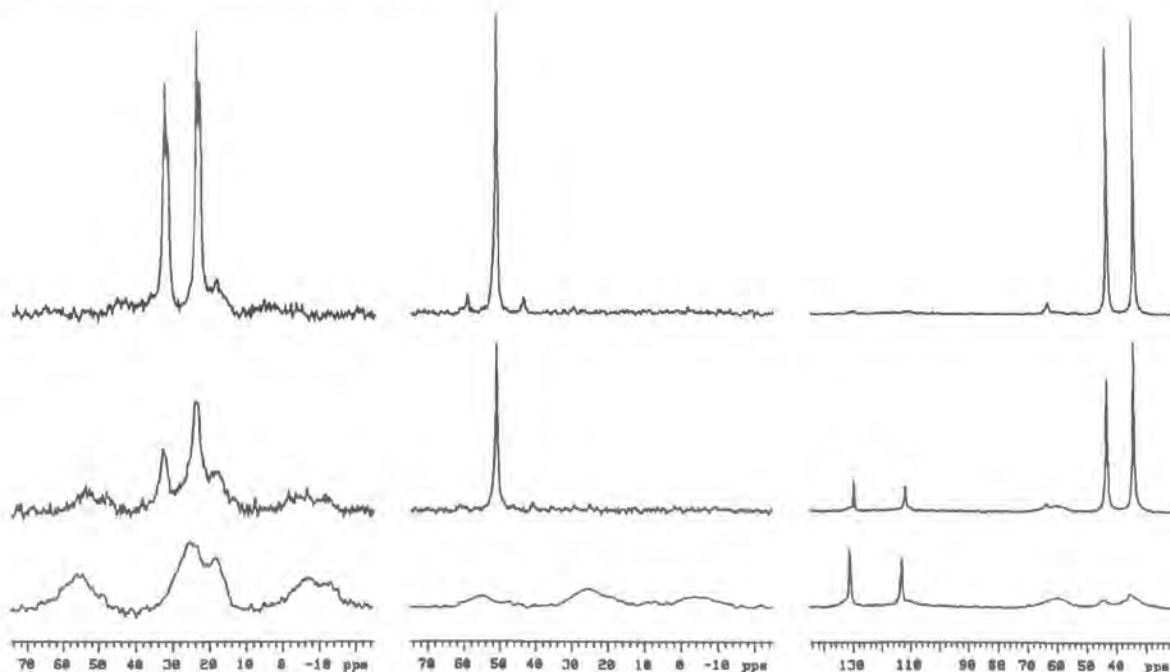


Figure 1. MAS NMR spectra obtained for agents added to AP-MgO: (left) GD at (top to bottom) $t = 9.5$ min, 1.0 h, and 23 h; (middle) VX at $t = 8.5$ min, 24 h, and 3 months; (right) HD at $t = 9.5$ min, 3.8 h, and 1 week.

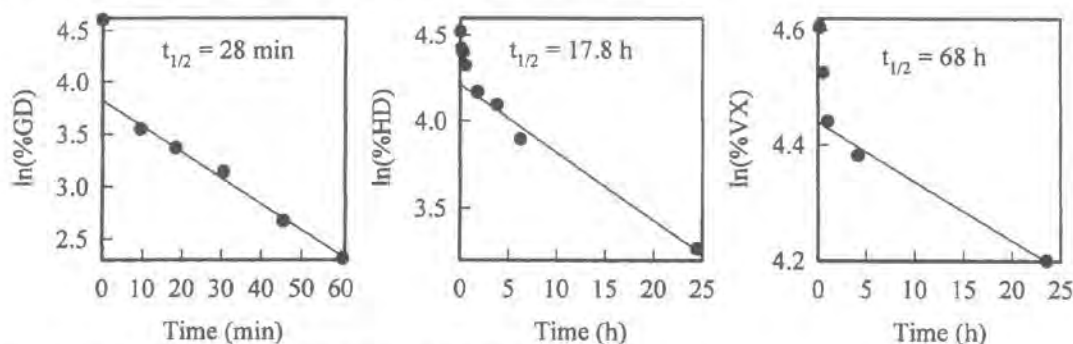
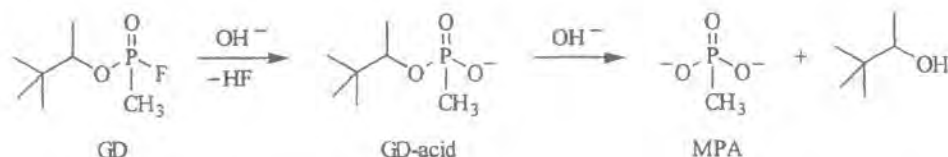


Figure 2. Reaction profiles for GD, HD, and VX liquid on AP-MgO.

SCHEME 1



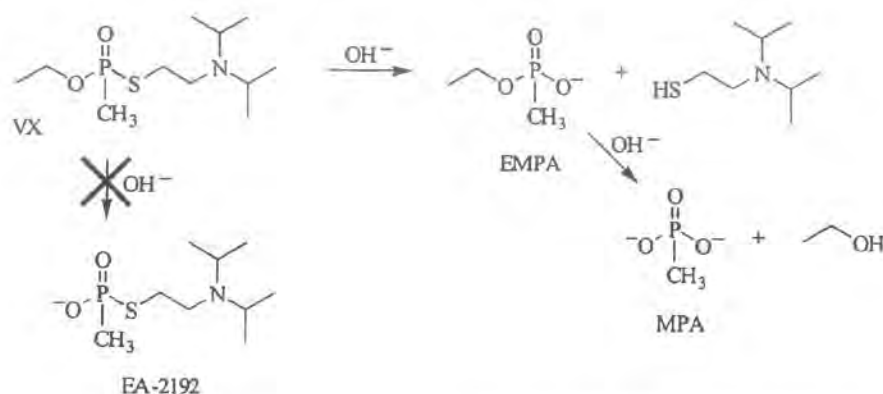
^{31}P NMR peaks is indicative of a strong interaction with the surface (see Discussion). The reaction profile is shown in Figure 2. After a fast initial reaction, a steady state is achieved exhibiting a first-order half-life of 28 min.

VX. Selected ^{31}P MAS NMR spectra obtained for 6 μL of VX added to 104 mg of AP-MgO are shown in the middle column of Figure 1. The intense singlet in the top spectrum at 51.6 ppm is due to VX, and the two smaller peaks are spinning sidebands. VX is slowly hydrolyzed by surface hydroxyls and/or physisorbed water to yield ethyl methylphosphonic acid (EMPA) and MPA, as evidenced by the broad peaks at 25.2 and 19.8 ppm, respectively. No toxic EA-2192 (expected to yield a peak near 40 ppm), which is known to form during hydrolysis in aqueous solution,¹ is observed. The acidic VX products are shown in the ionized form in Scheme 2. Again, the broad lines

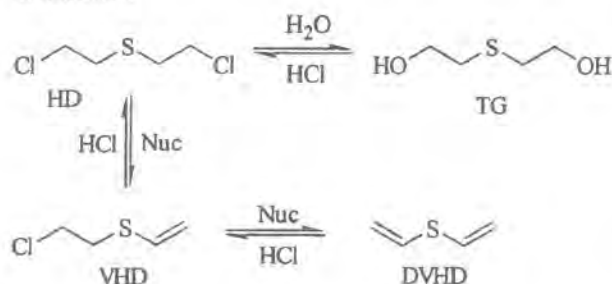
detected for EMPA and MPA reveal a very strong interaction of these species with the surface (see Discussion). The reaction profile is shown in Figure 2. As with GD, the fast initial reaction slows to a steady-state, first-order reaction with $t_{1/2} = 68$ h.

HD. Selected ^{13}C MAS NMR spectra obtained for 5 μL of HD* added to 111 mg of AP-MgO are shown in the right column of Figure 1. The two intense peaks in the top spectra are due to HD* (43.2 ppm, CH_2Cl ; 34.0 ppm, SCH_2). The small peak at 63.3 ppm is due to an impurity in the HD* ($\text{CH}_3\text{C}(\text{O})\text{O}^*\text{CH}_2\text{CH}_2\text{SCH}_2\text{CH}_2\text{Cl}$). Three products are observed during the course of the reaction: thiodiglycol (TG, broad peaks at 60.5 and 33.4 ppm), vinyl HD (VHD, 132.8, 111.0, 44.7, and 35.4 ppm), and divinyl HD (DVHD, 131.2 and 113.1 ppm). Thus, HD undergoes both hydrolysis and elimination of HCl. These reversible reactions are shown in Scheme 3. The precise

SCHEME 2



SCHEME 3

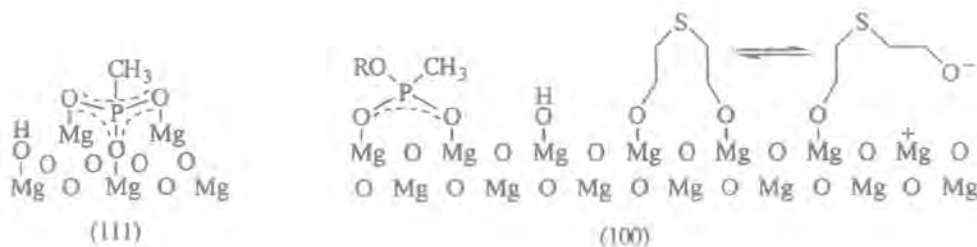


nature of the nucleophile performing the elimination is not clear since this reaction is not afforded by hydroxide in solution (see Discussion). The VHD eventually undergoes a second elimination of HCl to quantitatively yield DVHD. The final product ratio is about 50% TG and 50% DVHD. The broadened ^{13}C NMR lines detected for TG indicate a strong interaction of this compound with the surface (see Discussion). Conversely, the sharp lines for DVHD reveal a distinct lack of surface interaction. The reaction profile is shown in Figure 2. As with the other agents, the fast initial reaction is replaced by a pseudo-first-order reaction with $t_{1/2} = 17.8$ h.

Discussion

Surface Reactions. The hydrolysis reactions observed for GD, VX, and HD are as expected due to the basic MgO surface and are strictly analogous to the known solution chemistry of the agents.^{1a,b} But the final state of the products is quite different from that in solution. For VX and GD, the broad ^{31}P NMR lines observed for their products are consistent with the formation of surface-bound magnesium phosphonates, which are only soluble in water at low pH.⁶ Thus G and V agent products are not extracted from inorganic oxides using water⁷ or organic solvents but may be "dissolved" and extracted by acidic media.^{3c} Proposed structures for the surface-bound metal phosphonates^{1c,8} are shown in Scheme 4. Owing to exposure to air, the MgO

SCHEME 4



surface surely contains surface hydroxyl groups, as shown. The precise role of such surface hydroxyls and/or physisorbed water on the observed agent reactions is not yet known. The geometry of the predominant (100) plane of conventional MgO is suitable for the bidentate species GD-acid and EMPA, as shown, but the tridentate MPA may require the trigonal symmetry of sites found on the (111) face (thought to be favored in AP-MgO⁴) or at an edge or corner site.^{4a} Indeed, such sites may actually encourage MPA formation since they possess the proper geometry to hydrolyze the bound bidentate species.⁹ For HD, the strong surface interaction evidenced by the broadened ^{13}C NMR lines for TG may be due to either hydrogen-bonding with the surface or the formation of a reactive magnesium alkoxide, as shown in Scheme 4. Additional evidence for the latter surface species is provided by the VHD and DVHD products. Alkoxides are known to effect rapid elimination of HCl from HD in homogeneous solution.^{1a,b} But the ability of various sites on the AP-MgO surface to perform the observed HCl elimination cannot be ruled out.

Surface Kinetics. The kinetic behavior of the reactions is actually consistent with the immediate, destructive adsorption of all three agents on the AP-MgO surface, which is highly reactive. However, the agents react in a stoichiometric fashion; i.e., the surface sites do not "turn over" (in the catalytic sense) to react with additional agent. The peculiar nature of the reaction, i.e., a fast initial reaction followed by a slow, pseudo-first-order reaction, is merely reflective of the ability of the agent molecules to reach fresh, unreacted surface from the bulk liquid. This process is controlled by various physical properties of the agents. The salient properties are shown in Table 1.

The fast reaction results from the spreading of the liquid agent through the pore structure of the AP-MgO^{4b} to form a "wet spot". As a minor fraction of the bulk, liquid agent rapidly reacts along the wave front, the surface becomes poisoned or passivated against further reaction by the strongly-bound products discussed above. The spreading stops at the point where the liquid achieves its volume in the pores (the "wet spot");

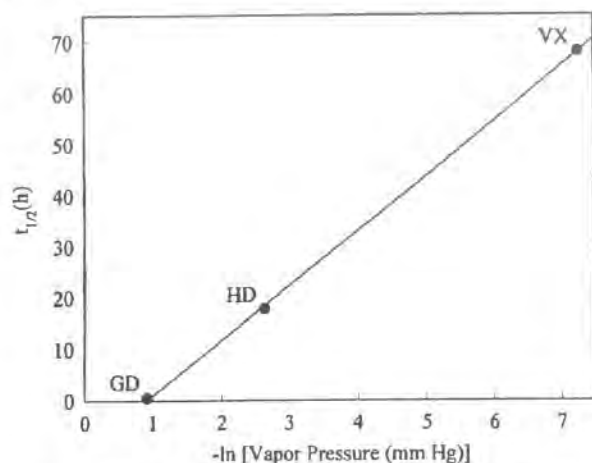


Figure 3. Dependence of steady-state half-life on vapor pressure.

TABLE 1: Physical Properties of GD, HD, and VX at 25 °C

	surface tension (dynes/cm)	viscosity (cS)	vapor diffusion coeff (cm ² /s)	vapor pressure (mm Hg)
GD	24.5	3.098	0.047	0.4
HD	42.5	3.1147	0.060	0.072
VX	31.3	9.958	0.034	0.0007

and the fast reaction ceases. The spreading process is presumably mediated by the surface tension and viscosity of the agent. Thus GD, possessing the lowest surface tension and viscosity, spreads the fastest. In the reaction profile shown in Figure 2, it is evident that this process for GD takes less than 10 min, the time at which the steady-state reaction begins. For HD and VX, the steady-state reaction begins at about 2 and 1 h, respectively. The viscosity of VX is much greater than that of HD, but it has a smaller surface tension. Therefore, it appears that surface tension (the ability of the liquid to expand its surface area) is more important with regard to spreading through AP-MgO than viscosity (the resistance to flow).

Once the liquid spreading ceases and the "wet spot" is established, the only mechanism by which agent molecules (present as bulk liquid within the pores) can reach fresh surface is by evaporation and diffusion in the gas phase. Diffusion-limited reactions exhibit first-order behavior, but gas phase diffusion is most likely not limiting the reactions as all three agents have vapor diffusion coefficients of the same order of magnitude. Rather, it is the disparate vapor pressures, a measure of the rate of evaporation, that is responsible for the slow, steady-state reaction of the agents with AP-MgO. GD has a significantly higher vapor pressure than either HD or VX. Therefore, GD has the fastest steady-state reaction ($t_{1/2} = 28$ min). HD has an intermediate vapor pressure and reaction rate ($t_{1/2} = 17.8$ h), and VX has the lowest vapor pressure and

slowest reaction rate ($t_{1/2} = 68$ h). Definitive evidence that the steady-state reaction is mediated by evaporation of the ensconced liquid agent in the "wet spot" is given by the dependence of the pseudo-first-order steady-state half-lives on the vapor pressure, as shown in Figure 3. This empirical relationship may provide the ability to predict the persistence of various agents on AP-MgO based solely on their vapor pressure.

Conclusions

The surface of AP-MgO is highly reactive toward GD, VX, and HD. The reaction is only limited by the physical processes of liquid spreading and evaporation, mediated primarily by the liquid surface tension and vapor pressure, respectively. These physical processes are responsible for the fast, initial reaction (liquid spreading) and the ensuing slow, steady-state pseudo-first-order reaction (evaporation) observed for all three agents. A simple empirical relationship exists between the steady-state half-life and the liquid vapor pressure of the agent, which allows the prediction of the persistence of other agents on AP-MgO.

Acknowledgment. Acknowledgments We thank Ms. Patrice Abercrombie, ERDEC, and Ms. Ann Butrow, ERDEC, for providing the physical property data for GD, VX, and HD.

References and Notes

- (1) (a) Yang, Y.-C.; Baker, J. A.; Ward, J. R. *Chem. Rev.* **1992**, *92*, 1729–1743. (b) Yang, Y.-C. *Chem. Ind.* **1995**, 334–337. (c) Ekerdt, J. G.; Klabunde, K. J.; Shapley, J. R.; White, J. M.; Yates, J. T., Jr. *J. Phys. Chem.* **1988**, *92*, 6182–6188.
- (2) Wagner, G. W.; Bartram, P. W. Unpublished results.
- (3) (a) Wagner, G. W.; Bartram, P. W. *Interaction of VX-, G- and HD-Simulants with Self-Decontaminating Sorbents: A Solid State MAS NMR Study*, ERDEC-TR-375; Aberdeen Proving Ground, MD, Nov 1996. (b) Wagner, G. W.; Bartram, P. W. *J. Mol. Catal. A: Chem.* **1996**, *111*, 175–180. (c) Wagner, G. W.; Bartram, P. W. *J. Mol. Catal. A: Chem.* **1995**, *99*, 175–181. (d) Wagner, G. W.; Bartram, P. W. *J. Mol. Catal. A: Chem.*, in press.
- (4) (a) Klabunde, K. J.; Stark, J.; Koper, O.; Mohs, C.; Park, D. G.; Decker, S.; Jiang, Y.; Lagadic, I.; Zhang, D. *J. Phys. Chem.* **1996**, *100*, 12142–12153. (b) Stark, J. V.; Park, D. G.; Lagadic, I.; Klabunde, K. J. *Chem. Mater.* **1996**, *8*, 1904–1912.
- (5) Reiff, L. P.; Taber, D. F.; Yet, L. *Synthesis of ¹⁴C-Labeled Mustard (HD)*, in *Proceedings of the 1996 ERDEC Scientific Conference on Chemical Defense Research*, ERDEC-SP-048; Aberdeen Proving Ground, MD, Oct 1997; pp 799–802.
- (6) Cao, G.; Lee, H.; Lynch, V. M.; Mallouk, T. E. *Inorg. Chem.* **1988**, *27*, 2781–2785.
- (7) Sides, G. D.; Mason, D. W.; Seiders, R. P. *Interaction of Agents HD, GD and VX with Alumina*. In *Proceedings of the 1983 Scientific Conference on Chemical Defense Research*, CRDC-SP-84014; Aberdeen Proving Ground, MD, Oct 1984; pp 285–291.
- (8) Templeton, M. K.; Weinberg, W. H. *J. Am. Chem. Soc.* **1985**, *107*, 97–108.
- (9) For the bidentate species bound to the (111) face, which possess trigonal symmetry, a nearest neighbor hydroxyl can easily assume the axial position of the trigonal bipyramid intermediate.¹⁰
- (10) Westheimer, F. H. *Acc. Chem. Res.* **1968**, *1*, 70–78.

Reactions of VX, GD, and HD with Nanosize CaO: Autocatalytic Dehydrohalogenation of HD

George W. Wagner,^{*,†} Olga B. Koper,[‡] Erik Lucas,[‡] Shawn Decker,[‡] and Kenneth J. Klabunde[†]

Research and Technology Directorate, U.S. Army Edgewood Chemical Biological Center, Aberdeen Proving Ground, Maryland 21010-5424 and Department of Chemistry, Kansas State University and Nantek, Inc., 1500 Hayes Dr., Manhattan, Kansas 66502

Received: January 6, 2000; In Final Form: March 13, 2000

Room-temperature reactions of the chemical warfare agents VX, GD, and HD with nanosize CaO (AP-CaO), and HD with commercial CaO have been studied using solid-state MAS NMR. VX and GD hydrolyze to yield surface-bound complexes of nontoxic ethyl methylphosphonate and pinacolyl methylphosphonate, respectively. The kinetics are characterized by an initial fast reaction followed by a slower, diffusion-limited reaction. Similar behavior is observed for HD on either dried or hydrated AP-CaO and CaO. On partially hydrated AP-CaO (but not CaO), a rather fast steady-state elimination of HCl occurs after an induction period. This behavior is attributed to acid-catalyzed surface reconstruction (to regenerate fresh surface) and the formation of CaCl₂, which is known to be more reactive than CaO. The product distribution for HD is about 80% divinyl sulfide and 20% thiodiglycol and/or sulfonium ions, which apparently reside as surface alkoxides. Such kinetic behavior was not evident for the common mustard simulant 2-chloroethyl ethyl sulfide (CEES) on partially hydrated AP-CaO, which exhibited only the typical fast/diffusion-limited reaction.

Introduction

Inorganic oxide particles are currently under consideration as reactive adsorbents for the decontamination of chemical warfare agents.¹ Enhancement in the reactivity of nanosize oxides is anticipated owing to increased surface area, greater amounts of highly reactive edge and corner "defect" sites, and unusual, stabilized lattice planes.² We recently reported results for the room-temperature reactions of neat liquid VX, GD, and HD with nanosize MgO (AP-MgO), which showed facile room-

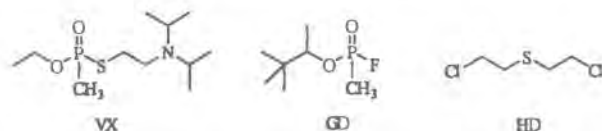
the dehydrohalogenation of chlorinated alkanes is anticipated, and water should affect the extent of this conversion. In situ generation of CaCl₂ and the conversion of bulk CaO to CaCl₂ are both potentially important processes to achieve a fast, catalytic elimination of HCl from HD.

Elimination of HCl from HD was observed on AP-MgO, although a large amount of hydrolysis (ca. 50%) also occurred (Scheme 1).³ GD and VX were observed to simply hydrolyze on AP-MgO (Schemes 2 and 3). These hydrolysis reactions are quite similar to those observed in solution,^{1a} except that the resulting products form surface-bound metal phosphonates (VX and GD) and metal alkoxides⁶ (HD). The vinyl and divinyl HD products are not bound to the surface and thus remain volatile. Another exception is that basic hydrolysis of VX in solution yields significant amounts of toxic EA-2192 in addition to the major nontoxic ethyl methylphosphonic acid (EMPA) product.⁷ EA-2912 does not form on AP-MgO or on other inorganic oxides examined,⁸ including zeolites.⁹ Such product selectivity for EMPA is exhibited in solution for the slow reaction of VX with an equimolar amount of water.¹⁰

In the present study, solid-state MAS NMR is used to examine the reactions VX, GD, and HD with nanosize CaO (AP-CaO). An unusual and fast reaction was observed for HD on partially hydrated AP-CaO which did not appear to be diffusion-limited, implying a catalytic reaction with the surface. Therefore, reactions of HD with commercial CaO and the common HD-simulant 2-chloroethyl ethyl sulfide (CEES) with AP-CaO were also examined to determine if this behavior is peculiar to the HD/AP-CaO system.

Experimental Section

Materials. Nanosize CaO (aerogel-prepared, AP-CaO) was prepared as previously described.^{2a} Samples prepared using the "as received" material were manipulated in air. Thus brief exposure to humid air occurred resulting in an unknown degree



temperature reactivity for all three agents, although liquid-state diffusion limitations severely reduced the overall reaction rates.³ VX and GD (Soman) are "nerve" agents, and HD (mustard) is a "blister" agent.^{1a}

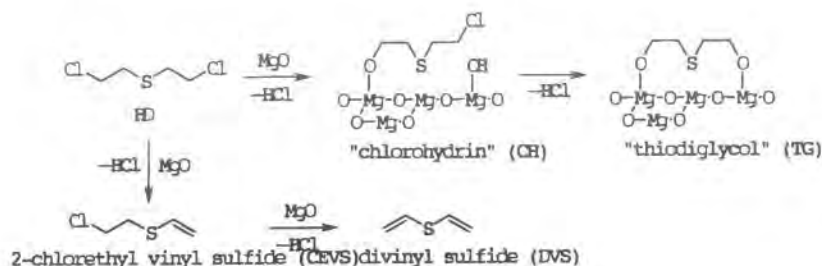
Metal oxides such as MgO and CaO are known to effect the elimination of HCl from chlorinated alkanes.⁴ Curiously, CaCl₂ (but apparently not MgCl₂) is reportedly even more active for this reaction than either of these oxides.^{4c} The reaction of CaO with acid-forming gases such as SO₂ is well-known, and water vapor has a favorable effect on its complete conversion to CaSO₃/CaSO₄.⁵ Thus the reaction is not limited to the surface, but continues through the bulk of the particle. The mechanism is not hard to envision as CaO is soluble in aqueous acid. Therefore, the formation of CaCl₂ from HCl generated during

* Corresponding author. E-mail: gwwagner@sbccom.apgea.army.mil

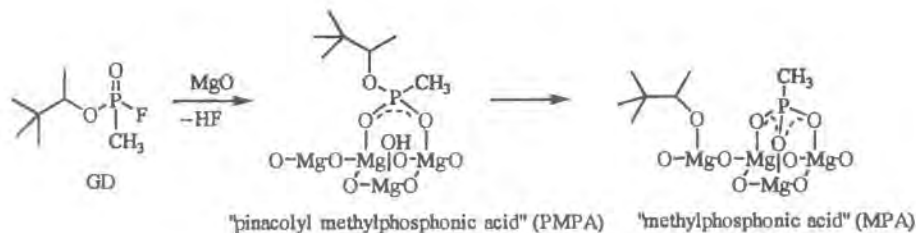
[†] Research and Technology Directorate, U.S. Army Edgewood Chemical Biological Center.

[‡] Department of Chemistry, Kansas State University and Nantek, Inc.

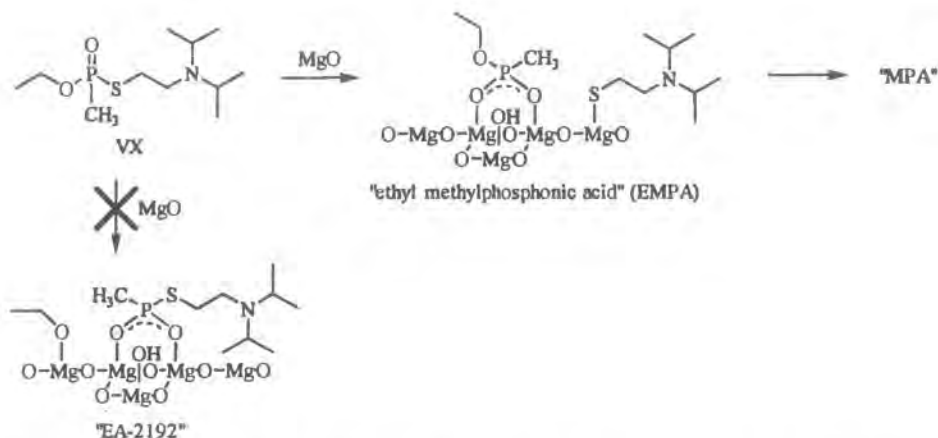
SCHEME 1



SCHEME 2



SCHEME 3



of partial hydration. Additional hydration may have occurred during prolonged storage. Dried AP-CaO was obtained by drying in air in an oven at 100 °C overnight, resulting in a 6.2% weight loss. Wet AP-CaO was prepared by standing in air overnight at room temperature, resulting in a 9.2% weight gain. Commercial CaO (99.9%, Aldrich) was used "as received". The CaO was allowed to stand in air overnight at room temperature to obtain the "wet" material, resulting in a 5.6% weight gain. Normal and ^{13}C -labeled HD (HD*) were used for ^1H and ^{13}C MAS NMR experiments, respectively. The HD* contained about 8% $\text{CH}_3\text{C}(\text{O})\text{OCH}_2\text{CH}_2\text{SCH}_2\text{CH}_2\text{Cl}$ as an impurity.¹¹ Normal 2-chloroethyl ethyl sulfide (Fairfield Chemical Company) was used as received in ^1H MAS NMR experiments.

NMR. ^{31}P and ^{13}C MAS NMR spectra were obtained using a Varian Unityplus 300 NMR spectrometer equipped with a Doty Scientific 7 mm high-speed VT-MAS probe as previously described.³ ^1H MAS NMR spectra were obtained using the same equipment. The nature of the HD and CEES adsorptions and reactions, i.e., no significant physisorption prior to destructive chemisorption (reaction), allowed monitoring by either ^{13}C or ^1H MAS NMR since the molecules remained highly mobile until their demise. In the case of ^1H MAS NMR spectra, relatively sharp peaks were evident for the mobile, volatile vinyl and divinyl products; however, peaks for the surface-bound hy-

drolysis products were too broad to detect. The latter products yielded broadened (compared to the vinyls), but detectable peaks in ^{13}C MAS NMR spectra.

Reaction Procedure. Caution: These experiments should only be performed by trained personnel using applicable safety procedures. In a typical run, 5 wt % neat, liquid agent or simulant (5–9 μL) was added via syringe to the center of a column of AP-CaO (ca. 120 mg) or CaO (ca. 200 mg) contained in the NMR rotor. The rotor was then sealed with the double O-ring cap, MAS NMR spectra were obtained periodically to monitor the reaction in situ.

Results

GD. Selected ^{31}P MAS NMR spectra obtained for 6 μL of GD added to 0.1157 g of "as received" AP-CaO are shown on the left side of Figure 1. Two doublets ($J_{\text{PF}} = 1049$ Hz) are apparent for the GD isomers centered at ca. 28.3 ppm. Over time, hydrolysis cleaves the P–F bond (Scheme 2) and the sharp doublets are replaced by a broad singlet for PMPA at 24.3 ppm. The broadness of the PMPA peak and the presence of intense spinning sidebands are indicative of surface binding of this product (Scheme 2). No further hydrolysis of PMPA to MPA was observed during the 24 h observation period. The reaction

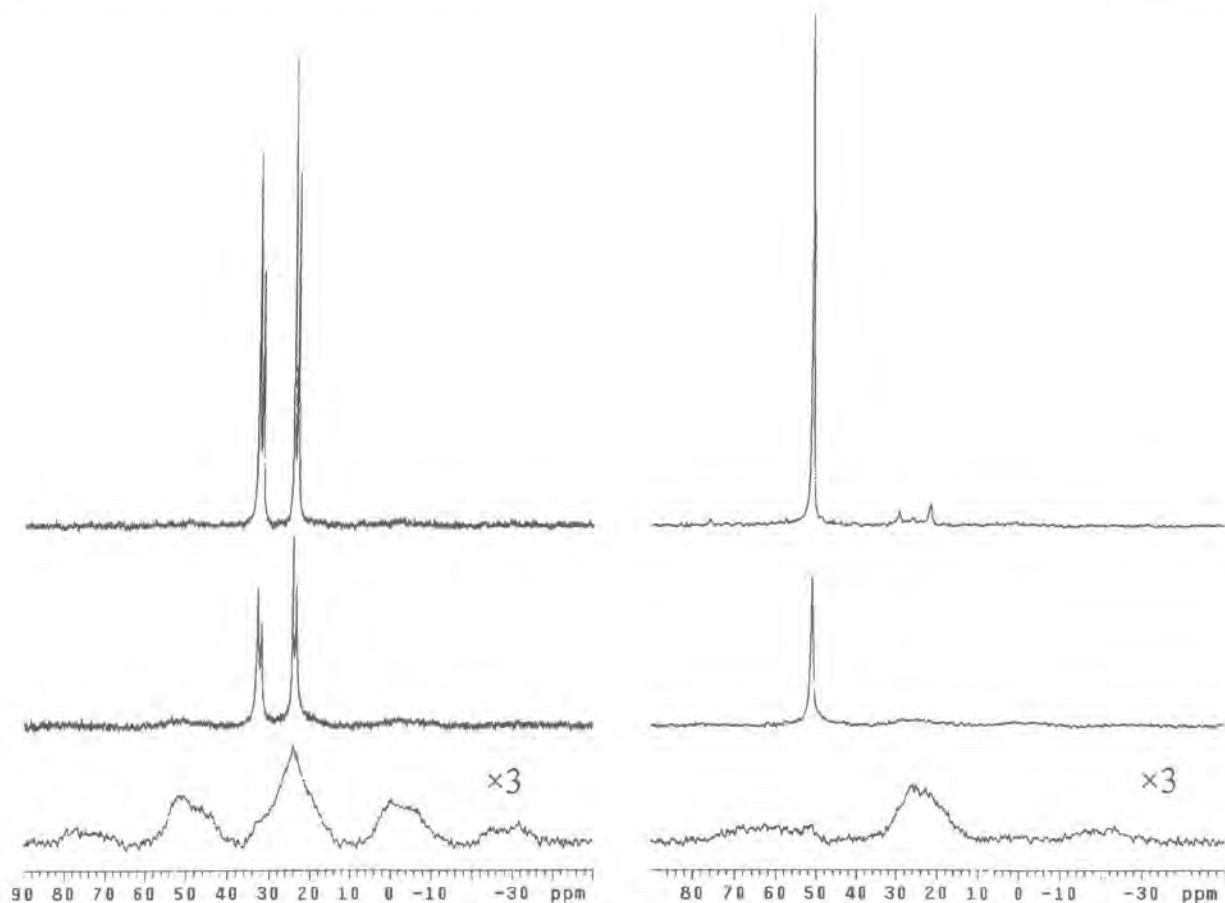


Figure 1. ^{31}P MAS NMR spectra obtained for nerve agents added to fresh, "as received" AP-CaO: (left) GD at (top to bottom) $t = 8.5$ min, 1.9 h, and 25 h; (right) VX at 8.5 min, 48 h, and 21 days. The bottom spectra for GD and VX have been expanded $3\times$ in vertical scale.

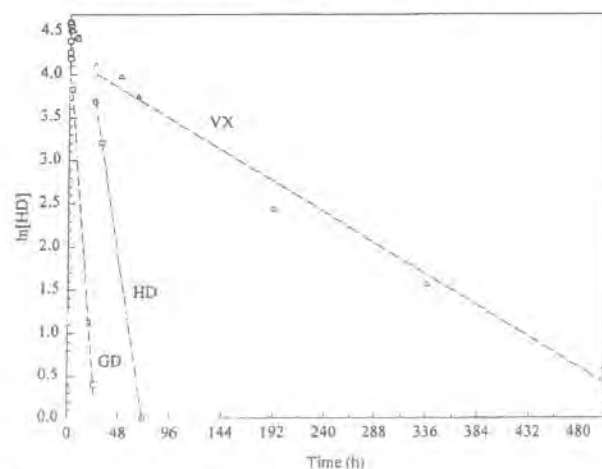


Figure 2. Reaction profiles for GD, VX, and HD* liquid on fresh, "as received" AP-CaO.

profile is shown in Figure 2. After a fast, initial reaction, a steady-state half-life of 4.5 h was observed.

VX. Selected ^{31}P MAS NMR spectra obtained for $6\ \mu\text{L}$ of VX added to $0.1106\ \text{g}$ of "as received" AP-CaO are shown on the right side of Figure 1. VX yields a sharp peak at $51.1\ \text{ppm}$. A small amount of an impurity, VX-pyro [$\text{EtOP}(\text{O})(\text{CH}_3)\text{OP}(\text{O})(\text{CH}_3)(\text{OEt})$], is evident as a small peak at $21.5\ \text{ppm}$. Gradually, VX (and VX-pyro) hydrolyzes to EMPA (Scheme 3), which emerges as a broad peak at $25.0\ \text{ppm}$. Spinning

sidebands are also apparent for this surface-bound species. No peak is evident for toxic EA-2192, which would occur near $40\ \text{ppm}$. The reaction profile in Figure 2 shows the same behavior exhibited by GD, except that the steady-state reaction is much slower, with a half-life of 93 h.

HD. Selected ^{13}C MAS NMR spectra obtained for $5\ \mu\text{L}$ of HD* added to $0.1152\ \text{g}$ of fresh, "as received" AP-CaO are shown on the left side of Figure 3. Peaks for HD* are present at 44.5 and $35.3\ \text{ppm}$. A small peak at $64.5\ \text{ppm}$ is due to an impurity. Over time sharp peaks appear for the elimination products (see Scheme 1) at 130.6 and $114.2\ \text{ppm}$ (DVS) and 132.0 , 112.3 , 43.3 , and $34.4\ \text{ppm}$ (CEVS), and broad peaks emerge for the hydrolysis product at ca. 61 and $33\ \text{ppm}$ (TG). The broadness of the TG product peaks is indicative of surface binding as shown in Scheme 1. The products indicate the reaction proceeds via 80% elimination and 20% hydrolysis. Minor amounts of sulfonium ions derived from the hydrolysis products (see below) were also detected, and these are included in the calculation of the elimination/hydrolysis distribution. The reaction profile is given in Figure 2, which exhibits an induction period of 5 h followed by a rather fast steady-state reaction with a half-life of 8.7 h. These results are summarized in Table 1.

On the right side of Figure 3 are shown selected ^1H MAS NMR spectra for $9\ \mu\text{L}$ of HD added to $0.1953\ \text{g}$ of "as received" commercial CaO. The HD peaks appear at 3.83 and $3.08\ \text{ppm}$. Over time the CEVS and DVS products yield overlapping vinyl proton peaks at 6.58 and $5.44\ \text{ppm}$; a third peak for CEVS at ca. $3.2\ \text{ppm}$ appears as a shoulder on the HD peak. ^1H peaks for surface-bound TG and/or sulfonium ion products are too

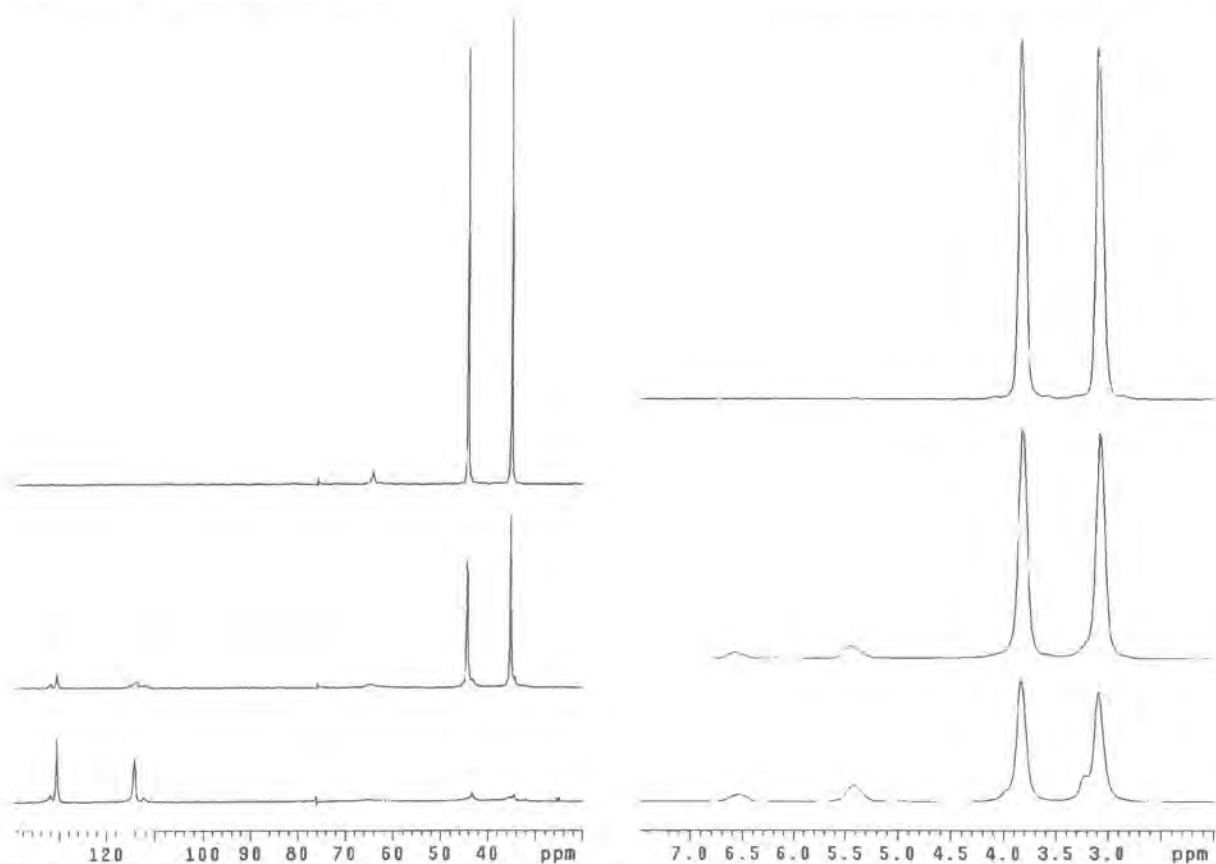


Figure 3. MAS NMR spectra obtained for (left, ^{13}C) HD* added to fresh, "as received" AP-CaO at (top to bottom) $t = 7.5$ min, 6.8 h, and 70 h, and (right, ^1H) HD added to fresh, "as received" CaO at $t = 8$ min, 24 h, and 17 days.

TABLE 1: HD and CEES Reactions on AP-CaO and CaO

compound/material/hydration	NMR method	induction period	initial half-life	steady-state half-life	elimination/hydrolysis
HD/AP-CaO/"as received"	^{13}C	5 h	8.7 h	8.7 h	80/20
HD/AP-CaO/ aged "as received"	^{13}C	1 h	3.5 h	3.5 h	80/20
HD/AP-CaO/ "wet"	^{13}C	none	3.1 h	> 46 h	80/20
HD/AP-CaO/ "dried"	^1H	none	4.0 h	> 11 days	5/95
HD/CaO/"as received"	^1H	40 min	31 h	> 49 days	80/20
HD/CaO/"wet"	^{13}C	none	9.1 h	> 49 days	60/40
CEES/AP-CaO/aged "as received"	^1H	none	< 12 min	> 135 h	5/95
CEES/AP-CaO/"dried"	^1H	none	1.7 h	> 156 h	30/70

broad to observe. The amount of vinyl product indicates about 20% elimination and 80% hydrolysis occurs. The reaction profile shown in Figure 4 exhibits a shorter induction period of about 40 min followed by a diffusion-limited reaction that continues to slow over time (final half-life > 49 days, Table 1).

Similar ^1H or ^{13}C MAS NMR spectra were obtained for 5 wt % HD or HD* on aged, "as received" AP-CaO (^{13}C), "dried" AP-CaO (^1H), "wet" AP-CaO (^{13}C), and "wet" CaO (^{13}C) (spectra not shown). These reaction profiles are also shown in Figure 4 and the results are summarized in Table 1. Compared to fresh, "as received" AP-CaO, the elimination of HCl from HD proceeded even faster on aged, "as received" AP-CaO, as the induction period was reduced to 1 h and the steady-state reaction exhibited a half-life of only 3.5 h. As before, about 80% elimination and 20% hydrolysis occurred. For "wet" AP-CaO, there is no discernible induction period, but the initially fast appearance of the reaction profile (initial half-life 3.1 h) is deceiving as the reaction continues to slow after 24 h (half-life > 46 h). The elimination/hydrolysis ratio for "wet" AP-CaO is still about 80/20. The "dried" AP-CaO also showed no induction period, had a somewhat slower initial half-life of 4.0 h, an even

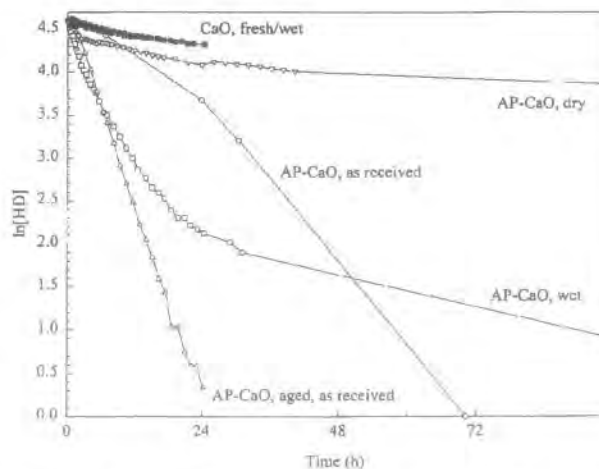


Figure 4. Reaction profiles for HD* and HD on AP-CaO and CaO. slower diffusion-limited reaction (half-life > 11 days), and yielded a small elimination/hydrolysis ratio of 5/95. However,

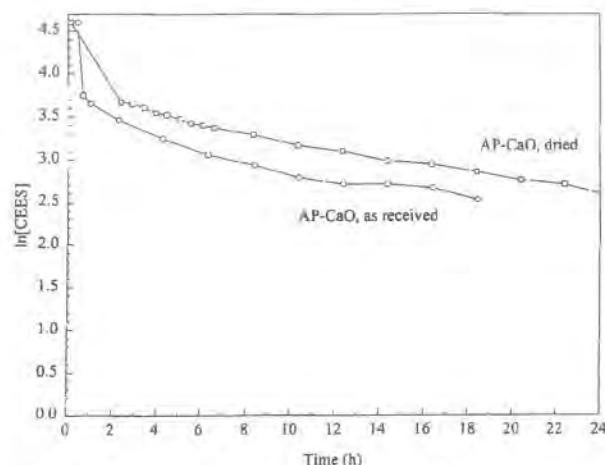


Figure 5. Reaction profiles for CEES on AP-CaO.

this material was still more reactive than the "as received" or "wet" CaO. "As received" CaO exhibited a short 40 min induction period and an initial half-life of 31 h, and "wet" CaO showed no induction period and a faster initial half-life of 9.1 h. However, both materials exhibited nearly identical, long-term diffusion-limited reaction profiles with extremely long half-lives greater than 49 days (Figure 4). The elimination/hydrolysis ratios were 80/20 for "as received" CaO and 60/40 for "wet" CaO.

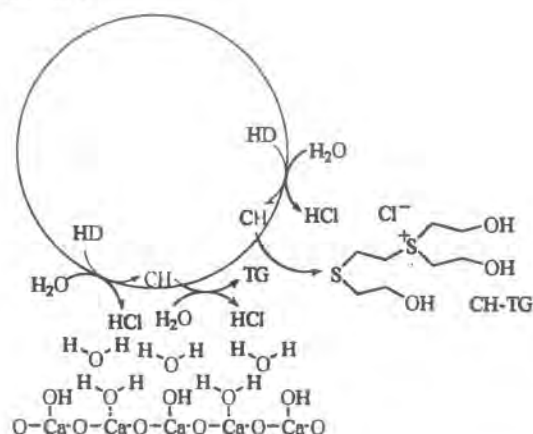
CEES. Reactions of 6 μ L of CEES added to ca. 0.123 g of aged, "as received" AP-CaO and "dried" AP-CaO were examined by ^1H MAS NMR (spectra not shown). The reaction profiles are shown in Figure 5. Unlike HD, no induction period is observed for CEES on either material. As shown in Table 1, the initial CEES reactions are faster than HD, but they eventually become diffusion-limited. CEES on aged, "as received" AP-CaO and "dried" AP-CaO yielded elimination/hydrolysis ratios of 5/95 and 30/70, respectively.

Discussion

GD and VX. Hydrolysis reactions observed for GD and VX are consistent with those previously observed on AP-MgO,³ and are adequately represented by Schemes 2 and 3. The reaction profiles are also quite similar to those observed on AP-MgO.³ The initial, fast reaction is attributed to liquid spreading and the reaction proceeds apace. However, once the liquid achieves its volume in the pore structure, spreading stops to form a "wet spot". Since the reaction with the surface is stoichiometric (Schemes 2 and 3), the reaction halts as well. At this point, evaporation appears to be the main mechanism by which molecules in the ensconced liquid may reach fresh surface and react, leading to the slow, diffusion-limited, steady-state reactions observed. Such reactions are mediated by the evaporation rate or vapor pressure.³ GD has a much higher vapor pressure than VX (0.4 vs 0.0007 mmHg), and thus has a much faster steady-state reaction (half-life 4.5 h) compared to VX (93 h). The half-lives observed for GD and VX are slower than those observed on AP-MgO, 28 min and 68 h,³ respectively.

HD. The major reaction for HD on "as received" or "wet" AP-CaO is elimination of HCl. The elimination/hydrolysis ratio is 80/20 compared to 50/50 on AP-MgO.³ The competing mechanisms are adequately represented by Scheme 1 with one exception, the formation of sulfonium ions. These were not detected on "as received" AP-MgO, but minor amounts were evident on AP-CaO. Sulfonium ions such as CH-TG result from the reaction of CH and TG hydrolysis products (see

SCHEME 4



Scheme 1), and tend to form when mustard droplets are in contact with water.¹² Scheme 4 depicts this reaction for a heavily hydrated CaO surface. Hydrolyzing environments which hinder sulfonium ion formation include dilute, homogeneous solutions¹² and surfaces where destructive adsorption occurs (i.e., Scheme 1, where hydrolysis occurs at the surface and products are immediately bound, rendering them unable to react with neighboring hydrolysis products). In solution and on surfaces HD droplet formation hinders the overall hydrolysis rate since only molecules at the droplet surface react.¹³ HD droplet formation is presumably also hindering the elimination reactions on the wetter materials.

HD on AP-MgO³ showed the same kinetic behavior exhibited by GD and VX above, i.e., a fast reaction due to liquid spreading, followed by a slower, steady-state reaction mediated by evaporation. The same behavior is observed for HD on "wet" or "dried" AP-CaO and "wet" CaO. However, on partially hydrated, "as received" AP-CaO, the behavior is quite different. On this material, the kinetic behavior is characterized by an induction period which precedes a rather fast steady-state reaction which does not become diffusion-limited. Also, the major mechanism is elimination. HD on "as received" CaO exhibits features of both kinetic behaviors; i.e., a short induction period precedes a brief, fast reaction which rapidly decays to a very slow diffusion-limited reaction. The induction period and fast steady-state reaction can be attributed to the formation of CaCl_2 on the AP-CaO surface. CaCl_2 is a more active elimination catalyst than CaO .^{4c} Water apparently assists in this endeavor, presumably by acid-catalyzed surface reconstruction. In this manner, the surface may be continually refreshed and expanded, resulting in the autocatalytic behavior observed. The nanosize nature of AP-CaO, i.e., small particle size and/or large amounts of unusual lattice planes and surface defect sites,² appears critical to achieving a sustained, catalytic elimination of HD. Moreover, AP-CaO must also possess the right amount of water. Although "as received" CaO showed evidence of a brief induction period and considerable elimination, a sustained catalytic reaction was not achieved, and this could be simply due to the larger particle size of the CaO.

CEES. CEES did not exhibit an induction period nor a fast, sustained catalytic elimination reaction on aged "as received" AP-CaO. On this material and on "dried" AP-CaO, the major reaction mechanism was hydrolysis, and the kinetic behavior is characterized by the typical fast/slow diffusion-limited reaction. However, the initial reactions were significantly faster than those observed for HD. The rapidity of the initial, fast CEES reaction is attributable to both its lower viscosity and

surface tension, providing for faster liquid spreading,³ and faster rate of hydrolysis relative to HD ($k = 0.0158 \text{ s}^{-1}$ for CEES,¹⁴ 0.00129 s^{-1} for HD¹⁵). Consistent with this picture, no elimination products were detected for CEES during the fast reaction, and only minor elimination occurred during the diffusion-limited reaction. It may be that the rapidity of the CEES hydrolysis and the concomitant substitution of the surface with alkoxide effectively hinders the formation of the CaCl_2 "islands" necessary for a sustained, catalytic reaction. Consistent with this rationale, "dried" AP-CaO showed enhanced elimination activity, presumably owing to reduced water content and hydrolytic activity.

Conclusions

AP-CaO exhibits room-temperature reactivity for VX, GD, and HD. For HD on partially hydrated AP-CaO, the presence of an induction period, the absence of a diffusion-limited reaction, and a predominant dehydrohalogenation reaction strongly suggests an autocatalytic surface reaction. Water plays a crucial role in this reaction as dried or heavily hydrated AP-CaO does not effect this behavior. The role of water may be to support an acid-catalyzed surface reconstruction to yield CaCl_2 , which is known to be a more active dehydrohalogenation catalyst than CaO. Too much water may prevent the necessary contact or spreading of HD on the surface of AP-CaO. Although an induction period can be observed for HD on partially hydrated commercial CaO, the material does not effect the sustained, catalytic reaction behavior seen for AP-CaO, possibly due to its larger particle size and/or lack of surface morphology unique to nanosize particles. Sustained, catalytic reaction behavior is also not observed for CEES on partially hydrated AP-CaO. As hydrolysis predominates over dehydrohalogenation for CEES on AP-CaO, its relatively fast hydrolysis rate (compared to HD) and concomitant surface-alkoxide formation could hinder the formation of CaCl_2 "islands" necessary for facile elimination of HCl.

Acknowledgment. We thank Messrs. Philip W. Bartram, Lawrence R. Procell, David C. Sorrick, and Richard J. O'Connor and Ms. Vikki D. Henderson for assistance with the agent operations.

References and Notes

- (1) (a) Yang, Y.-C.; Baker, J. A.; Ward, J. R. *Chem. Rev.* **1992**, *92*, 1729–1743. (b) Yang, Y.-C. *Chem. Ind.* **1995**, 334–337. (c) Ekerdt, J. G.; Klabunde, K. J.; Shapley, J. R.; White, J. M.; Yates, J. T., Jr. *J. Phys. Chem.* **1988**, *92*, 6182–6188.
- (2) (a) Klabunde, K. J.; Stark, J.; Koper, O.; Mohs, C.; Park, D. G.; Decker, S.; Jiang, Y.; Lagadic, I.; Zhang, D. *J. Phys. Chem.* **1996**, *100*, 12142–12153. (b) Stark, J. V.; Park, D. G.; Lagadic, I.; Klabunde, K. J. *Chem. Mater.* **1996**, *8*, 1904–1912.
- (3) Wagner, G. W.; Bartram, P. W.; Koper, O.; Klabunde, K. J. *J. Phys. Chem. B* **1999**, *103*, 3225–3228.
- (4) Misono, M.; Yoneda, Y. *J. Catal.* **1974**, *33*, 474–479. (2) Mochida, I.; Take, J.-I.; Saito, Y.; Yoneda, Y. *J. Org. Chem.* **1967**, *32*, 3894–3898. (c) Noller, H.; Hantsche, H.; Andreu, P. *J. Catal.* **1965**, *4*, 354–362. (d) Noller, H.; Hantsche, H.; Andreu, P. *Angew. Chem., Int. Ed.* **1964**, *3*, 584. (e) Andreu, P.; Schmitz, E.; Noller, H. *Angew. Chem., Int. Ed.* **1964**, *3*, 135.
- (5) Hartman, M.; Trnka, O. *AIChE J.* **1993**, *39*, 615–624.
- (6) Mawhinney, D. B.; Rossin, J. A.; Gerhart, K.; Yates, J. T., Jr. *Langmuir* **1999**, *15*, 4789–4795.
- (7) (a) Yang, Y.-C. *Acc. Chem. Res.* **1999**, *32*, 109–115. (b) Yang, Y.-C.; Szfraniec, L. L.; Beaudry, W. T. *J. Org. Chem.* **1993**, *58*, 6964–6965.
- (8) Wagner, G. W.; Bartram, P. W. Unpublished results.
- (9) Wagner, G. W.; Bartram, P. W. *Langmuir* **1999**, *15*, 8113–8118.
- (10) Yang, Y.-C.; Szfraniec, L. L.; Beaudry, W. T.; Rohrbaugh, D. K.; Procell, L. R.; Samuel, J. B. *J. Org. Chem.* **1996**, *61*, 8407–8413.
- (11) Reiff, L. P.; Taber, D. F.; Yet, L. Synthesis of ^{13}C -Labeled Mustard (HD). In *Proceedings of the 1996 ERDEC Scientific Conference on Chemical Defense Research*, ERDEC-SP-048; Aberdeen Proving Ground, MD, Oct. 1997; pp 799–802.
- (12) Yang, Y.-C.; Szfraniec, L. L.; Beaudry, W. T.; Ward, J. R. *J. Org. Chem.* **1988**, *53*, 3293–3297.
- (13) Wagner, G. W.; MacIver, B. K. *Langmuir* **1998**, *14*, 6930–6934.
- (14) Yang, Y.-C.; Ward, J. R.; Luteran, T. *J. Org. Chem.* **1986**, *51*, 2756–2759.
- (15) Bartlett, P. D.; Swain, C. G. *J. Am. Chem. Soc.* **1949**, *71*, 1406–1415.

Development of Reactive Topical Skin Protectants against Sulfur Mustard and Nerve Agents

Olga Koper, Eric Lucas and Kenneth J. Klabunde*

Nantek, Inc., 1500 Hayes Drive, and Department of Chemistry, Kansas State University, Manhattan, KS 66502, USA

Key words: reactive nanoparticles; GA; GB; HD; VX; topical skin protectant; metals; metal oxides.

The potential for highly reactive nanoparticles (RNP) to absorb destructively, i.e. to neutralize highly toxic substances such as the warfare agents GA, GB, HD and VX, has been demonstrated in the laboratory. Reactive nanoparticles represent a new class of nanoscale particles of metals and metal oxides that differ from other nanoparticles in reactivity and crystalline morphology.

The potential for incorporating RNP into a protective barrier skin cream also has been demonstrated. Preliminary studies indicate that RNP are physically and chemically compatible with a base cream provided by the Army Medical Research Office and, importantly, remain reactive with chemical agents while promising to be compatible with skin contact. Copyright © 1999 John Wiley & Sons, Ltd.

INTRODUCTION

Introduction to Nantek's destructive adsorption technology

The need for military personnel protective systems capable of neutralizing highly toxic substances such as the warfare agents GA, GB, HD, and VX has been identified as a significant problem facing the Department of Defense.^{1–24} For the specific application addressed in this paper, reactive adsorbent materials can be mixed into a base cream to provide protection for skin in the event of exposure to such highly toxic substances. Other counter-measures or protective uses for the adsorbents could include air purification, personnel ventilation systems and wide-area surface decontamination.

Significant work has been conducted at Kansas State University, resulting in the discovery of unique nanoparticle materials exhibiting extraordinary abilities to destroy highly toxic substances such as nerve agents, polychlorinated biphenyls (PCBs) and insecticides.^{20–24} Much of the basic research in nanoparticle synthesis and reactive chemistry has been funded by a variety of federal grant sources, including the Department of Army. From this basic research focusing on the synthesis, characterization and reaction chemistry of a broad range of nanoparticle materials, several patents are pending on the unique nanoparticles and the underlying destructive adsorption technology (DAT).

Essentially, the research conducted had demonstrated the ability of the unique nanoparticles to both adsorb and destroy hazardous compounds. Initial work focused on the use of DAT as an alternative to high-temperature

incineration for the bulk treatment of organophosphorus compounds, chlorinated hydrocarbons, PCBs, insecticides and other similar hazardous substances. On a laboratory scale, special metal oxide nanoparticles destructively adsorbed mimics of nerve gases, including paraoxon, one-armed mustard and dimethyl methyl phosphonate, as well as carbon tetrachloride, which is a fairly stable compound. Laboratory results strongly suggested that the nanoparticles indeed react with these substances at room temperature, thus opening the application to personal and building ventilation systems, protective skin products and wide-area surface decontamination.

The nanoparticles seem to provide a clear advantage over other competing decontamination technologies, such as activated carbon adsorbents and highly caustic solutions. Other decontaminants used primarily for surface decontamination, such as DS2, ozone and ethanol–NaOH–ammonia solutions,²⁵ are highly toxic for skin exposure and would not be compatible with the proposed base skin cream. Activated carbon, a possible solid adsorbent, has the disadvantages that:

- (i) carbon does not destroy the toxic chemical but merely 'holds it' by weak adsorption forces;
- (ii) inorganic pollutants such as hydrogen cyanide, cyanogen chloride and acid gases are not adsorbed well by activated carbon;
- (iii) clean-up and disposal of the contaminated carbon is difficult because the hazardous material is believed to be only adsorbed but still highly toxic.

Caustic sorbents are obviously unsuitable for this application, posing a significant hazard for humans. In fact, the solutions used for such purposes are so highly caustic that they corrode metals, paint and wood.

Thus, new materials or adsorbents offering rapid kinetics yet suitable from a safety and cost standpoint need to be developed that can protect skin from exposure to highly toxic nerve agents when combined

* Correspondence to: K. J. Klabunde, Nantek, Inc., 1500 Hayes Drive, Manhattan, KS 66502, USA.

RESULTS AND DISCUSSION

Several unique nanoparticles were developed during this work that were believed to be possible candidates for the skin cream protectant system. These included oxides of magnesium, titanium, calcium, zinc, nickel and copper, and composite samples consisting of transition metal-coated nanoparticles.

Extensive testing of the destructive adsorbent performance of a broad array of nanoparticle samples was conducted. These tests were conducted using mimics of nerve agents such as paraoxon and 2-CEES (the one-armed mustard). Figure 1 provides an illustration of the chemical composition of the military agents and their corresponding mimics.

Decomposition of paraoxon on various metal oxides

In the initial trials, a broad array of readily available samples (either commercial samples or particles previously produced at Nantek's laboratory) were tested for paraoxon decomposition, as detailed in Table 1. Figure 2 shows the disappearance of paraoxon on these sample compounds over time. In these experiments, the reaction was monitored over a period of 24 h. After the best samples were chosen, more detailed studies of the initial reaction of the adsorbent/mimic were

Table 1. Samples studied in preliminary mimic adsorption

Sample description	Designator	Surface area (m ² g ⁻¹)
Commercial copper oxide	CM-CuO	<1
Commercial nickel oxide	CM-NiO	4
Commercial iron oxide	CM-Fe ₂ O ₃	8
Commercial zinc oxide	CM-ZnO	24
Conventionally prepared zinc oxide	CP-ZnO	20
Commercial titanium dioxide	CM-TiO ₂	42

carried out. In addition to the UV-Vis spectra analysis, adsorption of the paraoxon was readily visible on most of the white powder samples due to the change in color of the powder from white to bright yellow. Note that paraoxon is a pale yellow, oily substance and its color does not duplicate the bright yellow observed. However, the anion O₂NC₆H₄O⁻ is bright yellow, and this observation coupled with IR data strongly suggests that the anion is formed very quickly on the surface of some of the nanoscale oxide adsorbents.

Some general conclusions can be drawn from Fig. 2. Materials with higher surface area appear to adsorb much better than those with lower surface area; however, some discrepancies were observed. For example,

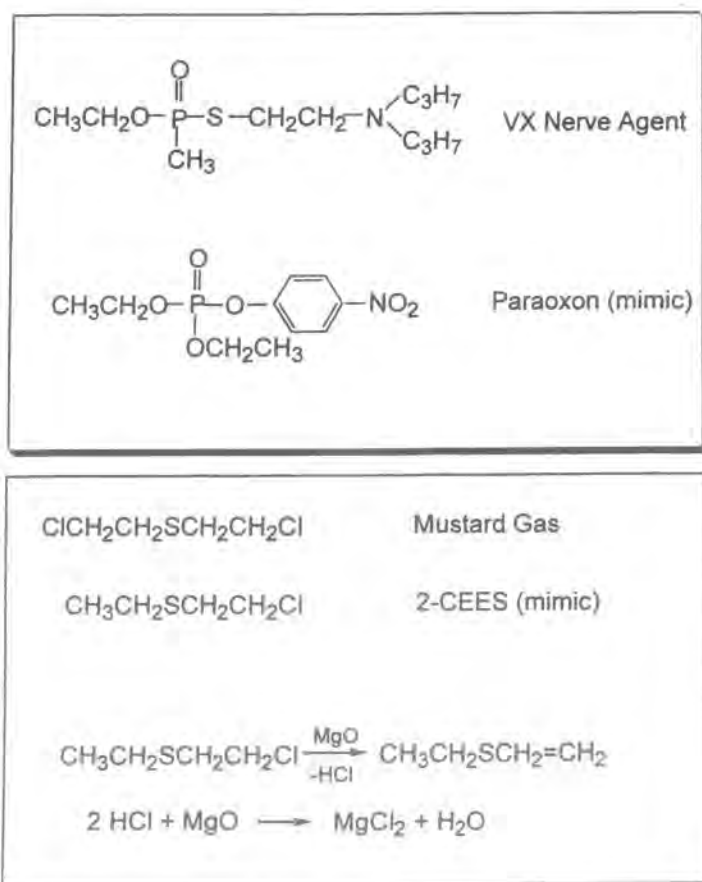


Figure 1. Military agents and their mimic counterparts.

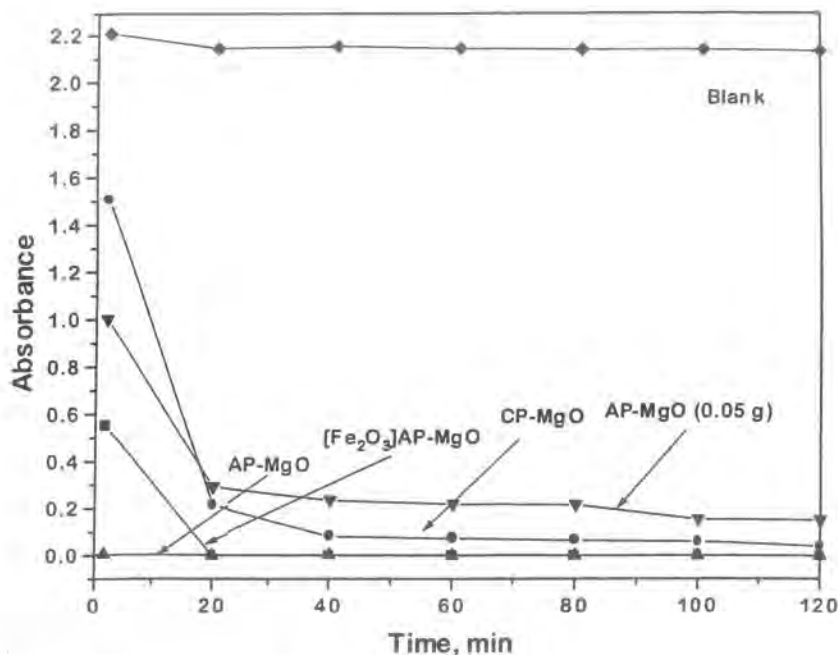


Figure 3. Rate of disappearance of paraoxon (4.5 μ l) on magnesium oxide samples.

the material's very high surface area of $562 \text{ m}^2 \text{ g}^{-1}$. The iron oxide-coated MgO sample ($[\text{Fe}_2\text{O}_3]\text{AP-MgO}$ with a surface area of $360 \text{ m}^2 \text{ g}^{-1}$) also behaved very well: after 20 min, no paraoxon was observed in the reaction flask. The amount of iron oxide was ca. 1% by weight of the sample. The conventionally prepared MgO samples ($340 \text{ m}^2 \text{ g}^{-1}$) also adsorbed paraoxon very efficiently.

The data obtained for calcium oxide are shown in Fig. 4. The iron oxide coating enhances the perform-

ance for both conventional and autoclave-prepared calcium oxide. For the iron-coated AP-CaO sample, only ca. 10% of the paraoxon was present after 2 h of reaction (based on the height of the paraoxon peak). The CP-CaO did not behave as well, even though its surface area was comparable to AP-CaO (ca. $120 \text{ m}^2 \text{ g}^{-1}$). However, when iron oxide was present, the surface area of CP-CaO decreased (from 110 to $68 \text{ m}^2 \text{ g}^{-1}$) but the amount of adsorbed paraoxon was much higher. The iron coating either enhances the

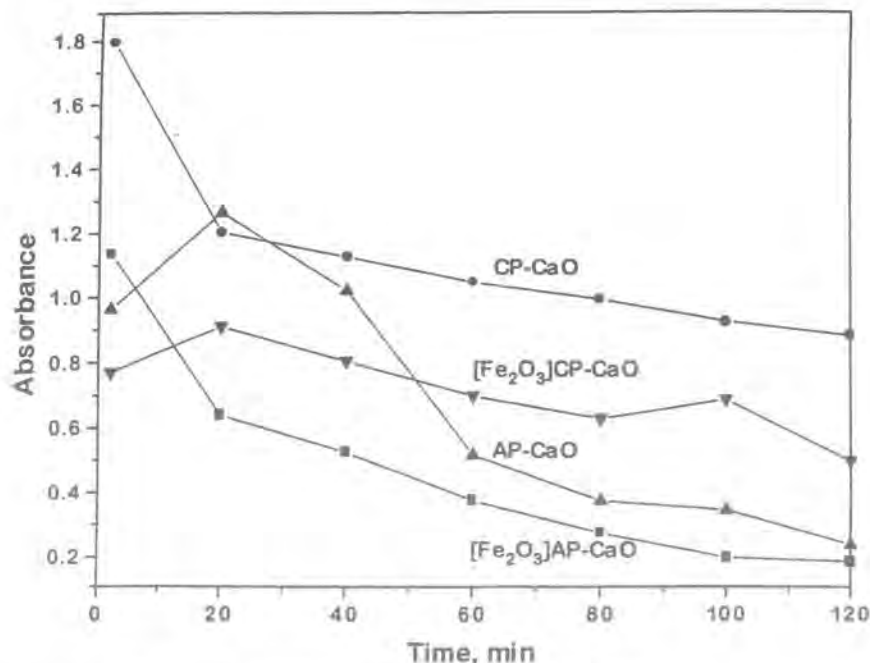


Figure 4. Rate of disappearance of paraoxon (4.5 μ l) on calcium oxide samples (0.1 g).

and its 'fragments' are on the surface. Further work is needed in order to elucidate what these fragments are.

Adsorption of mimics using activated carbon. We have performed preliminary benchmarking studies with a known adsorbent: activated carbon having an approximate surface area of $900 \text{ m}^2 \text{ g}^{-1}$. The same test conditions were utilized during the carbon testing. The activated carbon adsorbed the paraoxon well, as anticipated. After ca. 1 h, all of the paraoxon was adsorbed. However, when $10 \mu\text{l}$ of paraoxon was added to 0.1 g of the powder, only partial adsorption was observed. The same experiment was carried out with 15, 30 and $50 \mu\text{l}$ of paraoxon (per 0.1 g of activated carbon). However, in all three cases the absorbance of paraoxon was too high due to its high residual concentration, and thus out of range of the UV-Vis spectrophotometer.

For comparison purposes, similar experiments were conducted with Nantek's AP-MgO material, which has a surface area of ca. $400 \text{ m}^2 \text{ g}^{-1}$. It was found that AP-MgO works much better than activated carbon, despite its lower surface area. The AP-MgO was able to adsorb/decompose completely $15 \mu\text{L}$ of paraoxon after 1 h of exposure, whereas little adsorption was observed using the activated carbon. Interestingly, when AP-MgO was used with larger amounts of paraoxon, the peak of *p*-nitrophenol, a by-product of paraoxon decomposition, became more prominent. Most likely during the decomposition, *p*-nitrophenol is formed and subsequently back-adsorbed onto the surface if enough of the surface sites are still available. When larger amounts of paraoxon were used, the formed product could not completely adsorb on the surface and was therefore released into the organic solvent. Table 4 and Fig. 6 provide additional comparative data.

After the paraoxon reaction was complete, the powders were filtered in a glove bag to minimize exposure to moisture in the atmosphere and a KBr pellet for IR studies was made. The IR spectrum of AP-MgO changes completely upon adsorption of paraoxon, and resembles the spectrum of *p*-nitrophenol adsorbed on MgO.

When the paraoxon was adsorbed on activated carbon, a very different spectrum was observed. Preliminary extraction techniques were used to characterize the surface residues on the carbon sample. Methanol, a highly polar solvent, was added to the solid product in an attempt to remove the paraoxon residue. The extract was filtered and injected into a gas chromatograph mass spectrometer for analysis. For comparison, the spectra of the starting compound, paraoxon, and the product of reaction, *p*-nitrophenol were also injected into a methanol solution. However, the methanol extraction approach was unsuccessful at removing the paraoxon species from the surface of the carbon product.

To elucidate further those species that are on the surface after reaction, other extraction procedures were attempted. Toluene was added to the solid reaction product (AP-MgO and activated carbon after reaction with $10 \mu\text{l}$ of paraoxon) and the samples were sonicated for 20 min to remove all species from the surface. The extract then was filtered using a syringe filter and injected into the gas chromatography/mass spectrometer. For AP-MgO, no additional peaks were observed; however, in the case of the activated carbon, some non-decomposed paraoxon was detected.

In summary, Nantek's AP-MgO reactant appears to adsorb significantly more than activated carbon (Aldrich, Darco G60, 100-mesh). This finding was not necessarily expected, because the carbon material with its high surface area and large pore volume is recognized for its adsorbent capability. On a preliminary basis, we attempted to confirm our belief that activated carbon adsorbs but does not react or destroy the paraoxon. We have demonstrated that special high-surface-area metal oxide materials do indeed destroy the highly toxic substances through the formation of reaction by-products, including *p*-nitrophenol for paraoxon decomposition and vinyl sulfide for the one-armed mustard decomposition. The preliminary results do indicate that the solid products are indeed quite different. New extraction techniques for elucidation of the species on the surface of the activated carbon will need to be investigated.

Table 4. Comparison of the adsorption of different amounts of paraoxon on AP-MgO. (Surface area = $400 \text{ m}^2 \text{ g}^{-1}$) and activated carbon (Surface area = $900 \text{ m}^2 \text{ g}^{-1}$)

Sample	Paraoxon (μl)	Intensity of the paraoxon peak after 2 h	Intensity of the paraoxon peak after 20 h
AP-MgO	4.5	0	0
AP-MgO	10	0	0
AP-MgO	15	0.027	0
AP-MgO	30	Out of range	3.543
Activated carbon	4.5	(max = 5)	0
Activated carbon	10	0	1.205
Activated carbon	15	1.520	2.729
		Out of range (max = 5)	

Decomposition of 2-chloroethylethyl sulfide (2-CEES) on various metal oxides

Extensive test trials. In these experiments the samples exhibiting the best adsorbent activity in the paraoxon studies were used to study the dehydrochlorination of 2-chloroethylethyl sulfide (2-CEES), a mimic of mustard gas. This process can be monitored using IR spectroscopy by observing the growth of a peak assigned to ethylvinyl sulfide, a decomposition product. It is necessary to observe the product of the reaction because the disappearance of 2-CEES cannot be monitored directly, owing to the majority of the peaks of 2-CEES superimposing the peaks of ethylvinyl sulfide. The only significant difference between 2-CEES spectrum and ethylvinyl sulfide spectrum is the peak at 1595 cm^{-1} attributed to the double bond of ethylvinyl sulfide. The observation of the growth of this peak was therefore used as a fingerprint in the decomposition of 2-CEES.

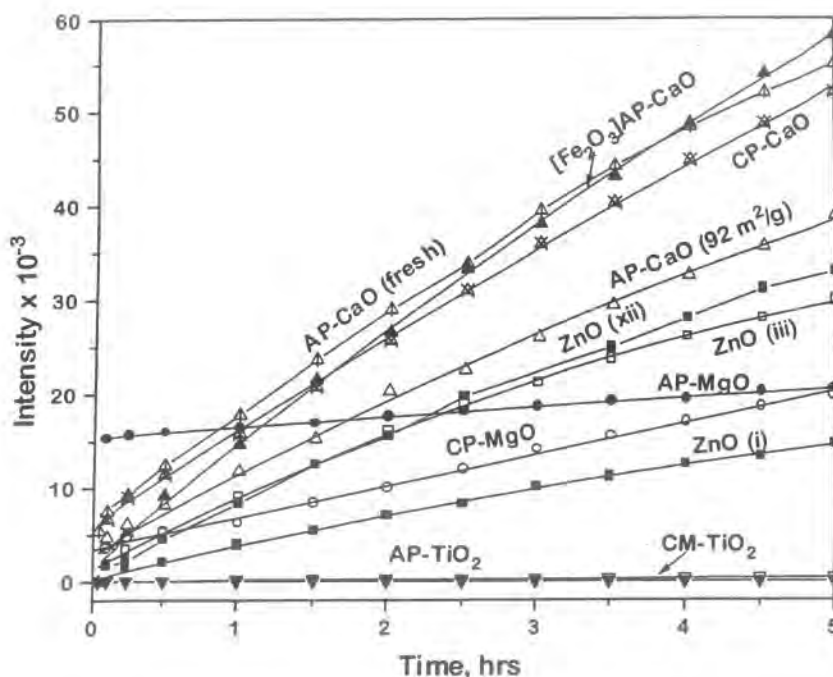


Figure 7. Appearance of ethylvinyl sulfide during 2-CEES decomposition on various metal oxides. Higher intensity indicates more destructive adsorption of 2-CEES.

oxides before and after exposure to 2-CEES. First we observed the formation of associated hydroxyl groups, as seen by the growth of a broad band at 3300 cm^{-1} ; secondly, we observed the broadening of a peak at 1082 cm^{-1} (assigned to calcium carbonate on the surface of CaO). To emphasize these differences, we removed the IR spectrum of the oxide before reaction from the spectrum of the same oxide after reaction. Although the differences appear more pronounced, they did not correspond to a simple adsorption of 2-CEES or ethylvinyl sulfide on the surface. Therefore, it is clear that the mustard mimic, 2-CEES, is not simply adsorbed. It is destroyed on the surface of the nano-scale oxide particles.

Physical compatibility of the metal oxides in the base cream

Magnesium, calcium and zinc oxides were mixed with the base cream provided by the Army and XRD of the paste was taken. For comparison, a diffraction pattern of the pure cream was also recorded. The cream by itself gives a high baseline in the spectrum. However, if enough oxide is present in the cream, it is possible to distinguish between the oxide pattern and the base cream. It appears that the cream does not change upon mixing with the oxide but the spectrum of MgO coincides with the cream spectrum. On the other hand, calcium oxide and zinc oxide give clearly distinctive peaks at different angles than the cream, as is shown in Fig. 8. The stability of the oxide in the base cream was studied further using XRD spectrum analysis after exposure to the atmosphere. Specifically, the XRD spectra of calcium oxide embedded in the

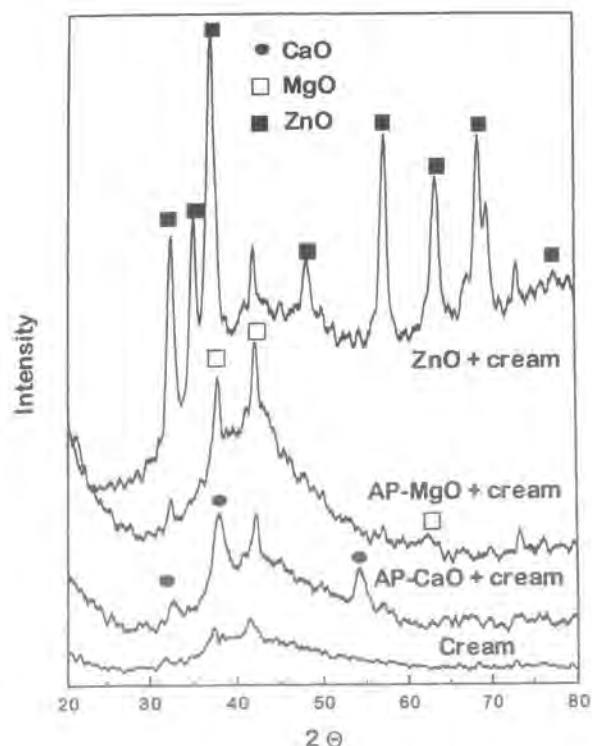


Figure 8. X-ray diffraction spectra of a skin cream system composed of metal oxides embedded in the base cream.

adsorbance during this effort. The following represents the major findings.

Identification of suitable nanoscale reactive adsorbent materials

The best formulations appear to be AP-MgO, [Fe₂O₃] AP-CaO and CP-CaO. At this time AP-MgO alone or in combination with a different metal oxide coating appears to be the most suitable reactive adsorbent for the topical skin cream application. However, substantial work is still needed to understand the products of the reaction, to custom design the most reactive adsorbent and to improve incrementally the reaction kinetics, especially to improve performance with HD.

Based on the preliminary paraoxon and 2-CEES decomposition studies, iron oxide coated CaO, coated and uncoated AP-MgO and high-surface-area ZnO provide significant promise for a reactive adsorbent in the skin protectant application. The Fe₂O₃ coating provides enhanced reaction, possibly due to a catalytic effect and/or due to the prevention of hydroxylation of the oxide powders.

As discussed previously, the enhancing effect of the outer metal oxide coating (the shell material of these core/shell nanoparticles) could be due to a catalytic effect where the outer oxide shuttles fragments of the mimic into the core oxide, where it is consumed. This catalytic effect has been demonstrated clearly in high-temperature (400–500°C) destructive adsorption work, but now appears to be viable possibly at room temperature as well. Further work to delineate the true function of the shell oxide (catalytic shuttle or protectant against hydrolysis or some other subtle effect) will be carried out in the future.

Autoclave-prepared MgO samples showed remarkable performance. These particles are the highest surface area samples tested, with a surface area of >500 m² g⁻¹. For the paraoxon studies, the AP-MgO nearly instantaneously destructively adsorbed all of the paraoxon before the first reading at 2 min after exposure. For the 2-CEES studies, it appears that the oxide reached a rapid equilibrium in <5 min where much of the 2-CEES was destroyed, but the ethylvinyl sulfide was also adsorbed on the particle surface. This result shows the need to develop additional tests suited for the case where rapid adsorption of both the starting material and products of reaction occurs. In addition, the solid samples of reacted AP-MgO were studied and significant evidence of reaction or destructive adsorption of the paraoxon was observed.

Comparison of nanoscale reactive particles with activated carbon

Although evidence of actual destruction of the mimic compound was observed for many of Nantek's custom

reactive adsorbents, we were able to confirm that destructive adsorption does not take place using activated carbon, a well-known highly adsorbent material. Activated carbon seems to adsorb quickly both paraoxon and 2-CEES; however, no evidence of decomposition of the mimic compounds was observed. An unexpected outcome of the research was that activated carbon actually has a lower adsorption capacity than Nantek's AP-MgO material on an equivalent gram basis. When 0.1 g of each adsorbent was used, only 4.5 µl of paraoxon was completely adsorbed on the activated carbon surface whereas the AP-MgO adsorbed/destroyed 20 µl of paraoxon.

Decomposition of the military nerve agents VX and HD

Nantek's AP-MgO showed exceptional results for the destruction of VX, with complete decomposition for both 4 µl and 20 µl loadings. In addition, no VX was extracted from the used AP-MgO sample using CH₂Cl₂ as an extraction solvent. Nantek's [Fe₂O₃]AP-CaO reactant also completely adsorbed 4 µl of VX; however, when 20 µl was used, ca. 60% of the VX remained after 6 h. The HD experiments indicated that some of the HD is adsorbed upon contact with the nanoscale reactants, but not all of it. Autoclave-prepared MgO behaved the best, destroying ca. 50% of the agent.

Chemical compatibility of the adsorbents with the base cream

Several nanoscale metal oxide samples, including magnesium, calcium and zinc, demonstrated compatibility upon mixing with the base cream provided by the Army. Furthermore, no significant changes in the cream were observed using XRD analysis upon prolonged exposure to atmospheric conditions.

Decomposition of mimics upon exposure to the prototype skin cream systems

In the preliminary tests, AP-MgO appears to remain reactive upon mixing with the base cream for both paraoxon and 2-CEES exposure. Owing to the barrier nature of the base cream, the reaction occurred at a slower rate than observed when the reactants were exposed directly to the mimic compounds.

Acknowledgements

We thank Donna R. Nichols of the Midwest Research Institute for carrying out experiments with VX and HD, and the Department of the Army, US Army Medical Research and Materiel Command for financial support.

Permeation of Chemical Agents

Final Report

For Nantek, Inc.

MRI Project No. 310086

August 2, 2000

Permeation of Chemical Agents

Final Report

**For Nantek, Inc.
1500 Hayes Drive
Manhattan, Kansas 66502**

MRI Project No. 310086

August 2, 2000

Preface

This report covers work performed to determine the resistance of Topical Skin Protectant formulations containing nanoparticles to permeation by chemical agents GD and HD. The work was performed for Nantek Inc. as MRI project 310086 in the Chemical Sciences Division of Midwest Research Institute.

This report is organized as follows:

Section 1—Summary

Section 2—Testing

Section 3—Test Results

Section 4—Discussion

Appendix—Mass Spectra and Library Searches

Raw data are in the appendix.

MIDWEST RESEARCH INSTITUTE

Donna R. Nichols
Senior Chemist

Approved:

Thomas M. Sack, Ph.D.
Director
Chemical Sciences Division

Contents

Preface	ii
Figures	iv
Tables	iv
 Section 1. Summary	 1
 Section 2. Testing	 6
2.1 Sample Preparation	6
2.2 Agent Challenges	8
 Section 3. Results and Discussion	 13
3.1 GD Test Results	13
3.2 HD Test Results	14
 Section 4. Discussion	 18

Appendix—Mass Spectra and Library Searches

Figures

Figure 1.	7
Figure 2. Permeation Cell Set-up.....	9
Figure 3. Photograph of GD Test Cells Showing the Transparent Areas.....	13

Tables

Table 1. GD Static Liquid Challenge of TSP: Permeation Results	3
Table 2. GD Static Liquid Challenge of TSP: Permeation Results	5
Table 3. Test Matrix.....	6
Table 4. Volumes of Proprietary Oil Added to the TSP Formulations.....	8
Table 5. Comparison of Extraction Efficiency of Hexane and Isopropyl Alcohol (IPA)	10
Table 6. GC/MS Analysis Conditions for Thermally Desorbed Blanks.....	11
Table 7. GC/MS Analysis Conditions for Liquid Standards and Isopropyl Alcohol Extracts of the GD Test Samples	11
Table 8. GC/MSD Analysis Parameters for HD Standards and Example Extracts.....	12
Table 9. GD Static Liquid Challenge of TSP: Permeation Results	15
Table 10. HD Static Vapor Challenge of TSP: Permeation Results.....	17

Section 1. Summary

This report presents results of proof-of-principle testing of Topical Skin Protectant (TSP) nanoparticle formulations for resistance to penetration by chemical agents GD and HD. A static liquid challenge/vapor permeation test was used for GD testing and a static vapor challenge/vapor permeation test was used for HD testing.

TSP formulations were applied at a known thickness on nitrocellulose filter supports sized for the permeation cells. Static liquid GD challenge involved direct application of neat GD to the TSP preparations. The tops of the cells were sealed to contain the agent. A stream of dry nitrogen swept the underside of the test assembly and collected volatile permeated components onto individual sorbent tubes. The static vapor HD challenge involved suspending a HD-saturated pad above each TSP preparation. The tops of the cells were sealed to contain the agent and volatile permeated components were collected on individual sorbent tubes.

At the end of the collection period, the sorbent tubes were disassembled and the sorbent packs separated and extracted. The extracts were analyzed by full scan GC/MS for permeated agent. Retention time and specific ion plots were used to identify permeated agent. Quantitation of agent was by comparison of the response of GD or HD found in the samples with a calibration curve. Mass spectra were collected of GD, HD, and non-agent components. The number varied with the samples. Non-agent components were not identified. The mass spectra of unknown permeated components are in the appendix of this report.

Both GD and HD permeated all of the TSP formulations. Results are in Tables 1 and 2.

Unforeseen technical and safety issues resulted in changes and additions to the scope of work after the March 2, 2000 proposal was signed. The changes were instated with concurrence of the Nantek project manager.

Overall, the TSP formulation retained the majority of GD. The 2.0% APMgO formulation produced the lowest breakthrough (0.76%). This was for a single sample however. The duplicate was lost due to a very large liquid GD breakthrough. The highest GD breakthrough was 2.2% (average of duplicates) from the 2.0% TiO₂ formulation.

The TSP formulations performed less efficiently with HD vapor. The TSP without nanoparticles (single sample) exposed to the HD vapor experienced a 1.48% breakthrough. The lowest breakthrough experienced by the TSP containing nanoparticles was 1.44% for the 5.0% TiO₂ formulation. The highest HD breakthrough, 4.8%, was

experienced by the 5.0% APMgO. This formulation also produced the highest GD breakthrough.

Except for the TSP sample without nanoparticles and the 2.0% APMgO GD test, breakthrough percentages given are averages of duplicate analyses.

Table 1. GD Static Liquid Challenge of TSP: Permeation Results

Duplicates of each TSP were prepared and tested. GD-1 and GD-2 are the two isomers detected by the analysis method. Agent weight is based on literature density of 1.02 g/mL. Permeation is based on a 2.5-inch (6.35-cm) diameter test swatch.

Sample name	Agent spiked	Amount spiked (µL—mg)	Spiking notebook no.	Analysis notebook no.	Analysis file name	Appearance after 20 hr	GD found (mg)	Permeation (µg/cm ²)	Percent breakthrough
Nitrocellulose filter blank	—	—	5983-5-1	5983-5-1	06200004 ¹	no change	0.00	0.00	0.00%
TSP Blank	—	—	5983-5-2	5983-5-2	06200005 ²	no change	0.00	0.00	0.00%
2.0 %APMgO GD 1	GD	94-96	5983-5-4	5983-12-4	06280004	"cracked," transparent filter	0.64	20.11	0.66%
2.0% APMgO GD 2	GD		5983-5-4	5983-12-4	06280004	"cracked," transparent filter	0.73	22.97	0.76%
Duplicate Lost Due to Safety Hazard									
5.0% APMgO GD 1	GD	94-96	5983-5-5	5983-12-5	06280005	"cracked," transparent filter	1.15	36.27	1.20%
5.0% APMgO GD 1	GD	94-96	5983-5-6	5983-12-6	06280006	"cracked"	1.41	44.59	1.47%
					Average		1.28	40.43	1.33%
5.0% APMgO GD 2	GD	94-96	5983-5-5	5983-12-5	06280005	"cracked," transparent filter	1.43	45.14	1.49%
5.0% APMgO GD 2	GD	94-96	5983-5-6	5983-12-6	06280006	"cracked"	2.03	64.04	2.11%
					Average		1.73	54.59	1.80%
2.0% APCaO GD 1	GD	94-96	5983-6-1	5983-12-7	06280007	"cracked," transparent filter, small holes	1.15	36.21	1.19%
2.0% APCaO GD 1	GD	94-96	5983-6-2	5983-12-8	06280008	"cracked," transparent filter, small holes	1.02	32.32	1.07%
					Average		1.08	34.27	1.13%
2.0% APCaO GD 2	GD	94-96	5983-6-1	5983-12-7	06280007	"cracked," transparent filter, small hole	1.25	39.49	1.30%
2.0% APCaO GD 2	GD	94-96	5983-6-2	5983-12-8	06280008	"cracked," transparent filter, small hole	1.24	39.19	1.29%
					Average		1.25	39.34	1.30%
5.0% TiO ₂ GD 1	GD	94-96	5983-6-3	5983-13-1	06280009	"cracked," transparent filter	1.84	58.02	1.91%
5.0% TiO ₂ GD 1	GD	94-96	5983-6-4	5983-13-2	06280010	"cracked," transparent filter	2.09	65.92	2.17%
					Average		1.96	61.97	2.04%

Table 1. GD Static Liquid Challenge of TSP: Permeation Results (Continued)

Sample name	Agent spiked	Amount spiked (μL —mg)	Spiking notebook no.	Analysis notebook no.	Analysis file name	Appearance after 20 hr	GD found (mg)	Permeation ($\mu\text{g}/\text{cm}^2$)	Percent breakthrough
Nitrocellulose filter blank	—	—	5983-5-1	5983-5-1	06200004	no change	0.00	0.00	0.00%
5.0% TiO_2 GD 2	GD	94-96	5983-6-3	5983-13-1	06280009	"cracked," transparent filter	2.01	63.49	2.09%
5.0% TiO_2 GD 2	GD	94-96	5983-6-4	5983-13-2	06280010	"cracked," transparent filter	2.25	71.20	2.35%
						Average	2.13	67.35	2.22%
2.0% ZnO GD 1	GD	94-96	5983-6-5	5983-13-3	06280011	"cracked," transparent filter	1.18	37.30	1.23%
2.0% ZnO GD 1	GD	94-96	5983-6-6	5983-13-4	06280012	"cracked," transparent filter	2.16	68.29	2.25%
						Average	1.67	52.80	1.74%
2.0% ZnO GD 2	GD	94-96	5983-6-5	5983-13-3	06280011	"cracked," transparent filter	1.16	36.51	1.20%
2.0% ZnO GD 2	GD	94-96	5983-6-6	5983-13-4	06280012	"cracked," transparent filter	1.95	61.67	2.03%
						Average	1.55	49.09	1.62%

Table 2. HD Static Liquid Challenge of TSP; Permeation Results

Agent weight is based on literature density of 1.27 g/mL. Permeation is based on a 2.5-inch (6.35-cm) diameter test swatch.

Sample name	Agent spiked	Amount spiked (μL—mg)	Spiking notebook no.	Analysis notebook no.	Analysis file name	Appearance after 20 hr	HD found (mg)	Permeation μg/cm ²	Percent breakthrough
Nitrocellulose filter blank	-	-	5983-17-1	5983-20-3	07100009	no change	0.00	0.00	0.00%
TSP Blank	HD	76-97	5983-17-2	5983-20-4	07100010	no change	1.43	45.20	1.48%
2.0 %APMgO HD 1	HD	76-97	5983-17-3	5983-20-5	07100011	no change	3.16	99.88	3.26%
2.0% APMgO HD 2	HD	76-97	5983-17-4	5983-20-6	07100012	no change	3.51	110.94	3.62%
5.0% APMgO HD 1	HD	76-97	5983-17-5	5983-20-7	07100013	no change	4.66	147.15	4.80%
5.0% APMgO HD 2	HD	76-97	5983-17-6	5983-20-8	07100014	no change	3.71	117.26	3.83%
2.0% APCaO HD 1	HD	76-97	5983-18-1	5983-20-9	07100015	no change	3.50	110.57	3.61%
2.0% APCaO HD 2	HD	76-97	5983-18-2	5983-20-10	07100016	no change	1.87	58.93	1.92%
5.0% TiO ₂ HD 1	HD	76-97	5983-18-3	5983-21-1	07100017	no change	1.39	43.99	1.44%
5.0% TiO ₂ HD 2	HD	76-97	5983-18-4	5983-21-2	07100018	no change	3.48	110.03	3.59%
2.0% ZnO HD 1	HD	76-97	5983-18-5	5983-21-3	07100020	no change	3.24	102.25	3.34%
2.0% ZnO HD 2	HD	76-97	5983-18-6	5983-21-4	07100021	no change	3.00	94.78	3.09%

Section 2. Testing

The test matrix consisted of five Topical Skin Protectant (TSP) formulations containing nanoparticles, one without nanoparticles, two chemical agents, and a nitrocellulose blank. Table 3 shows the test matrix.

Table 3. Test Matrix

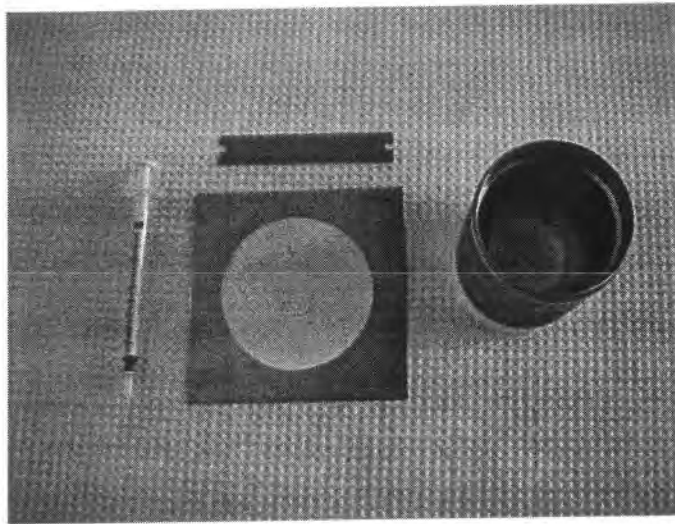
Test substance	GD—volume Static liquid challenge	HD—volume Static vapor challenge	Replicates
Cellulose nitrate filter blank	0	0	1
TSP Cream	0	76 μ L	1
2.0% AP-MgO in TSP	94 μ L	76 μ L	2
5.0% AP-MgO in TSP	94 μ L	76 μ L	2
2.0% AP-CaO in TSP	94 μ L	76 μ L	2
5.0% TiO ₂ in TSP	94 μ L	76 μ L	2
2.0% ZnO in TSP	94 μ L	76 μ L	2

2.1 Sample Preparation

Cellulose nitrate membrane filters (Whatman catalog number 7184 009) were used as a support for the TSP formulations. Custom-made brass templates (0.15 mm thick) were used to apply the TSP to the filters. A fresh template was used for each application to avoid cross-contamination of TSP types. To prepare the samples for testing, a fresh brass template was centered on a clean filter. The TSP was loaded into a disposable 1-mL syringe (Beckton Dickinson part number 309602). A bead of TSP was applied to the filter and spread across the filter surface using a microtome blade (Electron Microscopy Sciences part no. 63062-01).

Once the TSP was spread, a custom made punch was used to cut the TSP-coated filters to the correct size for insertion into the cell. A bead of the TSP used to coat the filter was applied to the cell bottom ledge to serve as a gasket. The filter was transferred to the cell bottom and the edges pressed into the TSP gasket. The cell was sealed until needed for agent challenge.

Figure 1 shows the items used to prepare the samples as well as a filter positioned in the cell bottom.



Left syringe, top microtome blade, right punch, center, brass template positioned on a cellulose nitrate filter.



Cell bottom with sample in place.

Figure 1.

The upper photograph shows components used to prepare the samples. The lower photograph shows a sample positioned in the bottom chamber of a permeation test cell.

The TSP formulations containing nanoparticles thickened over time even when sealed in containers. Thickening of the TSP resulted in reduced spreadability. This was solved by adding increments of the proprietary oil. A second and in some cases a third aliquot of oil was added. The oil was added using a disposable glass pipette. Approximately 150 drops from the pipettes equaled approximately one milliliter. The TSP base formulation, with no added nanoparticles, did not thicken with time. The amounts of oil added to the various formulations to bring them to a spreadable consistency are given in Table 4.

Table 4. Volumes of Proprietary Oil Added to the TSP Formulations

TSP	I.D.	No. Drops added	Comments
TSP Blank	LH2-52 (6/5/00)	20	
2% APMgO	LH2-52 (6/5/00)	100	Granular
5% APMgO	LH2-52 (6/5/00)	150	Granular
2% APCaO	LH2-52 (6/5/00)	50	Granular
5% TiO	LH2-52 (6/5/00)	10	Lumpy
5% ZnO	LH2-52 (6/5/00)	25	Lumpy

The increased surface area coupled with the quick-drying feature of the TSP formulations caused difficulties in obtaining an evenly spread testing surface. The apparent light- and air-sensitivity of the nanoparticles together with the extremely high surface area of the nanoparticles is thought to have caused the thickening. The TSP formulations also contained granules and aggregates in varying sizes. Neither Nantek nor MRI personnel were able to break up the aggregates with the mixing tools used to add the oil. These granules further complicated spreading of the TSP by generating uneven surfaces. The granules caused streaking in the TSP coating. These streaks resulted in uneven coating thicknesses.

2.2 Agent Challenges

The TSP formulations were challenged with two agents. GD challenges were by a “static liquid challenge/vapor permeation” method. HD challenges were by a “static vapor challenge/vapor permeation” method.

2.2.1 GD Testing

2.2.1.1 Challenge

The prepared TSP surfaces were contaminated with 94 microliters of neat GD by application in a drop-wise manner from a syringe. This represents a contamination density of 3 milligrams of GD per centimeter squared surface area. A liquid contamination density of 3 milligrams per centimeter squared is commonly used for testing the resistance of protective clothing to permeation by toxic chemical agents.

Samples were prepared and contaminated in duplicate. In addition, there were two uncontaminated cellulose nitrate filter blanks—one with and one without TSP base cream.

Immediately after contamination, samples were sealed in the cells and connected to the sampling train. The top half of the permeation cells were plugged with corks to contain agent liquid and vapors in a static state in the upper chamber. The lower half of the cell (normally the skin side) was continuously sampled by a stream of dry pre-purified nitrogen pulled through a Chromosorb 106 sorbent tube by a vacuum pump. Each cell was sampled for 20 hours with the total 20-hour permeated GD sample collected on an individual sorbent tube.

Figure 2 is a photograph of a permeation cell tower with six individual permeation cells in

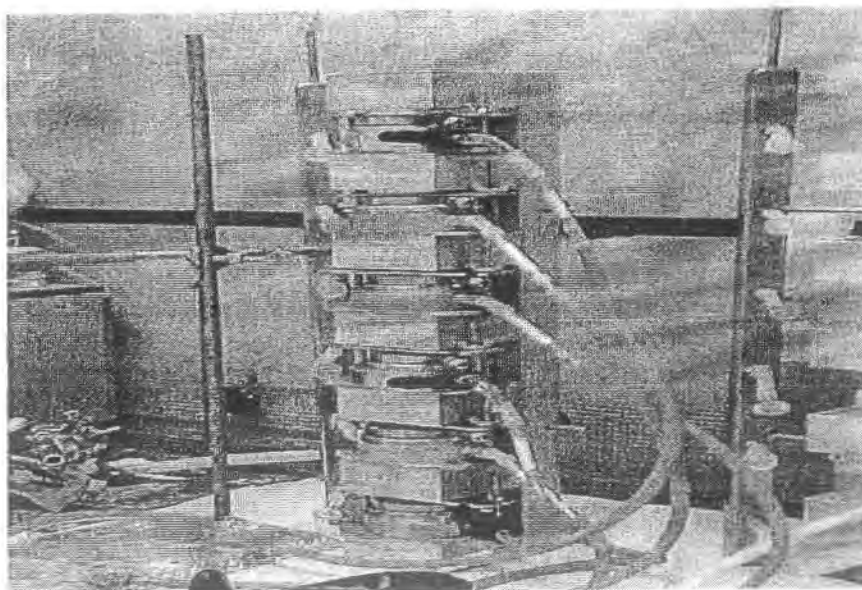


Figure 2. Permeation Cell Set-up

2.2.1.2 Extraction and Analysis

At the end of the 20-hour sampling period, the individual sorbent tubes were retrieved from the sampling train. The original plan was to thermally desorb the 8-mm sample tubes onto 3-mm tubes and analyze the 3-mm tubes by thermal desorption full scan GC/MS. The first 8-mm tube desorbed to a clean 3-mm tube presented a serious safety hazard. Although the tubes appeared normal, when the 8-mm tube was thermally desorbed onto the 3-mm tube, liquid GD wetted the sorbent and condensed in droplets on the glass barrels of both tubes. GD was confirmed by a positive M-8 paper contact test.

A solvent extraction approach was recommended to the client. An extraction efficiency study was performed with spiked tubes to compare hexane and isopropyl alcohol extraction. The tubes were dismantled and the sorbent was recovered and extracted with each solvent. Duplicate extractions were performed for each of the two solvents. Based on the data in Table 5 isopropyl alcohol was chosen as the extraction solvent.

Table 5. Comparison of Extraction Efficiency of Hexane and Isopropyl Alcohol (IPA)

Solvent	GD Spiked (µg)	GD Found (µg)	% Recovery	Average	RPD
Hexane	502	179	35.7	31.2	7.2
Hexane	502	134	26.7		
IPA	502	370	73.7	83.6	5.9
IPA	502	469	93.4		

2.2.2 GD Analysis

Vapor samples collected from the underside of the cellulose nitrate and TSP blank samples were analyzed by thermal desorption GC/MS. A 3-point calibration curve was analyzed by spiking aliquots of GD standard solutions and analyzing them by thermal desorption full scan GC/MS. The method detected both GD isomers. A response factor calculation was used for quantitation of permeated GD. Neither of the blanks produced peaks with a response above the low calibration standard in the GD window. Table 6 gives the analysis conditions for the blank samples.

Table 6. GC/MS Analysis Conditions for Thermally Desorbed Blanks

Parameter or component	Description or value
GC/MS System	HP5890 Series II GC interfaced with a HP 5971A MSD
Injection port	220°C
Initial GC temperature	40°C
Initial hold	4 min
Ramp	15 deg/min
Final temp	275°C
Final hold	1 min
Split/splitless injection	On at 1 minute
Injection volume	not applicable for thermal desorption
Solvent delay	3 min
Scan range	35 to 500
Quantitation Ion	<i>m/z</i> 126

Because of safety concerns, the remainder of the samples were solvent extracted with isopropyl alcohol and analyzed by direct liquid injection. For the remainder of the samples, a relative response factor (RRF) was calculated for three injections of a 50.2 ng GD standard. GD concentrations in the samples were calculated based on the standards RRF. Table 7 gives the analysis conditions for the extracts.

Table 7. GC/MS Analysis Conditions for Liquid Standards and Isopropyl Alcohol Extracts of the GD Test Samples

Parameter or component	Description or value
GC/MS System	HP5890 Series II GC interfaced with a HP 5971A MSD
Injection port	220°C
Initial GC temperature	40°C
Initial hold	4 min
Ramp	15 deg/min
Final temp	275 C
Final hold	2 min
Split/splitless injection	On at 1 minute
Injection volume	1 µL
Solvent delay	3 min
Scan range	35 to 500
Quantitation Ion	<i>m/z</i> 126

Both GD isomers were quantitated by the RRF method, then averaged. The average concentrations are reported.

2.2.3 HD Testing

2.2.3.1 Challenge

A static vapor challenge/vapor permeation test was performed on the TSP formulations. TSP samples for the HD test were prepared on cellulose nitrate membrane filter supports in the same way as those prepared for the GD test. Filter paper saturated with 76 microliters of neat HD was inserted into a slot in the upper chamber of each permeation cell as described in Table. When the cells were sealed, the HD-saturated filter was suspended above the TSP surface without touching it. The sealed cells were installed into the towers in the sampling train. Nitrogen flowing through the lower chamber collected any permeated vapor. The total flow through the chamber over a 20-hour period was captured on individual Tenax TA sorbent tubes for 20 hours.

The surface cracking and transparency that occurred with the liquid GD tests was not observed with the HD tests.

2.2.3.2 Extraction and Analysis

At the end of the 20-hour sampling period, the individual sorbent tubes were retrieved from the sampling train. The tubes were dismantled, the sorbent recovered and extracted with isopropyl alcohol. An extraction efficiency study was not performed for the HD samples.

A four-point calibration curve (range 20-100 ng injected) was analyzed. The R^2 for this curve was 1.00. Extracts were analyzed by GC/MSD using the conditions in Table 8.

Table 8. GC/MSD Analysis Parameters for HD Standards and Example Extracts

Parameter or component	Description or value
GC/MS System	HP5890 Series II GC interfaced with a HP 5971A MSD
Injection port	220°C
Initial GC temperature	40°C
Initial hold	4 min
Ramp	15 deg/min
Final temp	275°C
Final hold	2 min
Split/splitless injection	On at 1 minute
Injection volume	not applicable for thermal desorption
Solvent delay	3 min
Scan range	35 to 500
Quantitation ion	<i>m/z</i> 109

Section 3. Results and Discussion

3.1 GD Test Results

3.1.1 GD Data

GD was found in all of the breakthrough samples. Permeation ranged from a low of 23 micrograms per centimeter square to a high of 71 micrograms per centimeter squared. Table 9 presents the GD test data.

When the GD test cells were opened, all samples were observed to have extensive cracking and crazing across the surface of the TSP. Some (but not all) of the areas where GD was applied to the TSP had turned transparent during the 20-hour test period. Two of the samples had small holes after testing that were not present prior to testing (see Table 1 and Table 9).

A photograph of the post-test appearance of two of the test cells is shown in Figure 3. The camera used did not produce clear close-up photographs, neither did it have the resolution to obtain close-up of the fissures in the TSP surfaces. The single dark spot at the top of the left cell is one of the transparent areas. In the right-hand cell, there are two transparent spots that are not as definitive in the photograph as the one on the cell on the left. Although crazing was extensive on the TSP surface, cracks were not visible on the underside (the cellulose nitrate filter support). However, micro-cracks not visible to the eye may have been present.



Figure 3. Photograph of GD Test Cells Showing the Transparent Areas

3.2 HD Test Results

3.2.1 HD Data

HD was found in all of the samples. Permeation ranged from a low of 44 micrograms per centimeter square to a high of 147 micrograms per centimeter squared. Table 10 presents the HD test data.

Table 9. GD Static Liquid Challenge of TSP: Permeation Results

Duplicates of each TSP were prepared and tested. GD-1 and GD-2 are the two isomers detected by the analysis method. Agent weight is based on literature density of 1.02 g/mL. Permeation is based on a 2.5-inch (6.35-cm) diameter test swatch.

Sample name	Agent spiked	Amount Spiked (µL—mg)	Spiking Notebook #	Analysis Notebook #	Analysis File name	Appearance after 20 hr	GD found (mg)	Permeation(µg/cm ²)	Percent Breakthrough
Nitrocellulose filter blank	—	—	5983-5-1	5983-5-1	06200004 ¹	no change	0.00	0.00	0.00%
TSP Blank	—	—	5983-5-2	5983-5-2	06200005 ²	no change	0.00	0.00	0.00%
2.0 %APMgO GD 1	GD	94-96	5983-5-4	5983-12-4	06280004	"cracked," transparent filter	0.64	20.11	0.66%
2.0% APMgO GD 2	GD		5983-5-4	5983-12-4	06280004	"cracked," transparent filter	0.73	22.97	0.76%
Duplicate Lost Due to Safety Hazard									
5.0% APMgO GD 1	GD	94-96	5983-5-5	5983-12-5	06280005	"cracked," transparent filter	1.15	36.27	1.20%
5.0% APMgO GD 1	GD	94-96	5983-5-6	5983-12-6	06280006	"cracked"	1.41	44.59	1.47%
						Average	1.28	40.43	1.33%
5.0% APMgO GD 2	GD	94-96	5983-5-5	5983-12-5	06280005	"cracked," transparent filter	1.43	45.14	1.49%
5.0% APMgO GD 2	GD	94-96	5983-5-6	5983-12-6	06280006	"cracked"	2.03	64.04	2.11%
						Average	1.73	54.59	1.80%
2.0% APCaO GD 1	GD	94-96	5983-6-1	5983-12-7	06280007	"cracked," transparent filter, small holes	1.15	36.21	1.19%
2.0% APCaO GD 1	GD	94-96	5983-6-2	5983-12-8	06280008	"cracked," transparent filter, small holes	1.02	32.32	1.07%
						Average	1.08	34.27	1.13%
2.0% APCaO GD 2	GD	94-96	5983-6-1	5983-12-7	06280007	"cracked," transparent filter, small hole	1.25	39.49	1.30%
2.0% APCaO GD 2	GD	94-96	5983-6-2	5983-12-8	06280008	"cracked," transparent filter, small hole	1.24	39.19	1.29%
						Average	1.25	39.34	1.30%
5.0% TiO ₂ GD 1	GD	94-96	5983-6-3	5983-13-1	06280009	"cracked," transparent filter	1.84	58.02	1.91%
5.0% TiO ₂ GD 1	GD	94-96	5983-6-4	5983-13-2	06280010	"cracked," transparent filter	2.09	65.92	2.17%
						Average	1.96	61.97	2.04%

Table 9. GD Static Liquid Challenge of TSP: Permeation Results (Continued)

Sample name	Agent spiked	Amount Spiked (μL—mg)	Spiking Notebook #	Analysis Notebook #	Analysis File name	Appearance after 20 hr	GD found (mg)	Permeation(μg/cm ²)	Percent Breakthrough
5.0% TiO ₂ GD 2	GD	94-96	5983-6-3	5983-13-1	06280009	"cracked," transparent filter	2.01	63.49	2.09%
5.0% TiO ₂ GD 2	GD	94-96	5983-6-4	5983-13-2	06280010	"cracked," transparent filter	2.25	71.20	2.35%
						Average	2.13	67.35	2.22%
2.0% ZnO GD 1	GD	94-96	5983-6-5	5983-13-3	06280011	"cracked," transparent filter	1.18	37.30	1.23%
2.0% ZnO GD 1	GD	94-96	5983-6-6	5983-13-4	06280012	"cracked," transparent filter	2.16	68.29	2.25%
						Average	1.67	52.80	1.74%
2.0% ZnO GD 2	GD	94-96	5983-6-5	5983-13-3	06280011	"cracked," transparent filter	1.16	36.51	1.20%
2.0% ZnO GD 2	GD	94-96	5983-6-6	5983-13-4	06280012	"cracked," transparent filter	1.95	61.67	2.03%
						Average	1.55	49.09	1.62%

1 Error with MS, excessive signal, shut down after solvent delay.

2 Analyzed by SORBENT tube, remaining samples liquid extraction.

3 Sample was desorbed onto 3-mm sorbent tube and disposed of for safety reasons, 8-mm tube was still analyzed by liquid extraction but not reported due to loss of sample in the "desorb" step.

Table 10. HD Static Vapor Challenge of TSP: Permeation Results

Agent weight is based on literature density of 1.27 g/mL. Permeation is based on a 2.5-inch (6.35-cm) diameter test swatch.

Sample name	Agent spiked	Amount Spiked (μL—mg)	Spiking notebook no.	Analysis notebook no.	Analysis file name	Appearance after 20 hr	HD found (mg)	Permeation μg/cm ²	Percent breakthrough
Nitrocellulose filler blank	—	—	5983-17-1	5983-20-3	07100009	no change	0.00	0.00	0.00%
TSP Blank	HD	76-97	5983-17-2	5983-20-4	07100010	no change	1.43	45.20	1.48%
2.0 %APMgO HD 1	HD	76-97	5983-17-3	5983-20-5	07100011	no change	3.16	99.88	3.26%
2.0% APMgO HD 2	HD	76-97	5983-17-4	5983-20-6	07100012	no change	3.51	110.94	3.62%
5.0% APMgO HD 1	HD	76-97	5983-17-5	5983-20-7	07100013	no change	4.66	147.15	4.80%
5.0% APMgO HD 2	HD	76-97	5983-17-6	5983-20-8	07100014	no change	3.71	117.26	3.83%
2.0% APCaO HD 1	HD	76-97	5983-18-1	5983-20-9	07100015	no change	3.50	110.57	3.61%
2.0% APCaO HD 2	HD	76-97	5983-18-2	5983-20-10	07100016	no change	1.87	58.93	1.92%
5.0% TiO ₂ HD 1	HD	76-97	5983-18-3	5983-21-1	07100017	no change	1.39	43.99	1.44%
5.0% TiO ₂ HD 2	HD	76-97	5983-18-4	5983-21-2	07100018	no change	3.48	110.03	3.59%
2.0% ZnO HD 1	HD	76-97	5983-18-5	5983-21-3	07100020	no change	3.24	102.25	3.34%
2.0% ZnO HD 2	HD	76-97	5983-18-6	5983-21-4	07100021	no change	3.00	94.78	3.09%

Section 4. Discussion

Safety and technical difficulties were encountered during sample preparation and initial GD exposure. Most of the difficulties are related to the scale-up in the test area from 7/16-inch diameter (0.15 in^2) to 2.5-inch diameter (4.9 in^2)—a 33-fold increase in surface area. The agent loading per unit area for the larger test surfaces is about 30% of that for the smaller surface area. However, the total amount of agent is about 10 times that used for the smaller surface area. The technical and safety problems are discussed below.

All of the TSP formulations thickened over time resulting in schedule delays until an additional supply of the proprietary oil arrived. A second and in some cases a third aliquot of oil had to be added. The TSP base formulation, with no added nanoparticles, does not thicken with time. The increased surface area coupled with the quick-drying feature of the TSP formulations generated difficulties in obtaining an evenly spread testing surface. An apparent sensitivity of the nanoparticles to light and air exposure is thought to have contributed to the thickening.

Aggregates of the nanoparticles in the TSP contributed to uneven spreading. Neither Nantek nor MRI personnel were able to break up the aggregates with the mixing tools used to add the oil. The particles may have contributed to the breakthrough because they may have prevented a vapor-tight seal from forming between the upper and lower chambers of the cell. These granules further complicated spreading of the TSP by generating uneven surfaces. The granules caused streaking in the TSP coating. These streaks resulted in uneven coating thicknesses.

On completion of the GD exposure, the TSP surfaces containing nanoparticles exhibited numerous cracks and fissures. Some areas where agent had been applied were transparent. The nitrocellulose filter was intact, but the filter/TSP layers had been rendered transparent. Agent decomposition reactions using standard decontamination solutions are highly exothermic. Whether or not the reaction of the agents with the nanoparticles is exothermic is unknown. However, the appearance of the test layers after 20-hours would suggest an exothermic reaction. Heat from the reaction may have contributed to the surface fracturing of the TSP formulations. As the fissures formed in the TSP coatings, it is likely that micro fissures not detectable by visual inspection were formed in the nitrocellulose support as well. Two of the samples had small holes at the completion of testing that were not present at the start of the test. This would result in large breakthrough of the GD that resulted in condensation of neat agent within the sorbent collection tubes.

Breakthrough of large amounts of GD vapor condensed in the first of the sorbent tubes resulting in a positive M-8 response for liquid G-agent. The oil, a TSP formulation, and water were applied to the M-8 paper but none of these produced a positive response. The remaining tubes therefore were unsafe to desorb to 3-mm tubes for analyses by

thermal desorption GC/MS. Solvent extraction of the sorbent to recover was discussed with the client and performed by mutual agreement.

Overall, the TSP formulations retained the majority of GD. The 2.0% APMgO formulation produced the lowest breakthrough (0.76%). This was for a single sample however. The duplicate was lost due to a very large liquid GD breakthrough. the highest GD breakthrough was 2.2% (average of duplicates) from the 5.0% TiO₂ (GD-2) formulation.

The TSP formulations performed less efficiently with HD vapor. The TSP without nanoparticles (single sample) exposed to the HD vapor experienced a 1.48% breakthrough. The lowest breakthrough experienced by the TSP containing nanoparticles was 1.44% for the 5.0% TiO₂ formulation. The highest HD breakthrough, 4.8%, was experienced by the 5.0% APMgO. This formulation also produced the highest GD breakthrough.

Appendix

Mass Spectra and Library Searches

GD Tests: Mass Spectra and Library Searches for Non-Agent Components Detected

HD Tests: Mass Spectra and Library Searches for Non-Agent Components Detected

Sample name	Agent spiked	Amount spiked (μL—mg)	Spiking notebook no.	Analysis notebook no.	Analysis file name	Appearance after 20 hr	HD found (mg)	Permeation (μg/cm ²)	Percent breakthrough
Nitrocellulose filter blank	—	—	5983-17-1	5983-20-3	07100009	no change	0.00	0.00	0.00%

Sample name	Agent spiked	Amount spiked (μL—mg)	Spiking notebook no.	Analysis notebook no.	Analysis file name	Appearance after 20 hr	HD found (mg)	Permeation (μg/cm ²)	Percent breakthrough
TSP Blank	HD	76-97	5983-17-2	5983-20-4	07100010	no change	1.43	45.20	1.48%

Sample name	Agent spiked	Amount spiked (μL—mg)	Spiking notebook no.	Analysis notebook no.	Analysis file name	Appearance after 20 hr	HD found (mg)	Permeation (μg/cm ²)	Percent breakthrough
2.0 %APMgO HD 1	HD	76-97	5983-17-3	5983-20-5	07100011	no change	3.16	99.88	3.26%
2.0% APMgO HD 2	HD	76-97	5983-17-4	5983-20-6	07100012	no change	3.51	110.94	3.62%

Sample name	Agent spiked	Amount spiked (μL—mg)	Spiking notebook no.	Analysis notebook no.	Analysis file name	Appearance after 20 hr	HD found (mg)	Permeation (μg/cm ²)	Percent breakthrough
5.0% APMgO HD 1	HD	76-97	5983-17-5	5983-20-7	07100013	no change	4.66	147.15	4.80%
5.0% APMgO HD 2	HD	76-97	5983-17-6	5983-20-8	07100014	no change	3.71	117.26	3.83%

Sample name	Agent spiked	Amount spiked (µL—mg)	Spiking notebook no.	Analysis notebook no.	Analysis file name	Appearance after 20 hr	HD found (mg)	Permeation (µg/cm ²)	Percent breakthrough
2.0% APCaO HD 1	HD	76-97	5983-18-1	5983-20-9	07100015	no change	3.50	110.57	3.61%
2.0% APCaO HD 2	HD	76-97	5983-18-2	5983-20-10	07100016	no change	1.87	58.93	1.92%

Sample name	Agent spiked	Amount spiked (μL—mg)	Spiking notebook no.	Analysis notebook no.	Analysis file name	Appearance after 20 hr	HD found (mg)	Permeation (μg/cm ²)	Percent breakthrough
5.0% TiO ₂ HD 1	HD	76-97	5983-18-3	5983-21-1	07100017	no change	1.39	43.99	1.44%
5.0% TiO ₂ HD 2	HD	76-97	5983-18-4	5983-21-2	07100018	no change	3.48	110.03	3.59%

Sample name	Agent spiked	Amount spiked (μL—mg)	Spiking notebook no.	Analysis notebook no.	Analysis file name	Appearance after 20 hr	HD found (mg)	Permeation (μg/cm ²)	Percent breakthrough
2.0% ZnO HD 1	HD	76-97	5983-18-5	5983-21-3	07100020	no change	3.24	102.25	3.34%
2.0% ZnO HD 2	HD	76-97	5983-18-6	5983-21-4	07100021	no change	3.00	94.78	3.09%

Sample name	Agent spiked	Amount spiked (μL—mg)	Spiking notebook no.	Analysis notebook no.	Analysis file name	Appearance after 20 hr	HD found (mg)	Permeation (μg/cm ²)	Percent breakthrough
Nitrocellulose filter blank	—	—	5983-5-1	5983-5-1	06200004	no change	0.00	0.00	0.00%

Sample name	Agent spiked	Amount spiked (μL—mg)	Spiking notebook no.	Analysis notebook no.	Analysis file name	Appearance after 20 hr	HD found (mg)	Permeation (μg/cm ²)	Percent breakthrough
TSP Blank	-	-	5983-5-2	5983-5-2	06200005 ²	no change	0.00	0.00	0.00%

Sample name	Agent spiked	Amount spiked (μL—mg)	Spiking notebook no.	Analysis notebook no.	Analysis file name	Appearance after 20 hr	HD found (mg)	Permeation (μg/cm ²)	Percent breakthrough
2.0 %APMgO GD 1	GD	94-96	5983-5-4	5983-12-4	06280004	"cracked," transparent filter	0.64	20.11	0.66%
2.0% APMgO GD 2	GD		5983-5-4	5983-12-4	06280004	"cracked," transparent filter	0.73	22.97	0.76%
Duplicate Lost Due to Safety Hazard									

Sample name	Agent spiked	Amount spiked (µL—mg)	Spiking notebook no.	Analysis notebook no.	Analysis file name	Appearance after 20 hr	HD found (mg)	Permeation (µg/cm ²)	Percent breakthrough
5.0% APMgO GD 1	GD	94-96	5983-5-5	5983-12-5	06280005	"cracked," transparent filter	1.15	36.27	1.20%
5.0% APMgO GD 1	GD	94-96	5983-5-8	5983-12-6	06280006	"cracked"	1.41	44.59	1.47%
						Average	1.28	40.43	1.33%
5.0% APMgO GD 2	GD	94-96	5983-5-5	5983-12-5	06280005	"cracked," transparent filter	1.43	45.14	1.49%
5.0% APMgO GD 2	GD	94-96	5983-5-6	5983-12-6	06280006	"cracked"	2.03	64.04	2.11%
						Average	1.73	54.59	1.80%

Sample name	Agent spiked	Amount spiked (µL—mg)	Spiking notebook no.	Analysis notebook no.	Analysis file name	Appearance after 20 hr	HD found (mg)	Permeation (µg/cm ²)	Percent breakthrough
2.0% APCaO GD 1	GD	94-96	5983-6-1	5983-12-7	06280007	"cracked," transparent filter, small holes	1.15	36.21	1.19%
2.0% APCaO GD 1	GD	94-96	5983-6-2	5983-12-8	06280008	"cracked," transparent filter, small holes	1.02	32.32	1.07%
						Average	1.08	34.27	1.13%
2.0% APCaO GD 2	GD	94-96	5983-6-1	5983-12-7	06280007	"cracked," transparent filter, small hole	1.25	39.49	1.30%
2.0% APCaO GD 2	GD	94-96	5983-6-2	5983-12-8	06280008	"cracked," transparent filter, small hole	1.24	39.19	1.29%
						Average	1.25	39.34	1.30%

Sample name	Agent spiked	Amount spiked (µL—mg)	Spiking notebook no.	Analysis notebook no.	Analysis file name	Appearance after 20 hr	HD found (mg)	Permeation (µg/cm ²)	Percent breakthrough
5.0% TiO ₂ GD 1	GD	94-96	5983-6-3	5983-13-1	06280009	"cracked," transparent filter	1.84	58.02	1.91%
5.0% TiO ₂ GD 1	GD	94-96	5983-6-4	5983-13-2	06280010	"cracked," transparent filter	2.09	65.92	2.17%
						Average	1.96	61.97	2.04%
5.0% TiO ₂ GD 2	GD	94-96	5983-6-3	5983-13-1	06280009	"cracked," transparent filter	2.01	63.49	2.09%
5.0% TiO ₂ GD 2	GD	94-96	5983-6-4	5983-13-2	06280010	"cracked," transparent filter	2.25	71.20	2.35%
						Average	2.13	67.35	2.22%

Sample name	Agent spiked	Amount spiked (µL—mg)	Spiking notebook no.	Analysis notebook no.	Analysis file name	Appearance after 20 hr	HD found (mg)	Permeation (µg/cm ²)	Percent breakthrough
2.0% ZnO GD 1	GD	94-96	5983-6-5	5983-13-3	06280011	"cracked," transparent filter	1.18	37.30	1.23%
2.0% ZnO GD 1	GD	94-96	5983-6-6	5983-13-4	06280012	"cracked," transparent filter	2.16	68.29	2.25%
						Average	1.67	52.80	1.74%
2.0% ZnO GD 2	GD	94-96	5983-6-5	5983-13-3	06280011	"cracked," transparent filter	1.16	36.51	1.20%
2.0% ZnO GD 2	GD	94-96	5983-6-6	5983-13-4	06280012	"cracked," transparent filter	1.95	61.67	2.03%
						Average	1.55	49.09	1.62%

4. Error with MS, excessive signal, shut down after solvent delay.

SBIR final report from Nantek, Inc, Phase II

Award Number: DAMD17-99-C-9012

AD _____

Award Number: DAMD17-99-C-9012

TITLE: Catalytic Topical Skin Cream Protectants Based on
Nanoparticles and Polyoxometalates

PRINCIPAL INVESTIGATOR: Kenneth J. Klabunde, Ph.D.

CONTRACTING ORGANIZATION: NanoScale Materials, Incorporated
Manhattan, Kansas 66502

REPORT DATE: January 2003

TYPE OF REPORT: Final, Phase II

PREPARED FOR: U.S. Army Medical Research and Materiel Command
Fort Detrick, Maryland 21702-5012

DISTRIBUTION STATEMENT: Distribution authorized to U.S.
Government agencies only (specific authority). Other requests
for this document shall be referred to U.S. Army Medical
Research and Materiel Command, 504 Scott Street, Fort Detrick,
Maryland 21702-5012.

The views, opinions and/or findings contained in this report are
those of the author(s) and should not be construed as an official
Department of the Army position, policy or decision unless so
designated by other documentation.

NOTICE

USING GOVERNMENT DRAWINGS, SPECIFICATIONS, OR OTHER DATA INCLUDED IN THIS DOCUMENT FOR ANY PURPOSE OTHER THAN GOVERNMENT PROCUREMENT DOES NOT IN ANY WAY OBLIGATE THE US GOVERNMENT. THE FACT THAT THE GOVERNMENT FORMULATED OR SUPPLIED THE DRAWINGS, SPECIFICATIONS, OR OTHER DATA DOES NOT LICENSE THE HOLDER OR ANY OTHER PERSON OR CORPORATION; OR CONVEY ANY RIGHTS OR PERMISSION TO MANUFACTURE, USE, OR SELL ANY PATENTED INVENTION THAT MAY RELATE TO THEM.

SBIR DATA RIGHTS LEGEND

Contract: DAMD17-99-C-9012

Contractor: NanoScale Materials, Incorporated

For a period of five (5) years after completion of the project from which the data was generated, the Government's rights to use, modify, reproduce, release, perform, display, or disclose any technical data or computer software contained in this report are restricted as provided in paragraph (b)(4) of the Rights in Noncommercial Technical Data and Computer Software Small Business Innovative Research (SBIR) Program clause contained in the above-identified contract [DFARS 252.227-7018(Jun. 1995)]. No restrictions apply after expiration of that period. Any reproduction of technical data, computer software, or portions thereof marked as SBIR data must also reproduce those markings and this legend.

This technical report has been reviewed and is accepted under the provisions of the Small Business Innovation Research Program.

This report is published in the interest of scientific and technical information exchange and does not constitute approval or disapproval of its ideas or findings.

Do not return copies of this report unless contractual obligations or notice on a specific document requires its return.

REPORT DOCUMENTATION PAGEForm Approved
OMB No. 074-0188

Public reporting burden for this collection of information is estimated to average 1 hour per response, including the time for reviewing instructions, searching existing data sources, gathering and maintaining the data needed, and completing and reviewing this collection of information. Send comments regarding this burden estimate or any other aspect of this collection of information, including suggestions for reducing this burden to Washington Headquarters Services, Directorate for Information Operations and Reports, 1215 Jefferson Davis Highway, Suite 1204, Arlington, VA 22202-4302, and to the Office of Management and Budget, Paperwork Reduction Project (0704-0188), Washington, DC 20503

1. AGENCY USE ONLY (Leave blank)		2. REPORT DATE January 2003	3. REPORT TYPE AND DATES COVERED Final, Phase II (13 Dec 99 - 12 Dec 02)	
4. TITLE AND SUBTITLE Catalytic Topical Skin Cream Protectants Based on Nanoparticles and Polyoxometalates			5. FUNDING NUMBERS DAMD17-99-C-9012	
6. AUTHOR(S) Kenneth J. Klabunde, Ph.D.				
7. PERFORMING ORGANIZATION NAME(S) AND ADDRESS(ES) NanoScale Materials, Incorporated Manhattan, Kansas 66502 Email: kenj@nanmatinc.com			8. PERFORMING ORGANIZATION REPORT NUMBER	
9. SPONSORING / MONITORING AGENCY NAME(S) AND ADDRESS(ES) U.S. Army Medical Research and Materiel Command Fort Detrick, Maryland 21702-5012			10. SPONSORING / MONITORING AGENCY REPORT NUMBER	
11. SUPPLEMENTARY NOTES				
12a. DISTRIBUTION / AVAILABILITY STATEMENT Distribution authorized to U.S. Government agencies only (specific authority). Other requests for this document shall be referred to U.S. Army Medical Research and Materiel Command, 504 Scott Street, Fort Detrick, Maryland 21702-5012.				12b. DISTRIBUTION CODE
13. ABSTRACT (Maximum 200 words) The over-all goal of the research was to develop a reactive topical skin protectant (rTSP) for detoxification of multiple chemical warfare agents. During Phase II of this research, several formulations of reactive nanoparticles and nanoparticles-transition metal compounds hybrids were identified to be effective reagents for detoxification of mustard gas and nerve agents as well as their simulants. Effective detoxification continued to occur even after incorporation into TSP. Research was also done to understand formulation and stability aspects of rTSP. Detailed reactivity testing of various rTSP formulations using laboratory Miniature Automated Continuous Air Monitoring System (MINICAMS) was carried out and several promising formulations were identified. In Phase II extension study, new nanoparticles and nanoparticles based hybrids (salts or POMs) were prepared and investigated for their effectiveness using GC/MS and MINICAMS techniques. Several rTSP formulations performed better than base TSP. Especially, one formulation based on TiO ₂ reactive nanoparticles reduced the permeation of mustard simulant by 99% and of GD simulant by 80% relative to the TSP.				
14. SUBJECT TERMS chemical detoxification, topical skin protectant, reactive nanoparticles, polyoxometalates, catalytic demilitarization				15. NUMBER OF PAGES 114
				16. PRICE CODE
17. SECURITY CLASSIFICATION OF REPORT Unclassified	18. SECURITY CLASSIFICATION OF THIS PAGE Unclassified	19. SECURITY CLASSIFICATION OF ABSTRACT Unclassified	20. LIMITATION OF ABSTRACT Unlimited	

FOREWORD

Opinions, interpretation, conclusions and recommendations are those of the author and are not necessarily endorsed by the U.S. Army.

- (X) Where copyrighted material is quoted, permission has been obtained to use such material.
- (X) Where material from documents designated for limited distribution is quoted, permission has been obtained to use the material.
- (X) Citations of commercial organizations and trade names in this report do not constitute an official Department of the Army endorsement or approval of the products or services of these organizations.
- () In conducting research using animals, the investigator(s) have adhered to policies of applicable Federal Law 32 CFR 219 and 45 CFR 46.
- () In conduction research utilizing recombinant DNA technology, the investigator(s) adhered to current guidelines promulgated by the National Institutes of Health.

Kenneth J. Klebanski
Principal Investigator's Signature

Jan. 10, 2003
Date

Table of Contents

Cover.....	
SF 298.....	2
Foreword.....	3
Table of Contents.....	4
Introduction.....	5
Body.....	6
Key Research Accomplishments.....	106
Reportable Outcomes.....	108
Conclusions.....	109
References.....	111
Personnel Receiving Pay.....	113
Appendices.....	n/a

Introduction

Currently, the U.S. Army has a topical skin protectant (TSP) that is designed to provide an additional protective barrier to chemical warfare (CW) agents when used underneath Battle Dress Uniforms. While this TSP is a useful addition to the protection of soldiers under CW conditions, the protective ability of the TSP can be greatly enhanced by adding detoxifying agents. While many different additives have been proposed, the major problem is that they are only capable of detoxifying a single type of CW agent. In other words, a particular additive may be quite efficient at destroying mustard gas but is incapable of detoxifying sarin.

Five key requirements for an adsorbent/cream protectant system were considered during the development of the optimal system. These requirements were:

- 1) The active ingredient must be a non-toxic powder that can be blended and remain suspended within the cream.
- 2) It must destroy CW agents at acceptable rates under ambient temperature and humidity conditions.
- 3) It must be compatible with the base cream thereby retaining its reactivity and stability with the cream system.
- 4) It must have limited potential for irritation due to its close contact with human skin.
- 5) It must have a long shelf life.

Research conducted by NanoScale Materials and Emory University under a Phase I contract proved that the combination of polyoxometalates (POM) and reactive nanoparticles (RNPs) can provide protection against a multitude of chemical warfare agents. The project identified key species of POMs that are effective for the oxidation of a mustard gas simulant 2-chloroethyl-ethyl sulfide (CEES). When supporting the POMs on RNPs, the reactivity of these nanoparticles towards nerve agents is retained. Together, these results demonstrated that there is a synergy between POM and RNP technologies. Based upon these initial results, Phase II of this project has focused on

- 1) Identifying new highly catalytic RNPs and POMs (and combinations thereof).
- 2) Optimizing current catalytic POM and RNP formulations.
- 3) Incorporating these optimized POM/RNP formulations into currently available topical skin protectant (TSP) creams.
- 4) Testing the protective properties of the TSP/RNP/POM systems.

Project Results

A great number of advances in RNP technology were accomplished during the Phase II project. All of these enhanced the development of a POM/RNP hybrid for the U.S. Army that is capable of detoxifying multiple types of CW agents. Many additional POM species and transition metal compounds were identified to be excellent oxidizing agents of CEES. Since POMs alone have little if any reactivity towards nerve agents, combining them with reactive nanoparticles produces the desired protection against multiple threats. Also, it was shown that even when large amounts of these coatings were deposited on the RNP supports, excellent reactivity toward nerve agents was retained.

During the project, the mass production of nanoparticles has been accomplished. Significant increases in the reactivity of several nanoparticles (especially TiO_2), due to larger surface area, were obtained during the course of scale-up. The reduction of manufacturing costs has also been achieved.

A permeation cell apparatus (MINICAMS Series 3000) was obtained to examine the decomposition of CW simulants by POM/RNP formulations contained in TSP. This instrument is a continuous air monitoring system using gas chromatography to detect CW agents and simulants. This apparatus is identical to the unit used at U.S. Army Medical Research Institute of Chemical Defense (USAMRICD) at the Aberdeen Proving Grounds.

The problem encountered in Phase I of incorporating nanoparticles into the TSP to obtain a cream similar in consistency and texture as the base TSP was solved. This allowed for very reproducible results with the MINICAMS permeation testing. Also, aging studies were completed showing reactivity of the active ingredients in the POM/RNP/TSP creams does not decrease over time.

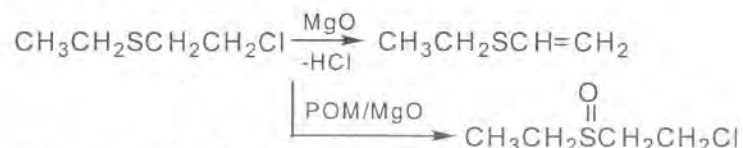
NanoScale Materials has participated in collaboration with researchers at USAMRICD to test the capability of POM/RNP/TSP combinations with real CW agents VX, GD, and HD. The result of these tests were extremely promising.

Task 1. Development of the optimal [POM]RNP formulation for the detoxification of HD, VX, and GD simulants.

The objective of Task 1 was to identify additional [POM]RNP formulations that can catalytically decompose CW agent simulants. (The brackets around POM indicate it is used as a coating on the reactive nanoparticles.) Data from Task 1 was used to select the most promising [POM]RNP formulations and utilize them in the topical skin protectant cream.

During the project, two main tests were used to compare the reactivity of the [POM]RNP samples towards decomposition of CW simulants. The simulants used in Task 1 were diethyl 4-nitrophenyl phosphate (paraoxon) and 2-chloroethyl ethyl sulfide (CEES). Paraoxon was used as a simulant of VX agent and the CEES as a simulant of mustard gas. Additional simulants of G-agents and a sulfur containing simulant of VX are discussed in detail in the Task 8 section. The general parameters for each of these reactivity tests are given below.

The decomposition chemistry of CEES differs between the stand-alone components of the POM/RNPs. In the case of reactive nanoparticles such as magnesium oxide, the decomposition of CEES involves the de-chlorination of the molecule to form ethyl vinyl sulfide ($\text{CH}_3\text{CH}_2\text{SCH}=\text{CH}_2$). In experiments with stand alone RNPs, we monitor the growth of the vinyl peak at circa 1585 cm^{-1} in the infrared spectrum to analyze the decomposition of the CEES. In the case of POMs, the deactivation of CEES occurs through oxidation to form chloroethyl ethyl sulfoxide ($\text{CH}_3\text{CH}_2\text{S}(=\text{O})\text{CH}_2\text{CH}_2\text{Cl}$ or CEESO).



In these experiments spectra were obtained on a Nicolet (Madison, WI) Protégé 460 FT-IR spectrophotometer. [POM]RNP powder (0.1 g) was added to the reaction flask of a special gas phase infrared cell that has been developed for these experiments. The cell was evacuated and transferred to the FT-IR and a background spectrum acquired. Next, 14 μL of neat CEES was carefully dropped onto the sample through a side-port of the cell. The vapor phase of the sample was then monitored as a function of time for up to five hours. In additional experiments, the cell was purged with air after preparation in order to perform the experiment under true ambient conditions.

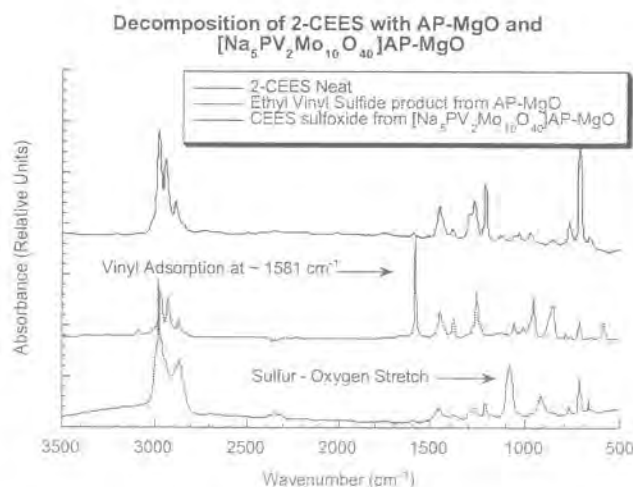


Figure 1. IR Spectra of the Reaction Products Of $[\text{Na}_5\text{PV}_2\text{Mo}_{10}\text{O}_{40}]\text{APMgO}$ and CEES.

The Government's rights to use, modify, reproduce, release, perform, display, or disclose technical data or computer software marked with this legend are restricted during the period shown on the cover page as provided in paragraph (b)(4) of the Rights in Noncommercial Technical Data and Computer Software--Small Business Innovative Research (SBIR) Program clause contained in the contract DAMD17-99-C-9012 with NanoScale Materials, Inc. (Formerly Nantek, Inc.). No restrictions apply after the expiration date (12 January 2007). Any reproduction of technical data, computer software, or portions thereof marked with this legend must also reproduce the markings.

Paraoxon Destructive Adsorption

Phase I research showed that the destructive adsorption of paraoxon over POM/RNP composites occurs through the chemistry of the RNP. Characterization of the reaction suggested that the major decomposition products are surface adsorbed p-nitrophenolate anion ($[\text{NO}_2\text{-C}_6\text{H}_4\text{-O}]^-$) and surface adsorbed diethyl phosphonate. These products are formed through the cleavage of the phosphorus – oxygen bond of the paraoxon molecule. Analysis of destructive adsorption of paraoxon is performed using UV-Vis spectrophotometry. Spectra were obtained on a Varian Cary 100 Bio UV-Vis spectrophotometer. In a typical experiment, neat paraoxon (9 μL) was added to a stirred round-bottom flask containing 200 mL pentane. The baseline spectrum was acquired by passing the pentane/paraoxon solution through a flow-through cuvette, and recording the spectrum. Once the baseline was obtained, the [POM]RNP sample (0.2 g) were added to the flask and spectra were collected at one-minute intervals for 10 minutes and then at 5-minute intervals for one hour. The adsorption of paraoxon onto the sample was assessed by the loss of the characteristic paraoxon absorption peak (267 nm) and formation of the yellow 4-nitrophenol product. Figure 2 compares paraoxon adsorption rates for uncoated and coated RNP samples and activated carbon.

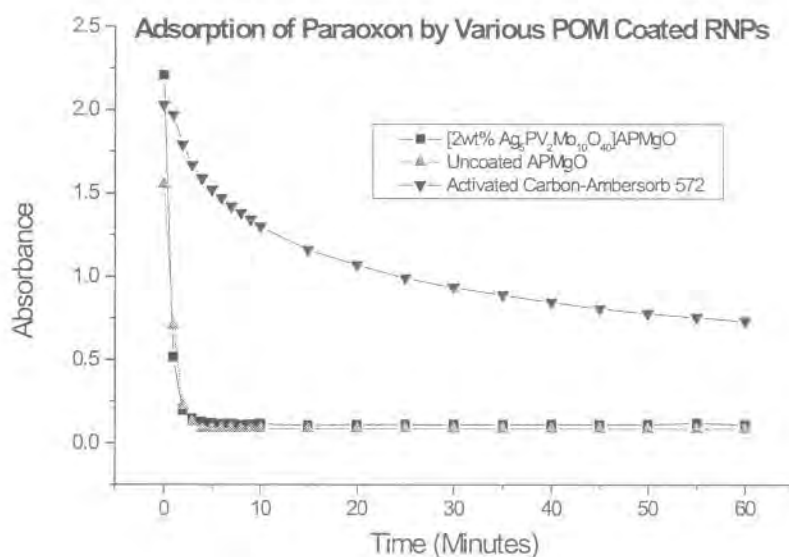


Figure 2. Adsorption of Paraoxon by Coated and Uncoated MgO Nanoparticles.

Phase II research has identified another POM/RNP formulation that performs as well, if not better than, the two most promising combinations identified in Phase I (namely $[\text{Na}_5\text{PV}_2\text{Mo}_{10}\text{O}_{40}]\text{APMgO}$ and $[\text{Ag}_5\text{PV}_2\text{Mo}_{10}\text{O}_{40}]\text{APMgO}$). The new formulation utilizes a high surface area titanium dioxide (TiO_2) nanoparticles as a support for the POM. Investigation initially involved the sodium salt POM supported on TiO_2 , which is designated as $[\text{Na}_5\text{PV}_2\text{Mo}_{10}\text{O}_{40}]\text{TiO}_2$. The mixed POM/RNP had a pale orange color that indicates the retention of the 5+ oxidation state of the vanadium heteroatom within the POM cage structure after deposition. Reduction of V(V) to V(IV) typically changes the color of the samples to dark

green, blue, or black which is often seen in “heteropoly blues”. Research with 2%, 5% and 10% wt/wt loadings of the POM onto the surface of TiO_2 indicates that relatively large amounts of the Na-POM can be deposited without significant effect on the nanoparticle support and its ability to chemically react with other simulants.

As in the case of the [POM]APMgO samples studied in Phase I, the oxidation chemistry involving the POM dominates in the $[\text{Na}_5\text{PV}_2\text{Mo}_{10}\text{O}_{40}]\text{TiO}_2$ system. The formation of CEESO occurs very rapidly, with no CEES peaks remaining in the vapor phase after five minutes reaction. Figure 3 shows CEESO in the vapor phase for the sample [10wt% $\text{Na}_5\text{PV}_2\text{Mo}_{10}\text{O}_{40}]\text{TiO}_2$ after five minutes reaction time and neat CEESO for comparison.

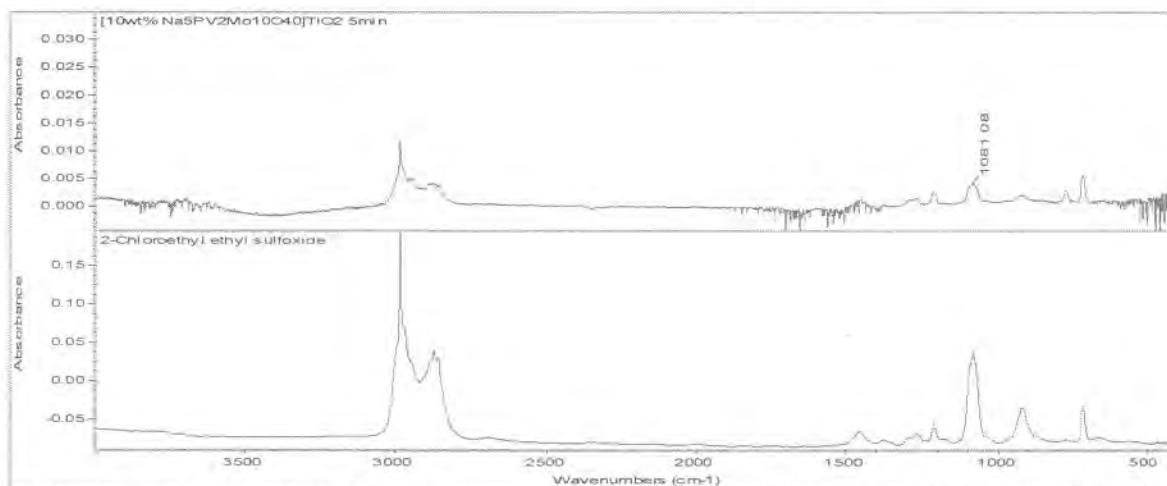
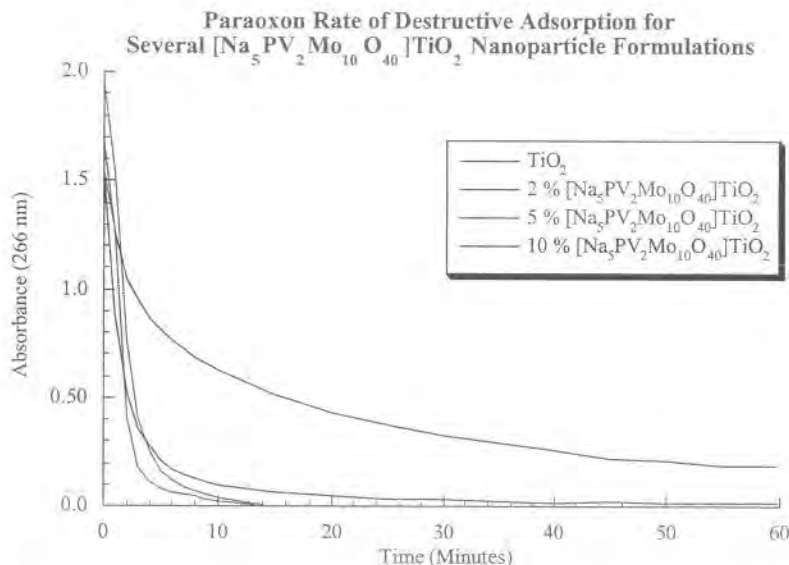


Figure 3. CEESO in the Vapor Phase After Reaction of [10wt% $\text{Na}_5\text{PV}_2\text{Mo}_{10}\text{O}_{40}]\text{TiO}_2$

While the paraoxon/MgO chemistry proceeded quite well for the $[\text{Na}_5\text{PV}_2\text{Mo}_{10}\text{O}_{40}]\text{APMgO}$ and $[\text{Ag}_5\text{PV}_2\text{Mo}_{10}\text{O}_{40}]\text{APMgO}$ samples in Phase I, it was determined that POM loadings higher than 5% started to hinder the access of paraoxon to the reactive sites of the MgO. $[\text{Na}_5\text{PV}_2\text{Mo}_{10}\text{O}_{40}]\text{TiO}_2$ provided a stark contrast to this observation. Research with this POM/RNP system shows that the addition of $\text{Na}_5\text{PV}_2\text{Mo}_{10}\text{O}_{40}$ does not hinder and may even increase the destructive adsorption capacity of the TiO_2 support. Figure 4 compares paraoxon adsorption rates for three different weight percentages of POM coated TiO_2 .



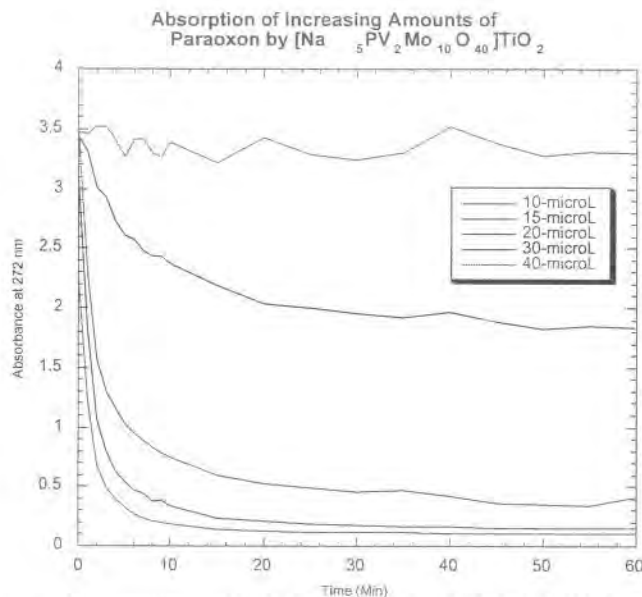
Can't tell which
 is the anisograph ✓

Figure 4: Adsorption of Paraoxon by POM Coated TiO_2 Compared with Uncoated TiO_2 .

Maximum Capacity Tests With Paraoxon

Experiments were then performed to examine the maximum absorption capacity of $[\text{Na}_5\text{PV}_2\text{Mo}_{10}\text{O}_{40}]\text{TiO}_2$ for paraoxon from pentane solution. Normal procedures for paraoxon destructive adsorption experiments utilizing UV-Vis were performed with the following exception. In order to evaluate the maximum amount of paraoxon that can be adsorbed by the POM/RNP nanoparticles, increasing amounts of paraoxon were injected for each 0.2-g sample. The amounts of paraoxon used in these experiments were 10 $\square\text{L}$, 15 $\square\text{L}$, 20 $\square\text{L}$, 30 $\square\text{L}$ and 40 $\square\text{L}$. The scanning kinetics program was utilized and the adsorption of paraoxon monitored for 60 minutes. The sample used was 5-wt% $[\text{Na}_5\text{PV}_2\text{Mo}_{10}\text{O}_{40}]\text{TiO}_2$ with a specific surface area of $378 \text{ m}^2/\text{g}$. The sample had previously been tested with paraoxon under normal experimental parameters (0.2g sample with 9 $\square\text{L}$ paraoxon). The results of these experiments are displayed in Figure 5.

? insert data ✓



could tell which line is which

Figure 5. Maximum Capacity Tests on 5-wt% $[\text{Na}_5\text{PV}_2\text{Mo}_{10}\text{O}_{40}]\text{TiO}_2$

It was shown that 0.2 g of 5wt% $[\text{Na}_5\text{PV}_2\text{Mo}_{10}\text{O}_{40}]\text{TiO}_2$ can effectively destroy upwards of 20 μL of paraoxon. With 30 μL paraoxon or more injected, there is a noticeable amount of un-adsorbed paraoxon even after 60 minutes. The molar ratios for the various amounts of paraoxon with 0.2 g (2.38×10^{-3} mol) 5wt% $[\text{Na}_5\text{PV}_2\text{Mo}_{10}\text{O}_{40}]\text{TiO}_2$ are as follows (1 mole paraoxon: 1 mole [POM]RNP):

- 9 μL (4.2×10^{-5} mol) paraoxon: 1:57
- 10 μL (4.6×10^{-5} mol) paraoxon: 1:52
- 15 μL (6.9×10^{-5} mol) paraoxon: 1:34
- 20 μL (9.2×10^{-5} mol) paraoxon: 1:26

ratio of paraoxon : pom/rnp

missing a

These results are promising since they indicate that the POM/RNP nanoparticles are capable of adsorbing paraoxon in amounts that are approaching that of stoichiometric (assuming surface reactions) for the formulation used. These results were comparable to the best stand-alone nanoparticle formulation identified from Phase I, namely nanocrystalline MgO.

Extraction Of Adsorbed Species After Paraaxon Reactions

The next set of experiments with $[\text{POM}]\text{TiO}_2$ samples determined the best way to extract the products after reaction with paraoxon from the surface of the nanoparticle. This experiment was to verify destruction of the paraoxon was occurring, not just adsorption. By using a standard calibration curve, this test was also used for quantification of the reaction products. Various extraction procedures were performed with a standard solution of p-nitrophenol until 100% recovery was obtained from a control. Distilled water was used as the solvent. To ensure that the substrate did not decompose under the extraction conditions, control experiments with paraoxon were also performed. The sample tested using these established protocols was $[\text{Na}_5\text{PV}_2\text{Mo}_{10}\text{O}_{40}]\text{TiO}_2$. The extract containing reaction products and any residual paraoxon was analyzed via UV-Vis spectroscopy. The product p-nitrophenol was identified as a major

decomposition product, observed at λ 399 nm in the spectrum (Figure 6). Using a calibration curve it was determined that 1.9×10^{-4} M p-nitrophenol was present after extraction compared to 2.1×10^{-4} M paraoxon initially injected in the reaction. This represents a 91% decomposition of paraoxon. It appears from Figure 6 that all the paraoxon was converted to p-nitrophenol upon adsorption on to the TiO_2 as no paraoxon peaks (located at 272 nm) are observed in the spectrum.

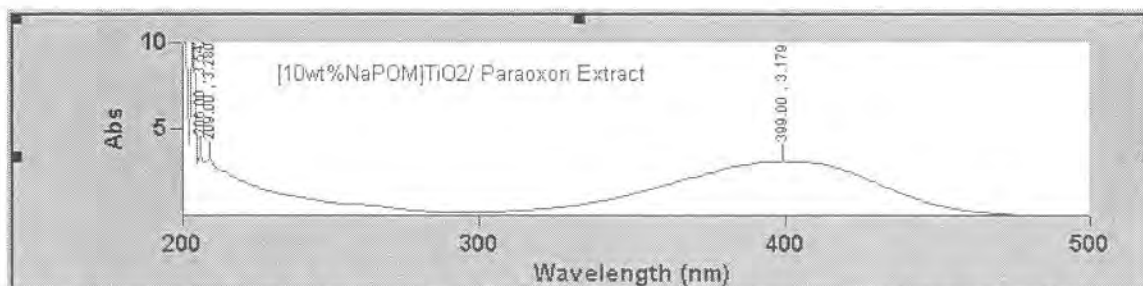


Figure 6. UV-Vis Spectrum of p-Nitrophenol Decomposition Product from Paraoxon Over $[\text{Na}_5\text{PV}_2\text{Mo}_{10}\text{O}_{40}]\text{TiO}_2$.

Structure of Adsorbed Species After Paraoxon Reactions

To verify the structure of the adsorbed species derived from paraoxon on coated and uncoated TiO_2 , solid state ^{31}P NMR experiments were performed and compared with prior NMR data from coated and uncoated AP-MgO. In a typical experiment, the solids after reaction with paraoxon were isolated and dried under vacuum. ^{31}P NMR spectra were obtained using a Tecmag 270 MHz spectrometer equipped with a Doty Scientific 7-mm high speed CP-MAS probe, using direct excitation and high power proton decoupling. The observation frequency for ^{31}P was 109.55 MHz. Samples were packed in a sapphire rotor with kel-F end caps and typically spun at 4700 Hz. Chemical shifts were referenced to external 85% H_3PO_4 (0 ppm).

Table 1 lists the solid state ^{31}P NMR data for several metal oxides and POM-coated metal oxide samples isolated after reaction with paraoxon. Included in this table are also the results of UV-Vis studies of these reactions that show, qualitatively, the extent of adsorption of paraoxon on these oxides.

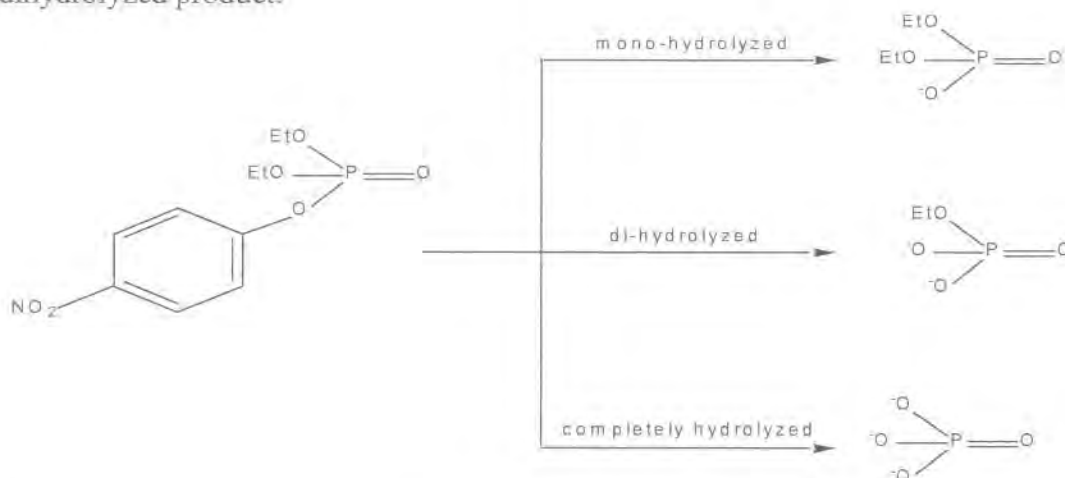
Table 1. ^{31}P NMR and UV Data for Samples Derived From Reaction of Paraoxon With Various Metal Oxides

Compound	^{31}P Chemical Shift (ppm)	Extent of Adsorption as Assessed by UV-Vis Analysis
AP-MgO	-0.85 (narrow)	Complete
$[\text{Na}_5\text{PV}_2\text{Mo}_{10}\text{O}_{40}]\text{APMgO}$	0.63 (broad, major) and -4.13 (narrow, minor)	Complete
TiO_2	-3.83 (broad)	Complete
$[\text{Ag}_5\text{PV}_2\text{Mo}_{10}\text{O}_{40}]\text{TiO}_2$	-3.63 (broad)	Complete

All ^{31}P NMR spectra showed one or two signals covering a wide range of chemical shifts. In addition, 1 or 2 pairs of spinning side bands were also observed in those spectra. Intense spinning sidebands are indicative of surface binding of the product.

For example, the ^{31}P NMR sample derived from reaction of paraoxon with APMgO showed a single, sharp signal centered on δ -0.85 ppm. UV analysis of the liquid phase revealed a near complete reaction on this adsorbent. It should also be noted that paraoxon in CDCl_3 exhibits a single peak around δ -6.50 ppm. Based on this information, and the fact that phosphorus in H_3PO_4 exhibits a signal at 0 ppm, we assigned the signal at -0.85 ppm to PO_4^{3-} , a product derived *via* complete hydrolysis of paraoxon.

The sample derived from $[\text{Na}_5\text{PV}_2\text{Mo}_{10}\text{O}_{40}]\text{APMgO}$ showed a broad and symmetrical major peak at δ 0.63 ppm attributable to PO_4^{3-} , and a narrow, relatively minor peak at δ -4.13 ppm, respectively. The latter peak is likely due to mono or di-hydrolyzed species, which are products derived from incomplete hydrolysis of paraoxon (below). However, the relatively narrow and symmetrical nature of this signal points to the existence of a single species. In view of the fact that the major peak is due to PO_4^{3-} , it appears likely that the other peak must be due to the dihydrolyzed product.



Samples derived from TiO_2 and 2 wt.% $[\text{Ag}_5\text{PV}_2\text{Mo}_{10}\text{O}_{40}]\text{TiO}_2$ exhibited a rather broad, unsymmetrical signal centered around δ -3.83 and -3.63 ppm, respectively. As mentioned above, it appears that this peak is probably due to mono and/or dihydrolyzed products derived from paraoxon. The broad, unsymmetrical nature of this signal indicates the existence of a heterogeneous product mixture (Figure 7).

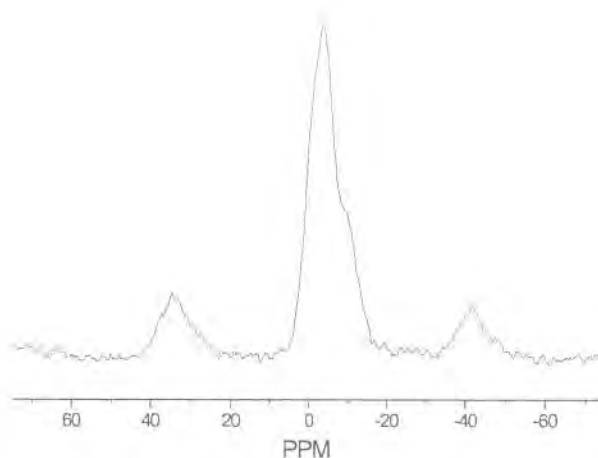


Figure 7. ^{31}P NMR Spectrum of Paraoxon/ $[\text{Ag}_5\text{PV}_2\text{Mo}_{10}\text{O}_{40}]\text{TiO}_2$

Study of Zinc Oxide Nanoparticles Coated with POMs

During the course of the project, a process for scaling up the synthesis of zinc oxide nanoparticles was optimized and kilogram quantities became available. (This research was performed under another project). The new, improved zinc oxide showed increased reactivity due to higher surface areas obtained. These ZnO nanoparticles were used as supports for POM coatings. In such experiments, 5% by weight of $\text{Ag}_5\text{PV}_2\text{Mo}_{10}\text{O}_{40}$ was used as the coating with tetrahydrofuran as a solvent. To study reactivity towards CEES, the typical experimental method on the FT-IR was performed. The vapor phase was monitored for up to five hours.

In the case of uncoated zinc oxide nanoparticles, de-chlorination of the CEES to form ethyl vinyl sulfide occurs as expected. When the zinc oxide nanoparticles are coated with silver POM, we find the oxidation chemistry of the POM dominates as in previous POM/RNP experiments. It appears that the chloroethyl ethyl sulfoxide product is formed in the vapor phase as indicated by the sulfoxide peak seen at circa 1079 cm^{-1} . However, growth of the vinyl peak at 1585 cm^{-1} is observed as well (Figure 8).

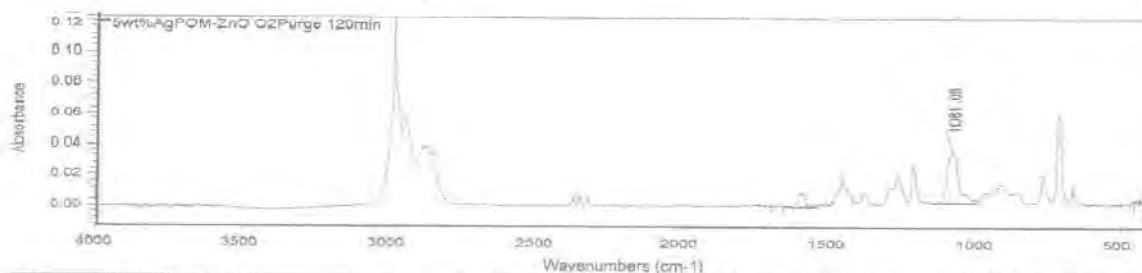


Figure 8. FT-IR Spectrum of 5 wt% $[\text{Ag}_5\text{PV}_2\text{Mo}_{10}\text{O}_{40}]\text{ZnO}$ After Reaction With CEES

The formation of this vinyl (de-chlorination) peak is graphed versus time for both the uncoated zinc oxide and the Ag-POM coated ZnO in Figure 9. This graph shows de-chlorination of CEES occurs in [AgPOM]ZnO as well as uncoated zinc oxide; however at a much slower rate.

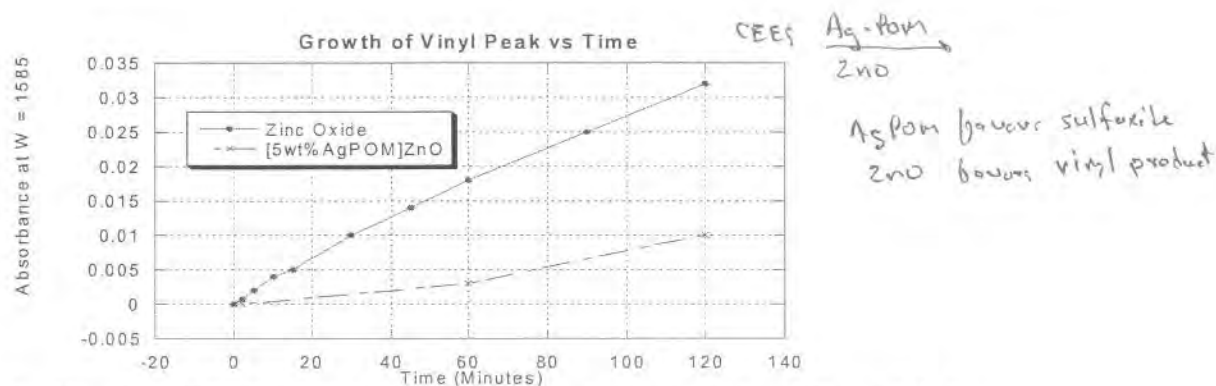


Figure 9: Kinetics of CEES to Ethyl Vinyl Sulfide for Uncoated and Coated ZnO

A kinetics graph of CEES oxidation (Figure 10) shows Ag-POM coated zinc oxide producing the sulfoxide peak indicative of oxidation but no sulfoxide growth over time for the uncoated zinc oxide.

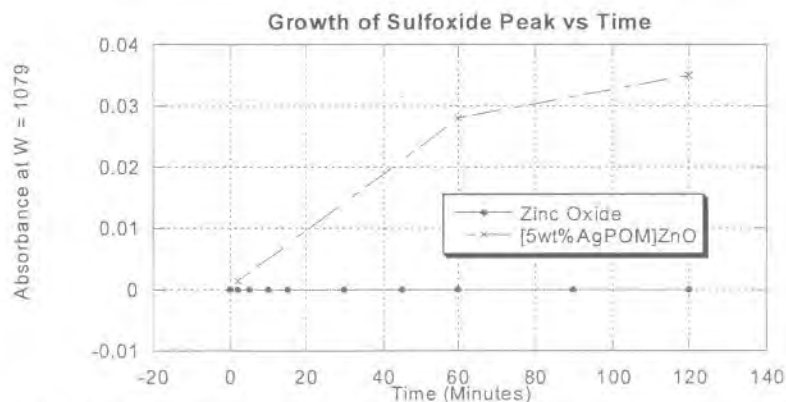


Figure 10: Oxidation of CEES to CEESO versus Time for Uncoated and Coated ZnO.

Figure 11 shows the relative rate of decomposition of paraoxon for the zinc oxide nanoparticles and the silver POM coated zinc oxide. The silver coated POM sample is slightly better at destructively adsorbing the paraoxon than the uncoated sample. This rate of destructive adsorption of paraoxon is typical for zinc oxide nanoparticles.

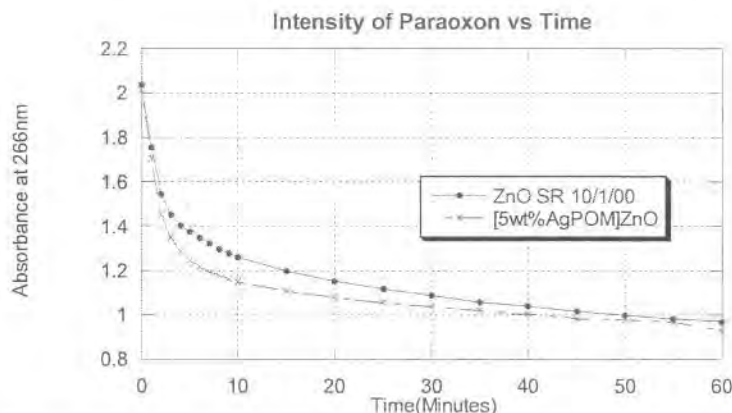


Figure 11. Destructive Adsorption of Paraaxon with Coated and Uncoated ZnO

Transition Metal Compounds Used as Coatings For Nanoparticles

Based on work performed at Emory University, various transition metal compounds including salts have shown great promise as oxidation catalysts of CEES¹. Consequently, samples were prepared using these catalysts as coatings for titanium dioxide and magnesium oxide nanoparticles. In a typical experiment, a 50-mL round bottom flask equipped with a stir bar, was charged with 25 mL tetrahydrofuran. A weighed amount of coating compound equivalent to 2 to 5 mole percent of the nanoparticles was added. The solid was allowed to dissolve completely before the nanoparticles were added. After two hours of stirring, the sample was attached to a vacuum line and the solvent evacuated from the flask. The powder was then placed into a drying oven for one hour at 120 °C.

The metal compounds used in these experiments were cerium nitrate, cerium oxide, copper nitrate, tetrabutylammonium dichloroaurate, cerium acetylacetonate and vanadyl acetylacetonate. The nanoparticles used for coating were AP-MgO (SSA 563 m²/g), and TiO₂ (SSA 200 m²/g). The various combinations were analyzed by typical paraoxon and CEES methods. The following samples were the most promising:

- 1) 5-mol% [VO(acac)₂]AP-MgO; SSA = 358 m²/g
- 2) 2-mol% [VO(acac)₂]TiO₂; SSA = 192 m²/g
- 3) 2-mol% [cerium nitrate]TiO₂; SSA = 176 m²/g
- 4) 2-mol% [cerium oxide]TiO₂; SSA = 173 m²/g
- 5) 2-mol% [copper nitrate]TiO₂; SSA = 173 m²/g

As is apparent from the above list, the best results were obtained when TiO₂ was used as the support. With other nanoparticle supports, there were either compatibility problems, or the coatings did not increase (in some cases prevented) destruction of the agent simulants. The results were encouraging with vanadyl acetylacetonate coated titanium dioxide and magnesium oxide (Samples 1 & 2). The CEES was oxidized to CEESO by 2-mol% [VO(acac)₂]TiO₂ as indicated by the sulfoxide peak at 1084 cm⁻¹ (Figure 12). Figure 13 shows the growth of the

sulfoxide peak versus time for the sample analyzed under vacuum and with an oxygen purge. The results were similar for 5-mol% $[\text{VO}(\text{acac})_2]\text{AP-MgO}$.

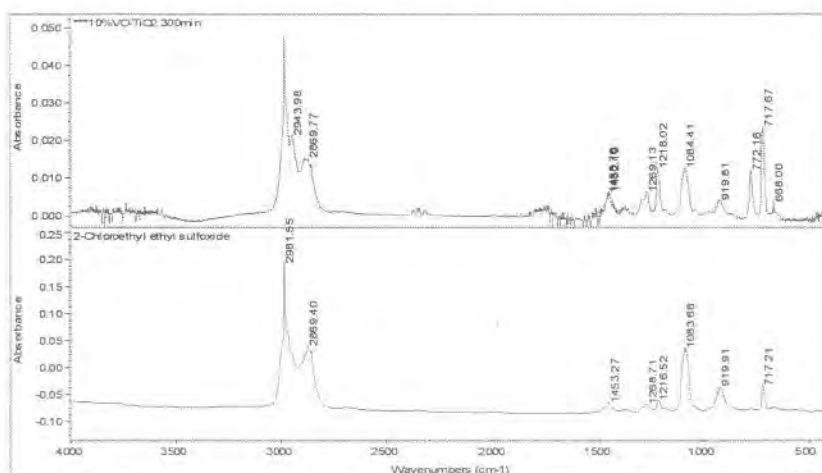


Figure 12. Oxidation of CEES With $[\text{VO}(\text{acac})_3]\text{TiO}_2$ to Form CEESO.

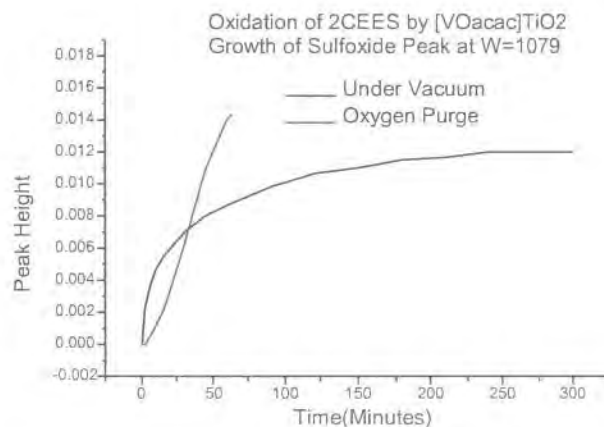


Figure 13. Rate of Oxidation of CEES with $[\text{VO}(\text{acac})_3]\text{TiO}_2$.

All the other samples performed as expected, oxidizing CEES into the product CEESO, over the period of the analysis. Figure 14 shows a typical spectrum of the oxidation of 2-CEES indicated by the growth of the sulfoxide peak at 1079 cm^{-1} . In this case, the sample $[2\text{mol}\% \text{CeNO}_3]\text{TiO}_2$ is shown after 300 minute reaction with 2-CEES. The reference spectrum of CEESO is included for comparison.

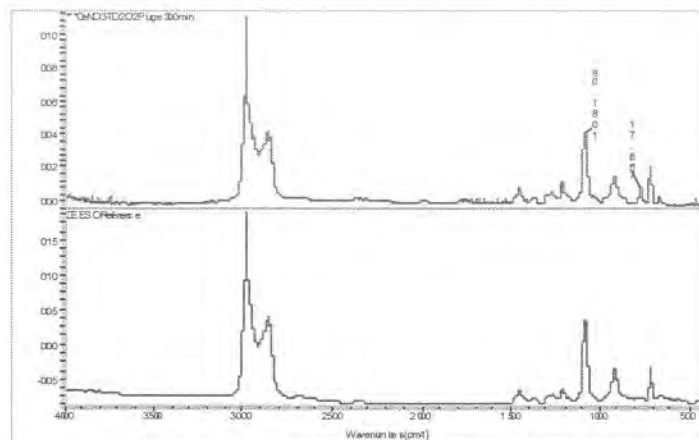


Figure 14. Oxidation of CEES by 2-mol% $[\text{Ce}(\text{NO}_3)_3]/\text{TiO}_2$ (Top) and CEESO Reference Spectrum (Bottom).

The peak at 1079 cm^{-1} (sulfoxide peak) was measured over the five hour reaction period for some of the samples. Figures 15 and 16 show the growth of the sulfoxide peak versus time for the samples both with oxygen purge and while under vacuum. It appears the nitrate compounds coated on TiO_2 are the most efficient at oxidizing 2-CEES under both conditions.

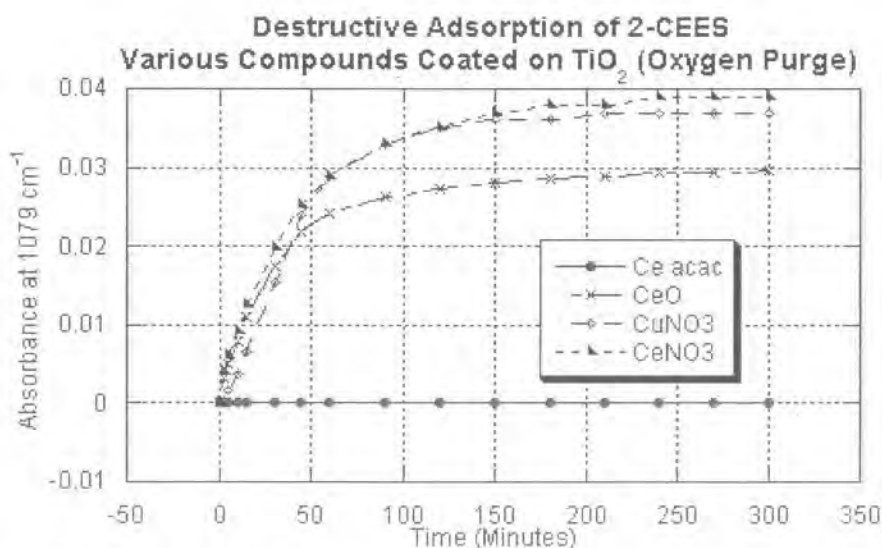


Figure 15. Growth of Sulfoxide Peak versus Time for TiO_2 Samples with Oxygen Purge.

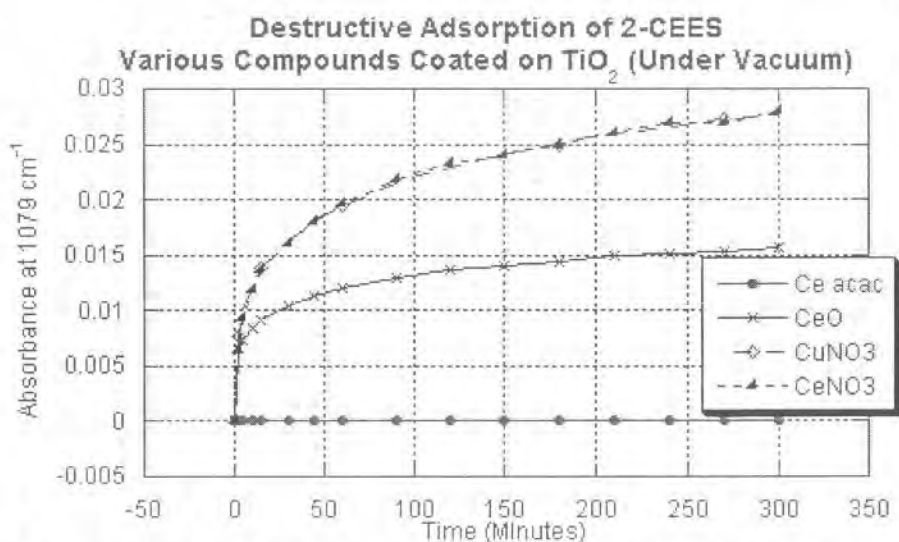


Figure 16. Growth of Sulfoxide versus Time for TiO₂ Samples Under Vacuum.

The paraoxon results of the samples that were successful at oxidizing CEES were more mixed. Only the sample 2-mol% [Cu(NO₃)₂]TiO₂ appears to be significantly faster at destructively adsorbing paraoxon than the titanium dioxide alone. Figure 17 shows the relative rate of adsorption and decomposition of paraoxon for the coated samples and titanium dioxide alone.

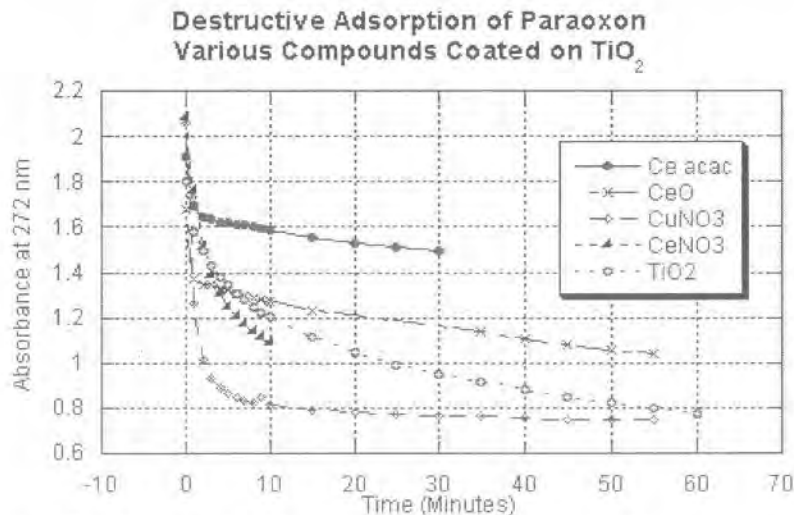


Figure 17. Destructive Adsorption of Paraoxon by Various Samples.

Transition Metal Mixtures as Coating For Titanium Dioxide Nanoparticles

Next, experiments were performed to evaluate a special formulation made by mixing one mole percent cerium nitrate and one mole percent copper nitrate together with titanium dioxide nanoparticles. The rationale was that combining these two metal salts might improve the reaction

with the chemical warfare agent simulants. Figure 17 on the previous page shows that coating cerium nitrate and copper nitrate separately on titanium dioxide improved the destructive adsorption of the VX simulant paraoxon over uncoated TiO_2 . These coated samples were also capable of oxidizing CEES. The sample was prepared by dissolving one mole percent cerium nitrate and one mole percent copper nitrate in tetrahydrofuran. To this solution the titanium dioxide nanoparticles ($\text{SSA} = 230 \text{ m}^2/\text{g}$) were added and stirred for two hours. After settling the supernatant THF was decanted and the remainder of the solvent evacuated via vacuum line until the solids were dry. The flask was then placed in a drying oven (110°C) for one hour. The specific surface area of the obtained powder was $180 \text{ m}^2/\text{g}$.

This sample performed extremely well at destructively adsorbing both paraoxon and CEES. It was capable of more rapid and complete oxidation of CEES than any of the previous samples, including the samples in which cerium nitrate and copper nitrate were coated separately on titanium dioxide. Figure 18 shows complete reaction of the CEES in the vapor phase to CEESO after the 300 minute reaction time, along with a reference spectrum of CEESO.

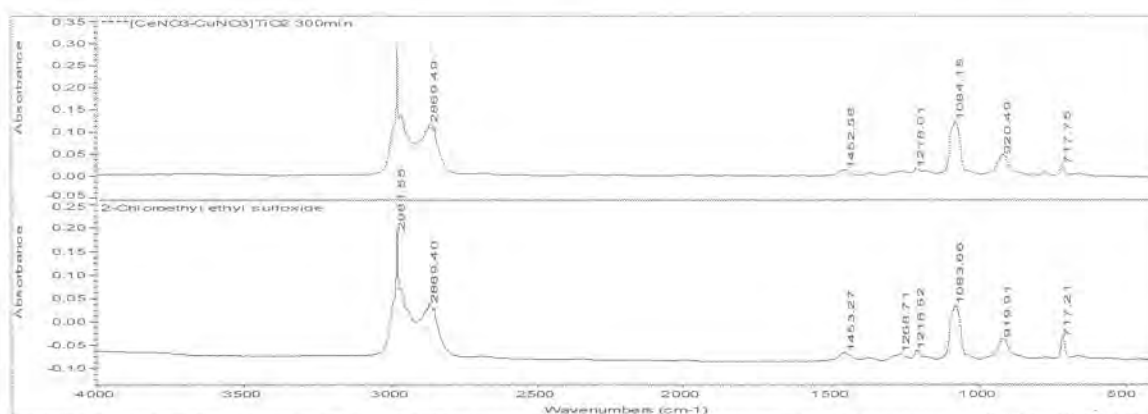


Figure 18. 2-mol% $[\text{Ce}(\text{NO}_3)_3\text{-Cu}(\text{NO}_3)_2]\text{TiO}_2$ After Reaction With CEES; and Neat CEESO.

The oxidation rate of CEES to chloroethyl ethyl sulfoxide (CEESO) was monitored over time. This result was graphed along with other similar samples for reference and comparison. Figure 19 shows the growth of the sulfoxide peak seen at 1084 cm^{-1} as a function of time.

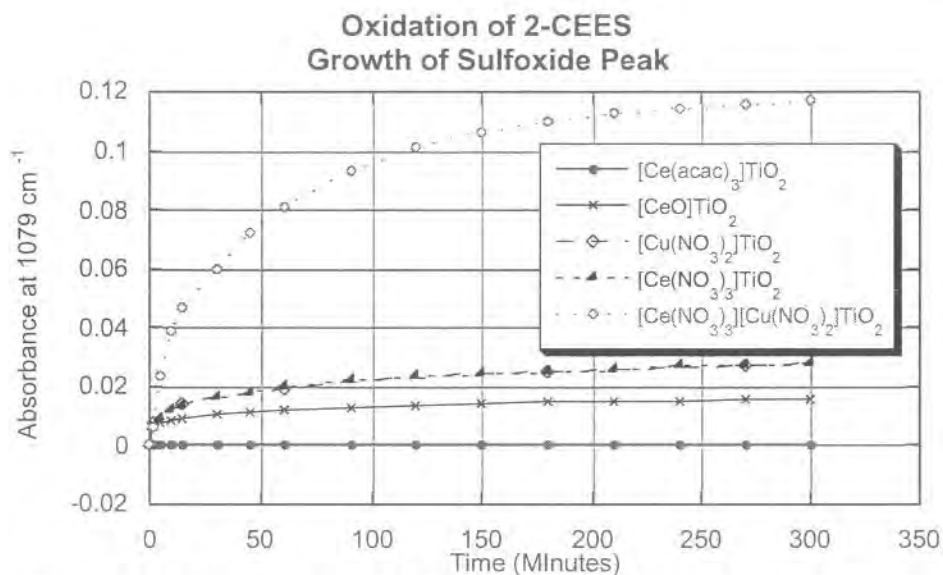


Figure 19. Oxidation of CEES: Growth of Sulfoxide Peak Versus Time

Destructive adsorption of paraoxon was just as promising. The combination of the cerium nitrate and copper nitrate coated on titanium dioxide appeared to substantially increase the rate of destruction of paraoxon even though the surface area of the sample was lower than the references. This is illustrated in Figure 20 below.

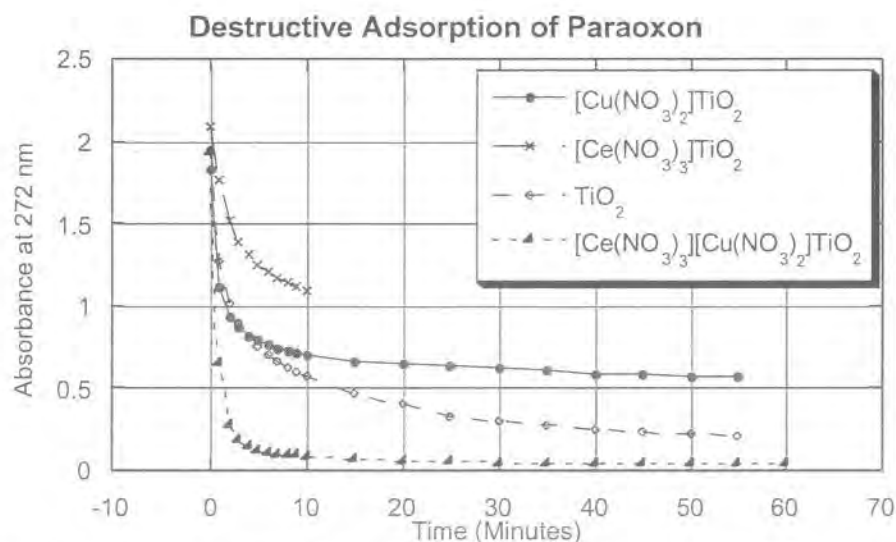


Figure 20. Destructive Adsorption of Paraaxon by Various TiO₂ Samples.

Transition Metal Mixtures as Coatings on Zinc Oxide Nanoparticles

As reported previously, the results were very promising when cerium and copper compounds were coated on titanium dioxide nanoparticles to aid in the oxidation of CEES. Also, at the same time, the presence of supported compounds did not diminish the reactive capabilities toward nerve agent simulants. In fact, we have shown how they may improve decomposition of these agents. Zinc oxide nanoparticles are known to be effective destructive adsorbents especially against CEES, where titanium dioxide alone is virtually unreactive. We investigate here whether we can improve on the reactivity of zinc oxide by coating the nanoparticles with cerium and copper compounds. Previously, experiments were conducted using polyoxometalates as a coating on zinc oxide nanoparticles, with mixed results.

To prepare these samples, the copper or cerium compound was dissolved in tetrahydrofuran in a small round bottom flask with stir bar. Zinc oxide nanoparticles (SSA = 116 m²/g) were added and this solution stirred for 2 hours. After settling, the supernatant THF was decanted and the solids dried under vacuum for several hours. The dry solids were then placed in a drying oven at 110°C for one hour. The samples prepared were:

- [2 mol% CeO]₂ZnO SSA = 102 m²/g
- [2 mol% Cu(NO₃)₂]₂ZnO, SSA = 73 m²/g
- [2 mol% Ce(NO₃)₃]₂ZnO, SSA = 64 m²/g

The results of these coated ZnO samples were not as promising as the coated TiO₂ samples. It appears the addition of copper and cerium compounds to zinc oxide hinders its ability to destructively adsorb paraoxon. Figure 21 below shows how the coated samples compare against zinc oxide alone.

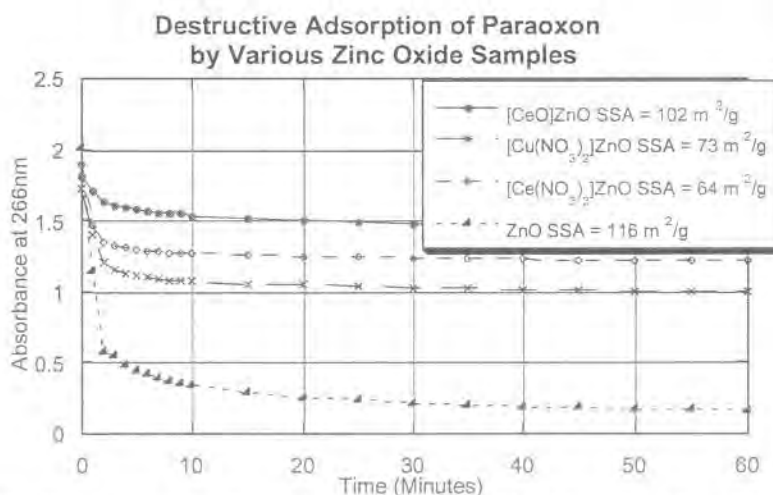


Figure 21. Destructive Adsorption of Paraoxon by Various Zinc Oxide Samples

The results of the CEES experiments are very interesting. When the coated samples were reacted with CEES, decomposition occurred in two different ways. Dehydrochlorination of the CEES to form ethyl vinyl sulfide was observed. This is indicated by the growth of the vinyl peak

at 1585 cm^{-1} . This pathway normally occurs with uncoated zinc oxide nanoparticles. But with the addition of cerium and copper compounds, oxidation to form chloroethyl ethyl sulfoxide (CEESO) occurs as well. This is observed by the growth of the sulfoxide peak at 1079 cm^{-1} . Figure 22 below is the spectrum of one of the samples showing both peaks. This spectrum appears to be a mixture of three compounds: ethyl vinyl sulfide, chloroethyl ethyl sulfoxide and still unreacted CEES.

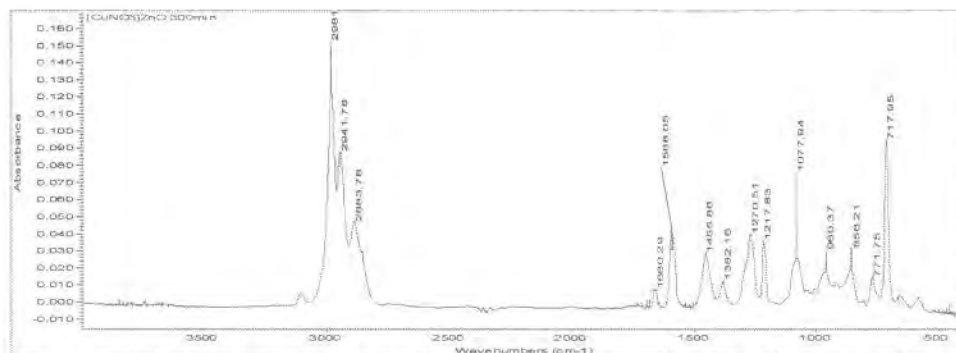


Figure 22. FT-IR Spectrum of Coated Zinc Oxide Sample After Reaction With CEES.

Also, it appears the copper nitrate coated zinc oxide far outperformed the other samples in oxidizing CEES (Figure 23).

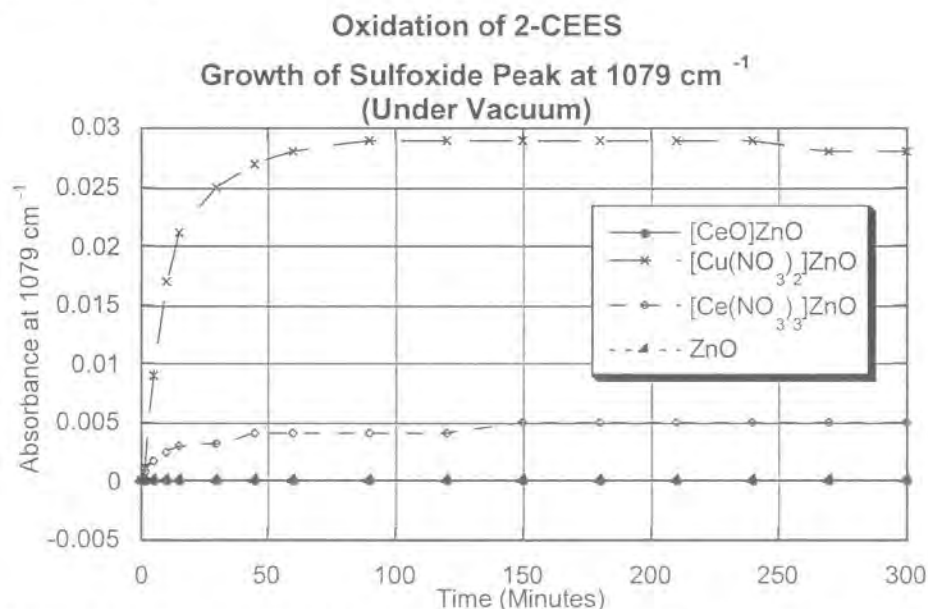


Figure 23. Growth of Sulfoxide Peak Versus Time for Zinc Oxide Samples.

Transition Metal Compounds As Coatings For Magnesium Oxide Nanoparticles

Magnesium oxide nanoparticles are known to be effective against CW agent simulants, especially CEES, where dehydrochlorination occurs to form the product ethyl vinyl sulfide. Previously, when AP-MgO nanoparticles were coated with polyoxometallates (POMs), we

showed how the oxidation chemistry dominated in the decomposition of CEES. In addition, the POM did not impede the destructive adsorption of paraoxon. The objective of these next experiments was to determine if coating AP-MgO with copper and cerium nitrates would also enhance the reactivity with agent simulants. These samples were prepared in the same fashion as the coated zinc oxide samples above.

The result of coating magnesium oxide nanoparticles with the cerium nitrate/copper nitrate mixture was interesting. This coating formulation did not impede the destructive adsorption of paraoxon. The paraoxon was adsorbed in the first three minutes after addition of the sample, which is typical of uncoated AP-MgO. With the CEES reaction however, oxidation to form CEESO does not occur. Dehydrochlorination to ethyl vinyl sulfide was formed as the reaction product. The cerium nitrate/copper nitrate coating does appear to improve the reaction kinetics when compared to the uncoated reference sample as seen in Figure 24. Although the reaction is slower at first, it appears to be a more complete reaction after the 300 minutes. Figure 24 shows the height of the vinyl peak, observed at 1585 cm^{-1} , increasing over time.

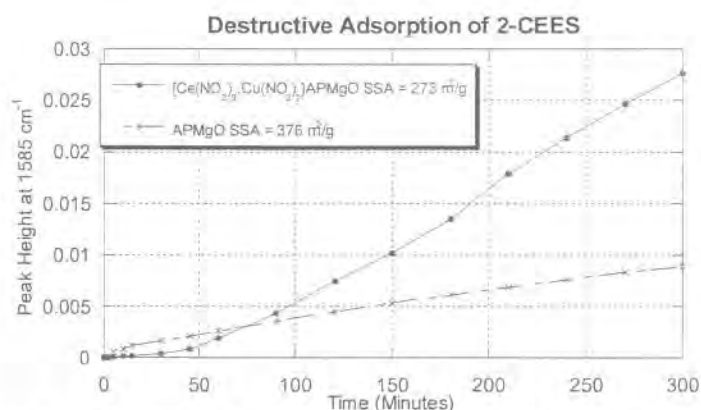


Figure 24. Growth of the Vinyl Peak Versus Time for Coated and Uncoated AP-MgO

Effect of Increased Loadings of Cerium Nitrate and Copper Nitrate Coated on TiO₂

The most promising formulations appear to be the samples prepared by mixing one mole percent cerium nitrate and one mole percent copper nitrate as coatings on titanium dioxide nanoparticles. These samples performed extremely well at destructively adsorbing paraoxon and oxidizing CEES. Additional samples were prepared using various other loadings of the cerium nitrate/copper nitrate on TiO₂ to optimize the loading on the TiO₂ support. Also, research at Emory University identified silver nitrate as an excellent oxidizer of CEES¹. Therefore, a sample was prepared with a coating of silver nitrate on TiO₂. These samples were tested against the chemical warfare agent simulants paraoxon and CEES.

The samples were prepared by dissolving various amounts of cerium nitrate and copper nitrate or silver nitrate in tetrahydrofuran. To this solution the titanium dioxide nanoparticles (SSA = $298\text{ m}^2/\text{g}$) were added and stirred for two hours. After settling, the supernatant THF was decanted and the remainder of the solvent evacuated via vacuum line until the solids were dry. The samples were then placed in a drying oven ($110\text{ }^{\circ}\text{C}$) for one hour. The samples prepared were:

[3 mol% $\text{Ce}(\text{NO}_3)_3\text{-Cu}(\text{NO}_3)_2\text{TiO}_2$,	SSA = 278 m^2/g
[5 mol% $\text{Ce}(\text{NO}_3)_3\text{-Cu}(\text{NO}_3)_2\text{TiO}_2$,	SSA = 157 m^2/g
[2 mol% $\text{AgNO}_3\text{TiO}_2$,	SSA = 281 m^2/g
Samples used for comparison were:	
[2 mol% $\text{Ce}(\text{NO}_3)_3\text{-Cu}(\text{NO}_3)_2\text{TiO}_2$,	SSA = 198 m^2/g
$\text{Ce}(\text{NO}_3)_3\text{-Cu}(\text{NO}_3)_2$	Physical Mixture
Uncoated TiO_2 ,	SSA = 298 m^2/g

All these samples appeared to work extremely well at oxidizing CEES. They are comparable with the previously prepared and reported [2mol% $\text{Ce}(\text{NO}_3)_3\text{-Cu}(\text{NO}_3)_2\text{TiO}_2$ sample, however, this sample still appears to be the best. All the samples showed oxidation of CEES in the vapor phase within 2 minutes after injection. There were no peaks indicative of CEES observed in the vapor phase after 5 minutes in all of the samples. Figure 25 shows the [3 mol% $\text{Ce}(\text{NO}_3)_3\text{-Cu}(\text{NO}_3)_2\text{TiO}_2$ sample after 5 minute reaction time as well as a reference spectrum of CEESO. This spectrum is representative of all the new samples tested including the silver nitrate coated sample. In all samples, the reaction in the vapor phase appeared complete, in other words, no typical CEES peaks were seen – only CEESO was observed in the vapor phase.

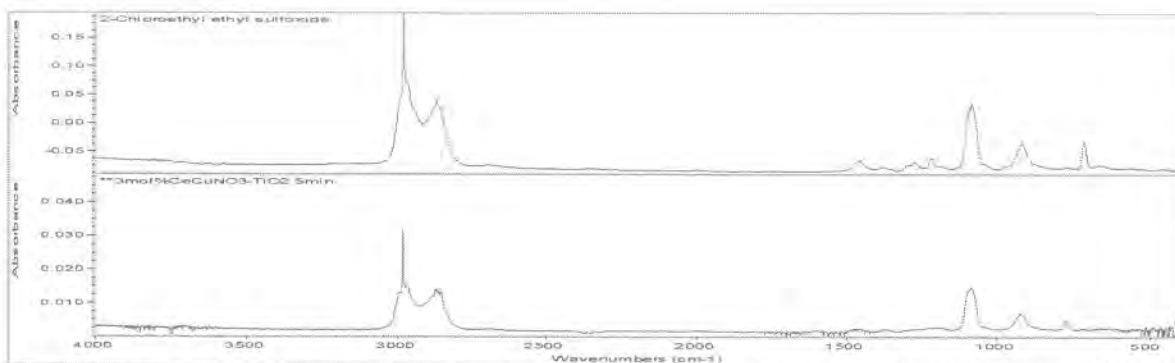


Figure 25. Reaction of [3 mol% $\text{Ce}(\text{NO}_3)_3\text{-Cu}(\text{NO}_3)_2\text{TiO}_2$ and CEES to Form CEESO

The oxidation rate of CEES to chloroethyl ethyl sulfoxide (CEESO) was monitored over the five hour reaction time for all these samples and compared to some other previous samples. Even though no CEES peaks are seen in the vapor phase 5 minutes after reaction, the height of the sulfoxide peak (1079 cm^{-1}) continues to grow over the five hour reaction time. Figure 26 shows this growth plotted as a function of time. It appears the original sample of [2 mol% $\text{Ce}(\text{NO}_3)_3\text{-Cu}(\text{NO}_3)_2\text{TiO}_2$ initially oxidizes CEES the fastest, however the largest sulfoxide peak was actually observed in the [5 mol% $\text{Ce}(\text{NO}_3)_3\text{-Cu}(\text{NO}_3)_2\text{TiO}_2$ sample after 120 minutes of reaction. When the physical mixture of cerium nitrate/copper nitrate is reacted with CEES and no nanoparticles are present, oxidation of CEES does not occur. What is observed after 300 minutes are typical CEES peaks as well as a large N-O stretch at 1367 cm^{-1} . No products of the destruction of CEES are observed.

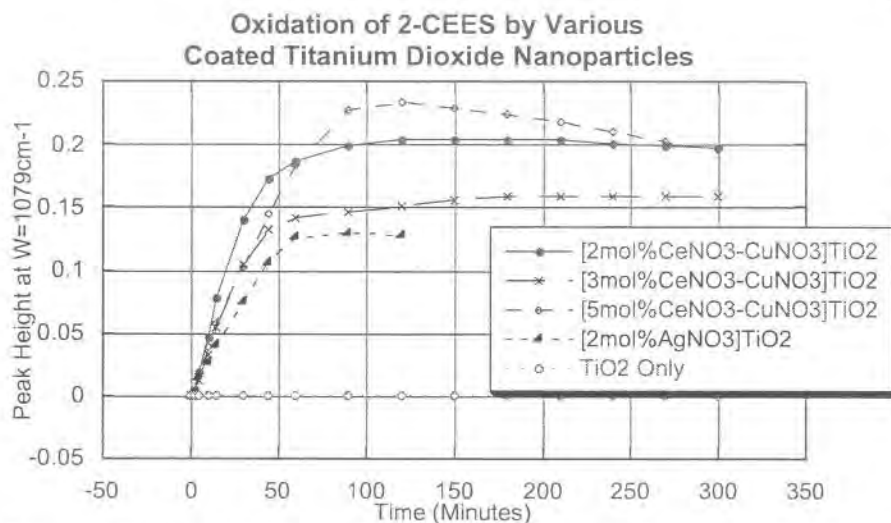


Figure 26. Oxidation of CEES by Various Loadings of $\text{Ce}(\text{NO}_3)_3\text{-Cu}(\text{NO}_3)_2$ Samples

With paraoxon, the original [2 mol% $\text{Ce}(\text{NO}_3)_3\text{-Cu}(\text{NO}_3)_2$] TiO_2 sample was the most effective in destructively adsorbing paraoxon over all the other samples except [2 mol% AgNO_3] TiO_2 . This sample performed just as well as [2 mol% $\text{Ce}(\text{NO}_3)_3\text{-Cu}(\text{NO}_3)_2$] TiO_2 . Figure 27 graphs the destructive adsorption of paraoxon by these samples over the 60 minute reaction time. As is apparent from the graph, the physical mixture of cerium nitrate and copper nitrate by themselves does nothing to destroy paraoxon. All the coated nanoparticle samples were an improvement over uncoated titanium dioxide.

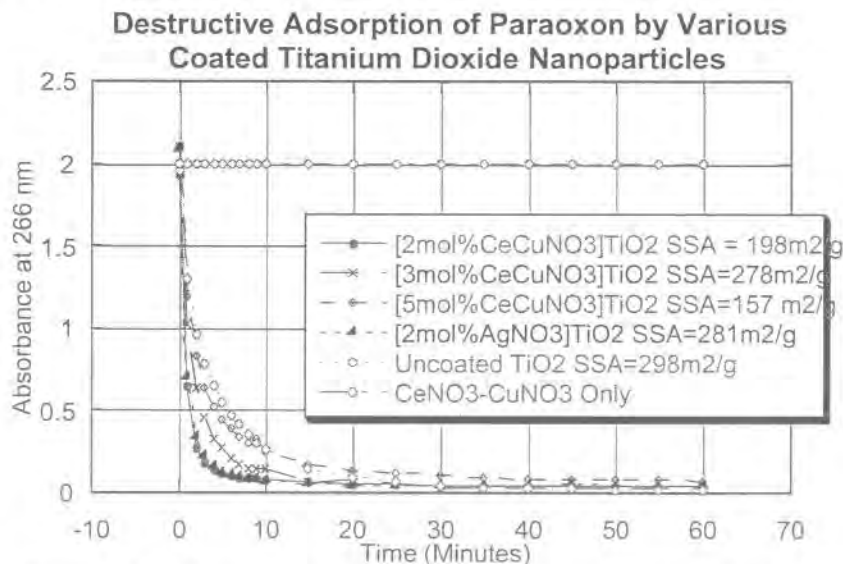


Figure 27. Destructive Adsorption of Paraoxon Over Sixty Minutes

Study of Adsorbed Species After Reaction of Paraoxon on $[\text{Ce}(\text{NO}_3)_3\text{-Cu}(\text{NO}_3)_2]\text{TiO}_2$

The structure of the adsorbed species after reaction of the cerium nitrate/copper nitrate samples and paraoxon were identified. ^{31}P NMR spectrum of uncoated titanium dioxide nanoparticles with adsorbed paraoxon was found to contain one large asymmetrical peak centered at $\delta -3.83$ ppm. (Figure 28) In previous studies, it was reported that reactions between paraoxon and AP-MgO showed a large peak centered around $\delta -0.85$ ppm. Since it is known that the phosphorus in H_3PO_4 exhibits a signal at 0 ppm, we assigned the signal at -0.85 ppm to PO_4^{3-} , a product derived via complete hydrolysis of paraoxon. Thus, the large asymmetrical peak in the uncoated TiO_2 is probably due to a mixture of mono and dihydrolyzed products. In the cerium nitrate/copper nitrate coated sample, there is again a large asymmetrical peak centered at $\delta -3.897$ ppm but also a small peak centered at $\delta -15.406$ ppm (see figure 29). The first peak is attributed to the mixture of mono and dihydrolyzed products and the second to unhydrolyzed adsorbed paraoxon.

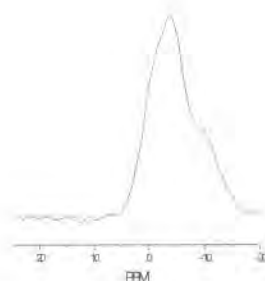


Figure 28. ^{31}P NMR Spectrum of Paraoxon/ TiO_2

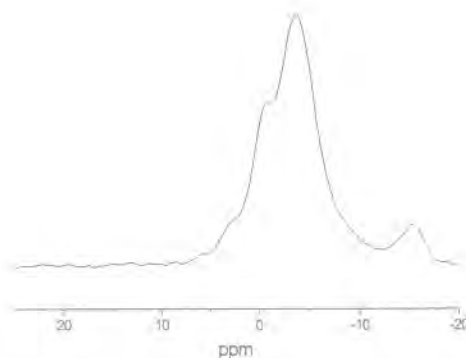


Figure 29. ^{31}P NMR Spectrum of Paraoxon/ $[\text{Ce}(\text{NO}_3)_3\text{-Cu}(\text{NO}_3)_2]\text{TiO}_2$

Study of Nanocrystalline Cerium Oxide As A Coating On TiO_2

Experiments to this point used commercial grade compounds as coatings for nanoparticles. Nanoparticle sized cerium (IV) oxide (CPCeO_2) was developed at NanoScale Materials, Inc. and was used these studies as a coating for TiO_2 . Experiments with the CPCeO_2 alone and coated on titanium dioxide were conducted to study the destructive capabilities against

CEES and paraoxon. These results are compared against uncoated titanium dioxide nanoparticles and commercial grade cerium oxide (CMCeO_2) coated TiO_2 .

The coated samples were prepared by dissolving the cerium (IV) oxide in tetrahydrofuran (THF). Titanium dioxide nanoparticles ($\text{SSA} = 318 \text{ m}^2/\text{g}$) were then added and the solution stirred for two hours. After settling, the supernatant THF was decanted and the remainder of the solvent evacuated via vacuum line until the solids were dry. The samples were then placed in a drying oven (110°C) for one hour. The samples were:

[10 wt% CPCeO_2] TiO_2 , $\text{SSA} = 177 \text{ m}^2/\text{g}$

CPCeO_2 , $\text{SSA} = 50 \text{ m}^2/\text{g}$

[5 wt% CMCeO_2] TiO_2 , $\text{SSA} = 173 \text{ m}^2/\text{g}$

Uncoated TiO_2 , $\text{SSA} = 318 \text{ m}^2/\text{g}$

The oxidation of CEES to chloroethyl ethyl sulfoxide (CEESO) by these samples was monitored by FT-IR over five hours. The height of the sulfoxide peak (1079 cm^{-1}) was recorded for each scan and the disappearance of the C-Cl bond at 720 cm^{-1} noted. For the sample CPCeO_2 alone, oxidation to CEESO does not occur in the vapor phase. Only CEES peaks are observed after the 300 minute reaction time. In the CMCeO_2 coated TiO_2 sample, there appears to be a mixture of CEES and the oxidation product CEESO in the vapor phase. The CPCeO_2 coated TiO_2 sample oxidizes CEES completely in the vapor phase as only the product CEESO is observed. This product appears after two minutes reaction time with very little if any CEES peaks remaining. Figure 30 shows the FT-IR spectra, which illustrate the differences noted among these three samples.

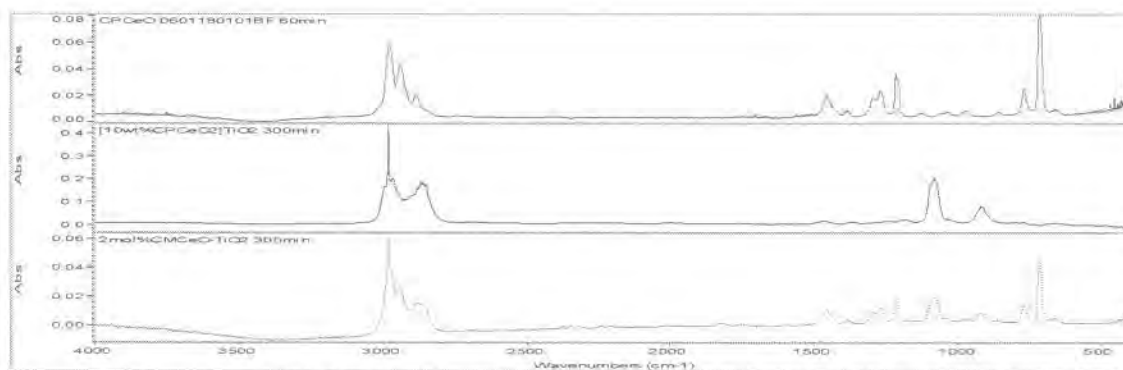


Figure 30. Reaction with CEES: (A) CPCeO_2 – CEES peaks, (B) $[\text{CPCeO}_2]\text{TiO}_2$ – CEESO Peaks, (C) $[\text{CMCeO}_2]\text{TiO}_2$ – Mixture of CEES and CEESO

With paraoxon, similar results are observed. The CPCeO_2 coated TiO_2 appears to have the highest reactivity towards adsorbing paraoxon over all the other samples. Figure 31 shows the destructive adsorption of paraoxon by these samples over the 60 minute reaction time. As is apparent from the graph, the CPCeO_2 sample by itself is very poor at adsorbing paraoxon. However, adding it as a coating does not diminish the capability of titanium dioxide nanoparticles to destructively adsorb paraoxon.

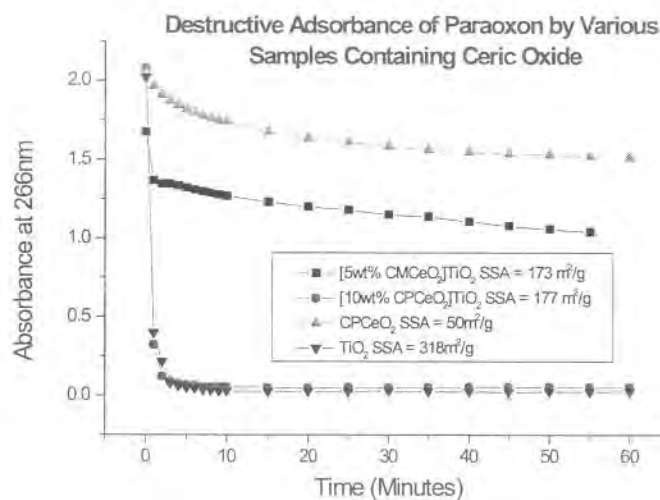


Figure 31: Adsorbance of Paraaxon over time for the coated and uncoated samples

Nanosized cerium (IV) oxide coated on titanium dioxide appears to be extremely good at destructively adsorbing all the chemical warfare agents studied. This sample is as efficient as any of the best performing samples reported here previously. These include the polyoxometalate coated titanium dioxide and magnesium oxide, and the cerium nitrate/copper nitrate coated titanium dioxide. As indicated above CPCeO₂ is a new product at NanoScale Materials, Inc., and while it does not perform well on its own, when coated onto titanium dioxide, the results are extremely promising.

Additional Experiments With Cerium and Copper Nitrates As Coatings

Previous UV-Vis spectroscopy experiments reported the rate and quantity of paraoxon adsorbed onto uncoated nanoparticulate TiO₂ (APTiO₂) versus coated APTiO₂ (2 mol % Ce(NO₃)₃-Cu(NO₃)₂). Based on this preliminary work, additional samples were analyzed to confirm the previously reported results. Commercial grade titanium dioxide (CMTiO₂) was coated with the cerium nitrate/copper nitrate mixture and compared to coated and uncoated APTiO₂. Additionally, solid-state FT-IR and ³¹P NMR were used to analyze the products resulting from paraoxon adsorption. The reacted samples were also extracted with an organic medium for additional characterization.

Coated samples were prepared by dissolving one mole percent of cerium nitrate and/or one mole percent copper nitrate in THF. To this solution either CMTiO₂ (SSA = 6.5 m²/g) or APTiO₂ (SSA = 298 m²/g) was added and stirred for 2 h. After settling, the clear supernatant was decanted, and the remaining solid was dried in vacuo then placed in a drying oven at 110 °C for one hour. The specific surface areas of the prepared samples were measured at 7.9 m²/g (CMTiO₂) and 198 m²/g (APTiO₂).

Extraction of adsorbed species was accomplished in the following manner. The RNP (0.2g) and paraoxon (9 µL) were placed in a small round bottom flask and stirred together for one hour. Distilled water (200 mL) was then added, and the mixture was refluxed for 2 h. After

cooling to room temperature, the supernatant was removed and the pH was adjusted to ≥ 7.6 by addition of sodium carbonate. The supernatant was then analyzed for the presence of paraoxon by UV-Vis spectroscopy.

UV-Vis analysis of the coated and uncoated APTiO₂ exhibited complete adsorption of the paraoxon onto the coated RNP within 60 min. In contrast, the CMTiO₂ samples exhibited no paraoxon adsorption onto the coated RNP after 60 min. Organic-phase extractions of the reaction products from the coated CMTiO₂ samples yielded ~10% hydrolyzed (~90% unhydrolyzed paraoxon) whereas extraction from the uncoated and coated APTiO₂ samples yielded ~50% hydrolyzed (~50% unhydrolyzed) and ~30% hydrolyzed (~70% unhydrolyzed) paraoxon, respectively (Table 2). The lower reactivity in the coated APTiO₂ over the uncoated APTiO₂ can be attributed to the cerium and copper coatings blocking the some of the active sites. Control experiments indicated that the APTiO₂ alone is responsible for paraoxon hydrolysis. Therefore, coating the surface with metal salts results in less surface area available for reaction.

Table 2. Results of UV-Vis Analysis

Sample	Extent of Adsorption as Assessed by UV Analysis	Unhydrolyzed Paraoxon As Determined by Extraction, %
Uncoated APTiO ₂	Complete (100%)	45%
[Ce(NO ₃) ₃ -Cu(NO ₃) ₂]APTiO ₂	Complete (100%)	68%
[Ce(NO ₃) ₃ -Cu(NO ₃) ₂]CMTiO ₂	Incomplete (<1%)	92%

Previous ³¹P NMR studies of paraoxon adsorbed on uncoated APTiO₂ displayed a single, broad asymmetrical peak centered at -3.83 ppm coupled with spinning side-bands (-43.00 and 43.00 ppm). The spinning side bands were assigned to paraoxon binding to the surface of the APTiO₂. In the cerium nitrate/copper nitrate coated APTiO₂, there also was a large asymmetrical peak centered at -3.90 ppm (also with spinning side bands), in addition to a small peak centered at -15.41 ppm (Figure 32). New ³¹P NMR analysis of paraoxon reacted APTiO₂ revealed a second smaller peak at -15.00 ppm. Since it was established that the paraoxon adsorbed on AP-MgO displayed large peak centered around -0.85 ppm and that the phosphorus in H₃PO₄ exhibits a signal at 0 ppm, the signal at -0.85 ppm was assigned to PO₄³⁻, resulting from complete hydrolysis of paraoxon. Additionally, the asymmetrical peak at -3.8 ppm probably arises from a mixture of mono- and dihydrolyzed products, with the small peak at δ -15.00 ppm attributed to unhydrolyzed RNP-adsorbed paraoxon. The coated CMTiO₂ sample with paraoxon showed no spinning side bands, suggesting a lack of paraoxon surface binding.

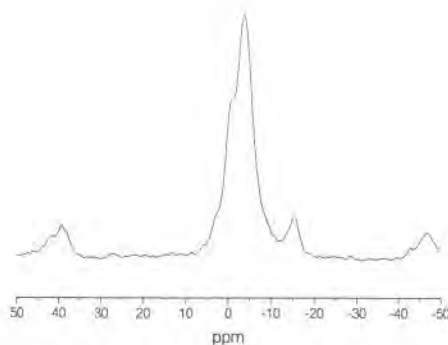


Figure 32. ^{31}P NMR Spectrum of Paraoxon/ $[\text{Ce}(\text{NO}_3)_3\text{-Cu}(\text{NO}_3)_2]\text{TiO}_2$

Comparison between CM and APTiO_2 provided striking difference toward paraoxon reactivity. The lack of reactivity in the CMTiO_2 sample can be attributed to the smaller surface area of the TiO_2 . Since paraoxon reaction occurs at the surface of the TiO_2 , a smaller surface area would yield lower reactivity. Indeed, this was confirmed by UV-Vis spectroscopy. Although the APTiO_2 had a much higher surface area (and hence propensity for reactivity), the cerium/copper coating did occlude the active sites somewhat and thus, mildly inhibited paraoxon reaction, as indicated by the organic-phase extractions.

Improvements in the Synthesis of Nanocrystalline Titanium Dioxide

During the course of the two years of this project, a significant increase in the surface area of titanium dioxide was achieved. This was due to the scaled-up processes initiated in our pilot plant. An increase in surface area from approximately $200 \text{ m}^2/\text{g}$ to the current average of $450 \text{ m}^2/\text{g}$ is a significant achievement. Consequently, the reactivity of the improved titanium dioxide nanoparticles towards paraoxon also increased. Figure 33 graphs the higher surface area TiO_2 against various coated samples. This shows how approximately 97% of the paraoxon is adsorbed within the first 3 minutes of reaction. This is now similar to the results of reactions of AP-MgO ($550 \text{ m}^2/\text{g}$) with paraoxon.

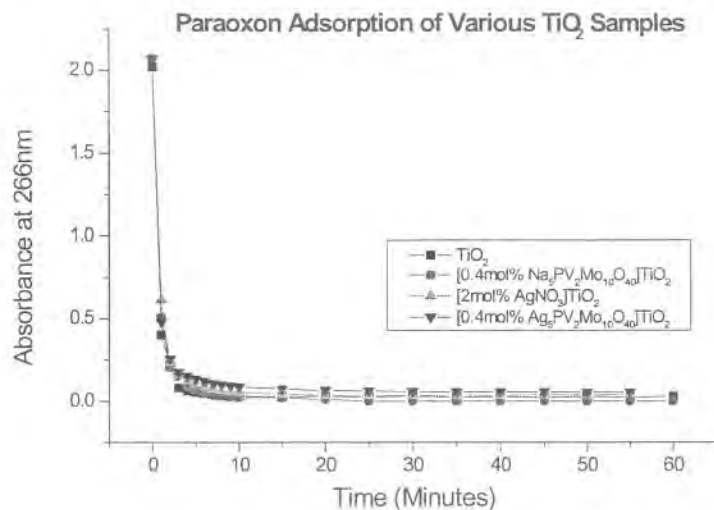


Figure 33. UV-Vis Analysis of Paraoxon Adsorption by Various Samples.

Summary of Cerium and Copper Nitrates as Coatings for TiO₂ Nanoparticles

The evolution of this project has lead to investigating new coatings for reactive nanoparticles (RNPs). While RNPs themselves do offer a decontaminating ability (through destructive adsorption) the incorporation of transition metal coatings onto the RNP surface has proven to compliment and enhance this ability. However, coating the RNP may inhibit the adsorption ability due to surface and active site blockage. Previous results have shown that TiO₂ alone destructively adsorbs paraoxon, while offering little reactivity towards CEES. Conversely, Ce(NO₃)₃ and Cu(NO₃)₂ (when used in combination) have demonstrated the ability to catalytically oxidize CEES with little or no reaction toward paraoxon. By coating TiO₂ with Ce(NO₃)₃ and Cu(NO₃)₂ a decontaminating system can be produced which offers activity against CEES and paraoxon without compromising the individual ability of either component.

Preparation of the Ce/Cu TiO₂ was accomplished, yielding a lightly colored, green powder. XRD analysis displayed diffraction patterns typical of anatase titanium dioxide with crystallite sizes of 4 - 6 nm. This data was consistent for the original uncoated TiO₂, indicating that the coating process did not adversely affect the original TiO₂.

UV-Vis analysis of the destructive adsorption of paraoxon (i.e. the paraoxon is adsorbed and subsequently destroyed) on the Ce/Cu TiO₂ showed completeness of reaction within 3 min (Figure 34).

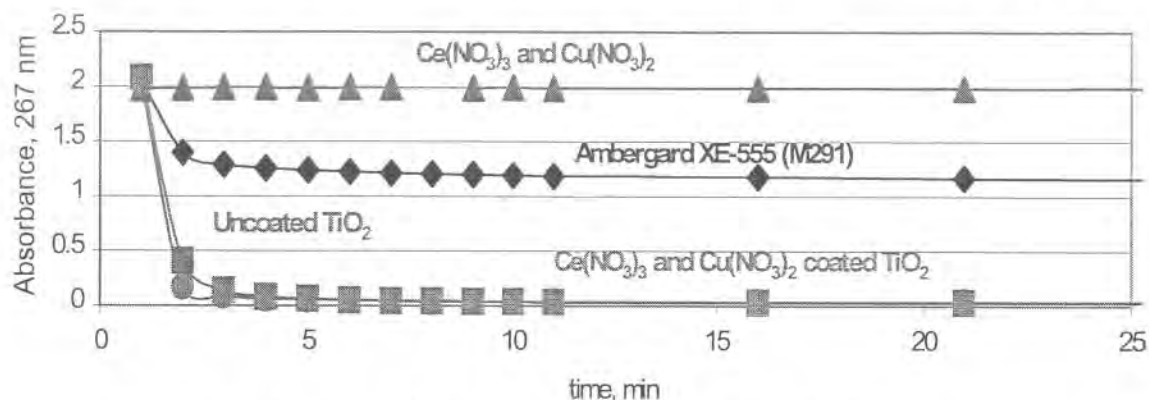


Figure 34. Paraoxon Adsorption Monitored by UV-Vis Spectroscopy.

In contrast, Ambergard XE-555 (the active component of the M291 SDK) adsorbed only ~30% of the paraoxon after 21 min. Control experiments with $\text{Ce}(\text{NO}_3)_3$ and $\text{Cu}(\text{NO}_3)_2$ indicated no adsorption, whereas uncoated TiO_2 provided similar performance to the Ce/Cu TiO_2 system. The advantage of using the Ce/Cu coated TiO_2 instead of the uncoated TiO_2 lies in the ability of the coating to oxidize and decontaminate the challenge agent (esp. against mustard agent simulants), rather than merely adsorbing.

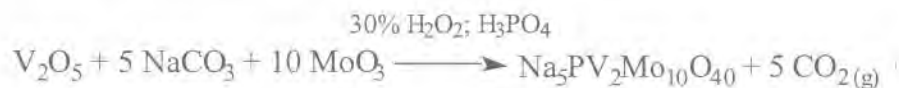
Coating TiO_2 with $\text{Ce}(\text{NO}_3)_3$ and $\text{Cu}(\text{NO}_3)_2$ does not impede the adsorptive capabilities of this RNP. Coated RNPs offer dual modes of protection, adsorption (derived from the RNP) and oxidative decontamination (derived from the transition metal coating). It was thought that coating the particles might adversely affect the ability of the RNPs to adsorb the challenge agent since the surface (and thus, the active sites) would be covered. However, Figure 34 clearly demonstrates that the presence of a 2 mol % covering does not inhibit adsorption. Even more significant, the Ce/Cu coated TiO_2 offers better adsorption ability toward paraoxon than the currently deployed M291 SDK.

Task 2. Synthesis of nanocrystalline POMs.

This objective was devoted to the development of a synthetic method for economically making *nanocrystalline POMs*. Such nanocrystals would greatly enhance the catalytic activity of the POMs. A description of the efforts to synthesize nanoparticulate POMs is given below:

1. Solvent removal techniques for the synthesis of high surface area POMs.

One attempt at producing nanocrystalline forms of POMs for this project was to investigate two techniques for the removal of solvent from the standard synthesis of proton, sodium, and silver salts of the $[\text{PV}_2\text{Mo}_{10}\text{O}_{40}]^{5-}$. One of the two methods of interest was supercritical drying, which is commonly used to remove solvent at temperatures and pressures that are above the supercritical point of the solvent. This is one approach for the production of nanoparticles. The second method was that of spray drying, which utilizes rapid expansion of a pressurized solution to rapidly remove solvent. Typically, fine powders are the result of spray drying solutions of inorganic salts and other materials. The most common synthesis of POM materials such as $\text{H}_5\text{PV}_2\text{Mo}_{10}\text{O}_{40}$ and $\text{Na}_5\text{PV}_2\text{Mo}_{10}\text{O}_{40}$ follows an aqueous route. The synthesis can be described by the following equation:



a. Supercritical drying of aqueous $\text{H}_5\text{PV}_2\text{Mo}_{10}\text{O}_{40}$ and $\text{Na}_5\text{PV}_2\text{Mo}_{10}\text{O}_{40}$ POM solutions.

The supercritical drying of both $\text{H}_5\text{PV}_2\text{Mo}_{10}\text{O}_{40}$ and $\text{Na}_5\text{PV}_2\text{Mo}_{10}\text{O}_{40}$ was performed in a 600-mL autoclave. In both cases, it was determined that the POM decomposes before the critical temperature and pressure is reached. The supercritical drying of these materials was performed several times under different solvent conditions (such as mixed with alcohols or acetonitrile) with the same resulting decomposition.

b. Spray drying of aqueous $\text{H}_5\text{PV}_2\text{Mo}_{10}\text{O}_{40}$ and $\text{Na}_5\text{PV}_2\text{Mo}_{10}\text{O}_{40}$ solutions.

This method resulted in some interesting initial results. It was discovered that the specific surface area of the $\text{Na}_5\text{PV}_2\text{Mo}_{10}\text{O}_{40}$ POM powder could be markedly increased from $1 \text{ m}^2/\text{g}$ to about $20 \text{ m}^2/\text{g}$. A series of experiments were set up to examine the effect of varying conditions related to the synthesis of the precursor solutions (concentration, solvents) and of the spray drying process itself (solution feed rates, gas flow rates, temperature of drying) on the specific surface area (SSA) of the POM powder. Changes in most of these parameters had very little effect on the SSA of the POM powders, typically the results were in the vicinity of $1\text{--}3 \text{ m}^2/\text{g}$. The parameter that yielded the most promising results was that of the POM solids concentration in the solution. The SSA was observed to increase from 1.4 to 7.6 to $19.2 \text{ m}^2/\text{g}$ for 3.0×10^{-2} , 3.0×10^{-3} and $3.0 \times 10^{-4} \text{ M}$ solutions of $\text{Na}_5\text{PV}_2\text{Mo}_{10}\text{O}_{40}$ respectively. $\text{H}_5\text{PV}_2\text{Mo}_{10}\text{O}_{40}$ solutions decomposed during the spray drying process.

2. Rapid crystallization of POMs from saturated solutions.

The rationale for the rapid crystallization of POMs from saturated solutions is similar to that of the other methods. Namely, the hindrance of the digestion of the crystals so that small crystallites are formed as opposed to large ones. Practically, these experiments involved the conventional synthesis of $\text{H}_5\text{PV}_2\text{Mo}_{10}\text{O}_{40}$ and $\text{Na}_5\text{PV}_2\text{Mo}_{10}\text{O}_{40}$ in aqueous solutions followed by the rapid introduction of this solution to solvents (alcohols, aromatics, acetonitrile, alkanes, etc.) in which the POMs are insoluble or of slight solubility. The goal was to "crash out" the POM powders before the crystallites can reach large sizes.

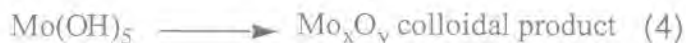
The results from these experiments were not promising. In many cases the POMs decomposed into vanadates and molybdates. In cases where the POM did not decompose, the SSA's of the resulting powders were in the range of 1-3 m^2/g .

3. Synthesis of molecular precursors for nanocrystalline POMs.

This approach was to synthesize nanocrystalline POMs using known sol-gel chemistry of the transition metal components of the POM. Sol-gel chemistry is at the heart of the method for the production of nanocrystalline MgO . Efforts had been to work with the sol-gel chemistry of molybdenum and vanadium with the ultimate goal of synthesizing nanocrystalline $\text{Na}_5\text{PV}_2\text{Mo}_{10}\text{O}_{40}$ and similar compounds.

a. Synthesis of molybdenum oxide via sol-gel chemistry.

While sol-gel chemistry of many transition metals is widely known, there has been relatively little work with molybdenum. However, there are several cases in the literature for the formation of molybdenum oxide sol-gels from the hydrolysis of molybdenum alkoxides that have been used as guides. Due to the enormous costs of commercially available molybdenum alkoxides, work was conducted on the synthesis of molybdenum ethoxides for use as precursors for the sol-gel synthesis. The entire synthetic scheme for the production of molybdenum oxide sol-gel is given in the equations below:



It is believed that under certain conditions, oxides such as Mo_8O_{23} and $\text{Mo}_{12}\text{O}_{40}$ can be produced via this set of reactions.

b. Synthesis of vanadium oxide via sol-gel chemistry.

The development of the vanadium oxide sol-gel chemistry is similar to that of molybdenum in that it proceeds through the hydrolysis of vanadium alkoxides. Vanadium oxides gels can be synthesized via the hydrolysis and condensation of vanadium oxo-alkoxides VO(OR)_3 with R representing Et, n-Bu, n-Pr, i-Pr, t-Am. Hydrolysis of commercially available vanadium ethoxide leads to the formation of reddish-orange vanadium oxide sol-gel.



Vanadium ethoxides are very reactive toward hydrolysis. This arises from the high electrophilic power of the vanadium atom and the possible coordination expansion from 4 to 5 or 6. Again, once the chemistry of the molybdenum sol-gels has advanced, it will be combined with the vanadium oxide in the attempt to produce molybdenum-vanadium mixed sol-gels for use as precursors in the production of POM nanocrystals.

The efforts involving the sol-gel chemistry of molybdenum and vanadium described above did not lead to the desired POM nanoparticle. We were successful in replicating the synthesis of the desired precursor materials, but the efforts to combine the molybdenum and vanadium solutions to form the desired nanoparticle POM have not been successful. However, it should be realized that the approach taken thus far is but a single one of a large number of possible routes. Unfortunately, we were unable to further pursue efforts in this area due to time constraints.

Task 3. Development of new POM formulations at Emory University.

The goal of this objective was to refine and enhance the catalytic activity of the POMs that were studied in Phase I. The need exists for a decontamination system that is heterogeneous, catalytic, selective and green for the destruction of HD and other deleterious thioethers. The need for such a systems is three-fold: (1) battlefield protection of troops and equipment against chemical warfare agents has become more important as the proliferation of these weapons of mass destruction (and despotic leaders willing to employ them) has increased dramatically, (2) large-scale decontamination of areas affected by chemical agent deployment and (3) destruction of large aging stockpiles of chemical warfare agents held by the US, UK, Russia et al. Heterogeneous systems are desirable over homogeneous systems because they allow for easier manipulation of the catalyst, fewer logistical burdens and incorporation into existing barrier protection technologies (notably topical skin protectant creams (TSPs)). Clearly, an effective system must be catalytic for protective and economic reasons. Selectivity is important to ensure the products of the decontamination are less toxic (ideally non-toxic) when compared to the offensive substrate. A problem with using bleach, peroxide or other harsh oxidants (currently employed technology) is that the oxidations are not selective and the products are only *slightly* less toxic than the substrate. Finally, the need for green materials is necessitated by the current demands of environmental friendliness in materials and process. Research conducted at Emory University (Atlanta, GA) focused on the development of new polyoxometalate systems to

catalyze the destruction/decontamination of chemical warfare agents under mild conditions. As a result, dozens of polyoxometalates, transition metal salt mixtures and combinations thereof were investigated. While many systems were efficacious towards chemical agent decontamination, $\text{Ag}_5\text{PV}_2\text{Mo}_{10}\text{O}_{40}$ was found to be the most effective for heterogeneous and selective oxidation.

Introduction to Polyoxometalates

Polyoxometalates (henceforth POMs for convenience) are early transition metal oxygen anion structures, akin to clusters. More specifically, they are oligomeric aggregates of metal cations bridged by oxide anions that form by self-assembly processes (see below). The number of POMs reported in the literature is greatly increasing with time, rendering a comprehensive review of all their physical, chemical and biological properties problematical. Interest in POMs extends into applications such as medicine,² and materials science.³ A unique feature of POMs is that nearly every molecular property can be systematically altered (i.e. POM molecular properties are “tunable”).⁴ These include polarity, redox potentials, surface charge distribution, shape, and acidity. Another attractive feature is that rational and reproducible synthetic methods are now available for the replacement of one or more of the skeletal d^0 or d^1 early transition metal cations in POMs with d- or p-block ions.

There are two generic families of POMs, the isopoly compounds, (also called isopolyanions or isopolyoxometalates) and the heteropoly compounds (also called heteropolyanions or heteropolyoxometalates).⁵ Isopolyanions are those POMs composed only of the MO_6 octahedra, represented by the formula $[\text{M}_x\text{O}_y]^{z-}$. Examples of isopolyanions are $\text{Nb}_6\text{O}_{19}^{8-}$, $\text{W}_{10}\text{O}_{32}^{4-}$ and $\text{Mo}_7\text{O}_{24}^{6-}$. Heteropolyanions are composed of the MO_6 octahedra in addition to central tetragonal MO_4 assemblies, represented by the formula $[\text{X}_r\text{M}_x\text{O}_y]^{z-}$ (where $r \leq x$). Examples of heteropolyanions include $\text{PMo}_{12}\text{O}_{40}^{3-}$, $\text{SiW}_{12}\text{O}_{40}^{4-}$, and $\text{P}_2\text{W}_{15}\text{O}_{56}^{12-}$. Depending on the POM type, differing numbers of heteroatoms can be present. The heteroatoms in the heteropoly compounds can reside in either buried (not solvent accessible) or surface (solvent accessible) positions in the POM structure. Over half of the elements in the periodic table are known to function as heteroatoms in heteropoly compounds. As heteropoly compounds are more numerous and their structural and electronic properties are easier to modify synthetically than those of the isopoly compounds, the former have dominated the application-oriented POM research to date. A variety of POM structural classes are shown below in Figure 35.²

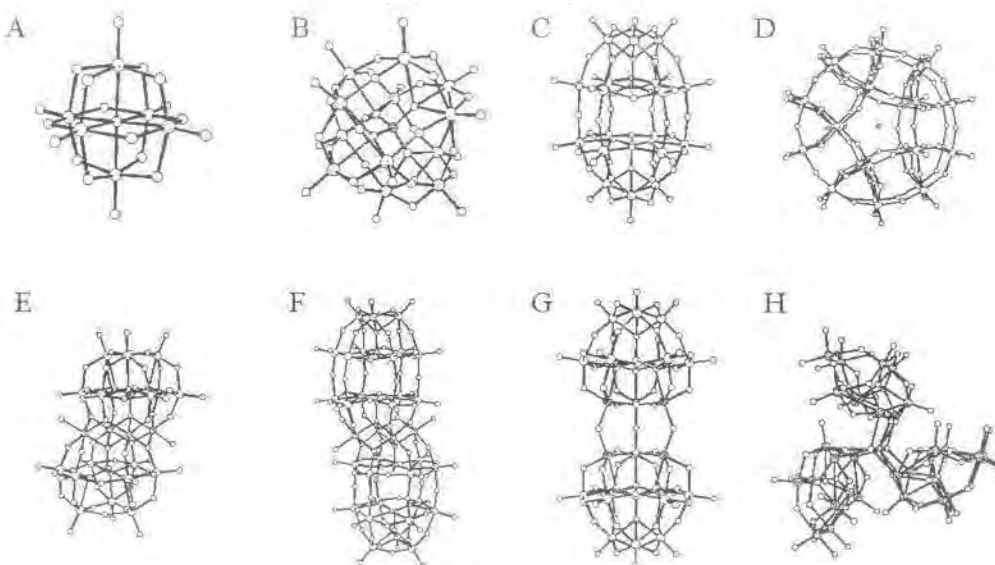
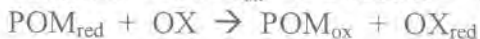


Figure 35. Atom notation ("ball-and-stick") drawings of 8 representative structural families of POMs. **A:** the hexametalate structure, $[M_6O_{19}]^{x-}$ (the charge, x, depends on M); **B:** common Keggin structure, $[XW_{12}O_{40}]^{x-}$ (the charge, x, depends on the heteroatom, X); **C:** the Wells-Dawson structure, $[X_2W_{18}O_{62}]^{x-}$ (x depends on X); **D:** the Pope-Jeannin-Preyssler structure, $[MP_5W_{30}O_{110}]^{x-}$ (x depends on the central metal ion, M); **E:** the trivacant Keggin-derived sandwich complex, $[(M^{II})_2(M^{II}L)_2(PW_9O_{34})_2]^{10-}$; **F:** the trivacant Wells-Dawson derived sandwich complex, $[(M^{II})_2(M^{II}L)_2(P_2W_{15}O_{56})_2]^{16-}$; **G:** the double-Keggin structure, $[\{A-SiO_4W_9O_{30}(OH)_3M_3\}_2(OH)_3]^{11-}$ and **H:** HPA-23, $[NaSb_9W_{21}O_{86}]^{18-}$.

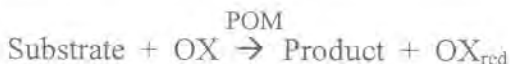
Substitution of one or more addenda atoms within the POM framework leads to the "mixed addenda" subclass of POMs. An example of a mixed-addenda POM is $PV_2Mo_{10}O_{40}^{5-}$. In this POM, two V atoms have replaced two of the Mo atoms, with the POM retaining its overall shape. However, the electronic properties of POM are often changed by the substitution of addenda atoms. Often POMs contain more than one type of addenda atom, resulting in a mixed-addenda POM.

POMs are exceptional redox catalysts based on their inherent ability to reversibly accept and subsequently release electrons. Further, POMs are thermodynamically resistant to oxidative decomposition because they are composed of metals in the highest oxidation state. Control of POM reduction and oxidation potentials can be exerted by selection of addenda atoms, heteroatoms and counteranions. For example, polyoxotungstates are more difficult to reduce (but more easily reoxidized) than polyoxovanadates, which are easier to reduce (but more difficult to reoxidize). Generally, polyoxotungstates are used for photocatalysis (where light is used to excite the POM, making it a strong oxidant) while vanado- and molybdo-POMs are more often used for thermal oxidations (usually in conjunction with a cooxidant).

As mentioned earlier, the utility of POM catalysts depends in large part on the POM redox potentials, which can be altered by the selection of addenda atoms. The redox series of POM addenda atoms is $V(V)$ (strongly oxidizing) $>$ $Mo(VI)$ $>$ $W(VI)$ (least oxidizing).⁶ The generic mechanism for thermal oxidation by POMs is outlined below:⁶

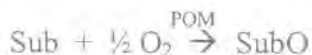
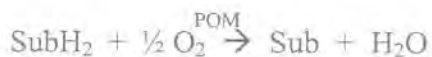


With the net equation:



Where POM_{ox} is the oxidized form of the POM, POM_{red} is the reduced form of the POM, OX is the oxidant, and OX_{red} is the reduced form of the oxidant.

The first step involves oxidation of the substrate to the product with concurrent reduction in the POM catalyst. This is followed by oxidation of the reduced POM back to the oxidized state with the reduction of the oxidant. This two-step mechanism results in two different types of thermal oxidations catalyzed by POMs - oxidative dehydrogenation and oxygenation (Eq. below).



Where SubH_2 is a hydrogen containing substrate, Sub is a substrate, and SubO is an oxidized substrate.

Catalytic Thermal Oxidation of Thioether Mustard Simulants by POMs and Metal Complexes

A comprehensive literature review of the last 10 years provides several references to thermal thioether oxidation by POMs and metal complexes. A brief review of this literature should be considered with the caveat that the majority of these papers use peroxides (and not molecular oxygen) as the terminal oxidant. Generally, mechanistic information is not presented; the point of this survey is to show the current state of the art rather than a critical review of the individual works. However, for particularly relevant studies, mechanistic and other data will be summarized.

In 1993, Hou and Hill published a study detailing the oxidation of the thioether tetrahydrothiophene (THT) by *tert*-butylhydroperoxide (TBHP) catalyzed by an organically modified Wells-Dawson POM.⁷ In this paper, the authors proposed that the POM activates the TBHP oxidant by a one-electron reduction, thereby forming alkylperoxy radicals. These radicals then selectively oxidize THT to THTO and reoxidize the catalyst.

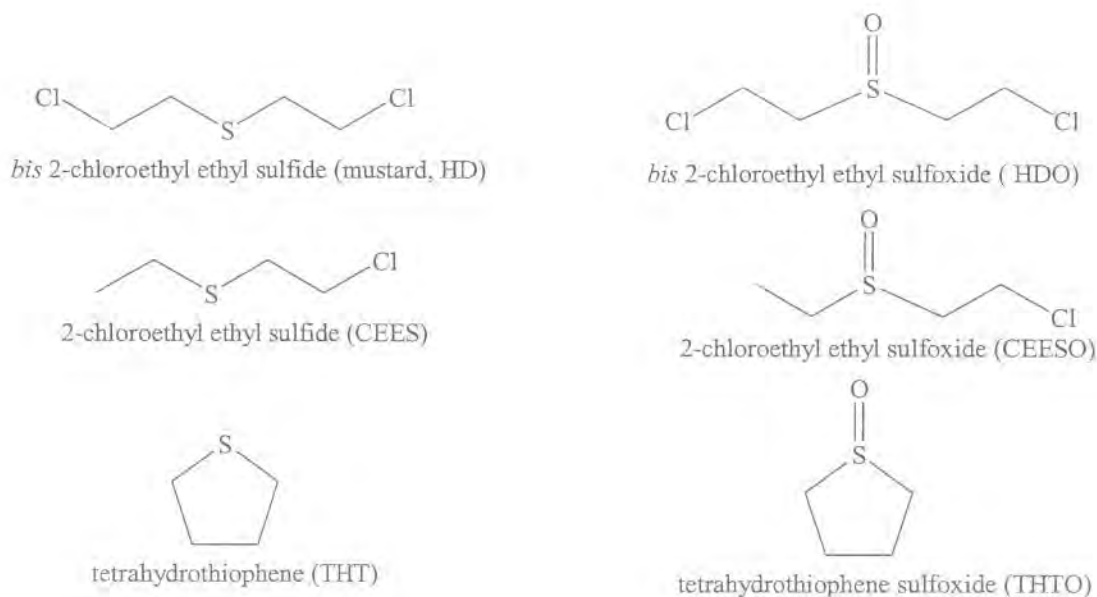


Figure 36. Chemical structures of the chemical warfare agent mustard, common thioether mustard simulants and their corresponding sulfoxides. Selective oxidation to the sulfoxide is preferred as these are less toxic than the sulfones.

Gall, Faraj and Hill provided a detailed kinetic study of THT oxidation by TBHP catalyzed by $H_5PV_2Mo_{10}O_{40}$.⁸ The authors noted that the selectivity of the oxidation was >99.9% for $H_5PV_2Mo_{10}O_{40}$, as opposed to 98 - 99% for the same reaction catalyzed by $H_3PMo_{12}O_{40}$ or $H_3PW_{12}O_{40}$. Further, mechanistic evidence and kinetic studies suggest initiation

of TBHP by the POM. Again, the overall reaction proceeds by initial thioether oxidation and POM reduction. This is followed by the reoxidation of the reduced POM by the TBHP.

Gall, Hill and Walker extended their examination of thioether oxidation by examining POMs supported on carbon materials as catalysts.^{9,10} The novelty of these papers stemmed from the heterogeneous nature of the catalysts. The carbon supports rendered the catalyst insoluble, while maintaining high selectivity (95 - 99% for THTO) and reasonable reaction rates at room temperature. Mechanistic studies provided data showing the oxidation began with a pre-association between the catalyst and substrate (POM:THT). The pre-associated catalyst then reduced the TBHP, initiating oxidation by a radical chain mechanism. Again, catalysis proceeds by an initial POM oxidation of the substrate (vide supra).

Recently, Kholdeeva et al. published the oxidation of thioethers by a novel Ti-containing POM using H_2O_2 as the oxidant.¹¹ Unfortunately, the oxidation was not very specific, and the thioether substrates were over-oxidized to the sulfone and other products.

Consideration of the literature to date has shown that POMs are capable of decontaminating (i.e. selectively oxidizing toxic reactants to non-toxic products) thioethers. However, the observation of significant reactivity in heterogeneous systems (catalyst totally insoluble) has been limited to reactions with a reactive cooxidant (TBHP) or elevated temperatures and pressures. Oxidation of thioethers using molecular oxygen by POMs or metal complexes has only recently been achieved.

Gall and Hill published a seminal paper in 1996 that demonstrated the oxidation of THT by molecular oxygen using POMs.¹² Selective oxidation of THT to THTO was achieved by a variety of combinatorially evaluated vanadium and molybdenum containing POMs at 95 °C and 1.52 atm. While these conditions are not ambient, this was the first paper to demonstrate that POMs are capable of catalyzing selective O_2 (air)-based oxidations of thioethers. Product distribution analysis showed that THTO₂ (the sulfone product resulting from further oxidation of THTO) was not produced in detectable quantities.

In 1999, Wagner and Bartram reported the decontamination of HD and the nerve agent VX¹³ by silver and sodium impregnated zeolites. This work demonstrated that Ag or Na doping of the zeolite increased the reactivity for HD decontamination at ambient temperature and pressure. However, the associated reaction products were toxic (i.e. the oxidation was not selective) rendering the usefulness of the chemistry questionable.

In 2000, Xu, Boring and Hill suspended $H_5PV_2Mo_{10}O_{40}$ on a variety of cloths and reported their heterogeneous activity for aerobic oxidation of THT.¹⁴ This work built on the earlier successful research of Gall, Hill and Walker.⁹ Significantly, these oxidations were accomplished at near ambient conditions. Again, the oxidation of THT was selective to THTO and conducted heterogeneously with the substrates in the liquid phase and the catalysts in the solid phase. While rigorous mechanistic information was not obtained, preliminary evidence (radical trapping) suggested that autoxidation was important in the reaction.

Building on the previous work in the Hill group, it was known that $PV_2Mo_{10}O_{40}^{5-}$ was an effective thermal catalyst for thioether oxidation. The work of Wagner and Bartram demonstrated the utility of Na and Ag as metals for heterogeneous thioether oxidation. Therefore, it was reasoned that synthesis of the Ag^+ salt of $PV_2Mo_{10}O_{40}^{5-}$ might yield a catalyst that displayed the desired properties.

Ag₅PV₂Mo₁₀O₄₀, a Heterogeneous Catalyst for Air-Based Selective Oxidation at Ambient Temperature

The development of molecules or materials that catalyze the selective oxidation of organic compounds using only air (or O₂) under ambient conditions is as potentially important technologically as it is challenging to achieve.^{15,16,17} Solid-state catalysts with such activity could be utilized for purifying air by the selective oxidation of the toxic agents therein including sulfur compounds (thioethers, thiols, H₂S),¹⁸ and others. Unfortunately, the ability to catalyze selective (non-radical-chain) organic oxidations by O₂ without the consumption of a reducing agent is difficult. With one exception,¹⁹ the few homogeneous species that catalyze non-radical chain, reductant-free O₂-based organic oxidations are all documented to proceed under conditions well above those in the ambient environment.²⁰⁻²⁴ The additional requirement of effective operation as a solid makes the task of catalyst development more problematical still.

We report here the preparation, structure and properties of a material, Ag₅PV₂Mo₁₀O₄₀ (Ag₅I), that catalyzes selective O₂ sulfoxidation of 2-chloroethyl ethyl sulfide (CEES, a common simulant for mustard) to its corresponding far less toxic sulfoxide (CEESO) when present simply as a low-surface-area powder using the ambient environment (room temperature and 1.0 atm of air).

All chemicals were obtained from Aldrich Chemical Co. (Milwaukee, WI) and used without further purification. Reactions were monitored with a Hewlett-Packard 6890 gas chromatograph equipped with a flame ionization detector and a 5% phenyl methyl silicone capillary column. Infrared spectra were determined as KBr pellets (2 - 5 wt % of the sample) using a Nicolet 510 M FTIR. ⁵¹V NMR spectra were acquired on a General Electric QE-300 (300 MHz) NMR referenced to a 10 mM H₄PVMo₁₁O₄₀ in 0.60 M NaCl (δ = -533.6 ppm relative to neat VOCl₃; chemical shifts are reported relative to VOCl₃ at δ = 0 ppm). X-ray data were collected on a Bruker XS D8 single crystal diffractometer equipped with a SMART-APEX CCD area detector. Elemental analyses were performed by Galbraith Laboratories Inc., Knoxville, TN. Specific Surface Areas (SSA) were determined with a Quantachrome NOVA 2200 Gas Sorption Analyzer using the 5-point Brunauer, Emmet and Teller (BET) method.

Na₅PV₂Mo₁₀O₄₀·xH₂O was synthesized and purified according to the literature procedure.²⁵ Na₅PV₂Mo₁₀O₄₀ (39.5 g, 21.4 mmol) was dissolved in 100 mL of distilled water at room temperature. Any undissolved POM was removed by filtration over a medium fritted funnel to yield a bright red-orange solution (0.214 M POM). An aliquot of this solution (40 mL, 8.55 mmol POM) was removed to which AgNO₃ (7.26g, 42.7 mmol) was added. Addition of AgNO₃ resulted in immediate precipitation of a red-orange amorphous powder. The precipitate was removed by suction filtration over a medium fritted funnel. The product was washed three times with room temperature water, three times with ether and then allowed to dry on the funnel (yield 5.07 g, 26.1% based on Na₅PV₂Mo₁₀O₄₀). TGA and DSC data showed Ag₅I was stable up to 832 °C. Water molecules of solvation (11 per POM, ~8.4 % weight loss) were driven off between 36 to 450 °C. Anal. Calcd. (found) for Ag₅PV₂Mo₁₀O₄₀: Ag, 23.74 (23.99); Mo, 42.82 (44.30); P, 1.36 (1.29); V, 4.50 (4.80) FTIR (KBr, 1100-400 cm⁻¹): 1073 (sh), 1062 (m), 1048

(m), 946 (s), 863 (m), 777 (vs) cm^{-1} . $\text{SSA} = 0.93 \text{ m}^2 \text{ g}^{-1}$. X-ray quality crystals were obtained by diffusion of diethyl ether into an acetonitrile solution of Ag_5I at 25°C .

A stock solution of CEES (0.275 M) was prepared in 2,2,2-trifluoroethanol with 1,3-dichlorobenzene added as an internal standard. The different catalysts were placed in 18-mL glass vials fitted with polytetrafluoroethylene (PTFE) septa and screw tops. Aliquots (2 mL) of CEES solution were added to each vial, and each reaction was allowed to proceed for 11.9 days at room temperature with stirring (400 rpm). All reactions were monitored by GC.

Confirmation of Reaction Stoichiometry.

Ag_5I (0.3008 g, 1.33×10^{-4} mol) was placed in a 25-mL Schlenk flask with 5.0 mL of a 0.2576 M solution of CEES in 2,2,2-trifluoroethanol. The flask was connected to a modified manometer and the system was purged with oxygen. The flask was then submerged in a 40°C water bath and allowed to thermally equilibrate. The volume of consumed oxygen versus time was recorded. The system was allowed to react for 36 hrs.

Confirmation that the Solid is the Active Catalyst by Filtration.

Ag_5I (0.292 g, 1.29×10^{-4} mol) was added to a glass vial fitted with a PTFE septum to which 4.5 mL of a 0.257 M solution of CEES in 2,2,2-trifluoroethanol was added. The reaction mixture was purged with O_2 , placed in a thermostated water bath at 40°C , and the suspension was stirred at 200 rpm. The reaction was monitored for 43 h during which aliquots were removed and analyzed by GC. After 43 h, the vial was removed from the water bath and the contents centrifuged and then filtered through a pipette that had been tightly packed with cellulose. The clear, very faint yellow supernatant was placed in a new vial fitted with a PTFE septum. The contents and vial were then purged with O_2 , placed back into the 40°C water bath, and stirred at 200 rpm. The recovered yellow-orange powder (POM) was mixed with 5.0 mL of fresh 0.257 M CEES solution in a second vial. The vial was fitted with a PTFE septum, and the vial and contents purged with O_2 . The vial was then placed back into the 40°C water bath, and the contents stirred at 200 rpm. All reactions were monitored by GC. The resuspended POM was allowed to react for 40 h, after which time the reaction vessel was removed from the water bath and the contents centrifuged and then filtered through a pipette that had been tightly packed with cellulose. The clear, very faint green supernatant was placed in a new vial, fitted with a PTFE septum and purged with O_2 . The reaction mixture was then put back into the 40°C water bath, and stirred at 200 rpm. The recovered yellow-green powder (POM) was placed into a vial which contained 5.0 mL of fresh 0.257 M CEES solution. The vial was fitted with a new PTFE septum and the contents and vial purged with O_2 . The vial was then placed back into the 40°C water bath and the reaction stirred at 200 rpm. GC was used to monitor all reactions.

Spectroscopic Assessment of Ag_5I Solubility.

Ag_5I (0.146 g, 6.43×10^{-5} mol) was suspended in the reaction mixture, containing TFE (2.0 mL), CEES (0.1 mL) and 1,3-dichlorobenzene (25 μL) as a reference. The mixture was stirred at 400 rpm for a 15 min and then centrifuged, followed by filtering through a pipette packed with cellulose. The clear supernatant was collected and the partially reacted Ag_5I was resuspended in a fresh reaction mixture. After stirring for 30 min, the reaction mixture was again centrifuged, followed by filtering through a cellulose packed pipette. This process was repeated

11 times at room temperature, at 40 °C, and at different stirring times (varying from 15 min to 18 h). At the conclusion, the collected supernatants (~20 mL) were combined, concentrated by roto-evaporation to a volume of 3 mL and filtered through a fine fritted funnel. The resulting solution was clear and very faintly yellow. An aliquot was removed and placed in an IR solution cell fitted with AgBr windows and a 0.015 mm Teflon spacer. Examination of the IR spectrum indicated no POM (absence of the M-O-M (797 cm^{-1}) and P-O (1046 cm^{-1}) bands). The solution (1 mL aliquot) was placed in a 5-mm NMR tube with a small amount of CD_3CN to achieve solvent lock. The sample was placed in the NMR and 3300 scans were acquired. No vanadium peaks were observed. To insure that any vanadium present was oxidized to diamagnetic $\text{d}^0 \text{V(V)}$ (reduced vanadium is paramagnetic and therefore would cause line-broadening and possibly no NMR signal at all) the sample was removed and bromine was added to the NMR tube. The sample was shaken vigorously and placed back into the NMR. Again, 3300 scans were acquired, and no vanadium peaks were observed. Finally, the 3 mL of concentrated solution was again concentrated by roto-evaporation until only a dark, oily substance remained. This was placed in an IR solution cell, fitted with AgBr windows and analyzed by IR. The spectrum did not display any bands associated with the $\text{Ag}_5\text{1}$ catalyst.

Inhibition of the Reaction by DMSO.

$\text{Ag}_5\text{1}$ (0.104 g, 4.58×10^{-5} mol) was suspended in 10 mL of a 0.185 M solution of CEES in 2,2,2-trifluoroethanol which had been placed in a glass vial with a PTFE septum. DMSO (0.14 mL, 2.0 mmol, used as a model for CEESO) was added to the system, and it was allowed to react under ambient conditions. A similar reaction (identical experimental conditions but without addition of DMSO) was run in parallel (see Figure 3). After 48 and 72 h, additional aliquots of DMSO (0.14 mL, 2.0 mmol) were added to the reaction mixture. Both reactions were monitored using quantitative GC.

Substrate Adsorption onto the Catalyst.

A stock solution of CEES (0.1047 M) was prepared in 2,2,2-trifluoroethanol with 1,3-dichlorobenzene added as an internal standard. The CEES solution was placed in a 18-mL glass vial fitted with a PTFE septum and screw-top. The solution was stirred at 400 rpm at room temperature for 2.6 hours, during which aliquots were removed and analyzed by GC. $\text{Ag}_5\text{1}$ (0.130 g, 5.26×10^{-5} mol) was then added to the stirring solution and the concentrations of CEES and $\text{CH}_3\text{CH}_2\text{SCH}_2\text{CH}_2\text{OH}$ (hydrolysis product of CEES) were monitored by GC. After 8.4 hours, 5.26×10^{-5} mols of CEES was absorbed onto 3.53×10^{-5} mols of catalyst. After reaction, the green (reduced form) catalyst was removed from the reaction mixture by suction filtration, suspended in TFE and washed for an hour, isolated and then dried in vacuo. This process was repeated three times, with the final in vacuo drying done overnight. Solid FTIR (5% KBr) analysis of the catalyst revealed new bands present at 3300 cm^{-1} (C – H stretching) and 1100 cm^{-1} (likely sulfoxide stretch) as well as the intact POM skeleton.

X-ray crystallography of $\text{Ag}_5\text{1}$ after reaction failed to yield a viable structure of CEESO bound to the catalyst. However, the X-ray data indicated CEESO molecules proximal to the Ag(I) centers. Elemental analysis confirmed the presence of S on the recovered catalyst.

Calculation of Surface Accessible Ag₅1.

1. What is the size of the Ag₅1 catalyst particles?

Assume spherical catalyst particles

Each Ag₅1 unit has a surface area of 1.2 nm²
 based on analysis of the packing diagram for crystalline Ag₅1.

Spherical catalyst particles have 0.93 m² g⁻¹ surface area from BET analysis

Density of Ag₅1 from X-ray crystallography = 3 • 10⁶ g m⁻³

$$\text{Volume (v)} = \frac{4}{3} \pi r^3$$

$$\text{Surface (s)} = 4 \pi r^2$$

$$\text{Density (d)} = \frac{\text{mass (m)}}{\text{volume (v)}}$$

$$\text{Specific Surface Area (SSA)} = \frac{s}{m} = \frac{4 \pi r^2}{\frac{4}{3} \pi r^3 d} = \frac{3}{rd}$$

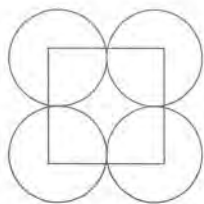
$$r = \frac{3}{\text{SSA} \times d} = \frac{3}{0.93 \text{ m}^2 \text{ g}^{-1} \times 3 \bullet 10^6 \text{ gm}^{-3}} = \frac{1}{10^6} \text{ m} = \sim 1 \mu\text{m}$$

thus, diameter of a Ag₅1 catalyst sphere = 2000 nm

2. How many Ag₅1 molecules are on the surface of the 1000 nm radius sphere?

$$n_s = \frac{s}{1.2 \text{ nm}^2} = \frac{4 \pi r^2}{1.2 \text{ nm}^2} = \frac{4 \pi (1000 \text{ nm})^2}{1.2 \text{ nm}^2} = 1.0 \bullet 10^7 \text{ molecules on the surface}$$

3. How many Ag₅1 molecules are in a 1000 nm radius sphere?



x = distance between catalytic
 spheres = $(1.2 \text{ nm}^2)^{-2} \cdot 1.2 \text{ nm} = 1.2 \text{ nm}$

$$n_{\theta} = \frac{\text{volume}}{x^3} = \frac{\frac{4}{3} \pi^3}{(1.2 \text{ nm})^3} = \frac{\frac{4}{3} \pi (1000 \text{ nm})^3}{(1.2 \text{ nm})^3} = 2.4 \cdot 10^9 \text{ Ag}_5\mathbf{1} \text{ molecules in the } 1 \mu\text{m sphere}$$

4. What percentage of $\text{Ag}_5\mathbf{1}$ molecules is on the surface?

$$\frac{n_s}{n_{\theta}} \times 100 = 0.41\% = \text{Ag}_5\mathbf{1} \text{ molecules are on the surface}$$

Thus, if there are 9.6 observed turnovers per mole of POM molecules and only 0.42% of these POMs are surface accessible then $(9.6/0.0041) = \sim 2300$ turnovers per surface exposed $\text{Ag}_5\mathbf{1}$ molecule

$\text{Ag}_5\mathbf{1}$, a salt of the redox active polyoxometalate (POM), $\text{PV}_2\text{Mo}_{10}\text{O}_{40}^{5-}$ (**1**) and a redox active d-block cation, Ag(I) is made by a simple metathesis precipitation between $\text{Na}_5\text{PV}_2\text{Mo}_{10}\text{O}_{40}$ and AgNO_3 in water. Two other Ag salts of POMs have been reported.^{26,27} Thermogravimetric analysis of $\text{Ag}_5\mathbf{1}$ indicates it is stable up to 832°C . Water molecules of solvation (11 per POM, $\sim 8.4\%$ weight loss) are evolved from 36 to 450°C . $\text{Ag}_5\mathbf{1}$ is more stable than the precursor, $\text{Na}_5\text{PV}_2\text{Mo}_{10}\text{O}_{40}$ (832°C versus 785°C). While the solubility of $\text{Ag}_5\mathbf{1}$ is too low to facilitate acquisition of NMR spectra, it is sufficiently soluble in acetonitrile for diffraction quality crystals to be grown.

The dominant structural feature of $\text{Ag}_5\mathbf{1}$ (Figure 37) recrystallized from MeCN and Et_2O involves two $\text{PV}_2\text{Mo}_{10}\text{O}_{40}^{5-}$ units bridged by two Ag(I) ions (Ag(7) and Ag(8)), each of which bonds to both bridging and terminal oxygens of the POM units. Each POM has, in addition, two non-bridging Ag(I) ions. All the Ag(I) centers are 4 coordinate, with terminally coordinated acetonitrile molecules (one each for the POM-bridging Ag centers and two each for the non-bridging Ag centers).

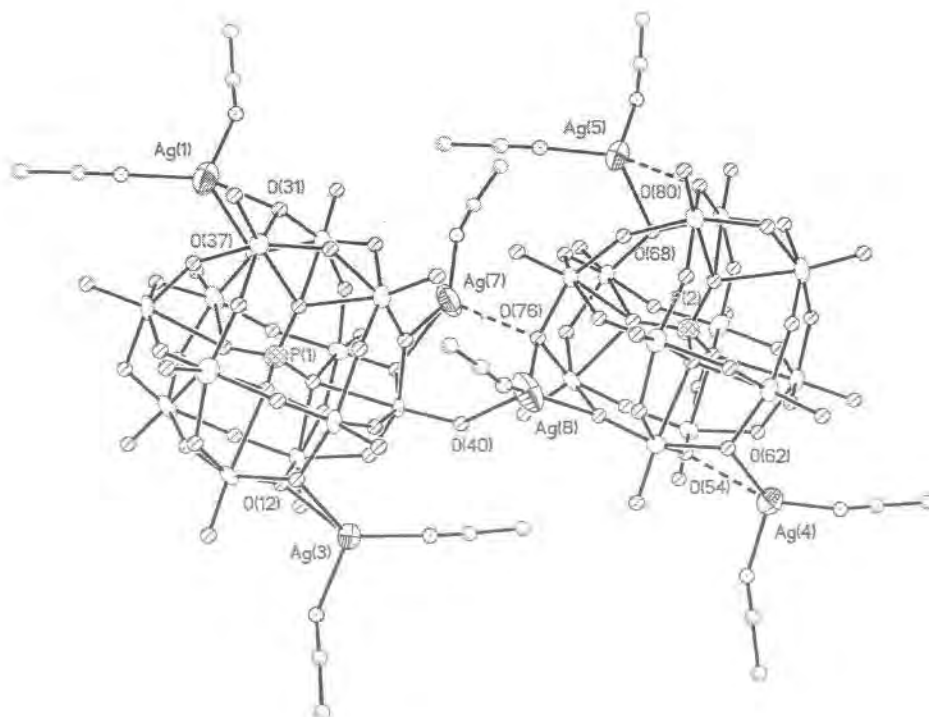


Figure 37. Structure of $\text{Ag}_5\text{1}$ crystallized from MeCN and Et_2O (formula: $\text{Ag}_{10.4}\text{P}_2\text{V}_4\text{Mo}_{20}\text{O}_{80}(\text{NO}_3)_{0.4} \cdot (\text{MeCN})_{17.3}(\text{H}_2\text{O})_{1.5}$). Each metal position on the POM has 1/6 V character and ca. 5/6 Mo character. Selected average bond lengths (\AA) and angles (deg): Ag - O_t , 2.40; Ag - O_b , 2.49; Ag - N_s , 2.24; P - O_c , 1.53; Mo - O_t , 1.68; Mo - O_b , 1.96; O_c - Mo, 2.42; O_b - Ag - O_b , 62.9; Mo - O_b - Mo, 89.0; O_c - P - O_c , 109.4; where O_t = terminal oxygen, O_b = μ_2 - oxo, O_c = μ_3 - oxo, N_s = acetonitrile (solvent) nitrogen. Solvent (MeCN and H_2O) and silver ions not bound to the POM units have been omitted for clarity.

Table 3. Crystal Data and Structure Refinement for $\text{Ag}_{10.4}\text{P}_2\text{V}_4\text{Mo}_{20}\text{O}_{80}(\text{NO}_3)_{0.4} \cdot (\text{MeCN})_{17.3}(\text{H}_2\text{O})_{1.5}$ (**Ag51**) Crystallized from $\text{CH}_3\text{CN}/\text{Et}_2\text{O}$.

Empirical formula	$\text{C}_{34.6} \text{Ag}_{10.4} \text{Mo}_{20} \text{N}_{17.7} \text{O}_{82.7} \text{P}_2 \text{V}_4$
Formula weight	5293.07
Temperature	100(2) K
Wavelength	0.71073 Å
Crystal system	Triclinic
Space group	P-1
Unit cell dimensions	$a = 13.038(5)$ Å $b = 21.175(8)$ Å $c = 22.353(8)$ Å $\alpha = 85.966(7)^\circ$ $\beta = 83.556(7)^\circ$ $\gamma = 77.854(7)^\circ$
Volume	$5988(4)$ Å ³
Z	2
Density (calculated)	2.936 Mg/m^3
Absorption coefficient	4.093 mm^{-1}
F(000)	4888
Theta range for data collection	1.61 to 30.69° .
Reflections collected	71417
Independent reflections	36109 [R(int) = 0.1276]
Completeness to $\theta = 30.69^\circ$	97.2 %
Absorption correction	Empirical
Goodness-of-fit on F^2	1.032
Final R indices [I > 2 sigma (I)]	$R_1 = 0.0937$, $wR_2 = 0.1731$

Figure 38 shows the selective oxidation of CEES to the corresponding sulfoxide, CEESO, in 2,2,2-trifluoroethanol (TFE) catalyzed by **Ag51** using the ambient environment (air = 21% O₂ at 1 atm pressure and room temperature). TFE was used as the solvent because it assured that CEES and CEESO were soluble but that the catalyst, **Ag51**, was completely insoluble. Further, fluorinated media are attractive for protective applications against toxic agents.²⁸ Significantly, there is no reaction in the absence of catalyst or in the presence of the POM precursor Na₅PV₂Mo₁₀O₄₀ (soluble), AgCl (insoluble) or both Na₅PV₂Mo₁₀O₄₀ and AgCl together. To our surprise, AgNO₃ also proved to have detectable activity for aerobic CEES oxidation under ambient conditions. However, a comparison between the AgNO₃, which is soluble, and **Ag51**, which is insoluble, is not meaningful. NaNO₃ alone is inactive indicating that NO₃⁻ is not the catalyst. Interestingly, the corresponding tungsten analogue of **Ag51**, Ag₅PV₂W₁₀O₄₀, and the Wells-Dawson complex, Ag₉P₂V₃W₁₅O₆₂, are both inactive under ambient conditions. Clearly, there is a synergistic effect between the Ag(I) cationic centers and the redox active V(V) centers

inside a fairly labile **1** (polymolybdates like **1** are far more labile than their polytungstate counterparts). Significantly, ~2300 molecules of CEESO are produced per mole of surface accessible $\text{Ag}_5\text{1}$ (based on a $\sim 1.2\text{-nm}^2$ cross-sectional area for $\text{Ag}_5\text{1}$ derived from the X-ray structure and a 5-point BET determined surface area of $0.93\text{ m}^2\text{ g}^{-1}$) after 7.1 days.

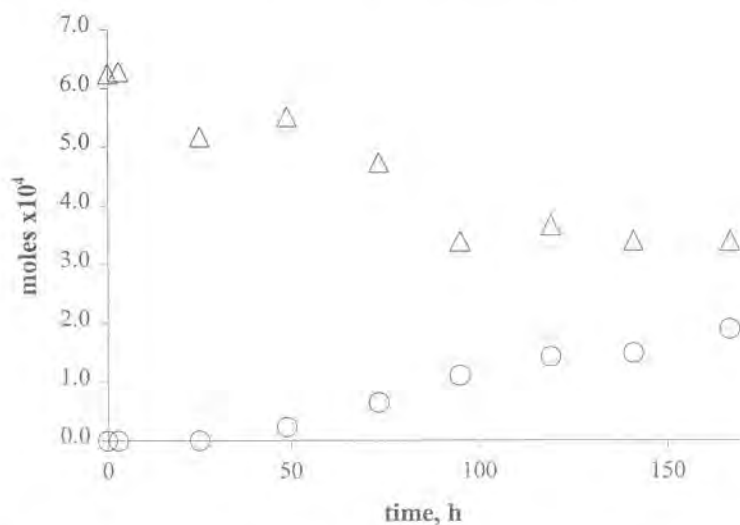


Figure 38. The heterogeneous, ambient-temperature air oxidation of $(\text{CH}_3\text{CH}_2\text{SCH}_2\text{CH}_2\text{Cl})$, CEES; \triangle) to $(\text{CH}_3\text{CH}_2\text{S(O)CH}_2\text{CH}_2\text{Cl})$, CEESO; \circ) catalyzed by $\text{Ag}_5\text{1}$ powder under ambient conditions (room temperature and 1.0 atm air). CEES (0.275 M) and $\text{Ag}_5\text{1}$ in 2,2,2-trifluoroethanol with 1,3-dichlorobenzene (internal standard) were stirred at 400 rpm in 18-mL glass vials fitted with Teflon septa. CEES and CEESO were quantified by GC.

Table 4. Ambient-Temperature Air Oxidation of CEES in 2,2,2-Trifluoroethanol Catalyzed by Selected Materials.^a

catalyst	mol of POM, 10^{-5}	mol of Ag salt, 10^{-5}	TON ^b
None	NA	NA	0 ^c
$\text{Ag}_5\text{1}$	2.30	NA	2300
$\text{Na}_5\text{PV}_2\text{Mo}_{10}\text{O}_{40}$	2.80	NA	0 ^c
AgCl	NA	3.35	0 ^c
$\text{Na}_5\text{PV}_2\text{Mo}_{10}\text{O}_{40} + \text{AgCl}$	2.90	14.5	0 ^c
$\text{Ag}_5\text{PV}_2\text{W}_{10}\text{O}_{40}$	2.45	NA	0 ^c
$\text{Ag}_9\text{P}_2\text{V}_3\text{W}_{15}\text{O}_{62}$	2.50	NA	0 ^c

^aReaction conditions: 0.275 M CEES (~20 mol CEES:1 mol catalyst) in 2,2,2-trifluoroethanol at room-temperature for 7.1 days. Reactions were quantified by GC (5% phenyl methyl siloxane column) using 1,3-dichlorobenzene as an internal standard. ^bTurnovers = [(mol of CEESO)/(mole of surface accessible $\text{Ag}_5\text{1}$)]. ^cBelow the detectable limit.

There is inhibition of the reaction by the CEESO product that is observable in Figure 39. When DMSO was used as a model for CEESO, inhibition of the initial reaction rate was observed (Figure 40). Further, CEES binds to the catalyst (1.6 mol of CEES per mol of catalyst after 8.4 hours) prior to oxidation to CEESO (Figure 41).

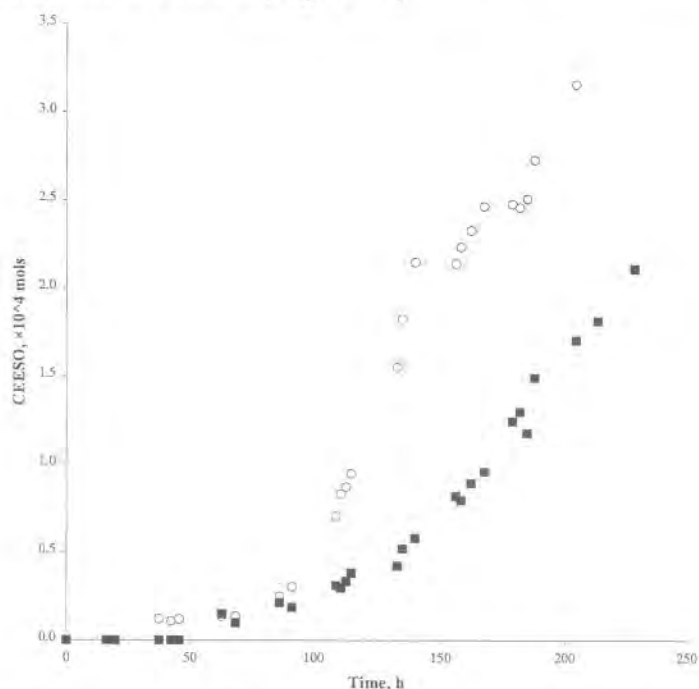


Figure 39. Reaction profile for the ambient-temperature air oxidation of CEES (O) to CEESO catalyzed by Ag_51 in 2,2,2-trifluoroethanol and its inhibition by added DMSO (■).

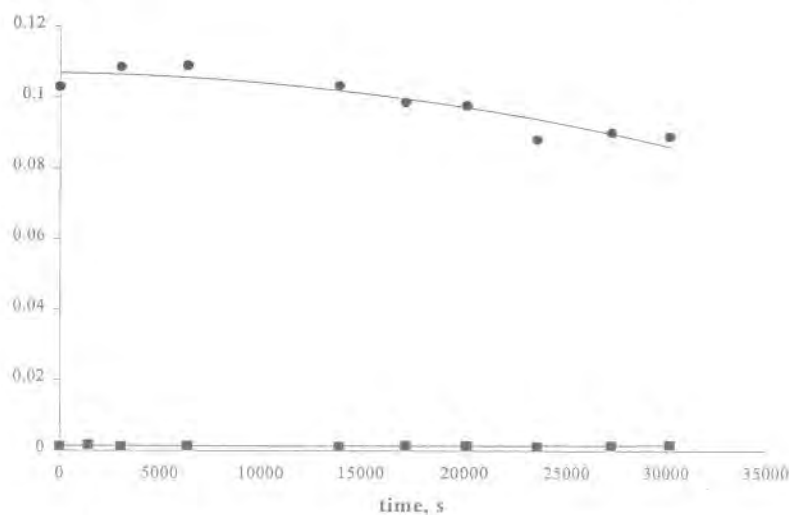


Figure 40. Adsorption of CEES onto the solid catalyst Ag_51 . Concentrations of CEES (●) and the hydrolysis product ($\text{CH}_3\text{CH}_2\text{SCH}_2\text{CH}_2\text{OH}$ (■)) are plotted versus time. After 8.4 hours, 5.26×10^{-5} mols of CEES was absorbed onto 3.53×10^{-5} mols of catalyst. No CEESO was detected.

A key concern regarding heterogeneous catalysts for liquid phase reactions is whether the observed reactivity derives from the actual insoluble solid catalyst or from a small quantity of dissolved catalyst. Two related experiments indicate that it is the actual Ag_5I powder that accounts for the catalysis. First, Ag_5I is extremely insoluble in the catalytic medium (2.0 mL of TFE, 0.257M in CEES; 1.0 atm of air). This was concluded by stirring the same sample of Ag_5I eleven consecutive times in this medium, filtering each, concentrating the combined supernatants to 3.0 mL and examining this solution by FTIR, UV-Vis and ^{51}V NMR spectroscopy. No Ag_5I was detectable. Second, Ag_5I was used in catalysis and filtered. The catalytic activity of both the separated solid and the supernatant were then evaluated by product distribution analysis (only CEESO present) and early reaction kinetics. This was done twice, and the recovered Ag_5I powder had the same catalytic activity after 1 and 2 recoveries. In contrast, the supernatants were all catalytically inactive. These combined results argue strongly that the solid Ag_5I is the actual catalyst, and that catalysis is not due to the dissolution and reactivity of any Ag_5I or any soluble AgNO_3 impurity.

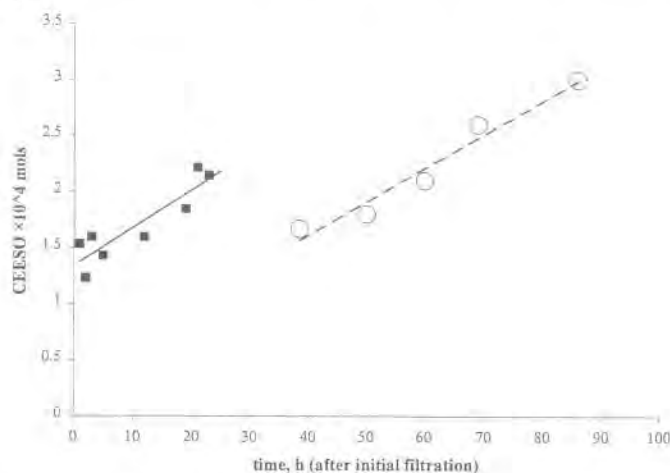


Figure 41. Continued oxidation of CEES to CEESO after isolation and resuspension of the heterogeneous catalyst.

The solid line is a plot of CEESO formation after Ag_5I was removed from the initial reaction mixture, isolated and resuspended in a reaction vial with fresh CEES solution. The dashed line is a plot of CEESO formation after Ag_5I was isolated a second time and resuspended in another reaction vial with fresh CEES solution. The catalytic activities of the clear filtrates from both trials were monitored. None showed any catalytic activity whatsoever. Reaction conditions: CEES was 0.275 M (~20 mol CEES : 1 mol catalyst) in 2,2,2-trifluoroethanol at 40 °C (higher temperature used to increase rate of reaction). Reactions were quantified by GC (5% phenyl methyl siloxane column) using 1,3-dichlorobenzene as an internal standard.

Unfortunately, the heterogeneity of the insoluble catalyst Ag_5I precludes a meaningful assessment of the full rate law to clarify the reactive species. However, Ag_5I was isolated and characterized after ~2300 turnovers per surface exposed Ag_5I . Elemental analysis, FTIR (bands present at 3300 cm^{-1} (C – H) and 1100 cm^{-1} (likely S = O) and X-ray crystallography confirm the presence of CEESO proximal to the Ag in the recovered catalyst. In addition, the characteristic

dark green-blue color of the one-electron reduced form of **1**, $PV_2Mo_{10}O_{40}^{6-}$, forms rapidly in the presence of CEES, indicating that catalytic turnover likely involves the reduction of the d^0 V(V) center, followed by reoxidation, a process observed in other thioether oxidations catalyzed by vanadium containing POMs.²⁹⁻³¹

$Ag_5PV_2Mo_{10}O_{40}$ (**Ag₅1**) was prepared, characterized and evaluated as a catalyst for the heterogeneous and selective O_2 oxidation of 2-chloroethyl ethyl sulfide (CEES) to its corresponding far less toxic sulfoxide (CEESO) under ambient conditions (room temperature and 1.0 atm of air). **Ag₅1** is a salt of a redox active polyoxometalate (POM), $PV_2Mo_{10}O_{40}^{5-}$ and a redox active d-block cation, Ag(I). X-ray crystallography reveals that the dominant structural feature of the crystallized complex is two $PV_2Mo_{10}O_{40}^{5-}$ units bridged by two Ag(I) ions, each of which bonds to both bridging and terminal oxygens of the POM units. In addition, each POM has two non-bridging Ag(I) ions. All the Ag(I) centers are 4 coordinate, with terminally coordinated acetonitrile molecules (one each for the POM-bridging Ag centers and two each for the non-bridging Ag centers)

As a catalyst, **Ag₅1** achieves ~2300 turnovers (moles of sulfoxide product per mole of surface accessible **Ag₅1** in the powder) in 7.1 days. The catalytic action of **Ag₅1** is inhibited by the binding of the sulfoxide product. Two lines of evidence, spectroscopy (UV-Vis and ^{51}V NMR) and a reaction-filtration-reaction sequence methodology confirm that the actual solid **Ag₅1**, and not a small quantity of dissolved **Ag₅1**, is responsible for the observed catalysis.

Task 4. Acquisition and setup of permeation cup test system based on Chemical Agent Monitoring System (CAMS).

This task involved the purchase and setup of a penetration cell apparatus with a laboratory MINICAMS unit from CMS Field Products Group. This apparatus was used to examine the decomposition of CW simulants by [POM]RNP formulations contained in TSP (rTSP). This apparatus is based on a design used for identical experiments at the U.S. Army Medical Research Institute of Chemical Defense at the Aberdeen Proving Grounds, Maryland.

The MINICAMS Series 3000 unit is an automatic continuous air monitoring system using gas chromatography and sample collection with a pre-concentrator tube. The MINICAMS collects a simulant sample, performs an analysis and reports the result. The unit is capable of detecting all CW agents and their simulants at levels below the US Surgeon Generals' 8-hour Time-Weighted Average (TWA) concentrations.

This apparatus was used for penetration tests of the rTSP and for the experiments outlined in Task 6. At the point of entering into this project there was a key issue to resolve prior to continuation of testing rTSP against CW agent simulants. The overall problem was that the cream failed by drying and cracking on the MINICAMS test cell leading to overloading the system with simulant and ruining the test for cells that have not failed. This led to studying this problem from a few different areas.

- 1) Rheology. It was noted that the rTSP creams prepared in the lab have a different "feel and texture" than that of the base cream. It was thought that if more of the physical parameters of the rTSP were closely matched to the supplied base cream this would help minimize the cracking and consequently the breakthrough of simulant. A Brookfield rheometer was purchased to study the rheological properties of the rTRP.
- 2) Technique. Cell preparation was studied. Cells of rTSP were prepared and tested on the MINICAMS without CW simulants. Cells were examined with a common magnifying glass and a flashlight to help detect cracks and to determine how long the rTSP will last on the test cell without failure.
- 3) Dispersion. Another problem was even dispersion of the RNP into the TSP. Uneven dispersion could lead to premature cell failure by affecting the rheology of the TSP or allowing cracking to occur along the edges of RNP clumps. A few methods of preparation were tested to determine which lead to the best dispersion.

A method provided by Dr. E. Braue & CPT S. Hobson of USAMRICD was effective for solving the problems of dispersion of RNP into TSP. This was accomplished by adding RNP to magnetically stirred oil component of the base cream. After 24 hrs of stirring, further mixing was done with a mechanical mixer. The teflon powder was added in three portions to the above mixture, followed by the addition of another gram of oil. In the case where the RNP formed large aggregates, the aggregates were processed through a 200-mesh sieve prior to addition into the oil component.

It was found that rTSP prepared as described above at NMI was much more viscous than the base cream. Therefore, an effort was placed on preparing a rTSP cream formulation with a viscosity similar to that of the base cream. After a series of experiments, it was found that a

relatively small increase in the oil component resulted in a large reduction in viscosity. The rheometer was used to measure the viscosity of the rTSP at a constant temperature of 20°C. The samples were tested at a linear increasing rate of shear from 0 to 1000 s⁻¹ over three minutes. The viscosity of the rTSP was modified by addition of oil to that of the base cream. The effect of adding increasing amounts of oil to the mixtures are illustrated in Table 5.

Table 5. Effect of Addition of Oil to Initial Viscosity of rTSP

Sample	Percentage of Components			Initial Viscosity, Pas @ 20°C
	RN P	Teflon Powder	Oil	
Base Cream (ICD 3005)	none	50	50	40
[POM]TiO ₂ -1	2.55	47.45	50.00	85
[POM]TiO ₂ -2	2.47	47.93	51.60	60
[POM]TiO ₂ -3	2.46	45.80	51.74	54
[POM]TiO ₂ -4	2.41	44.93	52.66	42
ZnO-1	2.55	47.6	49.8	86
ZnO-2	2.34	43.76	53.90	63
ZnO-3	2.31	43.01	54.60	48
ZnO-4	2.28	42.62	55.10	42

As shown by the viscosity curves in Figure 42, the initial viscosity and overall viscosity decreased with increasing amounts of oil.

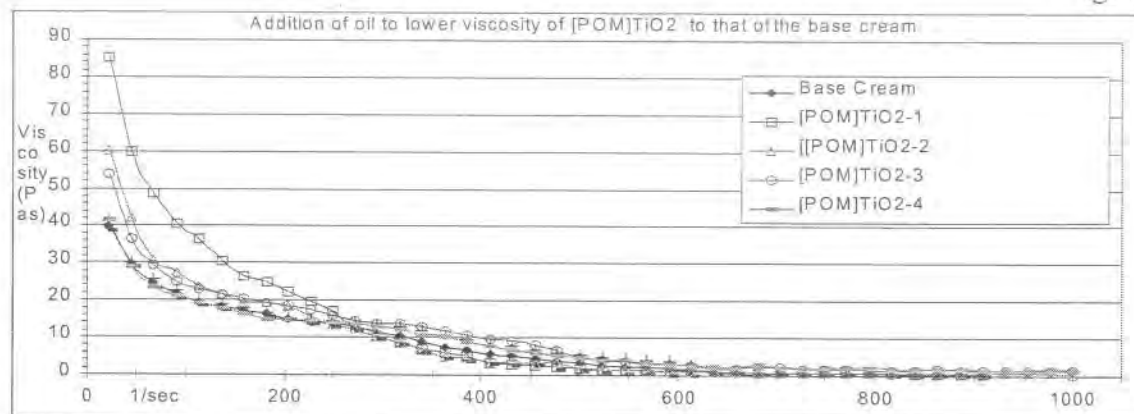


Figure 42. Effect of Oil Addition on the Viscosity of [POM]TiO₂ Containing Base Cream

This procedure was repeated successfully on the ZnO/TSP preparation from Table 6. In summary, we have produced rTSP with rheological characteristics similar to base cream with relatively minor changes in composition. The increased oil amounts helped minimize premature cream failure due to drying and cracking of the rTSP.

Task 5. Studies for the catalytic detoxification of simulants by POM/RNP in TSP.

This objective was designed to examine the catalytic decomposition of CW simulants by the [POM]RNP while it is embedded in the TSP.

Experiments with MINICAMS

The major thrust was to identify, and quantitate the amount of CEES that can be catalytically oxidized by the RNP supported POM (contained in the topical skin cream). However, it was quickly determined both experimentally and by review of the literature that CEES was a poor simulant for HD in vapor permeation studies. CEES was replaced by 2-chlorethyl phenyl sulfide (CEPS) as discussed in detail in NanoScale Materials' Interim Progress Report No. 18. A database was constructed using CEPS following protocol developed and utilized by Dr. E. Braue, and CPT S. Hobson, Drug Assessment Division at USAMRICD (Aberdeen Proving Grounds, MD). Permeation cells loaded with rTSP were each challenged with 10 μ l of CEPS in the vapor phase as a HD simulant.

Preparation of the rTSPs was accomplished by adding measured amounts of RNP or POM to the magnetically stirred perfluoropolyether oil component of the base cream. To prevent large aggregate formation, the RNP or POM was passed through a 200-mesh sieve prior to addition into the oil component. After 24 h of stirring, additional mixing was done with a mechanical mixer (Glas-Col GT Series Stirrer, Terre Haute, IN). The polytetrafluoroethylene powder was then added in separate portions to the stirring mixture, followed by the addition of more oil. Viscosity measurements were conducted at 20 °C with a Brookfield R/S-CPS rheometer (Middleboro, MA) at a linear increasing rate of shear from 0 to 1000 s⁻¹ over 3 min. The viscosities of the rTSP were normalized to the viscosity of the unmodified base TSP (ICD 3005). Penetration testing was performed using a Miniature Automated Continuous Air

Monitoring System (MINICAMS) with data collection and analysis using the Laboratory Monitoring System (LM-1001) (OI Analytical, CMS Field Products Group Pelham, AL). This multi-port sampling system collected samples on a sorbent bed followed by desorption and separation by gas chromatography and detection with a flame photometric detector. The permeation study was conducted by a two-step protocol developed and utilized at USAMRICD (Aberdeen Proving Grounds, MD). First, the amount of challenge agent that permeated the rTSP and TSP was monitored over a 20 h time frame. Second, the time required for 1000 ng of challenge agent to penetrate the cream was measured. Microsoft Excel and a proprietary DOS program (provided by Dr. E. Braue, and CPT S. Hobson, Drug Assessment Division, USAMRICD) were used to analyze the data obtained from the mini-CAMS permeation tests.

Results obtained throughout the project are summarized in Table 6 and Figures 43 and 44 below. The samples are listed in order of effectiveness of the rTSP to prevent simulant penetration.

Table 6. CEPS Permeation through Various rTSPs versus Time.

Ref.	Sample, weight %	% Oil	% Powder	Viscosity, Pas	Time (min) to 1000 ng CEPS Permeation	CEPS ng Permeation after 20 h
54.1	2.33% CommercialTiO ₂ /rTSP	53.24	44.43	44	401	3623
ICD 3005	Base Cream 08/03/01	50.00	50.00	37	525	2721
ICD 3005	Base Cream 11/27/01	50.00	50.00	37	594	2598
30.3	2.41%(10%CeO/TiO ₂)/rTSP	52.90	44.69	40	925	1695
26.1	2.41% [10%NaPOM TiO ₂]/rTSP	53.07	44.52	43	941	1670
36.1	2.40% RNP TiO ₂ /rTSP	53.06	44.54	41	992	1468
44.1	2.39%[2mol%(Ce(NO ₃) ₃ /Cu(NO ₃) ₂)/TiO ₂]/rTSP	53.48	44.13	38	1220	956
37.1	2.37% (0.4 mol % NaPOM/TiO ₂)/rTSP	53.65	43.99	40	1381	682
37.2	2.39% (2 mol%(AgNO ₃)/TiO ₂)/rTSP	53.23	44.38	44	1407	609
39.1	2.40% (0.4 mol % AgPOM/TiO ₂)/rTSP	53.24	44.36	44	1431	603
26.2	4.79% [10%NaPOM TiO ₂]/rTSP	53.26	41.96	38	1597	418
45.1	4.75%[2mol%(Ce(NO ₃) ₃ /Cu(NO ₃) ₂)/TiO ₂]/rTSP	53.33	41.92	39	2273	295
35.1	9.35% [10%NaPOM TiO ₂]/rTSP	52.55	38.10	42	2278	215
20.1	2.41% (2 mol%(AgNO ₃)/TiO ₂)/rTSP	52.66	44.93	42	5964	50

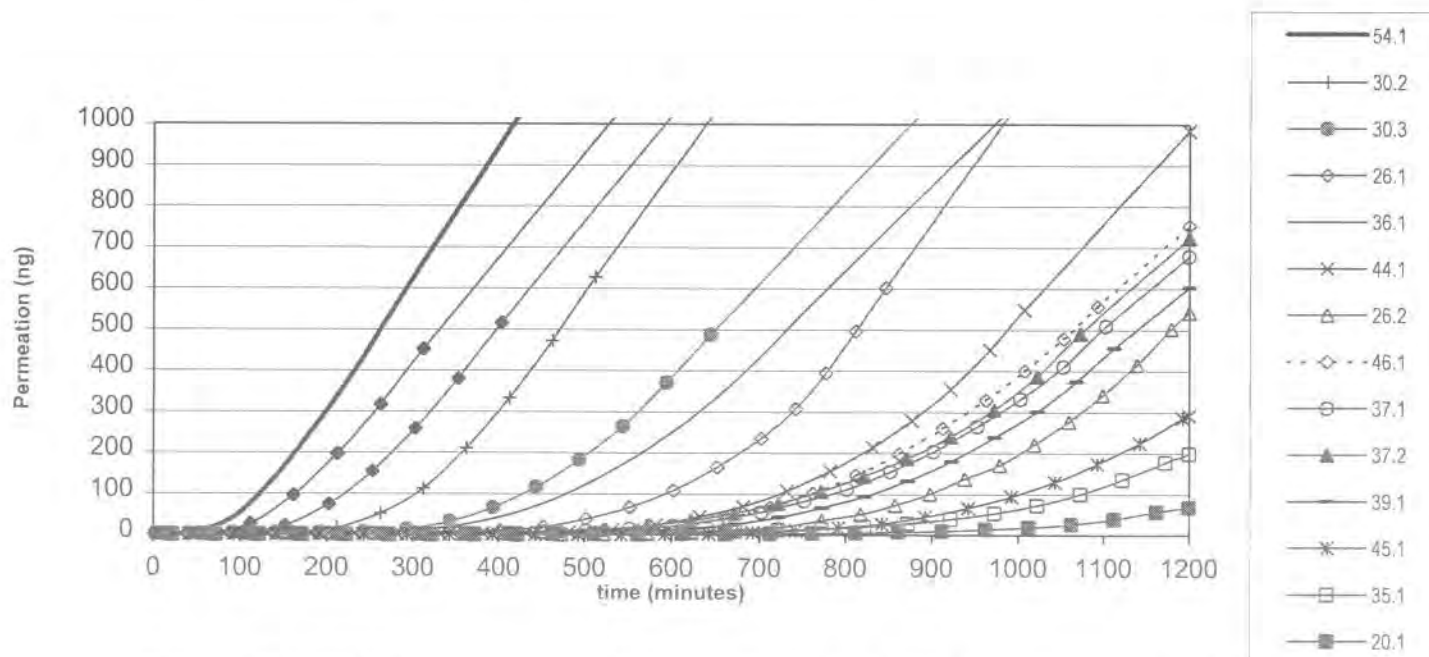


Figure 43. CEPS Permeation (ng) of rTSP vs Time (min). Reference Table 8 for Sample Labels.

The Government's rights to use, modify, reproduce, release, perform, display, or disclose technical data or computer software marked with this legend are restricted during the period shown on the cover page as provided in paragraph (b)(4) of the Rights in Noncommercial Technical Data and Computer Software--Small Business Innovative Research (SBIR) Program clause contained in the contract DAMD17-99-C-9012 with NanoScale Materials, Inc. (Formerly Nantek, Inc.). No restrictions apply after the expiration date (12 January 2007). Any reproduction of technical data, computer software, or portions thereof marked with this legend must also reproduce the markings.

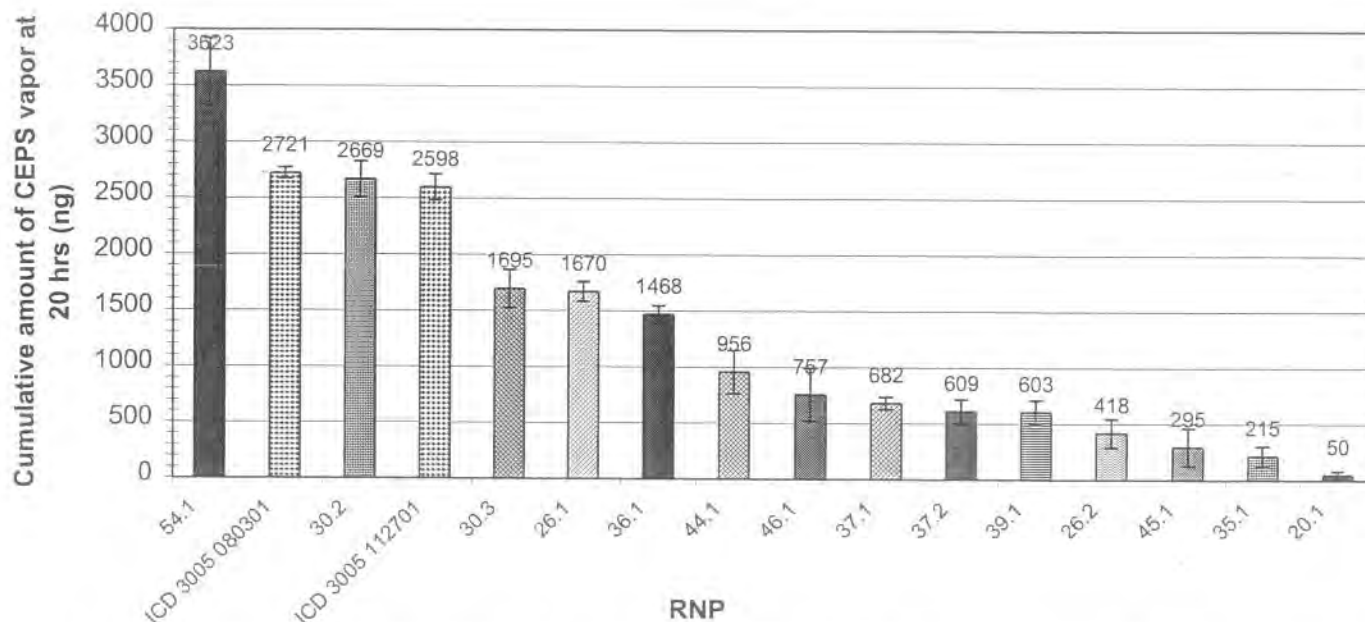


Figure 44. Cumulative Amount of 2-Chloroethyl Phenyl Sulfide (CEPS) Vapor Through a rTSP After 20 Hrs. Reference Table 8 for Sample Labels.

Incorporation of moieties that are active toward CWA simulant decontamination into the TSP dramatically improves the protective capabilities of TSPs (Figure 43). Importantly, by manipulation of the oil and powder components, loading the creams with catalysts can be accomplished without significantly altering the viscosity (and thus physical barrier properties) of the TSPs. In the data presented above, the AgNO_3 loaded cream (20.1) offered the greatest protective function, followed by the NaPOM loaded creams (35.1 and 26.2). rTSPs that were formulated with higher loadings of NaPOM offered increased protection. The data clearly shows a relationship between increased amount of NaPOM and the protective capability of the rTSP.

Experiments By FT-IR

The mixture of copper and cerium nitrates coated on titanium dioxide nanoparticles has been shown to be extremely effective for oxidation of CEES to the less toxic product CEESO. For these experiments, $[\text{Ce}(\text{NO}_3)_3\text{-Cu}(\text{NO}_3)_2]\text{TiO}_2$ was first incorporated into TSP cream (rTSP) and then challenged against CEES using typical FT-IR techniques to observe formation of CEESO. Uncoated titanium dioxide nanoparticles were also incorporated into TSP and analyzed for comparison.

The rTSP samples used for these experiments are the same that were prepared for the MINICAMS experiments listed above. Enough rTSP was added to the reaction flask of a special gas phase infrared cell equivalent to 0.1 g nanoparticles. A background spectrum was obtained and then CEES (14 μL) was injected into the reaction flask of the cell through a side-port. The

vapor phase of the sample was monitored as a function of time for up to five hours. The oxidation was observed by the formation of the sulfoxide peak at 1079 cm^{-1} .

Incorporation of the active component (Ce/Cu TiO_2 system) into the TSP does not impede reaction with CEES. While the reaction was slower due to the time for CEES to diffuse through the cream, the oxidation product CEESO (indicated by the growth of the sulfoxide peak at 1079 cm^{-1}) was clearly observed in the FT-IR spectrum (Figure 45). With uncoated TiO_2 in TSP no evidence of oxidation of CEES was observed in the five hour reaction time (Figure 45). Additionally, no other products of the destruction of CEES were observed in this spectrum, as expected with uncoated TiO_2 .

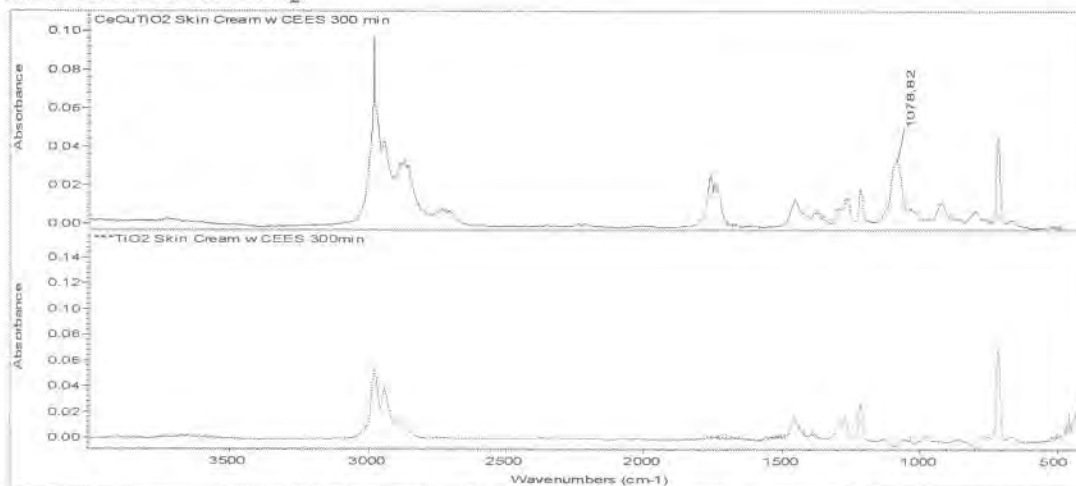


Figure 45. Spectra of CEESO in Ce/Cu TiO_2 rTSP (Top) and CEES With TiO_2 /rTSP (Bottom).

The oxidation of CEES to CEESO occurred as normally expected even after addition of the active component $[\text{Ce}(\text{NO}_3)_3\text{-Cu}(\text{NO}_3)_2]\text{TiO}_2$ to the TSP. The reaction was slower due to longer time needed for the CEES to diffuse through the cream.

Experiments By UV-Vis

Nanoparticles have been shown to be extremely effective at the destructive adsorption of paraoxon. When nanoparticles are coated with POMs to enhance reactivity with other agent simulants, the destructive adsorption ability with paraoxon is still intact and may actually be improved. For these experiments, coated and uncoated reactive nanoparticles (RNP) were incorporated into TSP cream (renamed rTSP for reactive topical skin protectants) and challenged with paraoxon to ensure the reactivity with paraoxon is not hindered by the skin cream. After extraction, analysis by UV-Vis was performed to quantify any remaining unadsorbed paraoxon.

The rTSPs used were the same as prepared for the above experiments on the FT-IR and MINICAMS. Reaction of rTSP samples with paraoxon was accomplished by adding a measured amount of rTSP (equal to 0.1 g nanoparticles) to screw cap jars. To the cream, neat paraoxon ($4.5\text{ }\mu\text{L}$) was injected and hand mixed for five minutes to ensure the paraoxon was evenly dispersed though out the cream. The color of the samples after the initial five minutes stirring period was recorded. The samples were then allowed to sit for 20 h during which the formation of p-nitrophenol (a product of the destruction of paraoxon) was monitored. Pentane (50 mL) was

then added to each jar with vigorous shaking for 2 h. An aliquot of the pentane layer was removed and the absorbance of the remaining paraoxon measured by UV-Vis spectroscopy.

From these experiments it was concluded that incorporation of nanoparticles as the active component in rTSP still allows destructive adsorption of paraoxon to occur. Table 7 shows each sample tested, the color observed, and the absorbance reading after 20 h of reaction with paraoxon. Hydrolysis of the paraoxon was apparent due to the deepening yellow color of the rTSP samples over time. Although impossible to extract all of the paraoxon from the cream samples, there is still apparent differences noted between the rTSP samples and the blank and control samples.

Table 7. Observations and absorbance of paraoxon after reaction with rTSP samples.

Sample	Color Observed (5 min)	Color Observed (20 h)	% Paraoxon Recovered
ICD 3005 (Blank)	Faint yellow tinge	White	32%
CMTiO ₂ /TSP (Control)	White	White	16%
APTiO ₂ /TSP	Pale yellow	Medium lemon yellow	3%
[2mol%AgNO ₃]TiO ₂ /TSP	Pale yellow	Medium lemon yellow	3%
[10wt%NaPOM]TiO ₂ /TSP	Light yellow	Medium yellow	5%
[2mol%Ce(NO ₃) ₃ -Cu(NO ₃) ₂]TiO ₂ /TSP	Pale yellow	Medium lemon yellow	4%

The absence of any color change in the ICD 3005 cream (blank) and the TSP with commercial TiO₂ (control) indicated minimal, if any reaction of the paraoxon. The amount of paraoxon recovered from the control was 50% of the amount recovered from the blank. This may be due to adsorption but not destruction of the paraoxon by the commercial TiO₂. The 88% decrease in absorbance of paraoxon in the rTSP samples over the blank and control also indicated destructive adsorption of paraoxon was occurring. Using this method, it is impossible to quantify exactly how much paraoxon is destroyed due to the difficulty of extracting the all of the remaining paraoxon from the cream. However, due to the color change over time of the rTSP samples and the decreased amount of paraoxon after extraction, it is concluded that the nanoparticles incorporated into skin cream are still actively destroying paraoxon.

Task 6. Compatibility Studies.

The purpose of this task was to examine the long term stability of the [POM]RNP formulation in the base skin cream. Prior to completion of Task 4 it was necessary to correct the physical properties of the rTSP. The addition of solids (e.g. [POM]RNP) to the TSP to form the rTSP resulted in increasing viscosity of the rTSP increasing, causing cracking. Obviously, cracking of the rTSP rendered it useless for permeation testing. However, by varying the ratios between solid and liquid components of the TSP, it was possible to produce rTSPs with similar viscosities to the unmodified base cream. The quantitative and comparative permeation testing was performed on the creams normalized for viscosity. Results reported below are based on repeating permeation testing on rTSP aged for 99 to 180 days.

After a period of storage, several of the rTSP along with the base cream or TSP (ICD 3005) were reevaluated by permeation testing method outlined previously. rTSP were stored in a sealed jar at room temperature in a lab drawer (no visible light).

After the desired storage time, visual inspection of all creams revealed slight separation of the oil component from the bulk of the cream. Therefore, prior to permeation testing, the cream components were remixed with a spatula. Qualitatively, the creams behaved similarly to the base cream, and as permeation cells were prepared there was no drying and cracking of the creams as was problematic prior to normalizing rTSP viscosity.

The base cream ICD3005 performed similarly when tested after 116 days. There was about a 15% increase in the time (min) for 1000 ng to permeate the cream. A 5% decrease was shown in nanograms of CEPS that permeated the base cream in 20 h. All rTSP performed better over time, showing an increased time for 1000ng permeation, and a decreased amount of CEPS permeated after 20 h. The only exception was rTSP containing [2 mol % (Ce(NO₃)₃/Cu(NO₃)₂), sample 2 from Table 8.

Particularly noteworthy was cream number 4: 9.35% [10% NaPOM / TiO₂]/TSP. It was retested 132 days after its initial tests and showed no CEPS permeation after 20 h. The time for 1000 ng permeation was beyond the calculating capacity of the software. This test was repeated and produced identical results.

Table 8. CEPS permeation changes over time.

rTSP	Percent		CEPS Permeation				Elapsed Time (days)
			Initial		Final		
	oil	powder	Time (min) to 1000 ng permeation	ng perm. After 20 h	Time (min) to 1000 ng permeation	ng perm. After 20 h	
ICD 3005	50.00	50.00	525	2,721	594	2,598	116
1	53.26	41.96	1,597	418	26,348	15	180
2	53.33	41.92	2,273	295	2,031	286	99
3	53.51	44.18	1,345	757	2,957	203	105
4 ^a	52.55	38.10	2,278	215	N/A _b	0	132
5	53.24	44.36	1,431	603	5,048	153	129
6	53.23	44.38	1,407	609	2,219	226	132

1) 4.79% [10% NaPOM / TiO₂]/TSP

2) 4.75% [2 mol % (Ce(NO₃)₃/Cu(NO₃)₂)/TSP

3) (1.5% [2 mol % (Ce(NO₃)₃/Cu(NO₃)₂), 1.5% [0.4 mol % NaPOM / TiO₂])/TSP

4) 9.35% [10% NaPOM / TiO₂]/TSP

5) 2.40% [0.4 mol % AgPOM / TiO₂]/TSP

6) 2.39% [2 mol % (Ag(NO₃) / TiO₂)/TSP

^a: Final permeation test was repeated two time with identical results.

^b: Time to 1000 ng permeation was unable to be calculated by software.

Task 7. Studies of optimized POM/RNP with real agents.

Testing of [POM]RNP hybrids with real CW agents was performed by researchers at U.S. Army Medical Research Institute of Chemical Defense (USAMRICD) at Aberdeen Proving Ground, MD and through a subcontract with Midwest Research Institute (MRI) in Kansas City, MO.

The active barrier cream against chemical warfare agents program is administered by Capt. Stephen Hobson, Ph.D. and Dr. Ernest H. Braue, Jr. of the Drug Assessment Division of USAMRICD. The following is a report from Dr. Braue and Capt. Hobson detailing the studies performed with our reactive nanoparticles.

Efficacy of Reactive Nanoparticles in the Active Topical Skin Protectant Program

A Skin Exposure Reduction Paste Against Chemical Warfare Agents (SERPACWA) has been developed by researchers at USAMRICD-APG to extend the protection afforded by the special chemical protective suit and allow a longer window for decontamination. It does not neutralize CWA nor does it protect well against HD vapor. To improve SERPACWA, researchers at USAMRICD have developed an *active* Topical Skin Protectant (aTSP).

The USAMRICD aTSP project is examining over 100 active moieties divided into four classes that are incorporated into the current SERPACWA material to afford additional protection to the U.S. warfighter. These include organic molecules, inorganic compounds, organic polymers and enzymes. Reactive nanoparticles (RNPs) from NanoScale Materials are included in the class of inorganic compounds.

The aTSPs are made by simply mixing small amounts of reactive moiety into the SERPACWA base material. The aTSPs are then challenged with HD and GD via a penetration cell test to determine the increase in protection of the aTSP versus TSP. A continuous air monitoring system (MINICAMS) was used for measuring the amount of CWA breaking through the aTSP barrier during a 20 hour period (Figure 46).

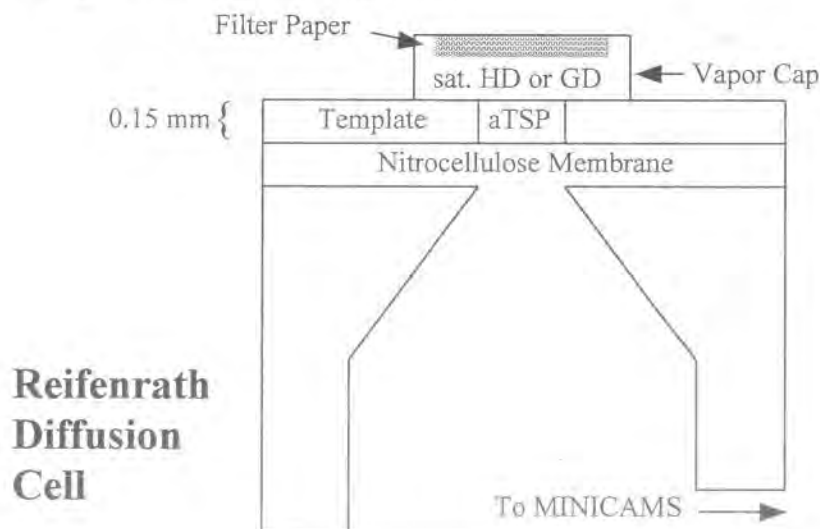


Figure 46. Schematic diagram of penetration cell with saturated vapor setup

The following are results from the USAMRICD project with regard to reactive nanoparticles. Reactive nanoparticles and RNP supported polyoxometalates are among the most effective compounds for the reduction of HD and GD permeation. The graphs below show the cumulative amount of each agent that passed through a 0.15 mm thick barrier of aTSP during a 20 hour period. Both figures show neat SERPACWA (no active component) as a reference. In Figure 47 XE 555, the current sorbent powder used in the M-291 and M-295 decontamination kits, is also shown as a reference. XE 555 was not effective enough against the GD to be shown on this graph. It should be noted that separate experiments have shown that the nanoparticulate materials adsorb *and neutralize* HD and GD. In contrast, XE 555 is simply an adsorbent material that does exhibit off-gassing problems.

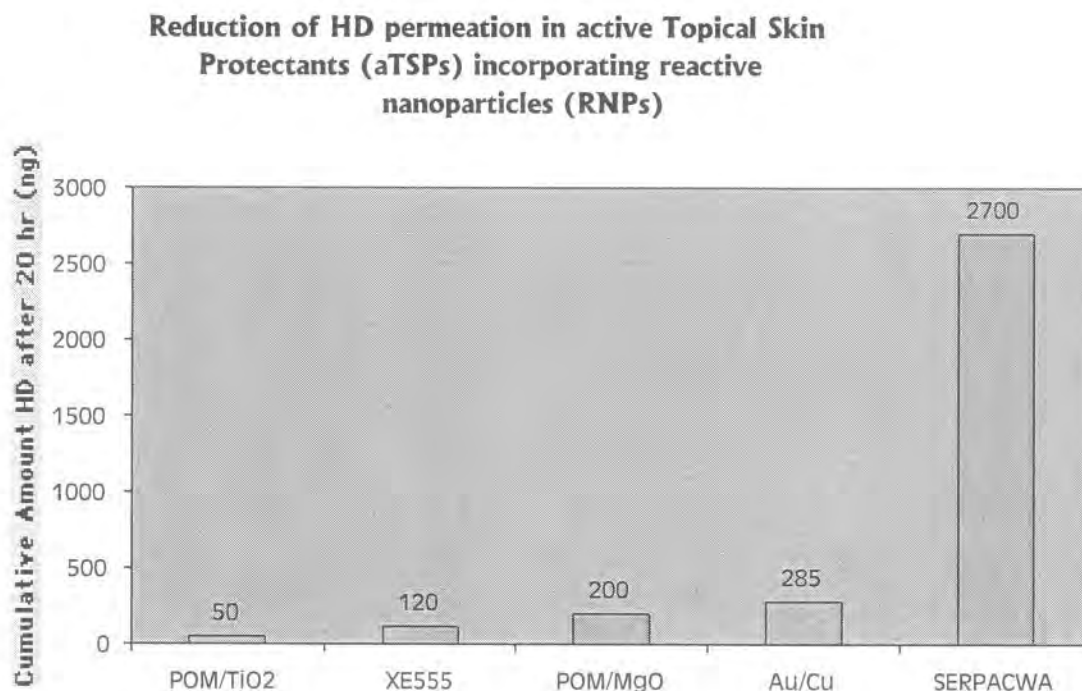


Figure 47. Cumulative amount of HD vapor permeating through the aTSP after 20 hrs as measured by penetration cell model / MINICAMS systems (saturated HD vapor, 0.15 mm thickness).

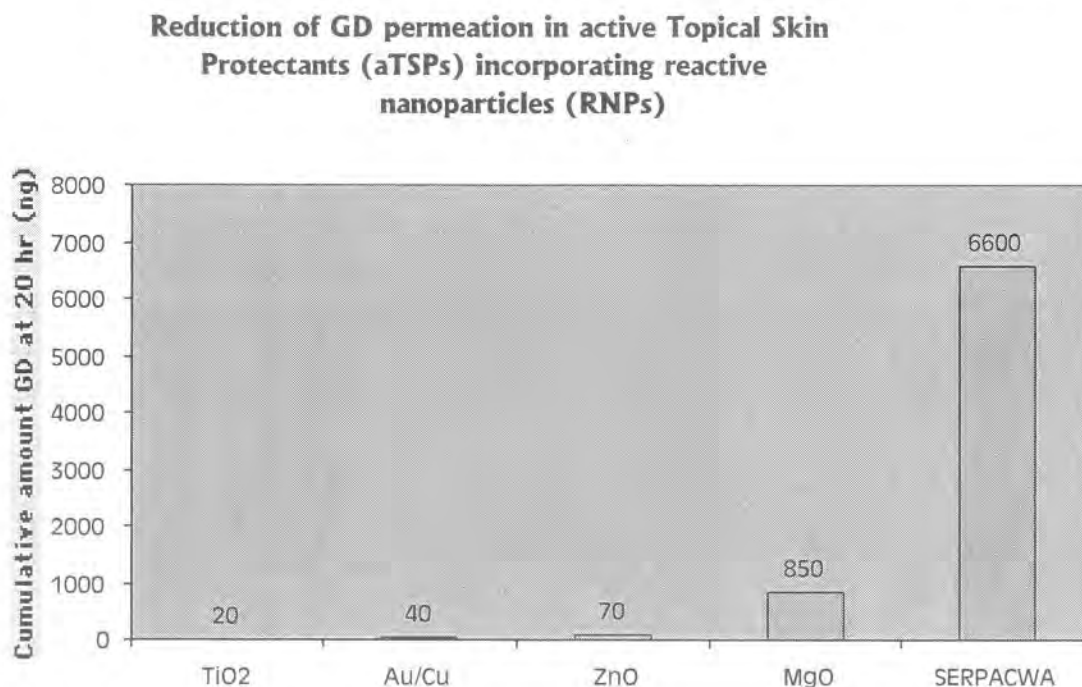


Figure 48. Cumulative amount GD vapor permeating through the aTSP after 20 hr as measured by penetration cell model / MINICAMs systems (saturated GD vapor, 0.15 mm thickness).

Real Agent Testing Through Midwest Research Institute

A subcontract with the Midwest Research Institute tested the efficacy of various [POM]RNP/TSP (rTSP) samples with mustard gas and GD. Unfortunately these experiments were conducted before the viscosity and thickening issues in the rTSP samples were resolved. The rTSP formulations thickened over time even when sealed in containers. After addition of the oil component, there were still difficulties in obtaining an evenly spread testing surface. The apparent light- and air-sensitivity of the nanoparticles together with the extremely high surface area of the nanoparticles is thought to have caused the thickening of the creams. The rTSP formulations also contained granules and aggregates in varying sizes. These granules further complicated spreading of the TSP by generating uneven surfaces. The granules caused streaking in the TSP coating. These streaks resulted in uneven coating thicknesses. The testing however was proceeded without resolving first these issues. Therefore, the results do not seem as promising as the real agent testing performed by Dr. E. Braue and CPT S. Hobson at USAMRICD (Aberdeen Proving Grounds, MD). A summary of the MRI testing protocol was as follows:

rTSP formulations were applied at a known thickness on nitrocellulose filter supports sized for the permeation cells. Static liquid GD challenge involved direct application of neat GD to the TSP preparations. The tops of the cells were sealed to contain the agent. A stream of dry

nitrogen swept the underside of the test assembly and collected volatile permeated components onto individual sorbent tubes. The static vapor HD challenge involved suspending a HD-saturated pad above each TSP preparation. The tops of the cells were sealed to contain the agent and volatile permeated components were collected on individual sorbent tubes.

At the end of the collection period, the sorbent tubes were disassembled and the sorbent packs separated and extracted. The extracts were analyzed by full scan GC/MS for permeated agent. Retention time and specific ion plots were used to identify permeated agent. Quantitation of agent was by comparison of the response of GD or HD found in the samples with a calibration curve. Mass spectra were collected of GD, HD, and non-agent components. The number varied with the samples. Non-agent components were not identified.

This is a summary of the results of proof-of-principle testing of rTSP for resistance to penetration by chemical agents GD and HD. A static liquid challenge/vapor permeation test was used for GD testing and a static vapor challenge/vapor permeation test was used for HD testing.

Overall, the TSP formulation retained the majority of GD. The 2.0% APMgO formulation produced the lowest breakthrough (0.76%). This was for a single sample however. The duplicate was lost due to a very large liquid GD breakthrough. The highest GD breakthrough was 2.2% (average of duplicates) from the 2.0% TiO₂ formulation.

The TSP formulations performed less efficiently with HD vapor. The base cream (single sample) exposed to the HD vapor experienced a 1.48% breakthrough. The lowest breakthrough experienced by the rTSP was 1.44% for the 5.0% TiO₂ formulation. The highest HD breakthrough, 4.8%, was experienced by the 5.0% APMgO. This formulation also produced the highest GD breakthrough.

Task 8. Studies of [POM]RNP with other simulants.

This task studied the detoxification of additional CW simulants by [POM]RNP formulations. These tests expanded the base of experiments that were used to evaluate the samples. The agent simulants studied here include diethyl phenylthiomethylphosphonate (DEPTMP - a sulfur containing VX simulant) and diisopropyl fluorophosphate (DFP - a GD simulant). Initial validation experiments on these methods were presented in an earlier project; however, some of that data will be presented here to compare with [POM]RNP samples.

Destructive Adsorption of Diethyl Phenylthiomethylphosphonate (DEPTMP), a Sulfur Containing VX Simulant.

An experimental method to investigate the destructive adsorption of the simulant diethyl phenylthiomethyl phosphonate was developed. This method described below, is similar to that for paraoxon. Initial adsorption studies with MgO nanoparticles and commercially available activated carbon materials are included for reference to compare with [POM]RNP samples. The structure of the adsorbed species after reaction was also determined in these experiments.

The UV spectrum of DEPTMP in pentane contains two absorption bands centered around 209 and 256 nm. Adsorption of DEPTMP by the solid adsorbent should result in a reduction of its concentration in the liquid phase and hence a decrease in the intensity of its absorption peaks. First, a calibration curve was constructed by measuring absorptions of a series of solutions of pentane containing known amounts of DEPTMP. Next, a 250 mL flask provided with a serum cap, stir bar and a magnetic stirrer was charged with dry pentane (200 mL). To the above was added sequentially, the solid adsorbent (0.2g) and DEPTMP (9 μ L, ~ 5% by wt.). After an hour at room temperature, stirring was stopped. Then, samples of the liquid phase derived from reactions using DEPTMP/adsorbent were analyzed by UV. Using the calibration curve the amount of unadsorbed DEPTMP left in the liquid phase of these reactions was calculated. Table 9 summarizes the results of the UV analysis of the liquid phase derived from DEPTMP and various adsorbents. In order to assess the adsorbed species, all the solvent was then decanted off and the solid dried overnight under vacuum and analyzed by IR and NMR to assess the structure of the adsorbed species.

Table 9. Amount of Unadsorbed DEPTMP As Determined by UV Analysis

Adsorbant	Unadsorbed DEPTMP ^a , %
APMgO	4
[Na ₅ PV ₂ Mo ₁₀ O ₄₀]APTiO ₂	7
APTiO ₂	9
CPMgO	26
CMMgO	83
Darco Activated Carbon	76
Norit Activated Carbon	65
Coconut Shell Activated Carbon	72
Ambersorb 572 Activated Carbon	41

From the table above, it is clear that nanoparticle formulations are superior to all other adsorbents. The ability to adsorb various reagents is attributed to their unique morphology and high surface area.

Samples for IR studies were prepared by grinding a sample of the dried solid (1-3 mg) with anhydrous KBr (100 mg). Pellets were made with a press. Spectrum of neat liquid was obtained by spreading a thin film of the liquid between a pair of salt plates. Figure 49 shows the IR spectra of neat DEPTMP (Bottom), uncoated APTiO₂ adsorbed DEPTMP (middle), and [POM]TiO₂ adsorbed DEPTMP (top).

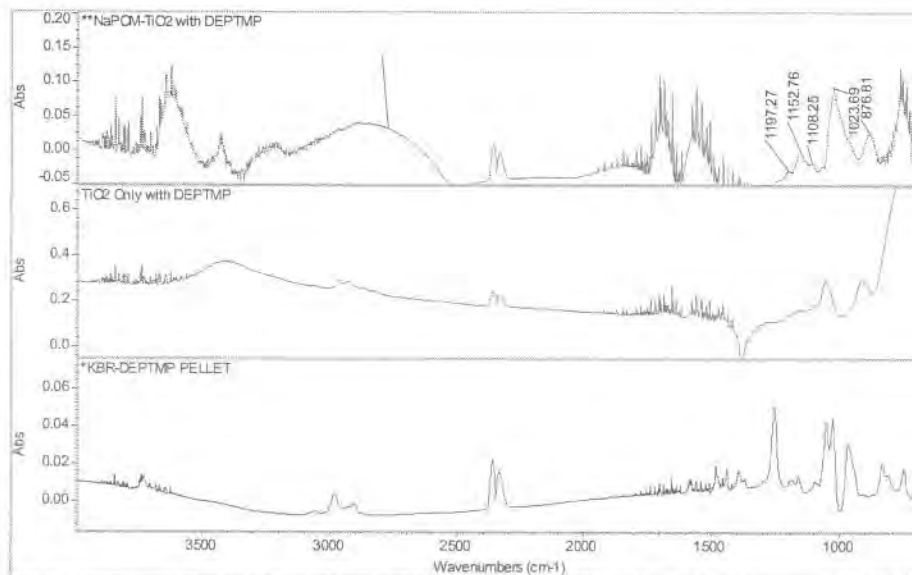
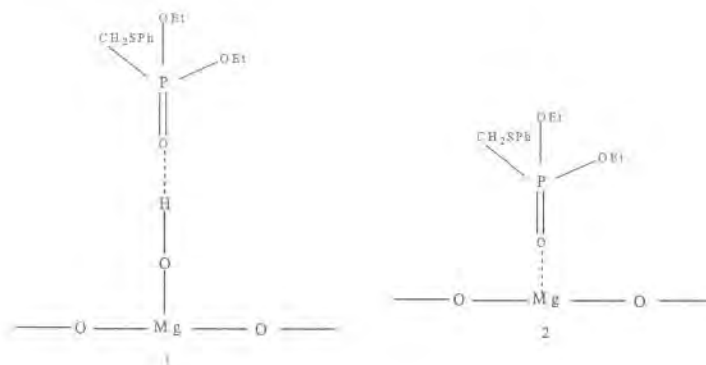


Figure 49. FT-IR Spectra (Solid Pellet) of DEPTMP/[NaPOM]TiO₂ (Top), DEPTMP/TiO₂ (Middle) and Neat DEPTMP (Bottom)

There is an appreciable amount of literature on the use of various IR techniques to explore the process of adsorption of phosphonates by inorganic oxides². The 1300-1000 cm⁻¹ region in the IR yields the most direct information about the nature of adsorbed species. The following points emerge from a close examination of Fig. 46. 49

- 1) Peaks after reaction appear broadened.
- 2) The $\nu_{P=O}$ band of DEPTMP shifted from 1250 cm⁻¹ to 1157 cm⁻¹ ($\Delta\nu = -93$ cm⁻¹).
- 3) The $\nu_{C-O(P)}$ band did not shift much in uncoated TiO₂, but shifted slightly ($\Delta\nu = -8$ cm⁻¹) in the [POM]TiO₂ sample.

These results indicate that the P=O bond is significantly perturbed upon adsorption. However, C-O stretch is not affected which suggests that adsorption does not involve the C-O(P) moiety. Thus, the initial adsorption might involve structures such as (1) and/or (2) as illustrated below using APMgO as the adsorbant.



In order to verify whether we have simple adsorption and/or decomposition *via* hydrolysis of DEPTMP, the solids recovered after adsorption reactions were analyzed by NMR. ^{31}P NMR spectra were obtained using a Tecmag-based 270 MHz spectrometer equipped with a Doty Scientific 7 mm high speed CP-MAS probe, using direct excitation and high power proton decoupling. The observation frequency for ^{31}P was 109.55 MHz. Samples were packed in a sapphire rotor with kel-F end caps and typically spun at 4700 Hz. Chemical shifts were referenced to external 85% H_3PO_4 (0 ppm).

Figure 50 shows the ^{31}P MAS NMR spectrum of AP-MgO adsorbed DEPTMP (5% by wt.). It displays two major peaks centered around 24.2 and 15.7 ppm and a set of two smaller peaks. The latter are attributed to spinning side bands. From a literature survey³², we found that for derivatives of type $(\text{EtO})_2\text{P}(\text{O})\text{R}$ wherein R is CH_3 , Et, or butyl, ^{31}P NMR δ value ranges from 29.6-32.6 ppm. Thus, it appears that the signals observed in the DEPTMP/AP-MgO sample are probably due to some products that contain a more shielded phosphorous nucleus.

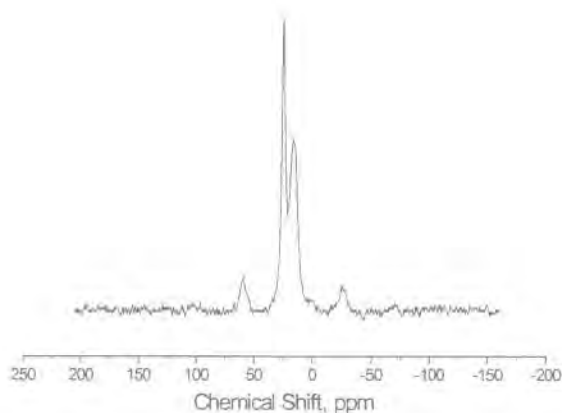
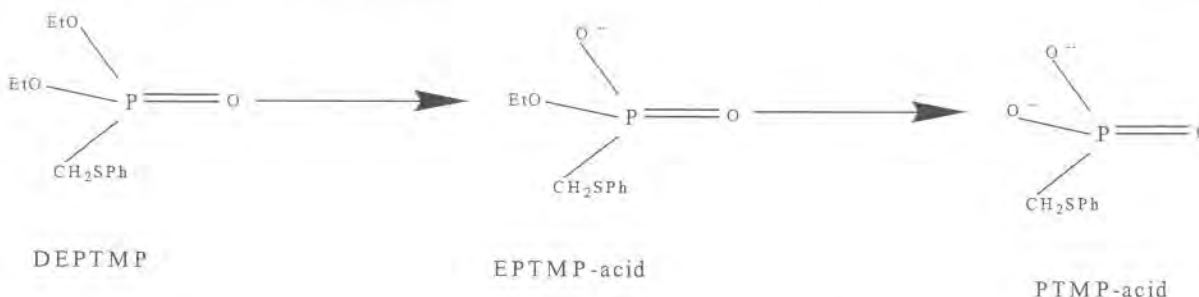


Figure 50. ^{31}P NMR Spectrum of DEPTMP (5% by wt.)/AP-MgO

Based on the work of Wagner *et al.*³³, we attribute the major peaks to ethyl phenylthiomethyl phosphonic acid (EPTMP) (24.2 ppm) and phenylthiomethyl phosphonic acid

(PTMP \square 15.7 ppm). Due to the basic nature of magnesium oxide, we showed the adsorbed species as the corresponding anions.



^{31}P NMR results indicate that the ethoxy groups of DEPTMP are hydrolyzed by surface hydroxyls and/or physisorbed water in AP-MgO to produce a mixture of mono and dianionic species. The $\text{P}=\text{O}$ group in these structures probably remain adsorbed as evidenced by IR. Even though ethoxy groups were hydrolyzed, the C-O stretching value remained the same. This may probably be because the IR stretching absorption values for $\text{CH}_2\text{O}(\text{P})$ and $\text{CH}_2\text{O}(\text{Mg})$ are not appreciably different.

^{31}P NMR results for $[\text{POM}]\text{TiO}_2$ and uncoated TiO_2 were similar to APMgO . The ^{31}P MAS NMR spectrum of APTiO_2 adsorbed DEPTMP is shown in Figure 51. There is a major peak centered at $\delta 18.04$ ppm, a smaller shoulder peak at $\delta 23.42$ and a set of two smaller peaks on either side. The latter are attributed to spinning side bands.

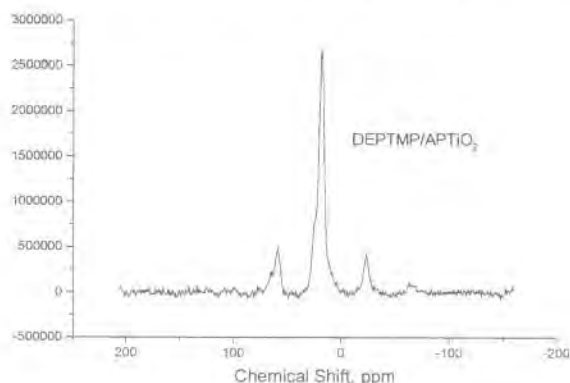


Figure 51. ^{31}P NMR Spectrum of DEPTMP/APTiO₂

The ^{31}P MAS NMR spectrum of $[\text{Na}_5\text{PV}_2\text{Mo}_{10}\text{O}_{40}]\text{TiO}_2$ adsorbed DEPTMP is shown in Figure 52. There is a major peak centered at $\delta 18.71$ ppm, a smaller shoulder peak at $\delta 24.84$ and a set of two smaller peaks on either side. The latter are attributed to spinning side bands.

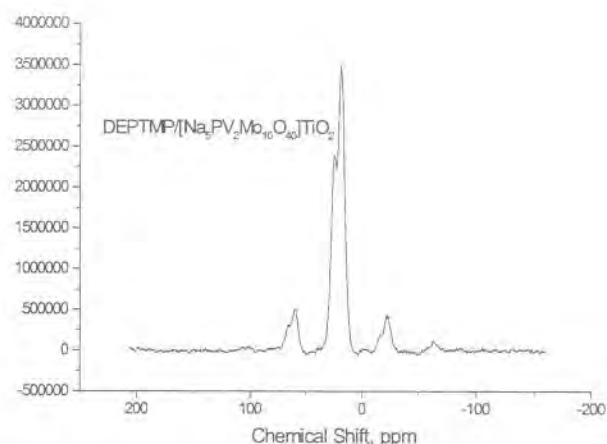


Figure 52. ^{31}P NMR Spectrum of DEPTMP/[$\text{Na}_5\text{PV}_2\text{Mo}_{10}\text{O}_{40}$]APTiO₂

These ^{31}P NMR results indicate that the ethoxy groups of DEPTMP are hydrolyzed to produce a mixture of mono and dianionic species (see above). The P=O groups in these structures remain adsorbed as evidenced by IR. Even though ethoxy groups were hydrolyzed, the C-O stretching value remained the same. This is probably because the IR stretching adsorption values for $\text{CH}_2\text{O}(\text{P})$ and $\text{CH}_2\text{O}(\text{Ti})$ are not appreciably different.

Kinetic Experiments with DEPTMP and [POM]RNP Formulations

During the course of the project, the most promising formulations of [POM]RNPs or transition metal coated RNPs were analyzed with DEPTMP in kinetic studies. The following are some of the formulations studied:

- TiO₂ (SSA = 446.9 m²/g)
- 2-wt% [$\text{Na}_5\text{PV}_2\text{Mo}_{10}\text{O}_{40}$]TiO₂ (SSA = 369 m²/g)
- 10-wt% [$\text{Na}_5\text{PV}_2\text{Mo}_{10}\text{O}_{40}$]TiO₂ (SSA = 317 m²/g)
- 2-wt% [$\text{Ag}_5\text{PV}_2\text{Mo}_{10}\text{O}_{40}$]TiO₂ (SSA = 515 m²/g)
- 5-wt% [$\text{Ag}_5\text{PV}_2\text{Mo}_{10}\text{O}_{40}$]TiO₂ (SSA = 420 m²/g)
- 10-wt% [$\text{Ag}_5\text{PV}_2\text{Mo}_{10}\text{O}_{40}$]TiO₂ (SSA = 491 m²/g)
- [2 mol% Cerium Oxide]TiO₂ SSA = 173 m²/g
- [2 mol% Copper Nitrate]TiO₂ SSA = 173 m²/g
- [2 mol% Cerium Nitrate]TiO₂ SSA = 176 m²/g

DEPTMP experiments were performed in the same manner as the paraoxon experiments. Briefly, a round bottom flask with stir bar, which contained 200-mL pentane, was placed on a stir plate. DEPTMP (9 μL) was injected and the solution stirred and pumped to a flow-through cuvette. The UV-Vis spectrum of the reference compound was obtained. Once this baseline has been established, 0.2g of sample was added to the stirring solution and spectra collected at 1 minute intervals up to 10 minutes and then at 5 minute intervals thereafter, up to 1 hour. The destructive adsorbance of DEPTMP is measured by monitoring the absorbance at 254nm. Figure

53 shows a typical UV-Vis spectra for a sixty minute reaction with DEPTMP. The top red trace is the DEPTMP dissolved in pentane, before addition of the sample.

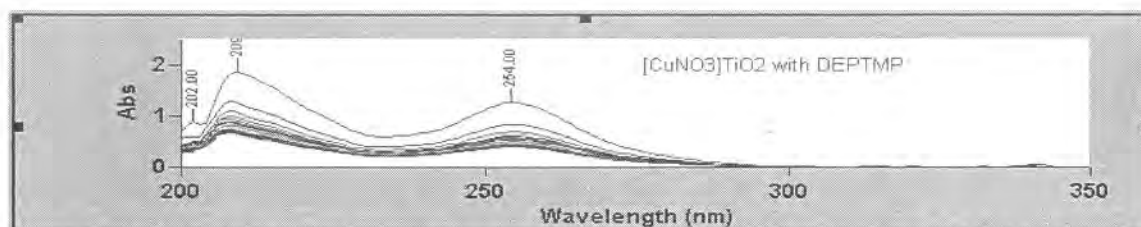


Figure 53. UV/VIS Spectra During Reaction of $[\text{Cu}(\text{NO}_3)_2]\text{TiO}_2$ and DEPTMP.

The results of DEPTMP studies with POM coated TiO_2 samples are shown in Figure 54. The sample that performed the best was 2-wt% $[\text{Ag}_5\text{PV}_2\text{Mo}_{10}\text{O}_{40}]\text{TiO}_2$. Since the other POM coated TiO_2 samples performed similarly to each other, only one is displayed in the graph for simplicity. Based on comparison with a standard curve, it appears that 0.2g of TiO_2 nanoparticles will adsorb approximately 94% DEPTMP after one hour with the bulk of the adsorption occurring within 20 minutes.

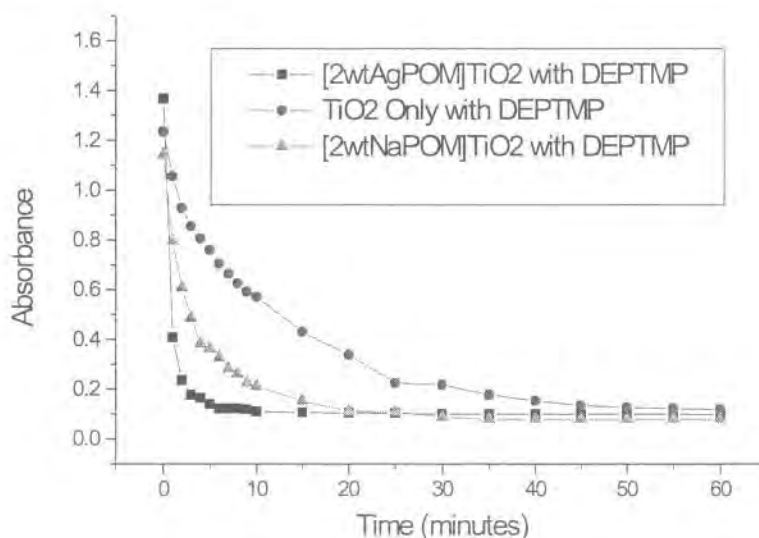


Figure 54. Comparison of DEPTMP Adsorption Rate with Various $[\text{POM}]\text{TiO}_2$ Samples.

The results of cerium and copper compounds coated on TiO_2 were interesting. When these compounds were coated separately on TiO_2 , they did not improve the destructive adsorbance of DEPTMP. Titanium dioxide alone reacted faster and there was less DEPTMP left unreacted after the sixty minute analysis time. However, addition of the mixture of cerium and copper nitrates on TiO_2 greatly improved its ability to destructively adsorb DEPTMP. All the samples performed much better than activated carbon, which was included for comparison. Figure 55 shows the relative rate of decomposition of DEPTMP for all the samples.

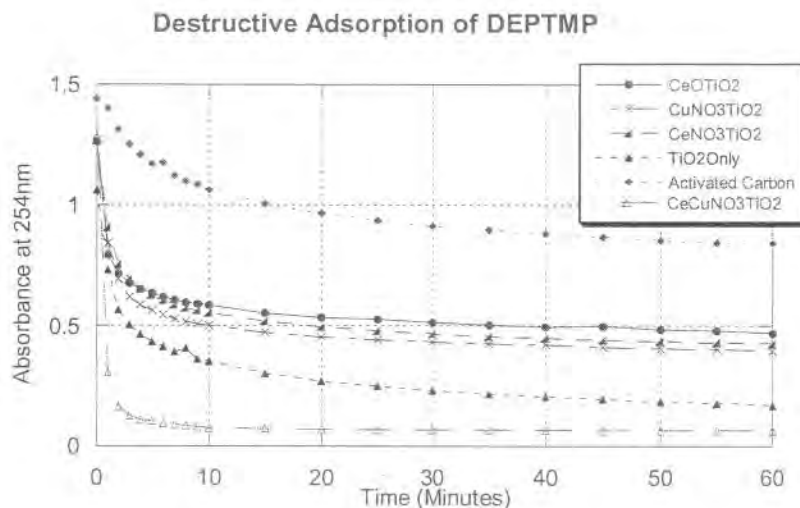


Figure 55. Destructive Adsorption of DEPTMP by Various Nanoparticles.

Destructive Adsorption of Diisopropyl Fluorophosphate (DFP), a GD Simulant.

Experimental methods to investigate the destructive adsorption of the simulant diisopropyl fluororophosphate (DFP) were developed. These experiments determined the efficacy of various reagents in adsorbing DFP and the structure of the adsorbed species. As in the previous experiments with DEPTMP, APMgO and various activated carbon samples were used for comparison with [POM]RNP formulations.

In a typical experiment, the appropriate adsorbent (~ 0.1 g) was weighed into an IR cell that could be connected to a vacuum line. Prior to adsorption, the adsorbents were evacuated at room temperature for ~ 15-30 min ($\sim 10^{-4}$ torr). After this treatment, a background spectrum was recorded. Subsequently, DFP was introduced (9 μ L) into the sample cell and the IR spectra of the vapor phase was recorded for up to five hours. In order to assess the structure of the adsorbed species, the DFP adsorbed solid was then isolated and analyzed.

The vapor phase IR spectra of neat DFP and that of the ones derived from reactions between DFP and APTiO_2 and DFP and $[\text{Na}_5\text{PV}_2\text{Mo}_{10}\text{O}_{40}]\text{APTiO}_2$ are shown in Figure 56. The DFP was completely adsorbed by both compounds. $[\text{Na}_5\text{PV}_2\text{Mo}_{10}\text{O}_{40}]\text{APTiO}_2$ adsorbed the reaction products as well. In the case of uncoated TiO_2 , products of reaction with DFP are still visible in the vapor phase.

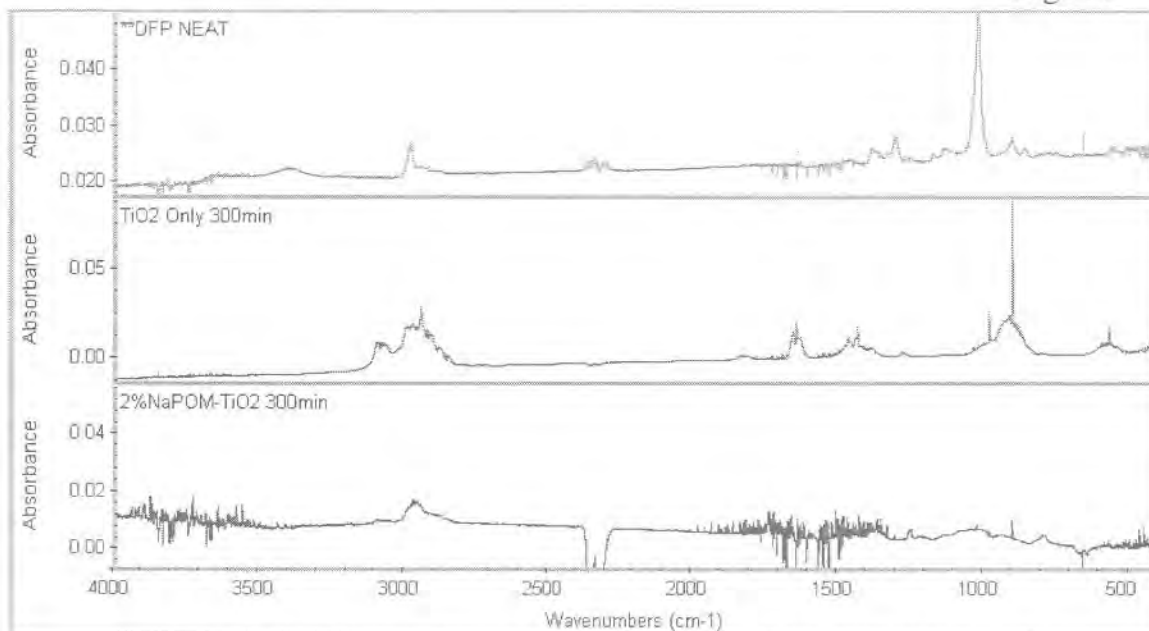


Figure 56. FT-IR Vapor Phase Spectra of (A) Neat DFP, (B) DFP/TiO₂ and (C) DFP/[NaPOM]TiO₂

After vapor phase analysis, the DFP adsorbed solid was isolated and pellets prepared using anhydrous KBr and a pellet press. Solid phase FT-IR and Solid State ³¹P NMR spectra were obtained and analyzed to assess the structure of the adsorbed species.

Figure 57 shows the solid phase spectra of these adsorbents as well as the spectrum of neat DFP obtained using a thin layer between salt plates. Table 10 includes data as to the prominent solid phase FT-IR bands in each of the three spectra.

Table 10. Prominent FT-IR Bands for Free DFP and Adsorbed DFP

Assignment	Adsorbed DFP		Neat DFP
	APTiO ₂	[NaPOM]TiO ₂	
P=O Stretch	---	---	1298(s)
CH ₃ rock	1175	1175,1152,1121	1180-1110(s)
C-O(p) Stretch	Obscured	Obscured	1016(s)
POO(bridged) Stretch	1068,1002	1068,1001	---

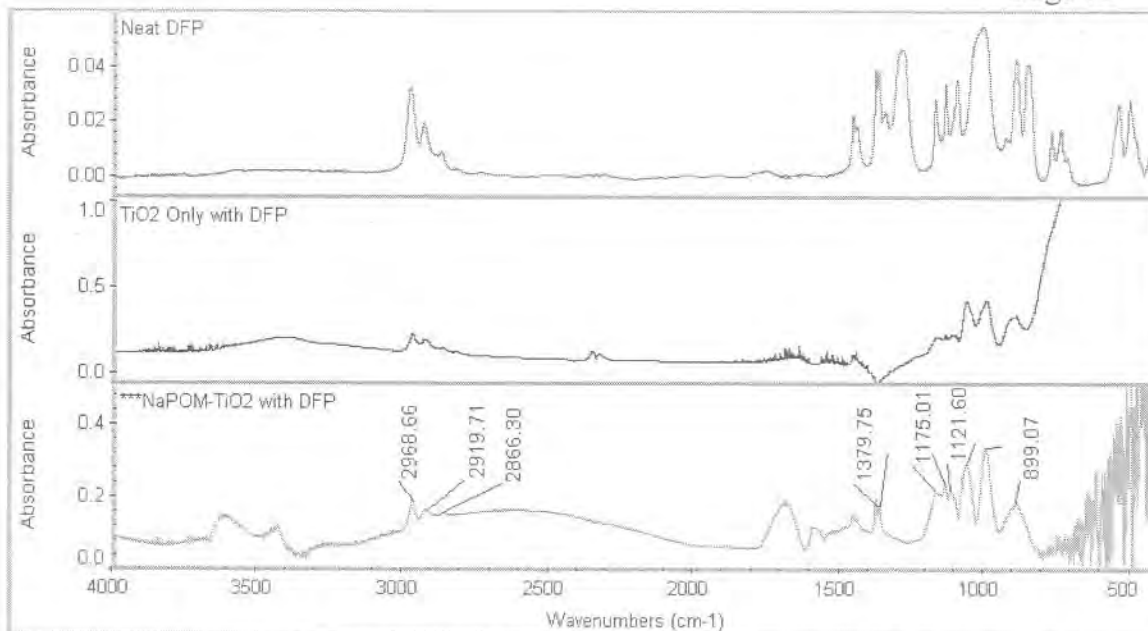
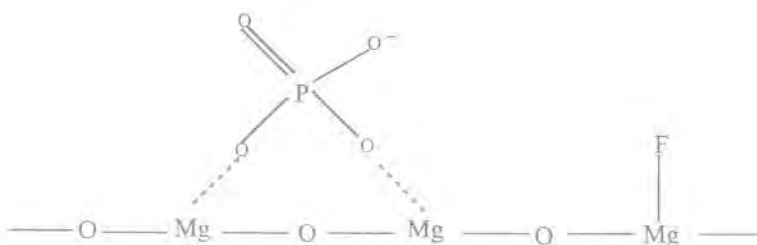


Figure 57. FT-IR Spectra (Solid Phase) of (A) Neat DFP, (B) DFP/TiO₂ and (C) DFP/[NaPOM]TiO₂

The following observations were made in comparing the spectra of neat DFP with DFP adsorbed on APTiO₂ and [Na₅PV₂Mo₁₀O₄₀]APTiO₂:

- 1) Broad adsorption bands were observed in the 3700-3000 cm⁻¹ region after reaction.
- 2) The alkyl C-H stretch region (3100-2800 cm⁻¹) did not change much upon adsorption.
- 3) The $\nu_{P=O}$ band of DFP (1298 cm⁻¹) did not appear in the adsorbed DFP samples.
- 4) The $\nu_{C-O(P)}$ band at 1016 cm⁻¹ is obscured by the peaks at 1001 & 1002 cm⁻¹ in the adsorbed samples.
- 5) The new peaks at 1068 cm⁻¹ and 1001 & 1002 cm⁻¹ are assigned to the bridged "POO" species whose existence was previously reported⁴.

We assigned the pair of new peaks (1068 & 1002 cm⁻¹) to the bridged "POO" species shown below. Existence of such structures have been proposed with dimethyl methylphosphonate/AP-MgO³⁴ and sarin and its related compounds adsorbed on alumina or magnesium oxide³⁵.



Direct evidence for the existence of PO_4^{3-} in DFP impregnated RNP samples comes from the ^{31}P NMR spectrum of DFP adsorbed on APMgO (Fig. 58). In this spectrum a major peak centered around δ -0.76 ppm and two sets of minor peaks were seen. The latter are attributed to spinning side bands.

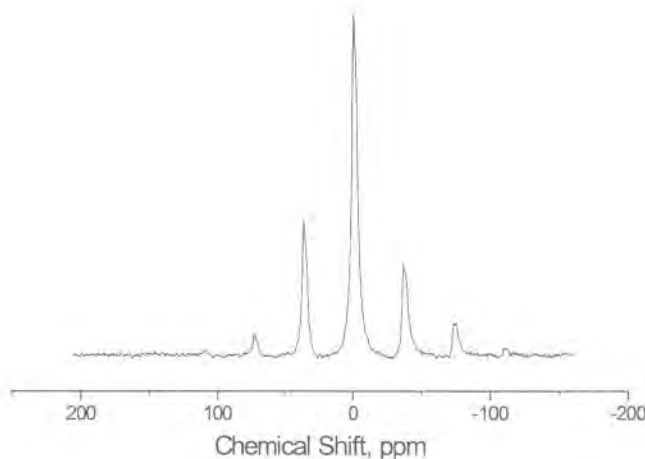
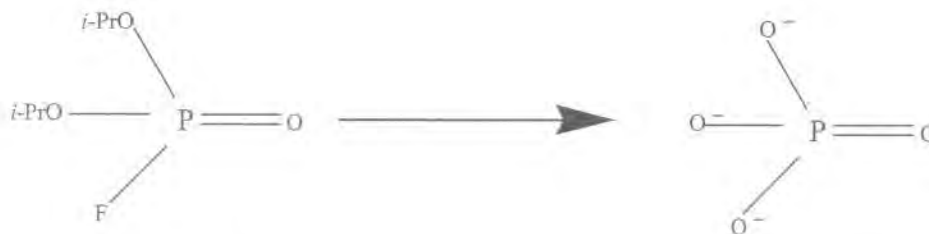


Figure 58. ^{31}P NMR Spectrum of DFP (5% by wt.)/AP-MgO

It is known that ^{31}P NMR of neat DFP shows a peak centered around δ 11.2 ppm³⁶. The appreciable up-field shift observed with the adsorbed sample indicates a highly shielded phosphorus nucleus such as a phosphate anion (PO_4^{3-}), a product derived *via* complete hydrolysis of DFP by surface hydroxyls and/or physisorbed water in AP-MgO.



In the case of the ^{31}P CP/MAS NMR spectra of APTiO_2 adsorbed DFP (Figure 59), there are two major peaks centered at δ -1.521 and δ -5.687 ppm. The set of two smaller peaks on either side is attributed to spinning side bands. The appreciable upward shift with this adsorbed sample indicates a highly shielded phosphorus nucleus as well. The larger of the two main peaks (δ -

1.521 ppm) indicates the completely hydrolyzed species PO_4^{3-} , and the peak at δ -5.687 ppm is attributed to the dihydrolyzed species.

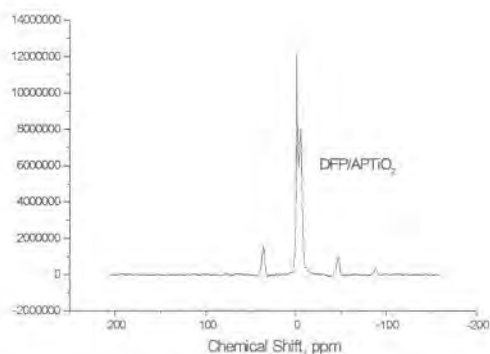


Figure 59. ^{31}P NMR Spectrum of DFP/APTiO₂

The ^{31}P CP/MAS NMR spectra of $[\text{Na}_5\text{PV}_2\text{Mo}_{10}\text{O}_{40}]\text{TiO}_2$ adsorbed DFP (Figure 60) appears to have only one major peak centered at δ -5.255 ppm. However, closer inspection of the enlarged spectrum reveals the peak to be broad and unsymmetrical indicating a mixture of the products shown above for uncoated TiO₂.

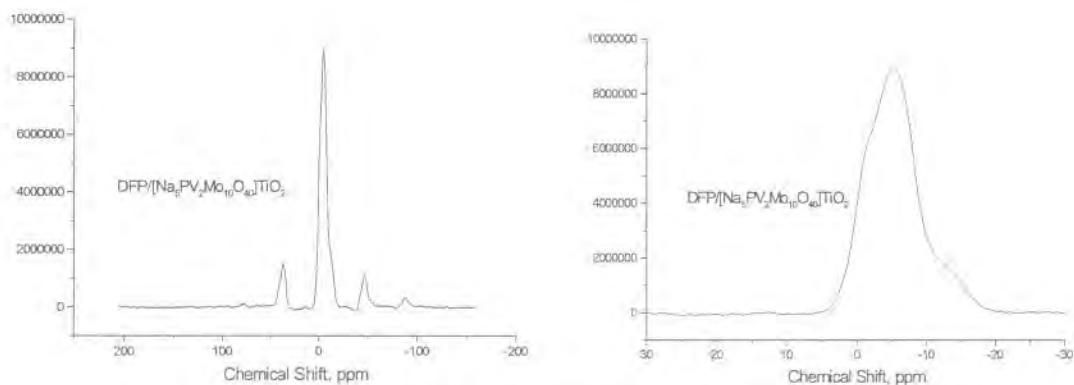


Figure 60. ^{31}P NMR Spectrum of DFP/ $[\text{Na}_5\text{PV}_2\text{Mo}_{10}\text{O}_{40}]\text{APTiO}_2$

The same experiments were conducted with DFP and the coated nanoparticle sample [2 mol% $\text{Ce}(\text{NO}_3)_3$ - $\text{Cu}(\text{NO}_3)_2$] TiO_2 . Figure 61 shows the solid phase spectra of the sample with adsorbed DFP and neat DFP. Table 11 includes data as to the prominent solid phase FT-IR bands in each spectrum.

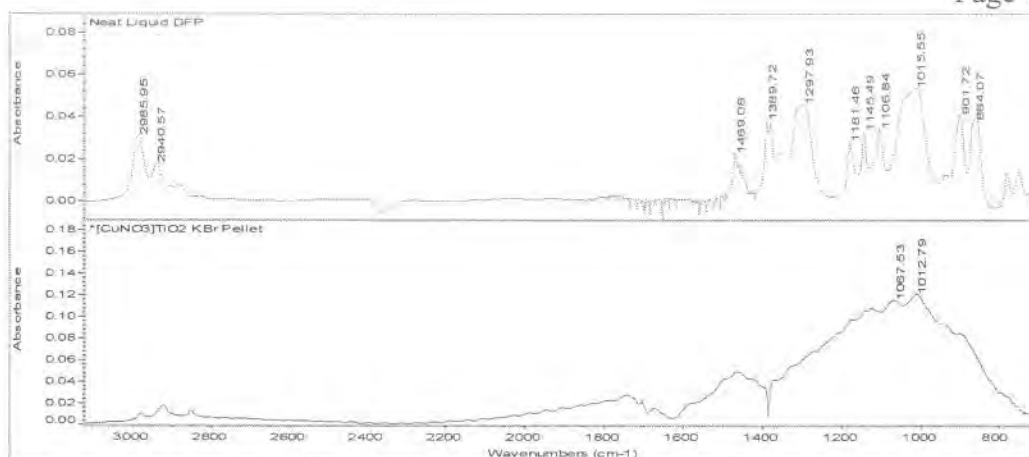


Figure 61. FT-IR Spectra (Solid Phase) of (Top) Neat DFP and (Bottom) DFP/[CeCuNO₃]TiO₂

The following observations were made in comparing the spectra of neat DFP and DFP adsorbed on the sample:

- 1) The alkyl C-H stretch region (3000 – 2800 cm⁻¹) did not change much upon adsorption.
- 2) The $\nu_{P=O}$ band of DFP (1298 cm⁻¹) does not appear prominently in the adsorbed DFP sample.
- 3) The stretch at 864 cm⁻¹ assigned to P-F does not appear in the adsorbed sample.
- 4) A new peak at 1065 cm⁻¹ is assigned to the bridged POO species whose existence was previously reported.

Table 11. Prominent FT-IR Bands for Free DFP and Adsorbed DFP

DFP Neat Liquid	Adsorbed DFP	Assignment
3000-2800	3000-2800	CH ₃ Stretch
1298	----	P=O Stretch
1180-1110	1122	CH ₃ Rock
----	1065	Bridged POO Species
1016	1012	C-O (P) Stretch
864	----	P-F Stretch

The ³¹P NMR spectrum of the sample with adsorbed DFP is shown in Figure 62. There appeared to be two major peaks centered at δ -5.489 and δ -18.149 ppm and a set of two smaller peaks on either side. The latter are attributed to spinning side bands. Close inspection of the spectrum reveals the large peak at δ -5.489 ppm to be broad and asymmetrical. This peak probably is a mixture of completely hydrolyzed and dihydrolyzed DFP. The smaller peak at δ -18.149 ppm probably indicated unhydrolyzed adsorbed DFP remaining in the solid.

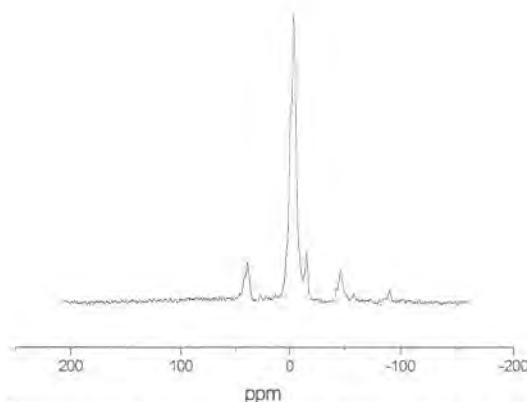


Figure 62. ^{31}P NMR Spectrum of $\text{DFP}/[\text{Ce}(\text{NO}_3)_3\text{-Cu}(\text{NO}_3)_2]\text{TiO}_2$

In conclusion, IR and ^{31}P NMR results on all the samples clearly show existence of PO_4^{3-} , a product after reaction, as a major phosphorus species in DFP/RNP systems.

Kinetic Experiments With DFP and [POM]RNP Formulations

The experiments were run in the same manner on the FTIR as the CEES experiments. Briefly, a vapor phase IR cell with 0.1g sample was evacuated. A background scan was obtained, then 9- μL of DFP (diisopropyl fluorophosphate) was injected into the sample cell and the 5-hour program started. The DFP vaporized upon injection into the IR cell. The destructive adsorption of DFP was measured by monitoring the decrease of the C-O(p) peak at 1029 cm^{-1} . The following samples were examined over the course of the project:

- Uncoated TiO_2 (SSA = $446\text{ m}^2/\text{g}$)
- 2-wt% $[\text{Na}_5\text{PV}_2\text{Mo}_{10}\text{O}_{40}]\text{TiO}_2$ (SSA = $369\text{ m}^2/\text{g}$)
- 10-wt% $[\text{Na}_5\text{PV}_2\text{Mo}_{10}\text{O}_{40}]\text{TiO}_2$ (SSA = $317\text{ m}^2/\text{g}$)
- 2-wt% $[\text{Ag}_5\text{PV}_2\text{Mo}_{10}\text{O}_{40}]\text{TiO}_2$ (SSA = $515\text{ m}^2/\text{g}$)
- 5-wt% $[\text{Ag}_5\text{PV}_2\text{Mo}_{10}\text{O}_{40}]\text{TiO}_2$ (SSA = $420\text{ m}^2/\text{g}$)
- 10-wt% $[\text{Ag}_5\text{PV}_2\text{Mo}_{10}\text{O}_{40}]\text{TiO}_2$ (SSA = $491\text{ m}^2/\text{g}$)
- 2-wt% $[\text{Ag}_5\text{PV}_2\text{Mo}_{10}\text{O}_{40}]\text{APMgO}$ (SSA = $473\text{ m}^2/\text{g}$)
- 5-wt% $[\text{Ag}_5\text{PV}_2\text{Mo}_{10}\text{O}_{40}]\text{APMgO}$ (SSA = $444\text{ m}^2/\text{g}$)
- 2-mol% $[\text{CeO}_2]\text{TiO}_2$ (SSA = $173\text{ m}^2/\text{g}$)
- 2-mol% $[\text{Ce}(\text{NO}_3)_3]\text{TiO}_2$ (SSA = $176\text{ m}^2/\text{g}$)
- 2-mol% $[\text{Cu}(\text{NO}_3)_2]\text{TiO}_2$ (SSA = $173\text{ m}^2/\text{g}$)

Figures 63 and 64 show data from measuring peak height versus time for the peak at 1029 cm^{-1} for several different formulations. For simplicity only the most promising or most representative samples were graphed. Figure 63 demonstrates that the adsorptive capacity of the [POM]MgO samples are approximately the same as that for [POM]TiO₂.

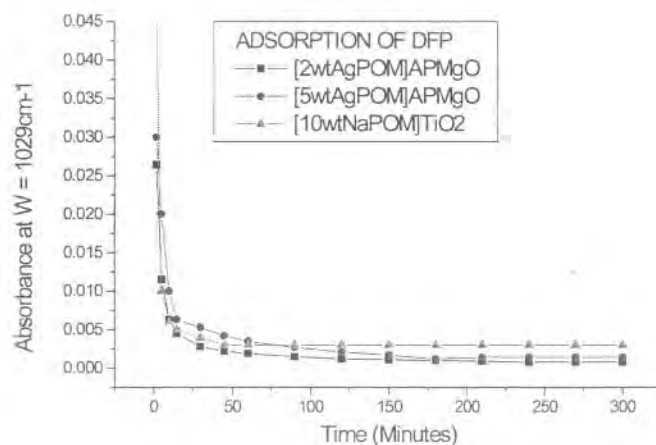


Figure 63. DFP Vapor Phase Adsorption Rate by Representative [POM]AP-MgO Samples Compared to [POM]TiO₂.

The cerium and copper compounds coated on titanium dioxide nanoparticles did not appear to benefit the destructive adsorption of DFP. Hydrolysis of DFP proceeded slightly faster in the uncoated TiO₂ than the coated samples.

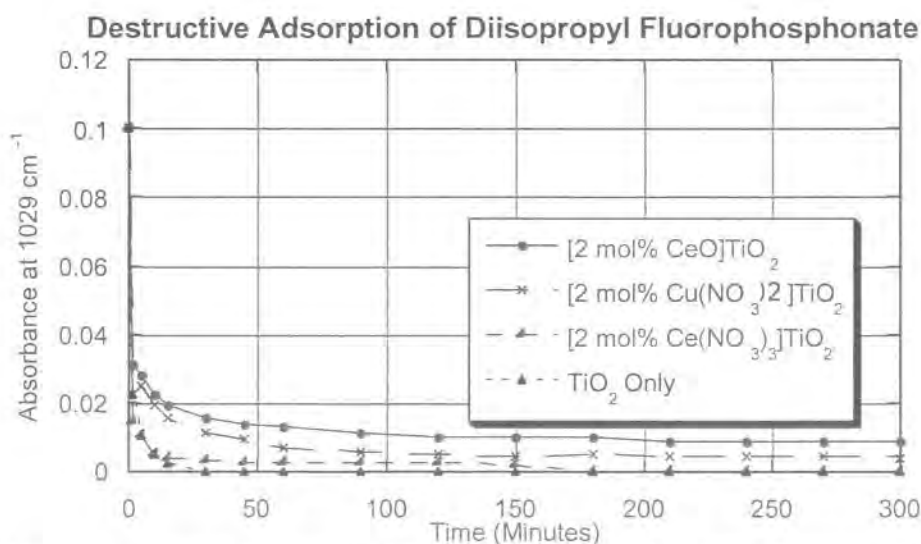


Figure 64. Destructive Adsorption of DFP by Cerium and Copper Compounds Coated On TiO₂.

Catalytic Destruction of VX Analogue Demeton S-Methyl Sulfone

Nerve agents pose a deadly concern in modern warfare. In particular, nerve agents possessing organophosphorous bonds are especially heinous. After showing great success towards the oxidation of CEES, an HD Analogue, we tried a similar approach towards the destruction of Demeton S-Methyl Sulfone, a VX analogue. As is evident in Fig. 65, the structures of the two compounds are very similar. Our approach was to design catalysts that oxidize the sulfur atom adjacent to the phosphorous atom (See Fig. 66). This will most likely have two significant effects and possibly three. First, the compound will become less volatile and therefore less dangerous, secondly the molecule would most likely become less stable and subject to decomposition into less harmful molecules. A third possibility, which is speculative, is that the oxidized molecule, although stable would be significantly less toxic than VX.

*VX is not
volatile to
begin with*

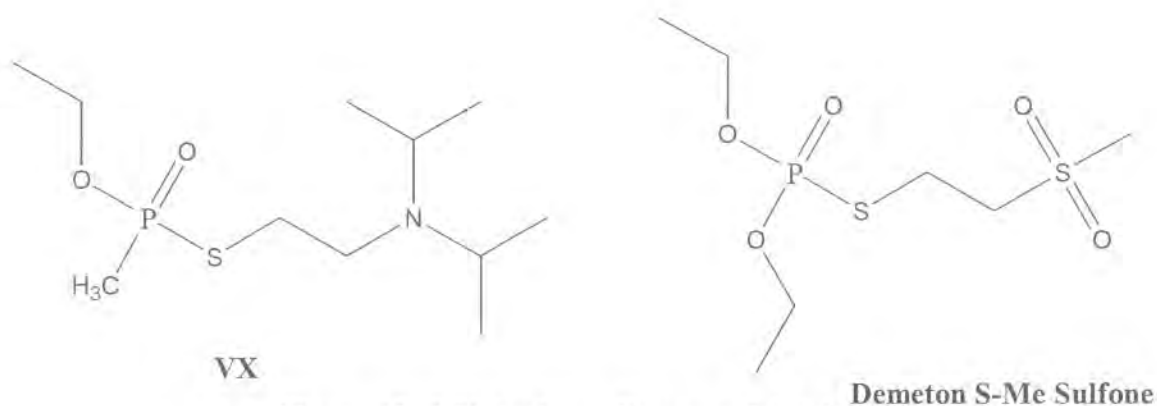


Figure 65. VX Analogue Demeton S-Methyl Sulfone.

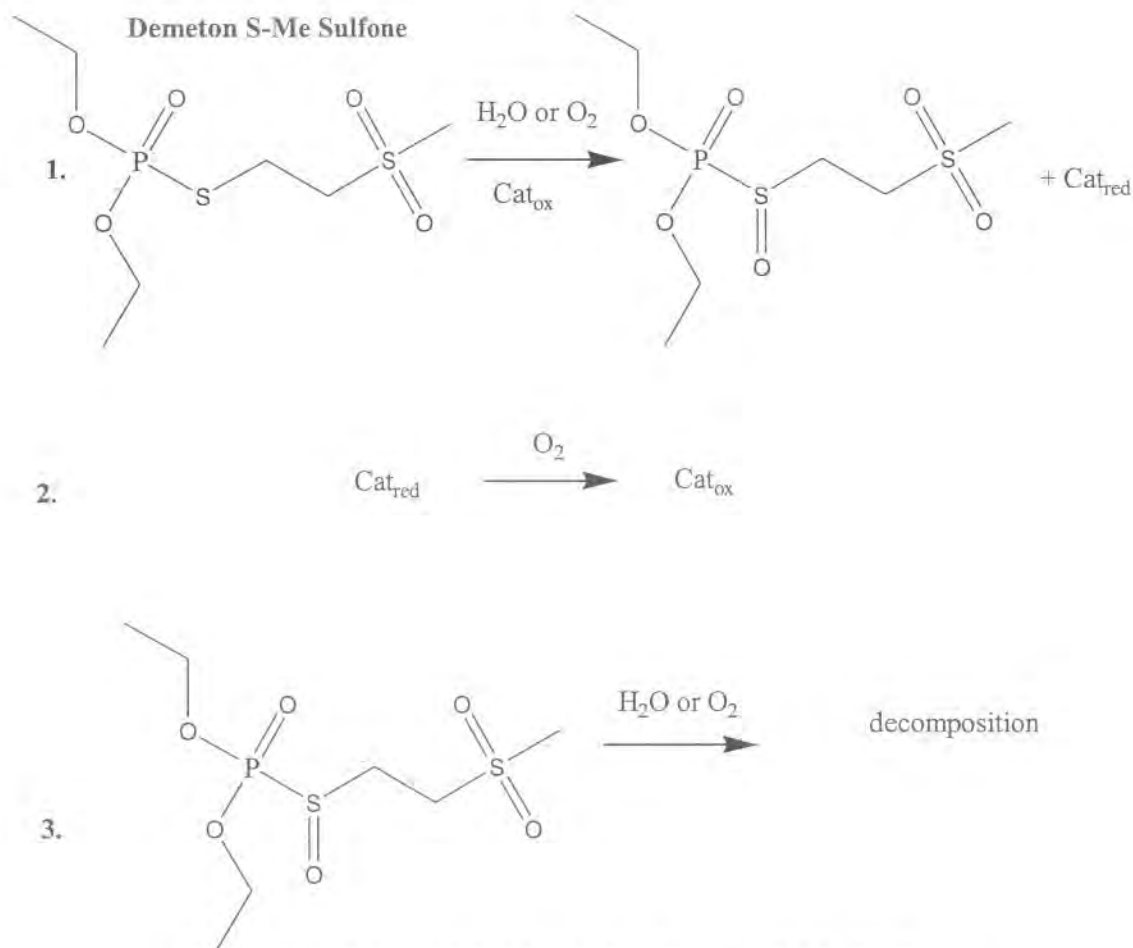


Figure 66. Proposed Oxidation for Demeton S-Me Sulfone.

In a 10 ml Schlenk flask, 0.005 g (1.0×10^{-5} mol, 1eq) of TEAAuCl₂, 0.004 g (2.0×10^{-5} mol, 2eq) of CuSO₄, 0.015 g (4×10^{-5} mol, 4 eq) of TBANO₃ were dissolved in 3.0 ml of acetonitrile. Under constant stirring the acetonitrile was removed by vacuum. To the flask, 1.0 ml of Fomblin was added. The flask was attached to a gas volume displacement apparatus and the system was purged with O₂ and equilibrated to atmospheric pressure. To the flask, 0.100 ml (7.5×10^{-4} mol, 75 eq) CEES was added and the solution allowed to stir for 70 min. A solution of 0.08 g (2.5×10^{-4} mol, 25 eq) of Demeton S-Me sulfone in 0.200 mL of acetonitrile was added and the solution was allowed to stir for 1400 min. At this point, an additional 0.08 g of Demeton S-Me sulfone in 0.200 mL of acetonitrile was added and the solution was allowed to stir 4123 min. O₂ consumption was monitored by volume displacement at periodic intervals.

Figure 67 illustrates a kinetic profile for the experiment mentioned above. Time 0 is defined as the time at which the solution of Demeton S-Me Sulfone is added and all of the CEES has been consumed.

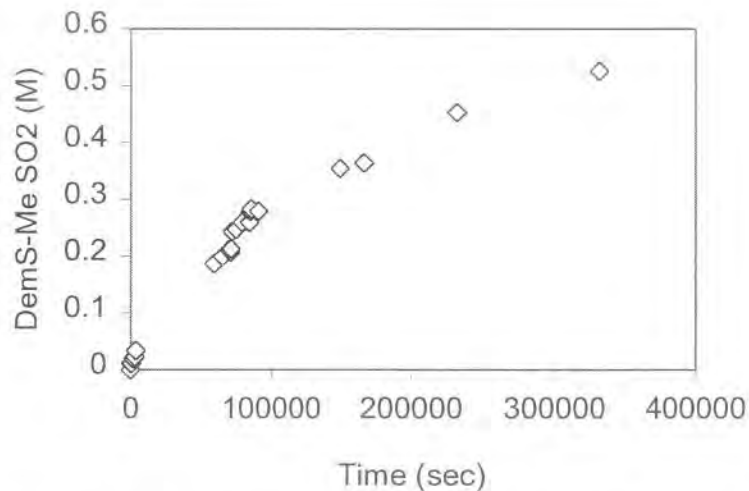


Figure 67. Kinetics Profile For Demeton S-Me Sulfone Oxidation

Although the results using the Au/Cu/NO₃ system show only preliminary evidence for Demeton S-Me Sulfone oxidation, which is the consumption of O₂, in our opinion this is a significant achievement and warrants further study.

Task 9. Economic Analysis.

Critical to NanoScale Materials' success is the production of reactive nanoparticles in commercial quantities at competitive prices. The Company has developed breakthrough manufacturing processes for its reactive metal oxide nanoparticles. The design and construction of a pilot plant to demonstrate scale-up economics and to produce increased quantities of nanoparticles for market development was completed in the fall of 2000. Currently, these processes are being further optimized to achieve the highest throughput at the lowest cost. The process breakthrough for aerogel prepared metal oxides involves replacing the costly, time-consuming hypercritical drying and vacuum heat treatment steps with a proprietary drying system for solvent removal and a hot stream of nitrogen gas for metal hydroxide dehydration. The resultant continuous process is environmentally friendly with byproducts that can be disposed of easily and safely.

The most promising nanoparticle formulations to be used in the topical protective skin cream are titanium dioxide, magnesium oxide and zinc oxide. Currently, NanoScale Materials is capable of producing aerogel prepared magnesium oxide, conventionally prepared magnesium oxide, titanium dioxide and zinc oxide in the demonstration plant. The production of aerogel prepared MgO is on the scale of 0.5 kg/hour, whereas the conventionally prepared MgO and zinc oxide on 4 kg/hour scale. Titanium dioxide is still prepared using a batch process. The estimated cost of production of these materials is in the range of \$125-1500 per kilogram using the demonstration plant. The low end pricing is for the zinc oxide and the high end for the titanium dioxide. These prices will be further reduced for a large scale production. Such reduction may be larger than an order of magnitude.

POMs are relatively easy to make, and will present no problems when scaling up to meet demand. POMs are also economical to produce. It has been estimated (Private communication from Emory) that on a production scale the cost may be as low as \$15 per kilogram.

Based on this preliminary data it appears that the cost of the reactive additive to the topical skin protectants can be synthesized on a large scale and the cost of this production is not prohibitive.

EXTENSION WORK PERFORMED AT NANOSCALE MATERIALS, INC.

Abstract

New highly catalytic POM/RNP combinations were discovered during the Phase II project. All of these were proven capable of destroying multiple types of CW agents. A major obstacle in past efforts was how to effectively incorporate the nanoparticles into the topical skin protectant (TSP) base cream. This issue was solved with the POM/RNP formulations by modifying the component ratios to obtain a consistency and texture similar to unmodified base cream. The effectiveness of the TSP formulations was shown not to decrease over time. A permeation cell apparatus was used to prove the POM/RNP/TSP systems offer increased protection against CW agent simulants. Through subcontracted testing, our formulations were also shown to be effective against real CW agents. Optimization and scale-up to kilogram quantities of TiO_2 was achieved. Significant increases in the reactivity of several nanoparticles, especially TiO_2 , were obtained during the course of scale-up. Titanium dioxide was identified as the most promising support for the variety of POM coatings. The most effective coatings were identified to be (1) a mixture of cerium nitrate and copper nitrate, (2) $\text{Na}_5\text{PV}_2\text{Mo}_{10}\text{O}_{40}$, (3) $\text{Ag}_5\text{PV}_2\text{Mo}_{10}\text{O}_{40}$, (4) silver nitrate, and (5) nanoparticulate cerium oxide.

Since the conclusion of Phase II of this project, there have been advancements in the metal oxide nanoparticle production at NanoScale. Samples of NanoActiveTM titanium dioxide, alumina, silica, and commercial silica were characterized by BET and XRD methods and sent to Dr. Hill group at Emory University to be coated with the most promising polyoxometalates (POM) and/or metal salt formulations. The 2 POM coatings were based on $\text{Cu}_2\text{HPV}_2\text{Mo}_{10}\text{O}_{40} \cdot 22\text{H}_2\text{O}$, $\text{K}_9[(\text{Fe}(\text{OH})_2)_3(\text{A}-\alpha\text{-PW}_9\text{O}_{34})_2] \cdot 20\text{H}_2\text{O}$ and/or two copper salts, $\text{Cu}(\text{NO}_3)_2 \cdot 2.5\text{H}_2\text{O}$, $\text{Cu}(\text{OTf})_2$. The first stage of testing involved a semi-dry GC procedure. In this, the adsorption of three chemical warfare agent simulants (CWAS) by various coated and uncoated nanoparticle formulations was studied in a dry state followed by solvent extraction and quantification by GC/MS. The CWAS used for HD were: 2-chloroethylethylsulfide (CEES), 2-chloroethylphenylsulfide (CEPS), GD simulants: dimethylmethylphosphonate (DMMP), Diisopropylfluorophosphate (DFP). The most promising materials were moved forward and incorporated into the topical skin protectant (TSP) forming a reactive TSP (rTSP) to increase its protective capability without compromising its physical protective function. CWAS permeation through the TSP and rTSPs was monitored over time by a laboratory Miniature Automated Continuous Air Monitoring System (MINICAMS) to evaluate the protective efficacies of rTSPs. The most effective rTSP formulation contained 9% NanoActiveTM TiO_2 . This formulation reduced CEPS permeation by 99% and DFP permeation by 80% relative to the TSP.

Experimental

Materials:

Diisopropylfluorophosphate (DFP) and dimethylmethylphosphonate (DMMP) were obtained from Aldrich Chemical Co. and used as GD simulants without further purification. 2-chloroethylphenylsulfide (CEPS) and 2-chloroethylethylsulfide (CEES) were obtained from Aldrich Chemical Co. and used as HD simulants without further purification. SiO₂ was from Aldrich and used without further purification.

Fomblin® perfluoropolyether oil was obtained from Ausimont and used without further purification. Unmodified TSP, and polytetrafluoroethylene powder were provided by Dr. E. Braue, and CPT S. Hobson, Drug Assessment Division, USAMRICD.

Materials from Emory: POMs: Cu₂HPV₂Mo₁₀O₄₀•22H₂O, K₉[(Fe(OH)₂)₂]₃(A-α-PW₉O₃₄)₂]•20H₂O. Copper salts: Cu(NO₃)₂•2.5H₂O, Cu(OTf)₂. Emory materials were also coated onto NanoScale materials at Emory.

NanoScale Materials: NanoActive™ alumina, NanoActive™ TiO₂, NanoActive™ SiO₂.

Metal Oxide Characterization

NanoActive™ titanium dioxide, alumina, silica and commercial silica were characterized by: surface area and pore volume determinations by BET (*Quantachrome* Nova 2200), and structural determination by XRD (*Kratos*, XDS-6000).

Procedure for GC Adsorption Experiments

The adsorbents (0.1 g) were placed in glass vials and treated with an amount of agent equal to a weight ratio of 1:10 (simulant:adsorbent). After brief vortex mixing, the samples were allowed to react for 75 minutes. The solid was extracted with *n*-hexane (10 mL). The amount of extracted agent was measured with a gas chromatograph/mass spectrometer (Hewlett Packard 5890 GC/5972 MSD) using *n*-decane as an internal standard.

Procedure for Permeation Experiments

Preparation of the rTSP was accomplished by adding measured amounts of appropriate additives to the magnetically stirred perfluoropolyether oil component of the base cream. After 24 h of stirring, additional mixing was done with a mechanical mixer. The polytetrafluoroethylene powder was then added in separate portions to the stirring mixture, followed by the addition of more oil. Viscosity measurements were conducted at 20 °C with a Brookfield R/S-CPS rheometer. The viscosities of the rTSP were normalized to the viscosity of the unmodified base TSP (ICD 3005). Permeation testing was performed using MINICAMS with data collection and analysis using the Laboratory Monitoring System (LM-1001) (OI Analytical, CMS Field Products Group Pelham, AL). This multi-port sampling system collected samples on a sorbent bed following desorption and separation by gas chromatography coupled with a flame photometric detector. The permeation study was conducted by a two-step protocol developed and utilized at USAMRICD (Aberdeen Proving Grounds, MD). First, the amount of challenge agent that permeated the rTSP and TSP was monitored over a 20 h time frame. Second, the time required for 1,000 ng of challenge agent to penetrate the cream was measured.

Microsoft Excel and a proprietary program (provided by Dr. E. Braue, and CPT S. Hobson, Drug Assessment Division, USAMRICD) were used to analyze the data obtained from the MINICAMS permeation tests.

Results and Discussion

Metal Oxide Characterization

Fig 68 displays the XRD of the various samples used in this study. Narrow peaks seen in the figure (2θ 37.8, 44.0, 64.4 and 77.5) are due to the sample holder itself. Table 12 summarizes the BET data for those samples. All the uncoated materials used in this study are amorphous, highly porous materials with high surface areas.

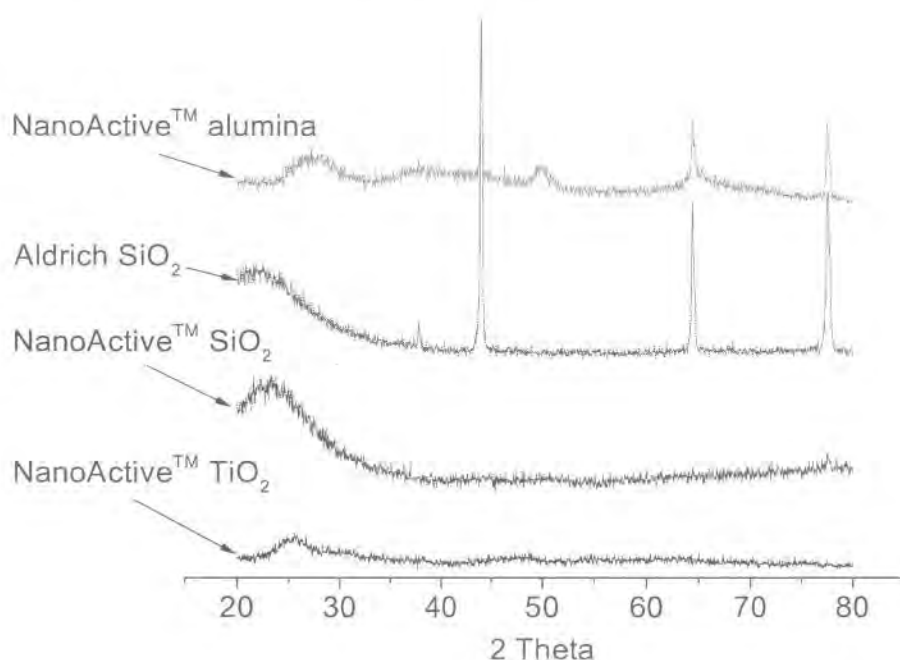


Fig 68. XRD data of Various High Surface Area Oxides

Table 12. BET data for Various Samples

<i>Sample</i>	<i>Surface area, m²/g</i>	<i>Average pore diameter, Å</i>	<i>Total pore volume, x 10³ cc/g</i>
NanoActive™ TiO ₂	443	12.332	272.97
NanoActive™ Al ₂ O ₃	707	38.552	1367.9
NanoActive™ SiO ₂	693	35.467	614.7
Aldrich SiO ₂	378	40.276	761.66

The Government's rights to use, modify, reproduce, release, perform, display, or disclose technical data or computer software marked with this legend are restricted during the period shown on the cover page as provided in paragraph (b)(4) of the Rights in Noncommercial Technical Data and Computer Software--Small Business Innovative Research (SBIR) Program clause contained in the contract DAMD17-99-C-9012 with NanoScale Materials, Inc. (Formerly Nantek, Inc.). No restrictions apply after the expiration date (12 January 2007). Any reproduction of technical data, computer software, or portions thereof marked with this legend must also reproduce the markings.

Adsorption

Results of the semi-dry adsorption experiments are summarized in Table 13. It should be mentioned lower amounts of extractable CWAS is the desired result.

Table 13. Amount of Chemical Warfare Agent Simulant Recovered From Uncoated and Coated Materials After 75 Minutes at Room Temperature. Sorbent/Simulant ratio 10:1 w/w.

Entry	Sample	Percent of simulant recovered in extract		
		HD simulants		GD simulant
		CEES	CEPS	DMMP
1	NanoActive™ Al ₂ O ₃	22.1±1.3	73.8±1.7	0.7±1.2
2	827 NanoActive™ Al ₂ O ₃	N/A	78.6±3.3	N/A
3	NSM2 NanoActive™ Al ₂ O ₃	31.1±2.6	80.1±2.0	5.6±1.4
4	NanoActive™ TiO ₂	11.8±3.3	40.4±1.6	3.7±1.2
5	827 NanoActive™ TiO ₂	N/A	71.7±3.5	N/A
6	NSM2 NanoActive™ TiO ₂	10.8±2.5	80.8±2.1	1.7±1.4
7	NanoActive™ SiO ₂	100.0±1.5	97.6±1.7	69.2±3.4
8	Comm. SiO ₂	51.0±1.5	89.1±1.8	4.2±1.4
9	827 Comm. SiO ₂	N/A	96.4±4.9	N/A
10	NSM2 Comm. SiO ₂	2.3±1.5	86.0±5.9	8.6±2.4

827: copper triflate - copper nitrate coating, (Cu(OTf)₂ and Cu(NO₃)₂•2.5H₂O)

NSM2: (Cu₂HPV₂Mo₁₀O₄₀•22H₂O and copper salts, Cu(OTf)₂ and Cu(NO₃)₂•2.5H₂O) coating.

The most effective adsorbent for CEES was the NSM2 coated commercial SiO₂ (entry 10). It showed a large improvement relative to the uncoated commercial SiO₂ (entry 8 vs. 10). The next most effective adsorbent was the NanoActive™ TiO₂ and NSM2 coated NanoActive™ TiO₂ (entries 4, 6) where the coating offered no additional benefit. The uncoated NanoActive™ Al₂O₃ was the next most effective adsorbent. Its effectiveness was decreased with the addition of the NSM2 coating (entry 1 vs. 3). The SiO₂ synthesized at NanoScale (entry 7) had no adsorption capability toward CEES. No coatings of this formulation were prepared or tested.

The most effective adsorbent for CEPS was the NanoActive™ TiO₂ (entry 4). Coating the NanoActive™ TiO₂ with Emory materials reduced its effectiveness (entry 4 vs. 5,6). The next most effective adsorbents were the 827 coated NanoActive™ TiO₂ and the uncoated NanoActive™ Al₂O₃ (entries 1,5). Coating the NanoActive™ Al₂O₃ only decreased its performance (entry 1 vs. 2,3). The commercial silica had little adsorption ability toward CEPS the 827 coated material reduced its performance further, while the NSM2 coated material offered

a slight improvement in performance (entries 8-10). The SiO₂ synthesized at NanoScale (entry 7) had little to no adsorption capability toward CEPS.

The most effective adsorbents for DMMP were the uncoated NanoActive™ Al₂O₃ and NSM2 coated NanoActive™ TiO₂ followed by the both the uncoated NanoActive™ TiO₂ and uncoated commercial SiO₂ (entries 1,6,4,8). The SiO₂ synthesized at NanoScale (entry 7) had the least adsorption capability toward DMMP.

Permeation

Table 14 displays all CEPS and DFP permeation results obtained over the course of this project and some previous relevant results. Several formulations of rTSP were tested for CEPS or DFP permeation on the MINICAMS and those formulations contained either nanoparticles or physical mixtures of TiO₂ nanoparticles and various additives. The additives used include silver nitrate, Emory's FePOM (iron substituted sandwich POM K₁₂[Fe(OH₂)₂Fe₂(P₂W₁₅O₅₆)₂]), Cu/Cu (Cu(II) salts Cu(NO₃)₂•2.5H₂O and Cu(OTf)₂) and a 1:1 mixture of FePOM and Cu/Cu mixture. Comparisons of the results were made relative to TSP (ICD 3005) as a baseline. The time for 1,000 ng CEPS and DFP permeation and nanogram amount of CEPS and DFP permeated after 20 h are shown in Table 14. The values reported are generally the average of 5 (but has ranged from 4 to 9) replicate samples plus/minus one standard deviation.

HD Simulant (CEPS)

Entries 2-6 show the results obtained with commercial and NanoActive™ TiO₂ containing formulations of rTSP. The following facts are apparent from this study.

- 1) Incorporation of commercial TiO₂ into the base cream does not offer any added advantage (entry 2 vs entry 1)
- 2) Barrier protection offered by NanoActive™ TiO₂ containing cream is superior to base cream (entries 3 and 4 vs entry 1)
- 3) Increasing amounts of TiO₂ results in increased protection as revealed by time for 1,000 ng permeation and the amount permeated after 20 h (entries 4-6)
- 4) *More importantly, relative to the base material, the composite material containing 8.93% TiO₂ exhibited a 99% reduction of CEPS vapor break-through after 20 h (entry 6 vs entry 1, from 2517 ng to 19 ng).*

Testing was also conducted with creams containing physical mixtures of NanoActive™ TiO₂ and AgNO₃ or NanoActive™ TiO₂ and Emory materials (FePOM, Cu/Cu, FePOM and Cu/Cu) to determine if there was any synergistic effect on the reduction of CEPS permeation. Additionally, a cream formulation containing 1:1 physical mixture of FePOM and Cu/Cu without any nanoparticles was prepared and tested.

All the different additives containing TiO₂ creams resulted in better barrier properties as revealed by time for 1,000 ng permeation and the amount permeated after 20 h, compared to TiO₂ only containing cream (entries 8-11 vs 4). However, at the levels used in this brief study, none of them met the goal of 99% reduction of CEPS vapor break-through after 20 h. It is very likely that increased amounts of these additives would bring about the desired protection.

Interestingly, the rTSP containing only the Emory materials 1:1 FePOM and Cu/Cu showed the lowest reduction (entry 12) of CEPS permeation of any of the rTSPs tested in current or past work. ***It is therefore concluded that the improved barrier properties imparted to rTSP is mainly due to the nanoparticles and not due to POMs or salts.***

Testing of creams containing NanoActiveTM alumina (entry 13) and SiO₂ (entries 14 and 15) revealed better performances compared to the base cream (entry 1). However, none of those formulations was as effective as the formulations containing NanoActiveTM TiO₂ (entries 4 & 5) both in terms of time for 1,000 ng permeation and the amount permeated after 20 h. Unfortunately, incorporation of commercial SiO₂ into the rTSP was unsuccessful. The SiO₂ sample had an extremely low apparent density and it adsorbed the oil during the preparation of the rTSP turning the formulation into a gel type material that was quite different visually from the TSP.

GD Simulants (DMMP, DFP)

Initially, permeation testing was carried out with dimethyl methyl phosphonate (DMMP). However, no notable permeation was observed with the unmodified base TSP (ICD 3005). The amount of permeation after 20 h of exposure to DMMP vapors was 19±23 ng. The extrapolated time until 1,000 ng of DMMP vapor permeation was 1.5±1.5 million minutes (slightly under 3 years). The TSP was obviously an effective permeation barrier to DMMP vapor. Hence, testing with DMMP was discontinued and use of DFP in the permeation testing was explored.

Barrier protection offered by NanoActiveTM TiO₂ containing cream is superior to base cream (entries 4 and 6 vs. entry 1). Additionally, increased amounts of TiO₂ results in increased protection as revealed by time for 1,000 ng permeation and the amount permeated after 20 h (entries 4, 6).

Testing was also conducted with creams containing physical mixtures of NanoActiveTM TiO₂ and AgNO₃ or NanoActiveTM TiO₂ and Emory materials (FePOM, Cu/Cu, FePOM and Cu/Cu) to determine if there was any synergistic effect on the reduction of DFP permeation. Additionally, a cream formulation containing 1:1 physical mixture of FePOM and Cu/Cu without any nanoparticles was prepared and tested.

The TiO₂ creams containing: AgNO₃, FePOM, FePOM and Cu/Cu were not considered significantly different from each other and the 2.36% NanoActiveTM TiO₂ cream in terms of the amount permeated after 20 h by one-way analysis of variance (ANOVA) at a 0.05 level of significance (entries 4, 8, 10, 11).

Testing of the cream containing NanoActiveTM SiO₂ revealed better performance compared to the base cream both in terms of time for 1,000 ng permeation and the amount permeated after 20 h (entry 14 vs. 1). Its performance was slightly greater than 2.36 % NanoActiveTM TiO₂ rTSP and slightly worse than the 8.93 % NanoActiveTM TiO₂ rTSP (entry 14 vs. 4 or 6) in terms of amount permeated after 20 h but the differences were not considered significant by ANOVA at a 0.05 level of significance.

Table 14. CEPS, DFP Permeation through Various rTSPs as Measured by the MINICAMS System

#	Percent by weight Active Component	Time (min) to 1000ng permeation		Permeation after 20 hrs ng		% reduction in 20 hr permeation relative to unmodified TSP	
		CEPS	DFP	CEPS	DFP	CEPS	DFP
1	Unmodified TSP	631±36	214±16	2,517±22 8	12,420±2, 361	0	0
2	2.33% Comm. TiO ₂	401±33	ND	3,623±29 7	ND	ND	ND
3 ^a	2.40% NanoActive TiO ₂	992±36	ND	1,468±79	ND	42	ND
4 ^b	2.36% NanoActive TiO ₂	1,823±14 0	365±49	307±93	6,949±1,5 59	88	44
5 ^b	4.76% NanoActive TiO ₂	31,968±1 3,848	ND	52±19	ND	98	ND
6 ^b	8.93% NanoActive TiO ₂	50,066±5 8,816	873±330	19±7	2,544±1,8 83	99	80
7 ^a	2.41% (AgNO ₃ , AgNO ₃ coated NanoActive TiO ₂)	5,964±4,2 86	ND	50±33	ND	98	ND
8 ^b	2.27% (AgNO ₃ , AgNO ₃ coated NanoActive TiO ₂)	5,606±4,3 01	433±115	126±116	7,916±2,0 27	95	36
9 ^b	2.30% (physical mixture: Cu/Cu, NanoActive TiO ₂)	2,822±1,5 17	501±177	241±208	5,950±1,1 91	90	52
10 ^b	2.28% (physical mixture: FePOM, NanoActive TiO ₂)	8,554±6,6 57	433±19	142±148	7,569±1,8 20	94	39
11 ^b	2.29% (physical mixture: Cu/Cu, FePOM, NanoActive TiO ₂)	12,148±5, 752	499±54	57±18	5,871±1,0 52	98	53
12	4.51% (physical mixture of 1:1 w/w: Cu/Cu, FePOM)	803±39	626±151	1,932±13 6	3,599±1,1 08	23	71
13	2.02% NanoActive AlOH	1,181±85	ND	1,038±18 8	ND	59	ND
14	2.25% NanoActive SiO ₂	1,396±12 5	390±57	615±200	4,863±1,3 60	76	61
15	4.55% NanoActive SiO ₂	1,951±53 3	ND	283±120	ND	89	ND

^a Results obtained during Phase II using TiO₂ prepared by existing procedures.

^b Results obtained using TiO₂ prepared by new and improved procedure, during the current extension phase of this project.

ND = not determined.

EXTENSION WORK PERFORMED AT EMORY UNIVERSITY

Purpose and scope of the research effort

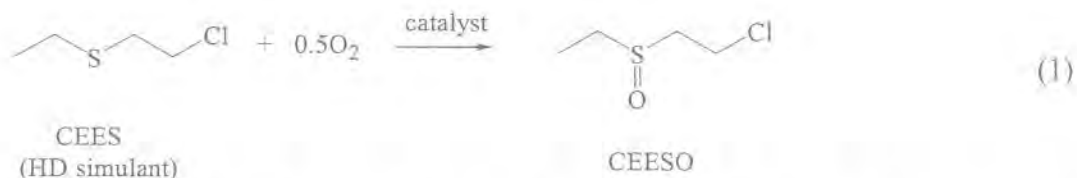
Develop new effective catalytic additives based on reactive nanoparticles (RNPs) and polyoxometalates (POMs) for topical skin protectants (TSPs) designed for oxidative decontamination of mustard (HD) and hydrolysis of G agents under ambient conditions.

Abstract

The most reactive catalytic compositions yet for mustard (HD) (and the HD analogue CEES) aerobic sulfoxidation decontamination comprise a Cu(II) salt having weakly bound counter anions, such as triflate, perchlorate, tetrafluoroborate, copper or tetra-*n*-butylammonium nitrate (the systems containing Cu(II) salts with two different anions are henceforth referred to as "Cu/Cu"), and an Fe-containing polyoxometalate (POM). Some systems result in hundreds of turnovers to the corresponding sulfoxide in 100% selectivity under ambient conditions in a short period of time (hours). The POMs that contain more than one adjacent Fe center in the surface sites, such as $[\text{Fe}_3\text{PW}_9\text{O}_{37}\bullet\text{NO}_3]^{7-}$ and $[\text{Fe}_3\text{PW}_9\text{O}_{37}]^{6-}$ are among the most effective POM catalyst components. The addition of NanoActive™ TiO_2 or binding of Cu/Cu and POM to NanoActive™ TiO_2 , Al_2O_3 and SiO_2 did not result in higher catalytic activity in acetonitrile and hexane. However, our results indicate that the rates of sulfoxidation are higher in perfluoropolyether (PFPE) media such as Fomblin® and Fluorolink™ than in any other solvents.

Introduction

The development of new materials to catalyze the selective aerobic oxidation of HD under ambient conditions (1 atm air/ O_2 and 25 °C) is of both intellectual and practical interest. The ideal catalyst should not only be selective and reasonably rapid, but it should also be efficient in the solid state. To date there are very few molecules or materials that catalyze rapid air-based oxidations under ambient conditions.³⁷ We report here new compositions of dual mode decontamination catalysts that potentially catalyze effective hydrolysis of G agents and air (O_2) oxidative decontamination of HD (mustard) under ambient conditions.



These catalysts comprise a Cu(II) salt having weakly bound counter anions, such as triflate, perchlorate, tetrafluoroborate, copper or tetra-*n*-butylammonium nitrate, and/or anionic metal oxygen clusters (polyoxometalates or POMs for short)^{38,39}. POMs that contain more than one Fe center in the surface sites, such as $[\text{Fe}_3\text{PW}_9\text{O}_{34}]^{6-}$, $[\text{Fe}_3\text{PW}_9\text{O}_{34}(\text{NO}_3)]^{7-}$ and $[\text{Fe}_3(\text{A}-\alpha\text{-PW}_9\text{O}_{34})_2]^{9-}$ are among the most effective of these POM catalyst components. In the presence of these catalysts the rates of sulfoxidation are faster in perfluoropolyether (PFPE) media such as Fomblin® and Fluorolink™, than in any other solvents. PFPEs constitute a major component of existing topical skin protectants (TSPs).

Experimental

General methods and materials

A- α - $\text{Na}_9\text{PW}_9\text{O}_{34} \cdot 7\text{H}_2\text{O}$ and $\text{Na}_5\text{PV}_2\text{Mo}_{10}\text{O}_{40}$ were prepared by the literature methods, and their purities were checked by FT-IR. NanoActive™ particles and unmodified TSP samples were obtained from NanoScale Materials Inc. and were used as received. $\text{Fe}(\text{NO}_3)_3 \cdot 9\text{H}_2\text{O}$, tetra-*n*-butylammonium bromide (TBABr), acetonitrile, 2-chlorethyl ethyl sulfide (CEES), 2-chlorethyl phenyl sulfide (CEPS), tetrahydrothiophene (THT) and 1,3-dichlorobenzene were purchased from Aldrich and used without further purification. The perfluoropolyether (PFPE) Fluorolink™ 7004 was purchased from Ausimont USA, Inc., and was used as received. The infrared spectra were recorded on a Nicolet 510 FT-IR spectrometer. Oxidation products were identified and quantified by gas chromatography (GC; Hewlett Packard 5890 series gas chromatograph equipped with a flame ionization detector, 5% phenyl methyl silicone capillary column, N_2 carrier gas, and a Hewlett Packard 3390A series integrator). Gas chromatography-mass spectrometry measurements were performed on a Hewlett Packard 5890 series II gas chromatograph connected to a Hewlett Packard 5971 mass selective detector. Elemental analyses were performed by Atlantic Microlab, Inc. in Atlanta, GA and Desert Analytics in Tucson, AZ.

Synthesis of the Cu substituted $\text{PV}_2\text{Mo}_{10}\text{O}_{40}^{5-}$.

$\text{H}_5\text{PV}_2\text{Mo}_{10}\text{O}_{40} \cdot 10\text{H}_2\text{O}$ (0.5 g, 0.26 mmol) was dissolved in 90 mL of water with stirring. $\text{Cu}(\text{NO}_3)_2 \cdot 2.5\text{H}_2\text{O}$ 0.3 g (1.3 mmol) and $\text{Cu}(\text{OTf})_2$ (0.7 g, 1.95 mmol) were slowly added to the solution while stirring. The solution was heated at 50 °C for 3 hours with stirring, cooled to room temperature, and allowed to crystallize at 15 °C. After 8 days, large orange crystals formed. Anal. Calcd. for $\text{Cu}_2\text{HPV}_2\text{Mo}_{10}\text{O}_{40} \cdot 22\text{H}_2\text{O}$: Cu, 5.63; P, 1.37; V, 4.51. Found: Cu, 5.64; P, 1.38; V, 4.62.

X-ray Crystallographic Structure Determination.

A suitable crystal was coated with Paratone N oil, suspended in a small fiber loop and placed in a cooled nitrogen gas stream at 100 K on a Bruker D8 SMART APEX CCD sealed tube diffractometer with graphite monochromated MoK_α (0.71073 Å) radiation. Data were measured using a series of combinations of phi and omega scans with 10 second frame exposure and 0.3° frame width. Data collection, indexing and initial cell refinements were all carried out using SMART⁴⁰ software. Frame integration and final cell refinements were done using SAINT⁴¹ software. The final cell parameters were determined from least-squares refinement on 9618 reflections. The SADABS⁴² program was used to carry out absorption corrections. The structure was solved using Direct methods and difference Fourier techniques (SHELXTL, V5.10).⁴³ All non-hydrogen atoms were refined anisotopically. Scattering factors and anomalous dispersion corrections are taken from the *International Tables for X-ray Crystallography*.⁴⁴ Structure solution, refinement, graphics and generation of publication materials were performed by using SHELXTL, V5.10 software. The structural data on Cu^{II} substituted $\text{PV}_2\text{Mo}_{10}\text{O}_{40}^{5-}$ are summarized in Figures 69 and 70.

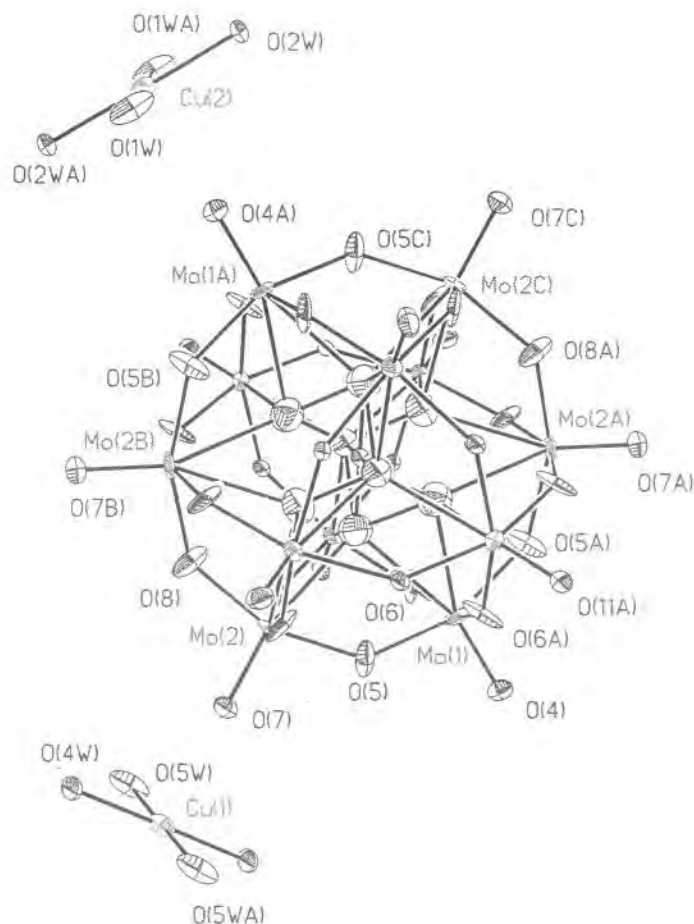


Figure 69. Thermal ellipsoid plot of the Cu^{II} substituted $\alpha\text{-PV}_2\text{Mo}_{10}\text{O}_{40}^{5-}$.

Although this structure was similar to one previously reported,³⁷ the space group and intermolecular bonding in this structure was different. The Keggin units are held together by relatively strong O-Cu-O bonds as follows: Cu1 has four water molecules in a plane with bond lengths 1.91 and 1.96 Å and two longer bonds to the O7 atoms on two different Keggin units of 2.46 Å. Similarly, Cu2 has four planar waters at 1.92 and 1.96 Å and two longer bonds to the O4 atoms on nearby Keggin units of 2.46 Å. The crystal consists of a three dimensional array of Keggin ions held together by O-Cu bonds through the O7 and O4 oxygen atoms of the Keggin moieties. In addition, there are several dispersed solvent waters in the lattice. This X-ray structure of copper(II) salt of the decamolybdovanadate anion, $\alpha\text{-PV}_2\text{Mo}_{10}\text{O}_{40}^{5-}$ suggests that the redox-active copper counterions completely surround the cluster and are loosely associated with the anion (the average distance between each copper center and the terminal oxo ligand of the anion is 2.5 Å) (see Figure 70).



Figure 70. Polyhedral drawing of Cu^{II} substituted $\text{PV}_2\text{Mo}_{10}\text{O}_{40}^{5-}$ showing the redox-active copper counterions surrounding the cluster.

Elemental analyses established that the stoichiometric ratio of $\text{Cu}(\text{II})$ to $\text{PV}_2\text{Mo}_{10}\text{O}_{40}^{5-}$ is 2:1. The overall quality of the crystals prevented the precise determination of the identity or geometry of the ligands surrounding each copper center. In addition, the complex $\alpha\text{-PV}_2\text{Mo}_{10}\text{O}_{40}^{5-}$ is a mixture of five positional isomers. Therefore, each of the twelve MO_6 centers of the anion is occupied by vanadium $1/6^{\text{th}}$ of the time and by molybdenum $5/6^{\text{th}}$ of the time.

Synthesis of $[\text{Fe}_3\text{PW}_9\text{O}_{37} \bullet \text{NO}_3]^{7-}$

To $\text{A-}\alpha\text{-Na}_9\text{PW}_9\text{O}_{34} \bullet 7\text{H}_2\text{O}$ (2.5 g) dissolved in 50 mL of H_2O was added TBABr (20 g) dissolved in 80 mL of H_2O . The mixture was stirred for 30 min and centrifuged. The precipitate was removed by filtration and dissolved in acetonitrile (80 mL). To this solution $\text{Fe}(\text{NO}_3)_3$ (1.2 g) was added quickly with vigorous stirring. A dark reddish-brown solution and a small amount of water soluble precipitate immediately formed. The solution was filtered, stirred for 4 h at room temperature, and left to evaporate in air. Orange crystals formed from the solution were recrystallized from acetonitrile and exhibit a sharp nitrate infrared band at 1389 cm^{-1} . Anal. Calcd. for $[\text{Fe}_3\text{PW}_9\text{O}_{37} \bullet \text{NO}_3]^{7-}$: Br, 0.0; N, 0.56; O, 20.51. Found: H, 4.39; N, 0.56; O, 20.50. This Keggin monomer has resisted characterization by X-ray crystallography. The polyhedral structure of the proposed POM is shown along with other POMs used in this study (Fig. 71, B).

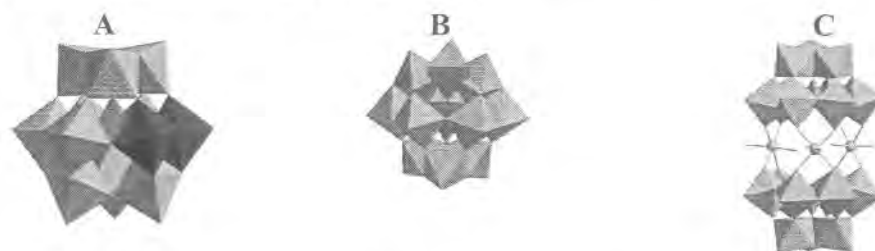


Figure 71. Polyhedral structures of the 3 polyoxometalates (POMs) used in this study. A: a mixed addenda Keggin heteropolyanion $\text{PV}_2\text{Mo}_{10}\text{O}_{40}^{5-}$ (only one positional isomer shown), B: the A-type Keggin POM of formula $\text{Fe}_3\text{PW}_9\text{O}_{37}^{6-}$ C: the A-type sandwich POM of formula $(\text{Fe}((\text{OH}_2)_2)_3)(\text{A-}\alpha\text{-PW}_9\text{O}_{34})_2^{9-}$.

Optimization of Cu/Cu and preparation of Cu/Cu

A stock solution of 15 mM $\text{Cu}(\text{NO}_3)_2$ was prepared in 25-mL vials using anhydrous CH_3CN . The concentration of $\text{Cu}(\text{OTf})_2$ was varied from 10 mM to 37.5 mM. The concentration of $\text{Cu}(\text{NO}_3)_2$ was kept constant in all reactions (15 mM). Aliquots (0.5 mL) of the $\text{Cu}(\text{OTf})_2/\text{Cu}(\text{NO}_3)_2$ solution were placed in 20-mL vials and 0.876 mmol of 1,3-dichlorobenzene (GC internal standard) was added to each. The total volume of each solution was adjusted to 2.395 mL (4 significant figures justified) by addition of anhydrous CH_3CN , and each vial was sealed and fitted with a PTFE septum. After stirring for 1-20 min, 0.100 mL of 2-chloroethyl ethyl sulfide (CEES) was added via syringe. Air access during the reaction was provided through the needle in the cap. Each reaction was stirred continuously and monitored for 20-24 hours, and aliquots were removed for GC analysis every 15 minutes. Importantly, the optimal ratio of $\text{Cu}(\text{OTf})_2/\text{Cu}(\text{NO}_3)_2$ was subsequently used in all experiments. The $\text{Cu}(\text{OTf})_2/\text{Cu}(\text{NO}_3)_2$ solution was evaluated for activity after catalysis (9 and 13 turnovers, respectively) and no change in activity was apparent. Blue-green crystals of $\text{Cu}(\text{OTf})_2$ (identified by X-ray crystallography) were re-isolated in high yield after catalysis (aerobic CEES oxidation). The Cu/Cu catalyst was prepared by mixing (grinding in a pestle) $\text{Cu}(\text{OTf})_2$ and $\text{Cu}(\text{NO}_3)_2$ in the optimum ratio. Cu/Cu/POM catalysts were prepared by mixing of the solid POMs with Cu/Cu. The compositions were dried in vacuo overnight prior to use.

Optimization and preparation of Cu/OTf/NO₃

Because the catalyst was designed to be used in perfluorinated media its optimization was performed in 96% PFPE/4% CH_3CN (4% CH_3CN used to insure solubility). In all experiments, 0.018 g of $\text{Cu}(\text{OTf})_2$ (5.0×10^{-5} mol) was used. TBANO_3 was varied from 0.5×10^{-5} to 8.0×10^{-5} mol. The mixtures were placed in 20-mL vials and 2 mL of 96% PFPE/4% CH_3CN was added. After the mixture dissolved (from 20 to 40 min) the total volume of the solution was adjusted to 2.395 mL (4 significant figures justified) by addition of 96% PFPE/4% CH_3CN , and the vial was sealed and fitted with a PTFE septum. The mixture was stirred for 1-5 min, and 0.105 mL of 2-chloroethyl ethyl sulfide (CEES) was added via syringe. Air access during the experiment was provided through the needle in the cap. The reaction was stirred continuously for 1 hour. At the end of the reaction, an extraction was performed using 2.4 mL of methylene chloride and the top fraction was collected (prior to the use of CH_2Cl_2 for extraction, it was established that CEES is not oxidized in CH_2Cl_2 under these conditions, and the partition coefficient of CEES between CH_2Cl_2 and 96% PFPE/4% CH_3CN was determined as $P_{\text{CEES}} = [\text{CEES}]_{\text{CH}_2\text{Cl}_2} / [\text{CEES}]_{\text{PFPE/CH}_3\text{CN}} = 1.692$). An internal standard (0.876 mmol of 1,3-dichlorobenzene) was added and 1.0 μL aliquots of the solution were analyzed by GC.

Preparation of coated NanoActive™ particles

POM (0.00005 moles) and/or $\text{Cu}(\text{OTf})_2$ (0.00125 moles) and $\text{Cu}(\text{NO}_3)_2 \cdot 2.5 \text{H}_2\text{O}$ (0.00085 moles) were dissolved in 50 mL of DI water; the pH of the solution was adjusted by the addition of trifluoromethanesulfonic acid (0.1 M) or sodium hydroxide (0.1 M) to keep the NanoActive™ particles surface positively or negatively charged. (The following pHs values were used to keep the negative charge on the RNP surface: for TiO_2 nanoparticles - 8.65, for

SiO₂ nanoparticles - 4.55, for Al₂O₃ nanoparticles - 8.94). To this solution, 2 g of NanoActive™ particles were added.

Suspensions were mixed at RT for 2 hrs and centrifuged for 55 min at 4000 rpm (from 12 to 15 mL of gels were produced); gels were washed twice with addition of 40 mL of DI water and dried at 100 °C for 1 hr and at 120 °C for 2 hrs.

Preparation of TSPs with additives

To 2.4375 g of unmodified cream 0.0625 g of active ingredients (NanoActive™ TiO₂, POM, Cu/Cu catalyst or their mixtures containing 0.060 g of TiO₂ and 0.0025 g of POM and/or Cu/Cu catalyst) were mixed (grinded in a mortar).

Catalytic oxidation of HD analogues (2-chloroethyl ethyl sulfide (CEES), 2-chlorethyl phenyl sulfide (CEPS) and tetrahydrothiophene (THT))

In a typical experiment, 15-25 mg of the catalyst was weighed out into 20-mL vial and dissolved or suspended in 1.0 mL of CH₃CN, 0.876 mmol of 1,3-dichlorobenzene (GC internal standard) was added and the total volume was adjusted to 2.395 mL. The vial was sealed and fitted with a PTFE septum. After the solution/suspension was stirred for 1-20 min, 0.105 mL of HD analogue was added to initiate the reaction. Air access to the mixture was provided through a needle in the cap.

Evaluation of TSPs

In a typical experiment, 2.5 g of cream containing 62.5 mg of additive was weighed out into a 15-mL centrifuge vial, 6.25 mg (0.05 mmol) of CEES was spread over the cream (the weight ratio of CEES to active additives was 1:10), the vial was shaken for 1 min, and left to sit at room temperature for 60 min. Hexane or acetonitrile (4.8 ml) was added into a vial for extraction of CEES, the vial was shaken again for 1 min, and then sonicated for 5 min and centrifuged at 5000 rpm for 5 min. The solvent was separated from the cream, 0.05 mmol of 1,3-dichlorobenzene (GC internal standard) was added, and the total volume was adjusted to 5.0 mL. Three 1 µL portions of this solution were analyzed by GC.

Results and Discussion

Soluble binary cupric nitrate and triflate systems catalyze the air oxidation of the mustard (HD) analogue, 2-chloroethyl ethyl sulfide (CEES) to the corresponding desired sulfoxide (CEESO) with effectively quantitative selectivity in acetonitrile under ambient conditions (eq. 1 and Table 15, line 2). CEESO is far less toxic than the corresponding vesicant sulfone (CEESO₂) and other products.⁹⁴⁵ This Cu(NO₃)₂/Cu(OTf)₂ system (henceforth referred to as "Cu/Cu" for convenience) was determined to be optimal after examining several other Cu(II) salts alone and in combinations. These optimization experiments indicated that both nitrate and an additional weakly binding counter anion such as trifluoromethane sulfonate (triflate or OTf) were required for optimal activity of the Cu(II)-based system. Isolation of high yields of blue-green crystals of Cu(OTf)₂ (characterized by X-ray diffraction) after 10 turnovers shows that this salt is not consumed significantly if at all during catalytic turnover. However, based on the diminution of the intensity of the NO₃⁻ peaks in the mid-infrared (826, 1380, 1790, 2428 cm⁻¹

after 13 turnovers) and the production of NO₂, nitrate is reduced during the reaction. Since each Cu(II) ion turns over many times (produces many equivalents of CEESO product per equivalent of Cu(II), as does each NO₃⁻ ion) during reaction (see Table 15, line 2 and footnote g) and only one equivalent of nitrate is present, nitrate clearly isn't the terminal oxidant. Significantly however, Kochi has clearly demonstrated that NO₂ can catalyze the aerobic oxidation of thioethers in dichloromethane solution under mild conditions.^{37b} Thus some CEESO production in the systems we report here is doubtless taking place by NO₂ generated in situ and by the Cu(II) or Cu(II)/POM systems themselves. Significantly, when only Cu(NO₃)₂ was present under otherwise identical conditions, there was almost no production of CEESO. The experimental conditions make it very problematical to quantify how much CEESO is derived from the different catalytic processes taking place simultaneously. Figure 72 indicates that the optimal ratio of triflate to nitrate for catalytic turnover is 1.5. Both anions clearly play roles in catalytic turnover. Triflate associates with the most active form(s) of the catalyst for selective sulfoxidation, but the nitrate dependence could derive solely from its role as a precursor for NO₂. The non-integer value of the optimal [OTf]/[NO₃⁻] ratio is consistent with simultaneous sulfoxide production by a cupric triflate complex and by NO₂ generated in situ.

Table 15. Aerobic Oxidation/Adsorption of 2-Chloroethyl Ethyl Sulfide (CEES) in Acetonitrile by TiO₂ and TiO₂/Cu(II) and/or Polyoxometalate (POM)-based Homogeneous and Heterogeneous Catalysts^a

Catalyst ^b	9 hrs ^c		20 hrs ^c		70 hrs ^c	
	% conv. ^d	% yield ^e	% conv. ^d	% yield ^e	% conv. ^d	% yield ^e
TiO ₂ ^f (1)	0	0	0	0	0	0
Cu(NO ₃) ₂ / Cu(OTf) ₂ (Cu/Cu) ^g	51	51	56	56	65	65
TBA ₅ PV ₂ Mo ₁₀ O ₄₀ (2) ^h	1	1.5	2.5	2.4	6	5
Cu ₂ HPV ₂ Mo ₁₀ O ₄₀ (3) ^h	1.5	2	4	4.5	7	7
TBA ₉ (Fe ^{III} (OH ₂) ₂) ₃ (A-α-PW ₉ O ₃₄) ₂ (4) ^h	0	0	0	0	0	0
TBA ₆ Fe ₃ PW ₉ O ₃₇ (5) ^h	0	0	0	0	0	0
TBA ₇ Fe ₃ PW ₉ O ₃₇ (NO ₃) (6) ^h	31	31	45	45	50	50
Cu/Cu/ 1 ^j	0	0	0	0	0	0
Cu/Cu +1 ⁱ	37	37	39	39	41	41
Cu/Cu +2	51	51	56	56	65	65
Cu/Cu +3	50	50	57	57	68	68
Cu/Cu +4	50	50	57	57	68	68
Cu/Cu +5	70	70	81	81	85	85
Cu/Cu +6	77	77	90	90	92	92
Cu/Cu +2+1 ^k	31	31	42	42	60	60

^aGeneral conditions: 0.875 mmol (0.35 M) of CEES, 1 atm of air, 0.876 mmol (0.35 M) of 1,3-dichlorobenzene (internal standard) were stirred in 2.5 mL of acetonitrile at 25 °C; ^bno product was observed in the presence of TiO₂, Cu(II), POM or TiO₂; ^c reaction time; ^d% conversion = (moles of CEES consumed / moles of initial CEES) x 100; ^e% yield = (moles of

CEESO / moles of initial CEES) $\times 100$; ^f1 = NanoActive™ TiO₂ (37 mg suspended in solution);
^g(Cu/Cu) = 15 mM Cu(NO₃)₂ + 22.5 mM Cu(OTf)₂; ^h 0.8 mM of TBA₅PV₂Mo₁₀O₄₀ (2),
 Cu₂HPV₂Mo₁₀O₄₀ (3), TBA₉(Fe^{III}(OH₂)₂)₃(A- α -PW₉O₃₄)₂ (4), TBA₆Fe₃PW₉O₃₇ (5),
 TBA₇PW₉O₃₇(NO₃) (6); ^jCu/Cu bound to NanoActive™ TiO₂ (60 mg suspended in solution);
ⁱNanoActive™ TiO₂ (30 mg suspended in a solution of Cu/Cu); ^kNanoActive™ TiO₂ (30 mg
 suspended in a solution of Cu/Cu + 0.8 mM of TBA₉(Fe^{III}(OH₂)₂)₃(A- α -PW₉O₃₄)₂.

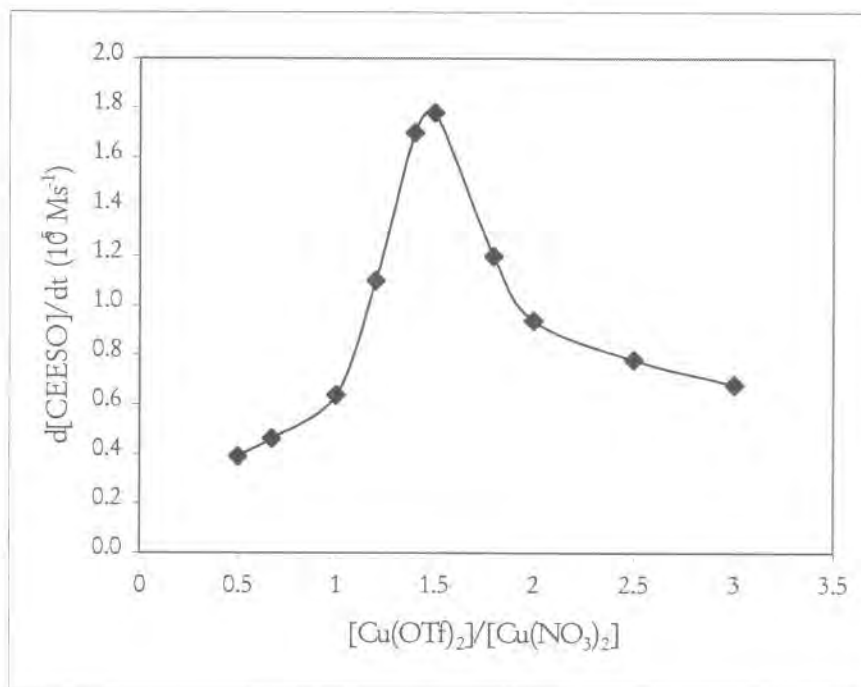


Figure 72. Rate of CEESO formation as a function of ratio of [Cu(OTf)₂] to [Cu(NO₃)₂].
 Conditions: 1 atm of air, 25 °C; [Cu(NO₃)₂] = 15 mM in acetonitrile in all reactions with
 [Cu(OTf)₂] adjusted accordingly; [CEES] = 0.35 M for all reactions.

The four acetonitrile-soluble tetra-*n*-butylammonium (TBA) salts and one non-soluble Cu(II) salt of polyoxometalates (POMs) from three representative families of POMs (Figure 71), each with extensive and reversible redox chemistry, were also prepared and evaluated as catalysts for the aerobic sulfoxidation of CEES under ambient conditions (Table 15, lines 3-7). These include PV₂Mo₁₀O₄₀⁵⁻ (2), the mixed addenda heteropolyanion, a POM with considerable documented ability to catalyze homogeneous oxidations, including some by O₂,⁴⁶⁻⁵¹ the Cu(II) salt of this heteropolyanion (3), a new POM prepared and characterized in the course of this study, the A-type sandwich POM (Fe((OH₂)₂)₃(A- α -PW₉O₃₄)₂)⁹⁻ (4), a POM recently prepared and showed to catalyze oxidations when bound to positive surfaces.⁵² Two new POMs that appear to be a Keggin monomer and analyze for “Fe₃PW₉O₃₇” (5) and “Fe₃PW₉O₃₇(NO₃)” but

have thus far resisted characterization by X-ray crystallography were also evaluated. Among all of the evaluated complexes only **6** exhibited a significant activity, **4** and **5** were effectively inactive, **2** and **3** showed a reproducible but quite low activity.

When three POMs (**2**, **3** and **4**) were added to the optimized homogenous binary cupric system (Cu/Cu) (Table 15, lines 10-12), the activity of the latter was basically unaffected.

Significantly, however, when Fe-containing Keggin POMs are added to the optimized Cu/Cu solution, there is a remarkable and reproducible increase in catalytic activity of these two of the Fe-containing POMs, **5** and **6** (Table 15, lines 13, 14).

NanoActive™ TiO₂ was completely inactive for CEES oxidation or adsorption in acetonitrile Table 15, line 1). Interestingly when TiO₂ was added to the optimized homogenous binary cupric system (Cu/Cu) (Table 15, line 10), the activity of the latter was drastically lowered. When Cu/Cu was bound to TiO₂ its activity totally vanished (Table 15, line 8).

Very similar results were observed for THT oxidation in acetonitrile (Table 16).

Table 16. Aerobic Oxidation/Adsorption of Tetrahydrothiophene (THT) in Acetonitrile by TiO₂ and TiO₂/Cu(II) and/or Polyoxometalate (POM)-based Homogeneous and Heterogeneous Catalysts^a

Catalyst ^b	9 hrs ^c		20 hrs ^c		70 hrs ^c	
	% conv. ^d	% yield ^e	% conv. ^d	% yield ^e	% conv. ^d	% yield ^e
TiO ₂ ^f (1)	0	0	0	0	0	0
Cu(NO ₃) ₂ / Cu(OTf) ₂ (Cu/Cu) ^g	55	55	58	58	70	70
TBA ₅ PV ₂ Mo ₁₀ O ₄₀ (2) ^h	1	1.5	2.5	2.4	6	5
Cu ₂ HPV ₂ Mo ₁₀ O ₄₀ (3) ^h	1.5	2	4	4.5	7	7
TBA ₉ (Fe ^{III} (OH ₂) ₂) ₃ (A-α-PW ₉ O ₃₄) ₂ (4) ^h	0	0	0	0	0	0
TBA ₆ Fe ₃ PW ₉ O ₃₇ (5) ^h	0	0	0	0	0	0
TBA ₇ Fe ₃ PW ₉ O ₃₇ (NO ₃) (6) ^h	39	38	53.8	53.3	56	56
Cu/Cu + 1 ^j	0	0	0	0	0	0
Cu/Cu + 1 ^k	38	38	39	38	43	42
Cu/Cu + 2	51	51	56	56	65	65
Cu/Cu + 3	50	50	57	57	68	68
Cu/Cu + 4	50	50	57	57	68	68
Cu/Cu + 5	72	72	83	82	86	85
Cu/Cu + 6	78	78	92	91	95	94

^aGeneral conditions: 0.88 mmol (0.347 M) of THT, 1 atm of air, 0.875 mmol (0.35 M) of 1,3-dichlorobenzene (internal standard) were stirred in 2.5 mL of acetonitrile at 25 °C; ^bno product was observed in the presence of TiO₂, Cu(II), POM or TiO₂; ^c reaction time; ^d% conversion = (moles of THT consumed / moles of initial THT) x 100; ^e% yield = (moles of THTO / moles of initial CEES) x 100; ^f**1** = NanoActive™ TiO₂ (37 mg suspended in solution); ^g(Cu/Cu) = 15 mM Cu(NO₃)₂ + 22.5 mM Cu(OTf)₂; ^h0.8mM TBA₅PV₂Mo₁₀O₄₀ (**2**), Cu₂HPV₂Mo₁₀O₄₀ (**3**), TBA₉(Fe^{III}(OH₂)₂)₃(A-α-PW₉O₃₄)₂ (**4**), TBA₆Fe₃PW₉O₃₇ (**5**),

TBA₇PW₉O₃₇(NO₃) (6); ¹Cu/Cu bound to NanoActive™ TiO₂ (60 mg suspended in solution); ¹NanoActive™ TiO₂ (30 mg suspended in a solution of Cu/Cu).

All of these catalysts were effectively inactive for 2-chlorethyl phenyl sulfide (CEPS) aerobic oxidation in acetonitrile. This is difficult to explain and shall be studied in future studies.

The rates of sulfoxidation of CEES were dramatically increased in perfluoropolyether (PFPE) media such as Fomblin® and Fluorolink™, relative to other solvents. PFPEs constitute a major component of existing topical skin protectants (TSPs).

Job's method of continues variation was used to find the optimum stoichiometry of NO₃⁻/OTf (Figure 73).

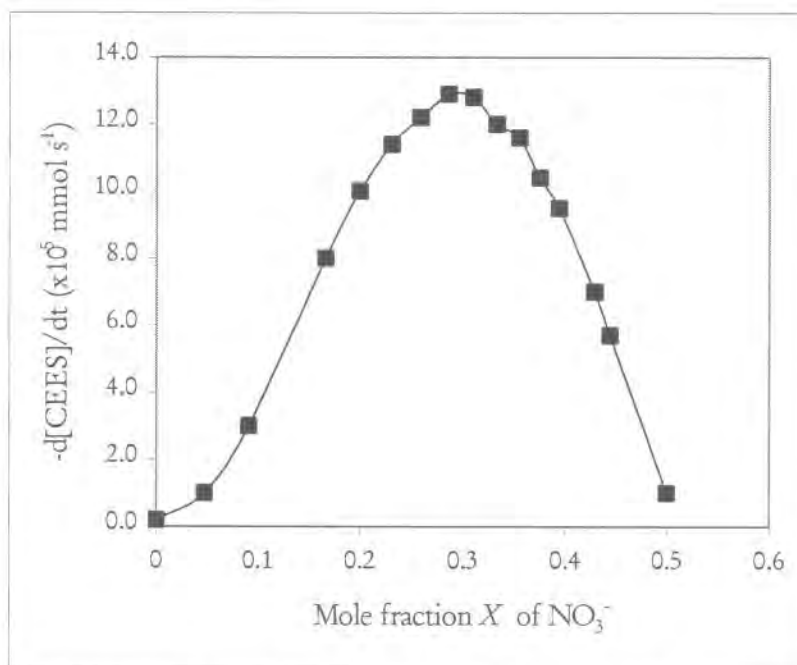


Figure 73. Aerobic oxidation of CEES in 96% Fomblin MF-300/4% CH₃CN catalyzed by Cu(OTf)₂/TBANO₃ systems as a function of the mole fraction, X, of nitrate. $X = [\text{NO}_3^-] / ([\text{NO}_3^-] + [\text{OTf}])$. [OTf] = 40 mM. Conditions: 25 °C; 1 atm of air.

Job's plot (Figure 73) indicated that the optimal ratio of [NO₃⁻]/[OTf] for maximum catalytic turnover efficiency was equal 0.4. Similarly, the optimum mole fraction of [NO₃⁻] in the Cu(II)/OTf/NO₃⁻ catalytic system was determined to be 0.286.

Fluorolink™ 7004 (Fluorolink for short) surfactant was used as a model solvent for the TSP. It forms homogeneous solutions with acetonitrile. The Cu(II)/OTf/NO₃⁻ catalyst dissolves in Fluorolink and in acetonitrile-Fluorolink mixtures after CEES addition. The replacement of acetonitrile by Fluorolink increases the efficiency of Cu(II)-based catalytic system for the aerobic oxidation of CEES (Figure 74).

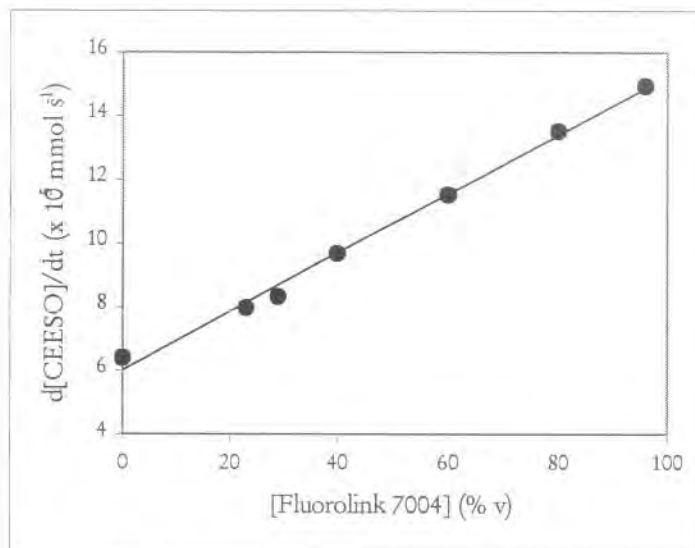


Figure 74. Effect of Fluorolink™ 7004 (volume %) on the rate of Cu(II)/OTf/NO₃⁻ catalyzed air oxidation of CEES. Conditions: 1 atm of air, 25 °C. [TBANO₃] = 16 mM. [Cu(OTf)₂] = 20 mM; [CEES] = 0.35 M.

Table 17 summarizes aerobic oxidation of CEES to CEESO catalyzed by Cu(II) triflates/nitrates and/or POMs in fluorinated media and other solvents.

The substitution of acetonitrile with 96% PFPE/4% CH₃CN significantly increases the rate of CEE oxidation catalyzed by Cu/OTf/NO₃ from 6.45 x 10⁻⁵ to 13 x 10⁻⁵ mmol s⁻¹. Three uncoated Active Nanoparticles, TiO₂, SiO₂ and Al₂O₃, in three different forms, as is, coated with Cu₂HPV₂Mo₁₀O₄₀ (**3**), or coated with **3**/Cu/Cu, were screened for catalytic activity. The results are shown in Table 18.

Table 17. Aerobic Oxidation of 2-Chloroethyl Ethyl Sulfide (CEES) in Fluorinated Fluids and Other solvents by Cu(II)-Based Catalysts^a

Catalyst ^b	Solvent	% conv. ^c	$-(d[\text{CEES}]/dt)$ (10 ⁵ , mmol s ⁻¹) ^d
CuCl ₂	PFPE ^e	0	0
CuSO ₄	PFPE ^e	0	0
Cu(NO ₃) ₂	PFPE ^e	0.50	0.13
Cu(BF ₄) ₂	PFPE ^e	0.44	0.11
Cu(ClO ₄) ₂	PFPE ^e	0.61	0.15
Cu(OTf) ₂	PFPE ^e	0.85	0.21
CuCl ₂ /TBANO ₃	PFPE ^e	3.2	0.80
CuSO ₄ /TBANO ₃	PFPE ^e	5.3	1.30
Cu(BF ₄) ₂ /TBANO ₃	PFPE ^e	33.5	8.13
Cu(ClO ₄) ₂ /TBANO ₃	PFPE ^e	46.3	11.30
Cu(OTf) ₂ /TBANO ₃ (Cu/OTf/NO ₃ ⁻)	PFPE ^e	53.0	12.90
Cu/OTf/NO ₃ ⁻	CH ₃ CN	26.5	6.45
Cu/OTf/NO ₃ ⁻	MeOH	0	0
Cu/OTf/NO ₃ ⁻	EtOH	0	0
Cu/OTf/NO ₃ ⁻	acetone	0	0
Cu/OTf/NO ₃ ⁻	CH ₂ Cl ₂	0	0
Cu/OTf/NO ₃ ⁻	C ₂ H ₄ Cl ₂	0	0
Cu/OTf/NO ₃ ⁻	TFE ^f	0	0
Cu(BF ₄) ₂ /TBANO ₃	PFPE ^g	38.5	9.40
Cu(ClO ₄) ₂ /TBANO ₃	PFPE ^g	53.3	13.0
Cu/OTf/NO ₃ ⁻	PFPE ^g	61.5	15.0

^aGeneral conditions: 0.875 mmol (0.35 M) of CEES, 1 atm of air, 0.876 mmol (0.35 M) of 1,3-dichlorobenzene (internal standard) were stirred in 2.5 mL of solvent at 25 °C for 1 h; ^b[Cu²⁺] = 20 mM in all reactions, [NO₃⁻] = 16 mM in all reactions except in reaction 3 (reaction with only Cu(NO₃)₂); [SO₄²⁻] = 20 mM in reactions with this anion; the total concentration of the other anions (OTf⁻, ClO₄⁻, BF₄⁻ and/or Cl⁻) = 40 mM in all reactions, no product was observed in the absence of Cu(II) salts (for example in the presence of only TBAX, X = ClO₄⁻, OTf⁻, BF₄⁻, NO₃⁻, Cl⁻ or SO₄²⁻); ^c% conversion = (moles of CEES consumed / moles of initial CEES) x 100; ^dreaction (conversion) rate = mmol of CEES consumed/s; ^e96% Fomblin[®] (MF-300)/4% CH₃CN (4% CH₃CN used to insure solubility); ^fTrifluoroethanol; ^g96% Fluorolink[™] (7004)/4% CH₃CN.

Table 18. Aerobic Oxidation of 2-Chloroethyl Ethyl Sulfide (CEES) in Fluorolink 7004 Catalyzed by Coated and Uncoated NanoActive™ particles.^a

Catalyst ^b	% conv. ^c	-(d[CEES]/dt) (10 ⁵ , mmol s ⁻¹) ^d
TiO ₂	10.3	1.32
Al ₂ O ₃	12.4	1.60
SiO ₂	3.2	0.41
Cu ₂ HPV ₂ Mo ₁₀ O ₄₀ •x H ₂ O (3)	20.0	2.57
Cu(OTf) ₂ /Cu(NO ₃) ₂ (Cu/Cu)	61.5	7.90
3 /Cu/Cu ^e	65.0	8.35
3 /TiO ₂ ^e	22.1	2.84
3 /Al ₂ O ₃ ^e	21.6	2.77
3 /SiO ₂ ^e	11.4	1.45
3 /Cu/Cu/TiO ₂ ^e	32.4	4.16
3 /Cu/Cu/Al ₂ O ₃ ^e	44.4	5.71
3 /Cu/Cu/SiO ₂ ^e	16.2	2.08

^aGeneral conditions: 0.463 mmol (0.185 M) of CEES (21 mg of catalyst in all reactions), 1 atm of air, were stirred in 2.5 mL of 96% PFPE/4% CH₃CN solution at 25 °C for 1 h; ^bno oxidation was observed in the absence of catalyst; ^c% conversion = (moles of CEES consumed/moles of initial CEES) x 100; ^dreaction (conversion) rate = mmol of CEES consumed/s; ^e3 mol % of **3** or **3**/Cu/Cu in all coatings.

The catalytic activity of NanoActive™ particles TiO₂, SiO₂ and Al₂O₃, were improved via coating with Cu₂HPV₂Mo₁₀•22H₂O. This catalytic enhancement is fairly impressive when the coating is a combination of Cu₂HPV₂Mo₁₀•22 H₂O, Cu(NO₃)₂•2.5 H₂O and Cu(OTf)₂ in 1: 4.3 : 6.5 mole ratio.

TSP creams with eight different additives were evaluated using two different solvents for extraction of CEES and CEESO, hexane and acetonitrile (Table 19). These include NanoActive™ TiO₂ (**1**); NanoActive™ TiO₂ (96%) + Cu/Cu (4%) (**2**); NanoActive™ TiO₂ (96%)+Cu/Cu (3.5%) + [(Fe^{III}(OH₂)₂)₃(A-α-PW₉O₃₄)₂]⁹⁻ (0.5%) (**3**); Cu/Cu (**4**); Cu/Cu (87.5%) + [(Fe^{III}(OH₂)₂)₃(A-α-PW₉O₃₄)₂]⁹⁻ (12.5%) (**5**); [Fe₃PW₉(NO₃)]⁷⁻ (**6**); Cu/Cu (87.5%) + [Fe₃PW₉(NO₃)]⁷⁻ (12.5%) (**7**), NanoActive™ TiO₂ (96%) + [Fe₃PW₉(NO₃)]⁷⁻ (4%) (**8**).

Table 19. Aerobic Oxidation/adsorption of 2-Chloroethyl Ethyl Sulfide (CEES) in TSP with Catalytically active additives.^a

Additive	Hexane ^b		Acetonitrile ^b	
	% cons. ^c	% conv. ^d	% cons. ^c	% conv. ^d
Blank	n/d ^e	n/d ^e	0	0
TiO ₂ ^f	n/d ^e	n/d ^e	3.7	0
TiO ₂ + Cu/Cu ^g	n/d ^e	n/d ^e	11.2	6.2
TiO ₂ + Cu/Cu+[(Fe ^{III} (OH ₂) ₂) ₃ (A-α-PW ₉ O ₃₄) ₂] ^{9- n}	n/d ^e	n/d ^e	9.2	5.0
Cu/Cu+[(Fe ^{III} (OH ₂) ₂) ₃ (A-α-PW ₉ O ₃₄) ₂] ^{9- i}	n/d ^e	n/d ^e	0	0
Cu/Cu ^j	n/d ^e	n/d ^e	31.9	28.3
[Fe ₃ PW ₉ (NO ₃)] ^{7- k}	n/d ^e	n/d ^e	28.5	20.0
Cu/Cu + [Fe ₃ PW ₉ (NO ₃)] ^{7- l}	n/d ^e	n/d ^e	56	49.8
TiO ₂ (96%) + [Fe ₃ PW ₉ (NO ₃)] ^{7- m}	n/d ^e	n/d ^e	4.5	0

^aGeneral conditions: 0.05 mmol (6.25 mg) of CEES, 0.05 mmol of 1,3-dichlorobenzene (internal standard), 6.35 mg of active additive (2.5 g of cream in all reactions), 1 atm of air, 25 °C; extraction was performed by 5.0 mL of acetonitrile (see Experimental section for details); ^bsolvent used for extraction; ^c% consumed = (moles of CEES consumed / moles of initial CEES) x 100; ^d% conversion = (moles of CEESO / moles of initial CEES) x 100; ^en/d=CEES or CEESO were not detected; ^fNanoActive™ TiO₂; ^gNanoActive™ TiO₂ (96%) + Cu/Cu (4%); ^hNanoActive™ TiO₂ (96%) + Cu/Cu (3.5%) + [(Fe^{III}(OH₂)₂)₃(A-α-PW₉O₃₄)₂]^{9- n} (0.5%); ⁱCu/Cu (87.5%) + [(Fe^{III}(OH₂)₂)₃(A-α-PW₉O₃₄)₂]^{9- i} (12.5%); ^jCu/Cu; ^k[Fe₃PW₉(NO₃)]^{7- k}; ^lCu/Cu (87.5%) + [Fe₃PW₉(NO₃)]^{7- l} (12.5%); ^mNanoActive™ TiO₂ (96%) + [Fe₃PW₉(NO₃)]^{7- m}.

Significantly, when the hexane was used for the extraction, there no measurable amounts of CEES or CEESO extracted from any of the samples. However, when the acetonitrile was used for extraction, reproducible amounts of CEES and CEESO (Fig.75) were present.

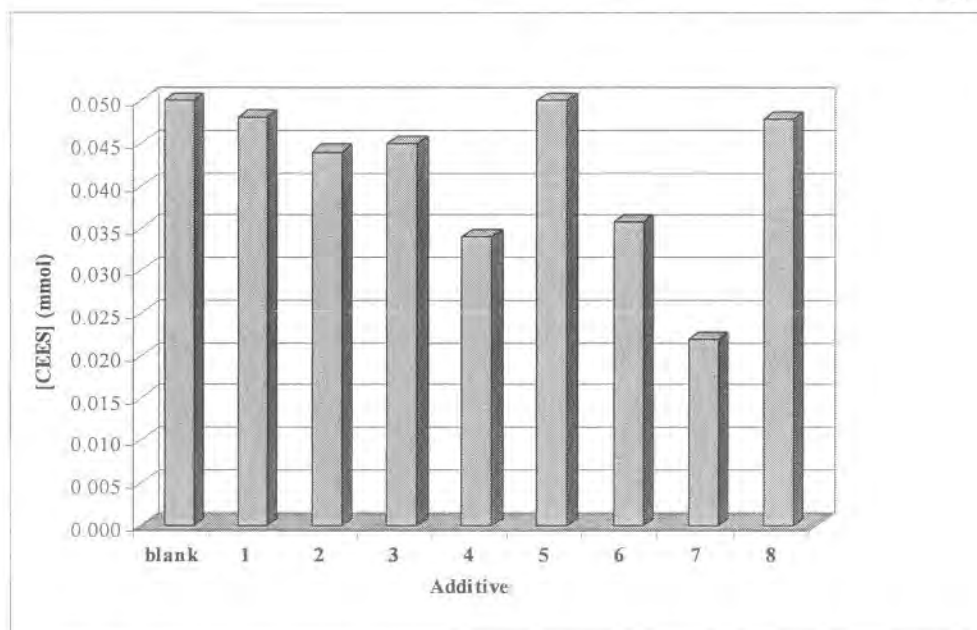


Figure 75. Aerobic oxidation/adsorption of 2-chloroethyl ethyl sulfide (CEES) in

TSP with catalytically active additives. General conditions: 0.05 mmol (6.25 mg) of CEES, 0.05 mmol of 1,3-dichlorobenzene (internal standard), 1 atm of air, 25 °C; extraction was performed by 5.0 mL of acetonitrile (see Experimental section for details); 2.5 g of cream with 62.5 mg of active additives (2.5%) in all reactions; NanoActive™ TiO₂ (1); NanoActive™ TiO₂ (96%) + Cu/Cu (4%) (2); NanoActive™ TiO₂ (96%) + Cu/Cu (3.5%) + [(Fe^{III}(OH)₂)₃(A-α-PW₉O₃₄)₂]⁹⁻ (0.5%) (3); Cu/Cu (4); Cu/Cu (87.5%) + [(Fe^{III}(OH)₂)₃(A-α-PW₉O₃₄)₂]⁹⁻ (12.5%) (5); [Fe₃PW₉(NO₃)]⁷⁻ (6); Cu/Cu (87.5%) + [Fe₃PW₉(NO₃)]⁷⁻ (12.5%) (7), NanoActive™ TiO₂ (96%) + [Fe₃PW₉(NO₃)]⁷⁻ (4%) (8).

Our results indicate that the binary cupric system, [Fe₃PW₉(NO₃)]⁷⁻, and a mixture of the two (Table 19, lines 6-8), exhibit the highest activity for consumption of CEES and oxidation of CEES to CEESO. NanoActive™ TiO₂ showed quite low activity, and addition of TiO₂ to the Cu/Cu system or to [Fe₃PW₉(NO₃)]⁷⁻ strongly inhibited CEES consumption.

Key Research Accomplishments

This Phase II project has led to the following key research accomplishments:

1. Proved that incorporation of POM/RNPs into topical skin protectants significantly increases afforded protection.
2. Identified/characterized of additional transition metal/polyoxometalates for room temperature, heterogeneous oxidation of chemical warfare agent simulants.
3. Coated new higher surface area reactive nanoparticles with transition metal salts/polyoxometalates for increased decontaminating ability.

The Government's rights to use, modify, reproduce, release, perform, display, or disclose technical data or computer software marked with this legend are restricted during the period shown on the cover page as provided in paragraph (b)(4) of the Rights in Noncommercial Technical Data and Computer Software--Small Business Innovative Research (SBIR) Program clause contained in the contract DAMD17-99-C-9012 with NanoScale Materials, Inc. (Formerly Nantek, Inc.). No restrictions apply after the expiration date (12 January 2007). Any reproduction of technical data, computer software, or portions thereof marked with this legend must also reproduce the markings.

4. Optimized incorporation of POM/RNP formulations into TSP creams, obtaining consistency between samples.
5. Determined optimum viscosity for maximum barrier protection of topical skin protectants.
6. Determined that aging of POM/RNP/TSP samples does not decrease reactivity over time.
7. Developed a standard method using the MINICAMS for permeation testing of topical skin protectants.
8. Evaluated several reactive nanoparticle and/or polyoxometalate mixtures incorporated into topical skin protectants.
9. Characterized decontamination products from coated and uncoated reactive nanoparticle reactions with CW simulants.
10. Optimized scale-up process for kilogram quantities of TiO_2 .

This Phase II project Extension has led to the following key research accomplishments:

1. Incorporation of advanced formulations of NanoActiveTM TiO_2 into topical skin protectants reduced the permeation of HD CW simulant by 99% and the permeation of GD CW simulant by 80% relative to the unmodified TSP.
2. Incorporation of Emory materials FePOM and a Cu/Cu salt physically mixed with an advanced formulation of NanoActiveTM TiO_2 into a topical skin protectant reduced the permeation of HD CW simulant by 98% and the permeation of GD CW simulant by 53% relative to the unmodified TSP.

Reportable Outcomes

Work from this project has directly or partially led to the following patents, publications and conference presentations (Phase II Extension N/A):

Patents

International Patent Application No. PCt/US99/07889. "Creams for the Catalytic Destruction of Mustard (HD) Under Ambient Conditions." Emory University File No. 00073. Inventors: Eric Boring and Craig Hill, Ph.D.

Patent Application, No. 6,403,653. "Active Topical Skin Protectants Using Reactive Nanoparticles." NanoScale Materials, Inc.

Patent Application, No. 6,410,603. "Active Topical Skin Protectants Using Combinations of Reactive Nanoparticles And Polyoxometalates or Metal Salts." NanoScale Materials, Inc.

Publications:

Rhule, J. T., Do, B. T., Hardcastle, K. I., and Hill, C. L. "Polyoxometalate Complexes that Catalyze Heterogeneous, Ambient Temperature Aldehyde Autoxidation." 2001 Scientific Conference on Chemical & Biological Weapon Defense Research, Hunt Valley, MD, 2001.

Rhule, J. T., Neiwert, W. A., Hardcastle, K. I., Do, B. T., and Hill, C. L. "Ag₅PV₂Mo₁₀O₄₀, a Heterogeneous Catalyst for Air-Based Selective Oxidation at Ambient Temperature." Journal of the American Chemical Society, 2001, Vol. 123, 12101.

Conference Presentations

Bioscience 2000, "Addition of Reactive Nanoparticles to a Topical Skin Protectant to Enhance its Protective Properties", presented by Dr. Shawn Decker, NanoScale Materials, Inc.

Bioscience 2002 "Incorporation of Reactive Nanoparticles into Topical Skin Protectants", presented by Dr. Jeffrey T. Rhule, NanoScale Materials, Inc.

Conclusions from the Phase II

New highly catalytic POM/RNP combinations were discovered during the Phase II and Phase II Extension projects. All of these were proven to be capable of destroying multiple types of CW agents. A major obstacle in past efforts was how to effectively incorporate the nanoparticles into the topical skin protectant (TSP) base cream. This issue was solved with the POM/RNP formulations by modifying the component ratios to obtain a consistency and texture similar to unmodified base cream. The effectiveness of the TSP formulations was shown not to decrease over time.

A permeation cell apparatus was used to prove the POM/RNP/TSP systems offer increased protection against CW agent simulants. Through subcontracted testing, our formulations were also shown to be effective against real CW agents.

Optimization and scale-up to kilogram quantities of TiO_2 was achieved. Significant increases in the reactivity of several nanoparticles, especially TiO_2 , were obtained during the course of scale-up.

Titanium dioxide was identified as the most promising support for the variety of POM coatings. The most effective coatings were identified to be (1) a mixture of cerium nitrate and copper nitrate, (2) $\text{Na}_5\text{PV}_2\text{Mo}_{10}\text{O}_{40}$, (3) $\text{Ag}_5\text{PV}_2\text{Mo}_{10}\text{O}_{40}$, (4) silver nitrate, and (5) nanoparticulate cerium oxide.

The requirements for a successful POM/RNP/TSP formulation defined in the introduction have been met.

1) All of the reactive nanoparticles and POM coatings examined in this study are non-toxic to humans.

a. POMs are non-toxic. In fact, hundreds of POMs have been evaluated for their antiviral and antitumoral activity. In 1998 Rhule et al. published a comprehensive review of POMs as medicinal agents. Included within that publication is a comprehensive review of POM toxicity. The reader is invited to consult that reference for additional information: Rhule, J. T., Hill, C. L., Judd, D. A., and Schinazi, R. F. "Polyoxometalates in Medicine." Chemical Reviews, 1998, Vol. 98, No. 1, p 317.

b. Toxicity testing of the reactive nanoparticles TiO_2 and ZnO have been conducted under another project. The skin irritation and sensitivity tests were all positive. Only moderate eye irritation was reported with ZnO . MgO nanoparticles are currently being tested.

what degree is mostly "pink"

2) The reactive nanoparticles were shown to destroy the three major types of CW agents – VX, HD, and GD.

3) The POM/RNP systems and the TSP cream are chemically compatible. Retention of the nanoparticle reactivity in the TSP cream has been retained over time.

4) The nanoparticle/POM hybrids are not skin irritants, see 1.b. above. (TiO_2 is a common component in sunscreen).

5) The POM/RNP/TSP formulations have shown long shelf life after they were appropriately mixed.

Conclusions from Phase II Extension

The objective of the GC adsorption testing was to screen additional candidates, nanoparticles, polyoxometalates and metal salts, for insertion as a component into the reactive topical skin protectant (rTSP). There were several promising materials identified depending on the simulant used. The uncoated NanoActive™ TiO₂ was found to be the most promising against all simulants tested.

The most effective (100% selective and fast) *catalytic* systems yet for air oxidation of mustard (HD) simulants have been developed at Emory. These include: binary Cu(II) nitrate/triflate complexes and/or Fe-containing POMs. These Cu/Cu/FePOM systems are highly effective for air oxidation of two very close mustard (HD) analogues 2-chloroethyl ethyl sulfide (CEES) and tetrahydrothiophene (THT) in acetonitrile, perfluoropolyethers, and TSP cream. The results indicate that 2-chloroethyl phenyl sulfide (CEPS) cannot be oxidized by these systems.

The objective of MINICAMS testing was to establish the effectiveness of promising materials under more realistic testing conditions. Based on a poster presentation given by the Technical Monitor, a goal was set for a 99% reduction of HD and GD vapor break-through after 20 h (Development of Multifunctional Perfluorinated Polymer Blends as an Active Barrier Cream Against Chemical Warfare Agents, 04/17/01). This goal for HD simulant CEPS was reached with the 8.93% NanoActive™ TiO₂ rTSP. For the GD simulant, DFP, this goal has not been reached with the materials reported so far. The most effective material to date is the 8.93% NanoActive™ TiO₂ rTSP showing an 80% reduction of DFP vapor break-through after 20 h. It should be noted that DFP may not be the best simulant for GD and if possible, testing with real agent should be carried out. Inclusion of Emory materials or AgNO₃ offered small benefits to its performance. Surprisingly, NanoActive™ SiO₂ performed better in the cream than in GC testing conditions. rTSP containing NanoActive™ alumina was comparable to NanoActive™ SiO₂ in its performance.

References

1. Rhule, J. T., Neiwert, W. A., Hardcastle, K. I., Do, B. T., and Hill, C. L. "Ag₅PV₂Mo₁₀O₄₀, a Heterogeneous Catalyst for Air-Based Selective Oxidation at Ambient Temperature." *Journal of the American Chemical Society*, 2001, Vol. 123, 12101.
2. Rhule, J. T.; Hill, C. L.; Judd, D. A.; Schinazi, R. F. *Chem. Rev.* **1998**, *98*, 327-357.
3. Pope, M. T.; Mueller, A.; Editors, Eds. *Polyoxometalates: From Platonic Solids to Anti-Retroviral Activity. [In: Top. Mol. Organ. Eng., 1994; 10]*.
4. Hill, C. L. *Chem. Rev.* **1998**, *98*, 1-2. Pope, M. T. *Heteropoly and Isopoly Oxometalates*; Springer-Verlag: Berlin, 1983.
5. Pope, M. T.; Mueller, A.; Editors, Eds. *Polyoxometalates: From Platonic Solids to Anti-Retroviral Activity. [In: Top. Mol. Organ. Eng., 1994; 10]*.
6. Hill, C. L.; Prosser-McCartha, C. M. *Coord. Chem. Rev.* **1995**, *143*, 407-455.
7. Hou, Y.; Hill, C. L. *J. Am. Chem. Soc.* **1993**, *115*, 11823-11830.
8. Gall, R. D.; Faraj, M.; Hill, C. L. *Inorg. Chem.* **1994**, *33*, 5015-5021.
9. Gall, R. D.; Hill, C. L.; Walker, J. E. *Chem. Mat.* **1996**, *8*, 2523-2527.
10. Gall, R. D.; Hill, C. L.; Walker, J. E. *J. Catal.* **1996**, *159*, 473-478.
11. Kholdeeva, O. A. M.; Gennadii M.; Maksimovskaya, Raisa I.; Kovaleva, Lyubov A.; Fedotov, Martin A.; Grigoriev, Vladimir A.; Hill, Craig L. *Inorg. Chem.* **2000**, *39*, 3828-3837.
12. Hill, C. L.; Gall, R. D. *J. Mol. Catal. A: Chem.* **1996**, *114*, 103-111.
13. Wagner, G. W.; Bartram, P. W. *Langmuir* **1999**, *15*, 8113-8118.
14. Xu, L.; Boring, E. A.; Hill, C. L. *J. Catal.* **2000**, *195*, 394-405.
15. Brink, G.-J. T.; Arends, I. W. C. E.; Sheldon, R. A. *Science* **2000**, *287*, 1636-1639.
16. Johnson, R. P.; Hill, C. L. *J. Appl. Toxicol.* **1999**, *19*, S71-S75.
17. Xu, L.; Boring, E. A.; Hill, C. L. *J. Catal.* **2000**, *195*, 394-405.
18. Dimotakis, E. D.; Cal, M. P.; Economy, J. *Environ. Sci. Technol.* **1995**, *29*, 1876-1880.
19. Boring, E. A. *J. Am. Chem. Soc.* **2001**, *123*, 1625-1635.
20. Groves, J. T.; Quinn, R. *J. Am. Chem. Soc.* **1985**, *107*, 5790-5792.
21. Neumann, R.; Dahan, M. *Nature* **1997**, *388*, 353-355.
22. Neumann, R. *Prog. Inorg. Chem.* **1998**, *47*, 317-370.
23. Weiner, H.; Finke, R. G. *J. Am. Chem. Soc.* **1999**, *121*, 9831-9842.
24. Shapley, P. A.; Zhang, N.; Allen, J. L.; Pool, D. H.; Liang, H.-C. *J. Am. Chem. Soc.* **2000**, *122*, 1079-1091.
25. Pettersson, L.; Andersson, I.; Selling, A.; Grate, G. H. *Inorg. Chem.* **1994**, *33*, 982-993.
26. Villanneau, R.; Proust, A.; Robert, F.; Gouzerh, P. *J. Chem. Soc., Chem. Comm.* **1998**, 1491-1492.
27. Kinne, M.; Barteau, M. A. *Surface Science* **2000**, *447*, 105-111.
28. McCreery, M. J.; USA, Secy of the Army: US, 1997.
29. Gall, R. D.; Faraj, M.; Hill, C. L. *Inorg. Chem.* **1994**, *33*, 5015-5021.
30. Gall, R. D.; Hill, C. L.; Walker, J. E. *J. Catal.* **1996**, *159*, 473-478.
31. Hill, C. L.; Prosser-McCartha, C. M. *Coord. Chem. Rev.* **1995**, *143*, 407-455.

32. *Phosphorous-31 NMR: Principles and Applications*. Edited by David G. Gorenstein. **1984**, Chap. 18, 549, Academic Press, Inc. Orlando, Florida.
33. Wagner, G. W.; Bartram, P. W.; Koper, O.; Klabundae, K.J. *J. Phys. Chem B*. **1999**, *103*, 3225.
34. Li, Y.-X.; Schlup, J. R. Klabundae, K. J. *Langmuir*, **1991**, *7*, 1394.
35. Kuiper, A. E. T.; van Bokhoven, J. J. G. M.; Medema, J. *J. Catal.* **1976**, *43*, 154.
36. Reddy, G.S.; Schmutzler, R. Z. *Naturforsch. Part B*. **1970**, *25*, 1199.
37. Srivastava, R. S.; Milani, B.; Alessio, E.; Mestroni, G. *Inorg. Chim. Acta*, **1992**, *191*, 15-17;
 (b) Bosch, E.; Kochi, J. K. *J. Org. Chem.* **1995**, *60*, 3172-3183;
 (c) Xu, L.; Boring, E.; Hill, C. L. *J. Catal.* **2000**, *195*, 394-405;
 (d) Boring, E.; Geletii, Y. V.; Hill, C. L. *J. Am. Chem. Soc.* **2001**, *123*, 1625-1635;
 (e) Martin, S. E.; Rossi, L. I. *Tetrahedron Lett.* **2001**, *42*, 7147-7152;
 (f) Boring, E.; Geletii, Y.; Hill, C. L. *J. Mol. Catal.* **2001**, *176*, 49-63.
 (g) Rhule, J. T.; Neiwert, W. A.; Hardcastle, K. I.; Hill, C. L. *J. Am. Chem. Soc.* **2001**, *123*, 12101-12102.
38. Topical issue on polyoxometalates: *Chem. Rev.* **1998**, *98*, 1-389.
39. *Polyoxometalate Chemistry: From Topology via Self-Assembly to Applications*; Pope, M. T., Müller, A., Eds.; Kluwer Academic Publishers: Dordrecht, Netherlands, 2001.
40. SMART, version 5.55; Bruker AXS, Inc., Analytical X-ray Systems: Madison, WI, **2000**.
41. SAINT, version 6.02; Bruker AXS, Inc., Analytical X-ray Systems: Madison, WI, **1999**.
42. Sheldrick, G., SADABS, University of Göttingen, **1996**.
43. SHELXTL, version 5.10; Bruker AXS, Inc., Analytical X-ray Systems: Madison, WI, **1997**.
44. *International Tables for X-ray Crystallography, Volume C*; Kypoch Academic Publishers: Dordrecht, **1992**.
45. Y. C. Yang, J. A. Baker, J. R. Ward *Chem. Rev.* **92** (**1992**) 1729.
46. Representative reviews on POMs in catalysis: (a) I. V. Kozhevnikov, K. I. Matveev *Russian Chem. Rev.* **51** (**1982**) 1075; (b) C. L. Hill, C. M. Prosser-McCartha *Coord. Chem. Rev.* **143** (**1995**) 407; (c) T. Okuhara, N. Mizuno, M. Misono *Advan. Catal.* **41** (**1996**) 113; (d) R. Neumann *Prog. Inorg. Chem.* **47** (**1998**) 317.
47. C. L. Hill, R. D. Gall *J. Mol. Catal. A: Chem.* **114** (**1996**) 103.
48. L. Xu, E. Boring, C. L. Hill, *J. Catal.* **195** (**2000**) 394.
49. R. Neumann, M. Levin *J. Am. Chem. Soc.* **114** (**1992**) 7278.
50. R. D. Gall, M. Faraj, C. L. Hill *Inorg. Chem.* **33** (**1994**) 5015.
51. R. D. Gall, C. L. Hill, J. E. Waker *J. Catal.* **159** (**1996**) 473.
52. N. M. Okun, T. M. Anderson, C. L. Hill *J. Am. Chem. Soc.* **124** (**2003**) in press.

List of Personnel Receiving Pay From This Research Effort

Dr. Kenneth Klabunde – Principal Investigator
Dr. Craig Hill - Professor
Dr. Olga Koper – Director of Research and Development
Dr. Shawn Decker – Project Leader
Dr. Shyamala Rajogopalan – Project Extension Leader, Senior Scientist
Laura Hladky – Project Chemist
Dr. Jeff Rhule – Scientist
Dr. Nelya Okun – Post-doc
Dr. Ravichandra Mulukutla – Senior Scientist
John Rasinski – Chemist II
Jennifer John – Staff Chemist
John Klabunde – Staff Chemist
Michael Sigel – Staff Chemist
David Jones – Process Engineer
Stephen Wanamaker – Chemical Engineer
Chet Davidson – Chemical Engineer
Jeffrey Woirhaye – Chemical Engineer

SBIR final report from METSS Corp. Phase II

Award Number: DAMD17-99-C-9046

AD _____

Award Number: DAMD17-99-C-9046

TITLE: Development of a Catalytically Reactive Topical Skin
Protectant Against Chemical Warfare Agents

PRINCIPAL INVESTIGATOR: Kenneth Heater, Ph.D.
Richard Sapienza, Ph.D.
Janet Gariano Ricks

CONTRACTING ORGANIZATION: METSS Corporation
Columbus, Ohio 43085

REPORT DATE: February 2003

TYPE OF REPORT: Final, Phase II

PREPARED FOR: U.S. Army Medical Research and Materiel Command
Fort Detrick, Maryland 21702-5012

DISTRIBUTION STATEMENT: Distribution authorized to U.S.
Government agencies only (specific authority). Other requests
for this document shall be referred to U.S. Army Medical
Research and Materiel Command, 504 Scott Street, Fort Detrick,
Maryland 21702-5012.

The views, opinions and/or findings contained in this report are
those of the author(s) and should not be construed as an official
Department of the Army position, policy or decision unless so
designated by other documentation.

NOTICE

USING GOVERNMENT DRAWINGS, SPECIFICATIONS, OR OTHER DATA INCLUDED IN THIS DOCUMENT FOR ANY PURPOSE OTHER THAN GOVERNMENT PROCUREMENT DOES NOT IN ANY WAY OBLIGATE THE US GOVERNMENT. THE FACT THAT THE GOVERNMENT FORMULATED OR SUPPLIED THE DRAWINGS, SPECIFICATIONS, OR OTHER DATA DOES NOT LICENSE THE HOLDER OR ANY OTHER PERSON OR CORPORATION; OR CONVEY ANY RIGHTS OR PERMISSION TO MANUFACTURE, USE, OR SELL ANY PATENTED INVENTION THAT MAY RELATE TO THEM.

SBIR DATA RIGHTS LEGEND

Contract: DAMD17-99-C-9046

Contractor: METSS Corporation

For a period of five (5) years after completion of the project from which the data was generated, the Government's rights to use, modify, reproduce, release, perform, display, or disclose any technical data or computer software contained in this report are restricted as provided in paragraph (b)(4) of the Rights in Noncommercial Technical Data and Computer Software Small Business Innovative Research (SBIR) Program clause contained in the above-identified contract [DFARS 252.227-7018(Jun. 1995)]. No restrictions apply after expiration of that period. Any reproduction of technical data, computer software, or portions thereof marked as SBIR data must also reproduce those markings and this legend.

This technical report has been reviewed and is accepted under the provisions of the Small Business Innovation Research Program.

This report is published in the interest of scientific and technical information exchange and does not constitute approval or disapproval of its ideas or findings.

Do not return copies of this report unless contractual obligations or notice on a specific document requires its return.

REPORT DOCUMENTATION PAGE			Form Approved OMB No. 074-0188	
Public reporting burden for this collection of information is estimated to average 1 hour per response, including the time for reviewing instructions, searching existing data sources, gathering and maintaining the data needed, and completing and reviewing this collection of information. Send comments regarding this burden estimate or any other aspect of this collection of information, including suggestions for reducing this burden to Washington Headquarters Services, Directorate for Information Operations and Reports, 1215 Jefferson Davis Highway, Suite 1204, Arlington, VA 22202-4302, and to the Office of Management and Budget, Paperwork Reduction Project (0704-0188), Washington, DC 20503				
1. AGENCY USE ONLY (Leave blank)	2. REPORT DATE February 2003	3. REPORT TYPE AND DATES COVERED Final, Phase II (2 Jan 01 - 1 Jan 03)		
4. TITLE AND SUBTITLE Development of a Catalytically Reactive Topical Skin Protectant Against Chemical Warfare Agents		5. FUNDING NUMBERS DAMD17-99-C-9046		
6. AUTHOR(S) Kenneth Heater, Ph.D. Richard Sapienza, Ph.D. Janet Gariano Ricks				
7. PERFORMING ORGANIZATION NAME(S) AND ADDRESS(ES) METSS Corporation Columbus, Ohio 43085 E-mail: kheater@metss.com		8. PERFORMING ORGANIZATION REPORT NUMBER		
9. SPONSORING / MONITORING AGENCY NAME(S) AND ADDRESS(ES) U.S. Army Medical Research and Materiel Command Fort Detrick, Maryland 21702-5012		10. SPONSORING / MONITORING AGENCY REPORT NUMBER		
11. SUPPLEMENTARY NOTES Original contains color plates: All DTIC reproductions will be in black and white.				
12a. DISTRIBUTION / AVAILABILITY STATEMENT Distribution authorized to U.S. Government agencies only (specific authority). Other requests for this document shall be referred to U.S. Army Medical Research and Materiel Command, 504 Scott Street, Fort Detrick, Maryland 21702-5012.			12b. DISTRIBUTION CODE	
13. ABSTRACT (Maximum 200 Words) This report was developed under SBIR Topic OSD98-038. Topical Skin Protectants (TSPs) comprised of perfluorinated polyether oil thickened with PTFE are currently used to protect military personnel from Chemical Warfare Agents (CWAs). The existing TSPs provide an effective physical barrier to CWAs but have no destructive capacity toward CWAs, thus limiting their long-term effectiveness and posing an unnecessary hazard to personnel. The incorporation of reactive materials capable of neutralizing appreciable quantities of CWAs (nerve agents and/or vesicants) would markedly enhance the efficacy of TSPs and reduce risk to personnel. During this Phase II SBIR program METSS was able to identify compounds capable of completely neutralizing common CWA simulants in a time effective manner. Furthermore, METSS was able to incorporate these chemistries into existing TSP formulations.				
14. SUBJECT TERMS chemical warfare agent, topical skin protectant, organophosphorous compounds, vesicant, barrier creams, protection			15. NUMBER OF PAGES 70	
			16. PRICE CODE	
17. SECURITY CLASSIFICATION OF REPORT Unclassified	18. SECURITY CLASSIFICATION OF THIS PAGE Unclassified	19. SECURITY CLASSIFICATION OF ABSTRACT Unclassified	20. LIMITATION OF ABSTRACT Unlimited	

Table of Contents

	<u>Page</u>
1.0 Introduction	1
2.0 Experimental - Analytical Methods and Materials	3
2.1 Analytical Methodology	3
2.2 Simulants	10
2.3 Reactive compounds	10
3.0 Reactivity Studies	16
3.1 Metal Complexes	16
3.2 Krytox® Compounds	17
3.3 Perfluorinated Acids	20
3.4 Perfluorinated Sulfonates	22
3.5 Functionalized Styrene/Divinylbenzene and Clays	24
3.6 Sulfonated Polystyrene	27
3.7 Oxidizers	27
4.0 Reaction Capacity Studies	29
5.0 Permeation Studies	32
5.1 Cream Preparation	32
5.2 Permeation Test Results	33
6.0 Materiel Compatibility	36
6.1 rTSP compatibility with DEET	36
6.2 rTSP compatibility with Camouflage paint	38
7.0 Research Accomplishments and Conclusions	41
7.1 Reportable Outcomes	41
7.2 Key RESEARCH accomplishments	41
7.3 Prototype Delivery and Commercial potential	42
7.4 Conclusions	43
8.0 Appendices	44
8.1 METSS SOP# 02.001.01	44
8.2 METSS SOP# 02.002.01	44
8.3 METSS SOP# 02.003.01	44

List of Figures

	<u>Page</u>
Figure 1. Chromatogram of 5 µg/ml DFP in Hexane.....	5
Figure 2. Regression Line - DFP.....	5
Figure 3. Chromatogram of 5 µg/ml CEES in Hexane	6
Figure 4. Regression Line - CEES	6
Figure 5. Chromatogram of 5 µg/ml Malathion in Hexane.....	7
Figure 6. Regression Line - Malathion.....	7
Figure 7. Chromatogram of 5 µg/ml Paraoxon in Methylene Chloride.....	8
Figure 8. Regression Line - Paraoxon.....	8
Figure 9. Chromatogram of 5 µg/ml CEPS in Methylene Chloride.....	9
Figure 10. Regression Line - CEPS	9
Figure 11. Simulant Depletion with Time Using Krytox® Acid	18
Figure 12. Simulant Depletion with Time Using Cu(Krytox®) ₂	18
Figure 13. Simulant Depletion with Time Using Ni(Krytox®) ₂	19
Figure 14. Simulant Depletion with Time Using Fe(Krytox®) ₃	19
Figure 15. Simulant Depletion with Time Using La(Krytox®) ₂	20
Figure 16. Simulant Depletion with Time Using Perfluoropropionic Acid.....	21
Figure 17. Simulant Depletion with Time Using Perfluorotetradecanoic Acid	21
Figure 18. Simulant Depletion with Time Using METSS 2-8-13.....	26
Figure 19. Simulant Depletion with Time Using METSS 2-8-14.....	26
Figure 20. Reaction Capacity of Candidate Reactants with DFP.....	30
Figure 21. Reaction Capacity of Candidate Reactants with CEES	30
Figure 22. Reaction Capacity of Candidate Reactants with Paraoxon.....	31
Figure 23. Reaction Capacity of Candidate Reactants with Malathion	31
Figure 24. DFP Permeation Summary	35
Figure 25. CEPS Permeation Summary	35
Figure 26. 5 µg/mL DEET in Methylene Chloride	36
Figure 27. Regression Line - DEET.....	37
Figure 28. Depletion of DEET in Cu(Krytox®) ₂ and METSS 2-8-14.....	37
Figure 29. DFP Reactivity with Black Camouflage Paint Mixtures	39
Figure 30. CEES Reactivity with Red Camouflage Paint Mixtures.....	39
Figure 31. CEES Reactivity with Black Camouflage Paint Mixtures.....	40
Figure 32. CEES Reactivity with Red Camouflage Paint Mixtures.....	40

List of Tables

	<u>Page</u>
Table 1. Results of the Synthesis of Copper Complexes	11
Table 2. Results of the Synthesis of Iron Complexes	12
Table 3. Results of the Synthesis of Lanthanum Complexes.....	12
Table 4. Results of Metal Analyses - Krytox® Complexes.....	13
Table 5. Reactivity of Metal Complexes with Simulants.....	16
Table 6. Summary of Simulant Reactivity with Krytox Compounds	17
Table 7. Simulant Reactivity with Perfluorinated Sulfonates	23
Table 8. Simulant Reactivity of Functionalized Styrene/Divinylbenzene and Clays	25
Table 9. Simulant Reactivity with Sulfonated Polystyrene.....	27
Table 10. Eight Hour Reactivity Data for Benzoyl Peroxide and Mixtures.....	28
Table 11. 24-hour Permeation Test Results	34

1.0 INTRODUCTION

Topical Skin Protectants (TSPs) comprised of perfluorinated poly(alkyl)ether oil (PFAE) thickened with polytetrafluoroethylene (PTFE) are currently used to protect of military personnel from Chemical Warfare Agents (CWAs). TSPs were developed to provide an effective physical barrier to CWAs, thereby effecting protection of personnel exposed to CWAs by preventing direct agent contact with any exposed skin surfaces. The existing creams may be applied up to 24 hours prior to entry into a contaminated environment and remain effective for a period of 4 to 6 hours when exposed to a CWA threat. The effective mission profile of the existing TSPs presumably affords the soldier enough time to complete his/her immediate mission and return to a personnel decontamination station to remove any live agent contamination before the agents have a chance to render an effect.

The primary limitation of the existing TSPs is their inability to incapacitate CWAs contacting the cream. This limits their long-term effectiveness and poses an unnecessary hazard to personnel. The incorporation of catalytically reactive materials capable of neutralizing chemical warfare agents, nerve agents and/or vesicants, would markedly enhance the efficacy of TSPs and reduce risk to personnel. Thus, the objectives of this program were to develop additives that would catalytically destroy the CWAs; to incorporate these additives into existing TSPs; to demonstrate improved mission profile and personnel protection capability; and to demonstrate that the technologies developed under the Phase II program can be transferred to the field in a commercially viable manner.

The initial focus of Phase II program was to study the reactivity of Krytox® compounds, as well as, metal complexes of various organic acids (including Krytox® acid) with chemical warfare agent simulants. The use of Krytox® compounds and reactants based on Krytox® compounds were emphasized as a starting point since they are composed of a perfluorinated polyether backbone similar to the TSPs in current use and, as a result, can be more readily incorporated into the TSP cream. The use of metal complexes was supported by the literature, which contains numerous references to the effectiveness of metal complexes as catalysts, including specific applications to CWA destruction. Following the study of these compounds, reactivity data were obtained for several types of perfluorinated sulfonates with the CWA simulants. Since sulfonic acids are known to be stronger acids than carboxylic acids, it was expected that these compounds would be even more effective in simulant destruction. The perfluorinated sulfonates also have the advantage of a perfluorinated polyether backbone, which would theoretically facilitate their incorporation into a cream. The perfluorinated sulfonates are; however, relatively expensive and the commercial form of

these materials are not readily amenable to TSP preparation. For these reasons, sulfonated polymers, specifically sulfonated styrene/divinyl benzene and sulfonated polystyrene, were also investigated for their effectiveness in simulant destruction. Styrene/divinyl benzene and polystyrene resins are low cost, very effective and readily available; however, they are somewhat brittle and difficult to incorporate into a cream unless the size of the particles is significantly reduced.

2.0 EXPERIMENTAL - ANALYTICAL METHODS AND MATERIALS

2.1 ANALYTICAL METHODOLOGY

2.1.1. Gas Chromatography

All reported Phase II chromatographic work was performed using a Hewlett Packard 5890 Series II gas chromatograph with flame ionization detector (FID). Using an RTX-5 capillary column (30m X 0.25mm X 0.25 μ m), the detection limits of all simulants were found to be approximately 5 μ g/ml with linear ranges between 5 and 500 μ g/ml. Since 1 μ l injection volumes with a split ratio of approximately 1:80 were used, the overall amount of simulant injected onto the column was on the order of nanograms (ng), thus demonstrating an appropriate level of sensitivity to support the program efforts.

Did any reaction occur after extraction?

Interferences due to the test compounds were greatly eliminated by extracting the simulant into appropriate solvent and analyzing the extracts. More importantly, the effect of the extraction served to "quench" the reaction so that data relating reactivity as a function of time could be obtained. Since DFP, CEES and Malathion are very soluble in hexane, while the Krytox® compounds are not, it initially was used for extractions. Hexane also possesses physical characteristics, which make it favorable for use in a gas chromatographic system. As the program progressed, methylene chloride was also used to support the extraction of Paraoxon. Methylene chloride also performs well in a chromatographic system and Paraoxon is much more soluble in methylene chloride than in hexane. In addition, fillers added to some of the commercial perfluorinated sulfonates were found to effectively "adsorb" the simulants so methylene chloride, which is a stronger solvent than hexane, had to be used to obtain valid reactivity data. However, use of methylene chloride had the negative effect of extracting materials that were detrimental to column performance. Malathion and Paraoxon are particularly sensitive to active sites in the injection port and column. This complication was relatively easily managed by insuring that matrix blanks were analyzed with every analytical run and by frequent replacement of the gold seal and silanized injection port liner. The injection port end of the column was routinely clipped to remove decomposition products. Baking out the column and conditioning the column with high concentrations of the simulant of interest was also advantageous. In summary, the choice of solvent was not always clear; a balance had to be reached between complete extraction of the simulant and extraction of reactive compounds, which would have a negative effect on the instrumentation or add interferences leading to artificially high simulant

What was % Recovery?

recovery values. In many cases, extractions were performed using both solvents and the data compared.

2.1.2. Reactivity and Reaction Capacity Measurements

A detailed description of the testing methodology used to determine the reactivity of the test compounds toward the CWA simulants is included in the standard operating procedure (SOP) provided in Appendix 8.1, which is summarized as follows:

- 50 mg of test compound is weighed into a series of screw-capped vials
- Each vial is spiked with known amounts of simulant (in most cases 1 to 10 μ l) and allowed to react with the test compound for various periods of time (up to 8 hours)
- Any remaining simulant is extracted from the simulant/test compound mixture and the extract analyzed by gas chromatography
- Data charts, which relate the amount of simulant remaining after a given period of time, are then generated for each test compound.

Representative chromatograms and regression lines for each of the simulants used to support the program efforts are provided in Figures 1-10. *(I Hope the COR has a better copy to review)*

2.1.3. Permeation Measurements

A detailed SOP for the permeation studies performed under the program is presented in Appendix 8.2. In summary, the procedure for measuring permeation involved spiking a known volume of DFP or CEPS onto nitrocellulose filter paper over which a 0.15 mm layer of cream had been spread. The filter paper with the cream was contained in a glass cell. Air flowed through the bottom portion of the cell to cartridges containing XAD-2 resin. Any simulant permeating through the cream was absorbed by the XAD-2. The resin was subsequently desorbed using a known quantity of methylene chloride and the extracts analyzed by gas chromatography. The same instrument, column and instrument conditions were used to analyze the permeation extracts as were used for analysis of the reactivity extracts. Methylene chloride was used for the XAD-2 extractions since the extraction efficiency of the simulants using hexane is low.

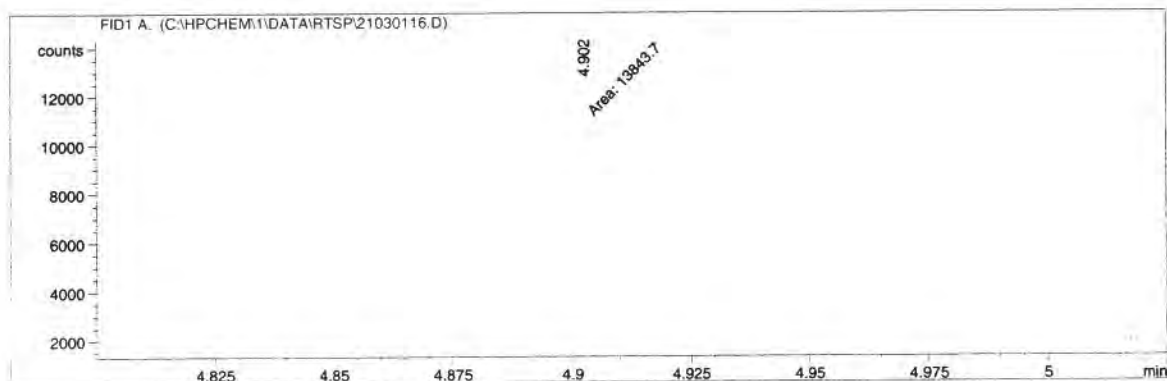


Figure 1. Chromatogram of 5 µg/ml DFP in Hexane

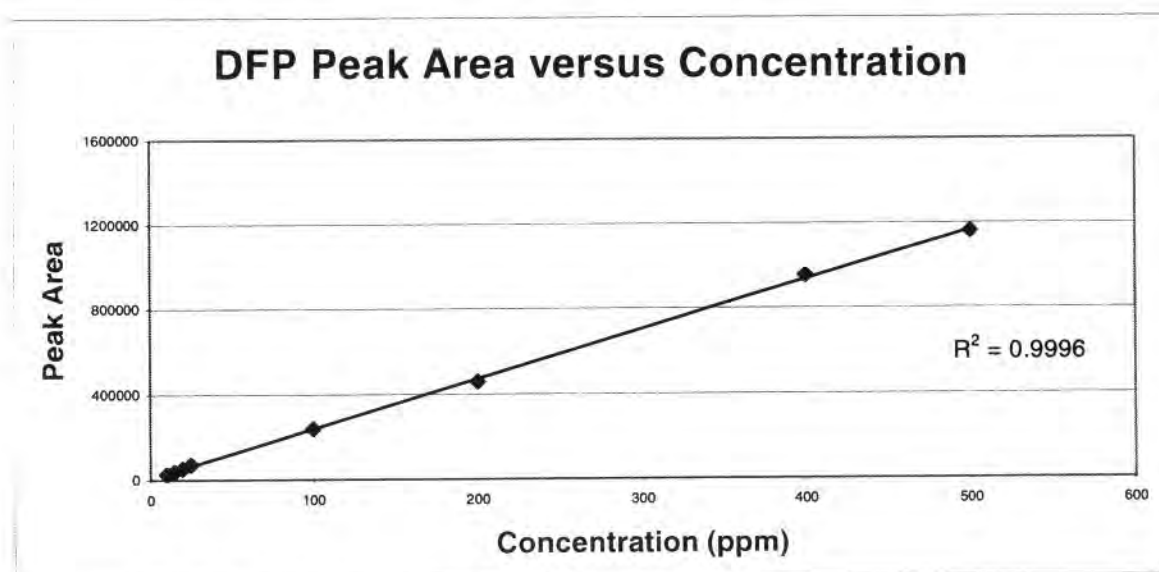


Figure 2. Regression Line - DFP

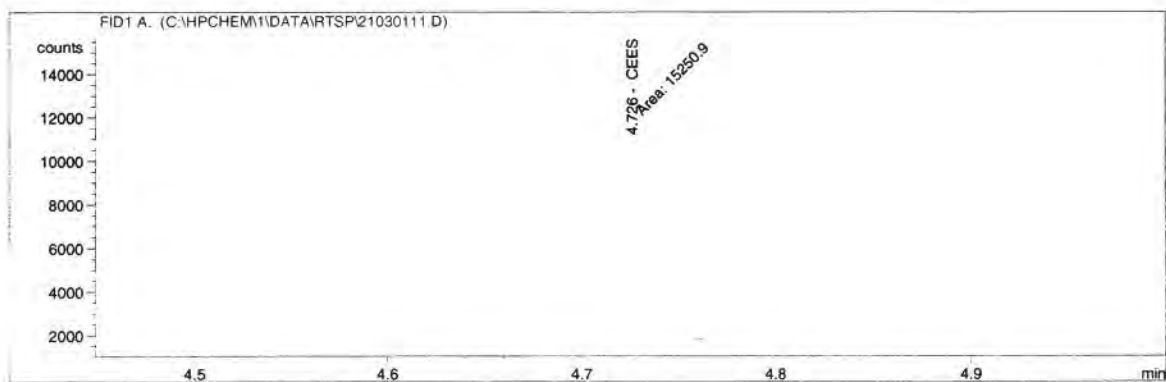


Figure 3. Chromatogram of 5 µg/ml CEES in Hexane

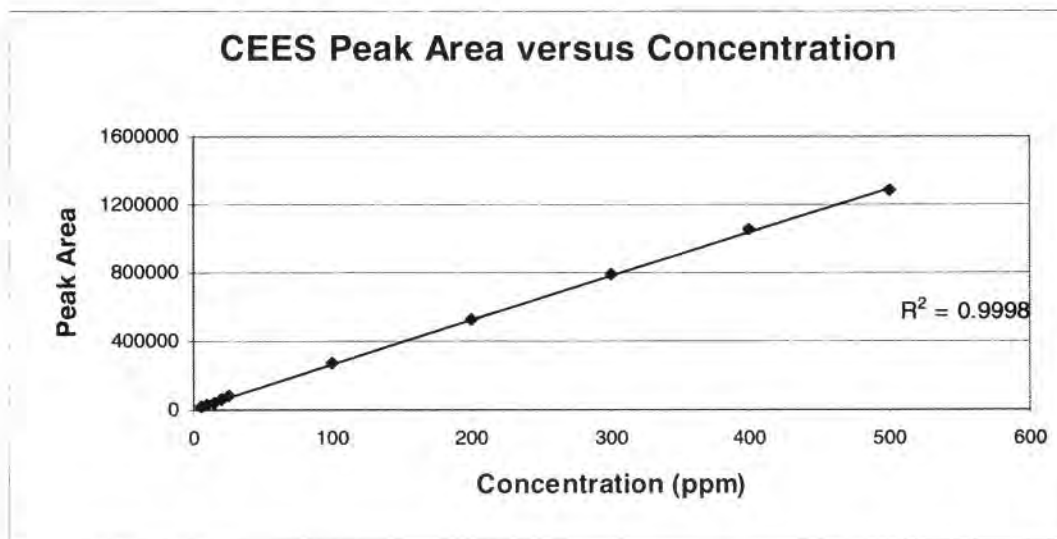


Figure 4. Regression Line - CEES

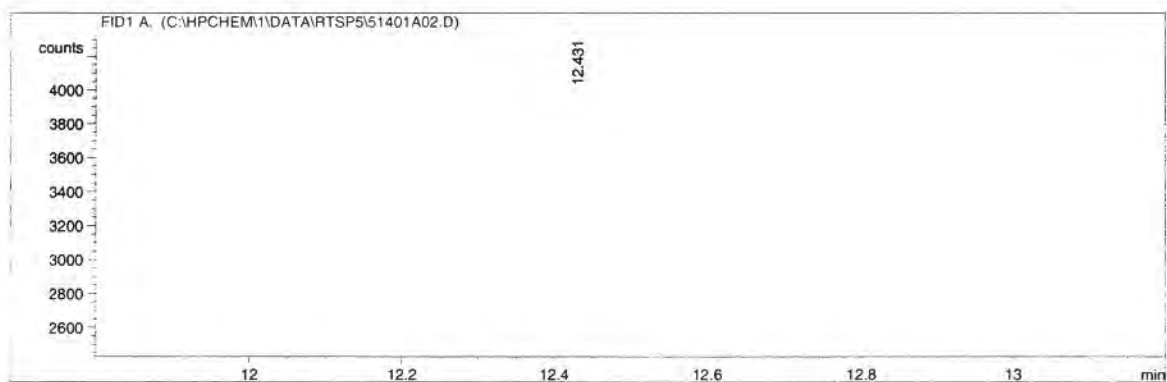


Figure 5. Chromatogram of 5 µg/ml Malathion in Hexane

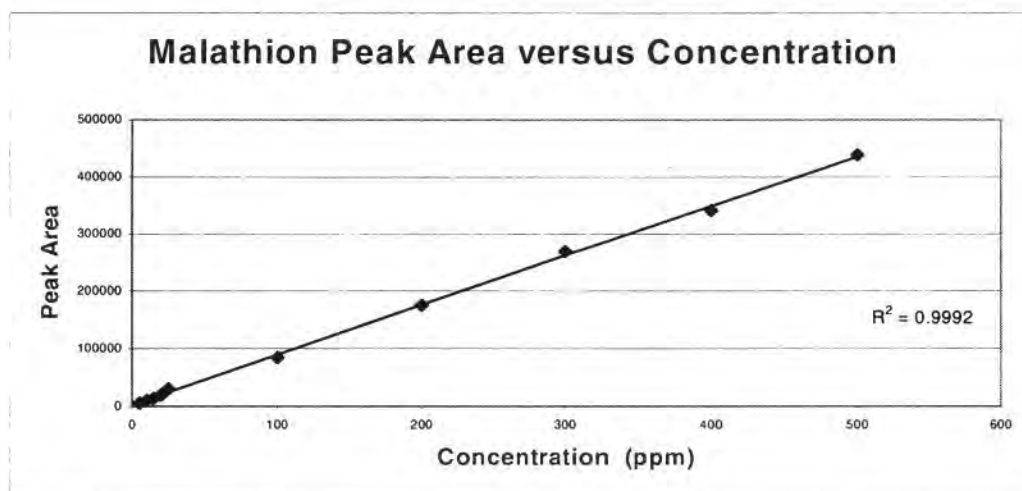


Figure 6. Regression Line - Malathion

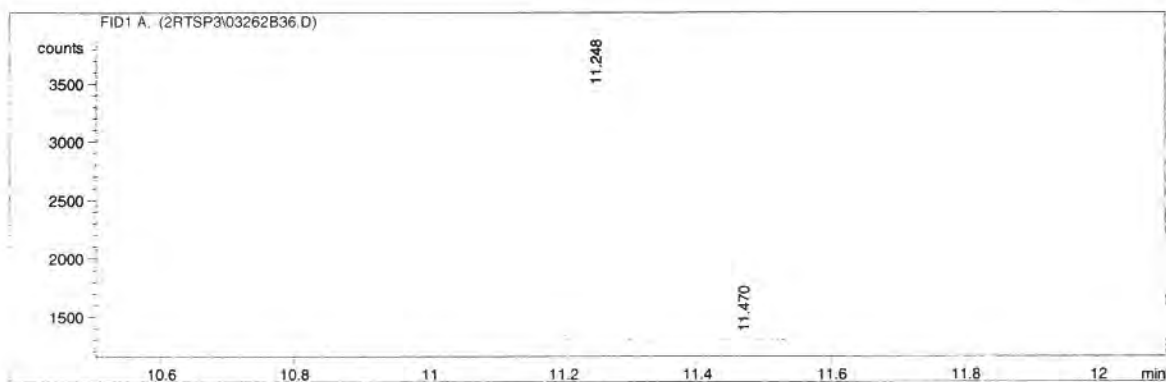


Figure 7. Chromatogram of 5 µg/ml Paraaxon in Methylene Chloride

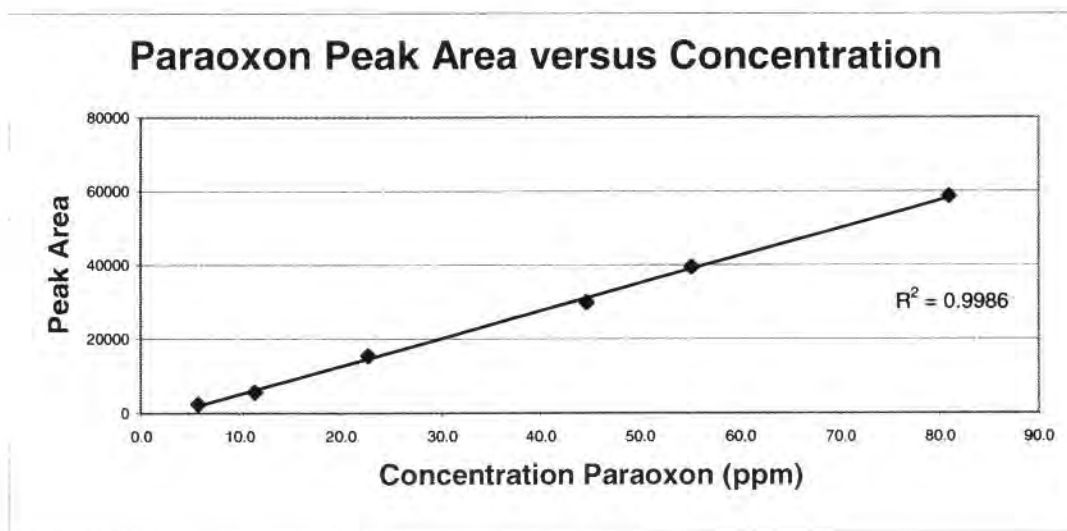


Figure 8. Regression Line - Paraaxon

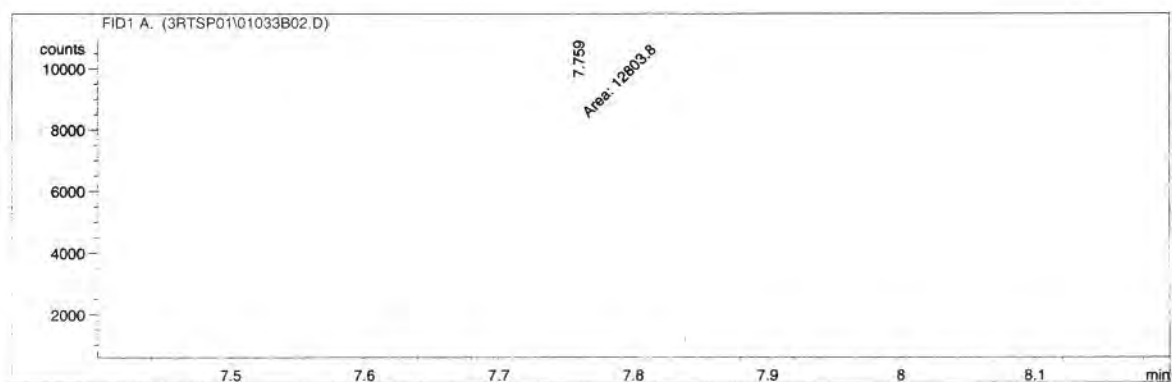


Figure 9. Chromatogram of 5 µg/ml CEPS in Methylene Chloride

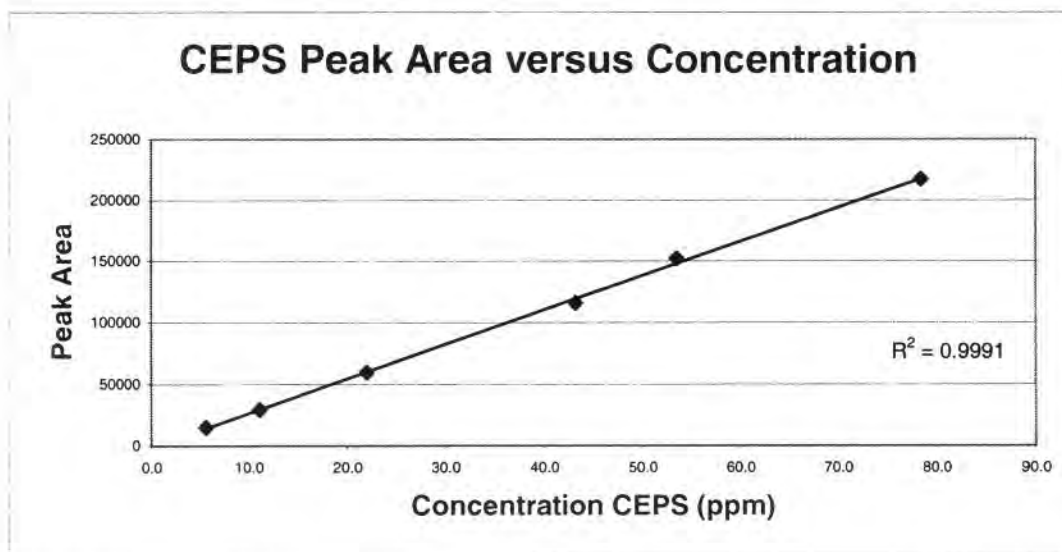


Figure 10. Regression Line - CEPS

2.2 SIMULANTS

The simulants used in this program were diisopropylfluorophosphate (DFP), 2-chloroethylethylsulfide (CEES), and Malathion (for GD, HD and VX agents, respectively). Since recent publications suggested that Paraoxon (diethyl p-nitro-phenyl phosphate) might more closely mimic VX chemical properties, testing of reactive compounds with Paraoxon was initiated in the second year of the program.¹ 2-Chloroethyl phenyl sulfide (CEPS) was substituted for CEES as an HD simulant in permeation work, as requested by USAMRICD.

2.3 REACTIVE COMPOUNDS

2.3.1 Metal Complexes

Commercially available compounds based on copper, iron, and lanthanum complexes of acetylacetone were evaluated for reactivity toward the target CWA simulants and rTSPs incorporation. In addition to the commercial complexes of acetylacetone, chelates of urocanic acid, 2,3-pyridinecarboxylic acid, 4(5)-imidazolidithiocarboxylic acid, 2,2'-dipyridyl, 1,1'-ethylenebis(5-oxo-3-pyrrolidine carboxylic acid), ethylenediaminetetraacetic acid (EDTA), and Krytox®157FSL (perfluoroalkylether carboxylic acid) were prepared and evaluated.

The methodology used to synthesize the solid complexes involved the initial conversion of the carboxylic acid group of the chelating agents to the corresponding sodium salt. This was accomplished by dissolving the compound in an aqueous sodium hydroxide solution. The appropriate metal chloride was then added. In some cases, the precipitate formed immediately. In others, it was necessary to adjust the pH, add an excess of metal chloride, and/or cool the solution to accelerate precipitate formation. After the precipitate formed, it was filtered, washed with de-ionized water to remove excess reagents, and dried in a forced air oven at 38°C.

The copper, iron and lanthanum complexes of Krytox®157FSL were formed by dissolving stoichiometric amounts of the Krytox acid and the appropriate metal acetate in 2,3-dihydrodecafluoropentane (DuPont Vertrel XF®). These reagents were then refluxed in a round bottom flask equipped with water condenser. A complete reaction was taken to be complete

¹ O. Koper, E. Lucas, K.J. Klabunde, "Development of Reactive Topical Skin Protectants against Sulfur Mustard and Nerve Agents", *J. Appl. Toxicol.*, 19, S59-S70 (1999).

dissolution of the acetate and formation of a clear, homogeneous solution. In the case of copper/Krytox® acid, this was accomplished after approximately four hours of refluxing. The iron and lanthanum complexes were refluxed for 12 hours with no appreciable reaction; however, with the addition of a catalyst consisting of two milliliters of 1N NaOH, the reaction was able to go to completion. The Vertrel® was distilled off and the resulting oils were placed in a vacuum oven at 70°C to remove residual acetic acid. Ni(Krytox®)₂ was also prepared and evaluated under the program. The initial preparation was similar to that used for the other Krytox® complexes but was found to be unsuccessful. It was necessary to remove hydrated water from the nickel acetate by a toluene/water azeotropic distillation prior to refluxing with Krytox® acid in Vertrel®, followed by liquid extraction to remove the unreacted Krytox® acid. While successful, the reaction yield (approximately 49%) was considerably less than that for the other metal Krytox® compounds.

Metal analyses of the Krytox® complexes synthesized during the program were performed by dry ashing the complexes, dissolving the residue in acid and analyzing the resulting solution using atomic absorption (AA) spectroscopy. The yields and appearances of all complexes are shown in Tables 1 through 3. The percentages reported assume theoretical product yields. However, it is anticipated that some of the complexes may be hydrated and contain metal oxides and/or hydroxides. Table 4 contains the results of metal analyses by atomic absorption spectroscopy performed on three of the metal complexes of Krytox®157FSL.

Table 1. Results of the Synthesis of Copper Complexes

Chelating Agent	Yield (grams)	Percent Yield	Appearance
Urocanic acid	0.8563	71.5	Blue solid
2,3-pyridinedicarboxylic acid	0.7414	49.7	Blue solid
4(5)-imidazoledithio-carboxylic acid	0.8871	73.2	Black solid
2,2'-dipyridyl	1.1987	97.7	Blue solid
1,1'-ethylenebis(5-oxo-3-pyrrolidine carboxylic acid)	0.3241	29.3	Black solid
Ethylenediaminetetraacetic acid (EDTA)	0.1778	13.1	Light blue solid
Krytox®157FSL	13.5837	96.7	Clear, blue oil

Table 2. Results of the Synthesis of Iron Complexes

Chelating Agent	Yield (grams)	Percent Yield	Appearance
Urocanic acid	0.3505	30.5	Red, black solid
2,3-pyridinedicarboxylic acid	0.2120	16.7	Black solid
4(5)-imidazoledithio-carboxylic acid	1.3857	118.7	Black solid
2,2'-dipyridyl	0.9811	85.4	Red, black solid
1,1'-ethylenebis(5-oxo-3-pyrrolidine carboxylic acid)	0.3547	33.5	Black solid
Ethylenediaminetetraacetic acid (EDTA)	0.1609	12.3	Red, black solid
Krytox®157FSL	14.0881	91.0	Dark red oil

Table 3. Results of the Synthesis of Lanthanum Complexes

Chelating Agent	Yield (grams)	Percent Yield	Appearance
Urocanic acid	0.3129	25.9	Beige solid
2,3-pyridinedicarboxylic acid	0.5539	41.5	White solid
4(5)-imidazoledithio-carboxylic acid	0.5044	38.4	White solid
2,2'-dipyridyl	1.0744	77.6	White solid
1,1'-ethylenebis(5-oxo-3-pyrrolidine carboxylic acid)	0.7819	63.9	White solid
Ethylenediaminetetraacetic acid (EDTA)	0.7514	57.5	White solid
Krytox®157FSL	14.7165	94.4	Colorless grease

Table 4. Results of Metal Analyses - Krytox® Complexes

Complex	Experimental Metal Content	Theoretical Metal Content
Ni(Krytox®) ₂	1.13%	1.16%
Cu(Krytox®) ₂	1.14%	1.26%
Fe(Krytox®) ₃	0.66%	0.74%

Reliable results regarding the lanthanum concentration of the lanthanum/ Krytox® compound could not be obtained using the same analytical methodology used for the other three compounds, i.e. dry ashing of the complex followed by dissolution of the residue in concentrated acid and subsequent analysis of the solution. This was due to two factors – the relative volatility of lanthanum metal and the thermal stability of the fluorinated Krytox® backbone. At the temperatures necessary to breakdown the fluorocarbon portion of the material, the lanthanum was volatilized leading to artificially low values. Wet ashing techniques, hot plate or microwave, and/or the method of standard additions are possible techniques, which could have been utilized. However, it was decided that the expenditure of time and resources for method development was not warranted since the compound's reactivity with simulants was less than that of the other complexes.

2.3.2 Krytox® Compounds

All Krytox® products were supplied by DuPont. Included were perfluorinated poly(alkyl)ether, as well as, the ether functionalized with amine, amide, alcohol and acid groups. DuPont also prepared reactive TSP cream samples containing reactive compounds identified in this program.

2.3.3 Perfluorinated Acids

Perfluoropropionic acid and perfluorotetradecanoic acid (ACS grade or better) and were purchased from Aldrich Chemical.

2.3.4 Perfluorinated Sulfonates

Since sulfonates are known to be much stronger acids than carboxylic acids and a perfluorinated sulfonate could, theoretically, be readily incorporated into the TSP cream, several types of these classes of compounds were tested under the program. Perfluorinated sulfonate (2-7-2) is supplied in bead form and has an equivalent weight of approximately 1100. Perfluorinated sulfonate (2-7-9) is a powder and a by-product of sulfonate (2-7-2) production. Perfluorinated sulfonate (1-10-13) is an experimental DuPont product based on perfluorinated sulfonate (2-7-9), which has been adsorbed onto an inorganic reactive base. In addition, a copper perfluorinated sulfonate was prepared, in-house, by refluxing a mixture of copper acetate and perfluorinated sulfonate (1-10-13) in Vertrel® using methods similar to those previously described.

2.3.5 Functionalized Styrene/Divinylbenzene and Clays

Functionalized styrene/divinylbenzenes were purchased from Sybron Chemical, Fluka Chemical Corporation and Dow Chemical. The clays were obtained from Southern Clay Products.

2.3.6 Sulfonated Polystyrene

Limited supplies of sulfonated polystyrene with varying degrees of sulfonation were evaluated under the program.² Due to the marginal success of these materials, it was decided to synthesize polymer with a higher degree of sulfonation (50%) in-house, using Dr. Weiss' methodology. The complete text of the method, as received from Dr. Weiss, is included in Appendix 8.3. In summary, a 1M solution of acetyl sulfate was prepared by measuring the appropriate amount of acetic anhydride into dry 1,2-dichloroethane followed by the addition of concentrated sulfuric acid. A known quantity of the acetyl sulfate, based on the desired degree of sulfonation, was added to a solution of polystyrene (M_w 280,000) in dry dichloroethane. The mixture was heated to 50°C with constant stirring for approximately 60 minutes after which the reaction was terminated by the addition of 2-propanol. After distilling off the solvent, the polymer was ground to a fine powder. The degree of sulfonation was determined by acid-base titration to a phenolphthalein endpoint.

² Sulfonated polystyrene samples were obtained from Dr. Robert Weiss of the University of Connecticut, Chemical Engineering Department.

2.3.7 Oxidizing Materials and Mixtures

The possible use of oxidation mechanisms for agent destruction was evaluated using benzoyl peroxide (Aldrich Chemical), an oxidizing agent commonly used in over-the-counter creams and medicinal products. The use of benzoyl peroxide in decomposition of the simulants was tested alone and in mixtures with other materials evaluated under the program. Compositions of mixtures were tested with the goal of achieving reactivity to both nerve agents and vesicants.

3.0 REACTIVITY STUDIES

The reactivity of the candidate materials with each of the target simulants was determined by methods summarized in Section 2.1.2 and detailed in the standard operating procedure (SOP) provided in Appendix 8.1. The results of these measurements are presented in this section. The percent of the initial simulant challenge remaining after 8 hours is reported in tabular format. Data are also presented in graphical form to demonstrate the rate of the reaction process.

3.1 METAL COMPLEXES

As shown in Table 5, the non-Krytox® complexes discussed in Section 2.2 generally demonstrated little reactivity with the target simulants. For this reason, the majority of program efforts concentrated upon testing of the metal/Krytox® compounds and sulfonates. It should be noted that early in the program, a spiking level of 5 or 10 µl was used for reactivity studies of, not only the metal complexes but also, the metal/Krytox® compounds. Upon the recommendation of USAMRICD, this level was changed to 1 µl. As necessary, a limited amount of the testing, which had been performed with the higher spiking levels was repeated using the lower values.

Table 5. Reactivity of Metal Complexes with Simulants

Compound	Percent of Challenge Remaining After 8 hours (µl challenge)			
	DFP	CEES	Malathion	Paraoxon
Cu ₂ (acetylacetonate)	100 (5 µl) 90 (1 µl)	85 (5 µl)	90 (5 µl)	NT
Cu ₂ (2,2'-dipyridyl)	100 (1 µl)	80 (1 µl)	95 (1 µl)	NT
Cu ₂ (urocanate)	100 (1 µl)	100 (1 µl)	95 (1 µl)	NT
Cu ₂ (EDTA)	90 (1 µl)	95 (1 µl)	NT	NT
Fe ₃ (acetylacetonate)	95 (1 µl)	NT	80 (1 µl)	90 (1 µl)

NT – not tested

None of this are effective!

3.2 KRYTOX® COMPOUNDS

Table 6 summarizes the final amounts of simulant remaining after an 8-hour reaction period with all of the Krytox® compounds and mixtures discussed in Section 2.2 (best performers are highlighted). Eight-hour reaction data for these compounds against 1µL challenges of the target simulants are presented in Figures 11 through 15. Testing of metal/Krytox® complexes, as well as mixtures of Krytox® acid and several of the complexes demonstrated these materials to be reactive to DFP, CEES and, to a lesser degree, Paraoxon. Reaction of all Krytox® compounds with Malathion is minimal. Cu(Krytox®)₂ and Ni(Krytox®)₂ show the largest amount of activity. Fe(Krytox®)₃ and La(Krytox®)₂ reactions are simulant dependent, with greater activity toward DFP than CEES. In general, DFP reacts quickly— within the first thirty minutes. With CEES, the reaction rate is slower, leveling off within the first few hours. It is interesting to note the differences in reactivity between Malathion and Paraoxon, as Paraoxon is approximately twice as reactive. Due to the large difference in reactivity, testing with all four simulants was continued throughout the program.

Table 6. Summary of Simulant Reactivity with Krytox Compounds

Compound	Percent of 1 µl Challenge Remaining After 8 hours			
	DFP	CEES	Malathion	Paraoxon
Krytox® Acid	35	25	70	85
Cu(Krytox®) ₂	5	10	80	40
Fe(Krytox®) ₃	15	50	80	30
La(Krytox®) ₂	10	80	95	NT
Ni(Krytox®) ₂	10	15	85	45
37% Cu(Krytox®) ₂ in Krytox® Acid	30	10	85	NT
Equal mix of Cu(Krytox®) ₂ , Fe(Krytox®) ₃ , Krytox® Acid	20	10	85	NT
10% Cu(Krytox®) ₂ in Krytox® 1525	70	80	NT	NT

NT - not tested

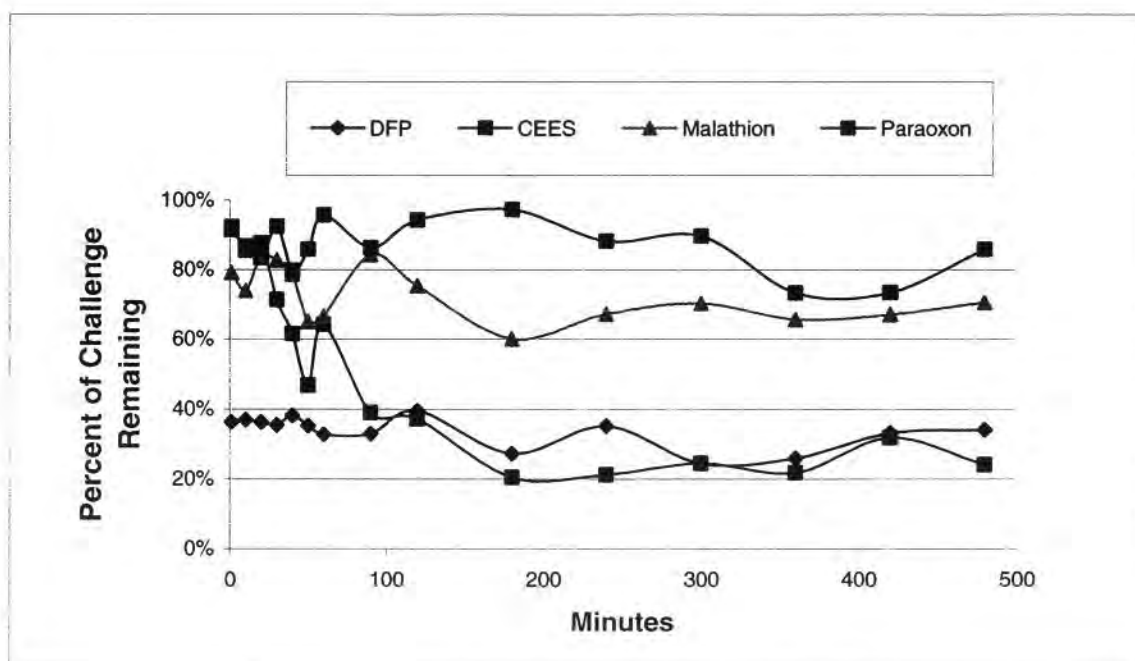


Figure 11. Simulant Depletion with Time Using Krytox® Acid

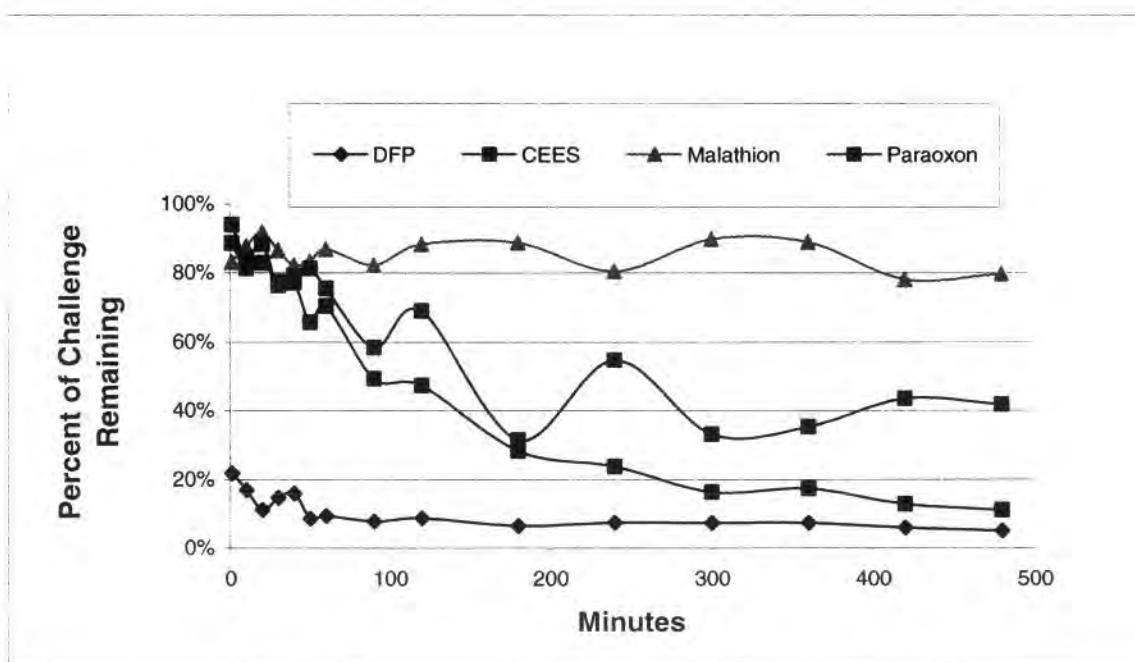


Figure 12. Simulant Depletion with Time Using Cu(Krytox®)₂

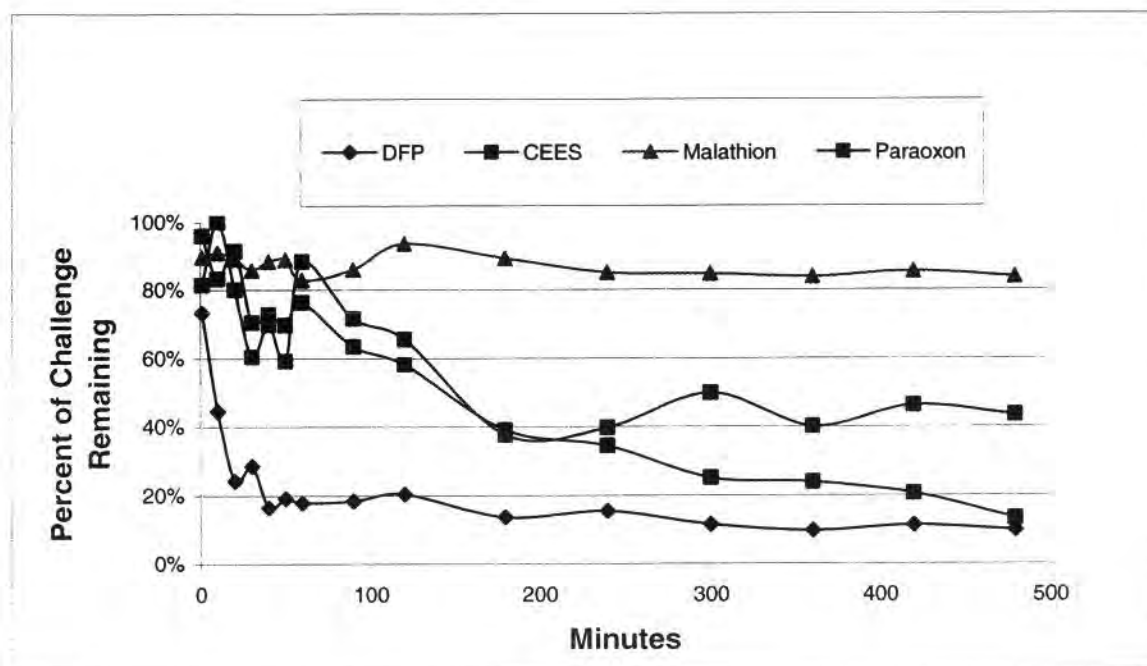


Figure 13. Simulant Depletion with Time Using Ni(Krytox®)₂

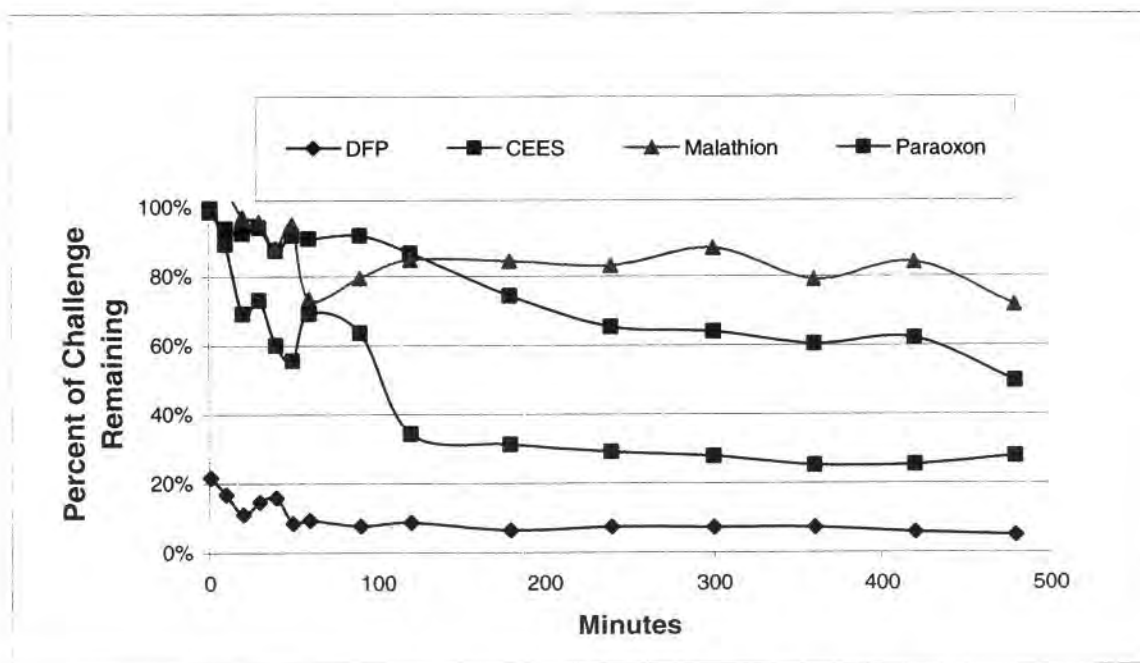


Figure 14. Simulant Depletion with Time Using Fe(Krytox®)₃

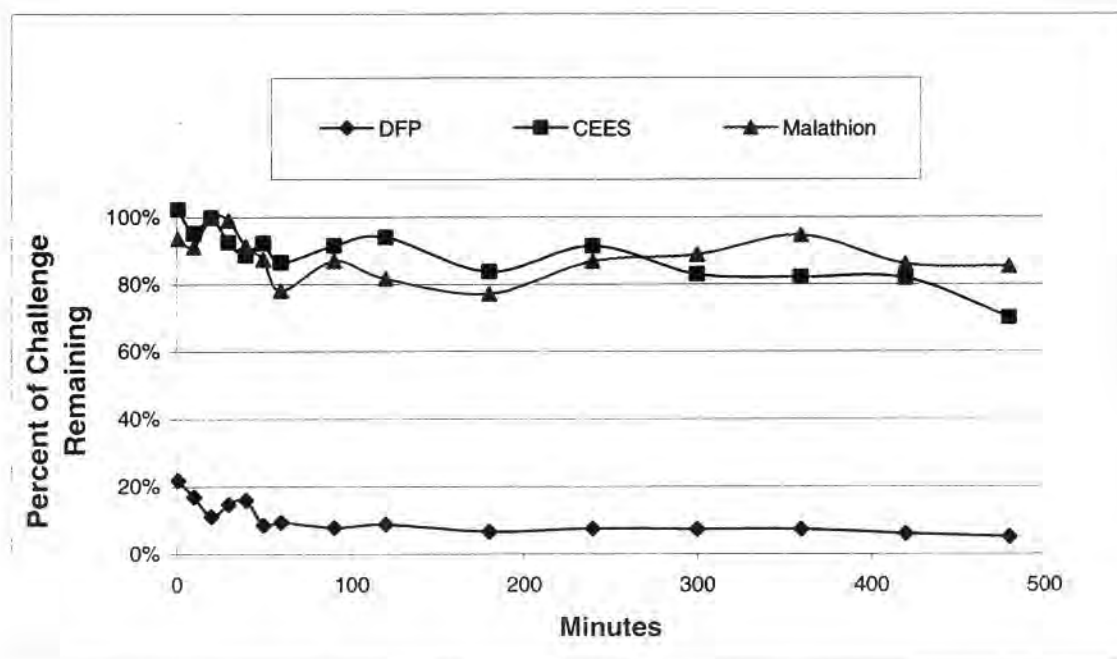


Figure 15. Simulant Depletion with Time Using La(Krytox®),

3.3 PERFLUORINATED ACIDS

The overall effect of a fluorocarbon backbone is to increase acidity due to the electron-withdrawing ability of the fluorine atoms. Decreasing the chain length of an organic carboxylic acid will also increase its acidity. Since the simulants were shown to breakdown in the presence of Krytox® acid (a perfluorinated carboxylic acid), other shorter chain perfluorinated acids (e.g., perfluoropropionic acid and perfluorotetradecanoic acid) were purchased and tested for reactivity toward the target simulants. While both acids are too corrosive to actually be used in TSPs, the information obtained from these experiments provided insight into the possible mechanisms involved in the decomposition reactions being studied. Data from these experiments are summarized in Figures 16 and 17.

Malathion reactivity is similar for all three acids, which suggests that either the Malathion is not affected by acidic conditions or these particular acids are not aggressive enough to cause its decomposition. DFP's reactivity is the opposite of what would be expected if acidity were the only factor in the deactivation, i.e. with a shorter the fluorocarbon backbone and increasing acid strength, the DFP reactivity would be expected to increase not decrease. In the case of CEES, the reactivity does not follow the acidity.

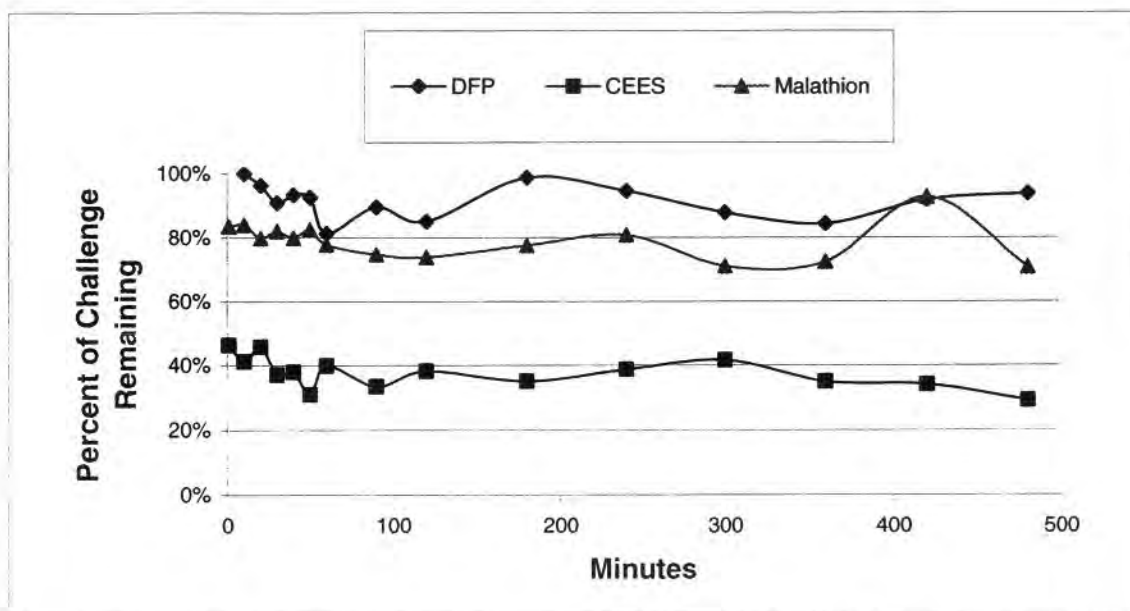


Figure 16. Simulant Depletion with Time Using Perfluoropropionic Acid

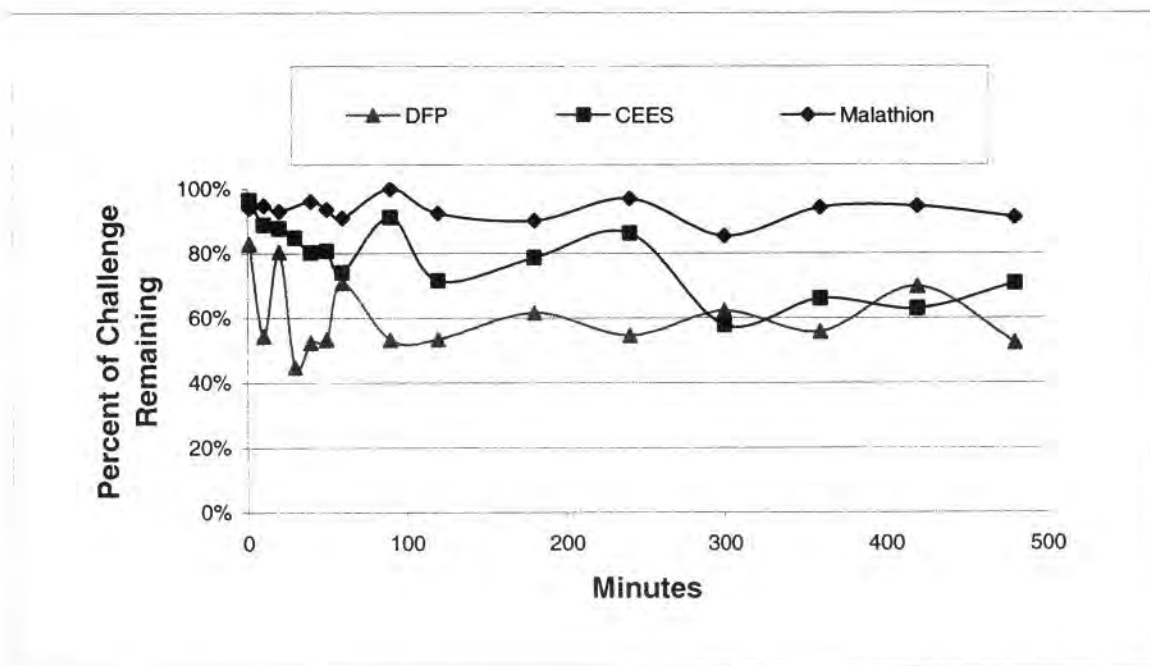


Figure 17. Simulant Depletion with Time Using Perfluorotetradecanoic Acid

✓ correct
The reactivity of CEES with Krytox® acid and perfluoropropionic acid are similar. However, the reactivity of CEES ~~reactivity~~ with perfluorotetradecanoic acid is less than would be expected. These results suggest that in the case of DFP and CEES, in addition to acid hydrolysis, there is probably another mechanism involved in the decomposition reaction.

3.4 PERFLUORINATED SULFONATES

Cu(Krytox®)₂ is the most reactive of the compounds discussed thus far. However, the performance of Cu(Krytox®)₂ is not optimal as it demonstrates limited reactivity with Malathion. Since sulfonates are known to be much stronger acids than carboxylic acids and a perfluorinated sulfonate could, theoretically, be readily incorporated into the TSP cream, a number of perfluorinated sulfonates were identified for evaluation under the program, including:

- Perfluorinated sulfonate (2-7-2) - supplied in bead form and has an equivalent weight of approximately 1100
- Perfluorinated sulfonate (2-7-9) - a powder and a by-product of sulfonate (2-7-2) production
- Perfluorinated sulfonate (1-10-13) - an experimental DuPont product based on perfluorinated sulfonate (2-7-9), which has been adsorbed on an inorganic reactive base
- Copper perfluorinated sulfonate was prepared, in-house, by refluxing a mixture of copper acetate and perfluorinated sulfonate (1-10-13) in Vertrel®.

As shown in Table 7, the reactivity of these materials with the target simulants is dependent on the simulant and the actual perfluorinated sulfonate involved. Of the three simulants tested, the rate and amount of reaction with CEES demonstrates the most significant improvement relative to the Krytox® compounds. The reactivity of the CEES is highly dependent upon the available surface area of the test material, as shown by the widely divergent values for sulfonates (2-7-9, a powder form) and (2-7-2, a bead form). In the case of DFP and Malathion, the apparent reaction with perfluorinated sulfonate (1-10-13), and the copper complex made from this material, is a result of adsorption of the simulant onto the surface of the inorganic material present in this particular sulfonate. Extractions were performed with hexane and methylene chloride to confirm this behavior. It is unknown whether the adsorption may lead to decomposition of the simulant at reaction times greater than 8 hours. The data indicate that adsorption is not a factor with CEES.

Table 7. Simulant Reactivity with Perfluorinated Sulfonates

Compound	Percent of Challenge Remaining After 8 hours	
	Hexane Extraction	Methylene Chloride Extraction
DFP		
Perfluorinated Sulfonate (1-10-13)	2 (1µl)	67
	18 (5µl)	NT
	43 (10µl)	NT
Perfluorinated Sulfonate (2-7-2)	3.5 (1µl)	12
	4.0 (5µl)	NT
Perfluorinated Sulfonate (2-7-9)	13	22
Copper Perfluorinated Sulfonate (1-10-13)	0	81
CEES		
Perfluorinated Sulfonate (1-10-13)	2 (1µl)	8
	13 (5µl)	NT
	46 (10µl)	NT
Perfluorinated Sulfonate (2-7-2)	92	85
Perfluorinated Sulfonate (2-7-9)	0	2
Copper Perfluorinated Sulfonate (1-10-13)	2	4
Malathion		
Perfluorinated Sulfonate (1-10-13)	10 (1µl)	80
	31 (5µl)	NT
Perfluorinated Sulfonate (2-7-2)	100	91
Perfluorinated Sulfonate (2-7-9)	75	67
Copper Perfluorinated Sulfonate (1-10-13)	0	100

NT - not tested

After the overall adsorption effect has been accounted for, the effectiveness of the fluorinated sulfonates, in general, is disappointing. The results do, however, add more credence to the theory that reactivity involves more than just acid hydrolysis. In addition, the high cost of the materials, along with their limited availability, makes the fluorinated sulfonates unfavorable candidates for use in reactive TSPs. *

3.5 FUNCTIONALIZED STYRENE/DIVINYLBENZENE AND CLAYS

Since results obtained with fluorinated sulfonates and carboxylates indicate that factors other than acid strength alone may affect reactivity, a number of non-fluorinated functionalized compounds were evaluated. Styrene/divinylbenzene resins and clays with sulfonic acid (acid and salt form) and various basic groups are very inexpensive and widely available commercially. Tests results, as well as, the functional group present in each material tested are presented in Table 8 (best performers are highlighted).

Several of the functionalized styrene/divinylbenzenes exhibited very favorable results with not only DFP and CEES, but also Malathion and Paraoxon. For example, all four simulants are completely destroyed or almost completely destroyed within the first 10 to 20 minutes of contact with METSS 2-8-13 and METSS 2-8-14 (see Figures 18 and 19).

The sodium salt of several of the sulfonated polymers reacts with DFP and CEES, which again points to the observation that acidity or even basic character may not be the only factor involved in the selection of active compounds. The clays tested show no apparent advantage over other materials.

A disadvantage to obtaining compounds commercially is that the information concerning a particular material is limited. Information was not available on the average molecular weight, degree of crosslinking and percent of active functional group for the first eight compounds listed in Table 8. For the last eight compounds, only limited information on crosslinking was available. The most significant effect, which may be attributed to crosslinking, is the reactivity of the amines, METSS 3-7-12, 3-7-13 and 3-7-14, with CEES, as the reactivity was noted to increase with increasing crosslink density.

Table 8. Simulant Reactivity of Functionalized Styrene/Divinylbenzene and Clays

Compound	Active Functional Group	Percent of 1 µl Challenge Remaining After 8 hours			
		DFP	CEES	Malathion	Paraoxon
Stryene/divinylbenzene Sulfonate (C 267)	Sulfonic/H	10	2	70	55
Stryene/divinylbenzene Sulfonate (C 253)	Sulfonic/Na	20	0	90	NT
Stryene/divinylbenzene Sulfonate (2-8-10)	Sulfonic/Na	25	1	95	NT
Stryene/divinylbenzene Sulfonate (C 251)	Sulfonic/H	10	1	80	NT
Stryene/divinylbenzene Sulfonate (2-8-13)	NH4	0	0	0	NT
Stryene/divinylbenzene Sulfonate (2-8-14)	Sulfonic/NH4	0	1	1	10
Perfluorinated Sulfonate (2-7-9)	Sulfonic/H	20	2	65	35
Modified Clay (3-7-1)	NH4	55	45	80	NT
Modified Clay (3-7-2)	Sulfonic/NH4	80	55	NT	NT
Modified Clay (3-7-8)	NH4	NT	100	NT	NT
Modified Clay (3-8-4)	NH4	60	80	NT	NT
Modified Clay (3-7-7)	NH4	NT	95	NT	NT
Styrene/divinylbenzene Amine (3-7-12)	Quat. methyl amine	90	4	75	NT
Styrene/divinylbenzene Amine (3-7-13)	Quat. methyl amine	90	20	85	NT
Styrene/divinylbenzene Amine (3-7-14)	Quat. methyl amine	80	50	25	NT
Styrene/divinylbenzene Amine (3-7-18)	Dimethyl amine	65	70	65	NT
Styrene/divinylbenzene Sulfonate (3-7-15)	Sulfonic/H	5	0	80	80
Styrene/divinylbenzene Sulfonate (3-7-16)	Sulfonic/H	5	0	80	60
Styrene/divinylbenzene Sulfonate (3-7-17)	Sulfonic/H	10	0	65	60
Styrene/divinylbenzene Sulfonate (3-8-13)	Sulfonic/H	5	5	60	45

NT - not tested

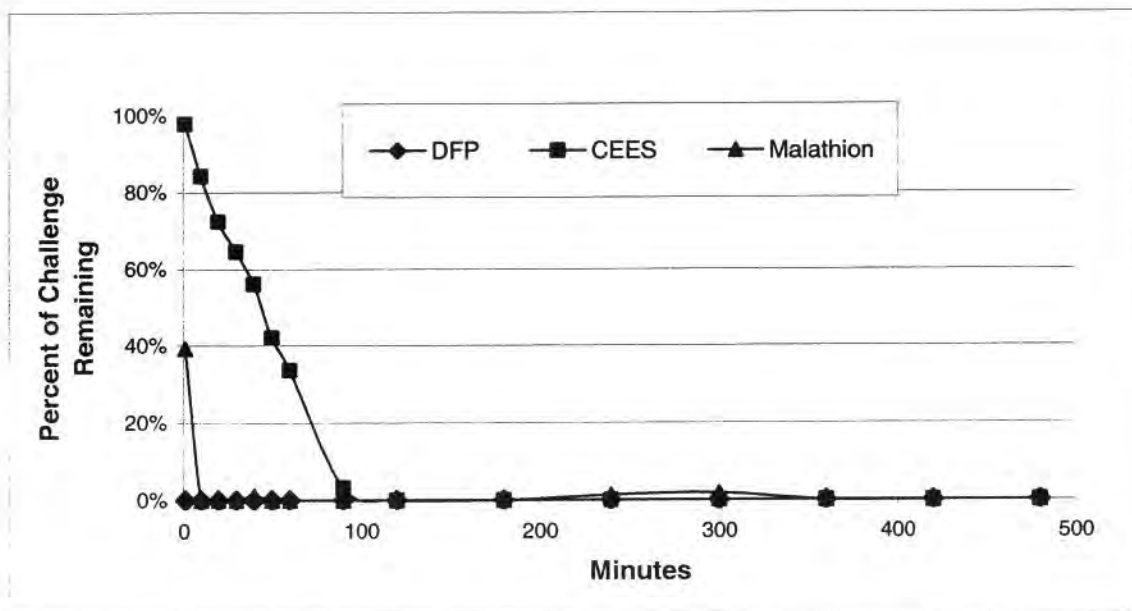


Figure 18. Simulant Depletion with Time Using METSS 2-8-13

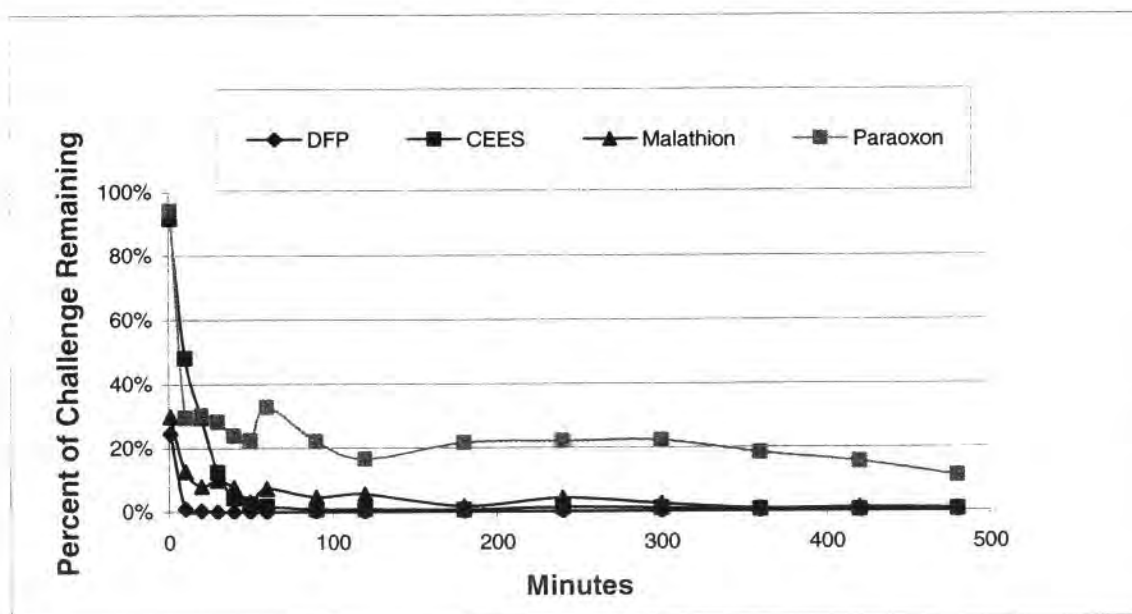


Figure 19. Simulant Depletion with Time Using METSS 2-8-14

3.6 SULFONATED POLYSTYRENE

Several samples of sulfonated polystyrene were obtained from Dr. Robert Weiss of the University of Connecticut for evaluation under the program (Table 9). As these samples were custom synthesized, considerably more information was available regarding these resins. The starting point for all was polystyrene with M_w of 280,000. The percent sulfonation for each sample was also supplied and is included in the identification for each compound tested. The last resin, with 50% sulfonation was prepared by METSS. With the exception of reactivity with Malathion, the reactivity of the sulfonated polystyrene materials with the target simulants is related to the degree of sulfonation.

Table 9. Simulant Reactivity with Sulfonated Polystyrene

Compound	Active Functional Group	Percent of 1 μ l Challenge Remaining After 8 hours			
		DFP	CEES	Malathion	Paraoxon
Sulfonated Polystyrene (11 mole %)	Sulfonic/H	85	90	NT	90
Sulfonated Polystyrene (6.4 mole %)	Sulfonic/H	75	60	75	80
Sulfonated Polystyrene (17.9 mole %)	Sulfonic/H	40	55	90	25
Sulfonated Polystyrene (50 mole %)	Sulfonic/H	30	20	90	30

NT - not tested

3.7 OXIDIZERS

Hydrolysis mechanisms of decomposition, both acid and base catalyzed, were investigated extensively under the program. The possible use of oxidation mechanisms for agent destruction was evaluated using benzoyl peroxide, an oxidizing agent commonly used in over-the-counter creams and medicinal products. The use of benzoyl peroxide for decomposition of the simulants was tested alone and in mixtures with other materials evaluated under the program.

When tested alone, benzoyl peroxide was found to be ineffective, most likely due to the lack of available water to support the reaction process. In most cases, preparation of mixtures did not give definitive results, e.g., the mixture may have performed better than one component of the mixture when tested individually, but agent neutralization performance was worse with respect to the other component. Mixtures of benzoyl peroxide in Cu(Krytox®)₂ were the one exception to this (Table

10). As little as 5% benzoyl peroxide had a noticeable effect on Paraoxon reactivity without being detrimental to DFP and CEES reactivity (see Table 6 for comparison with Cu(Krytox®)₂ alone). This mixture is a liquid, so it can be readily formulated into a reactive cream.

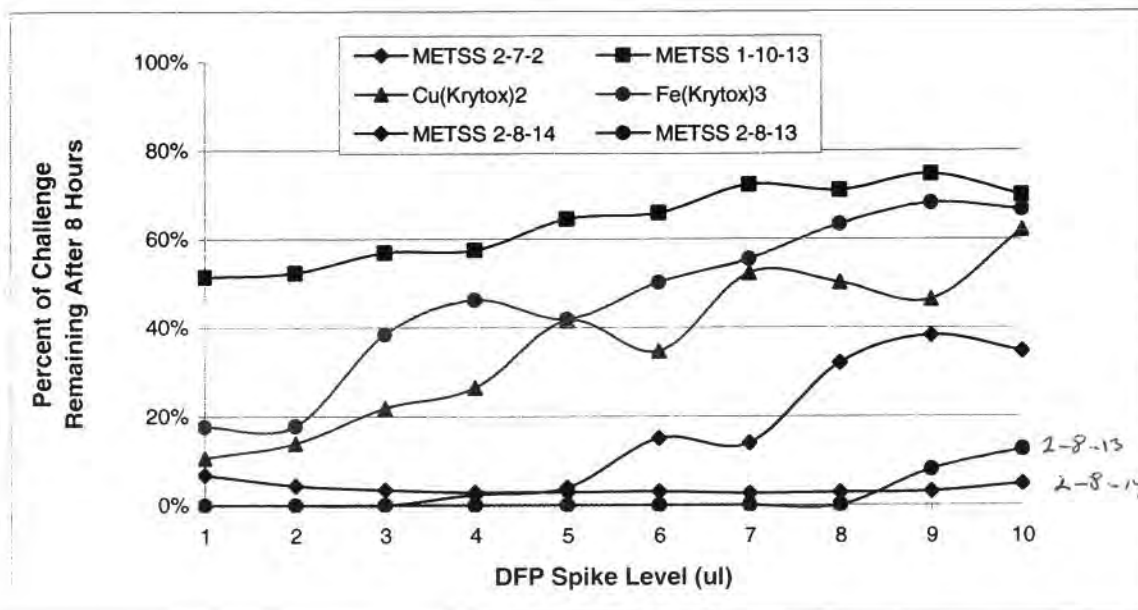
Table 10. Eight Hour Reactivity Data for Benzoyl Peroxide and Mixtures

Compound	Type	Percent of 1 µl Challenge Remaining After 8 hours			
		DFP	CEES	Malathion	Paraoxon
5% Benzoyl Peroxide in Cu(Krytox) ₂	Mixture	15	7	60	2
9% Benzoyl Peroxide in Cu(Krytox) ₂	Mixture	15	0	75	30
20% Benzoyl Peroxide in Cu(Krytox) ₂	Mixture	20	5	65	5
5% Benzoyl Peroxide & 0.5% METSS 2-8-14 in Cu(Krytox®) ₂	Mixture	20	5	75	35

4.0 REACTION CAPACITY STUDIES

A second series of experiments was conducted on materials demonstrating the most reactivity with one or more of the target simulants to determine the amount of simulant (1 to 10 μL) that could be destroyed within an 8 hour time period by 50 mg of each of the reactive materials. The reactivity of the candidate materials with varying amounts of each of the target simulants was determined by methods summarized in Section 2.1.2 and detailed in the standard operating procedure (SOP) provided in Appendix 8.1. The results of these measurements are presented in Figures 20, 21, 22 and 23 for DFP, CEES, Paraoxon and Malathion respectively. The trends presented in these tables are consistent with the results of the reaction studied presented in the previous section.

The reaction capacity of the styrene/divinylbenzene sulfonate materials (METSS 2-8-13 and METSS 2-8-14) toward DFP was exceptional, with the 50 mg test sample of METSS 2-8-13 completely destroying up to 8 μL of DFP in the 8 hour reaction period before showing signs of depletion and the 2-8-14 destroying up to 3 to 5 μL of the DFP challenge in the 8 hour reaction period before showing signs of depletion. METSS 2-7-2 (a perfluorinated sulfonate) destroyed more than 90% of the DFP simulant challenge after 8 hours, even at the 10 μL challenge level. The metal-Krytox® samples demonstrated less overall reactivity during the same 8 hour time period and a much more limited capacity toward the level of simulant challenge, showing a steady decrease in reaction capacity with each increasing level of challenge. As expected (based on previous DFP test results), the experimental perfluorinated sulfonate (METSS 1-10-13) demonstrated poor performance. METSS 2-8-13 and METSS 2-8-14 also demonstrated exceptional reaction capacity toward CEES, with both materials destroying up to 7 μL of CEES in the 8-hour reaction period before showing signs of depletion. METSS 1-10-13 demonstrated much better performance against CEES than DFP, while METSS 2-7-2 demonstrated very poor performance against CEES. Once again, the metal-Krytox® samples showed a decrease in reaction capacity with each increasing level of challenge. All of the test samples demonstrated less overall reactivity with Paraoxon, with the best performers destroying only 30% of the initial 1 μL challenge. While the amount of simulant remaining after 8 hours was much higher in this data set, the trends in the reactivity data were very similar to the trends seen in the DFP data, with the exception of METSS 2-7-2, which was much less reactive with Paraoxon than DFP. Reaction capacity data for Malathion was limited due to simulant availability. However, the overall performance of the reactants tested against Malathion was limited, regardless of the level of challenge.



use different
symbol for
Fe 2-8-13
and
2-7-2 / 2-8-1
which is not Fe
same compound
for Fig 20-22

Figure 20. Reaction Capacity of Candidate Reactants with DFP

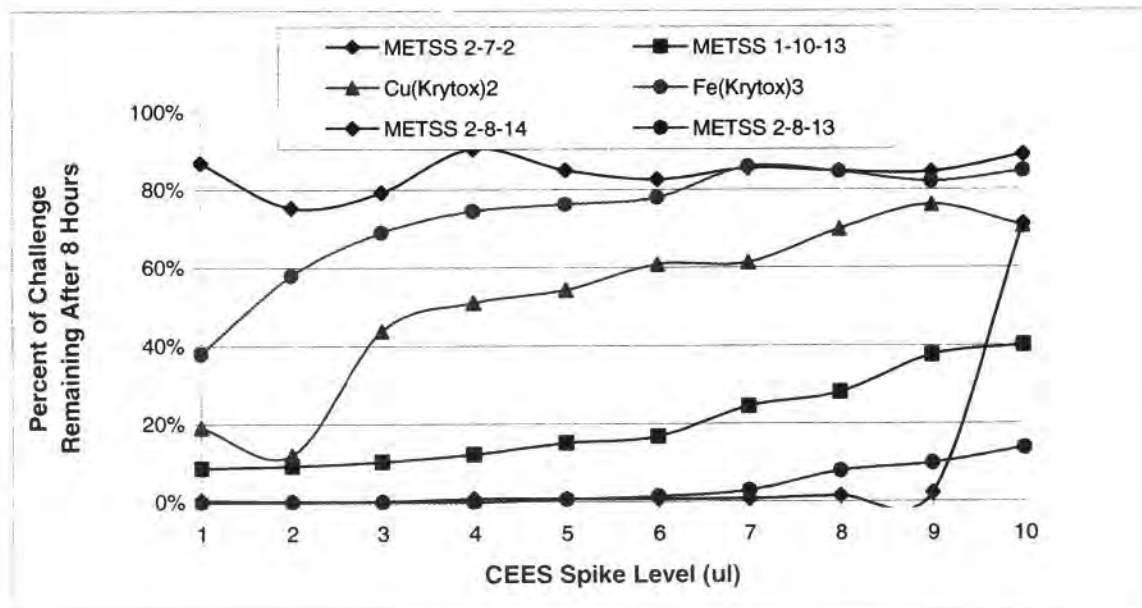


Figure 21. Reaction Capacity of Candidate Reactants with CEES

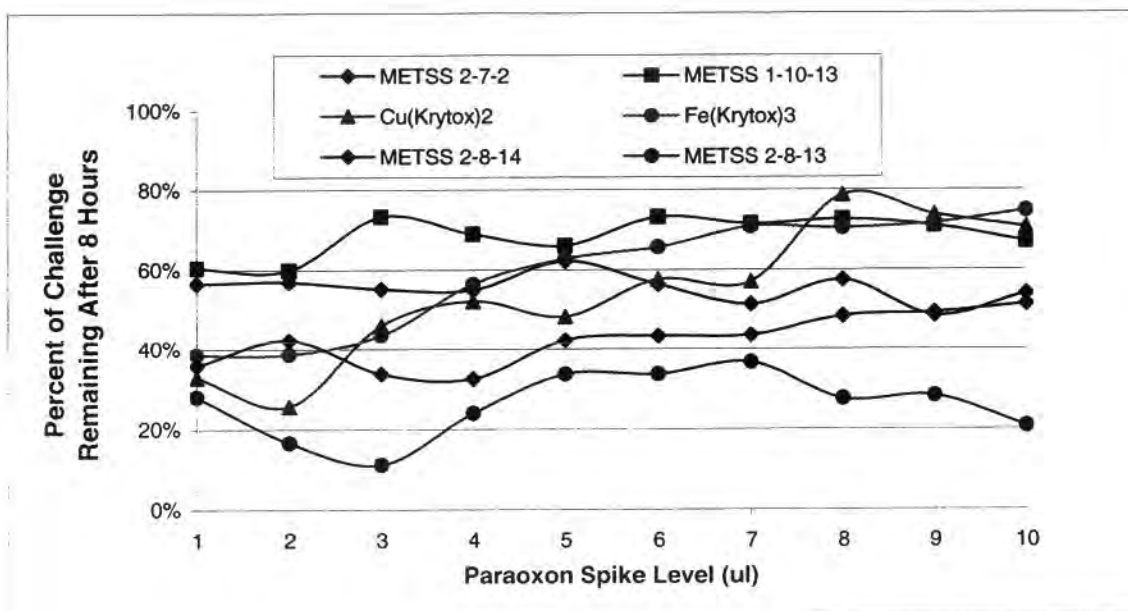


Figure 22. Reaction Capacity of Candidate Reactants with Paraoxon

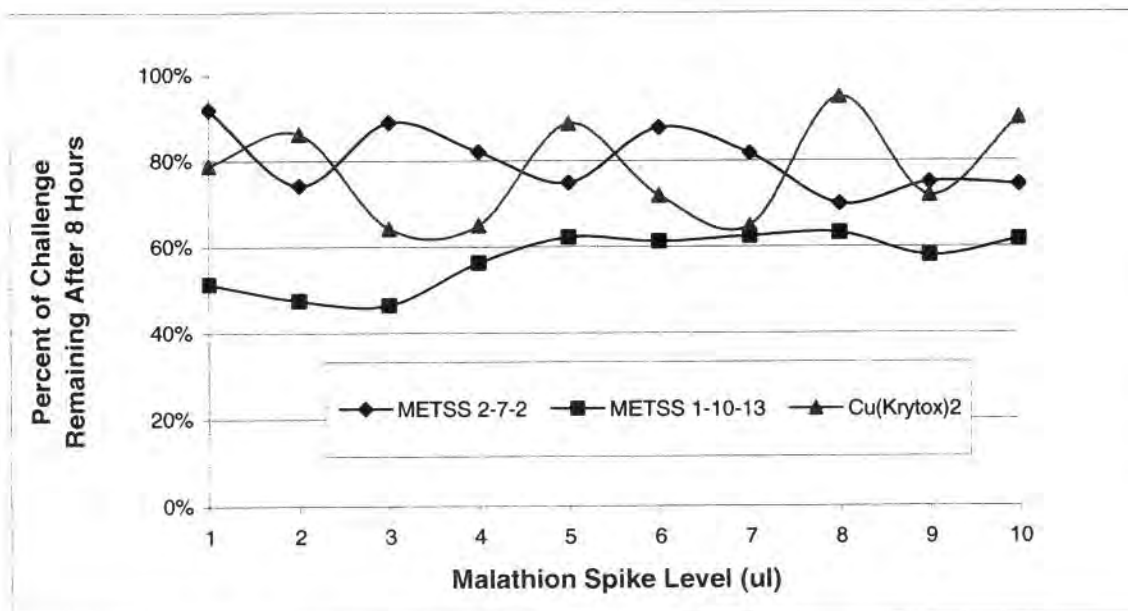


Figure 23. Reaction Capacity of Candidate Reactants with Malathion

5.0 PERMEATION STUDIES

5.1 CREAM PREPARATION

The TSP creams used to support the program efforts were obtained from DuPont and USAMRICD. The material from DuPont was formulated to have a viscosity of Grade 4 grease by dispersing appropriately sized PTFE particles in Krytox® 1525 PFAE oil.³ During permeation studies, it was discovered that this material was too thick to be applied to the nitrocellulose filter paper used in the permeation cell, leading to tearing of this very brittle material and subsequent disruption in obtaining appropriate experimental data. The ICD 3005 TSP cream provided by the Army was a much thinner material with a consistency of a thick liquid rather than grease. This material was much more compatible with the permeation test method and apparatus.

Various methods were used to incorporate the reactants evaluated under the program into the ICD 3005 TSP cream, depending on the form of the reacting material. Liquid compounds were added to the TSP cream using a mortar and pestle to thoroughly mix the two components. The addition of solid compounds proved to be much more challenging as it was first necessary to use various methods to reduce the size of the solid particulates down to a very small size domain to facilitate introduction into the TSP cream without adversely affecting the consistency of the cream. In some cases, it was also necessary to add additional Krytox® 1525 or a fluorinated emulsifier to thin the material to the same initial viscosity as the control cream and facilitate the introduction of the solid reactants into the cream.

METSS 2-8-14, one of the best performing reactive compounds, was particularly difficult to incorporate into the base cream. Several grinding methods were used to reduce the size of the 2-8-14 particles, including:

- mortar and pestle
- mortar and pestle with dry ice
- mortar and pestle with liquid nitrogen
- mortar and pestle with toluene
- coffee grinder
- Gilson planetary mill with and without added water

³ According to the specifications provided by the Army during Phase I program.

- Sturtevant Micronizer
- Lehman Mills three roll mill.

Of these, only the Micronizer and three roll mill were able to successfully reduce the particle size of this material to a level required to facilitate incorporation into the cream without disrupting the physical properties and protection afforded by the base cream.

Size reduction using the three roll mill was accomplished by passing a 50% mixture of METSS 2-8-14 in Krytox® 1525 through the mill and then adding this mix to the control cream. There did not appear to be any loss in reactivity due to dehydration of the METSS 2-8-14 when using this method. This may be attributed to the presence of the Krytox® 1525 in the initial mixture as the hydrophobic nature of the Krytox® may act to 'seal' in the hydrated water

Size reduction using the Micronizer was found to remove approximately half of the coordinated water in METSS 2-8-14, which was detrimental to the reactivity of this material toward the target simulants. However, it was determined that the powder could be re-hydrated with full restoration of the reactivity by simply mixing the reduced powder with water in a mortar and pestle prior to addition to the cream. This problem may also be avoided by using wet-milling procedures.

5.2 PERMEATION TEST RESULTS

A summary of the general methodology used in permeation studies was provided in Section 2.1, with a full description provided in Appendix 2. As the program progressed, minor changes were required to the initial test methodology to achieve proper performance. The main problems were associated with tearing of the nitrocellulose paper during experimental setup. This problem was ultimately solved by reducing the internal diameter of the glass cell from 23 mm to 12 mm and reducing the air flow through the cell from approximately 1.0 L/min to 0.5 L/min.

The initial method of purging the cell with air was by means of a pump that would pull air from the laboratory through two XAD-2 cartridges to purify the air before it entered the cell. From the cell, the air would pass through two XAD-2 cartridges used to collect simulant and then into the pump. However, it was found that volatile materials in the laboratory air were high enough at times to saturate the initial XAD cartridges and contaminate the cell. For this reason, the pump was eliminated and replaced with high purity compressed air (Zero air) from a cylinder.

A summary of the permeation results using several of the most reactive materials identified under the program is provided in Table 11. Graphs summarizing the twenty-four hour permeation data for these formulations are presented in Figures 24 and 25 for DFP and CEPS permeability, respectively. The data are reported as the total amount of simulant (as a percent of the initial 10 µl liquid challenge) permeating through the test cream after 24 hours.

Table 11. 24-hour Permeation Test Results

Sample	Percent Breakthrough of 10 µl Liquid DFP Challenge	Percent Breakthrough of 10 µl Liquid CEPS Challenge
Base Cream (ICD 3005)	1.7	0.12
10% Cu(Krytox®) ₂ in Base Cream	< 0.1*	< 0.1*
10% Fe(Krytox®) ₃ in Base Cream	0.2	< 0.1*
10% METSS 2-8-14 in Base Cream	0.6	< 0.1*
10% METSS 2-8-13 in Base Cream	< 0.1*	< 0.1*
10% Sulfonated (50%) polystyrene	< 0.1*	< 0.1*

*less than the method detection limits.

The total simulant breakthrough for all of the reactive creams was less than that of the base TSP cream, clearly demonstrating the positive effects of incorporating a reactive component. The 10% Cu(Krytox®)₂ system demonstrated exceptional performance against DFP and CEPS, as did the reactive creams with 10% METSS 2-8-13 and 10% sulfonated (50%) polystyrene.

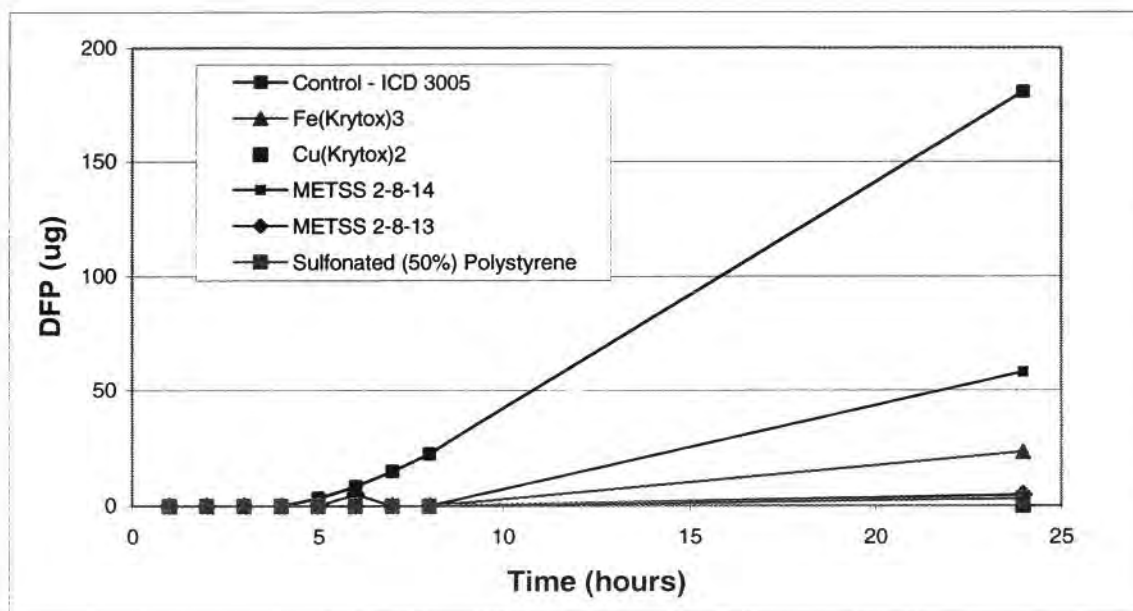


Figure 24. DFP Permeation Summary

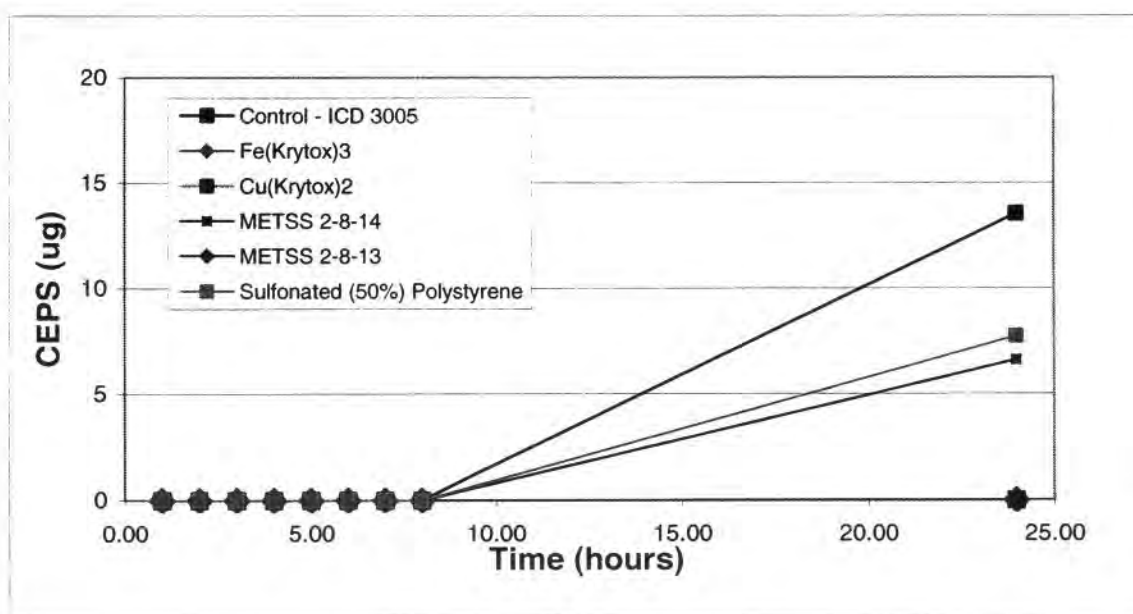


Figure 25. CEPS Permeation Summary

6.0 MATERIEL COMPATIBILITY

The performance of the best performing reactive TSP formulations was evaluated for compatibility with camouflage paint and a DEET-based (N, N-diethyl-m-toluamide) insecticide purchased from a local military surplus store. Specifically, the following materials were obtained:

- 30% DEET in an alcohol base
- three color (red, black, green) “compact” style camouflage paint
- light green and loam, dual stick camouflage paint
- black and olive drab, dual stick camouflage paint.

6.1 RTSP COMPATIBILITY WITH DEET

Since the alcohol in military issued DEET will evaporate almost immediately upon use, the decision was made to use analytical reagent grade DEET for stability testing. Compatibility with the reactive compounds Cu(Krytox®)₂ and METSS 2-8-14 (sulfonated styrene/divinylbenzene) was determined by spiking 50 mg of each of these reactants with 1 µL of DEET and then measuring the amount of DEET remaining at known intervals of time. The amount of DEET remaining was determined using the same gas chromatography methodology used to determine the residual simulant concentrations during the reactivity testing (see Section 2.1.2). Examples of a DEET chromatogram and calibration curve are shown in Figures 26 and 27, respectively. The detection limit and linear range is similar to that of the simulants.

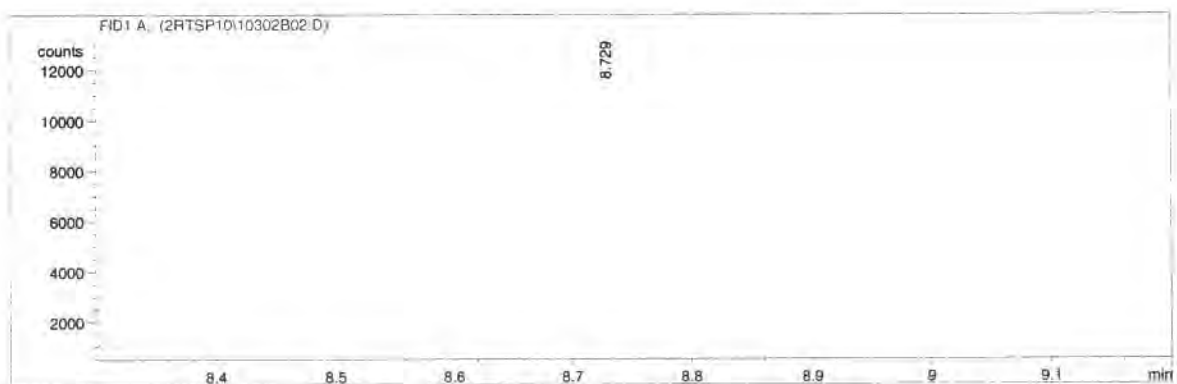


Figure 26. 5 µg/mL DEET in Methylene Chloride

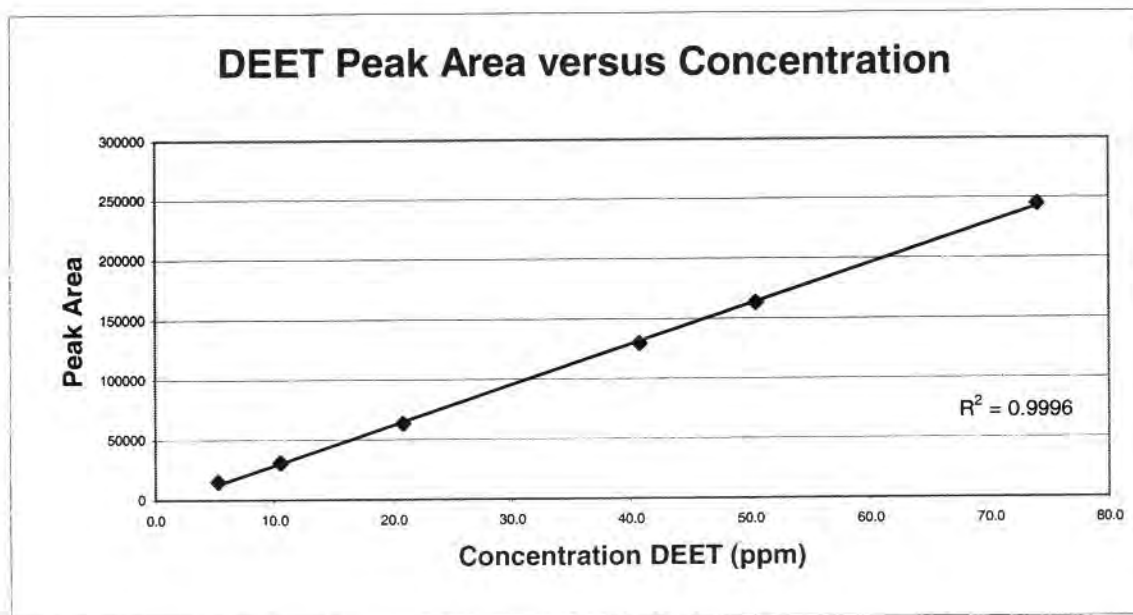


Figure 27. Regression Line - DEET

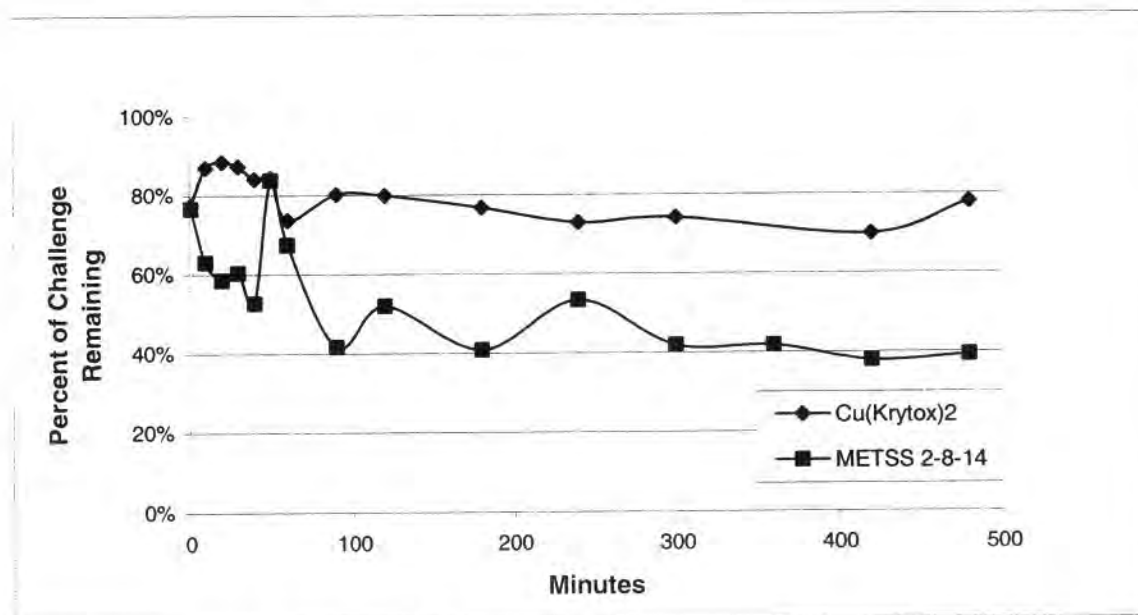


Figure 28. Depletion of DEET in Cu(Krytox®)₂ and METSS 2-8-14

The amount of DEET remaining during an 8-hour period after initial exposure to the two reactive compounds is presented graphically in Figure 28. The reactivity of DEET with Cu(Krytox®)₂ was found to be minimal. However, the interaction between DEET and METSS 2-8-14 was much more pronounced, causing some concern about the potential use of DEET with a reactive TSP containing this particular compound.

6.2 RTSP COMPATIBILITY WITH CAMOUFLAGE PAINT

The affect of various types of camouflage paints on the reactivity of Cu(Krytox®)₂ and METSS 2-8-14 with DFP and CEES was also investigated. An equal amount of black or red paint was blended with both Cu(Krytox®)₂ and METSS 2-8-14. The reactivity of these mixtures was then determined by spiking 50 mg of each of these two mixtures with 1 µL of DFP or CEES and then measuring the amount of simulant remaining at known intervals of time using the same gas chromatography methodology used to determine the residual simulant concentrations during the reactivity testing (see Section 2.1.2).

The results of these experiments are presented in Figures 29 through 32. Mixtures of Cu(Krytox®)₂ with the camouflage paint did not perform as well as the Cu(Krytox®)₂ by itself. As the apparent difference in capacity was not directly proportional to the dilution factor with the paints, it might be concluded that there is some physical or chemical degenerative interaction between the Cu(Krytox®)₂ and the paints. In the case of METSS 2-8-14, both of the paints slowed the rate of reaction with each of the simulants; however, the amount of simulant destroyed after 8 hours was virtually unchanged.

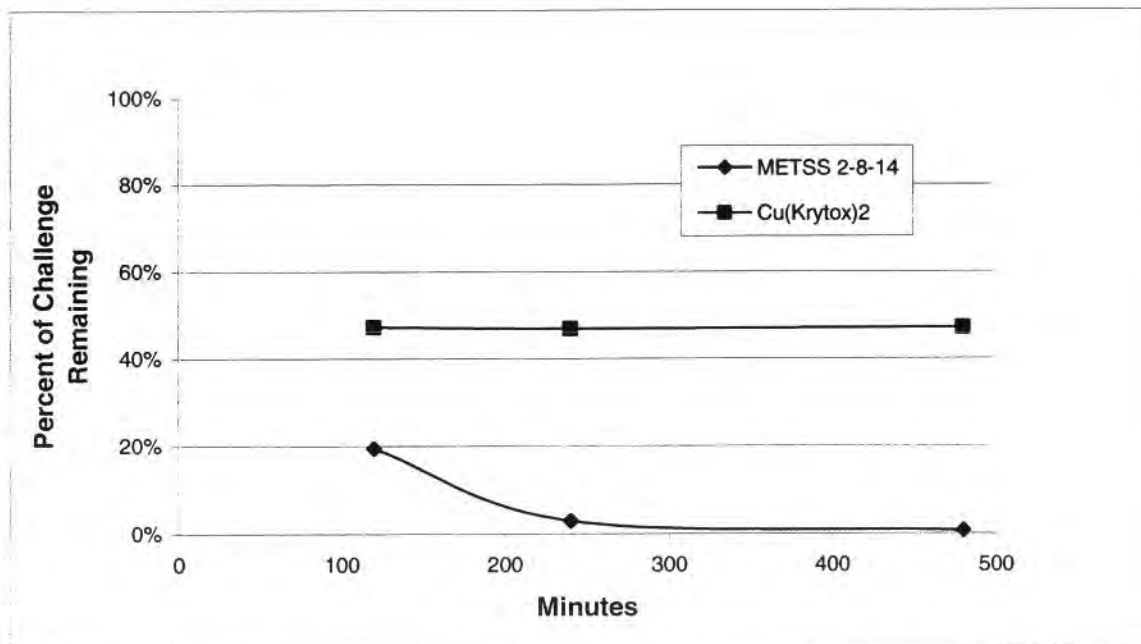


Figure 29. DFP Reactivity with Black Camouflage Paint Mixtures

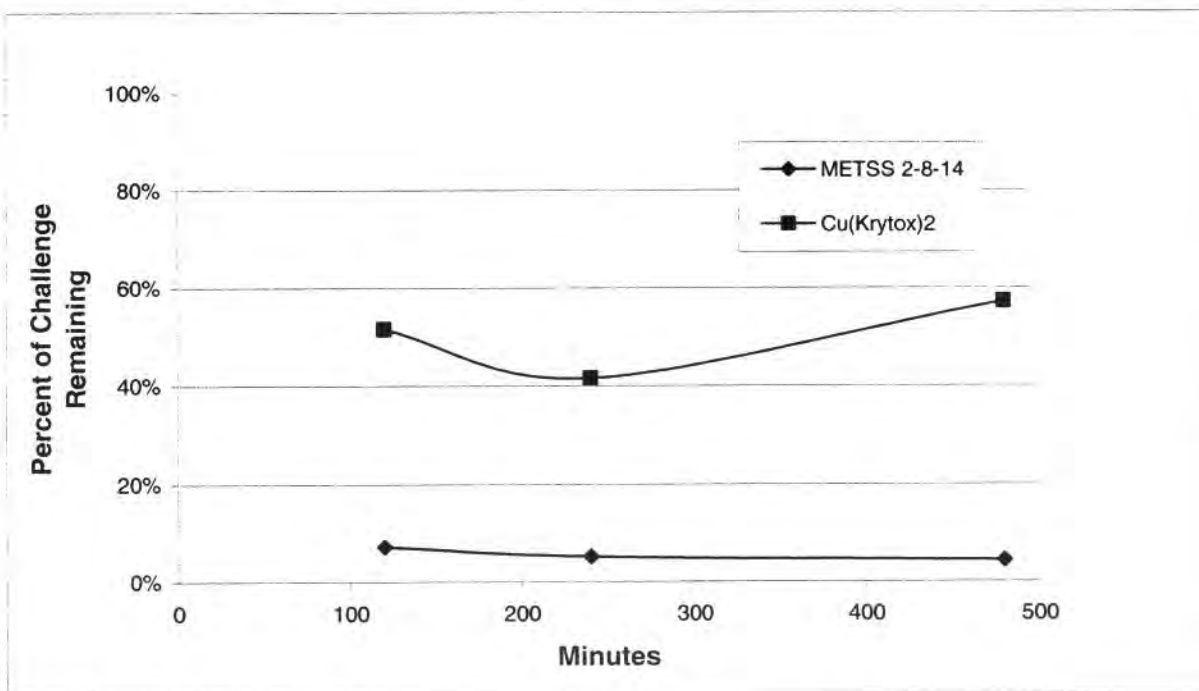


Figure 30. CEES Reactivity with Red Camouflage Paint Mixtures

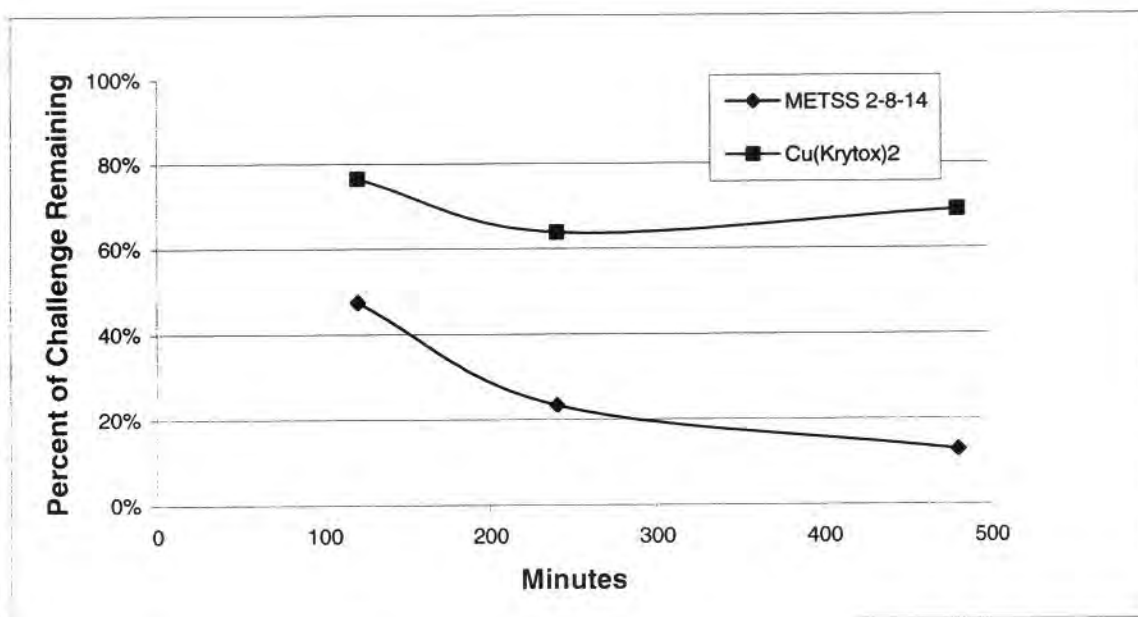


Figure 31. CEES Reactivity with Black Camouflage Paint Mixtures

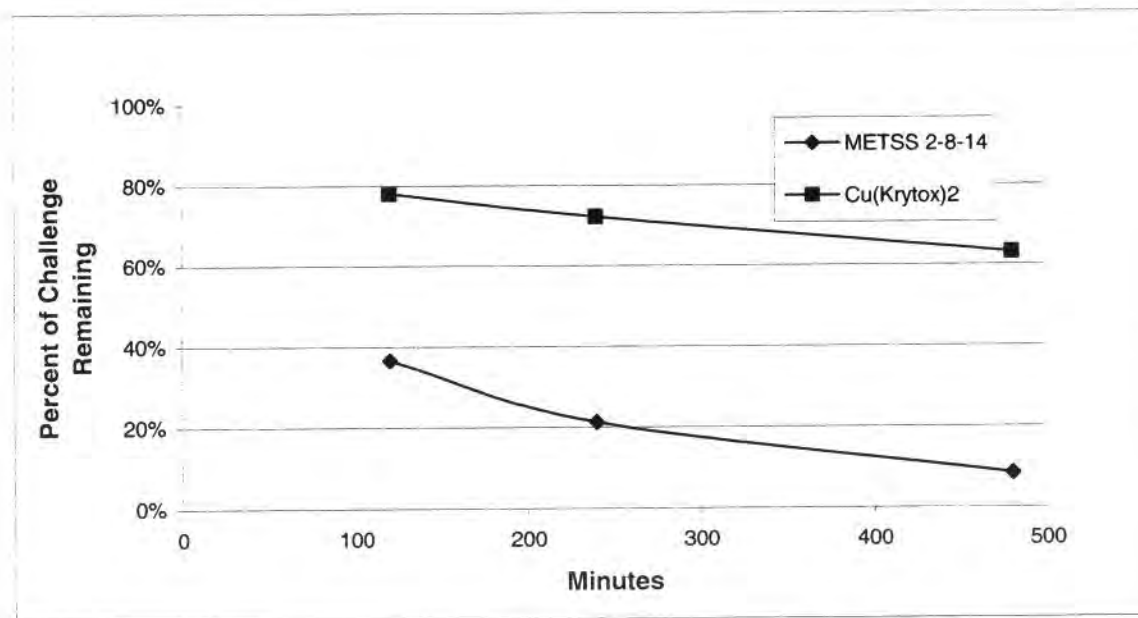


Figure 32. CEES Reactivity with Red Camouflage Paint Mixtures

7.0 RESEARCH ACCOMPLISHMENTS AND CONCLUSIONS

7.1 REPORTABLE OUTCOMES

Through the course of the program efforts, METSS has gained a better understanding of the mechanism that is effecting CWA simulant destruction by the types of compounds identified under SBIR program. METSS has used this knowledge base to identify and prepare new reactants that have demonstrated steady progression in CWA simulant destruction capability. A number of these compounds have been found to destroy DFP, CEES quickly and effectively, and to a lesser degree, Paraoxon. Destruction of the VX simulant, Malathion, continues to be a major challenge; however, Paraoxon may more closely correspond with VX chemical properties.

In sticking with the original objectives, METSS has continued to focus on reactant chemistries that are commercially available and viable. Furthermore, METSS has continued to work with materials that contain a fluorinated backbone so that the reactant chemistries can be readily incorporated into the existing PFAE based TSP creams with minimum impact on physical property performance. METSS has also identified non-fluorinated materials, which can be successfully incorporated into the creams using size reduction methods and emulsifiers to support rTSP formulation without adversely affecting the physical performance of the cream.

7.2 KEY RESEARCH ACCOMPLISHMENTS

Key accomplishments during this Phase II SBIR program include the following:

- GC methods were developed to provide an effective means of characterizing reactivity toward CWA simulants with nanogram sensitivity.
- A permeation cell was constructed and performance tested to support in-house characterization of rTSP breakthrough time performance.
- During the course of the program efforts, METSS has gained a better understanding of the reaction mechanism governing CWA destruction and has used this knowledge to identify, design and prepare reactants with improved performance and capability for CWA destruction.
- Reactants based on the following classes of materials have demonstrated good reactivity toward CWA simulant with potential applicability in rTSP formulations:

- perfluorinated acids and metal complexes of a perfluorinated acids
- perfluorinated sulfonic acids
- functionalized styrene/divinylbenzene
- sulfonated polystyrene.

7.3 PROTOTYPE DELIVERY AND COMMERCIAL POTENTIAL

As required under the program, METSS submitted samples to USAMRICD for additional testing and evaluation, including TSP incorporation, live agent reactivity testing and permeation cell testing. Prototype samples provided to USAMRICD for evaluation included samples of METSS 2-8-14 and Cu(Krytox®)₂. The results of the testing and evaluation efforts performed by USAMRICD were not reported to METSS.

While the US Government will retain rights to utilize the technology developed under this program for internal purposes, commercialization of the technology developed under this program will be pursued through the private sector. The Army has recently licensed the SERPACWA patent (McCreery 5,607,979) to DFB Pharmaceuticals of Fort Worth, Texas. DFB is currently in the process of working toward FDA approval for the base cream. Initial conversations have been held between METSS and DFB Pharmaceuticals to discuss the commercial potential of the technology developed under this program for military and consumer applications. As commercialization of the products developed this program will also be subject to FDA approval, a considerable commercial investment (in time and money) will have to be made to support commercial introduction. However, as the toxicology of the materials used to support the rTSP development efforts pursued under this program is similar in nature to the base TSP cream, additional approvals should be readily forthcoming once the base TSP is approved. This is especially true of the metal-Krytox® systems, as these systems are identical in character to the base PFAE oil used in the existing TSP formulation, with the exception of the metal-coordinated reaction sites that have been incorporated into the basic structure of the PFAE backbone at a very low level of relative concentration.

Cost should not be an issue that hinders the commercialization of products developed under this program. The major cost associated with the production of the base TSP cream is the cost of the PFAE oil (at (\$110/lb for Krytox®1525) and the Teflon® powder (approximately \$30/lb). At \$230/lb, the cost of Krytox®157FS, the starting material for Cu(Krytox®)₂ and Fe(Krytox®)₃, is somewhat more expensive than the base Krytox®1525 PFAE oil. However, since the final

concentration of the metal complexes is expected to be less than 10% of the overall rTSP formulation, the relative increase in cost for the raw materials is only expected to increase between 10 and 20% over the cost of the base TSP cream. At approximately \$2200/lb, the perfluorinated sulfonate materials tested under the program, are currently too expensive for program consideration. However, the sulfonated styrene/divinylbenzene compounds, which demonstrated exceptional performance under the program, are very low cost (typically pricing out at less than \$1.00/lb), thereby providing an extremely cost effective means of the reactive materials into rTSPs and other CWA decontamination systems.

7.4 CONCLUSIONS

As a result of the research carried out under this program, a number of compounds have been identified or prepared which will degrade the CWA simulants DFP, CEES, Paraoxon and to a lesser degree Malathion. All compounds can be blended into the TSP creams currently in use by the military. Although results of live agent testing have not yet been reported, METSS has demonstrated the improved performance of actual rTSP cream formulations using in-house permeation cell studies with CWA simulants. Based on the data obtained during this program, the following compounds are recommended for rTSP preparation:

- Cu(Krytox®)₂, Fe(Krytox®)₃, Ni(Krytox®)₂
- Cu(Krytox®)₂ with the addition of small amounts of benzoyl peroxide
- METSS 2-8-14, functionalized styrene/divinylbenzene
- METSS 2-8-13, functionalized styrene/divinylbenzene.

8.0 APPENDICES

8.1 METSS SOP# 02.001.01

GAS CHROMATOGRAPHIC ANALYSIS OF THE SIMULANTS DIISOPROPYL FLUOROPHOSPHATE (DFP), 2-CHLOROETHYL ETHYL SULFIDE (CEES) AND MALATHION.

8.2 METSS SOP# 02.002.01

PERMEABILITY OF MATERIALS TO THE SIMULANTS DIISOPROPYL FLUOROPHOSPHATE (DFP) AND 2-CHLOROETHYL ETHYL SULFIDE (CEES) USING GAS CHROMATOGRAPHY

8.3 METSS SOP# 02.003.01

PREPARATION OF SULFONATED POLYSTYRENE; Provided By Dr. Robert Weiss, Professor of Chemical Engineering, University of Connecticut

**GAS CHROMATOGRAPHIC ANALYSIS OF THE SIMULANTS
DIISOPROPYL FLUOROPHOSPHATE (DFP),
2-CHLOROETHYL ETHYL SULFIDE (CEES) AND MALATHION**

Relevant Program(s): *rTSP*

SOP Written by: Janet Ricks

Date: January 10, 2002

1.0 Definition:

This method describes the extraction of the chemical warfare agent (CWA) simulants diisopropyl fluorophosphate (DFP), 2-chloroethyl ethylsulfide (CEES) and Malathion from various test compounds and their detection and quantitation using gas chromatography with flame ionization detection (FID). Known amounts of test compound are spiked with simulant and, at specified times, the simulant is extracted and analyzed. From the amount of simulant remaining, the reactivity of the simulant with the test compound is determined.

2.0 Scope:

This method may be used to quantitate simulants dissolved in or adhering to almost any solid material. Care must be taken to ensure that the solvent used to extract the simulant from the test article is one in which the simulant is soluble but that does not dissolve the test article. The method may also be used for the analysis of simulants dissolved in a liquid provided that the liquid is not miscible with the extraction solvent. The solvents of choice for dissolving the simulants, as well as, for acceptable chromatographic behavior, are hexane or methylene chloride. For this reason, these are the only two solvents covered by this method.

The approximate detection limit for all three simulants is 5 µg/mL. The linear ranges are approximately 5-100 µg/mL.

3.0 References: none

4.0 Materials:

1. n-Hexane, Pesticide residue grade or better, Burdick and Jackson Labs, VWR catalog number BJGC217-4, [CAS 110-54-3].
2. Methylene chloride, Pesticide residue grade or better, Burdick and Jackson Labs, VWR catalog number BJ300-4, [CAS 75-09-2].
3. Diisopropyl fluorophosphate (DFP), 99+%, Aldrich catalog number D12,600-4 [CAS 55-91-4].
4. 2-Chloroethyl ethyl sulfide (CEES), 98%, Aldrich catalog number 24,264-0 [CAS 693-07-2].
5. Malathion (Pestanal), Riedel-deHaen, 98.5%, Aldrich catalog number 4555 [CAS 1221-75-5].

6. Bleach, ordinary Clorox for household use is acceptable. It is not advisable to substitute discount brand bleach since many of these have been diluted with water.
7. Compressed nitrogen gas, 99.9+%, UHP, size T-304, DeLille number 0125-4000.
8. Compressed hydrogen gas, 99.9+%, UHP, size T-261, DeLille number 0125-3005.
9. Compressed air, Zero air, size T-308, DeLille number 0125-0550.

5.0 Apparatus:

1. Gas chromatograph, Hewlett Packard/Agilent, 5890 Series II equipped with flame ionization detector, 100 vial auto sampler and Chemstation software Rev. A.08.01
2. Chromatography vials, 2-mL, National Scientific number C4011-88 (VWR number Supleco) or Hewlett Packard (VWR catalog number HP-5181-3400) equipped with aluminum crimp cap vials and Teflon/red rubber septa.
3. Assorted GAS TIGHT, cemented needle syringes:
 25 μ L, Hamilton number 80200, VWR catalog number 60376-230
 50 μ L, Hamilton number 80900, VWR catalog number 60376-241
 100 μ L, Hamilton number 81000, VWR catalog number 60376-252 or Supelco catalog number 20688
 1-mL, Hamilton number 81317, Supelco catalog number 20740-U
 5.0-mL, Hamilton number 81517, Supelco catalog number 20692
 10 μ L auto sampler syringes, six pack, 701 ASN, 26s gauge, Supelco catalog number 21316
4. Vortex mixer, single tube sufficient.
5. General purpose, tabletop centrifuge with rotor capable of holding 4-mL vials.
6. Analytical balance, capable of weighing to 0.1mg, Mettler or equivalent.
7. Septa, LB-2, Supelco catalog number 20654.
8. Disposable pipets, 5- $\frac{3}{4}$ in., VWR catalog number 52283-910.
9. Pipet bulbs, VWR catalog number 56310-240, 56310-002, 56310-060 or 56310-062.
10. 25 mL glass volumetric flask, Class A, VWR catalog number 29623-424.
11. TimeMed tape, VWR catalog number 36432-164.
12. Kimwipes, VWR catalog number 21905-026.
13. Gloves (powder free), latex or, for additional, protection Nitrile. Assorted sizes.
14. Underpads, (absorbent, plastic backed paper) at least 2 ft. x 2 ft. in size.
15. Plastic bucket of approximately 2-3 gallon capacity with handle.
16. Inlet liners, 2mm, Supelco catalog number 2051305 or 2051301.
17. Gold seals, Supelco catalog number 23318-U.

NOTE: Substitution of equivalent materials may be made for some of those previously listed, after approval by the Principal Investigator. The initial selection of these materials was made to insure accurate results and minimize contamination from containers used to hold both samples and standards; therefore, any changes must be made judiciously.

6.0 Stock Standard Preparation

1. Remove neat simulant from the refrigerator and allow it to reach room temperature.
2. Into a clean, 25 mL volumetric flask add approximately 10 mL of hexane and cap.
3. Using a 50 μ L gas tight syringe and ensuring that there are no air bubbles visible in the glass barrel of the syringe, add exactly 25 μ L of simulant to the volumetric flask and recap. It may be necessary to pump the syringe several times to remove any bubbles present.

4. Fill the volumetric flask to the line with hexane and recap.
5. Vortex the volumetric flask for a minimum of one minute.
6. Transfer the solution in the volumetric flask into 5-6 four mL vials and cap each tightly.
7. Record all data in the laboratory notebook (LRB) and assign an identification number to the standard based on the page number and line number where the standard preparation has been recorded.
8. Using TimeMed tape, label the vial with sample identification number, description, date and initials of analyst.
9. Use TimeMed tape to wrap the cap of each vial. Place the vials in a secondary container and store in the refrigerator when not in use.
10. Thoroughly clean the 50 μ L syringe using a minimum of five volumes of solvent and wiping the barrel and needle with a Kimwipe.

Calculations

$$\text{DFP (mg/mL)} = \frac{(25 \mu\text{L})(1.055 \text{ mg}/\mu\text{L})}{25 \text{ mL}} = 1.055 \text{ mg/mL}$$

$$\text{CEES (mg/mL)} = \frac{(25 \mu\text{L})(1.070 \text{ mg}/\mu\text{L})}{25 \text{ mL}} = 1.070 \text{ mg/mL}$$

$$\text{Malathion (mg/mL)} = \frac{(25 \mu\text{L})(1.23 \text{ mg}/\mu\text{L})}{25 \text{ mL}} = 1.23 \text{ mg/mL}$$

7.0 Test Procedure

1. Label eighteen 4-mL vials with appropriate sample numbers i.e. LRB page number – line number (see Section 8.0).
2. Label eighteen chromatography vials with the same numbers in Step 1. Label an additional seven chromatography vials, as follows: hexane (or methylene chloride), 5, 10, 20, 40, 50 and 75. The last seven will be used to prepare working standards. The number represents the number of μ L of stock standard to be added to each vial.
3. Into each of the sixteen 4-mL vials (Step 1) labeled (LRB#) 5 through 20, weigh 50 ± 5 mg of the compound to be tested. Record all four decimal places in the appropriate place in the program notebook (see Section 8.0). (Note: the amount of test compound may change as dictated by program requirements per Principal Investigator). Keep vials tightly capped at all times except for the actual addition of test compound. Since the analysis of a single set requires a full eight hours, the test samples should be weighed out, as a minimum, the day before the analysis is to be done.
4. Using a clean 1-mL gas tight syringe, add 1-mL of solvent (hexane or methylene chloride) to each of the chromatography vials in step 2 with the exception of that labeled LRB#-5. Cap each vial immediately after the solvent is added to prevent evaporation
5. Remove the simulant from the refrigerator and allow it to come to room temperature before proceeding. Using a CLEAN, gas tight 10-mL syringe draw up the requisite

amount of simulant. In most cases, this amount will be 1 μ L but may change as necessary to meet

program goals. Ensure that there are no bubbles visible in the glass portion of the syringe. It may be necessary to pump the syringe several times to remove any bubbles present. In the case of Malathion, fill the syringe very slowly – do not pump the syringe. Due to the viscosity of the Malathion, it may take one to two minutes to fill the syringe without air bubbles.

6. Unscrew the cap of the appropriate 4-mL vial (start with 8-hour vial) and spike simulant onto the side of the vial just above the test compound. Quickly recap the vial. NOTE: TO AVOID CONTAMINATION OF THE SYRINGE DO NOT TOUCH THE TEST COMPOUND WITH TIP OF THE SYRINGE. CLEAN SYRINGE WITH SOLVENT IF THIS SHOULD OCCUR.
7. Vortex the vial for a minimum of one minute. Visually insure that all simulant has been uniformly distributed in the test compound. Using a laboratory marker, mark the top of the cap of the vial. Marking of the cap helps to prevent erroneously re-spiking of the same vial.
8. Record the spiking time (military time) in the appropriate place in the LRB (see Section 8.0).
9. Repeat steps 4 through 6 for all vials except that labeled (LRB#)-5. Continue spiking the vials with an 8-hour time period (Section 8.0) -(LRB#)-20 containing 50 mg test compound and (LRB#)-4A and 4B which contain no test compound - and proceed to the vial with the shortest sample time, 1 minute (LRB#)-6. THOROUGHLY CLEAN THE 10 μ L SYRINGE WITH SOLVENT AFTER SPIKING HAS BEEN COMPLETED. RINSE WITH A MINIMUM OF FIVE VOLUMES OF SOLVENT AND WIPE PLUNGER AND NEEDLE WITH A CLEAN KIMWIPE.
10. At the appropriate time for each vial, as listed in the LRB (see Section 8.0), uncap the vial and add 3-mL of solvent (hexane or methylene chloride) using a 3-mL gas tight syringe. Quickly recap vial.
11. Vortex the vial for 1 minute.
12. Centrifuge the vial for 5 minutes. (Insure that there is a balance vial in the position opposite that to be used for the sample.)
13. Using a 100 μ L syringe, remove 100 μ L of extract from the 4 mL vial and add immediately to the appropriately labeled 1mL chromatography vial containing solvent as prepared in step 4.
14. Vortex the vial and thoroughly clean the 100 μ L syringe with solvent. RINSE WITH A MINIMUM OF FIVE VOLUMES OF SOLVENT AND WIPE PLUNGER AND NEEDLE WITH A CLEAN KIMWIPE.
15. Repeat steps 10-14 for all vials at the appropriate time.

Interference check. (LRB#)-5 contains test compound only and is used to verify that the test compound contains no extractable components, which will interfere with the analysis of the simulant. This sample is referred to as METHOD BLANK.

16. For the vial labeled (LRB#)-5, add 1 mL of solvent (hexane or methylene chloride) using a gas tight syringe. Cap tightly.
17. Vortex vial (LRB#)-5 for 1 minute.
18. Centrifuge vial (LRB#)-5 for 5 minutes.
19. Using a disposable glass pipet and bulb, transfer as much of the solvent from the vial as possible (without removing test material) into the chromatography vial labeled LRB-5 (see step 1). Cap immediately.

Standards Preparation:

20. Remove the standard stock solution (approximately 1 mg/mL) from the refrigerator and allow it to come to room temperature before proceeding. To each of the standards vials containing 1 mL of solvent (prepared in step 4) add the appropriate amount of stock standard (5, 10, 20, 40, 50, 75 μ L), using CLEAN, gas tight syringe. Use a 10 μ L syringe for the two lower concentration standards and a 100 μ L syringe for the four higher concentration standards.
21. Vortex each standard after the addition of stock solution.
22. Place all vials (samples and standards) upright into a capped, secondary container. Store in the laboratory freezer until they can be analyzed.
23. Set up the gas chromatograph to run samples and standards prepared in steps 1-20. The method to do this is based on manufacturer's instructions and accepted analytical practices. Refer to SOP 2.004.01 for details.

8.0 Data Recording

Table 1 provides a template to be used for the recording of data in the laboratory notebook for every analytical run. Replace LRB with the number of the page in the LRB where the actual data is recorded. In addition to adding the name of the test compound, simulant and solvent used, the inventory identification number for each must be recorded.

Also, include on this page:

- The date the test samples were weighed out.
- The extraction date.
- Appropriate dilution information.
- Lot number of stock solution used to make the working standards.
- Initial and date of all analysts involved in the procedure.

When the chromatographic analysis is complete, enter all data into an Excel spreadsheet (see SOP 02.004.001 for further information). After the data is reviewed by the Principal Investigator, print the spreadsheet, the calibration curve and summary chart. Tape the copies

of the spreadsheet and charts to the two pages of the laboratory notebook immediately following the page containing Table 1. Transfer an electronic version of the Excel spreadsheet to the company server in the data file folder for the appropriate program.

Table 1. Data Template

ID #	Amount of Test Compound (ID#)(g)	Amount of Simulant (ID#) (μL)	Start Time (military)	Stop Time (military)	Reaction time (minutes)	Amount solvent added (ID#) (mL)
LRB-4A	-	1			480	3
LRB-4B	-	1			480	3
LRB-5		-			-	1
LRB-6		1			1	3
LRB-7		1			10	3
LRB-8		1			20	3
LRB-9		1			30	3
LRB-10		1			40	3
LRB-11		1			50	3
LRB-12		1			60	3
LRB-13		1			90	3
LRB-14		1			120	3
LRB-15		1			180	3
LRB-16		1			240	3
LRB-17		1			300	3
LRB-18		1			360	3
LRB-19		1			420	3
LRB-20		1			480	3

9.0 Quality Control

To ensure the quality of data and data reporting, the following must be followed:

- All reagents used must be analytical reagent grade or better. Solvents must be MS/pesticide grade or better.
- All volumetric glassware used must be Grade A and be washed with deionized water and appropriate solvents before being used.
- Analytical balances must be checked on an annual basis by the manufacturer (calibration will be checked weekly by METSS personnel)
- A minimum of three concentration levels (preferably five) must be used to generate calibration curves. All regression lines must have an R^2 value of at least 0.995. Either a linear or a quadratic fit to the data is acceptable. All standards analyzed during a particular sequence are to be used to generate one line or curve that is used to back calculate all unknown concentrations within that analytical run.
- For a given chromatographic sequence, all standards must be analyzed at the beginning and again at the end of the sequence with additional injections of standards for every fifth unknown sample.

- The difference between known standard concentrations and that calculated using the regression line must be less than 15% for the lowest concentration standard. For all others this value must be less than or equal to 10%.
- All unknown extracts must be within the range of the standards. For those with concentration greater than the highest standard, a dilution must be made and the sample reanalyzed. Those below the lowest standard must be listed as “none detected” with the appropriate detection limit, stated.
- All data must be verified for accuracy by a second person other than the original analyst and the Principal Investigator.
- All data will be recorded in a bound notebook with numbered pages, preferably with a black pen. Under no circumstances is pencil acceptable. Errors will be crossed out, the correct value added next to the incorrect one along with the reason for changing the value and the initial and date of the person making the change.
- A laboratory notebook must be maintained for each program. This notebook must have a table of contents and a listing of all reagents and apparatus used at the beginning of the book. Any information added to the book at any time, no matter how minute, must be initialed and dated by the analyst making the notation.
- The chromatogram of the Method Blank must not contain peaks with an area count of greater than 10% of the lowest standard at a retention time of ± 0.05 minutes of the simulant being analyzed.
- The average concentration of simulant in the recovery samples must be $\pm 20\%$ of the challenge concentration.

10.0 Safety

While the materials used in this method are simulants to nerve agents and sulfur mustard, not the original compounds, they are still extremely hazardous.

PRIOR TO INITIATING ANY TESTING, ALL ANALYSTS MUST READ AND UNDERSTAND THE INFORMATION PRESENTED IN THE MATERIAL SAFETY DATA SHEETS FOR THESE COMPOUNDS.

Additionally, the following procedures must be followed when working with simulants:

- Neat simulant or dilutions must be kept tightly closed and refrigerated in secondary containers when not in use.
- All work with the simulants must take place in a fume hood operating at 100 ± 20 fpm. Specific METSS personnel have been assigned to test the functioning of laboratory hoods. It is the responsibility of the analyst working with simulant to periodically ensure that this has been done.
- A lab coat, gloves and safety glasses must be worn when working with simulants.
- The counter inside the lab hood must be covered with absorbent Underpads to absorb spills.
- A bucket and wash bottle containing bleach must be kept in the hood at all times to decontaminate extracts and vials. Any materials being decontaminated must remain immersed in the bleach for a minimum of 24 hours. A steel rod has been placed inside the bucket to aid in the immersion of materials that would normally float on the surface of the bleach. The bleach should be changed weekly, preferably on Monday mornings, to maintain the 24 hours minimum decontamination time. At the end of this time, the

bleach may be flushed down the drain with large amounts of water. The remaining vials etc. are to be double bagged in plastic and placed immediately in the outside dumpster.

- Any equipment being removed from the hood must be washed with soap and water prior to being used outside the hood.
- Work must be conducted at least 6 inches inside the hood sash. At no time should the analyst put his or her head inside the hood.
- The Safety Officer must be notified of any spills or other accidents.

Approved: _____

Date: _____

PERMEABILITY OF MATERIALS TO THE SIMULANTS DIISOPROPYL FLUOROPHOSPHATE (DFP) AND 2-CHLOROETHYL ETHYL SULFIDE (CEES) USING GAS CHROMATOGRAPHY

Relevant Program(s): rTSP, Facemasks

SOP Written by: Janet Ricks

Date: January 14, 2002

1.0 Definition:

This method describes the measurement of the permeability of various test materials to the chemical warfare agent (CWA) simulants diisopropyl fluorophosphate (DFP) and 2-chloroethyl ethylsulfide (CEES). The article to be tested is placed into a permeation cell and spiked with a known amount of simulant. Airflow of a known rate is maintained on the opposite side of the test article. The air passes through absorbent tubes and, at specified times, the tubes are removed, the absorbent material is extracted with solvent and the extracts analyzed by gas chromatography (FID). Based on the amount of simulant detected in each tube, the permeability of the test article as a function of time is determined.

2.0 Scope:

This method may be used to measure the permeation of simulants or other volatile organic compounds through almost any solid material. Compounds of limited volatility may be used if the bottom portion of the cell is heated to prevent their condensation. This is not covered by this SOP. The test material must be capable of being cut into a circle of approximately 2 inches in diameter and must not compromise the seal between the top and bottom pieces of the cell. Very high viscosity liquids or greases may also be tested for permeability if they can be applied in a uniform film onto a solid of known high permeability.

The approximate detection limits for both simulants is 5 µg/tube. Linear ranges are approximately 5-100 µg/mL of sample extract.

3.0 References: none

4.0 Materials:

1. Methylene chloride, Pesticide residue grade or better, Burdick and Jackson Labs, VWR catalog number BJ300-4, [CAS 75-09-2].
2. Diisopropyl fluorophosphate (DFP), 99+%, Aldrich catalog number D12,600-4 [CAS 55-91-4].
3. 2-Chloroethyl ethyl sulfide (CEES), 98%, Aldrich catalog number 24,264-0 [CAS 693-07-2].

4. Bleach, ordinary Clorox for household use is acceptable. It is not advisable to substitute discount brand bleach since many of these have been diluted with water.
5. Compressed nitrogen gas, 99.9+%, UHP, size T-304, DeLille number 0125-4000.
6. Compressed hydrogen gas, 99.9+%, UHP, size T-261, DeLille number 0125-3005.
7. Compressed air, Zero air, size T-308, DeLille number 0125-0550.
8. XAD-2 resin, a polystyrene/divinyl benzene based polymer, SKC, Inc. catalog number P22601
9. Silanized glass wool, Supelco part number 20411 or 20410.

5.0 Apparatus:

1. Gas chromatograph, Hewlett Packard/Agilent, 5890 Series II equipped with flame ionization detector, 100 vial auto sampler and Chemstation software Rev. A.08.01
2. Chromatography vials, 2-mL, National Scientific number C4011-88 (VWR number Supleco) or Hewlett Packard (VWR catalog number HP-5181-3400) equipped with aluminum crimp cap vials and Teflon/red rubber septa.
3. Assorted GAS TIGHT, cemented needle syringes:
4. 25 μ L, Hamilton number 80200, VWR catalog number 60376-230
5. 50 μ L, Hamilton number 80900, VWR catalog number 60376-241
6. 100 μ L, Hamilton number 81000, VWR catalog number 60376-252 or Supelco catalog number 20688
7. 1-mL, Hamilton number 81317, Supelco catalog number 20740-U
8. 5.0-mL, Hamilton number 81517, Supelco catalog number 20692
9. 10 μ L autosampler syringes, six pack, 701 ASN, 26s gauge, Supelco catalog number 21316
- 10.
11. Vortex mixer, single tube sufficient.
12. Analytical balance, capable of weighing to 0.1mg, Mettler or equivalent.
13. Septa (for gas chromatograph), LB-2, Supelco catalog number 20654.
14. Disposable pipets, 5- $\frac{3}{4}$ in., VWR catalog number 52283-910.
15. Pipet bulbs, VWR catalog number 56310-240, 56310-002, 56310-060 or 56310-062.
16. 25 mL glass volumetric flask, Class A, VWR catalog number 29623-424.
17. 10.TimeMed tape, VWR catalog number 36432-164.
18. Kimwipes, VWR catalog number 21905-026.
19. Gloves (powder free), latex or, for additional, protection Nitrile. Assorted sizes.
20. Underpads, (absorbent, plastic backed paper) at least 2 ft. x 2 ft. in size.
21. Plastic bucket of approximately 2-3 gallon capacity with handle.
22. Pump, Airchek 52, SKC catalog number 224-52.
23. Airchek 52 Battery Eliminator, SKC catalog number 223-300.
24. Triangular metal file, VWR catalog number 28130-047.
25. Permeation cell, as shown in Figure 1.
26. Aluminum template, as shown in Figure 2.
27. Tygon tubing, 8 mm I.D.
28. Viton o-rings, 36 mm O.D., ChemGlass, CG-305-29.
29. Septa (for permeation cell), Hamilton 65006, Supelco catalog number 20418.
30. Glass wool puller/insertor tool, Supelco catalog number 22406.

NOTE: Substitution of equivalent materials may be made for some of those previously listed, after approval by the Principal Investigator. The initial selection of these materials was made to insure accurate results and minimize contamination from

containers used to hold both samples and standards; therefore, any changes must be made judiciously.

6.0 Stock Standard Preparation:

1. Remove neat simulant from the refrigerator and allow it to reach room temperature.
2. Into a **clean**, 25 mL volumetric flask add approximately 10 mL of hexane and cap.
3. Using a 50 μ L gas tight syringe and ensuring that there are no air bubbles visible in the glass barrel of the syringe, add **exactly** 25 μ L of simulant to the volumetric flask and recap. It may be necessary to pump the syringe several times to remove any bubbles present.
4. Fill the volumetric flask to the line with hexane and recap.
5. Vortex the volumetric flask for a minimum of one minute.
6. Transfer the solution in the volumetric flask into 5-6 four mL vials and cap each tightly.
7. Record all data in the laboratory notebook (LRB) and assign an identification number to the standard based on the page number and line number where the standard preparation has been recorded.
8. Using TimeMed tape, label the vial with sample identification number, description, date and initials of analyst.
9. Use TimeMed tape to wrap the cap of each vial. Place the vials in a secondary container and store in the refrigerator when not in use.
10. Thoroughly clean the 50 μ L syringe using a minimum of five volumes of solvent and wiping the barrel and needle with a Kimwipe.

Calculations

$$\text{DFP (mg/mL)} = \frac{(25 \mu\text{L})(1.055 \text{ mg}/\mu\text{L})}{25 \text{ mL}} = 1.055 \text{ mg/mL}$$

$$\text{CEES (mg/mL)} = \frac{(25 \mu\text{L})(1.070 \text{ mg}/\mu\text{L})}{25 \text{ mL}} = 1.070 \text{ mg/mL}$$

7.0 Absorption Tube Preparation

As mentioned previously, the simulant permeating through a given test article is collected on tubes containing XAD-2 resin absorbent. These tubes may be purchased commercially, however, the cost involved is prohibitive. The procedure for in-house preparation is as follows:

1. Using a triangular file, cut the thin glass tips off approximately 25 glass disposable pipets. This should be done just below the point that the glass begins to flare out to form the body of the pipet.
2. Cut off the opposite ends of these pipets such that the overall length of the remaining tube is approximately 1.5 – 2 inches in length.
3. Using silanized glass wool, form a plug approximately 0.25-0.5 inch in length. Fold the glass wool so that one end is smooth. Avoid fracturing the glass wool. Having a smooth plug will prevent the XAD-2 resin from mixing into the glass wool.

4. Insert the glass wool, smooth side up, into the glass tube using the glass wool puller. Repeat this for all tubes.
5. Using an analytical balance, weigh 100 ± 5 mg of XAD into each tube.
6. Add an additional plug of glass wool on top of the resin, this time smooth side down, facing the resin.
7. Repeat steps 5 and 6 for all tubes.

XAD-2 RESIN WILL ABSORB ORGANIC MATERIAL FROM THE AIR. STORE TUBES IN AN AIRTIGHT CONTAINER UNTIL THEY ARE READY TO BE USED FOR AN ANALYSIS.

8.0 Permeation Cell Set-up

Figures 1 and 2 show the basic features of the permeation cell and aluminum template used in this method.

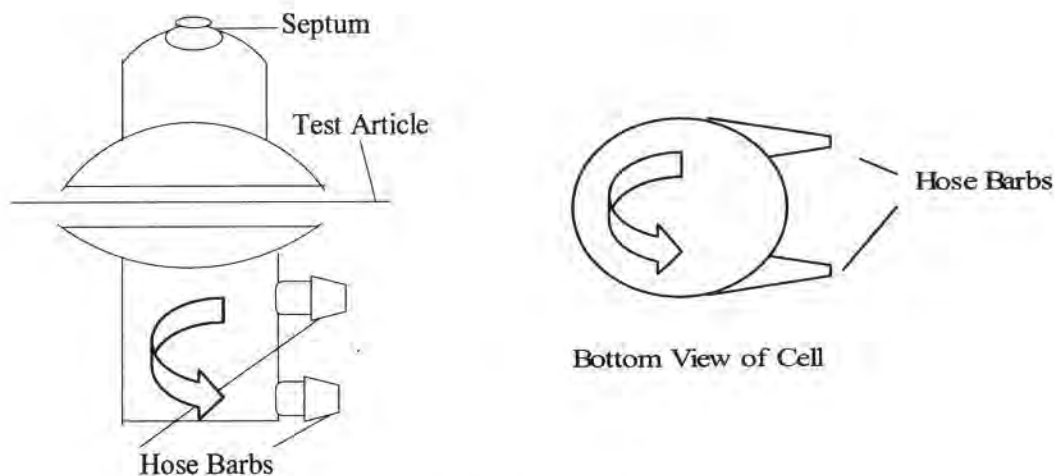


Figure 1. Permeation Cell

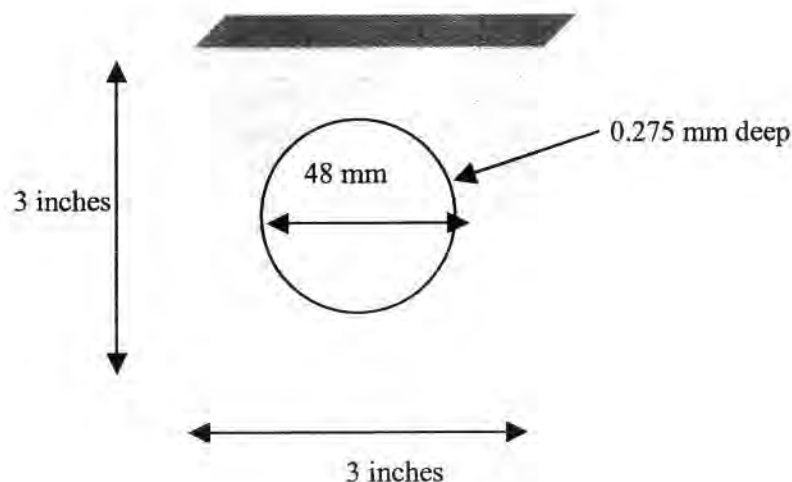


Figure 2. Aluminum Form

To set the cell up for testing follow the procedure summarized below:

1. Cut a circular piece (at least 2 inches in diameter) of the material to be tested.
2. Place an o-ring into the groove on the bottom glass piece of the permeation cell.
3. Center the test article on top of this o-ring.
4. Add a second o-ring on top of the test article, followed by the top piece of the permeation cell.
5. Clamp the cell pieces, o-rings and test article in place. Ensure that the o-rings are directly above one another and that they are both in the grooves of the permeation cell. Lock clamp in place.
6. Screw a septum and nut onto the top piece of the cell. Clamp the cell to a ring stand in the hood.
7. Using a bubble flow meter, ensure that the airflow into the cell is approximately 1L/min.
8. Cut approximately 10 pieces of Tygon tubing with length 0.5-0.75 inches.
9. Attach one piece to each of the ports on the cell.
10. Use another to connect the wide end of one tube to the narrow end of another as shown in Figure 3.

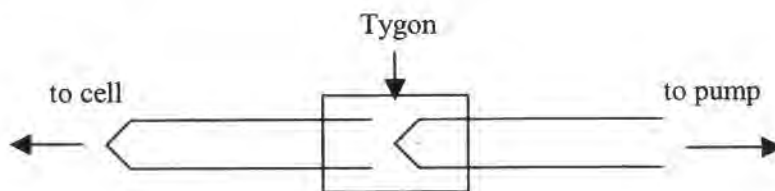


Figure 3. XAD-2 tubes connected in series

11. Insert the cell end of the tube in Figure 3 into the Tygon tubing on the BOTTOM port of the permeation cell.
12. Attach a longer piece of Tygon tubing (6-10 inch) to the pump end of the tubes shown in Figure 3.
13. Insert a third XAD-2 tube into the Tygon piece on the TOP port of the permeation cell. This tube serves to remove contaminants from the air before they enter the permeation cell.
14. Attach a 3-4 foot section of tygon tubing to the opposite end of the tube in step 8.
15. Run the tubing (in step 9) outside of the hood and fasten to the hood structure as close to the ceiling as possible. Since most organic vapors are heavier than air, placing the tubing as close to the ceiling as possible helps minimize solvent contamination from the lab. Placing the tubing outside of the hood ensures that other work can continue in the hood without affecting the permeation study.
16. Ensure that all connections are tight. TimeMed tape may be used, especially at the inlet airline, to ensure that none of the connections come loose.
17. If a cream or viscous liquid is to be tested, cut out a circle of appropriate support material (filter paper, copier paper) 48 mm in diameter and place into the template (Figure 2). Using the back of a metal scupula, coat the support uniformly with the test cream. Using this particular template, the thickness of the support material plus cream will be 0.275 mm.

9.0

Test Procedure

1. Label eighteen 4-mL vials and eighteen chromatography vials with appropriate sample numbers i.e. LRB page number – line number (see Section 10.0, Table 1).
2. Label an additional three 4-mL vials and three chromatography vials for recovery samples (see Section 10.0, Table 2).
3. Label six chromatography vials for working standards preparation (see Section 10.0, Table 2.)

Standards Preparation

4. Using a 1-mL gas tight syringe, add 1-mL of methylene chloride to each of the six standard chromatography vials. Cap each vial immediately after the solvent has been added to prevent evaporation.
5. Remove the standard stock solution (approximately 1 mg/mL) from the refrigerator and allow it to come to room temperature before proceeding. To each of the standards vials containing 1 mL of solvent (prepared in step 4) add the appropriate amount of stock standard (5, 10, 20, 40, 50, 75 μ L), using CLEAN, gas tight syringe. Use a 10 μ L syringe for the two lower concentration standards and a 100 μ L syringe for the four higher concentration standards.
6. Vortex each standard after the addition of stock solution.

Spike Recovery Sample Preparation

7. Into each of the three 4-mL vials (Step 2), weigh 100 ± 5 mg of the XAD-2 resin. Tightly cap the vials after the addition of resin.
8. Using CLEAN, gas tight 10 and 100 μ L syringes draw up the requisite amount of stock standard (5, 10, and 40 μ L) and spike into the appropriate 4 ml vial (see Section 10.0). Ensure that there are no bubbles visible in the glass portion of the syringe. It may be

necessary to pump the syringe several times to remove any bubbles present. Use a 10 μ L syringe for the two lower concentration standards and a 100 μ L syringe for the higher concentration standard.

9. Vortex each vial for a minimum of one minute. Visually insure that all stock solution has been uniformly distributed in the resin. Using a laboratory marker, mark the top of the cap of the vial. Marking of the cap helps to prevent erroneously re-spiking of the same vial. THOROUGHLY CLEAN THE SYRINGES WITH SOLVENT AFTER SPIKING HAS BEEN COMPLETED. RINSE WITH A MINIMUM OF FIVE VOLUMES OF SOLVENT AND WIPE PLUNGER AND NEEDLE WITH A CLEAN KIMWIPE.
10. Ensure the permeation has been sent up as in Section 9 and that the pump is plugged in and operational.
11. Fill a gas tight syringe with the appropriate amount and type of simulant. Insert the needle of the syringe through the septum at the top of the permeation cell and dispense the simulant onto the surface of the test material. DO NOT TOUCH OR PUNCTURE THE TEST MATERIAL WITH THE POINT OF THE SYRINGE.
12. Immediately turn on the pump and record the start time in the notebook (see Section 10).
13. Several minutes before the end of the testing period, remove two absorption tubes from their container and connect them together as in Figure 3.
14. At the end of the testing time, turn the pump off and quickly replace the initial XAD-2 tubes with fresh ones from step 13.
15. Quickly turn the pump back on and record the counter number and sampling times in the LRB.
16. Using the glass wool inserter/puller, immediately remove the glass wool from the top of an absorption tube and pour all of the resin into a 4 mL vial.
17. Add 3 mL of methylene chloride to the vial, cap tightly and vortex. Repeat with the second adsorption tube.
18. Place used glass tubing and glass wool directly into the decon bucket.
19. After a minimum of 30 minutes, vortex the vials and allow the resin to separate (1-2 minutes).
20. With a disposable glass pipet and bulb, transfer approximately 1 mL of extract to the appropriately labeled chromatography vial.
21. After at least 30 minutes, extract the recovery samples (step 9) and the XAD-2 tube on inlet of cell following the same procedures as in step 17-19.
22. Place all vials (samples, standards and recoveries) upright into a capped, secondary container. Store in the laboratory freezer until they can be analyzed.
23. Set up the gas chromatograph to run samples and standards prepared in steps 1-22. The method to do this is based on manufacturer's instructions and accepted analytical practices. Refer to SOP 2.004.01 for details.

10. Data Recording

Tables 1 and 2 provide templates to be used for the recording of data in the laboratory notebook for every analytical run. Replace LRB with the number of the page in the LRB where the actual data is recorded.

Also, include on the data page:

- The date the testing was performed.
- Appropriate dilution information.

- Lot number of stock solution used to make the working standards.
- Initial and date of all analysts involved in the procedure.
- Spike recovery amounts

Table 1. Data Template

ID #	Start Time (military)	Stop Time (military)	Counter	Tube Position
LRB-8				Front
LRB-9				Back
LRB-10				Front
LRB-11				Back
LRB-12				Front
LRB-13				Back
LRB-14				Front
LRB-15				Back
LRB-16				Front
LRB-17				Back
LRB-18				Front
LRB-19				Back
LRB-20				Front
LRB-21				Back
LRB-22				Front
LRB-23				Back
LRB-24				Front
LRB-25				Back
LRB-26	AIR	PURIFYING	TUBE	-

Table 2. Standards and Spike Recovery Template

	Amount of Stock Standard (μ L)	Final Concentration (μ g/mL)
Spike Recoveries		
LRB-8	5	
LRB-9	10	
LRB-10	40	
Standards		
LRB-12	5	
LRB-13	10	
LRB-14	20	
LRB-15	40	
LRB-16	50	
LRB-17	75	

When the chromatographic analysis is complete, enter all data into an Excel spreadsheet (see SOP 02.004.001 for further information). After the data is reviewed by the Principal

Investigator, print the spreadsheet, the calibration curve and summary chart. Tape the copies of the spreadsheet and charts to the two pages of the laboratory notebook immediately following the page containing Table 1. Transfer an electronic version of the Excel spreadsheet to the company server in the data file folder for the appropriate program.

11.0 Quality Control

To ensure the quality of data and data reporting, the following must be followed:

- All reagents used must be analytical reagent grade or better. Solvents must be MS/pesticide grade or better.
- All volumetric glassware used must be Grade A and be washed with deionized water and appropriate solvents before being used.
- Analytical balances must be checked on an annual basis by the manufacturer (calibration will be checked weekly by METSS personnel)
- A minimum of three concentration levels (preferably five) must be used to generate calibration curves. All regression lines must have an R^2 value of at least 0.995. Either a linear or a quadratic fit to the data is acceptable. All standards analyzed during a particular sequence are to be used to generate one line or curve that is used to back calculate all unknown concentrations within that analytical run.
- For a given chromatographic sequence, all standards must be analyzed at the beginning and again at the end of the sequence with additional injections of standards for every fifth unknown sample.
- The difference between known standard concentrations and that calculated using the regression line must be less than 15% for the lowest concentration standard. For all others this value must be less than or equal to 10%.
- All unknown extracts must be within the range of the standards. For those with concentration greater than the highest standard, a dilution must be made and the sample reanalyzed. Those below the lowest standard must be listed as "none detected" with the appropriate detection limit stated.
- All data must be verified for accuracy by a second person other than the original analyst and the Principal Investigator.
- All data will be recorded in a bound notebook with numbered pages, using a black pen. Under no circumstances is pencil acceptable. Errors will be crossed out, the correct value added next to the incorrect one along with the reason for changing the value and the initial and date of the person making the change.
- A laboratory notebook must be maintained for each program. This notebook must have a table of contents and a listing of all reagents and apparatus used at the beginning of the book. Any information added to the book at any time, no matter how minute, must be initialed and dated by the analyst making the notation.
- The average concentration of simulant in the recovery samples must be $100 \pm 20\%$ of the challenge concentration.

12.0 Safety

While the materials used in this method are simulants to nerve agents and sulfur mustard, not the original compounds, they are still extremely hazardous.

PRIOR TO INITIATING ANY TESTING, ALL ANALYSTS MUST READ AND UNDERSTAND THE INFORMATION PRESENTED IN THE MATERIAL SAFETY DATA SHEETS FOR THESE COMPOUNDS.

Additionally, the following procedures must be followed when working with simulants:

- Neat simulant or dilutions must be kept tightly closed and refrigerated in secondary containers when not in use.
- All work with the simulants must take place in a fume hood operating at 100 ± 20 fpm. Specific METSS personnel have been assigned to test the functioning of laboratory hoods. It is the responsibility of the analyst working with simulant to periodically ensure that this has been done.
- A lab coat, gloves and safety glasses must be worn when working with simulants.
- The counter inside the lab hood must be covered with absorbent Underpads to absorb spills.
- A bucket and wash bottle containing bleach must be kept in the hood at all times to decontaminate extracts and vials. Any materials being decontaminated must remain immersed in the bleach for a minimum of 24 hours. A steel rod has been placed inside the bucket to aid in the immersion of materials that would normally float on the surface of the bleach. The bleach should be changed weekly, preferably on Monday mornings, to maintain the 24 hours minimum decontamination time. At the end of this time, the bleach may be flushed down the drain with large amounts of water. The remaining vials etc. are to be double bagged in plastic and placed immediately in the outside dumpster.
- Any equipment being removed from the hood must be washed with soap and water prior to being used outside the hood.
- Work must be conducted at least 6 inches inside the hood sash. At no time should the analyst put his or her head inside the hood.
- The Safety Officer must be notified of any spills or other accidents.

Approved: _____

Date: _____

PROCEDURE FOR PREPARING SULFONATED POLYSTYRENE

Provided By Dr. Robert Weiss, Professor of Chemical Engineering, University of Connecticut

Preparation of 0.996 M acetyl sulfate

Basis: preparation of 500 ml of 0.996 M acetyl sulfate

To 395.7 ml of 1,2-dichloroethane, add 76.3 ml (82.4 g, 0.808 mole) of acetic anhydride. Cool solution to below 10°C and add 28.0 ml of 95% sulfuric acid (48.9 g sulfuric acid, 0.498 mole). A clear solution should result. The acetyl sulfate concentration of the resulting solution should be 0.498 moles acetyl sulfate/500 ml = 0.996M.

Sulfonation of polystyrene (Target sulfonation = 1 mol%)

Use freshly prepared acetyl sulfate. Dissolve 100 g polystyrene in 500 ml of dry dichloroethane. Heat solution to 50°C and add 9.7 ml of 0.996 molar acetyl sulfate (9.66 meq). Stir solution for 60 minutes at 50°C. Terminate the reaction by adding 25 ml 2-propanol and precipitate the polymer in a highly agitated bath of 2-propanol or methanol**. If needed, pulverize polymer in water with a Waring blender. Wash with ethanol and water, filter, air dry and finally vacuum dry at 50°C for 5 days. For a 100% yield, this reaction should result in a sulfonated polystyrene with 1.0 sulfonic acid groups per 100 styrene repeat units (i.e., 1 mol% sulfonation). In practice, we generally achieve ca. 80-90% yield. The dried polymer should be soluble in a 90/10 mixture of toluene/methanol and may be neutralized by the addition of an appropriate metal hydroxide or acetate (e.g., NaOH or Zn-acetate).

** An alternative isolation procedure is to steam-strip the reaction solution instead of precipitating the polymer in alcohol. This usually works well; except in several isolated instances, we have experienced that the isolated polymer will not re-dissolve in solvent.

Sulfonation of polystyrene (Target sulfonation = x mol%)

Use the procedure above for a target sulfonation of 1 mol%, but multiply the amount of acetyl sulfate used by x . For example, for a target sulfonation of 6 mol%, use 58.2 ml of 0.996 M acetyl sulfate.

Determination of sulfonation

Two methods may be used to determine the amount of sulfonation: (1) elemental analysis of sulfur or (2) titration of the sulfonic acid derivative.

1. Elemental sulfur analysis. The mol% sulfonation may be calculated from the wt% S in the sulfonic acid derivative by the following equation:

$$x = (10400S)/(3200 - 80S)$$

where S = sulfur content in wt. percent and x = the mol% sulfonation (number of sulfonate groups per 100 styrene repeat units).

2. Titration of sulfonic acid. Prepare a standard sodium hydroxide solution in methanol, nominally 0.1 N (1 g NaOH in 250 ml absolute methanol). A minimal amount of distilled water may be necessary to facilitate dissolution of the NaOH. The normality of the standard solution is determined by titrating with a 0.1 N solution of p-toluene sulfonic acid in methanol using phenolphthalein as an indicator. Prepare a 0.2% solution of the sulfonated polystyrene in a 90/10 mixture of toluene/methanol (v/v). Bubble nitrogen through the solution for 30 min. in order to remove any dissolved CO_2 . Dilute the standardized NaOH solution five times with absolute methanol and titrate the polymer solution to a phenolphthalein endpoint.

SBIR final report from Cape Cod Research, Inc. Phase I

Award Number: W81XWH-05-C-0123

AD _____

Award Number: W81XWH-05-C-0123

TITLE: TOXIN-NEUTRALIZING BARRIER SKIN CREAM FOR CWA PROTECTION

PRINCIPAL INVESTIGATOR: FRANCIS L. KEOHAN AND JOHN E. DARGA

CONTRACTING ORGANIZATION:

Cape Cod Research, Inc.
19 Research Road
East Falmouth, MA 02536

REPORT DATE: December, 2005

TYPE OF REPORT: Final Report

PREPARED FOR: U.S. Army Medical Research and Materiel Command
Fort Detrick, Maryland 21702-5012

DISTRIBUTION STATEMENT: (Check one)

- ☐ Approved for public release; distribution unlimited
- ☒ Distribution limited to U.S. Government agencies only;
report contains proprietary information

The views, opinions and/or findings contained in this report are those of the author(s) and should not be construed as an official Department of the Army position, policy or decision unless so designated by other documentation.

REPORT DOCUMENTATION PAGE				Form Approved OMB No. 0704-0188	
Public reporting burden for this collection of information is estimated to average 1 hour per response, including the time for reviewing instructions, searching existing data sources, gathering and maintaining the data needed, and completing and reviewing this collection of information. Send comments regarding this burden estimate or any other aspect of this collection of information, including suggestions for reducing this burden to Department of Defense, Washington Headquarters Services, Directorate for Information Operations and Reports (0704-0188), 1215 Jefferson Davis Highway, Suite 1204, Arlington, VA 22202-4302. Respondents should be aware that notwithstanding any other provision of law, no person shall be subject to any penalty for failing to comply with a collection of information if it does not display a currently valid OMB control number. PLEASE DO NOT RETURN YOUR FORM TO THE ABOVE ADDRESS.					
1. REPORT DATE (DD-MM-YYYY) 12-12-2005		2. REPORT TYPE Final Report		3. DATES COVERED (From - To) 5/13/2005 - 11/12/2005	
4. TITLE AND SUBTITLE Toxin-Neutralizing Barrier Skin Cream For CWA Protection				5a. CONTRACT NUMBER Contract No. W81XWH-05-C-0123	
				5b. GRANT NUMBER	
				5c. PROGRAM ELEMENT NUMBER	
6. AUTHOR(S) Francis L. Keohan and John Darga				5d. PROJECT NUMBER	
				5e. TASK NUMBER	
				5f. WORK UNIT NUMBER	
7. PERFORMING ORGANIZATION NAME(S) AND ADDRESS(ES) Cape Cod Research 19 Research Road East Falmouth, MA 02536				8. PERFORMING ORGANIZATION REPORT NUMBER	
9. SPONSORING / MONITORING AGENCY NAME(S) AND ADDRESS(ES) US Army Medical Research and Materiel Command 820 Chandler Street Fort Detrick, MD 21702-5014				10. SPONSOR/MONITOR'S ACRONYM(S)	
				11. SPONSOR/MONITOR'S REPORT NUMBER(S)	
12. DISTRIBUTION / AVAILABILITY STATEMENT Distribution authorized to US Government Agencies only; contains proprietary information.					
13. SUPPLEMENTARY NOTES					
14. ABSTRACT Report developed under SBIR contract for Topic number CBD05-118. The threat of chemical warfare agent (CWA) exposure requires a variety of measures to protect military personnel. CWA agent entry through the skin can potentially be reduced through the application of chemical barrier creams. A new protective skin cream was developed that utilizes a self-stratifying matrix and known CWA neutralizing chemicals to defend against multiple threats. The Phase I objective was to identify reactive topical skin protectant (rTSP) systems that meet the goals of low toxicity, simple application, self-stratification for combined CWA barrier and active CWA detoxification. A combination of surfactants, hydrophilic polymers, micronized supported catalysts, mild oxidants, and fluoropolymer additives were used to formulate new aqueous-based rTSP systems. The ability of selected formulations to form self-stratified films and efficiently promote the degradation of several CWA simulants was demonstrated. Hydrolytic degradation of the VX simulant Malathion was observed for some formulations. Certain CWA detoxification agents used in the products may also show activity against biological threats. The new rTSP formulations were found to be more easily removed than purely fluoropolymer-based controls. Formulation and processing variables were identified for optimizing the rTSP products for ultimate integration with warfighter protection systems.					
15. SUBJECT TERMS SBIR Report, Skin cream, barrier, self-assemble, fluorocarbon, CWA, neutralize					
16. SECURITY CLASSIFICATION OF:			17. LIMITATION OF ABSTRACT SAR	18. NUMBER OF PAGES 52	19a. NAME OF RESPONSIBLE PERSON Frank Keohan
a. REPORT Unclassified	b. ABSTRACT Unclassified	c. THIS PAGE Unclassified			19b. TELEPHONE NUMBER (include area code) 508-540-4400

TABLE OF CONTENTS

	Page
COVER	i
SF 298	ii
LIST OF FIGURES	vii
LIST OF TABLES	ix
PREFACE	x
EXECUTIVE SUMMARY	1
1.0 INTRODUCTION	4
1.1 Background	4
1.2 Technical Objective	5
1.3 Technical Approach	5
1.4 Commercial Applications for Chemical Agent Protective Skin Creams	7
2.0 BODY	9
2.1 EXPERIMENTAL PROGRAM	9

TABLE OF CONTENTS (continued)

	Page
2.1.1 Preparation of Amino-Functional Fluorocarbon-Stabilized Copper (II) Salts	9
2.1.2 Preparation of Surfactant-Stabilized Micronized Basic Ion Exchange Resins	9
2.1.3 Formulation of Experimental Water-Based CWA-Degrading Skin Creams	9
2.1.4 Physical Properties of Candidate Skin Creams Formulations	9
2.1.5 Skin Cream Film Analysis	10
2.1.5.1 Morphological Analysis of Experimental Skin Cream Films	10
2.1.5.2 Morphological Analysis of Experimental Skin Cream Films	10
2.1.6 Film Removal Demonstration	10
2.1.7 CWA Simulant Penetration Resistance of Applied Skin Cream Films	10
2.1.8 CWA Simulant Degradation Testing	11
2.1.8.1 CWA Simulant Degradation Product Analysis	11
2.2 RESULTS AND DISCUSSION	12
2.2.1 Screening for Candidate rTSP Cream Base Materials	12

TABLE OF CONTENTS (continued)

	Page
2.2.2 Fluorocarbon-Compatible Copper Complexes for Surface Destruction of CWAs	12
2.2.3 Preparation of Fatty Acid-Stabilized Micronized Basic Ion Exchange Resins	13
2.2.4 Evaluation of Commercial Nano-Sized Metal Oxide Particles for Simulant Neutralizing Ability	14
2.2.5 Skin Cream Formulation and Application Properties	14
2.2.5.1 Viscosity of Experimental Skin Cream Films	16
2.2.5.2 Morphological Analysis of Experimental Skin Cream Films	17
2.2.5.3 Adhesion and Flexibility of Experimental Skin Cream Films	20
2.2.5.4 Removability of Experimental Skin Cream Films	20
2.2.6 CWA Simulant Barrier Properties of Experimental rTSP Films	20
2.2.7 CWA Simulant Decomposition Testing of Experimental Skin Cream Films	21
2.2.7.1 Decomposition Chemistry for Selected CWA Simulants	22

TABLE OF CONTENTS (continued)

	Page
2.2.7.2 Decomposition Testing of CWA Simulants with Experimental rTSPs	23
2.2.7.3 CWA Simulant Degradation Product Analysis	31
3.0 KEY RESEARCH ACCOMPLISHMENTS	33
4.0 REPORTABLE OUTCOMES	34
5.0 CONCLUSIONS	35
6.0 REFERENCES	37
APPENDICES	
A) Fourier Transform Infrared Spectra	38
B) Hazards and Safety	41

LIST OF FIGURES

Figure	Page
1 Self-assembly and stratified morphology produced by new rTSPs applied to skin	6
2 Synthesis of fluorocarbon-functional-amine-copper catalysts	13
3 Chemical structures of commercially available fluorocarbon-functional-amines	13
4 FTIR (MIR) spectra overlay of JD5-94C (upper-TSP applied directly to MIR crystal; lower- TSP applied to aluminum foil, dried and coated foil placed in contact with MIR crystal)	18
5 FTIR (MIR) spectra overlay of Formulation JD5-119 with fluoroether additive (upper-TSP applied directly to MIR crystal; lower- TSP applied to aluminum foil, dried and coated foil placed in contact with MIR crystal)	19
6 Base-catalyzed hydrolysis of VX simulant Malathion	22
7 Secondary base-catalyzed hydrolysis of VX simulant Malathion	22
8 Base-catalyzed hydrolysis of HD simulant chloroethylethyl sulfide (CEES)	23
9 Oxidation of HD simulant chloroethylethyl sulfide (CEES)	23
10 Base-catalyzed hydrolysis of GD simulant diisopropylmethyl fluorophosphate (DIFP)	23

LIST OF FIGURES (continued)

Figure	Page
11 Effect of skin cream formulation composition and aging on the degradation of CWA simulant DEEP	24
12 Effect of skin cream formulation composition and aging on the degradation of CWA simulant CEES	25
13 Effect of oxidizing additives on the degradation of CWA simulant CEES	26
14 Effect of ion exchange and oxidizing additives on the degradation of CWA simulant CEES	27
15 Effect of skin cream formulation composition and film age on the degradation of CWA simulant Malathion	28
16 Effect of ion exchange additives on the degradation of CWA simulant Malathion by experimental water-based rTSPs	29
17 Effect of ion exchange and oxidizing additives on the degradation of CWA simulant Malathion	30
18 Effect of ion exchange, oxidizing, and perfluoroether oil additives on the degradation of CWA simulant Malathion	31
19 FTIR spectra overlay upper Malathion applied over JD5-129; lower- Malathion-alkaline hydrogen peroxide reaction product	32

LIST OF TABLES

Table		Page
1	Experimental rTSP Compositions Formulated with Cu(II) Agents	15
2	Experimental Reactive and Non-Reactive TSP Compositions	15
3	Experimental Water-Based rTSP Compositions Formulated with Oxidizing CWA Decontaminating Agents	16
4	Viscosity of Experimental rTSP and Control TSP Formulations	16
5	Removability of Experimental rTSP and Control TSP Formulations	20
6	CWA Simulant Barrier Properties of Experimental rTSP Formulations	21

PREFACE

This final report covers work performed during the period May 13, 2005 through November 12, 2005 under U.S. Army Medical Research and Materiel Command Contract No W81XWH-05-C-0123. The work was administered by the U.S. Army Medical Research Institute of Chemical Defense, Aberdeen Proving Ground, MD and U.S. Army Medical Research Acquisition Activity, Fort Detrick, MD. Dr. Ernest Braue, AMEDD, was the Project Engineer for this program.

The contract was performed by Cape Cod Research, Inc. under the supervision of Francis L. Keohan, Principal Investigator. This technical report was submitted in December, 2005.

EXECUTIVE SUMMARY

This SBIR Phase I research explores the feasibility of developing an improved topical skin protectant (TSP). The threat of chemical and biological (CB) warfare agent exposure requires a variety of measures to protect military personnel. CB agent entry through the skin can potentially be reduced through the application of chemical barrier creams. Low surface energy fluoropolymers have been shown to resist penetration of both polar and nonpolar chemicals. A new protective skin cream is proposed that utilizes fluorochemical intermediates and known CB neutralizing chemicals to defend against multiple threats. The new protective skin cream is based on a blend of non-irritating film-forming compounds, chemical agent hydrolysis catalysts that concentrate at the film surface and solid particulate neutralization agents that combine to form a highly resistant barrier to the transmission of both hydrophobic and hydrophilic chemicals. The novelty of the approach stems from the dual protection mode offered by a system that self assembles into a multi-layered film for resisting CB agent penetration while quickly neutralizing harmful agents before they reach the skin. The advanced reactive TSP (rTSP) will be simple to apply and effectively render the skin highly resistant to the penetration of harmful chemicals and biological agents. The new CB-blocking compounds were formulated and tested for CB simulant barrier properties, self-decontaminating ability and longevity.

- New reactive skin cream formulations were successfully formulated as water-thinned suspensions of commodity surfactants, hydrophilic resins, reactive additives and fluoropolymers.
- Experimental skin cream formulations have shown efficacy in the decomposition of three different CWA simulants: chloroethyl ethyl sulfide (CEES), a simulant for mustard vapor (HD), diethyl ethylphosphonate (DEEP), a simulant for GB, and Malathion which is a simulant for nerve agent VX.
- Ball milling ion exchange resins with ceramic media in the presence of surfactants appears to be an effective means of reducing the resin particles to a size compatible with a skin cream product.
- Alkaline ion exchange resins appear to have the greatest positive effect on the skin cream's ability to degrade hydrolysable CWA simulants.
- rTSP formulations prepared with an oxidative chloro amide additive promote degradation of HD simulant CEES and VX simulant Malathion.
- rTSP formulations prepared with micronized alkaline ion exchange resin additives promote degradation of VX simulant Malathion.
- The ability of the experimental rTSP formulations to decompose different CWA simulants was found to depend on the level of micronized ion exchange resin fillers.

- Formulations based on physiologically inert polymers and ionic surfactants displayed self-assembling properties as inferred by surface FTIR analysis.
- The hydrophilic polymer additive PVP was found to preferentially absorb onto a polar substrate and away from the air-coating interface from an rTSP formulation.
- Fluorocarbon-rich components of the experimental rTSP formulations were found to favor the film-air interface.
- The level of perfluoroether oil additive could be used to modulate the barrier properties of the experimental water-based rTSPs.
- The level of perfluoroether oil additive could be used to reduce water sensitivity of the experimental water-based rTSPs and provide stable, cleanable films.
- Formulation and processing variables were identified for optimizing the rTSP products.

The results of this feasibility study provide a foundation for new high performance TSP formulations for broad range protection against a variety of CWA threats. Developing suitable self-assembling skin cream base materials that can readily be formulated into TSP products to provide enhanced chemical barrier and CWA-degrading properties would be the main goal of the expanded program. The Phase II effort will explore extending and validating the self-assembling film/rTSP concept using systematic formulation optimization techniques leading up to animal testing. The most promising formulations developed in Phase I would serve as the starting point for process optimization and scale-up to production volumes. The validation testing will be coordinated with the Army sponsor and a collaborating organization with experience in CWA handling and personnel protective technologies

The feasibility of formulating skin creams based combinations of micronized ion exchange resins, mildly oxidizing compounds, nanoparticulate metal oxides, PTFE powders, and non-irritating surfactants that actively degrade CWA's has been demonstrated in the Phase I program. An expanded Phase II effort is recommended in order to more completely develop and characterize the skin cream compositions and application methodology developed during the Phase I. The primary objective of this Phase II research effort is to develop an easily applied, physiologically benign protective skin cream system that both blocks the transmission of CWA to the skin and actively detoxifies these chemical toxins. The new skin cream products will be designed for maximum physiological tolerance, effective repellency of chemicals, and high capacity for CWA detoxification. The proposed approach should lead to skin cream formulations which can be readily applied to in the field, exhibit long term efficacy in preventing CWA transmission through the skin, provide efficient degradation of a variety of chemical threats and allow simple removal. The specific Phase II objectives are:

- Establish material processing parameters for optimizing the critical components of the proposed CWA-degrading skin cream system.

- Optimize polymeric components, surfactants, fluoropolymer barrier materials, micronized ion exchange resins, and nano-scale metal oxide particulates and formulation to achieve specified CWA-degrading and barrier properties
- Develop CWA degrading agents engineered to concentrate in outer layers of a self-stratifying rTSP film
- Optimize skin cream formulation process to yield uniform products for facile application in the field.
- Demonstrate the ability to apply the rTSPs in a manner compatible with practical and accepted soldier field operations
- Demonstrate the ability to safely remove rTSPs in a manner compatible with battlefield operations
- Validate efficacy of optimized rTSP formulations using actual CWAs
 - Demonstrate *in vitro* performance of rTSPs using chronic barrier and head space testing
 - Demonstrate *in vivo* performance of rTSPs using animal skin exposure and acetylcholinesterase inhibitor tests
- Demonstrate that the rTSP coatings that have been challenged with CWAs or simulants can be effectively removed without exposing skin to harmful chemicals.
- Demonstrate durability of applied rTSPs in terms of resistance to sweat, sunscreen, insect repellent, and incidental contact.
- Develop production plan for optimized rTSP products

1.0 INTRODUCTION

The threat of chemical warfare agent (CWA) exposure requires a variety of measures to protect military personnel. CWA agent entry through the skin can potentially be reduced through the application of chemical barrier creams. A new protective skin cream was developed that utilizes a self-stratifying matrix and known CWA neutralizing chemicals to defend against multiple threats. The Phase I objective was to identify reactive topical skin protectant (rTSP) systems that meet the goals of low toxicity, simple application, self-stratification for combined CWA barrier and active CWA detoxification. A combination of surfactants, hydrophilic polymers, micronized supported catalysts, mild oxidants, and fluoropolymer additives were used to formulate new aqueous-based rTSP systems. The ability of selected formulations to form self-stratified films and efficiently promote the degradation of several CWA simulants, including Malathion and chloroethylethyl sulfide was demonstrated. Hydrolytic degradation of the VX simulant Malathion was observed for some formulations. The new rTSP formulations were found to be more easily removed than purely fluoropolymer-based controls. Formulation and processing variables were identified for optimizing the rTSP products for ultimate integration with warfighter protection systems.

1.1 Background

Military personnel face a variety of potential chemical threats on the modern battlefield. These hazardous chemicals include chemical warfare agents such as the nerve agents GB and GA as well as toxic industrial solvents such as benzene. Conventional protective measures include variety of outer garments that present barriers to CWA penetration or absorb and chemically neutralize the harmful agents. A new protective skin cream has been developed that uses fluorocarbon resins to shield the skin against CWAs.¹ The military has identified a need for a pre-exposure skin cream that will neutralize CWAs before they reach the skin.

A number of CWA neutralization products have been developed but do not possess the necessary physiological compatibility to be used for long-term contact with the skin. One liquid product called DF-200, reported to be based on a mixture of surfactants and aqueous hydrogen peroxide can be used to decontaminate both CWA chemicals and microbiological threats such as anthrax.² The military currently uses a mixture of carbonaceous absorbing agent and ground basic ion exchange resin and plastic particles (M291 Resin Kit) for field decontamination of skin.³⁻⁴ One of the latest developments for protecting exposed skin from CWAs is a family of skin barrier creams termed topical skin protectants or TSPs.⁵⁻⁶ These products, based on blends of perfluorinated oils and resin powders function by preventing the transmission of liquid CWAs to the skin. Newer versions of the TSPs containing CWA-detoxifying agents termed reactive TSPs or rTSPs have also been reported.⁴ Additives such as halogenated organonitrogen compounds, nano-scale metal oxides, polysilsesquioxanes, and ion exchange resins have been used successfully to provide rTSPs with active CWA decomposing properties.⁵⁻⁷ Some of these additives, however can be irritating to the skin when formulated in the quantities necessary for efficient CWA detoxification.

1.2 Technical Objective

The prime objective of this research is to identify promising low-toxicity chemical barrier/chemical neutralization cream candidates that can effectively protect military personnel from the threat of chemical warfare agent (CWA) exposure. A new protective skin cream is proposed that utilizes fluorochemical intermediates and known CWA neutralizing chemicals to provide a first line of defense against these threats. The new protective skin cream is based on a blend of non-irritating film-forming compounds and solid particulate neutralization agents that combine to form a highly resistant barrier to the transmission of both hydrophobic and hydrophilic chemicals. Demonstrating the feasibility of using state-of-the-art polymer self assembly techniques with active CWA neutralizing compounds in a form that allows easy application and removal from the skin was a main goal of the program. The approach should significantly improve the readiness of military forces against CWA threats and provide valuable technology for protecting hazardous material handlers. Questions that must be answered to prove the feasibility of the proposed approach include:

- What factors govern the self assembly and controlled microphase separation of the proposed skin cream coating precursors?
- What factors govern the ability of the deposited films to remain intact for the desired duration and can they be readily recoated without removing the first layer?
- What are the best ways for producing self-stratifying films having different CWA detoxifying capacity over skin?
- How can the neutralizing agents be incorporated into the multi-layered coating system to maximize CWA destruction while minimizing interaction with the protected skin?
- How readily and by what means can the coating residues be removed from the skin?

Demonstrating the efficacy of these personal protective coatings would help to expedite the technological and commercial development of catalysis-based CWA decontaminating systems. The benefits of an effective single-component barrier cream that quickly neutralizes CWAs include: reversible adhesion to skin, environmental durability, reduced toxic effluents, and simplified application in the field. Potential commercial applications lie in personal protection products for military, law enforcement, civil defense, health care, emergency response, agriculture, and petroleum and chemical processing industries. In Phase II the most promising detoxifying reactants and rTSP formulations will be optimized and their efficacy demonstrated against simulants and chemical warfare agents.

1.3 Technical Approach

The overall approach involves a thorough definition of the permeability of typical CWAs in the proposed coating film components, chemical and morphological properties of the films derived from the skin creams, and CWA neutralization mechanisms required for this application. The technical approach involves the formulation and testing of dual-phase coating materials derived

from self-assembled polyelectrolytes, fluorosurfactants and fatty acid-based surfactants. These temporary binder matrix materials will be filled with a mixture of nano-sized metal oxides and finely ground basic ion exchange resins that have been stabilized with fatty acid surfactants. Another key ingredient will be potent CWA hydrolysis catalysts based on fluorocarbon-substituted organic copper complexes that preferentially concentrate at the applied coating surface.

The film morphology expected from the phase segregation and self assembly of the polyelectrolyte-surfactant precursors is represented in Figure 1. This formulation approach has been reported to produce remarkably uniform and robust films. Complex formation occurs spontaneously as a result of electrostatic and hydrophobic interactions.⁸ The films formed over hydrophilic skin surfaces should have a distinctly stratified morphology due to the tendency of hydrophobic fluorinated organics to migrate towards the air interface and hydrophilic polymers such as polyvinylpyrrolidone to absorb at the polar skin surface. The anticipated morphology for a multi-functional, self-segregating CWA skin barrier coating applied to a skin substrate is illustrated in Figure 1.

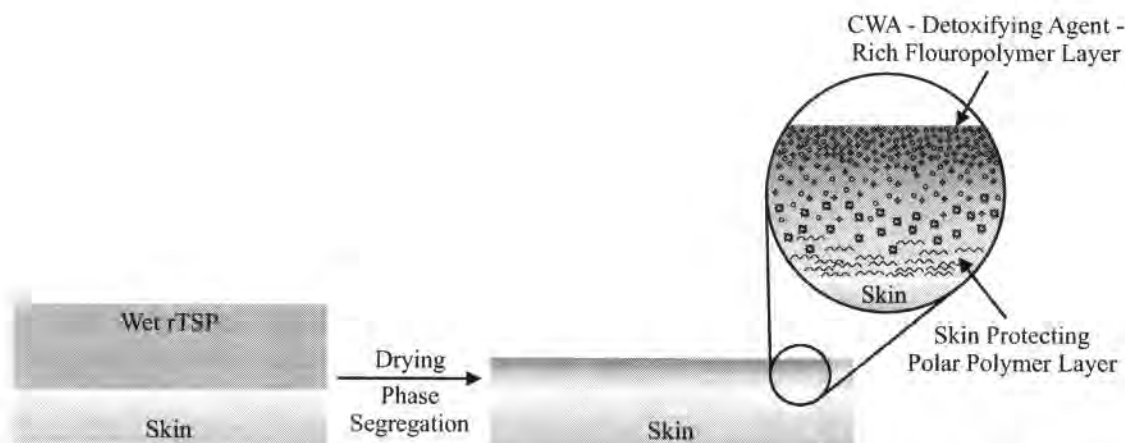


Figure 1 Self-assembly and stratified morphology produced by new rTSPs applied to skin

In the generalized structure fatty acid surfactants are shown surrounding amine-functional basic ion exchange resin particles, and metal oxide nano-scale particles providing stabilization within the coating layer. The sheath of self-assembled stearic acid groups and the hydrophilic collagen layer should aid in keeping the potentially irritating basic ion exchange resins from contacting the skin. The copper-amine catalytic agents that should preferentially concentrate in the fluorocarbon-rich outer layers of the applied coating readily decompose many hydrolytically-sensitive CWAs and leave behind a catalytic residue due that provides for additional detoxifying capacity. PTFE microparticles and the fluorocarbon residues of fluorosurfactants should provide an effective barrier to both polar and non-polar CWAs.

Some of the problems associated with this CWA agent protective cream application include: slowing the diffusion of CWAs through the protective film to allow neutralization time, providing a strong decontaminating capability at the outer surface of the cream-derived coating, formulating skin creams with sufficiently micronized neutralization agents for uniform application and film formation, protecting the skin from the potentially irritating effects of the

basic neutralization additives, and providing a means for readily removing the deposited film from the skin when desired. Logistical improvements in dealing with chemical battlefield scenarios could be made if more actively decontaminating skin protectants were available that resulted in rapid and thorough destruction of different CWAs. Previous research has shown that certain transition metal complexes, most notably copper (II) complexes can catalyze the decomposition of certain CWAs such as GB and GD by hydrolysis.⁴ Copper ions can also catalyze the oxidation of organic compounds, particularly in the presence of co-oxidants such as hydrogen peroxide.⁹ The proposed approach seeks to use a combination of copper (II) complexes for CWA hydrolysis, fluoropolymer and fluorocarbon surfactants for enhanced chemical barrier properties and different CWA-neutralizing additives for multi-level protection.

1.4 Commercial Applications for Chemical Agent Protective Skin Creams

Successful demonstration of the feasibility of the proposed self-assembling skin cream concept will establish that the combination of CWA-neutralizing additives in a fluorocarbon-based vehicle yields film-forming systems for a variety of protective applications. This product could be used in a broad range of military and civilian applications. For example, industrial workers exposed to materials similar to CWAs including pesticides, herbicides, and other chemicals that represent health hazards. In addition, this product would greatly improve the protection of civilian first responders to a chemical warfare agent terrorist attack.

Potential customers for this new skin cream product are military personnel, emergency response workers, and chemical plant personnel. The proposed skin cream formulations could be successfully marketed to both military and civilian customers. The pricing of the product(s) will be determined through analysis of the market for competitive product pricing and the cost structure for producing the skin cream products. Premiums for added value such as improved physiological inertness, excellent chemical neutralization rates, easy removability, and wider applicability would also be factored into the pricing strategy. The sales results of the test marketing study will provide valuable information for price adjustment before any full-scale product launch. Advertising and promotion plans for this product would begin with the preparation of detailed technical data sheets, product brochures and press releases to targeted personal protective product industry publications.

Competing Technologies

Currently, the main methods for protecting the skin from CWA poisoning are through the use of protective garments or with a newly developed perfluoropolymer-based skin barrier cream. The use of protective garments presents logistical problems in fitting properly and donning them in time to stop CWA contamination. The new Teflon-like skin creams act as a barrier without actively decontaminating the chemical agents on the surface. A secondary detoxifying agent would be needed with these products, which would increase the cost of using them. These materials would not necessarily detoxify CWAs at the outer film surface in the manner of the proposed coatings. The combination of partial chemical barrier resistance and rapid CWA neutralization ability will be the principal means of differentiating the proposed skin cream products from the competition.

Patent Protection

Patent protection for technology developed under the SBIR Phase I and Phase II should significantly improve its marketability to potential corporate partners as well as to strengthen the position of the small firm. New skin cream coating precursors and CWA neutralizing additives developed during the course of this research that displayed outstanding protective properties and acceptable physiological compatibility could be protected by concept of matter patents.

2.0 BODY

2.1 EXPERIMENTAL PROGRAM

The experimental effort was designed to test the feasibility of self-assembling reactive topical skin protectants (rTSPs) formulated from surfactants, fillers, hydrolysis catalysts, micronized ion exchange resins, PTFE powders, and metal oxide nanoparticles for blocking the transmission and detoxifying chemical warfare agent (CWA) simulants.

2.1.1 Preparation of Amino-Functional Fluorocarbon-Stabilized Copper (II) Salts

Copper (II) acetate was reacted with the fluorocarbon-based amine pentafluoroaniline in different solvents including water, methanol, and tetrahydrofuran. The reactions were followed by UV-visible light spectroscopy. A Shimadzu Model 160 PMT double beam UV/Visible Spectrophotometer was used for this analysis.

2.1.2 Preparation of Surfactant-Stabilized Micronized Basic Ion Exchange Resins

A commercial basic ion exchange resin Amberlite IRA-400 was micronized by ball milling. Ball milling with ceramic media appears to be an effective means of reducing the resin particles to a size compatible with a skin cream product. Treating the ground ion exchange resins with surfactants was evaluated as a means of preventing skin irritation. Examples of the surfactants include fatty acids and alkyl polyethoxylates.

A commercial polyethylene glycol-stearyl ether surfactant (Hetoxol STA-30) was employed as a base-stable processing aid for the ion exchange resin milling. The protective surfactants were applied from alcohol dispersions of the ion exchange resins before milling. The micronized and treated resins were dried under reduced pressure before formulating.

2.1.3 Formulation of Experimental Water-Based CWA-Degrading Skin Creams

The most promising resins, CWA detoxifying agents, surfactants, and fillers were formulated via high-speed dispersion. Water-soluble polymers were predissolved in deionized water before adding to the mixtures. Stirring rates of up to 5000 rpm were used to obtain stable emulsions of the different resins with water. The formulated samples were stored in screw-top polyethylene bottles.

2.1.4 Physical Properties of Candidate Skin Creams Formulations

The initial viscosity characteristics of skin cream dispersions was determined by traditional viscometry using a Brookfield model LVT rotary viscometer, small sample adapter, and temperature-controlled sample chamber. Viscosity measurements were conducted at room temperature.

2.1.5 Skin Cream Film Analysis

The dried films resulting from draw down blade application of the experimental skin cream formulations were evaluated for tackiness, permanence, appearance, thickness, and the ability to self-stratify after applying.

2.1.5.1 Morphological Analysis of Experimental Skin Cream Films

Infrared spectra were recorded from opposing surfaces of deposited skin cream films in order to test for self assembly and stratification within the films. A Perkin Elmer Paragon 1000 FTIR spectrophotometer with the multiple internal reflectance (MIR) attachment was used for this analysis. In MIR, an IR beam is passed through a thin, IR transmitting sample in a manner such that it alternately undergoes internal reflection from the front and rear faces of the sample.¹¹ In order to test for preferential phase separation and self assembly within the applied TSP films, the MIR studies were performed in two different ways. To study the chemical composition of the applied films' outer or air interface, the TSP samples were applied to aluminum foil-covered rubber spacer sheets. The latter are used to block light from the sides of the MIR crystal and compress the sample film against the opposite crystal surfaces where the reflecting IR beam can impinge the sample to be analyzed. The coated foil-covered rubber spacers were allowed to air dry overnight at ambient temperature before analyzing. The chemical composition of the TSP films at the opposite (skin-to-coating) interface was analyzed by applying the TSP directly to both sides of the zinc selenide crystal, drying for the same period and using uncoated aluminum foil-covered rubber spacers.

2.1.5.2 Adhesion of Skin Cream Film to Skin

The adhesion of the proposed skin cream-derived films was qualitatively determined by applying the products to a skin surface surrogate. Estane polyurethane film was used as a surrogate skin for this feasibility study. After drying, the coatings were tested for adhesion and flexibility by bending the coated elastomer sheet over standard size mandrels ranging in diameter from 0.5 inch to 1/8 inch. The ability of the films to remain intact and adhered to the polyurethane substrate was observed and recorded.

2.1.6 Film Removal Demonstration

The ability to remove the skin cream films was demonstrated with different hand cleaning agents including simple soap and water and liquid hand soaps. Softsoap® liquid hand cleaner from Colgate-Palmolive Co. was used in this testing. The soap and water were applied to a paper towel and the wetted towel wiped over the rTSP-coated polyurethane sheet specimens. The ability to remove the applied coatings was qualitatively assessed by visually noting how easily and completely the coatings could be cleaned from these skin-substitutes.

2.1.7 CWA Simulant Penetration Resistance of Applied Skin Cream Films

Experimental TSP formulations were applied to C8 Chemical Agent Detector paper using a film drawdown blade. The nominal thickness of the films was 0.15 mm. The films appeared uniform

and were easily spread over the paper substrate. Microdrops (8 μ L) of diethyl ethylphosphonate (DEEP), a simulant for GB, 2-chloroethyl ethyl sulfide (CEES), a simulant for HD, and Malathion, a simulant for VX were applied to the film surfaces in triplicate and their ability to penetrate through to the indicator paper was monitored over a period of 6 hours at approximately 25°C.

2.1.8 CWA Simulant Degradation Testing

The ability of the proposed skin cream coatings to actively decontaminate different CWA simulants was tested using a version of the head space method. Coated polyurethane film samples are exposed to a carefully measured amount of simulant for a specified period of time in a closed container. The coatings are applied to the rubber sheet using a wet film drawdown blade having a gap of 0.050 in. This typically yields films with thicknesses of approximately 0.035 in. The headspace of the closed system is periodically sampled and analyzed by gas chromatography (GC) for quantitative reduction of the target CWA simulants. The CWA decomposition studies are being conducted at Cape Cod Research using a Hewlett-Packard Model 5890 GC equipped with a capillary column (HP-5, 12 m length, 0.2 mm ID), split-splitless injector and a flame ionization detector.

The experimental procedure for the decontamination testing consists of placing a 0.25 in X 0.25 in square piece of polyurethane sheet at the bottom of a 40 ml glass scintillation vial fitted with a rubber septum-centered screw cap. 5-60 μ l of the CWA simulant test fluid is injected onto the surface of the sheet and the vial placed in a temperature regulated water bath. The temperature is being varied from room temperature (21°C to 50°C) in order to produce enough volatilized CWA simulant in the sample chamber head space to be reliably detected by CG. The sampling is conducted using a 500 μ l syringe.

2.1.8.1 CWA simulant degradation product analysis

The products and intermediates of the rTSP CWA simulant decomposition testing were characterized by Cape Cod Research FTIR spectroscopy. rTSP-coated aluminum film samples were exposed to a carefully measured amount of simulant for a specified period of time in a closed container. The coatings are applied to the aluminum sheet using a wet film drawdown blade having a gap of 0.050 in. After different dwell times, the simulant-challenged films were removed and immediately exposed to the surface of a zinc selenide MIR crystal and analyzed by FTIR. These spectra were compared to those obtained from aqueous base/ hydrogen peroxide-induced hydrolysis of Malathion.

2.2 RESULTS AND DISCUSSION

2.2.1 Screening for Candidate rTSP Cream Base Materials

The new multi-action, CWA- detoxifying skin creams were formulated to meet the following application and final property objectives:

- low skin irritation potential
- low initial viscosity for easy application similar to sun screens
- fast film-forming properties
- durable adhesion to skin substrates under normal operating conditions
- breathable coating films that allow water vapor to escape from the skin
- highly flexible and resistant to hydrocarbons, water, and host of CWAs
- contain a surface rich in catalysts for the hydrolytic degradation of certain common CWAs
- readily able to dissolve, neutralize and bind CWAs that penetrate the fluorocarbon-rich outer phase before they reach the skin
- able to be removed from the skin with soap and water

The laboratory research involved developing a simple-to-apply skin cream that protects soldiers from CWA agents via multiple mechanisms: a fluorocarbon-rich outer layer for resisting the initial penetration of toxic agents; agents for catalytically detoxifying CWAs at the film surface; a nanoscale particulate filler that chemically neutralizes CWAs; and another particulate filler that both absorbs and neutralizes CWA chemicals. Experimentation focused on the processing of ion exchange resins, nano-scale metal oxides and mildly oxidizing agents for skin cream applications, and the formulation of lotion vehicles that self-assemble in stratified layers. The skin cream coating components contained blends anionic fluorosurfactants such as ammonium phosphoric acid fluoroalkyl ester, (Zonyl® FSE, DuPont Co.). Ionic surfactants and oppositely charged polyelectrolytes have been shown to spontaneously form well-defined complexes, which precipitate from aqueous solutions as a result of electrostatic and hydrophobic interactions. Representative skin cream binder constituents including PTFE powders, polyfluoroether fluids, polyelectrolytes such as PVP, fluorosurfactants, and low irritation organo-polyether surfactants were used in these systems. These materials were screened for compatibility and film-forming characteristics.

2.2.2 Fluorocarbon-Compatible Copper Complexes for Surface Destruction of CWAs

Key components of the new protective skin creams are CWA-decomposing agents that enrich the outer portions of the applied product. An example of these types of agents is a copper-amine CWA hydrolysis catalyst that possesses the capability to migrate to the outer layer of the applied cream film. Copper (II)-amine complexes have been shown to rapidly catalyze the hydrolysis of GB-type CWAs.⁴ By synthesizing copper (II) salts from fluorocarbon-functional amines, a catalyst with a high affinity for fluorocarbon media can potentially be obtained. The outer surface of the proposed skin creams should be enriched in materials such as poly(tetrafluoroethylene) particles and fluorosurfactant residues. The fluorocarbon amine-copper complexes were synthesized from Cu(II) salts such as copper (II) chloride or copper (II)

acetate and commercially available fluorocarbon-based amines. Figure 2 illustrates the chemical structures and synthetic route for these CWA hydrolysis catalysts.

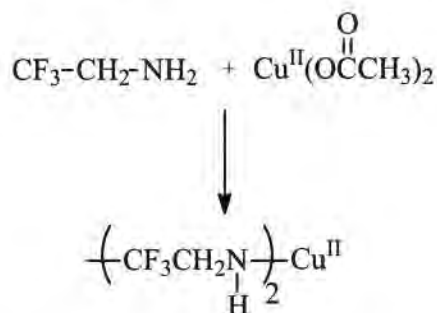


Figure 2 Synthesis of fluorocarbon-functional-amine-copper catalysts

Several different fluorocarbon-based amines are commercially available as potential precursors for synthesizing these catalysts. Illustrations of candidate fluoroamine structures are provided in Figure 3.

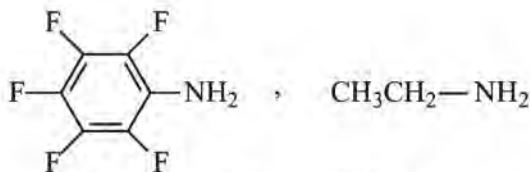


Figure 3 Chemical structures of commercially available fluorocarbon-functional-amines

In the feasibility study, the pentafluoroaniline was used to prepare copper complexes for evaluation as surface-enriching hydrolysis catalysts. Copper II acetate was reacted with the fluorocarbon-based amine pentafluoroaniline in different solvents including water, methanol, and tetrahydrofuran. The reactions are being followed by UV-visible light spectroscopy. The copper II salt has a maximum absorbance peak at approximately 710 nm. Changes in this absorbance and those attributable to the fluorinated amine would indicate complex formation.

Another potential copper II-based CWA hydrolysis catalyst containing fluorinated organic ligands that was also evaluated in this system was copper (II) hexafluoroacetylacetonate. This complex may also possess the ability to migrate to the fluorocarbon-enriched surface where it can be most effective in catalyzing the destruction of CWA's such as GB.

2.2.3 Preparation of Fatty Acid-Stabilized Micronized Basic Ion Exchange Resins

CWAs neutralization will be partially effected by including a micronized basic ion exchange resin that has been used successfully for field level CWA destruction. Different commercial basic ion exchange resins (e.g. Amberlite IRA-400) were procured, micronized by ball milling and tested alone and in the proposed coating vehicles for the ability to rapidly neutralize CWA simulants to non-hazardous compounds. Ball milling with ceramic media appeared to be an

effective means of reducing the resin particles to a size compatible with a skin cream product. Treating the ground ion exchange resins with surfactants was done to prevent skin irritation. Examples of the surfactants include fatty acids and alkyl polyethoxylates.

A promising system utilized a commercial polyethylene glycol-stearyl ether surfactant (Hetoxol STA-30). The protective surfactants were applied from alcohol dispersions of the ion exchange resins after milling. The treated resins were evaluated for their capacity to detoxify base-sensitive CWA simulants.

2.2.4 Evaluation of Commercial Nano-Sized Metal Oxide Particles for Simulant Neutralizing Ability

The proposed skin creams were also formulated with nano-particulate metal oxides for neutralizing CWA's. A commercial product from Nanoscale, Inc. called FAST-Act is a propriety formulation of non-toxic reactive nanomaterials that have been shown to effectively hydrolyze and dehydrohalogenate a variety of CWAs. A sample of FAST-Act was procured and tested for its effectiveness in neutralizing CWA simulants after formulating with the proposed skin cream film binder materials. The oxide powder appeared to blend well with the other materials in the proposed skin cream formulations and did not produce agglomeration.

2.2.5 Skin Cream Formulation and Application Properties

The application properties of proposed skin cream formulations are being studied. The effects of binder precursor loadings and additives on viscosity and dispersion stability are being determined. Blending of the experimental water-thinned skin cream formulations was carried out with a high speed laboratory disperser. A Brookfield viscometer was used to measure formulation viscosities and compared to a control consisting of a PTFE powder-perfluoroether oil formulation analogous to SERPACWA.

The addition of a poly(vinylpyrrolidone) (PVP) as a modifier for forming a skin- barrier coating protective intermediary layer was investigated. A formulation containing approximately 40 % water, 10 % commercial PVP and the remainder different fillers, PTFE powder, perfluoroether oil and surfactants on a weight:weight basis were prepared using high speed dispersion. The product was a stable, smooth dispersion with enhanced spreadability. Additional formulations, designed to allow more penetration of the organic CWA simulants into the coatings for more effective neutralization were also prepared without the perfluoroether additive. These formulations were evaluated for film-forming ability, CWA simulant barrier and decontaminating properties. The compositions of the Cu(II) complex-containing, water-thinned and perfluoroether oil-based barrier cream formulations are provided in Table 1

Table 1
Experimental rTSP Compositions Formulated with Cu(II) Agents

Formulation ID	JD4-191 (Exp. rTSP)	JD4-43 (Exp. rTSP)	JD4-51 (Exp. rTSP)	JD5-70A (Exp. rTSP)	JD5-70B (Exp. rTSP)
Component	Weight (%)	Weight (%)	Weight (%)	Weight (%)	Weight (%)
Fomblin Y 25/6 (fluoroether oil)	63.0	31.4			
PTFE powder ¹	8.0	9.1	9.1	8.0	8.0
Micronized ion exchange resin ²	18.4	7.9	7.9	8.0	4.0
Zonyl FSE	2.1	1.3	32.6	0.8	0.8
Fast Act nanoparticles ³	8.0				4.0
Polyvinylpyrrolidone		9.5	10.0	5.8	5.8
Cu(II) trifluoroacetylacetonate	0.5	0.8	0.4	0.4	0.4
PEGMTE				8.0	8.0
Deionized water		40	40	69	69

1. PTFE powder (12 micron diameter powder)
2. Amberlite IRA-400 emulsion w/ Polyethylene glycol myristyl tallow ether (PEGMTE)
3. Fast Act (nanometer-scale titanium and magnesium oxides)

A series of formulations were prepared without copper complex additives. The compositions of the water-thinned reactive agent and non-active TSPs as well as a perfluoroether oil-based control barrier cream formulations are provided in Table 2.

Table 2
Experimental Reactive and Non-Reactive TSP Compositions

Formulation ID	JD4-186 (control)	JD5-94C (Exp. TSP)	JD5-119 (Exp. TSP)	JD5-94A (Exp. rTSP)	JD5-94B (Exp. rTSP)
Component	Weight (%)	Weight (%)	Weight (%)	Weight (%)	Weight (%)
PTFE powder ¹	37.0	9.4	9.2	8.5	8.5
Micronized ion exchange resin ²				9.4	9.4
Zonyl FSE		0.9		0.9	0.9
Fomblin Y 25/6	63.0		3.0		
Polyvinylpyrrolidone		8.5	8.4	7.7	7.7
PEGMTE		9.4	9.2	8.5	8.5
Deionized water		71.8	70.2	65.0	65.0

1. PTFE powder (12 micron diameter powder)

Several water-thinned formulations were prepared using the mildly oxidizing chloramine-T reactive additive. The compositions of these water-thinned rTSP formulations are provided in Table 3.

Table 3
Experimental Water-Based rTSP Compositions Formulated with Oxidizing CWA
Decontaminating Agents

Formulation ID	JD5-111 (Exp. rTSP)	JD5-123 (Exp. TSP)	JD5-129 (Exp. TSP)	JD5-134 (Exp. TSP)
Component	Weight (%)	Weight (%)	Weight (%)	Weight (%)
PTFE powder ¹	8.5	8.1	6.2	5.9
Micronized ion exchange resin ²		9.7	9.7	9.3
Zonyl FSE	0.9	1.0	1.0	1.0
Fomblin Y 25/6			1.9	6.0
Chloramine-T hydrate	9.4	4.7	4.7	4.5
Polyvinylpyrrolidone	7.7	7.2	7.2	6.9
PEGMTE	8.5	8.1	8.1	7.8
Deionized water	65.0	61.2	61.2	58.6

1. PTFE powder (12 micron diameter powder)

These formulations were tested for application viscosity and their ability to be applied in uniform layers to polyurethane sheets.

2.2.5.1 Viscosity of Experimental Skin Cream Films

The ambient temperature viscosity values of several water-based experimental rTSPs and a control formulated to approximate the composition of a SERPACWA TSP are provided in Table 4.

Table 4
Viscosity of Experimental rTSP and Control TSP Formulations

Formulation ID	Weight % Solids	Viscosity (cps)
SERPACWA-type control	50.0	> 100000
JD5-94C	28.2	54000
JD5-123	38.8	19500

The PTFE powder/perfluoroether oil based control was quite viscous and its viscosity could not be measured with this viscometer. The experimental rTSP formulations JD5-94C and JD5-123, which used water as the thinning agent showed significantly lower viscosities. Formulation JD5-123, which possessed a higher solids content than the JD5-94C control had only about half the viscosity.

2.2.5.2 Morphological Analysis of Experimental Skin Cream Films

Self-Segregation Testing of Experimental Skin Cream Formulations

Infrared spectra were recorded from opposing surfaces of deposited skin cream films in order to test for self assembly and stratification within the films. A Perkin Elmer Paragon 1000 FTIR spectrophotometer with the multiple internal reflectance (MIR) attachment was used for this analysis. In MIR, an IR beam is passed through a thin, IR transmitting sample in a manner such that it alternately undergoes internal reflection from the front and rear faces of the sample. In order to test for preferential phase separation and self-assembly within the applied TSP films, the MIR studies were performed in two different ways.

To study the chemical composition of the applied films' outer or air interface, the TSP samples were applied to aluminum foil-covered rubber spacer sheets. The latter are used to block light from the sides of the MIR crystal and compress the sample film against the opposite crystal surfaces where the reflecting IR beam can impinge the sample to be analyzed. The coated foil-covered rubber spacers were allowed to air dry overnight at ambient temperature before analyzing. The chemical composition of the TSP films at the opposite (skin-to-coating) interface was analyzed by applying the TSP directly to both sides of the zinc selenide crystal, drying for the same period and using uncoated aluminum foil-covered rubber spacers.

In Figure 4, the overlaid spectra of the two opposing sides of the film resulting from the deposition of formulation JD5-94C shows differences in chemical composition. The most prominent differences are the presence of strong absorbance bands at approximately 3387 cm^{-1} , attributable to phosphonic acid salts with associated water and at approximately 1650 cm^{-1} , attributable to phosphonic acid and carbonyl groups from the polyvinylpyrrolidone (PVP). These are not observed in the MIR spectrum of the air-film interface. This suggests that the experimental TSP formulation undergoes a form of self-segregation with the more polar PVP and anionic fluorosurfactant showing preferential migration to the polar MIR crystal surface. Strong absorbance bands attributed to fluorocarbon-based coating components were observed at both the air and substrate interfaces, e.g., 963 , 1208 , and 1289 cm^{-1} . It appears that the PVP and anionic fluorosurfactant may form a complex that bonds strongly to polar surfaces such as skin. This may be very advantageous in the proposed rTSPs as the self-assembled PVP-fluorosurfactant layer absorbing at the skin may be a better barrier to harmful agent permeation than a simple hydrophilic polymer layer alone.

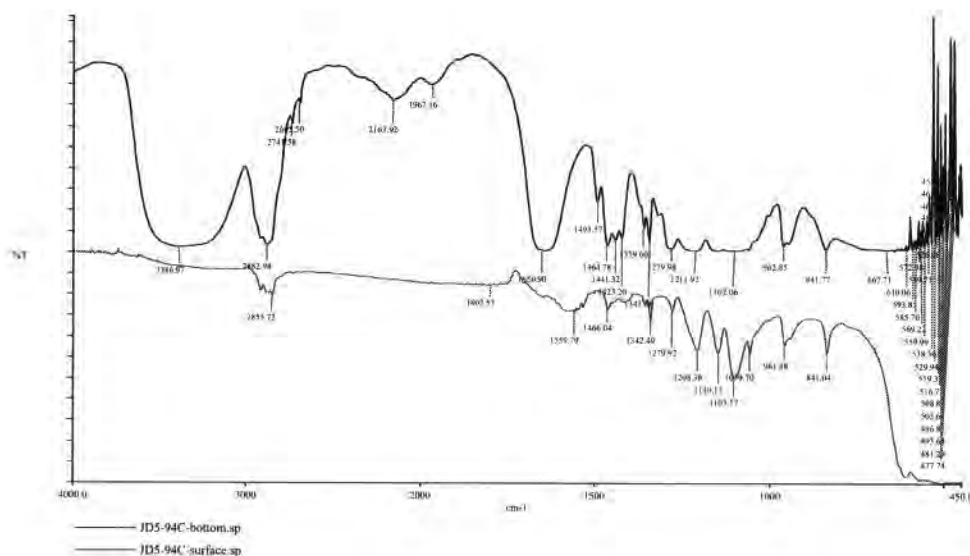


Figure 4 FTIR (MIR) spectra overlay of JD5-94C (upper-TSP applied directly to MIR crystal; lower- TSP applied to aluminum foil, dried and coated foil placed in contact with MIR crystal)

Sample JD5-119, a fluoroether-modified version of formulation JD5-94C was applied to aluminum foil and directly to the MIR crystal for FTIR analysis. The overlaid spectra from opposing sides are shown in Figure 5.

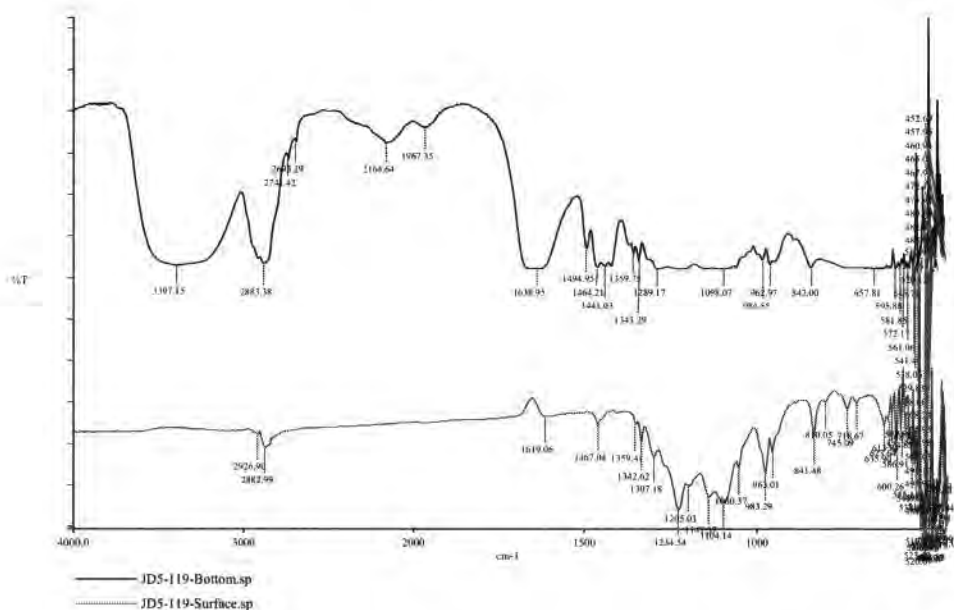


Figure 5 FTIR (MIR) spectra overlay of Formulation JD5-119 with fluoroether additive (upper-TSP applied directly to MIR crystal; lower- TSP applied to aluminum foil, dried and coated foil placed in contact with MIR crystal)

There again appears to be evidence of preferential segregation within the applied TSP film. The film layer at the crystal interface shows strong absorbance bands at approximately 3400 cm^{-1} , attributable to associated water and at approximately 1640 cm^{-1} , attributable to carbonyl groups from the polyvinylpyrrolidone (PVP). The film-substrate interface also appears to retain significant amounts of water after drying for 24 hour. This water-rich reservoir may be valuable in CWA detoxification since water-induced hydrolysis is an important reaction for these systems. The substitution of perfluoroether oil for the fluorosurfactant did not appear to prevent the preferential absorption of PVP at the polar substrate. Strong absorbance bands attributed to fluorocarbon-based coating components were observed over the region between 960 and 1300 cm^{-1} in the spectrum taken at the air-film interface. FTIR spectra for the PVP and Zonyl FSE fluorosurfactant are provided in Appendix A.

2.2.5.3 Adhesion and Flexibility of Experimental Skin Cream Films

The adhesion of the films from experimental rTSP formulation JD5-129 and control formulation JD5-94C was qualitatively determined by applying the products to a skin surface surrogate. Estane polyurethane film was used as a surrogate skin for this feasibility study. After drying, the coatings were tested for adhesion and flexibility by bending the coated elastomer sheet over standard size mandrels ranging in diameter from 0.5 inch to 0.25 inch. The ability of the films to remain intact and adhered to the polyurethane substrate was observed and recorded. Both film-covered polyurethane sheets could be bent over the smaller diameter (0.25 inch) mandrel without disadhering the films.

2.2.5.4 Removability of Experimental Skin Cream Films

The ability to remove selected experimental and control skin cream films was tested with different hand cleaning agents including simple water and liquid hand soaps. The soap and water were applied to a paper towel and the wetted towel wiped over the rTSP-coated polyurethane sheet specimens. The ability to remove the applied coatings was qualitatively assessed by visually noting how easily and completely the coatings could be cleaned from these skin-substitutes. Table 5 summarizes the cleaning test results.

Table 5
Removability of Experimental rTSP and Control TSP Formulations

Formulation ID	Cleaning Results	
	Water Only	Liquid Hand Soap and Water
SERPACWA-type control	no removal	incomplete removal
JD5-94C	nearly complete removal	complete removal
JD5-129	some removal	complete removal
JD5-134	little removal	complete removal

Overall, the ability to remove the experimental rTSPs and TSPs was mostly affected by the level of perfluoroether oil in the formulation. The SERPACWA-like control formulation was very difficult to remove with common hand soap and left residual material on the polyurethane substrate. The perfluoroether oil-free formulation JD5-94C showed an unacceptable level of water sensitivity in that it could be easily removed with water alone. This tendency can be effectively counteracted by using the perfluoroether oil additive in levels far below the SERPACWA control. The application of hydrophilic polymers and organic surfactants in combination with perfluoroether oil components provides for rTSP products that display both effective barrier properties and practical removability. It is recommended that the levels of the different rTSP matrix materials be systematically varied to achieve the optimal combination of CWA barrier, detoxification rate and removability characteristics.

2.2.6 CWA Simulant Barrier Properties of Experimental rTSP Films

The CWA barrier properties of experimental TSPs were tested by applying the skin cream formulations over polyurethane sheets, exposing the coated-sides to specific quantities of different CWA simulants and analyzing for CWA penetration. Simulants for chemical warfare

agents were used to test the ability of the proposed coatings to block chemical transmission.¹⁰ The transmission testing was conducted according to a literature procedure that measures chemical penetration through a film of the TSP applied over a chemical indicator paper. Control films such as PTFE powder in perfluoroether oil were used as controls. The proposed films should slow the penetration of CWAs to allow reaction with the formulated decomposition agents and target permeability values should reside between unprotected indicator paper and the substrate coated with Teflon powder-filled TSP controls.

The experimental and control formulations were applied to C8 Chemical Agent Detector paper using a film drawdown blade. The nominal thickness of the films was 0.15 mm. The films appeared uniform and were easily spread over the paper substrate. The decomposition additive-filled experimental formulations were typically brown-tan color while the control had very little color and appeared translucent.

Microdrops (8 μ L) of diethyl ethylphosphonate (DEEP), a simulant for GB, 2-chloroethyl ethyl sulfide (CEES), a simulant for HD, and Malathion a simulant for VX were applied to the film surfaces in triplicate and their ability to penetrate through to the indicator paper monitored. The results are summarized in Table 6.

Table 6
CWA Simulant Barrier Properties of Experimental rTSP Formulations

Formulation ID	Time to Penetrate (minutes)		
	DEEP	Malathion	CEES
Control	> 360	> 360	> 360
JD4-191	> 360	NT	> 360
JD5-123	NT	30	30
JD5-129	NT	45	90
JD5-134	NT	60	120

The CWA simulant penetrant testing suggests that the level of perfluoroether oil additive significantly alters the chemical barrier properties of experimental rTSP films. Conversely, the level of hydrophilic components such as PVP and organic surfactants allow increased transmission of these agents. By balancing the levels of these TSP matrix components and reactive additives, a rTSP product with the ability to both prevent CWA transmission and actively detoxify these toxic agents within the film can be formulated.

2.2.7 CWA Simulant Decomposition Testing of Experimental Skin Cream Films

The ability of the proposed skin cream coatings to actively decontaminate different CWA simulants was tested by the head space concentration method. Coated polyurethane film samples are exposed to a carefully measured amount of simulant for a specified period of time in a closed container. The headspace of the closed system is periodically sampled and analyzed by gas chromatography (GC) for quantitative reduction of the target CWA simulants. The majority of the experiments was conducted at body temperature (37°C) or slightly above to better simulate application conditions.

Three different CWA simulants, namely diethyl ethylphosphonate (DEEP), a simulant for GB; chloroethyl ethyl sulfide (CEES), a simulant for mustard vapor; and Malathion which is a simulant for the nerve agent VX were used for the skin cream coating decontamination testing.

2.2.7.1 Decomposition Chemistry for Selected CWA Simulants

The primary modes of CWA simulant decomposition explored in this feasibility study for experimental reactive TSPs included base-catalyzed hydrolysis, oxidation, and nucleophilic attack by basic inorganic oxides. For Malathion, a thiophosphoryl-based insecticide, and a simulant for VX CWA, the simple base-catalyzed ester hydrolysis reaction is illustrated in Figure 6.

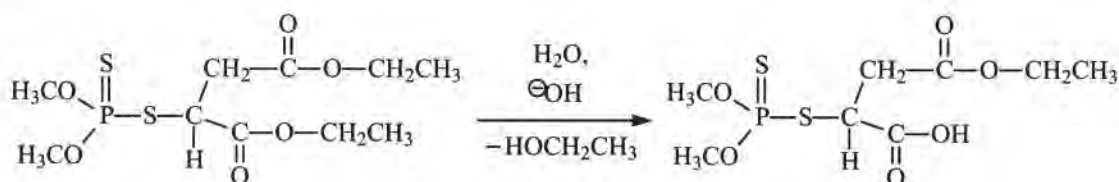


Figure 6 Base-catalyzed hydrolysis of VX simulant Malathion

Malathion is known to undergo this reaction rapidly in the environment.¹² Other possible hydrolysis reactions include attack at phosphorus yielding P-O scission and loss of methanol and P-S scission leaving thiolate-functional esters and thiophosphoric acid-esters. These reactions are illustrated in Figure 7.

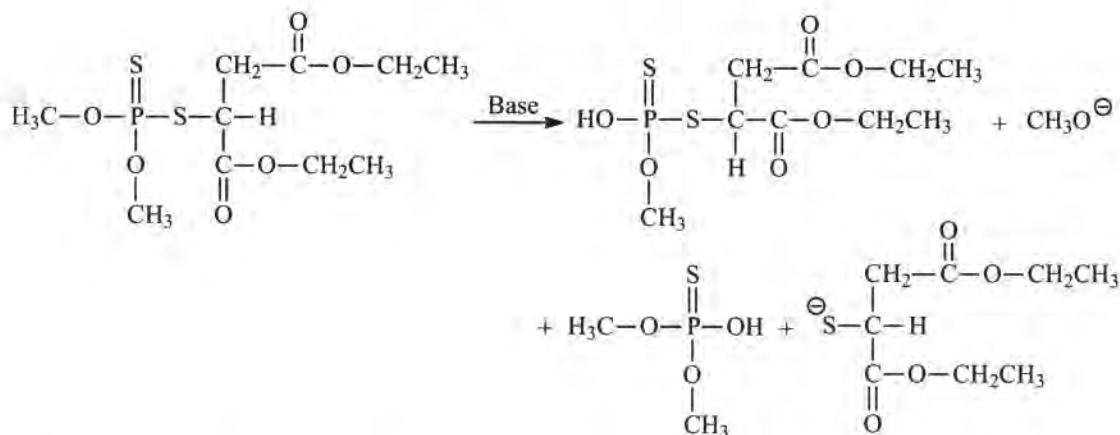


Figure 7 Secondary base-catalyzed hydrolysis of VX simulant Malathion

Scission of P-S bonds in VX has been demonstrated with acid catalysis and oxidative agents such as chloramines B.⁴ Care must be taken in using this mechanism as the sole means of detoxification since it has been shown that some VX oxidation byproducts can also be quite toxic. Oxidative and hydrolytic degradation are also possible means of removing HD. The base-catalyzed hydrolysis of HD simulant chloroethylethyl sulfide (CEES) is illustrated in Figure 8.

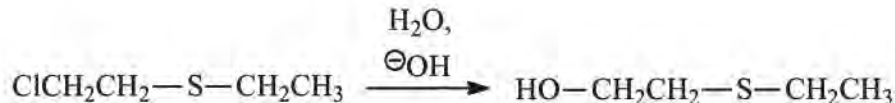


Figure 8 Base-catalyzed hydrolysis of HD simulant chloroethylethyl sulfide (CEES)

This reaction may be better described as a hydroxide ion nucleophilic displacement. The sulfide link in this compound is also susceptible to oxidation. Peroxygen- and persulfate-based oxidizers have been used to oxidatively detoxify HD.⁴ The oxidation of HD simulant chloroethylethyl sulfide (CEES) is illustrated in Figure 8.

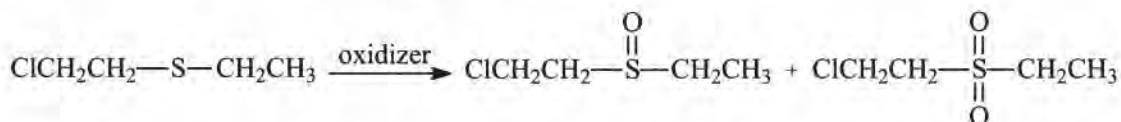


Figure 9 Oxidation of HD simulant chloroethylethyl sulfide (CEES)

The high reactivity of fluorophosphate-based CWAs such as GD towards nucleophilic attack allows them to be hydrolyzed with water, base and hypochlorite, defluorinated with nucleophilic organic compounds such as sodium 2-nitro-4 iodoxybenzoate, or reacted with high surface area alkaline metal oxides such as calcium oxide.⁴ The simple base-catalyzed hydrolysis of GD simulant diisopropylmethyl fluorophosphates is illustrated in Figure 10.

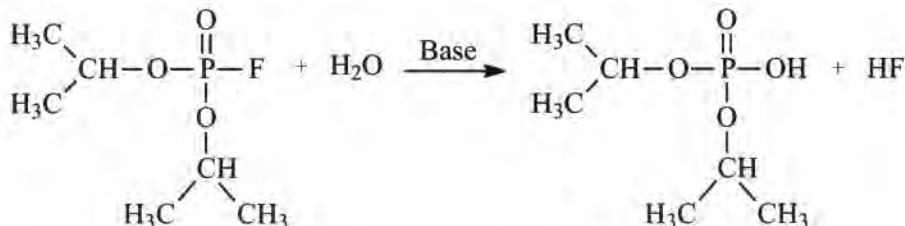


Figure 10 Base-catalyzed hydrolysis of GD simulant diisopropylmethyl fluorophosphate (DIFP)

The proposed rTSPs should maintain a high level of water in their structures and thus should provide rapid hydrolysis of fluorophosphate-based CWAs.

2.2.7.2 Decomposition Testing of CWA Simulants with Experimental rTSPs

The ability of the experimental skin cream coatings to actively decontaminate different CWA simulants was tested. Coated polyurethane film samples were exposed to a carefully measured amount of simulant for a specified period of time in a closed container. The headspace of the closed system was periodically sampled and analyzed by gas chromatography (GC) for quantitative reduction of the target CWA simulants. The surrogate CWA compounds used in

this study were: HD simulant chloroethylethyl sulfide (CEES), GB simulant diethyl ethylphosphonate (DEEP), and VX simulant Malathion.

DEEP Decontamination Test Results for Formulations JD5-70A and JD5-70B

Samples of formulations JD5-70A and JD5-70B were applied to the polyurethane sheet specimens and tested within one hour (wet condition) for ability to degrade DEEP simulant. The samples and control (empty vial) were challenged with 60µl of DEEP. This amount was found to produce a saturated vapor phase under these conditions. The time-zero points were collected at ambient temperature (20-22°C) immediately after adding the DEEP to the vial. The vials were then held at 40°C for all additional head space sampling. A graph of the DEEP headspace level in terms of CG peak height over time at 40°C for the different test conditions is shown in Figure 11.

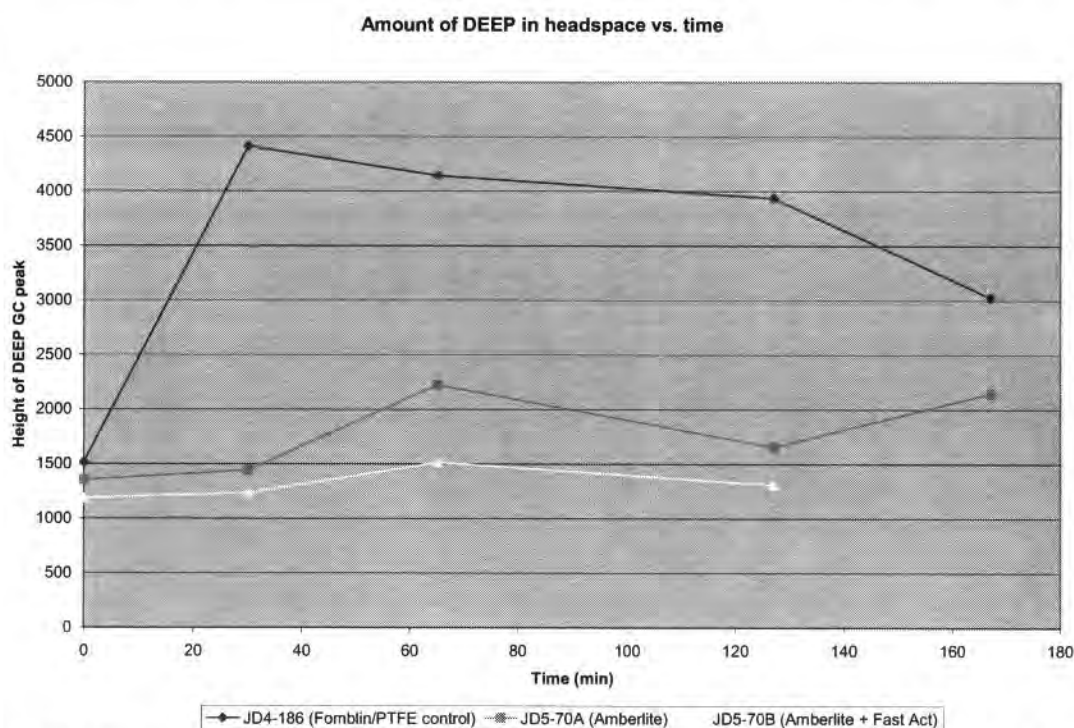


Figure 11 Effect of skin cream formulation composition and aging on the degradation of CWA simulant DEEP

The headspace analysis results for the two experimental formulations suggested significant activity in degrading the DEEP simulant when tested within an hour of skin cream film application. The JD5-70B formulation, which contained a blend of micronized ion exchange resin with nano-scale metal oxides, appeared to yield the best results for degrading the DEEP simulant although more testing would be needed to prove this statistically. In Phase II, a more reactive simulant for GB such as diisopropylfluorophosphonate (DIFP) should be used to optimize the detoxifying activity of the new rTSP formulations.

CEES Decontamination Screening Test Results for Formulations JD5-70A and JD5-70B

Two different test conditions were used to evaluate the decontaminating properties of formulations JD5-70A and JD5-70B compared to an empty vial control. In one case, the skin cream formulations were applied over the polyurethane substrate and allowed to dry in air for 16 hours before applying the simulant. In the second case, the formulations were applied over the polyurethane and the simulant added after about 30 minutes of dry time.

Samples of formulations JD5-70A and JD5-70B were applied to the polyurethane sheet specimens and tested within one hour (wet condition) and after drying in air at room temperature for 16 hours (dry condition) for ability to degrade CEES, a simulant for mustard. The samples and control (empty vial) were challenged with 5 μ l of CEES. This amount was found to produce a saturated vapor phase under these conditions. The time zero points were collected at ambient temperature (20-22°C) immediately after adding the CEES to the vial. The vials were then held at 40°C for all additional head space sampling. A graph of the CEES headspace level in terms of CG peak height over time at 40°C for the different test conditions is shown in Figure 12.

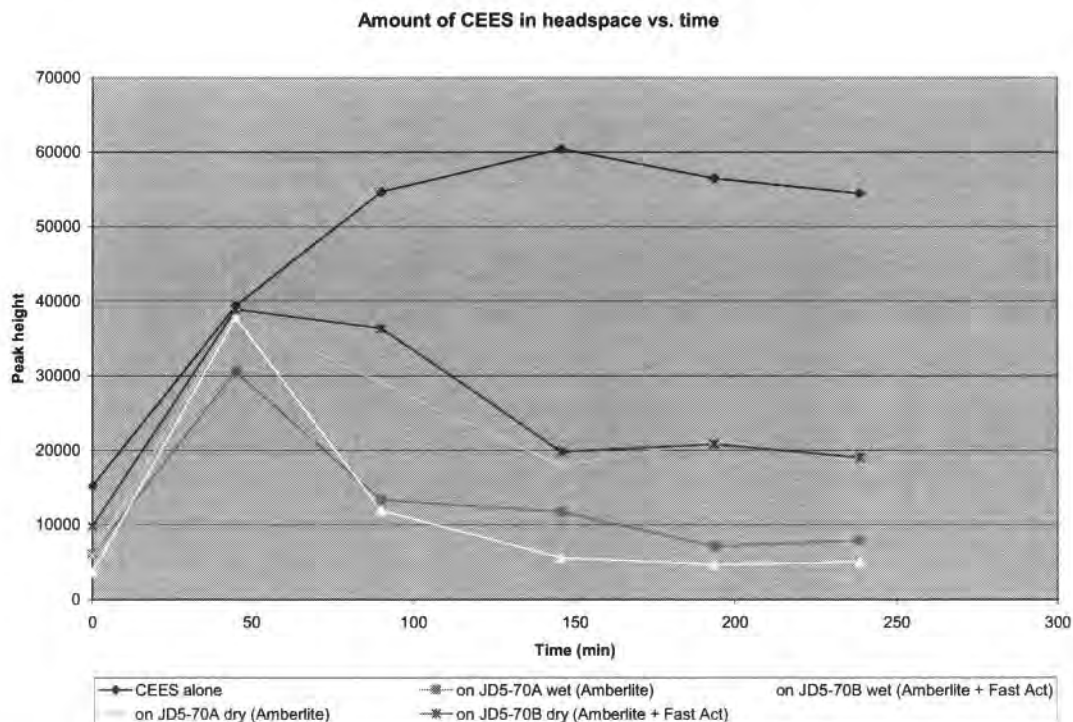


Figure 12 Effect of skin cream composition and film age on the degradation of CWA simulant CEES

The headspace analysis results suggested that the two experimental formulations actively removed the CEES simulant. The JD5-70A and JD5-70B formulations, which contained micronized ion exchange resin and a blend of this with nano-scale metal oxides respectively as the principle active ingredients appeared to degrade the CEES more readily when freshly applied than when tested after 16 hours of drying on the polyurethane substrate. The presence of water

in the films may assist in the hydrolysis rate of the CEES. In practice, the films would presumably be continuously rehydrated by contact with the skin through normal perspiration. More testing would be required to determine which of the two formulations was more effective against this family of CWA compounds.

CEES Decontamination Test Results for Formulations JD5-94A and JD5-111

Samples of formulations JD5-94C and JD5-111 were applied to the polyurethane sheet specimens and tested within one hour (wet condition) for ability to degrade CEES simulant. Formulation JD5-94C is a control consisting of the non-active components such as PTFE, fluorinated and non-fluorinated surfactants, and PVP. Formulation JD5-111 employs the same matrix with Chloramine-B additive. The time-zero points were collected at ambient temperature (20-22°C) immediately after adding the DEEP to the vial. The vials were then held at 40°C for all additional head space sampling. The samples were challenged with 5µl of CEES. The time zero points were collected at ambient temperature (20-22°C) immediately after adding the CEES to the vial. The vials were then held at 40°C for all additional head space sampling. A graph of the CEES headspace concentration obtained from standardization experiments over time at 40°C for the different test conditions is shown in Figure 13. Each point on the graph represents the average of three experimental measurements.

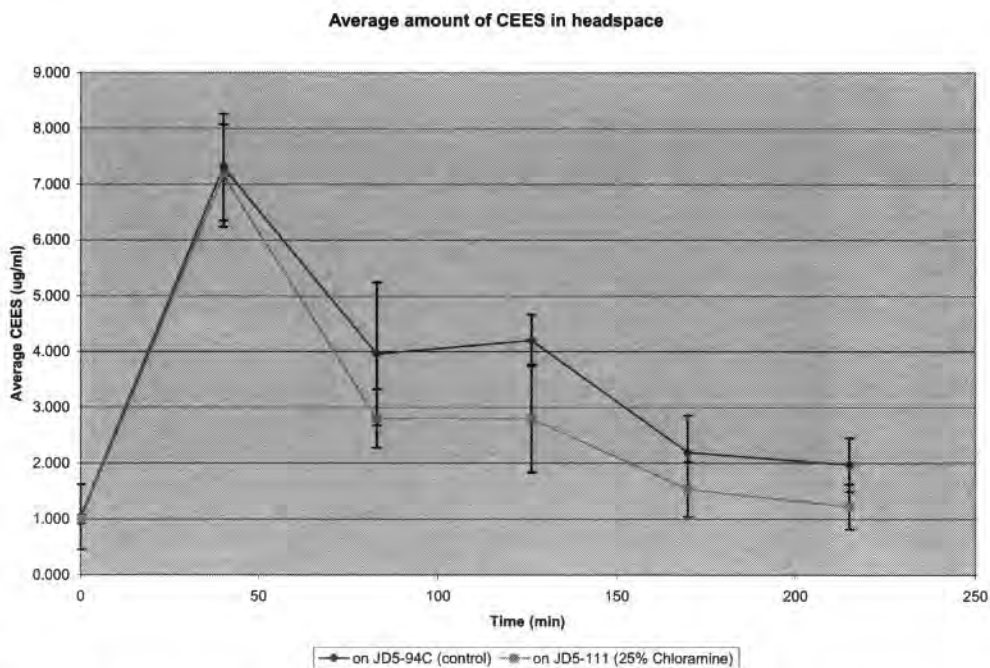


Figure 13 Effect of oxidizing additives on the degradation of CWA simulant CEES

The two experimental formulations showed significant activity in degrading the CEES simulant. Since no ion exchange resins were used in either formulation, the removal of the CEES compound most likely does not result from a simple absorption effect. The JD5-111 formulation, which contains the oxidizing agent Chloramine-B, and JD5-111 formulations,

appeared to degrade the CEES more readily and completely than the unmodified JD5-94C sample. The presence of water in both of the films may assist in the hydrolysis rate of the CEES. In practice, the films would presumably be continuously rehydrated by contact with the skin through normal perspiration. The CEES-degrading activity of a formulation containing both hydrolysis-promoting basic ion exchange resins and mild oxidants was also tested. These results are shown in Figure 14.

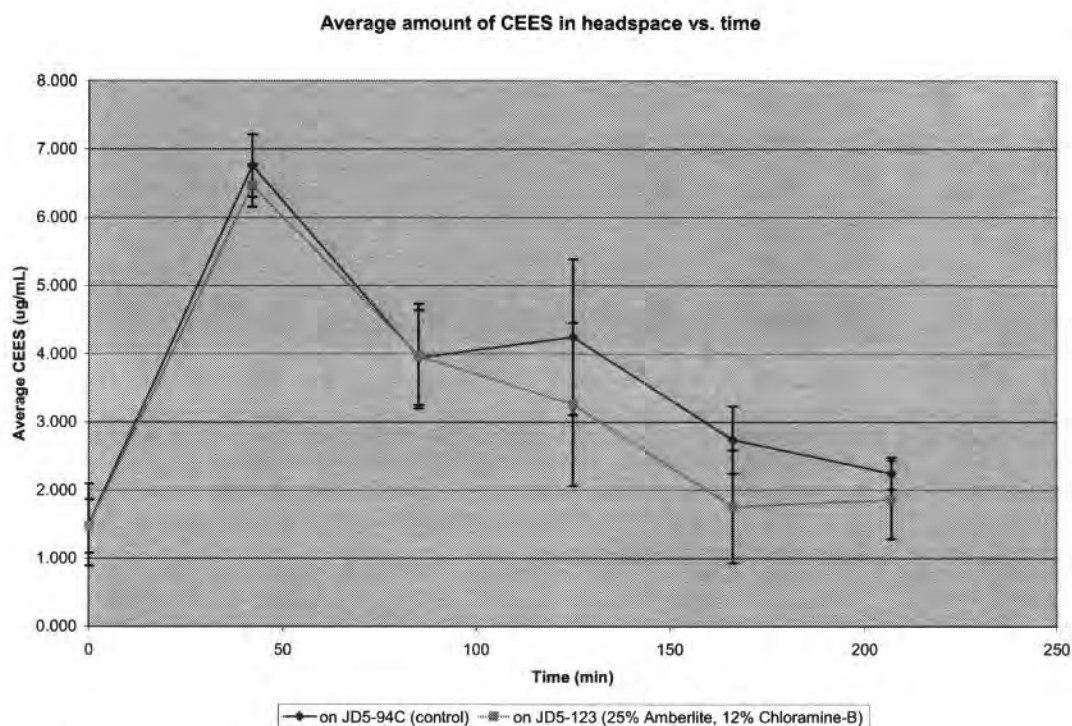


Figure 14 Effect of ion exchange and oxidizing additives on the degradation of CWA simulant CEES

The same types of experimental rTSPs were tested for efficacy with the VX simulant Malathion.

Malathion Simulant Decontamination Screening Test Results for Formulations JD5-70A and JD5-70B

The samples and control (empty vial) were challenged with 20 μ l of Malathion. The time zero points were collected at ambient temperature (20-22°C) immediately after adding the Malathion to the vial. The vials were then held at 37°C for all additional head space sampling. A graph of the Malathion headspace level in terms of CG peak height over time at 37°C for the different test conditions is shown in Figure 15.

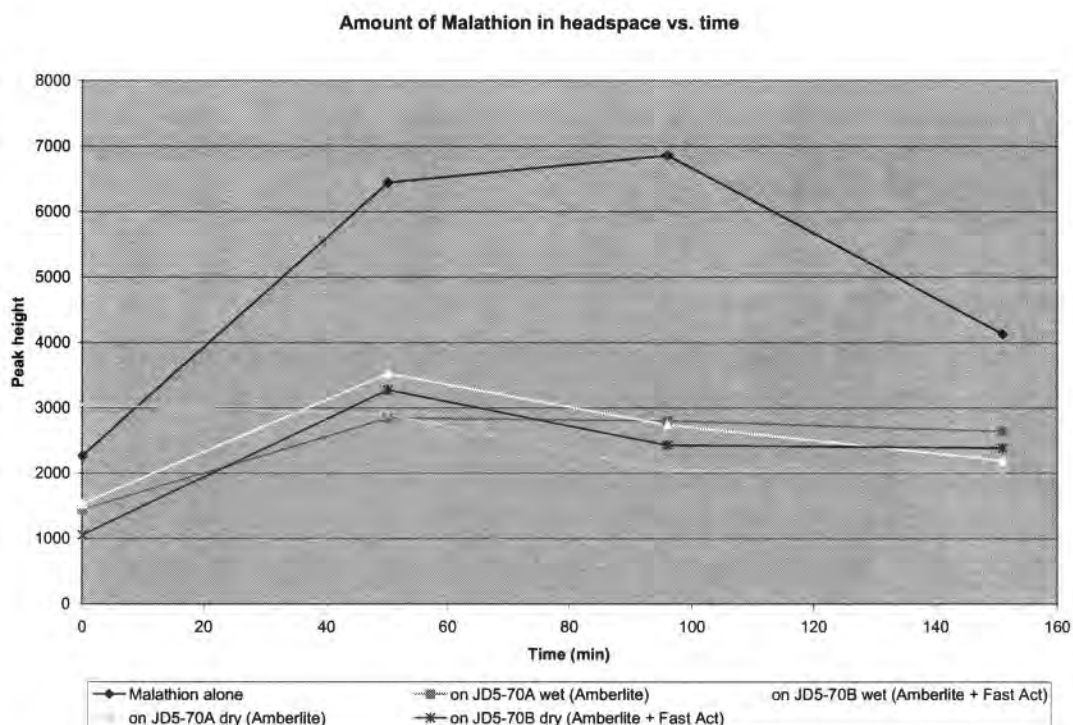


Figure 15 Effect of skin cream formulation composition and film age on the degradation of CWA simulant Malathion

The two skin cream formulations JD5-70A and JD5-70B both appeared to rapidly degrade the Malathion with respect to the control condition. The reactivity of the experimental skin creams did not seem to be significantly affected by the presence of water in the films as the air-dried samples showed comparable Malathion-degrading activity. The JD5-70A formulation, which contained micronized ion exchange resin as the principle active ingredient appeared to have a slight latency period when tested after 16 hours of drying on the polyurethane substrate. This sample showed excellent Malathion-degrading reactivity after exposure to the 37°C reaction condition. More testing is required to determine which of these formulations is more effective against this family of CWA compounds.

These experiments were continued to study the behavior of the coatings in further reducing the concentration of this simulant. Additional formulation work was performed to isolate the effects of the different reactive additives as well as the addition of perfluoroether oil additive for increased barrier protection. Also, the testing of the Malathion simulant detoxification was conducted in triplicate treated in order to obtain more statistically meaningful product performance measures.

Malathion Decontamination Test Results for Formulations JD5-94C and JD5-94A

Samples of formulations JD5-94C and JD5-94A were applied to polyurethane sheet specimens and tested within one hour (wet condition) for ability to degrade Malathion simulant.

Formulation JD5-94C is a control consisting of the non-active self-stratifying TSP components and JD5-94A employs the same matrix with micronized basic ion exchange resins. The samples and control (empty vial) were challenged with 20 μ l of Malathion. The time zero points were collected at ambient temperature (20-22°C) immediately after adding the Malathion to the vial. The vials were then held at 37°C for all additional head space sampling. A graph of the Malathion headspace level in terms of CG peak height over time at 37°C for the different experimental rTSPs is shown in Figure 16. Each point on the graph represents the average of three experimental measurements.

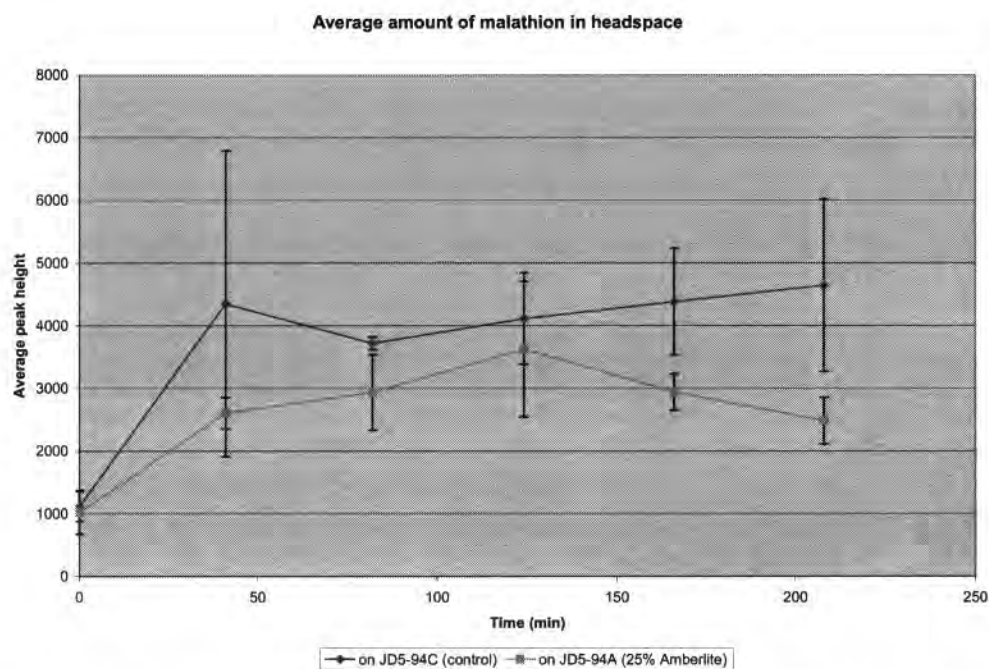


Figure 16 Effect of ion exchange additives on the degradation of CWA simulant Malathion by experimental water-based rTSPs

The JD5-94A appeared to consistently remove more of the Malathion with respect to the control formulation, JD5-94C. The quantification of Malathion headspace concentration as it relates to GC peak height was attempted but insufficient separation between Malathion and any of the solvents used for serial dilution precluded calibration curve creation. The general Malathion-degrading activity of formulations containing both hydrolysis-promoting basic ion exchange resins and mild oxidants were also tested in triplicate for more statistically significant comparisons to TSP controls.

Malathion Decontamination Test Results for Formulations JD5-94C and JD5-123

Samples of formulations JD5-94C and JD5-123 were applied to polyurethane sheet specimens and tested within one hour (wet condition) for ability to degrade Malathion simulant. Formulation JD5-94C is a non-reactive control consisting of the non-active self-stratifying TSP

components while JD5-123 employs micronized alkaline ion exchange resins and Chloramine-B in the same matrix. The performance against CWA simulant Malathion is shown in Figure 17.

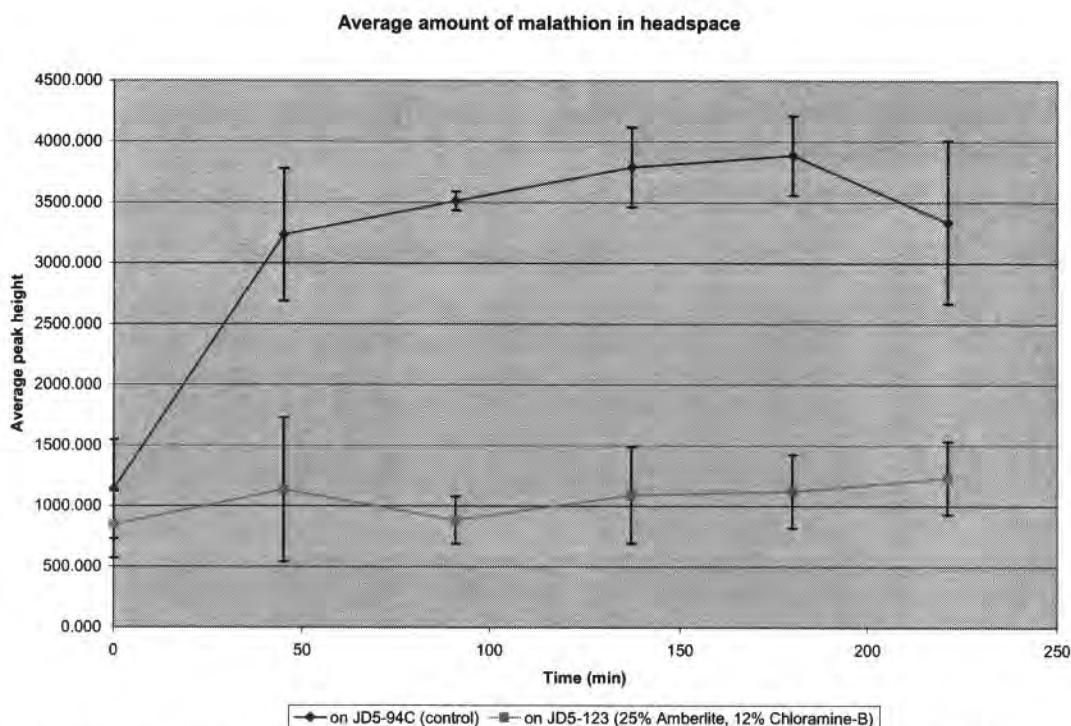


Figure 17 Effect of ion exchange and oxidizing additives on the degradation of CWA simulant Malathion

The JD5-123 formulation appeared to consistently remove more of the Malathion with respect to the control formulation, JD5-94C. The combination of basic ion exchange resin microparticulate and Chloramine-B additives appeared to out perform both the control and the JD5-94A formulation, which was filled with the ion exchange resin alone. The effect of adding perfluoroether oil to the JD5-123 formulation on Malathion removal was also explored.

Malathion Decontamination Test Results for Formulations JD5-94C and JD5-129

Samples of formulations JD5-94C and JD5-129 were applied to polyurethane sheet specimens and tested within one hour (wet condition) for ability to degrade Malathion simulant. Formulation JD5-94C is a non-reactive control consisting of the non-active self-stratifying TSP components while JD5-129 employs micronized alkaline ion exchange resins, Chloramine-B and perfluoroether oil in the same matrix. The performance against CWA simulant Malathion is shown in Figure 18. Each point on the graph represents the average of three experimental measurements.

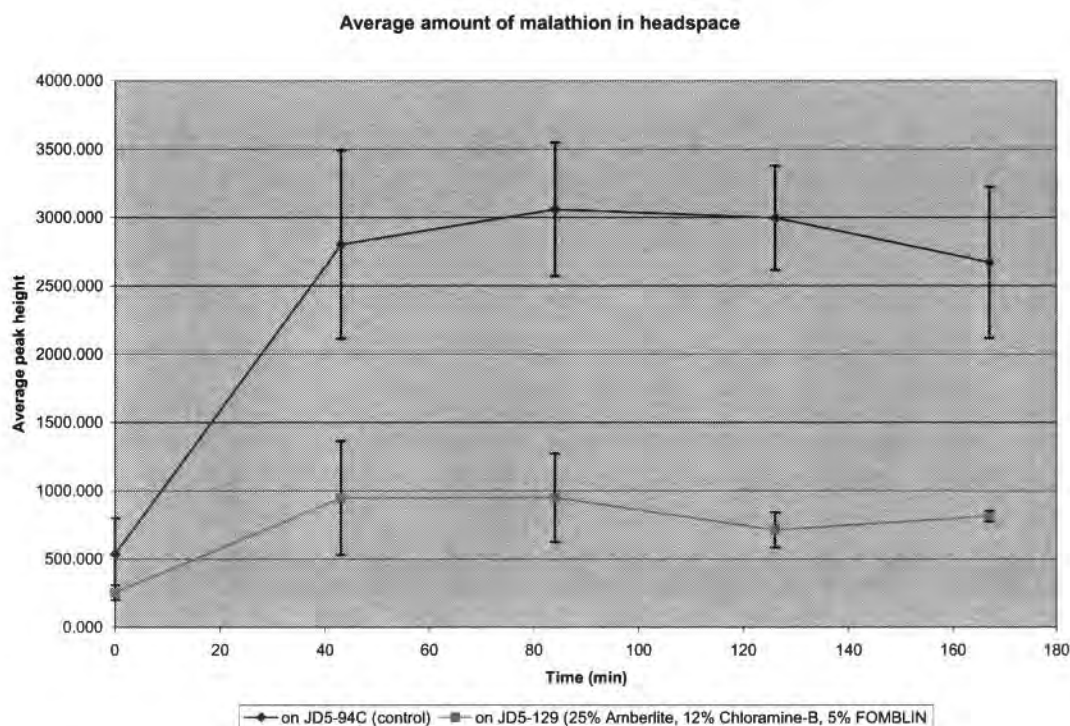


Figure 18 Effect of ion exchange, oxidizing, and perfluoroether oil additives on the degradation of CWA simulant Malathion

The JD5-129 formulation appeared to consistently remove more of the Malathion with respect to the control formulation, JD5-94C. The addition of perfluoroether oil to the JD5-123 formulation, which contained basic ion exchange resin microparticulate and Chloramine-B additives appeared to have no effect on Malathion removal. This is an important finding since the final rTSP products will most likely need to contain this inert additive for controlling CWA penetration through the applied skin creams.

2.2.7.3 CWA Simulant Degradation Product Analysis

The products and intermediates of the rTSP-promoted CWA simulant decomposition testing were characterized by GC and FTIR spectroscopy. rTSP-coated aluminum film samples JD5-129 were exposed to a carefully measured amount of simulant for a specified period of time in a closed container. The coatings are applied to the aluminum sheet using a wet film drawdown blade having a gap of 0.050 in. After different dwell times, the simulant-challenged films were removed and immediately exposed to the surface of a zinc selenide MIR crystal and analyzed by FTIR. These spectra were compared to those obtained from aqueous base/hydrogen peroxide-promoted hydrolysis and oxidation of Malathion. The overlaid spectra of the reaction product from Malathion with basic hydrogen peroxide solution and that obtained from Malathion applied to a coating film of experimental rTSP JD5-129 are shown in Figure 19.

3.0 KEY RESEARCH ACCOMPLISHMENTS

The important observations and results of this feasibility study on new CWA-degrading, skin barrier creams technology for protecting military personnel on the chemical battlefield are:

- New reactive skin cream formulations were successfully formulated as water-thinned suspensions of commodity surfactants, resins, reactive additives and fluoropolymers.
- Experimental skin cream formulations have shown efficacy in the decomposition of three different CWA simulants, namely diethyl ethylphosphonate (DEEP), a simulant for GB, chloroethyl ethyl sulfide (CEES), which is a simulant for mustard vapor (HD) and Malathion which is a simulant for nerve agents GB and GA.
- Ball milling ion exchange resins with ceramic media in the presence of surfactants appears to be an effective means of reducing the resin particles to a size compatible with a skin cream product.
- Alkaline ion exchange resins appear to have the greatest positive effect on the skin cream's ability to degrade hydrolysable CWA simulants.
- rTSP formulations prepared with a oxidative chloro amide additive promote degradation of HD simulant CEES.
- rTSP formulations prepared with micronized alkaline ion exchange resin additives promote degradation of VX simulant Malathion.
- The ability of the experimental rTSP formulations to decompose different CWA simulants was found to depend on the level of micronized ion exchange resin fillers.
- Formulations based on physiologically inert polymers and ionic surfactants displayed self-assembling properties as inferred by surface FTIR analysis.
- The hydrophilic polymer additive PVP was found to preferentially absorb onto a polar substrate and away from the air-coating interface from a rTSP formulation.
- Fluorocarbon-rich components of the experimental rTSP formulations were found to favor the film-air interface.
- The level of perfluoroether oil additive could be used to modulate the barrier properties of the experimental water-based rTSPs against CWA simulant penetration.
- The level of perfluoroether oil additive could be used to reduce water sensitivity of the experimental water-based rTSPs and provide stable, cleanable films.
- Formulation and processing variables were identified for optimizing the rTSP products.

4.0 REPORTABLE OUTCOMES

Cape Cod Research personnel were trained in the handling and analysis of highly toxic chemicals. The firm plans to seek further financial support for developing alternative CWA decontaminating technology based on the results of this feasibility study.

5.0 CONCLUSIONS

The primary objective of the Phase I research program was to demonstrate the feasibility of developing an easily applicable skin cream that prevents chemical warfare agents (CWAs) from penetrating to the skin as well as actively detoxifying the agents. The Phase I experimental approach involved the identification and feasibility testing of new barrier cream systems for limiting chemical warfare agent (CWA) penetration and decomposing absorbed toxins to non-harmful compounds. The experimental work focused on screening potential self-assembling resin systems and reactive additives for formulating topical skin protectant (TSP) creams with the necessary properties for rapidly decomposing CWAs and providing the simple application properties required for skin protective products. Skin cream formulations based on blends of micronized ion exchange resins, nano-sized metal oxides, hydrolysis catalysts, PTFE powder and a blend of surfactants and resins were prepared and shown to possess CWA detoxifying properties.

A system that met many of these goals was successfully demonstrated and could be an enabling technology in the development of a comprehensive protective system for military personnel exposed to these toxic agents. The new rTSPs showed the ability to be applied like a commercial skin cream product, possessed controllable levels of CWA simulant barrier properties, provided multi-agent decomposition capacity, and could be effectively removed from surfaces with soap and water.

A Phase II program is recommended to explore variations in composition and application of the new CWA protective skin cream formulations. Specific efforts in this developmental program would include:

- Establishment of material processing parameters for optimizing the critical components of the proposed CWA-degrading skin cream system.
- Optimization of polymeric components, surfactants, fluoropolymer barrier materials, micronized ion exchange resins, and nano-scale metal oxide particulates and formulation to achieve specified CWA-degrading and barrier properties
- Development of CWA degrading agents engineered to concentrate in outer layers of a self-stratifying rTSP film
- Demonstrate the ability to reduce the penetration and actively degrade more reactive CWA simulants such as diisopropylfluorophosphate (DIFP).

- Optimization of skin cream formulation process to yield uniform products for facile application in the field.
- Demonstration the ability to apply the rTSPs in a manner compatible with practical and accepted soldier field operations
- Demonstrate the ability to safely remove rTSPs in a manner compatible with battlefield operations
- Validation of efficacy of optimized rTSP formulations using actual CWAs
 - Demonstration of *in vitro* performance of rTSPs using chronic barrier and head space testing
 - Demonstration of *in vivo* performance of rTSPs using animal skin exposure and acetylcholinesterase inhibitor tests
- Demonstration that the rTSP coatings that have been challenged with CWAs or simulants can be effectively removed without exposing skin to harmful chemicals.
- Demonstration of the durability of applied rTSPs in terms of resistance to sweat, sunscreen, insect repellent, and incidental contact.
- Development of a production plan for optimized rTSP products

6.0 REFERENCES

1. "US Army Grants DPT Labs License for Topical Skin Cream," San Antonio Business Journal, November, 2002, www.bizjournals.com/sanantonio.
2. Schactman, N., "Army Brews Potions that Protect," Wired News, January, 2003, www.Wirednews.com/news/print.
3. Decontamination 660 AD, Virtual Naval Hospital, www://vnh.org/CHEMCASU/08Decontamination
4. Yang, Y.-C., Baker, J. A., Ward, J. R., *Chem. Rev.*, **92**, 1729-1743, 1992.
5. Braue, E. H, Jr., *J. Applied Toxicology*, **19**, S47-S53, 1999.
6. Hobson, S. T., Lehnert, E. K., and Braue, E. H, Jr., *Mat. Res. Symp. Proc.*, Vol. **628**, CC108.1, Materials Research Soc., 2000
7. Hobson, S. T., Braue, E. H., Shea, K., "Active Topical Skin Protectants Using Hybrid Organic Polysilisesquioxane Materials," U. S. Patent No. 6,417, 336 B1, July 9, 2002.
8. Lochhaas, K. H., Thunemann, A. F., Antonietti, M., *Surface Coatings International*, **9**, 451-455, 1999.
9. Edwards, J. O., Ruggero, C., "Fenton Type Activation and Chemistry of Hydroxyl Radical," Ch. 4 in Catalytic Oxidations with Hydrogen Peroxide as Oxidant, p. 126, Strukul, G., Ed., Kluwer Acad. Pub., Dordrecht, The Netherlands, 1992.
10. Lewis, R. E., Liebman, S.A., Grasso, P. S., Sarver, E. W., "Chemical Agent Simulants for Testing Transparent Materials," DTIC Report No. AD-A197-138, May, 1988.
11. "Multiple Internal Reflection Accessory Instructions," Perkin Elmer Instruments, Doc. No. 0186-0799, Shelton, CT, 1987
12. Corbridge, D.E.C., Ch. 6 in Phosphorus, An Outline of Its Chemistry, Biochemistry, and Technology, pp. 574-581, Elsevier, Amsterdam, the Netherlands, 1995.
13. Silverstein, R. M., Bassler, G. C., and Morrill, T. C, in Spectrometric Identification of Organic Compounds, 4th Ed., p131-132, John Wiley & Sons, New York, 1981.

APPENDIX A

Fourier Transform Infrared Spectra

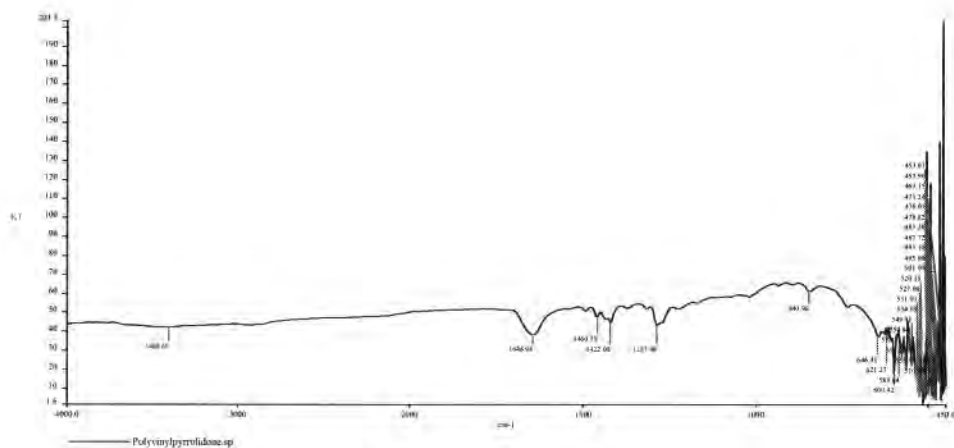


Figure A1 FTIR (MIR) spectrum of PVP applied to aluminum foil

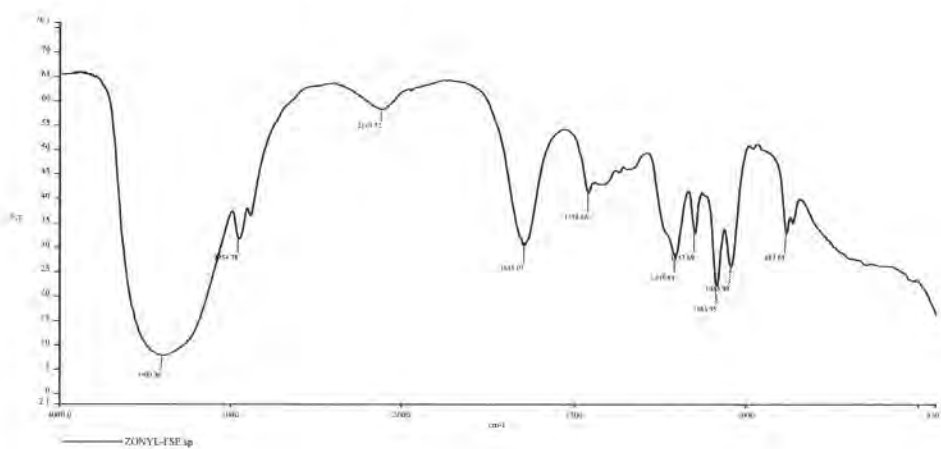


Figure A2 FTIR transmission mode spectrum of fluoroalkyl phosphate surfactant (Zonyl FSE)

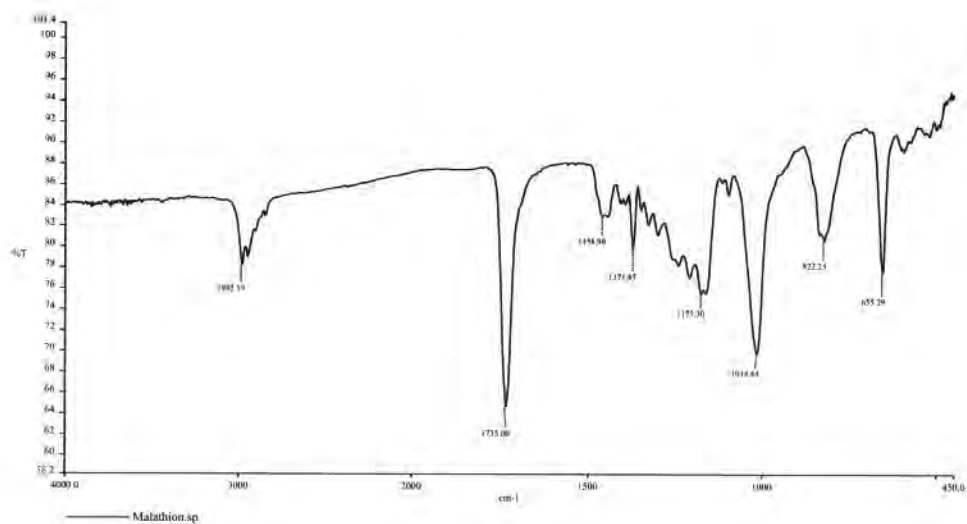


Figure A3 FTIR (MIR) spectrum for Malathion

APPENDIX B

Hazards and Safety

Hazards and Safety Issues with New rTSP Materials

The hazards associated with the new skin screen materials are considered low in terms of toxicological effects. The basic ion exchange resins, when micronized and in the dry state should not be inhaled, ingested, or exposed to the skin. After formulation with surfactants and perfluorinated oils, this hazard should be significantly reduced. The primary mode of entry would be expected to be through vapor inhalation and absorption through the skin. Exposure of personnel to toxic substances shall not be in excess of the threshold values contained in the American Conference of Government Industrial Hygienists Threshold Limit Values. The limits for these materials will be calculated according to the environment within which they are expected to be used. Appropriate precautionary procedures, safety equipment and clothing will be specified.

SBIR final report from Eltron Research, Inc., Phase I

Award Number: DAMD17-99-C-9007

AD _____

Award Number: DAMD17-99-C-9007

TITLE: Polyoxometalates as Topical Skin Protectants

PRINCIPAL INVESTIGATOR: James H. White

CONTRACTING ORGANIZATION: Eltron Research, Incorporated
Boulder, Colorado 80301

REPORT DATE: June 1999

TYPE OF REPORT: Final, Phase 1

PREPARED FOR: U.S. Army Medical Research and Materiel Command
Fort Detrick, Maryland 21702-5400

DISTRIBUTION STATEMENT: Distribution authorized to U.S. Government agencies only (specific authority). Other requests for this document shall be referred to U.S. Army Medical Research and Materiel Command, 504 Scott Street, Fort Detrick, Maryland 21702-5012

The views, opinions and/or findings contained in this report are those of the author(s) and should not be construed as an official Department of the Army position, policy or decision unless so designated by other documentation.

REPORT DOCUMENTATION PAGE

Form Approved
OMB No. 0704-0188

Public reporting burden for this collection of information is estimated to average 1 hour per response, including the time for reviewing instructions, searching existing data sources, gathering and maintaining the data needed, and completing and reviewing the collection of information. Send comments regarding this burden estimate or any other aspect of this collection of information, including suggestions for reducing this burden, to Washington Headquarters Services, Directorate for Information Operations and Reports, 1215 Jefferson Davis Highway, Suite 1204, Arlington, VA 22202-4302, and to the Office of Management and Budget, Paperwork Reduction Project (0704-0188), Washington, DC 20503.

1. AGENCY USE ONLY (Leave blank)

2. REPORT DATE
June 1999

3. REPORT TYPE AND DATES COVERED
Final, Phase I (18 Dec 98 - 17 Jun 99)

4. TITLE AND SUBTITLE
Polyoxometalates as Topical Skin Protectants

5. FUNDING NUMBERS
DAMD17-99-C-9007

6. AUTHOR(S)
James H. White

7. PERFORMING ORGANIZATION NAME(S) AND ADDRESS(ES)
Eltron Research, Incorporated
Boulder, Colorado 80301

8. PERFORMING ORGANIZATION
REPORT NUMBER

9. SPONSORING / MONITORING AGENCY NAME(S) AND ADDRESS(ES)
U.S. Army Medical Research and Materiel Command
Fort Detrick, Maryland 21702-5012

10. SPONSORING / MONITORING
AGENCY REPORT NUMBER

11. SUPPLEMENTARY NOTES

12a. DISTRIBUTION / AVAILABILITY STATEMENT
Authorized to U.S. Government agencies only (specific authority)

12b. DISTRIBUTION CODE

13. ABSTRACT (Maximum 200 words)

This program was directed at the development of reactive topical skin protectants (rTSP) using polyoxometalates (POM) as catalytic reactive moieties. The approach relied on the activity of POM for the selective conversion of simulated vesicants and other organosulfides to innocuous forms, e.g., sulfoxides. Such an approach is anticipated useful in the decontamination of chemical warfare agents (CWA) incident upon U.S. troops in battlefield scenarios involving the use of CWA. The approach was verified by the activity of catalysts in both aqueous environments as well as in skin creams. Results point to preferred catalysts as well as to the superiority of hydrogen peroxide as oxidant. Cerium oxide support of POM appeared to greatly enhance POM activity in skin cream.

14. SUBJECT TERMS

Polyoxometalates, chemical warfare agents, vesicants,
oxidation, catalysts

15. NUMBER OF PAGES
29

16. PRICE CODE

17. SECURITY CLASSIFICATION
OF REPORT
Unclassified

18. SECURITY CLASSIFICATION
OF THIS PAGE
Unclassified

19. SECURITY CLASSIFICATION
OF ABSTRACT
Unclassified

20. LIMITATION OF
ABSTRACT
Limited

FOREWORD

Opinions, interpretations, conclusions and recommendations are those of the author and are not necessarily endorsed by the U.S. Army.

____ Where copyrighted material is quoted, permission has been obtained to use such material.

____ Where material from documents designated for limited distribution is quoted, permission has been obtained to use the material.

____ Citations of commercial organizations and trade names in this report do not constitute an official Department of Army endorsement or approval of the products or services of these organizations.

____ In conducting research using animals, the investigator(s) adhered to the "Guide for the Care and Use of Laboratory Animals," prepared by the Committee on Care and use of Laboratory Animals of the Institute of Laboratory Resources, national Research Council (NIH Publication No. 86-23, Revised 1985).

____ For the protection of human subjects, the investigator(s) adhered to policies of applicable Federal Law 45 CFR 46.

____ In conducting research utilizing recombinant DNA technology, the investigator(s) adhered to current guidelines promulgated by the National Institutes of Health.

____ In the conduct of research utilizing recombinant DNA, the investigator(s) adhered to the NIH Guidelines for Research Involving Recombinant DNA Molecules.

____ In the conduct of research involving hazardous organisms, the investigator(s) adhered to the CDC-NIH Guide for Biosafety in Microbiological and Biomedical Laboratories.

 6/16/99
PI - Signature Date

TABLE OF CONTENTS

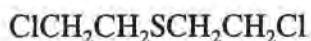
	<u>Page</u>
Report Documentation Page	2
Foreword	3
I. Introduction	4
II. Phase I Technical Objectives	4
III. Work Performed and Results Obtained	5
A. Task 1 - Synthesis and Characterization of Heteropolyacids	5
1. $H_5PMo_{10}V_2O_{40}$	5
2. $Na_7PTi_2W_{10}O_{40}^4$	8
3. $K_7PTi_2W_{10}O_{40}^4$	8
4. Synthesis of $(n\text{-Butyl}_4N)_4H_3PMo_{11}O_{39}$ (Product #1) ⁵	8
5. Synthesis of $(n\text{-Butyl}_4N)_4HPMo_{11}Cu(CH_3CN)O_{39}$	8
6. Synthesis of $(n\text{-Butyl}_4N)_4HPMo_{11}Co(CH_3CN)O_{39}$ ⁵	9
7. Synthesis of $(n\text{-Butyl}_4N)_4HPMo_{11}Zn(CH_3CN)O_{39}$ ⁵	9
8. Synthesis of $K_7PW_{11}O_{39} \cdot 12H_2O$ ⁶	9
9. Synthesis of $K_4PFe(OH_2)W_{11}O_{39} \cdot 14H_2O$ ⁶	9
10. Synthesis of $K_5PRh(OH)W_{11}O_{39} \cdot 11H_2O$	10
B. Task 2 - Evaluation of POM and Incorporation into Simulated Skin Creams	11
1. Analysis	11
2. Initial Gas Phase Experiments	11
3. Liquid Phase Screening	12

i)	Oxidation with Dioxygen	12
ii)	Oxidation by Hydrogen Peroxide	14
4.	Evaluation in Base Cream	16
i)	Pre-Assembly Preparations	16
ii)	Assembly Procedures	17
iii)	Assay Procedures	17
C.	Optimization of rTSP	18
D.	Evaluation of Barrier Effectiveness and Duration of POM-Based rTSP ..	19
IV.	Conclusions	24
A.	Summary of Phase I Results	24
B.	Conclusions	26
C.	Recommended Future Work	26
V.	References	27

I. INTRODUCTION

This project is directed towards the development of barrier skin creams containing a catalytic moiety for use as reactive topical skin protectants. The chemistry of the proposed approach is based on the use of polyoxometalates (POM) as catalysts for promoting the partial or complete oxidation of functionalities of chemical warfare and nerve agents. Potential military application would be in the destruction of chemical warfare agents - primarily vesicants such as sulfur mustard and lewisite. Of particular interest in this program are simulants such as methyl sulfide and chloroethylethyl sulfide, which present a functionality of mustard agents for characterization in partial oxidation of the sulfide moieties to sulfoxides. Mustard agents are rendered nontoxic by this partial oxidation. However, selectivity is critical, as the corresponding sulfones (doubly oxidized sulfide) is also highly toxic. The catalytic approach being pursued has solid literature support: selectivity of the order of 99% to the sulfoxide^{1,2} has been obtained in the oxidation of mustard analogs.

Base skin cream formulations have demonstrated the ability to substantially reduce percutaneous exposure and toxicity. However, the base cream still allows for a substantial permeation rate of vesicants such as dichlorodiethyl sulfide (sulfur mustard)



and permit the continued toxicity of these species subsequent to challenge by the agent. Consequently, the incorporation of a reactive species in the skin cream, whose purpose is to increase the decontamination efficacy of a TSP, appears to be necessary.

The approach proposed here relies on catalytic activity of a reactive moiety (in this case, a polyoxometalate). The other general category of reactive moieties are the stoichiometric kinds. These react only up to a stoichiometric ratio with a CWA. Consequently, such moieties are ineffective against liquid phase challenges of CWA and necessitate the use of catalytic species such as POM. Development of rTSP incorporating these catalysts is the goal of this overall program. The use of either oxygen (in air) or hydrogen peroxide as oxidant are possible. However, hydrogen peroxide would have to be continuously resupplied, probably by a chemical process occurring within the film. Consequently, we were quite interested in evaluating rTSP using dioxygen as the oxidant. Nevertheless, hydrogen peroxide at medicinal concentrations was found to rapidly oxidize organosulfides.

II. PHASE I TECHNICAL OBJECTIVES

The overall objective of this program was to experimentally verify the use of polyoxometalate catalysts, incorporated into a simulated barrier skin cream, for the selective and high rate air or hydrogen peroxide oxidation of chemical warfare or nerve agent analogs.

Specific objectives to be addressed in this program will be:

- Prepare and spectroscopically, microscopically, and crystallographically characterize vanadium, titanium, iron, and ruthenium substituted polyoxomolybdates and tungstates. Prepare (where possible) water insoluble versions of these materials or versions of the materials incorporated onto silica, alumina, ceria, or high surface area carbon.

- Perform experiments to characterize relative activities of the POM catalysts prepared above. Test activity toward a mustard analog (tetrahydrothiophene) and another organosulfide (methyl sulfide) in aqueous solutions prepared using a solubilizing agent. Also, measure reactivity of POM with solubilizing agent.
- Incorporate preferred POM into a simulated barrier skin cream prepared from perfluorinated polyether oil and polytetrafluoroethylene to create a simulated rTSP. Test activity toward a mustard analog using an aqueous stream containing the mustard analog and a solubilizing agent brought into contact with the rTSP.
- Using a statistical experimental design, determine the variables exerting the most influence on rTSP activity.
- Using the most influential variables determined above, optimize the rTSP for activity toward the mustard analog.
- Evaluate the long term stability of optimized preferred rTSP.

III. WORK PERFORMED AND RESULTS OBTAINED

A. Catalyst Synthesis (Task 1)

During this task, a total of ten polyoxometalates were synthesized, either by direct reaction of starting materials or by synthesis of lacunary complexes followed by their metallation. Procedures for synthesis of each material are given in the following paragraphs.

1. $H_5PMo_{10}V_2O_{40}$

The syntheses of this POM were generally in accord with a procedure described in the literature.³ This consisted generally of first dissolving $NaVO_3$ and Na_2HPO_4 in boiling water, cooling, then adding concentrated sulfuric acid to obtain a red solution. A solution of Na_2MoO_4 in water was added, followed by the further addition of concentrated sulfuric acid, and cooling. The cooled solution was then extracted in a separation funnel using diethyl ether, producing three layers. The bottom two layers were air evaporated and the solids recrystallized from water. A more complete description follows. Three syntheses were attempted here.

Synthesis 1:

Added 6.05 g of sodium metavanadate to 31 mls of boiling deionized water. Once this species was dissolved, 3.52 g of sodium hydrogen phosphate was added and the solution mixed until a clear, slightly yellow solution was obtained. Solution was allowed to cool to room temperature. Concentrated sulfuric acid was added drop wise until a red color was obtained.

A solution 2.5M in $Na_2MoO_4 \cdot 2H_2O$ was added to the red colored solution with vigorous stirring using a magnetic stirrer. Once the solution was thoroughly mixed, concentrated sulfuric

acid (4.4ml) was added to produce a nominal acid concentration of .5M. The solution was allowed to cool to room temperature.

Using a 125 ml separatory funnel 25 ml of the acidified solution above was extracted with 50 ml of ethyl ether and shaken vigorously. However, no product (etherate layer) was recovered. Consequently, additional acid was added to bring the solution pH to between 2 and 3 and solvent air evaporated. This step proved to be crucial, producing a viscous liquid, while forming a layer of yellow solid on the top. Extraction of this viscous liquid produced a three layer system. The three separate layers were placed in crystallizing dishes and the solvent removed by air evaporation.

The crude solids obtained above were dissolved in a minimal amount of boiling deionized water. The hot liquid was gravity filtered and the filtrate cooled to ambient temperature in a covered crystallizing dish. The purified products were allowed to dry, then characterized by FTIR.

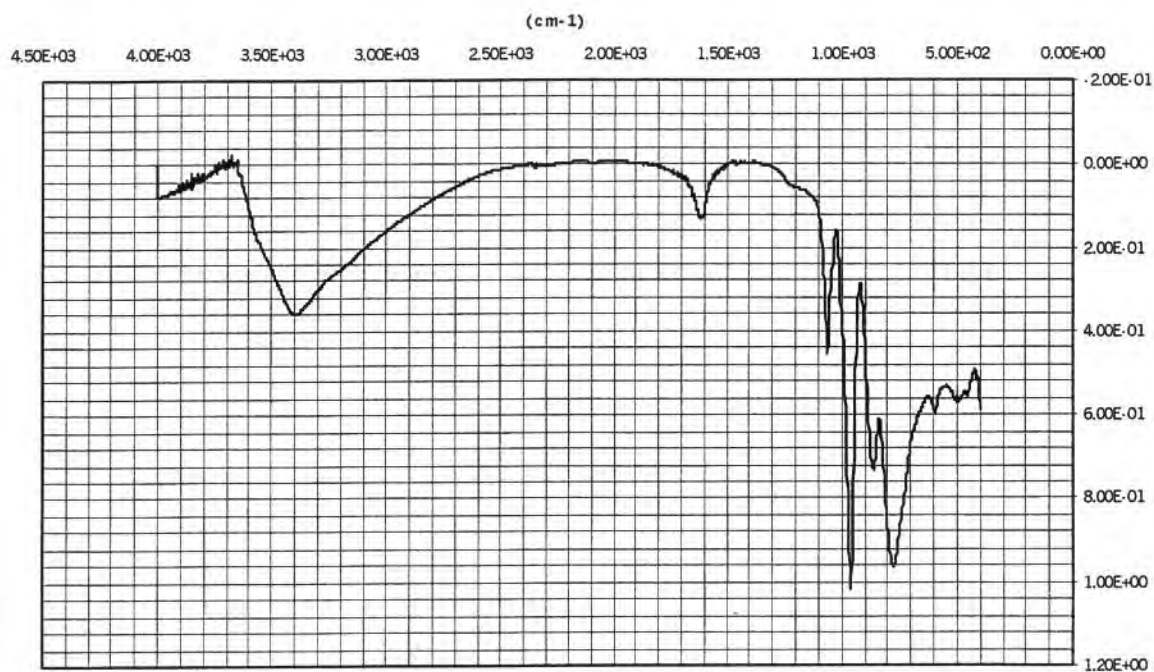
Synthesis 2:

The procedure here was the same as for Synthesis 1, except that the reaction mixture was cooled in an ice bath during the acidification steps. During the final acidification step, the pH was brought initially to between 7 and 8 and, finally, to between 3 and 4. Ether extraction was attempted at both pH's, yielding only two layers in either case. Solvent was evaporated from both layers and the remaining solids recrystallized and characterized with FTIR.

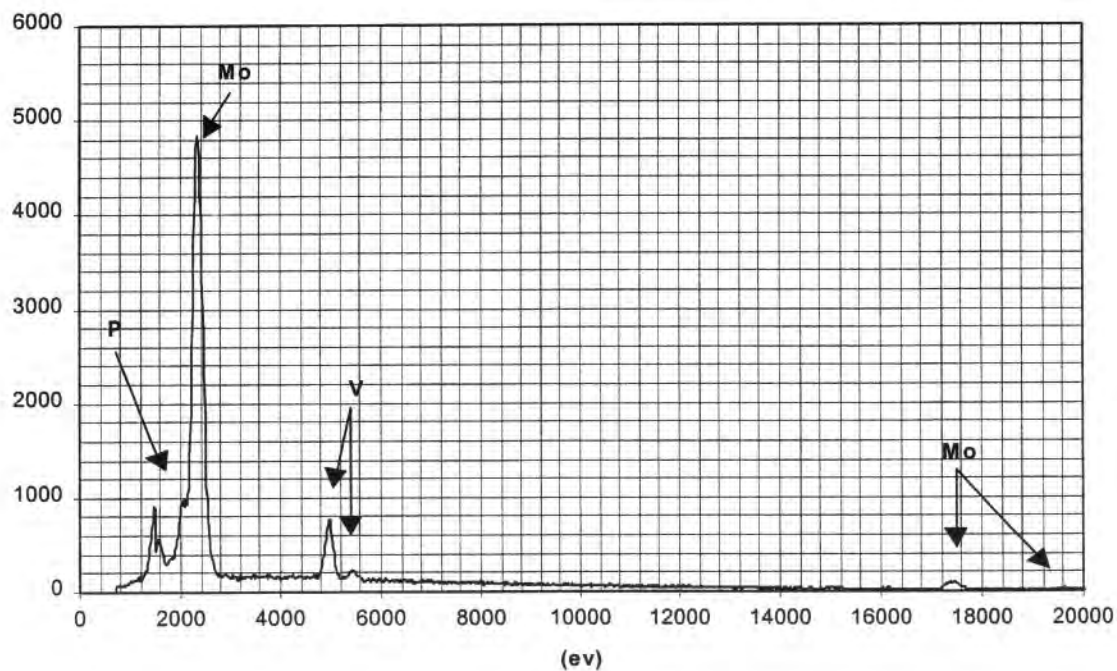
Synthesis 3:

This was a repetition of Synthesis 2, except that the final pH was brought to about 2. Three distinct, well-defined layers were obtained. This seems to be the best of the three synthesis procedures employed.

Products of synthesis were characterized using Fourier Transform InfraRed (FTIR) (Figure 1A) spectroscopy. A Nicolet Impact 410 FTIR spectrometer interfaced to a computer was used for this purpose. The lower wavenumber ($< 1500\text{cm}^{-1}$) region was of particular interest, as metal-oxygen vibrations are manifested there. IR spectra for all starting materials as well as for sodium sulfate (a product of acidification) were obtained. In addition, a spectrum for phosphomolybdic acid ($\text{H}_5\text{PMo}_{12}\text{O}_{40}$) was obtained for direct comparison with that for phosphomolybdic acid so that an initial indication of product identity could be obtained, since it is expected that the vanadium substituted species will possess the same structure as the unsubstituted Mo-based Keggin structure. Indeed, it was found that the two heaviest layers obtained from the ether extraction gave IR spectra that were very similar to that of phosphomolybdic acid, indicating structural similarity. The EDX spectrum (Figure 1B) shows strong lines for Mo and a weak line for phosphorus.



A



B

Figure 1. A) FT-IR and B) EDX spectra for the POM material $H_5PV_2Mo_{10}O_{40}$.

2. $\text{Na}_7\text{PTi}_2\text{W}_{10}\text{O}_{40}$ ⁴

6.0g of NaH_2PO_4 was dissolved in 100 mL of deionized H_2O followed by the addition of 30.0g of $\text{Na}_2\text{WO}_4 \cdot 2\text{H}_2\text{O}$. This solution was then placed in a helium glove bag and 1.8 mL of TiCl_4 added dropwise, producing a white suspension. This mixture was then refluxed for 20 minutes at 97°C and the solution vacuum filtered. The clear filtrate had a pH of 8.2. To this filtrate 30g of NaCl was added and the mixture magnetically stirred for 30 minutes. The precipitate that formed was vacuum filtered and recrystallized with a minimum amount of boiling water. The purified product was exposed to air overnight to evaporate solvent.

We were unable to obtain a material with an FT-IR spectrum characteristic of a polyoxometalate.

3. $\text{K}_7\text{PTi}_2\text{W}_{10}\text{O}_{40}$ ⁴

6.0g of NaH_2PO_4 was dissolved in 100 mL of deionized H_2O followed by the addition of 30.0g of $\text{Na}_2\text{WO}_4 \cdot 2\text{H}_2\text{O}$. The resulting solution was placed in a He glove bag and 1.8 mL of TiCl_4 added drop wise to the solution. This produced a cloudy white mixture that was subsequently refluxed for 20 minutes at 97°C . The solution was then vacuum filtered, producing a clear filtrate with a pH of 8.2. To this filtrate solution 30g of KCl was added, followed by magnetic stirring for 30 minutes. The precipitate that formed was vacuum filtered and recrystallized with a minimum amount of boiling water. The purified product was exposed to air overnight to evaporate solvent.

FT-IR spectra were characteristic of the material, as indicated in the literature.⁴ The EDX spectrum clearly showed potassium, tungsten, and titanium lines.

4. *Synthesis of (n-Butyl₄N)₄H₃PMo₁₁O₃₉ (Product #1)*⁵

11.9g of $\text{H}_3\text{PMO}_{12}\text{O}_{40} \cdot 14\text{H}_2\text{O}$ was dissolved in 50 mL of deionized water. Li_2CO_3 was then added until a pH of 4.3 was obtained. 24.5g of (n-butyl₄N)Br was then added, giving a yellow precipitate. The precipitate was recovered by vacuum filtration and the solvent removed by overnight air evaporation. This precipitate was then recrystallized from 250 mL of CH_3CN , which involved dissolving the crude material and allowing the solvent to air evaporate. Once the crystals had formed the CH_3CN was decanted away from the solid and the remaining solvent evaporated by exposure to air.

EDX of the recrystallized product clearly showed strong phosphorus and molybdenum lines.

5. *Synthesis of (n-Butyl₄N)₄HPMo₁₁Cu(CH₃CN)O₃₉*⁵

1.0g of product 1 was added, with stirring, to 60 mL of CH_3CN . 40 mls of toluene was then added to this solution and the mixture stirred for 10 minutes. A second solution, consisting of 90 mg of CuSO_4 in 25 mL of deionized H_2O was prepared. These solutions were then combined in a separatory funnel and shaken vigorously for 2 to 4 minutes. The organic layer was separated from the aqueous layer and the organic solvent evaporated by exposure to air. The crude product obtained was subjected to recrystallization in CH_3CN . Solvent was removed from the purified product by air evaporation.

Although phosphorus and molybdenum were readily detected in the EDX spectrum of the recrystallized material, a strong copper line was not evident.

6. *Synthesis of (n-Butyl₄N)₄HPMo₁₁Co(CH₃CN)O₃₉*⁵

1.0g of product 1 was added, with stirring, to 60 mL of CH₃CN. 40 mls of toluene was then added and the mixture stirred for 10 minutes. A second solution, consisting of 87 mg of CoSO₄ in 25 mL of deionized H₂O was prepared. These solutions were combined in a separatory funnel and

shaken vigorously for 2 to 4 minutes. The organic layer was separated from the aqueous layer and the organic solvent removed from the nonaqueous phase by air evaporation. The crude product obtained was recrystallized in CH₃CN and the solvent removed by overnight air evaporation.

7. *Synthesis of (n-Butyl₄N)₄HPMo₁₁Zn(CH₃CN)O₃₉*⁵

1.0g of product 1 was added, with stirring, to 60 mL of CH₃CN. 40 mls of toluene was then added and the mixture stirred for 10 minutes. A second solution, consisting of .10g of ZnSO₄·H₂O and deionized H₂O was prepared. These solutions were combined in a separatory funnel and shaken vigorously for 2 to 4 minutes. The organic layer was separated from the water layer and the organic solvent removed from the nonaqueous phase by air evaporation. The crude product obtained was recrystallized in CH₃CN and the solvent removed by overnight air evaporation.

Phosphorus, molybdenum, and zinc all gave strong x-ray emission lines in the EDX spectrum.

8. *Synthesis of K₇PW₁₁O₃₉·12H₂O*⁶

135.3g of Na₂WO₄·2H₂O was added, with stirring, to 225 mL of deionized water. 6.99g of Na₂HPO₄ was then added and the mixture stirred for 1 hour. 150 mL of 4M HCl was slowly added and the mixture stirred for 1 hour. The final step involved the addition of 56.4g of KCl to the solution, resulting in the formation of a white precipitate that was recovered by vacuum filtration. Solvent was removed by air evaporation.

Strong tungsten, phosphorus, and potassium signals were evident in the EDX spectrum for the purified material synthesized here. However, a strong chlorine signal was also obtained, pointing to the presence of KCl.

9. *Synthesis of K₄PFe(OH₂)W₁₁O₃₉·14H₂O*⁶

47.25g of K₇PW₁₁O₃₉·12H₂O was added, with stirring, to 93.75mL of deionized water and heated to 95 °C. 6.11g of Fe(NO₃)₃·9H₂O was added very slowly, yielding a brown solution. The solution was stirred for 10 minutes with the temperature-being maintained at 95 °C. A precipitate formed and was recovered by vacuum filtration. The filtrate was then cooled to room temperature and 150 mL of a 50% methanol/50% ethanol mixture added. A precipitate formed immediately and was recovered by vacuum filtration. The crude product was then recrystallized by adding to

45°C deionized water followed by adding methanol until a precipitate formed. The solvent was then removed by overnight air evaporation.

The EDX pattern for this material showed strong lines for tungsten and potassium as well as weaker lines for iron and phosphorus.

10. Synthesis of $K_5PRh(OH)W_{11}O_{39} \cdot 11H_2O$

10.7g of $K_7PW_{11}O_{39} \cdot 12H_2O$ was added, with stirring, to 33.33 mL of deionized H_2O and heated to a temperature of 90°C. The pH was adjusted, using a 1M solution of HNO_3 , to between 2 and 2.5. A second solution was prepared by dissolving 0.51g of $Rh(NO_3)_3$ in 33.33 mL of deionized water. The second solution was added drop wise to the first at a temperature of 90°C. The mixture was then heated for 30 minutes and allowed to cool. The solution was vacuum filtered and the filtrate exposed to air to evaporate solvent. The crude product obtained was purified by recrystallization using minimal amount of hot H_2O .

The EDX spectrum of the product obtained from this synthesis showed a strong tungsten signal and weaker potassium and rhodium signals.

Elemental analyses performed by Huffman Laboratories, Inc. using inductively coupled plasma (ICP) atomic absorption spectroscopy for two of the catalysts synthesized and used in a number of experiments are presented in Table 1 below. These two catalysts were selected because their FT-IR and EDX spectra were strongly suggestive of vibrational modes characteristic of POM and the presence of elements anticipated, respectively.

The analysis for the material $H_5PV_2Mo_{10}O_{40}$ shows ratios of elements in good approximation to the nominal composition. However, this was not the case for the material $K_7PTi_2W_{10}O_{40}$, where tungsten and titanium appeared to be present, but at deficits relative to the other elements. This suggests the presence of impurity in this material.

Table 1.
Elemental Analysis for Two Catalysts Evaluated During Phase I

Material	Parameter	Mo	P	K	Ti	W	V	O	H	Sum w/w%
$H_5PV_2Mo_{10}O_{40}$	atomic weight	95.94	31.0	39.10	47.90	183.9	50.94	16.00	1.008	
	found w/w%	44.96	1.39				5.20			
	theory w/w%	55.22	1.78				5.865	36.84	0.290	100.001
	theory a/a%	17.24	1.72				3.449	68.97	8.618	100.00
	#atoms/molecule	10	1				2	40	5	58
$K_7PTi_2W_{10}O_{40}$	found w/w%		2.07	17.27	2.25	49.77				
	theory w/w%		1.076	9.507	3.328	63.86		22.23		100.001
	theory a/a%		1.667	11.67	3.334	16.67		66.67		100.000
	#atoms/molecule		1	7	2	10		40		60

B. Evaluation of POM (Task 2)

1. Analysis

The quantitation method used was gas chromatography (GC). A Shimadzu GC-8A gas chromatograph equipped with a flame ionization detector (FID) and an Alltech Teflon 30' X 1/8" Super Q column with 18" packing (80/100 mesh) was used for separation. The conditions employed were as follows: injector temp 220°C, detector temp 220°C, column temp 210°C. The carrier gas for these experiments was helium, the flow rate set at 35 ml/min. The gas sample injection size used was 1 ml. Relative retention times for $(\text{CH}_3)_2\text{S}$, DMSO, $\text{DI}\cdot\text{H}_2\text{O}$, 1-methyl-2-pyrrolidinone were determined and are as follows. $(\text{CH}_3)_2\text{S}$ eluted in 30 seconds, DMSO eluted in 9 minutes, H_2O eluted almost instantaneously and 1-methyl-2-pyrrolidinone eluted in 25 minutes.

2. Initial Gas Phase Experiments

Initial screening experiments were conducted using the apparatus shown in Figure 2. The apparatus consisted of a quartz tube of inside diameter 14 mm into which a POM impregnated piece of quartz wool of length 1cm was inserted. The catalyst used for all experiments reported here was $\text{H}_3\text{PV}_2\text{Mo}_{10}\text{O}_{40}$. The quartz wool was impregnated with 0.5ml of 0.1M POM followed by air drying overnight. The reactor was connected to a bubbler containing $(\text{CH}_3)_2\text{S}$ (methyl sulfide). Connections to glassware were made using stainless steel fittings and teflon tubing was used to carry gas mixtures between the bubbler reactor and scrubber (copper). Gases were supplied to the bubbler via polypropylene tubing and gas flow rates were controlled using needle valves and measured with flowmeters. Inlet and exit gases were sampled through injection ports using a gas tight syringe. 1ml gas samples were analyzed using gas chromatography. In the first experiment, air was bubbled through 10 ml of $(\text{CH}_3)_2\text{S}$ at a GHSV of 750h^{-1} (12.5 ml/min) with a reactor temp of 45°C. The result was the appearance of DMSO in the product vapor stream.

Solubilization of organosulfide in water was achieved by use of the solubilizing agent 1-methyl-2-pyrrolidinone. A solution of 1% $(\text{CH}_3)_2\text{S}$ and 1-methyl-2-pyrrolidinone was placed in the bubbler and the gaseous effluent from the bubbler passed over the POM impregnated quartz wool. The experiment produced the same results as the previous one, a rise in DMSO concentration over time. Experiments were also conducted at room temperature ($\sim 23^\circ\text{C}$) using the solubilized organosulfide. A solution of 1% $(\text{CH}_3)_2\text{S}$ and 1-methyl-2-pyrrolidinone was placed to the bubbler and air at a flow rate of 26 mls/min. was bubbled through the mixture for 30 seconds and a sample taken from the reactor exit. After 17 minutes (the time required for elution of all components from the GC column) a sample was taken from the reactor inlet. This cycle was repeated four times. Upon the first injection there was no DMSO peak. After 17 minutes there was a significant rise in DMSO concentration. However, this DMSO was found in both the reactor inlets and effluent, pointing to air oxidation of the bubbler contents. We are unable to conclude at this time that any activity was observed in these experiments.

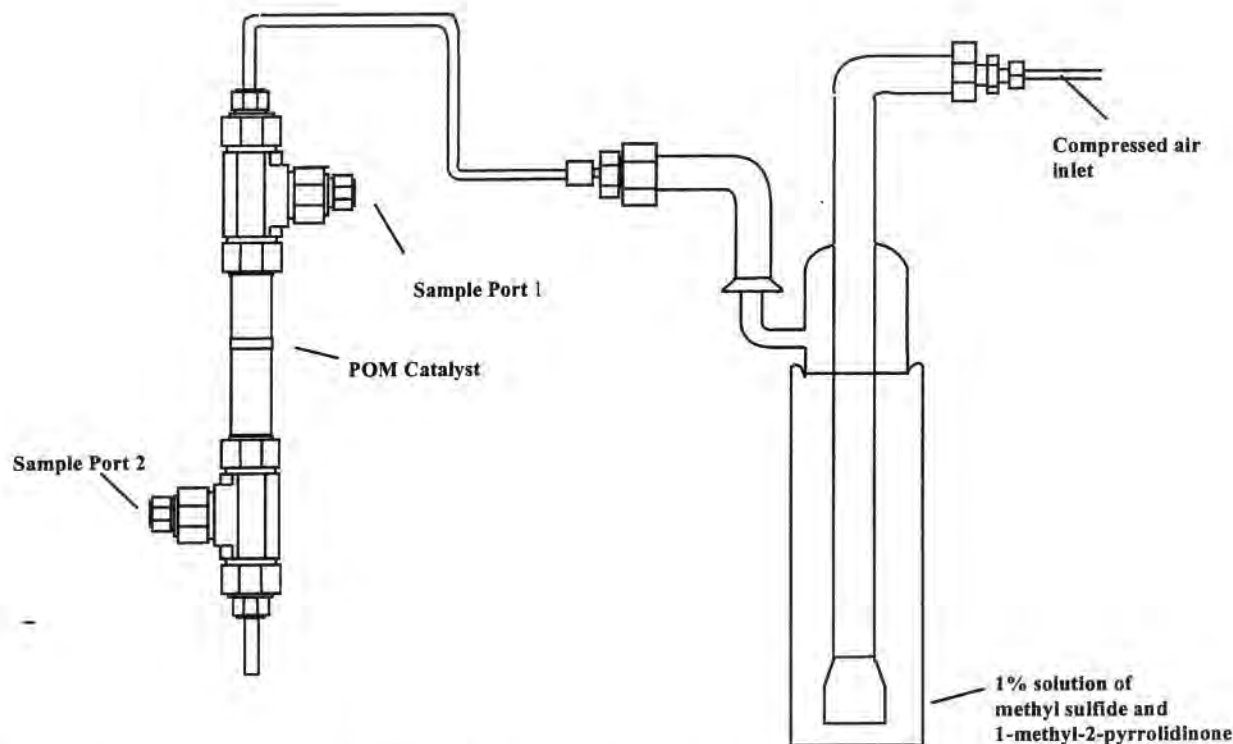


Figure 2. Schematic diagram of reactor used for initial screening of catalysts.

3. Liquid Phase Screening

i) Oxidation with Dioxygen

In this instance, O_2 was used as the oxidant in the removal of dimethyl sulfide from an aqueous medium.

The catalysts $H_5PV_2Mo_{10}O_{40}$ and $K_7PtTi_2W_{10}O_{40}$ were investigated here. 20 mL of 0.1M solution of each catalyst was prepared in deionized water followed by the addition of 9.6 microliters of 1-methyl-2-pyrrolidinone to make a 500 ppm solution. This mixture was then sparged with prepurified O_2 for 15 minutes in order to saturate the solution. The mixture was poured into a 50 mL erlenmeyer flask containing a stir bar and immediately capped with an airtight rubber septum and slow stirring initiated. Dimethyl sulfide (11.8 microliters) was introduced with a microliter syringe through the septum in 2 to 3 microliter aliquots with stirring. Gas chromatographic monitoring of the dimethyl sulfide and dimethyl sulfoxide concentrations was performed at 1 hour increments by injecting 0.5 microliter volumes of the reaction mixture into a GC. Data for aqueous phase reaction of dimethyl sulfide with oxygen are presented in Table 2.

All of the catalysts showed activity, in the order $H_5PV_2Mo_{10}O_{40} > K_7PtTi_2W_{10}O_{40} > K_4PFe(OH_2)W_{11}O_{39} \cdot 14H_2O$. There appeared to be very large spread in the area of the water peak so that the DMS/ H_2O normalization does not appear to be meaningful here. However, we are not certain of the product distribution obtained. We can only say that apparent activity was obtained. The material $H_5PV_2Mo_{10}O_{40}$ was selected for subsequent incorporation into a reactive TSP, prior

Table 2.
Data for Aqueous Phase Oxidation of Dimethyl Sulfide. Oxidant = O₂.

Catalyst	Elapsed Time (min)	Water Area	Dimethyl Sulfide (DMS) Area	DMS/H ₂ O
$K_4PFe(OH_2)W_{11}O_{39} \cdot 14H_2O$	10	71.7	69.93	0.97
	120	48	66.4	1.38
	220	48	65.1	1.30
	290	51	63.4	1.24
	1320	30.7	52.3	1.70
	1400	77.9	51.9	0.66
$H_5PV_2Mo_{10}O_{40}$	10	48.9	111.3	2.27
	40	35.6	115	3.23
	80	120.9	157.4	1.30
	120	96	100.8	1.05
	160	91.4	80	0.87
	200	79.7	73.1	0.91
	290	79	90.6	1.14
	330	70	64.4	0.92
	370	36	68	1.88
	410	42	74.6	1.77
$K_7PTi_2W_{10}O_{40}$		89.2	254.4	2.85
		48.4	464.7	9.60
		52.6	272.5	5.18
		49.5	139.4	2.82
	3900	50.3	172.1	3.42

to acquisition of this data. Consequently, we chose $K_7PTi_2W_{10}O_{40}$ for initial use in the rTSP and this will be described next. We were unable to assess into which channels (e.g., DMSO, etc.) product was evolving.

ii) Oxidation by Hydrogen Peroxide

In this case, dilute hydrogen peroxide was used as the oxidant. The experimental procedure was as follows. POM catalyst was dissolved in hydrogen peroxide of medicinal concentration (3 %) to give a solution 0.05M in the desired catalyst. For example, 1.74g of $\text{H}_5\text{PV}_2\text{Mo}_{10}\text{O}_{40}$ was added to 20 ml of 3 % H_2O_2 in a 50 ml erlenmeyer flask with 1-methyl-2-pyrrolidinone (1000ppm) being used as a solubilizing agent for the sulfide. A silicone rubber septum was placed over the mouth of the erlenmeyer flask and enough of the organosulfide injected to make a solution 500ppm in the sulfide. Data is presented in Figure 3. This data shows that dimethyl sulfide is rapidly removed from solution in both gas and liquid phases. In fact, in either case, over 90% removal was achieved within approximately 90 minutes. Sampling of the liquid phase showed that a peak characteristic of DMSO increased with time in the reaction medium, suggesting a selective pathway for conversion of DMS to the sulfoxide. We are somewhat cautious about this DMSO data, since an interference was obtained upon injection of water, as well. An additional consideration is that removal in the absence of catalyst was much slower, clearly indicating that the catalyst was serving a useful role.

Data for the evolution of gas phase concentration of dimethyl sulfide with time over two POM catalysts is shown in Figure 4. This data shows that the $\text{K}_5\text{PRh}(\text{OH})\text{W}_{11}\text{O}_{39}$ catalyst is considerably more active for the removal of dimethyl sulfide than is $\text{H}_5\text{PV}_2\text{Mo}_{10}\text{O}_{40}$ when hydrogen peroxide is used as the oxidant. However, we were unable to perform product analysis in the gas phase, so that the $\text{H}_5\text{PV}_2\text{Mo}_{10}\text{O}_{40}$ species must be regarded as preferred catalyst at this point.

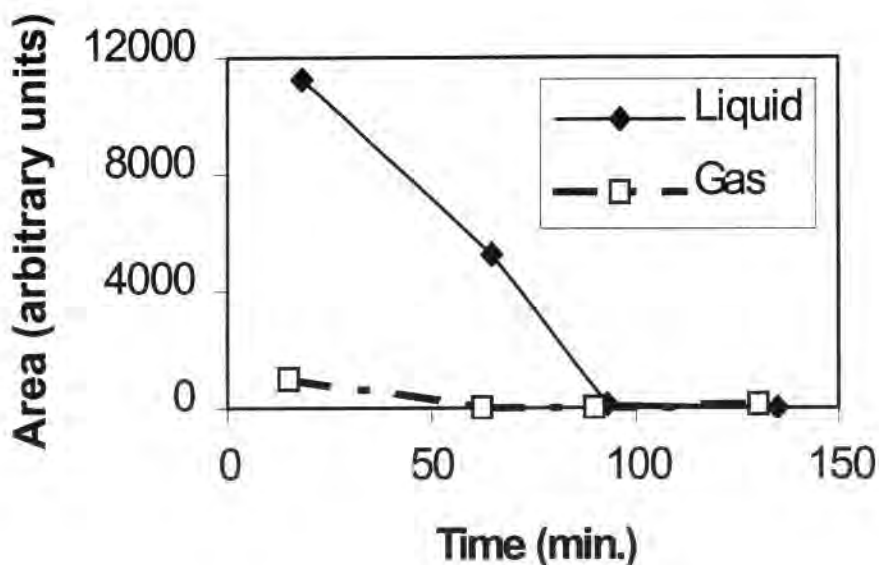


Figure 3. Plot of area of dimethyl sulfide GC peak versus time using a 3% H_2O_2 oxidant and a $\text{H}_5\text{PV}_2\text{Mo}_{10}\text{O}_{40}$ catalyst.

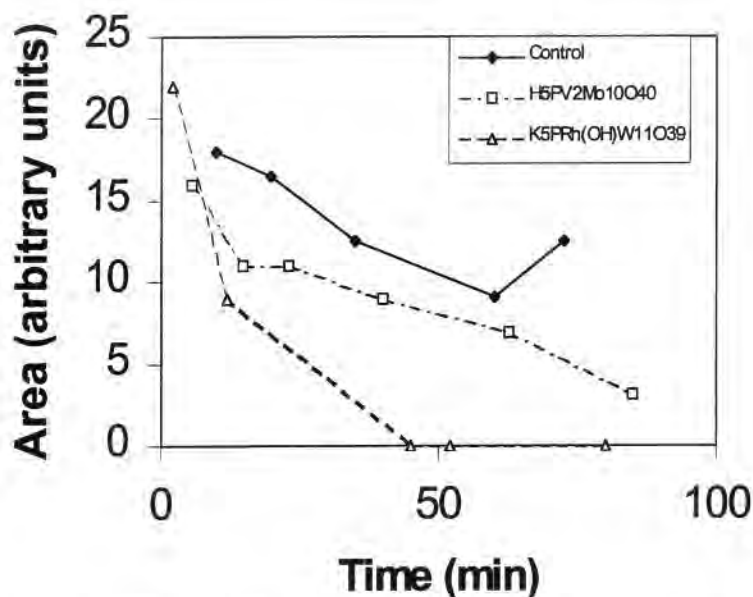


Figure 4. Plots of gas phase concentration of dimethyl sulfide versus time for the hydrogen peroxide oxidation of dimethyl sulfide using POM catalysts.

The same catalyst was found to be active for removal of the sulfur half-mustard (Figure 5). The simulant concentration was found to decrease in both liquid and gas phases. It should be pointed out that this is probably a pessimistic estimate of activity since it was found that injection of water resulted in an interfering ghost peak.

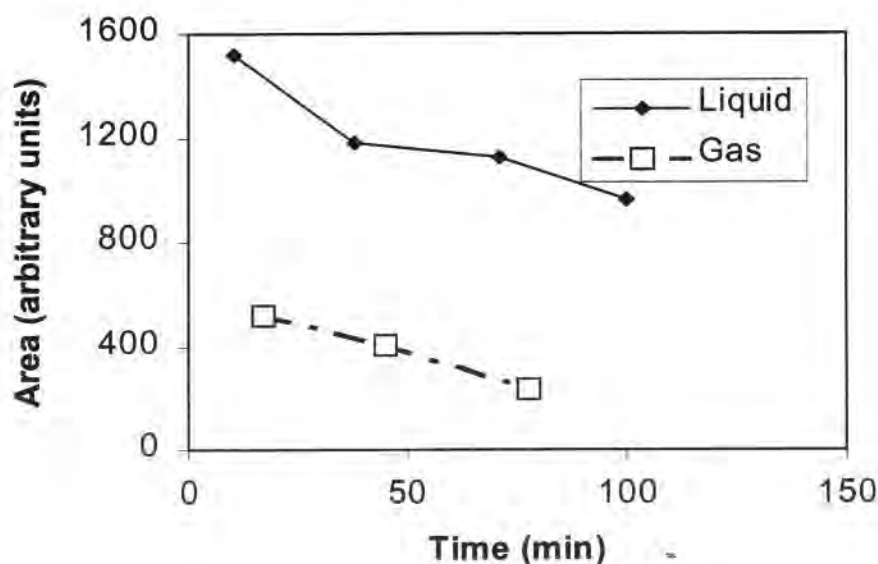


Figure 5. Plot of area of chloroethylethyl sulfide GC peak versus time using a 3% H₂O₂ oxidant and a H₅PV₂Mo₁₀O₄₀ catalyst.

4. Evaluation in Base Creams

A Reifenrath diffusion cell (Figure 6) was employed here. Procedures are described in the following narrative.

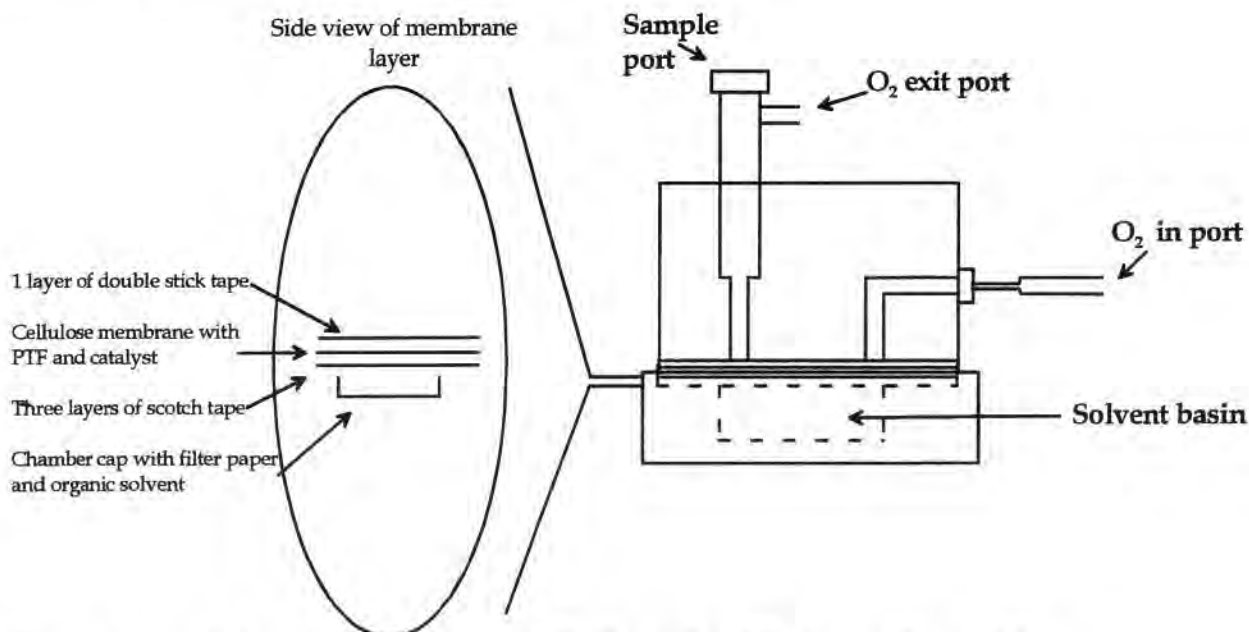


Figure 6. Schematic diagram of Reifenrath diffusion cell used for screening reactive topical skin protectants based on polyoxometalates.

i) Pre-assembly Preparations

The acrylic cell body and plastic screw cap of the minicell were first cleaned with pressurized helium to remove any traces of dimethyl sulfide or half-mustard. The PTFE cream was prepared for each run by mixing PTFE powder (ICD 2478) with PFPE oil (ICD 2959) until a thick, but readily spreadable cream was obtained. A Whatman 25 mm X 0.45 micrometer cellulose nitrate membrane filter was trimmed to fit inside the minicell and double sided plastic tape was used to hold the filter to the acrylic body face of the upper cell chamber. Initially, eight layers of single sided plastic tape were combined to make a 0.46 mm thick layer, indicating a mean thickness of about 0.058mm for the tape and establishing a metric for layer thickness. The layered tape was cut with a coring tool to expose the membrane surface to both sides of the cell chamber before the tape was placed on the cell body. In the case of a vapor phase challenge, a piece of filter paper was cut to size and placed inside the Teflon cell cap to hold the dimethyl sulfide in the lower cell chamber, and a bead of PTFE cream was drawn along the bottom edge of the cap before assembly. In the case of liquid phase challenges, the cell was oriented so that the skin cream faced upward.

ii) Assembly Procedures

Assembly of the tape layers and membrane was performed very carefully but once the cream was applied, the final assembly was performed quickly to assure dimethyl sulfide or half-mustard saturation within the cell.

The tape layers and membrane were then assembled such that the multilayered tape was on top, forming a well above the membrane, into which the PTFE cream was spread in an even layer with a glass slide. The layer of cream was spread such that it was level with the plastic tape well and set aside.

One drop of 98% dimethyl sulfide (Aldrich) was placed on the filter paper in the cell cap and the liquid allowed to vaporize, but before the filter paper dried, the cell cap was placed on top of the Teflon cream layer. A bead of Teflon cream was then drawn around the perimeter of the cell cap to seal the lower cell chamber, and the plastic screw cap placed on top of the cell cap.

The assembled cell was placed into a clamp and a luer-tipped syringe inserted into one upper chamber port of the acrylic cell body. Teflon tubing connected the syringe to a water bubbler and a rubber sampling septum capped the syringe. Another rubber septum was placed in the second cell port and pierced with a needle to supply purified oxygen at 4.8 mL/minute.

iii) Assay Procedures

The assay was begun as soon as the cell was assembled and oxygen flow verified. Assays lasted 60 to 90 minutes and 0.5 mL gas samples were taken from the sampling port at 2 minutes and every 10 minutes thereafter. Samples were analyzed in the Shimadzu Gas Chromatograph GC-8A described above. Peak areas were calculated using Peak Fit.

Using dimethyl sulfide as a simulant resulted in very poor reproducibility of measured breakthrough times using a control (base cream) barrier. Consequently use of dimethyl sulfide as a simulant was suspended and use of chloroethylethyl sulfide (half-mustard) initiated.

Data obtained here suggested that incorporation of catalyst into a skin cream results in enhanced permeation of sulfide through the skin cream, implying nonuniformity of the layer or formation of channels along chains of catalyst crystallites in the skin cream. However, using a bilayer system in which catalyst is incorporated into the layer(s) nearest the simulant source and an additional layer consisting of base cream furthest from the source resulted in considerable improvement. Data obtained using half-mustard is presented in Table 3. The data presented for the base cream suggests that reproducibility of measurements is obtainable. This contrasts with data obtained previously with dimethyl sulfide, which showed very large variance in the data. This was attributed to volatility of the dimethyl sulfide. The data above, using chloroethylethyl sulfide, suggests that this is indeed the case. However, incorporation of catalyst into the base skin cream again resulted in enhanced permeation of sulfide through the skin cream, implying nonuniformity of the layer or formation of channels along chains of catalyst crystallites in the skin cream. For that reason, we tried a dual layer system, in which one (bottom) layer consisted of base cream and the other consisted of base cream plus $K_7Pt_{12}W_{10}O_{40}$. A marked improvement in the performance of the barrier was noted. Initial results indicated the possibility of improved activity.

Table 3.
Permeation Data for Chloroethylethyl Sulfide. Liquid Phase Challenge. Base Cream:1.2g
ICD 2959/1.0g ICD 2478

Experiment	Breakthrough Time (min)	# Replications	Total Thickness (mm)
1 layer base cream	100 ± 14	5	0.17
1 layer (base cream + 5wt. % $K_7PTi_2W_{10}O_{40}$)	5	1	0.17
2 layers (1 layer base cream + 1 layer base cream including 5 wt. % $K_7PTi_2W_{10}O_{40}$)	260	1	0.34

– In summary, completion of this task resulted in testing of POM catalysts using both dioxygen and hydrogen peroxide oxidants. Medicinal hydrogen peroxide was found to be a better oxidant than oxygen, probably because of the higher solution concentration of the former.

C. Optimization of rTSP (Task 3)

Variable studies were performed in catalyst type ($K_7PTi_2W_{10}O_{40}$, $H_5PV_2Mo_{10}O_{40}$, and $K_4PFe(OH_2)W_{11}O_{39}$), catalyst loading, layer thickness, type of challenge (liquid or vapor), and simulant type. Using a model linear in these variables would give rise to an experimental layout with the following form (Table 4).

The problem that emerged in attempting to assess the relative influence of experimental variables is that within-sample variances were quite large (e.g., > 14% after five trials in measuring breakthrough times through a control base cream film). This requirement imposed severe time requirements and did not allow the experiments in a layout arising from a design of experiments to be completed .

In summary, completion of this task resulted in the construction of an experimental layout. However, owing to the large within-sample variance obtained during the conduct of experiments, the needed statistics were too demanding to allow completion of the design.

Table 4.
Plackett-Burman Screening Design for Determining the Most Influential Experimental Variables for rTSP

Experiment No.	X_1	X_2	X_3	X_4	X_5
1	+	+	-	-	-
2	+	-	-	+	-
3	+	-	-	-	+
4	-	-	+	-	+
5	-	+	+	-	-
6	-	-	-	-	-
+					-
X_1	Catalyst Type		$H_5PV_2Mo_{10}O_{40}$		$K_7PTi_2W_{10}O_{40}$
X_2	Catalyst Loading		15%		0
X_3	Layer Thickness		0.51		0.17
X_4	Type of Challenge		Vapor		Liquid
X_5	Simulant Type		Dimethyl Sulfide		Half-Mustard

D. Evaluation of Barrier Effectiveness (Task 4)

In this task, the permeation of a simulated vesicant through skin protectants was determined under a number of configurations and conditions. A summary of this data is presented in Table 5.

Table 5.
Summary of Data Obtained from Liquid Phase Challenges to Various Skin Creams.
Evaluations Performed at Ambient Temperature Using Reifenrath Diffusion Cell.
Simulant: Chloroethyl ethyl Sulfide > "Layer" Refers to Thickness of Tape (0.06mm)

Cell #	Layer System	Catalyst	Time (min)	Area
2	double-double	15% $H_5PV_2Mo_{10}O_{40}$	165	11.7
			195	6.4
			225	13.7
			255	28.1
			295	32.5
2	double-double	15% $H_5PV_2Mo_{10}O_{40}$	85	6.1
			280	16.1
			310	8.3
			340	19.6
			370	52
			400	28.6
1	double-double	15% $H_5PV_2Mo_{10}O_{40}$	75	20.7
			105	28
			135	33.1
			165	43.8
			195	44.3
			225	66.8
			255	86.4
			285	67.4
1	double-double	15% $H_5PV_2Mo_{10}O_{40}$	175	10.8
			205	10.2
			235	36

Cell #	Layer System	Catalyst	Time (min)	Area
			265	51
			295	30.9
			325	37.4
			365	56
1	double-double	None	115	2.4
			145	10.7
			175	8.5
			205	9.36
			235	9.3
			265	18.5
			295	37.7
1	double-double	None	90	6.8
			130	15.1
			150	15.1
			180	10.6
			220	28.1
2	double-double	5% $K_4PFe(OH_2)W_{11}O_{39}$	160	12.3
			195	40.8
			225	56.6
			255	57.2
			285	54.68
2	double-double	5% $K_4PFe(OH_2)W_{11}O_{39}$	190	605
			255	860
			285	704

Cell #	Layer System	Catalyst	Time (min)	Area
1	double-double	15% $K_7Pt_{12}W_{10}O_{40}$	140	39.1
			175	60.2
			205	76.9
			265	68.2
			295	60.6
1	double-double	15% $K_7Pt_{12}W_{10}O_{40}$	135	86.1
			165	1713.9
			195	1828.5
2	double-triple	None	300	22.5
			330	20.7
			360	21
2	double-triple	None	210	9.2
			240	20.8
			270	24.31
			300	29.12

The data in this table show that there is a large spread in the data within each set of experimental conditions. The following can be said of the data: 1) There is considerable spread in breakthrough times and simulant peak areas at fixed times between replications of experiments for the same configuration and catalyst. 2) As expected, increasing layer thickness increased breakthrough time. 3) Breakthrough times were generally later for creams incorporating catalysts. To further illustrate this point, comparison of averaged data for each configuration and catalyst is made in Table 6.

Table 6.
Comparison of Average Breakthrough Times/Simulant Peak Areas at Fixed Time

Cell #	Layer system	Catalyst	Average Breakthrough Time (min)	Ave. Simulant Peak Area at 280 - 300min
1	double-double	None	102.5	33
1	double-double	15% $\text{H}_5\text{PV}_2\text{Mo}_{10}\text{O}_{40}$	125	49
2	double-double	15% $\text{H}_5\text{PV}_2\text{Mo}_{10}\text{O}_{40}$	125	24
1	double-double	15% $\text{K}_7\text{PTi}_2\text{W}_{10}\text{O}_{40}$	137.5	61
2	double-double	5% $\text{K}_4\text{PFe}(\text{OH})_2\text{W}_{11}\text{O}_{39}$	175	55

From this table, it appears that, although breakthrough times were generally longer with creams incorporating catalyst, peak areas at a fixed time of between 280 and 300 minutes were found generally to be greater than that for the control. An exception was obtained with the POM $\text{H}_5\text{PV}_2\text{Mo}_{10}\text{O}_{40}$. However, from Table 5, it is readily apparent that the spread in peak areas was so great as to preclude using peak area as a metric.

Ceria supported $\text{H}_5\text{PV}_2\text{Mo}_{10}\text{O}_{40}$ was prepared as follows. 0.1 g of $\text{H}_5\text{PV}_2\text{Mo}_{10}\text{O}_{40}$ was dissolved in 0.46 ml of water. This solution was then added to 0.9g of high surface area ($> 60\text{m}^2/\text{g}$) ceria, previously prepared by precipitation so that the support was wetted up to the point that excess liquid had begun to appear. The water was removed by air evaporation. A cream 15wt % in ceria supported $\text{H}_5\text{PV}_2\text{Mo}_{10}\text{O}_{40}$ was prepared using the base cream used previously during the program. A bilayer skin cream configuration was used here, i.e., a 0.12mm layer of base cream supported a 0.12mm layer of cream 15wt. % in the supported catalyst. Experiments were performed as above. A breakthrough time of 255 min (versus 102.5 for the control breakthrough time) with initial half-mustard area of 35.6 was obtained (Table 7).

This was considerably better than for the unsupported catalyst and may be due to the superior oxidation activity of the supported catalyst: ceria is known to promote oxidation chemistry.⁷ Nevertheless, the level of half-mustard that appears on breakthrough is considerably higher with the catalyst than without.

To summarize, Task 4 resulted in the testing of POM catalysts in skin creams. It was found that there was possibly some positive effect on inhibiting breakthrough of a half-mustard simulant.

Table 7.
Data for Test of Chloroethylethyl Sulfide Permeation Through Bilayer Skin Cream
Incorporating as the Catalytic Layer 15wt% $\text{H}_5\text{PV}_2\text{Mo}_{10}\text{O}_{40}/\text{CeO}_2$ (1.5wt% Catalyst).
Oxidant: Air

System	Breakthrough Time (minutes)	Half-Mustard GC Peak Area Upon Breakthrough
Control (double-double, with all layers base cream defined as in Table 3)	102.5	4.6
Double-double, with catalytic layer 15 wt % $\text{H}_5\text{PV}_2\text{Mo}_{10}\text{O}_{40}/\text{CeO}_2$ (1.5wt% catalyst)	255	35.6

IV. CONCLUSIONS

A. Summary of Phase I Results

- The polyoxometalate species $\text{H}_5\text{PV}_2\text{Mo}_{10}\text{O}_{40}$ was prepared by direct reaction of starting materials (molybdates, vanadates, and phosphates). It was found that careful control of pH was necessary to obtain the desired product. Product was purified by means of ether extraction and recrystallization.
- Products of syntheses were characterized using fourier transform infrared (FT-IR) spectroscopy and energy dispersive x-ray spectroscopy (EDX).
- Synthesis of $\text{Na}_7\text{PW}_{10}\text{Ti}_2\text{O}_{40}$ by direct reaction of sodium tungstate, titanium tetrachloride, and sodium phosphate was unsuccessful. FT-IR did not display a metal oxide fingerprint region indicative of a polyoxometalate, but rather, of partially reacted starting materials.
- $\text{K}_7\text{PW}_{10}\text{Ti}_2\text{O}_{40}$ was successfully synthesized using a procedure essentially identical to that attempted for the sodium analog. FT-IR indicated that the material was a POM and EDX indicated the presence of the constituent elements.
- The lacunary complexes $(n\text{-Butyl}_4\text{N})_4\text{H}_3\text{PMo}_{11}\text{O}_{39}$ and $\text{K}_7\text{PW}_{11}\text{O}_{39} \cdot 12\text{H}_2\text{O}$ were prepared by directly reacting starting materials for each species. The former material was recrystallized from acetonitrile whereas the latter was recovered as a precipitate by the addition of KCl to a precursor.

- The lacunary complex $(n\text{-Butyl}_4\text{N})_4\text{H}_3\text{PMo}_{11}\text{O}_{39}$ was metallated by first solubilizing in acetonitrile, followed by addition of aqueous solutions of the appropriate metal ion. In this manner, $(n\text{-Butyl}_4\text{N})_4\text{HPMo}_{11}\text{Cu}(\text{CH}_3\text{CN})\text{O}_{39}$, $(n\text{-Butyl}_4\text{N})_4\text{HPMo}_{11}\text{Co}(\text{CH}_3\text{CN})\text{O}_{39}$, and $(n\text{-Butyl}_4\text{N})_4\text{HPMo}_{11}\text{Zn}(\text{CH}_3\text{CN})\text{O}_{39}$ were synthesized. Identities of the materials were established by FT-IR and EDX fingerprints.
- $\text{K}_4\text{PFe}(\text{OH}_2)\text{W}_{11}\text{O}_{39} \cdot 14\text{H}_2\text{O}$ was synthesized by metallation of the lacunary complex $\text{K}_7\text{PW}_{11}\text{O}_{39} \cdot 12\text{H}_2\text{O}$ using an aqueous solution of iron(III) nitrate. The identity of the material was established, as above, by the FT-IR and EDX.
- The POM $\text{H}_5\text{PV}_2\text{Mo}_{10}\text{O}_{40}$ was supported on quartz wool. However, exposure of the supported catalyst to vapor phase dimethyl sulfide resulted in no apparent conversion. However, the catalyst appeared to change state, as its color changed from orange to green.
- An aqueous solution, 0.1M in the POM $\text{H}_5\text{PV}_2\text{Mo}_{10}\text{O}_{40}$, was found to be inactive toward dimethyl sulfide.
- A 0.1M solution of $\text{K}_7\text{PW}_{10}\text{Ti}_2\text{O}_{40}$ was found to remove a significant fraction (up to 80 %) of dimethyl sulfide in both liquid and gas phases using oxygen as oxidant.
- Films of ICD 2289 of thickness up to 0.46mm were found not to reproducibly prevent permeation of dimethyl sulfide. This is attributable to the volatility of the molecule and the poor reproducibility of films produced.
- Films of a base cream consisting of 1.2g ICD 2959 PFPE oil/1.0g ICD 2478 PTFE powder were found, at thicknesses of 0.17mm to reproducibly prevent measurable breakthrough of monochloroethylethyl sulfide (half-mustard) for approximately 100 minutes when a liquid phase challenge with this simulant was presented to the skin cream.
- Incorporation of 5 wt. % $\text{K}_7\text{PW}_{10}\text{Ti}_2\text{O}_{40}$ into the above base cream resulted in breakthrough in only 5 minutes.
- A bilayer system, of total thickness of 0.34mm, and consisting of a layer of the above base cream and a second layer of base cream plus 5 wt. % $\text{K}_7\text{PW}_{10}\text{Ti}_2\text{O}_{40}$ resulted in no measurable breakthrough until 260 minutes after initiation of a liquid phase challenge by half-mustard. This result points to possible increased efficacy upon incorporation of POM catalysts into TSP's.
- Bilayer systems incorporating the catalysts $\text{K}_7\text{PTi}_2\text{W}_{10}\text{O}_{40}$, $\text{H}_5\text{PV}_2\text{Mo}_{10}\text{O}_{40}$, and $\text{K}_4\text{PFe}(\text{OH}_2)\text{W}_{11}\text{O}_{39}$ were found, possibly, to inhibit the permeation of chloroethylethyl sulfide through a barrier skin cream when exposure of the membrane to air was allowed.

- Hydrogen peroxide was found to be a much more effective oxidant in aqueous systems than oxygen. This was true with both dimethyl sulfide and sulfur half-mustard (chloroethylethyl sulfide). The greater effectiveness of H_2O_2 versus O_2 was probably due to a concentration effect, i.e., more of the former oxidant was available than of the latter because of its much greater solubility.
- A cerium oxide supported $\text{H}_5\text{PV}_2\text{Mo}_{10}\text{O}_{40}$ (15 wt. %) catalyst was found to significantly inhibit the permeation of sulfur half-mustard through a rTSP incorporating this catalyst.

B. Conclusions

Results obtained during Phase I indicate that: 1) Catalysts synthesized during Phase I are active for oxygen and hydrogen peroxide oxidation of dimethyl sulfide and chloroethylethyl sulfide in aqueous solution. 2) Incorporation of some catalysts into base skin creams resulted in enhancement of base skin cream permeability to half-mustard, apparently due to the presence of catalyst crystallites in the cream. 3) A bilayer skin cream, in which the layer(s) nearest the simulated vesicant contain catalyst, and the other layer(s) furthest from the simulant is (are) comprised of base skin cream, was most effective for use as a rTSP. 4) Some activity (inhibited breakthrough) using an air oxidant was possibly obtained when the catalysts $\text{H}_5\text{PMo}_{10}\text{V}_2\text{O}_{40}$, $\text{K}_4\text{PFe}(\text{OH})_2\text{W}_{11}\text{O}_{39}$, and $\text{K}_7\text{PW}_{10}\text{Ti}_2\text{O}_{40}$ were incorporated into skin creams. 5) Hydrogen peroxide is the preferred oxidant, at least for aqueous phase oxidation. 6) $\text{H}_5\text{PMo}_{10}\text{V}_2\text{O}_{40}$ was the preferred catalyst, both in terms of activity and compatibility for incorporation into skin creams.

C. Recommended Future Work

Work done during Phase I points to several areas to be pursued in future work: 1) The use of hydrogen peroxide as oxidant and its incorporation into hydrophobic skin creams. 2) The breakthrough of simulant due to the presence of catalyst crystallites. The mechanical grinding of acid forms of POM appears to lead to regelation, leading to limitations in the dispersion of the catalyst. Large particle size may result in leakage along particle agglomerations. Consequently, supporting the catalysts on teflon powder may be the preferred approach. 3) Full identification of reaction product distributions in skin creams will be necessary, as we have not yet accounted for disappearance of sulfur half-mustard and have only tentatively measured DMSO as a product of dimethyl sulfide oxidation in the aqueous phase. 4) Improved sensitivity to target molecules is needed, as we have been analyzing at points-in-time rather than by integrated product accumulation. 5) Issues concerning skin irritation need to be identified, so that that criterion can be included in the optimization of rTSP.

V. REFERENCES

1. Gall, R.D., Faraj, M., Hill, C.L., *Inorg. Chem.* **33** 5015 (1994).
2. Gall, R.D., Hill, C.L., Walker, J.E., *J. Catal.* **159** 473 (1996).
3. G.A. Tsigdinos and C.J. Hallada, *Inorg. Chem.* **7** 437(1968).
4. P.J.Domaille and W.H. Knoth, *Inorg. Chem.* **22** 818(1983).
5. L.A. Coombs-Walker and C.L. Hill, *Inorg. Chem.* **30** 4016(1991).
6. F. Zonnevjlle, C. M. Tourne, and G.F. Tourne, *Inorg. Chem.* **21** 2751(1982).
7. A. Trovarelli, *Sci. and Eng.*, **38** 439 (1996).

SBIR final report from TIAX LLC, Phase I

Award Number: W81XWH-05-C-0131

Reviewed by E. Braun
3 Aug 06

AD _____

Award Number: W81XWH-05-C-0131

TITLE: Novel Polymeric Formulations for Skin Protection and decontamination

PRINCIPAL INVESTIGATOR: Emily L. Reichert, Ph.D.

CONTRACTING ORGANIZATION: TIAX LLC
Cambridge, Massachusetts 02140

REPORT DATE: April 2006

TYPE OF REPORT: Final, Phase I

PREPARED FOR: U.S. Army Medical Research and Materiel Command
Fort Detrick, Maryland 21702-5012

DISTRIBUTION STATEMENT: Distribution authorized to U.S. Government agencies only (specific authority). Other requests for this document shall be referred to U.S. Army Medical Research and Materiel Command, 504 Scott Street, Fort Detrick, Maryland 21702-5012.

The views, opinions and/or findings contained in this report are those of the author(s) and should not be construed as an official Department of the Army position, policy or decision unless so designated by other documentation.

NOTICE

USING GOVERNMENT DRAWINGS, SPECIFICATIONS, OR OTHER DATA INCLUDED IN THIS DOCUMENT FOR ANY PURPOSE OTHER THAN GOVERNMENT PROCUREMENT DOES NOT IN ANY WAY OBLIGATE THE US GOVERNMENT. THE FACT THAT THE GOVERNMENT FORMULATED OR SUPPLIED THE DRAWINGS, SPECIFICATIONS, OR OTHER DATA DOES NOT LICENSE THE HOLDER OR ANY OTHER PERSON OR CORPORATION; OR CONVEY ANY RIGHTS OR PERMISSION TO MANUFACTURE, USE, OR SELL ANY PATENTED INVENTION THAT MAY RELATE TO THEM.

SBIR DATA RIGHTS LEGEND

Award: W81XWH-05-C-0131

Organization: TIAX LLC

For a period of five (5) years after completion of the project from which the data was generated, the Government's rights to use, modify, reproduce, release, perform, display, or disclose any technical data or computer software contained in this report are restricted as provided in paragraph (b)(4) of the Rights in Noncommercial Technical Data and Computer Software Small Business Innovative Research (SBIR) Program clause contained in the above-identified contract [DFARS 252.227-7018(Jun. 1995)]. No restrictions apply after expiration of that period. Any reproduction of technical data, computer software, or portions thereof marked as SBIR data must also reproduce those markings and this legend.

This technical report has been reviewed and is accepted under the provisions of the Small Business Innovation Research Program.

Dr. Ernest Braue

This report is published in the interest of scientific and technical information exchange and does not constitute approval or disapproval of its ideas or findings.

Do not return copies of this report unless contractual obligations or notice on a specific document requires its return.

REPORT DOCUMENTATION PAGE				Form Approved OMB No. 0704-0188	
Public reporting burden for this collection of information is estimated to average 1 hour per response, including the time for reviewing instructions, searching existing data sources, gathering and maintaining the data needed, and completing and reviewing this collection of information. Send comments regarding this burden estimate or any other aspect of this collection of information, including suggestions for reducing this burden to Department of Defense, Washington Headquarters Services, Directorate for Information Operations and Reports (0704-0188), 1215 Jefferson Davis Highway, Suite 1204, Arlington, VA 22202-4302. Respondents should be aware that notwithstanding any other provision of law, no person shall be subject to any penalty for failing to comply with a collection of information if it does not display a currently valid OMB control number. PLEASE DO NOT RETURN YOUR FORM TO THE ABOVE ADDRESS.					
1. REPORT DATE (DD-MM-YYYY) April 2006		2. REPORT TYPE Final, Phase I		3. DATES COVERED (From - To) 25 May 05 – 24 Mar 06	
4. TITLE AND SUBTITLE Novel Polymeric Formulations for Skin Protection and decontamination				5a. CONTRACT NUMBER W81XWH-05-C-0131	
				5b. GRANT NUMBER	
				5c. PROGRAM ELEMENT NUMBER	
6. AUTHOR(S) Emily L. Reichert, Ph.D. E-Mail: reichert.emily@tiaxllc.com				5d. PROJECT NUMBER	
				5e. TASK NUMBER	
				5f. WORK UNIT NUMBER	
7. PERFORMING ORGANIZATION NAME(S) AND ADDRESS(ES) TIAX LLC Cambridge, Massachusetts 02140				8. PERFORMING ORGANIZATION REPORT NUMBER	
9. SPONSORING / MONITORING AGENCY NAME(S) AND ADDRESS(ES) U.S. Army Medical Research and Materiel Command Fort Detrick, Maryland 21702-5012				10. SPONSOR/MONITOR'S ACRONYM(S)	
				11. SPONSOR/MONITOR'S REPORT NUMBER(S)	
12. DISTRIBUTION / AVAILABILITY STATEMENT Distribution authorized to U.S. Government agencies only (proprietary information, specific authority). Other request for this document shall be referred to U.S. Army Medical Research and Materiel Command, 504 Scott Street, Fort Detrick, Maryland 21702-5012.					
13. SUPPLEMENTARY NOTES					
14. ABSTRACT: Currently there is a need for a pre-exposure decontamination skin cream that will neutralize chemical warfare agents (CWA) on contact. Current approaches to this problem cannot both dissolve a CWA challenge and neutralize the agent into less toxic products before it reaches the skin surface. We are currently developing an innovative Neutralizing Skin Protectant (NSP). The NSP will employ physiochemical means to protect exposed skin from chemical agents while solubilizing both an active moiety and the CWA, enabling a neutralization reaction to occur within the matrix. This Phase I Final Report details our proof-of-concept studies demonstrating the efficacy of our approach against nerve and sulfur mustard (HD) simulants.					
15. SUBJECT TERMS decontamination, neutralization, CWA, skin protection, topical skin protectant, skin cream, chemical warfare agent, CWA protection					
16. SECURITY CLASSIFICATION OF:			17. LIMITATION OF ABSTRACT	18. NUMBER OF PAGES	19a. NAME OF RESPONSIBLE PERSON
a. REPORT	b. ABSTRACT	c. THIS PAGE			USAMRMC
Unclassified	Unclassified	Unclassified	Unclassified	28	19b. TELEPHONE NUMBER (include area code)

Table of Contents

Cover.....	3
SF 298.....	3
Introduction.....	5
Body.....	5
Key Research Accomplishments.....	19
Reportable Outcomes.....	20
Conclusions.....	20
References.....	21
Appendices.....	23

1.0 Introduction

Given recent domestic and global events there is a need for a decontaminating skin cream that neutralizes chemical warfare agents (CWAs) on contact. The current technologies available to US soldiers, SERPACWA and M291 SDK, cannot both *dissolve* a CWA challenge and *neutralize* the agent into less toxic products before it reaches the skin surface. TIAX's technical approach will result in a Neutralizing Skin Protectant (NSP) formulation that protects exposed skin by solubilizing both the neutralizing active and the CWA, enabling a chemical reaction to occur within the matrix. This Phase I Final Report details our evaluation of the feasibility of incorporating active neutralizing moieties (polyethylenimines) into a polymer base material that is substantive (but not occlusive) to skin. In these proof-of-concept studies, polyethylenimine/polymer base combinations were challenged by CWA simulants and then monitored for neutralization efficacy using a head-space solid phase microextraction (HS-SPME) method. Proof of neutralization (relative to control samples containing no active) was observed against both nerve and sulfur mustard agent simulants.

2.0 Report Body

This section of the report describes the research accomplishments of Phase I, associated with each task as outlined in the original proposal (below).

Task 1: Compatibility Assessment of Polymer-Active Combinations <ul style="list-style-type: none">• Select active neutralization moieties and confirm with Army COR• Confirm appropriate CWA simulants with Army COR• Develop specific protocols for laboratory compatibility assessment (Task 2)• Develop specific protocols for proof-of-neutralization testing (Task 3)• Assess compatibility of polymer-active combinations (paper study)
Task 2: Formulation of Polymer-Active Combinations <ul style="list-style-type: none">• Prepare samples of polymer-active combinations• Laboratory verification of compatibility (e.g., phase separation, turbidity measurements)• Eliminate non-compatible combinations• Select formulations for efficacy testing in Task 3
Task 3: Concept Feasibility Determination via Efficacy Testing using CWA simulants <ul style="list-style-type: none">• Validate HS-SPME GC/MS analysis method• Chemical analysis of simulant spiked samples (from Task 2) for proof of neutralization• Analyze results of efficacy testing• Identify "most promising" polymer-active formulation
Task 4: Program Communication and Reporting <ul style="list-style-type: none">• Kick-off meeting• Monthly teleconferences• Final Report

2.1 Task 1: Compatibility Assessment of Polymer-Active Combinations

2.1.1 Objectives

- Select active neutralization moieties and confirm with Army COR
- Confirm appropriate CWA simulants with Army COR
- Develop specific protocols for compatibility assessment (Task 2)
- Develop specific protocols for proof-of-neutralization testing (Task 3)
- Assess compatibility of polymer-active combinations (paper study)

2.1.2 Change in Cationic Polymer from Phase I Proposal

Our original Phase I proposal sought to evaluate the feasibility of an approach based on MacroChem Corporation's (Lexington, MA) patented MacroDerm™ technology, a series of proprietary urethane polymers with a range of possible chemical structures (including cationic). MacroChem had demonstrated via percutaneous absorption studies the ability of MacroDerms to reduce the penetration of sunscreen and insect repellent actives into the skin.

Shortly after our Phase I Kickoff (06 July 05), MacroChem Corporation announced on 01 Sept 05 it was ceasing all R&D activity and would sell its intellectual property, including the three patents covering the MacroDerm technology. Due to the unforeseen change in their situation, MacroChem was now unable to provide MacroDerm samples to TIAX for testing. Following MacroChem's announcement, TIAX quickly identified a cationic polymer with a similar structure sold commercially by Croda Inc. (Edison, NJ) under the trade name Incroquat QLC. The chemical structure of Incroquat QLC is shown in Figure 1 below.

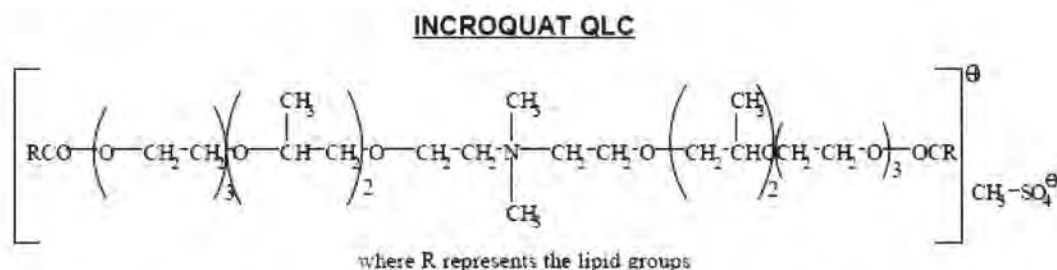


Figure 1 - INCROQUAT QLC Chemical Structure (Croda Incroquat QLC Data Sheet DS-177, 2003).

Incroquat QLC (N,N-Di(Ethoxy-polyoxypropylene-2-polyoxyethylene-3-lanolinoyl)-N,N-dimethyl methosulfate) is structurally very similar to the cationic MacroDerms we had originally proposed to evaluate in our Phase I Technical Approach. It is a quaternary ammonium salt with symmetrical repeating propoxy (PPO) groups, ethoxy (EO) groups, and long chain alkyl end groups. We believed that neither the lack of urethane linkages (which resulted from the synthesis route to MacroDerms) nor the lack of rigidity building moieties would strongly affect the functionality for which the polymer was to be used in our application: skin-friendly (non-sensitizing), substantive to skin, physical and chemical compatibility with actives, and able to retard the penetration of actives/agents into the skin.

Incroquat QLC quats were developed by Croda especially for personal care (skin) applications. As with the cationic MacroDerms, the quaternary character of Incroquat QLC gives this polymer high substantivity to skin. According to Croda these quats are non-sensitizing and even provide skin smoothing and moisturizing benefits that have been proven in clinical studies. The ability of Incroquat QLC to retard penetration of actives through the skin has not been tested to our knowledge.

For our Phase I effort, we have demonstrated proof of concept by incorporating active neutralizing moieties into the skin-friendly Incroquat QLC polymer instead of the MacroDerms as originally proposed. The change of polymers from MacroDerms to Incroquats was approved by the Army COR, Dr. Ernest Braue on 21 Dec 05 in an e-mail. Croda's Incroquat OSC was also considered but the high melting point of this compound made it difficult to work with for this application. We have been selected for award for Phase II and anticipate that we will work closely with Croda (as a commercialization partner) to optimize the structure of the quat to meet the functional needs of the skin decontamination application. A meeting with Croda is being planned for Jul 06 to correspond with the kick-off of Phase II.

2.1.3 Selection of Neutralization Actives and CWA Simulants

The selection of active neutralization moieties and CWA simulants occurred during the Program Kick-Off meeting on 6 Jul 05 which involved the full team from TIAX, MacroChem, and the COR, Dr. Ernie Braue of USAMRICD. Based on previous results with SERPACWA, the Lupasol® polyethylenimines (BASF Corporation, Charlotte, NC) were chosen as the neutralization actives (Figure 2); the selection of CEES and DFP as simulants (Figure 3) for the Phase I testing were confirmed by the COR.

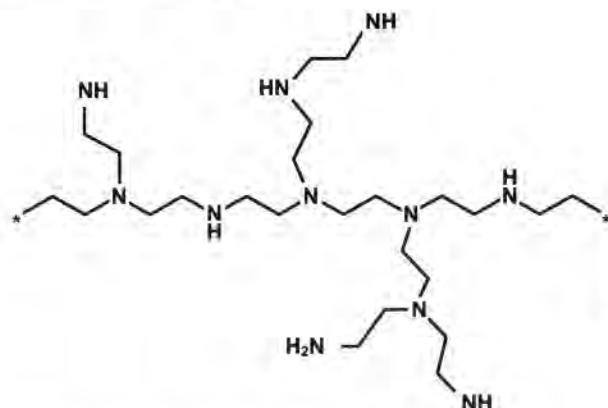
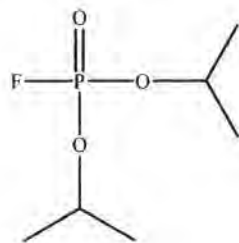
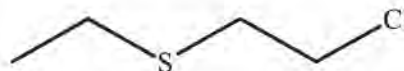


Figure 2 – Representative structure of the Lupasol® polyethylenimines (BASF Corp.) selected for evaluation in Phase I as neutralization actives.

Further review of the SERPACWA test results with Lupasol (US Patent Application – 2004/0067205) after the Kick-Off meeting identified Lupasol® FG, Lupasol® P, Lupasol® WF, and Lupasol® G20 WF as the most efficacious against nerve (GD) and mustard (HD) agents. These choices for active moieties were confirmed by the COR 25 Jul 05. Table 1 below gives relevant properties of the Lupasols selected for evaluation.



DFP



CEES

Figure 3 – CWA simulants selected for testing in Phase I, DFP (difluorophosphate) and CEES (chloroethyl ethyl sulfide).

Table 1. Properties of BASF Lupasols® Selected for Evaluation in the Phase I Program

Lupasol®	MW	Composition	Description	Solubility	Viscosity	Water Content
FG	800	99% NH ₂ CH ₂ CH ₂ NH ₂ - CH ₂ NHCH ₂ ethylene diamine- ethylenimine copolymer	Slightly yellow, viscous liquid, amine odor	Miscible in water	2-10 ps (20C)	1.50%
G20 WF	1300	100% (CH ₂ H ₅ N) copolymer	Slightly yellow, viscous	Miscible in water, soluble in	3-15 ps (20C)	2%

PROPRIETARY INFORMATION – NOT APPROVED FOR PUBLIC RELEASE
SBIR Data – See Cover Page for Use, Release, and Disclosure Restrictions

			liquid, mild amine odor	alcohol		
WF	25000	100% (CH ₂ CH ₂ NH) Aziridine (ethylenimine) homopolymer	Clear, viscous liquid, odorless	Soluble in water	13-18ps (50C)	1%
P	750000	50% Aziridine (ethylenimine) homopolymer, 50% water	Slightly yellow, honey-like liquid, faint amine odor	Soluble in water	18-40 ps (20C)	50%

Source: BASF MSDS and Technical Data Sheets

2.1.4 Protocol Development

To evaluate the efficacy of candidate formulations, we proposed to conduct "proof of neutralization" testing. In the proof of neutralization test method, a sample of the polymer/active (e.g., Incroquat QLC/Lupasol FG) is challenged with a known amount of chemical agent simulant. The headspace of the sample is monitored for simulant loss of concentration vs. time by Head Space - Solid Phase MicroExtraction (HS-SPME) with GC/MS detection. The percent loss of simulant vs. time is compared to a control sample (no active). The HS-SPME GC MS method protocol used in Phase I was developed with input from Dr. Kevin Morrissey of EAI Corp., who carried out similar proof-of-neutralization testing on SERPACWA for USAMRICD. The final version of the protocol used in the experiments described below can be found in Appendix A.

2.1.5 Theoretical Compatibility Assessment of Polymer/Neutralization Active Combinations

We carried out a brief theoretical (paper) compatibility assessment of our polymer base material, Incroquat QLC (Croda) with the Lupasol polyethylenimines. We calculated solubility parameters for PEIs and Incroquat QLC using the Hoy method, the results of which are shown in Table 2 below:

Table 2. Calculated Solubility Parameters for Polyethylenimines (PEIs) and Incroquat QLC

	δT	δH	δP	δNP
PEI	10.95	4.85	6.26	4.85
Incroquat QLC	9.53	4.00	3.45	7.94

Units are cal^{1/2}/cm^{3/2}. Source data from Tables of Solubility Parameters, Union Carbide Corporation, 1975.

The Hoy Solubility method is used to predict whether an organic material is compatible with (or soluble in) another organic material (solvent or polymer). The method assumes that each chemical group in the molecule contributes to the total solubility. Predictions of solubility are based on the total (δT) of three different contributions: non-polar (δNP), polar (δP), and hydrogen bonding (δH). The more similar δT values are for two materials, the more soluble they will be, according to the theory. For solubility with PEI actives ($\delta T = 10.95$), the value for Incroquat QLC at 9.53 compares favorably to δT for PTFE (SERPACWA), which is 6.2. By way of comparison, we had previously calculated the δT for the cationic MacroDermis at 10.42-10.44.

Additional physical properties considered in the paper assessment were molecular weight and viscosity. Based on the moderate viscosity (syrup-like) and molecular weight (MW) of the Croda quat (1400), we considered Lupasols FG (MW 800) and Lupasols G20 WF (MW 1300) the most likely to be compatible.

2.2 Task 2: Laboratory formulation of candidate polymer-active combinations

2.2.1 Objectives

- Prepare samples of polymer-active combinations
- Laboratory verification of compatibility (e.g., phase separation, turbidity measurements)

PROPRIETARY INFORMATION – NOT APPROVED FOR PUBLIC RELEASE
SBIR Data – See Cover Page for Use, Release, and Disclosure Restrictions

- Eliminate non-compatible combinations
- Select formulations for efficacy testing in Task 3

2.2.2 Laboratory Compatibility Assessment via Phase Separation Testing

Laboratory compatibility testing was carried out by simple mixing of Incroquat QLC with the four Lupasols, followed by observation of the mixtures for several hours to several days. (No additional protocol was developed). Phase separation was easily observable due to the color difference in the components – Lupasols are clear to slightly yellow-tinged, while Croda's Incroquat QLC is yellow. Phase separation could also be observed due to the different viscosities of the two components – the Lupasols were considerably more viscous than the Croda material. If phase separation was observed, additional means of solubilizing the two components such as sonication, magnetic stirring, heating to 55C, reducing the weight % of Lupasol component and adding compatibilizers were tried in succession. Table 3 below summarizes the results of our compatibility tests.

Table 3. Results of Laboratory Compatibility Assessment of Incroquat QLC with Lupasols.

	Lupasols			
	FG	G20 WF	WF	P
Sample -test condition				
1:1 (by weight) Incroquat QLC /Lupasol	Two phases apparent	Two phases apparent	Two phases apparent	Two phases apparent
- sonication	No change	No change	No change	No change
-heat to 55C	No change	No change	No change	No change
-magnetic stir/heat to 40C	Slight clouding, two phases apparent	Slight clouding, two phases apparent	Slight clouding, two phases apparent	Slight clouding, two phases apparent
-after one week set time	Slightly cloudy yellow viscous liquid, one phase	Slightly cloudy yellow viscous liquid, one phase	Two phases, more viscous layer very cloudy	Two phases with different viscosity apparent
10% (by wt.) Incroquat QLC/Lupasol	Slightly cloudy yellow viscous liquid, one phase	Slightly cloudy yellow viscous liquid, one phase		
5% (by wt.) Incroquat QLC/Lupasol	Slightly cloudy yellow viscous liquid, one phase	Slightly cloudy yellow viscous liquid, one phase		
-1-3 drops diethanolamine	Slightly cloudy yellow viscous liquid, one phase	Slightly cloudy yellow viscous liquid, one phase		
-1-3 drops Triton X-100*	Clear yellow viscous liquid, one phase	Slightly cloudy yellow viscous liquid, one phase		

*Alkyl phenoxy polyethoxy ethanol (Rohm and Haas)

2.2.3 Selection of Candidate Formulation for Efficacy Testing

From our initial compatibility assessment, we observed that Incroquat QLC appears to be more soluble in the lower molecular weight, lower viscosity, lower % water Lupasols. Further, it appears that the addition of small amount of Triton X-100 (alkyl phenoxy polyethoxy ethanol, Rohm and Haas, Philadelphia, PA) enhances the solubility of Lupasol FG in Incroquat QLC. **Based on these results, we selected a mixture of 10% (by wt.) Lupasol FG and 2.5% (by wt.) Triton X-100 in Incroquat QLC for the primary formulation to test against DFP and CEES challenges.**

PROPRIETARY INFORMATION – NOT APPROVED FOR PUBLIC RELEASE
SBIR Data – See Cover Page for Use, Release, and Disclosure Restrictions

2.3 Task 3: Efficacy Testing of Candidate Polymer-Active Combinations

2.3.1 Objectives

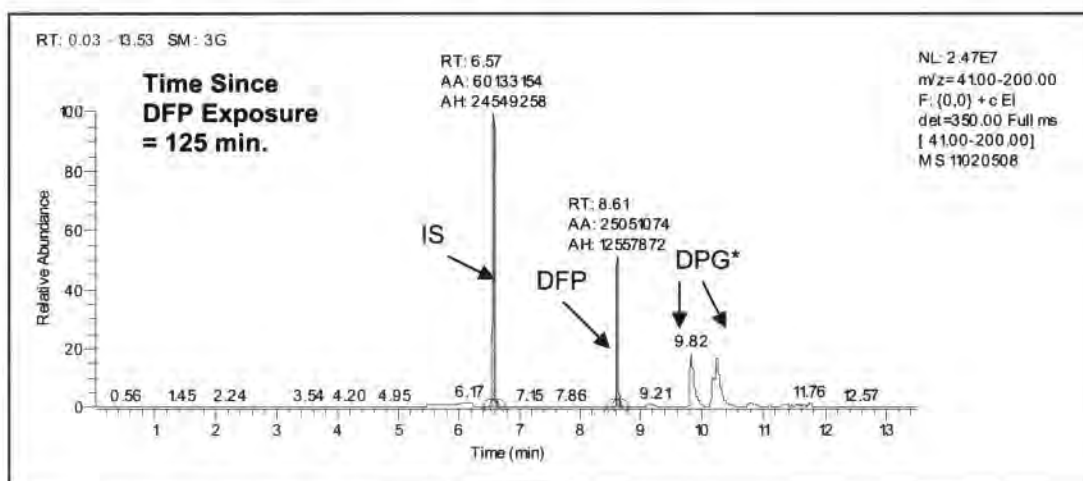
- Validate HS-SPME GC/MS analysis method
- Chemical analysis of simulant spiked samples (from Task 2) for proof of neutralization
- Analyze results of efficacy testing
- Identify "most promising" polymer-active formulation

2.3.2 Overview of Proof of Neutralization Test

To evaluate the efficacy of candidate formulations, we conducted "proof of neutralization" testing using HS-SPME with GC/MS detection. In the test, a sample of the polymer/active (e.g., Incroquat QLC/Lupasol) is challenged with a known amount of chemical agent simulant, DFP or CEES. The headspace of the sample is extracted periodically using a SPME fiber, which is then desorbed into a hot injector port of the GC/MS. Identification and measurement of the DFP or CEES in the headspace by GC/MS enables tracking of the decrease in simulant concentration vs. time. This result is compared to a control sample (no active) analyzed under the same conditions. The detailed method protocol, developed in Task 1 and refined in Task 3, is attached to this report as Appendix A.

2.3.3 Chromatography and Mass Spectra for Simulants Using HS-SPME Method

A sample chromatogram from a 5 minute extraction 125 minutes after exposure to DFP is shown in Figure 4. IS denotes the internal standard, p-xylene. We have included p-xylene as an internal standard to correct for any instrument fluctuations over the course of an experiment, which can be up to 7 hours. A mass spectrum corresponding to the DFP peak (Retention Time = 8.61) is also provided as well as automated search output of the NIST Mass Spectral Library positively identifying this peak (Figure 5 and Table 4).



*DPG = Dipropylene Glycol (present in Incroquat QLC)

Figure 4 - HS-SPME GC/MS Analysis of Incroquat QLC/ 10% by wt. Lupasol FG Sample

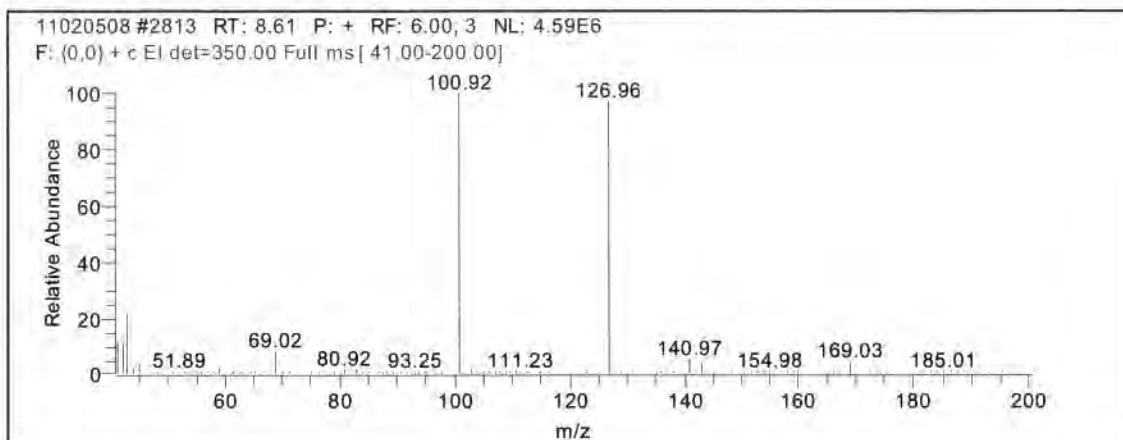


Figure 5 - Mass Spectrum for DFP (Figure 4, Time = 8.61 minutes)

Table 4. Results from NIST Mass Spectral Library Database Search (Figure 4, Time = 8.61 minutes)

RT	Name	Molecular Formula	Probability	NIST Library
8.61	Isofluorophate*	C6H14FO3P	98.63	MAINLIB
8.61	Cyclohexane, 1,1-dimethoxy-2-methyl-	C9H18O2	0.98	MAINLIB
8.61	2-Cyclohexyl-hexan-2-ol	C12H24O	0.20	MAINLIB
8.61	Phosphorocyanidothioic difluoride	CF2NPS	0.05	MAINLIB
8.61	Cyclohexanone, 4,4-dimethoxy-	C8H14O3	0.04	MAINLIB

*Isofluorophate is a synonym for DFP.

In Figure 6, a sample chromatogram from a 15 minute extraction 15 minutes after exposure to CEES is shown. Figure 7 contains the corresponding Mass Spectrum (RT = 11.00 min.) positively identified by an automated NIST library search program (Table 5).

RT: 0.03 - 12.93 SM: 3G

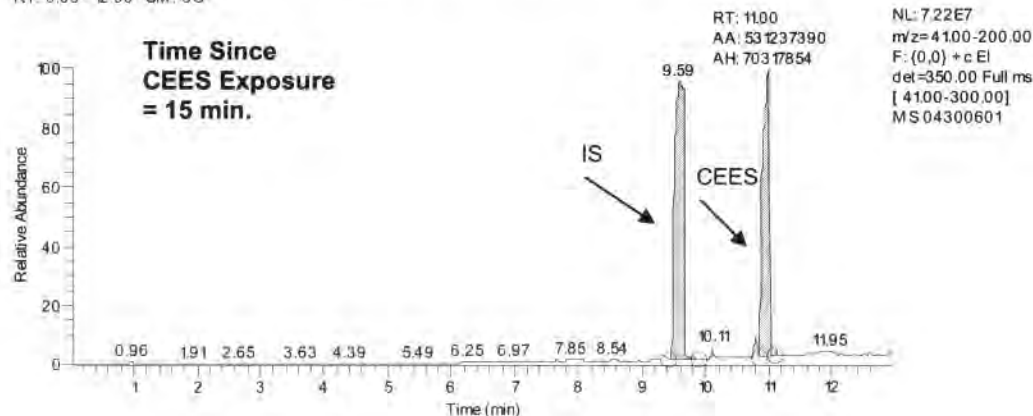


Figure 6 - HS-SPME Gas chromatogram of CEES

04300601 #2476 RT: 11.00 P: + NL: 5.98E6
F: {0,0} + c EI det=350.00 Full ms [41.00-300.00]

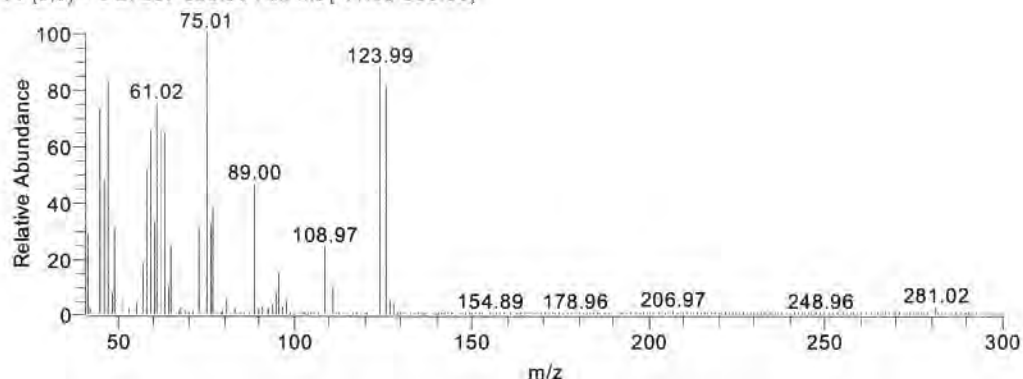


Figure 7 - Mass spectrum of CEES from (Figure 6, Time = 11.00 minutes)

Table 5. Results from NIST Mass Spectral Library Database Search (Figure 6, Time = 11.00 minutes)

RT	Name	Molecular Formula	Probability	NIST Library
11.00	2-Chloroethyl ethyl sulfide	C4H9ClS	97.05	MAINLIB
11.00	2-Chloroethyl ethyl sulfide	C4H9ClS	97.05	REPLIB
11.00	Carbonochloridothioic acid, S-ethyl ester	C3H5ClOS	2.40	REPLIB
11.00	Carbonochloridothioic acid, S-ethyl ester	C3H5ClOS	2.40	MAINLIB
11.00	Chloromethyl n-propyl sulfide	C4H9ClS	0.20	MAINLIB

In the description that follows, peak areas from the chromatograms (such as those shown in Figure 5 and 7) are used as a semi-quantitative measure of the simulant concentration in the headspace. Peak areas were calculated using the Xcalibur software application that also runs the instrument. Variation in the integration parameters did not change peak areas significantly enough to change the outcome of the results reported here.

2.3.4 Optimization and Validation of HS-SPME GC/MS Method - Overview

To optimize a HS-SPME method, several factors must be considered, as described in *Solid Phase Microextraction: Theory and Practice* (Pawliszyn, 1997). These include:

- Desorption Conditions
 - Injector Temperature
 - Fiber Desorption Time
 - Needle Exposure Depth
- Extraction Conditions
 - Extraction Time Profile
 - Fiber Extraction Time
- Calibration Method

The testing required to optimize/validate each of the parameters above for DFP and CEES is discussed in detail in Appendix B.

2.3.6 Proof-of-Neutralization Results - Overview

In the following sections, we present the key outcomes of this program: the results of our efficacy testing against chemical agents simulants DFP and CEES. For each simulant, the results of control testing are presented first, then results with inclusion of the neutralization active. This is followed by a brief discussion relating current results to previous outcomes (USAMRICD work with SERPACWA).

Against DFP, significant efficacy (70% headspace reduction in 2-3 hours) was observed for the Incroquat QLC/10% Lupasol FG combination. Several additional experiments were performed including an aging study and a study varying the concentration of active. For the Incroquat QL/10% Lupasol FG combination, we fit the data to an exponential curve and also plotted log DFP concentration vs. time, which was linear.

Against CEES, we did not initially see any proof of neutralization using the Incroquat QLC/10% Lupasol FG combination. Several scoping experiments were performed in an effort to increase efficacy. With the addition of the solvent methanol, we observed a reproducible reduction in headspace concentration of 8-10% over 5-7 hours. We plan to continue to work on improving efficacy against CEES during the Phase I Option period.

2.3.6 Proof-of-Neutralization Results for DFP

2.3.6.1 Control Samples – Incroquat QLC – No Lupasol FG

The data shown in Figure 8 illustrates a typical experimental result for a *control* sample containing Incroquat QLC and Triton X-100 (2.5%, mixing aid), but *no* neutralizing active, spiked with DFP. In this experiment, we injected 0.5 μ L of DFP into a sample vial containing 100 mg control sample at $t = 0$, then extracted the vial headspace over a period of 4-5 hours, at $t = 15, 45, 75, 105, 135, 165, 195, 225$ and 255 minutes. The sample was maintained at 28-30C in a constant temperature bath throughout the experiment. As can be seen in Figure 8, the raw DFP response (blue diamonds) over time is nearly constant, with slight fluctuations in experimental conditions causing variability of about 4% of the average value over the experimental period. These fluctuations are corrected using an internal standard p-xylene (IS, pink squares) also present in the sample. The IS-corrected DFP response (yellow triangles) deviates about 3% from the mean value over the experimental period of over 4 hours. This "control" experiment was repeated on several different days to ensure that the result was reproducible.

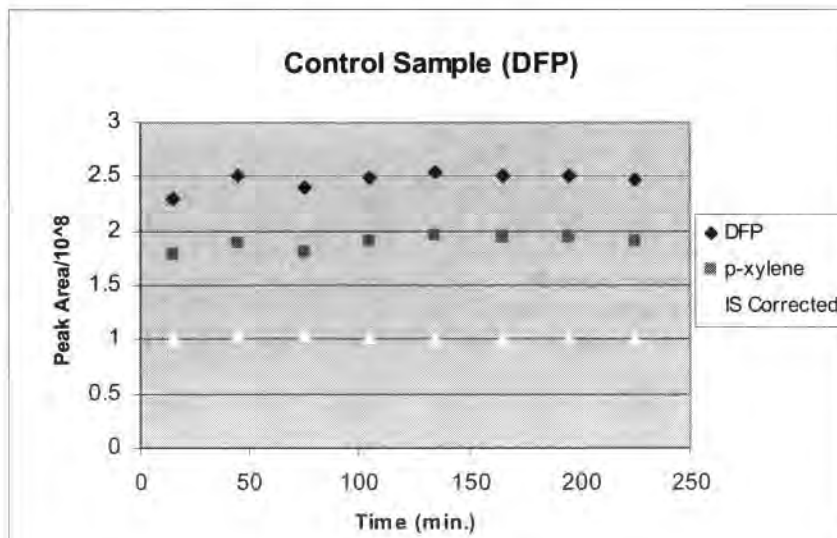
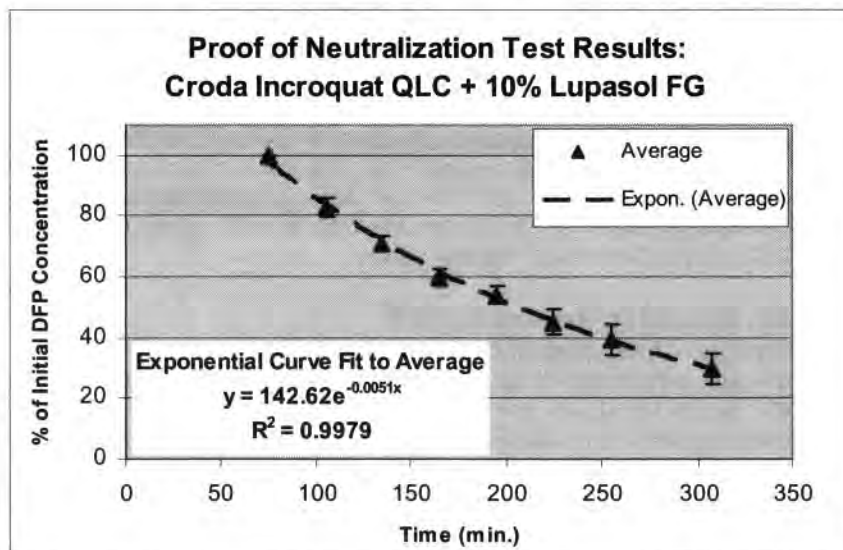


Figure 8- Comparison of raw data vs. internal standard-corrected data for DFP spike of a control sample (Incroquat QLC/Triton X-100)

PROPRIETARY INFORMATION – NOT APPROVED FOR PUBLIC RELEASE
SBIR Data – See Cover Page for Use, Release, and Disclosure Restrictions

2.3.6.2 Active Samples - Incroquat QLC – Lupasol FG (10% by wt.)

Figure 9 shows proof of neutralization test results for five active samples containing 10% by wt. Lupasol FG in Incroquat QLC (with 2.5% by wt. Triton X-100). As can be seen in Figure 9, when the active Lupasol FG is present, the concentration of DFP in the headspace (100% at $t = 75$ min.) is reduced by 70% over a period of 2-3 hours. Figure 9 indicates the average of all five measurements, which were made on five different days. The error bars indicate \pm one standard deviation from the mean value.



Note: I took
75 min to start
seeing a decrease
In ECBC exit we
started in 30 min

Figure 9 - Percent Loss of DFP vs. time for the average of five Incroquat QLC/10% by wt. Lupasol FG samples. Measurements made over 5 days. The black dotted line is a best fit to the average.

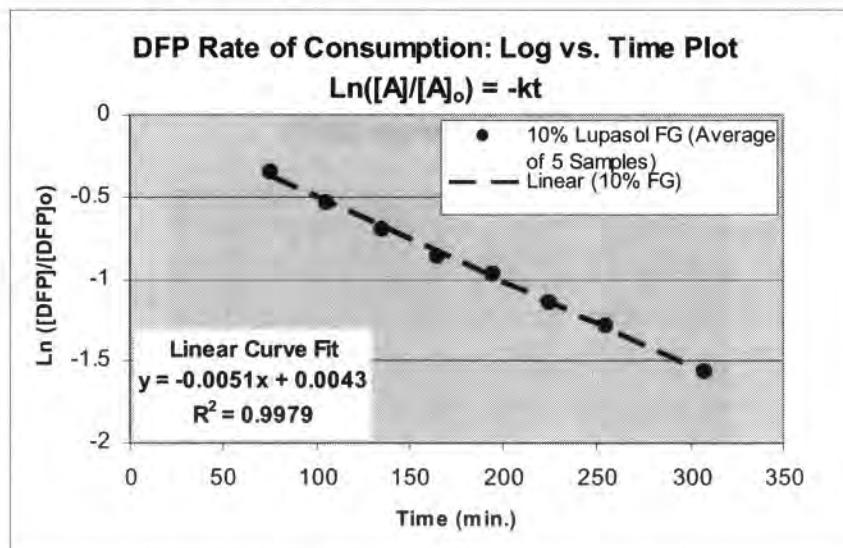


Figure 10 – Plot of $\ln([DFP]/[DFP]_0)$ vs. time for the average of five Incroquat/10% by wt. Lupasol FG samples. The dotted black dotted line is a linear curve fit.

We attempted to fit the data in Figure 9 using linear, 2nd order polynomial, power, exponential and log functions. The best fit to the average (as judged by R^2 value) were log and exponential functions (fit shown above in Figure 9), followed by the 2nd order polynomial function. Based on the good fit of the data to an exponential curve, we next plotted $\ln([DFP]/[DFP]_0)$ vs. time (Figure 10). Based on the linearity of this plot, we can postulate that the rate of DFP removal from the headspace is first order or pseudo-first order; as we are not measuring any other reactants or products, it is not possible to determine further a rate law for the reaction.

2.3.6.3 Aging study – Incroquat QLC – 10% by wt. Lupasol FG

Figure 11 shows the results of an aging study performed on a 10% by wt. Lupasol FG (active) sample. As the graph indicates, there is minimal change in the rate of DFP removal from the headspace for a sample that has aged up to 16 days. The average % standard deviation over all time points (3 measurements each) was 3.5%.

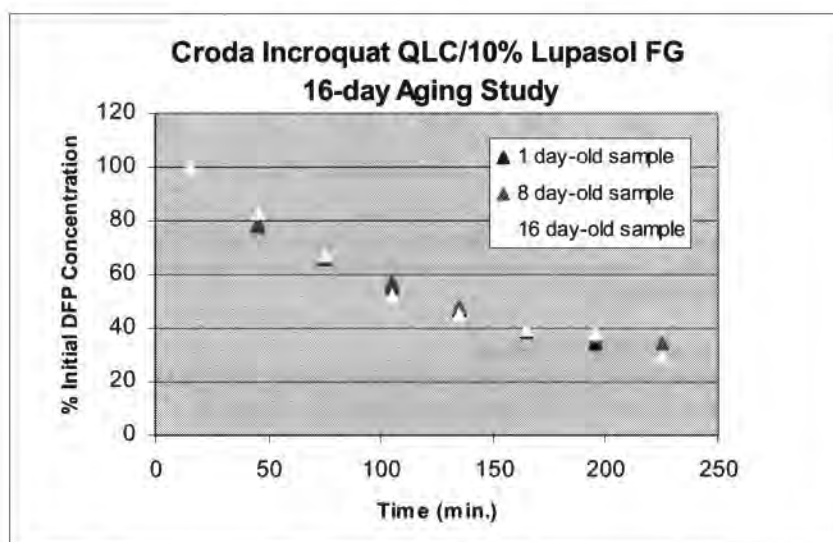


Figure 11 - Percent Loss of DFP vs. time for a Incroquat QLC/10% by wt. Lupasol FG sample over 16 days.

2.3.6.4 Concentration study – Incroquat QLC – 5%, 10%, and 20% by wt. Lupasol FG

Figure 12 (below) shows the results of a concentration study in which we evaluated the rate of removal of DFP from the headspace for half and double the typical Lupasol FG concentration of 10% by wt. Data was collected at each concentration level in triplicate; the data points shown in the chart are averages of three data sets each. As can be seen in the graph, the curve shape changes based on the concentration level of Lupasol FG. As expected, the 20% by wt. Lupasol FG curve drops more sharply than the 10% curve, which drops more sharply than the 5% curve. Fits to the three averaged data sets are shown by the dotted lines; the corresponding equations are shown next to each curve fit.

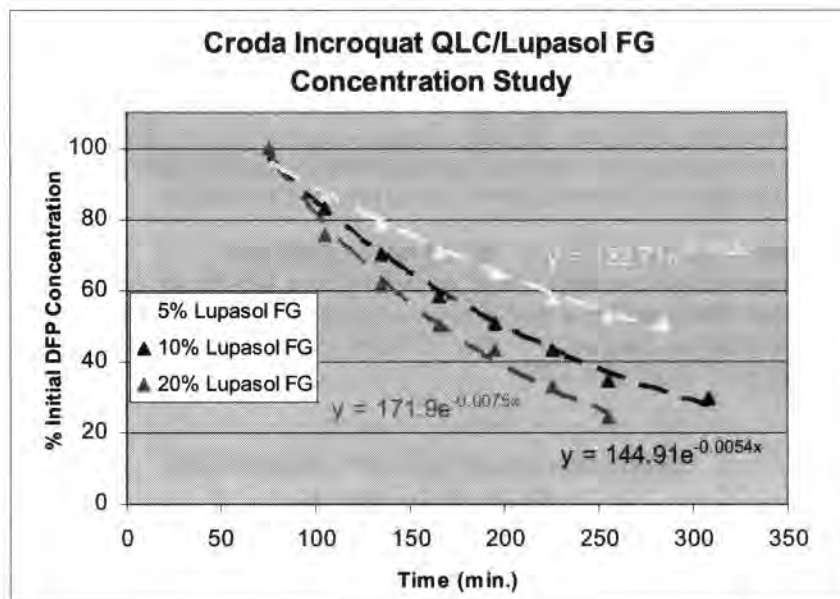


Figure 12 - Percent Loss of DFP vs. time for three concentration levels (5%, 10%, and 20%) of Lupasol FG in Incroquat QLC. Dotted lines show exponential curve fits; the corresponding equations are the same colors as the dotted lines.

2.3.6.5 Review of previous PEI/DFP results

US Patent Application 2004/0067205 describes the work performed by USAMRICD on incorporating PEIs into the SERPACWA-like base materials. Braue *et al.* evaluated the relative activity of five different Lupasol polyalkenimines including Lupasol FG, Lupasol WF, Lupasol G-20 WF, and Lupasol P by monitoring the extent of hydrolysis (ratio of hydrolysis products to DFP) in D₂O by phosphorus-31 NMR. After 2 hours, the extent of hydrolysis for the four solutions containing 2.5% by wt. Lupasol was 60-80% compared to that for D₂O alone (approximately 5% hydrolysis extent). After 12 hours, the extent of hydrolysis for the four solutions containing Lupasols ranged from 70-95% compared to D₂O alone, about 50%. Of the four Lupasols, FG and WF appear the most efficacious on both short (2 hour) and long (12 hour) time scales; Lupasol G20 WF and P were also shown to be more efficacious than D₂O.

A brief review of the technical and patent literature did not reveal additional examples of experimental data for the reaction of DFP with PEIs.

2.3.6.6 Comparison of previous results to current PEI/DFP

Although the methodology and matrix of the USAMRICD testing of PEI actives against DFP was quite different from the HS-SPME GC/MS testing we performed, the results we observed are in line with USAMRICD's results for Lupasol FG against DFP in D₂O. We observed a disappearance of DFP in the headspace of 70% of the initial value in 2-3 hours with 10% by wt. Lupasol FG; 55% reduction was observed after 2-3 hours for samples containing 5% by wt Lupasol FG. They observed an extent of hydrolysis of 75-80% during the same time period in their experiment with 2.5% Lupasol FG in D₂O.

2.3.7 Proof-of-Neutralization Test Results Against CEES

2.3.7.1 Control Samples – Incroquat QLC – No Lupasol FG

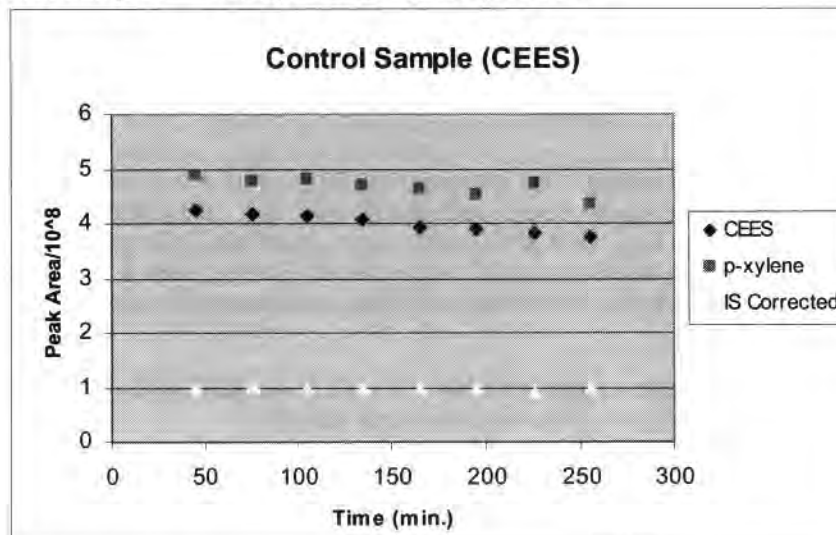


Figure 13 - Comparison of raw data vs. internal standard-corrected data for CEES challenge of a control sample (Incroquat QLC/Triton X-100)

The data shown in Figure 13 below illustrates a typical experimental result for a *control* sample containing Incroquat QLC and Triton X-100 (2.5%, mixing aid), but *no* neutralizing active. In this experiment, we injected 0.50 μ L of CEES into a sample vial containing 100 mg control sample at $t = 0$, then extracted the vial headspace over a period of 4-5 hours, at $t = 45, 75, 105, 135, 165, 195, 225$ and 255 minutes. The sample was maintained at 28-30C in a constant temperature bath throughout the experiment. As can be seen in Figure 13, the raw CEES response (blue diamonds) over time is nearly constant, with slight fluctuations in experimental conditions causing variability of about 4% of the average value over the experimental period. These fluctuations are corrected using an internal standard (p-xylene, pink squares) also present in the sample. The IS-corrected CEES response (yellow triangles) deviates about 2% from the mean value over the experimental period of over 4 hours. This "control" experiment was repeated on several different days to ensure that the result was reproducible.

2.3.7.2 Active Samples - Incroquat QLC – Lupasol FG

Our initial proof of neutralization test results using 10% by wt. Lupasol FG in Incroquat QLC (with 2.5% by wt. Triton X-100) did not show efficacy against a CEES challenge (to within experimental error) under the same conditions which had been used for the DFP experiments. Increasing the concentration of Lupasol FG to 30% by wt. also did not show a decrease in the % CEES in the headspace vs. time, up to 5.75 hours. In a third experiment, we applied CEES to neat Lupasol FG. After 2.5 hrs, a 10% drop in CEES headspace concentration was observed. For the same sample after 18 hours, 47% of the initial CEES concentration in the headspace remained. Relative to our previous results with DFP (70% decrease over 2-3 hours), it was apparent that Lupasol FG was less efficacious over an equivalent time period. Due to these initial results, we reviewed previous CEES results with SERPACWA and then identified and tested several hypotheses to explain this efficacy difference, as discussed below.

2.3.6.3 Review of previous PEI/CEES results

We reviewed US Patent Application 2004/0067205 describing the work performed by USAMRICD on incorporating PEIs into the SERPACWA-like base materials, to see if similar results for CEES relative to DFP were obtained. In the Patent Application, one proton NMR "degree of neutralization" study was reported in which a 2.5% Lupasol WF in D₂O was challenged with

CEES. The results (US 2004/0067205 Figures 3-5) showed no evidence of CEES or hydrolysis products remaining after a 12 hour time period, compared to some hydrolysis products remaining after 18 hours for CEES in D₂O with no Lupasol WF present. Results for a similar study with DFP reported in the Application indicated 70-80% DFP hydrolysis in the presence of 2.5 % Lupasol WF or Lupasol FG after 2 hours.

For the remainder of the PEI/SERPACWA results reported in 2004/0067205, sulfur mustard (not CEES) was used. Increased efficacy (relative to SERPACWA alone) with the inclusion of PEIs is evident from these results. Several formulations containing Lupasol FG at levels of 13-26% were among those showing the greatest efficacy against HD vapor, e.g., ICD# 3833, 3782, 3792, and 4051 and against HD liquid, e.g., ICD# 3792, 3833. Although no time information is given for the HD liquid (LAR) studies, the weanling pig (HD vapor) module showed a 66.6-88.4% decrease in erythema vs. control in a period of 30 minutes, indicating a neutralization reaction occurred during this time period.

A brief review of the technical and patent literature did not reveal additional examples of experimental data for the reaction of mustard simulants with PEIs.

2.3.6.4 Comparison of previous PEI/CEES results with current results

Since CEES has a chemical structure that is nearly identical to sulfur mustard (excluding one chlorine), and since there are many examples of CEES use as a simulant agent in the literature, it is assumed the molecule should have similar reactivity to HD with PEIs. Although the HD liquid results (US 2004/0067205) showed considerable neutralization in as little as 30 minutes for the PEI/SERPACWA formulation, we have not observed this under our experimental conditions using a similar % by wt. Lupasol FG formulation during a time period of up to 6.75 hours. It is possible that the reactivity of Lupasol FG or WF may be somewhat different for HD than for CEES. No comparable time scales (minimum of 12 hours) were given for CEES in the SERPACWA work to allow comparison. Other experimental conditions (e.g., time window of our experiment) may also factor into the different results as well.

2.3.6.5 Optimization of Efficacy Against CEES

To better understand the results of our Incroquat QLC/Lupasol FG formulations observed against CEES, we performed a several scoping experiments. These were based on the following hypotheses:

- *We may not see the extent of the reaction during our time window of 2-3 hours.*
Even at high levels of Lupasol FG (30-100%), the reaction rate appears slow. Extending the time window (up to 7 hours) allowed us to see a measurable decrease in headspace concentration.
- *Lupasol FG reaction may be slowed by "dryness" of the formulation.*
A consultation with a TIAX polymer expert (Dr. Peter Kopf) resulted in the suggestion of adding water to the formulation. Water (2.5 and 10% by wt.) was added to 30% Lupasol FG in Incroquat QLC formulations. Any decrease in the CEES headspace concentration for 2.5% water added was within the experimental error; while for 10% water the decrease was 2-4% over 4.5 hours.
- *CEES is not sufficiently soluble in Incroquat QLC/Lupasol FG formulation.*
CEES solubility is likely to be similar to HD, which is nearly insoluble in water. The Incroquat QLC/Lupasol FG is highly polar (hydrophilic). We surmised that an additional solvent may be needed to enable reaction to occur across this phase boundary. Methanol (2.5%) was added to a 10% Lupasol FG in Incroquat QLC sample. An 8% decrease in the CEES headspace concentration was observed over 6.75 hours. Figure 14 shows this result for an average of 5 runs over 5 different days. The error bars indicate \pm one standard deviation from the mean value. Even considering the large error bars, a clear decrease in CEES headspace concentration can be seen over the time period of the experiment.

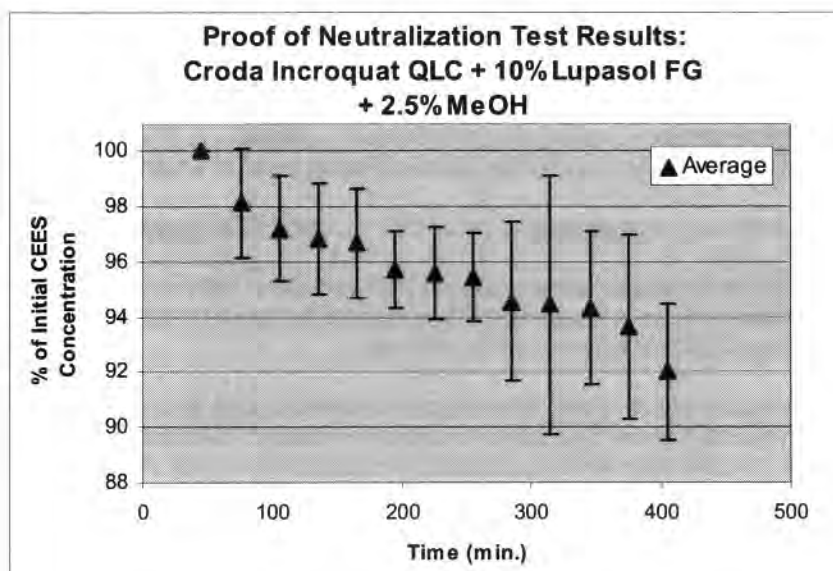


Figure 14 - Percent loss of DFP vs. time for the average of five Incroquat QLC/10% by wt. Lupasol FG samples. Measurements made over 5 days.

We realize that methanol is not an ideal solvent for inclusion in our final skin protection formulation, and plan to identify alternatives to methanol in the Phase I option period.

- Another Lupasol may be more effective than Lupasol FG.
At a level of 2.5% methanol/10% Lupasol in Incroquat QLC, a 5% decrease of CEES headspace concentration over 4.25 hours was observed.

2.3.6.6 Planned further experiments

Based on our initial scoping experiments using Lupasol FG and Lupasol WF with the addition of methanol against CEES, we plan to continue efforts to optimize our formulation by addition of solvents other than methanol, such as 1-propanol, 2-propanol, ethylene glycol, and others during the Phase I Option period.

2.4 Task 4: Program Communication and Reporting

We proposed to begin Phase I of this program with a kick-off meeting by teleconference, which occurred 06 July 05. The deliverable for Task 4 was (monthly) technical reports describing progress throughout the effort and a final report, detailing the activities and results of Phase I. Five technical monthly reports and one final report have been produced as part of this effort.

III. Key Research Accomplishments

- Identified substitute cationic polymer material (Croda's Incroquat QLC) to formulate with Lupasol (BASF Corp.) polyethylenimines following loss of access to originally proposed cationic polymer materials after technical partner's (MacroChem Corp.) unexpected bankruptcy announcement.
- Assessed compatibility of Incroquat QLC with four polyethylenimines (Lupasol FG, Lupasol WF, Lupasol G20 WF, Lupasol P) in theoretical and laboratory studies.
- Identified best candidate combination for testing against chemical agent simulants DFP and CEES: 10% Lupasol FG in Incroquat QLC with 2.5% Triton X-100 as a mixing aid.
- Optimized/validated and developed protocol for HS-SPME GC/MS method to measure DFP and CEES headspace concentrations.

PROPRIETARY INFORMATION – NOT APPROVED FOR PUBLIC RELEASE
SBIR Data – See Cover Page for Use, Release, and Disclosure Restrictions

- Evaluated efficacy of candidate Incroquat QLC/Lupasol FG formulation against DFP and CEES.
- Observed 70% decrease in headspace concentration of DFP over 2-3 hours for 10% Incroquat QLC/Lupasol FG combination, demonstrating proof of neutralization.
- Demonstrated efficacy is unchanged against DFP in a short term aging study of 16 days.
- Demonstrated that increased efficacy against DFP correlates with concentration of Lupasol present; increasing the wt % of Lupasol FG increases the rate of reduction of DFP from the headspace under identical experimental conditions.
- Optimized Incroquat QLC/Lupasol formulation to achieve 8-10% decrease in CEES concentration over 5-7 hours by addition of solvent methanol, demonstrating proof of neutralization. (We will identify an alternative to methanol during the Phase I Option period).

IV. Reportable Outcomes

- On 27 July 05, we submitted the following abstract for the PITTCON 2006 meeting (12-17 March 06, Orlando, FL). The abstract was accepted as an oral presentation. Unfortunately, a unanticipated scheduling contract prevented us from attending. We have been invited to re-submit for PITTCON 2007.

HS-SPME Analysis Method for Evaluating the Efficacy of Candidate Skin

Decontamination Formulations Against Chemical Warfare Agent (CWA) Simulants

US Armed Forces personnel abroad face the threat of chemical warfare agent (CWA) attack daily. Currently available to soldiers are creams that temporarily protect the skin at openings in MOPP (mission oriented protective posture) gear but do not neutralize the threat. Following exposure, thorough decontamination of the skin is required within hours to minimize permanent tissue damage, often a logistical challenge in the field. We are developing an alternative cream incorporating active moieties into a proprietary polymer base material. This new formulation will both protect the soldier's skin and neutralize CWAs into less toxic products on contact, reducing or eliminating the need for immediate decontamination in the field. To evaluate the efficacy of the candidate formulations, we have used Head Space-Solid Phase Micro Extraction (HS-SPME) GC/MS. HS-SPME is a solvent-less extraction technique that involves the exposure of a coated fused-silica fiber to the headspace of a solid or liquid sample. SPME is ideal for rapid screening due to reduced sample preparation time and analysis costs. In this paper, we present the results of challenge testing candidate skin protection formulations with two chemical agent simulants, and discuss the optimization of the HS-SPME technique for this unique application. This work was supported by the US Army Medical Research Institute for Chemical Defense under the SBIR program (Contract No. W81XWH-05-C-0131).

- We anticipate filing of a provisional patent application prior to the end of the Phase I option period.

V. Conclusion

Our Phase I results demonstrate proof-of-concept towards the development of a new topical skin protectant technology that will neutralize chemical warfare agents (CWA) on contact. **The key outcome of our Phase I program is the identification of a promising cationic polymer-neutralization active combination, Incroquat QLC/Lupasol FG, based on results of HS-SPME proof of neutralization testing against chemical agent simulants DFP and CEES.** We have demonstrated significant efficacy against nerve agent simulant DFP for the Incroquat

QLC/Lupasol FG polymer-active combination (70% reduction over 2-3 hours). Proof of neutralization was also observed against CEES (8-10% reduction over 5-7 hours); we are continuing optimization against this mustard agent simulant during the Phase I option period.

Our Phase I proof-of-concept work will be built upon during Phase II, in which we will extend these polymer-active combinations into prototype cream or gel formulations. We plan to evaluate the skin protective capacity of prototype formulations in a series of skin permeation tests using a Franz Cell apparatus. These prototypes may incorporate Incroquat QLC as well as other polymers of similar structure synthesized for us by our commercialization partner, Croda Inc. Our final Phase II prototype formulations will be tested for efficacy using both simulants and chemical warfare agents (conducted by USAMRICD).

This work extends earlier research conducted by USAMRICD (US 2004/0067205). Braue *et al.* conducted a series of experiments evaluating the feasibility of incorporating neutralizing actives (including the Lupasol polyethylenimines) into Skin Exposure Reduction Paste Against Chemical Warfare Agents (SERPACWA). Consisting of fine particulates of polytetrafluoroethylene (PTFE) resins dispersed in perfluorinated polyether (PFPE) oils, it provides an occlusive physical barrier to percutaneous contamination. Incorporating neutralizing actives does increase efficacy of SERPACWA by neutralizing CWAs that penetrate into the base cream; however, contamination remaining on the surface of the barrier coating remains unreacted. Thus, despite some increase in efficacy against nerve (GD, VX) and mustard agent (HD) Braue *et al.* observed by incorporating PEIs (relative to SERPACWA alone), the PTFE/PFPE vehicle is less than ideal. Our approach is to both dissolve the CWA challenge and neutralize the agent before it reaches the skin surface, which will result in a neutralizing skin protectant that is effective and more comfortable than SERPACWA, the product currently available to soldiers.

VI. References

Braue, E.H. Jr., "Development of a Reactive Topical Skin Protectant," J Appl Toxicol, 19, S47-53, 1999.

Braue, E.H., Hobson, S.T., Boecker, J.D., Smith, B.M., "Active Topical Skin Protectants Containing Amines, Polyalkenimines and/or Derivatives," 2004, U.S. Patent Application 2004/0067205.

"Decontamination" www.nbcdefense.net/nore/decon.html

Ellen, S. "Personal decontamination products protect the warfighter from battlefield health hazards," Military Medical Technology [Online Edition]. www.military-medical-technology.com

Hobson, S. T., Lehnert, E. K., and Braue, E. H. Jr., "The U. S. Army Reactive Topical Skin Protectant (rTSP): Challenges and Successes," MRS Symposium Series CC: Hybrid Organic Inorganic Materials [Online], 628, CC10.8.1-CC10.8.8, 2000.

Hurst, C. G. 1997. "Chapter 15: Decontamination." P. 351-359 in Medical Aspects of Chemical and Biological Warfare, edited by Sidell, F.R., Takafuji, E.T., Franz, D.R. Washington, DC: TMM Publications.

"Incroquat QLC: Quaternized Lipid Conditioner," Croda, Inc. Datasheet DS-177, 2003.

Information Paper DASG-HCF 20 Feb. 03: Skin Exposure Reduction Paste Against Chemical Warfare Agents (SERPACWA). 2003. www.wood.army.mil

"Lupasol® Product Range: Preliminary Technical Information," BASF, 1996.
<http://www.basf.com/businesses/coatcolor/printingink/pdfs/lupasol/lupasol%20web/lupasol%20ag.pdf>

"Lupasol® FG Polyethylenimine," Technical Bulletin, BASF Corporation, 2002.

"Lupasol® 20G Waterfree Polyethylenimine," Technical Bulletin, BASF Corporation, 2002.

"Lupasol® P Polyethylenimine," Technical Bulletin, BASF Corporation, 2002.

"Lupasol® Waterfree Polyethylenimine," Technical Bulletin, BASF Corporation, 2002.

Samour, C., Krauser, S. F. MacroChem Corporation. "Cationic film-forming polymer compositions, and use thereof in topical agent delivery system and method of delivering agents to the skin." 1998. U.S. Pat. 5,807,957.

Samour, C., Krauser, S. F. MacroChem Corporation. "Cationic film-forming polymer compositions, and use thereof in topical agent delivery system and method of delivering agents to the skin." 1999. U.S. Pat. 5,906,822.

"Skin Exposure Paste Indications, Dosage, Stability."
www.rxlist.com/cgi/generic3/skinexpose_ids.html

Vas, G., Vekey, K., "Solid-phase microextraction: a powerful sample preparation tool prior to mass spectrometric analysis" J. Mass Spectrom., 39, 233–254, 2004.

VII. Appendices

Appendix A: Proof of Neutralization Testing GC/MS HS-SPME Method Protocol

Objective:

Verify that sample formulations neutralize simulant CWAs (DFP and CEES) into less toxic products using the Headspace Solid Phase Micro-Extraction (HS-SPME) technique to collect the simulants in headspace above the samples vs. time.

Equipment:

Thermoelectron Trace GC/Trace MS system
Rtx -5 Capillary GC column (30 m x .25 mm x 1 μ m, Restek #10253)
SPME Fiber Holder, 23 gauge, for use with manual sampling (Sigma Aldrich PN 57330-U)
Fiber Assembly – 100 μ m PDMS fiber, SPME fiber assembly, for manual holder (Sigma Aldrich PN 57342-U)
4 mL clear glass screw top vials with hole cap, pre-assembled (Sigma Aldrich PN 27136)
Syringes, 1 μ L, 10 μ L (Hamilton)
Magnetic Stir/Hot Plate (Corning)
Constant Temperature Bath, Digital thermometer
Stopwatch

Fiber Pre-Conditioning Protocol:

0.5 hr at 250 C (Max desorption temperature is 280C) as prescribed by Sigma-Aldrich Data Sheet T794123M

Sample/Controls(s) Run Protocol:

1. Weigh 100 mg polymer/active sample into tared 4 mL headspace vial, add Teflon-coated stir-bar, cap vial.
2. Allow sample to equilibrate with 28-30 C constant temperature bath for a minimum of 30 minutes.
3. Remove sample from bath, using syringe add 5 μ L internal standard through vial septum, magnetic stir for 5 sec. at setting 2.
4. Using second syringe, add 5 μ L simulant through vial septum, magnetic stir for 5 second at setting 2, return to constant temperature bath. Mark time. Decontaminate syringe.
5. Equilibrate sample with constant temperature bath for 15 min.
6. Extract sample headspace by injecting SPME fiber into vial (still in constant temperature bath).
7. Retract fiber into SPME holder, transfer to GC injector port. Hold at 250C for 2.5 min. to desorb fiber.
8. Run GC program: 2.5 min. hold at 40C, ramp 10C/min. to 150 min., hold 1 min.
9. Repeat steps 7-9 until the desired number of data points are gathered.
10. Integrate peak areas (internal standard and simulant) using automated processing method.
11. Use internal standard peak areas to correct for any fluctuation in instrument performance.

Appendix B - Optimization and Validation of HS-SPME GC/MS Method

B.1 Optimization of Desorption Conditions

Desorption of the sample involves placing the SPME fiber into the hot GC injector port to release an absorbed analyte from the coating of the fiber.

B.1.1 Desorption Temperature Selection

The maximum temperature for the 100 μ m PDMS fiber we are using is 280C. For DFP, a slightly lower desorption temperature of 250C was selected to maximize the life of the fiber. 250C is a fairly standard literature value for a desorption temperature. Due to the experimental observation that CEES required additional time to desorb from the fiber relative to DFP (see discussion below in B.1.3), we raised the desorption temperature from 250C to 265C for the CEES experiments. During a conversation (27 Jul 05) about the SPME method, Dr. Kevin Morrissey (who performed the SERPACWA work) recommended desorption temperatures of 250C and 260C for DFP and CEES respectively.



B.1.2 Needle Depth Optimization

The depth of the fiber should be adjusted to place it in the center of the hot injector zone of the GC to ensure efficient, reproducible desorption (Pawliszyn, 1997). A schematic of an HS-SPME device is shown in Figure B1. This parameter was optimized by observing the GC response for three different fiber depths in the GC injector port as determined by needle guide/fiber depth gauge positions 2.4, 3.4, and 4.4. Three replicates for each fiber position were obtained. The sample was 0.100 g Incroquat QLC/Triton X-100 (2.5 % by wt.) in a 4 mL sample vial, with 0.5 μ L injections of DFP and p-xylene (IS). After injection, each sample was allowed to equilibrate in a constant temperature bath at 28-30 C for approximately 1 hour (prior to extraction). The extraction time was 2 minutes per sample.

Results of this study are shown in Figure B2.

The DFP and p-xylene peak areas increase (45-55%) as the needle guide/fiber depth gauge position increases from 2.4 to 4.4, indicating this change moves the fiber towards the hottest part of the GC injector port. The *ratio* of DFP to p-xylene (which is reported in the efficacy studies) is constant within 2% of the average value over all nine measurements; it increases 4% over position 2.4-4.4. For repeated measurements, practical considerations limit the position of the fiber to 4.0 or less, therefore the fiber will be held constant at this position. The needle guide/fiber depth position can be locked in place and is easily reproduced over multiple measurements. The fiber depth was held at position 4.0 for the CEES studies as well.

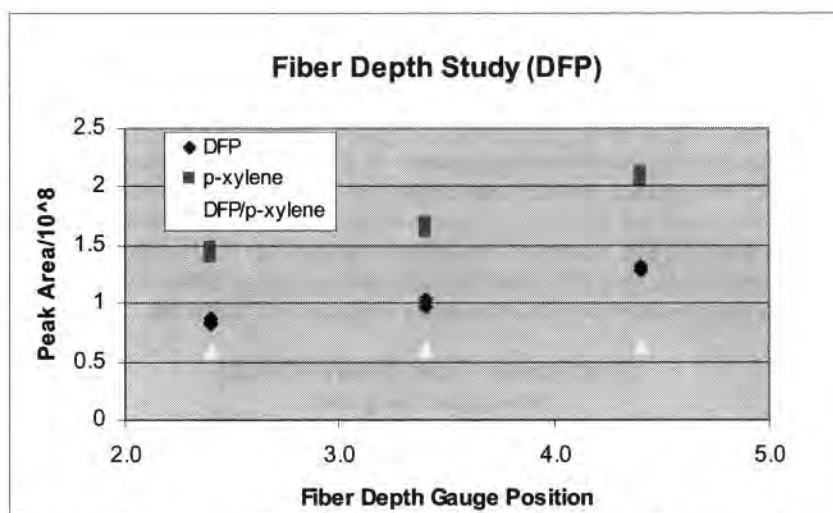


Figure B2- GC Response at Fiber Depth Positions 2.4, 3.4, and 4.4 for DFP and p-xylene (IS).

B.1.3 Fiber Desorption Time Optimization

To determine the optimal desorption for the DFP experiments, measurements were made (in triplicate) at desorption times of 1, 4, and 8 minutes for a sample of 0.100 g Incroquat QLC/Triton X-100 (2.5 % by wt.) under the same conditions referenced above for the fiber depth measurements (2 minute extraction time). The results of this study for DFP and internal standard p-xylene are displayed in Figure B3.

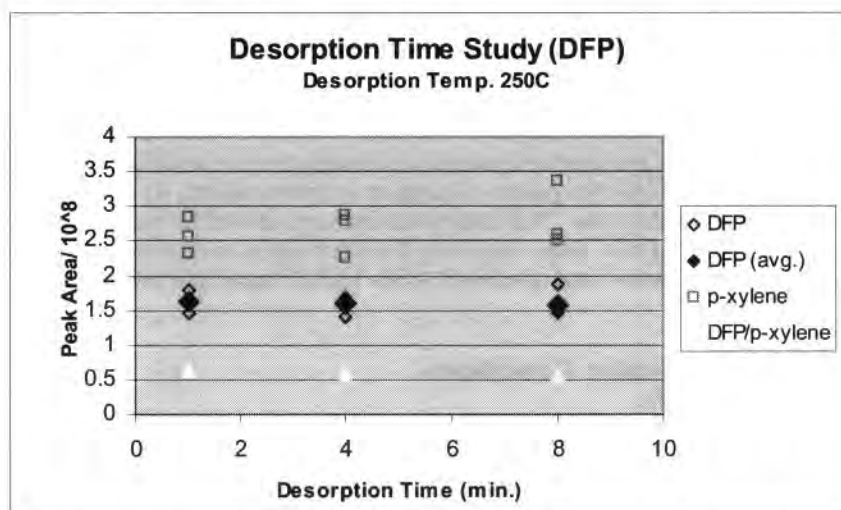


Figure B3- GC Response at Desorption Times of 1, 4, and 8 min. for DFP and p-xylene (IS).

The unusual scatter in this data set obscures the slight trend toward increasing peak area with increasing desorption time for p-xylene; the opposite trend is observed for DFP. However, if the averages of the measurements at each desorption time are considered, the % deviation is 1.5% for DFP, 3.2% for p-xylene over the range of desorption times. For a given compound, variability increases as desorption time increases. We selected a desorption time of 2.5 minutes for the DFP experiments based on the need to minimize the time of each extraction-desorption step and also the variability between measurements.

To optimize the desorption time for CEES, measurements were made (in triplicate) at desorption times over 1-8 minutes for a sample of 0.100 g Incroquat QLC/Triton X-100 (2.5 % by wt.) spiked with 0.5 μ L CEES for a 15 minute extraction time and desorption temperature 250C. At this desorption temperature, we observed an increase in GC response with increasing desorption time of 23%, indicating that all of the CEES was not being fully desorbed at the shorter (1-2 min.) desorption times. We then repeated the experiment (in triplicate) at a higher desorption temperature of 265C, the results of which are shown as filled blue diamonds in Figure B4. An additional data point was added. Based on these results, we selected a desorption time of 5 min. to ensure that all of the CEES is desorbed and due to the greater fluctuations at shorter desorption times (Figure B4). The instrumental fluctuations are corrected by inclusion of the internal standard, p-xylene, as shown by the yellow triangles of Figure B4.

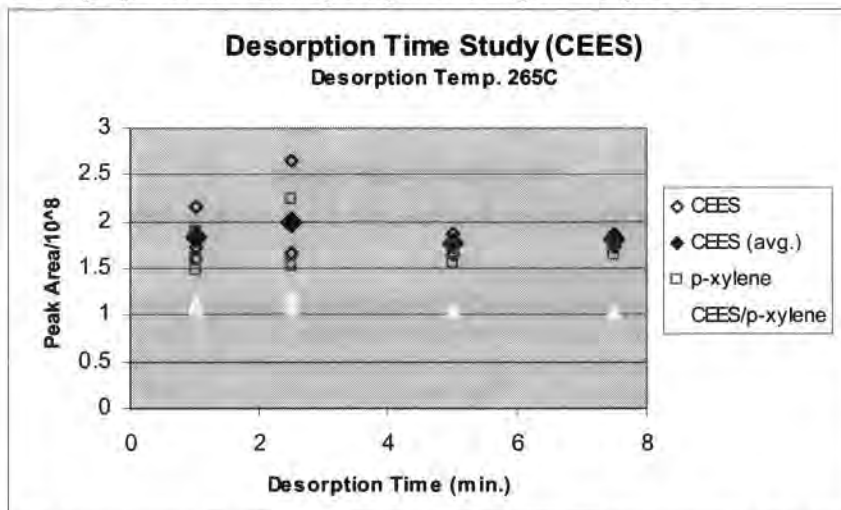


Figure B4- GC Response at Desorption Times of 1, 2.5, 5, and 7.5 min. for CEES and p-xylene (IS).

Other parameters used to optimize desorption conditions include: 1) use of a narrow bore GC injector insert, 2) exposure of the fiber *immediately* following needle introduction into the injector, 3) regular examination of the inlet for pieces of septum (contamination), 4) analysis of the fiber following an extraction for carry-over. The lattermost test was carried by capping the end of the fiber holder following a desorption, then desorbing the fiber again immediately after the previous run was completed. No carryover was observed under typical experimental conditions for DFP or CEES.

B.2 Optimization of Extraction Conditions

B.2.1 Extraction Time Profile

The extraction time is the period that the fiber is exposed to the sample; increasing the time of extraction therefore increases the amount of analyte absorbed by the fiber coating. As extraction time increases, an "equilibrium" state is reached at which a small variation in extraction time does not result in a large variation in GC response. The most desirable extraction time for quantitative measurements will therefore be at shortest possible extraction time after which equilibrium is reached.

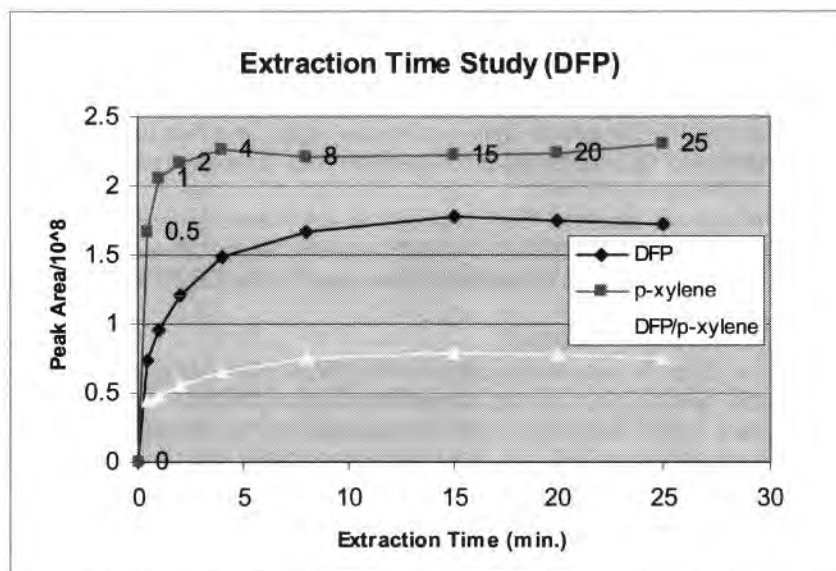


Figure B5- Extraction Time Profile for DFP and p-xylene(IS).

An example of an extraction time profile for DFP and p-xylene is shown in Figure B5 and for CEES and p-xylene in Figure B6. The extraction time profile was obtained by making a series of measurements with progressively longer extraction times over a period of about 4 hours, using the optimized desorption time and fiber position for each simulant. The sample was prepared as described in the Desorption Optimization section above.

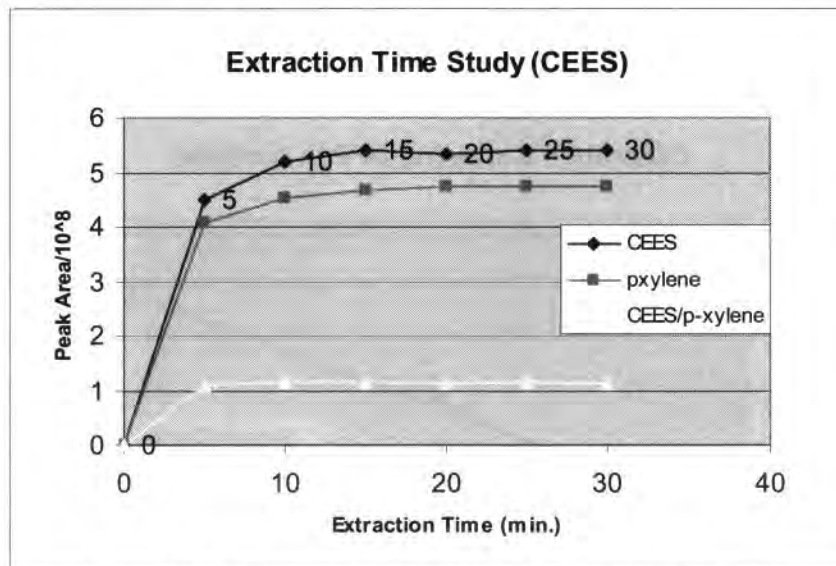


Figure B6- Extraction Time Profile for CEES and p-xylene (IS).

B.2.2 Selection of Extraction Time

As can be seen from the extraction time profile displayed in Figure B5, the p-xylene concentration (pink squares) reaches an equilibrium state very rapidly (~4 min.) while for DFP (blue diamonds), the equilibrium state is not apparent until an extraction time of 15 minutes. The ratio of DFP/p-xylene (yellow triangles) on which our quantitative results will be based reaches equilibrium at 15

minutes. We have therefore selected 15 minutes as the extraction time for the remainder of the experiments with DFP.

CEES and p-xylene have both reached an equilibrium state at an extraction time of 15 minutes (Figure B6). The ratio of CEES/p-xylene (yellow triangles) again reaches equilibrium by 15 minutes. We have selected 15 minutes as the extraction time for experiments with CEES as well.

During extraction, the sample (and the fiber) was held in a constant temperature bath at 28-30C, selected to minimize the degradation of DFP, which occurs at temperatures above 30C according to the manufacturer's MSDS. The same temperature was used in the CEES experiments as well.

B.3 Selection of Calibration Method

It is not our intention to provide quantitative data in this efficacy screening study (our experiments are relative to a control sample), but we did attempt to roughly correlate mass transfer of DFP from the vial headspace to GC response. To do this we selected a calibration method based on injecting known concentrations of DFP in a non-interfering solvent (acetone) directly into the GC. By non-interfering, it is meant that the solvent should not effect the GC response to DFP. This is a reasonable assumption based on the fact acetone is commonly used as a solvent in the quantitative analysis of organophosphorous pesticides (e.g., NIOSH Method 5600) via GC and GC/MS. We evaluated GC response (in triplicate) for standards containing 10.6 ng, 265 ng, and 530 ng DFP in a 1 μ L acetone injection. The experimental conditions were otherwise the same as in the measurements discussed above.

Typical GC response for our control samples (Croda/Triton) with a 0.5 μ L DFP spike has been in the range of 10-20 $\times 10^7$. As can be observed in Figure B7, the GC response (peak area) in this range is quite linear. Assuming 100% transfer of the DFP onto the GC column, the typical 10-20 $\times 10^7$ response indicates mass transfer in the range of 300-500 ng from the fiber into the GC. As a typical DFP spike is 50 μ L (53 μ g), this is a 0.6-1.0% transfer of DFP from the sample matrix (Croda/Triton/DFP) to the fiber under typical experimental conditions. We did not identify a calibration method for CEES beyond that which we used for DFP.

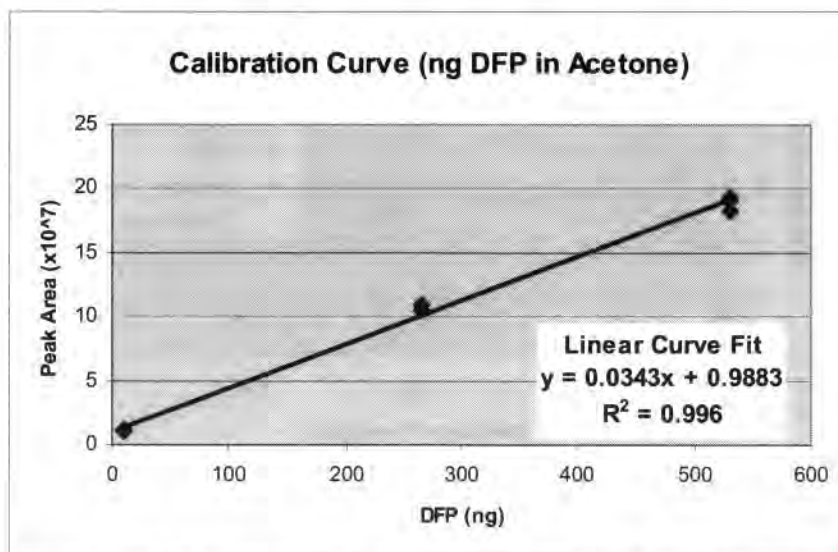


Figure B7 - GC Response vs. ng DFP for direct injection of DFP in acetone.

VIII. Supporting Data

Included within body of report.

PROPRIETARY INFORMATION – NOT APPROVED FOR PUBLIC RELEASE
SBIR Data – See Cover Page for Use, Release, and Disclosure Restrictions

SBIR final report from TIAX LLC, Phase II

Award Number: W81XWH-05-C-0131

Contract Number: W81XWH-05-C-0131

TITLE: Novel Polymeric Formulations for Skin Protection and Decontamination

PRINCIPAL INVESTIGATOR: Arthur Schwope, Ph.D.

CONTRACTING ORGANIZATION:

US Army Medical Research Acquisition Activity (USAMRAA)
Fort Detrick, MD 21702

REPORT DATE: December 2012

TYPE OF REPORT: SBIR Phase II Final Report

PREPARED FOR:

U.S. Army Medical Research and Materiel Command (USAMRMC)
Fort Detrick, MD 21702-5012

DISTRIBUTION STATEMENT:

Distribution limited to U.S. Government agencies only; report contains proprietary information



The views, opinions and/or findings contained in this report are those of the author(s) and should not be construed as an official Department of the Army position, policy or decision unless so designated by other documentation.

SBIR DATA RIGHTS

Contract Number	W81XWH-05-C-0131
Contractor Name	TIAX LLC
Contractor Address	35 Hartwell Ave, Lexington MA 02421
Expiration of SBIR Data Rights Period	09/31/2017 unless extended

The government's right to use, modify, reproduce, release, perform, display or disclose technical data or computer software marked with this legend are restricted during the period shown as provided in paragraph (b)(4) of the Rights in Noncommercial Technical Data and Computer Software—Small Business Innovative Research (SBIR) Program clause contained in the above identified contract. No restrictions apply after the expiration date shown above. Any reproduction of technical data, computer software, or portions thereof marked with this legend must also reproduce the markings.

Novel Polymeric Formulations for Skin Protection and Decontamination

SBIR Phase II Final Report

Contract # W81XWH-05-C-0131

REPORT DOCUMENTATION PAGE			Form Approved OMB No. 0704-0188		
Public reporting burden for this collection of information is estimated to average 1 hour per response, including the time for reviewing instructions, searching existing data sources, gathering and maintaining the data needed, and completing and reviewing this collection of information. Send comments regarding this burden estimate or any other aspect of this collection of information, including suggestions for reducing this burden to Department of Defense, Washington Headquarters Services, Directorate for Information Operations and Reports (0704-0188), 1215 Jefferson Davis Highway, Suite 1204, Arlington, VA 22202-4302. Respondents should be aware that notwithstanding any other provision of law, no person shall be subject to any penalty for failing to comply with a collection of information if it does not display a currently valid OMB control number. PLEASE DO NOT RETURN YOUR FORM TO THE ABOVE ADDRESS.					
1. REPORT DATE 21-12-2012		2. REPORT TYPE SBIR Phase II Final Report		3. DATES COVERED 24-03-2006 - 21-12-2012	
4. TITLE AND SUBTITLE Novel Polymeric Formulations for Skin Protection and Decontamination			5a. CONTRACT NUMBER W81XWH-05-C-0131		
			5b. GRANT NUMBER		
			5c. PROGRAM ELEMENT NUMBER		
6. AUTHOR(S) Arthur Schwope, Ph.D. Michael J. Jakubowski E-Mail: Schowpe.A@tiaxllc.com			5d. PROJECT NUMBER		
			5e. TASK NUMBER		
			5f. WORK UNIT NUMBER		
7. PERFORMING ORGANIZATION NAME(S) AND ADDRESS(ES) TIAx LLC 35 Hartwell Ave. Lexington, MA 0242			8. PERFORMING ORGANIZATION REPORT NUMBER D0323-FINAL		
9. SPONSORING / MONITORING AGENCY NAME(S) AND ADDRESS(ES) U.S. Army Medical Research and Materiel Command Fort Detrick, Maryland 21702-5012			10. SPONSOR/MONITOR'S ACRONYM(S) USAMRMC		
			11. SPONSOR/MONITOR'S REPORT NUMBER(S)		
12. DISTRIBUTION / AVAILABILITY STATEMENT Distribution authorized to U.S. Government Agencies only, Proprietary Information. The data delivered to the Government is marked with the SBIR Data Rights Notice; the Government may use the data for government purposes only, and cannot disclose the data outside the Government (except for use by support contractors) for a specified period of time.					
13. SUPPLEMENTARY NOTES SBIR Data Rights					
14. ABSTRACT: Currently there is a need for a pre-exposure decontaminating skin cream that will neutralize chemical warfare agents (CWA) on contact. Current approaches to this problem cannot both dissolve a CWA challenge and neutralize the agent into less toxic products before it reaches the skin surface. During Phase II, we developed a number of Neutralizing Skin Protectant (NSP) formulations that utilize physiochemical means to absorb and neutralize CWA simulants, five of which were tested against live agents.					
15. SUBJECT TERMS Decontamination, neutralization, CWA, skin protection, topical skin protection, skin cream, chemical warfare agent, CWA protection					
16. SECURITY CLASSIFICATION OF:			17. LIMITATION OF ABSTRACT	18. NUMBER OF PAGES	19a. NAME OF RESPONSIBLE PERSON
a. REPORT Unclassified	b. ABSTRACT Unclassified	c. THIS PAGE Unclassified	Unclassified	60	USAMRMC
					19b. TELEPHONE NUMBER (include area code)

Standard Form 298 (Rev. 8-98)
Prescribed by ANSI Std. Z39.18

TABLE OF CONTENTS

1.0	Introduction.....	4
2.0	Report Body	5
2.1	Task 1: Program Needs Update and FDA Approval Planning	6
2.2	Task 2: Pre-Formulation of Neutralizing Skin Protectant.....	7
2.3	Task 3: Formulation of Neutralizing Skin Protectant.....	27
2.4	Task 4: In vitro Skin Permeation Assessment Studies with CWA Surrogate Challenges ...	35
2.5	Task 5: Program Communication and Reporting	40
2.6	Task 6: Finalize Phase II Commercialization Partner	41
3.0	Key Research Accomplishments.....	46
4.0	Reportable Outcomes.....	46
5.0	Conclusion	47
6.0	References	48
7.0	Appendix	49
7.1	Head Space Test Protocol, Validation and Method Development.....	49
7.2	Proof of Neutralization Testing GC/MS HS-SPME Method Protocol	51
7.3	Skin Barrier GC/MS Standard Operating Procedure.	54
7.4	Summary of NSP Preparation Procedures and Results	55

1.0 Introduction

Given recent domestic and global events there is a need for a decontaminating skin cream that neutralizes chemical warfare agents (CWAs) on contact. The technology currently available to soldiers, Skin Exposure Reduction Paste Against Chemical Warfare Agents (SERPACWA) provides effective *pre-exposure* protection. However, efforts to incorporate reactive moieties into SERPACWA in order to neutralize CWAs have met with varied success. Other personal decontamination products currently in use by the military, such as the M291 SDK, provide only *post-exposure* CWA neutralization. None of these approaches can both *dissolve* a CWA challenge and *neutralize* the agent into less toxic products before it reaches the skin surface, providing both *pre- and post-exposure* protection.

TIAX's approach to this problem is an innovative solution for *pre/post-exposure* skin-decontamination using a Neutralizing Skin Protectant (NSP). As illustrated in Figure 1, we envision the final TIAX NSP prototype to protect exposed skin from chemical agents by solubilizing the CWA and enabling a neutralization reaction to occur with the help of a dissolved neutralizing "active", polyethyleneimine (PEI), while reducing the diffusion rate of the CWA through the formulation.

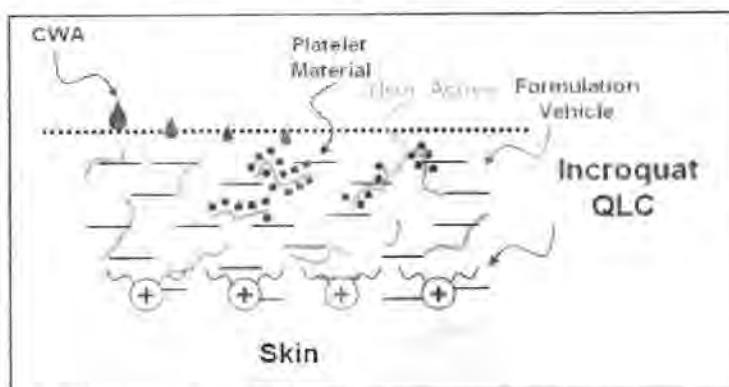


Figure 1: Mechanism of action against CWAs using TIAX's NSP.

Our approach built upon our preliminary Phase I results demonstrating the efficacy of neutralizing active/cationic polymer combinations against chemical agent surrogates. In Phase I, we evaluated the feasibility of incorporating neutralizing actives (polyethylenimines) into the skin-friendly polymer base, Incroquat QLC (Croda, Inc.). Our results showed proof-of-neutralization against surrogates for mustard and nerve agents, chloroethyl(ethyl) sulfide (CEES) and difluorophosphate (DFP), respectively. During the Phase I Option period, we further optimized the formulation against CEES by addition of selected solvents that increase the solubility of CEES in Incroquat QLC/Lupasol FG combination.

During Phase II we built upon Phase I "pre-formulations", developing prototype cream formulations, and submitted them for *in vitro* permeation assessment against live chemical agents at the USAMRICD. In addition, we are seeking additional funding to further optimize the final prototypes to be tested against live chemical agents. We have also identified two companies interested in helping to commercialize the NSP product: Steris Corporation and EZ-EM Inc., the manufacturer of currently fielded Reactive Skin Decontamination Lotion (RSDL). While a pre-exposure skin protectant for the US Military is the primary goal of this work, skin protection for first responders may be our first civilian product. The platform technology developed during Phase II program also has considerable appeal for other civilian companies, such as manufacturers of personal care products like sunscreens and insect repellants, in which there is value to consumers in reducing percutaneous absorption of actives. Proctor & Gamble and Reckitt-Benckiser, both multi-million dollar consumer products companies, have expressed interest in our platform technology.

2.0 Report Body

This section of the report describes the research accomplishments of Phase II associated with each task as outlined in the original Phase II proposal (Figure 2).

Task 1: Program Needs Update and FDA Approval Planning <ul style="list-style-type: none"> Kick-off Meeting Summary Phase II Regulatory Issues Plan
Task 2: Pre-Formulation of Neutralizing Skin Protectant <ul style="list-style-type: none"> Selection of Ingredients Draft Processing Protocol for Task 3
Task 3: Formulation of Neutralizing Skin Protectant <ul style="list-style-type: none"> Neutralizing Skin Protectant Formulations for Task 4 Testing Designed Experiment(s) for Testing Formulations Draft Protocol for <i>In vitro</i> Skin Permeation Assessment
Task 4: <i>In vitro</i> Skin Permeation Assessment Studies with CWA Surrogate Challenges* <ul style="list-style-type: none"> Skin Permeation Testing Results* Prototype Formulations for Testing with Live Agents at USAMRICD
Task 5: Program Communication and Reporting <ul style="list-style-type: none"> Monthly Status Reports Final Report Presentation of Phase II Programs Results
Task 6: Finalize Phase II Commercialization Partner <ul style="list-style-type: none"> Description of our Selection Criteria and Process Final Identification of our Technology Transformation Partner

* This task was modified after extensive discussions with the COR. The deliverables represented here are as they were originally stated in the proposal.

Figure 2: Tasks and Deliverables of Phase II SBIR Program

2.1 Task 1: Program Needs Update and FDA Approval Planning

Objectives

- Program Kick-off Meeting
- Initiate Discussions with FDA to Accelerate Regulatory Approvals

Summary of Task 1

To facilitate good communication and alignment of goals throughout the effort, we proposed to begin the Phase II program with a kick-off meeting. A summary of this teleconference was submitted to the COR in a monthly report and via email.

A key consideration guiding our Phase II work is the need for eventual FDA approval of the skin protectant prior to use by the US Military or civilian applications. We sought to begin discussions with the FDA to inform them of the project and our approach, soliciting their guidance on proceeding as quickly as possible through the necessary regulatory steps. Via discussions with FDA staff and review of the FDA website, we have determined the most appropriate type of meeting (Pre-IND, Type C) and have drafted a Pre-IND Meeting Request form. The Meeting Request form has been reviewed and approved by the COR. We have had some difficulty in determining who the representative would be (besides the COR) from the Army; hence, we have not yet submitted the Meeting Request form to the FDA. Once it is submitted, it is anticipated that the meeting would occur in approximately 90 days. As a result of these discussions we will better understand the requirements for classification of the product as a cosmetic, medical device, or drug. We realize we may need to petition the FDA to consider our final product a medical device, instead of a drug. Guided by conversations with the FDA, we can then address any issues with our approach and make the appropriate filings as early as possible.

Our interim reports have detailed our efforts to obtain a representative from the CBD to help us with the FDA approval process. As of July 2008, we had identified "Gary" Guilin Qiao, DVM, PhD, Sr. Pharmacologist/Subject Matter Expert-Regulatory (703-767-3375) within the CBD JSTO as someone who could attend the FDA meeting along with the SBIR COR, Dr. Ernie Braue. Due to the positive results from the *in vitro* Skin Permeation Assessment of our final NSP prototypes, we will restart discussions with Dr. Qiao and send a FDA form request for him to review before submission to the FDA.

2.2 Task 2: Pre-Formulation of Neutralizing Skin Protectant

Objectives

- Compilation of Physical and Chemical Data of Actives, Functional and Inactive Excipients
- Select Vehicle for NSP Formulations
- Develop Formulation Processing Protocol
- Identify and Obtain Chemicals, Materials, and Equipment required for Formulation/Testing

Summary of Task 2

In Task 2 we compiled physical and chemical data for the actives, skin-friendly polymer (Incroquat QLC), and diffusion-inhibiting materials that would be used in the NSP formulations from available literature. Based on the compilation of physical/chemical properties, we selected suitable vehicles and excipients, and developed a processing method. We also identified a source of human cadaver skin and selected and purchased the Franz cell apparatus that were to be used in Task 4 testing.

Compilation of Physical and Chemical Data of Actives, Functional and Inactive Excipients

The pre-formulation approach to developing NSP formulations involved compiling physical and chemical data for the neutralizing actives and other key materials in the formulation, such as the Incroquat polymer and the diffusion inhibiting platelets. During this pre-formulation step, laboratory tests were performed to fill in gaps in the physical/chemicals properties data from the literature as needed.

Physiochemical properties of neutralization active, polyethyleneimine (Lupasol FG)

During our Phase I work and based on previous results with SERPACWA, the Lupasol[®] polyethylenimines (BASF Corporation, Charlotte, NC) were chosen as the neutralization actives. According to the BASF literature,¹ Lupasol FG is a copolymer of ethylenediamine and ethyleneimine (aziridine). It is likely that one "initiator" molecule of ethylenediamine reacts by addition of the amine groups to form four branches (Figure 3, nitrogens in blue). The amines then build on one another to form primary, secondary, and tertiary amine functional groups. According to the BASF literature, the measured ratio of primary to secondary to tertiary groups in Lupasol FG is 1.0:0.85:0.53 respectively. A possible structure, with 8 -RNH₂, 6 -R₂NH, and 4 -R₃N groups (MW~800 g/mol) is shown in Figure 3. Table 1 lists the key physical and chemical properties of Lupasol FG provided by BASF.

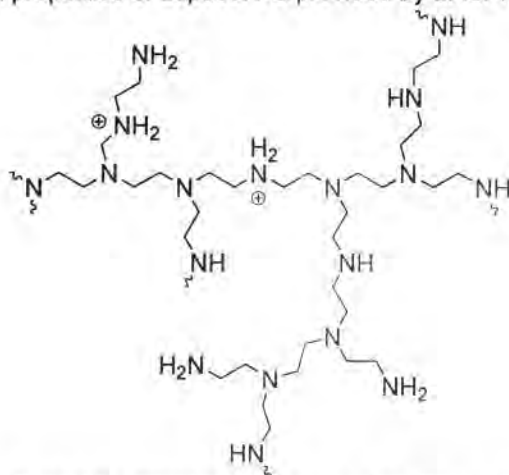


Figure 3: Example structure of Lupasol FG (MW = 800 g/mol)

¹ "Lupasol[®] Product Range: Preliminary Technical Information," BASF, 1996.

<http://www.basf.com/businesses/coatcolor/printingink/pdfs/lupasol/lupasol%20web/lupasol%20ag.pdf>

"Lupasol[®] FG Polyethylenimine," Technical Bulletin, BASF Corporation, 2002.

Table 1: Compilation of Physical and Chemical Properties of Lupasols

Lupasol FG (CAS 25987-06-8) Chemical/Physical Properties			
MW (g/mol)	800	Pour Point	-18 C
Viscosity (mPas)	~5000 @ 20C	Boiling Point	>>200 C
Density	1.03 g/mL	Decomposition Temp	340 C
Amine groups 1°:2°:3°	1.0:0.85:0.53	Solubility	Water (infinite), polar solvents, some aprotic non-polar solvents
Acid-Base Properties		Solvents	Water and polar solvents: alcohols, DMF, ethylene glycol, propylene glycol, NMP
pH (1% soln)	~11	Incompatibilities	Heavy metal ions, organochlorides, chlorine, bromine, aldehydes, ketones, oxides of carbon, nitrogen or sulfur
pK _a	7-10		

Although a considerable amount of data is available on Lupasols from BASF, pH was one property which required further study in the pre-formulation stage. According to the product literature, the pH of Lupasol FG solutions (1-10%) is in the range of pH 11. Our experience with personal care products for direct contact with skin indicates pHs in the range of 4.5-8 are more typical. A potential concern with lowering the pH in a Lupasol-containing skin decontamination formulation is a resulting decrease in neutralizing efficacy. In chemical terms, the decreasing pH would protonate the primary, secondary, and tertiary amines, making these groups potentially "unavailable" for reaction with surrogates and agents.

To better understand the effect decreasing the pH might have on the neutralizing activity of the Lupasols, we carried out a literature search on pH effects on PEIs. We also carried out a brief laboratory study. Solutions of Lupasol FG (PEI) in deionized H₂O (1%, 5%, 10%, 15% and 25% w/w) and three measurements were made with a calibrated pH meter (Table 2). Measurement of pH = 10.95 for 1% Lupasol FG solution compared well to the pH 11 value from the BASF product literature. The pH measurements with the remaining Lupasol concentrations enabled calculation of primary, secondary, tertiary amines, showing an approximate K_b of 1×10^{-4} to 10×10^{-4} and pK_a's of 10.9 – 11.1, both of which are typical values for protonated amines. The reported pK_a range from the BASF Lupasol FG literature¹ is 7-10.

Table 2: pH measurements of 1-25% Lupasol FG in deionized water solutions, and calculated equilibrium constants. Typical K_b's for amines are in the range of 1×10^{-4} to 10×10^{-4}

Lupasol FG % by wt.	Measured pH	Calc'd ~K _b	Calc'd ~K _a	Calc'd ~pK _a
1	10.95	1.37E-03	7.31E-12	11.14
5	11.15	6.53E-04	1.53E-11	10.82
10	11.23	4.68E-04	2.14E-11	10.67
15	11.34	5.17E-04	1.94E-11	10.71
25	11.56	8.54E-04	1.17E-11	10.93
Averages:		7.72E-04	1.50E-11	10.85

Next, we titrated a 10% Lupasol FG in deionized water solution with 0.100 M HCl. A calibrated pH meter was used to measure the pH after each addition of the HCl solution. No clear equivalence point was apparent; the data are shown in Figure 4. The titration was repeated twice.

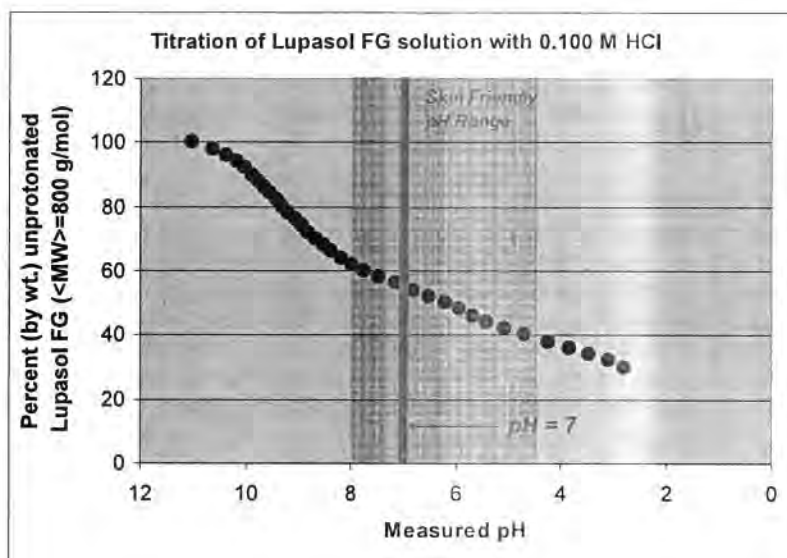


Figure 4: Titration of 10% Lupasol FG solution with 0.100M HCl (blue dots). Red area indicates pH range of typical skin contact personal care products.

In Figure 4, weight percent unprotonated Lupasol FG is plotted vs the pH. This calculation is based on several assumptions.

- 100% ionization of HCl; 100% reaction of H^+ with polymer reactive groups
- Each polymer molecule has ~20 reactive N groups, which react* identically
- Given enough protons are present, all 20 reactive N groups will react on each PEI molecule
- Stoichiometry: 1 mol PEI reacts with 20 mol H^+

A literature search revealed several examples studies of pH effects on PEIs. In one study² by researchers from Cardiff University in Stockholm, electrophoretic NMR was used to probe the electrophoretic mobility of PEIs as a function of pH. The results of the study indicated that at pH 7, PEI is about 50% protonated, implying that about 50% of the original amine groups are available for reaction. In a second, earlier study³, ~50% protonation was again shown at pH in a study of the effect of PEI flocculation of silica particles on molecular weight, pH, and salt concentration (as surrogates for the number of cationic charges per molecule). Based on the literature and our own pH study (Figure 4), we planned to create a formulation in the skin-friendly pH range while maintaining approximately 50% efficacy of the PEI actives. It is possible that we will need to increase the amount of PEI we used in the Phase I study (~10% by wt.).

In addition to pH, other properties of Lupasols we considered closely in the pre-formulation study included viscosity, which can create difficulties for formulating if it is too high. Reviewing the datasheets for water-Lupasol mixtures revealed that viscosity can be made to drop quite rapidly with the addition of water or low molecular weight alcohols.

Reactions of PEIs - Catalytic vs. stoichiometric – Literature Review

Literature studies on the reactions of polyethylenimine (PEI) with various electrophiles shows that PEI may promote a catalytic decomposition of the CWAs and their simulants chloroethylethylsulfide (CEES) and diisopropylfluorophosphate (DFP). The catalytic mechanism can occur by general base catalysis or enzyme-like catalysis.

² Macromolecules **2005**, 38, 3539-3542

³ Journal of Colloid and Interface Science, **1976**, 55, 45-59.

General base catalysis occurs in aqueous solutions when uncharged amino groups in PEI deprotonate water molecules and produce hydroxide ions, which could readily hydrolyze CEES or DFP. Figure 5 shows the proposed general base catalytic pathway for CEES and DFP hydrolysis as well as the direct aminolysis that would also occur with CEES and DFP.

Kudryastev et al.⁴ have shown that PEI promotes the hydrolysis of O-alkyl-O-p-nitrophenyl phosphates by this general base-catalyzed mechanism. Their studies show that the catalytic activity of linear and branched PEI increases with increasing pH, presumably due to the increasing amount of unprotonated amine groups. In addition, the cationic centers in PEI promote the alkaline hydrolysis due to electrostatic interactions with the hydroxide ions, increasing the contribution of alkaline hydrolysis in the observed rate of the reaction. For branched PEI (MW = 80K) the catalytic activity is optimal at pH > 9.5. Their studies also showed that the general-basic catalyzed hydrolysis was observed over the direct aminolysis of O-alkyl-O-p-nitrophenyl phosphates. This indicates that in our NSP formulations, the PEI would perform the same action against the nerve agents (and the simulant DFP) which share structure similarity to phosphates used in the Kudryastev studies. Other studies by Arcelli et al.,⁵ however, shows that direct aminolysis may also be observed. In their work, the rate of aminolysis of branched PEI with several phenyl acetates was studied. The authors showed that direct aminolysis (amide formation), occurs at a wide pH range (4 – 11). This would indicate that PEI action may be substrate dependent and we might still observe aminolysis of the sulfur mustard (and simulant CEES) and the nerve agents (and simulant DFP). Since non-protonated PEI is required for both the general base catalysis and the direct aminolysis, both mechanisms most likely will contribute to the neutralization of CWAs and their simulants.

⁴ Bakeeva, R. F.; Kudryavtseva, L. A.; Bel'skii, V. E.; Ivanov, B. E. *J. Gen. Chem. USSR (Engl. Transl.)* **1983**, 53, 935-938.

⁵ a) Arcelli, A.; Concillio, C. *J. Org. Chem.* **1996**, 61, 1682-1688. b) Arcelli, A. *Macromolecules* **1999**, 32, 2910-2919. c) Arcelli, A.; Cecchi, R.; Porzi, G.; Sandri, M. *J. Phys. Org. Chem.* **2005**, 18, 255-263.

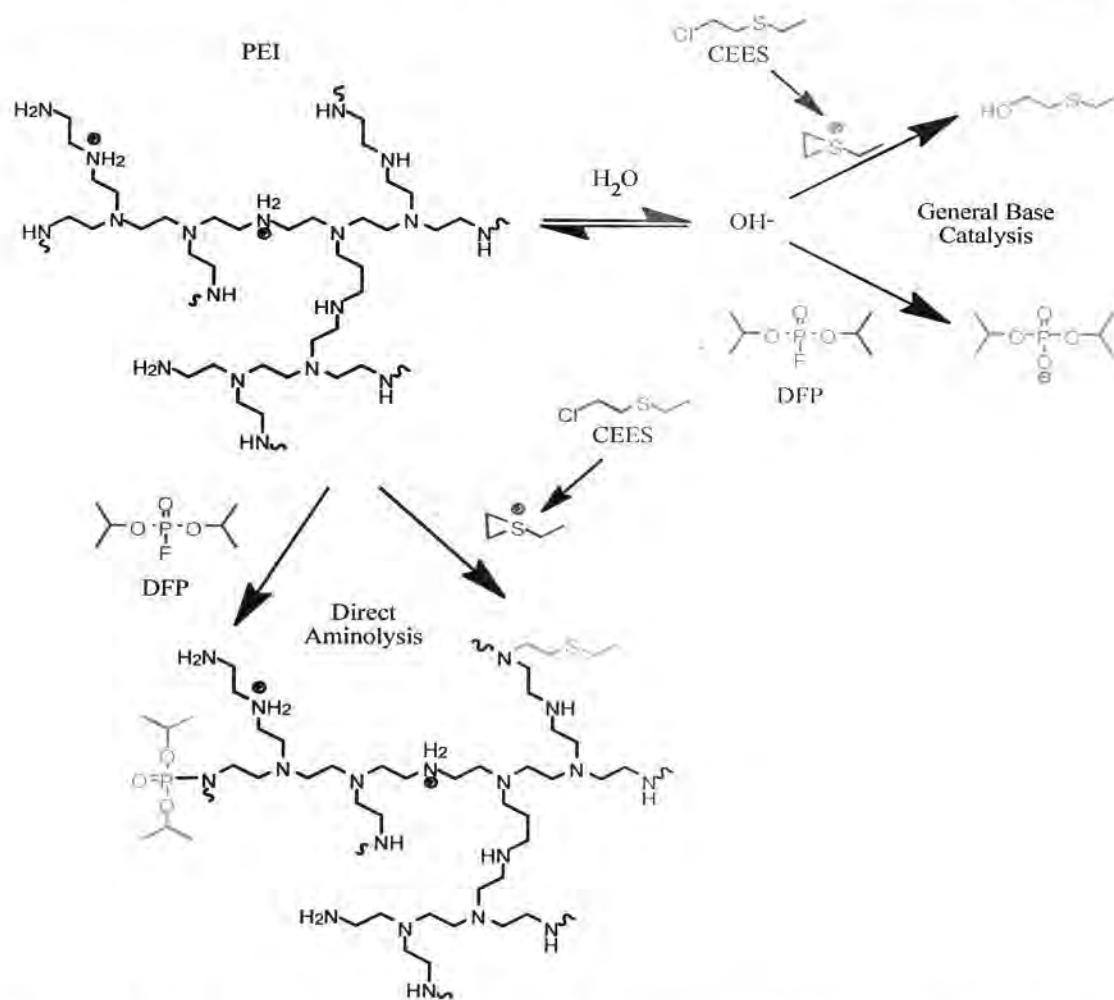


Figure 5: Direct aminolysis and general base catalysis promoted hydrolysis of CWA simulants, CEES and DFP.

Arcelli et al.⁵ also indicate that the aminolysis of phenyl acetates is promoted due to an enzyme-like stabilization of the tetrahedral intermediate during amide formation. Hence, although a direct aminolysis of CEES and DFP may also occur, the highly branched nature of PEI with its range of amine bases may stabilize the transition state or intermediates during aminolysis, and accelerate the rate of CEES and DFP aminolysis. Several studies also indicate that enzyme-type catalysis is particularly promoted by alkylated/acetylated PEI.⁶ The alkylated/acetylated PEIs form a range of hydrophobic cavities that drives substrate binding and the positively charged framework serves to stabilize negatively charged transition states. (For example, Tawfik et al.⁷ developed an optimal alkylated PEI that promoted the enzyme-like catalysis of the Kemp elimination of isooxazole in aqueous solutions.) Obviously, the structure of PEI could be altered by alkylation or acylation specifically for CEES and DFP; however, our studies so far indicate that sufficient CEES and/or DFP neutralization takes place without such modification.

⁶ Klotz, I. In *Enzyme Mechanisms*; Williams, A., Page, M., Eds.; The Royal Society of Chemistry: London, 1987, pp 14-34.

⁷ Hollfelder, F.; Kirby, A. J.; Tawfik, D. S. *J. Am. Chem. Soc.* 1997, 119, 9578-9570.

Finally, since PEI will likely be incorporated in an oil/water or water/oil emulsion, micellar type structures are likely to form and micellar catalysis of CEES/DFP hydrolysis may also take place. Kudryavstev et al.⁸ have also shown that cationic micelles accelerate the PEI-catalyzed hydrolysis of O-alkyl-O-p-nitrophenyl phosphonate due to the concentrating of the reactive substrates within the micelles. However, they also indicate that the micellar catalysis is highly dependent on the nature of the substrate, indicating that CEES and DFP might be hydrolyzed at different rates via the PEI catalysis pathway.

Diffusion Inhibitors – Creating a “Tortuous Path”

A key to the success of our prototype formulation is balancing the need for migration of the active and agent into the matrix with the need to protect the skin from any exposure to agent by providing chemical and/or physical resistance. Therefore, the goal involves creating a “tortuous path”, reducing the rate of diffusion of agent through the matrix. Materials we considered for inclusion in the skin protectant are typically used in pharmaceutical, cosmetic, and personal care product formulations (Table 3).

Table 3: Platelets and particles typically used in pharmaceutical, cosmetic, and personal care product formulations.

Platelet/Particle Type	Chemical Formula	Comments
Bentonite	$\text{Al}_2\text{O}_3 \cdot 4\text{SiO}_2$	Used to adsorb cationic drugs sustaining release, likely interaction with PEIs if untreated. Examples include Bentone (Elementis) and Bentonite (Southern Clay) grades
Treated Clays	various	Typically bentonites, hectorites, modified with organics, e.g., stearylaluminum hectorite. Resides in oil phase. Available from Elementis and Southern Clay.
Colloidal Silicon Dioxide	SiO_2	Cab-o-Sil from Cabot Corp. Insoluble in organics and water, but will dissolve at pH >10.5. Nanoparticles; may affect viscosity of formulation. Surface area varies with grade.
Kaolin	$\text{Al}_2\text{O}_3 \cdot 2\text{SiO}_2 \cdot 2\text{H}_2\text{O}$	Hydrated aluminum silicate, larger particle size than Bentonite clays. Needs evaluation for potential incompatibility with PEIs.
Magnesium Aluminum Silicate	Polymeric complex of Mg, Al, and oxides	Trade name: Veegum (Vanderbilt). Not soluble in water or organic solvents. Fairly inert, with few incompatibilities; unstable below pH 3.5. Some base-exchange capacity.
Magnesium Trisilicate	$2\text{MgO} \cdot 3\text{SiO}_2 \cdot x\text{H}_2\text{O}$	Adsorbs some active drug compounds. Insoluble in water and alcohol.
Calcium Phosphate Tribasic	$\text{Ca}_5(\text{OH})(\text{PO}_4)_3$	Slightly soluble in water, more soluble in dilute mineral acids.
Cellulose	$(\text{C}_6\text{H}_{10}\text{O}_5)_x$	Only incompatible with oxidizing agents. Practically insoluble. Slightly soluble in bases. Many grades with varying viscosity.
Talc	$\text{H}_2\text{O} \cdot 3\text{Si} \cdot 3/4 \text{ Mg}$	Incompatible with quaternary ammonium compounds.

⁸ a) Kudryavtsev, D. B.; Bakeeva, R. F.; Kudryavsteva, L. A.; Zakharova, L. Y.; Sopin, V. F. *Mendeleev Commun.* **2000**, 202-204. b) Zakharova, L. Y.; Shagidullina, R. A.; Valeeva, F. G.; Kudryavtseva, L. A. *Mendeleev Commun.* **1999**, 5, 171-173.

Key criteria for selection of the particle or platelet material included:

- Potential for interaction/deactivation of PEI ***Most important***
- Shape: oblong and flat is most desirable for tortuous path effect.
- Incompatibilities: insoluble in all possible excipients (e.g., water, emulsifiers, fats)
- Phase: residence of platelets in oil or water phase.

Selection of Diffusion Inhibitors

Representative samples of several treated and non-treated materials we obtained are listed in Table 4 below.

Table 4: Platelets and particles obtained for initial testing with Lupasol polyethylenimines

Trade name/Grade	Product Description	pH in solution	Formulation Phase
Elementis Bentone EW	Hectorite clay	8.5-9.5 @ 2%	Water
Elementis Bentone LT	Organically modified hectorite clay	8.5-9.5 @ 2%	Oil
Southern Clay Gelwhite H	Highly purified white bentonite clay	9.5-10.5 @ 5%	Water
Southern Clay Tixogel VP-V	Q-90 modified bentonite clay	NA	Oil
Southern Clay Gelwhite MAS 102	Highly purified mixture of smectite clays	9.0-10.0 @ 5%	Water
Southern Clay Laponite XLG	Synthetic layered silicate (hectorite-like) with polyphosphate dispersing agent	9.8 @ 5%	Water
Southern Clay Laponite RD	Synthetic layered silicate (hectorite-like)	9.8 @ 5%	Water
RT Vanderbilt Veegum Granules	Highly purified smectite clay (Al:Mg = 0.5-1.2)	9.0-10.0 @ 5%	Water
RT Vanderbilt Veegum HS Granules	Highly purified smectite clay (Al:Mg = 3.5-5.5)	9.0-10.0 @ 5%	Water
RT Vanderbilt Veegum Ultra Granules	Acidic smectite clay	4.3-5.3 @ 5%	Water
RT Vanderbilt Veegum PRO Granules	Tromethamine-modified smectite clay	8.0-9.0 @ 1%	Water
Degussa Aerosil 200	Hydrophilic fumed silica	3.7-4.7 @ 4%	Water

Most of these particles/platelets fall into the category of natural and synthetic smectite clays. Smectites are layered silicate clay particles in which substitutions of metal atoms (e.g., a Mg^{+2} for an Al^{+3}) have resulted in a net negative charge on the "faces" of the particles. To balance this charge, interlayers of cations (Na^{+} , Ca^{+2} , and K^{+}) form between the clay particles (Figure 6, left). These larger particles expand ("swell") and separate with the addition of water, alcohols or glycols (Figure 6, right). The resulting colloidal-sized particles then may form a dispersion or may flocculate ("gel") depending on their composition and the conditions (pH, salt concentration, etc.).

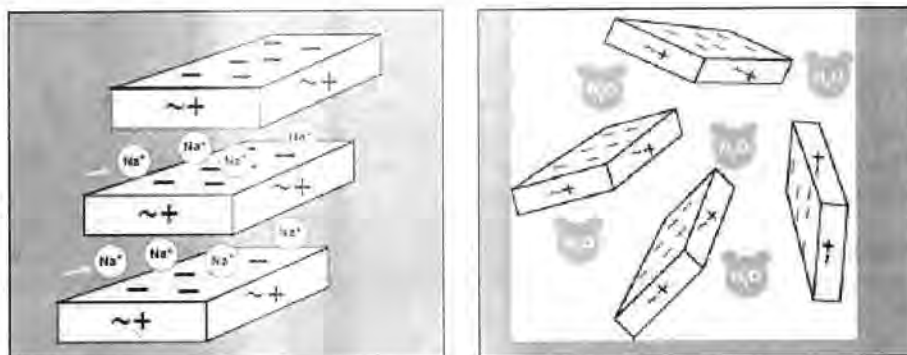


Figure 6: Schematic diagram of smectite-type clay (left) and the swelling of smectite clays in an aqueous environment (right). Ref: RT Vanderbilt Veegum Data Sheet

Smectite clays used in personal care applications include montmorillonites (from bentonite rock) and hectorite which differ in their mineral makeup. Montmorillonites (bentonites) are based on the structure of pyrophyllite ($\text{Al}_2\text{Si}_4\text{O}_{10}(\text{OH})_2$) with significant substitutions of Mg for Al; hectorites are similar to the structure of talc ($\text{Mg}_3\text{Si}_4\text{O}_{10}(\text{OH})_2$) with substitutions of Li for Mg. Particular grades of a single clay type vary in their exact elemental composition, their purity, and in treatments applied. With the exception of those that are organic-treated, all of these clays will reside in the water (or polar) phase of the formulation.

We also selected a hydrophilic fumed silica (SiO_2). This material is typically used in pharma/cosmetic and personal care formulations to adjust rheological properties. Unlike smectite clays, fumed silicas do not have appreciable charge.

Compatibility Evaluation of Clays with Polyethylenimines

Originally, a key concern we had with the use of clays as diffusion inhibitors in our formulation is the possibility of flocculation. Lupasols (PEIs) are known to flocculate clay particles in solution. We carried out several experiments to determine if the Lupasols are compatible with the selected clays and silicas. If they interact, we could not use the clays in the water phase of the skin protectant formulations to be developed, since the PEIs will also reside in the water phase.

Three Lupasols (FG, WF, and P) were evaluated for their compatibility with ten representative clays and one fumed silica (Table 4). 1-2% solutions of 1) Lupasol and water and 2) clay or silica in water were prepared, mixed together, and observed initially and at 24 hours after mixing. pH and viscosity were also monitored and recorded.

We observed that all of the clays and the fumed silica tested flocculated with all three Lupasols under the conditions of the experiments. Additional experiments were carried out to further understand this effect. One such experiment evaluated whether adjusting the pH of the mixtures reduced the tendency of the Lupasols to flocculate the clays/particles. We had previously used medium and low capacity buffers at pH~8 (potassium phosphate dibasic and potassium phosphate monobasic). For this experiment we instead used a high capacity (high concentration) phosphate buffer which had a measured pH of 8.2. We found that the degree of flocking increased with the presence of the buffer, probably due to the increased ionic strength of the solution.

While experiments to reduce flocking behavior were ongoing for the smectite clays and silica, we tested several additional clays (Table 5) for flocking behavior with polyethylenimines, these include talcs, synthetic mica, kaolin, microcrystalline cellulose and calcium phosphate tribasic. Properties and typical uses of these materials are listed in Chart 1, below. All of these materials would reside in the water phase of the formulation.

Table 5: Additional platelets and particles selected for initial testing with Lupasol polyethylenimines.

Supplier	Trade name	Composition	Formulation Phase
Sensient Cosmetic Technologies	Submica E	Synthetic Aluminium Fluoro Magnesium Sodium Silicate (Mica)	Water
Mineral and Pigment Solutions, Inc.	Talc – BC Grade (Cosmetic) Imperial 400	$Mg_3Si_4O_{10}(OH)_2$	Water
Mineral and Pigment Solutions, Inc.	Talc – BC Grade (Cosmetic)	$Mg_3Si_4O_{10}(OH)_2$	Water
Mineral and Pigment Solutions, Inc.	Colloidal Kaolin - 2749 BC Grade: (Cosmetic / Pharmaceutical)	Hydrated aluminum silicate	Water
Mineral and Pigment Solutions, Inc.	Colloidal Kaolin – 2457 - BC Grade (Cosmetic / Pharmaceutical)	Hydrated aluminum silicate	Water
FMC Corporation	Avicel RC/CL Microcrystalline Cellulose	Cellulose/Sodium Carboxymethylcellulose	Water
Spectrum Chemical	N/A	Calcium Phosphate Tribasic	Water

Talc ($Mg_3Si_4O_{10}(OH)_2$), a white powder, is used as a filler in many cosmetic products and as an absorbent for perspiration and excess skin oils. The two grades of talc tested were in the particle size range of 3-5 μm . Unlike hectorites, talc should not swell water or solvents.

Mica is an aluminum fluoro magnesium potassium silicate mineral. We used a synthetic grade from Sensient Technologies, Submica E, commonly used in skin care and make-up products. This mineral is expected to swell in water, but have limited potential for cation exchange (relative to the smectite minerals). Submica E is an off-white powder.

Kaolin, a white powder, is used as an extender and suspending agent in a variety of cosmetic and pharmaceutical preparations. It is widely used in creams and lotions as a suspending agent and opacifier. In veterinary applications, it functions as a topical and G.I. absorbent and as a component of poultices. The colloidal Kaolin evaluated had a (non-dispersed) particle size of 0.6-1 μm . Kaolin does not swell in water per se, but is attractive for the platelet-shaped particles which are in the form "books" of platelets prior to dispersion, and the neutral charge of these particles.

Microcrystalline cellulose is a white, crystalline powder. In water, with shear, MCC forms a three-dimensional matrix comprised of millions of insoluble microcrystals that form an extremely stable, thixotropic gel. Typical particle size when dispersed is less than 0.2 μm . MCC is used in food, cosmetic, and pharmaceutical properties for stabilization and anti-caking purposes.

Calcium phosphate tribasic ($Ca_5(OH)(PO_4)_3$) is a fine white powder frequently used in pharmaceutical preparations as an antacid. It is also used as a calcium supplement and as a component of baby powder.

Chart 1 – Descriptions and typical uses of particles/platelets selected for compatibility testing with polyethylenimines

For the talc, kaolin, mica and calcium phosphate tribasic, minimal flocking was apparent in the presence of Lupasol FG. Tests were performed in which a 1-2% solution of the powdered material was combined

with a 1% solution of Lupasol FG. The mixtures were observed for flocking immediately and after 24 hours standing time. Unlike the smectite clay/Lupasol FG mixtures, these materials only coalesce slightly and can be easily re-suspended in the solution with shaking, similar to control samples containing only water (no Lupasol FG). This was very different behavior from the smectite clays, which we observed form flocs in the presence of PEIs that cannot be easily broken up to re-suspend particles in the solution by simple shaking. A summary of the results of compatibility testing for all materials tested thus far is found in Table 6 below.

Table 6: Results of compatibility tests of platelets and particles selected for initial testing with Lupasol polyethylenimines. Size of the particles determined by SEM photos.

Particle Description	Supplier/Grade	Function	Particle size (dry, undispersed)	Compatibility Test Results 1% Lupasol FG
Pure hectorite clay	Elementis/ Bentone EW	Rheology Modifier	5-30 μm	Strong flocking, increasing pH increases flocking
Pure bentonite clay	Southern Clay/ Gel-white H	Rheology Modifier	1-30 μm	Strong flocking, no apparent pH effect
Hydroxyethylcellulose-modified hectorite clay	Elementis/ Bentone LT	Rheology Modifier	n/a	Forms solid mass , increasing pH increases this effect
Synthetic hectorite clay	Southern Clay/ Laponite XLG, Laponite RD	Rheology Modifier	1-200 μm	Strong flocking, increasing pH increases flocking
Magnesium aluminum silicate (water-washed smectite clay)	Vanderbilt GT/ Veegum Granules, Veegum HS Granules, Veegum Ultra, Veegum Pro/ Rheology Modifier	Rheology Modifier	50-200 μm	Strong flocking, increasing pH increases flocking
Hydrophilic Fumed Silica	Degussa/ Aerosil 200	Rheology Modifier	0.2-0.3 μm	Strong flocking, increasing pH increases flocking
Synthetic Aluminium Fluoro Magnesium Sodium Silicate (Mica)	Sensient Cosmetic Technologies/ Submica E	Rheology Modifier	1-10 μm	Weak flocking, re-disperses when shaken
Talc	Mineral & Pigment Solutions, Inc./ Talc – BC Grade	Filler, absorbent	1-20 μm	Weak flocking, re-disperses when shaken
Kaolin clay	Mineral & Pigment Solutions, Inc./ Colloidal Kaolin – BC Grade	Filler, suspending agent	<2 μm	Weak flocking, re-disperses when shaken

Microcrystalline cellulose	FMC Biopolymer/ Avicel RC/CL	Rheology Modifier	5-40 μm	Some flocking
Calcium Phosphate Tribasic	Spectrum Chemical	Filler, Antacid	<10 μm	Weak flocking, re-disperses when shaken

Based on the above results, it seemed we should initially proceed with the weakly flocking materials, including the mica, talc and kaolin to create a tortuous path through the water phase. However, the issue of flocking led us to carry out a review of the primary literature. We came across two articles^{9,10} that discussed rheology effects of PEIs added to bentonite dispersions. These researchers found that at a certain concentration of PEI, flocculation will actually diminish due to repulsion among PEI-saturated particles. The main difference between their work and our application is the MW of the polymer they used; 10^5 - 10^6 MW vs. our preferred 800 MW polymer (Lupasol FG). We explored experimentally the possibility that flocculation would diminish with increasing PEI concentration using Lupasol FG and Gelwhite H (pure bentonite clay). The results of this qualitative study are shown in Figure 7. As can be seen from the figure, at increasing concentrations of PEI we've observed a visual max (via light microscope) in floc size at 5 g/L PEI, above which floc size decreases again with increasing concentration, confirming this behavior (qualitatively) for the smaller MW PEI relevant to this project. Perhaps coincidentally, 5 g/L PEI is very similar to the concentration "max" identified in the rheology effects study of 4.5 g/L PEI.⁹

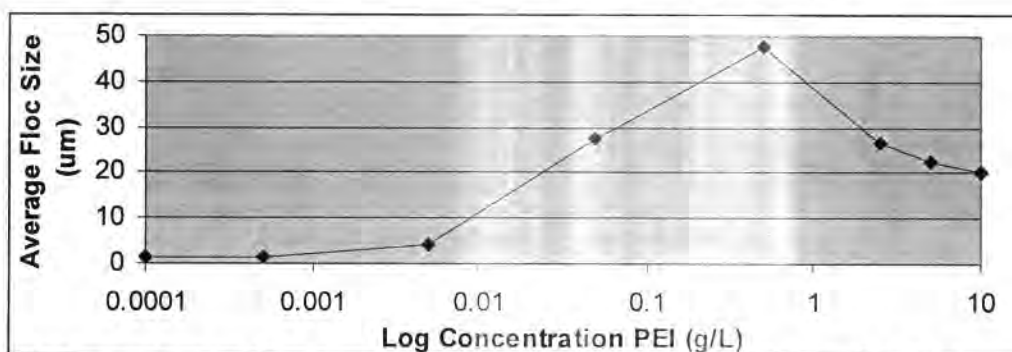


Figure 7: Dependence of Floc size on the concentration of Lupasol FG PEI in a 2% Gelwhite H bentonite clay dispersion.

This new information increased the desirability of using an aqueous (oil-in-water, O/W) vehicle for our NSP formulations. Above the "saturation concentration" of the clay with PEIs, the O/W matrix will consist of PEI-coated particles, presumably with some functionality remaining against CWAs, and additional PEI in solution also reactive with CWAs. Our hypothesis is that the functionality against CWAs can then be maintained in the presence of the tortuous path materials in the continuous (water) phase.

Shape of the particles is another important factor, as it influences the ability of these materials to obstruct the passage of harmful molecules through the cream. From our review of the literature, we have identified bentonites (and montmorillites) as having the most desirable shape: $800\text{ nm} \times 800\text{ nm} \times 1\text{ nm}$; natural hectorites are more needle shaped, $800\text{ nm} \times 80\text{ nm} \times 1\text{ nm}$. Synthetic hectorites are much smaller: $25\text{ nm} \times 25\text{ nm} \times 1\text{ nm}$. Cosmetic grade magnesium aluminum silicates have dimensions of $100\text{ nm} \times 100\text{ nm} \times 1\text{ nm}$. We used a scanning electron microscope (SEM) to confirm both the size and the shape of the particles in Table 6 above. Figure 8a-d displays the plate-like nature of samples of talc, bentonite, kaolin and organically modified bentonite.

⁹ Bull. Mater. Sci., 28 (3), 2005, pp. 287-291.

¹⁰ Mat. Lett., 55, 2002, pp. 73-76.

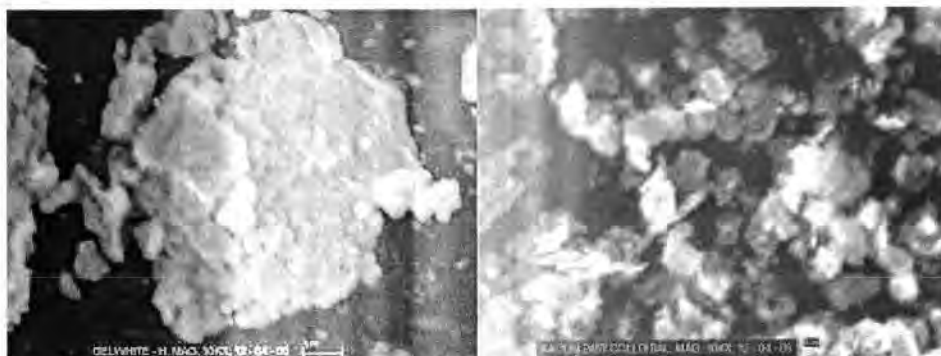


Figure 8a and Figure 8b: SEM photos of bentonite (Southern Clay Gelwhite-H, 10,000x) and kaolin (MPSI Colloidal, 10,000x)

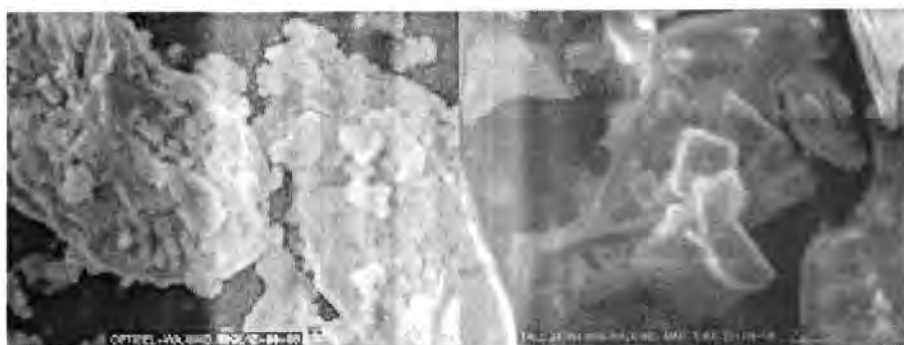


Figure 8c and Figure 8d: SEM photos of organically modified bentonite (Southern Clay Optigel WA, 10,000x) and talc (MPSI Cosmetic, 10,000x)

As can be seen in the pictures, the bentonites (8a and 8c) consist of large 1-30 μm particles that can be dispersed in water to form much smaller platelets. The colloidal kaolin sample also appears to be made up of platelets of less than 2 μm . The talc sample also appears to be platy in nature, with particle sizes (unexfoliated) of 1-20 μm .

Selection of Vehicle(s) for Skin Protectant Formulation

With a selection of PEI actives and diffusion inhibitors in hand, we next examined possible formulation vehicles, namely emulsions, gel or ointment forms.

The possible vehicle forms are defined as follows:

Emulsion, Oil-in-Water (O/W): Colloidal dispersion comprising two immiscible phases (oil and water), in which the oil phase is dispersed as droplets within the water phase.

Emulsion, Water-in-Oil (W/O): Colloidal dispersion comprising two immiscible phases (oil and water), in which the water phase is dispersed as droplets within the oil phase.

Gel: Gels are semisolids, either large organic molecules (polymers) or small inorganic particles interpenetrated with liquid. Both oleogels and hydrogels can be considered.

Ointment: Ointments are typically a single phase containing a suspension of the active ingredient.

Initially, we identified a large number of sample topical formulations for each vehicle type. A base formulation and processing method, drawn from the sample formulations we identified, was developed for each type of vehicle. Probable excipients (inactive ingredients) for each vehicle type were included in these base formulations. Our selection of excipients depended upon the chosen vehicle form,

compatibility with the PEI actives, the cationic polymer, and the diffusion inhibiting (platelet) materials, as well as the attributes that they offer to the final preparation. Additionally, in the analysis of each vehicle type below we discuss where each of the key components of the formulation, the PEI actives, cationic polymer, and the diffusion inhibiting (platelet) materials will reside in the phases of the vehicle, and the resulting desirability of each vehicle.

O/W Emulsion

Oil in water emulsions make up the majority of skin care products on the market today, including most lotions and many creams. The main advantages of O/W emulsions are skin feel, solubility of many actives in water and reduced cost to manufacture relative to oil-based forms. The water component of the formulation rapidly evaporates from the skin, resulting in a light cooling feeling. Disadvantages include greater risk of microbial contamination than oil-based formulations.

A base formulation for an O/W emulsion skin cream is shown in the box below. Examples and descriptions of each of the components in the O/W emulsion are found in Table 7. Typically, in processing an O/W emulsion, both the oil phase and the water phase are separately pre-mixed and heated to 75-80 °C; the heated oil phase is added to the heated water phase vortex while stirring. Stirring and heating

O/W Emulsion: Base Formulation	
Oil Phase	
Emulsifier(s) (HLB 8-16)	5-7%
Emollient(s)	10-40%
(Oleophilic thickener	0-1%)
Water Phase	
Water	to 100%
Humectants	4-7%
Preservatives	0-1%
Chelating Agents	0-0.02%
Antioxidants	0.01-0.05%
Buffer/pH adjuster	
(Hydrophilic thickener	0-1%)

continues until a homogeneous mixture is formed; it is then allowed to cool to 30-40 °C. Additives such as preservatives, antioxidants, buffers and other heat labile ingredients such as fragrance (as needed) may be added to the cooled mixture with continued stirring. Hydrophilic or oleophilic thickeners are typically pre-mixed (with heating) to the water or oil component prior to the addition of the rest of the phase ingredients. Preservatives are essential to O/W formulations which are subject to microbial contamination.

In an O/W emulsion the PEI would reside in the continuous (water) phase; the Incroquat polymer is also dispersible in water. Diffusion inhibiting hydrophilic platelets would also be expected to reside

in the continuous phase. Organoclays as diffusion inhibitors may be an option, but it is unclear whether they can reside within oil droplets dispersed within the continuous phase. Additionally, it was conveyed to us by the program COR that "cream-like" consistency is less desirable than a gel or ointment form (especially if the cream will become dry on application). For these reasons, we placed the O/W vehicle formulation as a lower priority in our initial development efforts.

Table 7: Excipients that are typical components of topical formulations (O/W, W/O, gel and emulsion vehicles).

Component	Purpose	Preferred Examples
Emulsifier (surfactant)	Stabilizes emulsion (O/W emulsions require HLB 8-16; W/O requires HLB 4-6); surfactants can also be used to solubilize actives as needed	Non-ionic preferred to minimize skin irritation (e.g., lanolin alcohols, POE fatty ester, polysorbates (10-17), sorbitan esters)
Emollient	Improve skin feel, spreadability of product, improve lipid content of skin upper layers	Synthetic esters
Humectant	Prevents drying of formulation	Dipropylene glycol is a humectant and is also a component of Incroquat QLC
Preservative	Prevents microbial contamination and degradation	Parabens, Diazolidinyl urea

Chelating Agent	Prevents degradation by oxidation reactions	Citric acid, EDTA, and tartaric acid
Antioxidant	Protection of unsaturated lipids	Butylated hydroxyanisole (BHA), butylated hydroxytoluene (BHT)
Buffer, acid or base	Maintain optimal pH of the formulation	HCl, KOH, Triethanolamine
Salt	Stabilize W/O emulsion	MgSO ₄ ·7H ₂ O
Thickeners	Viscosity modification	Oleophilic example: microcrystalline wax Hydrophilic example: colloidal dispersed solids (e.g., bentonite, magnesium aluminum sulfate, MCC)
Gelling Agent (gel vehicle only)	Viscosity builder	Polysaccharides, Acrylic polymers, Cellulose derivatives, Colloidal dispersed solids

W/O Emulsion

W/O Emulsion: Base Formulation	
Oil Phase	
Emulsifier(s) (HLB 3-8)	7-10%
Emollient(s)	20%
(Oleophilic thickener	0-1%)
Water Phase	
Water	to 100%
Humectants	4-7%
Preservatives	0-1%
Chelating Agents	0-0.02%
Antioxidants	0.01-0.05%
MgSO ₄ ·7H ₂ O	0.5%
Buffer/pH adjuster	
(Hydrophilic thickener	0-1%)

Examples of water in oil emulsions include diaper creams, makeup (foundation), water-proof sunscreens and other heavy cream formulations. Advantages of this vehicle include the chemical similarity of the major component (oils) to the natural protective lipid layer of the stratum corneum and the potential formation of a continuous lipid layer after application, providing a semi-occlusive barrier. There is a lower risk of microbial growth compared to O/W formulations. Disadvantages include the heavy, greasy feeling sometimes associated with waxes and oils that make up the major component of the vehicle; however, modern synthetic esters and silicone materials can often improve skin feel.

A sample formulation for an W/O vehicle is shown in the box above. Many of the same ingredients are

found in the O/W vehicle and are described in Table 7. The processing method is very similar except that the heated water phase is added to the heated and stirring oil phase for a W/O emulsion.

If a W/O vehicle is used for the skin protectant, the PEI will reside in the inner phase of the emulsion. The Incroquat polymer is dispersible, but not soluble in water; it is soluble in alcohols, and moderate molecular weight synthetic esters (e.g., PPG-2 myristyl ether propionate). It is insoluble in mineral oil. Therefore, it is likely to partition in some fraction into both the oil and water phases. Thus, including a lower molecular weight component in the oil phase, such as diisopropyl adipate as an emollient could be valuable. Additionally, the result of our interaction with Croda may produce a higher molecular weight cationic polymer than the Incroquat QLC polymer we are currently using, which could increase its solubility in the oil phase.

In the W/O type formulation, the continuous (oil) phase would need to contain the platelets for diffusion reduction through the matrix. We have identified several organoclays: hydrophobically modified bentonites and hectorites, e.g., Southern Clay's Tixogel VP (Quarternium-18 Bentonite), Tixogel VP-V (Quarternium-90 Bentonite) and Elementis' Bentone-38 (Quarternium-18 Hectorite). Several of these organoclays can be purchased "pre-activated" (dispersed) in mixtures of various fats/oils and activator (typically propylene carbonate). The mixtures are attractive for ease of formulation.

When dried, the W/O type formulation would lose less volume than the O/W formulation (PEI would be expected to have a humectant effect holding water in a formulation of either type). The oil-phase residue remaining behind would contain the organoclays, providing the barrier and dispersed PEI/water for continuing decontamination efficacy. The oil phase residue should also provide a semi-occlusive barrier. The addition of silicones, a common component of the oil phase could increase "breathability" and improve skin feel of the lipid layer remaining behind. However, is it possible that when water evaporates from the W/O vehicle it may leave behind "holes" that could be weak points of the coverage. This possibility would have to be further evaluated experimentally. Based on this analysis, the W/O vehicle seems appropriate to pursue further.

Gels

Hydrogel: Base Formulation

Water Phase

Water/Alcohol	to 100%
Gelling Agent	0.5-10%
Preservatives	0-1%

Gels have a single phase, water (hydrogels) or oil (oleogels), made up of a uniform matrix of a swellable polymer or clay. An example formulation for a hydrogel is given in the box. The primary components for a swellable polymer hydrogel are water and alcohol; typically this type of vehicle must be protected against anti-microbial growth. Water and alcohol are also the

primary components of a dispersed clay-based hydrogel. Oleogels are obtained by adding a hydrophobic thickening agent to an oil or a liquid lipid. This vehicle is less likely to suffer from microbial contamination.

The solubility of the PEI active excludes oleogels from consideration. Thus the two types of hydrogels can be considered. In both cases, it is likely that the formulation will lose considerable volume on drying, even in the presence of PEIs. Remaining residue will include PEIs, Incroquat QLC, and some water, in addition to the swelling material. In the case of the hydrophilic clay minerals, we have already observed that undesirable flocking behavior occurs in the presence of PEIs. Thus hydrogels do not seem a very attractive option in our initial analysis.

Ointments (Suspensions)

This vehicle does not seem immediately attractive for the skin protectant application, again due to the lack solubility of the PEI actives in oil or petroleum. This form, particles/powders suspended in an oily base, is essentially the same concept as the SERPACWA, the starting point for this and the aTSP.

Our analysis of the four vehicles mentioned above is summarized in Table 8.

Table 8: Results of Initial Paper Analysis of O/W, W/O, gel and emulsion vehicles

Vehicle Type	Desirability/Reasoning
Emulsion (O/W)	Moderate. In an O/W emulsion, the PEI would reside in the continuous (water) phase; the Incroquat polymer is also dispersible in water. Diffusion inhibiting, hydrophilic platelets would also be expected to reside in the continuous phase. Experiments have demonstrated that many of the hydrophilic platelets undergo some degree of flocking with PEIs.
Emulsion (W/O)	High. When dried, the W/O type formulation would lose less volume than the O/W formulation (PEI would be expected to have a humectant effect holding water in a formulation of either type). The oil-phase residue remaining behind would contain the organoclays, providing the barrier and dispersed PEI/water for continuing decontamination efficacy. The oil phase residue should also provide a semi-occlusive barrier. However, is it possible that when water evaporates from the W/O vehicle it may leave behind "holes" that could be weak points of the coverage, which would need to be evaluated experimentally.
Gel	Moderate. The solubility of the PEI active excludes oleogels (single lipophilic

	phase) from consideration. Thus the two types of hydrogels (organic polymer and inorganic particle-based) can be considered. In both cases, it is likely that the formulation will lose considerable volume on drying, even in the presence of PEIs. Remaining residue will include PEIs, Incroquat QLC, and some water, in addition to the swelling material. In the case of the hydrophilic clay minerals, we have already observed that undesirable flocking behavior occurs in the presence of PEIs.
Ointment	Low. This vehicle does not seem immediately attractive for the skin protectant application, due to the lack solubility of the PEI actives in oil or petroleum.

Two-Clay Gels

Following the analysis summarized in Table 8 above, our continued reviews of the patent literature related to hydrophilic and lipophilic clays and high solids formulation vehicles yielded two other possible formulation vehicles. We identified two no-emulsion, two-clay "gel" vehicle examples, discussed in patent US6660277 assigned to Avon, and patent US5702709 assigned to Enviroderm.

The Avon patent (US6660277) formulation is described as a "cosmetic composition comprising a lipophilic clay gel and a hydrophilic clay gel" combined to create a "gel matrix" that "functions like an emulsion" as both a cosmetic base and a carrier for other active cosmetic ingredients. The patent discloses use of two water-swellaable montmorillonite clays, one of which has been treated with di(octadecyl) dimethyl ammonium chloride to create a hydrophobic surface, commercially available as Claytones (Southern Clay). The two gels are prepared separately and then mixed, forming a single phase into which additional active ingredients can be incorporated. A specific formulation modeled on this type of vehicle is described in detail below. According to the patent, benefits of this type of formulation include: good spreadability, smooth and creamy feel, superior high temperature stability, excellent suspension properties, and freedom from use of surfactants which may be irritating to skin. This type of dual gel matrix formulation is attractive for consideration in the skin protectant formulation selection process due to the use of two clays (tortuous path) with additional incorporated actives.

The Enviroderm patent (US5702709) also describes a formulation with two clays (hydrophilic and lipophilic), which has direct benefits for the skin by providing a barrier against irritants and allergens. The patent discusses the use of the smectite-derived organophilic clay as an adsorbent and barrier for the urushiol allergen found in poison ivy. The hydrophilic clay is used as a thickener in this formulation. The two clay formulation creates "a cosmetically acceptable emollient vehicle" that conveniently spreads over the skin providing protection. A specific formulation modeled on this type of vehicle is described in detail below. The two-clay mixture is delivered to the skin in a mainly water/alcoholic solution that evaporates, leaving behind "a coating of the organophilic clay which provides a barrier against environmental allergens and irritants." This type of barrier coating, which remains on the skin following evaporation of a volatile solvent could also be attractive for the skin protectant application. The invention of this patent has been embodied in the commercial product "Ivy Block®," which is readily available from several distributors.

Emollient Selection

As discussed above, commercial creams made of O/W or W/O emulsions contain emollients in the oil layer and are typically there to improve skin feel, spreadability, as well as the lipid content of skin upper layers. For our purposes, an emollient is also necessary that would dissolve the CWAs and their simulants into the cream to allow it to react effectively with the PEI neutralizing agents incorporated within the cream.

We used solubility parameter theory to select known emollients that would be compatible with CWAs and simulants. Solubility parameter theory is used to predict whether one organic material is compatible with (or soluble in) another organic material (solvent or polymer). The method assumes that each chemical group in the molecule contributes to the total solubility. Predictions of solubility are based on the total (δT) of three different contributions: non-polar (δNP), polar (δP), and hydrogen bonding (δH). In our analysis,

we have focused on the polar and the hydrogen bonding parameters. We have used solubility parameter theory to select the most promising emollients for our formulations. The total solubility parameter for untreated SC is between 9 and 10 (cal/cm)^{3/2}, HD (sulfur mustard) has a total solubility parameter of 7.22 (cal/cm)^{3/2}, while GD (Soman) has a total solubility parameter of 6.31 (cal/cm)^{3/2}. Thus, selecting a vehicle with a continuous phase in the range of the surrogates (but differing from the SC), ~7 (cal/cm)^{3/2} is the strategy we have employed in selecting vehicle components.

We have calculated the solubility parameters of numerous emollient candidates Table 9. Based on this initial analysis we determined that ester-based emollients were the most promising general class. They provide hydrogen bonding and polar parameters that are much closer to the agents (and PEI) than more petrolatum-like carriers. This is illustrated in the solubility parameter plot shown in Figure 9. The plot shows the range of polar (2.00-7.00) and hydrogen bonding parameters (2.00-6.00). Lanolin, long chain triglycerides, ester waxes, beeswax, mineral oil, and petroleum, etc. fall in the range of 0-3.00 on both of the axes of interest (not shown), indicating low solubility with the agents and PEI. Small polar solvents, which occupy the opposite quadrant (>5.00, both axes, not shown), are also not ideal. Specific data is found in Table 9.

Table 9: Hoy Solubility Parameters (δ_P , δ_H , δ_D and δ_N) for agents, surrogates, PEI, and a series of esters. Units are cal^{1/2}/cm^{3/2}. Source data from Tables of Solubility Parameters, Union Carbide Corporation, 1975.

Chemical	Abbrev.	δ_T	δ_H	δ_P	δ_{NP}	Chemical	Abbrev.	δ_T	δ_H	δ_P	δ_{NP}
Mustard	MUS	10.22	3.28	6.46	7.22	<i>Esters - Phthalates</i>					
CEES	CEES	9.38	2.61	5.52	7.12	Dibutyl phthalate	DBP	9.56	3.87	4.71	7.37
GD-Soman	GD	7.94	2.27	4.24	6.31	Butyl benzyl phthalate	BBP	10.11	3.76	5.38	7.69
DFP	DFP	8.22	3.23	4.71	5.92	<i>Esters - Citrates</i>					
Polyethylenimine	PEI	10.95	4.65	6.26	7.56	Triethyl Citrate	TEC	10.23	5.96	5.44	6.29
<i>Esters - Benzoates</i>						Tributyl Citrate	TBC	9.45	3.69	4.92	7.17
Ethyl benzoate	EB	9.95	3.19	5.50	7.65	Acetyl tributyl citrate	ATBC	9.16	2.27	4.89	7.41
Butyl benzoate	BB	9.67	3.02	4.83	7.69	Acetyl trihexyl citrate	ATHC	8.93	2.22	4.29	7.23
C12-C15 Alkyl benzoate	CCAB	8.75	2.51	3.28	7.71	<i>Esters - Maleates</i>					
Phenyl ethyl benzoate	PEB	10.13	2.56	5.53	8.09	Dibutyl maleate	DBM	9.22	4.20	4.40	6.92
Diethylene glycol dibenzoate	DEGDB	10.12	3.87	5.69	7.43	Dioctyl maleate	DOM	9.77	3.55	3.77	8.29
Butylene glycol dibenzoate	BGDB	10.19	3.76	5.57	7.66	Di-2-Ethylhexyl maleate	DEHM	8.59	3.10	3.51	7.20
Dipropylene glycol dibenzoate	DPGDB	9.83	3.27	5.43	7.51	<i>Esters - Glycerol esters</i>					
<i>Esters - Adipates</i>						Triacetin	GTA	10.60	5.73	5.73	6.83
Diisopropyl adipate	DIPA	8.67	3.22	4.13	6.91	Glycerol Tricapronate (C6)	GTH	8.84	3.19	3.95	7.24
Di-n-propyl adipate	DNPA	9.07	4.04	4.11	7.01	Triethylhexanoate	GEH	8.54	3.09	3.47	7.17
Dibutyl adipate	DBA	8.93	3.85	3.84	7.09	Caprylic/Capric Triglyceride	GCC	8.64	3.12	3.32	7.34
Di-2-ethylhexyl adipate	DEHA	8.49	3.07	3.14	7.27	Caprylic/Capric Succinic	M829	9.05	3.27	3.98	7.44
<i>Esters - Succinates</i>						Triglyceride					
Dimethyl succinate	DMS	10.30	5.32	5.73	6.70	<i>Silicones</i>					
Diethyl succinate	DES	10.21	5.30	5.14	7.05	Dimethicone - PDMS	PDMS	8.69	3.14	3.95	7.07
Diisopropyl succinate	DIPS	8.83	3.30	4.52	6.83	Cyclotetrasiloxane	CTSi	6.12	2.21	2.78	4.99
Dibutyl succinate	DBS	9.06	4.02	4.11	7.01	Cyclopentasiloxane	CPSi	6.10	2.20	2.77	4.97
Diethoxyethyl succinate	DEES	8.85	3.88	4.53	6.54	Phenyl Trimethicone	PTM	7.02	2.53	2.93	5.85
Diethylhexyl succinate	DEHS	8.78	2.79	3.44	7.58						
<i>Miscellaneous Esters</i>											
Isopropyl myristate	IPM	8.10	2.47	2.50	7.29	PEG12 Dilaurate	PEG12DL	8.93	3.23	3.81	7.41
Isopropyl palmitate	IPP	8.09	2.17	2.40	7.41	Lauryl Lactate	LL	9.00	4.57	3.52	6.00
Propylene glycol dicaprate	PGDC	8.36	3.02	3.02	7.19	Propylene glycol laurate	PGML	9.64	5.35	3.64	7.15
Neopentyl Glycol Dicaprate	NGDC	8.29	2.99	2.90	7.17	Cradamol STS	CSTS	8.38	3.02	3.27	7.09
PEG4 Dilaurate	PEG4DL	9.05	3.27	3.44	7.70						

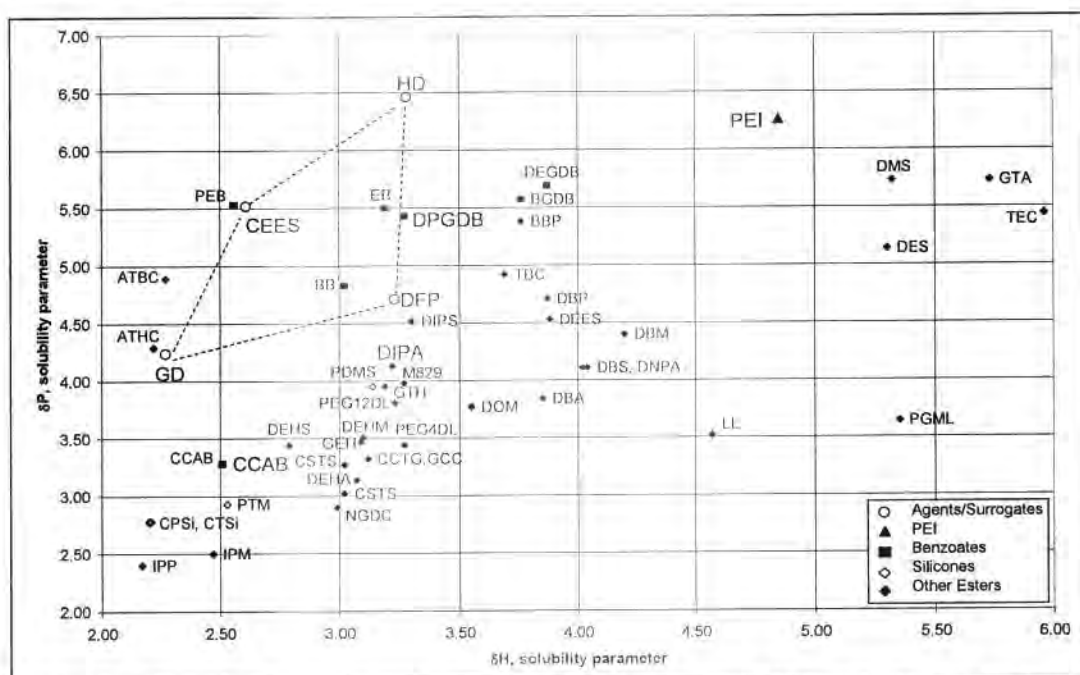


Figure 9: Analysis of emollients using Hoy solubility parameters. The plot shows Hoy Solubility Parameters (δ_P and δ_H , Table 9) for agents, surrogates, PEI, and a series of esters. Units are $\text{cal}^{1/2}/\text{cm}^{3/2}$. Source data from Tables of Solubility Parameters, Union Carbide Corporation, 1975.

Examples of the families of esters that would be appropriate to use as the oil phase of the NSP include adipates, benzoates, citrates, fatty esters such as palmitates, myristates, caprates, laureates, glycerol esters, maleates, phthalates and succinates. The benzoate esters are preferred, as they provide the highest polar solubility parameters. The most preferred benzoate ester is Dipropylene glycol dibenzoate (DPGDB), because of its excellent fit with our criteria and commercial availability of this ester as a cosmetic ingredient. C12-C15 alkyl benzoate (AB) is also preferred; it is a moderate fit with the solubility criteria, but is extensively used as an emollient in skin cream formulations.

Development of Formulation Processing Protocols

We prepared several preliminary formulations that incorporated clays to enable set-up and optimization of our mixing equipment/apparatus and rheology testing procedures. We first sought to reproduce the Ivy Block formulation (see "Two Clay Gels" section above), since it could be easily obtained for comparison purposes and provided an example of a two-clay formulation. We were also interested in evaluating our hypotheses about dried form of various vehicles. The following five formulas describe preliminary "base" formulations and do not contain the key active ingredients.

Formulation #1

Objective: Reproduce Ivy Block formulation (US Patent 5702709)

Phase A (Oil)

Q-90 Bentonite (Tixogel VP-V)*	5%
Diisopropyl adipate (ISP Ceraphyl 230)	20%

Phase B (Water)

Water	45%
Bentonite Clay	5%
Ethanol (SD denatured alcohol)	25%

Combine Phase A and Phase B components *separately*, heating as necessary to make homogeneous. Mix Phase A & Phase B until homogeneous.

Notes: Diisopropyl adipate is an emollient, selected for its relatively short chain length to minimize interaction with long chains of Q-90 Bentonite. Isopropanol may be substituted for ethanol. 0.3% preservative (methyl paraben) can be added to water phase as needed.

Expected wet form: watery lotion

Expected dry form: oily film, containing organoclay

Barrier function: Oil, clays act as barrier

The product mixed using the ingredients and components above was similar, but not identical to the commercial product Ivy Block. Formulation #1 was tackier (oil component was more apparent) in wet and dry form. The Formulation #1 and Ivy Block both formed slightly oily white films when dried on watch glasses.

Formulation #2

Objective: Create formulation described in Avon Patent #6660277

Phase A – (~10% clay, ~90% oil)

Tixogel FTN-1564	5%
C12-15-Alkyl Benzoate (Crodamol AB)	30%

Phase B – (~4% clay, ~96% water)

Bentonite clay (Gelwhite H)	3%
Deionized Water	62%

Combine components of each phase separately to form two gels. Use heat if necessary to create homogeneity.

Tixogel FTN-1564: Stearalkonium Bentonite 90 + C12-C15 Alkyl Benzoate + Propylene Carbonate (activator)

According to the patent, a 1:1 ratio of Phase A/Phase B is used; 2:1 produces a heavier cream, while 1:2 produces a lighter cream.

Expected wet form: "spreadable cement"

Expected dry form: oily film, containing clays

Barrier function: Oil, clays act as barrier

Formulation #2 was similar to Formulation #1 with increased oily hand feel.

Based on these initial results with Formulations #1 and #2, we speculated that the clay had not fully swelled (exfoliated) under the conditions of moderate mixing (300 rpm, 3-way paddle) and no heating (~25 °C) we had initially employed. Complete exfoliation of the clay is important not only for formulation stability but also to create the best possible tortuous path. Using a Wells-Brookfield R/S CPS Rheometer, we evaluated the effects via rheology measurements of increasing mixing speed (to ~1100 rpm, Cowles blade) and adding heat (up to 80 °C) of 2% and 4% hydrophilic clays (Gelwhite H, pure bentonite). An example of the effect of heating and stirring speed on a 2% Gel-white H solution is shown in Figure 10. In Figure 11, a viscosity measurement of the Ivy Block product is shown.

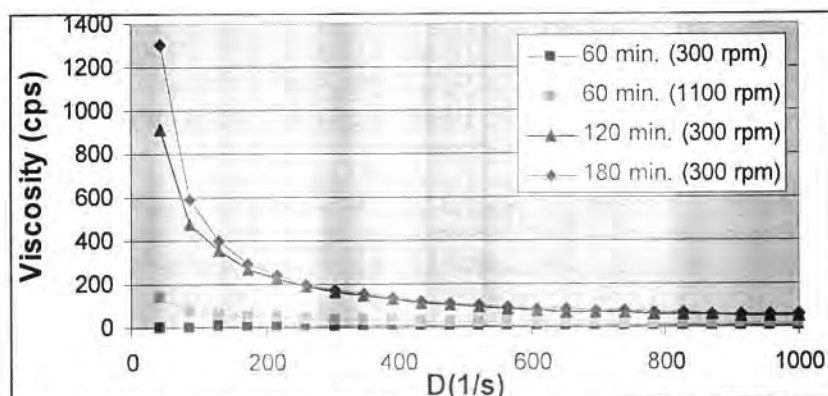


Figure 10: Viscosity Vs. Shear Rate (D) of 2% Gelwhite H heated to 80°C at different times and mixing speeds (rpm).

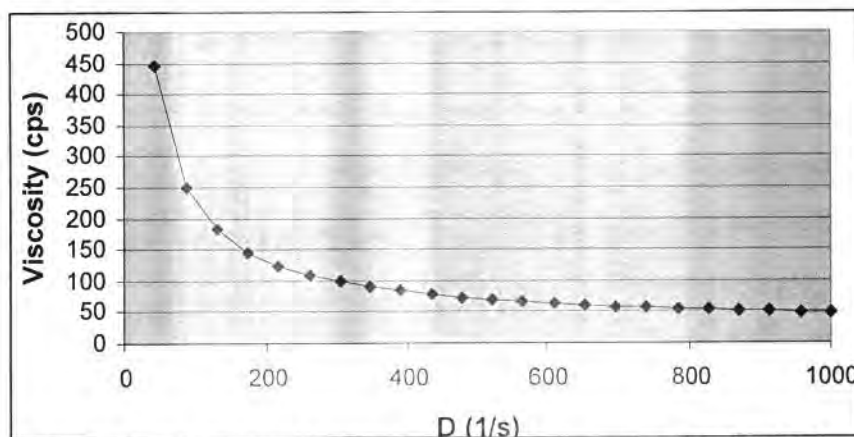


Figure 11: Ivy Block® product viscosity measurement using Brookfield rheometer

Based on our learning of optimal heating and mixing (1100 rpm, 75°C) on the swelling of hydrophilic clays, we developed a reproducible processing method enabling us to move forward with building up additional formulation vehicles containing clays.

2.3 Task 3: Formulation of Neutralizing Skin Protectant

Objectives

- Development of Candidate Formulations
- Screening of Candidate Formulations
- Develop *In vitro* Skin Permeation Assessment Protocol

Summary of Task 3

Our objective for Task 3 was to create several specific formulations for testing in Task 4. Using the processing methods we developed in Task 2, we created a series of formulations. We created over 26 formulations, which were reduced to 5 through physical evaluation and screening.

To evaluate the ability of the prototype NSP formulations to protect skin, we proposed a series of *in vitro* skin permeation experiments using a Franz Cell apparatus. *In vitro* skin permeation experiments were to be performed in Task 4. However, in consultation with the COR, we decided to discontinue the use of the Franz cell apparatus for formulation testing and evaluation and instead performed headspace GC analysis which is described in the next section. The description of the Franz Cell apparatus are described in detail in previous reports and are not repeated here, since it was not used for testing the final formulations, as agreed upon by the Army COR and TIAX program manager.

Development of Candidate Formulations

Initial Base Formulations Containing Neutralizing Actives (PEIs)

In a section 2.2, we described base formulations #1 and #2, which were used to develop and refine our processing method. These two-clay base formulations were used as a starting point for a two-clay formulation containing the active neutralizing and diffusion inhibiting materials, as follows:

TIAX Two-Clay Barrier Paste Formulation Example (building on Base Formulation #1 & #2)

Q-18 Bentonite Clay	5%
Activator for Clay	2.5%
Emollient	to 20%
Hydrophilic Clay	5%
Lupasol FG	10%
H ₂ O	10%
Croda Incroquat QLC	2%
DPG+H ₂ O	42.5%
Preservatives	1%
Buffer	2%

1. Pre-swell hydrophilic clay in H₂O/DPG mixture (~20%) in 60C bath for 60 min.
2. Pre-activate hydrophobic clay by high speed mixing for 60 min. in presence of activator.
3. Dissolve Lupasol FG initially in water in equal parts; after adding all other water phase ingredients make up the rest of the volume with combination of DPG/H₂O.
4. Combine remaining, non-heat labile ingredients. Continue mixing at high speed until mixture is homogeneous at 75-80C.
5. Cool to room temperature.
6. Add heat-labile ingredients (e.g., preservatives)

We also created W/O and O/W "starter formulations" that contain PEIs, building from the base formulations and processing methods identified in our review of sample topical formulations for each vehicle type.

W/O Formulation with Hydrophobic Clay**Phase A: Oil Phase**

Tixogel MIO-1584*	15%
Mineral Oil (Emollient)	20%
Emulsifier (HLB 5)	7%

Phase B: Water Phase

H ₂ O	46%
Incroquat QLC	2%
PEI	10%

1. Combine Phase A and Phase B components separately with high speed mixing and heating to 75-80C.
2. Add Phase B to Phase A. Continue mixing at high speed until mixture is homogeneous at 75-80C.
3. Once homogenous, begin cooling.

*Tixogel MIO-1584: Quaternium-90 Bentonite + NF Light Mineral Oil + Propylene carbonate)

O/W Formulation with Hydrophilic Clay**Phase A: Water phase**

PEI	10%
H ₂ O	10%
Croda Incroquat QLC	2%
DPG+H ₂ O	to 32%
Hydrophilic Clay	5%
Preservatives	1%
Buffer	2%

Phase B: Oil Phase

Emollient	36%
Emulsifier	2%

1. Pre-swell hydrophilic clay in H₂O/DPG mixture (~20%) in 60C bath for 60 min.
2. Dissolve Lupasol FG initially in water in equal parts; after adding all other water phase ingredients make up the rest of the volume with combination of DPG/H₂O.
3. Combine Phase A and Phase B components separately with high speed mixing and heating to 75-80C.
4. Add Phase B to Phase A. Continue mixing at high speed until mixture is homogeneous at 75-80C.
5. Cool to room temperature.
6. Add heat-labile ingredients (e.g., preservatives)

Building on Initial Base Formulations containing PEIs

Building on the starting formulations above, over 26 formulations were made in approximately 300g batches. We focused our effort on incorporating the maximum amount of polyethylenimines (PEI) into physically stable W/O emulsions and two-clay O/W emulsions. These new, physically stable base formulations and the most promising formulation of each type are provided below.

Two-Clay Gel (Formulation #1)

As discussed above, our starting point for the two-clay type formulations arises from two patents we identified earlier in the program. The Enviroderm patent (US5702709) describes a two-clay formulation that provides a barrier against irritants and allergens. The invention has been embodied in the commercial product "Ivy Block®," which we have purchased to compare and evaluate relative to the same

formulation made in our lab, enabling "tuning up" of our processing method. We provided a specific formulation modeled on the Enviroderm patent discussed above. This formulation did not contain PEIs. Updated versions of the formulation, with and without PEIs, are provided below.

Formulation #1 "Ivy Block" (Updated)

US Patent 5702709

Phase A (Oil)

Q-90 Bentonite (Tixogel VP-V)*	5%
Diisopropyl adipate (ISP Ceraphyl 230)	20%
Ethanol (organoclay activator)	2.5%

Add diisopropyl adipate (solvent) to beaker. Slowly add organoclay to stirring solvent vortex. Mix for 5 minutes at 1100 rpm. Add ethanol and mix for an additional 5 minutes at 1100 rpm. Organoclay is now activated and ready to use.

Phase B (Water)

Water (distilled)	45%
Bentonite Clay (Gelwhite H)	5%
Ethanol (SD denatured alcohol)	22.5%

Add hydrophilic clay to stirring 75C water vortex. Mix for 10 minutes at 1100 rpm. Cool to 40 C and add ethanol while stirring.

Add Phase A to Phase B while stirring; mix at 1100 rpm until homogeneous.

Formulation #1 was altered from its previous version, to include the activator of the clay (ethanol) in the oil phase. Propylene carbonate could also be used. The mixture is somewhat more viscous than the commercial product Ivy Block formulation (pH 7.5) and has a pH of 7-7.5. Otherwise the consistency is qualitatively similar to the commercial product, validating our processing method. (A thinner consistency would have indicated that we were not exfoliating the clays comparably to the Ivy Block product).

Next we sought to include PEIs (Formulation #1A). The first version of this formulation included PEI (Lupasol FG, BASF) at a level of 5% by weight. We tried two processing methods. In one method we first exfoliated the clay in Phase C, and then added a pre-combined mixture of the PEI and an equal weight of water (Phase B). In the second (Formulation #1B, not shown), we simply added the 5% PEI to Phase B, the water phase. Formulation #1A resulted in a thick, pasty mixture with a pH of 9-9.5. For Formulation #1B, no thickening was observed in Phase B when the clay was added, indicating the clay did not exfoliate in the presence of PEIs. Addition of the oil phase (Phase A) resulted in complete separation of the mixture. We therefore moved forward with revising Formulation #1A, raising the level of PEI by 5% (by weight) intervals. Formulation #1A, Revision 2 (below) contains 15% PEI. This mixture forms a whitish-brown cream of moderate viscosity with a pH of 10, which does not separate. Attempts to include Incroquat QLC (2.5%) as part of Phase C or as a separate phase (D) with the ethanol were unsuccessful. We continued to experiment on this front as well as to increase the content of PEI, and improve consistency.

Formulation #1A (Revision 2) "Ivy Block" with 15% PEI**Phase A (Oil)**

Q-90 Bentonite (Tixogel VP-V)*	5%
Diisopropyl adipate (ISP Ceraphyl 230)	20%
Ethanol (organoclay activator)	2.5%

Add diisopropyl adipate (solvent) to beaker. Slowly add organoclay to stirring solvent vortex. Mix for 5 minutes at 1100 rpm. Add ethanol and mix for an additional 5 minutes at 1100 rpm. Organoclay is now activated and ready to use.

Phase B (Water)

PEI (Lupasol FG)	15%
Water (distilled)	15%

Combine ingredients with magnetic stirring.

Phase C (Clay)

Water (distilled)	30%
Bentonite Clay (Gelwhite H)	2.5%
Ethanol (SD denatured alcohol)	10%

Add hydrophilic clay to stirring 75°C water vortex. Mix for 10 minutes at 1100 rpm. Cool to 40 °C and add ethanol while stirring.

Add Phase B very slowly (drop wise) to Phase C while mixing vigorously (close to 1100 rpm). Observe result. If phase separation is apparent after all Phase B is added, do not proceed to Phase A. Otherwise, add Phase A to Phase B/C while stirring; mix at 1100 rpm until homogeneous.

Two-Clay Gel (Formulation #2)

US patent (US6660277) assigned to Avon describes a formulation that is a "cosmetic composition comprising a lipophilic clay gel and a hydrophilic clay gel" combined to create a "gel matrix" that "functions like an emulsion." We identified this formulation base as attractive for consideration in the NSP formulation selection process due to the use of two clays (tortuous path) with additional incorporated actives. We provided a specific formulation modeled on this type of vehicle in an earlier section. Formulation #2 was updated mainly in the processing method. We learned through experience that the hydrophilic clay does not exfoliate (thicken) at room temperature under our mixing conditions (~1100 rpm, Cowles blade). Heating to 75 °C has been added in the preparation of Phase B. The mixture thickens to a creamy texture with a pH of 7.5-8.

Formulation #2 "Avon 2-Clay" (Updated)
 US Patent 6660277
Phase A (Oil)

Q-90 Bentonite (Tixogel VP-V)	5%
C12-15-Alkyl Benzoate (Crodamol AB)	30%
Ethanol (organoclay activator)	2.5%

Add Alkyl Benzoates (solvent) to beaker. Slowly add organoclay to stirring solvent vortex. Mix for 5 minutes at 1100 rpm. Add ethanol and mix for an additional 5 minutes at 1100 rpm. Organoclay is now activated and ready to use.

Phase B (Water)

Bentonite clay (Gelwhite H)	2.5%
Deionized Water	60%

Add hydrophilic clay to stirring 75°C water vortex. Mix for 10 minutes at 1100 rpm.

Cool Phase B to room temperature. Add Phase A to Phase B while stirring. Heat mixture to 75°C while stirring at 1100 rpm until homogeneous.

Formulation #2A (Revision 3) "Avon 2-Clay" with 20% PEI
Phase A (Oil)

Q-90 Bentonite (Tixogel VP-V)	5%
C12-15-Alkyl Benzoate (Crodamol AB)	20%
Ethanol (organoclay activator)	2.5%

Add Alkyl Benzoates (solvent) to beaker. Slowly add organoclay to stirring solvent vortex. Mix for 5 minutes at 1100 rpm. Add ethanol and mix for an additional 5 minutes at 1100 rpm. Organoclay is now activated and ready to use.

Phase B (Water)

Deionized Water	20%
PEI (Lupasol FG)	20%

Combine ingredients with magnetic stirring.

Phase C (Clay)

Bentonite clay (Gelwhite H)	2.5%
Deionized Water	30%

Add hydrophilic clay to stirring 75°C water vortex. Mix for 10 minutes at 1100 rpm.

Add Phase B very slowly (drop wise) to Phase C while mixing vigorously (close to 1100 rpm). Observe result. If phase separation is apparent once all Phase B is added, do not proceed to Phase A. Otherwise, add Phase A to Phase B/C while stirring; mix at 1100 rpm until homogeneous.

We next added PEI at a level of 1% by weight. (Formulations #2A and #2B). As with formulation #1A, in Formulation #2A, we created a separate phase (C) in which the hydrophilic clay is first exfoliated separately. Then a pre-combined 50:50 PEI:water mixture (Phase B) is added drop wise into Phase C. In

Formulation #2B (not shown) we combined the PEI directly into Phase B. Formulation #2A was observed to form a smooth creamy mixture of pH 10, while Formulation #2B completely separated as Phase A was added. Therefore we moved forward with Formulation #2A, adding PEI by 5% intervals to each revision of this formulation. Formulation #2A, Revision 3, containing 20% by weight PEI (below) results in a thick creamy textured mixture with no separation and pH of 10. Our next steps were to add in Incroquat QLC, increase PEI further, and continue to improve consistency.

W/O Emulsion (Formulation #3)

An updated version of the water in oil (W/O) emulsion base formulation presented in an earlier section is shown below. In this formulation, we replaced mineral oil with C12-15 Alkyl Benzoates and the organoclay with an organoclay gel. Tixogel FTN-1564 contains organoclay pre-activated with propylene carbonate and C12-15 Alkyl Benzoates (emollient) for ease of mixing into personal care formulations.

Formulation #3 – W/O Emulsion

Phase A (Oil Phase)

Tixogel FTN-1564	10%
C12-15 Alkyl Benzoates	15%
Emulsifier HLB 5 (Crill 3)	5%

Combine Phase A components with mixing and heating to 80C.

Phase B (Water)

Water (distilled)	65%
Clay (Gelwhite H)	2.5%
Incroquat QLC	2.5%

Combine Phase B components with mixing and heating to 80C.

Add Phase B to Phase A with vigorous mixing at 80C. Continue mixing intensively until mixture is homogeneous.

Once homogenous, begin cooling.

The use of the Alkyl Benzoates are preferred to the mineral oil because it is commonly used as an emollient in skin preparations of the consistency/"staying power" we are seeking for this formulation. Additionally, based on solubility parameter calculations, Alkyl Benzoates have favorable solubility for solubilizing the CWAs as well. We have also selected an emulsifier (Crill 3 Sorbitan Ester, HLB 4.7, Croda) for the formulation. The resulting W/O formulation (#3) results in a thick, creamy textured gel that is white in color with a pH of 8.5-9. No separation was apparent. Oil was confirmed as the continuous phase using a drop test (water or oil) on microscope slides.

Based on our successful (non-separating) 2-Clay Formulations, we started at a higher level of PEI in the W/O Formulation (#3A, not shown), 10% by weight. As with the 2-Clay Formulations described above, we created a separate Phase C in which the water and bentonite clay were combined. Incroquat QLC was added to Phase C. Phase B (50:50 water:PEI) was added to Phase C drop wise. However, separation of the phases was observed when Phase A was added to Phase B/C. Next we tried lowering the PEI to 5% (Formulation #3A, Revision 1). A very small amount of separation was observed; the mixture was homogeneous except for a few beads of water within the sample jar on cooling. We surmised that the oil phase was not sufficient to contain the high water content of the formulation and substantially increased the oil phase (from 30% to 47.5% by weight of the formulation). To simplify the formulation, we also removed the Incroquat QLC for now.

Formulation #3C, W/O Emulsion with 5% PEI**Phase A (Oil Phase)**

Tixogel FTN-1564	15%
C12-15 Alkyl Benzoates	27.5%
Emulsifier HLB 5 (Crill 3)	5%

Combine Phase A components with mixing and heating to 80C.
Split Phase A in half (A-1, A-2)

Phase B (Water/PEI)

PEI (Lupasol FG)	5%
Water (distilled)	5%

Combine ingredients with magnetic stirring.

Phase C (Clay)

Water (distilled)	40%
Bentonite Clay (Gelwhite H)	2.5%

Add hydrophilic clay to stirring 80C water vortex. Mix for 10 minutes at 1100 rpm.
Add Phase B into Phase A-1 while mixing vigorously at 80 C (close to 1100 rpm).
Add Phase C into Phase A-2 while mixing vigorously at 80 C (close to 1100 rpm).

Add Phase A/B to Phase A/C with vigorous mixing at 80C. Continue mixing vigorously (close to 1100 rpm) until mixture is homogeneous. Once homogenous, begin cooling.

Finally, we tried two modified processing methods. In Formulation #3B (not shown), we pre-combined Phase C (water + clay) and added this into (Oil) Phase A, then added Phase B into Phase A/C. In Formulation #3C (below), we pre-combined Phase C (water + clay) and added it into 1/2 of Phase A, add Phase B into 1/2 of Phase A. Phase A/B and A/C were then combined. The mixture resulting from the Formulation #3C was the most homogeneous during processing, but had a minimal water layer upon cooling

Formulation for Screening by Headspace Solid Phase Micro-Extraction (HS-SPME)

The formulations shown above were iteratively improved and nine formulations were developed for *in vitro* testing, four oil-in-water (O/W), three water-in-oil (W/O), and two waterless systems.

Polyethylenimine was used as the active ingredient to react with the surrogates. Both hydrophobic and hydrophilic clays, in the exfoliated state, were used as barrier materials to produce "tortuous paths" in the applied creams. Four of the samples were controls, containing no polyethylenimine, but were formulated with approximately the same level of exfoliated clays. Table 10 below summarizes the compositions of the final formulations.

Table 10: Summary of final TIAx NSP (TNSP) Formulations for Testing Against CWA Surrogates and CWAs

Sample Name	Type of Formulation	% PEI Active	Non-Volatiles (Composition)	Volatiles	Internal TIAx I.D.
TNSP 1	Oil-in-Water	15	Hydrophobic Clay Hydrophilic Clay C12-C15 Alkyl Benzoate*	Ethanol Water	357-107; 419-26
TNSP 1 Control	Oil-in-Water	0	Hydrophobic Clay Hydrophilic Clay C12-C15 Alkyl Benzoate*	Ethanol Water	357-106; 419-27
TNSP 2	Oil-in-Water	15	Hydrophobic Clay Hydrophilic Clay Dipropylene Glycol Benzoate*	Propylene Carbonate Water	357-112; 419-28
TNSP 2 Control	Oil-in-Water	0	Hydrophobic Clay Hydrophilic Clay Dipropylene Glycol Benzoate*	Propylene Carbonate Water	357-111; 419-25
TNSP 3	Water-in-Oil	10	Hydrophobic Clay Dipropylene Glycol Benzoate* Emulsifier Lipid Conditioner	Ethanol Water	357-109; 419-21
TNSP 4	Water-in-Oil	15	Hydrophobic Clay Dipropylene Glycol Benzoate* Emulsifier Lipid Conditioner	Ethanol Water	357-110; 419-22
TNSP 3/4 Control	Water-in-Oil	0	Hydrophobic Clay Dipropylene Glycol Benzoate* Emulsifier	Ethanol Water	357-108; 419-20
TNSP 5	Waterless	20	Hydrophobic Clay Dipropylene Glycol Benzoate*	Propylene Carbonate	357-114; 419-24
TNSP 5 Control	Waterless	0	Hydrophobic Clay Dipropylene Glycol Benzoate*	Propylene Carbonate	357-113; 419-23

*Emollient

More detailed formulation and composition information are shown in the Appendix.

2.4 Task 4: *In vitro* Skin Permeation Assessment Studies with CWA Surrogate Challenges

Objectives (as stated in Phase II Proposal)

- Validation of Franz Cell Skin Permeation Assessment Method
- Evaluation of Formulations for Skin Permeation of Chemical Agent Surrogates using Franz Cell Apparatus

Modified Objectives*

- Pre-screening of down-selected NSP formulations from Task 3 with Headspace Solid Phase Micro-Extraction (HS-SPME) (using CWA surrogates)
- Replacement of Franz Cell Skin Permeation Assessment Method with neutralization testing against live CWAs

*Modified objectives reflect the change in the Task that took place in consultation and mutual agreement with the COR

Summary of Task 4

A conference call with the COR was held on 28 April 2008. During the call we mutually agreed to substitute Penetration Cell testing to be performed at Battelle, using live agents, for the Franz cell-based *in vitro* Skin Permeation Assessment testing using chemical agent surrogates that was to be performed at TIAX, originally proposed as Task 4 of the Phase II proposal. In September 2011, it was decided that a neutralization test of CWAs (GB, HD and VX) would take place at USAMRICD under the supervision of the COTR instead of the penetration cell testing. The deliverables for Task 4 as stated in the Phase II proposal were 1) Skin permeation testing results and 2) Prototype formulations for testing with live agents at USAMRICD. The new deliverables are: 1) results of the NSP pre-screening studies (TIAX) and 2) results of the CWA neutralization testing at the United States Army Medical Research Institute of Chemical Defense (USAMRICD). We agreed to perform initial screening tests of NSP formulations at TIAX using the HS-SPME test method developed in the Phase I program (Task 4, Deliverable 1), and use the neutralization testing as the final, definitive evaluation of the most promising NSP formulations. These formulations will be evaluated against three agents in liquid form, HD, GD and VX (Task 4, Deliverable 2). The results of these two testing protocols are discussed below.

NSP Pre-screening - Headspace Solid Phase Micro-Extraction (HS-SPME) Results.

We evaluated the efficacy of PEIs against chemical agent surrogates CEES (for HD) and DFP (for GD) using a "proof of neutralization" test method based on HS-SPME with GC/MS detection. In the test, a sample formulation containing the active neutralizing moiety is challenged with a known amount of chemical agent surrogate, DFP or CEES. The headspace of the sample is extracted periodically using a SPME fiber, which is then desorbed into a hot injector port of the GC/MS. Identification and measurement of the DFP or CEES in the headspace by GC/MS enables tracking of the decrease in surrogate concentration vs. time. This result is compared to a control sample (no active) analyzed under the same conditions. The details of the HS-SPME process are described in the Appendix. Four series of experiments were carried out using the HS-SPME procedure on the TNSP 1, 2, 3, 4 and 5, containing the PEI active, and the corresponding controls which contained no actives. The results are shown in Figure 12 - Figure 19, below. In all figures, the concentration of the CEES or DFP in the headspace is plotted against time of exposure to the surrogate. We found that of the five formulations containing PEI actives, TNSP 1 appeared to have the highest potential as a NSP cream against CWAs, as the amount of CEES and DFP decreased significantly more than the corresponding non-active containing control. TNSP 1 is an OW 2-clay system with 15% PEI and alkyl benzoate emollient. TNSP 2 was the next most promising candidate for similar reasons, however, the reproducibility was poorer. TNSP 3 and 4 show mixed results as the control (TNSP 3/4 Control) showed significant amount of CEES/DFP decrease in the headspace. Finally, the waterless formulation (TNSP 5) showed promising results against the nerve agent simulant, DFP, but not against the vesicant simulant, CEES.

Although the results of this pre-screening show mixed results, the down selected TNSP formulations may show better results in the live agent neutralization testing. This is because the HS-SPME testing only

shows the disappearance of the CWA surrogates in the headspace, and not the neutralization that may be taking place within the NSP.

Series 1: CEES and DFP against TNSP 1 and TNSP 1 control.

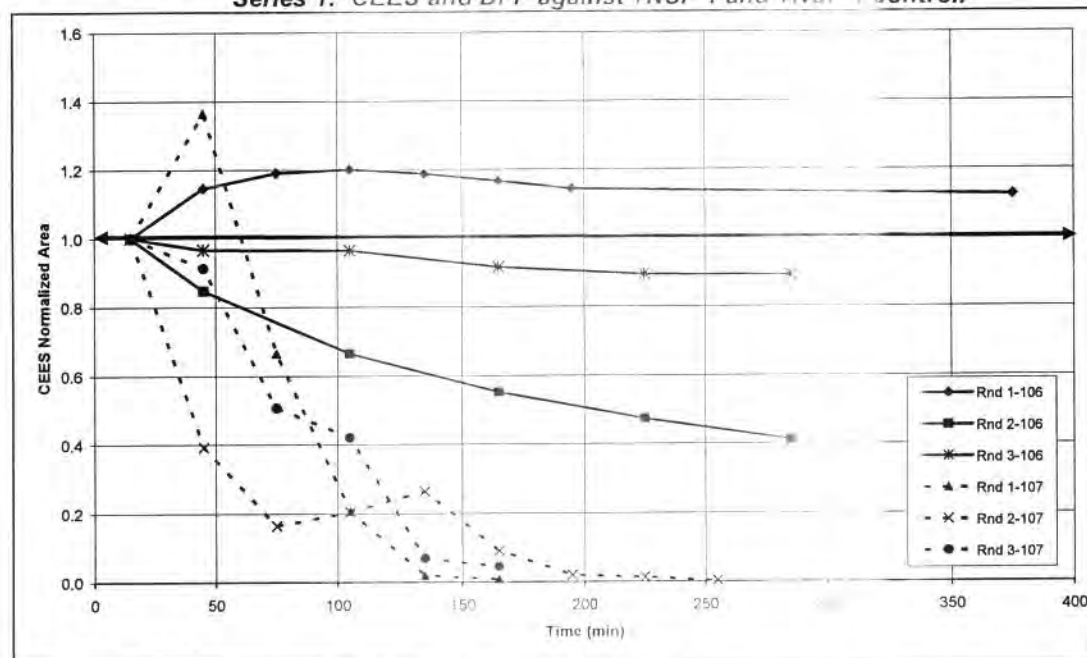


Figure 12: Relative amount of CEES in headspace of designated samples vs. time, as measured by HS-SPME and GC-MS. TNSP 1 (dotted line) and TNSP 1 Control (solid line). Formulations are Oil-in-Water, 2-Clays, Alkyl Benzoate Emollient.

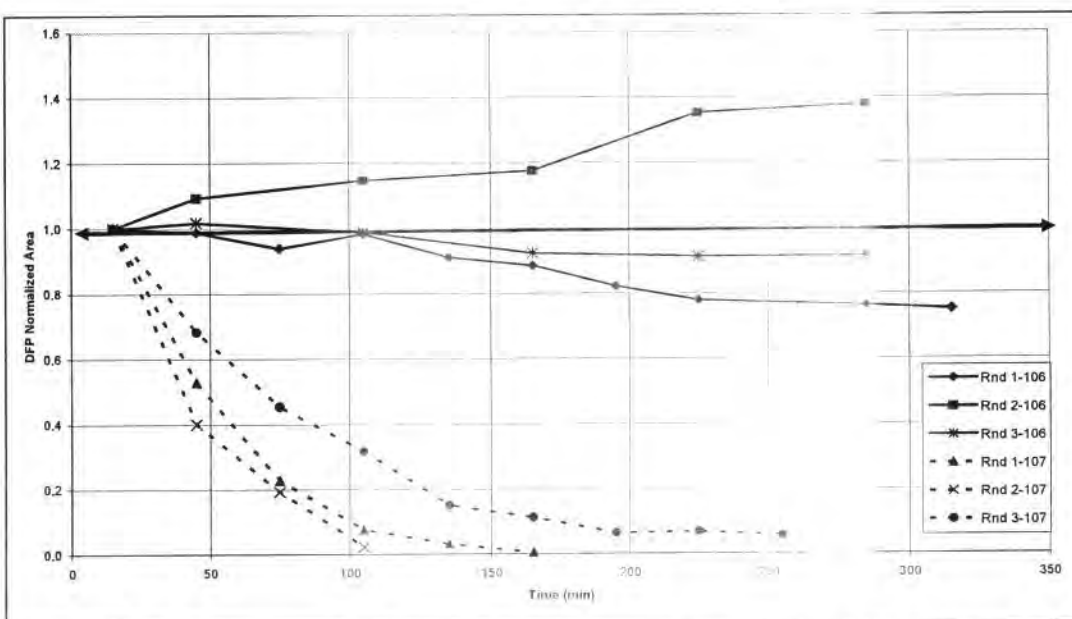


Figure 13: Relative amount of DFP in headspace of designated samples vs. time, as measured by HS-SPME and GC-MS. TNSP 1 (dotted line) and TNSP 1 Control (solid line). Formulations are Oil-in-Water, 2-Clays, Alkyl Benzoate Emollient.

Series 2: CEES and DFP against TNSP 2 and TNSP 2 control.

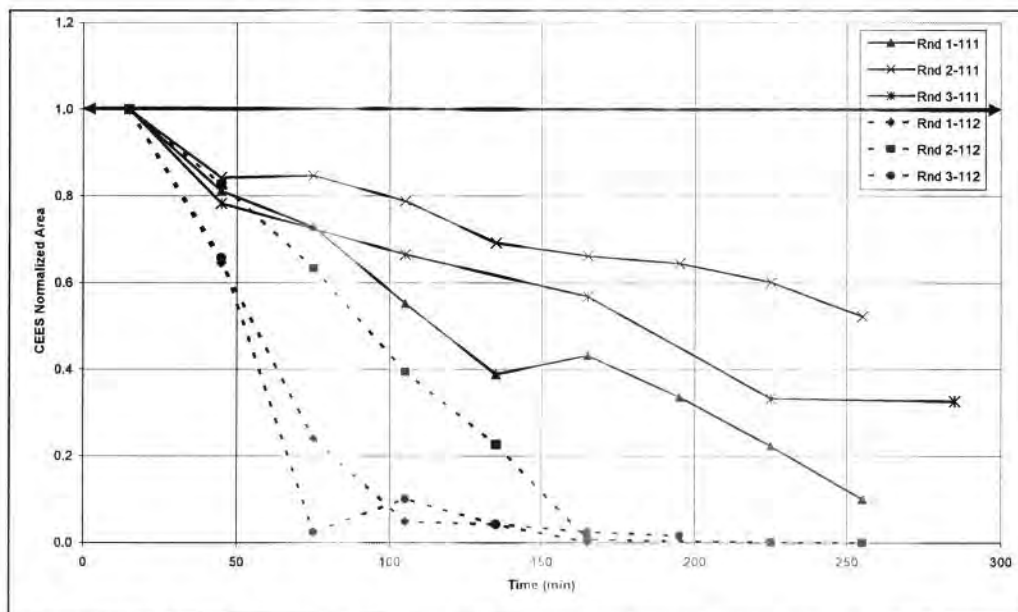


Figure 14: Relative amount of CEES in headspace of designated samples vs. time, as measured by HS-SPME and GC-MS. TNSP 2 (dotted line) and TNSP 2 Control (solid line). Formulations are Oil-in-Water, 2-Clays, Dipropylene Glycol Dibenzoate Emollient.

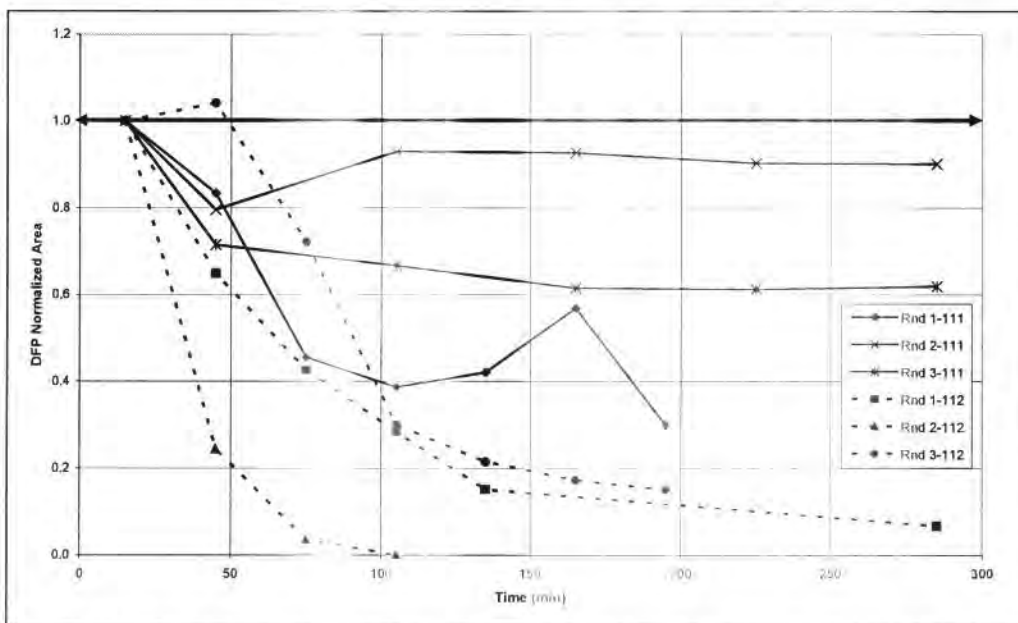


Figure 15: Relative amount of DFP in headspace of designated samples vs. time, as measured by HS-SPME and GC-MS. TNSP 2 (dotted line) and TNSP 2 Control (solid line). Formulations are Oil-in-Water, 2-Clays, Dipropylene Glycol Dibenzoate Emollient.

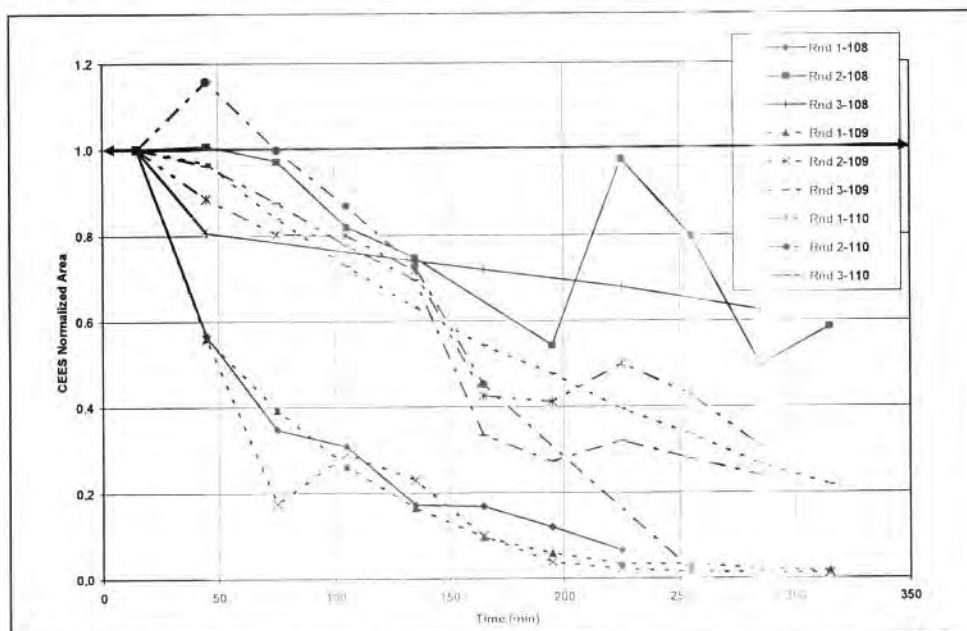
Series 3: CEES and DFP against TNSP 3, TNSP 4 and TNSP 3/4 control.

Figure 16: Relative amount of CEES in headspace of designated samples vs. time, as measured by HS-SPME and GC-MS. TNSP 3 (dotted line), TNSP 4 (dotted/dashed line) and TNSP 3/4 Control (solid line). Formulations are Water-in-Oil, Hydrophobic Clay Dipropylene Glycol Dibenzoate Emollient.

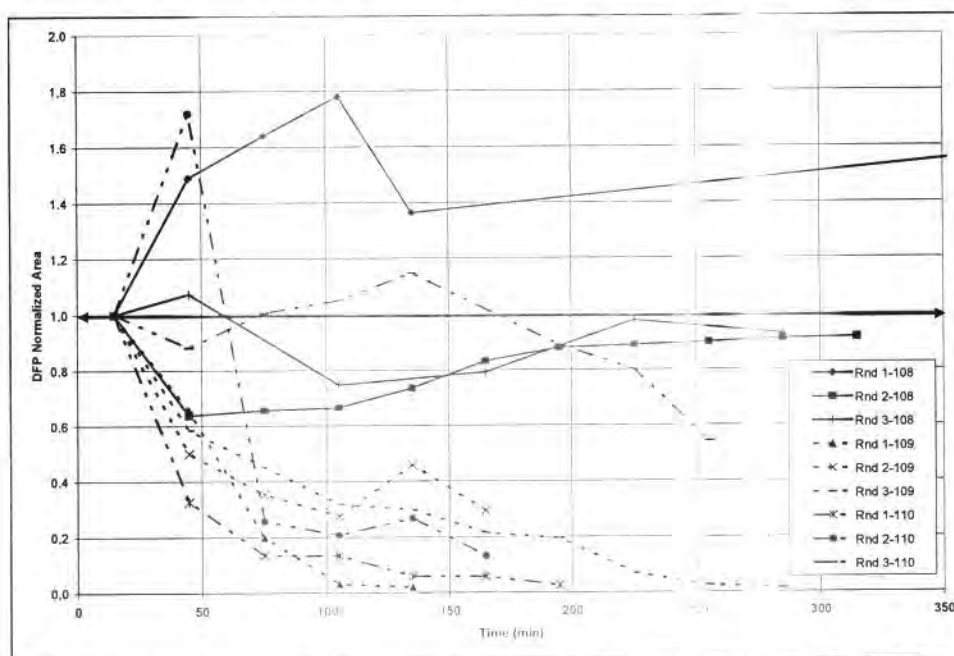


Figure 17: Relative amount of DFP in headspace of designated samples vs. time, as measured by HS-SPME and GC-MS. TNSP 3 (dotted line), TNSP 4 (dotted/dashed line) and TNSP 3/4 Control (solid line). Formulations are Water-in-Oil, Hydrophobic Clay Dipropylene Glycol Dibenzoate Emollient.

Series 4: CEES and DFP against TNSP 5 and TNSP 5 Control.

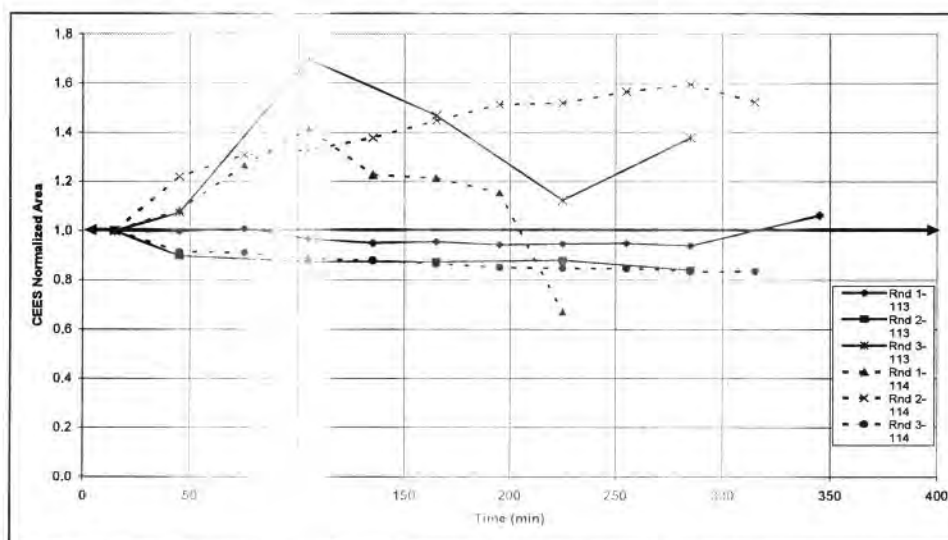


Figure 18: Relative amount of CEES in headspace of designated samples vs. time, as measured by HS-SPME and GC-MS. TNSP 5 (dotted line), and TNSP 5 Control (solid line). Formulations are Waterless, Hydrophobic Poly in Dipropylene Glycol Dibenzate Emollient.

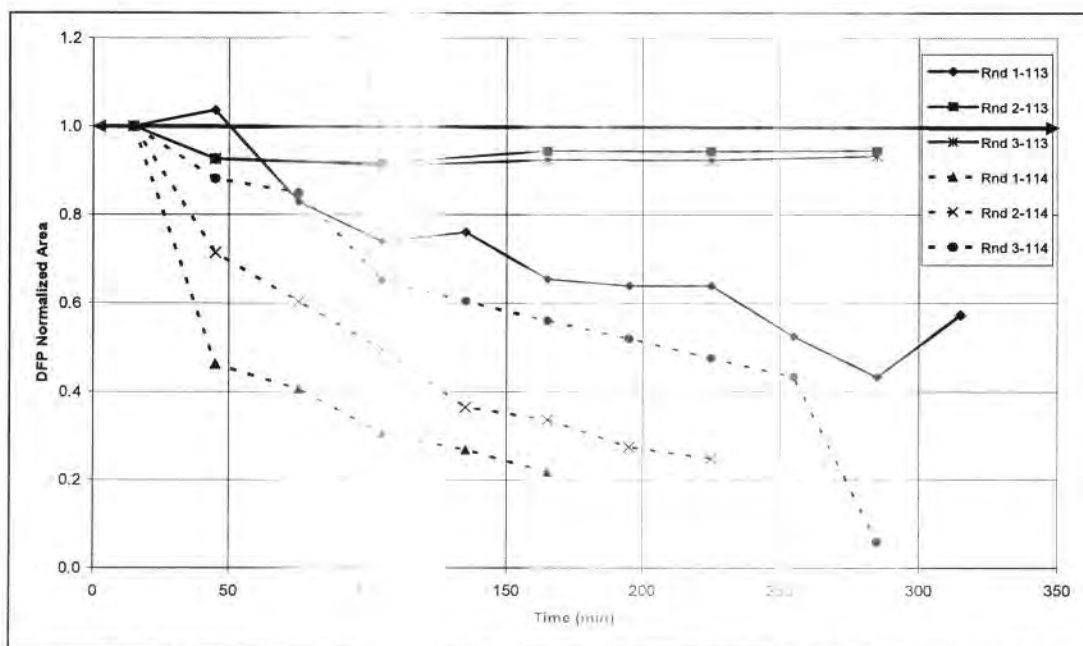


Figure 19: Relative amount of DFP in headspace of designated samples vs. time, as measured by HS-SPME and GC-MS. TNSP 5 (dotted line), and TNSP 5 Control (solid line). Formulations are Waterless, Hydrophobic Poly in Dipropylene Glycol Dibenzate Emollient.

Live Agent Neutralization Tests with live CWAs, GD, HD and VX

The purpose of the neutralization testing with live CWAs was to obtain the true neutralization efficacy about TIAX's NSP formulations shown in Table 10. The method for the testing is described below, which occurred under the supervision of the COTR at USAMRICD.

Methods:

A "test tube" methodology was utilized in which the designated formulation (TNSP1, 2, 3, 4 or 5) was mixed with the test agents (GD, VX or HD) and the headspace was monitored for the presence of the agent. Sampling of the headspace occurred after 40 minutes of equilibration and 60 minutes of absorption time. The amount of agent left in the headspace was then compared to that left in the headspace of the corresponding control. Each formulation and control experiment was analyzed in triplicate. The final methodology was reviewed and agreed upon by the COTR before testing began.

The results are summarized in Table 11 below, and are partially consistent with our testing for DFP, but not for CEES. Specifically, TNSP1 and TNSP2 both absorbed the GD in similar fashion to its analogue DFP; however, TNSP1 and TNSP2 were not able to absorb HD or VX, showing inconsistent results when compared to our simulants. However TNSP1 and TNSP2 seem to be the most promising and their formulations may have to be modified in order to see HD and VX neutralization.

Table 11: Each value indicates the chemical agent peak area in the headspace after 100 minutes equilibration and absorption by the TNSP containing the active or control.

	GD Peak Area		HD Peak Area		VX Peak Area	
	<i>Active</i>	<i>Control</i>	<i>Active</i>	<i>Control</i>	<i>Active</i>	<i>Control</i>
TNSP1	4.92×10^4 ($\pm 1.44 \times 10^4$)	4.59×10^7 ($\pm 1.08 \times 10^7$)	1.11×10^7 ($\pm 0.08 \times 10^7$)	7.78×10^6 ($\pm 0.81 \times 10^6$)	6.31×10^6 ($\pm 2.68 \times 10^6$)	1.55×10^7 ($\pm 3.93 \times 10^6$)
TNSP2	4.64×10^4 ($\pm 6.54 \times 10^4$)	5.30×10^7 ($\pm 0.35 \times 10^7$)	1.33×10^7 ($\pm 0.20 \times 10^7$)	7.31×10^6 ($\pm 1.99 \times 10^6$)	4.89×10^6 ($\pm 5.04 \times 10^5$)	3.80×10^6 ($\pm 2.90 \times 10^6$)
TNSP3	3.05×10^7 ($\pm 1.85 \times 10^7$)	5.01×10^7 ($\pm 1.58 \times 10^7$)	8.23×10^9 ($\pm 0.14 \times 10^9$)	6.39×10^9 ($\pm 0.10 \times 10^9$)	4.19×10^6 ($\pm 3.85 \times 10^6$)	1.93×10^6 ($\pm 3.73 \times 10^6$)
TNSP4	2.09×10^7 ($\pm 1.48 \times 10^7$)		8.47×10^6 ($\pm 0.34 \times 10^6$)		4.42×10^6 ($\pm 1.74 \times 10^6$)	
TNSP5	6.67×10^6 ($\pm 0.99 \times 10^6$)	4.77×10^7 ($\pm 0.25 \times 10^7$)	7.57×10^6 ($\pm 0.86 \times 10^6$)	6.38×10^6 ($\pm 1.47 \times 10^5$)	1.26×10^6 ($\pm 1.98 \times 10^5$)	1.76×10^6 ($\pm 2.36 \times 10^5$)

2.5 Task 5: Program Communication and Reporting**Objectives**

- Monthly Reports/Teleconferences
- Final Report

Summary of Task 5

During the period covered in this final report, we have communicated with the COR through monthly reports, informal teleconferences, and emails. All teleconferences were summarized and reported in emails to the COR and subsequent monthly reports.

The deliverables for Task 5 were monthly status reports, a Phase II annual report and this final report, detailing the activities and results of Phase II.

2.6 Task 6: Finalize Phase II Commercialization Partner

Below, we highlight the commercialization partner(s) with whom we discussed commercializing our technology.

Objectives

- Discussions with Previously Identified Commercialization Partners
- Down-select from Potential Commercialization Partners
- Develop Plan for Regulatory Issues, Manufacturing, Pricing, and Marketing the Product

Summary of Task 6

Final Identification of our Technology Transformation Partner

1. Technology Transformation TIAX LLC is a collaborative technology development firm that accelerates innovation to help customers create an impact in the marketplace. We position us to address the interface between research labs and universities, private-sector "implementation" of government S&T, such as the

Technology Transformation Partner - Definition

Technology development firm that accelerates innovation to help customers create an impact in the marketplace. Our combined scientific/technical and business expertise uniquely address a long-standing, highly problematic gap that exists between sources of ideas, such as research labs and universities, private-sector manufacturers that would deliver them to market. This emergent technology development program is analogous to the "valley of death" that persists between research and development, government S&T, and the acquisition community.

Our products are partial technologies. We typically develop these kernel technologies and achieve market impact via "Technology Transformation" partnerships including:

Our products are partial technologies (called "kernels") organized around several platforms. We typically develop these kernel technologies and achieve market impact via "Technology Transformation" partnerships – multifaceted business arrangements

- o **Technology Transfer**: Transfer of technology rights to our partners for an up-front license fee, plus a tapering royalty fee.
- o **Implementation Services**: Our expert team collaborates with our commercialization partner's R&D team to transform our technology into marketable products, and enable our partner's team to continue moving forward independently.
- o **Ongoing Upgrades** (as needed): TIAX continues active work in the technology area, and provides general updates and improvements to the technologies transferred, for a fixed annual fee.

Our products are partial technologies (called "kernels") organized around several platforms. We typically develop these kernel technologies and achieve market impact via "Technology Transformation" partnerships – multifaceted business arrangements

This is typically not a one-time licensing and services revenue deal; it is an ongoing relationship from which TIAX derives revenue. Our customers enjoy faster time to market with superior products – a key enabler of growth and economic benefits in their communities. Two successful examples of TIAX Technology Transformation agreements include:

Our products are partial technologies (called "kernels") organized around several platforms. We typically develop these kernel technologies and achieve market impact via "Technology Transformation" partnerships – multifaceted business arrangements

- o TIAX licensed its Integrated Aircrew Flight Equipment (IAFE) technology (originally developed under Phase I and II SBIR grants) to two, world-class aircrew flight equipment companies—Mustang Survival and RFD Beaufort, who are teaming to develop a current IAFE contract for the U.S. Air Force.
- o TIAX has developed and commercialized advanced lithium ion battery technologies to several major international firms.

Our products are partial technologies (called "kernels") organized around several platforms. We typically develop these kernel technologies and achieve market impact via "Technology Transformation" partnerships – multifaceted business arrangements

We consider the NSP as a key enabler of growth and economic benefits in their communities. Two successful examples of TIAX Technology Transformation agreements include:

Our products are partial technologies (called "kernels") organized around several platforms. We typically develop these kernel technologies and achieve market impact via "Technology Transformation" partnerships – multifaceted business arrangements

2. Description of Process

Identification of Technology Transformation Partner

Prior to the start of the Phase II program, we identified two potential candidates for our Technology Transformation partner: Procter & Gamble (Cincinnati, OH), a \$MM consumer products company and Croda (Edison, NJ) a leading supplier of cosmetic raw materials for the Personal Care Industry. We had initial discussions and secured letters of interest from both companies. From our discussions, we learned that Croda was interested in the possibility of helping to commercialize the neutralizing skin protectant based on a Croda ingredient, Incroquat QLC. P&G expressed interest in collaborative development of the skin protectant platform for personal care applications, such as insect repellent. Later in the course of Phase II, Reckitt-Benckiser, another \$MM consumer products company also expressed interest in the platform technology. Summaries of meetings with P&G, Croda, and Reckitt-Benckiser can be found in previous monthly reports.

As we moved further into the program and as a result of meetings with our potential partners, our understanding of what would constitute an ideal Technology Transformation partner evolved. TIAX's baseline strategy was to team with Croda on the commercialization of the neutralizing skin protectant for the military and first responder markets. Croda's size, market presence in skin care ingredients, and existing manufacturing and distribution channels made them an attractive partner initially. However, one disadvantage of working with Croda was the company's lack of interest or presence in military markets. Thus, we have now shifted towards partners who have a greater financial interest in commercialization of the product of immediate interest to the military. We believe such a partner will be more motivated help us push the project forward through Phase III commercialization, as well as providing the benefit of a military market presence.

In Oct '07, we attended the National Defense Industry Association (NDIA) Chemical & Biological Decontamination and Protection Conference and Exhibition in Virginia Beach, VA, and presented a poster "Development of a Neutralizing Skin Protectant" on the NSP and proposed commercialization path. (We attended the conference at no cost to the government). Our purpose in attending was to raise awareness of the SBIR program and interest potential commercial and government partners in funding the testing of the final prototypes for efficacy against CWAs using animal models. During this meeting, two companies expressed interest in NSP; Steris Corp., and EZ-EM, Inc. EZ-EM is a contract pharmaceutical manufacturer who currently makes and sells RSDL, the existing post-exposure skin decontamination product. Steris manufactures a wide variety of sterilization products; they also have a line of skin decontamination products which they'd like to extend. Both companies expressed interest in having further discussions with us, and in helping to commercialize the NSP via licensing the technology from us. Steris expressed interest in possibly funding the live agent testing with animals at the end of the Phase II SBIR program if the results of our testing with chemical agent surrogates were promising.

On 19 Dec 07, we met with representatives from Steris Corp. at TIAX's facility, including Tim Giddens, P.E., Director of Strategic Technology Enterprises, Inc. (Steris), Dr. Ian McCreary, Program Manager, Defense and Industrial group, and Dr. Dan Klein, project leader on Steris' Personnel Decontamination projects within the Defense and Industrial group. Our objective was first and foremost to learn more about each other's companies, and more specifically how the NSP would fit Steris' overall product portfolio. As we did not have an NDA in place we did not discuss specific details of the technology. We agreed that TIAX would contact Steris with a non-disclosure agreement when we have data that we are ready to share. However, our initial discussions were very encouraging in the sense of Steris' strong interest in the NSP technology and apparent fit with a growth area of their business.

3. Description of Criteria for Selection of Technology Transformation Partner

In our Phase II SBIR proposal, we described an initial list of criteria that would be important in choosing our Technology Transformation partner. Because TIAX is a technology development company, and not a manufacturing nor distribution company, key among these criteria will be that the partner has the interest and capability to collaborate with us in Phase III as we work towards the final formulation that optimizes efficacy, safety, cost, and usability. We have now updated our initial key criteria:

- o Established manufacturing capability for skin care products
- o Financial stability and capacity to bring NSP to market
- o Experience with regulatory agencies/processes, especially FDA
- o Experience supplying military markets

SBIR Phase II Final Report

Contract # W81XWH-05-C-0131

- o Established channels to
- o US-based operations
- o Represents a strategic

nd global markets.

A area for the partner

We believe that Steris meets all qualifications to be our preferred representative from the company forward to learning any additional missed.

the criteria outlined above. Below is a detailed description of Steris' Technology Transformation partner, based on our discussions with as well as publicly available information (www.steris.com). We look for the criteria the Army TPOC believes are important that we might have

Overview – Steris Corporation

A \$1.2 billion business headquartered around the world to prevent infection of sterility are required to ensure pharmaceutical manufacturing environments.

In Mentor, OH, Steris develops and creates products that are used and contamination in critical environments where the highest levels of successful outcomes. These include hospitals, outpatient clinics, pharmaceutical medical device, research labs and other industrial

Since Steris was involved in this area for the company has been in this area currently is based on developed in cooperation with the chemical and biological warfare in the area of biological and chemical steam sterilization systems, bio

in a DPC mail facility after the anthrax scare in 2003, a key growth product for chemical and biological defense. Steris' main product is a hydrogen peroxide (VHP) decontamination technology, Army Edgewood Chemical Biological Center for use against biological in buildings, aircraft and other environments. Additional products include Steris' Spor-Klenz® cold sterilant, chemical indicators, and anti-microbial skin care solutions.

Technology Transformation**a. Established manufacturing**

Steris has the chemical formula development as well as the manufacturing a variety of skin care and sterilization facilities are either

Key Criteria**Ability for skin care products**

testing and manufacturing expertise relevant to the advanced manufacturing of the NSP. They currently develop, manufacture, market, and global solutions. All of the Company's manufacturing and contract facilities are ISO 9000 or ISO 13485:2003 certified, at a minimum.

Steris' skin care product categories

- o Alcohol Hand rinses and
- o Body Wash and Shampoo
- o High Risk Hand washing
- o Incontinence Products
- o Lotions and Conditioners
- o Routine Skin Care
- o Surgical Scrubs
- o Acute-Kare® Healthcare

currently includes:

Acute-Kare Antiseptic Hand rub

Specific examples of Steris' der

- o Alcare Plus® Antiseptic
- o Bactoshield® CHG 2%
- o CV® Medicated Lotion
- o Medicated Soft N Sure
- o Prima-Kare® 0.75% Chlor
- o Septisol® NPD with Tri

dermatology-related skin care products include:

Acute-Kare Emollients

Acute-Kare Skin Cleanser

Acute-Kare Personnel Hand Wash

b. Financial stability and cap

Steris is a \$1.2 billion company experienced similar growth in product sales dates back to the founding of the innovator of sterilization products in countries.

growing NSP to market

achieved revenue growth of 4-6% in fiscal 2008. It has

While the Corporation was founded in 1987, Steris' history

Steris Company in 1894, a long-time, globally leading

employs 5,100 people, with representation in more than 60

SBIR Phase II Final Report

Contract # W81XWH-05-C-0131

Steris' key business areas are healthcare (~70%), life sciences (~20%), and sterilization services (~10%). The bulk of their revenues are derived from the pharmaceutical industries. These markets are driven by the aging of the population and an increasing number of individuals are now entering their prime health years. Other factors favorably influencing the Steris' financial stability include increasing hospital-acquired infections around the world. Finally, infection-control is a global concern, and emerging threats have gained prominence in the past few years. Steris has new opportunities to adapt their VHP technologies to meet the needs of biodefense, aerospace, and industrial decontamination. The company's long-term strategy to continue to innovate in research and development as part of their long-term strategy to continue to innovate. In 2007, 2006, and 2005, research and development expenses were \$1.1 million, \$1.0 million, and \$0.9 million, respectively, primarily incurred for the research and development of new products. Based on past and recent performance of the company and the emphasis on innovation, it is clear that Steris has the financial stability and capacity to bring NSP to market.

c. Experience with regulatory agencies/processes, especially FDA
Steris has a number of FDA approved products, and has considerable experience navigating through the US and international regulatory processes. Two recent examples are highlighted below:

1. Reliance™ Endoscope Processing System. In July 2006, Steris introduced the Reliance™ Endoscope Processing System. This product, available in Canada, Australia and parts of Europe, meets a significant unmet need for high-level disinfection capability in gastrointestinal suites at hospitals.

Other products for which Steris has obtained FDA approval to market include the Amsco Millennium Steam Sterilizer; Amsco V-PRO™ Low Temperature phase hydrogen peroxide sterilizer; SparView PA Culture Set, Castlog Indicator Kit, and VERIFY® SYSTEM 1 Biological Monitoring Kit Versi indicators; HERMES® O.R. Control Center, a laparoscope for use in gynecology; Vis-U-All Heat Seal Pouch and Tubing, a sterilization wrap.

2. Vaprox® sterilant. The Environmental Protection Agency cleared Vaprox® for expanded commercial use on surfaces in large enclosed areas. Vaprox® is an effective solution for treating patient rooms, ambulances, laboratory rooms, hotel rooms, offices, cruise ships, recreational facilities and more. Steris has also received EPA approval for Spor-Klenz RTU Cold Sterilant and Peroxide 35%.

Steris' regulatory experience with a variety of products will be valuable in the process for NSP.

d. Experience supplying military markets

Steris has a recent and expanding track record of working with the military. In December 2007, the DHS (designated and certified Steris system as a Qualified Anti-Terrorism Technology which is the highest level of recognition under the Support Antiterrorism by Fostering Effective Technologies Act of 2002). In 2003, Steris completed the decontamination of a United States Department of State facility in Sterling, Virginia using the Company's VHP technology, which launched biological defense as a business area.

Other partnerships with U.S. government include the Army and NASA's application of Steris' mVHP technology to new uses. Specific examples include:

Steris' subsidiary, Strategic Technology Enterprises, Inc., was awarded a contract by the Jet Propulsion Laboratory (JPL), a NASA contract laboratory, to conduct research and

biodefense), and healthcare and throughout the world; assumption years. Other factors regarding the level of infection in general are becoming a global concern. Steris is actively pursuing new markets such as biodefense, aerospace, and industrial decontamination. Steris ended March 31, 2007, with \$33.6 million, and \$31.5 million in commercial products. Based on past and recent performance, it is clear that

the following products are highlighted below:

approval from the FDA to market the Reliance™ Endoscope Processing System. This product, available in Canada, Australia and parts of Europe, meets a significant unmet need for high-level disinfection capability in gastrointestinal suites at hospitals.

Other products for which Steris has obtained FDA approval to market include the Amsco Millennium Steam Sterilizer; Amsco V-PRO™ Low Temperature phase hydrogen peroxide sterilizer; SparView PA Culture Set, Castlog Indicator Kit, and VERIFY® SYSTEM 1 Biological Monitoring Kit Versi indicators; HERMES® O.R. Control Center, a laparoscope for use in gynecology; Vis-U-All Heat Seal Pouch and Tubing, a sterilization wrap.

Vaprox® sterilant in November 2007. Vaprox® can now be sold as an effective solution for treating patient rooms, ambulances, laboratory rooms, hotel rooms, offices, cruise ships, recreational facilities and more. Steris has also received EPA approval for Spor-Klenz RTU Cold Sterilant and Peroxide 35%.

Steris' regulatory experience with a variety of products will be valuable in the process for NSP.

Steris has a recent and expanding track record of working with the military. In December 2007, the DHS (designated and certified Steris system as a Qualified Anti-Terrorism Technology which is the highest level of recognition under the Support Antiterrorism by Fostering Effective Technologies Act of 2002). In 2003, Steris completed the decontamination of a United States Department of State facility in Sterling, Virginia using the Company's VHP technology, which launched biological defense as a business area.

Other partnerships with U.S. government include the Army and NASA's application of Steris' mVHP technology to new uses. Specific examples include:

Steris' subsidiary, Strategic Technology Enterprises, Inc., was awarded a contract by the Jet Propulsion Laboratory (JPL), a NASA contract laboratory, to conduct research and

and certify a Steris patented planetary sterilization technology for application in the sterilization of robotic planetary spacecraft systems and sub-systems. JPL is pursuing this certification to meet NASA's sterility requirements on future space exploration missions.

In 2004, Steris demonstrated its modified vapor-phased mVHP®/Vaprox® technology was effective at inactivating both chemical and biological agents. The research and development effort was conducted jointly by the U.S. Army Edgewood Chemical and Biological Center (ECBC) and Steris Corporation's subsidiary, Strategic Technologies, Inc., as part of an ongoing cooperative research and development agreement that was initiated in July 2002 to evaluate, optimize, and modify Steris technologies for use against chemical and biological warfare agents. ECBC provided chemical activation facilities for conducting the research.

e. Established channels to US and global markets

Steris currently has approximately 5,100 employees worldwide, with production/manufacturing operations in the United States, Canada, and Europe, including the United Kingdom, France, Mexico and Switzerland. They have sales offices in 17 countries with 2,300 direct sales, service and field support worldwide. Sales and service activities are supported by a staff of regionally based clinical specialists, system planners, corporate account managers, and in-house customer service and field support departments. Dealers represent Steris' products in more than 60 countries. International revenues were \$263.9 million, or 22.0%, of our total revenues for the year ended March 31, 2007. Revenues from Europe, Canada, and other international locations were 55.3%, 2.5%, and 21.1%, respectively, of total international revenues for the year ended March 31, 2007. Clearly, then, Steris possesses the channels to market that are desirable for the successful marketing and sales of the NSP both in the US and eventually, internationally.

f. US based operations

Steris is US-based, with headquarters in Mentor, Ohio. Its skin decontamination product development capabilities are mainly based in St. Louis, MO (about 260 people).

g. Represents a strategic opportunity for the partner

Representatives from Steris indicated that they envision the NSP technology as extending their line of products to include decontamination of chemical threats as well. They would like to enter the market with a product containing both biological and chemical neutralization functionality. Eventually Steris would like to come up with a product that is effective against C/BWA as well as standard infectious bacteria, e.g. MRSA, influenza, etc. The Steris representatives we met with would be interested in testing the NSP technology to see if it has any efficacy against hospital infectants, in addition to chemical decontamination functionality.

4. Next Steps with Technology Transformation Partner, Steris

We had originally anticipated a collaboration with our commercialization partner in Phase II. However, because of the delay in the live agent testing, we did not feel we had the necessary data to enter an agreement, and we anticipated we would have it only at the end of the Phase II program. Given the disappointing results from the live agent testing, we do not plan to pursue this further at this time.

3.0 Key Research Accomplishments

- Compiled physiochemical data/properties of PEI for formulation and laboratory studies.
- Identified and obtained 13 different potential diffusion-inhibitors from the literature and platelets.
- Assessed compatibility of key active PEI and diffusion-inhibitors in laboratory and paper studies.
- Developed preferred list of emollients based on solubility parameters to identify candidates most compatible with surrogates and agents.
- Identified best formulation vehicles for the skin protectant, based on compatibility with actives/excipients, anticipated diffusion, and laboratory testing.
- Developed base (non-active) formulations for vehicles of interest including "two-clay" W/O, O/W, and waterless ointment types.
- Developed processing protocol for formulation vehicles of interest including "two-clay" W/O, and O/W, and waterless ointment types.
- Developed active formulations and processing method for vehicles of interest, including "two-clay" W/O, O/W and waterless ointment types.
- Developed *in vitro* skin permeation assessment method and protocol.
- Developed HS-SPME method. The method was used to verify that the formulations neutralize chemical warfare agents.
- Identified several NSP formulations (TNSP 1, 2, 3, 4, 5) for testing with CWA surrogates and live agent testing with against CWAs, GD and HD.
- Identified most promising formulation (TNSP 1 and 2) with live agent testing against live CWA agents. Absorption of GD was shown, but not HD or VX.

4.0 Reportable Outcomes

- We filed a provisional patent application in December 2008.

5.0 Conclusion

This work extends earlier work by a series of experiments with Lupasol polyethylenimine (SERPACWA). Consistent with perfluorinated polyether coatings, contamination that penetrates the coating remains unreacted and the agent before it reaches the skin. This is an effective and more com-

patible formulation by USAMRICD (US 2004/0067205). Braue *et al.* conducted a study on the ability of incorporating neutralizing actives (including the active ingredient of the Reduction Paste Against Chemical Warfare Agents (RPACWA)) into polytetrafluoroethylene (PTFE) resins dispersed in a matrix. This provides an occlusive physical barrier to percutaneous contamination. Incorporation of neutralizing actives does increase efficacy of SERPACWA by neutralizing the agent. However, contamination remaining on the surface of the barrier must be removed to both dissolve the CWA challenge and neutralize the agent. This would result in a neutralizing skin protectant that is more effective than SERPACWA, the product currently available to soldiers.

This Phase II SBIR project has demonstrated a skin protectant formulation for protection and decontamination in one step. We developed 1) a skin permeation assay and 2) a skin permeation assay. We then validated this method. We then analyzed analysis issues and the results.

Significant progress towards the ultimate goal of development of a skin protectant for *pre-exposure* protection and *post-exposure* decontamination. We developed 1) a number of prototype formulations (26 total) and 2) a skin permeation assay and protocol using the Franz cell apparatus. We then validated this method. We then analyzed analysis issues and the results.

Two TIAX formulations were tested on HS-SPME/GC-MS for absorption of GD was determined. Absorption of VX nerve agent was determined via *in vitro* neutralization tests.

The most potential for advancing to a final prototype based on the results of the above agent neutralization testing. However, only the results of the above agent neutralization testing will be necessary to show better results. Finally, to show to true efficacy, we need to show proof of efficacy via *in vivo* assessment tests.

6.0 References

Additional references can be found as footnotes within the body of the report.

Braue, E.H. Jr., "Development of a Reactive Topical Skin Protectant," J Appl Polym Sci, 19, S47-53, 1999.

Braue, E.H., Hobson, S.T., Boecker, J.D., Smith, B.M., "Active Ingredients Containing Amines, Polyalkenimines and/or Derivatives," 2004, U.S. Patent Application # 20067205.

Hobson, S. T., Lehnert, E. K., and Braue, E. H. Jr., "The U. S. Army Reactive Topical Skin Protectant (rTSP): Challenges and Successes," MRS Symposium Series C Hybrid Organic-Inorganic Materials [Online], 628, CC10.8.1-CC10.8.8, 2000.

"Incroquat QLC: Quaternized Lipid Conditioner," Croda, Inc. Data Sheet DS-1003.

Information Paper DASG-HCF 20 Feb. 03: Skin Exposure Reduction Paste (SERPACWA). 2003. www.wood.army.mil

"Skin Exposure Paste Indications, Dosage, Stability," www.rxlist.com/cgile/inexpose_ids.html

Vas, G., Vekey, K., "Solid-phase microextraction: a powerful sample preparation tool prior to mass spectrometric analysis" J. Mass Spectrom., 39, 233-254, 2004.

7.0 Appendix

7.1 Head Space Test Procedure

HS-SPME GC-FID Method

Objective:

To validate a HS-SPME method for the determination of surrogate CWAs (DFP and DFP-*d*₅) in water, the concentration of surrogate

Equipment:

- Agilent 6890 GC
- Rtx-5 Capillary GC
- SPME Fiber Holder
- Fiber Assembly – PN 57342-U)
- 4 mL clear glass
- Syringes, 10 uL (1
- Magnetic Stir/Hot
- Magnetic stir bars
- Constant Temper
- Stopwatch
- Analytical Balance
- Spatula

IT IS VERY EASY TO BR
injector port, always ma
vial/injector first if neces

Step 1. Pre-Condition the
0.5 hr at 250 C (Max desc
T794123M

Step 2. Method Validation
GC Conditions:

An SPME specific (narrow injection port. Use pre-cut Note: the maximum temperature should be 10-20 C lower to minimize peak broadening program. Check the liner

Temperature Control:

During extraction, the same steps should be followed to minimize the degradation of the sample. Refer to the manufacturer's MSDS. To prepare the bath, you will need to prepare the bath at one time, you will need to (height) every time when

Samples for Method Var

Use Incroquat QLC/2.5 %
be in lab 15-318. You ma
vials at the beginning of e

Validation and Method Development

method is to be used to verify that sample formulations neutralize headspace above the samples will be monitored for the

1 m x .25 mm x 1 μ m, Restek #10253) or equivalent
for use with manual sampling (Sigma Aldrich PN 57330-U)
3 fiber, SPME fiber assembly, for manual holder (Sigma Aldrich
5 with hole cap, pre-assembled (Sigma Aldrich PN 27136)

Digital thermometer

ER. Especially when injecting the fiber into a vial or the fiber will not hit anything as it extends. Practice outside the

ture is 280C) as prescribed by Sigma-Aldrich Data Sheet

and low bleed septum (thermogreen LB-2) should be installed in the tube (or pre-cut manually). The injection port is 280 C. The final temperature of the oven ramp is 260 C. A low initial temperature (e.g., 40C) will reduce sorption time should be included as part of the oven temperature program. Septa pieces during testing.

ber) is held in a constant temperature bath at 28-30°C, selected to occur at temperatures above 30°C according the temperature should be used in the CEES experiments as well. You will any experiments. Although multiple vials can be stored in the a ring stand to hold the SPME holder device at the same position one particular vial.

X-100, as was used in the previous studies. Both of these should layout the appropriate number of 0.100 g samples in 4 mL SPME step, plus a few extras.

A. Desorption Temperature Selection

We will use the same desorption temperatures as determined in the DFP. 265C for CEES. This is the setting of the injector temperature.

B. Needle Depth Optimization

The depth of the fiber should be adjusted to place it in the center to ensure efficient, reproducible desorption. This parameter is optimized at least three different fiber depths in the GC injector port as the gauge positions. For the GC/MS, positions 2.4, 3.4, and 4.4 (all measured); the optimal position 4.0. At least two replicates should be measured. **positions for the GC-FID will need to be determined prior to as for the GC/MS.** You may want to stick a marked syringe plunger to determine the depth to hit something. Once you know this, determine the depths to use in this study. **We will do this study**

1. Weigh a minimum of nine 100 mg polymer/active samples and label each vial.
2. Allow samples to equilibrate with 28-30 C constant temperature. Longer is okay.
3. Remove a sample from the bath, add a magnetic stir bar, or standard through vial septum, magnetic stir for 5 sec. at setting 2.
4. Using a second syringe, add 0.5 µL surrogate through vial septum, setting 2, return to constant temperature bath. Mark time. Decontaminate.
5. Equilibrate sample in constant temperature bath for 30 min.
6. Set the guide/fiber depth gauge position according to the position.
7. Extract sample headspace by injecting SPME fiber into vial for 1 min.
8. Retract fiber into SPME holder, transfer to GC injector port.
9. Immediately hit start to run GC program: 2.5 min. hold at 400 C. You will need to leave the fiber in the injector for the entire duration.
10. Repeat steps 3-9 until at least 2 points at each depth are measured. Third point for each depth.
11. Integrate peak areas (internal standard and surrogate) using GC/MS.
12. Plot data (Area vs. Fiber Depth Position). Use internal standard to correct for any fluctuation in instrument performance.

B. Fiber Desorption Time Optimization

To determine the optimal desorption for the DFP experiments, we will run at desorption times of 1, 4, and 8 minutes for a sample of 0.10 µg referenced above for the fiber depth measurements (2.5 min). **we determined that the optimal desorption time for DFP was 2.5 min.** For CEES, we determined that the optimal desorption time for DFP was 2.5 min. This optimization will require changing the desorption time. **so it would be a good idea to create multiple method copies ahead of time: CEES_1 min., etc and enter these into the pre-programmed sequence. CEES requires a higher desorption temperature of 265 C and include this in your validation step with both DFP and CEES.**

1. Weigh nine (x 2 surrogates) 100 mg polymer/active samples in vials and label each vial.
2. Allow samples to equilibrate with 28-30 C constant temperature. Longer is okay.
3. Remove a sample from the bath, add a magnetic stir bar, use standard through vial septum, magnetic stir for 5 sec. at setting 2.
4. Using a second syringe, add 0.5 µL surrogate (DFP or CEES), 5 seconds at setting 2, return to constant temperature bath. Mark time.

GC work: 250C for

one of the GC to
the GC response for
guide/fiber depth
(of the o-ring) were
position. **Reasonable
may not be the same
injection port to
the extended fiber to**

ce vials. Cap and

of 30 minutes.

0.5 µL internal

5 seconds at

desired setting.
temperature bath) for 2.5

0 C, hold 1 min.

of scatter, do a

g method.
correct for any

made (in triplicate)
same conditions
GC/MS studies,
required a longer
(initial hold time),
DFP_4 min,
at CEES requires a
ed to do this

space vials. Cap and

of 30 minutes.

internal standard

magnetic stir for 5
syringe.

5. Equilibrate sample in constant temperature bath for 15 min.
6. Extract sample headspace using SPME fiber into vial (still in constant temperature bath) for 2.5 min.
7. Retract fiber into SPME vial and insert into GC injector port.
8. Immediately hit start button and wait 1, 4, or 8 min. hold at 40C, ramp 10C/min. to 150 C, hold 1 min. in injector for the entire desorption time.
9. Repeat steps 3-8 until 10 measurements are made. Peak areas at desorption time are measured.
10. Integrate peak areas for DFP and surrogate) using automated processing method.
11. Plot data (Area vs. Desorption time) for each surrogate. Use internal standard peak areas to correct for any fluctuation in instrument response.

C. Extraction Time Optimization

The extraction time is the time the SPME fiber is exposed to the sample; increasing the time of extraction therefore increases the amount of chemical absorbed by the fiber coating. As extraction time increases, an "equilibrium" state is reached where a small variation in extraction time does not result in a large variation in GC response. The extraction time for quantitative measurements will therefore be at shortest possible time after which equilibrium is reached. This was 15 minutes for both DFP and CEES in the presence of neutralizing agents. An extraction time profile is obtained by making a series of measurements with increasing extraction times over a period of time, using the optimized desorption time and fiber response determined previously for each surrogate. This validation step only needs to be done with 1 surrogate.

1. Weigh at least eight identical samples into tared 4 mL headspace vials, Cap and label each vial.
2. Allow samples to equilibrate in constant temperature bath for a minimum of 30 minutes. Longer is okay.
3. Remove a sample from bath using syringe, add 0.5 µL internal standard through vial septum, magnetic stir for 5 seconds.
4. Using a second syringe, add 0.5 µL surrogate (DFP) through vial septum, magnetic stir for 5 seconds at setting 2. Mark time. Decontaminate syringe.
5. Equilibrate sample in constant temperature bath for 15 min.
6. Extract sample headspace using SPME fiber into vial (still in constant temperature bath) for 0.5, 1, 2, 4, 8, 15, 20, or 25 min.
7. Retract fiber into SPME vial and insert into GC injector port.
8. Immediately hit start button and wait 2.5 min. hold at 40C, ramp 10C/min. to 150 C, hold 1 min. in injector for the entire desorption time of 2.5 min.
9. Repeat steps 3-8 until 10 measurements are made. Peak areas for DFP and surrogate) using automated processing method.
10. Integrate peak areas for DFP and surrogate) using automated processing method.
11. Plot data (Area vs. Desorption time) for each surrogate. Use internal standard peak areas to correct for any fluctuation in instrument response.

7.2 Proof of Neutralization

Objective:

Verify that sample formulations neutralize the surrogate CWAs (DFP and CEES) using the Headspace Solid Phase Micro-Extraction (HS-SPME) method.

1. Compare neutralizing efficacy of neutralizing agents.
2. Compare neutralizing efficacy of neutralizing agents.

Efficacy is determined by the amount of surrogate CWA in the headspace of the sample. An initial measurement of the surrogate concentration is taken at a specified time, followed by one or more subsequent measurements at increasing time points.

HS-SPME Method Protocol

Collect surrogate CWAs (DFP and CEES) using the Headspace Solid Phase Micro-Extraction (HS-SPME) method to collect the surrogates in headspace above the samples.

Compare the neutralizing active to identical formulations containing no neutralizing agent to determine increased efficacy relative to control. Compare each other for relative neutralizing efficacy.

Measure the surrogate at a certain time point (or time points) relative to the initial measurement of the surrogate concentration in the headspace of the sample. An initial measurement of the surrogate concentration is taken at a specified time, followed by one or more subsequent measurements at increasing time points.

Note: Since all of the formulations will have water in them, the "control" concentration level of surrogate. This is okay as long as the control and

are reproducible.

Equipment:

- Thermoelectron Trace GC/Trace MS system
- Rtx -5 Capillary GC column (30 m x .25 mm x 1 μ m, Restek)
- SPME Fiber Holder, 23 gauge, for use with manual sample
- Fiber Assembly – 100 μ m PDMS fiber, SPME fiber assembly, Aldrich PN 57342-U)
- 4 mL clear glass screw top vials with hole cap, pre-assembled
- Syringes, 1 μ L, 10 μ L (Hamilton)
- Magnetic Stir/Hot Plate (Corning)
- Constant Temperature Bath, Digital thermometer
- Stopwatch
- Analytical Balance
- Spatula

polyvalent
PN 57330-U)
holder (Sigma Aldrich
Aldrich PN 27136)

IT IS VERY EASY TO BREAK THE FIBER. Especially when injecting, always make sure the fiber will not hit anything as it extends. If necessary,

vial or the injector port,
hold the vial/injector first

Step 1. Pre-Condition the Fiber

0.5 hr at 250 C (Max desorption temperature is 280C) as prescribed T794123M

Aldrich Data Sheet

Step 2. Method Validation

GC Conditions:

An SPME specific (narrow bore) liner and low bleed septum (thermo) injection port. Use pre-cut septa if available (or pre-cut manually).

Note: the maximum temperature of the injection port is 280 C. The temperature should be 10-20 C lower than the max. fiber temperature. A low initial temperature broadening. The fiber desorption time should be included as part of the temperature program. Check the liner frequently for septa pieces during testing.

should be installed in the
temperature of the oven ramp
temperature will minimize peak
temperature program.

Temperature Control:

During extraction, the sample (and the fiber) is held in a constant temperature to minimize the degradation of DFP, which occurs at temperatures above 280C. The same temperature should be used in the CEES experiments. The bath prior to starting any experiments. Although multiple vials can be used, you will need to rig up a ring stand to hold the SPME holder device. Check the bath temperature every time when you are extracting one particular vial.

at 28-30C, selected to
the manufacturer's
You will need to prepare
in the bath at one time,
position (height) every

Samples for Method Validation:

Use Incroquat QLC/2.5 % (by wt.) Triton X-100, as was used in the lab 15-318. You may want to weigh out the appropriate number of vials at the beginning of each validation step, plus a few extras.

Both of these should
samples in 4 mL SPME

A. Desorption Temperature Selection

We will use the same desorption temperatures as determined in the DFP. 265C for CEES. The maximum temperature for the 100 μ m PL

PME work; 250C for
are using is 280C.

B. Needle Depth Optimization

The depth of the fiber should be adjusted to place it in the center of the injection zone of the GC to ensure efficient, reproducible desorption. A schematic of an HS-SPME

injection zone of the GC to
is shown below. This

ing the GC response for at least three different fiber depths in the GC
dle gauge/fiber depth gauge positions. For the GC/MS, positions 2.4,
tion (the o-ring) were measured; the optimal position 4.0. At least two
position. **Reasonable positions for the GC-FID will need to be**
they may not be the same as for the GC/MS. You may want to stick a
GC-FID injection port to determine the depth to hit something. Once you
of the extended fiber to determine the depths to use in this study. **We**

- (s) into tared 4 mL headspace vial, add Teflon-coated stir-bar,
 with 28-30 °C constant temperature bath for a minimum of 30 minutes.
 Using a syringe add 0.5 µL internal standard through vial septum,
 stir surrogate through vial septum, magnetic stir for 5 second at setting
 bath. Park time. Decontaminate syringe.
 temperature bath for 30 min.
 position according to the position of the o-ring to the desired setting.
 Injecting SPME fiber into vial (still in constant temperature bath) for 2.5
 transfer to GC injector port.
 program: 2.5 min. hold at 40°C, ramp 10°C/min. to 150 °C, hold 1 min.
 2 points at each depth are measured. If there is a lot of scatter, do a
 standard and surrogate) using automated processing method.
 (Position). Use internal standard peak areas to correct for any
 loss.

77

In the DFP experiments, measurements will be made (in triplicate) at 1 minute for a sample of 0.100 g sample under the same conditions as the GC/MS studies (with measurements (2.5 minute extraction time)). For the GC/MS studies, sorption time for DFP was 2.5 minutes, while CEES required a longer sorption time. You will require changing the GC oven program (initial hold time at 60 °C). Create multiple method ahead of time, DFP_1 min, DFP_4 min, etc., and include them in your methods. Remember that CEES requires a 265 °C initial hold and include this in your methods. We will need to do this

- 1) into tared 4 mL headspace vial, add Teflon-coated stir-bar, 2) constant temperature bath for a minimum of 30 minutes. 3) syringe add 0.5 µL internal standard through vial septum, 4) purge (DFP or CEES) through vial septum, magnetic stir for 5 minutes, 5) constant temperature bath. Mark time. Decontaminate syringe, 6) constant temperature bath for 15 min. 7) SPME fiber into vial (still in constant temperature bath) for 2.5 minutes. 8) remove fiber to GC injector port. 9) 1, 4, or 8 min. hold at 40°C, ramp 10°C/min. to 150°C, hold 1 minute. 10) desorption time are measured. 11) (and surrogate) using automated processing method.

11. Plot data (Area vs. Desorption Time) for each surrogate, use internal peak areas to correct for any fluctuation in instrument performance.

C. Extraction time optimization

The extraction time is the period that the fiber is exposed to the sample, therefore increases the amount of analyte absorbed by the fiber coat. An "equilibrium" state is reached at which a small variation in extraction time results in a large variation in GC response. The most desirable extraction time for quantitative analysis will therefore be at shortest possible extraction time after which equilibrium is reached. For DFP and CEES in the previous GC/MS studies. An extraction time protocol of measurements with progressively longer extraction times over a period of 30 minutes and fiber position determined previously for each surrogate needs to be done with DFP.

1. Weigh 100 mg polymer/active sample(s) into tared 4 mL headspace vial and label the vial.
2. Allow samples to equilibrate with 28-30 C constant temperature bath. Longer is okay.
3. Remove a sample from the bath, using syringe add 0.5 µL internal standard through vial septum, magnetic stir for 5 sec. at setting 2.
4. Using second syringe, add 0.5 µL surrogate (DFP) through vial septum, setting 2, return to constant temperature bath. Mark time. Decontaminate syringe.
5. Equilibrate sample in constant temperature bath for 15 min.
6. Extract sample headspace by injecting SPME fiber into vial (still in bath) for 0.5, 1, 2, 4, 8, 15, 20, or 25 minutes.
7. Retract fiber into SPME holder, transfer to GC injector port.
8. Immediately hit start to run GC program: 2.5 min. hold at 40C, ramp to 250C, hold 1 min.
9. Integrate peak areas (internal standard and surrogate) using auto method.
10. Plot data (Area vs. Extraction Time) for each surrogate. Use internal peak areas to correct for any fluctuation in instrument performance.

7.3 Skin Barrier GC/MS Standard Operating Procedure.

Surrogate Neutralization Testing GC/MS HS-SPME Method Protocol

1. Weigh 100 mg polymer/active sample(s) into tared 4 mL headspace vial and label the vial.
2. Allow samples to equilibrate with 28-30 C constant temperature bath. Longer is okay.
3. Remove a sample from the bath, using syringe add 0.5 µL internal standard through vial septum, magnetic stir for 5 sec. at setting 2.
4. Using second syringe, add 0.5 µL surrogate (DFP or CEES) through vial septum, setting 2, return to constant temperature bath. Mark time.
5. Equilibrate sample in constant temperature bath for 15 min.
6. Extract sample headspace by injecting SPME fiber into vial (still in bath) for 5, 10, 15, 20, or 25 min.
7. Retract fiber into SPME holder, transfer to GC injector port.
8. Immediately hit start to run GC program: Hold at 35C, ramp to 250C, hold 3 min. for DFP.
9. Repeat steps 6-8 every 30 or 60 min until surrogate falls below detection limit after at least 3 hours.
10. Repeat steps 3-8 until at least 3 points at desorption time.
11. Identify peaks using their mass spectrum data.
12. Integrate peak areas (internal standard and surrogate) using auto method.

internal peak areas to correct

time of extraction
time increases, an
in a large
points will therefore
minutes for both
making a series
the optimized
ation step only

T
coated stir-bar,
30 minutes.
al septum,
for 5 second at
bath) for 0.5,
hold 1 min.
method.
areas to correct

coated stir-bar,
30 minutes.
standard through
magnetic stir for 5
age.
bath) for 5
min. for CEES,
peak area or
method.

SBIR Phase II Final Report

Contract # W81XWH-05-C-0131

13. Plot data (Area vs. Desorption) for any fluctuation in instrument response.

7.4 Summary of NSP Preparation

Summary: 2- Clay System, C

Procedure:

Phase A (Oil)

Material
Q-90 Bentonite
C12-15-Alkyl
Ethanol

Add Alkyl Benzoates (solvent) for 5 minutes at 1100 rpm. Add

Phase B (Water)

Material
Distilled water
Bentonite

Add hydrophilic clay to stirring

Cool Phase B to room temperature stirring at 1100 rpm. Leave to cool at room temperature.

Results:

A thick, creamy dispersion

Summary: 2- Clay System, B

Procedure: Prepare Phase A

Phase A (Oil)

Material
Q-90 Bentonite
C12-15-Alkyl
Ethanol

Add Alkyl Benzoates (solvent) speed=20. Mix for 5 minutes.

Phase B (Water)

Material
Distilled water
PEI (Lupine)

Combine ingredients

Phase C (Clay)

M
D
B

Add hydrophilic clay to stirring

for each surrogate. Use internal standard peak areas to correct for any fluctuation in instrument response.

Procedures and Results

TNSP 1 Control

LBN: 357-106/ 419-27

Alkyl Benzoate Emollient Control

	Weight Percent (%)	Mass (g)
	5	15.0
	30	90.0
	2.5	7.5

beaker. Slowly add organoclay to solvent vortex (speed =20). Mix and mix for an additional 5 minutes at 1100 rpm.

	Weight Percent (%)	Mass (g)
	60	180.0
	2.5	7.5

er vortex. Mix for 45 minutes at 1100 rpm.

Phase A to Phase B while stirring. Heat mixture to 75°C while stirring at 1100 rpm and 75°C for 20 minutes. Remove from vortex and leave

TNSP 1

LBN: 357-107/ 419-26

Alkyl Benzoate Emollient, 15% PEI Active

Formulation made first. B+C were made on 10/4/11.

	Weight Percent (%)	Mass (g)
	5	15.0
	30	90.0
	2.5	7.5

beaker. Slowly add organoclay to stirring solvent vortex at 1100 rpm. Add ethanol and mix for an additional 5 minutes at 1100 rpm.

	Weight Percent (%)	Mass (g)
	15	45.1
	15	47.1

	Weight Percent (%)	Mass (g)
	30	90.0
	2.5	7.5

er vortex. Mix for 10 minutes at 1100 rpm.

SBIR Phase II Final Report

Add Phase B very slowly (drop wise) to Phase C while mixing vigorously for 5 minutes.

Let B+C cool in air. Once the temperature cools to 25°C, slowly add Phase A and stir for 5 minutes.

Results:

A thick, tan, creamy dispersion with no separation.

TNSP 2 Control
LBN: 357-111/ 419-25

Summary: 2- Clay System, Oil in Water, Dipropylene Glycol Benzoate

Procedure: Prepare "organoclay activator" comprising 95% propylene glycol and 5% DI water. Make only enough for this trial.

Phase A (Oil)

Material	Weight Percent (%)
Stearalkonium bentonite	3
Dipropylene Glycol Dibenzoate	45
Propylene carbonate/Water	2

Add Dipropylene glycol dibenzoate to metal beaker. Slowly add organoclay activator. Mix for 5 minutes at 1100 rpm (speed =26). Add propylene carbonate/water and mix for an additional 5 minutes at 1100 rpm.

Phase C (Clay/Water)

Material	Weight Percent
Distilled water	46
Bentonite clay	4

Phase C: Add hydrophilic clay to stirring 75°C water vortex. Mix for 5 minutes.

Add Phase A to Phase C while stirring at 1100rpm; mix at high speed for 5 minutes. Remove from heat and let cool at room temperature.

Results:

A very thick, off-white creamy dispersion with an airy texture.

TNSP 2
LBN: 357-112/ 419-28

Summary: 2- Clay System, Oil in Water, Dipropylene Glycol Benzoate

Procedure: Prepare "organoclay activator" comprising 95% propylene glycol and 5% DI water. Make only enough for this trial.

Phase A (Oil)

Material	Weight Percent (%)
Stearalkonium bentonite	3
Propylene carbonate/water	2
Dipropylene Glycol Dibenzoate	30

Procedure:

Contract # W81XWH-05-C-0131

1100 rpm, 75°C) for 5 minutes.

stir at 1100rpm for 20 minutes.

Control

ate, 5% DI water. Make only enough for this trial.

stirring (speed =20) for 5 minutes. Add propylene carbonate/water and mix for an additional 5 minutes.

Weight (g)
1
2

1100 rpm.

20 minutes. Remove from heat and let cool at room temperature.

5% PEI Active

5% DI water.

1
2
3

to metal beaker. Slowly (and at speed = 20 to reduce powder stirring solvent vortex. Mix for 5 minutes at 1100 rpm. Add propylene glycol 5 minutes at 1100 rpm.

	Weight Percent (%)	Mass (g)
	5	15.1
b)	15	45.0

2 stirring.

Material	Weight Percent (%)	Mass (g)
Distilled water	41	123.0
Bentonite clay	4	12.0

id =20) 75°C water vortex. Mix for 10 minutes at 1100 rpm.

5. Remove beaker from vortex, and let cool at room temperature.

pourable.

Summary: Hydrophobic Clay, Water in Oil, Dipropylene Glycol Benzoate Emollient, Control.

Phase A (Oil Phase)

Material		Weight Percent (%)	Mass (g)
Stearalkonium	tonite	2	6.02
Ethanol		1	3.03
Dipropylene Gly	benzoate	42	126.03
Emulsifier HLB		5	15.0145

to metal beaker. Place beaker in vortex holder. Slowly add organoclay (0.25 g) = 20. Mix for 5 minutes at 1100 rpm (speed= 26). Add ethanol and 100 rpm. Add grill with mixing at 1100rpm and heating to 80°C.

Material	Weight Percent (%)	Mass (g)
Distilled Water	50	150.04

vigorous mixing at 80°C. Continue mixing intensively at 80°C for 20 min and turn off heat. Let sample cool at room temperature.

A thick, white, creamy disper

PROFFER STATEMENT - NOT APPROVED FOR PUBLIC RELEASE
 Page 57 of 60

Summary: Hydrophobic Clay System, Water in Oil, Dipropylene Glycol, 10% PEI Active

Procedure: Prepare "organoclay activator" comprising 95% propylene carbonate only enough for this trial. Incroquat QLC is retained since it forms a

Phase A (Oil Phase)

Material	Weight Percent (%)
Stearalkonium-90 Bentonite	4
Propylene Carbonate/ water	2.4
Dipropylene Glycol Dibenzoate	43.6
Emulsifier HLB 5	5

Add dipropylene glycol dibenzoate to metal beaker. Place beaker in to stirring (speed = 20) solvent vortex. Mix for 5 minutes at 1100 rpm. Add propylene carbonate/water and mix for an additional 5 minutes at 1100 rpm. Add emulsifier with mixing at 1100rpm and heating to 80°C.

Phase B (Water)

Material	Weight Percent (%)
Distilled water	32.5
PEI (Lupasol FG)	10
Incroquat QLC (Liquid Conditioner)	2.5

Combine ingredients in glass beaker on stir plate.

Once T=80°C, add Phase B to Phase A with mixing at 1100rpm. Stop mixing and remove beaker from vortex machine; turn heating system off at room temperature.

Results:

A very thick, tan, creamy dispersion

TNSP 4 LBN: 357-110/ 419-022

Summary: Hydrophobic Clay System, Water in Oil, Dipropylene Glycol, 15% PEI Active

Procedure: Prepare "organoclay activator" comprising 95% propylene carbonate only enough for this trial.

Phase A (Oil Phase)

Material	Weight Percent (%)
Stearalkonium-90 Bentonite	4
Propylene Carbonate/ water	2.4
Dipropylene Glycol Dibenzoate	43.6
Emulsifier HLB 5	5

Add dipropylene glycol dibenzoate to metal beaker. Place beaker in to stirring (speed = 20) solvent vortex. Mix for 5 minutes at 1100 rpm. Add propylene carbonate/water and mix for an additional 5 minutes at 1100 rpm. Add emulsifier with mixing at 1100rpm and heating to 80°C.

Phase B (Water)

Material	Weight Percent	Mass (g)
Distilled Water	27.5	82.5
PEI (Lugol's)	15	45.153
Incroquat	2.5	7.518

Combine ingredients in glass beaker with magnetic stirring.

Once T=80°C, add Phase B to Phase A with mixing at 1100rpm. Set timer for 20 min. After 20 min, stop mixing and remove beaker from vortex machine; turn heating system off. Leave to cool at room temperature.

Results:

A thick, creamy dispersion

TNSP 5 Control LBN: 357-113/ 419-23

Summary: Hydrophobic system, Waterless, Dipropylene Glycol Benzoate Emollient Control

Procedure: Prepare "organoclay activator" comprising 95% propylene carbonate, 5% H₂O water. All done at room temperature.

Phase A (Oil Phase)

Material	Weight Percent (%)	Mass (g)
Stearal	6	18.0
Propylene carbonate/ water	4	11.4/ 0.65
Dipropylene Glycol Benzoate	70	210.1

Add dipropylene glycol benzoate to metal beaker. Place beaker in vortex holder (since vortex takes long time to cool, beaker will be the water). Slowly add organoclay to stirring (speed = 20) solvent vortex. Mix for 5 minutes. Add propylene carbonate/water and mix for an additional 5 minutes at

Phase B (Waterless)

Material	Weight Percent	Mass (g)
Dipropylene Glycol Benzoate	20	60.1

Slowly add Phase B to Phase A with mixing at 1100rpm. Set timer for 10 min. After 10 min, stop mixing and remove beaker from machine.

Results:

A thick, greasy, pourable emulsion. Sticky.

TNSP 5 LBN: 357-114/ 419-24

Summary: Hydrophobic system, Waterless, Dipropylene Glycol Benzoate Emollient 20% PEI Active

Procedure: Prepare "organoclay activator" comprising 95% propylene carbonate, 5% H₂O water. Make emulsion performed at room temperature.

Phase A (Oil Phase)

Material	Weight Percent (%)	Mass (g)
Stearalkonium-90 Bentonite	6	13.1
Propylene Carbonate/ water	4	11.4/ 0.63
Dipropylene Glycol Dibenzoate	70	210.1

Add dipropylene glycol dibenzoate to metal beaker. Place beaker in vortex mixer (since vortex takes long time to cool, beaker was held above the water). Slowly add organoclay to solvent (speed = 20) vortex. Mix for 5 minutes at 1100 rpm (speed= 26). Add propylene carbonate/ water and mix for an additional 5 minutes at 1100 rpm.

Phase B (Waterless)

Material	Weight Percent	Mass (g)
PEI (Lupasol FG)	20	60.6

Slowly add Phase B to Phase A with mixing at 1100rpm. Set timer for 10 min. After 10 min, stop mixing and remove beaker from vortex machine.

Results:

A slightly thick, pourable dispersion.

STAS final report from Emory University, Dr. Craig Hill

Award Number: DAAH04-96-C-0086, TCN 98-18

POSTDOC FOR RESEARCH ON POLYOXOMETALATES (POMs) IN TOPICAL SKIN
PROTECTANTS

By

Craig L. Hill

Goodrich C. White Professor of Science
Department of Chemistry, Emory University
1515 Pierce Drive, Atlanta, GA 30322
phone: 404-727-6611; fax: 404-727-6076
E-mail: chill@emory.edu

for

Battelle and the U.S. Army Research Office

January 27, 2000

Contract No. DAAH04-96-C-0086
TCN 98-138
Scientific Services Program

The views, opinions, and/or findings contained in this report are those of the author(s) and should not be construed as an official Department of the Army position, policy, or decision, unless so designated by other documentation.

REPORT DOCUMENTATION PAGE

Form Approved
OMB No. 0704-0188

Public reporting burden for this collection of information is estimated to average 1 hour per response, including the time for reviewing instructions, searching existing data sources, gathering and maintaining the data needed, and completing and reviewing the collection of information. Send comments regarding this burden estimate or any other aspect of this collection of information, including suggestions for reducing this burden, to Washington Headquarters Services, Directorate for Information Operations and Reports, 1215 Jefferson Davis Highway, Suite 1204, Arlington, VA 22202-4302, and to the Office of Management and Budget, Paperwork Reduction Project (0704-0188), Washington, DC 20503.

1. AGENCY USE ONLY (Leave blank)		2. REPORT DATE January 28, 2000		3. REPORT TYPE AND DATES COVERED FINAL REPORT; FROM: 8/24/98 TO: 12/31/99	
4. TITLE AND SUBTITLE POSTDOC FOR RESEARCH ON POLYOXOMETALATES (POMs) IN TOPICAL SKIN PROTECTANTS				5. FUNDING NUMBERS DAAH04-96-C-0086	
6. AUTHOR(S) Craig L. Hill Goodrich C. White Professor of Science					
7. PERFORMING ORGANIZATION NAME(S) AND ADDRESS(ES) Department of Chemistry, Emory University 1515 Pierce Drive, Atlanta, GA 30322				8. PERFORMING ORGANIZATION REPORT NUMBER Delivery Order 0321	
9. SPONSORING/MONITORING AGENCY NAME(S) AND ADDRESS(ES) U.S. Army Research Office P.O. Box 12211, Research Triangle Park, NC 27709				10. SPONSORING/MONITORING AGENCY REPORT NUMBER TCN 98138	
11. SUPPLEMENTARY NOTES Task was performed under a Scientific Services Agreement issued by Battelle, Research Triangle Park Office, 200 Park Drive, P.O. Box 12297, Research Triangle Park, NC 27709					
12a. DISTRIBUTION/AVAILABILITY STATEMENT May not be released by other than sponsoring organization without approval of US Army Research Office				12b. DISTRIBUTION CODE	
13. ABSTRACT (Maximum 200 words) The contracted research successfully achieved its stated goal of developing POM systems that catalytically decontaminate chemical warfare agents (CWAs) when formulated into reactive topical skin protectants (rTSPs). Using combinatorial libraries and considerable background knowledge on POMs, 3 prototype systems that all decontaminate mustard (HD) analogs using only the environment (air) under ambient conditions have been identified. The systems are silver, gold and ceric salts of vanadium-containing polytungstates. All 3 systems work not only in solution but also as powders, even powders with very low surface area. While these systems should be amenable to significant optimization (POM elemental composition, choice of counter cation(s), powder surface area, etc.), no such optimization has yet been attempted (and was beyond the mandate of the contract initial research effort)					
14. SUBJECT TERMS catalytic decontamination, topical skin protectants, polyoxometalates (POMs)				15. NUMBER OF PAGES	
				16. PRICE CODE	
17. SECURITY CLASSIFICATION OF REPORT	18. SECURITY CLASSIFICATION OF THIS PAGE	19. SECURITY CLASSIFICATION OF ABSTRACT	20. LIMITATION OF ABSTRACT		

Final Report:

POSTDOC FOR RESEARCH ON POLYOXOMETALATES (POMs) IN TOPICAL SKIN PROTECTANTS

By

Craig L. Hill

January 27, 2000

Introduction

The development of effective catalytic methods to decontaminate chemical warfare agents (CWAs) using simply the environment (no requirement for reagents, energy sources, or even water) is as formidable as it is attractive. No systems yet exist for this. Such catalysts would likely be of value in every type of decontamination as they would entail an absolutely minimal logistics burden for deployment.

Barrier creams for protection against CWAs (topical skin protectants = TSPs) without caustic additives currently lack an effective chemical decontamination capability against sulfur mustard (HD). The fluorinated nature of the existing TSPs, typically polytetrafluoroethylene powders suspended in perfluoropolyether (PFPE) oil with or without a fluorinated co-solvent such as trifluoroethanol (TFE), impart good barrier properties. Furthermore, these barrier properties can be improved by the addition of some stoichiometric reagents including N-chloro oxidants that can oxidize HD. No TSP, however, has a durable catalytic HD decon capability. Once the oxidant in the cream is consumed, the barrier properties of the cream revert to those of the TSP alone. It is also far from clear if these potent stoichiometric oxidant additives would be compatible with skin (dermatitis and skin damage can result from extended contact with many such agents).

As a consequence, our goal in this contracted research was and is to develop decontamination catalysts that not only work with the environment (air/O₂) under ambient conditions but also are compatible with the existing TSPs of interest to the US Army. Such catalyst additives should render the TSPs not only reactive (rTSPs) but also catalytic (cTSPs).

Our research has focused on HD because HD is the CWA agent of greatest concern. It is prevalent and generally harder to decontaminate than the other major treats (GB, GD and VX). The principal catalysts in this research have been polyoxometalates (POMs) because preliminary research indicated that several classes of POMs had promise as catalysts for O₂ oxidation, and

because POMs are extensively modifiable synthetically. Literally thousands of different POMs of the Keggin structural class can be made readily and the counter cations of the POM anions could also be widely varied. We have used combinatorial and other approaches to identify the top POM catalysts. In the course of such catalyst discovery efforts, we also identified some POM-free catalysts for O₂ oxidation.

Our research has used both regular solvents such as acetonitrile and fluorinated ones that model the PFPEs such as TFE, as well as limited work with the PFPEs themselves. The former solvents have been used because they dissolve the HD simulants, and in many cases the catalysts as well, while the PFPEs do not. Thus the studies with acetonitrile and TFE facilitated detailed and informative kinetics and mechanistic studies that were impossible with the heterogeneous PFPE-based systems.

This preliminary 15-month research program has been very successful in that several catalytic systems have been identified that do in fact catalyze oxidation of a range of compounds, including thioether HD simulants, by air under ambient conditions, and thus effectively function without any significant logistical requirement (energy, water, etc.). Furthermore, several of these systems are active not only in solution but also as solids.

In both the Experimental and Results sections, we first address a recently discovered yet thoroughly investigated homogeneous Au/Ag/NO₃⁻ based catalyst for CEES oxidation by O₂. We subsequently address other catalysts developed in this last year that are as yet less thoroughly investigated either because they are heterogeneous and thus not amenable to kinetics investigations or are too new (discovered too recently) for extensive research to have been conducted.

Experimental section

The next 11 paragraphs are on the homogeneous Au/Ag/NO₃⁻ catalytic O₂-based oxidation system for CEES, and the last paragraph is on additional recently discovered heterogeneous and other catalysts for the same process.

Materials. HAuCl₄, AgNO₃, AgClO₄, TBANO₃, TBACl, TBAHSO₄, TMAOH, TBAClO₄, TBABPh₄, CH₃CO₂TBA, TBAH₂PO₄, anhydrous acetonitrile (CH₃CN), 2-chloroethyl ethyl sulfide (CEES), dimethyl sulfoxide (DMSO), 1,3-dichlorobenzene, and 95 atom % labeled H₂¹⁸O were purchased from Aldrich. TBANO₂ was purchased from Fluka (TBA and TMA are abbreviations for tetra-*n*-butylammonium and tetramethylammonium cations, respectively). Diethyl ether and acetone were purchased from Aldrich and filtered through a column of neutral alumina before use. All POMs were synthesized from literature preparations. All reagents except for H₂¹⁸O (Aldrich) were dried *in vacuo* overnight. Stock solutions were prepared using anhydrous CH₃CN.

General Procedures. All gas chromatography analyses were performed on an HP5890 Gas Chromatograph equipped with an FID detector and a 5% phenyl methyl silicone capillary column. 1,3-Dichlorobenzene was used an internal standard in all cases. Mass abundance

determinations were performed using a HP 5890 GC with a 5% phenyl methyl silicone capillary column and a 5971A Mass Selective Detector. UV-visible spectra were run on a HP 8452A Diode Array Spectrophotometer. The percentages of O₂ of the reaction atmosphere were varied using a Series 810 Mass Trak flowmeter with dried argon as the other gas.

Fitting of the Reaction Kinetics. Fitting was performed using a standard Solver subprogram of the MS Excel software package by minimizing the sum of the squares of the difference between experimental and theoretical values. When fitting was performed varying two parameters at once, several minima could be found. In this case the parameters giving the least deviation from experimental data were used.

Evaluation of the Library of Catalysts. A total of 150 combinations of substituted polyoxometalate anions and counter cations were generated, and each was evaluated for the ability to catalyze the oxidation of CEES by O₂. For each of the 150 reactions, 1.0 eq of a POM was mixed with 5 eq of HAuCl₄ in a 20-mL vial. The vial was purged with O₂, and a 1.0-mL solution containing 100 eq of CEES and 50 eq of 1,3-dichlorobenzene in CH₃CN was added via syringe. Each reaction was monitored at 4 and 11 hrs for turnovers of CEESO. Product distributions were quantified by GC.

General Procedure for Sample Preparation. Stock solutions of HAuCl₄, AgNO₃, and AgClO₄, TBANO₃, TBACl, TBAClO₄ were prepared in anhydrous CH₃CN and wrapped with aluminum foil to prevent light exposure. All reagents were dried *in vacuo* before they were dissolved in anhydrous CH₃CN. Appropriate amounts of each stock solution were added via syringe to a 20-mL glass vial fitted with a PTFE septum that was first purged with O₂. The atmospheric pressure was adjusted to approximately 1.0 atm by inserting a needle into the septum for several seconds. The reactions were carried out at 25 ± 1 °C.

Rate Law Determination for CEES Oxidation by O₂ Catalyzed by the HAuCl₄/AgNO₃/AgClO₄ System. Screening of a combinatorial library identified the most reactive O₂-based catalyst as one comprised of AgNO₃, AgClO₄ and HAuCl₄, thus this system was chosen for further investigation. When 1.0 eq of HAuCl₄ was used, the optimal reactivity was achieved with 0.75 and 1.25 eq of Ag(I) and NO₃⁻ respectively. The order of each component was determined by varying its concentration over the range given below while the concentrations of all other components were held constant. Unless otherwise noted the initial concentration of HAuCl₄, [HAuCl₄]₀, used in each reaction was 4.77 mM. [CEES]₀ was varied from 0.153 M to 3.06 M. [Ag(I)]₀ was varied from 0 to 15.2 mM, [HAuCl₄]₀ was varied from 0 to 11.9 mM, and [NO₃⁻]₀ was varied from 0 to 54 mM. To establish the order in the active multi-component catalyst itself, the following ratio of concentrations of catalyst components [2 Ag(I)/1 Au(III)/0.75 NO₃⁻] was varied from 1.2 mM to 7.4 mM (based on total Au concentration). [Cl]₀ was varied from 0 to 6.3 mM, and [ClO₄]₀ was varied from 0 to 0.1 M. The kinetic impact of the product sulfoxide was assessed using DMSO as a model for CEESO (CEESO itself could not, of course, be used because it is the actual product). [DMSO]₀ was varied from 0 to 0.36 M, [H₂O]₀ was varied from 0 to 0.91 M, and the percentage of O₂ in the gas phase (head space over reaction) was varied from 0 to 100%. For rate order determinations, the reaction was monitored until at least 10% of the starting CEES was consumed.

H₂¹⁸O Labeling Experiment. In order to determine the atomic origin of oxygen in the sulfoxide product (H₂O, H₂O₂, or O₂) an experiment using H₂¹⁸O was performed. For this experiment, a stock solution of 1.53 M H₂¹⁸O in anhydrous CH₃CN was prepared using 95 atom % ¹⁸O labeled H₂O. All other stock solutions used were the same as those in the previous experiments. In a 20-mL vial purged with O₂, 0.100 mL (4.77 × 10⁻⁶ mol, 1 eq) of HAuCl₄, 0.035 mL (3.58 × 10⁻⁶ mol, 0.75 eq) of AgNO₃, 0.060 mL (5.96 × 10⁻⁶ mol, 1.25 eq) of AgClO₄, and 0.083 mL (7.15 × 10⁻⁴ mol, 150 eq) of the internal standard 1,3-dichlorobenzene were added by syringe. The volume was adjusted to 0.820 mL with anhydrous CH₃CN. After the solution was stirred for 60 s, 0.042 mL of CEES (3.58 × 10⁻⁴ mol, 75 eq) were added followed immediately by 0.140 mL of H₂¹⁸O (3.58 × 10⁻⁴ mol, 75 eq). The isotopic composition of the products was quantified by GC-MS.

Assessment of H₂O₂-Based Sulfoxidation. To assess sulfoxidation arising from any H₂O₂ generated *in situ*, an experiment using H₂O₂ was performed. In a Schlenk flask, 2.0 mL of a 30% aqueous H₂O₂ solution was reduced in volume to 0.7 mL resulting in 85% v/v H₂O₂. *Caution. The procedure of concentrating H₂O₂ or any other peroxide is potentially dangerous. There is some risk of explosion.* The concentrated H₂O₂ solution was immediately diluted with anhydrous CH₃CN and titrated iodometrically; Final [H₂O₂] = 1.2 M in CH₃CN. The same concentrations of each component were used as in the H₂¹⁸O experiment except that the H₂¹⁸O was omitted. After allowing the solution to react for 2 hrs, 0.060 mL of the 1.2 M H₂O₂ solution (7.15 × 10⁻⁵ mol, 15.0 eq) was added by syringe.

Attempted Oxidation of Dimethyl Sulfoxide to Dimethyl Sulfone. In a 20-mL vial purged with O₂, 0.100 mL (4.77 × 10⁻⁶ mol, 1 eq) of HAuCl₄, 0.035 mL (3.58 × 10⁻⁶ mol, 0.75 eq) of AgNO₃, 0.060 mL (5.96 × 10⁻⁶ mol, 1.25 eq) of AgClO₄, and 0.083 mL (7.15 × 10⁻⁴ mol, 150 eq) of 1,3-dichlorobenzene were added by syringe. The volume was adjusted to 0.820 mL with anhydrous CH₃CN. To this solution, 0.025 mL (3.58 × 10⁻⁴ mol, 75 eq) of DMSO was added by syringe. The reaction products were quantified as a function of time by GC and GC-MS as described above.

Assessment of Au(III). A blank consisting of 1.50 mL of CH₃CN and 0.083 mL of 1,3-dichlorobenzene was prepared in a 1.0-cm quartz cuvette fitted with a stir bar and septum stopper. This background absorbance was measured on a HP 8452A Diode Array Spectrophotometer. To this cuvette was added by syringe stock solutions of 0.070 mL (7.15 × 10⁻⁶ mol, 0.75 eq) of AgNO₃, 0.119 mL (1.19 × 10⁻⁵ mol, 1.25 eq) of AgClO₄, and 0.200 mL (9.54 × 10⁻⁶ mol, 1.0 eq) of HAuCl₄. After acquiring 1 spectrum of the solution, it was apparent that 400 nm was the optimal wavelength for assessing the Au(III). The solution was immediately transferred to a 20-mL vial that was purged with O₂. To this solution was added 0.033 mL (2.86 × 10⁻⁴ mol, 30 eq) of CEES. After shaking for 60 s, the vial was centrifuged and the solution was transferred back to the cuvette previously purged with O₂. Spectra were collected every 30 s for 2 hrs.

Substituting NO₃⁻ with Other Anions. These experiments were conducted using similar protocols and solutions as those in the experiments described above. Solutions of 0.095 mL (9.54 × 10⁻⁶ mol, 2 eq) of AgClO₄, 0.100 mL (4.77 × 10⁻⁶ mol, 1 eq) of HAuCl₄, and 0.083 mL (7.16 × 10⁻⁴ mol, 150 eq) of 1,3-dichlorobenzene were added by syringe to a 20-mL vial that was purged with O₂. The solutions of the following in anhydrous CH₃CN (all 0.2 M) were prepared

in 20-mL vials: TBANO_2 , TBABPh_4 , TBAHSO_4 , TMAOH , TBAPF_6 , $\text{CH}_3\text{CO}_2\text{TBA}$, and TBAH_2PO_4 . Each of the aforementioned 0.2 M solutions (0.024 mL, 4.77×10^{-6} mol, 1 eq) was added to vials containing the Au/Ag solution. The volume was adjusted to 0.958 mL with anhydrous CH_3CN . After stirring for 60 s, 0.042 mL CEES was added by syringe. Aliquots were analyzed by GC every 15 min.

Conditions for Tables 1-3. The conditions for the reactions in these tables are given in the table captions at the bottom of each table. All the products were quantified by GC and GC-MS by the same techniques used for the Au/Ag/ NO_3^- system outlined above.

Results and Discussion.

Compounds have been discovered that are as active as any known for the catalytic oxidation of organic compounds, including thioether HD simulants, by air/ O_2 . Many of them are active under ambient conditions without additives. Furthermore, many are active not only in solution but also as powders. Thus they should be effective for catalytic decontamination of HD either as solutions or suspensions in PFPEs, the liquid base of TSPs.

Figures 1-9 (captions immediately below) establish that when Ag(I), Au(III) and NO_3^- are dissolved in CH_3CN solution (or other solvents including TFE), a highly active catalyst for the O_2 oxidation of CEES to the much less toxic sulfoxide, CEESO, is produced.

Figure Captions:

Figure 1. Combinatorial library of catalysts for the oxidation of 2-chloroethyl ethyl sulfide (CEES). Catalytic activity (turnovers of CEESO after 11 hours) is depicted on the z axis. Each entry on the x,y plane (base plane) represents a distinct catalyst. Formulas of all the entries (primarily POM derivatives) are given in the Supporting Information (Table S1). Catalytic activity was assessed in an identical manner for all 150 members of the library (see Experimental Section for details). Catalyst number 131 was the Au/Ag/ NO_3^- combination (in less than ideal mole ratios) that lead to discovery of the parent system (optimized mole ratios) that was subsequently investigated in depth.

Figure 2. Kinetics of CEES oxidation by the $\text{HAuCl}_4/0.75\text{AgNO}_3/1.25\text{AgClO}_4/\text{O}_2$ system. CEES consumption as a function of time (\circ). CEESO formation as a function of time (\square). Vinyl chloride formation as a function of time (\diamond). Insert: Absorbance at 400 nm as a function of time (the absorbance remains constant after 5000 s). Conditions: 25 °C; 1 atm O_2 ; $[\text{HAuCl}_4] = 0.0048$ M; $[\text{AgNO}_3] = 0.0036$ M; $[\text{AgClO}_4] = 0.0060$ M.

Figure 3. Induction period as a function of initial O_2 concentration in the $\text{HAuCl}_4/0.75\text{AgNO}_3/1.25\text{AgClO}_4/\text{O}_2$ system. 100% $\text{O}_2 = 1.0$ atm O_2 ; 70% $\text{O}_2 = 0.7$ atm O_2 ; 50% $\text{O}_2 = 0.5$ atm O_2 ; 30% $\text{O}_2 = 0.3$ atm O_2 ; 20% $\text{O}_2 = 0.2$ atm O_2 . In every case except 100% O_2 ,

the total gas pressure is adjusted to 1.0 atm with Ar. Conditions: 25 °C; [HAuCl₄] = 0.0048 M; [AgNO₃] = 0.0036 M; [AgClO₄] = 0.0060 M; [CEES] = 0.15 M.

Figure 4. Rate of CEESO formation as a function of [NO₃⁻]/[Au(III)]. Conditions: 25 °C; 1 atm O₂; [HAuCl₄] = 0.0048 M; [CEES] = 0.37 M.

Figure 5. Rate of CEESO formation as a function of [Cl⁻]/[Au(III)]. Conditions: 25 °C; 1 atm O₂; [HAuCl₄] = 0.0048 M; [CEES] = 0.37 M.

Figure 6. Rate of CEESO formation as a function of initial CEES concentration. The best least squares line through the points is given (plot, equation and error). Conditions: 25 °C; 1 atm O₂; [HAuCl₄] = 0.0048 M; [AgNO₃] = 0.0036 M; [AgClO₄] = 0.0060 M.

Figure 7. Rate of CEESO formation as a function of H₂O concentration. Conditions: 25 °C; 1 atm O₂; [HAuCl₄] = 0.0048 M; [AgNO₃] = 0.0036 M; [AgClO₄] = 0.0060 M. [CEES] = 0.37 M.

Figure 8. Rate of CEESO formation as a function of [DMSO]. Conditions: 25 °C; 1 atm O₂; [HAuCl₄] = 0.0048 M; [AgNO₃] = 0.0036 M; [AgClO₄] = 0.0060 M. [CEES] = 0.037 M.

Figure 9. Fitting CEES consumption (o) and CEESO formation (□) experimental data to a theoretical model. The theoretical kinetic curve (simple exponential decay with pseudo first order rate constant; $k_{obs} = 7 \times 10^{-5} \text{ s}^{-1}$) for CEES consumption assuming no inhibition by CEESO (....). Conditions: 25 °C; 1 atm O₂; [HAuCl₄] = 0.0048 M; [AgNO₃] = 0.0036 M; [AgClO₄] = 0.0060 M.

The results presented in all these figures are consistent with the mechanism in Scheme 1 which involves an initiation period followed by effective catalysis with Au cycling between I and II oxidation states.

The ¹⁸O labeling experiment establishes that the oxygen of the sulfoxide derives from H₂O present and not O₂ (or H₂O₂ that can be generated from O₂ reduction *in situ*). The reaction is inhibited to some extent by H₂O (Figure 7) and somewhat more by sulfoxide (e.g. CEESO) itself (Figure 8); however both H₂O- and CEESO-ligated Au complexes that exist at high H₂O and CEESO concentrations, respectively, also exhibit some activity.

Reaction of a Au complex containing 2 CEES ligands and a nitrate ligand (1) is the rate-limiting step (Scheme 1). This process does not involve O₂. Determination of the exact mechanism of this step will require further research; however, it probably involves generation of a Au(II)(CEES⁺•) intermediate that undergoes rapid disproportionation with itself and/or reduction (of the Au(II)) by an additional CEES.

Since these informative investigations, we have determined that even faster catalysis is seen in fluorinated media (e.g. trifluoroethanol = TFE solvent) then in CH₃CN. This homogeneous Au/Ag/NO₃⁻ aerobic oxidation system hasn't yet been investigated in PFPE.

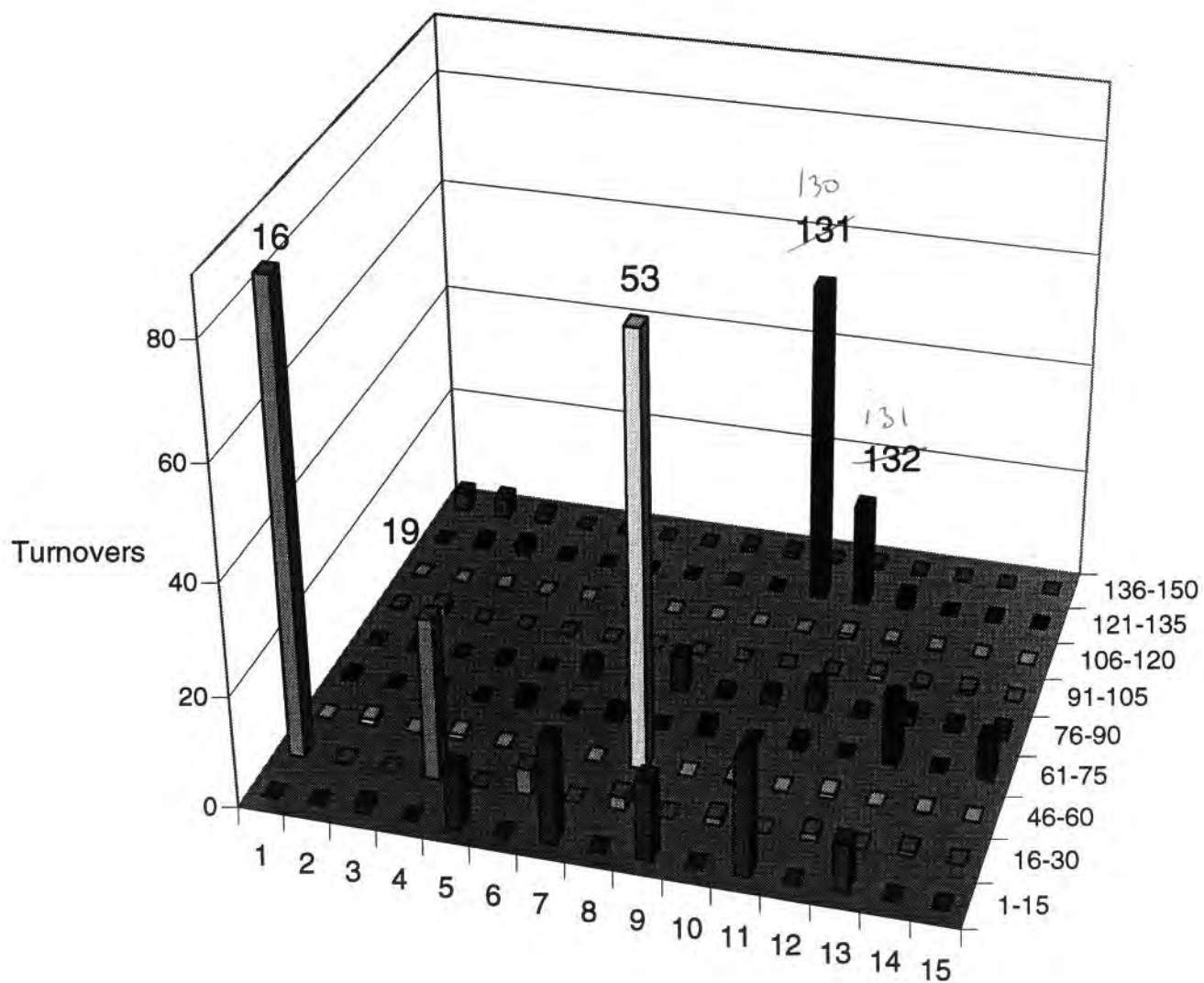


FIG 1

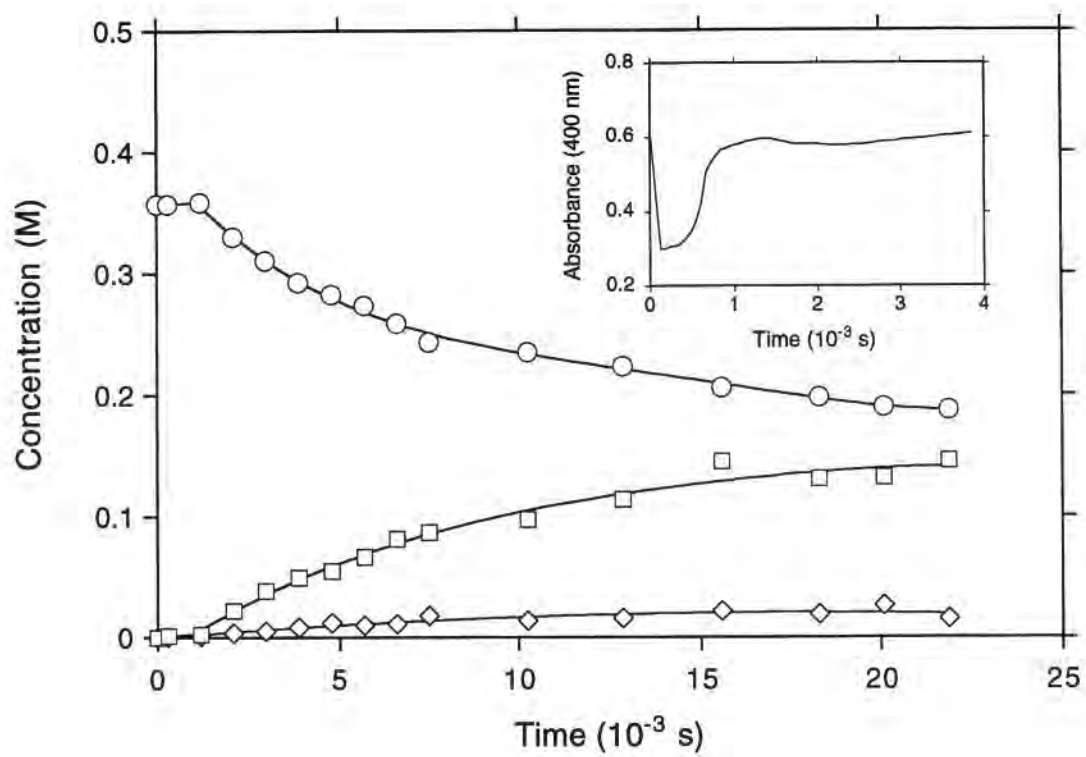


Fig. 9

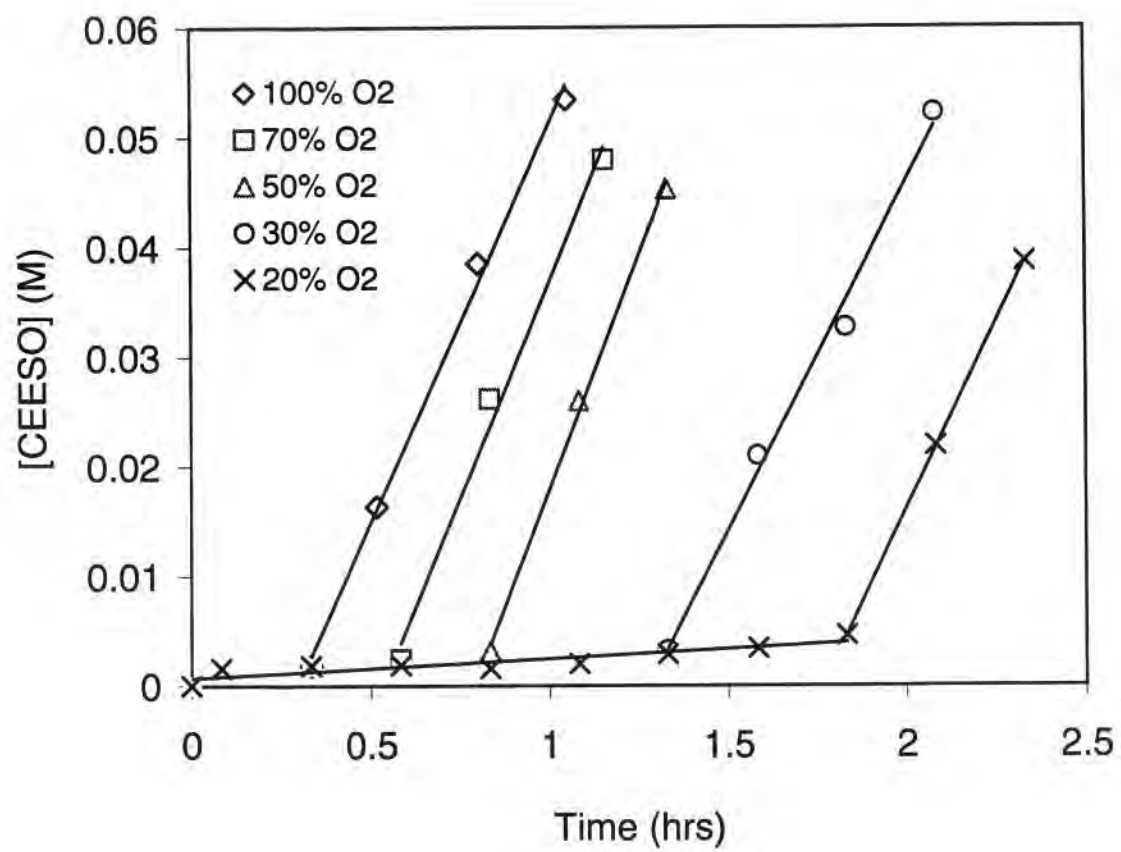


Fig. 3

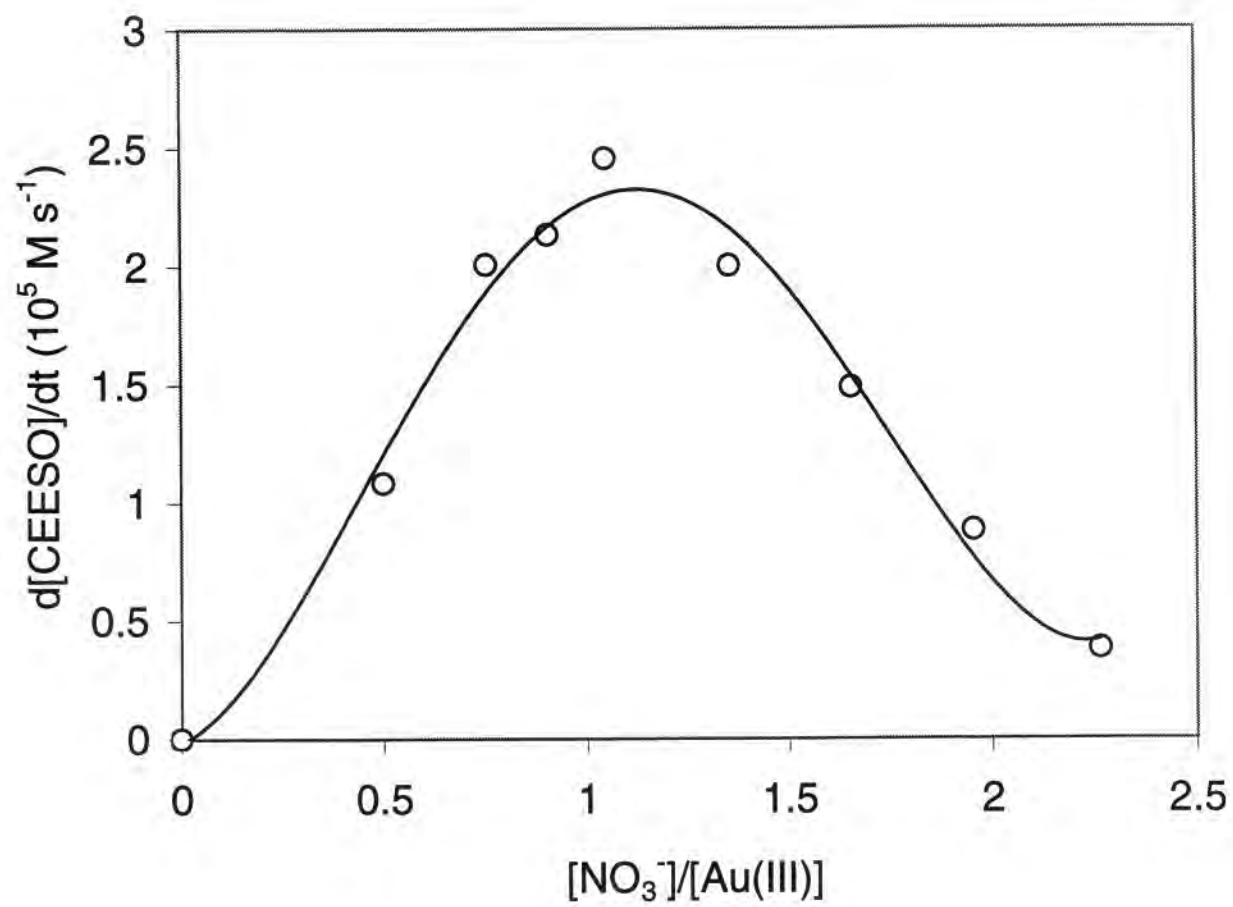


Fig 4

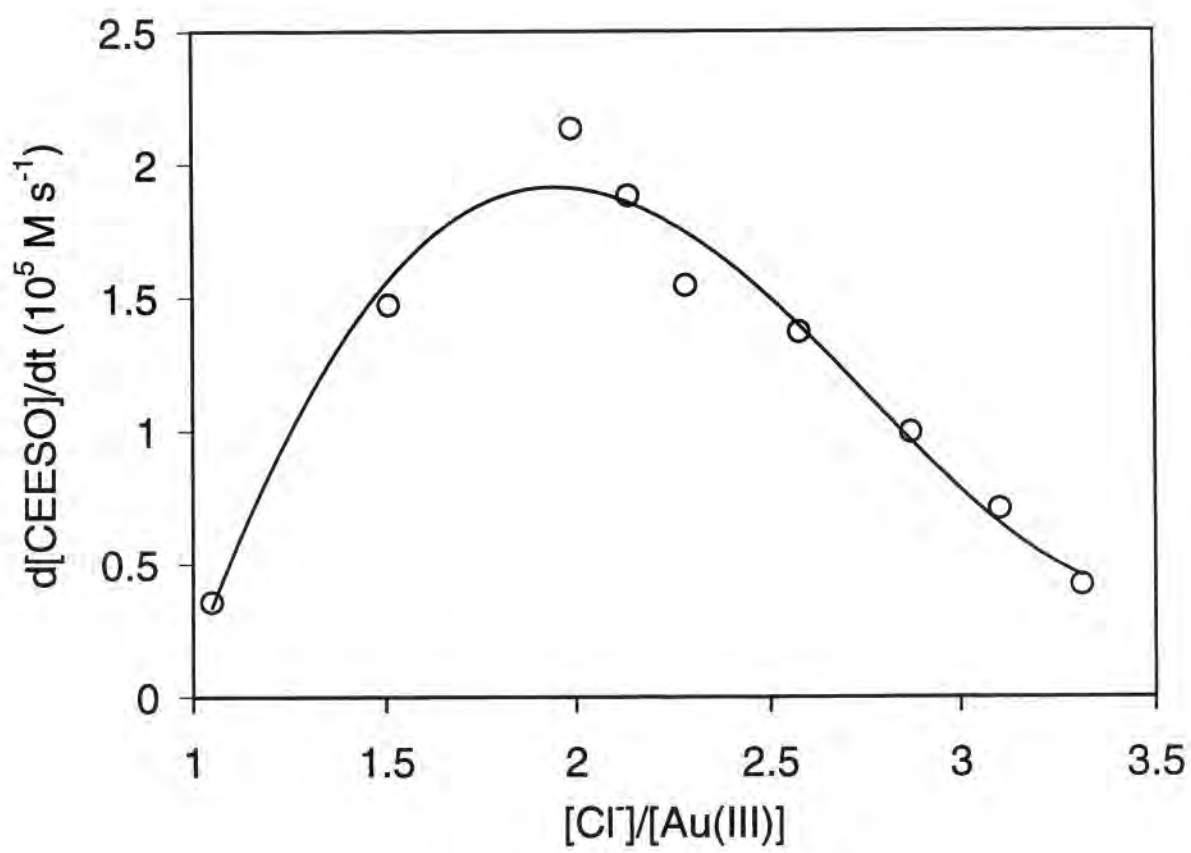


Fig. 5

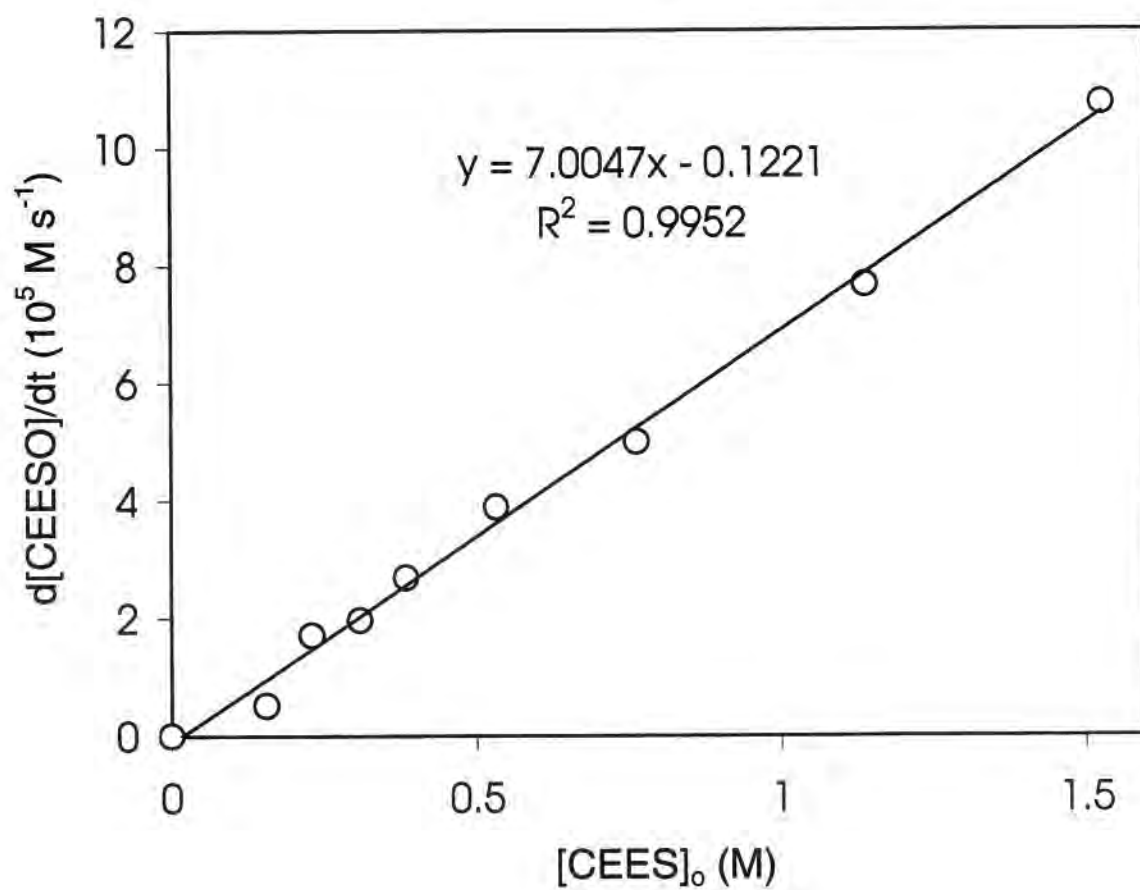


Fig. 6

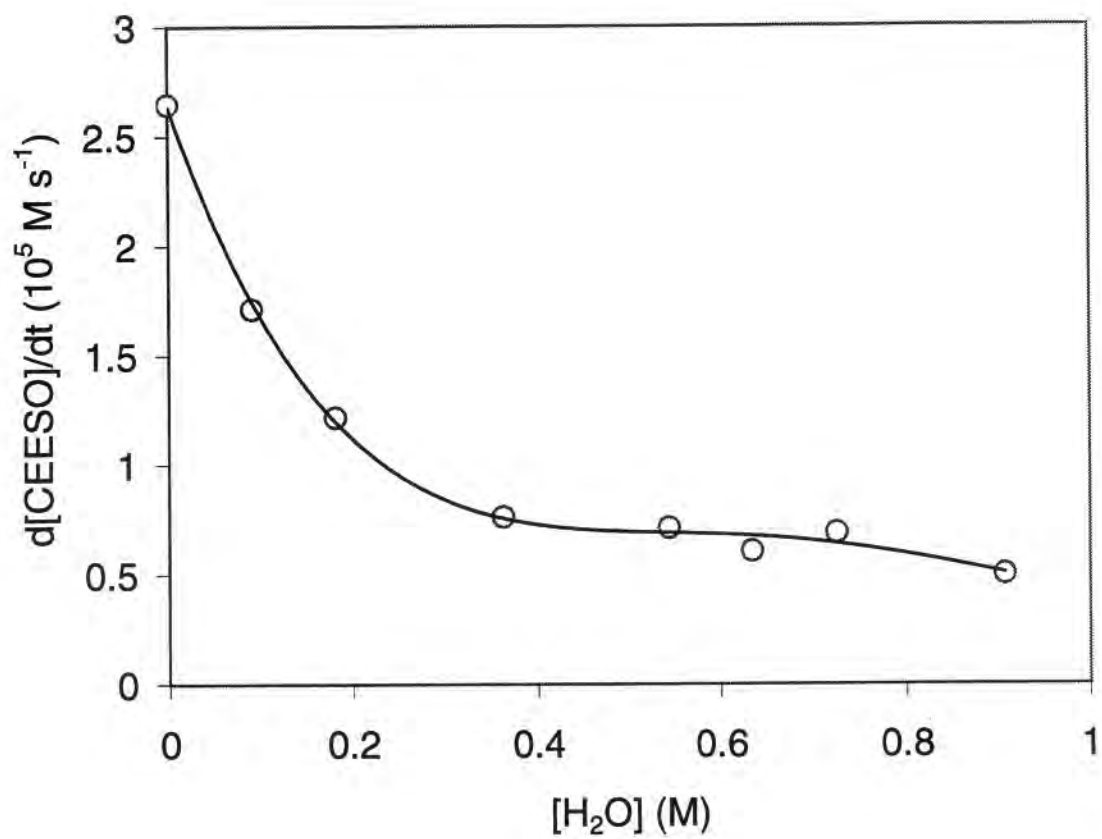


Fig. 7

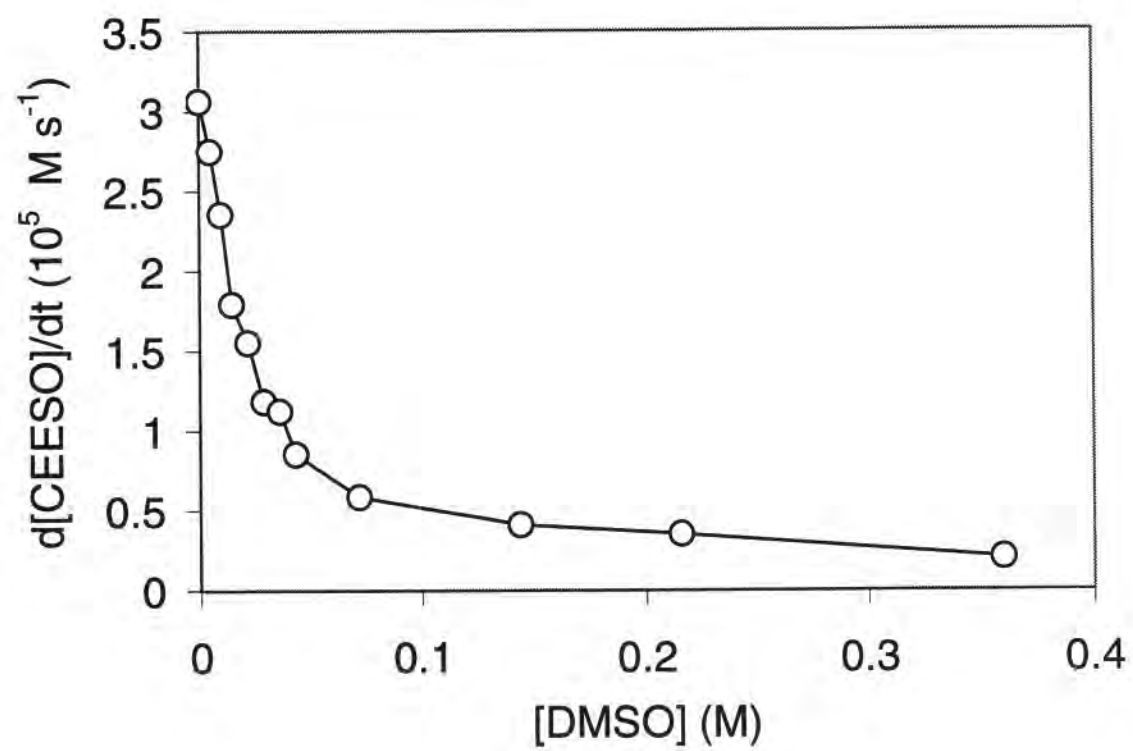


Fig 8

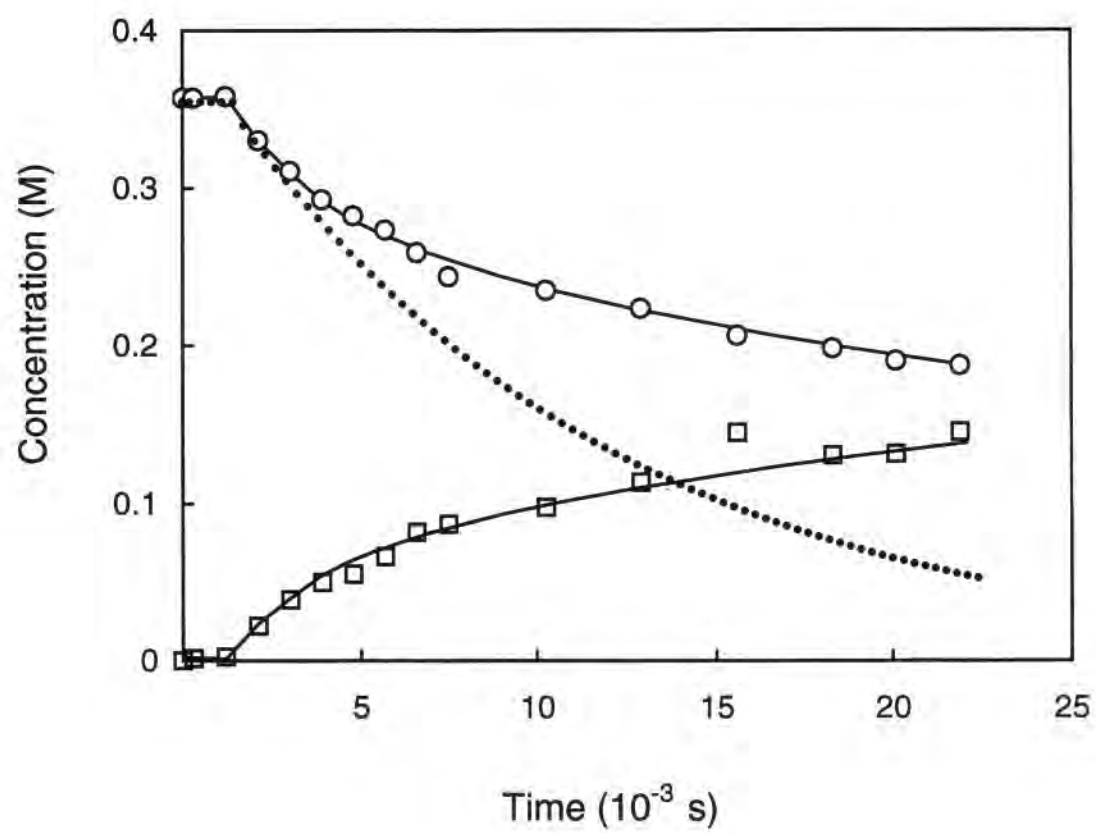
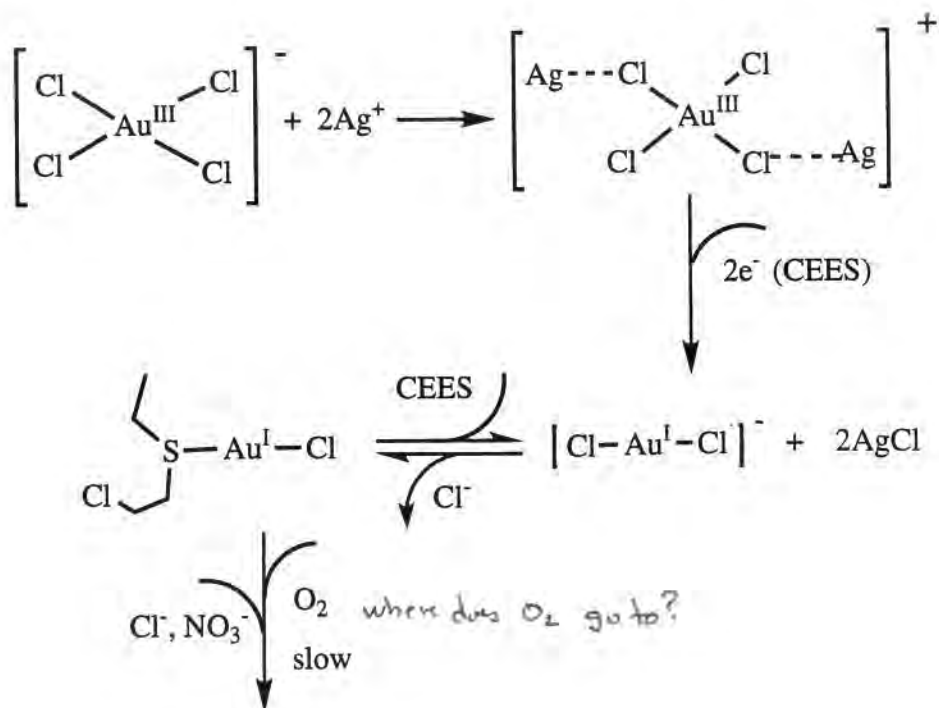


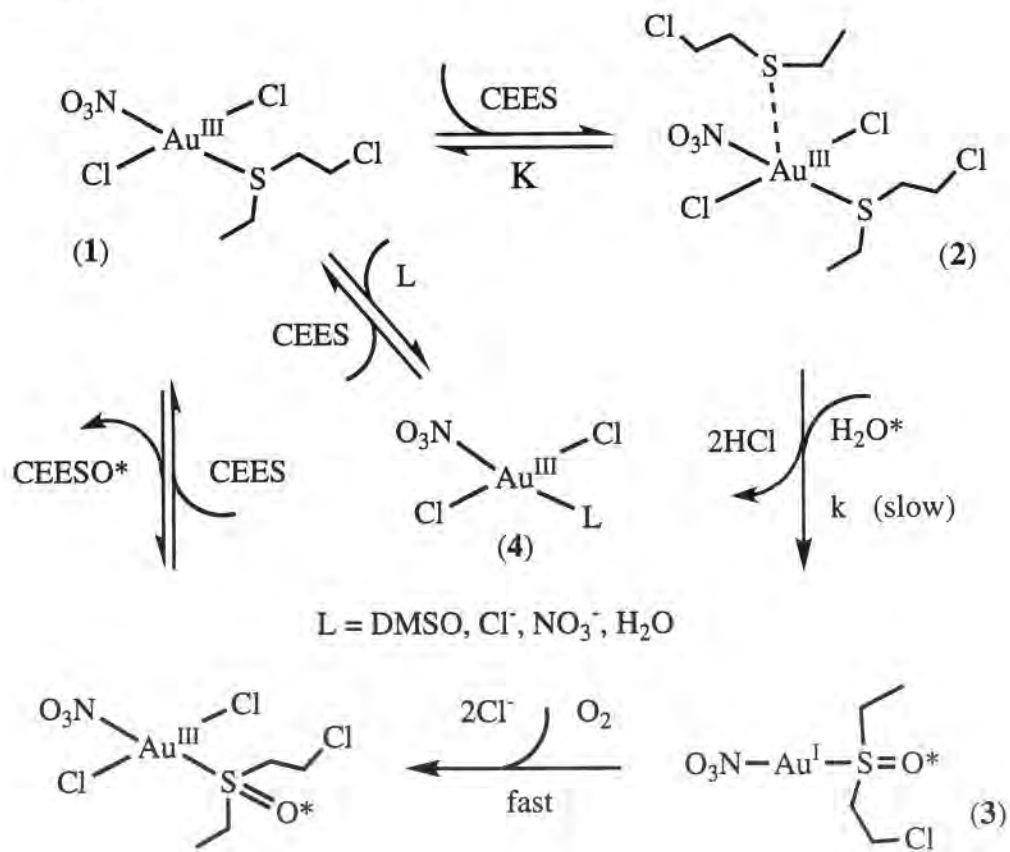
Fig. 9

Mass balance & electron balance not clear on this chart

Induction period



Catalytic cycle



Tables 1-3 on the next 3 pages also summarize data on other promising systems for O₂ oxidation of thioether HD simulants that should be compatible to varying degrees with the PFPE-based TSPs.

Table 1 addresses reactions involving insoluble Ag salts of some vanadium-containing POMs, and Table 2 gives reactivity (turnovers) for combinations of Au(III) and selected POMs evaluated after 4 and after 11 hours of reaction. Table 3 provides preliminary information on other POM-containing and POM-free systems with substantial activity.

Nearly all these systems can doubtless be improved with additional research. In particular the POM systems, given the ease with which POM compositions and consequent properties can be varied, can almost certainly be made more active.

Both developmental and mechanistic experiments are needed now to optimize the highly promising systems we have already identified. Also, however, additional exploratory research is warranted, because other aerobic oxidation catalysts of these classes doubtless exist and simply haven't been discovered yet. Combinations of active cations and POM anions are of particular interest because a myriad of molecular properties can be altered in such systems to make them more active.

Acknowledgment. We thank Dr. Ernie Braue for getting us interested in this area of research and the U.S. Army (administered by Battelle) for funding.

Table 1. Oxidation of the HD Simulant CEES in 2,2,2-Trifluoroethanol by Air and Catalyzed by Selected Insoluble Materials at Room Temperature^a

Entry	Catalyst ^b	Mol of catalyst, 10 ⁻⁵	Product yield, % ^c	TON ^d
1	None	NA	0	0
2	Ag ₅ PV ₂ Mo ₁₀ O ₄₀ + AgNO ₃	2.18	27.8	7.86
3	Ag _{3.5} Na _{1.5} PV ₂ Mo ₁₀ O ₄₀	2.30	35.1	8.65
4	Na ₅ PV ₂ Mo ₁₀ O ₄₀ + AgNO ₃	2.97	33.5	6.93
5	Na ₅ PV ₂ Mo ₁₀ O ₄₀	2.80	0	0
6	AgCl	3.35	0	0
7	Na ₅ PV ₂ Mo ₁₀ O ₄₀ + AgCl	2.90	0	0

^a Reaction conditions: CEES was 0.075 M (~50 mol CEES:1 mol catalyst) in 2,2,2-trifluoroethanol at 25 °C for 11.9 days. ^b "Catalyst" refers to POM in all cases except entry 6 where it refers to AgCl. Reactions were quantified by GC (5% phenyl methylsiloxane column) using 1,3-dichlorobenzene as an internal standard. ^c Yield based on [CEES]₀. ^d Turnovers = [(mol of CEESO)/(mol of POM)].

Table 2. Aerobic Oxidation of the HD Simulant CEES with Polyoxometalate using H₂AuCl₄ as a Cooxidant.^a

Catalyst	Time (h)	Turnovers ^b of CEESO	Time (h)	Turnovers ^b of CEESO
Na ₄ PVMo ₁₁ O ₄₀	4	0	11	1.1
Na ₄ PV ₂ Mo ₁₀ O ₄₀	4	5.0	11	10.6
Na ₆ PV ₃ Mo ₉ O ₄₀	4	7.0	11	18.3
Na ₅ H ₂ PV ₄ W ₈ O ₄₀	4	4.4	11	14.2
Na ₉ PV ₆ Mo ₆ O ₄₀	4	5.6	11	20.7
Na ₅ CuPW ₁₁ O ₃₉	4	59.2	11	83.6
H ₂ AuCl ₄	4	0	11	0

^a Reaction conditions: 9.61x10⁻⁶ mol POM, 4.8x10⁻⁵ mol H₂AuCl₄, 9.61x10⁻⁴ mol 1,2-dichlorobenzene, and 9.61x10⁻⁴ mol CEES were stirred in 4 mL of CH₃CN under 20 mL (0.82 mmol) of O₂ at 298 K. ^b Turnovers = [(moles of CEESO in the catalyst run) – moles of CEESO on the blank run)] / moles of catalyst.

Table 3. Catalytic Aerobic Oxidation of the HD Simulant Tetrahydrothiophene (THT) in Liquid Phase by Ce/Au/H₅PV₂Mo₁₀O₄₀ Combinations.^a

Catalyst	Time (h)	Yield % ^b	Turnover ^c
Blank ^d	3.5	0	-
	72 ^e	0	-
1	3.5	0	0
HAuCl ₄	3.5	0	0
	72 ^e	0	0
(NH ₄) ₂ Ce(NO ₃) ₆	3.5	14	12
	72 ^e	26	100
(NH ₄) ₂ Ce(NO ₃) ₆ + 1	3.5	14	12
(NH ₄) ₂ Ce(NO ₃) ₆ + HAuCl ₄	3.5	67	57
	72 ^e	76	293
(NH ₄) ₂ Ce(NO ₃) ₆ + HAuCl ₄ + 1	3.5	65	56
H ₂ PtCl ₆	3	0	0
(NH ₄) ₂ Ce(NO ₃) ₆ + H ₂ PtCl ₆	3	25	21
(NH ₄) ₂ Ce(NO ₃) ₆ + H ₂ PtCl ₆ + 1	3	26	23

^a Reaction conditions: 0.445 mmol (0.64 M) THT and 1,3-dichlorobenzene (internal standard) were stirred in 4 mL of CH₃CN in 20-mL vials under 1 atm O₂ at 25 °C. ^b Moles of THTO / moles of initial THT. ^c Moles of THTO / moles of catalyst. ^d No catalyst. ^e More THT and O₂ were added to the system after 24 hr of reaction.

Supplementary Information for Final Report:

Table S1. List of Catalysts Screened for Combinatorial Library (Figure 1):

Series Number	Compound A	Compound B
1		5 HAuCl ₄
2	Na ₄ PVMo ₁₁ O ₄₀	
3	Na ₄ PVMo ₁₁ O ₄₀	5 HAuCl ₄
4	Na ₅ PV ₂ Mo ₁₀ O ₄₀	
5	Na ₅ PV ₂ Mo ₁₀ O ₄₀	5 HAuCl ₄
6	Na ₆ PV ₃ Mo ₉ O ₄₀	
7	Na ₆ PV ₃ Mo ₉ O ₄₀	5 HAuCl ₄
8	Na ₅ H ₂ PV ₄ Mo ₈ O ₄₀	
9	Na ₅ H ₂ PV ₄ Mo ₈ O ₄₀	5 HAuCl ₄
10	Na ₉ PV ₆ Mo ₆ O ₄₀	
11	Na ₉ PV ₆ Mo ₆ O ₄₀	5 HAuCl ₄
12	Na ₄ PVW ₁₁ O ₄₀	
13	Na ₄ PVW ₁₁ O ₄₀	5 HAuCl ₄
14	Na ₃ PMo ₁₂ O ₄₀	
15	Na ₃ PMo ₁₂ O ₄₀	5 HAuCl ₄
16	Na ₅ CuPW ₁₁ O ₃₉	5 HAuCl ₄
17	(TBA) ₅ CuPW ₁₁ O ₃₉	5 HAuCl ₄
18	Na ₅ MnPW ₁₁ O ₃₉	
19	Na ₅ MnPW ₁₁ O ₃₉	5 HAuCl ₄
20	Na ₅ FeSiW ₁₁ O ₃₉	
21	Na ₅ FeSiW ₁₁ O ₃₉	
22	Na ₅ SiVW ₁₁ O ₄₀	
23	Na ₅ SiVW ₁₁ O ₄₀	5 HAuCl ₄
24	Na ₅ PV ₂ W ₁₀ O ₄₀	
25	Na ₅ PV ₂ W ₁₀ O ₄₀	5 HAuCl ₄
26	Na ₆ PV ₃ W ₉ O ₄₀	
27	Na ₆ PV ₃ W ₉ O ₄₀	5 HAuCl ₄
28	Na ₇ PV ₄ W ₈ O ₄₀	
29	Na ₇ PV ₄ W ₈ O ₄₀	5 HAuCl ₄
30	Na ₁₆ P ₄ W ₃₀ Cu ₄ O ₁₁₂	
31	Na ₁₆ P ₄ W ₃₀ Cu ₄ O ₁₁₂	5 HAuCl ₄
32	H ₂ Na ₁₄ [Fe(III) ₂ (NaH ₂ O) ₂ (P ₂ W ₁₅ O ₅₆) ₂	
33	H ₂ Na ₁₄ [Fe(III) ₂ (NaH ₂ O) ₂ (P ₂ W ₁₅ O ₅₆) ₂	5 HAuCl ₄
34	K ₁₀ Ce(PW ₁₁ O ₃₉) ₂	
35	K ₁₀ Ce(PW ₁₁ O ₃₉) ₂	5 HAuCl ₄
36	K ₇ CuSiW ₁₁ O ₃₉	
37	K ₇ CuSiW ₁₁ O ₃₉	5 HAuCl ₄

38	$K_8CoVW_{11}O_{39}$	
39	$K_8CoVW_{11}O_{39}$	5 $HAuCl_4$
40	$K_5CoPW_{11}O_{39}$	
41	$K_5CoPW_{11}O_{39}$	5 $HAuCl_4$
42	$K_8Co_2W_{11}O_{39}$	
43	$K_8Co_2W_{11}O_{39}$	5 $HAuCl_4$
44	$(NDec_4)_6HMnNb_3P_2W_{15}O_{62}$	
45	$(NDec_4)_6HMnNb_3P_2W_{15}O_{62}$	5 $HAuCl_4$
46	$Na_7CuSiW_{11}O_{39}$	
47	$Na_7CuSiW_{11}O_{39}$	5 $HAuCl_4$
48	$Na_5NiPW_{11}O_{39}$	
49	$Na_5NiPW_{11}O_{39}$	5 $HAuCl_4$
50	$Na_6SiVNbW_{11}O_{39}$	
51	$Na_6SiVNbW_{11}O_{39}$	5 $HAuCl_4$
52	$K_5PMnW_{11}O_{39}$	
53	$K_5PMnW_{11}O_{39}$	5 $HAuCl_4$
54	$K_6SiTiW_{11}O_{40}$	
55	$K_6SiTiW_{11}O_{40}$	5 $HAuCl_4$
56	$K(NH_4)_6RuBW_{11}O_{39}$	
57	$K(NH_4)_6RuBW_{11}O_{39}$	5 $HAuCl_4$
58	$Na_3AsW_{12}O_{40}$	
59	$Na_3AsW_{12}O_{40}$	5 $HAuCl_4$
60	$K_6FeSiW_{11}O_{39}$	
61	$K_6FeSiW_{11}O_{39}$	5 $HAuCl_4$
62	$K_8NiP_2W_{17}O_{61}$	
63	$K_8NiP_2W_{17}O_{61}$	5 $HAuCl_4$
64	$(Me_4N)_{10}(Co_3SiW_9O_{40}H_6)$	
65	$(Me_4N)_{10}(Co_3SiW_9O_{40}H_6)$	5 $HAuCl_4$
66	$K_{10}Co_4P_2W_{18}O_{68}$	
67	$K_{10}Co_4P_2W_{18}O_{68}$	5 $HAuCl_4$
68	$Na_3V_{10}O_{28}$	
69	$Na_3V_{10}O_{28}$	5 $HAuCl_4$
70	$K_{10}(Mn_4)(PW_9O_{34})_2$	
71	$K_{10}(Mn_4)(PW_9O_{34})_2$	5 $HAuCl_4$
72	$K_{12}Cu_3(W_9PO_{34})_2$	
73	$K_{12}Cu_3(W_9PO_{34})_2$	5 $HAuCl_4$
74	$K_{10}Ni_4P_2W_{17}O_{61}$	
75	$K_{10}Ni_4P_2W_{17}O_{61}$	5 $HAuCl_4$
76	$K_8P_2W_{17}(NbO_2)$	
77	$K_8P_2W_{17}(NbO_2)$	5 $HAuCl_4$
78	$(NH_4)_6P_2FeW_{17}O_{61}$	
79	$(NH_4)_6P_2FeW_{17}O_{61}$	5 $HAuCl_4$
80	$K_8Co(II)P_2W_{17}O_{61}$	
81	$K_8Co(II)P_2W_{17}O_{61}$	5 $HAuCl_4$

82	$K_{12}Pd_3(PW_9O_{34})_2$	
83	$K_{12}Pd_3(PW_9O_{34})_2$	5 $HAuCl_4$
84	$K_7Mn(II)P_2W_{17}O_{61}$	5 $HAuCl_4$
85	$K_{10}P_2W_{18}Cu_4O_{68}$	5 $HAuCl_4$
86	$K_8Cu(II)P_2W_{17}O_{61}$	5 $HAuCl_4$
87	$K_5Si(NbO_2)W_{11}O_{40}$	5 $HAuCl_4$
88	$K_{12}P_2W_{18}Ni_3O_{68}$	5 $HAuCl_4$
89	$Na_3H_6Mo_9O_{34}$	5 $HAuCl_4$
90	$Na_6P_4W_{30}Mn(II)_4O_{112}$	5 $HAuCl_4$
91	$(NH_4)_6P_2W_{18}O_{62}+5HAuCl_4$	5 $HAuCl_4$
92	$(NH_4)_{17}Na(NaSb_9W_{21})O_{86}$	5 $HAuCl_4$
93		5 $Cu(acetate)_2$
94	$Na_5PV_2Mo_{10}O_{40}$	5 $Cu(acetate)_2$
95		5 $Co(II)Acac$
96	$Na_5PV_2Mo_{10}O_{40}$	5 $Co(II)Acac$
97		5 $Fe(III)Acac$
98	$Na_5PV_2Mo_{10}O_{40}$	5 $Fe(III)Acac$
99		5 MnO_2
100	$Na_5PV_2Mo_{10}O_{40}$	5 MnO_2
101		5 $CuCl_2$
102	$Na_5PV_2Mo_{10}O_{40}$	5 $CuCl_2$
103		5 $FeCl_3$
104	$Na_5PV_2Mo_{10}O_{40}$	5 $FeCl_3$
105		5 $CrCl_3$
106	$Na_5PV_2Mo_{10}O_{40}$	5 $CrCl_3$
107		5 $CeCl_3$
108	$Na_5PV_2Mo_{10}O_{40}$	5 $CeCl_3$
109	$Na_9PV_6Mo_6O_{40}$	5 $FeCl_3$
110	$Na_9PV_6Mo_6O_{40}$	5 $CuCl_2$
111	$Na_9PV_6Mo_6O_{40}$	
112	$K_{12}Pd_3(PW_9O_{36})_2$	5 $FeCl_3$
113	$K_{12}Pd_3(PW_9O_{36})_2$	5 $CuCl_2$
114	$K_{12}Pd_3(PW_9O_{36})_2$	
115	$Na_5CuPW_{11}O_{39}$	
116	$Na_5CuPW_{11}O_{39}$	5 $Cr(NO_3)_3$
117		5 $CrNO_3$
118	$Na_5CuPW_{11}O_{39}$	5 $Co(NO_3)_2$
119		5 $Co(NO_3)_2$
120		5 $Zn(NO_3)_2$
121	$Na_5CuPW_{11}O_{39}$	5 $Zn(NO_3)_2$
122	$Na_5CuPW_{11}O_{39}$	5 $Cu(NO_3)_2$
123		5 $Cu(NO_3)_2$
124	$Na_5CuPW_{11}O_{39}$	5 $Zn(NO_3)_3$
125	$Na_5CuW_{11}O_{39}$	5 $Cu(acetate)_2$

126	$\text{Na}_5\text{CuW}_{11}\text{O}_{39}$	5 $\text{Fe}(\text{acetate})_2$
127	$\text{Na}_5\text{CuW}_{11}\text{O}_{39}$	5 MnO_2
128		5 NaNO_3
129	$\text{Li}_5\text{PVW}_{11}\text{O}_{40}$	5 HAuCl_4
130	AgNO_3	
131	AgNO_3	5 HAuCl_4
132	NaNO_3	5 HAuCl_4
133	NaClO_4	5 HAuCl_4
134	AgClO_4	5 HAuCl_4
135	LiClO_4	5 HAuCl_4
136		5 $(\text{NH}_4)_2\text{Ce}(\text{NO}_3)_6$
137	$\text{Na}_5\text{PVMo}_{11}\text{O}_{40}$	5 $(\text{NH}_4)_2\text{Ce}(\text{NO}_3)_6$
138	$\text{Na}_5\text{CuPW}_{11}\text{O}_{39}$	5 $(\text{NH}_4)_2\text{Ce}(\text{NO}_3)_6$
139	$\text{Na}_5\text{PVMo}_{11}\text{O}_{40}$	5 CoSO_4
140	$\text{Na}_5\text{CuPW}_{11}\text{O}_{39}$	5 CoSO_4
141	$\text{Na}_5\text{PVMo}_{11}\text{O}_{40}$	5 $\text{Ce}(\text{SO}_4)_2$
142	$\text{Na}_5\text{CuPW}_{11}\text{O}_{39}$	5 $\text{Ce}(\text{SO}_4)_2$
143	$\text{Na}_5\text{PVMo}_{11}\text{O}_{40}$	5 H_2PtCl_6
144	$\text{Na}_5\text{CuPW}_{11}\text{O}_{39}$	5 H_2PtCl_6
145	$\text{Na}_5\text{PVMo}_{11}\text{O}_{40}$	5 $\text{Pd}(\text{NO}_3)_2$
146	$\text{Na}_5\text{CuPW}_{11}\text{O}_{39}$	5 $\text{Pd}(\text{NO}_3)_2$
147	$\text{Na}_5\text{PVMo}_{11}\text{O}_{40}$	5 RhCl_3
148	$\text{Na}_5\text{CuPW}_{11}\text{O}_{39}$	5 RhCl_3
149	$\text{Na}_5\text{PVMo}_{11}\text{O}_{40}$	5 ReO_2
150	$\text{Na}_5\text{CuPW}_{11}\text{O}_{39}$	5 ReO_2

STAS Final report from Emory University, Dr. Craig Hill

Award Number: DAAH04-96-C-0086, TCN 01-125

REPORT DOCUMENTATION PAGE

Form Approved
OMB NO. 0704-0188

Public Reporting burden for this collection of information is estimated to average 1 hour per response, including the time for reviewing instructions, searching existing data sources, gathering and maintaining the data needed, and completing and reviewing the collection of information. Send comment regarding this burden estimates or any other aspect of this collection of information, including suggestions for reducing this burden, to Washington Headquarters Services, Directorate for information Operations and Reports, 1215 Jefferson Davis Highway, Suite 1204, Arlington, VA 22202-4302, and to the Office of Management and Budget, Paperwork Reduction Project (0704-0188,) Washington, DC 20503.

1. AGENCY USE ONLY (Leave Blank)

2. REPORT DATE
Nov. 19, 2002

3. REPORT TYPE AND DATES COVERED
FINAL REPORT From 9/18/01 to 10/31/02

4. TITLE AND SUBTITLE

Coinage-Metal Complexes for Catalytic Air-Based Ambient-Temperature Decontamination in Topical Skin Protectants

5. FUNDING NUMBERS

Contract DAAH04-96-C-0086

6. AUTHOR(S)

Craig L. Hill

7. PERFORMING ORGANIZATION NAME(S) AND ADDRESS(ES)

Emory University Dept. of Chemistry
1515 Pierce Dr.
Atlanta, GA 30322

8. PERFORMING ORGANIZATION

REPORT NUMBER
Delivery Order 791

9. SPONSORING / MONITORING AGENCY NAME(S) AND ADDRESS(ES)

U. S. Army Research Office
P.O. Box 12211
Research Triangle Park, NC 27709-2211

10. SPONSORING / MONITORING

AGENCY REPORT NUMBER
TCN 01125

11. SUPPLEMENTARY NOTES

Task was performed under a Scientific Services Agreement issued by Battelle, Research Triangle Park Office, 200 Park Drive, PO Box 12297, Research Triangle Park, NC 27709

12 a. DISTRIBUTION / AVAILABILITY STATEMENT

May not be released by other than sponsoring organization without approval of US Army Research Office

12 b. DISTRIBUTION CODE

13. ABSTRACT (Maximum 200 words)

Au(III)Cl(R₂S)²⁺-based systems, NO₃⁻/CuY₂ (Y = weakly coordinating ligand, e.g. triflate) systems, some multi-iron polyoxometalates (POMs), and POMs bound to cationic silica nanoparticles all catalyze the rapid oxidative decontamination of HD or its simulant CEES by O₂/air under ambient conditions. The features (active intermediates, structure-activity information) and the mechanism of the Au(III)Cl(R₂S)²⁺-based systems have now been thoroughly elucidated. Many of the features of the highly tunable NO₃⁻/CuY₂ systems have been established. At present little is known about the other systems and thus their catalytic decontamination chemistry hasn't been optimized. Activity against G agents hasn't been significantly studied yet. Some systems should be catalytically active against HD, GB/GD and, by virtue of combined hydrolysis and air-based thiol oxidation chemistry, VX as well.

14. SUBJECT TERMS

15. NUMBER OF PAGES
8 (including this one)

16. PRICE CODE

17. SECURITY CLASSIFICATION
OR REPORT

UNCLASSIFIED

18. SECURITY CLASSIFICATION
ON THIS PAGE

UNCLASSIFIED

19. SECURITY CLASSIFICATION
OF ABSTRACT

UNCLASSIFIED

20. LIMITATION OF ABSTRACT

UL

NSN 7540-01-280-5500

Standard Form 298 (Rev.2-89)
Prescribed by ANSI Std. Z39-18
298-102

Final report

Title of grant: Coinage-Metal Complexes for Catalytic Air-Based Ambient-Temperature Decontamination in Topical Skin Protectants

Report by:

Principal Investigator: Craig L. Hill, Goodrich C. White Professor, Department of Chemistry, Emory University, Atlanta, GA 30322; phone: 404-727-6611; E-mail: chill@emory.edu

U.S. Army (USAMRICD); administered by Battelle

DAAH04-96-C-086
TCN 01125, D.O. 0791

Goal: To develop *catalytically active* additives for active topical skin protectants (aTSPs), skin creams designed to function both as a protective barrier and as an active destructive matrix against chemical warfare agents (CWAs). Good leads are to be evaluated against live agent in various protocols by our USAMRICD collaborators (Drs. Braue and Hobson) or their colleagues. Since many of our complexes function catalytically, significantly less of them should be needed than the effective but stoichiometric reagents currently used in rTSPs as HD oxidants: 1,3,4,6-tetrachloro-7,8-diimino glycouril ("S-330") and iodobenzene diacetate ("IBDA"). Furthermore, the Au/Ag/Cu-O₂ systems are far milder agents (far less thermodynamically oxidizing and effectively pH neutral) than either S-330 or IBDA and are thus likely to be significantly better tolerated on the skin, than the latter stoichiometric oxidants. They are also indefinitely stable.

Summary: A three-year research program and statement of work were originally outlined. However, the funding was for 1 year with a brief no-cost extension. Within this limitation, much has been accomplished. Key findings: (1) The mechanism of the Au(III)Cl(R₂S)²⁺-based systems that rapidly and catalytically degrade HD (and CEES) using O₂/air were thoroughly elucidated. This is important because many of the findings in this work carry over to our other decon systems in current development. These include Cu- and Ag-based systems as well as the coinage metal (Cu, Ag, and Au) salts of polyoxometalates (POMs). (2) Binary systems comprised of a NO₃⁻ salt and a Cu(II) complex with weakly bound ligands (e.g. triflate, tetrafluoroborate, etc.) were found to be highly active in the oxidative decontamination of HD using air. (3) Two other types of catalysts with considerable promise for CWA decontamination were developed but have not yet been extensively investigated: multi-iron-containing polyoxometalates (POMs) and POMs bound to cationic silica nanoparticles. Both types of material catalyze air-based CEES oxidation in the absence of Cu complexes or other activators or co-catalysts. (The presence of such co-catalysts, however, accelerates air-based decon). (5) Although some of our catalysts have shown activity for the hydrolysis of G agents, and Cu(II) complexes of many kinds catalyze the hydrolysis of phosphonate esters (such as GB, GD and VX), we have not studied this kind of reactivity significantly and thus have not optimized it.

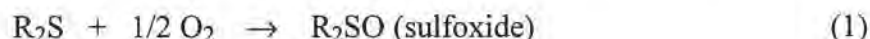
Proposed research:

The grant proposed experiments in three complementary directions: (1) further investigation of the original Au(III)Cl₂NO₃(thioether)/O₂/CEES system, because data generated therefrom was

deemed likely to yield additional fundamental insights of direct value in optimizing these systems for use in aTSPs; (2) exploratory work using combinatorial and multifactorial approaches with our currently active coinage-metal-based catalysts as starting points; and (3) investigation of coinage metal-fluorocarbon systems, particularly metal catalysts dissolved or suspended in perfluoropolyethers (PFPEs).

All three areas were addressed in the last year. The findings are now elaborated.

1. Understanding the Au(III)Cl(R₂S)²⁺-based catalysts for aerobic (air-based) HD decontamination. The principal chemistry of the prototype system for CEES and HD oxidative decontamination (selective sulfoxidation), Au(III)Cl₂NO₃(thioether)/O₂, was reported in the initial paper published just prior to the start of this grant.¹ This publication established the stoichiometry of the reaction is that given in eq 1. This is the desired reaction, because the sulfoxide of HD is far less toxic than HD or the sulfone, and also because the reaction proceeds by a dioxygenase stoichiometry (both atoms of O₂ end up in the desired product; no by-products are generated).



This paper also provided extensive structure-activity data, kinetics, and other information that defined the mechanism fairly well, including the nature of key active intermediates. A second paper on work just prior to the start of the grant was published about a year ago.² This paper reported the effects several variables on the rate for catalytic aerobic CEES sulfoxidation. The abstract of this article, which follows immediately, outlines these findings.

Abstract. The complexes Au(III)(Hal)₂(NO_x)(L), Hal = Cl⁻ or Br⁻, NO_x = NO₃⁻ or NO₂⁻, L = thioether, catalyze the selective aerobic sulfoxidation of thioethers, including the mustard simulant 2-chloroethyl ethyl sulfide (CEES), by dioxygen (stoichiometry: CEES + 0.5O₂ → CEESO) under ambient conditions (25 °C, 1 atm O₂) in both homogeneous solution (acetonitrile, trifluoroethanol, nitromethane, 1,2-dichloroethane) or non-toxic perfluoropolyether (PFPE) suspensions. The reaction rate, induction period, and the extent of product inhibition are dependent on the Au(III) ligands, the solvent, and the presence of additional redox active metals. This reaction in trifluoroethanol exhibits no induction period and is 2.8 times faster than in acetonitrile. Addition of 2 equivalents of Cu(II) per Au(III) to the system increases the rate by a factor of 2.7. The Au(III)/Br_n/NO₃⁻/Cu(II) system exhibits high rates for the selective aerobic oxidation of CEES to CEESO under ambient conditions (~68 turnovers per hour), with little if any inhibition by the CEESO product. At low concentrations, sulfoxides reduce the induction period and increase the rate of CEES oxidation in acetonitrile, but at high concentrations they inhibit the reaction. These Au(III) catalysts are extremely efficient for aerobic CEES sulfoxidation when suspended in the PFPE Fomblin® MF-300 (up to 200 turnovers in 10 min). This is a significant improvement from the Au system described in the first study, Au(III)(Cl)₂(NO₃)(CEES) in acetonitrile, which yielded approximately 5 turnovers of CEESO after 10 min. The catalytic reactivity of the Au(III)(Cl)₂(NO₃)(L) in Fomblin® MF-300 for aerobic CEES oxidation was evaluated in the presence of the common amino acids to assess the extent to which the various functional groups in human skin (epidermal polypeptides) might inhibit the catalysis. Some amino acids inhibit the reaction, but the reaction still proceeds even in the presence of 7.5 equiv. of the most inhibitory functional group, indole (tryptophan).

Since the start of the grant, additional aspects of this chemistry were clarified. A lengthy chapter on this chemistry in a book "Catalytic Activation of Dioxygen" will be published very shortly.³ The following abstract of this work succinctly summarizes the findings:

Abstract. Diversity-based methods for catalyst discovery coupled with the knowledge of lead systems for the catalysis of O₂-based organic oxidation reactions has led to the development of new species that actually catalyze rapid and selective (non-radical-chain), reductant-free, O₂ oxidation under ambient conditions (room temperature and 1.0 atmosphere of air). The first process of focus is selective sulfoxidation of thioethers (organic sulfides). The principal work reviewed here involves homogeneous catalysis, but highly reactive heterogeneous formulations have already been identified. The stoichiometry is that characteristic of dioxygenase enzymes: R₂S (thioether) + 1/2 O₂ → R₂S(O) (sulfoxide). Oxidative dehydrogenation, a less desirable net process, is not seen. Studies have primarily been conducted with 2-chloroethyl ethyl sulfide (CEES), which is both notoriously unreactive and a useful simulant for mustard. Extensive kinetics and product studies have identified the active catalyst, at least in acetonitrile solution, to be Au(III)Cl₂NO₃(thioether) (**1**), and the rate limiting step to be reaction of **1** with another molecule of the thioether substrate. Reoxidation of the resulting Au(I) to Au(III) by O₂ is a fast subsequent step. The solvent kinetic isotope effect ($k_{\text{H}_2\text{O}}/k_{\text{D}_2\text{O}} = 1.0$), rate of sulfoxidation when Cl is replaced by Br, and multiparameter fitting of the kinetic data establish that the mechanism of the rate-limiting step itself involves a bimolecular attack of CEES on a Au(III)-bound halide and it does not involve H₂O. Isotope labeling studies with H₂¹⁸O indicate that H₂O and not O₂ or H₂O₂ is the source of oxygen in the sulfoxide product. Interestingly, H₂O is consumed and subsequently regenerated in the mechanism. Despite the impressive (unique) reactivity attributes above, these recently developed catalytic systems have some limitations that include an induction period and inhibition by sulfoxide product. However, these two difficulties are eliminated in other solvents or in nontoxic developmentally attractive perfluoropolyether (PFPE) media. Another potential problem, is catalyst inactivation by precipitation of the Au as colloidal Au(0), but this can be largely avoided by use of appropriate reaction conditions. Finally, these Au-catalyzed aerobic sulfoxidation reactions can be co-catalyzed by some d-block ions. Cu(II) is particularly effective in this context resulting in severalfold increases in reaction rate at low Cu(II) concentrations. Co-catalysis by the d-block ions also results in elimination of the induction period in some cases.

Additional features of this chemistry have been identified in the last few months. These include the fact that a co-catalytic system based on nitrate/nitrite is also involved. This system alone catalyzes air-based sulfoxidation of sulfides, including CEES, at room temperature.

2. NO₃⁻/CuY₂ (Y = weakly coordinating ligand) Catalysts. Just prior to the start of the grant, we discovered that a combination of nitrate (almost any salt works) and some Cu(II) salts catalyze the rapid and selective air-based sulfoxidation of CEES. During the grant, the scope and key features of this chemistry were established. In the early months it was determined that only Cu complexes with weakly bound ligands such as perchlorate, tetrafluoroborate and triflate were effective; complexes with more conventional and more strongly binding ligands such as chloride, etc. were far less active or completely inactive, at least using air at ambient temperature. Many informative data (samples and controls) are presented in the Table 1 below.

Table 1. Aerobic oxidation of 2-chloroethyl ethyl sulfide (CEES) in fluorinated fluids and other solvents by Cu(II)-based catalysts^a

Catalyst ^b	Solvent	% conv. ^c	$-(d[\text{CEES}]/dt)$ ($10^5, \text{mmol s}^{-1}$) ^d
CuCl ₂	PFPE ^e	0.00	0.00
CuSO ₄	PFPE ^e	0.00	0.00
Cu(NO ₃) ₂	PFPE ^e	0.50	0.13
Cu(BF ₄) ₂	PFPE ^e	0.44	0.11
Cu(ClO ₄) ₂	PFPE ^e	0.61	0.15
Cu(OTf) ₂	PFPE ^e	0.85	0.21
CuCl ₂ /TBANO ₃	PFPE ^e	3.20	0.80
CuSO ₄ /TBANO ₃	PFPE ^e	5.30	1.30
Cu(BF ₄) ₂ /TBANO ₃	PFPE ^e	33.50	8.13
Cu(ClO ₄) ₂ /TBANO ₃	PFPE ^e	46.30	11.30
Cu(OTf) ₂ /TBANO ₃ (Cu/OTf/NO ₃ ⁻)	PFPE ^e	53.00	12.90
Cu/OTf/NO ₃ ⁻	CH ₃ CN	26.50	6.45
Cu/OTf/NO ₃ ⁻	MeOH	0.00	0.00
Cu/OTf/NO ₃ ⁻	EtOH	0.00	0.00
Cu/OTf/NO ₃ ⁻	acetone	0.00	0.00
Cu/OTf/NO ₃ ⁻	TFE ^f	0.00	0.00
Cu(BF ₄) ₂ /TBANO ₃ ^g	PFPE ^g	38.50	9.40
Cu(ClO ₄) ₂ /TBANO ₃ ^g	PFPE ^g	53.30	13.00
Cu/OTf/NO ₃ ⁻	PFPE ^g	61.50	15.00

^aGeneral conditions: 0.875 mmol (0.35 M) of CEES, 1 atm of air, 0.876 mmol (0.35 M) of 1,3-dichlorobenzene (internal standard) were stirred in 2.5 mL of solvent at 25 °C for 1 h; ^b0.09 mmol (0.036 M) of individual Cu(II) salt or 0.05 mmol of Cu²⁺ cations, 0.10 mmol of counter anions (ClO₄⁻, OTf⁻, BF₄⁻, NO₃⁻, Cl⁻ or SO₄²⁻) and 0.04 mmol of NO₃⁻ anions in composition; no product was observed in the absence of Cu(II) salts (for example in the presence of only TBAX, X = ClO₄⁻, OTf⁻, BF₄⁻, NO₃⁻, Cl⁻ or SO₄²⁻); ^c% conversion = (moles of CEES consumed / moles of initial CEES) x 100; ^dreaction (conversion) rate = mmol of CEES consumed / s; ^e96% Fomblin[®] (MD-300)/4% CH₃CN (4% CH₃CN used to insure solubility); ^fTrifluoroethanol; ^g96% Fluorolink[™] (7004)/4% CH₃CN.

Figure 1 below (catalytic oxidation of CEES by the $\text{Cu}(\text{NO}_3)_2\text{-Cu}(\text{OTf})_2/\text{air}$ system as a function of the concentration of nitrate) illustrates the accelerating affect of nitrate. This acceleration effect varies with the medium. Some nitrate-free systems are fairly fast.

Figure 2 illustrates the accelerating effect of a PFPE medium.

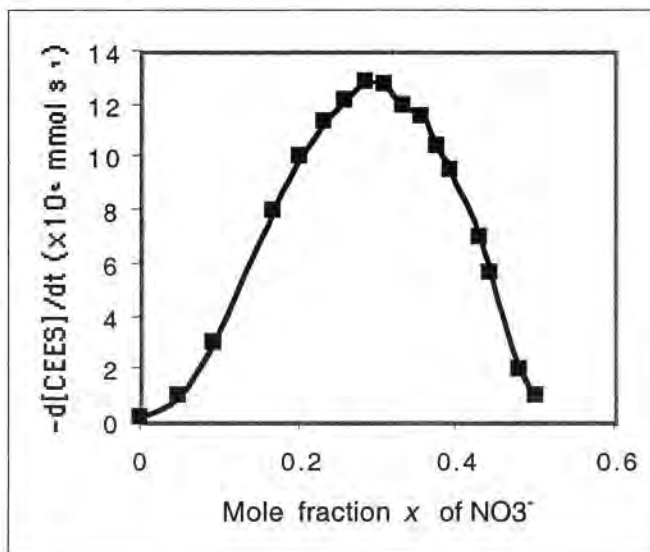


Figure 1. Rate of CEES sulfoxidation by air catalyzed by the $\text{Cu}(\text{NO}_3)_2\text{-Cu}(\text{OTf})_2$ system in perfluoropolyether (PFPE) media as a function of the mole fraction of nitrate (relative to all anionic ligands present).

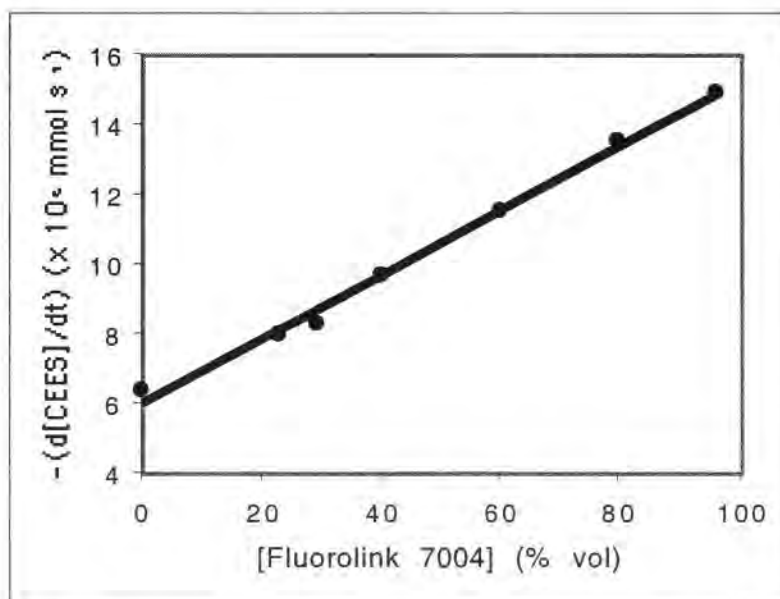


Figure 2. Rate of CEES sulfoxidation by air catalyzed by the $\text{Cu}(\text{NO}_3)_2\text{-Cu}(\text{OTf})_2$ system as a function of the mole fraction of PFPE (specifically “Fluorolink”) in acetonitrile.

3. Coinage metal salts of POMs. An initial effort in this area (just published as this grant started)⁴ was quite promising. This involved preparation of the silver salt of $PV_2Mo_{10}O_{40}^{5-}$, a much used POM that can be easily prepared in quantity. The actual complex (formula: $Ag_5PV_2Mo_{10}O_{40}$) was characterized by X-ray crystallography, NMR and elemental analysis in addition to other techniques. This microporous material is a powder that can be easily dispersed in PFPE media. As a totally unoptimized low-surface area solid, it catalyzes CEES oxidation by air at room temperature. The lack of time has precluded significant further work on these systems. However, since both the cations, and independently, the POM anions can be extensively varied and the surface area of these powders can very likely be increased 1-2 orders of magnitude without Herculean efforts, this area holds promise.

4. Fe-containing POMs. Recently new multi-iron-containing POMs have been prepared in our laboratory that appear to be the most active POM-based catalysts yet for air-based CEES oxidation in the absence of Cu salts or nitrate. They are more reactive still in the presence of the latter co-catalysts. We are in the early stages of this work.

5. Other systems. In the course of the proposed catalyst discovery and evaluation protocols, we found that certain POMs when supported on cationic silica nanoparticles become activated as oxidation catalysts.⁵ These nanoparticles appear to disperse readily in TSP (PFPE) media. One POM-catalyzed oxidation that is greatly accelerated is $CEES + O_2 \rightarrow CEESO$. Another is thiol oxidation by air/ O_2 . This is significant because VX hydrolysis involves generation of a thiol (2-*N,N*-diisopropylaminoethane-1-thiol), but this process is reversible. However, if the thiol were to be rapidly oxidized precluding back reaction, then the hydrolytic decontamination chemistry of VX should be greatly improved in general. This is also an exciting finding. Some preliminary work on activation of a POM for aerobic oxidation of sulfides has been submitted for publication.⁵

6. Some concluding thoughts on these various systems as catalytic additives for TSPs. At present, excellent activity against HD by several of our catalysts has been found in penetration cells tests. The 2 or 3 catalysts tested against GD in the pig model didn't show promise (erythema was similar to control), but these compounds weren't targeted for GD decon chemistry. It would be of interest to investigate the potency of our thiol oxidizing systems against VX, but this is problematical because VX simulants aren't readily available. It would also be of considerable interest to evaluate the catalytic decontamination efficacy of salts made from a cationic Cu, Ce and Zr complexes and anionic POMs. Some cationic Cu(II) species are known to be excellent hydrolysis catalysts of the nerve agents and some simple Ce(IV) and Zr(IV) compounds may be even better; POMs are the best catalysts for air-based HD decontamination. It should be possible to prepare a range of such Cu/Ce/Zr POM salts. Simultaneous rapid catalytic decontamination of GB/CD, VX and HD should be attainable by optimization of the proper components. It is too early at present to assess the promise of the new multi-iron POMs with or without co-catalysts as aTSP additives. It is also too early to assess the use of cationic nanopowders for catalyst activation in conjunction with this general program.

References

1. Boring, E.; Gueletii, Y.; Hill, C. L. "A Homogeneous Catalyst for Selective O₂ Oxidation at Ambient Temperature. Diversity-Based Discovery and Mechanistic Investigation of Thioether Oxidation by the Au(III)Cl₂NO₃(thioether) / O₂ System." *J. Am. Chem. Soc.* **2001**, *123*, 1625-1635. (Write-up in March 5 issue of *Chemical and Engineering News*, **2001**, *79*, 5) Also cited by the editors of *Chemical and Engineering News* in their year-end summary of "the most significant scientific achievements of 2001" (cover story by S. Borman, December 10, 2001 issue of *Chemical and Engineering News*, **2001**, *79*, 45-55).
2. Boring, E.; Gueletii, Y.; Hill, C. L. "Catalytic aerobic oxidation of 2-chloroethyl ethyl sulfide (CEES), an HD simulant, under ambient conditions. Effect of solvents, ligands, and transition metals on reactivity" *J Mol. Cat. A, Chem.* **2001**, *176*, 49-63.
3. Boring, E.; Geletii, Y.; Hill, C. L. "Catalysts for Selective Aerobic Oxidation under Ambient Conditions. Thioether Sulfoxidation Catalyzed by Gold Complexes" In "Catalytic Activation of Dioxygen" Simandi, L. I., Ed.; Kluwer: Dordrecht, The Netherlands, 2002, in press.
4. Rhule, J. T.; Neiwert, W. A.; Hardcastle, K. I.; Do, B. T.; Hill, C. L. "Ag₅PV₂Mo₁₀O₄₀, a Heterogeneous Catalyst for Air-Based Selective Oxidation at Ambient Temperature" *J. Am. Chem. Soc.* **2001**, *123*, 12101-12102.
5. Okun, N. M.; Anderson, T. M.; Hill, C. L. "[Fe^{III}(OH₂)₂)₃(A-α-PW₉O₃₄)₂]⁹⁻ on Cationic Silica Nanoparticles, a New Type of Material and Efficient Heterogeneous Catalyst for Aerobic Oxidations." *J. Am. Chem. Soc.* **2003** Submitted.

STAS Final report from University of California at Irvine, Dr. Kenneth Shea

Award Number: DAAH04-96-C-0086, TCN 00-089

SHORT TERM ANALYSIS SERVICE (STAS)

FINAL REPORT

on

Development of Hybrid Organic Bridged Polysilsesquioxanes
As Reactants for Reactive Topical Skin Protectants (rTSP's)

by

Dr. Kenneth Shea
University of California, Irvine
5042D Frederick Reines Hall
Irvine, CA 92697-2025

for

U.S. Army Medical Research Institute
of Chemical Defense
3100 Ricketts Point Road
Aberdeen Proving Ground, MD 21010-5425

31 May 2003

Contract No. DAAH04-96-C-0086
TCN 00089/D.O. 0592
Scientific Services Program

The views, opinions, and/or findings contained in this report are those of the author and should not be construed as an official Department of the Army position, policy, or decision, unless so designated by other documentation.

Final Report for STAS contract
with Dr. Ken Shea at UC Irvine
Date 20 Jun 2003

**Sulfur Containing Bridged Polysilsesquioxanes: Synthesis and Characterization of
High Capacity Adsorbents for CW Agents.**

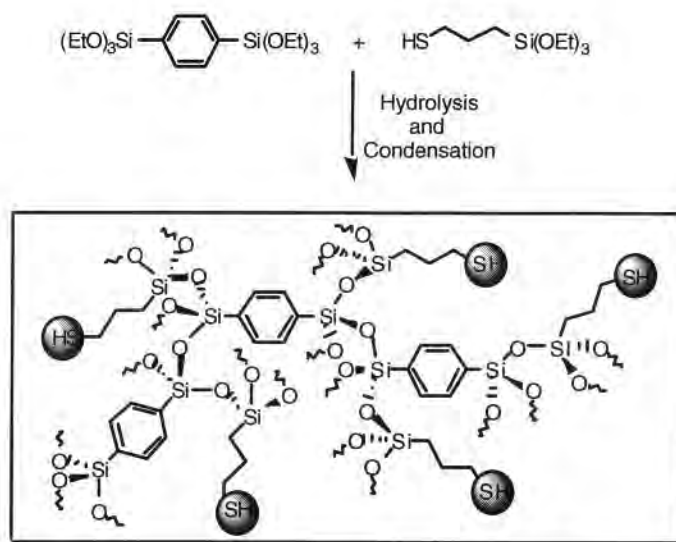
Stephen T. Hobson,¹ Joseph A. Tran, Kristine Muroya, and Kenneth J. Shea

Department of Chemistry, University of California, Irvine, Irvine CA 92697-2025

Hybrid materials are versatile substances that have a range of properties attainable from varying the organic and inorganic components. We will provide the U. S. Army with multigram quantities of mercaptopropyl functionalized bridged polysilsesquioxanes. These materials will be used for testing as a barrier and detoxifying agent against chemical warfare substances including mustard gas. These materials have high internal surface areas and high loadings of chemically active thiol functional groups. We will provide the Army with sufficient quantities to evaluate these materials against actual CW agents. The specific tasks will include (a) the synthesis of sol-gel polymerizable monomers that are used as starting materials for the materials synthesis. This step requires synthetic organic transformations under controlled reaction conditions. The products from these reactions must be isolated, purified then characterized by analytical and spectroscopic techniques. The next phase (2) involves the sol-gel polymerization and processing of the monomers. This step produces the materials that will be used for testing. To insure the identity, purity and correct properties of the material, the final stage (3) of our work involves spectroscopic characterization of the material (solid state NMR, FT-IR) as well as surface area analysis. All of these tasks will make use of the facilities and infrastructure of the University of California, Irvine.

To this end, we have prepared functionalized hybrid inorganic-organic materials with reactive thiol functional groups with high ligand loading. The thiol group was

chosen because of its high reactivity against electrophilic CW agents such as mustards. The reactive thiol groups are immobilized as part of a porous solid matrix removing any potential toxicity associated with the material or unpleasant odor. These materials are made from copolymerization of 1,4-bis(triethoxysilyl)benzene and 3-mercaptopropyltriethoxysilane (Scheme 1).



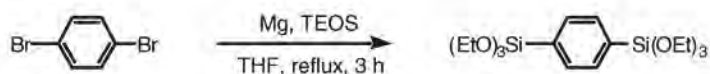
Scheme 1. Illustration of amorphous functionalized bridged polysilsesquioxane

This novel hybrid polymer allows the incorporation of the functional ligand within the pore structure, as well as, on the surface of the material. The ligand loadings that are achieved with this method can be varied and can be as high as 5.8 mmole of ligand per gram of adsorbent. This loading capacity is a significant improvement over the loading capacity of the functionalized highly ordered silicate materials. Optimization of the polymerization and processing conditions will allow design mechanically robust materials with high surface area and porosity and exceptionally high loading of reactive functionality .

Results and Discussion

Synthesis

Synthesis of 1,4-bis(triethoxysilyl)benzene was achieved under Barbier Grignard conditions using 1,4-dibromobenzene and tetraethylorthosilicate (TEOS), shown in Scheme 2.

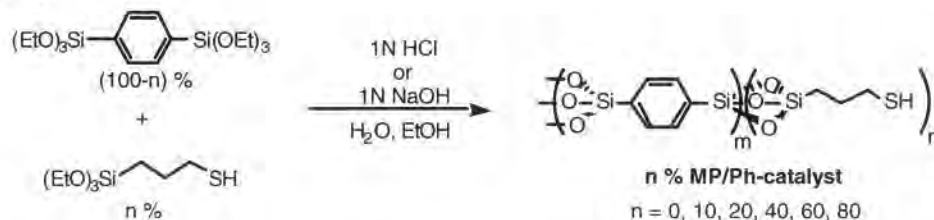


Scheme 2. Preparation of 1,4-Bis(triethoxysilyl)benzene

The monomer was isolated by high vacuum distillation in yields ranging from 43-47% (literature 55%). The by-product of the reaction resulted from double additions of the Grignard with TEOS. This by-product was not isolated.

Thiol Doped Polysilsesquioxanes

Sol-gel materials containing 3-mercaptopropyltriethoxysilane and 1,4-bis(triethoxysilyl)benzene were prepared under both acid and base catalyzed conditions. The gels were made at a total monomer concentration of 0.4M and water processed (Scheme 3).



Scheme 3. Mercaptopropylene doped/Phenylene Polysilsesquioxane

*MP = Mercaptopropyltriethoxysilane, Ph = 1,4-bis(triethoxysilyl)benzene, A = Acid or B = Base catalyzed

Both acid and base catalyzed materials were made in order to examine the effects of the catalyst on material properties. The gelation times for the various gels are shown in Table 1,

Sol-Gel Materials	Gelation Times	Sol-Gel Materials	Gelation Times
100% PH-A	2 days	100% PH-B	2 hrs
10% MP/Ph-A	5 days	10% MP/Ph-B	2 hrs
20% MP/Ph-A	7 days	20% MP/Ph-B	2 hrs
40% MP/Ph-A	1 month	40% MP/Ph-B	2 hrs
60% MP/Ph-A	no gel	60% MP/Ph-B	2 hrs
80% MP/Ph-A	no gel	80% MP/Ph-B	2 days

Table 1. Gelation times for various mercaptopropyltriethoxysilane doped/phenylene bridged materials. The descriptors A or B refer to acid or base catalyst. Fractional percentages refer to mole % mercaptopropyltriethoxysilane in the copolymerization mixture. Top two entries are pure phenylene polysilsesquioxane.

In general, the base catalyzed materials gelled within several hours to several days even at high mercaptopropyltriethoxysilane loading. In contrast, the acid catalyzed gels were slow to react and gelation times took several days to months. The acid catalyzed gels with high loadings of mercaptopropyltriethoxysilane (60% and 80%) did not gel after many months. All materials that gelled were aged for at least 48 hrs the "water processed", that is, crushed and soaked in water for 24 hrs then air dried. Following through drying under high vacuum at 100°C, the materials were characterized by nitrogen adsorption porosimetry.

Surface Area & Porosity

Nitrogen adsorption porosimetry analyses were performed on acid and base catalyzed 3-mercaptopropylsilane doped samples. Analysis of the acid catalyzed mercaptopropyltriethoxysilane doped/phenylene materials showed these materials to be essentially non-porous at high ligand loadings (Table 2).

Acid Cat. Materials (STH)	Surface Area (m ² /g)	Avg. Pore Diameter (Å)	Total Pore Vol. (cc/g)
100% Ph-A	527	22	0.29
10% MP/Ph-A	239	23	0.14
40% MP/Ph-A	6	-	0.02
60% MP/Ph-A	8	-	0.02

* surface area and pore diameter calculated using BET method and nitrogen as the adsorbate

Table 2. Surface area and porosity of MP doped/Ph acid catalyzed materials

The materials with higher ligand loadings of thiol groups (40% MP/Ph-A & 60% MP/Ph-A) would obviously be the most desirable as absorbents due to their potential for higher uptake. However, these materials lack porosity which can limit accessibility of the substrate with the mercaptopropyl ligands. (see Hg²⁺ uptake section).

In contrast to the acid catalyzed materials, the base catalyzed mercaptopropyltriethoxysilane doped/phenylene materials displayed high surface areas and porosity (Table 3). Interestingly, for pure phenylene materials the acid catalyzed polysilsesquioxanes are usually more porous than the base catalyzed materials.²

Base Cat. Materials (JAT)	Surface Area (m ² /g)	Avg. Pore Diameter (Å)	Total Pore Vol. (cc/g)
20% MP/Ph-B	928	32	0.73
40% MP/Ph-B	848	36	0.73

60% MP/Ph-B	707	51	0.91
80% MP/Ph-B	449 (443)	96 (58.2)	1.08 (0.64)

Table 3. Surface area and porosity of MP doped/Ph base catalyzed materials

The surface area analysis of the base catalyzed series showed that sol-gel materials could be made with high ligand loadings without sacrificing surface area and porosity. Especially noteworthy is that even at 80% ligand loading, a mesoporous sol-gel material formed in about one day. In comparison, 100% mercaptopropyltriethoxysilane does not form a gel under these conditions. Therefore a key determinant of the materials' bulk properties can be attributed to the phenylene bridged moiety.

A noticeable trend in the base catalyzed series was a corresponding decrease in surface area with increasing ligand loading. However, with the decrease in surface area, there was an increase in pore diameter. Furthermore, in all cases, including materials with the highest loading of mercaptopropyl groups, the internal pore volumes were substantial. This is important for mass transport which influences the rate of uptake. The trend of decreasing surface area may be the result of a greater compliance of the network resulting from an effective decreased crosslinking with higher loading of mercaptopropyltriethoxysilane. This in turn can cause collapse of the pore network during polymerization and processing.

Hg⁺² Adsorption Studies

The facilities at UCI do not permit the use of real CW agents. Nevertheless, it was important to evaluate accessibility of the thiol groups and the capacity of these materials for taking up electrophilic substances. To this end we examined their capacity to take up Hg²⁺ ions from an aqueous solution.

Mercury adsorption studies were conducted on various MP doped/phenylene materials. Mercury(II) nitrate in water was used as the Hg⁺² source. The experiment required taking 10 mg portions of the doped materials and stirring for 18-24 hours with

50 mL of $\text{Hg}(\text{NO}_3)_2$ solutions at initial concentrations ranging from 0-300 ppm. Mercury(II) concentrations were determined before and after treatment by colormetric analysis using diphenylthiocarbazone as an indicator. The results of the mercury adsorption studies for the base catalyzed mercaptopropyltriethoxysilane doped/phenylene series are shown below in Table 4.

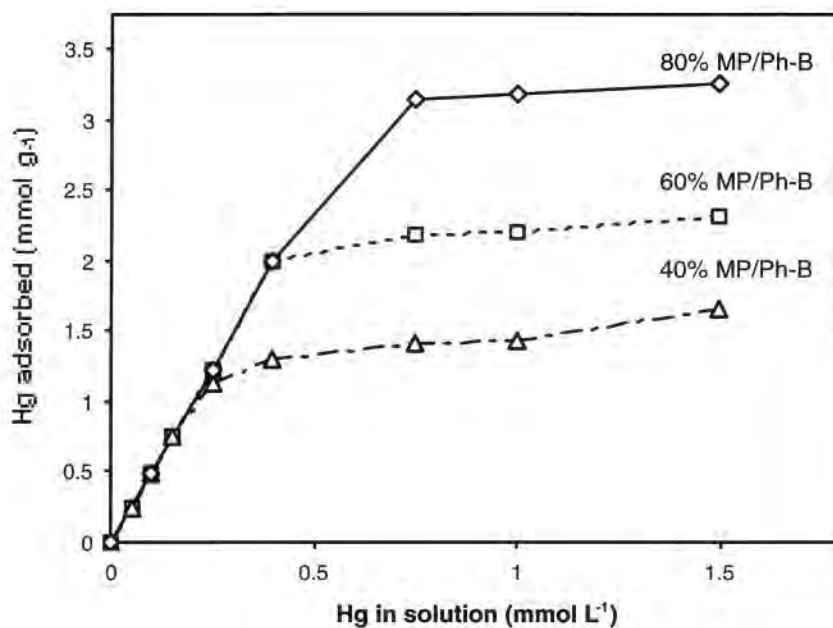


Figure 1. Graph of mercury adsorbed (mmol) per gram of polymer.

Base Catalyzed Materials	Hg ²⁺ Adsorbed (mmol/g)	Theoretical Max. (mmol/g)
100% Ph-B	-	0
20% MP/Ph-B	2.34	1.18
40% MP/Ph-B	1.66	2.51
60% MP/Ph-B	2.32	4.04
80% MP/Ph-B	3.26 (2.80)	5.8

Table 4. Maximum Hg²⁺ Uptake for MP doped/Ph base catalyzed materials

For the Hg²⁺ uptake experiments, pure phenyl bridged polysilsesquioxane was used as the control. Absorption of Hg²⁺ by 100% Ph-B was minimal and essentially negligible. Therefore, it can be concluded that the incorporated mercapto ligand was solely responsible for the uptake of Hg²⁺. As seen from Table 4, the uptake of Hg²⁺ in the doped materials was lower than the expected theoretical maximum. However, the mercury(II) adsorption capacity for these materials are still the highest that have been reported for any silicate material. A noticeable trend was that the Hg²⁺ uptake tended to deviate more from the theoretical maximum with increased ligand loading. For example, 40% MP/Ph-B adsorbed 66% of the theoretical loading capacity, whereas, 80% MP/Ph-B adsorbed only 57% of capacity. This trend can be correlated to the decrease in surface area with increasing in ligand loading. Decreased surface areas and porosity limits access of the substrate with functional ligands. Also, adsorption less than the theoretical maximum may have resulted from irregular pore shapes which can become blocked during Hg²⁺ uptake experiments.

Conclusion

An effective high capacity thiol containing Hg²⁺ adsorbent has been synthesized by incorporation of functional thiol ligands into a hybrid organic-inorganic matrix. The syntheses of these materials are straightforward and require only copolymerization of

commercially available 3-mercaptopropyltriethoxysilane with 1,4-bis(triethoxysilyl)benzene under base catalyzed sol-gel conditions. The polymerization gives functional gels within 24 hours and a benign water processing procedure followed by drying yields mesoporous materials with surface areas ranging from ~1000 to 450 m²/g. These materials displayed high capacity for Hg⁺² adsorption from aqueous Hg(NO₃)₂ solutions. Mercury(II) adsorption capacities have reached as high as 3.26 (2.80) mmol of Hg⁺²/g of adsorbent material. This adsorption capacity is currently the highest recorded for any functionalized silicate material. In preliminary studies conducted by the Army, these materials, in conjunction with a barrier cream, have provided significant protection against mustard gas.

Experimental Section

Instrumentation. ¹H NMR spectra were recorded on a General Electric GN-500 (500 MHz) or Bruker Omega-500 (500 MHz). The chemical shifts are reported in ppm using deuterated solvent peaks as the internal references. Coupling constant (*J*) is reported in Hz and the splitting abbreviations used are: s, single; d, doublet; t, triplet; q, quartet; m, multiplet; br, broad. ¹³C NMR spectra were obtained using the same instruments operating at 125.8 MHz. High-resolution mass spectra (HRMS) were recorded using a VG 7070E high-resolution mass spectrometer or Fisons Autospec mass spectrometer. Surface area measurements were made on a Micrometrics ASAP 2000 porosimeter using high purity nitrogen as the adsorbate at 77 K. Surface areas were calculated by the BET equation ($0.05 \leq P/P_0 \leq 0.35$ for N₂) and pore distributions characterized by Barret-Joyner-Halendg.

General Procedures. All glassware was oven-dried overnight, flame-dried and purged with nitrogen prior to use for all monomer preparations. All reactions were run under a N₂ atmosphere. Tetrahydrofuran was dried by filtering through alumina following a procedure described by Grubbs.³ All other solvents were dried over drying agents (CaH₂ for hexanes and Mg(OEt)₂ for ethanol). Removal of volatile solvents were performed

using a Büchi rotary evaporator and denoted by the statement, "removed *in vacuo*."

Tetraethylorthosilicate (TEOS) and 3-aminopropyltriethoxysilane was purchased from Aldrich Chemical Company, distilled over CaH_2 and stored over 4Å molecular sieves prior to use. 3-Mercaptopropyltriethoxysilane (**MP**) was purchased from Gelest, distilled over 4Å molecular sieves and stored over 4Å molecular sieves.

Monomer Preparation

1,4-Bis(triethoxysilyl)benzene, 1.⁶ To a suspension of magnesium turnings (3.00 g, 123 mmol), THF (60 mL) and a small crystal of iodine was added TEOS (90 mL, 403 mmol). After heating the solution to reflux, a solution of 1,4-dibromobenzene (9.61 g, 41 mmol) in THF (30 mL) was slowly added over a period of 1 h. The mixture was kept at reflux for 2 h after the addition of the dibromide. The solution was cooled and cold hexanes was added to precipitate magnesium salts. The mixture was filtered through celite into a dry flask. The solvent was removed *in vacuo* to afford a light brown solution. The remaining TEOS and TEOS oligomers were removed *in vacuo* (75 °C, 0.5 mm) leaving a brown oil. Further purification was performed by Kugelrohr distillation (130-135 °C, 0.5 mm) to collect a clear, colorless oil (**1**, 6.23 g, 39%): ^1H NMR (500 MHz, CDCl_3) δ 7.67 (s, 4H), 3.88-3.84 (q, $J = 7.0$, 12H), 1.25-1.22 (t, $J = 7.0$, 18H); ^{13}C NMR (125.8 MHz, CDCl_3) δ 134.0, 133.1, 58.7, 18.1; IR (neat) 3057, 2975, 1392, 1295, 961, 778, 704 cm^{-1} ; HRMS (FAB) m/z calcd for $\text{C}_{18}\text{H}_{34}\text{O}_6\text{Si}_2$ ($\text{M}+\text{H}$)⁺ 403.1972, found 403.1965.

Sol-gel Polymerization

Polysilsesquioxane from 1,4-bistriethoxysilylbenzene blank (x-3A(0%)). In volumetric flask (10 mL) rinsed with EtOH was added 1,4-bistriethoxysilylbenzene (1.613 g, 4.00 $\times 10^{-3}$ mol) and EtOH (~5 mL). The flask was agitated until a homogeneous solution results, $\text{HCl}_{(\text{aq})}$ (1.005-0.995 M, 0.425 mL, 6.0 eq H_2O) was added, the flask was diluted to the mark with EtOH, and was shaken for 2 minutes to give a homogenous solution.

The solution was transferred to a polypropylene vial (25 mL) and allowed to sit. The solution gelled after approximately 48 hours to give a clear gel. The gel was aged for 9 days, water processed, air dried (24 hours), rough ground, and dried *in vacuo* at 100° C for 4 hours to give a white powder (0.65 g, 92.2%): ¹³C NMR (50.29 MHz, solid state) CPMAS (4000 Hz) δ 132.0, 58.0, 15.3; MAS (4000 Hz) 131.8, 51.2, 14.5; ²⁹Si NMR (39.97 MHz, solid state); CPMAS (4000 Hz) δ -61.1 (T¹), -70.0 (T²), -78.9 (T³), MAS (4000 Hz), -61.1 (T¹), -70.0 (T²), -78.9 (T³) ppm; IR (KBr) cm⁻¹; Deconvolution for ²⁹Si MAS NMR: T¹ 14.9%; T² 63.1%; T³ 22.0%; 69.0 % condensed. Analysis calc'd for C₆H₄O₃Si₂: Carbon, 40.0; Hydrogen, 2.2; Silicon, 31.2; found: Carbon,; Hydrogen,; Sulfur,; Silicon. TGA rt-100°C, - 5%; 508-691°C, - 7.5%; DSC; Porsimetry: Nitrogen: 77 K. BET: 0.05 ≤ P/P₀ ≤ 0.35: 527 ± 15 m²/g; R=0.997; C=-66.3: BJH average pore diameter (adsorption) 45.4 Å; BJH average pore diameter (desorption) 28.3 Å; total pore volume (p/p₀=0.9966) 0.289 cc/g.

Polysilsesquioxane from 10% 3-Mercaptopropyltriethoxysilane and 90% 1,4-bistriethoxysilylbenzene (x-4(10%)). In volumetric flask (25 mL) rinsed with EtOH was added 3-Mercaptopropyltriethoxysilane (MPTES) (0.250 g, 9.78 x 10⁻⁴ mol), 1,4-bistriethoxysilylbenzene (3.62 g, 8.99 x 10⁻³ mol), and EtOH (~15 mL). The flask was agitated until a homogeneous solution results, HCl_(aq) (1.005-0.995 M, 1.06 mL, 6.0 eq H₂O) was added, the flask was diluted to the mark with EtOH, and was shaken for 2 minutes to give a homogenous solution. The solution was transferred to a polypropylene vial (25 mL) and allowed to sit. The solution gelled after 52 hours to give a opaque gel..

Gel was aged for 9 days, water processed, air dried (24 hours), rough ground, and dried *in vacuo* at 100° C for 4 hours to give a white powder (1.83 g, 99.3%): ¹³C NMR (50.29 MHz, solid state) CPMAS (4000 Hz) δ 132.2, 57.6, 26.2, 16.1, 12.1; MAS (4000 Hz) 132.2, 58.4, 26.2, 15.7, 11.6; ²⁹Si NMR (39.97 MHz, solid state); CPMAS (4000 Hz) δ - 61.1 (T¹), -70.0 (T²), -77.9 (T³), MAS (4000 Hz), -60.2 (T¹), -69.0 (T²), -78.9 (T³) ppm; IR (KBr) cm⁻¹; Deconvolution for ²⁹Si MAS NMR: T¹ 18.9%; T² 65.9%; T³ 15.2%; 65.4 % condensed. Analysis calc'd for C₂₂H₁₈O₈N₂Si₂: Carbon, 38.4; Hydrogen, 2.5; Sulfur, 1.9; Silicon, 30.2; found: Carbon,; Hydrogen,; Sulfur,; Silicon. TGA: DSC; Porsimetry: Nitrogen: 77 K. BET: 0.05 ≤ P/P₀ ≤ 0.35: 239 ± 6 m²/g; R=0.998: C=-136.5: BJH average pore diameter (adsorption) 38.1 Å; BJH average pore diameter (desorption) 3093 Å; total pore volume (p/p₀=0.9966) 0.139 cc/g.

80% 3-Mercaptopropyl/20% phenyl-bridged polymer, 80% MP/Ph-B. The sol-gel polymerization of **MP** and monomer **1** was carried out in capped 100 mL polyethylene bottles at room temperature. Solutions with total monomer concentration of 0.4 M in dry ethanol were made with **1** (0.805 g, 2.00 mmol), 3-mercaptopropyltriethoxysilane (1.907 g, 8.00 mmol) and ethanol (16.6 g, 21.2 mL). After the addition of 1 N NaOH (1.08 mL), in one portion, the bottle was capped tightly, shaken vigorously for 1 min, and allowed to stand at room temperature. The polymer gelled in 2 days and was aged for 4 days, before it was removed from the bottle and broken into smaller pieces with a spatula. The gel was washed with EtOH and soaked in water overnight. The water was removed by decanting and the polymer was allowed to air-dry for several days. After air-drying, the

polymer was ground into a powder and dried under reduced pressure (80 °C, 0.2 mm) overnight

- (1) Current Address: USAMRICD, MCMR-UV-DA, ATTN: CPT Stephen Hobson,
3100 Ricketts Pt. Rd, Aberdeen Proving Ground, MD 21010.
- 2 Shea, K.J.; Loy, D.A.; Webster, O.; *J. Am. Chem. Soc.* **1992**, *114*(17), 6700.
- 3 Pangborn, A. B.; Giardello, M. A.; Grubbs, R. H.; Rosen, R. K.; Timmons, F.
Organometallics **1996**, *15*, 1518–1520.

Toxicology Study No. 85-2594-99, Hubert Snodgrass

U.S. Army Center for Health Promotion
and Preventive Medicine

TOXICOLOGY STUDY NO. 85-2594-99
THE ACUTE SKIN AND EYE EFFECTS
OF THE TOPICAL SKIN PROTECTANTS ICD-2701,
ICD-3247, ICD-3248, AND ICD-3249 IN RABBITS
SEPTEMBER 1999

Approved for public release; distribution is unlimited.



Readiness Thru Health

U.S. Army Center for Health Promotion and Preventive Medicine

The lineage of the U.S. Army Center for Health Promotion and Preventive Medicine (USACHPPM) can be traced back over 50 years. This organization began as the U.S. Army Industrial Hygiene Laboratory, established during the industrial buildup for World War II, under the direct supervision of the Army Surgeon General. Its original location was at the Johns Hopkins School of Hygiene and Public Health. Its mission was to conduct occupational health surveys and investigations within the Department of Defense's (DOD's) industrial production base. It was staffed with three personnel and had a limited annual operating budget of three thousand dollars.

Most recently, it became internationally known as the U.S. Army Environmental Hygiene Agency (AEHA). Its mission expanded to support worldwide preventive medicine programs of the Army, DOD, and other Federal agencies as directed by the Army Medical Command or the Office of The Surgeon General, through consultations, support services, investigations, on-site visits, and training.

On 1 August 1994, AEHA was redesignated the U.S. Army Center for Health Promotion and Preventive Medicine with a provisional status and a commanding general officer. On 1 October 1995, the nonprovisional status was approved with a mission of providing preventive medicine and health promotion leadership, direction, and services for America's Army.

The organization's quest has always been one of excellence and the provision of quality service. Today, its goal is to be an established world-class center of excellence for achieving and maintaining a fit, healthy, and ready force. To achieve that end, the CHPPM holds firmly to its values which are steeped in rich military heritage:

- ★ *Integrity is the foundation*
 - ★ *Excellence is the standard*
 - ★ *Customer satisfaction is the focus*
 - ★ *Its people are the most valued resource*
 - ★ *Continuous quality improvement is the pathway*

This organization stands on the threshold of even greater challenges and responsibilities. It has been reorganized and reengineered to support the Army of the future. The CHPPM now has three direct support activities located in Fort Meade, Maryland; Fort McPherson, Georgia; and Fitzsimons Army Medical Center, Aurora, Colorado; to provide responsive regional health promotion and preventive medicine support across the U.S. There are also two CHPPM overseas commands in Landstuhl, Germany and Camp Zama, Japan who contribute to the success of CHPPM's increasing global mission. As CHPPM moves into the 21st Century, new programs relating to fitness, health promotion, wellness, and disease surveillance are being added. As always, CHPPM stands firm in its commitment to Army readiness. It is an organization proud of its fine history, yet equally excited about its challenging future.

REPORT DOCUMENTATION PAGE				Form Approved OMB No. 0704-0188	
<small>Public reporting burden for this collection of information is estimated to average 1 hour per response, including the time for reviewing instructions, searching existing data sources, gathering and maintaining the data needed, and completing and reviewing the collection of information. Send comments regarding this burden estimate or any other aspect of this collection of information, including suggestions for reducing this burden, to Washington Headquarters Services, Directorate for Information Operations and Reports, 1215 Jefferson Davis Highway, Suite 1204, Arlington, VA 22202-4302, and to the Office of Management and Budget, Paperwork Reduction Project (0704-0188), Washington, DC 20503.</small>					
1. AGENCY USE ONLY (Leave blank)		2. REPORT DATE 24 September 1999		3. REPORT TYPE AND DATES COVERED Final	
4. TITLE AND SUBTITLE Toxicology Study No. 85-2594-99 The Acute Skin and Eye Effects of the Topical Skin Protectants ICD-2710, ICD-3247, ICD-3248, and ICD-3249 in Rabbits. September 1999				5. FUNDING NUMBERS	
6. AUTHOR(S) Hubert L. Snodgrass					
7. PERFORMING ORGANIZATION NAME(S) AND ADDRESS(ES) U.S. Army Center for Health Promotion and Preventive Medicine 5158 Blackhawk Road Aberdeen Proving Ground, MD 21010-5403				8. PERFORMING ORGANIZATION REPORT NUMBER 85-2594-99	
9. SPONSORING / MONITORING AGENCY NAME(S) AND ADDRESS(ES) U.S. Army Medical Research Institute of Chemical Defense Advanced Assessment Branch Aberdeen Proving Ground, MD 21010-5425				10. SPONSORING / MONITORING AGENCY REPORT NUMBER	
11. SUPPLEMENTARY NOTES Name of responsible individual: Hubert L. Snodgrass Telephone: 410-436-3980 Office symbol: MCHB-TS-TTE					
12a. DISTRIBUTION / AVAILABILITY STATEMENT Approved for Public Release; Distribution Unlimited				12b. DISTRIBUTION CODE	
13. ABSTRACT (Maximum 200 words) <p>Toxicity tests were performed to determine the skin and eye irritation effects of four candidate topical skin protectant formulations (TSP) in rabbits. The test substances were identified as ICD-2701, ICD-3247, ICD-3248, and ICD-3249. For the skin studies, 0.5 gm of the material was placed on the skin under a gauze pad and gauze overwrap. The exposure was for four hours. For testing in the eyes, 0.1 gm of the material was placed in the conjunctival sac of the test eyes. Scoring of irritation was performed at 24-hour intervals.</p> <p>The topical skin protectants ICD-2701, ICD-3247, ICD-3248, and ICD-3249, did not produce skin or eye irritation in rabbits. No toxic effects were observed.</p> <p>No adverse skin or eye effects in man are anticipated following an acute exposure.</p>					
14. SUBJECT TERMS animals ICD-3247 rabbit TSP eye irritation ICD-3248 topical skin protectant skin irritation ICD-2701 ICD-3249 toxicity skin protectant				15. NUMBER OF PAGES 21	
				16. PRICE CODE	
17. SECURITY CLASSIFICATION OF REPORT UNCLASSIFIED	18. SECURITY CLASSIFICATION OF THIS PAGE UNCLASSIFIED	19. SECURITY CLASSIFICATION OF ABSTRACT UNCLASSIFIED	20. LIMITATION OF ABSTRACT UL		



REPLY TO
ATTENTION OF

DEPARTMENT OF THE ARMY
U.S. ARMY CENTER FOR HEALTH PROMOTION AND PREVENTIVE MEDICINE
5168 BLACKHAWK ROAD
ABERDEEN PROVING GROUND, MARYLAND 21010-5422

EXECUTIVE SUMMARY
TOXICOLOGY STUDY NO. 85-2594-99
THE ACUTE SKIN AND EYE EFFECTS
OF THE TOPICAL SKIN PROTECTANTS ICD-2701,
ICD-3247, ICD-3248, AND ICD-3249 IN RABBITS
SEPTEMBER 1999

1. PURPOSE. To determine the acute skin and eye irritant effects of the topical skin protectant formulations ICD-2701, ICD-3247, ICD-3248, and ICD-3249 in animals.
2. CONCLUSIONS. The topical skin protectants ICD-2701, ICD-3247, ICD-3248, and ICD-3249 did not produce skin or eye irritation in rabbits. No adverse skin or eye effects in man are anticipated following acute exposure.

Readiness thru Health

TABLE OF CONTENTS

Paragraph	Page
1. REFERENCES	1
2. AUTHORITY	1
3. PURPOSE	1
4. MATERIALS	1
a. Test Substance	1
b. Animals	1
5. METHODS.....	2
a. Primary Skin Irritation	2
b. Primary Eye Irritation.....	2
6. RESULTS	2
a. Primary Skin Irritation	2
b. Primary Eye Irritation.....	3
7. CONCLUSION.....	3
Appendices	
A - REFERENCES.....	A-1
B - USACHPPM CATEGORIES FOR SKIN IRRITATION EFFECTS	B-1
C - EPA TOXICITY CATEGORIES CRITERIA	C-1
D - USACHPPM CATEGORIES FOR EYE IRRITATION EFFECTS.....	D-1
E - PRIMARY SKIN IRRITATION DATA (ICD-2701).....	E-1
F - PRIMARY SKIN IRRITATION DATA (ICD-3247).....	F-1
G - PRIMARY SKIN IRRITATION DATA (ICD-3248)	G-1
H - PRIMARY SKIN IRRITATION DATA (ICD-3249)	H-1
I - PRIMARY EYE IRRITATION DATA (ICD-2701)	I-1
J - PRIMARY EYE IRRITATION DATA (ICD-3247)	J-1
K - PRIMARY EYE IRRITATION DATA (ICD-3248)	K-1
L - PRIMARY EYE IRRITATION DATA (ICD-3249)	L-1



REPLY TO
ATTENTION OF

DEPARTMENT OF THE ARMY
U.S. ARMY CENTER FOR HEALTH PROMOTION AND PREVENTIVE MEDICINE
5158 BLACKHAWK ROAD
ABERDEEN PROVING GROUND, MARYLAND 21010-5422

MCHB-TS-TTE

TOXICOLOGY STUDY NO. 85-2594-99
THE ACUTE SKIN AND EYE EFFECTS
OF THE TOPICAL SKIN PROTECTANTS ICD-2701,
ICD-3247, ICD-3248, AND ICD-3249 IN RABBITS
SEPTEMBER 1999

1. REFERENCES. See Appendix A for a listing of references.
2. AUTHORITY. Letter, U.S. Army Medical Research Institute of Chemical Defense (MRICD), 3 June 1999, subject: [Request for Acute Eye and Skin Evaluations of rTSP Formulations.]
3. PURPOSE. To determine the acute skin and eye irritant effects of the topical skin protectant (TSP) formulations ICD-2701, ICD-3247, ICD-3248, and ICD-3249 in animals.
4. MATERIALS.

a. Test Substance. Dr. Ernest Braue, MRICD, provided the four test substances labeled ICD-2701, ICD-3247, ICD-3248, and ICD-3249. Each substance was a heavy, smooth, white cream, having no noticeable odor. Chemical characterization of the test substance was the responsibility of the sponsor.

b. Animals.^{*†} The acute skin and eye irritation studies were conducted using New Zealand white rabbits purchased from Covance Research Products, Inc., Denver, Pennsylvania. A total of 24 animals of either sex were used. At the start of testing, rabbits weighed between 2.32 and 4.26 kilograms (kg). Rabbits were identified by cage card and were housed in individual wire-bottom stainless steel cages. Drinking-quality water and feed (Teklad Certified 15% Rabbit Diet (W) 8630C, Harlan/Teklad, Madison, Wisconsin) were available *ad libitum*. Ambient temperatures in the animal rooms were maintained at 64 to 70°F with relative humidity between 40 and 60 percent. The light/dark cycle was at 12-hour intervals.

^{*} In conducting the studies described herein, the investigators adhered to the *Guide for the Care and Use of Laboratory Animals*, U.S. Department of Health, Education and Welfare Publication No. (NIH) 85-23, 1985.

[†] The studies reported herein were performed in animal facilities fully accredited by the American Association for the Accreditation of Laboratory Animal Care.

5. METHODS.

a. Primary Skin Irritation.

(1) A primary skin irritation test was conducted using six rabbits. The procedure (reference 1) involved the single application of 0.5 gram (gm) of each test substance to one site on the clipped back of each rabbit. The rabbits' backs were divided into four sites, two on either side of the mid-line, such that each animal received all four test materials. The pre-weighed substance was dispensed under a 2-by-2-inch gauze pad secured to the skin surface with nonirritating tape. The site was then overwrapped with roll gauze. Animals were not restrained during the exposure but wore Elizabethan collars to prevent probing of the covered exposure site. Exposure was for 4 hours, after which the coverings were removed and the irritation scored 1 hour later. Evaluations were also made 24, 48, and 72 hours after treatment.

(2) Scoring of irritation was based on the Draize method in which erythema and edema were evaluated on a scale of 0 to 4 for severity. The sum of the mean erythema and mean edema values at 24 and 72 hours were used for the rating of skin irritation. The USACHPPM skin irritation rating system that appears at Appendix B was followed. The U.S. Environmental Protection Agency (EPA) Toxicity Categories Criteria that appear at Appendix C were also used. In addition to the observations for skin irritation, any signs of systemic toxicity were recorded.

b. Primary Eye Irritation. An acute eye irritation test was conducted using six rabbits per test substance. The procedure (reference 2) involved the application of 0.1 gm of the substance weighed onto a disposable autopipette tip, in the form of a small suspended ball, and then placed in the conjunctival sac of each rabbit. The eye was momentarily held closed, then the animal returned to its cage. After 24 hours, the cornea, iris and conjunctiva were observed for signs of irritation and scored using the Draize method. The eyes were also evaluated at 48 and 72 hours. If irritation was observed at 72 hours, observations were made at 7 and 14 days after treatment to assess recovery. The USACHPPM eye irritation rating system that appears at Appendix D was followed. The EPA Toxicity Categories Criteria that appear at Appendix C were also used. In addition to the observations for eye irritation, any signs of systemic toxicity were recorded.

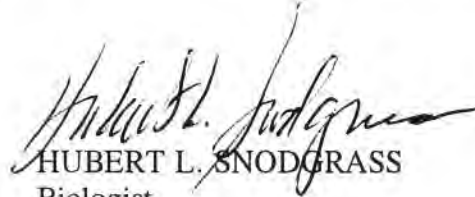
6. RESULTS.

a. Primary Skin Irritation. Under the conditions of the described study, the test substances ICD-2701, ICD-3247, ICD-3248, and ICD-3249 did not produce primary irritation to the skin of rabbits. Appendices E through H present the individual animal results.

Toxicology Study No. 85-2594-99, Sep 99

b. Primary Eye Irritation. Under the conditions of the described study, the test substances ICD-2701, ICD-3247, ICD-3248, and ICD-3249 did not produce primary irritation to the eyes of rabbits. Appendices I through L present the individual animal results.

7. CONCLUSION. The topical skin protectants ICD-2701, ICD-3247, ICD-3248, and ICD-3249 did not produce skin or eye irritation in rabbits. No adverse skin or eye effects in man are anticipated following acute exposure.



HUBERT L. SNODGRASS

Biologist

Master Consultant

Toxicity Evaluation Program

APPROVED:



for LEROY W. METKER
Program Manager
Toxicity Evaluation

Date 14 Oct 99

APPENDIX A

REFERENCES

1. Standing Operating Procedure (SOP) No. 08.98, Primary Dermal Irritation Study, U.S. Army Center for Health Promotion and Preventive Medicine (USACHPPM), Directorate of Toxicology, 20 August 1998.
2. SOP No. 07.99, Primary Eye Irritation Study, USACHPPM, Directorate of Toxicology, 29 July 1999.
3. *Guide for the Care and Use of Laboratory Animals*, U.S. Department of Health, Education and Welfare Publication No. (NIH) 85-23, 1985.
4. Title 40, Code of Federal Regulations (CFR), Part 156.10, Labeling requirements, revised 1 July 1995.

APPENDIX B

USACHPPM CATEGORIES FOR SKIN IRRITATION EFFECTS

CATEGORY I - Compounds producing no primary irritation of the intact skin or no greater than mild primary irritation of the skin surrounding an abrasion. Score Limits: Intact 0-0.5; Abraded 0.51-2.0; Total 0-2.0. INTERPRETATION: *No restriction for acute application to the human skin.*

CATEGORY II - Compounds producing mild primary irritation of the intact skin and the skin surrounding an abrasion. Score Limits: Intact >0.5; Total 0.51-2.0. INTERPRETATION: *Should be used only on human skin found by examination to have no abrasions or may be used as clothing impregnant.*

CATEGORY III - Compounds producing moderate primary irritation of the intact skin and the skin surrounding an abrasion. Score Limits: Total 2.1-5.0. INTERPRETATION: *Should not be used directly without a prophetic patch test having been conducted on humans to determine irritation potential to human skin. May be used without patch testing, with extreme caution, as clothing impregnants. Compound should be resubmitted in the form and at the intended use concentration, so that its irritation potential can be reexamined using other test techniques on animals.*

CATEGORY IV - Compounds producing moderate to severe primary irritation of the intact skin and of the skin surrounding an abrasion. Score Limits: Total 2.1-7.9. INTERPRETATION: *Should be resubmitted for testing in the form and at the intended use concentration. Upon resubmission, and prior to its possible prophetic patch testing in humans, its irritation potential will be reexamined using other test techniques on animals, at concentrations that have been shown not to produce primary irritation in animals.*

CATEGORY V - Compounds impossible to classify because of staining of the skin or other masking effects owing to physical properties of the compound or compounds producing necrosis, vesiculation, or eschars. Score Limits: Total 8.0 or not scorable. INTERPRETATION: *Not suitable for use on humans.*

APPENDIX C

EPA TOXICITY CATEGORIES CRITERIA*

Hazard Indicators	Category I <i>Highly Toxic</i>[†]	Category II <i>Moderately Toxic</i>	Category III <i>Slightly Toxic</i>	Category IV <i>Practically Nontoxic</i>
Oral LD ₅₀ mg/kg	Up to and incl 50	50 through 500	500 through 5,000	Greater than 5,000
Inhalation LC ₅₀ mg/L	Up to and incl 0.2	0.2 through 2.0	2.0 through 20	Greater than 20
Dermal LD ₅₀	Up to and incl 200	200 through 2,000	2,000 through 20,000	Greater than 20,000
Eye Effects	Corrosive; corneal opacity not revers-ible within 7 da	Corneal opacity reversible within 7 da; irritation persisting for 7 da	No corneal opacity; irritation reversible within 72 hr	No irritation
Skin Effects	Corrosive	Severe irritation at 72 hr	Moderate irritation at 72 hr	Mild or slight irritation at 72 hr

* 40 CFR 156.10, Labeling requirements, revised 1 July 1995.

[†] Descriptive terms, e.g., Highly Toxic, Moderately Toxic, etc., inserted for clarification only; not a part of 40 CFR156.10.

APPENDIX D

USACHPPM CATEGORIES FOR EYE IRRITATION EFFECTS

CATEGORY A – Compounds noninjurious to the eye. Score Limits: 0-10 (individual conjunctival score for chemosis, redness or discharge not to exceed 1). **INTERPRETATION:** *Irritation of human eyes is not expected if the compound should accidentally get into the eyes, provided it is washed out as soon as possible.*

CATEGORY B – Compounds producing mild injury to the cornea. Score Limits: 10-20 (individual conjunctival score for chemosis, redness or discharge not to exceed 1). **INTERPRETATION:** *To be used with caution around the eyes.*

CATEGORY C – Compounds producing mild injury to the cornea and, in addition, some injury to the conjunctiva. Score Limits: 5-30 (individual conjunctival score for chemosis, redness or discharge exceeds 1). **INTERPRETATION:** *To be used with caution around the eyes and mucosa (e.g., nose and mouth).*

CATEGORY D – Compounds producing moderate injury to the cornea. Score Limits: <20-50 (individual conjunctival score for chemosis, redness or discharge not to exceed 1). **INTERPRETATION:** *To be used with extreme caution around the eyes.*

CATEGORY E – Compounds producing moderate injury to the cornea and, in addition, producing some injury to the conjunctiva. Score Limits: 20-50 (individual conjunctival score for chemosis, redness or discharge exceeds 1). **INTERPRETATION:** *To be used with extreme caution around the eyes and mucosa.*

CATEGORY F – Compounds producing severe injury to the cornea and to the conjunctiva. Score Limits: 50 or greater. **INTERPRETATION:** *To be used with extreme caution; it is recommended that the use be restricted to areas other than the face.*

APPENDIX E

PRIMARY SKIN IRRITATION DATA (ICD-2701)

Study No.: 85-2594-99 Protocol No.: 2594a-11-98-02-05 SOP No.: 08.98								
Chemical Substance: Topical Skin Protectant ICD-2701								
Amount Applied: 0.5 gm					Concentration: NEAT			
Species: Rabbit			Sex: Mixed		Weight: 3.04 - 3.53 kg			
Conditions: 4-hour exposure. Non-occluded.								
Tm (hr)	Observation	Animal Number / Score						
		99.01	99.02	99.03	99.04	99.05	99.06	SUM
24	Erythema	0	0	0	0	0	0	0
72		0	0	0	0	0	0	0
7 da		0	0	0	0	0	0	0
Subtotal (24 and 72 hour)								0
24	Edema	0	0	0	0	0	0	0
72		0	0	0	0	0	0	0
7 da		0	0	0	0	0	0	0
Subtotal (24 and 72 hour)								0
Total Score (SUM of All Scores ÷ X No. of Animals)								0.0

Study Conclusions:

EPA Toxicity Category **IV**. [No precautionary statement required]

USACHPPM Category **I**. Interpretation: *No restriction for acute application to the human skin.*

APPENDIX F

PRIMARY SKIN IRRITATION DATA (ICD-3247)

Study No.: 85-2594-99 Protocol No.: 2594b-11-98-02-05 SOP No.: 08.98								
Chemical Substance: Topical Skin Protectant ICD-3247								
Amount Applied: 0.5 gm					Concentration: NEAT			
Species: Rabbit			Sex: Mixed		Weight: 3.04 - 3.53 kg			
Conditions: 4-hour exposure. Non-occluded.								
Tm (hr)	Observation	Animal Number / Score						
		99.01	99.02	99.03	99.04	99.05	99.06	SUM
24	Erythema	0	0	0	0	0	0	0
72		0	0	0	0	0	0	0
7 da		0	0	0	0	0	0	
Subtotal (24 and 72 hour)								0
24	Edema	0	0	0	0	0	0	0
72		0	0	0	0	0	0	0
7 da		0	0	0	0	0	0	
Subtotal (24 and 72 hour)								0
Total Score (SUM of All Scores ÷ X No. of Animals)								0.0

Study Conclusions:

EPA Toxicity Category IV. [No precautionary statement required]

USACHPPM Category I. Interpretation: *No restriction for acute application to the human skin.*

APPENDIX G

PRIMARY SKIN IRRITATION DATA (ICD-3248)

Study No.: 85-2594-99 Protocol No.: 2594c-11-98-02-05 SOP No.: 08.98								
Chemical Substance: Topical Skin Protectant ICD-3248								
Amount Applied: 0.5 gm					Concentration: NEAT			
Species: Rabbit			Sex: Mixed		Weight: 3.04 - 3.53 kg			
Conditions: 4-hour exposure. Non-occluded.								
Tm (hr)	Observation	Animal Number / Score						
		99.01	99.02	99.03	99.04	99.05	99.06	SUM
24	Erythema	0	0	0	0	0	0	0
72		0	0	0	0	0	0	0
7 da		0	0	0	0	0	0	
Subtotal (24 and 72 hour)								0
24	Edema	0	0	0	0	0	0	0
72		0	0	0	0	0	0	0
7 da		0	0	0	0	0	0	
Subtotal (24 and 72 hour)								0
Total Score (SUM of All Scores ÷ X No. of Animals)								0.0

Study Conclusions:

EPA Toxicity Category **IV**. [No precautionary statement required]

USACHPPM Category **I**. Interpretation: *No restriction for acute application to the human skin.*

APPENDIX H

PRIMARY SKIN IRRITATION DATA (ICD-3249)

Study No.: 85-2594-99 Protocol No.: 2594d-11-98-02-05 SOP No.: 08.98								
Chemical Substance: Topical Skin Protectant ICD-3249								
Amount Applied: 0.5 gm					Concentration: NEAT			
Species: Rabbit			Sex: Mixed		Weight: 3.04 - 3.53 kg			
Conditions: 4-hour exposure. Non-occluded.								
Tm (hr)	Observation	Animal Number / Score						
		99.01	99.02	99.03	99.04	99.05	99.06	SUM
24	Erythema	0	0	0	0	0	0	0
72		0	0	0	0	0	0	0
7 da		0	0	0	0	0	0	0
Subtotal (24 and 72 hour)								0
24	Edema	0	0	0	0	0	0	0
72		0	0	0	0	0	0	0
7 da		0	0	0	0	0	0	0
Subtotal (24 and 72 hour)								0
Total Score (SUM of All Scores ÷ X No. of Animals)								0.0

Study Conclusions:

EPA Toxicity Category IV. [No precautionary statement required]

USACHPPM Category I. Interpretation: *No restriction for acute application to the human skin.*

APPENDIX I

PRIMARY EYE IRRITATION DATA (ICD-2701)

Study No.: 85-2594-99 Protocol No.: 2594a-10-99-06-01 SOP No.: 07.99

Chemical Substance: Topical Skin Protectant ICD-2701

Amount Applied: 0.1 gm Concentration: NEAT

Species: Rabbit Sex: Mixed Weight: 3.43 – 4.26 kg

Conditions: Left eye - test

Tm (hr)	Observation	Animal Number / Score						
		99.01	99.02	99.03	99.04	99.05	99.06	MEAN
24	Cornea	0	0	0	0	0	0	0
	Iris	0	0	0	0	0	0	0
	Conjunctiva	0	0	0	0	0	0	0
48	Cornea	0	0	0	0	0	0	0
	Iris	0	0	0	0	0	0	0
	Conjunctiva	0	0	0	0	0	0	0
72	Cornea	0	0	0	0	0	0	0
	Iris	0	0	0	0	0	0	0
	Conjunctiva	0	0	0	0	0	0	0

Study Conclusions:

EPA Toxicity Category **IV**. [No precautionary statement required]

USACHPPM Category **A**. Interpretation: *Irritation of human eyes is not expected if the substance should accidentally get into the eyes, provided it is washed out as soon as possible.*

APPENDIX J

PRIMARY EYE IRRITATION DATA (ICD-3247)

Study No.: 85-2594-99

Protocol No.: 2594b-10-99-06-01

SOP No.: 07.99

Chemical Substance: Topical Skin Protectant

ICD-3247

Amount Applied: 0.1 gm

Concentration: NEAT

Species: Rabbit

Sex: Mixed

Weight: 2.32 – 2.76 kg

Conditions: Right eye - test

Tm (hr)	Observation	Animal Number / Score						
		99.19	99.20	99.21	99.22	99.23	99.24	MEAN
24	Cornea	0	0	0	0	0	0	0
	Iris	0	0	0	0	0	0	0
	Conjunctiva	0	0	0	0	0	0	0
48	Cornea	0	0	0	0	0	0	0
	Iris	0	0	0	0	0	0	0
	Conjunctiva	0	0	0	0	0	0	0
72	Cornea	0	0	0	0	0	0	0
	Iris	0	0	0	0	0	0	0
	Conjunctiva	0	0	0	0	0	0	0

Study Conclusions:

EPA Toxicity Category IV. No precautionary statement required]

USACHPPM Category A. Interpretation: *Irritation of human eyes is not expected if the substance should accidentally get into the eyes, provided it is washed out as soon as possible.*

APPENDIX K

PRIMARY EYE IRRITATION DATA (ICD-3248)

Study No.: 85-2594-99 Protocol No.: 2594c10-99-06-01 SOP No.: 07.99 Chemical Substance: Topical Skin Protectant ICD-3248 Amount Applied: 0.1 gm Concentration: NEAT Species: Rabbit Sex: Mixed Weight: 2.48 – 2.82 kg Conditions: Right eye – test								
Tm (hr)	Observation	Animal Number / Score						MEAN
		99.25	99.26	99.27	99.28	99.29	99.30	
24	Cornea	0	0	0	0	0	0	0
	Iris	0	0	0	0	0	0	0
	Conjunctiva	0	0	0	0	0	0	0
48	Cornea	0	0	0	0	0	0	0
	Iris	0	0	0	0	0	0	0
	Conjunctiva	0	0	0	0	0	0	0
72	Cornea	0	0	0	0	0	0	0
	Iris	0	0	0	0	0	0	0
	Conjunctiva	0	0	0	0	0	0	0

Study Conclusions:

EPA Toxicity Category IV. [No precautionary statement required]

USACHPPM Category A. Interpretation: *Irritation of human eyes is not expected if the substance should accidentally get into the eyes, provided it is washed out as soon as possible.*

Toxicology Study No. 85-MA-6631, Hubert Snodgrass

REPORT DOCUMENTATION PAGE					Form Approved OMB No. 0704-0188	
Public reporting burden for this collection of information is estimated to average 1 hour per response, including the time for reviewing instructions, searching existing data sources, gathering and maintaining the data needed, and completing and reviewing the collection of information. Send comments regarding this burden estimate or any other aspect of this collection of information, including suggestions for reducing this burden, to Washington Headquarters Services, Directorate for Information Operations and Reports, 1215 Jefferson Davis Highway, Suite 1204, Arlington, VA 22202-4302, and to the Office of Management and Budget, Paperwork Reduction Project (0704-0188), Washington, DC 20503.						
1. AGENCY USE ONLY (Leave blank)		2. REPORT DATE September 2001		3. REPORT TYPE AND DATES COVERED Final		
4. TITLE AND SUBTITLE Toxicology Study No. 85MA6631, The Acute Skin and Eye Effects of the Active Topical Skin Protectant (aTSP) Formulations ICD-3151, ICD-3308, ICD-3471, ICD-3533, ICD-3551, ICD-3665, and ICD-3673 in Rabbits. September 2001					5. FUNDING NUMBERS	
6. AUTHOR(S) Hubert L. Snodgrass						
7. PERFORMING ORGANIZATION NAME(S) AND ADDRESS(ES) U.S. Army Center for Health Promotion and Preventive Medicine 5158 Blackhawk Road Aberdeen Proving Ground, MD 21010-5403					8. PERFORMING ORGANIZATION REPORT NUMBER Toxicology Study No. 85MA6631	
9. SPONSORING / MONITORING AGENCY NAME(S) AND ADDRESS(ES) Drug Assessment Division U.S. Army Medical Research Institute of Chemical Defense 3100 Ricketts Point Road Aberdeen Proving Ground, MD 21010-5400					10. SPONSORING / MONITORING AGENCY REPORT NUMBER	
11. SUPPLEMENTARY NOTES						
12a. DISTRIBUTION / AVAILABILITY STATEMENT Approved for public release; distribution unlimited					12b. DISTRIBUTION CODE	
13. ABSTRACT (Maximum 200 words) Toxicity tests were performed to determine the skin and eye irritation effects of seven candidate active topical skin protectant (aTSP) formulations in rabbits. The test substances were identified as ICD-3151, ICD-3308, ICD-3471, ICD-3533, ICD-3551, ICD-3665, and ICD-3673. For the skin studies, 0.5 gm of the material was placed on the clipped skin surface under a gauze pad and gauze overwrap. The exposure was for four hours. For testing in the eyes, 0.1 gm of the material was placed in the conjunctival sac of the test eyes. Scoring of the irritation was performed at 24-hour intervals. The topical skin protectants ICD-3151, ICD-3308, ICD-3471, ICD-3533, ICD-3551, ICD-3665, and ICD-3673, did not produce skin or eye irritation in rabbits. No toxic effects were observed. No adverse skin or eye effects in man are anticipated following an acute exposure.						
14. SUBJECT TERMS eye irritation ICD-3471 ICD-3665 rabbit aTSP ICD-3151 ICD-3533 ICD-3673 topical skin protectant TSP ICD-3308 ICD-3551 skin irritation toxicity					15. NUMBER OF PAGES 30	
					16. PRICE CODE	
17. SECURITY CLASSIFICATION OF REPORT UNCLASSIFIED		18. SECURITY CLASSIFICATION OF THIS PAGE UNCLASSIFIED		19. SECURITY CLASSIFICATION OF ABSTRACT UNCLASSIFIED		20. LIMITATION OF ABSTRACT UL

Toxicology Study No. 85-MA-6631, Sep 01

Sponsor

Ernest H. Braue, Jr., Ph.D.
Advanced Assessment Branch
Drug Assessment Division
U.S. Army Medical Research Institute of Chemical Defense
3100 Ricketts Point Road
Aberdeen Proving Ground, MD 21010-5400

Study Title

Toxicology Study No. 85-MA-6631-01
The Acute Skin and Eye Effects of the Active Topical
Skin Protectant (aTSP) Formulations ICD-3151, ICD-3308,
ICD-3471, ICD-3533, ICD-3551, ICD-3665,
and ICD-3673 in Rabbits
September 2001

Data Requirement

FDA Guidelines
Reference No. 81-4
Reference No. 81-5

Author

Hubert L. Snodgrass

Study Completed

27 September 2001

Performing Laboratory

U.S. Army Center for Health Promotion and Preventive Medicine
Toxicology Program, ATTN: MCHB-TS-TTE
5158 Blackhawk Road
Aberdeen Proving Ground, MD 21010-5403

Quality Assurance Statement

For: Toxicology Study No. 85MA6631, The Acute Skin and Eye Effects of the Active Topical Skin Protectant (aTSP) Formulations ICD-3151, ICD-3308, ICD-3471, ICD-3533, ICD-3665, and ICD-3673 in Rabbits, the following critical phases were audited by the Quality Assurance Team:

<u>Critical Phase Audited (QSO Checklist #)</u>	<u>Date Audited</u>	<u>Date reported to Mngmt.</u>
1) Protocol Review (QSO #1.1)	05/12/01	05/12/01
2) DTOX Personnel Training Files (QSO# 3.1)	09/19/01	10/02/01
3) Test System – Facilities (QSO # 4.1)	09/19/01	10/02/01
a. Test System Receipt (4.2)	09/19/01	10/02/01
b. Test System Identification (4.3)	09/19/01	10/02/01
c. Test System Husbandry (4.4)	09/19/01	10/02/01
d. Test System Observations (4.5)	09/19/01	10/02/01
e. Test System Food and Water (4.6)	09/19/01	10/02/01
4) Test Article – Facilities (QSO # 5.1)	09/20/01	10/03/01
a. Test Article Control (5.2)	09/20/01	10/03/01
b. Test Article Receipt (5.3)	09/20/01	10/03/01
c. Test Article Preparation (5.4)	09/19/01	10/02/01
d. Test Article Handling (5.5)	09/19/01	10/02/01
e. Test Article Administration	09/19/01	10/02/01
5) Maintenance and Calibration of Equipment (9.1)	09/20/01	10/03/01
6) Compliance w/ DTOX SOPs (QSO # 11.1)	09/20/01	10/03/01
7) Compliance w/ DTOX protocols (QSO # 12.1)	09/20/01	10/03/01
8) Final Study Report Review (QSO # 13.1)	10/03/01	10/03/01
9) Study Data Review (QSO # 14.1)	10/03/01	10/03/01

- Any findings made during the audits were made known at the time of the audit to the Study Director.




Michael P. Kefauver
GLP Assessor, Quality Systems Office

Study Compliance Statement

The study described in this report was conducted in compliance with Title 21, Code of Federal Regulations (CFR), Food and Drug Administration (FDA); Part 58, Good Laboratory Practice Standards. There were no deviations from the aforementioned regulation that affected the quality or integrity of the study or the interpretation of the results.

Submitted By:

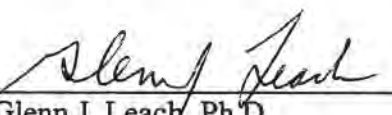
Study Director:


Hubert L. Snodgrass
Biologist/Master Consultant
Toxicity Evaluation Program
Directorate of Toxicology

23 Oct 01

Date

Approved By:


Glenn J. Leach, Ph.D.
Supervisory Toxicologist
Program Manager,
Toxicity Evaluation

23 Oct 01

Date

Applicant/Submitter

Date



REPLY TO
ATTENTION OF

DEPARTMENT OF THE ARMY
U.S. ARMY CENTER FOR HEALTH PROMOTION AND PREVENTIVE MEDICINE
5158 BLACKHAWK ROAD
ABERDEEN PROVING GROUND, MARYLAND 21010-5403

EXECUTIVE SUMMARY
TOXICOLOGY STUDY NO. 85-MA-6631-01
THE ACUTE SKIN AND EYE EFFECTS OF THE ACTIVE TOPICAL
SKIN PROTECTANT (aTSP) FORMULATIONS ICD-3151, ICD-3308,
ICD-3471, ICD-3533, ICD-3551, ICD-3665,
AND ICD-3673 IN RABBITS
SEPTEMBER 2001

1. **PURPOSE.** To determine the acute skin and eye irritation effects of the active topical skin protectant (aTSP) formulations ICD-3151, ICD-3308, ICD-3471, ICD-3533, ICD-3551, ICD-3665, and ICD-3673 in rabbits.
2. **CONCLUSIONS.** The aTSP products ICD-3151, ICD-3308, ICD-3471, ICD-3533, ICD-3551, ICD-3665, and ICD-3673 did not produce skin or eye irritation in rabbits. No adverse skin or eye effects in man are anticipated following acute exposure.

TABLE OF CONTENTS

Paragraph	Page
1. REFERENCES	1
2. AUTHORITY	1
3. PURPOSE	1
4. MATERIALS	1
a. Test Substance.....	1
b. Animal.....	2
5. METHODS	2
a. Primary Skin Irritation	2
b. Primary Eye Irritation	2
6. Results	3
a. Primary Skin Irritation	3
b. Primary Eye Irritation	3
9. CONCLUSIONS.....	3

Appendices

APPENDIX A - References.....	A-1
APPENDIX B - USACHPPM Categories for Skin Irritation Effects	B-1
APPENDIX C - USACHPPM Categories for Eye Irritation Effects.....	C-1
APPENDIX D - EPA Toxicity Categories Criteria	D-1
APPENDIX E - Primary Skin Irritation Data; ICD-3151	E-1
APPENDIX F - Primary Skin Irritation Data; ICD-3308	F-1
APPENDIX G - Primary Skin Irritation Data; ICD-3471	G-1
APPENDIX H - Primary Skin Irritation Data; ICD-3533	H-1
APPENDIX I - Primary Skin Irritation Data; ICD-3551	I-1
APPENDIX J - Primary Skin Irritation Data; ICD-3665.....	J-1
APPENDIX K - Primary Skin Irritation Data; ICD-3673	K-1
APPENDIX L - Primary Eye Irritation Data; ICD-3151	L-1
APPENDIX M - Primary Eye Irritation Data; ICD-3308	M-1
APPENDIX N - Primary Eye Irritation Data; ICD-3471	N-1
APPENDIX O - Primary Eye Irritation Data; ICD-3533	O-1
APPENDIX P - Primary Eye Irritation Data; ICD-3551	P-1
APPENDIX Q - Primary Eye Irritation Data; ICD-3665	Q-1
APPENDIX R - Primary Eye Irritation Data; ICD-3673.....	R-1
APPENDIX S - Archives/Personnel.....	S-1



REPLY TO
ATTENTION OF

MCHB-TS-TTE

DEPARTMENT OF THE ARMY
U.S. ARMY CENTER FOR HEALTH PROMOTION AND PREVENTIVE MEDICINE
5158 BLACKHAWK ROAD
ABERDEEN PROVING GROUND, MARYLAND 21010-5403

TOXICOLOGY STUDY NO. 85-MA-6631-01
THE ACUTE SKIN AND EYE EFFECTS OF THE ACTIVE TOPICAL
SKIN PROTECTANT (aTSP) FORMULATIONS ICD-3151, ICD-3308,
ICD-3471, ICD-3533, ICD-3551, ICD-3665,
AND ICD-3673 IN RABBITS
SEPTEMBER 2001

1. REFERENCES. See Appendix A for a listing of references.
2. AUTHORITY. Letter, U.S. Army Medical Research Institute of Chemical Defense (MRICD), 9 August 2001, subject: [Request for Acute Eye and Skin Evaluations of aTSP Formulations.]
3. PURPOSE. To determine the acute skin and eye irritant effects in animals of the topical skin protectant (aTSP) formulations ICD-3151, ICD-3308, ICD-3471, ICD-3533, ICD-3551, ICD-3665, and ICD-36731.
4. MATERIALS.
 - a. Test Substances. Dr. Ernest Braue, Medical Research Institute of Chemical Defense (MRICD) provided the test substances. Two of the substances, ICD-3151 and ICD-3308, were heavy, smooth, black creams. The remaining five were heavy, smooth, white creams. ICD-3471 was exceptionally stiff in texture. None of the materials had any noticeable odor. Chemical characterization of each substance was the responsibility of the sponsor.
 - b. Animals.*† The acute skin and eye irritation studies were conducted using New Zealand white rabbits purchased from Covance Research Products, Inc., Denver, Pennsylvania. A total of 12 animals of either sex were used. At the start of testing, rabbits weighed between 2.01 and 2.67 kilograms (kg). The rabbits were identified by ear tags and were housed in individual wire-bottom stainless steel cages. Drinking quality water and feed (Teklad Certified 15 percent (%) Rabbit Diet (W) 8630C, Harlan/Teklad, Madison, Wisconsin) were available *ad libitum*. Ambient temperatures in the animal rooms were maintained at 64 to 70 degrees Fahrenheit (°F) with relative humidity between 40 and 60 %. The light/dark cycle was a 12-hour interval.

Use of trademarked names does not imply endorsement by the U.S. Army
but is intended only to assist in identification of a specific product.

Readiness thru Health

5. METHODS.

a. A primary skin irritation test was conducted using twelve rabbits. The procedure (reference 1) involved the single application of 0.5 grams (gms) of each test substance to one site on the clipped back of each rabbit. The rabbits' backs were divided into four sites, two on either side of the mid-line; such that each animal received up to four test materials. The pre-weighed substance was dispensed under a 2by2-inch gauze pad secured to the skin surface with nonirritating tape. It was then overwrapped with roll gauze. The animals were not restrained during the exposure but wore Elizabethan collars to prevent probing of the covered exposure site. Exposure was for 4 hours, after which the coverings were removed and irritation scored within 1 hour. Evaluations were also made at 24, 48 and 72 hours after treatment. Scoring of irritation was based on the Draize method (reference 2) in which erythema and edema were evaluated on a scale of 0 to 4 for severity. The sum of the mean erythema and mean edema values at 24 and 72 hours were used for the rating of skin irritation. The USACHPPM Skin Irritation rating system was followed and appears at Appendix B. The U.S. Environmental Protection Agency (EPA) Toxicity Categories (reference 4) were also applied and appear at Appendix D. In addition to the observations for skin irritation, any signs of systemic toxicity were recorded.

b. An acute eye irritation test was conducted using three rabbits per test substance. The procedure (reference 3) involved the application of 0.1 gm of the substance to the conjunctival sac of each rabbit. The eye was momentarily held closed, then the animal returned to its cage. After 24 hours, the cornea, iris and conjunctiva were observed for signs of irritation and scored using the Draize method. The eyes were also evaluated at 48 and 72 hours. If irritation was observed at 72 hours, observations were made at 7 and 14 days after treatment to assess recovery. The USACHPPM eye irritation rating system was followed and appears at Appendix C. The U.S. EPA Toxicity Categories were also applied and appear at Appendix D. In addition to the observations for eye irritation, any signs of systemic toxicity were recorded.

c. Each test substance for skin application was weighed (0.5 gm) onto a 2-by-2 inch gauze pad, which was then taped onto the test site. For the eye irritation studies, 0.1 gm of the material was weighed onto a disposable autopipette tip, in the form of a small suspended ball, and then placed in the conjunctival sac of the animal.

* In conducting the studies described herein, the investigators adhered to the "*Guide for the Care and Use of Laboratory Animals*," U.S. Department of Health Education and Welfare Publication No. (NIH) 85-23, 1985.

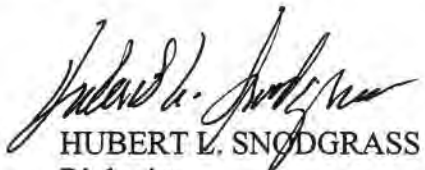
† The studies reported herein were performed in animal facilities fully accredited by the American Association for the Accreditation of Laboratory Animal Care.

6. RESULTS.

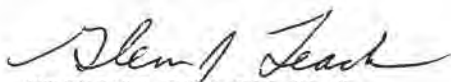
a. Skin Irritation. Under the conditions of the described study, the test substances ICD-3151, ICD-3308, ICD-3471, ICD-3533, ICD-3551, ICD-3665, and ICD-36731 did not produce primary irritation to the skin of rabbits. However, ICD-3471 bonded to the skin surface and required moistening of the gauze pad to aid removal. The individual animal results for each test substance are presented in Appendices E through K.

b. Eye Irritation. Under the conditions of the described study, the test substances ICD-3151, ICD-3308, ICD-3471, ICD-3533, ICD-3551, ICD-3665, and ICD-36731 did not produce primary irritation to the eyes of rabbits. The individual animal results for each test substance are presented in Appendices L through R.

7. CONCLUSION. The topical skin protectants ICD-3151, ICD-3308, ICD-3471, ICD-3533, ICD-3551, ICD-3665, and ICD-36731, did not produce skin or eye irritation in rabbits. No adverse skin or eye effects in man are anticipated following acute exposure.

 10/23/01
HUBERT L. SNODGRASS
Biologist
Master Consultant
Toxicity Evaluation Program

APPROVED:


GLENN J. LEACH, Ph.D.
Program Manager
Toxicity Evaluation

Date 10/23/01

APPENDIX A

REFERENCES

1. Standing Operating Procedure (SOP) No. 08.01, Primary Dermal Irritation Study, USACHPPM, Directorate of Toxicology, 2 August 2001.
2. Draize, J.H., Woodward, G., and Calvery, H.O. 1944. Methods for the study of irritation and toxicity of substances applied topically to the skin and mucous membranes, *J. Pharmacol. Exp. Ther.* 82:377-390.
3. SOP No. 07.01, Primary Eye Irritation Study, USACHPPM, Directorate of Toxicology, 2 August 2001.
4. Title 40, Code of Federal Regulations (CFR), Part 156.10, Labeling requirements, revised 1 July 1995.

APPENDIX B

USACHPPM CATEGORIES FOR SKIN IRRITATION EFFECTS

CATEGORY I - Compounds producing no primary irritation of the intact skin or no greater than mild primary irritation of the skin surrounding an abrasion. Score Limits: Intact 0-0.5; Abraded 0.51-2.0; Total 0-2.0 INTERPRETATION: *No restriction for acute application to the human skin.*

CATEGORY II - Compounds producing mild primary irritation of the intact skin and the skin surrounding an abrasion. Score Limits: Intact >0.5; Total 0.51-2.0 INTERPRETATION: *Should be used only on human skin found by examination to have no abrasions or may be used as clothing impregnant.*

CATEGORY III - Compounds producing moderate primary irritation of the intact skin and the skin surrounding an abrasion. Score Limits: Total 2.1-5.0 INTERPRETATION: *Should not be used directly without a prophetic patch test having been conducted on humans to determine irritation potential to human skin. May be used without patch testing, with extreme caution, as clothing impregnants. Compound should be resubmitted in the form and at the intended use concentration so that its irritation potential can be reexamined using other test techniques on animals.*

CATEGORY IV - Compounds producing moderate to severe primary irritation of the intact skin and of the skin surrounding an abrasion. Score Limits: Total 2.1-7.9 INTERPRETATION: *Should be resubmitted for testing in the form and at the intended use concentration. Upon resubmission, its irritation potential will be reexamined using other test techniques on animals, prior to possible prophetic patch testing in humans, at concentrations that have been shown not to produce primary irritation in animals.*

CATEGORY V - Compounds impossible to classify because of staining of the skin or other masking effects owing to physical properties of the compound or compounds producing necrosis, vesiculation, or eschars. Score Limits: Total 8.0 or not scorable. INTERPRETATION: *Not suitable for use on humans.*

APPENDIX C

USACHPPM CATEGORIES FOR EYE IRRITATION EFFECTS

CATEGORY A - Compounds noninjurious to the eye. Score Limits: 0-10 (individual conjunctival score for chemosis, redness or discharge not to exceed 1). **INTERPRETATION:** *Irritation of human eyes is not expected if the compound should accidentally get into the eyes, provided it is washed out as soon as possible.*

CATEGORY B - Compounds producing mild injury to the cornea. Score Limits: 10-20 (individual conjunctival score for chemosis, redness or discharge not to exceed 1). **INTERPRETATION:** *To be used with caution around the eyes.*

CATEGORY C - Compounds producing mild injury to the cornea, and in addition some injury to the conjunctiva. Score Limits: 5-30 (individual conjunctival score for chemosis, redness or discharge exceed 1). **INTERPRETATION:** *To be used with caution around the eyes and mucosa (e.g., nose and mouth).*

CATEGORY D - Compounds producing moderate injury to the cornea. Score Limits: <20-50 (individual conjunctival score for chemosis, redness or discharge not to exceed 1). **INTERPRETATION:** *To be used with extreme caution around eyes.*

CATEGORY E - Compounds producing moderate injury to the cornea and in addition producing some injury to the conjunctiva. Score Limits: 20-50 (individual conjunctival score for chemosis, redness or discharge exceed 1). **INTERPRETATION:** *To be used with extreme caution around the eyes and mucosa.*

CATEGORY F - Compounds producing severe injury to the cornea and to the conjunctiva. Score Limits: 50 or greater. **INTERPRETATION:** *To be used only with extreme caution; it is recommended that the use be restricted to areas other than the face.*

APPENDIX D

EPA TOXICITY CATEGORY CRITERIA*

Hazard Indicators	Category I <i>Highly Toxic†</i>	Category II <i>Moderately Toxic</i>	Category III <i>Slightly Toxic</i>	Category IV <i>Practically nontoxic</i>
Oral LD ₅₀ mg/kg	Up to and incl 50	50 through 500	500 through 5,000	Greater than 5,000
Inhalation LC ₅₀ mg/L	Up to and incl 0.2	0.2 through 2.0	2.0 through 20	Greater than 20
Dermal LD ₅₀	Up to and incl 200	200 through 2,000	2,000 through 20,000	Greater than 20,000
Eye Effects	Corrosive; corneal opacity not reversible within 7 da	Corneal opacity reversible within 7 da; irritation persisting for 7 da	No corneal opacity; irritation reversible within 72 hr	No irritation
Skin Effects	Corrosive	Severe irritation at 72 hr	Moderate irritation at 72 hr	Mild or slight irritation at 72 hr

* 40 CFR 156.10 Labeling Requirements, revised 1 July 2000.

† Descriptive terms, e.g., Highly Toxic, Moderately Toxic, etc., inserted for clarification only; not a part of 40 CFR156.10.

APPENDIX E

PRIMARY SKIN IRRITATION DATA

Protocol No.: 85MA6631a-11-01-07-04					SOP Number: 08.01			
Chemical Substance: ICD 3151								
Amount Applied: 0.5 gm					Concentration: NEAT			
Species: Rabbit			Sex: Mixed			Weight: 2.03 – 2.76 kg		
Conditions: 4-hour nonoccluded exposure.								
Tm (hr)	Observation	Animal Number / Score						
		13.01	14.01	15.01	16.01	17.01	18.01	SUM
24	Erythema	0	0	0	0	0	0	0
72		0	0	0	0	0	0	0
7 da								
Subtotal (24 and 72 hour)								0
24	Edema	0	0	0	0	0	0	0
72		0	0	0	0	0	0	0
7 da								
Subtotal (24 and 72 hour)								0
Total Score (SUM of All Scores ÷ 2X No. of Animals)								0.00
Study Conclusions: Nonirritating to the intact skin of rabbits. Study discontinued after 72 hrs since no irritant effects were observed.								
USACHPPM Category I. Interpretation: No restriction for acute application to the human skin.								
EPA Toxicity Category IV.								

APPENDIX F

PRIMARY SKIN IRRITATION DATA

Protocol No.: 85MA6631b-11-01-07-04					SOP Number: 08.01			
Chemical Substance: ICD 3308								
Amount Applied: 0.5 gm					Concentration: NEAT			
Species: Rabbit			Sex: Mixed			Weight: 2.03 – 2.76 kg		
Conditions: 4-hour nonoccluded exposure.								
Tm (hr)	Observation	Animal Number / Score						
		13.01	14.01	15.01	16.01	17.01	18.01	SUM
24	Erythema	0	0	0	0	0	0	0
72		0	0	0	0	0	0	0
7 da								
Subtotal (24 and 72 hour)								0
24	Edema	0	0	0	0	0	0	0
72		0	0	0	0	0	0	0
7 da								
Subtotal (24 and 72 hour)								0
Total Score (SUM of All Scores ÷ 2X No. of Animals)								0.00

Study Conclusions: Nonirritating to the intact skin of rabbits. Study discontinued after 72 hrs since no irritant effects were observed.

USACHPPM Category I. Interpretation: *No restriction for acute application to the human skin.*

EPA Toxicity Category IV.

APPENDIX G

PRIMARY SKIN IRRITATION DATA

Protocol No.: 85MA6631c-11-01-07-04					SOP Number: 08.01			
Chemical Substance: ICD 3471								
Amount Applied: 0.5 gm					Concentration: NEAT			
Species: Rabbit			Sex: Mixed			Weight: 2.03 – 2.76 kg		
Conditions: 4-hour nonoccluded exposure.								
Tm (hr)	Observation	Animal Number / Score						
		13.01	14.01	15.01	16.01	17.01	18.01	SUM
24	Erythema	0	0	0	0	0	0	0
72		0	0	0	0	0	0	0
7 da								
Subtotal (24 and 72 hour)								0
24	Edema	0	0	0	0	0	0	0
72		0	0	0	0	0	0	0
7 da								
Subtotal (24 and 72 hour)								0
Total Score (SUM of All Scores ÷ 2X No. of Animals)								0.00

Study Conclusions: Nonirritating to the intact skin of rabbits. Study discontinued after 72 hrs since no irritant effects were observed.

USACHPPM Category I. Interpretation: *No restriction for acute application to the human skin.*

EPA Toxicity Category IV.

APPENDIX H

PRIMARY SKIN IRRITATION DATA

Protocol No.: 85MA6631d-11-01-07-04						SOP Number: 08.01		
Chemical Substance: ICD 3533								
Amount Applied: 0.5 gm						Concentration: NEAT		
Species: Rabbit			Sex: Mixed			Weight: 2.03 – 2.76 kg		
Conditions: 4-hour nonoccluded exposure.								
Tm (hr)	Observation	Animal Number / Score						
		13.01	14.01	15.01	16.01	17.01	18.01	SUM
24	Erythema	0	0	0	0	0	0	0
72		0	0	0	0	0	0	0
7 da								
Subtotal (24 and 72 hour)								0
24	Edema	0	0	0	0	0	0	0
72		0	0	0	0	0	0	0
7 da								
Subtotal (24 and 72 hour)								0
Total Score (SUM of All Scores ÷ 2X No. of Animals)								0.00

Study Conclusions: Nonirritating to the intact skin of rabbits. Study discontinued after 72 hrs since no irritant effects were observed.

USACHPPM Category I. Interpretation: *No restriction for acute application to the human skin.*

EPA Toxicity Category IV.

APPENDIX I

PRIMARY SKIN IRRITATION DATA

Protocol No.: 85MA6631e-11-01-07-04						SOP Number: 08.01		
Chemical Substance: ICD 3551								
Amount Applied: 0.5 gm						Concentration: NEAT		
Species: Rabbit			Sex: Mixed			Weight: 2.25– 2.73 kg		
Conditions: 4-hour nonoccluded exposure.								
Tm	Observation	Animal Number / Score						
(hr)		19.01	20.01	21.01	22.01	23.01	24.01	SUM
24	Erythema	0	0	0	0	0	0	0
72		0	0	0	0	0	0	0
7 da								
Subtotal (24 and 72 hour)								0
24	Edema	0	0	0	0	0	0	0
72		0	0	0	0	0	0	0
7 da								
Subtotal (24 and 72 hour)								0
Total Score (SUM of All Scores ÷ 2X No. of Animals)								0.00

Study Conclusions: Nonirritating to the intact skin of rabbits. Study discontinued after 72 hrs since no irritant effects were observed.

USACHPPM Category I. Interpretation: *No restriction for acute application to the human skin.*

EPA Toxicity Category IV.

APPENDIX J

PRIMARY SKIN IRRITATION DATA

Protocol No.: 85MA6631f-11-01-07-04					SOP Number: 08.01			
Chemical Substance: ICD 3665								
Amount Applied: 0.5 gm					Concentration: NEAT			
Species: Rabbit			Sex: Mixed			Weight: 2.25– 2.73 kg		
Conditions: 4-hour nonoccluded exposure.								
Tm	Observation	Animal Number / Score						
(hr)		19.01	20.01	21.01	22.01	23.01	24.01	SUM
24	Erythema	0	0	0	0	0	0	0
72		0	0	0	0	0	0	0
7 da								
Subtotal (24 and 72 hour)								0
24	Edema	0	0	0	0	0	0	0
72		0	0	0	0	0	0	0
7 da								
Subtotal (24 and 72 hour)								0
Total Score (SUM of All Scores ÷ 2X No. of Animals)								0.00

Study Conclusions: Nonirritating to the intact skin of rabbits. Study discontinued after 72 hrs since no irritant effects were observed.

USACHPPM Category I. Interpretation: *No restriction for acute application to the human skin.*

EPA Toxicity Category IV.

APPENDIX K

PRIMARY SKIN IRRITATION DATA

Protocol No.: 85MA6631g-11-01-07-04					SOP Number: 08.01			
Chemical Substance: ICD 3673								
Amount Applied: 0.5 gm					Concentration: NEAT			
Species: Rabbit			Sex: Mixed			Weight: 2.25 – 2.73kg		
Conditions: 4-hour nonoccluded exposure.								
Tm (hr)	Observation	Animal Number / Score						
		19.01	21.01	22.01	23.01	24.01	25.01	SUM
24	Erythema	0	0	0	0	0	0	0
72		0	0	0	0	0	0	0
7 da								
Subtotal (24 and 72 hour)								0
24	Edema	0	0	0	0	0	0	0
72		0	0	0	0	0	0	0
7 da								
Subtotal (24 and 72 hour)								0
Total Score (SUM of All Scores ÷ 2X No. of Animals)								0.00

Study Conclusions: Nonirritating to the intact skin of rabbits. Study discontinued after 72 hrs since no irritant effects were observed.

USACHPPM Category I. Interpretation: *No restriction for acute application to the human skin.*

EPA Toxicity Category IV.

APPENDIX L

PRIMARY EYE IRRITATION DATA

Protocol No.: 85MA6631a-10-99-06-01				SOP Number: 07.01				
Chemical Substance: ICD – 3151								
Amount Applied: 0.1 gm				Concentration: NEAT				
Species: Rabbit				Sex: Mixed		Weight: 2.18-2.70		
Conditions: Applied to the conjunctival sac; right eye								
Tissue	Effect	Rabbit Number / 24-Hour Score						
		13.01	14.01	15.01				Subtotal
Cornea	A. Opacity	0	0	0				0
	B. Area Involved	0	0	0				
	Score = (AxBx5)	0	0	0				
Iris	A. Iritis	0	0	0				0
	B. Score = Ax5	0	0	0				
Conjunctiva	A. Redness	0	0	0				0
	B. Chemosis	0	0	0				
	C. Discharge	0	0	0				
	Score = (A+B+C) x2	0	0	0				

Total Irritation Score 00

Eye Injury Score (Total Score ÷ No. of Eyes). . 00

Study Conclusions: The test substance did not produce irritation or injury in rabbit eyes. Test discontinued at 72 hrs due to lack of eye effects.

USACHPPM Category: A Interpretation: *Irritation of human eyes is not expected if the substance should accidentally get into the eyes, provided it is washed out as soon as possible.*

EPA Toxicity Category: IV

APPENDIX M

PRIMARY EYE IRRITATION DATA

Protocol No.: 85MA6631b-10-99-06-01				SOP Number: 07.01				
Chemical Substance: ICD – 3308								
Amount Applied: 0.1 gm				Concentration: NEAT				
Species: Rabbit				Sex: Mixed		Weight: 2.47-2.75		
Conditions: Applied to the conjunctival sac; right eye								
Tissue	Effect	Rabbit Number / 24-Hour Score						
		16.01	17.01	18.01				Subtotal
Cornea	A. Opacity	0	0	0				
	B. Area Involved	0	0	0				
	Score = (AxBx5)	0	0	0				
Iris	A. Iritis	0	0	0				0
	B. Score = Ax5	0	0	0				
Conjunctiva	A. Redness	0	0	0				
	B. Chemosis	0	0	0				
	C. Discharge	0	0	0				
	Score = (A+B+C) x2	0	0	0				0

Total Irritation Score 00

Eye Injury Score (Total Score ÷ No. of Eyes).. 00

Study Conclusions: The test substance did not produce irritation or injury in rabbit eyes. Test discontinued at 72 hrs due to lack of eye effects.

USACHPPM Category: A Interpretation: *Irritation of human eyes is not expected if the substance should accidentally get into the eyes, provided it is washed out as soon as possible.*

EPA Toxicity Category: IV

APPENDIX N

PRIMARY EYE IRRITATION DATA

Protocol No.: 85MA6631c-10-99-06-01					SOP Number: 07.01			
Chemical Substance: ICD – 3471								
Amount Applied: 0.1 gm			Concentration: NEAT					
Species: Rabbit			Sex: Mixed			Weight: 2.45-2.60		
Conditions: Applied to the conjunctival sac; right eye								
Tissue	Effect	Rabbit Number / 24-Hour Score						Subtotal
		19.01	20.01	21.01				
Cornea	A. Opacity	0	0	0				
	B. Area Involved	0	0	0				
	Score = (AxBx5)	0	0	0				
Iris	A. Iritis	0	0	0				0
	B. Score = Ax5	0	0	0				
Conjunctiva	A. Redness	0	0	0				
	B. Chemosis	0	0	0				
	C. Discharge	0	0	0				
	Score = (A+B+C) x2	0	0	0				0

Total Irritation Score 00

Eye Injury Score (Total Score ÷ No. of Eyes). . . 00

Study Conclusions: The test substance did not produce irritation or injury in rabbit eyes. Test discontinued at 72 hrs due to lack of eye effects.

USACHPPM Category: A Interpretation: *Irritation of human eyes is not expected if the substance should accidentally get into the eyes, provided it is washed out as soon as possible.*

EPA Toxicity Category: IV

APPENDIX O

PRIMARY EYE IRRITATION DATA

Protocol No.: 85MA6631d-10-99-06-01

SOP Number: 07.01

Chemical Substance: ICD – 3533

Amount Applied: 0.1 gm

Concentration: NEAT

Species: Rabbit

Sex: Mixed

Weight: 2.69-2.77

Conditions: Applied to the conjunctival sac; right eye

Tissue	Effect	Rabbit Number / 24-Hour Score						
		22.01	23.01	24.01				Subtotal
Cornea	A. Opacity	0	0	0				
	B. Area Involved	0	0	0				
	Score = (AxBx5)	0	0	0				
Iris	A. Iritis	0	0	0				0
	B. Score = Ax5	0	0	0				
Conjunctiva	A. Redness	0	0	0				
	B. Chemosis	0	0	0				
	C. Discharge	0	0	0				
	Score = (A+B+C) x2	0	0	0				0

Total Irritation Score 00

Eye Injury Score (Total Score ÷ No. of Eyes).. 00

Study Conclusions: The test substance did not produce irritation or injury in rabbit eyes. Test discontinued at 72 hrs due to lack of eye effects.

USACHPPM Category: A Interpretation: *Irritation of human eyes is not expected if the substance should accidentally get into the eyes, provided it is washed out as soon as possible.*

EPA Toxicity Category: IV

APPENDIX P

PRIMARY EYE IRRITATION DATA

Protocol No.: 85MA6631e-10-99-06-01				SOP Number: 07.01				
Chemical Substance: ICD – 3551								
Amount Applied: 0.1 gm				Concentration: NEAT				
Species: Rabbit				Sex: Mixed		Weight: 2.42-2.71		
Conditions: Applied to the conjunctival sac; left eye								
Tissue	Effect	Rabbit Number / 24-Hour Score						
		13.01	14.01	15.01				Subtotal
Cornea	A. Opacity	0	0	0				
	B. Area Involved	0	0	0				
	Score = (AxBx5)	0	0	0				0
Iris	A. Iritis	0	0	0				0
	B. Score = Ax5	0	0	0				
Conjunctiva	A. Redness	0	0	0				
	B. Chemosis	0	0	0				
	C. Discharge	0	0	0				
	Score = (A+B+C) x2	0	0	0				0

Total Irritation Score 00

Eye Injury Score (Total Score ÷ No. of Eyes)... 00

Study Conclusions: The test substance did not produce irritation or injury in rabbit eyes. Test discontinued at 72 hrs due to lack of eye effects.

USACHPPM Category: A Interpretation: *Irritation of human eyes is not expected if the substance should accidentally get into the eyes, provided it is washed out as soon as possible.*

EPA Toxicity Category: IV

APPENDIX Q

PRIMARY EYE IRRITATION DATA

Protocol No.: 85MA6631f-10-99-06-01				SOP Number: 07.01				
Chemical Substance: ICD – 3665								
Amount Applied: 0.1 gm				Concentration: NEAT				
Species: Rabbit				Sex: Mixed		Weight: 2.57-2.80		
Conditions: Applied to the conjunctival sac; left eye								
Tissue	Effect	Rabbit Number / 24-Hour Score						
		16.01	17.01	18.01				Subtotal
Cornea	A. Opacity	0	0	0				
	B. Area Involved	0	0	0				
	Score = (AxBx5)	0	0	0				
Iris	A. Iritis	0	0	0				0
	B. Score = Ax5	0	0	0				
Conjunctiva	A. Redness	0	0	0				
	B. Chemosis	0	0	0				
	C. Discharge	0	0	0				
	Score = (A+B+C) x2	0	0	0				0

Total Irritation Score 00

Eye Injury Score (Total Score ÷ No. of Eyes)... 00

Study Conclusions: The test substance did not produce irritation or injury in rabbit eyes. Test discontinued at 72 hrs due to lack of eye effects.

USACHPPM Category: A Interpretation: *Irritation of human eyes is not expected if the substance should accidentally get into the eyes, provided it is washed out as soon as possible.*

EPA Toxicity Category: IV

APPENDIX R

PRIMARY EYE IRRITATION DATA

Protocol No.: 85MA6631g-10-99-06-01				SOP Number: 07.01				
Chemical Substance: ICD – 3673								
Amount Applied: 0.1 gm				Concentration: NEAT				
Species: Rabbit				Sex: Mixed		Weight: 2.53-2.65		
Conditions: Applied to the conjunctival sac; left eye								
Tissue	Effect	Rabbit Number / 24-Hour Score						
		19.01	20.01	21.01				Subtotal
Cornea	A. Opacity	0	0	0				0
	B. Area Involved	0	0	0				
	Score = (AxBx5)	0	0	0				
Iris	A. Iritis	0	0	0				0
	B. Score = Ax5	0	0	0				
Conjunctiva	A. Redness	0	0	0				0
	B. Chemosis	0	0	0				
	C. Discharge	0	0	0				
	Score = (A+B+C) x2	0	0	0				

Total Irritation Score 00

Eye Injury Score (Total Score ÷ No. of Eyes). . 00

Study Conclusions: The test substance did not produce irritation or injury in rabbit eyes. Test discontinued at 72 hrs due to lack of eye effects.

USACHPPM Category: A Interpretation: *Irritation of human eyes is not expected if the substance should accidentally get into the eyes, provided it is washed out as soon as possible.*

EPA Toxicity Category: IV

APPENDIX S

ARCHIVES/PERSONNEL

1. ARCHIVES.

a. All raw data, documentation, records, protocol and a copy of the final report generated as a result of this study will be archived in the storage facilities of the Toxicology Directorate, USACHPPM, for a minimum of five (5) years following submission of the final report to the Sponsor.

b. The present study used the laboratory project number 85-MA-6631-01 for all filings.

2. PERSONNEL. The following personnel participated in the studies reported herein:

a. Toxicology Directorate:

Mr. Hubert L. Snodgrass, Ms. Terry L. Hanna, and Newton H. Foster, MAJ, VC

b. Quality Assurance Office:

Mr. Michael Kefauver

Toxicology Study No. 85-XC-5154_02, Hubert Snodgrass

REPORT DOCUMENTATION PAGE			Form Approved OMB No 0704-0188	
Public reporting burden for this collection of information is estimated to average 1 hour per response, including the time for reviewing instructions, searching existing data sources, gathering and maintaining the data needed, and completing and reviewing the collection of information. Send comments regarding this burden estimate or any other aspect of this collection of information, including suggestions for reducing this burden, to Washington Headquarters Services, Directorate for Information Operations and Reports, 1215 Jefferson Davis Highway, Suite 1204, Arlington, VA 22202-4302, and to the Office of Management and Budget, Paperwork Reduction Project (0704-0188), Washington, DC 20503				
1 AGENCY USE ONLY (Leave blank)		2 REPORT DATE August 2002	3 REPORT TYPE AND DATES COVERED Final Jun - Aug 2002	
4 TITLE AND SUBTITLE Toxicology Study No 85-XC-5154-02, The Acute Skin and Eye Effects of the Active Topical Skin Protectant (aTSP) Formulations ICD-3829, ICD-3830, ICD-3831, ICD-3832, ICD-3833, ICD-3834, and ICD-3792 in Rabbits, August 2002			5 FUNDING NUMBERS	
6 AUTHOR(S) Hubert L. Snodgrass				
7 PERFORMING ORGANIZATION NAME(S) AND ADDRESS(ES) U.S. Army Center for Health Promotion and Preventive Medicine Toxicology Program, ATTN: MCHB-TS-TTE 5158 Blackhawk Road Aberdeen Proving Ground, MD 21010-5403			8 PERFORMING ORGANIZATION REPORT NUMBER Toxicology Study No 85-XC-5154-02	
9 SPONSORING / MONITORING AGENCY NAME(S) AND ADDRESS(ES) Advanced Assessment Branch Drug Assessment Division U.S. Army Medical Research Institute of Chemical Defense 3100 Ricketts Point Road Aberdeen Proving Ground, MD 21010-5400			10 SPONSORING / MONITORING AGENCY REPORT NUMBER	
11 SUPPLEMENTARY NOTES				
12a DISTRIBUTION / AVAILABILITY STATEMENT Approved for public release, distribution unlimited			12b DISTRIBUTION CODE	
13 ABSTRACT (Maximum 200 words) The purpose of the study was to determine the acute skin and eye irritation effects of the active topical skin protectant (TSP) formulations ICD-3829, ICD-3830, ICD-3831, ICD-3832, ICD-3833, ICD-3834, and ICD-3792 in Rabbits For the skin irritation study, the animals were treated with 0.5 g of each substance to the clipped back for four hours. No significant skin irritation was observed in rabbits through seven days following treatment with any of the test substances. No adverse skin effects in humans are anticipated following an acute exposure. For the skin irritation study, each rabbit received 0.1 g of a single test substance applied to the conjunctival sac of one eye. The opposite eye served as an untreated control. The TSP formulations ICD-3829, ICD-3830, ICD-3831, ICD-3832, ICD-3834, and ICD-3792, did not produce significant eye irritation in rabbits. No adverse ocular effects in humans are anticipated following an acute exposure. ICD-3833 produced moderate irritation in rabbit eyes which was resolved within 72 hours. In humans, ICD-3833 should be used with caution around the eyes and mucosa.				
14 SUBJECT TERMS ICD-3829 ICD-3832 ICD-3792 Skin irritation ICD-3830 ICD-3833 eye irritation topical skin protectant ICD-3831 ICD-3834 rabbit			15 NUMBER OF PAGES 37	
			16 PRICE CODE	
17 SECURITY CLASSIFICATION OF REPORT UNCLASSIFIED	18 SECURITY CLASSIFICATION OF THIS PAGE UNCLASSIFIED	19 SECURITY CLASSIFICATION OF ABSTRACT UNCLASSIFIED	20 LIMITATION OF ABSTRACT UNLIMITED	

Toxicology Study No. 85-XC-5154-02, Jun-Jul 02

Sponsor

Ernest H. Braue, Jr., Ph.D.
Advanced Assessment Branch
Drug Assessment Division
U.S. Army Medical Research Institute of Chemical Defense
3100 Ricketts Point Road
Aberdeen Proving Ground, MD 21010-5400

Study Title

Toxicology Study No. 85-XC-5154-02,
The Acute Skin and Eye Effects of the Active Topical Skin Protectant (aTSP)
Formulations ICD-3829, ICD-3830, ICD-3831, ICD-3832, ICD-3833, ICD-3834,
and ICD-3792 in Rabbits
June-July 2002

Data Requirement

Guideline
Reference No. 81-4
Reference No. 81-5

Author

Hubert L. Snodgrass

Study Initiation Date

17 June 2002

Study Completion Date

16 July 2002

Performing Laboratory

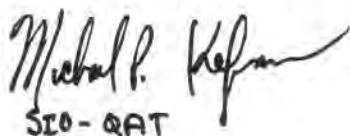
U.S. Army Center for Health Promotion and Preventive Medicine
Toxicology Directorate, ATTN: MCHB-TS-TTE
5158 Blackhawk Road
Aberdeen Proving Ground, MD 21010-5403

Quality Assurance Statement

For: Toxicology Study No. 85-XC-5154-02, titled "The Acute Skin and Eye Effects of the Active Topical Skin Protectant (aTSP) Formulations ICD-3829, ICD-3830, ICD-3831, ICD-3832, ICD-3833, ICD-3834, and ICD-3792 in Rabbits", the following critical phases were audited by the Strategic Initiatives Office-Quality Assurance Team:

<u>Critical Phase Audited (QSO Checklist #)</u>	<u>Date Audited</u>	<u>Date reported to Mngmt.</u>
<u>(For the Eye Irritation portion)</u>		
1) Protocol Review (SIO-QAT #1.1)	05/12/99	05/12/99
2) Test System – Facilities (SIO-QAT # 4.1)	06/27/02	07/09/02 (ICD-3829-3832)
3) Test System – Identification (SIO-QAT # 4.3)	06/27/02	07/09/02 (ICD-3829-3832)
4) Test System - Husbandry (# 4.4)	06/27/02	07/09/02 (ICD-3829-3832)
5) Test System – Observations (# 4.5)	07/02/02	07/12/02 (ICD-3833,34, 3792)
6) Test System - Food and Water (# 4.6)	06/27/02	07/09/02 (ICD-3829-3832)
7) Test System – Facilities (# 4.1)	07/01/02	07/12/02 (ICD-3833,34, 3792)
8) Test System – Identification (# 4.3)	07/01/02	07/12/02 (ICD-3833,34, 3792)
9) Test System - Husbandry (# 4.4)	07/01/02	07/12/02 (ICD-3833,34, 3792)
10) Test System - Food and Water (# 4.6)	07/01/02	07/12/02 (ICD-3833,34, 3792)
11) Test Article – Facilities (# 5.1)	06/27/02	07/09/02 (ICD-3829-3832)
12) Test Article – Control (# 5.2)	06/27/02	07/09/02 (ICD-3829-3832)
13) Test Article – Preparation (# 5.4)	06/27/02	07/09/02 (ICD-3829-3832)
14) Test Article – Administration (# 5.6)	06/27/02	07/09/02 (ICD-3829-3832)
15) Test Article – Facilities (# 5.1)	07/02/02	07/12/02 (ICD-3833,34, 3792)
16) Test Article – Control (# 5.2)	07/02/02	07/12/02 (ICD-3833,34, 3792)
17) Test Article – Preparation (# 5.4)	07/02/02	07/12/02 (ICD-3833,34, 3792)
18) Test Article – Administration (# 5.6)	07/02/02	07/12/02 (ICD-3833,34, 3792)
19) Maintenance and Calibration of Equipment (# 9.1)	06/27/02	07/09/02 (ICD-3829-3832)
20) Maintenance and Calibration of Equipment (# 9.1)	07/01/02	07/12/02 (ICD-3833,34, 3792)
<u>(For the Skin Irritation portion – All ICDs)</u>		
21) Protocol Review (SIO-QAT # 1.0)	07/12/01	07/12/01
21) Test System – Facilities (SIO-QAT # 4.1)	06/17/02	07/01/02
22) Test System – Identification (SIO-QAT # 4.3)	06/17/02	07/01/02
23) Test System - Husbandry (# 4.4)	06/17/02	07/01/02
24) Test System - Food and Water (# 4.6)	06/17/02	07/01/02
25) DTOX Personnel Training Records (# 3.1)	06/17/02	07/01/02
26) Test Article – Facilities (# 5.1)	06/17/02	07/01/02
12) Test Article – Control (# 5.2)	06/17/02	07/01/02
13) Test Article – Preparation (# 5.4)	06/17/02	07/01/02
14) Test Article – Administration (# 5.6)	06/17/02	07/01/02
20) Maintenance and Calibration of Equipment (# 9.1)	06/17/02	07/09/02
30) Compliance w/ DTOX SOPs (# 11.1)	07/09/02	07/15/02
Final Study Report Review (# 13.1) (Entire Study)	08/09/02	08/09/02
Study Raw Data Review (# 14.1) (Entire Study)	08/09/02	08/09/02

➤ Any findings made during the audits were made known at the time of the audit to the Study Director.


SIO - QAT

08/09/02

Toxicology Study No. 85-XC-5154-02, Jun-Jul 02

(Reserved for Confidentiality Claim)

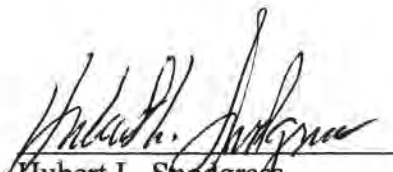
Toxicology Study No. 85-XC-5154-02, Jun-Jul 02

Study Compliance Statement

The study described in this report was conducted in compliance with Title 21, Code of Federal Regulations (CFR), Food and Drug Administration (FDA); Part 58, Good Laboratory Practice Standards. There were no deviations from the aforementioned regulation that affected the quality or integrity of the study or the interpretation of the results.


Submitted By:

Study Director:


Hubert L. Snodgrass
Biologist/Master Consultant
Toxicity Evaluation Program
Directorate of Toxicology

7 Oct 02
Date

Approved By:


Glenn J. Leach
Program Manager,
Toxicity Evaluation

7 Oct 02
Date

Applicant/Submitter

Date



REPLY TO
ATTENTION OF

DEPARTMENT OF THE ARMY
U.S. ARMY CENTER FOR HEALTH PROMOTION AND PREVENTIVE MEDICINE
5158 BLACKHAWK ROAD
ABERDEEN PROVING GROUND, MARYLAND 21010-5403

EXECUTIVE SUMMARY
TOXICOLOGY STUDY NO. 85-XC-5154-02
THE ACUTE SKIN AND EYE EFFECTS OF THE ACTIVE TOPICAL
SKIN PROTECTANT (aTSP) FORMULATIONS ICD-3829, ICD-3830,
ICD-3831, ICD-3832, ICD-3833, ICD-3834,
AND ICD-3792 IN RABBITS
JUNE-JULY 2002

1. **PURPOSE.** To determine the acute skin and eye irritation effects of the active topical skin protectant (aTSP) formulations ICD-3829, ICD-3830, ICD-3831, ICD-3832, ICD-3833, ICD-3834, and ICD-3792 in rabbits.

2. **CONCLUSIONS.**

a. The topical skin protectants ICD-3829, ICD-3830, ICD-3831, ICD-3832, ICD-3833, ICD-3834, and ICD-3792 did not produce significant skin irritation in rabbits. No adverse skin effects in humans are anticipated following an acute exposure.

b. The topical skin protectants ICD-3829, ICD-3830, ICD-3831, ICD-3832, ICD-3834, and ICD-3792 did not produce significant eye irritation in rabbits. No adverse ocular effects in humans are anticipated following an acute exposure. ICD-3833 produced moderate irritation in rabbit eyes that was resolved within 72 hours. In humans, ICD-3833 should be used with caution around the eyes and mucosa.

TABLE OF CONTENTS

Paragraph	Page
1. REFERENCES	1
2. AUTHORITY	1
3. PURPOSE	1
4. MATERIALS	1
a. Test Substance	1
b. Animal	1
5. METHODS	2
a. Primary Skin Irritation	2
b. Primary Eye Irritation	2
c. Test Substance Preparation	2
6. RESULTS	3
a. Primary Skin Irritation	3
b. Primary Eye Irritation	3
7. CONCLUSIONS	3

Appendices

APPENDIX A - References	A-1
APPENDIX B - USACHPPM Categories for Skin Irritation Effects	B-1
APPENDIX C - USACHPPM Categories for Eye Irritation Effects	C-1
APPENDIX D - EPA Toxicity Categories Criteria	D-1
APPENDIX E - Primary Skin Irritation Data; ICD-3829	E-1
APPENDIX F - Primary Skin Irritation Data; ICD-3830	F-1
APPENDIX G - Primary Skin Irritation Data; ICD-3831	G-1
APPENDIX H - Primary Skin Irritation Data; ICD-3832	H-1
APPENDIX I - Primary Skin Irritation Data; ICD-3833	I-1
APPENDIX J - Primary Skin Irritation Data; ICD-3834	J-1
APPENDIX K - Primary Skin Irritation Data; ICD-3792	K-1
APPENDIX L - Primary Eye Irritation Data; ICD-3829	L-1
APPENDIX M - Primary Eye Irritation Data; ICD-3830	M-1
APPENDIX N - Primary Eye Irritation Data; ICD-3831	N-1
APPENDIX O - Primary Eye Irritation Data; ICD-3832	O-1
APPENDIX P - Primary Eye Irritation Data; ICD-3833	P-1
APPENDIX Q - Primary Eye Irritation Data; ICD-3834	Q-1
APPENDIX R - Primary Eye Irritation Data; ICD-3792	R-1
APPENDIX S - Archives/Personnel	S-1



REPLY TO
ATTENTION OF

DEPARTMENT OF THE ARMY
U.S. ARMY CENTER FOR HEALTH PROMOTION AND PREVENTIVE MEDICINE
5158 BLACKHAWK ROAD
ABERDEEN PROVING GROUND, MARYLAND 21010-5403

MCHB-TS-TTE

TOXICOLOGY STUDY NO. 85-XC-5154-02
THE ACUTE SKIN AND EYE EFFECTS OF THE ACTIVE TOPICAL
SKIN PROTECTANT (aTSP) FORMULATIONS ICD-3829, ICD-3830,
ICD-3831, ICD-3832, ICD-3833, ICD-3834,
AND ICD-3792 IN RABBITS
JUNE-JULY 2002

1. REFERENCES. See Appendix A for a listing of references.
2. AUTHORITY. Letter, U.S. Army Medical Research Institute of Chemical Defense (MRICD), 7 May 2002, Subject: Toxicity Testing of aTSP Formulation(s).
3. PURPOSE. To determine the acute skin and eye irritant effects in animals of the topical skin protectant (aTSP) formulations ICD-3829, ICD-3830, ICD-3831, ICD-3832, ICD-3833, ICD-3834, and ICD-3792.
4. MATERIALS.
 - a. Test Substances. Dr. Ernest Braue, Medical Research Institute of Chemical Defense (MRICD) provided the test substances. All seven test substances were heavy to stiff, smooth, white creams. None of the materials had any noticeable odor. Chemical characterization of each substance was the responsibility of the sponsor.
 - b. Animals.^{*±} The acute skin and eye irritation studies were conducted using New Zealand white rabbits purchased from Covance Research Products, Inc., Denver, Pennsylvania. A total of 12 animals of either sex were used. At the start of testing, rabbits weighed between 2.55 and 2.84 kilograms (kg). The rabbits were identified by ear tags and were housed in individual wire-bottom stainless steel cages. Drinking quality water and feed (Teklad Certified 15 percent (%) Rabbit Diet (W) 8630C, Harlan/Teklad, Madison, Wisconsin) were available *ad libitum*. Ambient temperatures in the animal rooms were maintained at 64 to 70 degrees Fahrenheit (°F) with relative humidity between 40 and 60 %. The light/dark cycle was a 12-hour interval.

* In conducting the studies described herein, the investigators adhered to the "Guide for the Care and Use of Laboratory Animals," U S Department of Health Education and Welfare Publication No (NIH) 85-23, 1985.

± The studies reported herein were performed in animal facilities fully accredited by the American Association for the Accreditation of Laboratory Animal Care.

Use of trademarked names does not imply endorsement by the U S Army but is intended only to assist in identification of a specific product.

5. METHODS.

a. Primary Skin Irritation. A primary skin irritation test was conducted using twelve rabbits. Where the test results were equivocal and there was sufficient test material, additional rabbits were tested with the same substance and the scores combined. The procedure (reference 1) involved the single application of 0.5 grams (g) of each test substance to one site on the clipped back of each rabbit. The rabbits' backs were divided into four sites, two on either side of the mid-line; such that each animal received up to four test materials. The pre-weighed substance was dispensed under a 2-by-2 inch gauze pad secured to the skin surface with nonirritating tape. It was then over-wrapped with roll gauze. The animals were not restrained during the exposure but wore Elizabethan collars to prevent probing of the covered exposure site. Exposure was for 4 hours, after which the coverings were removed and irritation scored within 1 hour. Evaluations were also made at 24, 48 and 72 hours after treatment. Scoring of irritation was based on a method described by Draize (reference 2) in which erythema and edema were evaluated on a scale of 0 to 4 for severity. The sum of the mean erythema and mean edema values at 24 and 72 hours were used for the rating of skin irritation. The USACHPPM Skin Irritation rating system was followed and appears at Appendix B. The U.S. Environmental Protection Agency (EPA) Toxicity Categories (reference 4) were also applied and appear at Appendix D. In addition to the observations for skin irritation, any signs of systemic toxicity were recorded.

b. Primary Eye Irritation. An acute eye irritation test was conducted using three rabbits per test substance. The procedure (reference 3) involved the application of 0.1 gm of the substance to the conjunctival sac of each rabbit. The eye was momentarily held closed, then the animal returned to its cage. After 24 hours, the cornea, iris and conjunctiva were observed for signs of irritation and scored (0 to 4) using the Draize method. The total score from the worksheet was divided by the number of eyes scored (3), times the number of tissue systems evaluated (3). This value was the basis for applying the USACHPPM eye irritation rating system (see Appendix C). The eyes were also evaluated at 48 and 72 hours. If irritation was observed at 72 hours, observations were made at 7 and 14 days after treatment to assess recovery. The U.S. EPA Toxicity Categories were also applied and appear at Appendix D. In addition to the observations for eye irritation, any signs of systemic toxicity were recorded.

c. Test Substance Preparation. Each test substance for skin application was weighed (0.5 gm) onto a 2-by-2 inch gauze pad, which was then taped onto the test site. For the eye irritation studies, 0.1 gm of the material was weighed onto a disposable autopipette tip, in the form of a small, suspended ball, and then placed in the conjunctival sac of the animal.

6. RESULTS.

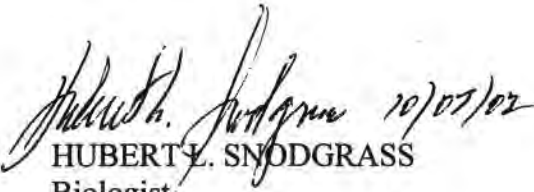
a. Primary Skin Irritation. Under the conditions of the described study, the test substances ICD-3829, ICD-3830, ICD-3831, ICD-3832, ICD-3833, ICD-3834, and ICD-3792 did not produce any significant skin irritation to rabbits. See Appendices E through L for individual animal results. The CHPPM Skin Irritation Category I was assigned for each substance (Appendix B). The EPA Toxicity Category IV (Practically Nontoxic) was assigned for each material (see Appendix D).

b. Primary Eye Irritation. Under the conditions of the described study, the test substances ICD-3829, ICD-3830, ICD-3831, ICD-3832, ICD-3834, and ICD-3792 did not produce primary irritation to the eyes of rabbits. See Appendices M through R for individual animal results. ICD-3833 caused moderate eye irritation but all of the effects were resolved within 7 days. The USACHPPM Eye Irritation Category C was assigned for ICD-3833 and EPA Toxicity Category III described the eye effects. The remaining six materials were without significant eye effects and received the Toxicity Ratings of USACHPPM - A and EPA - IV.

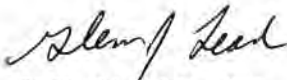
7. CONCLUSIONS.

a. The topical skin protectants ICD-3829, ICD-3830, ICD-3831, ICD-3832, ICD-3833, ICD-3834, and ICD-3792 did not produce significant skin irritation in rabbits. No adverse skin effects in humans are anticipated following an acute exposure.

b. The topical skin protectants ICD-3829, ICD-3830, ICD-3831, ICD-3832, ICD-3834, and ICD-3792 did not produce significant eye irritation in rabbits. No adverse ocular effects in humans are anticipated following an acute exposure. ICD-3833 produced moderate irritation in rabbit eyes that was resolved within 72 hours. In humans, ICD-3833 should be used with caution around the eyes and mucosa.


HUBERT L. SNODGRASS
Biologist
Master Consultant
Toxicity Evaluation Program

APPROVED:


GLENN J. LEACH
Program Manager,
Toxicity Evaluation

7 Oct 2002
Date

APPENDIX A

REFERENCES

1. Standing Operating Procedure (SOP) No. 08.01, Primary Dermal Irritation Study, USACHPPM, Directorate of Toxicology. 2 Aug 01.
2. Draize, J.H., Woodward, G., and Calvery, H.O. 1944. Methods for the study of irritation and toxicity of substances applied topically to the skin and mucous membranes, *J. Pharmacol. Exp. Ther.* 82:377-390.
3. SOP No. 07.01, Primary Eye Irritation Study, USACHPPM, Directorate of Toxicology. 2 Aug 01.
4. U.S. Environmental Protection Agency, Office of Prevention, Pesticides and Toxic Substances (OPPTS): Health Effects Test Guidelines, OPPTS 870.1000, Acute Toxicity Testing – Background. August 1998.

APPENDIX B

USACHPPM CATEGORIES FOR SKIN IRRITATION EFFECTS

CATEGORY I - Compounds producing no primary irritation of the intact skin or no greater than mild primary irritation of the skin surrounding an abrasion. Score Limits: Intact 0-0.5; Abraded 0.51-2.0; Total 0-2.0 INTERPRETATION: *No restriction for acute application to the human skin*

CATEGORY II - Compounds producing mild primary irritation of the intact skin and the skin surrounding an abrasion. Score Limits: Intact >0.5; Total 0.51-2.0 INTERPRETATION: *Should be used only on human skin found by examination to have no abrasions or may be used as clothing impregnant.*

CATEGORY III - Compounds producing moderate primary irritation of the intact skin and the skin surrounding an abrasion. Score Limits: Total 2.1-5.0 INTERPRETATION: *Should not be used directly without a prophetic patch test having been conducted on humans to determine irritation potential to human skin May be used without patch testing, with extreme caution, as clothing impregnants. Compound should be resubmitted in the form and at the intended use concentration so that its irritation potential can be reexamined using other test techniques on animals*

CATEGORY IV - Compounds producing moderate to severe primary irritation of the intact skin and of the skin surrounding an abrasion. Score Limits: Total 2.1-7.9 INTERPRETATION: *Should be resubmitted for testing in the form and at the intended use concentration Upon resubmission, its irritation potential will be reexamined using other test techniques on animals, prior to possible prophetic patch testing in humans, at concentrations that have been shown not to produce primary irritation in animals.*

CATEGORY V - Compounds impossible to classify because of staining of the skin or other masking effects owing to physical properties of the compound or compounds producing necrosis, vesiculation, or eschars. Score Limits: Total 8.0 or not scorable. INTERPRETATION: *Not suitable for use on humans*

APPENDIX C

USACHPPM CATEGORIES FOR EYE IRRITATION EFFECTS

CATEGORY A - Compounds noninjurious to the eye. Score Limits: 0-10 (individual conjunctival score for chemosis, redness or discharge not to exceed 1). **INTERPRETATION:** *Irritation of human eyes is not expected if the compound should accidentally get into the eyes, provided it is washed out as soon as possible.*

CATEGORY B - Compounds producing mild injury to the cornea. Score Limits: 10-20 (individual conjunctival score for chemosis, redness or discharge not to exceed 1). **INTERPRETATION:** *To be used with caution around the eyes.*

CATEGORY C - Compounds producing mild injury to the cornea, and in addition some injury to the conjunctiva. Score Limits: 5-30 (individual conjunctival score for chemosis, redness or discharge exceed 1). **INTERPRETATION:** *To be used with caution around the eyes and mucosa (e.g , nose and mouth).*

CATEGORY D - Compounds producing moderate injury to the cornea. Score Limits: <20-50 (individual conjunctival score for chemosis, redness or discharge not to exceed 1). **INTERPRETATION:** *To be used with extreme caution around eyes.*

CATEGORY E - Compounds producing moderate injury to the cornea and in addition producing some injury to the conjunctiva. Score Limits: 20-50 (individual conjunctival score for chemosis, redness or discharge exceed 1). **INTERPRETATION:** *To be used with extreme caution around the eyes and mucosa.*

CATEGORY F - Compounds producing severe injury to the cornea and to the conjunctiva. Score Limits: 50 or greater. **INTERPRETATION:** *To be used only with extreme caution, it is recommended that the use be restricted to areas other than the face.*

APPENDIX D

EPA TOXICITY CATEGORY CRITERIA*

Study	Category I <i>Highly Toxic</i> †	Category II <i>Moderately Toxic</i>	Category III <i>Slightly Toxic</i>	Category IV <i>Practically nontoxic</i>
Acute Oral mg/kg	Up to and including 50	> 50 through 500	> 500 through 5,000	> 5,000
Acute Inhalation mg/L	Up to and including 0.05	> 0.05 through 0.5	> 0.5 through 2.0	> 2.0
Acute Dermal mg/kg	Up to and including 200	> 200 through 2,000	> 2,000 through 5,000	> 5,000
Eye Irritation	Corrosive (irreversible destruction of ocular tissue) or corneal involvement or irritation persisting for more than 21 days	Corneal involvement or irritation clearing in 8- 21 days	Corneal involvement or irritation clearing in 7 days or less	Minimal effects clearing in less than 24 hours
Skin Irritation	Corrosive (tissue destruction into the dermis and/or scarring)	Severe irritation at 72 hours (severe erythema or edema)	Moderate irritation at 72 hours (moderate erythema)	Mild or slight irritation (no irritation or slight erythema)

Study	Study Results	Study Results
Dermal Sensitization	Product is a sensitizer or is positive for sensitization	Product is not a sensitizer or is negative for sensitization

* U.S. Environmental Protection Agency, Office of Prevention, Pesticides and Toxic Substances (OPPTS): Health Effects Test Guidelines, OPPTS 870.1000, Acute Toxicity Testing – Background. August 1998

† Descriptive terms, for example, Highly Toxic, Moderately toxic, etc., inserted for clarification only; not a part of OPPTS 870.1000

APPENDIX E

PRIMARY SKIN IRRITATION DATA

Protocol No.: 5154a-11-01-07-04					SOP Number: 08.01			
Chemical Substance: ICD-3829								
Amount Applied: 0.5 gm					Concentration: Technical			
Species: Rabbit			Sex: Mixed			Weight: 2.60 – 2.82 kg		
Conditions: 4-hour nonoccluded exposure.								
Tm (hr)	Observation	Animal Number / Score						
		02.13	02.14	02.15	02.16	02.17	02.18	SUM
24	Erythema	0	0	0	0	0	0	0
48		0	0	0	0	0	0	
72		0	0	0	0	0	0	
7 da		0	0	0	0	0	0	
Subtotal (24 and 72 hour)								0
24	Edema	0	0	0	0	0	0	0
48		0	0	0	0	0	0	
72		0	0	0	0	0	0	
7 da		0	0	0	0	0	0	
Subtotal (24 and 72 hour)								0
Total Score (SUM of All Scores ÷ 2X No. of Animals)								0.00
Study Conclusions: Nonirritating to the intact skin of rabbits. Study discontinued after 72 hrs since no irritant effects were observed.								
USACHPPM Category I. Interpretation: No restriction for acute application to the human skin.								
EPA Toxicity Category IV. Practically Nontoxic								

APPENDIX F

PRIMARY SKIN IRRITATION DATA

Protocol No.: 5154b-11-01-07-04					SOP Number: 08.01			
Chemical Substance: ICD-3830								
Amount Applied: 0.5 gm					Concentration: Technical			
Species: Rabbit			Sex: Mixed		Weight: 2.60 – 2.82 kg			
Conditions: 4-hour nonoccluded exposure.								
Tm (hr)	Observation	Animal Number / Score						
		02.13	02.14	02.15	02.16	02.17	02.18	SUM
24	Erythema	0	0	0	0	0	0	0
48		0	0	0	0	0	0	
72		0	0	0	0	0	0	
7 da		0	0	0	0	0	0	
Subtotal (24 and 72 hour)								0
24	Edema	0	0	0	0	0	0	0
48		0	0	0	0	0	0	
72		0	0	0	0	0	0	
7 da		0	0	0	0	0	0	
Subtotal (24 and 72 hour)								0
Total Score (SUM of All Scores ÷ 2X No. of Animals)								0.00
Study Conclusions: Nonirritating to the intact skin of rabbits. Study discontinued after 72 hrs since no irritant effects were observed.								
USACHPPM Category I. Interpretation: No restriction for acute application to the human skin.								
EPA Toxicity Category IV. Practically Nontoxic								

APPENDIX G

PRIMARY SKIN IRRITATION DATA

Protocol No.: 5154c-11-01-07-04					SOP Number: 08.01			
Chemical Substance: ICD-3831								
Amount Applied: 0.5 gm					Concentration: Technical			
Species: Rabbit		Sex: Mixed		Weight: 2.60 – 2.82 kg				
Conditions: 4-hour nonoccluded exposure.								
Tm (hr)	Observation	Animal Number / Score						
		02.13	02.14	02.15	02.16	02.17	02.18	SUM
24	Erythema	0	0	0	0	0	0	0
48		0	0	0	0	0	0	
72		0	0	0	0	0	0	
7 da		0	0	0	0	0	0	
Subtotal (24 and 72 hour)								0
24	Edema	0	0	0	0	0	0	0
48		0	0	0	0	0	0	
72		0	0	0	0	0	0	
7 da		0	0	0	0	0	0	
Subtotal (24 and 72 hour)								0
Total Score (SUM of All Scores ÷ 2X No. of Animals)								0.00
Study Conclusions: Nonirritating to the intact skin of rabbits. Study discontinued after 72 hrs since no irritant effects were observed.								
USACHPPM Category I. Interpretation: No restriction for acute application to the human skin.								
EPA Toxicity Category IV. Practically Nontoxic								

APPENDIX H

PRIMARY SKIN IRRITATION DATA

Protocol No.: 5154d-11-01-07-04					SOP Number: 08.01			
Chemical Substance: ICD-3832								
Amount Applied: 0.5 gm					Concentration: Technical			
Species: Rabbit			Sex: Mixed		Weight: 2.60 – 2.82 kg			
Conditions: 4-hour nonoccluded exposure.								
Tm (hr)	Observation	Animal Number / Score						
		02.13	02.14	02.15	02.16	02.17	02.18	SUM
24	Erythema	0	0	0	0	0	0	0
48		0	0	0	0	0	0	
72		0	0	0	0	0	0	
7 da		0	0	0	0	0	0	
Subtotal (24 and 72 hour)								0
24	Edema	0	0	0	0	0	0	0
48		0	0	0	0	0	0	
72		0	0	0	0	0	0	
7 da		0	0	0	0	0	0	
Subtotal (24 and 72 hour)								0
Total Score (SUM of All Scores ÷ 2X No. of Animals)								0.00
Study Conclusions: Nonirritating to the intact skin of rabbits. Study discontinued after 72 hrs since no irritant effects were observed.								
USACHPPM Category I. Interpretation: No restriction for acute application to the human skin.								
EPA Toxicity Category IV. Practically Nontoxic								

APPENDIX I

PRIMARY SKIN IRRITATION DATA

Protocol No.: 5154e-11-01-07-04				SOP Number: 08.01				
Chemical Substance: ICD-3833								
Amount Applied: 0.5 gm				Concentration: Technical				
Species: Rabbit		Sex: Mixed		Weight: 2.74 – 3.08 kg				
Conditions: 4-hour nonoccluded exposure.								
Tm (hr)	Observation	Animal Number / Score						
		02.19	02.20	02.21	02.23	02.24	02.13	SUM
24	Erythema	0	0	0	0	0	1	
48		0	0	1	0	0	1	
72		0	0	1	0	0	1	
7 da		0	0	0	0	0	0	
Subtotal (24 and 72 hour)								
24	Edema	0	0	0	0	0	0	
48		0	0	0	0	0	0	
72		0	0	0	0	0	0	
7 da		0	0	0	0	0	0	
Subtotal (24 and 72 hour)								
Total Score (SUM of All Scores ÷ 2X No. of Animals)								
Continued next page.								

Protocol No.: 5154e-11-01-07-04					SOP Number: 08.01			
Chemical Substance: ICD-3833								
Amount Applied: 0.5 gm					Concentration: Technical			
Species: Rabbit			Sex: Mixed		Weight: 2.74 – 3.08 kg			
Conditions: 4-hour nonoccluded exposure.								

Tm (hr)	Observation	Animal Number / Score						SUM
		02.14	02.15	02.16				
24	Erythema	0	0	0				1
48		0	0	1				
72		0	0	1				
7 da		0	0	0				
Subtotal (24 and 72 hour)								4
24	Edema	0	0	0				0
48		0	0	0				
72		0	0	0				
7 da		0	0	0				
Subtotal (24 and 72 hour)								0
Total Score (SUM of All Scores ÷ 2X No. of Animals)								0.22

Note: Nine animals tested.	
Study Conclusions: Nonirritating to the intact skin of rabbits.	
USACHPPM Category I. Interpretation: <i>No restriction for acute application to the human skin.</i>	
EPA Toxicity Category IV. <i>Practically Nontoxic</i>	

APPENDIX J

PRIMARY SKIN IRRITATION DATA

Protocol No.: 5154f-11-01-07-04				SOP Number: 08.01			
Chemical Substance: ICD-3834							
Amount Applied: 0.5 gm				Concentration: Technical			
Species: Rabbit		Sex: Mixed		Weight: 2.74 – 3.08 kg			
Conditions: 4-hour nonoccluded exposure.							

Tm (hr)	Observation	Animal Number / Score						SUM
		02.19	02.20	02.21	02.23	02.24	02.13	
24	Erythema	0	0	0	0	0	1	
48		0	0	1	0	0	1	
72		0	0	1	0	0	1	
7 da		0	0	0	0	0	0	
Subtotal (24 and 72 hour)								
24	Edema	0	0	0	0	0	0	
48		0	0	0	0	0	0	
72		0	0	0	0	0	0	
7 da		0	0	0	0	0	0	
Subtotal (24 and 72 hour)								
Total Score (SUM of All Scores ÷ 2X No. of Animals)								
Continued next page.								

Protocol No.: 5154f-11-01-07-04						SOP Number: 08.01		
Chemical Substance: ICD-3834								
Amount Applied: 0.5 gm						Concentration: Technical		
Species: Rabbit			Sex: Mixed			Weight: 2.74 – 3.08 kg		
Conditions: 4-hour nonoccluded exposure.								
Tm (hr)	Observation	Animal Number / Score						
		02.14	02.15	02.16	02.17			SUM
24	Erythema	0	0	0	0			1
48		0	0	1	0			3
72		0	0	1	0			
7 da		0	0	0	0			
Subtotal (24 and 72 hour)								4
24	Edema	0	0	0	0			0
48		0	0	0	0			0
72		0	0	0	0			
7 da		0	0	0	0			
Subtotal (24 and 72 hour)								0
Total Score (SUM of All Scores ÷ 2X No. of Animals)								0.20
Note: Ten animals tested.								
Study Conclusions: Nonirritating to the intact skin of rabbits								
USACHPPM Category I. Interpretation: No restriction for acute application to the human skin.								
EPA Toxicity Category IV. Practically Nontoxic								

APPENDIX K

PRIMARY SKIN IRRITATION DATA

Protocol No.: 5154g-11-01-07-04				SOP Number: 08.01			
Chemical Substance: ICD-3792							
Amount Applied: 0.5 gm				Concentration: Technical			
Species: Rabbit		Sex: Mixed		Weight: 2.74 – 3.08 kg			
Conditions: 4-hour nonoccluded exposure.							

Tm (hr)	Observation	Animal Number / Score						SUM
		02.19	02.20	02.21	02.23	02.24	02.13	
24	Erythema	0	0	0	0	0	0	
48		0	0	2	0	0	0	
72		0	0	2	0	0	0	
7 da		0	0	0	0	0	0	
Subtotal (24 and 72 hour)								
24	Edema	0	0	0	0	0	0	
48		0	0	1	0	0	0	
72		0	0	1	0	0	0	
7 da		0	0	0	0	0	0	
Subtotal (24 and 72 hour)								
Total Score (SUM of All Scores ÷ 2X No. of Animals)								
<i>Continued next page.</i>								

Protocol No.: 5154g-11-01-07-04				SOP Number: 08.01				
Chemical Substance: ICD-3792								
Amount Applied: 0.5 gm				Concentration: Technical				
Species: Rabbit		Sex: Mixed		Weight: 2.74 – 3.08 kg				
Conditions: 4-hour nonoccluded exposure.								
Tm (hr)	Observation	Animal Number / Score						
		02.14	02.25					SUM
24	Erythema	0	0					0
48		0	0					2
72		0	0					
7 da		0	0					
Subtotal (24 and 72 hour)								2
24	Edema	0	0					0
48		0	0					1
72		0	0					
7 da		0	0					
Subtotal (24 and 72 hour)								1
Total Score (SUM of All Scores ÷ 2X No. of Animals)								0.19
Note: Eight animals tested.								
Study Conclusions: Nonirritating to the intact skin of rabbits.								
USACHPPM Category I. Interpretation: No restriction for acute application to the human skin.								
EPA Toxicity Category IV. Practically Nontoxic								

APPENDIX L

PRIMARY EYE IRRITATION DATA

Protocol No.: 5154a-10-99-06-01		SOP Number: 07.01						
Chemical Substance: ICD – 3829								
Amount Applied: 0.1 gm			Concentration: NEAT					
Species: Rabbit			Sex: Male			Weight: 2.94-3.00 kg		
Conditions: Applied to the conjunctival sac; right eye								
Tissue	Effect	Rabbit Number / 24-Hour Score						Subtotal
		02.13	02.14	02.15				
Cornea	A. Opacity	0	0	0				
	B. Area Involved	0	0	0				
	Score = (AxBx5)	0	0	0				
Iris	A. Iritis	0	0	0				0
	B. Score = Ax5	0	0	0				
Conjunctiva	A. Redness	1	0	0				
	B. Chemosis	0	0	0				
	C. Discharge	0	0	0				
	Score = (A+B+C) x2	2	0	0				2

Total Irritation Score **2.00**

Eye Injury Score (Total Score ÷ No. of Eyes*) **0.22**

Study Conclusions: The test substance produced only minimal eye effects in one rabbit, which was resolved within 72 hours.

USACHPPM Category: A Interpretation: *Irritation of human eyes is not expected if the substance should accidentally get into the eyes, provided it is washed out as soon as possible.*

EPA Toxicity Category: IV *Practically nontoxic.*

* Number of eyes = 3 tissues observed x 3 eyes = 9

Toxicology Study No. 85-XC-5154-02, Jun-Jul 02

Raw Eye Irritation Scores By Time Period													
Protocol No. 5154a-10-99-06-01 Test Substance: ICD-3829		Animal Number 2.13				Animal Number 2.14				Animal Number 2.15			
		Observation Time											
Tissue	Effect (Score)	24 hr	48 hr	72 hr	7 da	24 hr	48 hr	72 hr	7 da	24 hr	48 hr	72 hr	7 da
Cornea	Opacity	0	0	0	0	0	0	0		0	0	0	
	Area	0	0	0	0	0	0	0		0	0	0	
Iris	Iritis	0	0	0	0	0	0	0		0	0	0	
Conjunctiva	Redness	1	1	0	0	0	0	0		0	0	0	
	Chemosis	0	0	0	0	0	0	0		0	0	0	
	Discharge	0	0	0	0	0	0	0		0	0	0	

APPENDIX M

PRIMARY EYE IRRITATION DATA

Protocol No.: 5154b-10-99-06-01		SOP Number: 07.01						
Chemical Substance: ICD – 3830								
Amount Applied: 0.1 gm			Concentration: NEAT					
Species: Rabbit			Sex: Male			Weight: 2.74-3.03 kg		
Conditions: Applied to the conjunctival sac; right eye								
Tissue	Effect	Rabbit Number / 24-Hour Score						Subtotal
		02.16	02.17	02.18				
Cornea	A. Opacity	0	0	0				
	B. Area Involved	0	0	0				
	Score = (AxBx5)	0	0	0				0
Iris	A. Iritis	0	0	0				0
	B. Score = Ax5	0	0	0				
Conjunctiva	A. Redness	0	0	0				
	B. Chemosis	0	0	0				
	C. Discharge	0	0	0				
	Score = (A+B+C) x2	0	0	0				0

Total Irritation Score **0.00**

Eye Injury Score (Total Score ÷ No. of Eyes) **0.00**

Study Conclusions: The test substance did not produce eye irritation in rabbits.

USACHPPM Category: A Interpretation: *Irritation of human eyes is not expected if the substance should accidentally get into the eyes, provided it is washed out as soon as possible.*

EPA Toxicity Category: IV *Practically nontoxic.*

Toxicology Study No. 85-XC-5154-02, Jun-Jul 02

Raw Eye Irritation Scores By Time Period													
Protocol No. 5154b-10-99-06-01 Test Substance: ICD-3830		Animal Number 2.16				Animal Number 2.17				Animal Number 2.18			
		Observation Time											
Tissue	Effect (Score)	24 hr	48 hr	72 hr	7 da	24 hr	48 hr	72 hr	7 da	24 hr	48 hr	72 hr	7 da
Cornea	Opacity	0	0	0		0	0	0		0	0	0	
	Area	0	0	0		0	0	0		0	0	0	
Iris	Iritis	0	0	0		0	0	0		0	0	0	
Conjunctiva	Redness	0	0	0		0	0	0		0	0	0	
	Chemosis	0	0	0		0	0	0		0	0	0	
	Discharge	0	0	0		0	0	0		0	0	0	

APPENDIX N

PRIMARY EYE IRRITATION DATA

Protocol No.: 5154c-10-99-06-01		SOP Number: 07.01						
Chemical Substance: ICD – 3831								
Amount Applied: 0.1 gm		Concentration: NEAT						
Species: Rabbit		Sex: Male		Weight: 2.76-2.99 kg				
Conditions: Applied to the conjunctival sac; right eye								
Tissue	Effect	Rabbit Number / 24-Hour Score						Subtotal
		02.19	02.20	02.21				
Cornea	A. Opacity	0	0	0				
	B. Area Involved	0	0	0				
	Score = (AxBx5)	0	0	0				0
Iris	A. Iritis	0	0	0				0
	B. Score = Ax5	0	0	0				
Conjunctiva	A. Redness	0	0	0				
	B. Chemosis	0	0	0				
	C. Discharge	0	0	0				
	Score = (A+B+C) x2	0	0	0				0

Total Irritation Score 0.00

Eye Injury Score (Total Score ÷No. of Eyes). 0.00

Study Conclusions: The test substance did not produce eye irritation in rabbits.

USACHPPM Category: A Interpretation: *Irritation of human eyes is not expected if the substance should accidentally get into the eyes, provided it is washed out as soon as possible.*

EPA Toxicity Category: IV *Practically nontoxic.*

Toxicology Study No. 85-XC-5154-02, Jun-Jul 02

Raw Eye Irritation Scores By Time Period													
Protocol No. 5154c-10-99-06-01 Test Substance: ICD-3831		Animal Number 2.19				Animal Number 2.20				Animal Number 2.21			
		Observation Time											
Tissue	Effect (Score)	24 hr	48 hr	72 hr	7 da	24 hr	48 hr	72 hr	7 da	24 hr	48 hr	72 hr	7 da
Cornea	Opacity	0	0	0		0	0	0		0	0	0	
	Area	0	0	0		0	0	0		0	0	0	
Iris	Iritis	0	0	0		0	0	0		0	0	0	
Conjunctiva	Redness	0	0	0		0	0	0		0	0	0	
	Chemosis	0	0	0		0	0	0		0	0	0	
	Discharge	0	0	0		0	0	0		0	0	0	

APPENDIX N

PRIMARY EYE IRRITATION DATA

Protocol No.: 5154c-10-99-06-01		SOP Number: 07.01						
Chemical Substance: ICD – 3831								
Amount Applied: 0.1 gm			Concentration: NEAT					
Species: Rabbit			Sex: Male			Weight: 2.76-2.99 kg		
Conditions: Applied to the conjunctival sac; right eye								
Tissue	Effect	Rabbit Number / 24-Hour Score						Subtotal
		02.19	02.20	02.21				
Cornea	A. Opacity	0	0	0				
	B. Area Involved	0	0	0				
	Score = (AxBx5)	0	0	0				0
Iris	A. Iritis	0	0	0				0
	B. Score = Ax5	0	0	0				
Conjunctiva	A. Redness	0	0	0				
	B. Chemosis	0	0	0				
	C. Discharge	0	0	0				
	Score = (A+B+C) x2	0	0	0				0

Total Irritation Score 0.00

Eye Injury Score (Total Score ÷No. of Eyes)..... 0.00

Study Conclusions: The test substance did not produce eye irritation in rabbits.

USACHPPM Category: A Interpretation: *Irritation of human eyes is not expected if the substance should accidentally get into the eyes, provided it is washed out as soon as possible.*

EPA Toxicity Category: IV *Practically nontoxic.*

Toxicology Study No. 85-XC-5154-02, Jun-Jul 02

Raw Eye Irritation Scores By Time Period													
Protocol No. 5154d-10-99-06-01 Test Substance: ICD-3832		Animal Number 2.22				Animal Number 2.23				Animal Number 2.24			
		Observation Time											
Tissue	Effect (Score)	24 hr	48 hr	72 hr	7 da	24 hr	48 hr	72 hr	7 da	24 hr	48 hr	72 hr	7 da
Cornea	Opacity	0	0	0		0	0	0		0	0	0	
	Area	0	0	0		0	0	0		0	0	0	
Iris	Iritis	0	0	0		0	0	0		0	0	0	
Conjunctiva	Redness	0	0	0		0	0	0		0	0	0	
	Chemosis	0	0	0		0	0	0		0	0	0	
	Discharge	0	0	0		0	0	0		0	0	0	

APPENDIX P

PRIMARY EYE IRRITATION DATA

Protocol No.: 5154e-10-99-06-01		SOP Number: 07.01						
Chemical Substance: ICD – 3833								
Amount Applied: 0.1 gm			Concentration: NEAT					
Species: Rabbit			Sex: Male			Weight: 3.04-3.10 kg		
Conditions: Applied to the conjunctival sac; right eye								
Tissue	Effect	Rabbit Number / 24-Hour Score						Subtotal
		02.13	02.14	02.15				
Cornea	A. Opacity	0	1	0				
	B. Area Involved	0	1	0				
	Score = (AxBx5)	0	5	0				
Iris	A. Iritis	0	0	0				0
	B. Score = Ax5	0	0	0				
Conjunctiva	A. Redness	2	2	1				
	B. Chemosis	0	1	0				
	C. Discharge	0	1	0				
	Score = (A+B+C) x2	4	8	2				14

Total Irritation Score 19.0

Eye Injury Score (Total Score ÷ No. of Eyes) 2.11

Study Conclusions: Moderate eye irritation. All injury resolved by 72 hours.**USACHPPM Category:** C Interpretation: *To be used with caution around the eyes and mucosa.***EPA Toxicity Category:** III. Slightly toxic.

Raw Eye Irritation Scores By Time Period													
Protocol No. 5154e-10-99-06-01 Test Substance: ICD-3833		Animal Number 2.13				Animal Number 2.14				Animal Number 2.15			
		Observation Time											
Tissue	Effect (Score)	24 hr	48 hr	72 hr	7 da	24 hr	48 hr	72 hr	7 da	24 hr	48 hr	72 hr	7 da
Cornea	Opacity	0	0	0	0	1	0	0	0	0	0	0	0
	Area	0	0	0	0	1	0	0	0	0	0	0	0
Iris	Iritis	0	0	0	0	0	0	0	0	0	0	0	0
Conjunctiva	Redness	2	1	0	0	2	1	0	0	1	1	0	0
	Chemosis	0	0	0	0	1	0	0	0	0	0	0	0
	Discharge	0	0	0	0	1	0	0	0	0	0	0	0

APPENDIX Q

PRIMARY EYE IRRITATION DATA

Protocol No.: 5154f-10-99-06-01		SOP Number: 07.01						
Chemical Substance: ICD – 3834								
Amount Applied: 0.1 gm		Concentration: NEAT						
Species: Rabbit		Sex: Male		Weight: 2.84-3.20 kg				
Conditions: Applied to the conjunctival sac; right eye								
Tissue	Effect	Rabbit Number / 24-Hour Score						
		2.16	2.17	2.18				Subtotal
Cornea	A. Opacity	0	0	0				
	B. Area Involved	0	0	0				
	Score = (AxBx5)	0	0	0				0
Iris	A. Iritis	0	0	0				0
	B. Score = Ax5	0	0	0				
Conjunctiva	A. Redness	0	0	0				
	B. Chemosis	0	0	0				
	C. Discharge	0	0	0				
	Score = (A+B+C) x2	0	0	0				0

Total Irritation Score 0.00

Eye Injury Score (Total Score ÷ No. of Eyes) 0.00

Study Conclusions: The test substance did not produce eye irritation in rabbits.

USACHPPM Category: A Interpretation: *Irritation of human eyes is not expected if the substance should accidentally get into the eyes, provided it is washed out as soon as possible.*

EPA Toxicity Category: IV *Practically nontoxic.*

Raw Eye Irritation Scores By Time Period													
Protocol No. 5154f-10-99-06-01 Test Substance: ICD-3834		Animal Number 2.16				Animal Number 2.17				Animal Number 2.18			
		Observation Time											
Tissue	Effect (Score)	24 hr	48 hr	72 hr	7 da	24 hr	48 hr	72 hr	7 da	24 hr	48 hr	72 hr	7 da
Cornea	Opacity	0	0	0		0	0	0		0	0	0	
	Area	0	0	0		0	0	0		0	0	0	
Iris	Iritis	0	0	0		0	0	0		0	0	0	
Conjunctiva	Redness	0	0	0		0	0	0		0	0	0	
	Chemosis	0	0	0		0	0	0		0	0	0	
	Discharge	0	0	0		0	0	0		0	0	0	

APPENDIX R

PRIMARY EYE IRRITATION DATA

Protocol No.: 5154g-10-99-06-01		SOP Number: 07.01						
Chemical Substance: ICD – 3792								
Amount Applied: 0.1 gm			Concentration: NEAT					
Species: Rabbit			Sex: Male			Weight: 2.98-3.16 kg		
Conditions: Applied to the conjunctival sac; right eye								
Tissue	Effect	Rabbit Number / 24-Hour Score						
		02.19	02.20	02.21				Subtotal
Cornea	A. Opacity	0	0	0				
	B. Area Involved	0	0	0				
	Score = (AxBx5)	0	0	0				
Iris	A. Iritis	0	0	0				0
	B. Score = Ax5	0	0	0				
Conjunctiva	A. Redness	0	1	1				
	B. Chemosis	0	0	0				
	C. Discharge	0	0	0				
	Score = (A+B+C) x2	0	2	2				4
Total Irritation Score								4.00
Eye Injury Score (Total Score ÷No. of Eyes)								0.44

Study Conclusions: Minimal eye irritation effects, resolved after 24 hours.

USACHPPM Category: A Interpretation: *Irritation of human eyes is not expected if the substance should accidentally get into the eyes, provided it is washed out as soon as possible.*

EPA Toxicity Category: IV *Practically nontoxic.*

Toxicology Study No. 85-XC-5154-02, Jun-Jul 02

Raw Eye Irritation Scores By Time Period													
Protocol No. 5154g-10-99-06-01 Test Substance: ICD-3792		Animal Number 2.19				Animal Number 2.20				Animal Number 2.21			
		Observation Time											
Tissue	Effect (Score)	24 hr	48 hr	72 hr	7 da	24 hr	48 hr	72 hr	7 da	24 hr	48 hr	72 hr	7 da
Cornea	Opacity	0	0	0		0	0	0		0	0	0	
	Area	0	0	0		0	0	0		0	0	0	
Iris	Iritis	0	0	0		0	0	0		0	0	0	
Conjunctiva	Redness	0	0	0		1	0	0		1	0	0	
	Chemosis	0	0	0		0	0	0		0	0	0	
	Discharge	0	0	0		0	0	0		0	0	0	

APPENDIX S

ARCHIVES/PERSONNEL

1. ARCHIVES.

a. All raw data, documentation, records, protocol, and a copy of the final report generated as a result of this study will be archived in the storage facilities of the Toxicology Directorate, USACHPPM, for a minimum of five (5) years following submission of the final report to the Sponsor.

b. The present study used the laboratory project number 85-MA-5154-01 for all filings.

c. The following protocol numbers identify the individual studies:

(1) Skin Irritation.

<u>Test Substance</u>	<u>Protocol Number</u>
ICD-3829	5154a-11-01-07-04
ICD-3830	5154b-11-01-07-04
ICD-3831	5154c-11-01-07-04
ICD-3832	5154d-11-01-07-04
ICD-3833	5154e-11-01-07-04
ICD-3834	5154f-11-01-07-04
ICD-3792	5154g-11-01-07-04

(2) Eye Irritation.

ICD-3829	5154a-10-99-06-01
ICD-3830	5154b-10-99-06-01
ICD-3831	5154c-10-99-06-01
ICD-3832	5154d-10-99-06-01
ICD-3833	5154e-10-99-06-01
ICD-3834	5154f-10-99-06-01
ICD-3792	5154g-10-99-06-01

2. PERSONNEL. The following personnel participated in the studies reported herein:

a. Toxicology Directorate:

Mr. Hubert L. Snodgrass, Ms. Terry L. Hanna, and Mr. John T. Houpt

b. Quality Assurance Office:

Mr. Michael Kefauver

Toxicology Study No. 85-XC-01FA-03, John Houpt

REPORT DOCUMENTATION PAGE			Form Approved OMB No. 0704-0188	
Public reporting burden for this collection of information is estimated to average 1 hour per response, including the time for reviewing instructions, searching existing data sources, gathering and maintaining the data needed, and completing and reviewing the collection of information. Send comments regarding this burden estimate or any other aspect of this collection of information, including suggestions for reducing this burden, to Washington Headquarters Services, Directorate for Information Operations and Reports, 1215 Jefferson Davis Highway, Suite 1204, Arlington, VA 22202-4302, and to the Office of Management and Budget, Paperwork Reduction Project (0704-0188), Washington, DC 20503.				
1. AGENCY USE ONLY (Leave blank)		2. REPORT DATE August 2003		3. REPORT TYPE AND DATES COVERED Technical Report (August 2003)
4. TITLE AND SUBTITLE Toxicology Study No. 85-XC-01FA-03, Protocol No. 01-07-04 and 02-09-03, The Acute Skin and Eye Effects of the Active Topical Skin Protectant (aTSP) Formulations ICD-4020, ICD-4029, ICD-4050, ICD 4051 and ICD 4052 in Rabbits, July 2003				5. FUNDING NUMBERS
6. AUTHOR(S) John T. Houpt,				
7. PERFORMING ORGANIZATION NAME(S) AND ADDRESS(ES) U.S. Army Center for Health Promotion and Preventive Medicine Toxicology Program, ATTN: MCHB-TS-TTE 5158 Blackhawk Road Aberdeen Proving Ground, MD 21010-5403				8. PERFORMING ORGANIZATION REPORT NUMBER Toxicology Study No. 85-XC-01FA-03 Protocol No. 01-07-04 and 02-09-03
9. SPONSORING / MONITORING AGENCY NAME(S) AND ADDRESS(ES) Drug Assessment Division U. S. Army Medical Research Institute of Chemical Defense 3100 Ricketts Point Road Aberdeen Proving Ground, MD 21010-5400				10. SPONSORING / MONITORING AGENCY REPORT NUMBER
11. SUPPLEMENTARY NOTES				
12a. DISTRIBUTION / AVAILABILITY STATEMENT Approved for public release; distribution unlimited			12b. DISTRIBUTION CODE	
13. ABSTRACT (Maximum 200 words) Toxicity tests were performed to determine the acute skin and eye irritation effects of the active topical skin protectant (aTSP) formulations ICD-4020, ICD-4029, ICD-4050, ICD-4051, and ICD-4052 in rabbits. For the skin studies, the preweighed substance (0.5 gm) was dispensed onto the center of a 25mm self-adhering patch (Webril System, Hill Top Research, Inc., Cincinnati, Ohio). The patch was applied to the appropriate site and then over-wrapped with roll gauze (ConformO Stretch Bandage, The Kendall Company, Mansfield, Massachusetts). The animals were not restrained during the exposure but wore Elizabethan collars to prevent probing of the covered exposure site. Exposure was for 4 hours, after which the coverings were removed and irritation scored within 1 hour. Evaluations were also made at 24, 48 and 72 hours after treatment. The acute eye irritation tests were conducted using three rabbits per test substance. The procedure involved the application of 0.1 g of the substance to the conjunctival sac of each rabbit. Following treatment the eye was momentarily held closed, and then the animal was returned to its cage. After 24 hours, the cornea, iris, and conjunctiva were examined for signs of irritation and were scored (0 to 4) using a method described by Draize. Scoring was also performed at 48 and 72 hour intervals. The topical skin protectants ICD-4020, ICD-4029, ICD-4050, ICD-4051, and ICD-4052 did not produce significant skin irritation in rabbits. No adverse skin effects in humans are anticipated following an acute exposure. The topical skin protectants ICD-4020, ICD-4029, ICD-4050, ICD-4051, and ICD-4052 did not produce eye irritation in rabbits. No adverse ocular effects in humans are anticipated following an acute exposure.				
14. SUBJECT TERMS eye irritation ICD-4020 ICD-4029 ICD-4050 ICD 405 ICD 4052 rabbit skin irritation toxicity topical skin protectant aTSP TSP				15. NUMBER OF PAGES 30
				16. PRICE CODE
17. SECURITY CLASSIFICATION OF REPORT UNCLASSIFIED		18. SECURITY CLASSIFICATION OF THIS PAGE UNCLASSIFIED		19. SECURITY CLASSIFICATION OF ABSTRACT UNCLASSIFIED
				20. LIMITATION OF ABSTRACT UNLIMITED

REPORT DOCUMENTATION PAGE

1. AGENCY USE ONLY (Leave blank)

2. AUTHOR

3. TITLE

4. AUTHORING ORGANIZATION NAME(S) AND ADDRESS(ES)

5. PERFORMING ORGANIZATION NAME(S) AND ADDRESS(ES)

6. AUTHORING ORGANIZATION NAME(S) AND ADDRESS(ES)

7. AUTHORING ORGANIZATION NAME(S) AND ADDRESS(ES)

8. AUTHORING ORGANIZATION NAME(S) AND ADDRESS(ES)

9. AUTHORING ORGANIZATION NAME(S) AND ADDRESS(ES)

10. AUTHORING ORGANIZATION NAME(S) AND ADDRESS(ES)

11. AUTHORING ORGANIZATION NAME(S) AND ADDRESS(ES)

12. AUTHORING ORGANIZATION NAME(S) AND ADDRESS(ES)

13. AUTHORING ORGANIZATION NAME(S) AND ADDRESS(ES)

14. AUTHORING ORGANIZATION NAME(S) AND ADDRESS(ES)

15. AUTHORING ORGANIZATION NAME(S) AND ADDRESS(ES)

16. AUTHORING ORGANIZATION NAME(S) AND ADDRESS(ES)

17. AUTHORING ORGANIZATION NAME(S) AND ADDRESS(ES)

18. AUTHORING ORGANIZATION NAME(S) AND ADDRESS(ES)

19. AUTHORING ORGANIZATION NAME(S) AND ADDRESS(ES)

20. AUTHORING ORGANIZATION NAME(S) AND ADDRESS(ES)

21. AUTHORING ORGANIZATION NAME(S) AND ADDRESS(ES)

22. AUTHORING ORGANIZATION NAME(S) AND ADDRESS(ES)

23. AUTHORING ORGANIZATION NAME(S) AND ADDRESS(ES)

24. AUTHORING ORGANIZATION NAME(S) AND ADDRESS(ES)

25. AUTHORING ORGANIZATION NAME(S) AND ADDRESS(ES)

26. AUTHORING ORGANIZATION NAME(S) AND ADDRESS(ES)

27. AUTHORING ORGANIZATION NAME(S) AND ADDRESS(ES)

28. AUTHORING ORGANIZATION NAME(S) AND ADDRESS(ES)

29. AUTHORING ORGANIZATION NAME(S) AND ADDRESS(ES)

30. AUTHORING ORGANIZATION NAME(S) AND ADDRESS(ES)

Toxicology Study No. 85-XC-01FA-03, Protocol Nos. 01-07-04 and 02-09-03, Jul 03

Sponsor

Ernest H. Braue, Jr., Ph.D.
Advanced Assessment Branch
Drug Assessment Division
U.S. Army Medical Research Institute of Chemical Defense
3100 Ricketts Point Road
Aberdeen Proving Ground, MD 21010-5425

Study Title

Toxicology Study No. 85-XC-01FA-03
Protocol Nos. 01-07-04 and 02-09-03
The Acute Skin and Eye Effects of the Active Topical Skin Protectant (aTSP)
Formulations ICD-4020, ICD-4029, ICD-4050, ICD-4051 and ICD-4052 in Rabbits
July 2003

Data Requirement

Guideline
Reference No. 81-4
Reference No. 81-5

Author

John T. Houpt

Study Initiation Date

23 June 2003

Study Completion Date

15 July 2003

Performing Laboratory

U.S. Army Center for Health Promotion and Preventive Medicine
Toxicology Program, ATTN: MCHB-TS-TTE
5158 Blackhawk Road
Aberdeen Proving Ground, MD 21010-5403

Section 1

Section 1.1
Section 1.2
Section 1.3
Section 1.4
Section 1.5
Section 1.6
Section 1.7
Section 1.8
Section 1.9
Section 1.10

Section 2

Section 2.1
Section 2.2
Section 2.3
Section 2.4
Section 2.5
Section 2.6
Section 2.7
Section 2.8
Section 2.9
Section 2.10

Section 3

Section 3.1
Section 3.2
Section 3.3
Section 3.4
Section 3.5
Section 3.6
Section 3.7
Section 3.8
Section 3.9
Section 3.10

Section 4

Section 4.1
Section 4.2
Section 4.3
Section 4.4
Section 4.5
Section 4.6
Section 4.7
Section 4.8
Section 4.9
Section 4.10

Section 5

Section 5.1
Section 5.2
Section 5.3
Section 5.4
Section 5.5
Section 5.6
Section 5.7
Section 5.8
Section 5.9
Section 5.10

Section 6

Section 6.1
Section 6.2
Section 6.3
Section 6.4
Section 6.5
Section 6.6
Section 6.7
Section 6.8
Section 6.9
Section 6.10

Section 7

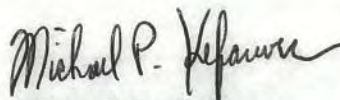
Section 7.1
Section 7.2
Section 7.3
Section 7.4
Section 7.5
Section 7.6
Section 7.7
Section 7.8
Section 7.9
Section 7.10

Toxicology Study No. 85-XC-01FA-03, Protocol Nos. 01-07-04 and 02-09-03, Jul 03

Quality Assurance Statement

For: Protocol Nos. 01-07-04 and 02-09-03, titled "The Acute Skin and Eye Effects of the Active Topical Skin Protectant (aTSP) Formulations ICD-4020, ICD-4029, ICD-4050, ICD-4051 and ICD-4052 in Rabbits the following critical phases were audited by the Strategic Initiatives Office-Quality Assurance Team:

<u>Critical Phase Audited (OSO Checklist #)</u>	<u>Date Audited</u>	<u>Date reported to Mngmt.</u>
1) Protocol Review (SIO-QAT #1.1)	06/04/03	06/04/03
2) Test System – Facilities (SIO-QAT # 4.1)	07/08/03	07/08/03
3) Test System – Identification (SIO-QAT # 4.3)	07/08/03	07/08/03
4) Test System - Husbandry (# 4.4)	07/08/03	07/08/03
5) Test System - Food and Water (# 4.6)	07/08/03	07/08/03
6) Maintenance and Calibration of Equip. (# 9.1)	07/08/03	07/08/03
7) Compliance w/ DTOX SOPs (SIO-QAT # 11.1)	07/08/03	07/08/03
8) Final Study Report Review (SIO-QAT # 13.1)	08/08/03	08/08/03
9) Study Raw Data Review (SIO-QAT # 14.1)	08/08/03	08/08/03
➤ Any findings made during the audits were made known at the time of the audit to the Study Director.		

 08/08/2003
Michael P. Kefauver
GLP Assessor, SIO-QAT

(Reserved for Confidentiality Claim)

Any changes made during the study were made known to the staff of the study in the study location.

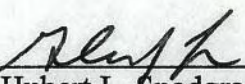
Signature: _____
Name: _____
Title: _____

Study Compliance Statement

The study described in this report was conducted in compliance with Title 21, Code of Federal Regulations (CFR), Food and Drug Administration (FDA); Part 58, Good Laboratory Practice Standards. There were no deviations from the aforementioned regulation that affected the quality or integrity of the study or the interpretation of the results.

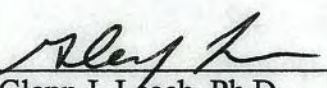
Submitted By:

Study Director:


for Hubert L. Snodgrass
Biologist/Master Consultant
Toxicity Evaluation Program
Directorate of Toxicology

25 Aug 2003
Date

Approved By:


Glenn J. Leach, Ph.D.
Supervisory Toxicologist
Program Manager
Toxicity Evaluation

25 Aug 2003
Date

Applicant/Submitter

Date

Reaction of Nitrogen Dioxide with Nitric Oxide

The reaction of nitrogen dioxide with nitric oxide has been studied in the gas phase at 25°C. The reaction is first order in each reactant and second order overall. The rate constant is $1.1 \times 10^4 \text{ liter/mole-sec}$. The activation energy is 11.5 kcal/mole . The reaction is exothermic by 10.5 kcal/mole . The equilibrium constant is $1.1 \times 10^4 \text{ liter/mole}$. The reaction is reversible.

Received May 1, 1952

Revised July 1, 1952

1. Introduction

The reaction of nitrogen dioxide with nitric oxide has been studied in the gas phase at 25°C. The reaction is first order in each reactant and second order overall. The rate constant is $1.1 \times 10^4 \text{ liter/mole-sec}$. The activation energy is 11.5 kcal/mole . The reaction is exothermic by 10.5 kcal/mole . The equilibrium constant is $1.1 \times 10^4 \text{ liter/mole}$. The reaction is reversible.

References

2. Discussion

The reaction of nitrogen dioxide with nitric oxide has been studied in the gas phase at 25°C. The reaction is first order in each reactant and second order overall. The rate constant is $1.1 \times 10^4 \text{ liter/mole-sec}$. The activation energy is 11.5 kcal/mole . The reaction is exothermic by 10.5 kcal/mole . The equilibrium constant is $1.1 \times 10^4 \text{ liter/mole}$. The reaction is reversible.

References



REPLY TO
ATTENTION OF

DEPARTMENT OF THE ARMY
U.S. ARMY CENTER FOR HEALTH PROMOTION AND PREVENTIVE MEDICINE
5158 BLACKHAWK ROAD
ABERDEEN PROVING GROUND, MARYLAND 21010-5403

EXECUTIVE SUMMARY
TOXICOLOGY STUDY NO. 85-XC-01FA-03
PROTOCOL NOS. 01-07-04 AND 02-09-03
THE ACUTE SKIN AND EYE EFFECTS OF THE ACTIVE TOPICAL
SKIN PROTECTANT (aTSP) FORMULATIONS ICD-4020, ICD-4029,
ICD-4050, ICD-4051 AND ICD-4052 IN RABBITS
JULY 2003

1. PURPOSE. To determine the acute skin and eye irritation effects of the active topical skin protectant (aTSP) formulations ICD-4020, ICD-4029, ICD-4050, ICD-4051, and ICD-4052 in rabbits.

2. CONCLUSIONS.

a. The topical skin protectants ICD-4020, ICD-4029, ICD-4050, ICD-4051, and ICD-4052 did not produce significant skin irritation in rabbits. No adverse skin effects in humans are anticipated following an acute exposure.

b. The topical skin protectants ICD-4020, ICD-4029, ICD-4050, ICD-4051, and ICD-4052 did not produce eye irritation in rabbits. No adverse ocular effects in humans are anticipated following an acute exposure.

TABLE OF CONTENTS

Paragraph	Page
1. REFERENCES	1
2. AUTHORITY	1
3. PURPOSE	1
4. MATERIALS	1
a. Test Substances	1
b. Animals	2
5. METHODS	2
a. Primary Skin Irritation	2
b. Primary Eye Irritation	2
c. Test Substance Preparation	3
6. RESULTS	3
a. Primary Skin Irritation	3
b. Primary Eye Irritation	3
7. CONCLUSIONS.....	3
Appendices	
A - References.....	A-1
B - USACHPPM Categories for Skin Irritation Effects	B-1
C - USACHPPM Categories for Eye Irritation Effects	C-1
D - EPA Toxicity Categories Criteria	D-1
E - Primary Skin Irritation Data; ICD-4020	E-1
F - Primary Skin Irritation Data; ICD-4029	F-1
G - Primary Skin Irritation Data; ICD-4050	G-1
H - Primary Skin Irritation Data; ICD-4051	H-1
I - Primary Skin Irritation Data; ICD-4052.....	I-1
J - Primary Eye Irritation Data; ICD-4020.....	J-1
K - Primary Eye Irritation Data; ICD-4029	K-1
L - Primary Eye Irritation Data; ICD-4050.....	L-1
M - Primary Eye Irritation Data; ICD-4051	M-1
N - Primary Eye Irritation Data; ICD-4052	N-1
O - Archives/Personnel	O-1

TABLE OF CONTENTS

Page	Section
1	1. INTRODUCTION
2	2. OBJECTIVES
3	3. SCOPE
4	4. METHODOLOGY
5	5. DATA SOURCES
6	6. ANALYSIS
7	7. RESULTS
8	8. CONCLUSIONS
9	9. REFERENCES
10	10. APPENDICES
11	11. GLOSSARY
12	12. INDEX
13	13. LIST OF FIGURES
14	14. LIST OF TABLES
15	15. SUMMARY
16	16. ACKNOWLEDGEMENTS
17	17. DECLARATION
18	18. CERTIFICATE
19	19. CURRICULUM VITAE
20	20. BIOGRAPHICAL SKETCH
21	21. STATEMENT OF WORK
22	22. STATEMENT OF ACHIEVEMENTS
23	23. STATEMENT OF INTERESTS
24	24. STATEMENT OF ACHIEVEMENTS
25	25. STATEMENT OF INTERESTS
26	26. STATEMENT OF ACHIEVEMENTS
27	27. STATEMENT OF INTERESTS
28	28. STATEMENT OF ACHIEVEMENTS
29	29. STATEMENT OF INTERESTS
30	30. STATEMENT OF ACHIEVEMENTS
31	31. STATEMENT OF INTERESTS
32	32. STATEMENT OF ACHIEVEMENTS
33	33. STATEMENT OF INTERESTS
34	34. STATEMENT OF ACHIEVEMENTS
35	35. STATEMENT OF INTERESTS
36	36. STATEMENT OF ACHIEVEMENTS
37	37. STATEMENT OF INTERESTS
38	38. STATEMENT OF ACHIEVEMENTS
39	39. STATEMENT OF INTERESTS
40	40. STATEMENT OF ACHIEVEMENTS
41	41. STATEMENT OF INTERESTS
42	42. STATEMENT OF ACHIEVEMENTS
43	43. STATEMENT OF INTERESTS
44	44. STATEMENT OF ACHIEVEMENTS
45	45. STATEMENT OF INTERESTS
46	46. STATEMENT OF ACHIEVEMENTS
47	47. STATEMENT OF INTERESTS
48	48. STATEMENT OF ACHIEVEMENTS
49	49. STATEMENT OF INTERESTS
50	50. STATEMENT OF ACHIEVEMENTS
51	51. STATEMENT OF INTERESTS
52	52. STATEMENT OF ACHIEVEMENTS
53	53. STATEMENT OF INTERESTS
54	54. STATEMENT OF ACHIEVEMENTS
55	55. STATEMENT OF INTERESTS
56	56. STATEMENT OF ACHIEVEMENTS
57	57. STATEMENT OF INTERESTS
58	58. STATEMENT OF ACHIEVEMENTS
59	59. STATEMENT OF INTERESTS
60	60. STATEMENT OF ACHIEVEMENTS
61	61. STATEMENT OF INTERESTS
62	62. STATEMENT OF ACHIEVEMENTS
63	63. STATEMENT OF INTERESTS
64	64. STATEMENT OF ACHIEVEMENTS
65	65. STATEMENT OF INTERESTS
66	66. STATEMENT OF ACHIEVEMENTS
67	67. STATEMENT OF INTERESTS
68	68. STATEMENT OF ACHIEVEMENTS
69	69. STATEMENT OF INTERESTS
70	70. STATEMENT OF ACHIEVEMENTS
71	71. STATEMENT OF INTERESTS
72	72. STATEMENT OF ACHIEVEMENTS
73	73. STATEMENT OF INTERESTS
74	74. STATEMENT OF ACHIEVEMENTS
75	75. STATEMENT OF INTERESTS
76	76. STATEMENT OF ACHIEVEMENTS
77	77. STATEMENT OF INTERESTS
78	78. STATEMENT OF ACHIEVEMENTS
79	79. STATEMENT OF INTERESTS
80	80. STATEMENT OF ACHIEVEMENTS
81	81. STATEMENT OF INTERESTS
82	82. STATEMENT OF ACHIEVEMENTS
83	83. STATEMENT OF INTERESTS
84	84. STATEMENT OF ACHIEVEMENTS
85	85. STATEMENT OF INTERESTS
86	86. STATEMENT OF ACHIEVEMENTS
87	87. STATEMENT OF INTERESTS
88	88. STATEMENT OF ACHIEVEMENTS
89	89. STATEMENT OF INTERESTS
90	90. STATEMENT OF ACHIEVEMENTS
91	91. STATEMENT OF INTERESTS
92	92. STATEMENT OF ACHIEVEMENTS
93	93. STATEMENT OF INTERESTS
94	94. STATEMENT OF ACHIEVEMENTS
95	95. STATEMENT OF INTERESTS
96	96. STATEMENT OF ACHIEVEMENTS
97	97. STATEMENT OF INTERESTS
98	98. STATEMENT OF ACHIEVEMENTS
99	99. STATEMENT OF INTERESTS
100	100. STATEMENT OF ACHIEVEMENTS



DEPARTMENT OF THE ARMY
U.S. ARMY CENTER FOR HEALTH PROMOTION AND PREVENTIVE MEDICINE
5158 BLACKHAWK ROAD
ABERDEEN PROVING GROUND, MARYLAND 21010-5403

REPLY TO
ATTENTION OF

MCHB-TS-TTE

TOXICOLOGY STUDY NO. 85-XC-01FA-03

PROTOCOL NOS. 01-07-04 AND 02-09-03

THE ACUTE SKIN AND EYE EFFECTS OF THE ACTIVE TOPICAL
SKIN PROTECTANT (aTSP) FORMULATIONS ICD-4020, ICD-4029,
ICD-4050, ICD-4051, AND ICD-4052 IN RABBITS
JULY 2003

1. REFERENCES. See Appendix A for a listing of references.
2. AUTHORITY. Letter, U.S. Army Medical Research Institute of Chemical Defense (MRICD), 20 March 2003, Subject: Toxicity Testing of Active Topical Skin Protectant Formulations.
3. PURPOSE. To determine the acute skin and eye irritant effects in animals of the topical skin protectant (aTSP) formulations ICD-4020, ICD-4029, ICD-4050, ICD-4051, and ICD-4052.
4. MATERIALS.

a. Test Substances. Dr. Ernest Braue, Medical Research Institute of Chemical Defense (MRICD), provided the test substances. None of the materials had any noticeable odor. Chemical characterization of each substance was the responsibility of the sponsor. Each material was identified by a lot number.

ICD-4020	Lot No. 4020-020828-ARL	Stiff, white cream
ICD 4029	Lot No. 4029-020904-ARL	Stiff, white cream
ICD-4050	Lot No. 4050-020906-ARL	Very stiff, white cream
ICD-4051	Lot No. 4051-020906-ARL	White, light cream
ICD-4052	Lot No. 4052-020906-ARL	Stiff, greenish cream

Use of trademarked names does not imply endorsement by the U.S. Army but is intended only to assist in identification of a specific product.

b. Animals. ⁺⁺The acute skin and eye irritation studies were conducted using New Zealand white rabbits purchased from Covance Research Products, Inc., Denver, Pennsylvania. A total of 12 animals of either sex were used. They were quarantined for 7 days prior to use. At the start of testing, rabbits weighed between 2.62 and 3.72 kilograms (kg). The rabbits were identified by ear tags and cage cards and were housed in individual wire-bottom stainless steel cages. Drinking quality water and feed [Teklad Certified 15 percent (%) Rabbit Diet[®] (W) 8630C] were available *ad libitum*. The rabbits were provided with Timothy Cubes[®], plastic barbells, and plastic ball toys as enrichment. Ambient temperatures in the animal rooms were maintained at 64 to 70 degrees Fahrenheit (°F) with relative humidity between 40 and 60%. The light/dark cycle was a 12-hour interval.

5. METHODS.

a. Primary Skin Irritation. A primary skin irritation test was conducted using six rabbits. The procedure (reference 1) involved the single application of 0.5 grams (g) of each test substance to one site on the clipped back of each rabbit. The rabbits' backs were divided into four sites, two on either side of the mid-line, such that each animal could receive up to four test materials. The preweighed substance was dispensed onto the center of a 25mm self-adhering patch (Webril System, Hill Top Research, Inc., Cincinnati, Ohio). The patch was applied to the appropriate site and then over-wrapped with roll gauze (Conform[®] Stretch Bandage, The Kendall Company, Mansfield, Massachusetts). The animals were not restrained during the exposure but wore Elizabethan collars to prevent probing of the covered exposure site. Exposure was for 4 hours, after which the coverings were removed and irritation scored within 1 hour. Evaluations were also made at 24, 48 and 72 hours after treatment and at 7 and 14 days, if necessary. Scoring of irritation was based on a method described by Draize (reference 2) in which erythema and edema were evaluated on a scale of 0 to 4 for severity. The sum of the mean erythema and mean edema values at 24 and 72 hours were used for the rating of skin irritation. The USACHPPM skin irritation rating system was followed (see Appendix B). The U.S. Environmental Protection Agency (EPA) Toxicity Categories (reference 4) were also applied (see Appendix D). In addition to the observations for skin irritation, any signs of systemic toxicity were recorded.

b. Primary Eye Irritation. An acute eye irritation test was conducted using three rabbits per test substance. The procedure (reference 3) involved the application of 0.1 g of the substance to the conjunctival sac of each rabbit. Following treatment the eye was momentarily held closed, and then the animal was returned to its cage. After 24 hours, the cornea, iris, and conjunctiva

* In conducting the studies described herein, the investigators adhered to the "Guide for the Care and Use of Laboratory Animals," National Research Council, National Academy Press, Washington, D.C. 1996.

+ The studies reported herein were performed in animal facilities fully accredited by the American Association for the Accreditation of Laboratory Animal Care.

® Teklad Certified Rabbit Diet is a registered trademark of Harlan, Teklad, Madison, Wisconsin.

® Timothy Cubes is a registered trademark of Bio-Serv, A Holton Industries Company, Frenchtown, New Jersey.

were examined for signs of irritation and were scored (0 to 4) using a method described by Draize (reference 2). The total score from the worksheet was divided by the number of eyes scored (3), times the number of tissue systems evaluated (3). This value was the basis for applying the USACHPPM eye irritation rating system (see Appendix C). The eyes were also evaluated at 48 and 72 hours. If irritation was observed at 72 hours, observations were made at 7 and 14 days after treatment to assess recovery. The EPA Toxicity Categories were also applied (see Appendix D). In addition to the observations for eye irritation, any signs of systemic toxicity were recorded.

c. Test Substance Preparation. For skin irritation testing, 0.5 g of each test substance was weighed onto an individual Webril patch and then applied to the skin. For the eye irritation studies, 0.1 g of the material was weighed onto a disposable autopipette tip, in the form of a small, suspended ball, and then placed in the conjunctival sac of the test animal.

6. RESULTS.

a. Primary Skin Irritation. Under the conditions of the described study, the test substances ICD-4020, ICD-4029, ICD-4050, ICD-4051, and ICD-4052 did not produce any significant skin irritation to rabbits following a 4-hour exposure. See Appendices E through N for individual animal results. The USACHPPM Skin Irritation Category I was assigned for each substance (Appendix B). The EPA Toxicity Category IV (Practically Nontoxic) was assigned for each material (see Appendix D).

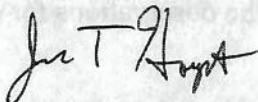
b. Primary Eye Irritation. Under the conditions of the described study, the test substances ICD-4020, ICD-4029, ICD-4050, ICD-4051, and ICD-4052 did not produce any primary irritation in the eyes of rabbits. See appendices M through R for individual animal results. The CHPPM Eye Irritation Category A was assigned for all five test materials. The EPA Toxicity Category IV was also assigned.

7. CONCLUSIONS.

a. The topical skin protectants ICD-4020, ICD-4029, ICD-4050, ICD-4051, and ICD-4052, did not produce significant skin irritation in rabbits. No adverse skin effects in humans are anticipated following an acute exposure.

Toxicology Study No. 85-XC-01FA-03, Protocol Nos. 01-07-04 and 02-09-03, Jul 03

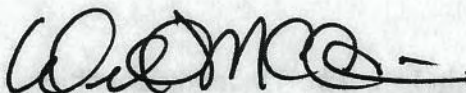
b. The topical skin protectants ICD-4020, ICD-4029, ICD-4050, ICD-4051, and ICD-4052, did not produce eye irritation in rabbits. No adverse ocular effects in humans are anticipated following an acute exposure.



JOHN T. HOUP

Biologist

Toxicity Evaluation Program



Wilfred McCain

Toxicologist

Toxicity Evaluation Program

APPROVED:



GLENN J. LEACH

Program Manager,

Toxicity Evaluation

Date 25 Aug 2003

APPENDIX A

REFERENCES

1. Standing Operating Procedure (SOP) No. 08.02, Primary Dermal Irritation Study, USACHPPM, Directorate of Toxicology. 2 Aug 02.
2. Draize, J.H., Woodward, G., and Calvery, H.O. 1944. Methods for the study of irritation and toxicity of substances applied topically to the skin and mucous membranes, *J. Pharmacol. Exp. Ther.* 82:377-390.
3. SOP No. 07.02, Primary Eye Irritation Study, USACHPPM, Directorate of Toxicology. 2 Aug 02.
4. U.S. Environmental Protection Agency, Office of Prevention, Pesticides and Toxic Substances (OPPTS): Health Effects Test Guidelines, OPPTS 870.1000, Acute Toxicity Testing – Background. August 1998.

APPENDIX B

USACHPPM CATEGORIES FOR SKIN IRRITATION EFFECTS

CATEGORY I - Compounds producing no primary irritation of the intact skin or no greater than mild primary irritation of the skin surrounding an abrasion. Score Limits: Intact 0-0.5; Abraded 0.51-2.0; Total 0-2.0 INTERPRETATION: *No restriction for acute application to the human skin.*

CATEGORY II - Compounds producing mild primary irritation of the intact skin and the skin surrounding an abrasion. Score Limits: Intact >0.5; Total 0.51-2.0 INTERPRETATION: *Should be used only on human skin found by examination to have no abrasions or may be used as clothing impregnant.*

CATEGORY III - Compounds producing moderate primary irritation of the intact skin and the skin surrounding an abrasion. Score Limits: Total 2.1-5.0 INTERPRETATION: *Should not be used directly without a prophetic patch test having been conducted on humans to determine irritation potential to human skin. May be used without patch testing, with extreme caution, as clothing impregnants. Compound should be resubmitted in the form and at the intended use concentration so that its irritation potential can be reexamined using other test techniques on animals.*

CATEGORY IV - Compounds producing moderate to severe primary irritation of the intact skin and of the skin surrounding an abrasion. Score Limits: Total 2.1-7.9 INTERPRETATION: *Should be resubmitted for testing in the form and at the intended use concentration. Upon resubmission, its irritation potential will be reexamined using other test techniques on animals, prior to possible prophetic patch testing in humans, at concentrations that have been shown not to produce primary irritation in animals.*

CATEGORY V - Compounds impossible to classify because of staining of the skin or other masking effects owing to physical properties of the compound or compounds producing necrosis, vesiculation, or eschars. Score Limits: Total 8.0 or not scorable. INTERPRETATION: *Not suitable for use on humans.*

APPENDIX C

USACHPPM CATEGORIES FOR EYE IRRITATION EFFECTS

CATEGORY A - Compounds noninjurious to the eye. Score Limits: 0-10 (individual conjunctival score for chemosis, redness or discharge not to exceed 1). **INTERPRETATION:** *Irritation of human eyes is not expected if the compound should accidentally get into the eyes, provided it is washed out as soon as possible.*

CATEGORY B - Compounds producing mild injury to the cornea. Score Limits: 10-20 (individual conjunctival score for chemosis, redness or discharge not to exceed 1). **INTERPRETATION:** *To be used with caution around the eyes.*

CATEGORY C - Compounds producing mild injury to the cornea, and in addition some injury to the conjunctiva. Score Limits: 5-30 (individual conjunctival score for chemosis, redness or discharge exceed 1). **INTERPRETATION:** *To be used with caution around the eyes and mucosa (e.g., nose and mouth).*

CATEGORY D - Compounds producing moderate injury to the cornea. Score Limits: <20-50 (individual conjunctival score for chemosis, redness or discharge not to exceed 1). **INTERPRETATION:** *To be used with extreme caution around eyes.*

CATEGORY E - Compounds producing moderate injury to the cornea and in addition producing some injury to the conjunctiva. Score Limits: 20-50 (individual conjunctival score for chemosis, redness or discharge exceed 1). **INTERPRETATION:** *To be used with extreme caution around the eyes and mucosa.*

CATEGORY F - Compounds producing severe injury to the cornea and to the conjunctiva. Score Limits: 50 or greater. **INTERPRETATION:** *To be used only with extreme caution; it is recommended that the use be restricted to areas other than the face.*

APPENDIX C

EXAMINER CATEGORY FOR EYE EXAMINATION

CATEGORY 1 - Examiner's responsibility is to the patient and the public. Examiner is responsible for the patient's safety and for the public's safety. Examiner is responsible for the patient's safety and for the public's safety. Examiner is responsible for the patient's safety and for the public's safety.

CATEGORY 2 - Examiner's responsibility is to the patient and the public. Examiner is responsible for the patient's safety and for the public's safety. Examiner is responsible for the patient's safety and for the public's safety. Examiner is responsible for the patient's safety and for the public's safety.

CATEGORY 3 - Examiner's responsibility is to the patient and the public. Examiner is responsible for the patient's safety and for the public's safety. Examiner is responsible for the patient's safety and for the public's safety. Examiner is responsible for the patient's safety and for the public's safety.

CATEGORY 4 - Examiner's responsibility is to the patient and the public. Examiner is responsible for the patient's safety and for the public's safety. Examiner is responsible for the patient's safety and for the public's safety. Examiner is responsible for the patient's safety and for the public's safety.

CATEGORY 5 - Examiner's responsibility is to the patient and the public. Examiner is responsible for the patient's safety and for the public's safety. Examiner is responsible for the patient's safety and for the public's safety. Examiner is responsible for the patient's safety and for the public's safety.

CATEGORY 6 - Examiner's responsibility is to the patient and the public. Examiner is responsible for the patient's safety and for the public's safety. Examiner is responsible for the patient's safety and for the public's safety. Examiner is responsible for the patient's safety and for the public's safety.

APPENDIX D

EPA TOXICITY CATEGORY CRITERIA*

Study	Category I <i>Highly Toxic</i> †	Category II <i>Moderately Toxic</i>	Category III <i>Slightly Toxic</i>	Category IV <i>Practically Nontoxic</i>
Acute Oral mg/kg	Up to and including 50	> 50 through 500	> 500 through 5,000	> 5,000
Acute Inhalation mg/L	Up to and including 0.05	> 0.05 through 0.5	> 0.5 through 2.0	> 2.0
Acute Dermal mg/kg	Up to and including 200	> 200 through 2,000	> 2,000 through 5,000	> 5,000
Eye Irritation	Corrosive (irreversible destruction of ocular tissue) or corneal involvement or irritation persisting for more than 21 days	Corneal involvement or irritation clearing in 8- 21 days	Corneal involvement or irritation clearing in 7 days or less	Minimal effects clearing in less than 24 hours
Skin Irritation	Corrosive (tissue destruction into the dermis and/or scarring)	Severe irritation at 72 hours (severe erythema or edema)	Moderate irritation at 72 hours (moderate erythema)	Mild or slight irritation (no irritation or slight erythema)

Study	Study Results	Study Results
Dermal Sensitization	Product is a sensitizer or is positive for sensitization	Product is not a sensitizer or is negative for sensitization

* U.S. Environmental Protection Agency, Office of Prevention, Pesticides and Toxic Substances (OPPTS): Health Effects Test Guidelines, OPPTS 870.1000, Acute Toxicity Testing –Back ground. August 1998.

† Descriptive terms, for example, Highly Toxic, Moderately toxic, etc., inserted for clarification only; not a part of OPPTS 870.1000.

APPENDIX B

DATA TO BE SUBMITTED BY CONTRACTOR

Category	Frequency	Location	Method of Collection	Data to be Submitted
1. Air Quality	Continuous	At the site	By using a continuous monitoring system	Hourly readings of particulate matter, sulfur dioxide, nitrogen dioxide, and carbon monoxide
2. Noise	Continuous	At the site	By using a continuous monitoring system	Hourly readings of noise level in dBA
3. Water Quality	Continuous	At the site	By using a continuous monitoring system	Hourly readings of pH, dissolved oxygen, temperature, and conductivity
4. Sedimentation	Continuous	At the site	By using a continuous monitoring system	Hourly readings of sedimentation rate in cm/hr
5. Air Pollution	Continuous	At the site	By using a continuous monitoring system	Hourly readings of particulate matter, sulfur dioxide, nitrogen dioxide, and carbon monoxide
6. Noise	Continuous	At the site	By using a continuous monitoring system	Hourly readings of noise level in dBA
7. Water Quality	Continuous	At the site	By using a continuous monitoring system	Hourly readings of pH, dissolved oxygen, temperature, and conductivity
8. Sedimentation	Continuous	At the site	By using a continuous monitoring system	Hourly readings of sedimentation rate in cm/hr

The contractor shall submit the data to the agency in the form of a report, which shall be submitted to the agency within 10 days of the completion of the project. The report shall include a summary of the data, a description of the methods used for data collection, and a discussion of the results. The report shall also include a copy of the data in the form of a table, which shall be submitted to the agency in the form of a separate document.

APPENDIX E

PRIMARY SKIN IRRITATION DATA

Protocol No.: 01FAa-11-01-07-04					SOP Number: 08.01			
Chemical Substance: ICD-4020 (aTSP) Lot No. 4020-020828-ARL								
Amount Applied: 0.5 gm					Concentration: Technical			
Species: Rabbit			Sex: Mixed		Weight: 2.63–3.32 kg			
Conditions: 4-hour nonoccluded exposure.								
Tm (hr)	Observation	Animal Number / Score						SUM
		03.02	03.05	03.06				
24	Erythema	0	0	0				0
48		0	0	0				
72		0	0	0				
7 da								
Subtotal (24 and 72 hour)								0
24	Edema	0	0	0				0
48		0	0	0				
72		0	0	0				
7 da								
Subtotal (24 and 72 hour)								0
Total Score (SUM of All Scores ÷ 2X No. of Animals)								0.00
<p>Study Conclusions: Nonirritating to the intact skin of rabbits. Discontinued after 72 hr since no irritant effects were observed.</p> <p>USACHPPM Category I. Interpretation: <i>No restriction for acute application to the human skin.</i></p> <p>EPA Toxicity Category IV. <i>Practically Nontoxic</i></p>								

APPENDIX F

PRIMARY SKIN IRRITATION DATA

Protocol No.: 01FAB-11-01-07-04					SOP Number: 08.01			
Chemical Substance: ICD-4029 (aTSP) Lot No. 4029-020904-ARL								
Amount Applied: 0.5 gm					Concentration: Technical			
Species: Rabbit			Sex: Mixed		Weight: 2.63 - 3.32 kg			
Conditions: 4-hour nonoccluded exposure.								

Tm (hr)	Observation	Animal Number / Score						SUM
		03.02	03.05	03.06				
24	Erythema	0	0	0				0
48		0	0	0				
72		0	0	0				
7 da								
Subtotal (24 and 72 hour)								0
24	Edema	0	0	0				0
48		0	0	0				
72		0	0	0				
7 da		0	0	0				
Subtotal (24 and 72 hour)								0
Total Score (SUM of All Scores ÷ 2X No. of Animals)								0.00

Study Conclusions: Nonirritating to the intact skin of rabbits. Discontinued after 72 hr since no irritant effects were observed.	
USACHPPM Category I. Interpretation: <i>No restriction for acute application to the human skin.</i>	
EPA Toxicity Category IV. <i>Practically Nontoxic</i>	

APPENDIX G

PRIMARY SKIN IRRITATION DATA

Protocol No.: 01FAc-11-01-07-04					OP Number: 08.01		
Chemical Substance: ICD-4050 (aTSP) Lot No. 4050-020906-AR1							
Amount Applied: 0.5 gm					Concentration: Technical		
Species: Rabbit		Sex: Mixed		Weight: 2.63-3.32 kg			
Conditions: 4-hour nonoccluded exposure.							

Tm (hr)	Observation	Animal Number / Score						SUM
		03.02	03.05	03.06				
24	Erythema	0	0	0				0
48		0	0	0				
72		0	0	0				
7 da								
Subtotal (24 and 72 hour)								0
24	Edema	0	0	0				0
48		0	0	0				
72		0	0	0				
7 da								
Subtotal (24 and 72 hour)								0
Total Score (SUM of All Scores ÷ 2X No. of Animals)								0.00

Study Conclusions: Nonirritating to the intact skin of rabbits. Discontinued after 72 hr since no irritant effects were observed.	
USACHPPM Category I. Interpretation: <i>No restriction for acute application to the human skin.</i>	
EPA Toxicity Category IV. <i>Practically Nontoxic</i>	

APPENDIX H

PRIMARY SKIN IRRITATION DATA

Protocol No.: 01FAd-11-01-07-04					SOP Number: 08.01			
Chemical Substance: ICD-4051								
Amount Applied: 0.5 gm					Concentration: Technical			
Species: Rabbit			Sex: Mixed		Weight: 2.79 – 3.35 kg			
Conditions: 4-hour nonoccluded exposure.								
Tm (hr)	Observation	03.08	03.10	03.12				SUM
24	Erythema	0	0	0				0
48		0	0	0				0
72		0	0	0				
7 da								
Subtotal (24 and 72 hour)								0
24	Edema	0	0	0				0
48		0	0	0				0
72		0	0	0				
7 da								
Subtotal (24 and 72 hour)								0
Total Score (SUM of All Scores ÷ 2X No. of Animals)								0.00
Study Conclusions: Nonirritating to the intact skin of rabbits. Discontinued after 72 hr since no irritant effects were observed. USACHPPM Category I. Interpretation: <i>No restriction for acute application to the human skin.</i> EPA Toxicity Category IV. <i>Practically Nontoxic</i>								

APPENDIX I

PRIMARY SKIN IRRITATION DATA

Protocol No.: 01FAe-11-01-07-04					SOP Number: 08.01			
Chemical Substance: ICD-4052 (sTSP) Lot No. 4052-020906-ARL								
Amount Applied: 0.5 gm					Concentration: Technical			
Species: Rabbit			Sex: Mixed			Weight: 2.79 – 3.35 kg		
Conditions: 4-hour nonoccluded exposure.								
Tm (hr)	Observation	Animal Number / Score						
		03.08	03.10	03.12				SUM
24	Erythema	1	1	0				2
48		1	0	0				1
72		1	0	0				
7 da		0	0	0				
Subtotal (24 and 72 hour)								3
24	Edema	0	0	0				0
48		0	0	0				0
72		0	0	0				
7 da		0	0	0				
Subtotal (24 and 72 hour)								3
Total Score (SUM of All Scores ÷ 2X No. of Animals)								0.5
Study Conclusions: Nonirritating to the intact skin of rabbits.								
USACHPPM Category I. Interpretation: No restriction for acute application to the human skin.								
EPA Toxicity Category IV. Practically Nontoxic								

APPENDIX J

PRIMARY EYE IRRITATION DATA

Protocol No.: 01FAa-10-02-09-03				SOP Number: 07.02				
Chemical Substance: ICD-4020 (aTSP) Lot No. 4020-020828-ARL								
Amount Applied: 0.1 gm				Concentration: Technical				
Species: Rabbit		Sex: Male		Weight: 2.95-3.23 kg				
Conditions: Applied to the conjunctival sac; right eye								
Tissue	Effect	Rabbit Number / 24-Hour Score						
		03.01	03.03	03.04				Subtotal
Cornea	A. Opacity	0	0	0				0
	B. Area Involved	0	0	0				
	Score = (Ax5)	0	0	0				
Iris	A. Iritis	0	0	0				0
	B. Score = Ax5	0	0	0				
Conjunctiva	A. Redness	0	0	0				0
	B. Chemosis	0	0	0				
	C. Discharge	0	0	0				
	Score = (A+B+C) x2	0	0	0				
Total Irritation Score							0	
Eye Injury Score (Total Score ÷ No. of Eyes*) ..							0.00	

Study Conclusions: The test substance was nonirritating to the eyes of rabbits.

USACHPPM Category: A Interpretation: *Irritation of human eyes is not expected if the substance should accidentally get into the eyes, provided it is washed out as soon as possible.*

EPA Toxicity Category: IV *Practically nontoxic.*

* Number of eyes = 3 tissues observed x 3 eyes = 9

Raw Irritation Scores By Time Period													
Protocol No. 01FAa-10-02-09-03 Test Substance: ICD-4020		Animal Number 03.01				Animal Number 03.03				Animal Number 03.04			
		Observation Time											
		Tissue	Effect (Score)	24 hr	48 hr	72 hr	7 da	24 hr	48 hr	72 hr	7 da	24 hr	48 hr
Cornea	Opacity	0	0	0		0	0	0		0	0	0	
	Area	0	0	0		0	0	0		0	0	0	
Iris	Iritis	0	0	0		0	0	0		0	0	0	
Conjunctiva	Redness	0	0	0		0	0	0		0	0	0	
	Chemosis	0	0	0		0	0	0		0	0	0	
	Discharge	0	0	0		0	0	0		0	0	0	

APPENDIX K

PRIMARY EYE IRRITATION DATA

Protocol No.: 01FAB-10-02-09-03		SOP Number: 07.02						
Chemical Substance: ICD - 402 9 (aTSP) Lot No. 4029-020904-ARL								
Amount Applied: 0.1 gm		Concentration: Technical						
Species: Rabbit		Sex: Male			Weight: 2.62-3.50 kg			
Conditions: Applied to the conjunctival sac; right eye								
Tissue	Effect	Rabbit Number / 24-Hour Score						
		03.07	03.09	03.11				Subtotal
Cornea	A. Opacity	0	0	0				0
	B. Area Involved	0	0	0				
	Score = (AxBx5)	0	0	0				
Iris	A. Iritis	0	0	0				0
	B. Score = Ax5	0	0	0				
Conjunctiva	A. Redness	0	0	0				0
	B. Chemosis	0	0	0				
	C. Discharge	0	0	0				
	Score = (A+B+C) x2	0	0	0				
Total Irritation Score							0.00	
Eye Injury Score (Total Score ÷ No. of Eyes)							0.00	

Study Conclusions: The test substance did not produce eye irritation in rabbits.

USACHPPM Category: A Interpretation: *Irritation of human eyes is not expected if the substance should accidentally get into the eyes, provided it is washed out as soon as possible.*

EPA Toxicity Category: IV *Practically nontoxic.*

Raw Eye Irritation Scores By Time Period													
Protocol No. 01FAB-10-0209-03 Test Substance: ICD-4029		Animal Number 3.07				Animal Number 3.09				Animal Number 3.11			
		Observation Time											
Tissue	Effect (Score)	24 hr	48 hr	72 hr	7 da	24 hr	48 hr	72 hr	7 da	24 hr	48 hr	72 hr	7 da
Cornea	Opacity	0	0	0		0	0	0		0	0	0	
	Area	0	0	0		0	0	0		0	0	0	
Iris	Iritis	0	0	0		0	0	0		0	0	0	
Conjunctiva	Redness	0	0	0		0	0	0		0	0	0	
	Chemosis	0	0	0		0	0	0		0	0	0	
	Discharge	0	0	0		0	0	0		0	0	0	

APPENDIX L

PRIMARY EYE IRRITATION DATA

Protocol No.: 01FAc-10-02-09-03		SOP Number: 07.02						
Chemical Substance: ICD-4050 (aTSP) Lot No. 4050-020906-ARL								
Amount Applied: 0.1 gm		Concentration: Technical						
Species: Rabbit		Sex: Male		Weight: 3.20-3.72 kg				
Conditions: Applied to the conjunctival sac; right eye								
Tissue	Effect	Rabbit Number / 24-Hour Score						Subtotal
		03.02	03.05	03.06				
Cornea	A. Opacity	0	0	0				0
	B. Area Involved	0	0	0				
	Score = (AxBx5)	0	0	0				
Iris	A. Iritis	0	0	0				0
	B. Score = Ax5	0	0	0				
Conjunctiva	A. Redness	0	0	0				0
	B. Chemosis	0	0	0				
	C. Discharge	0	0	0				
	Score = (A+B+C) x2	0	0	0				
Total Irritation Score							0.00	
Eye Injury Score (Total Score ÷ No. of Eyes).							0.00	

Study Conclusions: The test substance did not produce eye irritation in rabbits.

USACHPPM Category: A Interpretation: *Irritation of human eyes is not expected if the substance should accidentally get into the eyes, provided it is washed out as soon as possible.*

EPA Toxicity Category: IV *Practically nontoxic.*

Raw Eye Irritation Scores By Time Period													
Protocol No. 01FAc-10-02-09-03 Test Substance: ICD-4050		Animal Number 03.02				Animal Number 03.05				Animal Number 03.06			
		Observation Time											
Tissue	Effect (Score)	24 hr	48 hr	72 hr	7 da	24 hr	48 hr	72 hr	7 da	24 hr	48 hr	72 hr	7 da
Cornea	Opacity	0	0	0		0	0	0		0	0	0	
	Area	0	0	0		0	0	0		0	0	0	
Iris	Iritis	0	0	0		0	0	0		0	0	0	
Conjunctiva	Redness	0	0	0		0	0	0		0	0	0	
	Chemosis	0	0	0		0	0	0		0	0	0	
	Discharge	0	0	0		0	0	0		0	0	0	

APPENDIX M

PRIMARY EYE IRRITATION DATA

Protocol No.: 01FAd-10-02-09-03		SOP Number: 07.02						
Chemical Substance: ICD- 4051 (aTSP) Lot No. 4051-020906-ARL								
Amount Applied: 0.1 gm		Concentration: Technical						
Species: Rabbit		Sex: Male		Weight: 3.20-3.72 kg				
Conditions: Applied to the conjunctival sac; right eye								
Tissue	Effect	Rabbit Number / 24-Hour Score						Subtotal
		03.08	03.10	03.12				
Cornea	A. Opacity	0	0	0				
	B. Area Involved	0	0	0				
	Score = (AxBx5)	0	0	0				
Iris	A. Iritis	0	0	0				0
	B. Score = Ax5	0	0	0				
Conjunctiva	A. Redness	0	0	0				0
	B. Chemosis	0	0	0				
	C. Discharge	0	0	0				
	Score = (A+B+C) x2	0	0	0				
Total Irritation Score							0.00	
Eye Injury Score (Total Score ÷ No. of Eyes)							0.00	

Study Conclusions: The test substance did not produce eye irritation in rabbits.

USACHPPM Category: A Interpretation: *Irritation of human eyes is not expected if the substance should accidentally get into the eyes, provided it is washed out as soon as possible.*

EPA Toxicity Category: IV *Practically nontoxic.*

Raw Eye Irritation Scores By Time Period													
Protocol No. 01FAd-10-02—9-03 Test Substance: ICD-4051		Animal Number 03.08				Animal Number 03.10				Animal Number 03.12			
		Observation Time											
Tissue	Effect (Score)	24 hr	48 hr	72 hr	7 da	24 hr	48 hr	72 hr	7 da	24 hr	48 hr	72 hr	7 da
Cornea	Opacity	0	0	0		0	0	0		0	0	0	
	Area	0	0	0		0	0	0		0	0	0	
Iris	Iritis	0	0	0		0	0	0		0	0	0	
Conjunctiva	Redness	0	0	0		0	0	0		0	0	0	
	Chemosis	0	0	0		0	0	0		0	0	0	
	Discharge	0	0	0		0	0	0		0	0	0	

APPENDIX N

PRIMARY EYE IRRITATION DATA

Protocol No.: 01FAe-10-02-09-03		SOP Number: 07.02						
Chemical Substance: ICD -405 2 (aTSP) Lot No. 4052-020906-ARL								
Amount Applied: 0.1 gm		Concentration: Technical						
Species: Rabbit		Sex: Male		Weight: 3.18-3.42 kg				
Conditions: Applied to the conjunctival sac; left eye								
Tissue	Effect	Rabbit Number / 24-Hour Score						
		03.01	03.03	03.04				Subtotal
Cornea	A. Opacity	0	0	0				
	B. Area Involved	0	0	0				
	Score = (Ax5)	0	0	0				
Iris	A. Iritis	0	0	0				0
	B. Score = Ax5	0	0	0				
Conjunctiva	A. Redness	0	0	0				
	B. Chemosis	0	0	0				
	C. Discharge	0	0	0				
	Score = (A+B+C) x2	0	0	0				0

Total Irritation Score **0.00**

Eye Injury Score (Total Score ÷ No. of Eyes) **0.00**

Study Conclusions: The test substance did not produce eye irritation in rabbits

USACHPPM Category: A Interpretation: *Irritation of human eyes is not expected if the substance should accidentally get into the eyes, provided it is washed out as soon as possible.*

EPA Toxicity Category: IV *Practically nontoxic.*

Raw Eye Irritation Scores By Time Period													
Protocol No. 01FAe-10-02-09-03 Test Substance: ICD-4052		Animal Number 03.01				Animal Number 03.03				Animal Number 03.04			
		Observation Time											
		24 hr	48 hr	72 hr	7 da	24 hr	48 hr	72 hr	7 da	24 hr	48 hr	72 hr	7 da
Cornea	Opacity	0	0	0		0	0	0		0	0	0	
	Area	0	0	0		0	0	0		0	0	0	
Iris	Iritis	0	0	0		0	0	0		0	0	0	
Conjunctiva	Redness	0	0	0		0	0	0		0	0	0	
	Chemosis	0	0	0		0	0	0		0	0	0	
	Discharge	0	0	0		0	0	0		0	0	0	

APPENDIX O

ARCHIVES/PERSONNEL

1. ARCHIVES.

a. All raw data, documentation, records, protocol, and a copy of the final report generated as a result of this study will be archived in room 1026, Bldg E2100, USACHPPM, for a minimum of five (5) years following submission of the final report to the Sponsor. The archivist is Mark W. Michie, Toxicity Evaluation Program, 410-436-5089.

b. The present study used the laboratory project number 85-XC-01FA-03 for all filings.

c. The following protocol numbers identify the individual studies:

(1) Skin Irritation.

<u>Test Substance</u>	<u>Protocol Number</u>
ICD-4020	01FAa-11-01-07-04
ICD-4029	01FAb-11-01-07-04
ICD-4050	01FAc-11-01-07-04
ICD-4051	01FAd-11-01-07-04
ICD-4052	01FAe-11-01-07-04

(2) Eye Irritation.

ICD-4020	01FAa-10-02-09-02
ICD-4029	01FAb-10-02-09-02
ICD-4050	01FAc-10-02-09-02
ICD-4051	01FAd-10-02-09-02
ICD-4052	01FAe-10-02-09-02

2. PERSONNEL. The following personnel participated in the studies reported herein:

a. Toxicology Directorate:

Hubert L. Snodgrass, John T. Houpt, Wilfred C. McCain, Richard K. Arnold, and Theresa L. Hanna.

b. Quality Assurance Office:

Mr. Michael Kefauver